VOLUME 28 / NUMBER 1
JANUARY 8, 1990
ACC. NOS. N90-10001 TO N90-10827

STAR

AN ABSTRACT JOURNAL

Scientific and Technical Aerospace Reports

PRODUCED BY THE
SCIENTIFIC AND TECHNICAL
INFORMATION
DIVISION

NASA

NATIONAL AERONAUTICS AND SPACE ADMINISTRATION

WHAT YOU CAN DO FOR *STAR*

All users of this abstract service are urged to forward reports to be considered for announcement in *STAR*. This will aid NASA in its efforts to provide the fullest possible coverage of all scientific and technical publications that might support aeronautics and space research and development. If you have prepared relevant reports (other than those that you will transmit to NASA, DOD, or DOE through the usual contract- or grant-reporting channels), please send them for consideration to the NASA Scientific and Technical Information Facility, P.O. Box 8757, BWI Airport, MD 21240.

Reprints of journal articles, book chapters, and conference papers are also welcome. These will be considered for announcement in *STAR's* companion journal, *International Aerospace Abstracts.*

You may specify a particular source to be included in a report announcement if you wish; otherwise the report will be placed on public sale at the National Technical Information Service. Copyrighted publications will be announced but not distributed or sold.

PURCHASE OF *STAR*

The semimonthly issues are available to registered users on annual subscription from the NASA Scientific and Technical Information Facility, ATTN: Registration Services, P.O. Box 8757, BWI Airport, MD 21240. *STAR* is publicly available on annual subscription from the Superintendent of Documents, U.S. Government Printing Office, Washington, DC 20402.

PUBLISHED BY:

UNITED STATES GOVERNMENT
NATIONAL AERONAUTICS AND SPACE ADMINISTRATION
SCIENTIFIC AND TECHNICAL INFORMATION DIVISION
Scientific and Technical Aerospace Reports, Volume 28, is prepared by the NASA Scientific and Technical Information Facility operated for the National Aeronautics and Space Administration by RMS Associates.

The Administrator of the National Aeronautics and Space Administration has determined that the publication of this periodical is necessary in the transaction of the public business required by law of this agency. Use of funds for printing this periodical has been approved by the Director of the Office of Management and Budget through March 22, 1991.

US ISSN 0036-8741

Scientific and Technical Aerospace Reports (STAR) is issued twice a month and contains abstracts and indexes of meeting papers, conference proceedings, and unlimited distribution reports that have been added to the NASA Scientific and Technical Information Database during the preceding period. These citations may also be accessed online via NASA/RECON or via AIAA's Aerospace Database (File 108) through Dialog Information Services, Inc.

STAR subject coverage includes all aerospace-related areas that will help NASA achieve its mission. Material is gathered from all over the world and includes significant input from many countries under exchange and access agreements.

Consult the indexes at the back of this volume to help zero in on what you are looking for. These include:

Subject Index
Personal Author Index
Corporate Source Index
Contract Number Index
Report/Accession Number Index

STAR's companion abstract journal *International Aerospace Abstracts* should be used if you are looking for references to periodicals, books, and published meeting papers or conference proceedings.

Questions and comments should be addressed to:

NASA Scientific and Technical Information Facility
User Services
P.O. Box 8757
BWI Airport, MD 21240
301-621-0150

VOLUME 28 NUMBER 1 / JANUARY 8, 1990

TABLE OF CONTENTS

AERONAUTICS

Includes aeronautics (general); aerodynamics; air transportation and safety; aircraft communications and navigation; aircraft design, testing and performance; aircraft instrumentation; aircraft propulsion and power; aircraft stability and control; and research and support facilities (air).

For related information see also *Astronautics.*

01 AERONAUTICS (GENERAL) 1

02 AERODYNAMICS 1

Includes aerodynamics of bodies, combinations, wings, rotors, and control surfaces; and internal flow in ducts and turbomachinery.

For related information see also *34 Fluid Mechanics and Heat Transfer.*

03 AIR TRANSPORTATION AND SAFETY 4

Includes passenger and cargo air transport operations; and aircraft accidents.

For related information see also *16 Space Transportation* and *85 Urban Technology and Transportation.*

04 AIRCRAFT COMMUNICATIONS AND NAVIGATION 4

Includes digital and voice communication with aircraft; air navigation systems (satellite and ground based); and air traffic control.

For related information see also *17 Space Communications, Spacecraft Communications, Command and Tracking* and *32 Communications and Radar.*

05 AIRCRAFT DESIGN, TESTING AND PERFORMANCE 5

Includes aircraft simulation technology.

For related information see also *18 Spacecraft Design, Testing and Performance* and *39 Structural Mechanics.* For land transportation vehicles see *85 Urban Technology and Transportation.*

06 AIRCRAFT INSTRUMENTATION 7

Includes cockpit and cabin display devices; and flight instruments.

For related information see also *19 Spacecraft Instrumentation* and *35 Instrumentation and Photography.*

07 AIRCRAFT PROPULSION AND POWER 8

Includes prime propulsion systems and systems components, e.g., gas turbine engines and compressors; and onboard auxiliary power plants for aircraft.

For related information see also *20 Spacecraft Propulsion and Power, 28 Propellants and Fuels,* and *44 Energy Production and Conversion.*

08 AIRCRAFT STABILITY AND CONTROL 11

Includes aircraft handling qualities; piloting; flight controls; and autopilots.

For related information see also *05 Aircraft Design, Testing and Performance.*

09 RESEARCH AND SUPPORT FACILITIES (AIR) N.A.

Includes airports, hangars and runways; aircraft repair and overhaul facilities; wind tunnels; shock tubes; and aircraft engine test stands.

For related information see also *14 Ground Support Systems and Facilities (Space).*

ASTRONAUTICS

Includes astronautics (general); astrodynamics; ground support systems and facilities (space); launch vehicles and space vehicles; space transportation; space communications, spacecraft communications, command and tracking; spacecraft design, testing and performance; spacecraft instrumentation; and spacecraft propulsion and power.

For related information see also *Aeronautics.*

12 ASTRONAUTICS (GENERAL) 15

For extraterrestrial exploration see *91 Lunar and Planetary Exploration.*

13 ASTRODYNAMICS 16

Includes powered and free-flight trajectories; and orbital and launching dynamics.

14 GROUND SUPPORT SYSTEMS AND FACILITIES (SPACE) N.A.

Includes launch complexes, research and production facilities; ground support equipment, e.g., mobile transporters; and simulators.

For related information see also *09 Research and Support Facilities (Air).*

15 LAUNCH VEHICLES AND SPACE VEHICLES N.A.

Includes boosters; operating problems of launch/space vehicle systems; and reusable vehicles.

For related information see also *20 Spacecraft Propulsion and Power.*

16 SPACE TRANSPORTATION 16

Includes passenger and cargo space transportation, e.g., shuttle operations; and space rescue techniques.

For related information see also *03 Air Transportation and Safety* and *18 Spacecraft Design, Testing and Performance.* For space suits see *54 Man/System Technology and Life Support.*

17 SPACE COMMUNICATIONS, SPACECRAFT COMMUNICATIONS, COMMAND AND TRACKING N.A.

Includes telemetry; space communications networks; astronavigation and guidance; and radio blackout.

For related information see also *04 Aircraft Communications and Navigation* and *32 Communications and Radar.*

18 SPACECRAFT DESIGN, TESTING AND PERFORMANCE 17

Includes satellites; space platforms; space stations; spacecraft systems and components such as thermal and environmental controls; and attitude controls.

For life support systems see *54 Man/System Technology and Life Support.* For related information see also *05 Aircraft Design, Testing and Performance, 39 Structural Mechanics,* and *16 Space Transportation.*

19 SPACECRAFT INSTRUMENTATION 26

For related information see also *06 Aircraft Instrumentation* and *35 Instrumentation and Photography.*

20 SPACECRAFT PROPULSION AND POWER 26

Includes main propulsion systems and components, e.g. rocket engines; and spacecraft auxiliary power sources.

For related information see also *07 Aircraft Propulsion and Power, 28 Propellants and Fuels, 44 Energy Production and Conversion,* and *15 Launch Vehicles and Space Vehicles.*

CHEMISTRY AND MATERIALS

Includes chemistry and materials (general); composite materials; inorganic and physical chemistry; metallic materials; nonmetallic materials; propellants and fuels; and materials processing.

23 CHEMISTRY AND MATERIALS (GENERAL) 33

24 COMPOSITE MATERIALS 33

Includes physical, chemical, and mechanical properties of laminates and other composite materials.

For ceramic materials see *27 Nonmetallic Materials.*

25 INORGANIC AND PHYSICAL CHEMISTRY 35

Includes chemical analysis, e.g., chromatography; combustion theory; electrochemistry; and photochemistry.

For related information see also *77 Thermodynamics and Statistical Physics.*

26 METALLIC MATERIALS 42

Includes physical, chemical, and mechanical properties of metals, e.g., corrosion; and metallurgy.

27 NONMETALLIC MATERIALS 46

Includes physical, chemical, and mechanical properties of plastics, elastomers, lubricants, polymers, textiles, adhesives, and ceramic materials.

For composite materials see *24 Composite Materials.*

28 PROPELLANTS AND FUELS 53

Includes rocket propellants, igniters and oxidizers; their storage and handling procedures; and aircraft fuels.

For related information see also *07 Aircraft Propulsion and Power, 20 Spacecraft Propulsion and Power,* and *44 Energy Production and Conversion.*

29 MATERIALS PROCESSING N.A.

Includes space-based development of products and processes for commercial application.

For biological materials see *55 Space Biology.*

ENGINEERING

Includes engineering (general); communications and radar; electronics and electrical engineering; fluid mechanics and heat transfer; instrumentation and photography; lasers and masers; mechanical engineering; quality assurance and reliability; and structural mechanics.

For related information see also *Physics.*

31 ENGINEERING (GENERAL) 54

Includes vacuum technology; control engineering; display engineering; cryogenics; and fire prevention.

32 COMMUNICATIONS AND RADAR 55

Includes radar; land and global communications; communications theory; and optical communications.

For related information see also *04 Aircraft Communications and Navigation* and *17 Space Communications, Spacecraft Communications, Command and Tracking.* For search and rescue see *03 Air Transportation and Safety,* and *16 Space Transportation.*

33 ELECTRONICS AND ELECTRICAL ENGINEERING 58

Includes test equipment and maintainability; components, e.g., tunnel diodes and transistors; microminiaturization; and integrated circuitry.

For related information see also *60 Computer Operations and Hardware* and *76 Solid-State Physics.*

34 FLUID MECHANICS AND HEAT TRANSFER 62

Includes boundary layers; hydrodynamics; fluidics; mass transfer and ablation cooling.

For related information see also *02 Aerodynamics* and *77 Thermodynamics and Statistical Physics.*

35 INSTRUMENTATION AND PHOTOGRAPHY 72

Includes remote sensors; measuring instruments and gauges; detectors; cameras and photographic supplies; and holography.

For aerial photography see *43 Earth Resources and Remote Sensing.* For related information see also *06 Aircraft Instrumentation* and *19 Spacecraft Instrumentation.*

36 LASERS AND MASERS 74

Includes parametric amplifiers.

For related information see also *76 Solid-State Physics.*

37 MECHANICAL ENGINEERING 76

Includes auxiliary systems (nonpower); machine elements and processes; and mechanical equipment.

38 QUALITY ASSURANCE AND RELIABILITY N.A.

Includes product sampling procedures and techniques; and quality control.

39 STRUCTURAL MECHANICS 79

Includes structural element design and weight analysis; fatigue; and thermal stress.

For applications see *05 Aircraft Design, Testing and Performance* and *18 Spacecraft Design, Testing and Performance.*

GEOSCIENCES

Includes geosciences (general); earth resources and remote sensing; energy production and conversion; environment pollution; geophysics; meteorology and climatology; and oceanography.

For related information see also *Space Sciences.*

42 GEOSCIENCES (GENERAL) N.A.

43 EARTH RESOURCES AND REMOTE SENSING 82

Includes remote sensing of earth resources by aircraft and spacecraft; photogrammetry; and aerial photography.

For instrumentation see *35 Instrumentation and Photography.*

44 ENERGY PRODUCTION AND CONVERSION 82

Includes specific energy conversion systems, e.g., fuel cells; global sources of energy; geophysical conversion; and windpower.

For related information see also *07 Aircraft Propulsion and Power, 20 Spacecraft Propulsion and Power,* and *28 Propellants and Fuels.*

45 ENVIRONMENT POLLUTION 84

Includes atmospheric, noise, thermal, and water pollution.

46 GEOPHYSICS 85

Includes aeronomy; upper and lower atmosphere studies; ionospheric and magnetospheric physics; and geomagnetism.

For space radiation see *93 Space Radiation.*

47 METEOROLOGY AND CLIMATOLOGY 86

Includes weather forecasting and modification.

48 OCEANOGRAPHY 89

Includes biological, dynamic, and physical oceanography; and marine resources.

For related information see also *43 Earth Resources and Remote Sensing.*

LIFE SCIENCES

Includes life sciences (general); aerospace medicine; behavioral sciences; man/system technology and life support; and space biology.

51 LIFE SCIENCES (GENERAL) 91

52 AEROSPACE MEDICINE 92

Includes physiological factors; biological effects of radiation; and effects of weightlessness on man and animals.

53 BEHAVIORAL SCIENCES 94

Includes psychological factors; individual and group behavior; crew training and evaluation; and psychiatric research.

54 MAN/SYSTEM TECHNOLOGY AND LIFE SUPPORT 95

Includes human engineering; biotechnology; and space suits and protective clothing.

For related information see also *16 Space Transportation.*

55 SPACE BIOLOGY N.A.

Includes exobiology; planetary biology; and extraterrestrial life.

MATHEMATICAL AND COMPUTER SCIENCES

Includes mathematical and computer sciences (general); computer operations and hardware; computer programming and software; computer systems; cybernetics; numerical analysis; statistics and probability; systems analysis; and theoretical mathematics.

59 MATHEMATICAL AND COMPUTER SCIENCES (GENERAL) 102

60 COMPUTER OPERATIONS AND HARDWARE 102

Includes hardware for computer graphics, firmware, and data processing.

For components see *33 Electronics and Electrical Engineering.*

61 COMPUTER PROGRAMMING AND SOFTWARE 103

Includes computer programs, routines, algorithms, and specific applications, e.g., CAD/CAM.

62 COMPUTER SYSTEMS 107

Includes computer networks and special application computer systems.

63 CYBERNETICS 109

Includes feedback and control theory, artificial intelligence, robotics and expert systems.

For related information see also *54 Man/System Technology and Life Support.*

64 NUMERICAL ANALYSIS 111

Includes iteration, difference equations, and numerical approximation.

65 STATISTICS AND PROBABILITY 114

Includes data sampling and smoothing; Monte Carlo method; and stochastic processes.

66 SYSTEMS ANALYSIS 117

Includes mathematical modeling; network analysis; and operations research.

67 THEORETICAL MATHEMATICS 117

Includes topology and number theory.

PHYSICS

Includes physics (general); acoustics; atomic and molecular physics; nuclear and high-energy physics; optics; plasma physics; solid-state physics; and thermodynamics and statistical physics.

For related information see also *Engineering.*

70 PHYSICS (GENERAL) 118

For precision time and time interval (PTTI) see *35 Instrumentation and Photography;* for geophysics, astrophysics or solar physics see *46 Geophysics, 90 Astrophysics,* or *92 Solar Physics.*

71 ACOUSTICS 118
Includes sound generation, transmission, and attenuation.
For noise pollution see *45 Environment Pollution.*

72 ATOMIC AND MOLECULAR PHYSICS 119
Includes atomic structure, electron properties, and molecular spectra.

73 NUCLEAR AND HIGH-ENERGY PHYSICS 121
Includes elementary and nuclear particles; and reactor theory.
For space radiation see *93 Space Radiation.*

74 OPTICS 123
Includes light phenomena and optical devices.
For lasers see *36 Lasers and Masers.*

75 PLASMA PHYSICS 125
Includes magnetohydrodynamics and plasma fusion.
For ionospheric plasmas see *46 Geophysics.* For space plasmas see *90 Astrophysics.*

76 SOLID-STATE PHYSICS 127
Includes superconductivity.
For related information see also *33 Electronics and Electrical Engineering* and *36 Lasers and Masers.*

77 THERMODYNAMICS AND STATISTICAL PHYSICS 134
Includes quantum mechanics; theoretical physics; and Bose and Fermi statistics.
For related information see also *25 Inorganic and Physical Chemistry* and *34 Fluid Mechanics and Heat Transfer.*

SOCIAL SCIENCES

Includes social sciences (general); administration and management; documentation and information science; economics and cost analysis; law, political science, and space policy; and urban technology and transportation.

80 SOCIAL SCIENCES (GENERAL) N.A.
Includes educational matters.

81 ADMINISTRATION AND MANAGEMENT 135
Includes management planning and research.

82 DOCUMENTATION AND INFORMATION SCIENCE 136
Includes information management; information storage and retrieval technology; technical writing; graphic arts; and micrography.
For computer documentation see *61 Computer Programming and Software.*

83 ECONOMICS AND COST ANALYSIS N.A.
Includes cost effectiveness studies.

84 LAW, POLITICAL SCIENCE AND SPACE POLICY N.A.
Includes NASA appropriation hearings; aviation law; space law and policy; international law; international cooperation; and patent policy.

85 URBAN TECHNOLOGY AND TRANSPORTATION 137
Includes applications of space technology to urban problems; technology transfer; technology assessment; and surface and mass transportation.
For related information see *03 Air Transportation and Safety, 16 Space Transportation,* and *44 Energy Production and Conversion.*

SPACE SCIENCES

Includes space sciences (general); astronomy; astrophysics; lunar and planetary exploration; solar physics; and space radiation.
For related information see also *Geosciences.*

88 SPACE SCIENCES (GENERAL) 137

89 ASTRONOMY 139
Includes radio, gamma-ray, and infrared astronomy; and astrometry.

90 ASTROPHYSICS 140
Includes cosmology; celestial mechanics; space plasmas; and interstellar and interplanetary gases and dust.
For related information see also *75 Plasma Physics.*

91 LUNAR AND PLANETARY EXPLORATION 141
Includes planetology; and manned and unmanned flights.
For spacecraft design or space stations see *18 Spacecraft Design, Testing and Performance.*

92 SOLAR PHYSICS 142
Includes solar activity, solar flares, solar radiation and sunspots.
For related information see *93 Space Radiation.*

93 SPACE RADIATION N.A.
Includes cosmic radiation; and inner and outer earth's radiation belts.
For biological effects of radiation see *52 Aerospace Medicine.* For theory see *73 Nuclear and High-Energy Physics.*

GENERAL

Includes aeronautical, astronautical, and space science related histories, biographies, and pertinent reports too broad for categorization; histories or broad overviews of NASA programs.

99 GENERAL 143

Note: N.A. means that no abstracts were assigned to this category for this issue.

SUBJECT INDEX I-1
PERSONAL AUTHOR INDEX I-53
CORPORATE SOURCE INDEX I-61
CONTRACT NUMBER INDEX I-73
REPORT/ACCESSION NUMBER INDEX I-77
APPENDIX—ABOUT STAR A-1

TYPICAL CITATION AND ABSTRACT

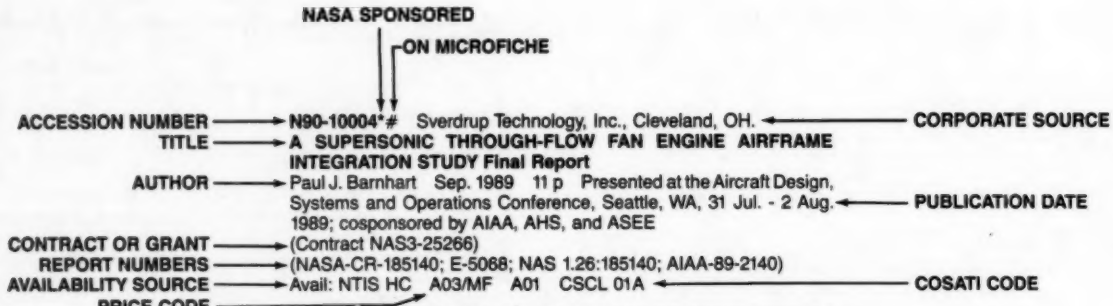
NASA SPONSORED
ON MICROFICHE
ACCESSION NUMBER
N90-10004*# Sverdrup Technology, Inc., Cleveland, OH.
CORPORATE SOURCE
TITLE
A SUPERSONIC THROUGH-FLOW FAN ENGINE AIRFRAME INTEGRATION STUDY Final Report
AUTHOR
Paul J. Barnhart Sep. 1989 11 p Presented at the Aircraft Design, Systems and Operations Conference, Seattle, WA, 31 Jul. - 2 Aug. 1989; cosponsored by AIAA, AHS, and ASEE
PUBLICATION DATE
CONTRACT OR GRANT
(Contract NAS3-25266)
REPORT NUMBERS
(NASA-CR-185140; E-5068; NAS 1.26:185140; AIAA-89-2140)
AVAILABILITY SOURCE
Avail: NTIS HC A03/MF A01 CSCL 01A
COSATI CODE
PRICE CODE

Engine airframe integration effects are investigated for supersonic through-flow fan engines installed on a Mach 3.20 supersonic cruise vehicle. Six different supersonic through-flow fan engine installations covering the effects of engine size, nacelle contour, nacelle placement, and approximate bypass plume effects are presented. The different supersonic through-flow fan installations are compared with a conventional turbine bypass engine configuration on the same basic airframe. The supersonic through-flow fan engine integrations are shown to be comparable to the turbine bypass engine configuration on the basis of installed nacelle wave drag. The supersonic through-flow fan engine airframe integrated vehicles have superior aerodynamic performance on the basis of maximum lift-to-drag ratio than the turbine bypass engine installation over the entire operating Mach number range from 1.10 to 3.20. When approximate bypass plume modeling is included, the supersonic through-flow fan engine configuration shows even larger improvements over the turbine bypass engine configuration. Author

VOLUME 28 NUMBER 1 / JANUARY 8, 1990

Scientific and Technical Aerospace Reports

A Semimonthly Publication of the National Aeronautics and Space Administration

01 AERONAUTICS (GENERAL)

N90-10001# Office of Air Force History, Washington, DC.
ENCYCLOPEDIA OF US AIR FORCE AIRCRAFT AND MISSILE SYSTEMS. VOLUME 2: POST-WORLD WAR 2 BOMBERS, 1945-1973
Marcelle S. Knaack 1988 618 p
(AD-A209273) Avail: NTIS HC A99/MF A02 CSCL 01/3

An overview is given of the basic development, technical and basic mission performance, and programs for the B-36 Peacemaker; B-45 Tornado; B-47 Stratojet; B-50 Superfortress; B-52 Stratofortress; B-57 Canberra; B-58 Hustler; B/RB-66 Destroyer; World War 2 bombers in the postwar period; and post-World War 2 experimental and prototype bombers. GRA

N90-10002*# National Aeronautics and Space Administration. Langley Research Center, Hampton, VA.
A STUDY OF HIGH-LIFT AIRFOILS AT HIGH REYNOLDS NUMBERS IN THE LANGLEY LOW-TURBULENCE PRESSURE TUNNEL
Harry L. Morgan, Jr., James C. Ferris, and Robert J. McGhee Jul. 1987 64 p
(NASA-TM-89125; L-16266; NAS 1.15:89125) Avail: NTIS HC A04/MF A01 CSCL 01A

An experimental study was conducted in the Langley Low Turbulence Pressure Tunnel to determine the effects of Reynolds number and Mach number on the two-dimensional aerodynamic performance of two supercritical type airfoils, one equipped with a conventional flap system and the other with an advanced high lift flap system. The conventional flap system consisted of a leading edge slat and a double slotted, trailing edge flap with a small chord vane and a large chord aft flap. The advanced flap system consisted of a leading edge slat and a double slotted, trailing edge flap with a large chord vane and a small chord aft flap. Both models were tested with all elements nested to form the cruise airfoil and with the leading edge slat and with a single or double slotted, trailing edge flap deflected to form the high lift airfoils. The experimental tests were conducted through a Reynolds number range from 2.8 to 20.9 x 1,000,000 and a Mach number range from 0.10 to 0.35. Lift and pitching moment data were obtained. Summaries of the test results obtained are presented and comparisons are made between the observed aerodynamic performance trends for both models. The results showing the effect of leading edge frost and glaze ice formation is given. Author

02 AERODYNAMICS

Includes aerodynamics of bodies, combinations, wings, rotors, and control surfaces; and internal flow in ducts and turbomachinery.

For related information see also *34 Fluid Mechanics and Heat Transfer.*

N90-10003# National Aerospace Lab., Tokyo (Japan).
A NUMERICAL METHOD FOR SOLVING TRANSONIC FLOW PAST AIRCRAFT IN CARTESIAN COORDINATES
Masayoshi Nakamura Dec. 1988 30 p In JAPANESE; ENGLISH summary
(NAL-TR-1008; ISSN-0389-4010) Avail: NTIS HC A03/MF A01

A numerical method for computing inviscid transonic flow around an arbitrary aircraft configuration is described. The basic formula consists of simultaneous equations for variables of velocity potential and Mach number. This formula is a permutation of the full potential equation. The simultaneous equations are solved numerically, satisfying given boundary conditions. The shock wave is captured as a discontinuous surface where the flow conditions satisfy the shock wave relationship. The calculation flow field is a rectangular box field. Grid points and boundary points are generated in Cartesian coordinates. The grid points are equidistant but their intervals can be varied with the location. External forms of the aircraft and vortex sheets are shaped from numerous small triangular planes. The majority of the boundary points are on these external forms. The basic formula is expressed as difference equations using the grid points and the boundary points. The difference equations are solved in the numerical procedure. Several calculated results of this method are compared with the experimental and other numerical results. Author

N90-10004*# Sverdrup Technology, Inc., Cleveland, OH.
A SUPERSONIC THROUGH-FLOW FAN ENGINE AIRFRAME INTEGRATION STUDY Final Report
Paul J. Barnhart Sep. 1989 11 p Presented at the Aircraft Design, Systems and Operations Conference, Seattle, WA, 31 Jul. - 2 Aug. 1989; cosponsored by AIAA, AHS, and ASEE
(Contract NAS3-25266)
(NASA-CR-185140; E-5068; NAS 1.26:185140; AIAA-89-2140)
Avail: NTIS HC A03/MF A01 CSCL 01A

Engine airframe integration effects are investigated for supersonic through-flow fan engines installed on a Mach 3.20 supersonic cruise vehicle. Six different supersonic through-flow fan engine installations covering the effects of engine size, nacelle contour, nacelle placement, and approximate bypass plume effects are presented. The different supersonic through-flow fan installations are compared with a conventional turbine bypass engine configuration on the same basic airframe. The supersonic through-flow fan engine integrations are shown to be comparable to the turbine bypass engine configuration on the basis of installed nacelle wave drag. The supersonic through-flow fan engine airframe integrated vehicles have superior aerodynamic performance on the basis of maximum lift-to-drag ratio than the turbine bypass engine installation over the entire operating Mach number range from 1.10 to 3.20. When approximate bypass plume modeling is included, the supersonic through-flow fan engine configuration shows even larger improvements over the turbine bypass engine configuration. Author

N90-10005 Mississippi State Univ., State College.
THREE-DIMENSIONAL UNSTEADY TRANSONIC VISCOUS-INVISCID INTERACTION Ph.D. Thesis
Shahyar Pirzadeh 1988 114 p
Avail: Univ. Microfilms Order No. DA8909851

The objective of this study is the development of a numerical technique which can provide three-dimensional, time-accurate, compressible, turbulent flow solutions in a practical and relatively economical way. The approach taken is that of the method of viscous-inviscid interaction. The Euler equations are assumed to

govern the outer inviscid portion of the flow, and the viscous layer close to the solid wall is described by a set of integral boundary-layer equations. The viscous solutions are obtained in a direct fashion with a weighted-average phase error scheme. The discretized integral form of the Euler equations are solved with an upwind, finite-volume scheme. The method of equivalent sources is used for viscous-inviscid coupling. Steady-state and unsteady computations for two AGARD airfoils and a wing show that satisfactory engineering solutions can be obtained for attached, high Reynolds number flows using this method. Quasi-unsteady interactions are shown to produce similar results to those provided by true-unsteady interactions. Considerable computer resources can be saved for some cases by using quasi-unsteady interactions. Dissert. Abstr.

N90-10006*# National Aeronautics and Space Administration. Ames Research Center, Moffett Field, CA.

AN INTEGRATED CFD/EXPERIMENTAL ANALYSIS OF AERODYNAMIC FORCES AND MOMENTS

John E. Melton, David D. Robertson, and Seth A. Moyer Aug. 1989 52 p

(NASA-TM-102195; A-89145; NAS 1.15:102195) Avail: NTIS HC A04/MF A01 CSCL 01A

Aerodynamic analysis using computational fluid dynamics (CFD) is most fruitful when it is combined with a thorough program of wind tunnel testing. The understanding of aerodynamic phenomena is enhanced by the synergistic use of both analysis methods. A technique is described for an integrated approach to determining the forces and moments acting on a wind tunnel model by using a combination of experimentally measured pressures and CFD predictions. The CFD code used was FLO57 (an Euler solver) and the wind tunnel model was a heavily instrumented delta wing with 62.5 deg of leading-edge sweep. A thorough comparison of the CFD results and the experimental data is presented for surface pressure distributions and longitudinal forces and moments. The experimental pressures were also integrated over the surface of the model and the resulting forces and moments are compared to the CFD and wind tunnel results. The accurate determination of various drag increments via the combined use of the CFD and experimental pressures is presented in detail. Author

N90-10007*# Institute for Computer Applications in Science and Engineering, Hampton, VA.

ON THE INTERACTION OF STATIONARY CROSSFLOW VORTICES AND TOLLMIEN-SCHLICHTING WAVES IN THE BOUNDARY LAYER ON A ROTATING DISC Final Report

Andrew P. Bassom and Philip Hall May 1989 54 p Submitted for publication

(Contract NAS1-18605)

(NASA-CR-181859; ICASE-89-34; NAS 1.26:181859) Avail: NTIS HC A04/MF A01 CSCL 01A

There are many fluid flows where the onset of transition can be caused by different instability mechanisms which compete among themselves. The interaction is considered of two types of instability mode (at an asymptotically large Reynolds number) which can occur in the flow above a rotating disc. In particular, the interaction is examined between lower branch Tollmien-Schlichting (TS) waves and the upper branch, stationary, inviscid crossflow vortex whose asymptotic structure has been described by Hall (1986). This problem is studied in the context of investigating the effect of the vortex on the stability characteristics of a small TS wave. Essentially, it is found that the primary effect is felt through the modification to the mean flow induced by the presence of the vortex. Initially, the TS wave is taken to be linear in character and it is shown (for the cases of both a linear and a nonlinear stationary vortex) that the vortex can exhibit both stabilizing and destabilizing effects on the TS wave and the nature of this influence is wholly dependent upon the orientation of this latter instability. Further, the problem is examined with a larger TS wave, whose size is chosen so as to ensure that this mode is nonlinear in its own right. An amplitude equation for the evolution of the TS wave is derived which admits solutions corresponding to finito amplitude, stable, traveling waves. Author

N90-10008# Florida Agricultural and Mechanical Univ., Tallahassee. Fluid Mechanics Research Lab.

BASIC STUDIES OF THE UNSTEADY FLOW PAST HIGH ANGLE OF ATTACK AIRFOILS Final Report, 1 Oct. 1986 - 30 Oct. 1988

Anjaneyulu Krothapalli, Luiz Lourenco, and Leon VanDommelen 15 May 1989 132 p

(Grant AF-AFOSR-0243-86; AF Proj. 2307)

(AD-A210252; AFOSR-89-0780TR) Avail: NTIS HC A07/MF A01 CSCL 20/4

Experimental and numerical simulations have been carried out to study the unsteady flow past an impulsively started NACA 0012 airfoil at different angles of attack. A novel experimental technique, commonly referred to as particle image displacement velocimetry (PIDV), is successfully implemented to measure the instantaneous velocity fields. The velocity field is measured with sufficient accuracy so that the distribution of vorticity can be calculated. The unsteady separated flow fields generated by these airfoils contain large scale vortical structures such as a primary vortex generated at the leading edge of the airfoil with secondary vortices upstream of it, a trailing vortex, and a vortex sheet type structure. The origins and time evolution of these structures are clearly depicted by the instantaneous velocity and vorticity fields. A random-walk vortex simulation of the full Navier-Stokes equations were performed as a comparison. GRA

N90-10009# Mississippi State Univ., Mississippi State. Dept. of Aerospace Engineering.

COMPUTATION OF TRANSONIC FLOW ABOUT STORES Final Report, Jun. 1984 - Sep. 1988

David L. Whitfield and Joe F. Thompson Jun. 1989 56 p

(Contract F08635-84-C-0228; AF Proj. 2307)

(AD-A210402; AD-E801954; AFATL-TR-89-20) Avail: NTIS HC A04/MF A01 CSCL 01/1

The objective of this program was to derive grid generation and fluid flow algorithms to predict the aerodynamics of aircraft/weapon configurations. Both captive carriage and the launch transient mode were considered in the design of the methods. The numerical grid generation techniques developed were both algebraic, based on transfinite interpolation, and elliptic, based on iterative solution of partial differential equations. The techniques were incorporated into one code that became the numerical grid generation for the Eglin Arbitrary Geometry Implicit Euler (EAGLE) code. In addition, an adaptive version of the grid generation code was developed and applied to missile configurations. The flow solvers developed were all upwind, finite volume schemes ranging from explicit, split flux vector to implicit, split flux difference algorithms. Both steady and unsteady, Euler and Navier-Stokes, were written and applied to various configurations. Two implicit algorithms were employed to form the EAGLE flow solver code. This code was run on complex aircraft/weapon configurations, including the launch transient problem of a weapon releasing from an aircraft pylon. GRA

N90-10010# Calspan Corp., Arnold AFS, TN.

WIND TUNNEL SUPPORT SYSTEM EFFECTS ON A FIGHTER AIRCRAFT MODEL AT MACH NUMBERS FROM 0.6 TO 2.0 Final Report, 23 Aug. - 1 Dec. 1988

David G. Whitby Jul. 1989 63 p Prepared in cooperation with AEDC, Arnold AFS, TN

(AD-A210614; AEDC-TR-89-4) Avail: NTIS HC A04/MF A01 CSCL 14/2

A wind tunnel investigation was conducted using a fighter aircraft model with various sting and blade support system arrangements to evaluate the effects of the model support system on the total body and component longitudinal force and moment data. Total aerodynamic force and moment data were determined from corrected strain-gage balance measured loads. Component data (i.e., tail loads) were obtained by subtracting tail-off balance data from tail-on data. Data taken at free-stream Mach numbers from 0.6 to 2.0 and model angles of attack from -2 to 8 deg were examined. The analysis indicates a significant change in total body and component force coefficients in the presence of various support

system configurations. The upper blade tends to decrease drag, lift, and pitching-moment coefficients, while the lower blade generally increases these coefficients. The influence of the sting on aerodynamic coefficients is a function of Mach number and angle of attack. A correction methodology using sting/blade tares is proposed and evaluated. GRA

N90-10011*# Lockheed-Georgia Co., Marietta.
ANALYSIS OF RESULTS FROM WIND TUNNEL TESTS OF INLETS FOR AN ADVANCED TURBOPROP NACELLE INSTALLATION Report, 1 Nov. 1982 - 30 Jun. 1985
J. P. Hancock, V. Lyman, and A. P. Pennock Jun. 1986 162 p (Contract NAS3-23710)
(NASA-CR-174937; NAS 1.26:174937; LG85ER0105) Avail: NTIS HC A08/MF A01 CSCL 01A

Inlets for tractor installations of advanced turboprop propulsion systems were tested in three phases, covering a period from November, 1982 to January, 1984. Nacelle inlet configuration types included single scoop, twin scoop, and annular arrangements. Tests were performed with and without boundary layer diverters and several different diverter heights were tested for the single scoop inlet. This same inlet was also tested at two different axial positions. Test Mach numbers ranged from Mach 0.20 to 0.80. Types of data taken were: (1) internal and external pressures, including inlet throat recoveries; (2) balance forces, including thrust-minus-drag; and (3) propellar blade stresses. Author

N90-10012*# Rockwell International Science Center, Thousand Oaks, CA.
SUPERSONIC FLOW COMPUTATIONS OVER AEROSPACE CONFIGURATIONS USING AN EULER MARCHING SOLVER
Kuo-Yen Szema, Sukumar Chakravarthy, and Vijaya Shankar Washington Jul. 1987 49 p
(Contract NAS1-15820)
(NASA-CR-4085; NAS 1.26:4085) Avail: NTIS HC A03/MF A01 CSCL 01A

For fully supersonic flows, an efficient strategy for obtaining numerical solutions is to employ space marching techniques. A full potential marching technique, known as the SIMP code and capable of handling such embedded subsonic regions, has achieved some success analyzing low supersonic Mach number flows. The extension of the full potential approach to the Euler equation which model the exact nonlinear inviscid gas dynamic flow processes is presented. Within the assumption of an inviscid flow, such an Euler marching solver can be applied to a wide class of shocked flows including the hypersonic range. The intent is to maintain some of the basic features of the full potential SIMP code within the Euler solver in dealing with geometry input, gridding techniques, and input/output routines including post processing of results. An Euler marching code known as EMTAC was developed. Results obtained for a variety of configurations involving canard, wing, horizontal tail, flow-through inlet, and fuselage using both the EMTAC and SIMP codes are reported. For shocked cases satisfying the isentropic assumption, the EMTAC and SIMP codes produced practically the same results. In terms of execution time, the EMTAC code is slower. Author

N90-10051*# National Aeronautics and Space Administration. Ames Research Center, Moffett Field, CA.
THE PRESENT STATUS AND THE FUTURE OF MISSILE AERODYNAMICS
Jack N. Nielsen *In* AGARD, Stability and Control of Tactical Missile Systems Mar. 1989 18 p (For primary document see N90-10050 01-08)
Avail: NTIS HC A15/MF A02 CSCL 01A

N90-10055# Dornier-Werke G.m.b.H., Friedrichshafen (Germany, F.R.).
PREDICTION OF DYNAMIC DERIVATIVES
Heinz Fuchs *In* AGARD, Stability and Control of Tactical Missile Systems Mar. 1989 19 p (For primary document see N90-10050 01-08)
Avail: NTIS HC A15/MF A02

N90-10056# Lockheed Missiles and Space Co., Sunnyvale, CA.
PREDICTION OF TACTICAL MISSILE DYNAMICS
L. E. Ericsson *In* AGARD, Stability and Control of Tactical Missile Systems Mar. 1989 22 p (For primary document see N90-10050 01-08)
Avail: NTIS HC A15/MF A02

N90-10359*# National Aeronautics and Space Administration. Langley Research Center, Hampton, VA.
STABILITY OF A SUPERSONIC BOUNDARY LAYER ALONG A SWEPT LEADING EDGE
Mujeeb R. Malik and Ivan E. Beckwith *In* AGARD, Fluid Dynamics of Three-Dimensional Turbulent Shear Flows and Transition Apr. 1989 9 p (For primary document see N90-10356 01-34)
Copyright Avail: NTIS HC A18/MF A03 CSCL 01A

N90-10360# Centre d'Etudes Aerodynamiques et Thermiques, Poitiers (France). Lab. d'Etudes Aerodynamiques.
LEADING EDGE TRANSITION BY CONTAMINATION IN HYPERSONIC FLOW [TRANSITION PAR CONTAMINATION DE BORD D'ATTAQUE EN ECOULEMENT HYPERSONIQUE]
J. L. DaCosta, D. Aymer delaChevalerie, and T. Alziary deRoquefort *In* AGARD, Fluid Dynamics of Three-Dimensional Turbulent Shear Flows and Transition Apr. 1989 14 p In FRENCH; ENGLISH summary (For primary document see N90-10356 01-34)
Copyright Avail: NTIS HC A18/MF A03

N90-10361*# National Aeronautics and Space Administration. Ames Research Center, Moffett Field, CA.
DIRECT NUMERICAL STUDY OF LEADING-EDGE CONTAMINATION
P. R. Spalart *In* AGARD, Fluid Dynamics of Three-Dimensional Turbulent Shear Flows and Transition Apr. 1989 13 p (For primary document see N90-10356 01-34)
Copyright Avail: NTIS HC A18/MF A03 CSCL 01A

N90-10364*# National Aeronautics and Space Administration. Langley Research Center, Hampton, VA.
GOERTLER INSTABILITY ON AN AIRFOIL: COMPARISON OF MARCHING SOLUTION WITH EXPERIMENTAL OBSERVATIONS
Vijay Kalburgi, Siva M. Mangalam (Analytical Services and Materials, Inc., Hampton, VA.), and J. Ray Dagenhart *In* AGARD, Fluid Dynamics of Three-Dimensional Turbulent Shear Flows and Transition Apr. 1989 16 p (For primary document see N90-10356 01-34)
Copyright Avail: NTIS HC A18/MF A03 CSCL 01A

N90-10367# Bristol Univ. (England). Dept. of Aerospace Engineering.
THE THREE-DIMENSIONAL VORTEX SHEET STRUCTURE ON DELTA WINGS
Martin V. Lowson *In* AGARD, Fluid Dynamics of Three-Dimensional Turbulent Shear Flows and Transition Apr. 1989 16 p (For primary document see N90-10356 01-34)
Copyright Avail: NTIS HC A18/MF A03

N90-10373# California State Univ., Long Beach. Dept. of Aerospace Engineering.
A THREE-DIMENSIONAL LINEAR STABILITY APPROACH TO TRANSITION ON WINGS AT INCIDENCE
Tuncer Cebeci, H. H. Chen, and D. Arnal *In* AGARD, Fluid Dynamics of Three-Dimensional Turbulent Shear Flows and Transition Apr. 1989 13 p Sponsored in part by Navy (For primary document see N90-10356 01-34)
Copyright Avail: NTIS HC A18/MF A03

N90-10379# McDonnell-Douglas Research Labs., Saint Louis, MO.
TRAILING-EDGE SWEEP AND THREE-DIMENSIONAL VORTEX INTERACTIONS IN JETS AND MIXING LAYERS
V. Kibens, R. W. Wlezien, F. W. Roos, and J. T. Kegelman *In* AGARD, Fluid Dynamics of Three-Dimensional Turbulent Shear

Flows and Transition Apr. 1989 12 p (For primary document see N90-10356 01-34)
Copyright Avail: NTIS HC A18/MF A03

N90-10380# National Aerospace Lab., Amsterdam (Netherlands). GARTEUR Action Group AD.
A EUROPEAN COLLABORATIVE INVESTIGATION OF THE THREE-DIMENSIONAL TURBULENT SHEAR LAYERS OF A SWEPT WING
B. vandenBerg *In* AGARD, Fluid Dynamics of Three-Dimensional Turbulent Shear Flows and Transition Apr. 1989 19 p (For primary document see N90-10356 01-34)
Copyright Avail: NTIS HC A18/MF A03

03 AIR TRANSPORTATION AND SAFETY

Includes passenger and cargo air transport operations; and aircraft accidents.

For related information see also *16 Space Transportation* and *85 Urban Technology and Transportation.*

N90-10013# National Transportation Safety Board, Washington, DC.
AIRCRAFT ACCIDENT REPORT: ALOHA AIRLINES, FLIGHT 243, BOEING 737-200, N73711, NEAR MAUI, HAWAII, APRIL 28, 1988
28 Apr. 1988 263 p
(PB89-910404; NTSB/AAR-89/03) Avail: NTIS HC A12/MF A02 CSCL 01C

On April 28, 1988, a Boeing 737-200, N73711, operated by Aloha Airlines Inc., experienced an explosive decompression and structural failure at 24,000 feet, while en route from Hilo, to Honolulu, Hawaii. Approximately 18 feet of the cabin skin and structure aft of the cabin entrance door and above the passenger floorline separated from the airplane during flight. There were 89 passengers and 6 crewmembers on board. One flight attendant was swept overboard during the decompression and is presumed to have been fatally injured; 7 passengers and 1 flight attendant received serious injuries. The flightcrew performed an emergency descent and landing at Kahului Airport on the Island of Maui. The safety issues raised in this report include: the quality of air carrier maintenance programs and the FAS surveillance of those programs, the engineering airworthiness of the B-737 with particular emphasis on multiple site fatigue cracking of the fuselage lap joints, the human factors aspects of air carrier maintenance and inspection for the continuing airworthiness of transport category airplanes, to include repair procedures and the training, certification and qualification of mechanics and inspectors. Author

N90-10014*# Boeing Commercial Airplane Co., Seattle, WA.
CLASSIFICATION AND REDUCTION OF PILOT ERROR Report, Jan. 1988 - Feb. 1989
W. H. Rogers, A. L. Logan, and G. D. Boley Sep. 1989 173 p
(Contract NAS1-18027)
(NASA-CR-181867; NAS 1.26:181867; DOT/FAA/DS-89/24)
Avail: NTIS HC A08/MF A01 CSCL 01C

Human error is a primary or contributing factor in about two-thirds of commercial aviation accidents worldwide. With the ultimate goal of reducing pilot error accidents, this contract effort is aimed at understanding the factors underlying error events and reducing the probability of certain types of errors by modifying underlying factors such as flight deck design and procedures. A review of the literature relevant to error classification was conducted. Classification includes categorizing types of errors, the information processing mechanisms and factors underlying them, and identifying factor-mechanism-error relationships. The classification scheme developed by Jens Rasmussen was adopted because it provided a comprehensive yet basic error classification shell or structure that could easily accommodate addition of details on domain-specific factors. For these purposes, factors specific to the aviation environment were incorporated. Hypotheses concerning the relationship of a small number of underlying factors, information processing mechanisms, and error types types identified in the classification scheme were formulated. ASRS data were reviewed and a simulation experiment was performed to evaluate and quantify the hypotheses. Author

N90-10015# Dayton Univ., OH. Research Inst.
DEFINITION AND REDUCTION OF THE F-18 WINDSHIELD BIRDSTRIKE HAZARD Interim Report, Feb. 1986 - Jul. 1988
G. J. Stenger, D. R. Bowman, and B. S. West Feb. 1989 143 p
(Contract F33615-84-C-3404; AF Proj. 1926)
(AD-A210700; UDR-TR-87-27; AFWAL-TR-88-3110) Avail: NTIS HC A07/MF A01 CSCL 01/3

Since 1983 there have been nine reported bird impacts on the F-18 windshield, resulting in one penetration and one injured pilot. The number of penetrations can be expected to increase as the F-18 fleet size increases. This program was initiated to develop a windshield system with an increased bird impact capability for the F-18 aircraft. The results of this seven-part study were incorporated into a design recommendation. GRA

04 AIRCRAFT COMMUNICATIONS AND NAVIGATION

Includes digital and voice communication with aircraft; air navigation systems (satellite and ground based); and air traffic control.

For related information see also *17 Space Communications, Spacecraft Communications, Command and Tracking* and *Communications and Radar.*

N90-10016# Office of Technology Assessment, Washington, DC.
SAFER SKIES WITH TCAS: TRAFFIC ALERT AND COLLISION AVOIDANCE SYSTEM Special Report
Feb. 1989 63 p
(PB89-169221; OTA-SET-431; LC-89-600725) Avail: NTIS HC A04/MF A01; SOD HC $2.50 as 052-003-01149-2 CSCL 17G

Because midair collisions between aircraft are nearly always catastrophic, the aviation community has been working for many years to develop technologies to help prevent such tragedies. These efforts have culminated in a cooperative government-industry program to develop, evaluate, and implement a traffic alert and collision avoidance system (TCAS 2) for commercial aviation. The 100th Congress passed legislation requiring that most commercial passenger aircraft be equipped with TCAS 2 by December 1991, or they would not be permitted to fly in U.S. airspace. However, during the second half of 1988, questions arose about the safety implications of the certification and implementation schedule for TCAS 2. The Office of Technology Assessment (OTA) was asked to assess these implications. This report contains the results of OTA's assessment. K.C.D.

N90-10017# Mitre Corp., McLean, VA.
NATIONAL AIRSPACE SYSTEM APPROACH AND DEPARTURE SEQUENCING OPERATIONAL CONCEPT Final Report, Jun. 1989
Joseph P. Iadeluca Mar. 1989 44 p
(Contract DTFA01-89-C-00001)
(NAS-SR-1322; DOT/FAA/DS-89/25) Avail: NTIS HC A03/MF A01

This concept of operations is one of many high level documents that will, in total, describe the operations of the National Airspace System (NAS) when the NAS Plan has been implemented. These documents as a set will assist in linking the requirements specified in NAS System Requirements Specification (NASSRS) with the NAS design. One of the functions of the NAS is to support approach and departure sequencing at specific airports. The objective of this document is to describe the relationship among subsystems, facilities, information, and operators/users involved in the approach and departure sequencing function. This document is intended as

a tool for system designers, analysts, and test planners. The document contains several types of block diagrams illustrating system connectivity, and operational flow. These diagrams in conjunction with the text are intended to provide perspective and insight into the NAS approach and departure sequencing function. Author

N90-10018# Federal Aviation Administration, Atlantic City, NJ.
ILS/MLS COMPARISON TESTS AT MIAMI/TAMIAMI, FLORIDA AIRPORT
John Townsend Jul. 1989 20 p
(Contract FAA-T0604-L)
(ACD-330; DOT/FAA/CT-TN89/39) Avail: NTIS HC A03/MF A01

A series of flight tests were performed by the Federal Aviation Administration (FAA) Technical Center at the Miami/Tamiami, Florida Airport, to compare the course quality of an instrumented landing system (ILS) with a collocated Microwave Landing System (MLS). The Technical Center's test bed MLS was transported to and collocated with the commissioned category 1 ILS on runway 9R at Tamiami. The flight data that was collected indicate that the MLS has less scalloping than the ILS and the MLS azimuth is unaffected by overflight interference. Author

N90-10019# Federal Aviation Administration, Atlantic City, NJ.
ILS (INSTRUMENT LANDING SYSTEM) MATHEMATICAL MODELING STUDY ON THE EFFECTS OF PROPOSED HANGAR CONSTRUCTION WEST OF RUNWAY 18R ON LOCALIZER PERFORMANCE AT DALLAS-FORT WORTH INTERNATIONAL AIRPORT Technical Note, period ending Mar. 1989
James D. Rambone and John E. Walls Jun. 1989 21 p
(AD-A210631; DOT/FAA/CT-TN89/29) Avail: NTIS HC A03/MF A01 CSCL 01/5

This Technical Note describes the instrument landing system (ILS) math modeling performed by the Federal Aviation Administration (FAA) Technical Center at the request of the Southwest Region. Computed data are presented showing the effects of several proposed hangar configurations on the performance of the ILS localizer for runway 18R at the Dallas-Fort Worth International Airport. The Southwest Region is concerned that reflections from the proposed hangars may degrade the localizer course beyond category II tolerances. Modeled course structure results indicate that category II localizer performance should be obtained with the existing 14/6 Type IB antenna for the proposed hangar configurations. Computed clearance orbit results indicate satisfactory linearity, course crossover, and signal clearance levels. GRA

N90-10020# Federal Aviation Administration, Atlantic City, NJ.
THE ADDITION OF BENDIX MLS (MICROWAVE LANDING SYSTEM) ANTENNA PATTERNS TO MLS MATHEMATICAL MODEL Technical Note, Jan. - Feb. 1989
Jesse D. Jones May 1989 120 p
(AD-A210633; DOT/FAA/CT-TN89/26) Avail: NTIS HC A06/MF A01 CSCL 17/7

Bendix Microwave Landing System (MLS) test bed antenna patterns were added to the MLS mathematical model. This report documents the method of installation, the required alterations of existing code to support the new patterns, and the results of testing of the new patterns with standard test scenario two. The tests yielded acceptable results. GRA

N90-10021*# Theory and Applications Unlimited Corp., Los Gatos, CA.
GUIDANCE SIMULATION AND TEST SUPPORT FOR DIFFERENTIAL GPS FLIGHT EXPERIMENT
G. J. Geier, P. V. W. Loomis, and A. Cabak Oct. 1987 47 p
(Contract NAS2-12378)
(NASA-CR-177471; NAS 1.26:177471) Avail: NTIS HC A03/MF A01 CSCL 17G

Three separate tasks which supported the test preparation, test operations, and post test analysis of the NASA Ames flight test evaluation of the differential Global Positioning System (GPS) are presented. Task 1 consisted of a navigation filter design, coding, and testing to optimally make use of GPS in a differential mode. The filter can be configured to accept inputs from external censors such as an accelerometer and a barometric or radar altimeter. The filter runs in real time onboard a NASA helicopter. It processes raw pseudo and delta range measurements from a single channel sequential GPS receiver. The Kalman filter software interfaces are described in detail, followed by a description of the filter algorithm, including the basic propagation and measurement update equations. The performance during flight tests is reviewed and discussed. Task 2 describes a refinement performed on the lateral and vertical steering algorithms developed on a previous contract. The refinements include modification of the internal logic to allow more diverse inflight initialization procedures, further data smoothing and compensation for system induced time delays. Task 3 describes the TAU Corp participation in the analysis of the real time Kalman navigation filter. The performance was compared to that of the Z-set filter in flight and to the laser tracker position data during post test analysis. This analysis allowed a more optimum selection of the parameters of the filter. Author

05 AIRCRAFT DESIGN, TESTING AND PERFORMANCE

Includes aircraft simulation technology.

For related information see also *18 Spacecraft Design, Testing and Performance* and *39 Structural Mechanics*.For land transportation vehicles see *85 Urban Technology and Transportation.*

N90-10022# Charles River Analytics, Inc., Cambridge, MA.
HIERARCHICAL DAMAGE TOLERANT CONTROLLERS FOR SMART STRUCTURES Final Report, Jun. - Dec. 1988
A. K. Caglayan, S. M. Allen, and S. J. Edwards Mar. 1989 68 p
(Contract F33615-88-C-3212)
(AD-A209422; AFWAL-TR-89-3009) Avail: NTIS HC A04/MF A01 CSCL 13/12

The research and development results are presented of the Hierarchical Damage Tolerant Controllers for Smart Structures. The major aim is the investigation and definition of a baseline architecture for a smart aerospace structure which can detect and isolate structural damage in real time and provide on-line reconfiguration of the structure's control system under the detected impairment conditions. In particular, how a smart aerospace structure can be implemented as a real-time knowledge based expert system was investigated by addressing issues involved with structural knowledge representation, structural damage detection and isolation strategies and real time performance in an embedded environment. GRA

N90-10023*# National Aeronautics and Space Administration. Hugh L. Dryden Flight Research Facility, Edwards, CA.
INITIAL FLIGHT QUALIFICATION AND OPERATIONAL MAINTENANCE OF X-29A FLIGHT SOFTWARE
Michael R. Earls and Joel R. Sitz Sep. 1989 28 p Presented at the AIAA Guidance, Navigation and Control Conference, Boston, MA, 14-16 Aug. 1989
(NASA-TM-101703; H-1558; NAS 1.15:101703; AIAA-89-3596)
Avail: NTIS HC A03/MF A01 CSCL 01C

A discussion is presented of some significant aspects of the initial flight qualification and operational maintenance of the flight control system softward for the X-29A technology demonstrator. Flight qualification and maintenance of complex, embedded flight control system software poses unique problems. The X-29A technology demonstrator aircraft has a digital flight control system which incorporates functions generally considered too complex for analog systems. Organizational responsibilities, software assurance issues, tools, and facilities are discussed. Author

N90-10024# Dayton Univ., OH. Systems Support Div.
CONFERENCE ON AEROSPACE TRANSPARENT MATERIALS AND ENCLOSURES (15TH) 16-20 JANUARY 1989. VOLUME 2: SESSIONS 6-9 Final Report
Samuel A. Marolo, comp. Apr. 1989 728 p Conference held 16-20 Jan. 1989
(Contract F33615-84-C-3404)
(AD-A210201; WRDC-TR-89-4044-Vol-2) Avail: NTIS HC A99/MF A04 CSCL 22/5

The technical papers presented at the 15th Conference on Aerospace Transparent Materials and Enclosures are reproduced. Seventy-two technical papers are presented in 9 sessions that address transparent material for enclosures, coatings for transparencies, transparency design; bird impact resistance; human factor and optics; operational problems; design criteria on transparent plastics, glasses and elastomers; aircraft-structural integration of windshields and canopies; computed design; testing techniques; and cost of ownership reduction. The papers were reproduced directly from the original manuscripts. GRA

N90-10025# Army Aviation Engineering Flight Activity, Edwards AFB, CA.
AIRWORTHINESS AND FLIGHT CHARACTERISTICS TEST OF THE UH-60A BLACK HAWK HELICOPTER EQUIPPED WITH THE XM-139 MULTIPLE MINE DISPENSING SYSTEM (VOLCANO) Final Report, 1 Sep. 1987 - 28 Jan. 1988
Randall W. Cason, Paul W. Losier, John I. Nagata, Christopher J. Young, and William D. Lewis Dec. 1988 186 p
(AD-A210271; USAAEFA-86-12) Avail: NTIS HC A09/MF A01 CSCL 01/3

An airworthiness and flight characteristics evaluation of the UH-60A helicopter (S/N 82-23748) with the XM-139 Multiple Mine Dispensing System (VOLCANO) installed was conducted by the U.S. Army Aviation Engineering Flight Activity. The tests required 59 productive flight hours. Performance and handling qualities tests were conducted. The change in equivalent flat plate area in forward flight varied as a function of the thrust coefficient and airspeed from approximately 36 to 50 square feet. The out-of-ground effect hover capability was reduced by approximately 520 pounds. The handling qualities of the UH-60A with the VOLCANO installed were slightly degraded when compared to the normal utility configuration. Seven shortcomings were noted in this configuration. They include the large position error for this ship's airspeed system, the negative longitudinal static stability at 100 KCAS during level flight, the neutral static longitudinal stability during intermediate rated power (IRP) climbs, and the neutral to slightly negative maneuver stability above a load factor of 1.4 at 116 KCAS. GRA

N90-10026# Aeronautical Research Labs., Melbourne (Australia).
A REVIEW OF AUSTRALIAN AND NEW ZEALAND INVESTIGATIONS ON AERONAUTICAL FATIGUE DURING THE PERIOD APRIL 1987 TO MARCH 1989 Aircraft Structures Technical Memorandum
G. S. Jost, ed. Apr. 1989 51 p Presented at the 21st Conference of the International Committee on Aeronautical Fatigue, Jerusalem, Israel, 19-20 Jun. 1989
(AD-A210373; ARL-STRUC-TM-506; DODA-AR-005-604) Avail: NTIS HC A04/MF A01 CSCL 20/11

This document was prepared for presentation to the 21st Conference of the International Committee on Aeronautical Fatigue scheduled to be held in Jerusalem, Israel, on June 19 and 20, 1989. A review is given of the aircraft fatigue research and associated activities which form part of the programs of the Aeronautical Research Laboratory, universities, the Civil Aviation Authority, the Australian aircraft industry and the Defence Scientific Establishment, New Zealand. The major topics discussed include the fatigue of both civil and military aircraft structures, fatigue damage detection, analysis and repair and fatigue life monitoring and assessment. GRA

N90-10027# Boeing Advanced Systems Co., Seattle, WA.
COMPATIBILITY OF FUEL SYSTEM COMPONENTS WITH HIGH DENSITY FUEL Final Report, Apr. 1987 - Jan. 1989
A. F. Grenich and A. M. Johnson May 1989 179 p
(Contract F33615-87-C-2711; AF Proj. 2480)
(AD-A210381; WRDC-TR-89-2034) Avail: NTIS HC A09/MF A01 CSCL 21/4

Environmental and endurance tests were conducted to evaluate the performance of typical fuel system components when exposed to high density aviation turbine engine fuel. The environment tests simulated the extreme high and low temperatures encountered in hot and cold day missions. The results revealed that the high density fuel (HDF) would not have any fuel boiling or freezing problems but the pump power required for HDF was higher than for JP-4 fuel as was expected and the lower heat capacity of HDF resulted in noticeably higher heat exchanger discharge temperatures. The endurance tests revealed that the HDF would not cause abnormal wear or component leakage. Nothing in the test results suggested that current inputs to fuel system life cycle cost models should be modified if HDF is used. GRA

N90-10028# Army Aeromedical Research Lab., Fort Rucker, AL.
COCKPIT LIGHTING COMPATIBILITY WITH IMAGE INTENSIFICATION NIGHT IMAGING SYSTEMS: ISSUES AND ANSWERS
Clarence E. Rash and Robert W. Verona May 1989 19 p
(AD-A210503; USAARL-89-6) Avail: NTIS HC A03/MF A01 CSCL 17/5

Night imaging systems based on image intensification (I sup 2) tubes are a major factor in the night operation capability of U.S. Army rotary-wing aircraft. A major problem associated with the use of these systems is the detrimental effect caused by internal cockpit lighting. Instrument lamps, caution lamps, utility lights, and other light sources inside the cockpit activate the bright source protection control circuits of the intensification tubes, thereby reducing their sensitivity to external, natural and artificial illumination. In 1986, a Tri-Service specification, MIL-L-85762, lighting, aircraft, interior, night vision imaging system compatible, was adopted to resolve the cockpit lighting problems. This specification defines the measurement instrumentation and techniques required to certify lighting components as ANVIS compatible. The specification does not address compatibility problems associated with AN/PVS-5 usage. Ongoing efforts related to MIL-L-85762 include characterization of lighting incompatibilities in current U.S. Army aircraft, implementation of programs to modify the lighting in incompatible cockpits, and certification of proposed lighting components for future aircraft systems. Additional work has been done to provide near compatible solutions to lighting problems associated with the use of AN/PVS5-systems. GRA

N90-10029# Naval Postgraduate School, Monterey, CA.
DEVELOPMENT OF A FLIGHT TEST METHODOLOGY FOR A US NAVY HALF-SCALE UNMANNED AIR VEHICLE M.S. Thesis
James C. Tanner Mar. 1989 106 p
(AD-A210563) Avail: NTIS HC A06/MF A01 CSCL 22/2

The development of a flight test methodology for predicting the performance characteristics of a half-scale Unmanned Air Vehicle (UAV) is discussed. This methodology is the first step in developing a UAV flight test program which will ultimately be used to help improve and/or validate the performance characteristics of these type of vehicles, currently being integrated into the U.S. Navy. The methodology determined powerplant characteristics through torque stand tests and aerodynamic characteristics through wind tunnel and flight tests. The data from these tests were used to construct power required and drag polar curves. These curves were then used to predict the basic performance characteristics of the half-scale Pioneer. GRA

N90-10030*# Lockheed-Georgia Co., Marietta. Advanced Structures Group.
APPLICATION OF SUPERPLASTICALLY FORMED AND DIFFUSION BONDED ALUMINUM TO A LAMINAR FLOW CONTROL LEADING EDGE Final Report
M. D. Goodyear Aug. 1987 74 p
(Contract NAS1-18036)
(NASA-CR-178316; NAS 1.26:178316; LG86ER0060) Avail: NTIS HC A04/MF A01 CSCL 01C

NASA sponsored the Aircraft Energy Efficiency (ACEE) program in 1976 to develop technologies to improve fuel efficiency. Laminar flow control was one such technology. Two approaches for achieving laminar flow were designed and manufactured under NASA sponsored programs: the perforated skin concept used at McDonnell Douglas and the slotted design used at Lockheed-Georgia. Both achieved laminar flow, with the slotted design to a lesser degree (JetStar flight test program). The latter design had several fabrication problems concerning springback and adhesive flow clogging the air flow passages. The Lockheed-Georgia Company accomplishments is documented in designing and fabricating a small section of a leading edge article addressing a simpler fabrication method to overcome the previous program's manufacturing problems, i.e., design and fabrication using advanced technologies such as diffusion bonding of aluminum, which has not been used on aerospace structures to date, and the superplastic forming of aluminum. Author

N90-10031*# Wichita State Univ., KS. Dept. of Aeronautical Engineering.
ELECTRO-IMPULSE DE-ICING TESTING ANALYSIS AND DESIGN Final Report
G. W. Zumwalt, R. L. Schrag, W. D. Bernhart, and R. A. Friedberg Sep. 1988 352 p
(Grant NAG3-284)
(NASA-CR-4175; E-4279; NAS 1.26:4175) Avail: NTIS HC A16/MF A02 CSCL 01C

Electro-Impulse De-Icing (EIDI) is a method of ice removal by sharp blows delivered by a transient electromagnetic field. Detailed results are given for studies of the electrodynamic phenomena. Structural dynamic tests and computations are described. Also reported are ten sets of tests at NASA's Icing Research Tunnel and flight tests by NASA and Cessna Aircraft Company. Fabrication of system components are described and illustrated. Fatigue and electromagnetic interference tests are reported. Here, the necessary information for the design of an EIDI system for aircraft is provided. Author

N90-10062*# National Aeronautics and Space Administration. Langley Research Center, Hampton, VA.
NEW TEST TECHNIQUES TO EVALUATE NEAR FIELD EFFECTS FOR SUPERSONIC STORE CARRIAGE AND SEPARATION
Wallace C. Sawyer, Robert L. Stallings, Jr., Floyd J. Wilcox, Jr., A. B. Blair, Jr., William J. Monta, and Elizabeth B. Plentovich *In* AGARD, Stability and Control of Tactical Missile Systems Mar. 1989 9 p (For primary document see N90-10050 01-08)
Avail: NTIS HC A15/MF A02 CSCL 01C

N90-10069# Naval Weapons Center, China Lake, CA. Dynamics and Control Branch.
ANALYSIS AND TESTING OF A HIGH PERFORMANCE AIR-AIR MISSILE
Gerald L. Stevens *In* AGARD, Stability and Control of Tactical Missile Systems Mar. 1989 15 p (For primary document see N90-10050 01-08)
Avail: NTIS HC A15/MF A02

N90-10070# Messerschmitt-Boelkow-Blohm G.m.b.H., Munich (Germany, F.R.).
MARGINAL RELEASE DISTURBANCES ON ADVANCED MISSILES
Ronald Deslandes *In* AGARD, Stability and Control of Tactical Missile Systems Mar. 1989 12 p (For primary document see N90-10050 01-08)
Avail: NTIS HC A15/MF A02

N90-10072# Selenia S.p.A., Rome (Italy). Missile System Div.
EXPERIENCE GAINED IN THE IMPROVEMENT OF THE ASPIDE AERODYNAMIC CONFIGURATION FOR THE SURFACE TO AIR ROLE
S. Mazzuca *In* AGARD, Stability and Control of Tactical Missile Systems Mar. 1989 10 p (For primary document see N90-10050 01-08)
Avail: NTIS HC A15/MF A02

N90-10073# Selenia S.p.A., Rome (Italy). Missile Systems Div.
WINGED VERSUS WINGLESS AIRFRAMES
A. Gazzina and S. Mazzuca *In* AGARD, Stability and Control of Tactical Missile Systems Mar. 1989 20 p (For primary document see N90-10050 01-08)
Avail: NTIS HC A15/MF A02

N90-10115*# Boeing Co., Seattle, WA.
AIRCRAFT MODAL SUPRESSION SYSTEM: EXISTING DESIGN APPROACH AND ITS SHORTCOMINGS
J. K. Ho, T. J. Goslin, and C. B. Tran *In* NASA. Langley Research Center, Proceedings of the Workshop on Computational Aspects in the Control of Flexible Systems, Part 2 May 1989 p 801-823 (For primary document see N90-10103 01-18)
Avail: NTIS HC A21/MF A03 CSCL 01C

N90-10116*# Boeing Commercial Airplane Co., Seattle, WA.
STRUCTURAL STABILITY AUGMENTATION SYSTEM DESIGN USING BODEDIRECT: A QUICK AND ACCURATE APPROACH
T. J. Goslin and J. K. Ho *In* NASA. Langley Research Center, Proceedings of the Workshop on Computational Aspects in the Control of Flexible Systems, Part 2 May 1989 p 825-851 (For primary document see N90-10103 01-18)
Avail: NTIS HC A21/MF A03 CSCL 01C

N90-10119*# National Aeronautics and Space Administration. Langley Research Center, Hampton, VA.
THE ACTIVE FLEXIBLE WING AEROSERVOELASTIC WIND-TUNNEL TEST PROGRAM
Thomas Noll and Boyd Perry *In its* Proceedings of the Workshop on Computational Aspects in the Control of Flexible Systems, Part 2 May 1989 p 903-941 (For primary document see N90-10103 01-18)
Avail: NTIS HC A21/MF A03 CSCL 01C

N90-10120*# Ottawa Univ. (Ontario).
MODELING AND STABILIZATION OF LARGE FLEXIBLE SPACE STATIONS
S. S. Lim and N. U. Ahmed *In* NASA. Langley Research Center, Proceedings of the Workshop on Computational Aspects in the Control of Flexible Systems, Part 2 May 1989 p 943-956 (For primary document see N90-10103 01-18)
Avail: NTIS HC A21/MF A03 CSCL 01C

06 AIRCRAFT INSTRUMENTATION

Includes cockpit and cabin display devices; and flight instruments.

For related information see also *19 Spacecraft Instrumentation* and *35 Instrumentation and Photography.*

N90-10032# National Center for Atmospheric Research, Boulder, CO. Atmospheric Technology Div.
MEETING REVIEW: WORKSHOP ON AIRBORNE INSTRUMENTATION
William A. Cooper and Darrel Baumgardner Mar. 1989 83 p Presented at the Workshop on Airborne Instrumentation, Boulder, CO, 19-21 Oct. 1988
(Grant NSF ATM-87-09659)

(PB89-174775; NCAR/TN-330+PROC) Avail: NTIS HC A05/MF A01 CSCL 01D

A workshop was held at NCAR (the National Center for Atmospheric Research) to review the needs for airborne instrumentation and to plan for the development of needed instruments. Areas covered included state parameters (pressure, temperature, wind, humidity measurement), air motion sensing, cloud physics, atmospheric electrification, remote sensing, gas-phase chemistry, aerosols, and deployable sensors in oceanography. Several measurement needs were identified and discussed. A summary of conclusions and recommendations is given. K.C.D.

07 AIRCRAFT PROPULSION AND POWER

Includes prime propulsion systems and systems components, e.g., gas turbine engines and compressors; and onboard auxilliary power plants for aircraft.

For related information see also *20 Spacecraft Propulsion and Power, 28 Propellants and Fuels,* and *44 Energy Production and Conversion.*

N90-10033*# Pratt and Whitney Aircraft, West Palm Beach, FL.
SSME ALTERNATE TURBOPUMP DEVELOPMENT PROGRAM: DESIGN VERIFICATION SPECIFICATION FOR HIGH-PRESSURE FUEL TURBOPUMP
21 Apr. 1989 88 p Revised
(Contract NAS8-36801)
(NASA-CR-183676; NAS 1.26:183676; DVS-30-Rev-3) Avail: NTIS HC A05/MF A01 CSCL 21E

The design and verification requirements are defined which are appropriate to hardware at the detail, subassembly, component, and engine levels and to correlate these requirements to the development demonstrations which provides verification that design objectives are achieved. The high pressure fuel turbopump requirements verification matrix provides correlation between design requirements and the tests required to verify that the requirement have been met. E.R.

N90-10034*# National Aeronautics and Space Administration. Langley Research Center, Hampton, VA.
PERFORMANCE POTENTIAL OF AN ADVANCED TECHNOLOGY MACH 3 TURBOJET ENGINE INSTALLED ON A CONCEPTUAL HIGH-SPEED CIVIL TRANSPORT
Shelby J. Morris, Jr., Karl A. Geiselhart (Planning Research Corp., Hampton, VA.), and Peter G. Coen Washington Nov. 1989 31 p
(NASA-TM-4144; L-16531; NAS 1.15:4144) Avail: NTIS HC A03/MF A01 CSCL 21E

The performance of an advanced technology conceptual turbojet optimized for a high-speed civil aircraft is presented. This information represents an estimate of performance of a Mach 3 Brayton (gas turbine) cycle engine optimized for minimum fuel burned at supersonic cruise. This conceptual engine had no noise or environmental constraints imposed upon it. The purpose of this data is to define an upper boundary on the propulsion performance for a conceptual commercial Mach 3 transport design. A comparison is presented demonstrating the impact of the technology proposed for this conceptual engine on the weight and other characteristics of a proposed high-speed civil transport. This comparison indicates that the advanced technology turbojet described could reduce the gross weight of a hypothetical Mach 3 high-speed civil transport design from about 714,000 pounds to about 545,000 pounds. The aircraft with the baseline engine and the aircraft with the advanced technology engine are described. Author

N90-10035# National Aerospace Lab., Tokyo (Japan).
CYCLE ANALYSIS OF SCRAMJET ENGINES
Takeshi Kanda, Goro Masuya, and Yoshio Wakamatsu Oct. 1988 16 p In JAPANESE; ENGLISH summary
(NAL-TR-1002; ISSN-0389-4010) Avail: NTIS HC A03/MF A01

Engine cycles for airframe-integrated scramjets employing hydrogen fuel are analyzed to investigate regenerative engine cooling characteristics, required pump exit pressure, and overall engine thrust. An expander cycle and a gas generator (G.G.) cycle are examined. It is found that the engine can function with either of these cycles. For flights at high Mach numbers, it is found that the hydrogen flow rate required for engine cooling exceeds the stoichiometric flow rate needed for combustion. The specific impulse of the G.G. cycle is lower than that of the expander cycle because oxygen is needed for the gas generator. If an advanced refractory material is available for the G.G. cycle engine wall, it is possible to decrease the hydrogen flow rate needed for engine cooling and thus to enlarge the range of engine operation. Author

N90-10036*# Detroit Diesel Allison, Indianapolis, IN. Dept. of Engineering.
ADVANCED TURBINE TECHNOLOGY APPLICATIONS PROJECT (ATTAP) Annual Report, Nov. 1987 - Dec. 1988
1 Jun. 1989 106 p
(Contracts DEN3-336; DE-AI01-85CE-50111)
(NASA-CR-185133; NAS 1.26:185133; EDR-14232; DOE/NASA/0336-1) Avail: NTIS HC A06/MF A01 CSCL 21E

ATTAP activities during the past year were highlighted by an extensive materials assessment, execution of a reference powertrain design, test-bed engine design and development, ceramic component design, materials and component characterization, ceramic component process development and fabrication, component rig design and fabrication, test-bed engine fabrication, and hot gasifier rig and engine testing. Materials assessment activities entailed engine environment evaluation of domestically supplied radial gasifier turbine rotors that were available at the conclusion of the Advanced Gas Turbine (AGT) Technology Development Project as well as an extensive survey of both domestic and foreign ceramic suppliers and Government laboratories performing ceramic materials research applicable to advanced heat engines. A reference powertrain design was executed to reflect the selection of the AGT-5 as the ceramic component test-bed engine for the ATTAP. Test-bed engine development activity focused on upgrading the AGT-5 from a 1038 C (1900 F) metal engine to a durable 1371 C (2500 F) structural ceramic component test-bed engine. Ceramic component design activities included the combustor, gasifier turbine static structure, and gasifier turbine rotor. The materials and component characterization efforts have included the testing and evaluation of several candidate ceramic materials and components being developed for use in the ATTAP. Ceramic component process development and fabrication activities were initiated for the gasifier turbine rotor, gasifier turbine vanes, gasifier turbine scroll, extruded regenerator disks, and thermal insulation. Component rig development activities included combustor, hot gasifier, and regenerator rigs. Test-bed engine fabrication activities consisted of the fabrication of an all-new AGT-5 durability test-bed engine and support of all engine test activities through instrumentation/build/repair. Hot gasifier rig and test-bed engine testing activities were performed. Author

N90-10037*# General Electric Co., Cincinnati, OH. Aircraft Engines.
PMR GRAPHITE ENGINE DUCT DEVELOPMENT Final Report
C. L. Stotler and S. A. Yokel Aug. 1989 190 p LIMITED REPRODUCIBILITY: More than 20% of this document may be affected by foldouts
(Contract NAS3-21854)
(NASA-CR-182228; NAS 1.26:182228) Avail: NTIS HC A09/MF A01 CSCL 21E

The objective was to demonstrate the cost and weight advantages that could be obtained by utilizing the graphite/PMR15 material system to replace titanium in selected turbofan engine applications. The first component to be selected as a basis for

evaluation was the outer bypass duct of the General Electric F404 engine. The operating environment of this duct was defined and then an extensive mechanical and physical property test program was conducted using material made by processing techniques which were also established by this program. Based on these properties, design concepts to fabricate a composite version of the duct were established and two complete ducts fabricated. One of these ducts was proof pressure tested and then run successfully on a factory test engine for over 1900 hours. The second duct was static tested to 210 percent design limit load without failure. An improved design was then developed which utilized integral composite end flanges. A complete duct was fabricated and successfully proof pressure tested. The net results of this effort showed that a composite version of the outer duct would be 14 percent lighter and 30 percent less expensive that the titanium duct. The other type of structure chosen for investigation was the F404 fan stator assembly, including the fan stator vanes. It was concluded that it was feasible to utilize composite materials for this type structure but that the requirements imposed by replacing an existing metal design resulted in an inefficient composite design. It was concluded that if composites were to be effectively used in this type structure, the design must be tailored for composite application from the outset. Author

N90-10038*# Pennsylvania State Univ., State College.
THE MEASUREMENT OF BOUNDARY LAYERS ON A COMPRESSOR BLADE IN CASCADE. VOLUME 1: EXPERIMENTAL TECHNIQUE, ANALYSIS AND RESULTS Final Report
William C. Zierke and Steven Deutsch Jul. 1989 212 p
(Grant NsG-3264)
(NASA-CR-185118-Vol-1; NAS 1.26:185118-Vol-1) Avail: NTIS HC A10/MF A02 CSCL 21E

Measurements were made of the boundary layers and wakes about a highly loaded, double-circular-arc compressor blade in cascade. These laser Doppler velocimetry measurements have yielded a very detailed and precise data base with which to test the application of viscous computational codes to turbomachinery. In order to test the computational codes at off-design conditions, the data were acquired at a chord Reynolds number of 500,000 and at three incidence angles. Moreover, these measurements have supplied some physical insight into these very complex flows. Although some natural transition is evident, laminar boundary layers usually detach and subsequently reattach as either fully or intermittently turbulent boundary layers. These transitional separation bubbles play an important role in the development of most of the boundary layers and wakes measured in this cascade and the modeling or computing of these bubbles should prove to be the key aspect in computing the entire cascade flow field. In addition, the nonequilibrium turbulent boundary layers on these highly loaded blades always have some region of separation near the trailing edge of the suction surface. These separated flows, as well as the subsequent near wakes, show no similarity and should prove to be a challenging test for the viscous computational codes. Author

N90-10039*# Pennsylvania State Univ., State College.
THE MEASUREMENT OF BOUNDARY LAYERS ON A COMPRESSOR BLADE IN CASCADE. VOLUME 2: DATA TABLES Final Report
William C. Zierke and Steven Deutsch Jul. 1989 224 p
(Grant NsG-3264)
(NASA-CR-185118-Vol-2; NAS 1.26:185118-Vol-2) Avail: NTIS HC A10/MF A02 CSCL 21E

Measurements were made of the boundary layers and wakes about a highly loaded, double-circular-arc compressor blade in cascade. These laser Doppler velocimetry measurements have yielded a very detailed and precise data base with which to test the application of viscous computational codes to turbomachinery. In order to test the computational codes at off-design conditions, the data have been acquired at a chord Reynolds number of 500,000 and at three incidence angles. Average values and 95 percent confidence bands were tabularized for the velocity, local turbulence intensity, skewness, kurtosis, and percent backflow. Tables also exist for the blade static-pressure distributions and boundary layer velocity profiles reconstructed to account for the normal pressure gradient. Author

N90-10040# Aeronautical Research Labs., Melbourne (Australia).
REPORT ON AN OVERSEAS VISIT, JUNE 1988 Propulsion Technical Memorandum
D. E. Glenny Feb. 1989 39 p
(AD-A210374; ARL-PROP-TM-455; DODA-AR-005-575) Avail: NTIS HC A03/MF A01 CSCL 13/8

A visit was undertaken in June 1988 to attend the 71st Symposium of the AGARD Propulsion and Energetics Panel (PEP) on Engine Condition Monitoring - Technology and Experience held in Quebec Canada and to visit selected industry, military and research facilities in Canada and USA. The latter visits were to discuss methods for assessing gas turbine performance when operating with and without faulty components. A total of 8 establishments were visited in Canada and USA. In the course of the visit an opportunity was taken to hold preliminary discussions on the establishment of Key Technical Areas (KTA) in the newly formed TTCP HTP-7. At the conclusion of the tour a visit was made to the Singapore Ministry of Defence (and Singapore Aircraft Industries) to discuss aspects of Performance Monitoring and the installation of the GE F404 in the Skyhawks of the Royal Singapore Air Force. GRA

N90-10041# Aeronautical Research Labs., Melbourne (Australia).
AN APPRAISAL OF A NUMBER OF POWER ASSESSMENT PROCEDURES BEING PROPOSED FOR USE IN CHINOOK-LYCOMING T55 ENGINE
D. E. Glenny Feb. 1989 27 p
(AD-A210482; ARL-PROP-TM-454; DODA-AR-005-574) Avail: NTIS HC A03/MF A01 CSCL 21/5

In response to a request from RAAF HQSC a number of power assessment procedures for application to the Chinook-Lycoming T55 engine were examined. The most satisfactory procedure was found to be the RAF Power Assurance Check (PAC). However because the method is not fully defined, and its monitoring period is currently set at 25 hour intervals, the procedure will require some refinement before it can be fully utilized. The potentially most attractive procedure is the Power Assurance Test (PAT) proposed in conjunction with the retrofitting of a full authority digital engine control (FADEC) to the T55-L11 engine. This latter procedure has a number of deficiencies associated with it and the RAAF should monitor its development closely before any decision is made to implement the procedures on a regular basis. GRA

N90-10042*# National Aeronautics and Space Administration. Ames Research Center, Moffett Field, CA.
STATIC AEROELASTIC ANALYSIS FOR GENERIC CONFIGURATION AIRCRAFT
In Lee, Hirokazu Miura, and Mladen K. Chargin Jun. 1987 53 p
(NASA-TM-89423; A-87091; NAS 1.15:89423) Avail: NTIS HC A04/MF A01 CSCL 21E

A static aeroelastic analysis capability that can calculate flexible air loads for generic configuration aircraft was developed. It was made possible by integrating a finite element structural analysis code (MSC/NASTRAN) and a panel code of aerodynamic analysis based on linear potential flow theory. The framework already built in MSC/NASTRAN was used and the aerodynamic influence coefficient matrix is computed externally and inserted in the NASTRAN by means of a DMAP program. It was shown that deformation and flexible airloads of an oblique wing aircraft can be calculated reliably by this code both in subsonic and supersonic speeds. Preliminary results indicating importance of flexibility in calculating air loads for this type of aircraft are presented.
Author

N90-10043*# Hamilton Standard, Windsor Locks, CT.
LARGE SCALE PROP-FAN STRUCTURAL DESIGN STUDY. VOLUME 1: INITIAL CONCEPTS
L. C. Billman, C. J. Gruska, R. M. Ladden, D. K. Leishman, and J. E. Turnberg 1988 258 p
(Contract NAS3-22394)
(NASA-CR-174992; NAS 1.26:174992; HSER-11518-Vol-1) Avail: NTIS HC A12/MF A02 CSCL 21E

In recent years, considerable attention has been directed toward improving aircraft fuel consumption. Studies have shown that the inherent efficiency advantage that turboprop propulsion systems have demonstrated at lower cruise speeds may now be extended to the higher speeds of today's turbofan and turbojet-powered aircraft. To achieve this goal, new propeller designs will require features such as thin, high speed airfoils and aerodynamic sweep, features currently found only in wing designs for high speed aircraft. This is Volume 1 of a 2 volume study to establish structural concepts for such advanced propeller blades, to define their structural properties, to identify any new design, analysis, or fabrication techniques which were required, and to determine the structural tradeoffs involved with several blade shapes selected primarily on the basis of aero/acoustic design considerations. The feasibility of fabricating and testing dynamically scaled models of these blades for aeroelastic testing was also established. The preliminary design of a blade suitable for flight use in a testbed advanced turboprop was conducted and is described in Volume 2. Author

N90-10044*# Hamilton Standard, Windsor Locks, CT.
LARGE SCALE PROP-FAN STRUCTURAL DESIGN STUDY. VOLUME 2: PRELIMINARY DESIGN OF SR-7
L. C. Billman, C. J. Gruska, R. M. Ladden, D. K. Leishman, and J. E. Turnberg 1988 282 p
(Contract NAS3-22394)
(NASA-CR-174993; NAS 1.26:174993; HSER-11518-Vol-2) Avail: NTIS HC A13/MF A02 CSCL 21E

In recent years, considerable attention has been directed toward improving aircraft fuel consumption. Studies have shown that the inherent efficiency advantage that turboprop propulsion systems have demonstrated at lower cruise speeds may now be extended to the higher speeds of today's turbofan and turbojet-powered aircraft. To achieve this goal, new propeller designs will require features such as thin, high speed airfoils and aerodynamic sweep, features currently found only in wing designs for high speed aircraft. This is Volume 2 of a 2 volume study to establish structural concepts for such advanced propeller blades, to define their structural properties, to identify any new design, analysis, or fabrication techniques which were required, and to determine the structural tradeoffs involved with several blade shapes selected primarily on the basis of aero/acoustic design considerations. The feasibility of fabricating and testing dynamically scaled models of these blades for aeroelastic testing was also established. The preliminary design of a blade suitable for flight use in a testbed advanced turboprop was conducted and is described. Author

N90-10045*# Hamilton Standard, Windsor Locks, CT.
LARGE-SCALE ADVANCED PROP-FAN (LAP) HIGH SPEED WIND TUNNEL TEST REPORT
William A. Campbell, Harold S. Wainauski, and Peter J. Arseneaux Jul. 1988 199 p
(Contract NAS3-23051)
(NASA-CR-182125; NAS 1.26:182125; HSER-11894) Avail: NTIS HC A09/MF A02 CSCL 21E

High Speed Wind Tunnel testing of the SR-7L Large Scale Advanced Prop-Fan (LAP) is reported. The LAP is a 2.74 meter (9.0 ft) diameter, 8-bladed tractor type rated for 4475 KW (6000 SHP) at 1698 rpm. It was designated and built by Hamilton Standard under contract to the NASA Lewis Research Center. The LAP employs thin swept blades to provide efficient propulsion at flight speeds up to Mach .85. Testing was conducted in the ONERA S1-MA Atmospheric Wind Tunnel in Modane, France. The test objectives were to confirm that the LAP is free from high speed classical flutter, determine the structural and aerodynamic response to angular inflow, measure blade surface pressures (static and dynamic) and evaluate the aerodynamic performance at various blade angles, rotational speeds and Mach numbers. The measured structural and aerodynamic performance of the LAP correlated well with analytical predictions thereby providing confidence in the computer prediction codes used for the design. There were no signs of classical flutter throughout all phases of the test up to and including the 0.84 maximum Mach number achieved. Steady and unsteady blade surface pressures were successfully measured for a wide range of Mach numbers, inflow angles, rotational speeds and blade angles. No barriers were discovered that would prevent proceeding with the PTA (Prop-Fan Test Assessment) Flight Test Program scheduled for early 1987. Author

N90-10046*# Hamilton Standard, Windsor Locks, CT.
LARGE-SCALE ADVANCED PROP-FAN (LAP) TECHNOLOGY ASSESSMENT REPORT
C. L. DeGeorge Sep. 1988 102 p
(Contract NAS3-23051)
(NASA-CR-182142; NAS 1.26:182142; HSER-11804) Avail: NTIS HC A06/MF A01 CSCL 21E

The technologically significant findings and accomplishments of the Large Scale Advanced Prop-Fan (LAP) program in the areas of aerodynamics, aeroelasticity, acoustics and materials and fabrication are described. The extent to which the program goals related to these disciplines were achieved is discussed, and recommendations for additional research are presented. The LAP program consisted of the design, manufacture and testing of a near full-scale Prop-Fan or advanced turboprop capable of operating efficiently at speeds to Mach .8. An aeroelastically scaled model of the LAP was also designed and fabricated. The goal of the program was to acquire data on Prop-Fan performance that would indicate the technology readiness of Prop-Fans for practical applications in commercial and military aviation. Author

N90-10047*# General Electric Co., Cincinnati, OH. Aircraft Engines Div.
FULL SCALE TECHNOLOGY DEMONSTRATION OF A MODERN COUNTERROTATING UNDUCTED FAN ENGINE CONCEPT: COMPONENT TEST
Dec. 1987 109 p
(Contract NAS3-24210)
(NASA-CR-180868; NAS 1.26:180868) Avail: NTIS HC A06/MF A01 CSCL 21E

The UDF trademark (Unducted Fan) engine is a new aircraft engine concept based on an ungeared, counterrotating, unducted, ultra-high-bypass turbofan configuration. This engine is being developed to provide a high thrust-to-weight ratio powerplant with exceptional fuel efficiency for subsonic aircraft application. This report covers the testing of pertinent components of this engine such as the fan blades, control and actuation system, turbine blades and spools, seals, and mixer frame. Author

N90-10048*# General Electric Co., Cincinnati, OH. Aircraft Engines Div.
FULL SCALE TECHNOLOGY DEMONSTRATION OF A MODERN COUNTERROTATING UNDUCTED FAN ENGINE CONCEPT. DESIGN REPORT
Dec. 1987 368 p
(Contract NAS3-24210)
(NASA-CR-180867; NAS 1.26:180867) Avail: NTIS HC A16/MF A02 CSCL 21E

The Unducted Fan engine (UDF trademark) concept is based on an ungeared, counterrotating, unducted, ultra-high-bypass turbofan configuration. This engine is being developed to provide a high thrust-to-weight ratio power plant with exceptional fuel efficiency for subsonic aircraft application. This report covers the design methodology and details for the major components of this engine. The design intent of the engine is to efficiently produce 25,000 pounds of static thrust while meeting life and stress requirements. The engine is required to operate at Mach numbers of 0.8 or above. Author

N90-10049*# General Electric Co., Cincinnati, OH. Aircraft Engines Div.
FULL SCALE TECHNOLOGY DEMONSTRATION OF A MODERN COUNTERROTATING UNDUCTED FAN ENGINE CONCEPT. ENGINE TEST
Dec. 1987 340 p
(Contract NAS3-24210)
(NASA-CR-180869; NAS 1.26:180869) Avail: NTIS HC A15/MF A02 CSCL 21E

The Unducted Fan (UDF) engine is an innovative aircraft engine concept based on an ungeared, counterrotating, unducted, ultra-high-bypass turbofan configuration. This engine is being developed to provide a high thrust-to-weight ratio power plant with exceptional fuel efficiency for subsonic aircraft application. This report covers the successful ground testing of this engine. A test program exceeding 100-hr duration was completed, in which all the major goals were achieved. The following accomplishments were demonstrated: (1) full thrust (25,000 lb); (2) full counterrotating rotor speeds (1393+ rpm); (3) low specific fuel consumption (less than 0.24 lb/hr/lb); (4) new composite fan design; (5) counterrotation of structures, turbines, and fan blades; (6) control system; (7) actuation system; and (8) reverse thrust. Author

N90-10195# General Electric Co., Cincinnati, OH. Aircraft Engines.
DYNAMIC INSTABILITY CHARACTERISTICS OF AIRCRAFT TURBINE ENGINE COMBUSTORS
M. J. Kenworthy, D. W. Bahr, P. Mungur, D. L. Burrus, J. M. Mehta, and Anthony J. Cifone (Naval Air Propulsion Test Center, Trenton, NJ.) *In* AGARD, Combustion Instabilities in Liquid-Fuelled Propulsion Systems Apr. 1989 13 p (For primary document see N90-10191 01-25)
Copyright Avail: NTIS HC A14/MF A03

N90-10198# Office National d'Etudes et de Recherches Aerospatiales, Paris (France).
EFFECTS OF LOW-FREQUENCY INSTABILITIES ON THE OPERATION OF RAMJET AIR INLETS [EFFETS DES INSTABILITES DE BASSE FREQUENCE SUR LE FONCTIONNEMENT DES PRISES D'AIR DE STATOREACTEUR]
C. Sans *In* AGARD, Combustion Instabilities in Liquid-Fuelled Propulsion Systems Apr. 1989 12 p In FRENCH; ENGLISH summary Previously announced in IAA as A89-29285 (For primary document see N90-10191 01-25)
Copyright Avail: NTIS HC A14/MF A03

N90-10199# Naval Weapons Center, China Lake, CA. Airbreathing Propulsion Branch.
RECENT DEVELOPMENTS IN RAMJET PRESSURE OSCILLATION TECHNOLOGY
P. A. Chun, J. A. Loundagin, J. A. Nabity, and S. E. Ayler *In* AGARD, Combustion Instabilities in Liquid-Fuelled Propulsion Systems Apr. 1989 13 p (For primary document see N90-10191 01-25)
Copyright Avail: NTIS HC A14/MF A03

N90-10200# Cambridge Univ. (England). Dept. of Engineering.
REHEAT BUZZ: AN ACOUSTICALLY COUPLED COMBUSTION INSTABILITY
A. P. Dowling *In* AGARD, Combustion Instabilities in Liquid-Fuelled Propulsion Systems Apr. 1989 16 p (For primary document see N90-10191 01-25)
Copyright Avail: NTIS HC A14/MF A02

N90-10201# Otago Univ., Dunedin (New Zealand). Dept. of Physics.
ATTENUATION OF REHEAT BUZZ BY ACTIVE CONTROL
P. J. Langhorne and N. Hooper (Cambridge Univ., England) *In* AGARD, Combustion Instabilities in Liquid-Fuelled Propulsion Systems Apr. 1989 17 p Sponsored in part by Rolls-Royce plc, London, England (For primary document see N90-10191 01-25)
Copyright Avail: NTIS HC A14/MF A02

N90-10202*# Flow Research, Inc., Kent, WA.
NUMERICAL SIMULATION OF PRESSURE OSCILLATIONS IN A RAMJET COMBUSTOR
Wen-Huei Jou and Suresh Menon *In* AGARD, Combustion Instabilities in Liquid-Fuelled Propulsion Systems Apr. 1989 25 p Sponsored in part by NASA. Lewis Research Center; and by NASA. Ames Research Center (For primary document see N90-10191 01-25)
(Contract N00014-84-C-0359)
Copyright Avail: NTIS HC A14/MF A02 CSCL 21E

N90-10203# Office National d'Etudes et de Recherches Aerospatiales, Paris (France).
NUMERICAL SIMULATION OF UNSTEADY COMBUSTION IN A DUMP COMBUSTOR [SIMULATION NUMERIQUE DU FONCTIONNEMENT INSTATIONNAIRE D'UN FOYER A ELARGISSEMENT BRUSQUE]
F. Garnier, B. Labegorre, M. Serrano, and A. Laverdant *In* AGARD, Combustion Instabilities in Liquid-Fuelled Propulsion Systems Apr. 1989 28 p In FRENCH; ENGLISH summary (For primary document see N90-10191 01-25)
Copyright Avail: NTIS HC A14/MF A02

N90-10204# California State Univ., Sacramento. Dept. of Mechanical Engineering.
VERY-LOW-FREQUENCY OSCILLATIONS IN LIQUID-FUELED RAMJETS
Frederick H. Reardon *In* AGARD, Combustion Instabilities in Liquid-Fuelled Propulsion Systems Apr. 1989 12 p (For primary document see N90-10191 01-25)
(Contract F33615-81-C-2078)
Copyright Avail: NTIS HC A14/MF A02

N90-10206# Naval Research Lab., Washington, DC. Lab. for Computational Physics and Fluid Dynamics.
ACOUSTIC-VORTEX-CHEMICAL INTERACTIONS IN AN IDEALIZED RAMJET
K. Kailasanath, J. H. Gardner, J. P. Boris, and Elaine S. Oran *In* AGARD, Combustion Instabilities in Liquid-Fuelled Propulsion Systems Apr. 1989 13 p Sponsored in part by Navy (For primary document see N90-10191 01-25)
Copyright Avail: NTIS HC A14/MF A02

08 AIRCRAFT STABILITY AND CONTROL

Includes aircraft handling qualities; piloting; flight controls; and autopilots.

For related information see also *05 Aircraft Design, Testing and Performance.*

N90-10050# Advisory Group for Aerospace Research and Development, Neuilly-Sur-Seine (France). Flight Mechanics Panel.
STABILITY AND CONTROL OF TACTICAL MISSILE SYSTEMS
Mar. 1989 332 p In ENGLISH and FRENCH Symposium held in Ankara, Turkey, 9-12 May 1988
(AGARD-CP-451; ISBN-92-835-0494-1) Avail: NTIS HC A15/MF A02

With recent advances in missile seekers and processors, and in the analysis of missile dynamics motions and the associated control subsystem designs, missile maneuver envelopes have significantly expanded. It was therefore appropriate and timely that the stability and controllability of such missiles be examined, and the different techniques currently involved in dealing with the various aspects of this subject. A wide selection of topics are covered: from prediction, simulation and test, through to a look at current development experience. The subject was deliberately

limited to tactical missiles, encompassing air-to-air, air-to-ground, and ground-to-air, but not ballistic missiles. For individual titles, see N90-10051 through N90-10073.

N90-10051*# National Aeronautics and Space Administration. Ames Research Center, Moffett Field, CA.
THE PRESENT STATUS AND THE FUTURE OF MISSILE AERODYNAMICS **c02**
Jack N. Nielsen *In* AGARD, Stability and Control of Tactical Missile Systems Mar. 1989 18 p (For primary document see N90-10050 01-08)
Avail: NTIS HC A15/MF A02 CSCL 01A

Recent developments in the state of the art in missile aerodynamics are reviewed. Among the subjects covered are: (1) Tri-service/NASA data base, (2) wing-body interference, (3) nonlinear controls, (4) hypersonic transition, (5) vortex interference, (6) airbreathers, supersonic inlets, (7) store separation problems, (8) correlation of missile data, (9) CFD codes for complete configurations, (10) engineering prediction methods, and (11) future configurations. Suggestions are made for future research and development to advance the state of the art of missile aerodynamics. Author

N90-10052# Office National d'Etudes et de Recherches Aerospatiales, Paris (France).
PREDICTION OF THE AERODYNAMIC STABILITY OF MISSILES [PREVISION DE LA STABILITE AERODYNAMIQUE DES MISSILES]
P. Champigny *In* AGARD, Stability and Control of Tactical Missile Systems Mar. 1989 13 p In FRENCH; ENGLISH summary (For primary document see N90-10050 01-08)
Avail: NTIS HC A15/MF A02

The development of new surface to air and air to air missiles with improved maneuverability in terms of load factor or time leg requires a better prediction of the aerodynamic coefficients, mainly those related to the static stability. Within this context, examples are presented of stability predictions based on several theoretical methods. Also underlined are the experimental problems for the evaluation of the static stability from wind-tunnel tests. Author

N90-10053# Messerschmitt-Boelkow-Blohm G.m.b.H., Munich (Germany, F.R.).
PREDICTION OF STABILITY DERIVATIVES FOR MISSILES USING THE HISSS PANEL CODE
L. Fornasier and P. DEspiney (Office National d'Etudes et de Recherches Aerospatiales, Paris, France) *In* AGARD, Stability and Control of Tactical Missile Systems Mar. 1989 20 p (For primary document see N90-10050 01-08)
Avail: NTIS HC A15/MF A02

The applicability of a higher order panel method code to the aerodynamic analysis of missile configurations is investigated. In a cooperative work between MBB and ONERA, the HISSS code (developed for the analysis of attached, subsonic and supersonic flow about complex aircraft configurations) was used for calculating a large variety of different missile geometries, including classical configurations, non-circular bodies and air-breathing configurations. Accuracy and limitations of the present theoretical approach are evaluated and discussed by comparison of calculated results with wind tunnel data available at ONERA. It is concluded that the method can be successfully used for the analysis of very complex missile geometries at both subsonic and supersonic Mach numbers, provided that the flow conditions prevent violation of the underlying linearized potential theory. Author

N90-10054# Air Force Wright Aeronautical Labs., Wright-Patterson AFB, OH.
MISSILE DATCOM: ENHANCEMENTS FOR DESIGN APPLICATIONS
Jerry E. Jenkins and William B. Blake *In* AGARD, Stability and Control of Tactical Missile Systems Mar. 1989 16 p (For primary document see N90-10050 01-08)
Avail: NTIS HC A15/MF A02

Missile Datcom, a stability and control prediction code tailored to conceptual and preliminary design applications, was developed. The program uses a component build-up approach based on the equivalent angle-of-attack concept. Simple vortex models are employed to allow for rapid and economical analyses. Two enhancements for design application were incorporated into the code. Experimental data substitution allows accuracy improvements to be attained by permitting the user to substitute experimental data for Missile Datcom predictions during the component build-up process. Its use is appropriate when more accurate data are available for vehicle components or for partial configurations. Configuration incrementing allows a user to more accurately investigate the effects of geometry changes on an existing configuration. In this case, experimental data for the complete baseline configuration are used to correct Missile Datcom predictions for the modified vehicle. Problem areas, in many cases related to vortex modeling, can degrade accuracy for some types of configurations. These are examined in the light of selected theory-to-test correlations. Finally, current efforts to improve existing methods and to develop new methods are briefly reviewed. Author

N90-10055# Dornier-Werke G.m.b.H., Friedrichshafen (Germany, F.R.).
PREDICTION OF DYNAMIC DERIVATIVES **c02**
Heinz Fuchs *In* AGARD, Stability and Control of Tactical Missile Systems Mar. 1989 19 p (For primary document see N90-10050 01-08)
Avail: NTIS HC A15/MF A02

The prediction methodology of dynamic derivatives is presented as derived from semiempirical calculation procedures like USAF Stability and Control Datcom in combination with some modifications necessary for tactical missile configurations at higher angles-of-attack. The main subject is the longitudinal stability derivatives and the roll damping derivativum. A comparison of theoretical and experimental results is presented where different dynamic wind tunnel test equipments are explained including the data evaluation theory. Some aspects of modification of the present linear data evaluation method to nonlinear terms at high angles-of-attack are shown with an example of a fighter aircraft configuration using the MOD test rig in the Dornier wind tunnel. Author

N90-10056# Lockheed Missiles and Space Co., Sunnyvale, CA.
PREDICTION OF TACTICAL MISSILE DYNAMICS **c02**
L. E. Ericsson *In* AGARD, Stability and Control of Tactical Missile Systems Mar. 1989 22 p (For primary document see N90-10050 01-08)
Avail: NTIS HC A15/MF A02

The aerodynamic information needed for preliminary design of tactical missiles was always obtained through the combined use of theory and experiments. In regard to the static aerodynamics this has resulted in a prediction capability that often is satisfactory for preliminary design. However, the vehicle dynamics cannot be predicted with the same confidence, especially not at the high angles of attack where high performance missiles often must operate. In this case dependence is still upon continuous efficient interactions between theoretical and experimental methods. The limitations of both methods are delineated and the means of how to circumvent them in order to predict tactical missile dynamics over the required range of operational parameters are described. Author

N90-10057# Nielsen Engineering and Research, Inc., Mountain View, CA.
VORTEX INDUCED CHARACTERISTICS OF MISSILES IN UNSTEADY MANEUVERS
Michael R. Mendenhall and Stanley C. Perkins, Jr. *In* AGARD, Stability and Control of Tactical Missile Systems Mar. 1989 13 p (For primary document see N90-10050 01-08)
Avail: NTIS HC A15/MF A02

A preliminary design method to predict the nonlinear aerodynamic characteristics of tactical missiles in unsteady maneuvers at high angles of attack in subsonic flow is described.

The approach is based on the accurate representation of the complex flow phenomena in the vicinity of the missile, including effects of forebody vortex shedding and lifting surface trailing vorticity. For specified motion of the missile, the time-dependent forces and moments on all missile components are calculated, including hysteresis effects due to vortex lag and the history of the motion, without the need for empirical information. This provides a capability to predict stability and control characteristics of advanced missile configurations for preliminary design analysis. When possible, comparison of experiment and theory are presented to validate the method. Author

N90-10058# Nielsen Engineering and Research, Inc., Mountain View, CA. Missile and Store Separation Aerodynamics.
AEROELASTIC TAILORING PROCEDURE FOR CONTROLLING FIN HINGE MOMENTS
M. F. E. Dillenius and S. C. McIntosh, Jr. (McIntosh Structural Dynamics, Inc., Palo Alto, CA.) *In* AGARD, Stability and Control of Tactical Missile Systems Mar. 1989 14 p (For primary document see N90-10050 01-08)
(Contract N00019-86-C-0032)
Avail: NTIS HC A15/MF A02

A combined static aeroelastic and optimization design method is presented which is aimed at controlling the center of pressure acting on a missile control fin made of composite material. Specifically, the material principal-axis directions of various segments of an orthotropic fin are varied in order to influence the chordwise location of the center of pressure through elastic fin deformation under nonlinear supersonic aerodynamic loading. The design problem is posed as an optimization problem, where the principal-axis directions are the design variables, and the objective is the difference between the current center of pressure location and its desired location. Constraints on flutter speeds, displacements, and natural frequencies are permitted, and the design variables have upper and lower bounds. Consistent fin deformations are obtained by iterating between the aerodynamic load and the fin displacement calculations. Results obtained by the present method are presented for a hypothetical supersonic missile control fin. An antisymmetric angle-ply layup of graphite fibers and epoxy is used for the fin material. The variation of chordwise center of pressure location with material principal-axis direction is mapped, and operation of the optimizer, with and without constraints, is demonstrated. The results demonstrate that locally optimum center of pressure locations can be calculated. Author

N90-10059# British Aerospace Dynamics Group, Hatfield (England). Systems Support Dept.
ALTERNATIVE POLAR HOMING STRATEGIES
M. S. Gate and R. S. Randall *In* AGARD, Stability and Control of Tactical Missile Systems Mar. 1989 14 p (For primary document see N90-10050 01-08)
Avail: NTIS HC A15/MF A02

The coupled lateral and roll requirements are considered for a twist-to-track missile which is constrained by the seeker to maintain the sight line at an approximately fixed polar angle from the body. Two alternative approaches, one based on roll profile optimization and the other on adopting a non-cruciform missile configuration, are described. Author

N90-10060# Selenia S.p.A., Rome (Italy). Missile System Div.
HOW TO CONTROL UNSTABLE MISSILE AIRFRAMES: METHODOLOGY AND LIMITATIONS
A. Gazzina *In* AGARD, Stability and Control of Tactical Missile Systems Mar. 1989 18 p (For primary document see N90-10050 01-08)
Avail: NTIS HC A15/MF A02

The problem of controlling static unstable airframes of tactical missiles through the proper choice both of gains and of the autopilot configuration is covered. Unlike other excellent treatments of the subject, the analytical description of the problem is simplified to the extreme in order to shorten the gap between the aerodynamicist and the control system designer. Classical feedback paths are described highlighting the key features of each of them and a method of direct synthesis is presented valid for both stable and unstable airframes. The maximum allowable instability of the airframe is derived. Author

N90-10061# Societe Francaise d'Equipments pour la Navigation Aerienne, Chatellerault (France).
MINIATURIZED TRIAXIAL LASER GYRO [GYROMETRE LASER TRIAXIAL MINIATURISE]
Serge Petit *In* AGARD, Stability and Control of Tactical Missile Systems Mar. 1989 9 p In FRENCH (For primary document see N90-10050 01-08)
Avail: NTIS HC A15/MF A02

The operating principles and advantages of the axial laser gyro concept are described and a technical description of a triaxial sensor developed for small-diameter missiles is presented. The performance characteristics of two prototype triaxial laser gyros are reported. Stability, biases, and scale factor characteristics are addressed. Finally, a brief description of a miniature accelerometer unit is given. Transl. by M.G.

N90-10062*# National Aeronautics and Space Administration. Langley Research Center, Hampton, VA.
NEW TEST TECHNIQUES TO EVALUATE NEAR FIELD EFFECTS FOR SUPERSONIC STORE CARRIAGE AND SEPARATION **c05**
Wallace C. Sawyer, Robert L. Stallings, Jr., Floyd J. Wilcox, Jr., A. B. Blair, Jr., William J. Monta, and Elizabeth B. Plentovich *In* AGARD, Stability and Control of Tactical Missile Systems Mar. 1989 9 p (For primary document see N90-10050 01-08)
Avail: NTIS HC A15/MF A02 CSCL 01C

Store separation and store carriage drag studies were conducted. A primary purpose is to develop new experimental methods to evaluate near field effects of store separation and levels of store carriage drag associated with a variety of carriage techniques for different store shapes and arrangements. Flow field measurements consisting of surface pressure distributions and vapor screen photographs are used to analyze the variations of the store separation characteristics with cavity geometry. Store carriage drag measurements representative of tangent, semi-submerged, and internal carriage installations are presented and discussed. Results are included from both fully metric models and models with only metric segments (metric pallets) and the relative merits of the two are discussed. Carriage drag measurements for store installations on an aircraft parent body are compared both with prediction methods and with installations on a generic parent body. Author

N90-10063*# National Aeronautics and Space Administration. Langley Research Center, Hampton, VA.
REMOTE CONTROL MISSILE MODEL TEST
Jerry M. Allen, David S. Shaw, and Wallace C. Sawyer *In* AGARD, Stability and Control of Tactical Missile Systems Mar. 1989 12 p (For primary document see N90-10050 01-08)
Avail: NTIS HC A15/MF A02 CSCL 01C

An extremely large, systematic, axisymmetric body/tail fin data base was gathered through tests of an innovative missile model design which is described herein. These data were originally obtained for incorporation into a missile aerodynamics code based on engineering methods (Program MISSILE3), but can also be used as diagnostic test cases for developing computational methods because of the individual-fin data included in the data base. Detailed analysis of four sample cases from these data are presented to illustrate interesting individual-fin force and moment trends. These samples quantitatively show how bow shock, fin orientation, fin deflection, and body vortices can produce strong, unusual, and computationally challenging effects on individual fin loads. Comparisons between these data and calculations from the SWINT Euler code are also presented. Author

N90-10064# Selenia S.p.A., Rome (Italy). Missile Systems Div.
WIND TUNNEL TESTS: THE ROLE OF THE MODEL **c09**
S. Mazzuca and B. Piacentini *In* AGARD, Stability and Control

of Tactical Missile Systems Mar. 1989 10 p (For primary document see N90-10050 01-08)
Avail: NTIS HC A15/MF A02

The role of the model in the overall wind tunnel test program is highlighted. Depending on the specific task to be achieved (i.e., improvement of an existing missile or a new missile development), the cost-effectiveness analysis leads to the best solution in terms of: scale of the model; number of configurations to be tested; degree of likelihood; wind tunnel facilities to be used; interoperability among different test sites; overall test time; and test time of each subphase. A further very important role is related to the test philosophy adopted in order to minimize the number of measurements while retaining the capability to obtain from the test useful information. A proper design of the model can fulfill these constraints, minimizing overall test time and the related costs. Author

N90-10065# Institut fuer Flugmechanik, Brunswick (Germany, F.R.).
IDENTIFICATION OF STABILITY AND CONTROL PARAMETERS OF A BRILLIANT AMMUNITION
K.-F. Doherr, G. Lehmann, and H. Schilling (Rheinmetall G.m.b.H., Duesseldorf, Germany, F.R.) *In* AGARD, Stability and Control of Tactical Missile Systems Mar. 1989 16 p (For primary document see N90-10050 01-08)
Avail: NTIS HC A15/MF A02

The efficient defense against armored ground vehicles depends heavily on precisely delivered warheads. New terminal guided warheads are under development presently which improve the hit accuracy and therefore the effectiveness drastically. One exampe is EPHRAM which employs a sophisticated detection and control system in order to achieve optimal results. A considerable part of the development of a brilliant ammunition is spent on the determination of its aerodynamic and control characteristics. For EPHRAM static and dynamic wind tunnel experiments were performed. A recoverable instrumented version was developed for the validation of the concept and the identification of aerodynamic parameters and thrust interference effects from flight tests. The test vehicle was dropped several times from a helicopter-lifted platform. During these first tests with reduced sensor equipment, which focused on the performance of EPHRAM, the desired footprint was achieved. An analysis of one of these flights confirmed the static wind tunnel results at low angle of attack. For the system identification at high angle of attack more flight tests are scheduled with complete instrumentation and selected thrust programs to fully excite the vehicle dynamics. Author

N90-10066# Messerschmitt-Boelkow-Blohm G.m.b.H., Munich (Germany, F.R.). Defense Systems Div.
VALIDATION OF MISSILE SIMULATION
Werner Bub *In* AGARD, Stability and Control of Tactical Missile Systems Mar. 1989 8 p (For primary document see N90-10050 01-08)
Avail: NTIS HC A15/MF A02

One of the key findings of AGARDograph No. 279, Survey of Missile Simulation and Flight Mechanics in NATO, was that very little effort was expended in missile simulation validation. No standard or well-defined techniques were in use adequate to communicate confidence in missile simulations to persons not directly involved in the process of simulation development. Missile simulation validation and confidence building techniques were examined. A simulation terminology was recommended that should simplify the validation process. In addition a hierarchical model representation called CLIMB was recommended in order to organize and document the knowledge base for simulation development as well as the data bases used for simulation validation. Author

N90-10067# Naval Weapons Center, China Lake, CA. Propulsion Control Technology Program.
INVESTIGATIONS OF THRUST VECTOR CONTROL FOR HIGH-ALPHA PITCHOVER
A. O. Danielson and R. B. Dillinger *In* AGARD, Stability and Control of Tactical Missile Systems Mar. 1989 14 p (For primary document see N90-10050 01-08)
Avail: NTIS HC A15/MF A02

Historically, thrust vector control (TVC) system investigations at the Naval Weapons Center have touched on a wide variety of technologies. Emphasis is on two technologies, the movable-nozzle and the jet-vane TVD, whose performance capabilities demonstrate the significant maneuvers achievable by thrust vector controlled missiles. Investigations have revealed an especially notable result of testing in the high-alpha vertical-launch pitchover environment; that is, despite high-performance TVC capability, missile subsystems such as seeker, airframe, actuation, autopilot, and rocket motor can limit the potential benefits otherwise offered by thrust vectoring. Some lessons learned in approaching such limits are delineated and referenced to assist systems engineers and designers of tactical missile airframes and control systems. Author

N90-10068# Naval Weapons Center, China Lake, CA.
A STRUCTURED SINGULAR VALUE APPROACH TO MISSILE AUTOPILOT ANALYSIS 2
G. A. Hewer, Richard Klabunde, and Charles Kenney *In* AGARD, Stability and Control of Tactical Missile Systems Mar. 1989 7 p (For primary document see N90-10050 01-08)
Avail: NTIS HC A15/MF A02

A state space model for additive errors that is algebraically and dynamically equivalent to Doyle's structured singular value is presented. Using this theory a new algorithm based on a Monte Carlo eigenvalue search is presented. Some examples are included that illustrate the convergence properties of the Monte Carlo technique. Author

N90-10069# Naval Weapons Center, China Lake, CA. Dynamics and Control Branch.
ANALYSIS AND TESTING OF A HIGH PERFORMANCE AIR-AIR MISSILE **c05**
Gerald L. Stevens *In* AGARD, Stability and Control of Tactical Missile Systems Mar. 1989 15 p (For primary document see N90-10050 01-08)
Avail: NTIS HC A15/MF A02

Hardware-in-the-loop (HWIL) testing of air-air missiles is performed at the Naval Weapons Center (NWC), China Lake. To illustrate the procedures, this presentation follows a highly maneuverable flight test vehicle from initial hardware testing, through the launch, to the subsequent postflight analysis. HWIL testing combines a real-time simulation with flight hardware. The purpose of the dynamic simulation is to validate stability and controllability of the missile system, debug flight hardware, help to characterize the missile subsystems and test interfaces used throughout the hardware. The simulation that results helps to characterize the air-air missile and its capabilities. Author

N90-10070# Messerschmitt-Boelkow-Blohm G.m.b.H., Munich (Germany, F.R.).
MARGINAL RELEASE DISTURBANCES ON ADVANCED MISSILES **c05**
Ronald Deslandes *In* AGARD, Stability and Control of Tactical Missile Systems Mar. 1989 12 p (For primary document see N90-10050 01-08)
Avail: NTIS HC A15/MF A02

Today's store separation analysis is more and more confronted to marginal clearance situations due to increasing requirements imposed by the aircraft operators. In fact, that an advanced missile has to be perfectly released during arbitrary aircraft maneuvers and variable installations affords the accurate knowledge of the missile's motion during tip-off. The engineering task is therefore no longer focussed exclusively on the analysis of safety aspects of separation, but is now to be extended on the consideration of compatibility between operator's requirements to allow any strength of release disturbances and the missile control system to overcome such situations. The results expected from such an analysis is an accurate indication of any marginal limitation respective to safety or to controllability. Based on simulations performed with a powerful

6-DOF code developed at MBB during the last decade, this paper deals with such inconsistancies implicated by excessive roll or pitch-motions during different rail-launch situations. After a short description of the basic algorithms, computed results involving data from flight test movie will be displayed by 3D-video, in order to prove that the problem area is well handled. Author

N90-10071# British Aerospace Dynamics Group, Hatfield (England). Systems Support Dept.
AEROELASTIC ANALYSIS OF MISSILE CONTROL SURFACES WITH STRUCTURAL NON-LINEARITY
D. Sepahy *In* AGARD, Stability and Control of Tactical Missile Systems Mar. 1989 12 p (For primary document see N90-10050 01-08)
Avail: NTIS HC A15/MF A02

An aeroelastic procedure is presented to deal with structural non-linearity of a missile control surface using the concept of linearized equivalent structural stiffness. This approach enables the use of standard software packages such as NASTRAN for linear aeroelastic analysis, i.e., divergence, flutter and dynamic response analysis. An example, backed up with experimental validation, is given for a flexible control surface with structural non-linearity due to free play at the root connection. A time simulation technique is also discussed for solution of the problem. Author

N90-10072# Selenia S.p.A., Rome (Italy). Missile System Div.
EXPERIENCE GAINED IN THE IMPROVEMENT OF THE ASPIDE AERODYNAMIC CONFIGURATION FOR THE SURFACE TO AIR ROLE **c05**
S. Mazzuca *In* AGARD, Stability and Control of Tactical Missile Systems Mar. 1989 10 p (For primary document see N90-10050 01-08)
Avail: NTIS HC A15/MF A02

From the beginning to the end, the development process of the new aerodynamic version of the Aspide in the surface to air roles is described. The aims, constraints and main activities of the project are reported. The entire decision process is also analyzed in great detail. The successful completion of the above process, with the new configuration in full production constitutes the solid background for further improvements or new designs. Author

N90-10073# Selenia S.p.A., Rome (Italy). Missile Systems Div.
WINGED VERSUS WINGLESS AIRFRAMES **c05**
A. Gazzina and S. Mazzuca *In* AGARD, Stability and Control of Tactical Missile Systems Mar. 1989 20 p (For primary document see N90-10050 01-08)
Avail: NTIS HC A15/MF A02

An analytical method developed with the purpose to compare the kinematic and dynamic performance of a winged configuration with respect to a wingless configuration of a tactical anti-air missile is described. A reference mission of the missile is firstly defined and the analytical method is built-up through the introduction of suitable assumptions and simplifications. The method is then applied to an actual missile for which wind tunnel results are available in its winged and wingless configuration. The peculiar aspects of both configurations are identified and highlighted. Even if the method was developed for a specific aim it revealed suitable and accurately enough for general application mainly for a quick evaluation of a missile kinematic performance and to conduct sensitivity analysis of the mass, propulsion, and aerodynamic properties of a generic tactical missile. Author

N90-10074*# National Aeronautics and Space Administration. Langley Research Center, Hampton, VA.
ANALYSIS OF FLIGHT DATA FROM A HIGH-INCIDENCE RESEARCH MODEL BY SYSTEM IDENTIFICATION METHODS
James G. Batterson and Vladislav Klein (Joint Inst. for Advancement of Flight Sciences, Hampton, VA.) Washington Nov. 1989 50 p
(NASA-TP-2940; L-16571; NAS 1.60:2940) Avail: NTIS HC A03/MF A01 CSCL 01C

Data partitioning and modified stepwise regression were applied to recorded flight data from a Royal Aerospace Establishment high incidence research model. An aerodynamic model structure and corresponding stability and control derivatives were determined for angles of attack between 18 and 30 deg. Several nonlinearities in angles of attack and sideslip as well as a unique roll-dominated set of lateral modes were found. All flight estimated values were compared to available wind tunnel measurements. Author

N90-10075*# California Univ., Los Angeles. Dept. of Computer Science.
REAL-TIME SUPPORT FOR HIGH PERFORMANCE AIRCRAFT OPERATION Final Report, 1986 - 1988
Jacques J. Vidal Jan. 1989 24 p
(Grant NAG2-302)
(NASA-CR-185475; NAS 1.26:185475) Avail: NTIS HC A03/MF A01 CSCL 01C

The feasibility of real-time processing schemes using artificial neural networks (ANNs) is investigated. A rationale for digital neural nets is presented and a general processor architecture for control applications is illustrated. Research results on ANN structures for real-time applications are given. Research results on ANN algorithms for real-time control are also shown. K.C.D.

09 RESEARCH AND SUPPORT FACILITIES (AIR)

Includes airports, hangars and runways; aircraft repair and overhaul facilities; wind tunnels; shock tubes; and aircraft engine test stands.

For related information see also *14 Ground Support Systems and Facilities (Space).*

N90-10064# Selenia S.p.A., Rome (Italy). Missile Systems Div.
WIND TUNNEL TESTS: THE ROLE OF THE MODEL
S. Mazzuca and B. Piacentini *In* AGARD, Stability and Control of Tactical Missile Systems Mar. 1989 10 p (For primary document see N90-10050 01-08)
Avail: NTIS HC A15/MF A02

12 ASTRONAUTICS (GENERAL)

For extraterrestrial exploration see *91 Lunar and Planetary Exploration.*

N90-10076* National Aeronautics and Space Administration, Washington, DC.
NASA VOYAGER 2 NEPTUNE ENCOUNTER PRESS KIT
Aug. 1989 26 p
(NASA-TM-101851; NAS 1.15:101851; P89-10131) Avail: Issuing Activity CSCL 22A

This is a press kit relating to the Voyager Project and the Voyager 2 encounter with Neptune. The scientific objectives of the mission are given. Also included is a quick look at the scientific instruments, the spacecraft's health, mission operations, telecommunications, and the Voyager management team. E.R.

N90-10077*# National Aeronautics and Space Administration. Goddard Space Flight Center, Greenbelt, MD.
THE SPARTAN 1 MISSION Final Report, 1980-1985
Raymond G. Cruddace, G. G. Fritz, D. J. Shrewsberry, D. J. Brandenstein, D. C. Creighton, G. Gutschewski, S. W. Lucid, J. M. Nagel, J. M. Fabian, and D. Zimmerman (National Aeronautics and Space Administration. John F. Kennedy Space Center, Cocoa Beach, FL.) et al 11 Jul. 1989 17 p Prepared in cooperation with NRL, Washington, DC, LANL, NM, and McDonnell-Douglas Corp., Saint Louis, MO Original contains color illustrations
(NASA-TM-101887; NAS 1.15:101887; AD-A210597; NRL-9207)
Avail: NTIS HC A03/MF A01 CSCL 22/1

The first Spartan mission is documented. The Spartan program, an outgrowth of a joint Naval Research Laboratory (NRL)/National

Aeronautics and Space Administration (NASA)-Goddard Space Flight Center (GSFC) development effort, was instituted by NASA for launching autonomous, recoverable payloads from the space shuttle. These payloads have a precise pointing system and are intended to support a wide range of space-science observations and experiments. The first Spartan, carrying an NRL X-ray astronomy instrument, was launched by the orbiter Discovery (STS51G) on June 20, 1985 and recovered successfully 45 h later, on June 22. During this period, Spartan 1 conducted a preprogrammed series of observations of two X-ray sources: the Perseus cluster of galaxies and the center of our galaxy. The mission was successful from both on engineering and a scientific viewpoint. Only one problem was encountered, the attitude control system (ACS) shut down earlier than planned because of high attitude control system gas consumption. A preplanned emergency mode then placed Spartan 1 into a stable, safe condition and allowed a safe recovery. The events are described of the mission and presents X-ray maps of the two observed sources, which were produced from the flight data. GRA

13 ASTRODYNAMICS

Includes powered and free-flight trajectories; and orbital and launching dynamics.

N90-10078# Massachusetts Inst. of Tech., Lexington. Lincoln Lab.
ON ANALYTIC MODELING OF LUNAR PERTURBATIONS OF ARTIFICIAL SATELLITES OF THE EARTH
M. T. Lane 13 Jun. 1989 87 p
(Contract F19628-85-C-0002)
(AD-A210440; TR-841; ESD-TR-88-315) Avail: NTIS HC A05/MF A01 CSCL 22/3

Two different procedures for analytically modeling the effects of the moon's direct gravitational force on artificial earth satellites are discussed from theoretical and numerical viewpoints. One is developed using classical series expansions of inclination and eccentricity for both the satellite and the moon, and the other employs the method of averaging. Both solutions are seen to have advantages, but it is shown that while the former is more accurate in special situations, the latter is quicker and more practical for the general orbit determination problem where observed data are used to correct the orbit in near real time. GRA

14 GROUND SUPPORT SYSTEMS AND FACILITIES (SPACE)

Includes launch complexes, research and production facilities; ground support equipment, e.g., mobile transporters; and simulators.

For related information see also *09 Research and Support Facilities (Air).*

No abstracts in this category.

15 LAUNCH VEHICLES AND SPACE VEHICLES

Includes boosters; operating problems of launch/space vehicle systems; and reusable vehicles.

For related information see also *20 Spacecraft Propulsion and Power.*

No abstracts in this category.

16 SPACE TRANSPORTATION

Includes passenger and cargo space transportation, e.g., shuttle operations; and space rescue techniques.

For related information see also *03 Air Transportation and Safety* and *18 Spacecraft Design, Testing and Performance.* For space suits see *54 Man/System Technology and Life Support.*

N90-10079*# National Aeronautics and Space Administration. John F. Kennedy Space Center, Cocoa Beach, FL.
DEBRIS/ICE/TPS ASSESSMENT AND PHOTOGRAPHIC ANALYSIS FOR SHUTTLE MISSION STS-28R
Charles G. Stevenson, Gregory N. Katnik, and Scott A. Higginbotham Sep. 1989 206 p
(NASA-TM-102152; NAS 1.15:102152) Avail: NTIS HC A10/MF A02 CSCL 22B

A Debris/Ice/TPS assessment and photographic analysis was conducted for Space Shuttle Mission STS-28R. Debris inspections of the flight elements and launch pad are performed before and after launch. Ice/Frost conditions on the External Tank are assessed by the use of computer programs, nomographs, and infrared scanner data during cryogenic loading of the nomographs, and infrared scanner data during cryogenic loading of the vehicle followed by on-pad visual inspection. High speed photography is analyzed after launch to identify ice/debris sources and evaluate potential vehicle damage and/or in-flight anomalies. The debris/ice/TPS conditions and photographic analysis of Mission STS-28R is documented along with their overall effect on the Space Shuttle Program. Author

17 SPACE COMM., SPACECRAFT COMM., COMMAND & TRACKING

Includes telemetry; space communications networks; astronavigation and guidance; and radio blackout.

For related information see also *04 Aircraft Communications and Navigation* and *32 Communications and Radar.*

No abstracts in this category.

18 SPACECRAFT DESIGN, TESTING AND PERFORMANCE

Includes satellites; space platforms; space stations; spacecraft systems and components such as thermal and environmental controls; and attitude controls.

For life support systems see *54 Man/System Technology and Life Support.* For related information see also *05 Aircraft Design, Testing and Performance, 39 Structural Mechanics,* and *16 Space Transportation.*

N90-10080*# National Aeronautics and Space Administration. Langley Research Center, Hampton, VA.
PROCEEDINGS OF THE WORKSHOP ON COMPUTATIONAL ASPECTS IN THE CONTROL OF FLEXIBLE SYSTEMS, PART 1
Lawrence W. Taylor, Jr., comp. May 1989 492 p Workshop held in Williamsburg, VA, 12-14 Jul. 1988
(NASA-TM-101578-Pt-1; NAS 1.15:101578-Pt-1) Avail: NTIS HC A21/MF A03 CSCL 22B

Control/Structures Integration program software needs, computer aided control engineering for flexible spacecraft, computer aided design, computational efficiency and capability, modeling and parameter estimation, and control synthesis and optimization software for flexible structures and robots are among the topics discussed. For individual titles, see N90-10081 through N90-10102.

N90-10081*# National Aeronautics and Space Administration. Langley Research Center, Hampton, VA.
NASA'S CONTROLS-STRUCTURES INTERACTION PROGRAM
Brantley R. Hanks *In its* Proceedings of the Workshop on Computational Aspects in the Control of Flexible Systems, Part 1 May 1989 p 21-32 (For primary document see N90-10080 01-18)
Avail: NTIS HC A21/MF A03 CSCL 22B

A NASA program is about to start which has the objective to advance Controls-Structures Interaction (CSI) technology to a point where it can be used in spacecraft design for future missions. Because of the close interrelationships between the structure, the control hardware, and the analysis/design, a highly interdisciplinary activity is defined in which structures, dynamics, controls, computer and electronics engineers work together on a daily basis and are co-located to a large extent. Methods will be developed which allow the controls and structures analysis and design functions to use the same mathematical models. Hardware tests and applications are emphasized and will require development of concepts and test methods to carry out. Because of a variety of mission application problem classes, several time-phased, focus ground test articles are planned. They will be located at the Langley Researdh Center (LaRC), the Marshall Space Flight Center (MSFC) and at the Jet Propulsion Laboratory (JPL). It is anticipated that the ground tests will be subject to gravity and other environmental effects to the extent that orbital flights tests will be needed for verification of some technology items. The need for orbital flight experiments will be quantified based on ground test results and mission needs. Candidate on-orbit experiments will be defined and preliminary design/definition and cost studies will be carried out for one or more high-priority experiments. Author

N90-10082*# Jet Propulsion Lab., California Inst. of Tech., Pasadena.
COMPUTATIONAL CONTROLS FOR AEROSPACE SYSTEMS
Guy K. Man, Robert A. Laskin, and A. Fernando Tolivar *In* NASA. Langley Research Center, Proceedings of the Workshop on Computational Aspects in the Control of Flexible Systems, Part 1 May 1989 p 33-48 (For primary document see N90-10080 01-18)
Avail: NTIS HC A21/MF A03 CSCL 22B

The goal is to develop the next generation guidance and control analysis and design tools to enable future missions and to improve productivity and reliability. Author

N90-10083*# Control Research Corp., Lexington, MA.
ADDITIONAL SOFTWARE DEVELOPMENTS WANTED FOR MODELING AND CONTROL OF FLEXIBLE SPACE SYSTEMS
Jiguan Gene Lin *In* NASA. Langley Research Center, Proceedings of the Workshop on Computational Aspects in the Control of Flexible Systems, Part 1 May 1989 p 49-63 (For primary document see N90-10080 01-18)
Avail: NTIS HC A21/MF A03 CSCL 22B

Existing modeling and control software packages are either inadequate or inefficient for applications to flexible space structures. Some additional software developments are wanted for effective design and evaluation of the control systems. The following are discussed: (1) linear-quadratic optimal regulators as usual can be designed using various modern control design software packages, (2) modal dashpots are very effective output-feedback vibration controllers for flexible structures, not only effective for augmenting a small amount of active damping to a large number of vibration modes (like the so-called low-authority structural controllers), but also effective for quick suppression of large vibrations (like high-authority structural controllers), and (3) the actual performance of any control design needs to be evaluated against a faithful model of the flexible structure to be controlled. The potential of destabilization or serious performance degradation needs to be detected by numerical simulation of the structure with the control loops being closed. Author

N90-10084*# Communications Research Centre, Ottawa (Ontario).
FLEXIBLE STRUCTURE CONTROL EXPERIMENTS USING A REAL-TIME WORKSTATION FOR COMPUTER-AIDED CONTROL ENGINEERING
Michael E. Stieber *In* NASA. Langley Research Center, Proceedings of the Workshop on Computational Aspects in the Control of Flexible Systems, Part 1 May 1989 p 67-88 (For primary document see N90-10080 01-18)
Avail: NTIS HC A21/MF A03 CSCL 22B

A Real-Time Workstation for Computer-Aided Control Engineering has been developed jointly by the Communications Research Centre (CRC) and Ruhr-Universitaet Bochum (RUB), West Germany. The system is presently used for the development and experimental verification of control techniques for large space systems with significant structural flexibility. The Real-Time Workstation essentially is an implementation of RUB's extensive Computer-Aided Control Engineering package KEDDC on an INTEL micro-computer running under the RMS real-time operating system. The portable system supports system identification, analysis, control design and simulation, as well as the immediate implementation and test of control systems. The Real-Time Workstation is currently being used by CRC to study control/structure interaction on a ground-based structure called DAISY, whose design was inspired by a reflector antenna. DAISY emulates the dynamics of a large flexible spacecraft with the following characteristics: rigid body modes, many clustered vibration modes with low frequencies and extremely low damping. The Real-Time Workstation was found to be a very powerful tool for experimental studies, supporting control design and simulation, and conducting and evaluating tests within one integrated environment. Author

N90-10085*# Maryland Univ., College Park.
CONSOLE: A CAD TANDEM FOR OPTIMIZATION-BASED DESIGN INTERACTING WITH USER-SUPPLIED SIMULATORS
Michael K. H. Fan, Li-Sheng Wang, Jan Koninckx, and Andre L. Tits *In* NASA. Langley Research Center, Proceedings of the Workshop on Computational Aspects in the Control of Flexible Systems, Part 1 May 1989 p 89-108 (For primary document see N90-10080 01-18)
Avail: NTIS HC A21/MF A03 CSCL 22B

CONSOLE employs a recently developed design methodology (International Journal of Control 43:1693-1721) which provides the designer with a congenial environment to express his problem as a multiple ojective constrained optimization problem and allows him to refine his characterization of optimality when a suboptimal

design is approached. To this end, in CONSOLE, the designed formulates the design problem using a high-level language and performs design task and explores tradeoff through a few short and clearly defined commands. The range of problems that can be solved efficiently using a CAD tools depends very much on the ability of this tool to be interfaced with user-supplied simulators. For instance, when designing a control system one makes use of the characteristics of the plant, and therefore, a model of the plant under study has to be made available to the CAD tool. CONSOLE allows for an easy interfacing of almost any simulator the user has available. To date CONSOLE has already been used successfully in many applications, including the design of controllers for a flexible arm and for a robotic manipulator and the solution of a parameter selection problem for a neural network. Author

N90-10086*# Royal Aerospace Establishment, Farnborough (England).
THE APPLICATION OF TSIM SOFTWARE TO ACT DESIGN AND ANALYSIS ON FLEXIBLE AIRCRAFT
Ian W. Kaynes *In* NASA. Langley Research Center, Proceedings of the Workshop on Computational Aspects in the Control of Flexible Systems, Part 1 May 1989 p 109-120 (For primary document see N90-10080 01-18)
Avail: NTIS HC A21/MF A03 CSCL 22B

The TSIM software is described. This is a package which uses an interactive FORTRAN-like simulation language for the simulation on nonlinear dynamic systems and offers facilities which include: mixed continuous and discrete time systems, time response calculations, numerical optimization, automatic trimming of nonlinear aircraft systems, and linearization of nonlinear equations for eigenvalues, frequency responses and power spectral response evaluation. Details are given of the application of TSIM to the analysis of aeroelastic systems under the RAE Farborough extension FLEX-SIM. The aerodynamic and structural data for the equations of motion of a flexible aircraft are prepared by a preprocessor program for incorporation in TSIM simulations. Within the simulation, the flexible aircraft model may then be selected interactively for different flight conditions and modal reduction techniques applied. The use of FLEX-SIM is demonstrated by an example of the flutter prediction for a simple aeroelastic model. By utilizing the numerical optimization facility of TSIM, it is possible to undertake identification of required parameters in the TSIM model within the simulation. Author

N90-10087*# Structural Dynamics Research Corp., San Diego, CA.
CONTROL/STRUCTURE INTERACTION METHODS FOR SPACE STATION POWER SYSTEMS
Paul Blelloch *In* NASA. Langley Research Center, Proceedings of the Workshop on Computational Aspects in the Control of Flexible Systems, Part 1 May 1989 p 121-137 (For primary document see N90-10080 01-18)
Avail: NTIS HC A21/MF A03 CSCL 22B

The Structural Dynamics Research Corporation and the NASA Lewis Research Center have been working together to develop tools and methods for the analysis of control/structure interaction problems related to the space station power systems. Flexible modes of the solar arrays below 0.1 Hz, suggest that even for relatively slow control systems, the potential for control/structure interaction exists. The emphasis of the effort has been to develop tools which couple NASTRAN's powerful capabilities in structural dynamics with EASY5's powerful capabilities in control systems analysis. One product is an interface software package called CO-ST-IN for COntrol-STructure-INteraction. CO-ST-IN acts to translate data between NASTRAN and EASY5, facilitating the analysis of complex coupled problems. Interfaces to SDRC I-DEAS and MATRIXx are also offered. Beside transferring standard modal information, CO-ST-IN implements a number of advanced methods. These include a modal ordering algorithm that helps eliminate uncontrollable or unobservable modes from the analysis, an implementation of the more accurate mode acceleration algorithm for recovery of element forces and stresses directly in EASY5 and an implementation of fixed interface modes in NASTRAN, which reduces the error in the closed-loop model due to the use of truncated mode sets. Author

N90-10088*# Johns Hopkins Univ., Laurel, MD. Applied Physics Lab.
FLEXIBLE MISSILE AUTOPILOT DESIGN STUDIES WITH PC-MATLAB/386
Michael J. Ruth *In* NASA. Langley Research Center, Proceedings of the Workshop on Computational Aspects in the Control of Flexible Systems, Part 1 May 1989 p 139-166 (For primary document see N90-10080 01-18)
Avail: NTIS HC A21/MF A03 CSCL 22B

Development of a responsive, high-bandwidth missile autopilot for airframes which have structural modes of unusually low frequency presents a challenging design task. Such systems are viable candidates for modern, state-space control design methods. The PC-MATLAB interactive software package provides an environment well-suited to the development of candidate linear control laws for flexible missile autopilots. The strengths of MATLAB include: (1) exceptionally high speed (MATLAB's version for 80386-based PC's offers benchmarks approaching minicomputer and mainframe performance); (2) ability to handle large design models of several hundred degrees of freedom, if necessary; and (3) broad extensibility through user-defined functions. To characterize MATLAB capabilities, a simplified design example is presented. This involves interactive definition of an observer-based state-space compensator for a flexible missile autopilot design task. MATLAB capabilities and limitations, in the context of this design task, are then summarized. Author

N90-10089*# Kaman Aerospace Corp., Bloomfield, CT.
DYSCO: A SOFTWARE SYSTEM FOR MODELING GENERAL DYNAMIC SYSTEMS
Alex Berman *In* NASA. Langley Research Center, Proceedings of the Workshop on Computational Aspects in the Control of Flexible Systems, Part 1 May 1989 p 167-219 (For primary document see N90-10080 01-18)
Avail: NTIS HC A21/MF A03 CSCL 22B

The DYSCO program has been under development since 1979. It has been funded by Army and Air Force laboratories and by the Kaman Aerospace Corporation. It is presently available at a number of government and nongovernment installations. It has been used to analyze a very broad range of dynamics problems. A principle feature of the software design of DYSCO is the separation of the executive from the technology. The executive, which controls all the operations, is intelligent in the sense that it knows that its function is to assemble differential equations and to prepare them for solution. The technology library contains FORTRAN routines which perform standard functions, such as, computing the equation coefficients of an element (or component) given the local state at any time. The technology library also contains algorithms and procedures for solving the coupled system equations. The system was designed to allow easy additional of technology to the library. Any linear or nonlinear structural entity, control system, or set of ordinary differential equations may be simply coded and added to the library, as well as algorithms for time or frequency domain solution. The program is described with emphasis on its usefulness in easily modeling unusual concepts and configurations, performing analysis of damage, evaluating new algorithms, and simulating dynamic tests. Author

N90-10090*# Boeing Co., Seattle, WA.
MODELING AND CONTROL SYSTEM DESIGN AND ANALYSIS TOOLS FOR FLEXIBLE STRUCTURES
Amir A. Anissipour, Russell A. Benson, and Edward E. Coleman *In* NASA. Langley Research Center, Proceedings of the Workshop on Computational Aspects in the Control of Flexible Systems, Part 1 May 1989 p 221-241 (For primary document see N90-10080 01-18)
Avail: NTIS HC A21/MF A03 CSCL 22B

Described here are Boeing software tools used for the development of control laws of flexible structures. The Boeing

Company has developed a software tool called Modern Control Software Package (MPAC). MPAC provides the environment necessary for linear model development, analysis, and controller design for large models of flexible structures. There are two features of MPAC which are particularly appropriate for use with large models: (1) numerical accuracy and (2) label-driven nature. With the first feature MPAC uses double precision arithmetic for all numerical operations and relies on EISPAC and LINPACK for the numerical foundation. With the second feature, all MPAC model inputs, outputs, and states are referenced by user-defined labels. This feature allows model modification while maintaining the same state, input, and output names. In addition, there is no need for the user to keep track of a model variable's matrix row and column locations. There is a wide range of model manipulation, analysis, and design features within the numerically robust and flexible environment provided by MPAC. Models can be built or modified using either state space or transfer function representations. Existing models can be combined via parallel, series, and feedback connections; and loops of a closed-loop model may be broken for analysis. Author

N90-10091*# Mechanical Dynamics, Inc., Ann Arbor, MI. Product Technology Group.

LUMPED MASS FORMULATIONS FOR MODELING FLEXIBLE BODY SYSTEMS

Rajiv Rampalli *In* NASA. Langley Research Center, Proceedings of the Workshop on Computational Aspects in the Control of Flexible Systems, Part 1 May 1989 p 243-264 (For primary document see N90-10080 01-18)

Avail: NTIS HC A21/MF A03 CSCL 22B

The efforts of Mechanical Dynamics, Inc. in obtaining a general formulation for flexible bodies in a multibody setting are discussed. The efforts being supported by MDI, both in house and externally are summarized. The feasibility of using lumped mass approaches to modeling flexibility in a multibody dynamics context is examined. The kinematics and kinetics for a simple system consisting of two rigid bodies connected together by an elastic beam are developed in detail. Accuracy, efficiency and ease of use using this approach are some of the issues that are then looked at. The formulation is then generalized to a superelement containing several nodes and connecting several bodies. Superelement kinematics and kinetics equations are developed. The feasibility and effectiveness of the method is illustrated by the use of some examples illustrating phenomena common in the context of spacecraft motions.

Author

N90-10092*# National Aeronautics and Space Administration. Langley Research Center, Hampton, VA.

A COMPARISON OF SOFTWARE FOR THE MODELING AND CONTROL OF FLEXIBLE SYSTEMS

Lawrence W. Taylor, Jr. *In its* Proceedings of the Workshop on Computational Aspects in the Control of Flexible Systems, Part 1 May 1989 p 265-279 (For primary document see N90-10080 01-18)

Avail: NTIS HC A21/MF A03 CSCL 22B

A researcher proposes a cooperative effort among specialists who use or develop software for simulating and analyzing the control of flexible aerospace systems. A comparison of existing software for modeling control systems and flexible structures, applied to several example problems would be quite valuable. The comparison would indicate computational efficiency and capabilities with respect to handling nonlinearities and graphical output. Because of the diversity of applications of such software, the researcher believes that the proposed cooperative effort can transcend projects involving specific applications. Comparisons of software capability and efficiency can be made and gaps can be identified. In this way the results of the cooperative effort can provide guidance for individual projects. Several charts which outline the objectives and approach of the proposed cooperative effort are given here. Author

N90-10093*# Comtek Co., Grafton, VA.

A FINITE ELEMENT APPROACH FOR LARGE MOTION DYNAMIC ANALYSIS OF MULTIBODY STRUCTURES IN SPACE

Che-Wei Chang *In* NASA. Langley Research Center, Proceedings of the Workshop on Computational Aspects in the Control of Flexible Systems, Part 1 May 1989 p 283-321 (For primary document see N90-10080 01-18)

Avail: NTIS HC A21/MF A03 CSCL 22B

A three-dimensional finite element formulation for modeling the transient dynamics of constrained multibody space sructures with truss-like configurations is presented. Convected coordinate systems are used to define rigid-body motion of individual elements in the system. These systems are located at one end of each element and are oriented such that one axis passes through the other end of the element. Deformation of each element, relative to its convected coordinate system, is defined by cubic flexural shape functions as used in finite element methods of structural analysis. The formulation is oriented toward joint dominated structures and places the generalized coordinates at the joint. A transformation matrix is derived to integrate joint degree-of-freedom into the equations of motion of the element. Based on the derivation, a general-purpose code LATDYN (Large Angle Transient DYNamics) was developed. Two examples are presented to illustrate the application of the code. For the spin-up of a flexible beam, results are compared with existing solutions available in the literature. For the deployment of one bay of a deployable space truss (the Minimast), results are verified by the geometric knowledge of the system and converged solution of a successively refined model. Author

N90-10094*# Michigan Univ., Ann Arbor.

ENHANCED ELEMENT-SPECIFIC MODAL FORMULATIONS FOR FLEXIBLE MULTIBODY DYNAMICS

Robert R. Ryan *In* NASA. Langley Research Center, Proceedings of the Workshop on Computational Aspects in the Control of Flexible Systems, Part 1 May 1989 p 323-348 (For primary document see N90-10080 01-18)

Avail: NTIS HC A21/MF A03 CSCL 22B

The accuracy of current flexible multibody formalisms based on assumed modes is examined in the context of standard spacecraft motions involving structural components undergoing both slow and fast overall translational and rotational motions as well as small deformations. Limitations of current techniques in treating: (1) element-specific coupling behavior of large motion and small deformation, and (2) motion-induced structural stiffness variations, are noted. The roles of nonlinear and linear elastic structural theories in accurately predicting transient large-displacement dynamic behavior of flexible multibody systems are examined in detail. Coupling effects between deformation and overall motion are carefully scrutinized in the context of assumed-mode discretization techniques. Consistently linearized beam, plate, and shell formulations involving in-plane stretch variables are proposed and shown to yield very accurate simulation results and extremely fast modal convergence for most motions involving small strains. In some particular cases, however, in which membrane stiffness dominates bending stiffness, a nonlinear strain formulation is required in order to capture proper coupling between deformation and overall motion. Author

N90-10095*# DYNACS Engineering Co., Inc., Clearwater, FL.

EFFICIENCY AND CAPABILITIES OF MULTI-BODY SIMULATIONS

R. J. VanderVoort *In* NASA. Langley Research Center, Proceedings of the Workshop on Computational Aspects in the Control of Flexible Systems, Part 1 May 1989 p 349-369 (For primary document see N90-10080 01-18)

Avail: NTIS HC A21/MF A03 CSCL 22B

Simulation efficiency and capability go hand in hand. The more capability you have the lower the efficiency will be. The efficiency and capabilities are discussed. The lesson learned about generic simulation is: Don't rule out any capabilities at the beginning, but

keep each one on a switch so it can be bypassed when warranted by a specific application. Author

N90-10096*# TRW Space Technology Labs., Redondo Beach, CA.
EXPLICIT MODELING AND COMPUTATIONAL LOAD DISTRIBUTION FOR CONCURRENT PROCESSING SIMULATION OF THE SPACE STATION
R. Gluck *In* NASA. Langley Research Center, Proceedings of the Workshop on Computational Aspects in the Control of Flexible Systems, Part 1 May 1989 p 371-413 (For primary document see N90-10080 01-18)
Avail: NTIS HC A21/MF A03 CSCL 22B

Two important aspects of concurrent processing under development at TRW are discussed. These are: (1) the derivation of explicit mathematical models of multibody dynamic systems, and (2) a balanced computational load distribution (BCLD) among loosely coupled computational units (processors) of a concurrent processing system. The developed methodologies are demonstrated by way of an application to the Phase 1 of the Space Station - a task being performed by TRW under NASA/JSC contract NAS9-17778. The mathematical model of the Space Station consists of three interconnected flexible bodies capable of undergoing large, rigid-body motion with respect to each other. Body 1 is the main central body and contains the pressurized modules inboard of the two Alpha gimbals. Bodies 2 and 3 are the starboard and port bodies connected to Body 1 at the Alpha gimbals and include all components on the transverse booms outboard of the Alpha gimbals (including the solar arrays). The control systems in the model maintain Body 1 in a prescribed 3-axis attitude control mode, while producing large-angle rotations of the flexible solar arrays to position them normal to the sun-line. Author

N90-10097*# Michigan Univ., Ann Arbor.
SIMULATION OF FLEXIBLE STRUCTURES WITH IMPACT: EXPERIMENTAL VALIDATION Abstract Only
A. Galip Ulsoy *In* NASA. Langley Research Center, Proceedings of the Workshop on Computational Aspects in the Control of Flexible Systems, Part 1 May 1989 p 415 (For primary document see N90-10080 01-18)
Avail: NTIS HC A21/MF A03 CSCL 22B

The simulation of the dynamic behavior of flexible structures with impact, is experimentally and numerically investigated. A radially rotating flexible beam attached to a rigid shaft is considered. Both experimental and numerical studies are undertaken. Experimental studies how excellent agreement with simulation studies using both the momentum balance (coefficient of friction), and spring-dashpot (impact pair) models. The simulation studies are even capable of predicting the high-speed multiple impacts which occur due to structural flexibility and which are experimentally observed using high-speed video photography. The results of the studies show that a simple momentum balance (coefficient of restitution) method for simulating the impact is sufficiently accurate in predicting the dynamic behavior of the system for most engineering applications. The momentum balance method cannot simulate the impact force which develops during the contact duration, but is computationally very efficient. The spring-dashpot model is more difficult to develop and requires significantly larger computation time, but can simulate impact forces and stresses due to impact. The momentum balance (coefficient of restitution) method, although strictly not applicable to flexible bodies, has been shown to provide an accurate and computationally efficient method for simulating the dynamic behavior of flexible structures with impact when contact stresses are not needed. Author

N90-10098*# Rutgers Univ., New Brunswick, NJ.
SIMULATION AND CONTROL PROBLEMS IN ELASTIC ROBOTS
S. S. K. Tadikonda and H. Baruh *In* NASA. Langley Research Center, Proceedings of the Workshop on Computational Aspects in the Control of Flexible Systems, Part 1 May 1989 p 417-439 (For primary document see N90-10080 01-18)
Avail: NTIS HC A21/MF A03 CSCL 22B

Computational issues associated with modeling and control of robots with revolute joints and elastic arms are considered. A manipulator with one arm and pinned at one end is considered to investigate various aspects of the modeling procedure and the model, and the effect of coupling between the rigid-body and the elastic motions. The rigid-body motion of a manipulator arm is described by means of a reference frame attached to the shadow beam, and the linear elastic operator denoting flexibility is defined with respect to this reference frame. The small elastic motion assumption coupled with the method of assumed modes is used to model the elasticity in the arm. It is shown that only terms up to quadratic in these model amplitudes need to be retained. An important aspect of the coupling between the rigid-body and the elastic motion is the centrifugal stiffening effect. This effect stiffens the elastic structure, as to be expected on physical grounds, gives rise to a time-varying inertia term for the rigid-body motion, and, in general, results in an effective inertia term smaller than the rigid-body inertia term. Simulation results are presented for an elastic beam pinned at one end and free at the other, and rotating in a horizontal plane, and control issues such as the order of the model, number of sensors, and modal extraction are examined within this context. Author

N90-10099*# Boeing Aerospace Co., Seattle, WA.
LINEARIZED FLEXIBILITY MODELS IN MULTIBODY DYNAMICS AND CONTROL
William W. Cimino *In* NASA. Langley Research Center, Proceedings of the Workshop on Computational Aspects in the Control of Flexible Systems, Part 1 May 1989 p 441-472 (For primary document see N90-10080 01-18)
Avail: NTIS HC A21/MF A03 CSCL 22B

Simulation of structural response of multi-flexible-body systems by linearized flexible motion combined with nonlinear rigid motion is discussed. Advantages and applicability of such an approach for accurate simulation with greatly reduced computational costs and turnaround times are described, restricting attention to the control design environment. Requirements for updating the linearized flexibility model to track large angular motions are discussed. Validation of such an approach by comparison with other existing codes is included. Application to a flexible robot manipulator system is described. Author

N90-10100*# Draper (Charles Stark) Lab., Inc., Cambridge, MA.
SIMULATION OF SHUTTLE FLIGHT CONTROL SYSTEM STRUCTURAL INTERACTION WITH RMS DEPLOYED PAYLOADS
Joe Turnball *In* NASA. Langley Research Center, Proceedings of the Workshop on Computational Aspects in the Control of Flexible Systems, Part 1 May 1989 p 473-494 (For primary document see N90-10080 01-18)
Avail: NTIS HC A21/MF A03 CSCL 22B

A simulation of the system made up of the Orbiter, Remote Manipulator System (RMS), and payload grappled by the RMS was completed. The simulation was used to study the stability of this overall system when its attitude is under control of the Orbiter's on-orbit Flight Control System (FCS). The simulation was also used to study the dynamics of the system when the RMS and its associated command software are in active control of the relative Orbiter to payload position and orientation. The simulation models all of the following elements: RMS boom bending (represented by two cubic bending models); RMS boom torsion; RMS joint gearbox compliance (represented by a non-linear wind-up model); flexibility at the RMS to Orbiter interface; flexibility at the RMS to payload interface; joint motor dynamics; joint servo-loop dynamics; RMS on-board computer command logic; data transfer delays between the RMS sensor and the RMS on-board computer and between the RMS on-board computer and RMS joint servos; on-orbit flight control nonlinear control logic; and the Reaction Control System (both Primary and Vernier) jet forces and moments. Author

N90-10101*# Michigan Univ., Ann Arbor. Applied Dynamics International.
A PERFORMANCE COMPARISON OF INTEGRATION ALGORITHMS IN SIMULATING FLEXIBLE STRUCTURES
R. M. Howe *In* NASA. Langley Research Center, Proceedings of the Workshop on Computational Aspects in the Control of Flexible Systems, Part 1 May 1989 p 495-514 (For primary document see N90-10080 01-18)
Avail: NTIS HC A21/MF A03 CSCL 22B

Asymptotic formulas for the characteristic root errors as well as transfer function gain and phase errors are presented for a number of traditional and new integration methods. Normalized stability regions in the lambda h plane are compared for the various methods. In particular, it is shown that a modified form of Euler integration with root matching is an especially efficient method for simulating lightly-damped structural modes. The method has been used successfully for structural bending modes in the real-time simulation of missiles. Performance of this algorithm is compared with other special algorithms, including the state-transition method. A predictor-corrector version of the modified Euler algorithm permits it to be extended to the simulation of nonlinear models of the type likely to be obtained when using the discretized structure approach. Performance of the different integration methods is also compared for integration step sizes larger than those for which the asymptotic formulas are valid. It is concluded that many traditional integration methods, such as RD-4, are not competitive in the simulation of lightly damped structures. Author

N90-10102*# National Aeronautics and Space Administration. Langley Research Center, Hampton, VA.
OPTICAL PROCESSING FOR DISTRIBUTED SENSORS IN CONTROL OF FLEXIBLE SPACECRAFT
Raymond C. Montgomery, Sharon S. Welch, Michael F. Barsky, and Ian T. Gallimore *In its* Proceedings of the Workshop on Computational Aspects in the Control of Flexible Systems, Part 1 May 1989 p 515-545 (For primary document see N90-10080 01-18)
Avail: NTIS HC A21/MF A03 CSCL 22B

A recent potential of distributed image processing is discussed. Applications in the control of flexible spacecraft are emphasized. Devices are currently being developed at NASA and in universities and industries that allow the real-time processing of holographic images. Within 5 years, it is expected that, in real-time, one may add or subtract holographic images at optical accuracy. Images are stored and processed in crystal mediums. The accuracy of their storage and processing is dictated by the grating level of laser holograms. It is far greater than that achievable using current analog-to-digital, pixel oriented, image digitizing and computing techniques. Processors using image processing algebra can conceptually be designed to mechanize Fourier transforms, least square lattice filters, and other complex control system operations. Thus, actuator command inputs derived from complex control laws involving distributed holographic images can be generated by such an image processor. Plans are revealed for the development of a Conjugate Optics Processor for control of a flexible object.
Author

N90-10103*# National Aeronautics and Space Administration. Langley Research Center, Hampton, VA.
PROCEEDINGS OF THE WORKSHOP ON COMPUTATIONAL ASPECTS IN THE CONTROL OF FLEXIBLE SYSTEMS, PART 2
Lawrence W. Taylor, Jr., comp. May 1989 482 p Workshop held in Williamsburg, VA, 12-14 Jul. 1988
(NASA-TM-101578-Pt-2; NAS 1.15:101578-Pt-2) Avail: NTIS HC A21/MF A03 CSCL 22B

The Control/Structures Integration Program, a survey of available software for control of flexible structures, computational efficiency and capability, modeling and parameter estimation, and control synthesis and optimization software are discussed. For individual titles, see N90-10104 through N90-10123.

N90-10104*# Carnegie-Mellon Univ., Pittsburgh, PA.
FLEXIBLE ROBOT CONTROL: MODELING AND EXPERIMENTS
Irving J. Oppenheim and Isao Shimoyama (Tokyo Univ., Japan) *In* NASA. Langley Research Center, Proceedings of the Workshop on Computational Aspects in the Control of Flexible Systems, Part 2 May 1989 p 549-579 (For primary document see N90-10103 01-18)
Avail: NTIS HC A21/MF A03 CSCL 22B

Described here is a model and its use in experimental studies of flexible manipulators. The analytical model uses the equivalent of Rayleigh's method to approximate the displaced shape of a flexible link as the static elastic displacement which would occur under end rotations as applied at the joints. The generalized coordinates are thereby expressly compatible with joint motions and rotations in serial link manipulators, because the amplitude variables are simply the end rotations between the flexible link and the chord connecting the end points. The equations for the system dynamics are quite simple and can readily be formulated for the multi-link, three-dimensional case. When the flexible links possess mass and (polar moment of) inertia which are small compared to the concentrated mass and inertia at the joints, the analytical model is exact and displays the additional advantage of reduction in system dimension for the governing equations. Four series of pilot tests have been completed. Studies on a planar single-link system were conducted at Carnegie-Mellon University, and tests conducted at Toshiba Corporation on a planar two-link system were then incorporated into the study. A single link system under three-dimensional motion, displaying biaxial flexure, was then tested at Carnegie-Mellon. Author

N90-10105*# Boeing Commercial Airplane Co., Seattle, WA.
MINIMUM-VARIANCE REDUCED-ORDER ESTIMATION ALGORITHMS FROM PONTRYGIN'S MINIMUM PRINCIPLE
Abstract Only
Yaghoob S. Ebrahimi *In* NASA. Langley Research Center, Proceedings of the Workshop on Computational Aspects in the Control of Flexible Systems, Part 2 May 1989 p 581 (For primary document see N90-10103 01-18)
Avail: NTIS HC A21/MF A03 CSCL 22B

A uniform derivation of minimum-variance reduced-order (MVRO) filter-smoother algorithms from Pontrygin's Minimum Principle is presented. An appropriate performance index for a general class of reduced order estimation problem is formulated herein to yield optimal results over the entire time interval of estimation. These results provide quantitative criteria for measuring the performance of certain classes of heuristically designed, suboptimal reduced-order estimators as well as explicit guidance to the suboptimal filter design process with both continuous and discrete filter-smoother algorithms being considered. By the duality principle, the algorithms of reduced-order estimation can be easily extended to the deterministic problems of optimal control (i.e., the regulator and linear tracking problem). Author

N90-10106*# Boeing Co., Seattle, WA.
MODIFYING HIGH-ORDER AEROELASTIC MATH MODEL OF A JET TRANSPORT USING MAXIMUM LIKELIHOOD ESTIMATION
Amir A. Anissipour and Russell A. Benson *In* NASA. Langley Research Center, Proceedings of the Workshop on Computational Aspects in the Control of Flexible Systems, Part 2 May 1989 p 583-629 (For primary document see N90-10103 01-18)
Avail: NTIS HC A21/MF A03 CSCL 22B

The design of control laws to damp flexible structural modes requires accurate math models. Unlike the design of control laws for rigid body motion (e.g., where robust control is used to compensate for modeling inaccuracies), structural mode damping usually employs narrow band notch filters. In order to obtain the required accuracy in the math model, maximum likelihood estimation technique is employed to improve the accuracy of the math model using flight data. Presented here are all phases of this methodology: (1) pre-flight analysis (i.e., optimal input signal design for flight test, sensor location determination, model reduction

technique, etc.), (2) data collection and preprocessing, and (3) post-flight analysis (i.e., estimation technique and model verification). In addition, a discussion is presented of the software tools used and the need for future study in this field. Author

N90-10107*# Georgia Inst. of Tech., Atlanta.
AUTOMATED MODEL FORMULATION FOR TIME-VARYING FLEXIBLE STRUCTURES Abstract Only
B. J. Glass and S. Hanagud *In* NASA. Langley Research Center, Proceedings of the Workshop on Computational Aspects in the Control of Flexible Systems, Part 2 May 1989 p 631 (For primary document see N90-10103 01-18)
Avail: NTIS HC A21/MF A03 CSCL 22B

Presented here is an identification technique that uses the sensor information to choose a new model out of a finite set of discrete model space, in order to follow the observed changes to the given time varying flexible structure. Boundary condition sets or other information on model variations are used to organize the set of possible models laterally into a search tree with levels of abstraction used to order the models vertically within branches. An object-oriented programming approach is used to represent the model set in the search tree. A modified A (asterisk) best first search algorithm finds the model where the model response best matches the current observations. Several extensions to this methodology are discussed. Methods of possible integration of rules with the current search algorithm are considered to give weight to interpreted trends that may be found in a series of observations. This capability might lead, for instance, to identifying a model that incorporates a progressive damage rather than with incorrect paramenters such as added mass. Another new direction is to consider the use of noisy time domain sensor feedback rather than frequency domain information in the search algorithm to improve the real-time capability of the developed procedure. Author

N90-10108*# Calspan Advanced Technology Center, Buffalo, NY.
NUMERICALLY EFFICIENT ALGORITHM FOR MODEL DEVELOPMENT OF HIGH-ORDER SYSTEMS
L. O. Parada *In* NASA. Langley Research Center, Proceedings of the Workshop on Computational Aspects in the Control of Flexible Systems, Part 2 May 1989 p 633-650 (For primary document see N90-10103 01-18)
Avail: NTIS HC A21/MF A03 CSCL 22B

A technique for estimating transfer functions in partial fraction expansion form from frequency response data for a high-order system is presented. The problem formulation avoids many of the numerical difficulties associated with high-order polynomials and has the advantage of having the option to fix the camping and frequency of a mode, if known, during the estimation process. The resulting transfer function(s) may be converted to Jordan-Form time domain equations directly. During the implementation of this technique, a frequency and amplitude normalizing window was developed that maximized the efficiency of the optimization algorithm. The combination of estimating the transfer function in factored form, the ability to fix preciously determined parameters and the effectiveness of the normalizing window led to a progressive approach to synthesizing transfer functions from frequency response data for high-order systems. Author

N90-10109*# California Univ., Los Angeles.
ON MODELLING NONLINEAR DAMPING IN DISTRIBUTED PARAMETER SYSTEMS
A. V. Balakrishnan *In* NASA. Langley Research Center, Proceedings of the Workshop n Computational Aspects in the Control of Flexible Systems, Part 2 May 1989 p 651-664 (For primary document see N90-10103 01-18)
Avail: NTIS HC A21/MF A03 CSCL 22B

Information is given in viewgraph form on the modeling of nonlinear damping in distributed parameter systems. Author

N90-10110*# Howard Univ., Washington, DC.
USE OF THE QUASILINEARIZATION ALGORITHM FOR THE SIMULATION OF LSS SLEWING
Feiyue Li and P. M. Bainum *In* NASA. Langley Research Center, Proceedings of the Workshop on Computational Aspects in the Control of Flexible Systems, Part 2 May 1989 p 665-690 (For primary document see N90-10103 01-18)
Avail: NTIS HC A21/MF A03 CSCL 22B

The use of the Maximum Principle for the large angle slewing of large space structures (LSS) usually results in the so-called two-point boundary-value problem, in which many requirements (e.g., minimum time, small amplitude, and limited control power, etc.) must be satisfied simultaneously. The successful solution of this problem depends largely on the use of an efficient numerical algorithm. There are many candidate algorithms available for this problem (e.g., quasilinearization, gradient, etc.). Here researchers discuss only the quasilinearization method which has been used for several cases of large angle slewing of LSS. The basic idea of this algorithm is to make a series of successive approximations of the solution from a particular solvable case (linear or nonlinear) to a more general practical case. For the rigid spacecraft slewing problem with no constraints on the controls, the solution procedure can be found in the literature. This procedure needs to be modified if a minimum time for the slewing problem is desired with control limits given. Recently, an indirect method for finding the minimum time was developed to meet all these requirements. For the general mixed (including both rigid and flexible parts) problem, an additional constraint of small vibrational amplitude on the flexible parts is imposed. Author

N90-10111*# National Aeronautics and Space Administration. Langley Research Center, Hampton, VA.
CONTROL LAW SYNTHESIS AND OPTIMIZATION SOFTWARE FOR LARGE ORDER AEROSERVOELASTIC SYSTEMS
V. Mukhopadhyay, A. Pototzky, and Thomas Noll *In its* Proceedings of the Workshop on Computational Aspects in the Control of Flexible Systems, Part 2 May 1989 p 693-707 (For primary document see N90-10103 01-18)
Avail: NTIS HC A21/MF A03 CSCL 22B

A flexible aircraft or space structure with active control is typically modeled by a large-order state space system of equations in order to accurately represent the rigid and flexible body modes, unsteady aerodynamic forces, actuator dynamics and gust spectra. The control law of this multi-input/multi-output (MIMO) system is expected to satisfy multiple design requirements on the dynamic loads, responses, actuator deflection and rate limitations, as well as maintain certain stability margins, yet should be simple enough to be implemented on an onboard digital microprocessor. A software package for performing an analog or digital control law synthesis for such a system, using optimal control theory and constrained optimization techniques is described. Author

N90-10112*# Purdue Univ., West Lafayette, IN.
FLEXIBLE AIRCRAFT DYNAMIC MODELING FOR DYNAMIC ANALYSIS AND CONTROL SYNTHESIS
David K. Schmidt *In* NASA. Langley Research Center, Proceedings of the Workshop on Computational Aspects in the Control of Flexible Systems, Part 2 May 1989 p 709-743 (For primary document see N90-10103 01-18)
Avail: NTIS HC A21/MF A03 CSCL 22B

The linearization and simplification of a nonlinear, literal model for flexible aircraft is highlighted. Areas of model fidelity that are critical if the model is to be used for control system synthesis are developed and several simplification techniques that can deliver the necessary model fidelity are discussed. These techniques include both numerical and analytical approaches. An analytical approach, based on first-order sensitivity theory is shown to lead not only to excellent numerical results, but also to closed-form analytical expressions for key system dynamic properties such as the pole/zero factors of the vehicle transfer-function matrix. The analytical results are expressed in terms of vehicle mass properties, vibrational characteristics, and rigid-body and aeroelastic stability

derivatives, thus leading to the underlying causes for critical dynamic characteristics. Author

N90-10113*# Michigan Univ., Ann Arbor. Mechanical Engineering and Applied Mechanics.
EXPERIMENTAL VALIDATION OF FLEXIBLE ROBOT ARM MODELING AND CONTROL
A. Galip Ulsoy *In* NASA. Langley Research Center, Proceedings of the Workshop on Computational Aspects in the Control of Flexible Systems, Part 2 May 1989 p 745-777 (For primary document see N90-10103 01-18)
Avail: NTIS HC A21/MF A03 CSCL 22B

Flexibility is important for high speed, high precision operation of lightweight manipulators. Accurate dynamic modeling of flexible robot arms is needed. Previous work has mostly been based on linear elasticity with prescribed rigid body motions (i.e., no effect of flexible motion on rigid body motion). Little or no experimental validation of dynamic models for flexible arms is available. Experimental results are also limited for flexible arm control. Researchers include the effects of prismatic as well as revolute joints. They investigate the effect of full coupling between the rigid and flexible motions, and of axial shortening, and consider the control of flexible arms using only additional sensors. Author

N90-10114*# Boeing Co., Seattle, WA.
CONTROLLING FLEXIBLE STRUCTURES: A SURVEY OF METHODS
Russell A. Benson and Edward E. Coleman *In* NASA. Langley Research Center, Proceedings of the Workshop on Computational Aspects in the Control of Flexible Systems, Part 2 May 1989 p 779-799 (For primary document see N90-10103 01-18)
Avail: NTIS HC A21/MF A03 CSCL 22B

Most of the presently available control system design techniques applicable to flexible structure problems were developed to design controllers for rigid body systems. Although many of these design methods can be applied to flexible dynamics problems, recently developed techniques may be more suitable for flexible structure controller design. The purpose of this presentation is to examine briefly the peculiarities of the dynamics of flexible structures and to stimulate discussion about top level controller design approaches when designing controllers for flexible structures. Presented here is a suggestion of a set of categories of design methods for designing controllers for flexible structures as well as a discussion of the advantages and disadvantages of each category. No attempt has been made herein to select one category of design techniques as the best for flexible structure controller design. Instead, it is hoped that the structure suggested by these categories will facilitate further discussion on the merits of particular methods that will eventually point to those design techniques suitable for further development. Author

N90-10115*# Boeing Co., Seattle, WA.
AIRCRAFT MODAL SUPRESSION SYSTEM: EXISTING DESIGN APPROACH AND ITS SHORTCOMINGS **c05**
J. K. Ho, T. J. Goslin, and C. B. Tran *In* NASA. Langley Research Center, Proceedings of the Workshop on Computational Aspects in the Control of Flexible Systems, Part 2 May 1989 p 801-823 (For primary document see N90-10103 01-18)
Avail: NTIS HC A21/MF A03 CSCL 01C

The bending of flexible body aircraft may degrade the ride coMfort of passengers. This is especially noticeable towards the aft end of the aircraft (due to the relatively large tail surfaces) which may easily be excited when flying through turbulence. In addition, some aircraft may experience a front body bending mode which can be annoying to the cabin crew and first class passengers. Normally, this dominant body bending mode falls between 1 to 5 Hz. This range is easily perceived by the human body. Also, in some situations, the rigid body control law may be out of phase with the mode and aggravate the vibration. Hence, an active modal suppression system is desirable for improving the ride quality of the airplane. The size of the mathematical model, which has both the airplane rigid body and flexible characteristics, could easily exceed 100 states. The computational burden and fidelity of this large structural model is addressed. Author

N90-10116*# Boeing Commercial Airplane Co., Seattle, WA.
STRUCTURAL STABILITY AUGMENTATION SYSTEM DESIGN USING BODEDIRECT: A QUICK AND ACCURATE APPROACH **c05**
T. J. Goslin and J. K. Ho *In* NASA. Langley Research Center, Proceedings of the Workshop on Computational Aspects in the Control of Flexible Systems, Part 2 May 1989 p 825-851 (For primary document see N90-10103 01-18)
Avail: NTIS HC A21/MF A03 CSCL 01C

A methodology is presented for a modal suppression control law design using flight test data instead of mathematical models to obtain the required gain and phase information about the flexible airplane. This approach is referred to as BODEDIRECT. The purpose of the BODEDIRECT program is to provide a method of analyzing the modal phase relationships measured directly from the airplane. These measurements can be achieved with a frequency sweep at the control surface input while measuring the outputs of interest. The measured Bode-models can be used directly for analysis in the frequency domain, and for control law design. Besides providing a more accurate representation for the system inputs and outputs of interest, this method is quick and relatively inexpensive. To date, the BODEDIRECT program has been tested and verified for computational integrity. Its capabilities include calculation of series, parallel and loop closure connections between Bode-model representations. System PSD, together with gain and phase margins of stability may be calculated for successive loop closures of multi-input/multi-output systems. Current plans include extensive flight testing to obtain a Bode-model representation of a commercial aircraft for design of a structural stability augmentation system. Author

N90-10117*# Australian National Univ., Canberra.
OPTIMAL q-MARKOV COVER FOR FINITE PRECISION IMPLEMENTATION **c61**
Darrell Williamson and Robert E. Skelton (Purdue Univ., West Lafayette, IN.) *In* NASA. Langley Research Center, Proceedings of the Workshop on Computational Aspects in the Control of Flexible Systems, Part 2 May 1989 p 853-881 (For primary document see N90-10103 01-18)
Avail: NTIS HC A21/MF A03 CSCL 09B

The existing q-Markov COVER realization theory does not take into account the problems of arithmetic errors due to both the quantization of states and coefficients of the reduced order model. All q-Markov COVERs allow some freedom in the choice of parameters. Here, researchers exploit this freedom in the existing theory to optimize the models with respect to these finite wordlength effects. Author

N90-10118*# General Electric Co., Schenectady, NY. Corporate Research and Development Center.
INPUT-OUTPUT ORIENTED COMPUTATION ALGORITHMS FOR THE CONTROL OF LARGE FLEXIBLE STRUCTURES
K. D. Minto *In* NASA. Langley Research Center, Proceedings of the Workshop on Computational Aspects in the Control of Flexible Systems, Part 2 May 1989 p 883-901 (For primary document see N90-10103 01-18)
Avail: NTIS HC A21/MF A03 CSCL 22B

An overview is given of work in progress aimed at developing computational algorithms addressing two important aspects in the control of large flexible space structures; namely, the selection and placement of sensors and actuators, and the resulting multivariable control law design problem. The issue of sensor/actuator set selection is particularly crucial to obtaining a satisfactory control design, as clearly a poor choice will inherently limit the degree to which good control can be achieved. With regard to control law design, the researchers are driven by concerns stemming from the practical issues associated with eventual implementation of multivariable control laws, such as reliability, limit protection, multimode operation, sampling rate selection, processor throughput, etc. Naturally, the burden imposed by dealing

with these aspects of the problem can be reduced by ensuring that the complexity of the compensator is minimized. Our approach to these problems is based on extensions to input/output oriented techniques that have proven useful in the design of multivariable control systems for aircraft engines. In particular, researchers are exploring the use of relative gain analysis and the condition number as a means of quantifying the process of sensor/actuator selection and placement for shape control of a large space platform.

Author

N90-10119*# National Aeronautics and Space Administration. Langley Research Center, Hampton, VA.

THE ACTIVE FLEXIBLE WING AEROSERVOELASTIC WIND-TUNNEL TEST PROGRAM **c05**

Thomas Noll and Boyd Perry *In its* Proceedings of the Workshop on Computational Aspects in the Control of Flexible Systems, Part 2 May 1989 p 903-941 (For primary document see N90-10103 01-18)

Avail: NTIS HC A21/MF A03 CSCL 01C

For a specific application of aeroservoelastic technology, Rockwell International Corporation developed a concept known as the Active Flexible Wing (AFW). The concept incorporates multiple active leading-and trailing-edge control surfaces with a very flexible wing such that wing shape is varied in an optimum manner resulting in improved performance and reduced weight. As a result of a cooperative program between the AFWAL's Flight Dynamics Laboratory, Rockwell, and NASA LaRC, a scaled aeroelastic wind-tunnel model of an advanced fighter was designed, fabricated, and tested in the NASA LaRC Transonic Dynamics Tunnel (TDT) to validate the AFW concept. Besides conducting the wind-tunnel tests NASA provided a design of an Active Roll Control (ARC) System that was implemented and evaluated during the tests. The ARC system used a concept referred to as Control Law Parameterization which involves maintaining constant performance, robustness, and stability while using different combinations of multiple control surface displacements. Since the ARC system used measured control surface stability derivatives during the design, the predicted performance and stability results correlated very well with test measurements. Author

N90-10120*# Ottawa Univ. (Ontario).

MODELING AND STABILIZATION OF LARGE FLEXIBLE SPACE STATIONS **c05**

S. S. Lim and N. U. Ahmed *In* NASA. Langley Research Center, Proceedings of the Workshop on Computational Aspects in the Control of Flexible Systems, Part 2 May 1989 p 943-956 (For primary document see N90-10103 01-18)

Avail: NTIS HC A21/MF A03 CSCL 01C

A preliminary formulation of a large space structure is presented. The system consists of a (rigid) massive body, which may play the role of experimental modules located at the center of the space station and a flexible configuration, consisting of several beams, which is rigidly attached to the main body. The equations that govern the motion of the complete system consist of several partial differential equations with boundary conditions describing the vibration of flexible components coupled with six ordinary differential equations that describe the rotational and translational motion of the central body. The problem of (feedback) stabilization of the system is discussed. This study is expected to provide an insight into the complexity of design and stabilization of actual space stations. Author

N90-10121*# Virginia Polytechnic Inst. and State Univ., Blacksburg.

ACTIVE VIBRATION MITIGATION OF DISTRIBUTED PARAMETER, SMART-TYPE STRUCTURES USING PSEUDO-FEEDBACK OPTIMAL CONTROL (PFOC)

W. N. Patten, H. H. Robertshaw, D. Pierpont, and R. H. Wynn *In* NASA. Langley Research Center, Proceedings of the Workshop on Computational Aspects in the Control of Flexible Systems, Part 2 May 1989 p 957-981 (For primary document see N90-10103 01-18)

Avail: NTIS HC A21/MF A03 CSCL 22B

A new, near-optimal feedback control technique is introduced that is shown to provide excellent vibration attenuation for those distributed parameter systems that are often encountered in the areas of aeroservoelasticity and large space systems. The technique relies on a novel solution methodology for the classical optimal control problem. Specifically, the quadratic regulator control problem for a flexible vibrating structure is first cast in a weak functional form that admits an approximate solution. The necessary conditions (first-order) are then solved via a time finite-element method. The procedure produces a low dimensional, algebraic parameterization of the optimal control problem that provides a rigorous basis for a discrete controller with a first-order like hold output. Simulation has shown that the algorithm can successfully control a wide variety of plant forms including multi-input/multi-output systems and systems exhibiting significant non-linearities. In order to firmly establish the efficacy of the algorithm, a laboratory control experiment was implemented to provide planar (bending) vibration attenuation of a highly flexible beam (with a first clamped-free mode of approximately 0.5 Hz).

Author

N90-10122*# Virginia Polytechnic Inst. and State Univ., Blacksburg.

SHAPE CONTROL OF HIGH DEGREE-OF-FREEDOM VARIABLE GEOMETRY TRUSSES

R. J. Salerno, C. F. Reinholtz, and H. H. Robertshaw *In* NASA. Langley Research Center, Proceedings of the Workshop on Computational Aspects in the Control of Flexible Systems, Part 2 May 1989 p 983-1002 (For primary document see N90-10103 01-18)

Avail: NTIS HC A21/MF A03 CSCL 22B

Common static trusses are constrained to permit no relative motion between truss elements. A Variable Geometry Truss (VGT), however, is a truss which contains some number of variable length links. The extensible links allow the truss to change shape in a precise, controllable manner. These changes can also be used to control the vibrational response of a truss structure or to perform robotic tasks. Many geometric configurations, both planar and spatial, are possible candidates for VGT manipulators. Here, only two geometries are discussed; the three degree-of-freedom (DOF) spatial octahedral/octahedral truss and the three DOF planar tetrahedral truss. These truss geometries are used as the fundamental element in a repeating chain of trusses. This results in a highly dexterous manipulator with perhaps 30 to 60 degrees of freedom that retains the favorable stiffness properties of a conventional truss. From a fixed base, this type of manipulator could perform shape or vibration control while extending and snaking through complex passageways or moving around obstacles to perform robotic tasks. The approach taken here is to first concentrate on fully understanding the forward and inverse kinematics of the fundamental elements and then utilizing the insight thus gained to solve the more complex problem of the kinematic chains. Author

N90-10123*# Old Dominion Univ., Norfolk, VA.

OPTIMAL INTEGRAL CONTROLLER WITH SENSOR FAILURE ACCOMMODATION

T. Alberts and T. Houlihan (Jonathan Corp., Norfolk, VA.) *In* NASA. Langley Research Center, Proceedings of the Workshop on Computational Aspects in the Control of Flexible Systems, Part 2 May 1989 p 1003-1023 (For primary document see N90-10103 01-18)

Avail: NTIS HC A21/MF A03 CSCL 22B

An Optimal Integral Controller that readily accommodates Sensor Failure - without resorting to (Kalman) filter or observer generation - has been designed. The system is based on Navy-sponsored research for the control of high performance aircraft. In conjunction with a NASA developed Numerical Optimization Code, the Integral Feedback Controller will provide optimal system response even in the case of incomplete state feedback. Hence, the need for costly replication of plant sensors is avoided since failure accommodation is effected by system software reconfiguration. The control design has been applied to

a particularly ill-behaved, third-order system. Dominant-root design in the classical sense produced an almost 100 percent overshoot for the third-order system response. An application of the newly-developed Optimal Integral Controller - assuming all state information available - produces a response with no overshoot. A further application of the controller design - assuming a one-third sensor failure scenario - produced a slight overshoot response that still preserved the steady state time-point of the full-state feedback response. The control design should have wide application in space systems. Author

N90-10124*# Alabama Univ., Huntsville. Dept. of Computer Science.
KNOWLEDGE-BASED MACHINE VISION SYSTEMS FOR SPACE STATION AUTOMATION Annual Report, 1 Aug. 1988 - 31 Jul. 1989
Heggere S. Ranganath and Laure J. Chipman 23 Aug. 1989 46 p
(Contract NCC8-016)
(NASA-CR-185710; NAS 1.26:185710) Avail: NTIS HC A03/MF A01 CSCL 22B

Computer vision techniques which have the potential for use on the space station and related applications are assessed. A knowledge-based vision system (expert vision system) and the development of a demonstration system for it are described. This system implements some of the capabilities that would be necessary in a machine vision system for the robot arm of the laboratory module in the space station. A Perceptics 9200e image processor, on a host VAXstation, was used to develop the demonstration system. In order to use realistic test images, photographs of actual space shuttle simulator panels were used. The system's capabilities of scene identification and scene matching are discussed. K.C.D.

N90-10125# Naval Postgraduate School, Monterey, CA.
MODELING, SIMULATION, AND ANALYSES OF ATTITUDE CONTROL FOR THE CREW/EQUIPMENT RETRIEVER (CER) PROPOSED FOR SPACE STATION M.S. Thesis
Daniel L. Hansen Mar. 1989 113 p
(AD-A208140) Avail: NTIS HC A06/MF A01 CSCL 22/3

The Crew/Equipment Retrieval System (CERS) is proposed for space station to provide the capability to rescue an EVA crewman or to retrieve equipment inadvertently detached from the station. Attitude control for the Crew/Equipment Retriever (CER) is modeled, simulated and analyzed with and without a target during autonomous attitude hold. Time-optimal and weighted-time-fuel optimal control laws are derived using Pontryagin's Minimum Principle. The CER baseline configuration is analyzed to accomplish some of the attitude control trade-off analyses planned for the CER preliminary design phase. Optimal thruster size and placement are evaluated for three-axis stabilization. Control stability when the moment of inertia tensor changes during target capture is evaluated for several worst-case scenarios. Attitude control performance results are computed through computer simulation. Simulation of the CER baseline configuration shows it does not provide effective control during capture of a worst-case 850 pound target. A new CER configuration scheme is proposed, evaluated to the baseline configuration. Fuel optimal and end-of-mission performance for the new CER configuration is evaluated. Simulation of the CER proposed configuration is evaluated. Simulation of the CER proposed configuration shows it provides effective control during target capture for modified locations in the capture for modified locations in the capture net. GRA

N90-10126 Texas Univ., Austin.
SYSTEM IDENTIFICATION FOR LARGE SPACE STRUCTURES Ph.D. Thesis
Hyoung Man Kim 1988 156 p
Avail: Univ. Microfilms Order No. DA8909689

A system identification procedure for large space structures is presented. A large space structure has a very large number of degrees of freedom - due to complexity as well as large size, and it is highly flexible and very lightly damped. Such structures should be tested and identified on orbit, and this may require a combination of on-line and off-line algorithms. System identification not only involves the selection of model, data, hardware, etc., but also requires those selected items to be properly combined. Therefore, the system identification method must be evaluated as a whole. An analytical model, as a mathematical model for simulation and as a base model for identification, is introduced. Model order-reduction techniques are considered to reduce the order of analytical models to a sufficiently small size. Among those, an unsymmetric block Lanczos method is outlined in detail. Some of the important signal processing techniques involved in system identification are introduced. The number of sampled data is first reduced in the frequency domain by using regression analysis or principal component analysis. Based on a reduced set of sampled data, an experimental model is found by using a least-squares algorithm. The order of the experimental model is reduced by a Lanczos method, and the Lanczos vectors are identified. Several examples are presented to illustrate various aspects of the proposed system identification procedure. They include an 8-degree of freedom beam-rotor assembly and a 474-degree of freedom Space Station model which are employed to evaluate an unsymmetric block Lanczos algorithm, an 8-degree of freedom cantilever beam which is employed to evaluate the whole system identification procedure, and a 60-degree of freedom Space Station model which is employed to apply the proposed system identification procedure to a large structure. It is found that the proposed system identification method works well with large space structures, which have very low frequency and very closely-spaced modes. Dissert. Abstr.

N90-10127*# National Aeronautics and Space Administration. Langley Research Center, Hampton, VA.
PRELIMINARY DESIGN OF A LARGE TETRAHEDRAL TRUSS/HEXAGONAL HEATSHIELD PANEL AEROBRAKE
John T. Dorsey and Martin M. Mikulas, Jr. Sep. 1989 46 p
(NASA-TM-101612; NAS 1.15:101612) Avail: NTIS HC A03/MF A01 CSCL 22B

An aerobrake structural concept is introduced which consists of two primary components: (1) a lightweight erectable tetrahedral support truss; and (2) sandwich hexagonal heatshield panels which, when attached to the truss, form a continuous impermeable aerobraking surface. Generic finite element models and a general analysis procedure to design tetrahedral truss/hexagonal heatshield panel aerobrakes is developed, and values of the aerobrake design parameters which minimize mass and packaging volume for a 120-foot-diameter aerobrake are determined. Sensitivity of the aerobrake design to variations in design parameters is also assessed. The results show that a 120-foot-diameter aerobrake is viable using the concept presented (i.e., the aerobrake mass is less than or equal to 15 percent of the payload spacecraft mass). Minimizing the aerobrake mass (by increasing the number of rings in the support truss) however, leads to aerobrakes with the highest part count. Author

N90-10128*# DWA Composite Specialities, Inc., Chatsworth, CA.
SPACE STRUCTURES CONCEPTS AND MATERIALS Final Report
A. M. Nowitzky and E. C. Supan 25 Jun. 1988 126 p
(Contract NAS8-37257)
(NASA-CR-183727; NAS 1.26:183727) Avail: NTIS HC A07/MF A01 CSCL 22B

An extension is preseted of the evaluation of graphite/aluminum metal matrix composites (MMC) for space structures application. A tubular DWG graphite/aluminum truss assembly was fabricated having the structural integrity and thermal stability needed for space application. DWG is a proprietary thin ply continuous graphite reinforced aluminum composite. The truss end fittings were constructed using the discontinuous ceramic particulate reinforced MMC DWAI 20 (trademark). Thermal stability was incorporated in the truss by utilizing high stiffness, negative coefficient of thermal expansion (CTE) P100 graphite fibers in a 6061 aluminum matrix,

crossplied to provide minimized CTE in the assembled truss. Tube CTE was designed to be slightly negative to offset the effects of the end fitting and sleeve, CTE values of which are approx. 1/2 that of aluminum. In the design of the truss configuration, the CTE contribution of each component was evaluated to establish the component dimension and layup configuration required to provide a net zero CTE in the subassemblies which would then translate to a zero CTE for the entire truss bay produced. E.R.

N90-10129*# Teledyne Brown Engineering, Huntsville, AL.
SPACE STATION RT AND E UTILIZATION STUDY
P. K. Wunsch and P. H. Anderson Sep. 1989 102 p
(Contract NAS1-18228)
(NASA-CR-181707; NAS 1.26:181707) Avail: NTIS HC A06/MF A01 CSCL 22B

Descriptive information on a set of 241 mission concepts was reviewed to establish preliminary Space Station outfitting needs for technology development missions. The missions studied covered the full range of in-space technology development activities envisioned for early Space Station operations and included both pressurized volume and attached payload requirements. Equipment needs were compared with outfitting plans for the life sciences and microgravity user communities, and a number of potential outfitting additions were identified. Outfitting implementation was addressed by selecting a strawman mission complement for each of seven technical themes, by organizing the missions into flight scenarios, and by assessing the associated outfitting buildup for planning impacts. Author

N90-10130* National Aeronautics and Space Administration, Washington, DC.
TECHNOLOGY FOR LARGE SPACE SYSTEMS: A BIBLIOGRAPHY WITH INDEXES (SUPPLEMENT 21)
Nov. 1988 195 p
(NASA-SP-7046(21); NAS 1.21:7046(21)) Avail: NTIS HC A07 CSCL 22B

This bibliography lists 745 reports, articles, and other documents introduced into the NASA scientific and technical information system between January 1, 1989 and June 30, 1989. Its purpose is to provide helpful information to the researcher, manager, and designer in technology development and mission design according to system, interactive analysis and design, structural and thermal analysis and design, structural concepts and control systems, electronics, advanced materials, assembly concepts, propulsion, and solar power satellite systems. Author

N90-10131* National Aeronautics and Space Administration, Washington, DC.
SPACE STATION SYSTEMS: A BIBLIOGRAPHY WITH INDEXES (SUPPLEMENT 8)
Dec. 1988 243 p
(NASA-SP-7056(08); NAS 1.21:7056(08)) Avail: NTIS HC A13 CSCL 22B

This bibliography lists 950 reports, articles, and other documents introduced into the NASA scientific and technical information system between July 1, 1989 and December 31, 1989. Its purpose is to provide helpful information to researchers, designers and managers engaged in Space Station technology development and mission design. Coverage includes documents that define major systems and subsystems related to structures and dynamic control, electronics and power supplies, propulsion, and payload integration. In addition, orbital construction methods, servicing and support requirements, procedures and operations, and missions for the current and future Space Station are included. Author

19 SPACECRAFT INSTRUMENTATION

For related information see also *06 Aircraft Instrumentation* and *35 Instrumentation and Photography.*

N90-10132*# National Aeronautics and Space Administration. Langley Research Center, Hampton, VA.
METHOD AND APPARATUS FOR DETERMINING TIME, DIRECTION AND COMPOSITION OF IMPACTING SPACE PARTICLES Patent Application
William H. Kinard, inventor (to NASA), Jim J. Wortman, inventor (to NASA), Philip C. Kassel, Jr., inventor (to NASA), Fred S. Singer, inventor (to NASA), Donald H. Humes, inventor (to NASA), and John E. Stanley, inventor (to NASA) (Virginia Univ., Charlottesville.) 21 Jun. 1989 19 p
(NASA-Case-LAR-13392-1-CU; NAS 1.71:LAR-13392-1-CU; US-Patent-Appl-SN-369490) Avail: NTIS HC A03/MF A01 CSCL 14B

A space particle collector for recording the time specific particles are captured, and its direction at the time of capture, utilizes an array of targets, each comprised of an MOS capacitor on a chip charges from an external source and discharged upon impact by a particle through a tab on the chip that serves as a fuse. Any impacting particle creates a crater, but only the first will cause a discharge of the capacitor. A substantial part of the metal film around the first crater is burned off by the discharge current. The time of the impulse which burns the tab, and the identification of the target, is recorded together with data from flight instruments. The metal film is partitioned into pie sections to provide a plurality of targets on each of an array of silicon wafers, thus increasing the total number of identified particles that can be collected. It is thus certain which particles were captured at what specific times. NASA

20 SPACECRAFT PROPULSION AND POWER

Includes main propulsion systems and components, e.g., rocket engines; and spacecraft auxilliary power sources.

For related information see also *07 Aircraft Propulsion and Power, 28 Propellants and Fuels, 44 Energy Production and Conversion,* and *15 Launch Vehicles and Space Vehicles.*

N90-10133*# General Dynamics Corp., San Diego, CA. Space Systems Div.
LIQUID ROCKET BOOSTER STUDY. VOLUME 2, BOOK 1 Final Report
Mar. 1989 485 p
(Contract NAS8-37137)
(NASA-CR-183600; NAS 1.26:183600) Avail: NTIS HC A21/MF A03 CSCL 21H

The recommended Liquid Rocket Booster (LRB) concept is shown which uses a common main engine with the Advanced Launch System (ALS) which burns LO2 and LH2. The central rationale is based on the belief that the U.S. can only afford one big new rocket engine development in the 1990's. A LO2/LH2 engine in the half million pound thrust class could satisfy STS LRB, ALS, and Shuttle C (instead of SSMEs). Development costs and higher production rates can be shared by NASA and USAF. If the ALS program does not occur, the LO2/RP-1 propellants would produce slight lower costs for and STS LRB. When the planned Booster Engine portion of the Civil Space Transportation Initiatives has provided data on large pressure fed LO2/RP-1 engines, then the choice should be reevaluated. E.R.

N90-10134*# General Dynamics Corp., San Diego, CA. Space Systems Div.
LIQUID ROCKET BOOSTER STUDY. VOLUME 2, BOOK 5, APPENDIX 9: LRB ALTERNATE APPLICATIONS AND EVOLUTIONARY GROWTH Final Report, Aug. 1988 - Jan. 1989

Feb. 1989 83 p
(Contract NAS8-37137)
(NASA-CR-183604; NAS 1.26:183604) Avail: NTIS HC A05/MF A01 CSCL 21H

The analyses performed in assessing the merit of the Liquid Rocket Booster concept for use in alternate applications such as for Shuttle C, for Standalone Expendable Launch Vehicles, and possibly for use with the Air Force's Advanced Launch System are presented. A comparison is also presented of the three LRB candidate designs, namely: (1) the LO2/LH2 pump fed, (2) the LO2/RP-1 pump fed, and (3) the LO2/RP-1 pressure fed propellant systems in terms of evolution along with design and cost factors, and other qualitative considerations. A further description is also presented of the recommended LRB standalone, core-to-orbit launch vehicle concept. E.R.

N90-10135*# General Dynamics Corp., San Diego, CA. Space Systems Div.
LIQUID ROCKET BOOSTER STUDY. VOLUME 2, BOOK 4, APPENDICES 6-8: REPORTS OF ROCKETDYNE, PRATT AND WHITNEY, AND TRW Final Report
8 Jun. 1988 559 p
(Contract NAS8-37137)
(NASA-CR-183603; NAS 1.26:183603) Avail: NTIS HC A24/MF A03 CSCL 21H

For the pressure fed engines, detailed trade studies were conducted defining engine features such as thrust vector control methods, thrust chamber construction, etc. This was followed by engine design layouts and booster propulsion configuration layouts. For the pump fed engines parametric performance and weight data was generated for both O2/H2 and O2/RP-1 engines. Subsequent studies resulted in the selection of both LOX/RP-1 and O2/H2 propellants for the pump fed engines. More detailed analysis of the selected LOX/RP-1 and O2/H2 engines was conducted during the final phase of the study. Author

N90-10136*# General Dynamics Corp., San Diego, CA. Space Systems Div.
LIQUID ROCKET BOOSTER STUDY. VOLUME 2, BOOK 2, APPENDIX 1: TRADES STUDIES Final Report, Nov. 1987 - Feb. 1988
Feb. 1988 374 p
(Contract NAS8-37137)
(NASA-CR-183601; NAS 1.26:183601; GDSS-LRB-MEM-88-01-Vol-2-Bk-2) Avail: NTIS HC A16/MF A02 CSCL 21H

A list is presented of the trade studies which were planned and the status to which they have been accomplished. Full descriptions are also given of the trade studies along with line drawings and graphs illustrating the studies. E.R.

N90-10137*# General Dynamics Corp., San Diego, CA. Space Systems Div.
LIQUID ROCKET BOOSTER STUDY. VOLUME 1: EXECUTIVE SUMMARY Final Report, Oct. 1987 - Jan. 1989
Mar. 1989 57 p
(Contract NAS8-37137)
(NASA-CR-183599; NAS 1.26:183599) Avail: NTIS HC A04/MF A01 CSCL 21H

The purpose of this study was to determine the feasibility of Liquid Rocket Boosters (LRBs) replacing Solid Rocket Boosters on the Space Shuttle program. The major findings are given. The most significant conclusion is that LRBs offer significantly safety and performance advantages over the SRBs currently used by the STS without major impact to the ongoing program. E.R.

N90-10138*# General Dynamics Corp., San Diego, CA. Space Systems Div.
LIQUID ROCKET BOOSTER STUDY. VOLUME 2, BOOK 6, APPENDIX 10: VEHICLE SYSTEMS EFFECTS Final Report
24 Mar. 1989 129 p Prepared in cooperation with Eagle Engineering, Inc., Houston, TX
(Contract NAS8-37137)
(NASA-CR-183605; NAS 1.26:183605) Avail: NTIS HC A07/MF A01 CSCL 21H

Three tasks were undertaken by Eagle Engineering as a part of the Liquid Rocket Booster (LRB) study. Task 1 required Eagle to supply current data relative to the Space Shuttle vehicle and systems affected by an LRB substitution. Tables listing data provided are presented. Task 2 was to evaluate and compare shuttle impacts of candidate LRB configuration in concert with overall trades of analysis activity. Three selected configurations with emphasis on flight loads, separation dynamics, and cost comparison are presented. Task 3 required the development of design guidelines and requirements to minimize impacts to the Space Shuttle system from all LRB substitution. Results are presented for progress to date. E.R.

N90-10139*# General Dynamics Corp., San Diego, CA. Space Systems Div.
LIQUID ROCKET BOOSTER STUDY. VOLUME 2, BOOK 3, APPENDICES 2-5: PPIP, TRANSITION PLAN, AMOS PLAN, AND ENVIRONMENTAL ANALYSIS Final Report
18 May 1988 208 p
(Contract NAS8-37137)
(NASA-CR-183602; NAS 1.26:183602) Avail: NTIS HC A10/MF A02 CSCL 21H

This Preliminary Project Implementation Plan (PPIP) was used to examine the feasibility of replacing the current Solid Rocket Boosters on the Space Shuttle with Liquid Rocket Boosters (LRBs). The need has determined the implications of integrating the LRB with the Space Transportation System as the earliest practical date. The purpose was to identify and define all elements required in a full scale development program for the LRB. This will be a reference guide for management of the LRB program, addressing such requirement as design and development, configuration management, performance measurement, manufacturing, product assurance and verification, launch operations, and mission operations support. E.R.

N90-10140*# National Aeronautics and Space Administration. Langley Research Center, Hampton, VA.
SECOND BEAMED SPACE-POWER WORKSHOP
Russell J. DeYoung, ed. Washington Jul. 1989 439 p Workshop held in Hampton, VA, 28 Feb. - 2 Mar. 1989
(NASA-CP-3037; L-16590; NAS 1.55:3037) Avail: NTIS HC A19/MF A03 CSCL 10B

Potential missions for microwave and laser power beaming in space are discussed. Power beaming options, millimeter wave technology, laser technology, lunar bases, spacecraft propulsion, and near-Earth applications are covered. For individual titles, see N90-10141 through N90-10167.

N90-10141*# National Aeronautics and Space Administration. Lyndon B. Johnson Space Center, Houston, TX.
OFFICE OF EXPLORATION OVERVIEW
John Alred *In* NASA. Langley Research Center, Second Beamed Space-Power Workshop Jul. 1989 p 3-18 (For primary document see N90-10140 01-20)
Avail: NTIS HC A19/MF A03 CSCL 10B

The NASA Office of Exploration case studies for FY89 are reviewed with regard to study ground rules and constraints. Three study scenarios are presented: lunar evolution, Mars evolution, and Mars expedition with emphasis on the key mission objectives. Author

N90-10142*# Kaman Aerospace Corp., Arlington, VA.
POWER BEAMING OPTIONS
John D. G. Rather *In* NASA. Langley Research Center, Second Beamed Space-Power Workshop Jul. 1989 p 21-40 (For primary document see N90-10140 01-20)
Avail: NTIS HC A19/MF A03 CSCL 10B

Some large scale power beaming applications are proposed for the purpose of stimulating research. The first proposal is for a combination of large phased arrays on the ground near power

stations and passive reflectors in geostationary orbit. The systems would beam excess electrical power in microwave form to areas in need of electrical power. Another proposal is to build solar arrays in deserts and beam the energy around the world. Another proposal is to use lasers to beam energy from earth to orbiting spacecraft. Author

N90-10143*# Dartmouth Coll., Hanover, NH.
LASER PROPULSION TO EARTH ORBIT. HAS ITS TIME COME?
Arthur Kantrowitz *In* NASA. Langley Research Center, Second Beamed Space-Power Workshop Jul. 1989 p 41-56 (For primary document see N90-10140 01-20)
Avail: NTIS HC A19/MF A03 CSCL 10B

Recent developments in high energy lasers, adaptive optics, and atmospheric transmission bring laser propulsion much closer to realization. Proposed here is a reference vehicle for study which consists of payload and solid propellant (e.g. ice). A suitable laser pulse is proposed for using a Laser Supported Detonation wave to produce thrust efficiently. It seems likely that a minimum system (10 Mw CO2 laser and 10 m dia. mirror) could be constructed for about $150 M. This minimum system could launch payloads of about 13 kg to a 400 km orbit every 10 minutes. The annual launch capability would be about 683 tons times the duty factor. Laser propulsion would be an order of magnitude cheaper than chemical rockets if the duty factor was 20 percent (10,000 launches/yr). Launches beyond that would be even cheaper. The chief problem which needs to be addressed before these possibilities could be realized is the design of a propellant to turn laser energy into thrust efficiently and to withstand the launch environment. Author

N90-10144*# Little (Arthur D.), Inc., Cambridge, MA.
POWER FROM SPACE FOR USE ON EARTH: AN EMERGING GLOBAL OPTION
Peter E. Glaser *In* NASA. Langley Research Center, Second Beamed Space-Power Workshop Jul. 1989 p 57-68 (For primary document see N90-10140 01-20)
Avail: NTIS HC A19/MF A03 CSCL 10B

The concept of the Earth as a closed ecological system is addressed from the point of view of the availability and use of energy from space and its potential influence on the economies of both developed and developing countries. The results of past studies of the solar power satellite (SPS) are reviewed, and the current international activities exploring various aspects of an SPS are mentioned. The functions of an SPS, including collection of solar energy in orbit, conversion to an intermediate form of energy, transmission of energy from orbit to Earth, and conversion to useful energy in the most appropriate form are discussed. Directions for future developments are addressed including a suggested planning framework. Salient aspects of SPS technologies are presented, and the potential benefits of the uses of lunar materials for the SPS construction are outlined. Scenarios within the context of international participation in a global SPS system are presented. The conclusion is drawn that an SPS system is one of the few promising, globally applicable power generation options that has the potential to meet energy demands in the 21st Century and to achieve the inevitable transition to inexhaustible and renewable energy sources. Author

N90-10145*# Washington Univ., Seattle.
NEW ENERGY CONVERSION TECHNIQUES IN SPACE, APPLICABLE TO PROPULSION
A. Hertzberg and K. C. Sun (Lockheed Missiles and Space Co., Palo Alto, CA.) *In* NASA. Langley Research Center, Second Beamed Space-Power Workshop Jul. 1989 p 69-103 Repr. from 15th AIAA, SAE and ASME Joint Propulsion Conference, Las Vegas, NV, 18-20 Jun. 1979 Previously announced in IAA as A79-40490 (For primary document see N90-10140 01-20)
(AIAA-79-1338) Avail: NTIS HC A19/MF A03 CSCL 10B

The powering of aircraft with laser energy from a solar power satellite may be a promising new approach to the critical problem of the rising cost of fuel for aircraft transportation systems. The result is a nearly fuelless, pollution-free flight transportation system which is cost-competitive with the fuel-conservative airplane of the future. The major components of this flight system include a laser power satellite, relay satellites, laser-powered turbofans and a conventional airframe. The relay satellites are orbiting optical systems which intercept the beam from a power satellite and refocus and redirect the beam to its next target. Author

N90-10146*# Naval Research Lab., Washington, DC.
VACUUM MICROELECTRONICS FOR BEAM POWER AND RECTENNAS
Henry F. Gray *In* NASA. Langley Research Center, Second Beamed Space-Power Workshop Jul. 1989 p 107-125 (For primary document see N90-10140 01-20)
Avail: NTIS HC A19/MF A03 CSCL 10B

Vacuum Microelectronic devices can be described as vacuum transistors or micro-miniature vacuum tubes, as one chooses. The fundamental reason behind this new technology is the very large current densities available from field emitters, namely as high as 10(8) A/sq cm. Array current densities as high as 1000 A/sq cm have been measured. Total electron transit times from source to drain for 1 micron feature size devices have been predicted to be about 150fs. This very short transit time implies the possibility of submillimeter wave transmitters and rectennas in devices which can operate with reasonably high voltages and which are small in size and are lightweight. In addition, they are expected to be extremely radiation hard and very temperature insensitive. That is, they are expected to have radiation hardness characteristics similar to vacuum tubes, and both the high temperature and low temperature limits should be determined by the package. That is, there should be no practical intrinsic temperature or carrier freezeout problems for devices based on metals or composites. But the technology is difficult to implement at the present time because it is based on 300 to 500 angstrom radius field emitters which must be relatively uniform. There is also the need to understand the non-equilibrium transport physics in the near-surface regions of the field emitters. Author

N90-10147*# Georgia Inst. of Tech., Atlanta.
MILLIMETER-WAVE/INFRARED RECTENNA DEVELOPMENT AT GEORGIA TECH
Mark A. Gouker *In* NASA. Langley Research Center, Second Beamed Space-Power Workshop Jul. 1989 p 127-137 (For primary document see N90-10140 01-20)
(Grant NAG3-202)
Avail: NTIS HC A19/MF A03 CSCL 10B

The key design issues of the Millimeter Wave/Infrared (MMW/IR) monolithic rectenna have been resolved. The work at Georgia Tech in the last year has focused on increasing the power received by the physically small MMW rectennas in order to increase the rectification efficiency. The solution to this problem is to place a focusing element on the back side of the substrate. The size of the focusing element can be adjusted to help maintain the optimum input power density not only for different power densities called for in various mission scenarios, but also for the nonuniform power density profile of a narrow EM-beam. Author

N90-10148*# Naval Research Lab., Washington, DC. High Power Electromagnetic Radiation Branch.
GYROTRON DEVELOPMENT FOR SPACE POWER BEAMING **c35**
Wallace M. Manheimer *In* NASA. Langley Research Center, Second Beamed Space-Power Workshop Jul. 1989 p 139-158 (For primary document see N90-10140 01-20)
Avail: NTIS HC A19/MF A03 CSCL 14B

The use of a gyrotron for space power beaming, especially in the form of a lunar orbiting power station is discussed. The advantages of phased array power beaming, output power, and the design of a quasi-optical gyrotron are discussed. Author

N90-10149*# Lockheed Missiles and Space Co., Palo Alto, CA. **c32**
ANTENNA TECHNOLOGY FOR BEAMED SPACE-POWER
W. S. Gregorwich *In* NASA. Langley Research Center, Second

Beamed Space-Power Workshop Jul. 1989 p 159-170 (For primary document see N90-10140 01-20)
Avail: NTIS HC A19/MF A03 CSCL 20N

Based on present technology, the efficient transfer of RF power in space is feasible. However, many parameters must be taken into consideration when designing the system and the interrelationships of these parameters must also be considered. Once the distance between the orbiting spacecraft is specified and the transmit frequency is chosen, then the maximum size for the transmit and receive antennas is fixed (i.e., Rayleigh Range). Once the level of transmit power and trasmit time is specified, then the minimum number of spacecraft batteries is determined. High power RF transmission allows the satellite designer another option in the design of spacecraft power systems. Author

N90-10150*# Raytheon Co., Waltham, MA. Microwave and Power Tube Div.
HISTORY AND STATUS OF BEAMED POWER TECHNOLOGY AND APPLICATIONS AT 2.45 GIGAHERTZ
William C. Brown *In* NASA. Langley Research Center, Second Beamed Space-Power Workshop Jul. 1989 p 171-185 (For primary document see N90-10140 01-20)
Avail: NTIS HC A19/MF A03 CSCL 10B

Various applications of beamed power technology are discussed. An experimental microwave powered helicopter, rectenna technology, the use of the Solar Power Satellite to beam energy to Earth via microwaves, the use of cyclotron resonance devices, microwave powered airships, and electric propulsion are discussed. Author

N90-10151*# Lawrence Livermore National Lab., CA.
TECHNICAL OPTIONS FOR HIGH AVERAGE POWER FREE ELECTRON MILIMETER-WAVE AND LASER DEVICES **c36**
James C. Swingle *In* NASA. Langley Research Center, Second Beamed Space-Power Workshop Jul. 1989 p 191-219 (For primary document see N90-10140 01-20)
Avail: NTIS HC A19/MF A03 CSCL 20E

Many of the potential space power beaming applications require the generation of directed energy beams with respectable amounts of average power (MWs). A tutorial summary is provided here on recent advances in the laboratory aimed at producing direct conversion of electrical energy to electromagnetic radiation over a wide spectral regime from microwaves to the ultraviolet. Author

N90-10152*# Hampton Inst., VA. Dept. of Physics.
LASER ENERGY CONVERSION **c36**
N. W. Jalufka *In* NASA. Langley Research Center, Second Beamed Space-Power Workshop Jul. 1989 p 221-238 (For primary document see N90-10140 01-20)
Avail: NTIS HC A19/MF A03 CSCL 20E

The conversion of laser energy to other, more useful, forms is an important element of any space power transmission system employing lasers. In general the user, at the receiving sight, will require the energy in a form other than laser radiation. In particular, conversion to rocket power and electricity are considered to be two major areas where one must consider various conversion techniques. Three systems (photovoltaic cells, MHD generators, and gas turbines) have been identified as the laser-to-electricity conversion systems that appear to meet most of the criteria for a space-based system. The laser thruster also shows considerable promise as a space propulsion system. At this time one cannot predict which of the three laser-to-electric converters will be best suited to particular mission needs. All three systems have some particular advantages, as well as disadvantages. It would be prudent to continue research on all three systems, as well as the laser rocket thruster. Research on novel energy conversion systems, such as the optical rectenna and the reverse free-electron laser, should continue due to their potential for high payoff. Author

N90-10153*# National Aeronautics and Space Administration. Langley Research Center, Hampton, VA.
STRUCTURAL CONCEPTS FOR VERY LARGE (400-METER-DIAMETER) SOLAR CONCENTRATORS **c44**
Martin M. Mikulas, Jr. and John M. Hedgepeth (Astro Aerospace Corp., Carpinteria, CA.) *In its* Second Beamed Space-Power Workshop Jul. 1989 p 239-257 (For primary document see N90-10140 01-20)
Avail: NTIS HC A19/MF A03 CSCL 10A

A general discussion of various types of large space structures is presented. A brief overview of the history of space structures is presented to provide insight into the current state-of-the art. Finally, the results of a structural study to assess the viability of very large solar concentrators are presented. These results include weight, stiffness, part count, and in-space construction time. Author

N90-10154*# National Aeronautics and Space Administration. Langley Research Center, Hampton, VA.
OVERVIEW OF LASER CONCEPTS **c36**
Edmund J. Conway *In its* Second Beamed Space-Power Workshop Jul. 1989 p 261-286 (For primary document see N90-10140 01-20)
Avail: NTIS HC A19/MF A03 CSCL 20E

The concepts of laser power-beaming applicable to advanced NASA missions are reviewed. The types of lasers, (the iodine lasers and the diode lasers) which are central to the laser miniworkshop presentations are discussed. Author

N90-10155*# National Aeronautics and Space Administration. Lewis Research Center, Cleveland, OH.
OVERVIEW OF MICROWAVE CONCEPTS **c32**
Karl A. Faymon *In* NASA. Langley Research Center, Second Beamed Space-Power Workshop Jul. 1989 p 287-290 (For primary document see N90-10140 01-20)
Avail: NTIS HC A19/MF A03 CSCL 20N

An overview of microwave beamed power concepts is given in outline form. Concepts such as power transmission to operational satellites, spacecraft propulsion, lunar/planetary outpost power and planetary rover propulsion are listed in chart form and characterized in columns titled power level, benefits, and comments. Author

N90-10156*# National Aeronautics and Space Administration. Langley Research Center, Hampton, VA.
LASER-POWERED LUNAR BASE **c36**
R. Costen, Donald H. Humes, G. H. Walker, M. D. Williams, and Russell J. DeYoung *In its* Second Beamed Space-Power Workshop Jul. 1989 p 293-316 (For primary document see N90-10140 01-20)
Avail: NTIS HC A19/MF A03 CSCL 20E

The objective was to compare a nuclear reactor-driven Sterling engine lunar base power source to a laser-to-electric converter with orbiting laser power station, each providing 1 MW of electricity to the lunar base. The comparison was made on the basis of total mass required in low-Earth-orbit for each system. This total mass includes transportation mass required to place systems in low-lunar orbit or on the lunar surface. The nuclear reactor with Sterling engines is considered the reference mission for lunar base power and is described first. The details of the laser-to-electric converter and mass are discussed. The next two solar-driven high-power laser concepts, the diode array laser or the iodine laser system, are discussed with associated masses in low-lunar-orbit. Finally, the payoff for laser-power beaming is summarized. Author

N90-10157*# National Aeronautics and Space Administration. Langley Research Center, Hampton, VA.
LASER-POWERED MARTIAN ROVER **c36**
W. L. Harries, W. E. Meador, G. A. Miner, Gregory L. Schuster, G. H. Walker, and M. D. Williams *In its* Second Beamed Space-Power Workshop Jul. 1989 p 317-327 (For primary document see N90-10140 01-20)
Avail: NTIS HC A19/MF A03 CSCL 20E

Two rover concepts were considered: an unpressurized skeleton vehicle having available 4.5 kW of electrical power and limited to a range of about 10 km from a temporary Martian base and a much larger surface exploration vehicle (SEV) operating on a maximum 75-kW power level and essentially unrestricted in range or mission. The only baseline reference system was a battery-operated skeleton vehicle with very limited mission capability and range and which would repeatedly return to its temporary base for battery recharging. It was quickly concluded that laser powering would be an uneconomical overkill for this concept. The SEV, on the other hand, is a new rover concept that is especially suited for powering by orbiting solar or electrically pumped lasers. Such vehicles are visualized as mobile habitats with full life-support systems onboard, having unlimited range over the Martian surface, and having extensive mission capability (e.g., core drilling and sampling, construction of shelters for protection from solar flares and dust storms, etc.). Laser power beaming to SEV's was shown to have the following advantages: (1) continuous energy supply by three orbiting lasers at 2000 km (no storage requirements as during Martian night with direct solar powering); (2) long-term supply without replacement; (3) very high power available (MW level possible); and (4) greatly enhanced mission enabling capability beyond anything currently conceived. Author

N90-10158*# National Aeronautics and Space Administration. Lewis Research Center, Cleveland, OH.
POWER FOR THE MOON: IS MICROWAVE POWER BEAMING AN OPTION?
Ronald C. Cull *In* NASA. Langley Research Center, Second Beamed Space-Power Workshop Jul. 1989 p 329-342 (For primary document see N90-10140 01-20)
Avail: NTIS HC A19/MF A03 CSCL 10C

Microwave power beaming options for powering lunar bases are presented in viewgraph form. Information is given on power dependent system masses, a solar source beam power system, a nuclear source beam power system, a three satellite beam power system, antenna configurations, and antenna design. Author

N90-10159*# National Aeronautics and Space Administration. Lewis Research Center, Cleveland, OH.
APPLICABILITY OF THE BEAMED POWER CONCEPT TO LUNAR ROVERS, CONSTRUCTION, MINING, EXPLORERS AND OTHER MOBILE EQUIPMENT
Jose L. Christian, Jr. *In* NASA. Langley Research Center, Second Beamed Space-Power Workshop Jul. 1989 p 343-356 (For primary document see N90-10140 01-20)
Avail: NTIS HC A19/MF A03 CSCL 10C

Some of the technical issues dealing with the feasibility of high power (10 Kw to 100 Kw) mobile manned equipment for settlement, exploration and exploitation of Lunar resources are addressed. Short range mining/construction equipment, a moderate range (50 Km) exploration vehicle, and an unlimited range explorer are discussed. Author

N90-10160*# National Aeronautics and Space Administration. Langley Research Center, Hampton, VA.
LOW-EARTH-ORBIT TO LOW-LUNAR-ORBIT LASER FREIGHTER Abstract Only
Russell J. DeYoung *In its* Second Beamed Space-Power Workshop Jul. 1989 p 363-364 (For primary document see N90-10140 01-20)
Avail: NTIS HC A19/MF A03 CSCL 10C

The objective of this mission study was to compare laser propulsion to chemical LOX/H2 and nuclear electric propulsion for the specific mission of delivering a 144-metric ton lunar base from low-Earth-orbit to low-lunar-orbit. The basis of comparison was total mass in low-Earth-orbit needed to accomplish this mission. The Office of Exploration approach to establishing the lunar base was to use two vehicles: a nuclear electric propulsion (NEP) vehicle to deliver cargo and a chemical vehicle to deliver humans. The NEP vehicle was reactor driven with a vehicle dry mass of 125 metric tons. The Office of Exploration study did not use chemical propulsion for cargo, but in the present study it was used for cargo for comparison to laser propulsion. This mission study assumes a high-power laser, either nuclear or solar electric-driven diode laser, is in orbit around Earth, beaming power to a laser propulsion vehicle. Laser power is only used for the LEO escape burn; other much lower-power burns are done with LOX/H2. Author

N90-10161*# National Aeronautics and Space Administration. Langley Research Center, Hampton, VA.
LASER PROPULSION OPTION **c36**
Donald H. Humes *In its* Second Beamed Space-Power Workshop Jul. 1989 p 365-375 (For primary document see N90-10140 01-20)
Avail: NTIS HC A19/MF A03 CSCL 20E

The use of laser thrusters with exhaust powers in the 25 MW to 250 MW range can reduce the fuel that would be needed to transport the lunar outpost equipment to low-lunar orbit with a chemical OTV by 57000 Kg to 105000 Kg with no significant penalty in trip time. This would save one or two launches of the heavy-load launch vehicle. Nuclear-electric OTVs would take 40 to 120 times as long to get to the moon and would spend 100 to 1700 times as long in the Van Allen radiation belts as OTVs that have laser thrusters. Author

N90-10162*# National Aeronautics and Space Administration. Langley Research Center, Hampton, VA.
EARTH ORBIT LASER SYSTEMS **c36**
Ja H. Lee *In its* Second Beamed Space-Power Workshop Jul. 1989 p 377-381 (For primary document see N90-10140 01-20)
Avail: NTIS HC A19/MF A03 CSCL 20E

At the state-of-the-art efficiencies, both nuclear and solar-driven systems require equal masses for the same laser powers in the 50 to 500 MW range, typically 3,700 tons for a 100-MW thruster. Future efficiency improvement of solar panel and laser diode array will realize significant reduction (by a factor of 3) in system masses. Beaming time for laser propulsion is relatively short and other missions should be considered for increasing the system duty cycle. Author

N90-10163*# Miami Univ., Oxford, OH.
LASER DIODE ARRAY AND TRANSMISSION OPTICS **c36**
Jin H. Kwon *In* NASA. Langley Research Center, Second Beamed Space-Power Workshop Jul. 1989 p 383-389 (For primary document see N90-10140 01-20)
Avail: NTIS HC A19/MF A03 CSCL 20E

Information on laser diode array and transmission optics is given in viewgraph form. Information is given on coherent combining of laser diode arrays, amplification through a laser diode array, the far field pattern of a laser diode transmitter, and beam diameter at receiver vs. transmission distance. Author

N90-10164*# Hampton Inst., VA. Dept. of Physics.
LASER THRUSTER **c36**
N. W. Jalufka *In* NASA. Langley Research Center, Second Beamed Space-Power Workshop Jul. 1989 p 391-396 (For primary document see N90-10140 01-20)
Avail: NTIS HC A19/MF A03 CSCL 20E

Laser propulsion can reduce fuel by 57 t to 105 t over chemical propulsion for a 144 t Lunar base, with no significant increase in trip time. Laser propulsion reduces trip time by a factor of 40 to 120 over nuclear electric propulsion and time in radiation belts by a factor of 100 to 1700. Either solar or nuclear driven laser diode arrays could produce multimegawatt beams, typically 3,700 t for a 235 MW laser system. Laser diode arrays have high payoff due to short wavelength (850 nm) and high diode efficiency (70 percent). A dry laser OTV of 8790 kg and 60 percent efficiency can transport a 144 t lunar base. Laser propulsion could carry both personnel and cargo safely to the lunar base. Author

N90-10165*# National Aeronautics and Space Administration. Lewis Research Center, Cleveland, OH.
MICROWAVE BEAM POWER

Karl A. Faymon *In* NASA. Langley Research Center, Second Beamed Space-Power Workshop Jul. 1989 p 397-403 (For primary document see N90-10140 01-20)
Avail: NTIS HC A19/MF A03 CSCL 10B

Information on microwave beam power is given in viewgraph form. Information is given on orbit transfer proulsion applications, costs of delivering 100 kWe of usable power, and costs of delivering a 1 kg payload into orbit. Author

N90-10166*# National Aeronautics and Space Administration. Lewis Research Center, Cleveland, OH.
CENTRAL ELECTRICAL UTILITY POWER FOR A SATELLITE RING CITY IN LOW EARTH ORBIT SPACE c33
Ira T. Myers, Karl A. Faymon, and A. D. Patton (Texas A&M Univ., College Station.) *In* NASA. Langley Research Center, Second Beamed Space-Power Workshop Jul. 1989 p 409-418 (For primary document see N90-10140 01-20)
Avail: NTIS HC A19/MF A03 CSCL 10C

Information is given in viewgraph form on central electrical power for a satellite ring city, defined as a group of large free flyers of 10 to 20 units with perhaps 100 people in each unit, and organized in a circle so that power can be fed from a central location. The free flyers would be located at 300 to 700 miles in altitude, and spaced about a kilometer apart. Potential activities of a ring city are listed as well as the electrical power needs. Information is given on costs and individual and centralized solar arrays and nuclear reactor systems. Author

N90-10167*# National Aeronautics and Space Administration. Langley Research Center, Hampton, VA.
BEAMED LASER POWER IN SUPPORT OF NEAR-EARTH MISSIONS c36
Edmund J. Conway, Gregory L. Schuster, Willard Weaver, and Donald H. Humes *In its* Second Beamed Space-Power Workshop Jul. 1989 p 419-429 (For primary document see N90-10140 01-20)
Avail: NTIS HC A19/MF A03 CSCL 20E

It was found that solar-pumped laser-beamed power is lighter than photovoltaic for power requirements of 150 KWe and above, and is competitive with combined photovoltaic/solar-dynamic over the entire power range investigated. A space station supported by laser-beamed power can be a lower-g facility (reduced drag) than with PV or PV + SD power; has greater freedom of orientation (small receiver moves rather than large arrays or concentrators); and requires less structure (arrays, alpha joints, booms) permitting easier control and fewer vibrational modes. Laser power beaming offers a revolutionary concept for planning designing, and powering large orbiting spacecraft. Author

N90-10168*# Sverdrup Technology, Inc., Bay Saint Louis, MS.
X-RAY SPECTROSCOPY OF THE SSME PLUME Report, May - Oct. 1988
Dan F. Olive Nov. 1988 20 p
(Contract NAS13-290)
(NASA-CR-185308; NAS 1.26:185308) Avail: NTIS HC A03/MF A01 CSCL 21H

In order to examine the potential of using SSME exhaust plume radiation in the soft X-ray spectrum as an early warning system of imminent engine failure, a low cost, low risk experiment was devised. An approach was established, equipment was leased, the system was installed and checked out, and data were successfully acquired demonstrating the proof-of-concept. One spectrum measurement of the SSME plume was acquired during a 300 second burn on the A-1 Test Stand. This spectrum showed a prominent, line emission feature at about 34.5 KeV, a result which was not expected, nor can it be explained at this time. If X-ray spectra are to be useful as a means of monitoring nominal engine operation, it will be necessary to explore this region of the EM spectrum in greater detail. The presence of structure in the spectrum indicates that this technology may prove to be useful as an engine health monitoring system. Author

N90-10169*# Morton Thiokol, Brigham City, UT. Space Div.
FLIGHT SET 360T004 (STS-30) INSULATION COMPONENT, INTERIM RELEASE, VOLUME 3 Final Report
James A. Passman 27 Jun. 1989 94 p
(Contract NAS8-30490)
(NASA-CR-183746; NAS 1.26:183746; TWR-17543-Vol-3; WBS-4B601-04-01; ECS-SS-1012) Avail: NTIS HC A05/MF A01 CSCL 21H

The insulation component of the Redesigned Solid Rocket Motor (RSRM) is discussed. The results of all visual evaluations and a thermal safety factor analysis are given. The data contained here supersedes the interim release and the insulation data presented in the Clearfield 10 day report. The objective is to document the postflight condition of the internal and external insulation of nozzle to case joints, the case field joints, the igniter to case joints, and the acreage insulation which made up RSRM-4A and RSRM-4B. Author

N90-10170*# Thiokol Corp., Brigham City, UT. Space Operations.
FLIGHT MOTOR SET 360L003 (STS-29R) Final Report
Glen A. Riehr Jul. 1989 326 p
(Contract NAS8-30490)
(NASA-CR-183739-Vol-1; NAS 1.26:183739-Vol-1; TWR-17542-1; WBS-4B601-03-08; ECS-SS-1011) Avail: NTIS HC A15/MF A02 CSCL 21H

The redesigned solid rocket motor (RSRM) flight set 360L003 was launched on March 13, 1989 as part of NASA space shuttle mission STS-29R. As was the case with flight sets 360L001 and 360L002 (STS-26R and STS-27R), both motors (360L003A and 360L003B) performed in an excellent manner. Evaluation of the ground environment instrumentation measurements verified thermal model analysis data and showed agreement with predicted environmental effects. The right-hand aft field joint primary heater failed during the countdown; the secondary heater was activated and performed as designed. All other field joint heaters and aft skirt thermal conditioning systems had no anomalies. Shuttle thermal imager infrared readings compared favorably with measured ground environment instrumentation data. No thermal launch commit criteria violations occurred at any time. Evaluation of the development flight instrumentation showed exceptional propulsion performance. All ballistic parameters closely matched the predicted values and were well within the required specification levels. Girth and biaxial strain gage measurements compared closely with corresponding gages on previous flight motors, static tests, and with preflight predictions. Adequate safety factors were verified. (Some ignition transient spiking was noted in a few girth gages; the spiking was determined not to be representative of actual case behavior, but an instrumentation phenomena.) The accelerometers again measured high vibration amplitude levels during the ignition transient and the reentry Max Q phases. Postflight inspection showed that all combustion gas was contained by the insulation in the field and case-to-nozzle joints. No anomalous insulation erosion patterns were found, and the seals that did directly contain motor pressure showed no heat effects, erosion, or blowby. All anomalies identified were a result of splashdown damage, with the exception of fretting in the case field joint interference (nonsealing) surfaces and a prelaunch field joint heater failure. The disposition of all anomalies and the complete results are reported. Author

N90-10171*# Thiokol Corp., Brigham City, UT. Space Operations.
GENERIC SYSTEM COMPONENTS OF THE THIOKOL ULTRASONIC RSRM CASE-TO-INSULATION BONDLINE INSPECTION SYSTEM Final Test Report
M. Cook 25 Jul. 1989 392 p
(Contract NAS8-30490)
(NASA-CR-183738; NAS 1.26:183738; TWR-18894; WBS-4B102-10-10; ECS-SS-2412) Avail: NTIS HC A17/MF A03 CSCL 21H

Qualification testing of the Ultrasonic Redesigned Solid Rocket Motor Bondline Inspection Systems (URBIS) was conducted at

the Thiokol Nondestructive Evaluation Test Facility M337A and at the Rotation Process Storage Facility at Kennedy Space Center. The test was performed on portions of the URBIS that are generic to redesigned solid rocket motor case-to-insulation bondline inspections. Testing began on Feb. 13, 1989 and was completed on May 26, 1989. The main purpose of the test was to verify that each URBIS performed to the manufacturer's specifications in the same manner and to make any procedural changes necessary for specific redesigned solid rocket motor inspections. All five URBISs passed every stage of the qualification test. Each URBIS is now qualified for use on redesigned solid rocket motors. Verifying the fact that each URBIS obtains and analyzes data in a similar fashion has eliminated concerns about variations in data between the five systems. The following recommendations were made as a result of this test: (1) each URBIS should be located within a stable environment; (2) an electronic preventative maintenance program should be established for each URBIS; (3) when the URBIS is being utilized to perform transducer analysis, the URBIS equipment setting should match the equipment setting noted on the manufacturer-supplied transducer certification sheet; and (4) optimum scan velocities for each inspection technique (clevis, capture feature, pinhole and membrane) should be determined through further testing. Author

N90-10172*# National Aeronautics and Space Administration. Lewis Research Center, Cleveland, OH.

A ROCKET ENGINE DESIGN EXPERT SYSTEM

Kenneth J. Davidian Oct. 1989 11 p Presented at the 26th JANNAF Combustion Meeting, Pasadena, CA, 23-27 Oct. 1989
(NASA-TM-102373; E-5107; NAS 1.15:102373) Avail: NTIS HC A03/MF A01 CSCL 21H

The overall structure and capabilities of an expert system designed to evaluate rocket engine performance are described. The expert system incorporates a JANNAF standard reference computer code to determine rocket engine performance and a state-of-the-art finite element computer code to calculate the interactions between propellant injection, energy release in the combustion chamber, and regenerative cooling heat transfer. Rule-of-thumb heuristics were incorporated for the hydrogen-oxygen coaxial injector design, including a minimum gap size constraint on the total number of injector elements. One-dimensional equilibrium chemistry was employed in the energy release analysis of the combustion chamber and three-dimensional finite-difference analysis of the regenerative cooling channels was used to calculate the pressure drop along the channels and the coolant temperature as it exits the coolant circuit. Inputting values to describe the geometry and state properties of the entire system is done directly from the computer keyboard. Graphical display of all output results from the computer code analyses is facilitated by menu selection of up to five dependent variables per plot. Author

N90-10173# Sandia National Labs., Albuquerque, NM.

CIRCUIT LEVEL MODELING OF INDUCTIVE ELEMENTS

G. P. Muyshondt and W. M. Portnoy (Texas Technological Univ., Lubbock.) 1989 5 p Presented at the 24th Intersociety Energy Conversion Engineering Conference, Washington, DC, 6-11 Aug. 1989
(Contract DE-AC04-76DP-00789)
(DE89-015122; SAND-89-1625C; CONF-890815-18) Avail: NTIS HC A01/MF A01

Design and analysis of spacecraft power systems have been difficult to perform because of the lack of circuit level models for nonlinear inductive elements. This paper reviews some of the models which have been proposed, their limitations, and applications. An improved saturation dependent model will be described. The model has been implemented in SPICE and with a commercial circuit program and demonstrated to be satisfactory in both implementations. DOE

N90-10174*# National Aeronautics and Space Administration. Lewis Research Center, Cleveland, OH.

A FEASIBILITY ASSESSMENT OF INSTALLATION, OPERATION AND DISPOSAL OPTIONS FOR NUCLEAR REACTOR POWER SYSTEM CONCEPTS FOR A NASA GROWTH SPACE STATION

Harvey S. Bloomfield and Jack A. Heller Jun. 1987 37 p
(NASA-TM-89923; E-3622; NAS 1.15:89923) Avail: NTIS HC A03/MF A01 CSCL 21H

A preliminary feasibility assessment of the integration of reactor power system concepts with a projected growth space station architecture was conducted to address a variety of installation, operational disposition, and safety issues. A previous NASA sponsored study, which showed the advantages of space station - attached concepts, served as the basis for this study. A study methodology was defined and implemented to assess compatible combinations of reactor power installation concepts, disposal destinations, and propulsion methods. Three installation concepts that met a set of integration criteria were characterized from a configuration and operational viewpoint, with end-of-life disposal mass identified. Disposal destinations that met current aerospace nuclear safety criteria were identified and characterized from an operational and energy requirements viewpoint, with delta-V energy requirement as a key parameter. Chemical propulsion methods that met current and near-term application criteria were identified and payload mass and delta-V capabilities were characterized. These capabilities were matched against concept disposal mass and destination delta-V requirements to provide the feasibility of each combination. Author

N90-10175*# General Dynamics Corp., San Diego, CA. Space Systems Div.

BIDIRECTIONAL POWER CONVERTER CONTROL ELECTRONICS Final Report

J. W. Mildice Nov. 1987 103 p
(Contract NAS3-23878)
(NASA-CR-175070; NAS 1.26:175070) Avail: NTIS HC A06/MF A01 CSCL 21H

The object of this program was to design, build, test, and deliver a set of control electronics suitable for control of bidirectional resonant power processing equipment of the direct output type. The program is described, including the technical background, and results discussed. Even though the initial program tested only the logic outputs, the hardware was subsequently tested with high-power breadboard equipment, and in the testbed of NASA contract NAS3-24399. The completed equipment is now operating as part of the Space Station Power System Test Facility at NASA Lewis Research Center. Author

N90-10176*# National Aeronautics and Space Administration. Ames Research Center, Moffett Field, CA.

BOOST-PHASE DISCRIMINATION RESEARCH ACTIVITIES Final Report, 1 Aug. 1986 - 31 Mar. 1989

David M. Cooper and George S. Deiwert 10 Jul. 1989 7 p
(Contract MIPR-ARO-118-87)
(NASA-TM-101889; NAS 1.15:101889; AD-A210912; ARO-24539.1-EG-SDI) Avail: NTIS HC A02/MF A01 CSCL 21/8

Theoretical research in two areas was performed. The aerothermodynamics research focused on the hard-body and rocket plume flows. Analytical real gas models to describe finite rate chemistry were developed and incorporated into the three-dimensional flow codes. New numerical algorithms capable of treating multi-species reacting gas equations and treating flows with large gradients were also developed. The computational chemistry research focused on the determination of spectral radiative intensity factors, transport properties and reaction rates. Ab initio solutions to the Schrodinger equation provided potential energy curves transition moments (radiative probabilities and strengths) and potential energy surfaces. These surfaces were then coupled with classical particle reactive trajectories to compute reaction cross-sections and rates. GRA

N90-10196# Office National d'Etudes et de Recherches Aerospatiales, Paris (France).
EXPERIMENTAL STUDY ON THE STABILITY OF SMALL ROCKET ENGINES WITH STORABLE LIQUID PROPELLANTS [RECHERCHE EXPERIMENTALE SUR LA STABILITE DES PETITS MOTEURS FUSEES A ERGOLS STOCKABLES]
Robert Foucaud and Renaud Lecourt *In* AGARD, Combustion Instabilities in Liquid-Fuelled Propulsion Systems Apr. 1989 8 p In FRENCH; ENGLISH summary Previously announced in IAA as A89-31804 (For primary document see N90-10191 01-25)
Copyright Avail: NTIS HC A14/MF A02

N90-10197# Messerschmitt-Boelkow-Blohm G.m.b.H., Munich (Germany, F.R.). Kommunikationssysteme und Antriebe.
LOW FREQUENCY AND HIGH FREQUENCY COMBUSTION OSCILLATION PHENOMENA INSIDE A ROCKET COMBUSTION CHAMBER FED BY LIQUID OR GASEOUS PROPELLANTS
D. Preclik and P. Spagna *In* AGARD, Combustion Instabilities in Liquid-Fuelled Propulsion Systems Apr. 1989 18 p (For primary document see N90-10191 01-25)
Copyright Avail: NTIS HC A14/MF A02

23 CHEMISTRY AND MATERIALS (GENERAL)

N90-10177# Purdue Univ., West Lafayette, IN. Dept. of Chemistry.
NMR EVIDENCE FOR A PLANAR ARENE INTERMEDIATE IN THE ELECTRON-TRANSFER INDUCED ETA 6 TO ETA 4 HAPTICITY CHANGE OF A RHODIUM ARENE COMPLEX
Technical Report No. 88, 1 Oct. 1987 - 30 Jun. 1989
Jon Merkert (Vermont Univ., Burlington.), Roger M. Nielson, Michael J. Weaver, and William E. Geiger 1 Jul. 1989 19 p Submitted for publication
(Contract N00014-86-K-0556)
(AD-A210211) Avail: NTIS HC A03/MF A01 CSCL 07/3

Hydrogen 1 NMR spectra were obtained for the Rhodium (II) complex (eta-C6Me6/RhCp*)+, Cp* = 5-C5Me5, at 200 MHz, and 470 MHz. A single resonance was observed for the arene CH3 protons between 298 K and 183 K in Methylene Chloride. The temperature dependence of the resonance was consistent with a doublet state formulation of the Rh(II) complex. At 298 K, the CH3 chemical shifts were 56 ppm for the arene substituents and 123 ppm for the cyclopentadienyl substituents. The magnetic equivalence of the methyl arene resonances is consistent with a planar arene structure in the complex. It is shown that a structural formulation including a highly fluxional bent arene is unlikely. The results demonstrate eta 4-arene hapticity, the one-electron intermediate can retain the planar arene structure, even if this results in a 19 e- metal. GRA

N90-10178# Turin Univ. (Italy).
INTERNATIONAL CONFERENCE ON ORGANOMETALLIC CHEMISTRY (13TH) HELD IN TORINO, EUROPE ON 4-9 SEPTEMBER 1988: ABSTRACTS
9 Sep. 1988 471 p Conference held in Turin, Italy, 4-9 Sep. 1988
(Contract DAJA45-88-M-0295)
(AD-A210617; R/D-6012-CH-02) Avail: NTIS HC A20/MF A03 CSCL 07/3

Organometallic Chemistry has grown considerably and covers many fields of interest from metal containing supports to biologically relevant molecules. Metal-carbon- and metal-hydrogen bond making and breaking are fundamental steps in many processes of interest to all chemists. Within the limits imposed by the tight schedule, the Scientific Organizing Committee has tried to aggregate the scientific contributions in meaningful and consistent clusters. GRA

24 COMPOSITE MATERIALS

Includes physical, chemical, and mechanical properties of laminates and other composite materials.
For ceramic materials see *27 Nonmetallic Materials.*

N90-10179*# National Aeronautics and Space Administration. Langley Research Center, Hampton, VA.
THE INTERLAMINAR FRACTURE TOUGHNESS OF WOVEN GRAPHITE/EPOXY COMPOSITES
Joan G. Funk and Jerry W. Deaton Washington Nov. 1989 28 p
(NASA-TP-2950; L-16629; NAS 1.60:2950) Avail: NTIS HC A03/MF A01 CSCL 11D

The interlaminar fracture toughness of 2-D graphite/epoxy woven composites was determined as a function of stacking sequence, thickness, and weave pattern. Plain, oxford, 5-harness satin, and 8-harness satin weaves of T300/934 material were evaluated by the double cantilever beam test. The fabric material had a G (sub Ic) ranging from 2 to 8 times greater than 0 degrees unidirectional T300/934 tape material. The interlaminar fracture toughness of a particular weave style was dependent on whether the stacking sequence was symmetric or asymmetric and, in some cases, on the fabric orientation. Author

N90-10180# Belden Wire and Cable, Geneva, IL.
MEASURING THE SHIELDING EFFECTIVENESS OF SUPERCONDUCTIVE COMPOSITES
Thomas Pienkowski, David Johnson, M. T. Lanagan, R. B. Poeppel, Steven Danyluk, and M. McGuire (Chicago Univ., IL.) 1989 3 p Presented at the IEEE International Symposium on Electromagnetic Compatibility, Denver, CO, 23-25 May 1989
(Contract W-31-109-eng-38)
(DE89-015164; CONF-890508-1) Avail: NTIS HC A01/MF A01

The ability to cool superconductors with liquid nitrogen instead of liquid helium has opened the door to a wide range of research. The well known Meissner effect, which states superconductors are perfectly diamagnetic, suggests shielding applications. One of the drawbacks to the new ceramic superconductors is the brittleness of the finished material. Because of this drawback any application which required any flexibility would be impractical. Therefore, the results of a preliminary investigation into the measuring of shielding effectiveness of YBa2Cu3O(7-x) both as a composite and as a monolithic material are presented. A flanged coaxial test fixture was selected to measure the shielding. The composite samples showed little or no shielding. The monolithic sample showed substantially less shielding than predicted. Possible explanations for this lack of shielding are discussed. DOE

N90-10181*# National Aeronautics and Space Administration. Lewis Research Center, Cleveland, OH.
COMPOSITE BLADE STRUCTURAL ANALYZER (COBSTRAN) THEORETICAL/PROGRAMMER'S MANUAL
Robert A. Aiello and Christos C. Chamis Aug. 1989 136 p
(NASA-TM-101958; E-4986; NAS 1.15:101958) Avail: NTIS HC A07/MF A01 CSCL 11D

This manual describes the organization and flow of data and analysis in the computer code, COBSTRAN (COmposite Blade STRuctural ANalyzer). This code combines composite mechanics and laminate theory with an internal data base of fiber and matrix properties and was developed for the design and analysis of composite turbofan and turboprop blades and composite wind turbine blades. Inputs to the code are constituent fiber and matrix material properties, factors reflecting the fabrication process, composite geometry and blade geometry. COBSTRAN performs the micromechanics and laminate analyses of these fiber composites and generates a NASTRAN finite element model of the blade. This manual describes the equations formulated and solved in the code and the function of each of the seventy-two subroutines. COBSTRAN is written in FORTRAN 77. Author

N90-10182 Florida Univ., Gainesville.
HYGROTHERMAL EFFECTS ON THE COMPLEX MODULI OF

COMPOSITE LAMINATES Ph.D. Thesis
Hacene Bouadi 1988 156 p
Avail: Univ. Microfilms Order No. DA8908214

The effects of absorbed moisture and temperature on the complex moduli of composite laminates are investigated and the mechanisms of moisture diffusion in a lamina are also analyzed. First, the variation of the complex moduli of epoxy in terms of temperature and moisture content are experimentally determined. Then, the hygrothermal effects on the complex moduli of composites are derived by using the complex moduli of the matrix, micromechanical formulas and experimental data. Only the hygrothermal effects on the complex moduli of pure epoxy need to be experimentally determined since these effects on the fibers properties are negligible. In addition, the effects of hygrothermal environment on the stress field and material damping of general laminated composite plates are analyzed. It is shown that hygrothermal stresses induced directly by moisture and indirectly by material property changes can be very high, but the effects on damping are less pronounced. Dissert. Abstr.

N90-10183*# National Aeronautics and Space Administration. Ames Research Center, Moffett Field, CA.
COMPOSITE MULTILAYER INSULATIONS FOR THERMAL PROTECTION OF AEROSPACE VEHICLES
D. A. Kourtides and W. C. Pitts Feb. 1989 15 p Presented at the Composites in Manufacturing 8 Exposition and Conference, Society of Manufacturing Engineers, Anaheim, CA, 9-12 Jan. 1989
(NASA-TM-101071; A-89035; NAS 1.15:101071) Avail: NTIS HC A03/MF A01 CSCL 11D

Composite flexible multilayer insulation systems (MLI), consisting of alternating layers of metal foil and scrim cloth or insulation quilted together using ceramic thread, were evaluated for thermal performance and compared with a silica fibrous (baseline) insulation system. The systems studied included: (1) alternating layers of aluminoborosilicate (ABS) scrim cloth and stainless steel foil, with silica, ABS, or alumina insulation; (2) alternating layers of scrim cloth and aluminum foil, with silica or ABS insulation; (3) alternating layers of alumininum foil and silica or ABS insulation; and (4) alternating layers of aluminum-coated polyimide placed on the bottom of the silica insulation. The MLIs containing aluminum were the most efficient, measuring as little as half the backface temperature increase of the baseline system. Author

N90-10184*# General Electric Co., Cincinnati, OH. Aircraft Engine Business Group.
REVOLUTIONARY OPPORTUNITIES FOR MATERIALS AND STRUCTURES STUDY
F. A. Schweiger Feb. 1987 169 p
(Contract NAS3-24622)
(NASA-CR-179642; NAS 1.26:179642) Avail: NTIS HC A08/MF A01 CSCL 11D

The revolutionary opportunities for materials and structures study was performed to provide Government and Industry focus for advanced materials technology. Both subsonic and supersonic engine studies and aircraft fuel burn and DOC evaluation are examined. Year 2010 goal materials were used in the advanced engine studies. These goal materials and improved component aero yielded subsonic fuel burn and DOC improvements of 13.4 percent and 5 percent, respectively and supersonic fuel burn and DOC improvements of 21.5 percent and 18 percent, respectively. Conclusions are that the supersonic study engine yielded fuel burn and DOC improvements well beyond the program goals; therefore, it is appropriate that advanced material programs be considered. Author

N90-10185*# National Aeronautics and Space Administration. Lewis Research Center, Cleveland, OH.
MECHANICS OF DAMPING FOR FIBER COMPOSITE LAMINATES INCLUDING HYGRO-THERMAL EFFECTS
D. A. Saravanos and Christos C. Chamis Apr. 1989 28 p Presented at the 30th Structures, Structural Dynamics, and Materials Conference, Mobile, AL, 3-5 Apr. 1989; sponsored in part by AIAA, ASME, ASCE, AHS, and ASC Previously announced in IAA as A89-30681
(NASA-TM-102329; E-5034; NAS 1.15:102329) Avail: NTIS HC A03/MF A01 CSCL 11D

An integrated mechanics theory was developed for the modeling of composite damping from the micromechanics to the laminate level. Simplified, design oriented equations based on hysteretic damping are presented for on-axis plies, off-axis plies, and laminates including the effect of temperature, moisture, and interply hysteretic damping. The temperature rise within vibrating composite laminates resulting from strain energy dissipation is also modeled, and their coupled hygro-thermo-mechanical response is predicted. The method correlates well with reported damping measurements. Application examples illustrate the effect of various ply, laminate, and hygro-thermal parameters on the overall damping performance of composite laminates. Author

N90-10186*# Boeing Aerospace Co., Seattle, WA.
DEVELOPMENT OF PRESSURE CONTAINMENT AND DAMAGE TOLERANCE TECHNOLOGY FOR COMPOSITE FUSELAGE STRUCTURES IN LARGE TRANSPORT AIRCRAFT
P. J. Smith, L. W. Thomson, and R. D. Wilson Washington Aug. 1986 187 p
(Contract NAS1-17740)
(NASA-CR-3996; NAS 1.26:3996) Avail: NTIS HC A09/MF A01 CSCL 11D

NASA sponsored composites research and development programs were set in place to develop the critical engineering technologies in large transport aircraft structures. This NASA-Boeing program focused on the critical issues of damage tolerance and pressure containment generic to the fuselage structure of large pressurized aircraft. Skin-stringer and honeycomb sandwich composite fuselage shell designs were evaluated to resolve these issues. Analyses were developed to model the structural response of the fuselage shell designs, and a development test program evaluated the selected design configurations to appropriate load conditions. Author

N90-10187*# McDonnell-Douglas Corp., Long Beach, CA.
LAMINAR FLOW CONTROL PERFORATED WING PANEL DEVELOPMENT
J. E. Fischler et al Oct. 1986 237 p
(Contract NAS1-17506)
(NASA-CR-178166; NAS 1.26:178166) Avail: NTIS HC A11/MF A02 CSCL 11D

Many structural concepts for a wing leading edge laminar flow control hybrid panel were analytically investigated. After many small, medium, and large tests, the selected design was verified. New analytic methods were developed to combine porous titanium sheet bonded to a substructure of fiberglass and carbon/epoxy cloth. At -65 and +160 F test conditions, the critical bond of the porous titanium to the composite failed at lower than anticipated test loads. New cure cycles, design improvements, and test improvements significantly improved the strength and reduced the deflections from thermal and lateral loadings. The wave tolerance limits for turbulence were not exceeded. Consideration of the beam column midbay deflections from the combinations of the axial and lateral loadings and thermal bowing at -65 F, room temperature, and +160 F were included. Many lap shear tests were performed at several cure cycles. Results indicate that sufficient verification was obtained to fabricate a demonstration vehicle. Author

N90-10188*# National Aeronautics and Space Administration. Lewis Research Center, Cleveland, OH.
MATERIALS FOR ENGINE APPLICATIONS ABOVE 3000 DEG F: AN OVERVIEW
Nancy J. Shaw, James A. DiCarlo, Nathan S. Jacobson, Stanley R. Levine, James A. Nesbitt, Hubert B. Probst, William A. Sanders, and Carl A. Stearns Oct. 1987 36 p
(NASA-TM-100169; E-3734; NAS 1.15:100169) Avail: NTIS HC A03/MF A01 CSCL 11D

Materials for future generations of aeropropulsion systems will

be required to perform at ever-increasing temperatures and have properties superior to the current state of the art. Improved engine efficiency can reduce specific fuel consumption and thus increase range and reduce operating costs. The ultimate payoff gain is expected to come when materials are developed which can perform without cooling at gas temperatures to 2200 C (4000 F). An overview is presented of materials for applications above 1650 C (3000 F), some pertinent physical property data, and the rationale used: (1) to arrive at recommendations of material systems that qualify for further investigation, and (2) to develop a proposed plan of research. From an analysis of available thermochemical data it was included that such materials systems must be composed of oxide ceramics. The required structural integrity will be achieved by developing these materials into fiber-reinforced ceramic composites. Author

N90-10189# Delaware Univ., Newark. Center for Composite Materials.
FAILURE BEHAVIOR OF PEEK AND ITS SHORT-FIBER COMPOSITE SYSTEMS Final Report, 1 Mar. 1985 - 28 Feb. 1989
Jerold M. Schultz 12 Jun. 1989 5 p
(Contract DAAG29-85-K-0042)
(AD-A210729; ARO-22301.7-MS) Avail: NTIS HC A01/MF A01 CSCL 11/4

The development of microstructure in PEEK and its short-fiber composites and the effects of such microstructure on mechanical failure were studied. A small-scale injection-molding machine installed in an X-ray diffractometer, was used to follow the development of crystallinity. For neat polymer, increasing the rate of injection increased the crystallization rate. Fibers sometimes slowed crystallization, due to polymer relaxation between the fibers. Fracture behavior in oriented PEEK was found to be highly anisotropy in the elastic modulus. Spherulite size was controlled by self-seeding. The fracture toughness was sound to increase with spherulite size. GRA

N90-10190# Army Materials Technology Lab., Watertown, MA.
FIELD REPAIR OF COMPOSITE MATERIALS IN ARMY SERVICE: PLANNING FOR THE FUTURE Final Report
Michael S. Sennett May 1989 20 p
(DA Proj. 1L2-63102-DO-71)
(AD-A210732; MTL-TR-89-45) Avail: NTIS HC A03/MF A01 CSCL 11/4

A discussion of fiber-reinforced polymer matrix composite repair technology as it relates to Army requirements is presented. The organizational of composite field repair research and development efforts within the Department of Defense (DOD) is reviewed. Recommendations are made for the establishment of a centralized Army composite field repair research and developement effort. Ongoing composite field repair programs in DOD are listed in the Appendix. GRA

25 INORGANIC AND PHYSICAL CHEMISTRY

Includes chemical analysis, e.g., chromatography; combustion theory; electrochemistry; and photochemistry.

For related information see also *77 Thermodynamics and Statistical Physics.*.

N90-10191# Advisory Group for Aerospace Research and Development, Neuilly-Sur-Seine (France). Propulsion and Energetics Panel.
COMBUSTION INSTABILITIES IN LIQUID-FUELLED PROPULSION SYSTEMS
Apr. 1989 306 p In ENGLISH and FRENCH Meeting held in Bath, England, 6-7 Oct. 1988
(AGARD-CP-450; ISBN-92-835-0503-4) Copyright Avail: NTIS HC A14/MF A02

The Specialists' Meeting was arranged in the following sessions: Keynote/Overview; Turbine Engine Development Experience; Rocket and Ramjet Development Experience; and Theoretical Modeling and Experimental Methods and Results. The technical evaluation report is included at the beginning of the proceedings. Questions and answers of the discussions follow each paper. For individual titles, see N90-10192 through N90-10207.

N90-10192# California Inst. of Tech., Pasadena.
COMBUSTION INSTABILITIES IN LIQUID-FUELED PROPULSION SYSTEMS: AN OVERVIEW
F. E. C. Culick *In* AGARD, Combustion Instabilities in Liquid-Fuelled Propulsion Systems Apr. 1989 73 p Sponsored in part by California Inst. of Technology; Navy; AF; and Hersh Acoustical Engineering (For primary document see N90-10191 01-25)
Copyright Avail: NTIS HC A14/MF A02

Combustion of reactants in a confined volume favors excitation of unsteady motions over a broad range of frequencies. A relatively small conversion of the energy released will produce both random fluctuations or noise, and, under many circumstances, organized oscillations generically called combustion instabilities. Owing to the high energy densities and low losses in combustion chambers designed for propulsion systems, the likelihood of combustion instabilities is high. The accompanying heat transfer to exposed surfaces, and structural vibrations are often unacceptable, causing failure in extreme cases. Combustion instabilities are briefly reviewed in liquid-fueled propulsion systems; rockets, ramjets, and thrust augmentors - with emphasis on work accomplished during the past decade. To provide a common framework for discussing the wide range of works, a theory of two-phase flow is reviewed as the basis for an approximate analysis of combustion instabilities. The analysis is directed primarily to treatment of linear stability; it is sufficiently general to accommodate all processes occurring in actual systems. A new result was obtained for an extended form of Rayleigh's criterion and its relation to the growth constant for unstable waves. The chief mechanisms for combustion instabilities in liquid-fueled systems are reviewed, followed by a summary of the common methods of analysis and applications to the three classes of propulsion systems. Control of instabilities by passive and active means is examined briefly. Author

N90-10193# Pratt and Whitney Aircraft, West Palm Beach, FL. Government Engine Business.
COMBUSTOR INFLUENCE ON FIGHTER ENGINE OPERABILITY
Thomas L. DuBell and Anthony J. Cifone (Naval Air Propulsion Test Center, Trenton, NJ.) *In* AGARD, Combustion Instabilities in Liquid-Fuelled Propulsion Systems Apr. 1989 5 p (For primary document see N90-10191 01-25)
Copyright Avail: NTIS HC A14/MF A02

An aspect of combustion instability that is generally unrecognized, but which has a critical influence on aircraft gas turbine engine operability is discussed. The basic lean combustion limit (static stability) of a combustor, when coupled with engine system dynamics, can result in the inability of an engine to recover from a compressor stall. This is a most serious event for a tactical fighter/attack aircraft engaged in air combat. The coupling of combustor static stability characteristics with engine system dynamics is reviewed, a hypothesis presented, solution approaches suggested and plans to address this challenge discussed. Author

N90-10194# Rolls-Royce Ltd., Bristol (England).
CHARACTERISTICS OF COMBUSTION DRIVEN PRESSURE OSCILLATIONS IN ADVANCED TURBO-FAN ENGINES WITH AFTERBURNER
B. E. Henderson and J. S. Lewis *In* AGARD, Combustion Instabilities in Liquid-Fuelled Propulsion Systems Apr. 1989 8 p (For primary document see N90-10191 01-25)
Copyright Avail: NTIS HC A14/MF A02

Development of a high thrust to weight ratio engine requires that the maximum afterburner thrust boost is achieved. The achievement of this thrust boost must be free of potentially damaging pressure oscillations. The characteristics of both low

and high frequency combustion driven pressure oscillations associated with the afterburner of an advanced turbo-fan engine are described. These oscillations are related to the geometry and flow conditions of the afterburner and engine. Models of the characteristics have been developed based on experimental and theoretical techniques. It is shown how these were used to ensure unrestricted operation of the afterburner system throughout the required operating range. Author

N90-10195# General Electric Co., Cincinnati, OH. Aircraft Engines.

DYNAMIC INSTABILITY CHARACTERISTICS OF AIRCRAFT TURBINE ENGINE COMBUSTORS **c07**

M. J. Kenworthy, D. W. Bahr, P. Mungur, D. L. Burrus, J. M. Mehta, and Anthony J. Cifone (Naval Air Propulsion Test Center, Trenton, NJ.) *In* AGARD, Combustion Instabilities in Liquid-Fuelled Propulsion Systems Apr. 1989 13 p (For primary document see N90-10191 01-25)

Copyright Avail: NTIS HC A14/MF A02

Many aircraft turbine engine combustors exhibit dynamic instabilities at subidle and idle operating conditions. These instabilities can result in objectionable noise and, in some instances, compressor stall problems. To permit analytical assessments of these phenomena, an aeroacoustic model of these combustor instabilities was developed. To calibrate and validate this model, sector rig tests of the CF6-80A engine combustor were conducted. In these tests, the frequencies and amplitudes of the instabilities and the acoustic characteristics of the combustor were measured. Additional tests in a F101/F110/CFM56 sector combustor rig are planned. The test results compare well with the theory. The following conclusions are drawn from the portion of the work completed to date: (1) audible noise is a resonant acoustic wave within the cavity as predicted by the analytical model; (2) the acoustic wave responds strongly at the fuel-air ratio with the optimum time lag between the fuel injector and the heat release region, consistent with the analytical model; and (3) the analytical model predictions are in generally good agreement with the CF6-80A combustor test data, but further experiments with better defined end conditions are being obtained for a more complete validation. Author

N90-10196# Office National d'Etudes et de Recherches Aerospatiales, Paris (France).

EXPERIMENTAL STUDY ON THE STABILITY OF SMALL ROCKET ENGINES WITH STORABLE LIQUID PROPELLANTS [RECHERCHE EXPERIMENTALE SUR LA STABILITE DES PETITS MOTEURS FUSEES A ERGOLS STOCKABLES] **c20**

Robert Foucaud and Renaud Lecourt *In* AGARD, Combustion Instabilities in Liquid-Fuelled Propulsion Systems Apr. 1989 8 p In FRENCH; ENGLISH summary Previously announced in IAA as A89-31804 (For primary document see N90-10191 01-25)

Copyright Avail: NTIS HC A14/MF A02

The stability of small rocket engines with storable liquid propellants was quantified and the sensitivity of the injection zone to an acoustic disturbance measured. In the method, the rocket is periodically destabilized near its first longitudinal acoustic mode by means of an intermittent modulation of the nozzle neck. Results are presented for axial injectors, where the acoustic disturbance is mainly a pressure oscillation, and radial injectors, where the acoustic disturbance is mainly a velocity oscillation. IAA

N90-10197# Messerschmitt-Boelkow-Blohm G.m.b.H., Munich (Germany, F.R.). Kommunikationssysteme und Antriebe.

LOW FREQUENCY AND HIGH FREQUENCY COMBUSTION OSCILLATION PHENOMENA INSIDE A ROCKET COMBUSTION CHAMBER FED BY LIQUID OR GASEOUS PROPELLANTS **c20**

D. Preclik and P. Spagna *In* AGARD, Combustion Instabilities in Liquid-Fuelled Propulsion Systems Apr. 1989 18 p (For primary document see N90-10191 01-25)

Copyright Avail: NTIS HC A14/MF A02

Combustion instability phenomena inside a rocket combustion chamber fed by liquid or gaseous propellants is investigated. The interpretation relies, among others, on the combustion time lag theory and the use of linear transfer functions for the different elements building the closed loop transfer function of the system. Author

N90-10198# Office National d'Etudes et de Recherches Aerospatiales, Paris (France).

EFFECTS OF LOW-FREQUENCY INSTABILITIES ON THE OPERATION OF RAMJET AIR INLETS [EFFETS DES INSTABILITES DE BASSE FREQUENCE SUR LE FONCTIONNEMENT DES PRISES D'AIR DE STATOREACTEUR] **c07**

C. Sans *In* AGARD, Combustion Instabilities in Liquid-Fuelled Propulsion Systems Apr. 1989 12 p In FRENCH; ENGLISH summary Previously announced in IAA as A89-29285 (For primary document see N90-10191 01-25)

Copyright Avail: NTIS HC A14/MF A02

The effect of low-frequency instabilities on ramjet air inlet performance was experimentally studied using an axisymmetric inlet equipped with a device providing large-pressure fluctuations of between 0 and 200 Hz. Results obtained at Mach 2 demonstrate that the instabilities do not interfere with the operation of the inlet, except for the case of subcritical conditions. The internal boundary-layer intake is shown to drastically reduce the pressure fluctuations. IAA

N90-10199# Naval Weapons Center, China Lake, CA. Airbreathing Propulsion Branch.

RECENT DEVELOPMENTS IN RAMJET PRESSURE OSCILLATION TECHNOLOGY **c07**

P. A. Chun, J. A. Loundagin, J. A. Nabity, and S. E. Ayler *In* AGARD, Combustion Instabilities in Liquid-Fuelled Propulsion Systems Apr. 1989 13 p (For primary document see N90-10191 01-25)

Copyright Avail: NTIS HC A14/MF A02

Dynamic matching of a supersonic inlet and combustor is a major consideration in ramjet propulsion development. The inlet shock system present under supersonic speeds must be kept stable under all engine operating conditions. An unstable shock system could result in inlet unstart and/or buzz and undesirable pressure oscillations in the ramjet engine. To date, there is no technique for determining if a particular ramjet engine configuration will have combustion-induced pressure oscillations. Current experimental and theoretical techniques applied to the characterization of liquid fuel ramjet combustors are summarized. Comparisons between steady-state and dynamic data are provided to show how both types of information are used to interpret engine behavior. Author

N90-10200# Cambridge Univ. (England). Dept. of Engineering.

REHEAT BUZZ: AN ACOUSTICALLY COUPLED COMBUSTION INSTABILITY **c07**

A. P. Dowling *In* AGARD, Combustion Instabilities in Liquid-Fuelled Propulsion Systems Apr. 1989 16 p (For primary document see N90-10191 01-25)

Copyright Avail: NTIS HC A14/MF A02

Reheat buzz is a low frequency instability of afterburners. It is caused by the interaction of combustion and acoustic waves within the reheat duct. The acoustic waves perturb the combustion, while the unsteady combustion generates yet more sound leading to the possibility of instability. A simple theory was developed and tested by comparison with results obtained on a premixed rig. The theory is able to predict the frequency of the instability and the mode shape, accurately reproducing the effect of changes in flow rate, inlet temperature, duct length and fuel-air ratio. Author

N90-10201# Otago Univ., Dunedin (New Zealand). Dept. of Physics.

ATTENUATION OF REHEAT BUZZ BY ACTIVE CONTROL **c07**

P. J. Langhorne and N. Hooper (Cambridge Univ., England) *In* AGARD, Combustion Instabilities in Liquid-Fuelled Propulsion

Systems Apr. 1989 17 p Sponsored in part by Rolls-Royce plc, London, England (For primary document see N90-10191 01-25)
Copyright Avail: NTIS HC A14/MF A02

Reheat buzz is a low frequency longitudinal pressure fluctuation which can be excited by flame/sound field interaction in the afterburner of a jet aeroengine operating at high fuel to air ratios. Active control techniques were already applied to control a similar combustion instability on a rig. In this previous case the controller modified the upstream boundary condition by unsteadily altering the mass flow of premixed gas. This method is not readily applicable to an engine. It is demonstrated that similar achievements are possible with the suitably-phased addition of extra fuel. The mechanical power requirements of this controller are modest and the system is easy to implement. Author

N90-10202*# Flow Research, Inc., Kent, WA.
NUMERICAL SIMULATION OF PRESSURE OSCILLATIONS IN A RAMJET COMBUSTOR **c07**
Wen-Huei Jou and Suresh Menon *In* AGARD, Combustion Instabilities in Liquid-Fuelled Propulsion Systems Apr. 1989 25 p Sponsored in part by NASA. Lewis Research Center; and by NASA. Ames Research Center (For primary document see N90-10191 01-25)
(Contract N00014-84-C-0359)
Copyright Avail: NTIS HC A14/MF A02 CSCL 21E

Large-eddy simulations of compressible cold flow in a ramjet combustor configuration were performed. The objectives were to investigate the mechanisms for vortex-acoustic interaction in such a device and to develop a simulation method that can be extended to cases with combustion heat release to study combustion instability. From the simulation, it was found that the separated shear layer rolls up into concentrated vortices that merge to form large coherent structures. These vortices interact with the choked nozzle downstream to produce an axial acoustic dipole. The spectrum of the pressure fluctuation at the base of the backward-facing step shows that there are two types of oscillations: an acoustic resonant mode and a vortex-acoustic coupled mode. Based on the flow physics observed in the simulations, a simple one-dimensional model for the vortex-acoustic coupled mode was proposed. The eigenvalue problem based on this model was solved to obtain the frequency of the coupled mode. Author

N90-10203# Office National d'Etudes et de Recherches Aerospatiales, Paris (France).
NUMERICAL SIMULATION OF UNSTEADY COMBUSTION IN A DUMP COMBUSTOR [SIMULATION NUMERIQUE DU FONCTIONNEMENT INSTATIONNAIRE D'UN FOYER A ELARGISSEMENT BRUSQUE] **c07**
F. Garnier, B. Labegorre, M. Serrano, and A. Laverdant *In* AGARD, Combustion Instabilities in Liquid-Fuelled Propulsion Systems Apr. 1989 28 p In FRENCH; ENGLISH summary (For primary document see N90-10191 01-25)
Copyright Avail: NTIS HC A14/MF A02

Basic investigations can be of great interest in the control of high frequency combustion instability in ramjets, in particular by identification of amplifying and damping mechanism of instabilities and of their coupling. With the advent of vectorized computers and the progress of numerical methods, simulation of unsteady, biphasic and three-dimensional combustion is now possible. In this perspective, ONERA has undertaken the adaptation of a computer code, KIVA, precedently developed by the Los Alamos National Laboratory for diesel engines study; this adaptation is essentially concerned with the introduction of inflow and outflow. The application is made on a dump combustor with liquid fuel injection. A detailed description of physico-chemical mechanism involved is presented and the first numerical results obtained are compared with similar ones. Author

N90-10204# California State Univ., Sacramento. Dept. of Mechanical Engineering.
VERY-LOW-FREQUENCY OSCILLATIONS IN LIQUID-FUELED RAMJETS **c07**
Frederick H. Reardon *In* AGARD, Combustion Instabilities in Liquid-Fuelled Propulsion Systems Apr. 1989 12 p (For primary document see N90-10191 01-25)
(Contract F33615-81-C-2078)
Copyright Avail: NTIS HC A14/MF A02

Very-low-frequency (bulk-mode) oscillations were studied, making use of experimental data gathered at the Air Force Wright Aeronautical Laboratories. Only those oscillations in which the acoustic resonance characteristics of the combustor were not excited were considered. More than 200 cases of such oscillations in coaxial-dump combustors were examined. Correlations of oscillation incidence, frequency and amplitude were made in terms of design and operating parameters, including inlet diameter and length, combustor diameter and length-to-diameter ratio, air inlet temperature and fuel-air ratio. An analytical model was developed with which the effects of various oscillation driving mechanisms were examined and compared with the experimental data. Mechanisms considered were: combustion rate fluctuations resulting from fluctuating flow rates of fuel and air, combustion energy release rate variations due to pressure and temperature fluctuations in the flame zone, distortion of the flame zone by vortices shed at the dump plane, generation of an oscillating pressure field by vortex shedding at the dump plane interacting with the exhaust nozzle contraction, and entropy (convective) waves, resulting from fuel/air ratio oscillations, that reflect from the nozzle as pressure waves. Calculations using the analytical model showed agreement with experimental results for nearly 70 percent of the tests examined. The vortex and entropy wave mechanisms did not substantially improve the model's predictive ability. Author

N90-10205# Imperial Coll. of Science and Technology, London (England).
OSCILLATIONS IN NON-AXISYMMETRIC DUMP COMBUSTORS
J. H. Whitelaw, S. Sivasegaram, K. C. Schadow, and E. Gutmark (Naval Weapons Center, China Lake, CA.) *In* AGARD, Combustion Instabilities in Liquid-Fuelled Propulsion Systems Apr. 1989 12 p (For primary document see N90-10191 01-25)
Copyright Avail: NTIS HC A14/MF A02

Instabilities in dump combustors with triangular and round ducts were investigated with expansion ratio, eccentricity of the dump, equivalence ratio and method of injecting the gaseous fuel as variables, and with and without exit nozzles. The shear flow developing from the vertex of a triangular duct is free from large-scale coherent structures, and the injection of fuel close to the vertices of a triangular upstream duct made the flow less susceptible to periodic heat release and resulted in wider ranges of flammability and stability. This effect is quantified for different arrangements of injection. The effect of eccentricity on flammability and stability characteristics is shown to be unimportant for dump-plane area ratios greater than 2.5 and rough combustion in open-ended ducts gave rise to quarter-wave oscillations while the presence of an exit nozzle caused bulk-mode frequencies to dominate. Author

N90-10206# Naval Research Lab., Washington, DC. Lab. for Computational Physics and Fluid Dynamics.
ACOUSTIC-VORTEX-CHEMICAL INTERACTIONS IN AN IDEALIZED RAMJET **c07**
K. Kailasanath, J. H. Gardner, J. P. Boris, and Elaine S. Oran *In* AGARD, Combustion Instabilities in Liquid-Fuelled Propulsion Systems Apr. 1989 13 p Sponsored in part by Navy (For primary document see N90-10191 01-25)
Copyright Avail: NTIS HC A14/MF A02

A potentially important source of large pressure oscillations in combustors is an instability induced by the interactions between large-scale vortex structures, acoustic waves, and chemical energy release. To study these interactions, time-dependent, compressible numerical simulations of the flow field in an idealized ramjet consisting of an axisymmetric inlet and combustor and a choked nozzle were performed. These simulations have allowed the isolation of the interactions between acoustic waves and large-scale

vortex structures and then to study the effects of energy release on the flow field. A number of parameters such as inflow Mach number, inlet and combustor acoustics and energy release rates have been systematically varied in the simulations. A summary of the observations from these various simulations are presented in this paper. The nonreactive flow calculations show complex interactions among the natural instability frequency of the shear layer at the inlet-combustor junction and the acoustics of both the inlet and the combustor. Vortex shedding usually occurs at the natural instability frequency of the initially laminar shear layer but vortex mergings are affected by the acoustic frequencies of the ramjet. When the frequency of the first longitudinal acoustic mode of the combustor is near the natural instability frequency of the shear layer, then vortex shedding is observed at the acoustic frequency. In many cases the entire flow oscillates at a low frequency which corresponds to that of a quarter-wave mode in the inlet. In these cases, the vortex-merging patterns in the combustor can be explained on the basis of an interaction between the acoustics of the inlet and the combustor. For the particular reactive flow case discussed, energy release alters the flow field substantially. In the first cycle after ignition, fluid expansion due to energy release quickly destroys the pattern of vortex mergings observed in the cold flow and a new pattern emerges that is dominated by a large vortex. In subsequent cycles, most of the energy release occurs after vortex mergings have produced this large vortex. Energy release in this large vortex is in phase with the pressure oscillation over a substantial region of the combustor. This results in the observed amplification of the low-frequency oscillations and leads to combustion instability. Author

N90-10207# Ente Nazionale per l'Energia Elettrica, Pisa (Italy).
COMBUSTION-DRIVEN OSCILLATION IN LARGE COMBUSTION SYSTEMS FOR POWER GENERATION
G. Benelli, V. Cossalter (Padua Univ., Italy), and G. DeMichele *In* AGARD, Combustion Instabilities in Liquid-Fuelled Propulsion Systems Apr. 1989 11 p (For primary document see N90-10191 01-25)
Copyright Avail: NTIS HC A14/MF A02

Intense pressure oscillations reaching peak values of about 1200 Pa in the 50 divided by 100 Hz range occurred in the combustion chamber of a 480 t/h steam generator, fed with gas or oil and gas together. Through experimental analysis it was possible to identify the acoustic modes of the furnace of the burner. Furthermore, a finite-element mathematical model was devised for modal analysis of the combustion chamber; the numerical results were in close agreement with the experimental data. The analysis carried out showed what modifications needed to be made to the geometry of the burners in order to reduce the self-excited vibrations to acceptable limits. Author

N90-10208# Kentucky Univ., Lexington. Dept. of Materials Science and Engineering.
STRUCTURAL AND SURFACE CHARACTERIZATION OF DISPERSED METAL CATALYSTS Final Report, 1 Sep. 1986 - 31 Dec. 1988
P. J. Reucroft, R. J. DeAngelis, and J. Bentley (Oak Ridge National Lab., TN.) 1988 13 p
(Contract DE-FG05-85ER-45186)
(DE89-014530; DOE/ER-45186/T1) Avail: NTIS HC A03/MF A01

The studies that were conducted in the last two year period have extended the research activities that were initiated in 1984. Dispersed metal catalyst systems and supports investigated in the most recent phase of the project include: Ni/Co/SiO2, Co/SiO2, Ni/SiO2 and ZrO2. A model catalyst system comprising Pt layers/particles on porous and non-porous silica was also investigated and a study was initiated on Co, Ni and Co/Ni layers on SiO2. Structural and surface characterization techniques that were employed include: transmission electron microscopy (TEM), scanning electron microscopy (SEM), analytical electron microscopy (AEM), X-ray diffraction (XRD) and ion scattering spectroscopy (ISS). In addition, catalyst activity was evaluated by measuring the kinetics of hydrocarbon formation from CO/H2 mixtures. DOE

N90-10209# Ultrasystems, Inc., Irvine, CA.
REACTIONS OF HYDROGEN CHLORIDE AND BORON TRICHLORIDE WITH TRIMETHYLSILYLAMINO GROUPS
K. J. Paciorek, R. H. Kratzer, J. H. Nakahara, and W. Krone-Schmidt 4 Apr. 1989 13 p Submitted for publication
(Contract N00014-87-C-0713)
(AD-A209006; TR-8) Avail: NTIS HC A03/MF A01 CSCL 07/4

Reactions of hydrogen chloride and triethylamine hydrochloride with the B-tris (bis-(trimethylsilyl)amino) borazine failed to give B-tris(trimethylsilylamino) borazine, but following liberation of Me3SiCl resulted in condensations. At lower temperatures ammonia was eliminated; at higher temperatures hexamethyldisilazane. The possible mechanisms are postulated. Boron trichloride action on tris(trimethylsilyl)amine and 1,3-trimethylsilyl 2,4-bis-(trimethylsilyl)amino 1,3,-diaza diboretane was investigated. In the first instance the clevage of the Si-N bond occurred to a very low degree, the major process was the replacement of the methyl groups on silicon by chlorine atoms. In the case of diboretane only the second reaction took place. GRA

N90-10210# Technische Univ., Vienna (Austria). Inst. fuer Technische Elektrochemie.
IMPEDANCE STUDIES OF THE CELL Pt/Ag+ CONDUCTING GLASS/Ag BETA-ALUMINA/Pt Technical Report No. 20, Aug. 1988 - Jul. 1989
H. Durakpasa, P. Linhardt, and M. W. Breiter 15 Jun. 1989 11 p Submitted for publication
(Contract N00014-83-K-0498)
(AD-A209820) Avail: NTIS HC A03/MF A01 CSCL 07/4

The qualitative comparison of the impedance behavior of the 3 cells platinum/silver(+) conducting glass/Ag beta alumina; Pt/glass/Pt and Pt/beta/Pt leads to the conclusion that the properties of the cell Pt/glass/beta/Pt are determined by those of the interfaces Pt/glass and beta/Pt at low and intermediate frequencies. At high frequencies the contributions of the bulk impedances become predominant. A contribution from the impedance of the interface glass/beta is small with respect to the other contributions. The transfer of the Ag(+) ion from the amorphous glass phase into the crystalline beta alumina is rapid. GRA

N90-10211# California Univ., Davis. Dept. of Chemistry.
SOLVENT EFFECTS ON THE KINETICS OF ELECTROREDUCTION OF Cu(I) AT MERCURY
W. Ronald Fawcett and Colby A. Foss, Jr. 1 Jun. 1989 9 p Presented at the ACS Central Regional Meeting, Symposium Honoring Professor E. Yeager, Cleveland, OH, Jun. 1989
(Contract N00014-87-K-0541)
(AD-A209423; TR-11) Avail: NTIS HC A02/MF A01 CSCL 07/4

The solvent plays an important role in amalgam formation reactions when it forms the primary solvation sheath of the reactant. A study is reported of the role of the solvent in the kinetics of reduction of copper (I) in nitrile solvents where the monovalent ion is stable. The standard rate constants for reduction of Cu (I) in acetonitrile (AN) and benzonitrile (BN) are virtually identical (0.13 and .16 cm/s, respectively) at mercury with close to unity for the reduction process in both solvents in spite of the fact that the double layer structure is very different. Kinetic parameters including heats of activation in these solvents and other nitriles are presented and discussed with respect to intrinsic asymmetry of the reaction barrier. GRA

N90-10212# California Univ., Davis. Dept. of Chemistry.
POTENTIAL DEPENDENCE OF THE ELEMENTARY STEPS IN THE KINETICS OF ELECTRODE REACTIONS INVOLVING AMALGAM FORMATION
W. Ronald Fawcett 15 Sep. 1988 45 p Submitted for publication

(Contract N00014-87-K-0541)
(AD-A209424; TR-7) Avail: NTIS HC A03/MF A01 CSCL 07/4

The effect of the double layer on the kinetics of the possible elementary steps in amalgam formation reactions are described in detail. The steps considered are electron transfer, ion transfer, adsorption, and metal incorporation. It is shown that the rate equations for all elementary steps have the same form, but that they differ considerably with respect to their kinetic parameters, namely, the standard rate constant and apparent transfer coefficient. As the location of the elementary step moves closer to the interface, its potential dependence increases and larger values of the apparent transfer coefficient are observed. Double layer effects are also considered for a more complex mechanism in which more than one step is rate determining. GRA

N90-10213# Massachusetts Inst. of Tech., Cambridge. Dept. of Chemistry.
COMBINING SPONTANEOUS MOLECULAR ASSEMBLY WITH MICROFABRICATION TO PATTERN SURFACES: SELECTIVE BINDING OF ISONITRILES TO PLATINUM MICROWIRES AND CHARACTERIZATION BY ELECTROCHEMISTRY AND SURFACE SPECTROSCOPY Technical Interim Report No. 31, 1 Jun. 1988 - 1 Jun. 1989
James J. Hickman, Chaofeng Zou, David Ofer, Pierre D. Harvey, and Mark S. Wrighton 12 Jun. 1989 16 p
(Contract N00014-84-K-0553)
(AD-A209528) Avail: NTIS HC A03/MF A01 CSCL 07/4

Platinum electrodes can be functionalized by spontaneous binding of p-(ferrocenyl) phenylisonitrile-I, or m-chloro-p (ferrocenyl)phenylisonitrile-II, by reaction of pretreated Pt with approx. 1 mM I or II in Acetonitrile at 298 K. FTIR is consistent with attachment of I or II via a -NC-Pt linkage. XPS, AES, and electromechanical characterizations are consistent with attachment of one monolayer of redox active material with a potential of approx. +0.6 V vs. silver due to the ferrocenyl moiety. XPS and AES show selective binding (greater than 100:1) of I or II to Pt compared to the silicon nitride substrate of Pt microelectrode arrays. An AES line scan shows the isonitrile to only be on the eight Pt electrodes each approx. 2 micrometers x approx. 90 micrometers long x 0.1 micrometer thick and separated from each other by 1.4 micrometers. The data show that spontaneous self-assembly and microfabrication can be used to pattern surfaces with redox active molecular reagents. GRA

N90-10214# Texas Univ., Austin. Dept. of Chemistry.
ELECTROCHEMISTRY IN NEAR-CRITICAL AND SUPERCRITICAL FLUIDS. PART 7: SO2
Carlos R. Cabrera, Edwin Garcia, and Allen J. Bard 12 May 1989 14 p Submitted for publication
(Contract N00014-84-K-0428)
(AD-A208207; TR-13) Avail: NTIS HC A03/MF A01 CSCL 07/2

We describe here the cyclic voltammetry (CV) and chronamperometry of Fe(bpy)3+2 (bpy = 2,2'-bipyridine) in SO2 at temperatures up to 174 C, above the critical point of SO2(Tc=158 C, Pc=77.8 atm), and discuss the effect of temperature on the diffusion coefficient (D) and the electrochemical behavior. Near critical and supercritical fluids are of interest because the solvent properties are very different than those of the liquid form and are adjustable over a wide range by variation of the temperature and pressure. Recent studies have demonstrated that electrochemical experiments can be carried out in supercritical H2O, NH3, CO2/H2O and MeCN. Extension of this methodology to SO2 is important because this solvent has been shown to be a very valuable one for electrochemical studies. GRA

N90-10215# Los Alamos National Lab., NM. Isotope and Nuclear Chemistry Div.
CHEMISTRY OF NITROMETHANE AT VERY HIGH PRESSURE
Stephen F. Agnew, Basil I. Swanson, John Kenney, and Inga Kenney (University of Eastern New Mexico, Portales.) 1989 4 p Presented at the 9th International Symposium on Detonation, Portland, OR, 28 Aug. - 1 Sep. 1989
(Contract W-7405-eng-36)
(DE89-008016; LA-UR-89-689; CONF-890811-7) Avail: NTIS HC A01/MF A02

Decomposition of nitromethane is reported over the range of 115 to 180 C and 0.6 to 8.5 GPa. About 5 (mu)g of nitromethane is compressed with a diamond-anvil cell, heated to the point that reaction occurs, and held typically 10 to 20 minutes at the reaction temperature. The cell is cooled and the volatile contents of the cell are frozen as a thin layer in vacuo and an infrared absorption spectrum is recorded. The three volatile products observed are N2O, CO2, and water, with N2O production peaking at 1.5 GPa, 135 C, and 35 percent of NME; CO2 production peaking at 3.5 GPa, 135 C, and 65 percent of NME, and water yields at 20 to 50 percent of NME at the highest pressure measured, 8.5 GPa and 175 C. Water yields were difficult to quantify due to background contamination. Results indicate three different reactions for solid NME dependent primarily on the pressure of the reaction, and that fluid NME does not decompose at 0.6 GPa and 175 C, although the solid decomposes readily at 1.1 GPa and 120 C. It is concluded that, while various decomposition mechanisms are possible, the initial step CH3NO2 yields CH3 + NO2 is very unlikely. DOE

N90-10216# California Univ., Berkeley. Dept. of Chemistry.
REACTION OF OXYGEN WITH ALLENE Ph.D. Thesis
Sheng-yu Huang Jul. 1988 231 p Prepared in cooperation with California Univ., Berkeley. Lawrence Berkeley Lab.
(Contract DE-AC03-76SF-00098)
(DE89-015219; LBL-26537) Avail: NTIS HC A11/MF A02

Elastic scattering studies carried out independently of the work related to the title forms the first section of the dissertation. The low-energy elastic scattering of He with Ar, Kr, Xe was studied by molecular beam techniques. Two potential forms, exponential-spline-Morse Morse spline-van de Waals (ESMMSV) and Simon-Parr-Finlan-Dunham (SPFD), were used to fit the measured differential cross section. Elastic scattering theory and experimental details are introduced. The reactive scattering of O((sup 3)P) with allene was studied using crossed molecular beams. Differing from the well known central carbon attack (CCA) mechanism in which the final products, carbon monoxide and ethylene, are obtained via a ring intermediate, a new mechanism, terminal carbon attack (TCA), was observed. The production of O(3 P) atoms by radio frequency discharge is also introduced. To assist understanding of the experiments a multi-configuration self-consistent field (MCSCF) study of the reaction of O(3 P) with allene was carried out. The key feature of the oxygen-allene potential energy surface for both CCA and TCA channels has been calculated with single-zeta (SZ), double-zeta (DZ), and double-zeta plus polarization (DZP) basis sets. Finally, an algorithm for optimizing the trial wavefunction in quantum Monte Carlo calculations was developed. With the application of group theory, a symmetry-constrained optimization process can yield an improved trial wavefunction for the calculation of excited electronic state energies as well as the ground-state energy. Several applications are discussed. DOE

N90-10217# Pennsylvania State Univ., University Park. Dept. of Mechanical Engineering.
UPWARD FLAME SPREAD ON VERTICAL WALLS Final Report
Anil K. Kulkarni Jun. 1989 70 p
(Grant NIST-60NANB4D0037)
(PB89-214787; NIST/GCR-89/565) Avail: NTIS HC A04/MF A01 CSCL 21B

Reported is a study of upward flame spread on vertical walls. First, a detailed review of literature on upward flame spread is presented. A complete procedure for predicting upward flame spread on practical materials, which can be used in a global fire hazard assessment model, is then described. Experimental results on upward flame spread on various materials are obtained and the validity of the model is established. Author

N90-10218# Flow Research, Inc., Kent, WA. Dept. of Mechanical Engineering.
DIRECT NUMERICAL SIMULATION OF TURBULENT FREE SHEAR FLOWS Final Report, 1 Jul. 1982 - 30 Apr. 1989
Ralph W. Metcalfe, Chia-fon Lee, and F. Hussain Jul. 1989 27 p Presented at the AIAA Conference, Clear Lake, TX, 18 May 1989
(Contract N00014-82-C-0600)
(AD-A210161; FLOW-RR-480) Avail: NTIS HC A03/MF A01 CSCL 21/2

In order to improve combustor efficiency, to reduce pollutant emissions, etc., the ability to accurately model turbulent chemical reactions in a combustor is essential. Several approaches involving statistical methods were conducted. An alternative method to solve this problem termed direct numerical simulations was proven to be very successful in gaining an understanding of the key features of a turbulent reacting flow. The role of large-scale coherent structures was investigated in enhancing mixing and chemical reaction in turbulent free shear flows by analyzing direct numerical simulations of temporally growing reacting mixing layers. The streamwise vortical modes are found to enhance the reaction rate by convoluting the reaction surface and enhancing the mixing of the two species, although the relative significance of this effect is very sensitive to species diffusivity. For certain Schmidt numbers, the effects of flame shortening are balanced by flame sheet stretching by the vortex pairing process. The behavior of the helicity density, dissipation, and enstrophy production in the braid region was examined. There does not appear to be a simple correlation between the amplitude of the helicity density and the position of some very strong coherent structures in this flow. GRA

N90-10219# California Univ., Berkeley. Lawrence Berkeley Lab. Materials and Chemical Sciences Div.
RAMAN CHARACTERIZATION OF HIGH TEMPERATURE MATERIALS USING AN IMAGING DETECTOR
Gerd M. Rosenblatt and D. Kirk Veirs 15 Mar. 1989 24 p Presented at the 6th International Conference on High Temperatures: Chemistry of Inorganic Materials, Gaithersburg, MD, 3-7 Apr. 1989
(Contract DE-AC03-76SF-00098)
(DE89-016308; LBL-26130; CONF-890435-5) Avail: NTIS HC A03/MF A01

The characterization of materials by Raman spectroscopy has been advanced by recent technological developments in light detectors. Imaging photomultiplier-tube detectors are now available that impart position information in two dimensions while retaining photon-counting sensitivity, effectively greatly reducing noise. The combination of sensitivity and reduced noise allows smaller amounts of material to be analyzed. The ability to observe small amount of material when coupled with position information makes possible Raman characterization in which many spatial elements are analyzed simultaneously. Raman spectroscopy making use of these capabilities has been used, for instance, to analyze the phases present in carbon films and fibers and to map phase-transformed zones accompanying crack propagation in toughened zirconia ceramics. DOE

N90-10220# Purdue Univ., West Lafayette, IN. Dept. of Chemistry.
SOLVENT RELAXATION IN ELECTRON-TRANSFER REACTIONS: COMPARISONS BETWEEN BARRIER-CROSSING DYNAMICS IN WATER AND POLAR APROTIC MEDIA Technical Report No. 89, 1 Oct. 1987 - 30 Jun. 1989
Roger M. Nielson, George E. McManis, and Michael J. Weaver 1 Jul. 1989 19 p Submitted for publication
(Contract N00014-86-K-0556)
(AD-A210212) Avail: NTIS HC A03/MF A01 CSCL 07/4

Rate constants, k sub ex, for electron self exchange of three metallocene redox couples, carboxymethyl (cobaltocenium-cobaltocene) ((CpCO2Me)2Co+o), hydroxymethyl (ferrocenium-ferrocene) ((Cp CpCH2OH)Fe+/o), and trimethylaminomethyl (ferrocenium-ferrocene) ((Cp CpCH2NMe3)-Fe2+/+), obtained using proton NMR line broadening, are utilized along with optical electron transfer energies for the mixed valence biferrocenylacetylene cation to obtain solvent dependent frequencies, Kappa sub el upsilon sub n, in water relative to those in methanol and six aprotic solvents. While (Kappa sub el)(upsilon sub n) for the ferrocene couples is insensitive to the solvent, indicative of nonadiabatic behavior (K sub el less than 1), K sub el upsilon sub n for the cobaltocene couple is responsive to the solvent dynamics. While rapid barrier crossing dynamics are obtained in water, comparable to acetonitrile, acetone, and nitromethane, the influence of high frequency relaxation components in water is less marked than for methanol. GRA

N90-10221# California Univ., Los Angeles. Dept. of Chemistry and Biochemistry.
MONOMERS, POLYMERS AND TRANSITION METAL COMPLEXES BASED UPON CARBORANES Final Report, 3 Mar. 1986 - 28 Feb. 1989
M. Frederick Hawthorne 20 Jun. 1989 6 p
(Contract N00014-86-K-0282)
(AD-A210226) Avail: NTIS HC A02/MF A01 CSCL 07/6

The research involved studies of the reactions of low valent metal carbonyl complexes with arylnitrile oxides resulting in the (3+2) cycloaddition of the arylnitrile oxide to the M-CO bond of metal carbonyl complex. A number of metallacycles were synthesized in good yield by this route, establishing the generality of this reaction. Recent studies were concerned with the nature and synthetic utility of the products resulting from the thermolysis of rhodium- and iridium-containing metallacycles. The accomplishment of an important goal was recently reported, the metallacycle-promoted thermal activation of C-H bonds of saturated hydrocarbons. In short, the thermolysis of selected metallacycles results in the loss of arylnitrile and Carbon dioxide to generate a coordinatively and electronically unsaturated metal fragment which is highly reactive. GRA

N90-10222# Weizmann Inst. of Science, Rehovoth (Israel). Dept. of Membrane Research.
ELECTRICAL FIELD DEPENDENCE OF PROTEIN CONFORMATION AND CHANNEL FUNCTION IN LIPID MEMBRANES OF DIFFERENT COMPOSITIONS Annual Report, 1 Jul. 1988 - 1 Jul. 1989
Israel R. Miller 1 Jul. 1989 11 p
(Contract N00014-87-G-0203; RR04108)
(AD-A210236) Avail: NTIS HC A03/MF A01 CSCL 06/2

The objective is to study the effect of electric field on membrane permeability and on the conformation of membrane proteins and channel forming polypeptides to gain insight on their function as channels or as signal transducing receptors. The research was conducted in model systems, namely lipid monolayers and lipid bilayer membranes. During the 2nd year of the research project, the investigation was continued of the membrane behavior and of the structure of its lipid and protein or polypeptide components under the influence of transmembrane electric fields. The model membranes investigated during this period were lipid monolayers at the mercury electrode/water interface and lipid bilayers with incorporated channel forming polypeptides alamethicin and melittin. The spread lipid monolayers were transferred after their interaction with the polypeptide in the aqueous solution, from the air/water to the mercury/water interface. Their properties were then inferred from their capacitance and ionic permeability at different electrode potentials. Ionic permeability of unilamellar vesicles upon interaction with the channel forming polypeptides and proteins was determined with and without applied diffusion potential. The change in conformation of specific membrane components with applied electric field was studied by circular dichrosim (CD) and Fourier transform infrared (FTIR) measurements. Transmembrane potentials induced were either diffusion potentials (K+ gradient valinomycin) in nonleaky membranes or Donnan potential when high channel concentrations made the membranes leaky to small ions. GRA

N90-10223# Utah Univ., Salt Lake City. Dept. of Chemical Engineering.
MULTIPLE INTERNAL REFLECTION FOURIER TRANSFORM INFRARED SPECTROSCOPY STUDIES OF THIOCYANATE ADSORPTION ON SILVER AND GOLD
Diane B. Parry, Joel M. Harris, and Kevin Ashley (San Jose State Univ., CA.) 1 Jul. 1989 40 p Submitted for publication
(Contract N00014-89-J-1412)
(AD-A210245; ONR-TR-12) Avail: NTIS HC A03/MF A01 CSCL 07/4

Conducting silver and gold coatings on silicon Attenuated Total Reflectance (ATR) plates were employed as transparent electrodes to monitor in situ surface electrochemistry. The multiple internal reflection Fourier transform infrared spectroscopy (MIRFTIRS) technique, used previously to study redox reactions on platinum and iron films, is applied to the study of adsorption processes in the double layer region, in particular, the adsorption of thiocyanate on silver and gold. The MIRFTIRS spectra were found to be essentially free of solution band interference and are compared to surface IR spectra of the same system obtained by other methods. Spectra of thiocyanate adsorbed on gold and silver surfaces were recorded as a function of applied potential and thiocyanate concentration. Evidence of thiocyanate species absorbed to gold via both nitrogen and sulfur atoms was obtained, while only S-bound thiocyanate was clearly observed on silver. GRA

N90-10224# Utah Univ., Salt Lake City. Dept. of Chemistry.
ATTENUATED TOTAL REFLECTION FTIR SPECTROSCOPY FOR MEASURING INTERFACIAL REACTION KINETICS AT SILICA SURFACES Technical Report No. 16, Jul. 1988 - Jul. 1989
Diane B. Parry and Joel M. Harris 1 Jul. 1989 12 p
(Contract N00014-89-J-1412)
(AD-A210314) Avail: NTIS HC A03/MF A01 CSCL 20/5

Attenuated total reflection (ATR) spectroscopy has been adapted to measure the rates of chemical reactions which modify silica surfaces. In this method, a silicon ATR substrate is oxidized to produce a silicon dioxide surface layer, which can be used as a model silica surface in measurements of the rates chemical modification. An ATR flow cell is filled with a solution of a surface active reagent, and spectra are obtained at regular intervals. Confinement of the infrared intensity to the interface by total internal reflection provides a measure of changes in concentrations of species which adsorb or bind to the surface. GRA

N90-10225# University of South Alabama, Mobile. Dept. of Biological Sciences.
POLYPEPTIDE INHIBITORS OF MINERAL SCALING AND CORROSION Annual Report, Jul. 1988 - Jun. 1989
C. S. Sikes, A. P. Wheeler, and Brenda J. Little Jun. 1989 16 p
(Contract N00014-88-K-0428)
(AD-A210507) Avail: NTIS HC A03/MF A01 CSCL 06/1

In the first year of the project, the work has been focused on: (1) synthesis of polypeptides; (2) evaluation of their activities as inhibitors of calcium carbonate and phosphate crystallization; and (3) measurement of their activities as inhibitors of corrosion of mild steel. A set of polyaspartate molecules of specific molecular sizes and other aspartate-enriched peptides were made by automated solid phase methods. Polyaspartate molecules with 1 to 3 serine residues at the N-terminus were phosphorylated post-synthesis using monochlorophosphoric acid. The polyaspartate molecules were very effective inhibitors of calcium carbonate but not calcium phosphate crystallization. Polyaspartate was most effective as an inhibitor of CaCO3 crystal growth at a length of about 15 residues, but a length of about 35 residues was required for maximum inhibition of crystal nucleation. The polyaspartate molecules with terminal phosphoserine residues were extraordinarily active inhibitors of both calcium carbonate and phosphate formation. By use of scanning electron microscopy, the polyaspartate was seen to be bound to electrode surfaces after brief exposures, where it appeared to inhibit both anodic and cathodic reactions at doses used in practice for corrosion inhibition. GRA

N90-10226# Pennsylvania State Univ., University Park. Materials Research Lab.
RAMAN SPECTROSCOPIC STUDY OF THE RARE EARTH SESQUISULFIDES
Diane S. Knight and William B. White 17 Jul. 1989 24 p
(Contract N00014-85-K-0129)
(AD-A210610; TR-1) Avail: NTIS HC A03/MF A01 CSCL 07/4

The sesquisulfides of the rare earths exists in six different crystallographic forms depending on temperature of synthesis and ionic radius of the rare earth. The structures and crystal chemistry were studied intensively. Because of the range of crystal structures and coordination polyhedra of the rare earth ions, it is of interests to examine the vibrational spectra of these compounds. The spectra may then be compared with the vibrational spectra of related ternary rare earth-containing sulfide structures. Raman spectra were measured on carefully synthesized and characterized sesquisulfides of the rare earth ions plus yttrium and scandium. Six structure types are represented. The Raman spectra are diagnostic of the structures type. Raman line widths indicate structural disorder only in the defect gamma type structure. High wavenumber bands shift with ionic radius of the rare earths and only slightly with cation coordination number. GRA

N90-10227# Virginia Univ., Charlottesville.
METAL-ASSISTED SYNTHESES OF BORANES AND CARBORANES Final Report, 14 Mar. 1986 - 14 May 1989
Russell N. Grimes 30 Jun. 1989 10 p
(Contract DAAL03-86-K-0048)
(AD-A210728; ARO-23508.7-CH) Avail: NTIS HC A02/MF A01 CSCL 07/1

Methods were developed for: (1) the systematic preparation of organosubstituted derivatives of small carboranes, especially of the type nido-RRC2B4H6 where R is alkyl, aryl, or arylalkyl groups; (2) oxidative fusion of these compounds to large R2C4B8H8 clusters via transition metal-promoted fusion; (3) conversion of the nido-carboranes to stable (arene)metal(carborane) complexes incorporating first-, second-, or third-row transition series metals; (4) stacking of the metal-carborane complexes to produce novel triple- and multi-decker sandwich complexes containing two or more metal centers; (5) synthesis of B-substituted carboranes and metallacarboranes via controlled regiospecific pathways; and (6) studies of the chemical reactivity of the nido-carboranes and their derived metal complexes. The nonmetallated new carboranes are potentially useful in VHBR (very high burning rate) applications, while the metal sandwich complexes are precursors to high molecular weight polymers or solid state materials having novel electronic properties. GRA

N90-10228# Oklahoma State Univ., Stillwater. Dept. of Chemistry.
HETEROGENEOUS CATALYSTS IN WATER Final Report, 1 Jun. 1986 - 31 May 1989
Warren T. Ford 21 Jul. 1989 23 p
(Contract DAAL03-86-K-0049)
(AD-A210742; ARO-22776.17-CH) Avail: NTIS HC A02/MF A01 CSCL 15/6

The feasibility of performing reactions of organic compounds in aqueous dispersions using catalysts supported on colloidal particles was determined. Such reactions could become the basis of new technology for decontamination of toxic substances, including chemical warfare agents. Oxidation reactions catalyzed by transition metal ions and complexes on latexes, and hydrolysis reactions catalyzed by silica sulfonic acids were studied because of the potential applicability of oxidation and hydrolysis to the decontamination of a wide range of toxic organic compounds. GRA

N90-10229# Massachusetts Inst. of Tech., Cambridge. Dept. Of Chemistry.
THE SYNTHESIS AND STRUCTURE OF NOVEL ANTIMONY THIAMETALLACYCLES Technical Report No. 1
Stephen L. Buchwald, Richard A. Fisher, and William M. Davis 1 Aug. 1989 16 p Submitted for publication
(Contract N00014-88-K-0307)
(AD-A210888; TR-1) Avail: NTIS HC A02/MF A01 CSCL 07/3

Recently a dramatic resurgence of interest in the organometallic chemistry of the main group elements has occurred. To a large degree this renewed activity derives from the utility of main group compounds in fields such as ceramics, electronic and thermochromic materials, and marine antifouling compounds. The development of general, efficient synthetic methods for the preparation of hitherto inaccessible main group organometallics should greatly enhance progress in many of these fields. The preparation and characterization are reported for a new class of main group metallacycle, 4, 5-didehydro-2-thiastibolanes, via a transmetallation from zirconium. GRA

N90-10230# California Univ., Berkeley. Lawrence Berkeley Lab.
THE STRUCTURE DETERMINATION OF MOLECULAR ADSORBATES WITH LARGE UNIT CELLS OR LATTICE-GAS DISORDER ON METAL SURFACES Final Report, 4 Dec. 1985 - 30 Jun. 1989
M. A. VanHove Jun. 1989 6 p
(Contracts MIPR-121-86; MIPR-102-88)
(AD-A210926; ARO-23011.6-CH) Avail: NTIS HC A02/MF A01 CSCL 07/4

For the purpose of structural determination of molecular adsorbates with large unit cells or lattice-gas disorder on metal surfaces, a novel method was developed to handle multiple scattering of electrons by surfaces. The method is particularly suitable for complex and disordered surfaces. It enables a great increase in computational efficiency for the determination of surface structures. In particular, a method of treating electron scattering by chains of atoms (these chains are to be thought of as components of a surface) was developed. These new methods were applied to the interpretation of experimental data, thereby extracting structural information about simple but non-trivial surfaces. The key to the approach is twofold: first, use kinetic electron energies above a few hundred electron volts, so as to obtain forward focusing by atoms; second, treat the surface as a cluster of atoms without regard to periodicity, thereby allowing complex and disordered surface structures. GRA

26 METALLIC MATERIALS

Includes physical, chemical, and mechanical properties of metals, e.g., corrosion; and metallurgy.

N90-10231# Advisory Group for Aerospace Research and Development, Neuilly-Sur-Seine (France). Structures and Materials Panel.
CASTINGS AIRWORTHINESS
May 1989 137 p In ENGLISH and FRENCH Meeting held in Mierlo, Netherlands, 3-7 Oct. 1988
(AGARD-R-762; ISBN-92-835-0507-7) Copyright Avail: NTIS HC A07/MF A01

The question of whether a casting factor, as such, need still be applied to premium quality castings given the improvements in casting technology obtained in recent years, was addressed. For individual titles, see N90-10232 through N90-10245.

N90-10232# Aeronautical Systems Div., Wright-Patterson AFB, OH.
US AIR FORCE CERTIFICATION OF CASTINGS
Walter L. Torrey and Edward A. Davidson *In* AGARD, Castings Airworthiness May 1989 6 p (For primary document see N90-10231 01-26)
Copyright Avail: NTIS HC A07/MF A01

The U.S. Air Force structural certification procedure is described. Static strength and durability and damage tolerance certification requirements are presented. Application to castings is explained, including supporting rationale. Elimination of the casting minimum margin of safety (i.e., factor of safety) can be allowed if a defined procedure is followed. Verification tests and quality assurance requirements are also addressed. Distinction between safety of flight versus non-safety of flight structure and manned versus unmanned applications is made. Author

N90-10233# Service Techniques des Programmes Aeronautiques, Paris (France). Responsable des Materiaux Structuraux.
CASTING FACTORS IMPOSED BY THE FRENCH REGULATION FOR FOUNDRY CASTINGS USED IN MILITARY AIRCRAFT [LES CASTINGS FACTORS IMPOSES PAR LA REGLEMENTATION FRANCAISE POUR LES PIECES DE FONDERIE UTILISEES DANS LES AVIONS MILITAIRES]
Michel Robert *In* AGARD, Castings Airworthiness May 1989 6 p In FRENCH (For primary document see N90-10231 01-26)
Copyright Avail: NTIS HC A07/MF A01

A table summarizing the casting factors imposed on foundry castings to be used in military aircraft is presented and discussed. The principle control and testing requirements for each of three functional classes -- vital, important, and secondary -- are described. Some comments are made regarding the future evolution of casting factors. Transl. by M.G.

N90-10234# Service Techniques des Programmes Aeronautiques, Paris (France).
CASTING AIRWORTHINESS JOINT EUROPEAN CIVIL AUTHORITIES VIEW-POINT
Michel Sancho *In* AGARD, Castings Airworthiness May 1989 6 p (For primary document see N90-10231 01-26)
Copyright Avail: NTIS HC A07/MF A01

After a short introduction on the European regulation, JAR 25 (Joint Airworthiness Requirements), the general certification procedures are described: static, fatigue, damage tolerance, manufacturing. Particular application to casting is discussed, particularly extra factors and damage tolerance evaluation. In conclusion a general overview of civil airworthiness authorities is given. Author

N90-10235# Royal Aircraft Establishment, Farnborough (England). Airworthiness Div.
ROYAL AEROSPACE ESTABLISHMENT: NO PLACE FOR A CASTINGS FACTOR
A. W. Cardrick and C. J. Peel *In* AGARD, Castings Airworthiness May 1989 3 p Presented at the AGARD Workshop on Castings Airworthiness, Mierlo, Netherlands, 5-6 Oct. 1988 (For primary document see N90-10231 01-26)
Copyright Avail: NTIS HC A07/MF A01

The structural design and airworthiness requirements for U.K. military aircraft are published in DEFSTAN 00-970. Once a cast material (and the associated process) has been approved it is treated like any other material; there is no castings factor. This note outlines acceptable procedures for the certification of advanced castings for use in the primary structure of airplanes and helicopters. Author

N90-10236# Messerschmitt-Boelkow-Blohm G.m.b.H., Bremen (Germany, F.R.). Unternehmensbereich Transporter.
CASTINGS, FROM THEORY TO PRACTICAL APPLICATION
R. Genoux *In* AGARD, Castings Airworthiness May 1989 19 p (For primary document see N90-10231 01-26)
Copyright Avail: NTIS HC A07/MF A01

A general summary of the state of the experience made by MBB-UT-Bremen with series castings is presented. From a designer's point of view an attempt is made to make valid statements on the following points: (1) Design/Cost Advantages; (2) Range of Application; (3) Designer's Confidence in Castings;

and (4) Handicap Reduction. These topics are treated in the following chapters: Introduction; Advantages of Casting Design; Designer's Handicap; and Conclusion and Prospects. Author

N90-10237# Aeritalia S.p.A., Turin (Italy). Direzione Tecnica.
EVALUATION OF TITANIUM CASTINGS FOR AEROSPACE COMPONENTS
G. Arsento *In* AGARD, Castings Airworthiness May 1989 18 p (For primary document see N90-10231 01-26)
Copyright Avail: NTIS HC A07/MF A01

A significant potential cost saving could be obtained by the introduction of titanium casting in lieu of parts machined from plate or conventional forging. In order to verify the production quality together with the behavior of the cast material and scatter of the results, a complete program of static, fatigue and cut-up tests has been performed. Three different structural components were analyzed in order to obtain a complete characterization of the cast material by dissection specimens and structural tests on full scale components. Parts were obtained using two different casting processes, rammed graphite and lost wax. The results obtained on the titanium cast parts in comparison to the machined ones. Author

N90-10238# Messier Fonderie, Arudy (France).
THE QUESTION OF THE CASTING FACTOR [LE FACTEUR DE FONDERIE EN QUESTION]
J. P. Mannant *In* AGARD, Castings Airworthiness May 1989 2 p In FRENCH (For primary document see N90-10231 01-26)
Copyright Avail: NTIS HC A07/MF A01

Aeronautical castings regulations such as FAR25 (U.S.), DEF STAN 00970 (U.K.), and AIR 2004/E (France) have not taken into account the recent progress in casting processes, production management, quality assurance and control, and also in user/foundry cooperation. Developments in aeronautical parts casting are described and the presuppositions underlying the introduction of casting factors are critically examined.
Transl. by M.G.

N90-10239# Hi-Tec Metals R and D Ltd., Chandler's Ford (England).
QUALITY CONTROL OF CASTINGS
G. A. Chadwick *In* AGARD, Castings Airworthiness May 1989 8 p (For primary document see N90-10231 01-26)
Copyright Avail: NTIS HC A07/MF A01

There is a degree of ambiguity about the word quality when applied to cast products: it can refer to the external engineering form of the casting, covering such parameters as dimensional tolerances and surface finish; or it can indicate some measure of performance expected of the cast material, such as the tensile load capability or fatigue behavior. The need for higher quality, in both senses, is of utmost importance if castings are to compete successfully with other manufacturing routes. Casting techniques have advanced significantly over the past 10 to 15 years and quality in the engineering sense is under much closer control now than it used to be. However, the internal metallurgical quality of castings has not shown the same general improvement in the same period of time, poor metallurgical quality being indicated by large casting factors that are applied by design engineers to load-bearing castings. Quality systems frequently refer to zero defect rate, whereas they really mean zero reject rate or zero scrap rate. Zero defect rate, in the sense of metallurgical quality, is the absolute quality limit: this is most closely approached at the present time by squeeze casting. Author

N90-10240# Getti Speciali S.p.A., Torino (Italy).
COMBINED ADVANCED FOUNDRY AND QUALITY CONTROL TECHNIQUES TO ENHANCE RELIABILITY OF CASTINGS FOR THE AEROSPACE INDUSTRY
G. P. Capello and M. Carosso *In* AGARD, Castings Airworthiness May 1989 10 p (For primary document see N90-10231 01-26)
Copyright Avail: NTIS HC A07/MF A01

Aspects of the technological innovation which can contribute, when fully inserted in the productive process, in improving the reliability of castings for use on aircraft are covered. Considered are: the development of processes and the use of means to ensure the absolute repeatability of the critical items with regard to the metallurgical condition of the castings; (mold filing hydraulics and thermal state of the casting; computer assisted management of specific chills; quality of liquid metal; and quenching conditions); and computerized quality control systems which guarantee systematic control of the qualitative conditions of the castings and non-destructive testing systems ensuring an adequate level of reading the internal soundness at acceptable costs (radioscopy linked to image processing systems and high-resolution equipment). Author

N90-10241# Honsel Werke A.G., Meschede (Germany, F.R.).
THE CREATION OF QUALITY: NEW DIRECTIONS IN THE PRODUCTION OF AERONAUTICS CASTINGS
N. Zeumer, G. Betz, and D. Brungs *In* AGARD, Castings Airworthiness May 1989 3 p (For primary document see N90-10231 01-26)
Copyright Avail: NTIS HC A07/MF A01

In order to ensure good consistent quality in aeronautics castings, it is necessary to introduce new quality control systems into production and inspection. To meet the constantly rising demands of the aircraft industry, the foundry must come considerably closer to the standard of reproducible quality. The challenge is to plan and create quality, instead of merely inspecting it. Author

N90-10242# Titan-Aluminum-Feinguss G.m.b.H., Bestwig (Germany, F.R.).
THIN WALLED CAST HIGH-STRENGTH STRUCTURAL PARTS
Ch. Liesner *In* AGARD, Castings Airworthiness May 1989 6 p (For primary document see N90-10231 01-26)
Copyright Avail: NTIS HC A07/MF A01

Production and reproducibility in series of thin-walled high-strength structural parts out of aluminum and titanium alloys produced to the investment casting process are reported. Limits referring to dimensions of parts, wall thicknesses and mechanical properties will be shown on choosen examples. Actions of quality assurance for reproducibility in series are necessary. First of all these include pre-material, melt, casting, ceramic coating, heat treatment. Also the good compatibility of the material combination titanium and CFA will be considered. Author

N90-10243# Settas S.A., Jumet (Belgium).
ADVANCES IN THE TECHNOLOGY OF TITANIUM CASTINGS
J. C. Carlier and P. J. Bridges (Inco Engineered Products Ltd., Birmingham, England) *In* AGARD, Castings Airworthiness May 1989 8 p (For primary document see N90-10231 01-26)
Copyright Avail: NTIS HC A07/MF A01

The techniques used for making titanium casting and how current mold making methods can produce pieces with good dimensional tolerances and surface finish are described. Both rammed sand and lost wax investment methods can be used for mold making, the choice depending on piece complexity, weight, required surface finish and economic considerations. Hot isostatic pressing is normally applied to castings for aerospace and results are presented showing the beneficial effect of this process in terms of reduction of internal porosity. The effect of HIP on mechanical properties is also presented. Author

N90-10244# Timminco Metals, Toronto (Ontario).
MICROSTRUCTURE MORPHOLOGY AND QUALITY OF Al-Si CASTINGS
Bernard Closset and Martin Bray (Grenville Castings, Merrickville, Ontario) *In* AGARD, Castings Airworthiness May 1989 11 p (For primary document see N90-10231 01-26)
Copyright Avail: NTIS HC A07/MF A01

The effect of strontium addition on the microstructure was investigated for Al-Si hypo-eutectic casting alloys. It is shown that strontium modification changes the eutectic morphology from

acicular or lamellar to fibrous. The study was carried out on samples cast in sand and in investment shell molds. The correlation between microstructure and mechanical properties was established. It was demonstrated that tensile strength and elongation, and impact strength are greatly improved by the Al-Si eutectic modification. Finally, techniques such as thermal analysis and electrical resistivity will be presented and their application as a quality control technique discussed. Author

N90-10245# Timminco Metals, Haley (Ontario).
THE IMPROVED CORROSION RESISTANCE OF ULTRA HIGH PURITY MAGNESIUM ALLOY CASTINGS
D. J. Zuliani *In* AGARD, Castings Airworthiness May 1989 14 p (For primary document see N90-10231 01-26)
Copyright Avail: NTIS HC A07/MF A01

The significant and still further improvement in the corrosion resistance of magnesium alloy castings attained by simultaneously reducing the iron, nickel, and copper impurities to ultra low levels (less than 15, 10, and 10 ppm, respectively) are reported. These ultra-high purity magnesium castings provide exceptionally high and consistent corrosion resistance as required for many critical or value added components where corrosion is a prime concern. Author

N90-10246# General Sciences Corp., Plymouth Meeting, PA.
NEW STRUCTURAL MATERIALS Final Report
25 Mar. 1989 23 p
(Contract N00014-88-C-0601)
(AD-A209425) Avail: NTIS HC A03/MF A01 CSCL 11/6

New high temperature structures need to be developed that are based on intermetallic materials and ceramic composites. High density borides and carbides previously were synthesized by self-propagating high temperature synthesis using reaction pressing techniques in the absence of external heating. Based on this technique, new materials (dense reinforced structures) were synthesized using titanium boride as a primary matrix, with second phase brittle components such as carbon particles, carbon cloths, silicon and silicon carbide filaments, as well as ductile second phase additions, such as several forms of nickel or chromium. The effects of the additions on the mechanical and physical properties of those materials were examined as a function of temperature and composition. The interaction of matrix/reinforcement during the exothermic formation was studied. A new filter material also was used with high temperature resin to demonstrate composites with higher temperature capabilities and low observable properties. The resulting materials were expected to have improved toughness, oxidation resistance, and high temperature survivability. GRA

N90-10247# Materials Research Labs., Melbourne (Australia).
PROPERTIES OF HY-100 FOR NAVAL CONSTRUCTION
J. C. Ritter and N. J. Baldwin Nov. 1988 21 p
(MRL-R-1149; AR-005-677) Avail: NTIS HC A03/MF A01

Data are presented on the chemical composition and mechanical properties of HY-100 steel manufactured by Broken Hill Proprietary Steel International, Slab and Plate Products Division and heat treated by Bunge Industrial Steels Pty Ltd. These data satisfy the requirements laid down by U.S. Naval Sea Systems Command for first article qualification following a procedure in which explosion bulge testing is waived, but where HY-80 steel from the same source is already qualified. The Australian-made HY-100 steel is found to be eminently suitable for Royal Australian Navy ship construction. Author

N90-10248*# National Aeronautics and Space Administration. Langley Research Center, Hampton, VA.
EMITTANCE, CATALYSIS, AND DYNAMIC OXIDATION OF Ti-14Al-21Nb
K. E. Wiedemann, R. K. Clark, and S. N. Sankaran (Analytical Services and Materials, Inc., Hampton, VA.) 1989 1 p Presented at the 1988 Annual Meeting of TMS AIME, Phoenix, AZ, Jan. 1988
(NASA-TP-2955; L-16606; NAS 1.60:2955) PREVIEW CSCL 11F

Emittance, catalytic efficiency, and dynamic oxidation resistance were determined for Ti-14Al-21Nb exposed to simulated hypersonic flight conditions at a surface temperature of 982 C for up to 8 hr. The emittance was low before testing (about 0.3), but high after testing (0.85 to 0.89). Catalytic efficiencies were high which means that during exposure to hypersonic conditions Ti-14Al-21Nb will experience a large amount of heating due to recombination of gaseous atoms at the surface. Oxides formed on the surface spalled readily, beginning with the first exposure cycle. Oxygen diffusion into the base metal was observed. The solubility limit of oxygen in the base metal was estimated to be 12.5 at.%, and the diffusion coefficient for oxygen in the base metal was 0.0234 (sq cm/sec) exp (-45090 (cal/mole. deg K)/RT) between 704 C and 982 C. The oxide was composed of several layers of different color but similar composition: TiO_2, Al_2O_3, TiN, and Ti_3O_5 were identified by x-ray diffraction. Author

N90-10249# Allied-Signal Aerospace Co., Kansas City, MO. Technical Communications Div.
GAUSSMETER DETERMINATION OF 302 STAINLESS STEEL MATERIAL CONDITION Final Report
R. E. ODonnell Aug. 1988 18 p
(Contract DE-AC04-76DP-00613)
(BDX-613-3941) Avail: NTIS HC A03/MF A01

A technique was developed to nondestructively distinguish between the annealed and spring tempered condition of a 302 stainless steel component inside a mechanical assembly. A gaussmeter was used to measure the difference in magnetic flux density between the two material conditions. This method provides an accurate way of distinguishing between low strength and high strength components inside mechanical assemblies. This determination can be made after the mechanical assembly is placed into a final assembly housing. Measurements of magnetic flux density were taken with fixturing that would allow evaluation of assemblies after they were placed into final assembly housings. Further development would be required before this could be implemented successfully on final assemblies. Author

N90-10250# Oak Ridge National Lab., TN. Metals and Ceramics Div.
THE QUANTITATIVE ANALYSIS OF FRACTURE SURFACES USING FRACTALS
D. J. Alexander 1988 26 p Presented at the ASTM Symposium on Evaluation and Techniques in Fractography, Atlanta, GA, 10 Nov. 1988
(Contract DE-AC05-84OR-21400)
(DE89-015361; CONF-8811253-1) Avail: NTIS HC A03/MF A01

The concept of fractals was used to analyze fracture surface profiles to determine whether fracture surfaces are fractal in nature, and whether the fractal character can be related to either the mechanical properties or the microstructure of the specimens. Sections taken through the fracture surface of fracture toughness specimens were metallographically prepared and photographed, and the fracture profiles were digitized. Simple computer programs which used different techniques to measure the length of the fracture profiles with differing degrees of precision were used to analyze the profiles by generating a fractal plot of apparent profile length versus the measurement step size. The accuracy of the computer programs was verified by examining artificially generated profiles which had a known fractal character. The analyses indicated that fracture surface profiles are indeed fractal, at least over a limited range of detail. However, it was not possible to match the fractal dimension of the fracture profiles to either the mechanical properties of the metals, or to their microstructures. In addition, different profiles taken from the same specimen had different fractal dimensions. Discontinuities in the fractal plot could not be related to the microstructural features. DOE

N90-10251# Lawrence Livermore National Lab., CA.
THE RESPONSE OF ISOTROPIC BRITTLE MATERIALS TO ABRASIVE PROCESSES
Norman J. Brown, Baruch A. Fuchs, P. Paul Hed, and Irving F. Stowers 24 Apr. 1989 7 p Presented at the American Society for Precision Engineering Spring Conference, Tucson, AZ, 25-27 Apr. 1989 Submitted for publication
(Contract W-7405-eng-48; AFWL Proj. 88-162)
(DE89-016637; UCRL-100647; CONF-8904259-1) Avail: NTIS HC A02/MF A01

This paper is an overview of brittle material responses to abrasion. It proposes a 3-region model for both 2-body and 3-body wear, two regions being where removal rate is nearly independent of abrasive size at otherwise identical conditions and a transition region where rate is proportional to abrasive size. The mechanics will be explored through these 3 regions in 2-body and 3-body wear and some comparisons will be made to the wear of nonbrittle materials. DOE

N90-10252# Lawrence Livermore National Lab., CA.
DELAYED FAILURE OF SILVER-AIDED DIFFUSION WELDS BETWEEN STEEL
M. E. Kassner, R. S. Rosen, G. A. Henshall, and W. E. King 17 Jul. 1989 19 p Presented at the 2nd International Conference on Brazing, High-Temperature Brazing and Diffusion Welding, Essen, Fed. Republic of Germany, 19-20 Sep. 1989 Submitted for publication
(Contract W-7405-eng-48)
(DE89-016652; UCRL-101547; CONF-8909171-1) Avail: NTIS HC A03/MF A01

Silver interlayer diffusion bonds that were fabricated using planar-magnetron sputtering exhibited very high tensile strengths. However, these joints undergo delayed failure at relatively low tensile stresses at ambient temperature, apparently by a microvoid coalescence mechanism at the bond interfaces. Two classes of delayed tensile failure were investigated. In the first case, the applied stress does not produce any plastic deformation in the base metal, and failure appears to be controlled by time-dependent plasticity within the silver interlayer. In the second case, modest time-dependent plasticity is observed in base metals, and concomitant shear occurs within the softer silver under a high triaxial stress state. Here, the time-dependent plasticity of the base metal may accelerate the failure. These findings are believed to be applicable to bonds for which the interlayers are prepared by processes different than physical vapor deposition. DOE

N90-10253# SRI International Corp., Menlo Park, CA.
INFLUENCE OF MICROSTRUCTURE AND MICRODAMAGE PROCESSES ON FRACTURE AT HIGH LOADING RATES Final Report, 1 Feb. 1986 - 30 Sep. 1988
J. H. Giovanola, R. W. Kloop, J. W. Simons, T. Kobayashi, and D. A. Shockey 26 Jun. 1989 48 p
(Contract F49620-86-K-0010)
(AD-A210307; TR-90; AFOSR-89-0992TR) Avail: NTIS HC A03/MF A01 CSCL 11/6

The objectives of this 3 year program were to establish how microstructure and loading rate influence the fracture behavior of Ti-10V-2Fe-3Al, a promising advanced titanium alloy increasingly used in aircraft structural components, and to relate the macroscopic fracture toughness results to microdeformation and microdamage processes with a view toward developing microstructurally based fracture models. Such models are desirable to develop compositions and processing conditions resulting in optimum mechanical properties. GRA

N90-10254# National Inst. of Standards and Technology, Gaithersburg, MD. Metallurgy Div.
DEVELOPMENT OF METASTABLE PROCESSING PATHS FOR HIGH TEMPERATURE ALLOYS Semiannual Technical Report, 1 Oct. 1988 - 31 Mar. 1989
William J. Boettinger 31 Mar. 1989 62 p
(AD-A210550) Avail: NTIS HC A04/MF A01 CSCL 11/6

The development of acceptable toughness and creep strength in high temperature intermetallic alloys is closely related to the formation of proper distributions of second phase particles. Phases are needed both to arrest crack growth at low temperatures and to resist creep at high temperatures. The possibility of developing new processing strategies for high temperature intermetallic compounds is being investigated. In particular rapid solidification and/or rapid solid state quenching followed by controlled heat treatment may provide new and unusual microstructures of multiphase materials. This report describes research performed in the Metallurgy Division at NIST to: (1) develop predictive models for solubility extension and metastable phase formation of intermetallic compounds by rapid solidification; (2) analyze the kinetics of decomposition of metastable phases involving ordering; and (3) improve the phase diagram modeling of systems involving ordered phases. GRA

N90-10255# Rockwell International Science Center, Thousand Oaks, CA.
FATIGUE CRACK INITIATION MECHANICS OF METAL AIRCRAFT STRUCTURES Final Report, 1 Aug. 1986 - 10 Oct. 1987
W. L. Morris, M. R. James, and B. N. Cox Aug. 1988 93 p
(Contract N62269-86-C-0261)
(AD-A210567; NADC-89044-60) Avail: NTIS HC A05/MF A01 CSCL 11/6

The understanding of deformation process that control the local stresses and strains at the grain size level in order to formulate a physically based model of crack initiation under spectrum loads was studied. Experimental techniques of high spatial resolution strain measurements developed at the Science Center were used to investigate the mechanical behavior of individual constrained grains in Al 2219-T851. Local mechanical properties and yield criteria were deduced from measurements of the local stress/strain hysteresis loop width. Two stages of flow are identified, each involving different yield locus behavior. Mathematical models of the local grain stiffness and the constrained plastic strain range are presented, and a phenomenological description of slip band nucleation and hardening are stated as functions of the local plastic strain range. These are then incorporated into a crack growth equation modified for plastic deformation to calculate the cycles required for a microcrack to reach the first subsurface grain boundary when propagating in a region of localized plastic flow. This provides a convenient engineering definition of crack initiation because it avoids the anomalous accelerated crack growth often found within the grain of initiation. GRA

N90-10256# Naval Ship Research and Development Center, Bethesda, MD. Ship Materials Engineering Dept.
MECHANISMS OF STRENGTH AND TOUGHNESS IN A MICROALLOYED, PRECIPITATION HARDENED STEEL
M. E. Natishan Apr. 1989 226 p
(AD-A210571; DTRC/SME-88-81) Avail: NTIS HC A11/MF A02 CSCL 11/6

The microstructural parameters contributing to the strength and toughness of low carbon, microalloyed, precipitation hardenable steels were identified in two ASTM A710, grade A, 50 mm thick plates in the reaustenitized, quenched and aged condition. Tensile, impact toughness and fracture toughness properties were determined over a full range of test temperatures to characterize the mechanical behavior and the fracture processes in the fracture mode transition temperature region, especially as related to cleavage failure and cracking parallel to the loading direction (longitudinal cracking). Microstructural and fractographic characterization, carbide precipitates (in the longitudinal direction) and a non-homogeneous grain size distribution as the primary contributing factors to lower toughness, while copper precipitation played a large role in strengthening. GRA

N90-10257# Cornell Univ., Ithaca, NY. Lab. of Atomic and Solid State Physics.
DYNAMICALLY COMPRESSED METALS: THEORY Final Report, 1 Feb. 1986 - 30 Apr. 1989
N. W. Ashcroft 28 Jun. 1989 7 p

(Contract DAAL03-86-K-0038)
(AD-A210741; ARO-23238.1-PH) Avail: NTIS HC A02/MF A01 CSCL 11/6

The major theme concerns the physics of systems that are subjected to conditions typical of shock or explosive environments. The focus is mainly but not exclusively on metallic systems; under shock loading they usually acquire a very substantial increase in temperature. In fact, for nuclear driven shocks the temperatures can become significant compared even with the Fermi temperature, and the systems are then taken quite far from degeneracy. Central to the theory of any metallic system is the physics of the underlying electron gas; what is required is a theory capable to giving its thermodynamic functions over a range spanning the extreme quantum to classical limits. Such a theory was developed and under the present grant was applied to nearly free electron metallic systems. GRA

N90-10258# Colorado School of Mines, Golden. Center for Welding Research.
INVESTIGATION OF THE PYROMETALLURGICAL, PHYSICAL AND MECHANICAL BEHAVIOR OF WELD METAL Final Report, 15 Apr. 1986 - 14 Apr. 1989
R. H. Frost and D. L. Olson Jun. 1989 18 p
(Contract DAAL03-86-K-0064)
(AD-A211114; MT-CWJR-089-034; ARO-23474.28-MS) Avail: NTIS HC A03/MF A01 CSCL 11/6

The physical and chemical behavior of welding consumables were investigated. The influence of strain and weld metal composition on weld metal microstructure, properties and cracking behavior were studied. Advanced concepts were evaluated to produce higher purity and more consistent welding consumables. New methods to quantify welding consumables were studied. Four different research areas are addressed. All are concerned with the pyrometallurgy and physical metallurgy of weld metals. These four research areas are: (1) steel weld metal phase transformation; (2) weld metal pore formation and methods to retard porosity; (3) advances in welding flux research; and (4) The hot cracking behavior of aluminum alloys. GRA

N90-10259# Army Lab. Command, Watertown, MA. Material Technology Lab.
STRAIN AGING IN TUNGSTEN-HEAVY ALLOYS Final Report
Robert J. Dowding and Kenneth J. Tauer Jul. 1989 15 p
(AD-A211166; MTL-TR-89-63) Avail: NTIS HC A03/MF A01 CSCL 11/6

It has been shown that strengthening of tungsten-heavy alloys is possible through the use of cold working and heat treatment. The source of the increased strength has been attributed to strain aging due to the presence of carbon. Further, it was shown that this increase in strength did not have to be at the expense of elongation. For a 90 percent tungsten-heavy alloy, the strength increased from 164.7 ksi in the as-swaged condition to 178.4 ksi when heat treated at 700 C for 1 hour. Under the same conditions the elongation increased from 10.8 percent to 12.2 percent. Similar results were observed for a 93 percent tungsten-heavy alloy. The strength increased from 173.9 ksi as-swaged, to 197.0 ksi when heat treated for 1 hour at 600 C. The elongation fully recovered at 800 C, held for 1 hour. GRA

27 NONMETALLIC MATERIALS

Includes physical, chemical, and mechanical properties of plastics, elastomers, lubricants, polymers, textiles, adhesives, and ceramic materials.

For composite materials see *24 Composite Materials.*

N90-10260# Case Inst. of Tech., Cleveland, OH. Dept. of Chemistry.
BONDING IN TRANSITION METAL SILYL DIMERS. MOLECULAR ORBITAL THEORY
Alfred B. Anderson, Paul Shiller, Eugene A. Zarate, Claire A. Tessier-Youngs, and Wiley J. Youngs 5 May 1989 19 p
(Contract N00014-86-K-0640)
(AD-A208269; TR-2) Avail: NTIS HC A03/MF A01 CSCL 07/3

Molecular orbital studies of Mn2(CO)8(Si(C6H5)2)2 and Pt2(H3P)4(SiC6H5Cl)2 have been made by interacting disilene fragments with transition metal dimers. In the former complex, it is found that the Mn-Mn distance is close to the sum of the atomic radii because the Mn-Mn bond order is 1. This leads to a long Si-Si distance and allows strong Si-Mn bond formation. In the latter complex, the Pt-Pt bond order is 0, so the disilene, with Si-Si bond intact, binds to the Pt atoms by means of ordinary Pi donation and back-donation to Pi(star). Based on these findings, the M-M and Si-Si distances in other known transition metal-silyl four-membered rings are discussed. GRA

N90-10261*# National Aeronautics and Space Administration. Pasadena Office, CA.
PREDICTIVE AGING OF POLYMERS Patent Application
Edward F. Cuddihy, inventor (to NASA) and Paul B. Willis, inventor (to NASA) (Jet Propulsion Lab., California Inst. of Tech., Pasadena.) 16 Jun. 1989 15 p Prepared in cooperation with Jet Propulsion Lab., California Inst. of Tech., Pasadena
(Contract NAS7-918)
(NASA-Case-NPO-17524-1-CU; NAS 1.71:NPO-17524-1-CU; US-Patent-Appl-SN-366957) Avail: NTIS HC A03/MF A01 CSCL 11C

A method of predicting aging of polymers operates by heating a polymer in the outdoors to an elevated temperature until a change of property is induced. The test is conducted at a plurality of temperatures to establish a linear Arrhenius plot which is extrapolated to predict the induction period for failure of the polymer at ambient temperature. An Outdoor Photo Thermal Aging Reactor (OPTAR) is also described including a heatable platen for receiving a sheet of polymer, means to heat the platen, and switching means such as a photoelectric switch for turning off the heater during dark periods. NASA

N90-10262*# National Aeronautics and Space Administration. Lewis Research Center, Cleveland, OH.
FRICTION AND WEAR OF OXIDE-CERAMIC SLIDING AGAINST IN-718 NICKEL BASE ALLOY AT 25 TO 800 C IN ATMOSPHERIC AIR
Harold E. Sliney and Daniel L. Deadmore Aug. 1989 27 p
(NASA-TM-102291; E-4963; NAS 1.15:102291) Avail: NTIS HC A03/MF A01 CSCL 11C

The friction and wear of oxide-ceramics sliding against the nickel base alloy IN-718 at 25 to 800 C were measured. The oxide materials tested were mullite (3Al2O3.2SiO2); lithium aluminum silicate (LiAlSi(x)O(y)); polycrystalline monolithic alpha alumina (alpha-Al2O3); single crystal alpha-Al2O3 (sapphire); zirconia (ZrO2); and silicon carbide (SiC) whisker-reinforced Al2O3 composites. At 25 C the mullite and zirconia had the lowest friction and the polycrystalline monolithic alumina had the lowest wear. At 800 C the Al2O3-8 vol/percent SiC whisker composite had the lowest friction and the Al2O3-25 vol/percent SiC composite had the lowest wear. The friction of the Al2O3-SiC whisker composites increased with increased whisker content while the wear decreased. In general, the wear-resistance of the ceramics improve with their hardness. Author

N90-10263# Burton Technologies, Inc., Raleigh, NC.
RESEARCH ON ULTRA LOW WEAR MATERIALS FOR ENERGY CONSERVATION Final Report, 30 Sep. 1988 - 30 Jun. 1989
Ralph A. Burton and R. Gaines Burton Jun. 1989 26 p
(Contract DE-AC02-88CE-90027)
(DE89-015096; DOE/CE-90027/1) Avail: NTIS HC A03/MF A01

This report summarizes a set of friction and wear measurements for glassy carbon based materials run against a broad range of counterfaces in ball on disk wear machines. The carbon based materials were operated as both riders and disks. The principal runs employed 1 N contact load, and special runs for the carbon

on its own kind extended the load to 20 N. Runs were carried out in laboratory air and in dry nitrogen and argon. Wear was measured on the rider, alone. The general trend of the results showed favorably low wear coefficient for the carbon based materials. They showed much less sensitivity of the wear rate to the replacement of the air by dry nitrogen than would have been experienced by graphitic carbon. DOE

N90-10264# Oak Ridge National Lab., TN. High Temperature Materials Section.
CERAMIC COMPONENTS IN MACHINES, COLOGNE AND AACHEN, WEST GERMANY; MAASTRICHT, THE NETHERLANDS AND BRUSSELS, BELGIUM Foreign Trip Report, 14-27 Jun. 1989
V. J. Tennery and E. L. Long, Jr. 18 Jul. 1989 23 p
(Contract DE-AC05-84OR-21400)
(DE89-015831; ORNL/FTR-3319) Avail: NTIS HC A03/MF A01

Structural ceramic research at the DLR is heavily focussed on silicon carbide whisker reinforced silicon nitride matrix composites and upon processing of monolithic silicon nitride compositions. Extensive research is also underway on aircraft alloys, including metal-polymer fiber and carbon-carbon composites. The IKKM, a new German research institute in Aachen, has a growing program focussed on characterizing ceramic components by techniques which can ultimately be used by German industry to produce highly reliable structural ceramic products. Residual stress, ultrasonic, and X-ray tomography techniques are the main thrust of the present program. The travelers attended the first meeting of the European Ceramic Society held at Maastricht, The Netherlands. The IEA Annex 2 Executive Committee held a meeting and voted approval of two new subtasks, Subtask 5 on mechanical properties and Subtask 6 on ceramic powders. An overview of the newly formed European Community Research and Development Program on Manufacturing Technologies and Advanced Materials for 1989 to 1992 was gained during a visit to the Commission of the European Communities in Brussels, Belgium. DOE

N90-10265# Sandia National Labs., Albuquerque, NM.
SHOCK COMPRESSION AND RELEASE IN HIGH-STRENGTH CERAMICS
Marlin E. Kipp and Dennis E. Grady Aug. 1989 54 p
(Contract DE-AC04-76DP-00789)
(DE89-013995; SAND-89-1461) Avail: NTIS HC A04/MF A01

A preliminary investigation of shock compression and release properties was performed on four ceramics: silicon carbide, titanium diboride, boron carbide and zirconium dioxide. Eight planar impact experiments using thin discs of similar ceramic as impactor and target have been completed. The particle velocity history at the interface between the back of the target ceramic and a lithium fluoride window material was acquired with a laser velocity interferometer (VISAR). These wave profiles indicate that each of these materials responds in a unique way to shock loading. Peak impact stresses in these experiments range between 20 and 50 GPa, leading to pronounced permanent deformation behavior of these materials. Dynamic compression and release stress-strain behavior of the ceramics, formulated with numerical iteration methods, is compared with compressive strength properties determined from the experimental data. The current experiments provide data for these ceramic materials which can be used to evaluate computational material models in wave propagation codes. DOE

N90-10266# Sandia National Labs., Livermore, CA.
X-RAY LITHOGRAPHY STUDIES OF POLYSILANE USING A LASER PLASMA X-RAY SOURCE
Glenn D. Kubiak, Duane A. Outka, and John M. Zeigler (Sandia National Labs., Albuquerque, NM.) 1988 6 p Presented at the Fall Meeting of the Materials Research Society, Boston, MA, 28 Nov. - 3 Dec. 1988
(Contract DE-AC04-76DP-00789)
(DE89-015390; SAND-88-3060C; CONF-881155-75) Avail: NTIS HC A02/MF A01

A laser-generated plasma source on monochromatized soft X-rays was used to study the X-ray lithographic resist properties of poly(cyclohexyl methysilane-co-dimethysilane). X-ray absorption spectra near the Si L sub 2,3 edge of unexposed samples were measured to guide the choice of exposure photon energy. It was found that poly(cyclohexyl methylsilane-co-dimethylsilane) exhibits positive tone at X-ray energies near 105 eV (Si 2p resonance), a sensitivity of 1000 mJ/sq cm and a contrast of 1.5. Sensitivity is found to increase markedly when exposed samples are held in air before development. Using simple wire mesh masks, estimates of the minimum achievable linewidth were made. DOE

N90-10267# Sandia National Labs., Albuquerque, NM.
ANALYSIS OF SURFACE MODIFIED COLLOIDAL SILICAS
Ricky D. Badley, Warren T. Ford, Frank J. McEnroe (Conoco, Inc., Ponca City, OK.), and Roger A. Assink 1989 9 p Presented at the Surface Modified Oxide Conference, 29 Jun. 1989
(Contract DE-AC04-76DP-00789)
(DE89-015849; SAND-89-0287C; CONF-8906187-1) Avail: NTIS HC A02/MF A01

Colloidal silica was prepared by hydrolysis of tetraethyl orthosilicate in water, ammonia, and ethanol, and its surface was modified with mercaptopropyl, aminopropyl, and octadecyl groups. The parent and modified silicas were analyzed by C-13 and (Si-29 NMR, elemental analysis, and thermogravimetric analysis (TGA). CP-MAS C-13 NMR failed to detect most of the mobile carbons, but direct polarization MAS NMR gave quantitative carbon analyses which agreed with elemental analyses. Direct polarization MAS Si-29 NMR showed that esterification of colloidal silica with octadecanol at 190 C did not cause additional crosslinking in the silica. But reaction with octadecyltrimethoxysilane did give a slight increase in siloxane linkages due to the surface reaction. TGA results show that the octadecylsiloxane linkage is thermally more stable than the octadecyloxysiloxane linkage. DOE

N90-10268# Central Research Inst. of Electric Power Industry, Tokyo (Japan).
THERMOPHYSICAL PROPERTIES OF CERAMICS. PART 2: DEVELOPMENT OF SPECIFIC-HEAT-MEASUREMENT APPARATUS AT HIGH TEMPERATURE
Takeshi Takahashi, Teruhide Hamamatsu, and Hiroshi Ishikawa Jun. 1988 22 p In JAPANESE; ENGLISH summary
(DE89-760382; CRIE-W-87042) Avail: NTIS (US Sales Only) HC A03/MF A01

It is necessary to study the thermal properties of ceramics in order to apply to high temperature field or high heat flux such as high temperature service in a gas turbine or abrasion protions, burners of a boiler. A specific heat measurement apparatus with measure temperature range of 500 to 2300 K was developed. A drop calorimeter method was adopted for the measurement, and a graphite furnace was used for the temperature increase, which is possible to increase up to 2600 K. A sample with M(g) weight and temperature of T sub m C is dropped into the calorimeter with water temperature of T sub r C. A specific heat C sub p of sample is represented by a following formula: C sub p = W*D sub t/M* T sub m - T sub r - D sub t where D sub t C is water temperature increasing, W(g) the sum of the water quality and a water equivalent of the calorimeter. Double insulating structure of the calorimeter showed superior performance. The specific heat of SiC were measured at the range of 800 to 2200 K with satisfactory results, and the measurement error is less than -3.0 percent at 1800 K. DOE

N90-10269# Aerospace Corp., El Segundo, CA. Chemistry and Physics Lab.
SILICON DIOXIDE DEPOSITION AT 100 DEG C USING VACUUM ULTRAVIOLET LIGHT
J. Marks and R. E. Robertson 5 Oct. 1988 12 p
(Contract F04701-85-C-0086)
(TR-0088(3945-07)-6; SD-TR-88-88) Avail: NTIS HC A03/MF A01

A new photochemical reation for low temperature deposition of silicon dioxide was developed. In this process silane is reacted

with nitrogen dioxide in the presence of vacuum ultraviolet radiation. The electrical and mechanical properties of films grown at 100 C are reported. Capacitance voltage measurements on metal oxide semiconductor structures on silicon indicate an interface state density less than 5 x 10(11)/sq cm. Several possible reaction mechanisms are discussed, and evidence is presented indicating surface photochemistry may be important. Author

N90-10270# Allied-Signal Aerospace Co., Kansas City, MO. Technical Communications Div.
INVESTIGATION OF MATERIALS AND BONDING USING THE SCANNING LASER ACOUSTIC MICROSCOPE Final Report
B. A. Jones and C. W. Boehning Dec. 1988 20 p
(Contract DE-AC04-76DP-00613)
(KCP-613-4033) Avail: NTIS HC A03/MF A01

The Scanning Laser Acoustic Microscope (SLAM) is a highly specialized device used to nondestructively examine material samples. The design of the SLAM is based on known properties of high frequency ultrasound. The sound waves penetrate materials at different depths, dependent upon material composition and the sound wave frequency level. In addition, sound waves are attenuated by flaws or discontinuities in the material. With the basic understanding of these properties, the SLAM system can be used to find and interpret the internal features of a variety of material samples. Some of the areas already investigated include heremetic seals, voids or delaminations in chip capacitors, die attachment, and cracks in ferrites. Author

N90-10271# Allied-Signal Aerospace Co., Kansas City, MO. Technical Communications Div.
ADHESION OF ENCAPSULATING ELASTOMER TO POLYOLEFIN SLEEVE Special Report
R. D. Holt Sep. 1988 24 p
(Contract DE-AC04-76DP-00613)
(BDX-613-3985) Avail: NTIS HC A03/MF A01

Surface treatments to heat shrinkable polyolefin were evaluated for their effects on the adhesion of a polyurethane encapsulation elastomer to the polyolefin. Peel strength measurements were provided and recommendations for surface treatments were made. Of the 18 different surface treatments evaluated, corona, treatment, flame treatment, and plasma treating were found to provide superior bonding. Author

N90-10272# Science Applications International Corp., McLean, VA.
JAPANESE STRUCTURAL CERAMICS RESEARCH AND DEVELOPMENT
J. B. Wachtman, Jr., R. C. Bradt, R. F. Davis, R. Raj, D. W. Richerson, N. J. Tighe, Barbara L. McKenney, ed., Moira McGrain, ed., and Renee G. Taub, ed. Jul. 1989 256 p
Avail: NTIS HC A12/MF A02

Japanese work on structural ceramics is reviewed in comparison with work in the United States. Key organizations involved in planning and conducting ceramics research and development are presented along with national plans for ceramics research. General themes including the Japanese commitment to ceramics and their approach to marketing and product development are discussed. Specific families of ceramic materials (silicon carbide, silicon nitride, zirconia, mullite, and alumina) are reviewed. Subjects that deal with more than one class of materials (hard coatings, e.g., diamond and cubic boron nitride, fabrication technology, borides and mixed compositions) are covered. It is concluded that Japanese and U.S. positions on science and technology are comparable but it is likely that the Japanese will be first in the introduction of significant load-bearing high-temperature parts in engines. K.C.D.

N90-10273# Los Alamos National Lab., NM. Theoretical Div.
MECHANICAL PROPERTIES, SOLUBILITIES, AND PROCESSABILITIES IN THE DESIGN OF THE FIRST SUPER-STRONG LIQUID-CRYSTALLINE POLYMERS
F. Dowell 1989 7 p Presented at the American Chemical Society National Meeting, Miami Beach, FL, 10-15 Sep. 1989
(Contract W-7405-eng-36)
(DE89-009252; LA-UR-89-1127; CONF-890902-1) Avail: NTIS HC A02/MF A01

Solidified super-strong (SS) liquid-crystalline polymers (LCPs) are designed to be the first polymers to have good compressive strengths, as well as to have tensile strengths and tensile moduli significantly greater than existing strong LCPs (i.e., backbone LCPs, such as Kevlar). These SS LCPs were also designed with certain features to give good solubilities and processabilities. The enhanced mechanical properties, solubilities, and processabilities of the super-strong liquid crystal polymers are covered. DOE

N90-10274# Oak Ridge National Lab., TN.
STRUCTURE-MECHANICAL PROPERTY RELATIONSHIPS IN ION IMPLANTED CERAMICS
C. J. McHargue, C. W. White, P. S. Sklad, M. E. OHern, D. L. Joslin, and G. C. Farlow (Wright State Univ., Dayton, OH.) 1989 15 p Presented at the 2nd International Seminar on Surface Engineering By High Energy Beams, Lisbon, Portugal, 5-7 Sep. 1989
(Contract DE-AC05-84OR-02140)
(DE89-010129; CONF-890995-1) Avail: NTIS HC A03/MF A01

Although the majority of research and development involving ion implantation was devoted to the doping of semiconductors, there was also much activity toward altering the chemical, physical, and mechanical properties of metals and alloys. In recent years, there was a resurgence of interest in the use of ion beams to alter the properties of insulating materials. As a class of materials, insulators exhibit a range of properties, structures, phases, and chemical bonding types. The portion of that class called ceramics, primarily the crystalline oxides and carbides that find technological applications today are considered. DOE

N90-10275# Oak Ridge National Lab., TN. Chemistry Div.
COMPUTER SIMULATIONS OF POLYMER DYNAMICS IN THE SOLID STATE
B. G. Sumpter, D. W. Noid, and B. Wunderlich 1989 4 p Presented at the American Physical Society Meeting, Miami, FL, 5-8 Sep. 1989 Prepared in cooperation with Tennessee Univ., Knoxville
(Contract DE-AC05-84OR-21400; NSF DMR-88-18412)
(DE89-010337; CONF-8909120-1) Avail: NTIS HC A01

Details at the atomic or molecular level are important for a more thorough understanding of polymer processes. A better knowledge of both structure and dynamics is needed. A method which is particularly suited for this task is the molecular dynamics method (MD). The method is well known, but its application to the solid state of polymers was not extensive. Indeed, polymer applications present some unique difficulties to be discussed in the next section. In the detailed computer simulations of the dynamics of solid polymers, the focus was on the following three topics: simulations of condis crystals and meso-phase transitions, melting and crystallization of polymers, and calculation of vibrational spectra and heat capacities of solids. DOE

N90-10276# Allied-Signal Aerospace Co., Kansas City, MO. Technical Communications Div.
ELECTRONIC ENCAPSULATION USING FOAM WITH BONDED METAL COVERS FOR A FILTER PACK
L. C. Davis Jul. 1989 20 p
(Contract DE-AC04-76DP-00613)
(DE89-014010; KCP-613-4076) Avail: NTIS HC A03/MF A01

This process investigation evaluated the feasibility of bonded metal covers to polyurethane foam in the non-electromagnetic radiation areas of a Filter Pack. This process would replace an epoxy microballoon encapsulation process presently used. Encapsulation samples and mock units underwent temperature and moisture testing for comparison against other similar processes and durability testing of adhesion. DOE

N90-10277# Connecticut Univ., Storrs. Dept. of Chemical Engineering.
CHARACTERIZATION OF POLYMERIC SURFACES AND INTERFACES Final Report, 1 Jul. 1986 - 1 Jan. 1989
Jeffrey T. Koberstein 13 Mar. 1989 10 p
(Contract DAAL03-86-K-0133)
(AD-A210227; ARO-24165.6-MS) Avail: NTIS HC A02/MF A01 CSCL 07/6

The purpose of this project was to gain a fundamental understanding of the behavior of polymer molecules at surfaces and interphases so as to provide a basis for the design of these important properties. The first accomplishment completed was the development of a technique for the determination of interfacial tension of polymers by robust shape analysis of the profiles of molten polymer pendant drops. This technique was then applied to several materials systems: concentrated polymer solutions, miscible polymer blends, binary homopolymer immiscible blends, functionally terminated homopolymers. GRA

N90-10278# Microelectronics Center of North Carolina, Research Triangle Park.
THE EFFECTS OF NORMAL ANNEALING CYCLES DURING IGFET FABRICATION ON INITIAL AND RADIATION INDUCED GATE INSULATOR DEFECTS Annual Progress Report, 1 Dec. 1988 - 7 Jul. 1989
M. Walters and A. Reisman 13 Jul. 1989 14 p Prepared in cooperation with North Carolina State Univ., Raleigh
(Contract N00014-88-C-0746)
(AD-A210282; TR-2) Avail: NTIS HC A03/MF A01 CSCL 20/12

The influence of three typical annealing cycles normally used in IGFET processing on as-fabricated and post-irradiated gate oxide defect levels was studied. These cycles were: (1) post-oxidation for 5 minutes at 1000 C in argon; (2) post-polysilicon for 30 minutes at 500 C in forming gas; and (3) post-metallization for 30 minutes at 400 C in hydrogen. Gate oxide defects were characterized using optically assisted electron injection of n-channel polysilicon-gated IGFET devices. It was found that the presence or absence of any of the three annealing cycles during the processing had no effect on measured interface state and bulk oxide defect levels in the as-fabricated devices. Following exposure to Al K (alpha) X-ray radiation, the increase in the number of bulk oxide defects was found to be independent also of the presence or absence of any of the cycles. The interface state density was found to increase only slightly following irradiation, with the smallest increase occurring for devices which had received either the post-oxidation or the post-metal anneal. These results may indicate that other high temperature steps which are present in IGFET processing, as well as the use of different electrode materials than were employed in the earlier studies, overshadow the effects of the three annealing cycles studied. Therefore, the entire processing sequence of IGFET fabrication must be considered in determining the factors which influence gate insulator defect levels and susceptibility to ionizing radiation. GRA

N90-10279# Colorado Univ., Boulder. Dept. of Chemistry.
NEW POLYMER PRECURSORS TO BORON AND SILICON NITRIDES Final Report, 1 Sep. 1987 - 31 Dec. 1988
Arlan D. Norman 8 Jun. 1989 15 p
(Contract N00014-87-K-0791)
(AD-A210287; CU-1-533835) Avail: NTIS HC A03/MF A01 CSCL 07/3

Phosphinosilanes and phosphino (halo) silanes E.G. MeSi(PH2)3 and MeSi (PH2)C12 have been obtained which can condense with amine borazane N-H bonds to form Si-N and B-N bonds cleanly. Polyborazane, polysilazane, and polyborosilazane 1,3,2-borodiazole C6H4 (NH)2BPh and 1,3,2-siladiazole C6H4(NH)-2R,R = Me, Ph precursors and the new C6H4(NH)2BPh and 1,3,2-siladiazole C6H4 (NH)2R, R = Me, Ph precursors and the new C6H4 (NHSiPh2)20 heterocycle have been synthesized. GRA

N90-10280# Alabama Univ., Birmingham. Lab. of Molecular Biophysics.
DEVELOPMENT OF ELASTOMERIC POLYPEPTIDE BIOMATERIALS Annual Report, 1 Jun. 1988 - 31 May 1989
Dan W. Urry, K. U. Prasad, and Casey Morrow 1 Jul. 1989 115 p
(Contract N00014-86-K-0402; RR04106)
(AD-A210295) Avail: NTIS HC A06/MF A01 CSCL 07/6

The purpose of this research was to design, prepare and characterize novel elastomeric polymers comprised of repeating peptide sequences, primarily the elastin pentamer and analogs of it alone and combined with repeating related hexapeptides and/or tetrapeptides. The purpose is to develop polymers with different elastic moduli and increased extension limits, polymers with different temperature ranges for their inverse temperature transitions over which elastomeric force dramatically changes, polymers in which different intensities and frequencies of their dielectric relaxations and polymers with wider temperature ranges over which they function as nearly ideal elastomers. In the elastomer design, the dominant repeat units will be pentamers and tetramers. Hexamers and alanine-rich, lysine-containing cross-linking sequences will be used to fine-tune properties. GRA

N90-10281# Washington Univ., Seattle. Dept. of Chemistry.
CONTROL OF SYNTHETIC PEPTIDE TERTIARY STRUCTURE Progress Report, Feb. - Jul. 1989
Paul B. Hopkins 1 Jul. 1989 3 p
(Contract N00014-88-K-0201; RR04106)
(AD-A210339) Avail: NTIS HC A01/MF A01 CSCL 06/2

The proposed research seeks to design and synthesize large organic molecules possessing precisely defined geometric shapes. A capability which will make possible the design of catalysis and receptors. The approach entails the design of unnatural amino acids which, when incorporated into peptides, will enforce tertiary structure on the overall molecule. Methods are also suggested whereby transiently stable noncovalent complexes of peptides might be permanently stabilized by covalent crosslinking, leading to the concept of self-assembly of large, highly ordered organic molecules. The additional possibility of assembling large structures from smaller pieces by incorporation of temporary functionality which will initially spatially orient small pieces prior to covalent assembly is suggested, a concept termed directed assembly. GRA

N90-10282# University of Southern Mississippi, Hattiesburg. Dept. of Polymer Science.
AN INVESTIGATION OF THE DEGRADATION AND STABILIZATION OF POLYMER SYSTEMS Final Report
Charles E. Hoyle and Gordon L. Nelson 14 Jul. 1989 6 p
(Contract N00014-85-K-0748)
(AD-A210362) Avail: NTIS HC A02/MF A01 CSCL 07/6

A detailed study was made of the factors which effect the photolytic decomposition of polyurethanes based on aromatic diisocyanates. An extensive investigation of the photophysics of 1,5-naphthalene diisocyanate based polyurethanes in solution was also conducted. In addition, ground work was laid to initiate studies on the photodegradation of polycarbonate, polyureas, and polymides. Employing both steady and time resolved fluorescence spectroscopy to analyze the photolysis products of model compounds and polyurethane films, photo-Fries and other cleavage products were identified at the very early stages of photolytic induced decomposition. The critical effect was established of polymer main-chain flexibility, crystalline content, and hydrogen bonding on the extent of degradation of polyurethane films and coatings. Laser flash photolysis results confirmed the contribution of peroxide and aromatic ketone impurities (incorporated into all commercial polyurethanes during the synthesis and processing steps) to the photodegradation process. For methylene 4,4' -diphenyl diisocyanate (MDI) based polyurethanes, transient spectra of diphenyl methyl radicals were detected under a variety of conditions, thus providing unequivocal evidence for one of the

primary modes of the initial stages of photooxidation of segmental polyurethane elastomers. GRA

N90-10283# Northeastern Univ., Boston, MA. Materials Science Div.
ESTABLISHMENT AND INITIAL OPERATION OF A RESOURCE FACILITY FOR RSR (RAPID SOLIDIFICATION RATE) PROCESSED ALLOYS IN PILOT QUANTITIES Final Report, 30 Sep. 1980 - 30 Sep. 1983
B. C. Giessen 22 Jun. 1989 19 p Sponsored by Army Research Office, Durham, NC
(Contract N00014-80-C-0986; NR Proj. 039-212)
(AD-A210369) Avail: NTIS HC A02/MF A01 CSCL 11/6

The program objective was to construct and operate a rapid solidification rate (RSR) processing resource facility based on melt spinning of pilot scale quantities. It consists of a controlled atmosphere melt spinner with a capacity of 1 lb of ferrous alloy, a 100 g capacity melt spinner (to establish experimental parameters and reduce cross contamination), and a high speed ribbon cutter for flake preparation. RSR processed materials were delivered to Government, industrial and academic users. GRA

N90-10284# Wisconsin Univ., Madison. Dept. of Chemical Engineering.
COMPARISON OF CARBOXYLATED AND SULFONATED MODEL POLYURETHANE IONOMERS Progress Report, 1 Jun. 1988 - 31 May 1989
Susan A. Visser and Stuart L. Cooper 30 May 1989 4 p
(Contract N00014-83-K-0423)
(AD-A210438; TR-20) Avail: NTIS HC A01/MF A01 CSCL 07/6

A series of model polyurethane ionomers containing uniform placement of the ionic groups along the chain has been synthesized in order to study the ionomer structure-property relationship in a well defined system. The materials were synthesized to vary in anion type (sulfonate vs. carboxylate), ionization level, and backbone soft segment polarity. The sulfonated ionomers possessed a higher degree of phase separation and superior mechanical properties compared to their carboxylated analogs. A critical minimum ionization level was found to be necessary for the development of good elastomeric properties. The model ionomers are 1:1 copolymers of either poly(tetramethylene oxide) (PTMO) or poly(propylene oxide) and tolylene diisocyanate. GRA

N90-10285# Wisconsin Univ., Madison. Dept. of Chemical Engineering.
UV-CURABLE POLYURETHANE-METHACRYLATE CO-NETWORKS AND INTERPENETRATING NETWORKS Summary Report, 1 Jun. 1988 - 31 May 1989
Xue-Hai Yu, James G. Homan, Timothy J. Connor, and Stuart L. Cooper 30 May 1989 25 p
(Contract N00014-83-K-0423)
(AD-A210445; TR-22) Avail: NTIS HC A01/MF A01 CSCL 07/6

Castor oil was reacted in varying ratios with Beta-isocyanatoethyl methacrylate to form a liquid urethane-methacrylate prepolymer. This prepolymer was then cured with ultraviolet radiation (to form a series of base networks) or with various methacrylates (to form a series of co-networks). By swelling the base networks with the appropriate methacrylate monomers, semi- and full interpenetrating networks (IPNs) were also prepared with similar compositions. All of the materials formed transparent films. Results of swelling experiments, dynamic mechanical analysis, differential scanning calorimetry, and small angle X-ray scattering are reported. GRA

N90-10286# Wisconsin Univ., Madison. Dept. of Chemical Engineering.
SYNTHESIS AND INTERFACIAL PROPERTIES OF NEW GENERATION POLYURETHANE SYSTEMS Final Project Report, 1 Jun. 1987 - 30 May 1989
Craig W. Myers and Stuart L. Cooper 30 May 1989 5 p
(Contract N00014-83-K-0423)
(AD-A210446) Avail: NTIS HC A01/MF A01 CSCL 11/10

The thrust of this research has been to synthesize and study the structure-property relationships of several families of modified polyurethanes in three main areas. First, we have attempted to improve the mechanical properties of environmentally stable polyurethanes by inserting polar groups into non-polar soft segments and by using blends of the conventional (polar) and non-polar soft-segments. Early work examined the effect on segmental compatibility of introducing polar (cyanomethylethyl) groups into a non-polar (siloxane) soft segment. Blends of polar poly(tetramethylene oxide) (PTMO) and non-polar poly(dimethylsiloxane) (PDMS) were later used in soft segments in an effort to reduce polyurethane moisture sensitivity while retaining good mechanical properties. Second, we have studied the incorporation of novel pendant structures (UV-curable groups and ionic groups) in segmented polyurethanes, and the material properties of the resulting polymers. A liquid urethane methacrylate prepolymer and various methacrylate monomers were used to form semi-and-full interpenetrating networks (IPNs). Third, because molecular characterization is a critical tool in the interpretation of structure-property relationships for these materials, we have investigated the analysis of polyurethane molecular weight distributions and their relationship to synthesis conditions. GRA

N90-10287# Wisconsin Univ., Madison. Dept. of Chemical Engineering.
SYNTHESIS AND PHYSICAL PROPERTIES OF POLY(PERFLUOROALKYLETHER) URETHANES Summary Report, 1 Jun. 1988 - 31 May 1989
Xue-Hai Yu, Ann Z. Okkema, and Stuart L. Cooper 30 May 1989 43 p
(Contract N00014-83-K-0423)
(AD-A210500; TR-21) Avail: NTIS HC A03/MF A01 CSCL 07/6

Polyurethane block copolymers were synthesized containing 33 and 50 wt percent soft segment, and hard segment based on 4,4-diphenylmethane dissocyanate (MDI) chain extender. The soft segments were mixtures of poly(tetramethylene oxide) (PTMO) and poly(perfluoroalkylether) (PFEG) glycols (Mn=1000 and 1900, respectively), ranging from 4 to 100 wt percent PFEG. The PMTO polyol in one sample was substituted with a PMTO/ethylene oxide polyol (75:25 mole ratio) (Mn=1140). The MDEA-extended polymer was ionized using 1,3-propane sultone. The morphology, bulk, and surface properties of these polymers were evaluated by a variety of techniques. Differential scanning calorimetry and dynamic mechanical analysis showed that the incorporation of PFEG into the soft segment phase slightly enhanced the degree of phase separation. GRA

N90-10288# Naval Weapons Center, China Lake, CA. Chemistry Div.
CHARACTERIZATION OF DIAMOND FILMS BY THERMOGRAVIMETRIC ANALYSIS AND INFRARED SPECTROSCOPY
Curtis E. Johnson, Wayne A. Weimer, and David C. Harris 1989 9 p
(AD-A210564) Avail: NTIS HC A02/MF A01 CSCL 20/12

Recent advances in the growth of diamond films by low pressure chemical vapor deposition (CVD) have generated a great deal of interest in developing diamond materials for a variety of technological applications. Unique optical, thermal and mechanical properties make diamond the material of choice for many purposes. A technique involving microwave plasma assisted chemical vapor deposition for the growth of diamond films was described recently by Chang, et. al. Results are reported which were obtained in characterizing free-standing diamond films produced by this technique. Diamond films were grown on silicon wafers at about 3 micrometers/hr by microwave plasma assisted chemical vapor deposition. The infrared transmission of a 3 micrometer thick film varied from near 61 percent at 5000/cm to near 75 percent at 1000/cm. Thermogravimetric analysis indicated that the diamond

films oxidize in air at about 650 C and are less resistant to oxidation than graphite. A film containing nitrogen was grown by adding N2 to the feed gas. GRA

N90-10289# Air Force Systems Command, Wright-Patterson AFB, OH. Foreign Technology Div.
THE HIGH-FREQUENCY DIELECTRIC PROPERTIES OF GLASS FIBRE REINFORCED PLASTIC AND HONEYCOMB LAYERS
Zhulin Zhou 29 Jun. 1989 13 p Transl. into ENGLISH from Wuli (Peoples Republic of China), v. 17, no. 4, Apr. 1988 p 225-228
(AD-A210581; FTD-ID(RS)T-0349-89) Avail: NTIS HC A03/MF A01 CSCL 11/9

The dielectric constant and the dielectric loss angle tangent of glass fibre reinforced plastic are both relatively small; it is a good wave-penetration rate of honeycomb layer structure. It is necessary to undertake a theoretical investigation of the properties and discover formulas with a practical value. This paper introduces the work we have done in this area. The dielectric properties of glass fibre reinforced plastic have a close relationship with the dielectric properties of the raw materials. GRA

N90-10290# Army Lab. Command, Watertown, MA. Materials Technology Lab.
ALTERNATIVE TEST METHODOLOGY FOR BALLISTIC PERFORMANCE RANKING OF ARMOR CERAMICS Final Report
Patrick Woolsey, David Kokidko, and Stephen A. Mariano May 1989 21 p
(DA Proj. 1L1-62105-AH-84)
(AD-A210587; MTL-TR-89-43) Avail: NTIS HC A03/MF A01 CSCL 11/2

A laboratory test method of ranking the ballistic performance of ceramic materials is under development at the U.S. Army Materials Technology Lab. by the Ballistic Impact Behavior Group and Armor Systems Team. Ranking are based on residual penetration of a tungsten long rod fired at constant velocity through a laterally confined ceramic into a semi-infinite steel backup. By varying the thickness or areal density of ceramic from zero to a value producing no residual penetration, a ballistic performance map for the ceramic is generated. Different materials can be compared on the basis of residual penetration observed for a given areal density. Ceramics tested to date include aluminum oxide in 90 percent and high purity forms, titanium diboride, silicon carbide, and boron carbide. Performance rankings observed for these materials are in agreement with the rankings yielded by conventional V50 protection ballistic limit test methods. This test method requires fewer shots than V50 tests, has sensitivity comparable to present test methods, and avoids the fundamental problem of V50 dependence on armor design. As a consequence, it should prove to be valuable for acceptance testing of production materials, comparison testing to rank the performance of new materials, and for parametric analysis of ballistic performance variations resulting from material properties, cell size, confinement, and similar factors. GRA

N90-10291# Pennsylvania State Univ., University Park. Materials Research Lab.
THE MEASUREMENT OF INFRARED SPECTRA OF DENSE CERAMICS BY SPECULAR REFLECTANCE SPECTROSCOPY
Mary Bliss (General Electric Co., Largo, FL.), Barbara L. Walden, and William B. White 17 Jul. 1989 30 p
(Contract N00014-85-K-0129)
(AD-A210609; TR-2) Avail: NTIS HC A03/MF A01 CSCL 11/2

It is shown that high quality IR specular reflectance spectra can be obtained from polished surface of dense ceramics. The reflectance spectra can be deconvoluted by the Kramers-Kronig transformation to yield absorption spectra or the real and imaginary parts of the dielectric function. IR line shapes and peak wavenumbers are comparable to single crystal data providing that the particle size is small compared with the IR wavelengths of interest. For non-cubic structures, the spectra are a superposition of polarization components. Modes separated by less than a band width are merged into a single band thus limiting the resolution of the measurement procedure. Grain size effects were modeled using the spectra of single crystal and polycrystal quartz as an example. GRA

N90-10292# Brookhaven National Lab., Upton, NY. Div. of Materials Science.
POLYHETEROCYCLE LANGMUIR-BLODGETT FILMS Technical Report No. 1, Jul. 1988 - Jul. 1989
X. Q. Yang, J. Chen, P. D. Hale, T. Inagaki, T. A. Skotheim, D. A. Fischer, Y. Okamoto, L. A. Samuelsen, Sukant K. Tripathy, and K. Hong (Massachusetts Inst. of Tech., Cambridge.) et al 31 May 1989 19 p Prepared in cooperation with Hunter Coll., New York, NY
(Contract N00014-87-K-0131)
(AD-A210625) Avail: NTIS HC A03/MF A01 CSCL 07/1

The increasing interest in organic and polymeric electroactive materials arises from their potential applications in synthetic membranes, nonlinear optical elements, sensors, and micro-electronic devices. Two types of polyheterocycle Langmuir-Blodgett films have been fabricated: (1) copolymers of pyrrole and 3-alkyl pyrrole (3-hexadecylpyrrole and octadecylpyrrole) LB films; and (2) mixtures of poly(3-alkyl thiophene) and stearic acid LB films. The orientation of single- and multi-layer films on platinum substrates have been studied by Near Edge X-ray Absorption Fine Structure (NEXAFS) spectroscopy which also provides information about interaction between the aromatic groups and the metallic substrate. The alkylsubstituted pyrrole are more disordered. In the case of mixtures of poly(3-alkyl thiophene) and stearic acid LB films, the hydrocarbon chains of the stearic acid molecules are highly ordered. The poly(3-alkyl thiophene) components, on the other hand exhibit random orientation of the thiophene moities. The orientation of the hydrocarbon chain of the poly(3-alkyl thiophene) varies with the chain length, from random to highly ordered along the surface normal of the substrate, as the chain length changes from 4 carbon units to 18 carbon units. GRA

N90-10293*# Ford Motor Co., Dearborn, MI. Scientific Lab.
IMPROVED SILICON CARBIDE FOR ADVANCED HEAT ENGINES Final Annual Report No. 2, 15 Feb. 1986 - 14 Feb. 1987
Thomas J. Whalen Oct. 1987 80 p
(Contract NAS3-24384)
(NASA-CR-180831; NAS 1.26:180831) Avail: NTIS HC A05/MF A01 CSCL 11C

This is the second annual technical report entitled, Improved Silicon Carbide for Advanced Heat Engines, and includes work performed during the period February 16, 1986 to February 15, 1987. The program is conducted for NASA under contract NAS3-24384. The objective is the development of high strength, high reliability silicon carbide parts with complex shapes suitable for use in advanced heat engines. The fabrication methods used are to be adaptable for mass production of such parts on an economically sound basis. Injection molding is the forming method selected. This objective is to be accomplished in a two-phase program: (1) to achieve a 20 percent improvement in strength and a 100 percent increase in Weibull modulus of the baseline material; and (2) to produce a complex shaped part, a gas turbine rotor, for example, with the improved mechanical properties attained in the first phase. Eight tasks are included in the first phase covering the characterization of the properties of a baseline material, the improvement of those properties and the fabrication of complex shaped parts. Activities during the first contract year concentrated on two of these areas: fabrication and characterization of the baseline material (Task 1) and improvement of material and processes (Task 7). Activities during the second contract year included an MOR bar matrix study to improve mechanical properties (Task 2), materials and process improvements (Task 7), and a Ford-funded task to mold a turbocharger rotor with an improved material (Task 8). Author

N90-10294*# Materials and Electrochemical Research Corp., Tucson, AZ.
ZIRCONIA TOUGHENED SiC WHISKER REINFORCED ALUMINA COMPOSITES SMALL BUSINESS INNOVATION RESEARCH Final Report, Dec. 1985 - Oct. 1986
R. O. Loutfy, K. L. Stuffle, J. C. Withers, and C. T. Lee Oct. 1987 48 p
(Contract NAS3-24872)
(NASA-CR-179629; NAS 1.26:179629) Avail: NTIS HC A03/MF A01 CSCL 11C

The objective of this phase 1 project was to develop a ceramic composite with superior fracture toughness and high strength, based on combining two toughness inducing materials: zirconia for transformation toughening and SiC whiskers for reinforcement, in a controlled microstructure alumina matrix. The controlled matrix microstructure is obtained by controlling the nucleation frequency of the alumina gel with seeds (submicron alpha-alumina). The results demonstrate the technical feasibility of producing superior binary composites (Al2O3-ZrO2) and tertiary composites (Al2O3-ZrO2-SiC). Thirty-two composites were prepared, consolidated, and fracture toughness tested. Statistical analysis of the results showed that: (1) the SiC type is the key statistically significant factor for increased toughness; (2) sol-gel processing with a-alumina seed had a statistically significant effect on increasing toughness of the binary and tertiary composites compared to the corresponding mixed powder processing; and (3) ZrO2 content within the range investigated had a minor effect. Binary composites with an average critical fracture toughness of 6.6MPam sup 1/2, were obtained. Tertiary composites with critical fracture toughness in the range of 9.3 to 10.1 MPam sup 1/2 were obtained. Results indicate that these composites are superior to zirconia toughened alumina and SiC whisker reinforced alumina ceramic composites produced by conventional techniques with similar composition from published data. Author

N90-10295# Minnesota Univ., Minneapolis. Corrosion Research Center.
QUARTZ CRYSTAL MICROBALANCE STUDIES OF ELECTROCHEMICAL GROWTH OF CONDUCTING POLYMERS Technical Report No. 5, Jul. 1988 - Jun. 1989
Katsuhiko Naoi, Mary M. Lien, and William H. Smyrl 15 Jun. 1989 3 p
(Contract N00014-88-K-0360)
(AD-A210788) Avail: NTIS HC A01/MF A01 CSCL 07/1

In-situ monitoring of the mass change occurring during electrochemical growth of conducting polymers is possible by use of quartz crystal microbalance (QCM). The mass change due to polymer formation as well as doping of anions and solvent up-take are monitored with time. Electro-polymerization factors, such as electrolysis mode (galvanostatic, potentiostatic, scan, pulse), electrolyte and solvent are compared. The electrochemistry of the resulting film is examined. QCM/Potentiostatic measurements have the advantage of providing simultaneous mass change and charge data. From these, 2 distinct growth phases are observed: (1) a fast, charge-efficient growth on substrate; and (2) a slower, inefficient growth on pyrrole. GRA

N90-10296# Albert Einstein Medical Center, Philadelphia, PA.
SYNTHETIC POLYPEPTIDE COMPOSITES FOR SENSOR APPLICATIONS Final Report, 1 Nov. 1985 - 30 Apr. 1989
S. Erhan, E. L. Cross, and A. Bhalla 10 Jul. 1989 73 p
(Contract DAAG29-85-K-0243)
(AD-A210797; ARO-23230.2-LS-A) Avail: NTIS HC A04/MF A01 CSCL 06/3

Due to technical difficulties, i.e., insolubility of the products, emphasis has been placed on modification of gelatin, using highly polar molecules, while trying to find a satisfactory solution to solubility problems. The modified gelatins have performed exceptionally well. Even at this early stage samples show under bias response comparable to best polar polymer (PVF2) and competitive with the inorganic LiTaO3. GRA

N90-10297# Bristol Univ. (England).
HIERARCHICAL STRUCTURE IN POLYMERIC SOLIDS AND ITS INFLUENCE ON PROPERTIES Final Report, Dec. 1984 - May 1989
A. Keller May 1989 174 p
(Contract DAJA45-85-C-0004; DA Proj. 1L1-61102-BH-57)
(AD-A210918; R/D-4794-MS-01) Avail: NTIS HC A08/MF A01 CSCL 07/6

The focuc was on main chain liquid crystal forming polymers (LCP-s) such as have potential structural applications as advanced materials. A close ongoing U.K.-U.S. collaboration was established where the U.S. workers are synthetizing tailor made rigid group-flexible spacer polyethers for physics based examination at Bristol. The varied lines of work and accomplishments are as follows. A broad thermodynamics based scheme was established providing unifying threads through hitherto disconnected phenomena in the LCP field with significant predictive power for ongoing works. Amongst others it encompasses the numerous situation where mesogens are not required for the formation of a liquid crystal (LC) state. Phase diagrams are being established as a function of molecular weight, chemical constitution and copolymer composition. This serves to identify and predict the LC region as a function of the above variables with due distinction between thermodynamic and kinetic factors. In aid of this, a new methodology was introduced: simultaneous X-ray diffraction and thermal analysis which was greatly facilitated by synchrotron generated X-rays. The importance of non-equilibrium states was recognized. A separate line of work was on the orientational behavior of rigid molecules, most of it on the fully rigid rod PBZT. A two-stage relaxational behavior was identified in semi-dilute (entangled) solutions by birefringence analysis. GRA

N90-10298# Naval Weapons Center, China Lake, CA. Chemistry Div.
PREPARATION, PURIFICATION AND DENSIFICATION OF ZINC SULFIDE POWDER FROM ORGANOMETALLICS
Curtis E. Johnson, Daniel C. Harris, and Charles B. Willingham (Raytheon Co., Lexington, MA.) 1989 46 p Submitted for publication
(AD-A210943) Avail: NTIS HC A03/MF A01 CSCL 11/2

Zinc sulfide powders were prepared from diethylzinc and hydrogen sulfide in toluene solution at 20 C. The powder consisted of agglomerates of 0.1 microm sized particles. The residual zinc ethyl group content was determined by acid hydrolysis followed by gas chromatography and varied from 10(-4) to 3 mol percent depending on reaction conditions. Reactivity varies with alkyl group as di-t-butylzinc greater than diethylzinc greater than dimethylzinc. Toluene and isopropylthiol were identified as organic impurities with isopropylthiol originating in the H2S reagent. Adventitious tetrahydrofuran impurity was converted to tetrahydrothiophene upon heating at 137 to 159 C. Organic impurities were oxidized by treatment of the powder with O2 at 400 C or 1 mol percent O3 in O2 at 25 C. Particle growth was evident in the O2 treated sample but not in the O3 treated sample. The oxidized samples contained about 2 mol percent ZnSO4 and EPR spectra provided evidence for SO2- radicals. The ZnSO4 impurity was converted to ZnO by heating at 800 C. Hot isostatic pressing of the treated powders at 775 C produced fragmented opaque compacts with grain sizes varying from 0.1 to 0.5 microns. The densified samples exhibited about twice the hardness of commercial RAYTRAN ZnS but only half the fracture toughness. GRA

N90-10299# Minnesota Univ., Minneapolis. Dept. of Chemical Engineering and Materials Science.
IMPEDANCE ANALYSIS OF IONIC TRANSPORT IN POLYPYRROLE-POLYAZULENE COPOLYMER AND ITS CHARGE-DISCHARGE CHARACTERISTICS Technical Report, Jul. 1988 - Jun. 1989
Katsuhiko Naoi, Ken-Ichi Ueyama, Tetsuya Osaka, and William H. Smyrl 15 Jun. 1989 27 p
(Contract N00014-88-K-0360)
(AD-A210979; AD-E501135; TR-7-ONR) Avail: NTIS HC A03/MF A01 CSCL 07/4

Ionic transport behavior across an electropolymerized polypyrrole/polyazulene composite film was investigated by using ac impedance analysis, and its charge-discharge characteristics were also studied. Coelectropolymerization of pyrrole and azulene was well defined and fairly stoichiometric in propylene carbonate solution. The charge capacity for the composite films, showed a remarkable increase for films around 50 to 75 percent of azulene monomer content, and the behavior was correlated with morphological and diffusivity changes. The charge-discharge characteristics were examined for cells with a lithium anode and various polypyrrole/polyazulene composite cathodes. Pure polypyrrole cathodes behaved exactly like a capacitor at low frequency, while pure polyazulene cathodes showed excellent rechargeable behavior with very flat discharge curves. Composite cathodes showed intermediate behavior. GRA

28 PROPELLANTS AND FUELS

Includes rocket propellants, igniters, and oxidizers; their storage and handling procedures; and aircraft fuels.

For related information see also *07 Aircraft Propulsion and Power, 20 Spacecraft Propulsion and Power,* and *44 Energy Production and Conversion.*

N90-10300# Center for Night Vision and Electro-Optics, Fort Belvoir, VA.

PHOTOREFLECTANCE STUDY OF BORON ION-IMPLANTED (100) CADMIUM TELLURIDE

P. M. Amirtharaj, M. S. Odell, R. C. Bowman, Jr., and R. L. Alt (Aerospace Corp., El Segundo, CA.) 3 Oct. 1988 23 p
(Contract F04701-85-C-0086-P00019)
(SD-TR-88-89; TR-0088(3945-07)-1) Avail: NTIS HC A03/MF A01

Ion implanted (100) cadmium telluride was studied using the contactless technique of photoreflectance. The implantations were performed using 50- to 400-keV boron ions to a maximum dosage of 1.5 x 10(16)/sq cm, and the annealing was accomplished at 500 C under vacuum. The spectral measurements were made at 77 K near the E(0) and E(1) critical points; all the spectra were computer-fitted to Aspnes' theory. The spectral line shapes from the ion damaged, partially recovered and undamaged, or fully recovered regions could be identified, and the respective volume fraction of each phase was estimated. Author

N90-10301# Los Alamos National Lab., NM.

EFFECTS OF BINDER CONCENTRATION ON THE PROPERTIES OF PLASTIC-BONDED EXPLOSIVES

Raymond D. Steele, Lawrence A. Stretz, Gene W. Taylor, and Thomas Rivera 1989 3 p Presented at the 9th International Symposium on Detonation, Portland, OR, 28 Aug. - 1 Sep. 1989
(Contract W-7405-eng-36)
(DE89-007744; LA-UR-89-407; CONF-890811-18) Avail: NTIS HC A01/MF A01

A series of plastic-bonded explosives (PBX) was formulated with more binder than is normally contained in high energy formulations. Adding a relatively small amount of binder to a material such as PBX 9501 (95/2.5/1.25/1.25 wt percent HMX/Estane/BDNPA/BDNPF (the BDNPA and BDNPF form a eutectic that is frequently called simply the eutectic)) was found to decrease the shock sensitivity while not decreasing the energy of the explosive. The best compromise for a PBX 9501-type material contains about 92 wt percent HMX. Adding additional binder does not continue to decrease the gap sensitivity of the formulation; however, the energy of the PBX decreases as expected. The higher-binder formulations are of potential use because of the possibility of formulating a PBX with energy similar to TATB formulations, such as PBX 9502 (95/5 wt percent TATB/Kel-F 800), and with a higher strain to failure. DOE

N90-10302# Los Alamos National Lab., NM. Chemical and Laser Sciences Div.

FREE-EXPANSION EXPERIMENTS AND MODELING IN DETONATION: CHEMISTRY AND HYDRODYNAMICS ON A LABORATORY SCALE

N. Roy Greiner and Normand Blais 1989 7 p Presented at the 9th International Symposium on Detonation, Portland, OR, 28 Aug. - 1 Sep. 1989
(Contract W-7405-eng-36)
(DE89-007748; LA-UR-89-376; CONF-890811-19) Avail: NTIS HC A02/MF A01

Laboratory-scale (25 to 50 mg) detonations of PETN, RDX, HNS, and TNT were carried out in a high vacuum chamber, and collisionless molecular beams of the freely expanding detonation products were analyzed as a function of time with a mass spectrometer. Concurrently, time sequenced schlieren and shadowgraph images of the initial expansion of the product plume are recorded using a pulsed laser for illumination. These data tie the chemistry and hydrodynamics of the detonation event together. The results, interpreted with the aid of a computer model, suggest that this experiment freezes the chemical reactions of detonation by rapid adiabatic cooling and provides a continuum of samples in the molecular beam, representing the sequence of reactions in the detonating charge. With a suitable model of the expansion hydrodynamics, the hydrodynamic histories of a sequence of volume elements can be associated with their frozen chemistries. Experiments like this are expected to provide a test for molecular models of detonation. DOE

N90-10303# Air Force Systems Command, Wright-Patterson AFB, OH. Fuels and Lubrication Div.

PROPERTIES OF F-34 (JP-8) FUEL FOR 1988 Summary Report, Jan. - Dec. 1988

Charles R. Martel Apr. 1989 27 p
(AD-A210188; WRDC-TR-89-2021) Avail: NTIS HC A03/MF A01 CSCL 21/4

This report summarizes the properties of 95 F-34 fuels delivered to U.S. military installations during calendar year 1988. Most of the fuel was obtained from refineries in Germany, Spain, Sicily and Greece, with one shipment obtained from Bahrain and seven shipments from Venezuela. F-34 destinations included the Central European Pipeline (via terminals in Germany and France), the United Kingdom Pipeline, the Azores, Spain, Italy, Korea and the United States. All of the F-34 fuels met Specification MIL-T-83133B requirements except for Particulate Matter (5 of the 95 fuels slightly exceeded the limit). Most fuel properties were well within specification limits. Two controversial specification limits are the 0.002 weight percent limit on mercaptan sulfur (commercial jet fuel specifications allow up to 0.003 weight percent) and the filtration-time limit. None of the fuels exceeded 0.001 weight percent mercaptan sulfur. Also, all fuels met the filtration time limit, although several fuels were at the specification limit of 15 minutes. GRA

N90-10304# Geo-Centers, Inc., Newton, MA.

HIGH ENERGY DENSITY SOLID AND LIQUID HYDROCARBON FUELS Final Report, Jul. 1987 - Dec. 1988

Alan P. Marchand Feb. 1989 37 p Prepared in cooperation with the University of North Texas, Denton
(Contract F33615-84-C-2412)
(AD-A210195; AFWAL-TR-88-2128) Avail: NTIS HC A03/MF A01 CSCL 21/4

The development of new high energy hydrocarbon fuels for use in air breathing missiles has been the objective of a number of investigations which have received support during the past decade through programs sponsored by the Air Force Systems Command and/or the Naval Air Systems Command. The key characteristics which must be met by potential cruise missile fuels have been described by Burdette and coworkers. A primary requirement in this regard is that candidate fuels must possess high net volumetric heat of combustion (preferably greater than 160,000 BTU/gallon). In order to meet the primary requirement of high net volumetric heat of combustion, hydrocarbon systems were

sought which maximize the ratio of carbon atom to hydrogen atom content were sought which maximize the ratio n/m. GRA

N90-10305# Fluorochem, Inc., Azusa, CA.
CUBANE DERIVATIVES FOR PROPELLANT APPLICATIONS Final Report, 1 Jun. 1987 - 31 May 1989
T. G. Archibald, S. B. Preston, S. A. Harding, N. V. Nguyen, F. O. Bonsu, and K. Baum 3 Jul. 1989 91 p
(Contract N00014-87-C-0676)
(AD-A210368; SDI-2-1) Avail: NTIS HC A05/MF A01 CSCL 07/3

Work during this program emphasized larger scale preparations of cubane-1,4-dicarboxylic acid and process improvements. In the first step, the reaction solvent was changed to toluene to shorten the reaction time and to avoid the use of the carcinogenic solvent, benzene. In the second step, p-dioxane could not be replaced by another solvent, but only molar amounts were needed. This material was destroyed during the reaction, avoiding disposal problem. In step three, the dehydrohalogenation was improved by using inexpensive sodium hydroxide and ethanol instead of potassium t-butoxide in tetrahydrofuran. GRA

N90-10306# Army Biomedical Research and Development Lab., Fort Detrick, MD.
ORGANIC EXPLOSIVES AND RELATED COMPOUNDS. ENVIRONMENTAL AND HEALTH CONSIDERATIONS Technical Report, Jan. 1988 - Mar. 1989
Elizabeth P. Burrows, David H. Rosenblatt, Wayne R. Mitchell, and David L. Parmer 1 Mar. 1989 62 p
(AD-A210554; USABRDL-TR-8901) Avail: NTIS HC A04/MF A01 CSCL 19/1

This report is a compendium of a large body of information currently available in the open literature and in government publications on organic compounds used as explosives and in propellant formulations. While a summary of synthetic processes is included, the emphasis is focused on behavior and fate of these compounds in the environment and their biological effects and potential for animal and human health concerns. Physicochemical properties likely to be of value in making environmental calculations and decisions are also listed and discussed. GRA

N90-10307# Army Missile Command, Redstone Arsenal, AL. Systems Simulation and Development Directorate.
REMARKS ON CERTAIN ASPECTS OF SOLID EXPLOSIVE DETONATION VIA SMALL PROJECTILE IMPACT Final Technical Report, Jul. 1986 - Jul. 1988
James P. Billingsley and Carl L. Adams May 1989 104 p
(AD-A210648; AD-E951366; AMSMI/TR-RD-SS-88-11) Avail: NTIS HC A06/MF A01 CSCL 19/1

Criteria for high explosive detonation via projectile impact have important lethality, survivability and safety implications. Five sets of classic projectile impact induced detonation data were reexamined and reevaluated with respect to Moulard's critical area concept. Some empirical relations were found which are simple functions of the critical area or the projectile cross-section area and known impact shock variables. These relations enhance and/or supplement current empirical detonation prediction methodology, and could lead to a better understanding of the underlying physical phenomena. Furthermore, results from this investigation imply that a minimum (or critical) area dependent shock energy input rate (or power) is necessary for detonation initiation. This minimum amount of power must be sustained for a minimum length of time. This result for solid explosives in analogous to a power input criterion for gaseous explosive detonation which is well documented in the technical literature. It is empirically shown that the area dependent energy rate (power) is inversely proportional to the shock velocity in the explosive. For true one-dimensional situations, the area dependent power requirement is indistinguishable from the constant energy (per unit area) criteria. GRA

29 MATERIALS PROCESSING

Includes space-based development of products and processes for commercial applications.
For biological materials see *55 Space Biology*.

No abstracts in this category.

31 ENGINEERING (GENERAL)

Includes vacuum technology; control engineering; display engineering; cryogenics; and fire prevention.

N90-10308*# National Aeronautics and Space Administration. Langley Research Center, Hampton, VA.
APPROXIMATE SIMULATION MODEL FOR ANALYSIS AND OPTIMIZATION IN ENGINEERING SYSTEM DESIGN
Jaroslaw Sobieszczanski-Sobieski Jun. 1989 13 p Presented at the ISAOC 1989 (International Symposium on Approximation, Optimization and Computing), Dalian, China, 3-7 Jul. 1989 Submitted for publication
(NASA-TM-101616; NAS 1.15:101616) Avail: NTIS HC A03/MF A01 CSCL 13B

Computational support of the engineering design process routinely requires mathematical models of behavior to inform designers of the system response to external stimuli. However, designers also need to know the effect of the changes in design variable values on the system behavior. For large engineering systems, the conventional way of evaluating these effects by repetitive simulation of behavior for perturbed variables is impractical because of excessive cost and inadequate accuracy. An alternative is described based on recently developed system sensitivity analysis that is combined with extrapolation to form a model of design. This design model is complementary to the model of behavior and capable of direct simulation of the effects of design variable changes. Author

N90-10309*# National Aeronautics and Space Administration. Lewis Research Center, Cleveland, OH.
TOTAL HEMISPHERICAL EMITTANCE MEASURED AT HIGH TEMPERATURES BY THE CALORIMETRIC METHOD
Frank DiFilippo, Michael J. Mirtich, Bruce A. Banks, Curtis Stidham, and Michael Kussmaul (Cleveland State Univ., OH.) 1989 19 p Presented at the 16th International Conference on Metallurgical Coatings, San Diego, CA, 17-21 Apr. 1989; sponsored by the American Vacuum Society
(NASA-TM-102322; E-4704; NAS 1.15:102322) Avail: NTIS HC A03/MF A01 CSCL 13B

A calorimetric vacuum emissometer (CVE) capable of measuring total hemispherical emittance of surfaces at elevated temperatures was designed, built, and tested. Several materials with a wide range of emittances were measured in the CVE between 773 to 923 K. These results were compared to values calculated from spectral emittance curves measured in a room temperature Hohlraum reflectometer and in an open-air elevated temperature emissometer. The results differed by as much as 0.2 for some materials but were in closer agreement for the more highly-emitting, diffuse-reflecting samples. The differences were attributed to temperature, atmospheric, and directional effects, and errors in the Hohlraum and emissometer measurements (plus or minus 5 percent). The probable error of the CVE measurements was typically less than 1 percent. Author

N90-10310*# National Aeronautics and Space Administration. Marshall Space Flight Center, Huntsville, AL.
ELECTROSTATICALLY SUSPENDED ROTOR FOR ANGULAR ENCODER Patent Application
Walter Polstorff, inventor (to NASA) 21 Aug. 1989 35 p
(NASA-Case-MFS-28294-1; NAS 1.71:MFS-28294-1;

US-Patent-Appl-SN-396262) Avail: NTIS HC A03/MF A01 CSCL 13H

An apparatus for engraving a code strip with coded markings is disclosed. The code strip is attached for rotation to a cylindrical rotor which is mounted within the cavity of a stator. The stator carries electrodes on its top and side walls to which high potentials are applied to electrostatically suspend the rotor. Circuit means sense the position of the rotor with respect to the stator electrodes and adjust the potential to maintain the rotor at its desired location. A drive motor is connected to the rotor through a drive shaft to initially life the rotor into the desired location within the stator and to rotate it at the desired speed. Thereafter, the drive shaft is disconnected from the rotor, and the rotor continues to spin at a highly stable angular velocity, supported only by the electrostatic fields. NASA

N90-10311# Carnegie-Mellon Univ., Pittsburgh, PA. Robotics Inst.

RELATING TOLERANCES AND KINEMATIC BEHAVIOR

D. A. Bourne, D. Navinchandra, and R. Ramaswamy Apr. 1989 28 p

(AD-A211125; CMU-RI-TR-89-10) Avail: NTIS HC A03/MF A01 CSCL 12/9

Designers usually complete the design with nominal dimensions and allocate tolerances only at the drawing stage. This practice can cause the following problems: (1) unnecessarily tight tolerances that require expensive manufacturing processes; (2) parts whose proper functioning is contingent on excessively tight tolerances; and (3) situations where slight wear on a part can seriously modify the behavior of the device. There is a need for computer-based techniques which allow designers to investigate the effect of manufacturing tolerances on the function their design performs. This paper presents a means for capturing the kinematic behavior of a device and relating it to the tolerances on its components. Behavior is represented using a configuration space representation, which we argue will be a useful tool for designers. GRA

32 COMMUNICATIONS AND RADAR

Includes radar; land and global communications; communications theory; and optical communications.

For related information see also *04 Aircraft Communications and Navigation* and *17 Space Communications, Spacecraft Communications, Command and Tracking.* For search and rescue see *03 Air Transportation and Safety,* and *16 Space Transportation.*

N90-10312# Office of Naval Research European Office, FPO New York, NY.

COHERENT MULTILCHANNEL TECHNIQUES FOR INTEGRATED BROADBAND COMMUNICATIONS SUBSCRIBER LINES

J. F. Blackburn 18 Jan. 1989 5 p

(AD-A209323; ONREUR-9-2-R) Avail: NTIS HC A01/MF A01 CSCL 25/3

The RACE program definition phase is summarized. The background and problems relating to coherent multichannel techniques for integrated communications subscriber lines, assumptions, and recent relevant state-of-the-art developments are discussed, including a commentary on Level III of the RACE definition phase scenario (ROPS-3). The main hardware advantage will occur in the central office in the implementation of broadband distribution services through a high degree of laser sharing. The selection of TV Channels is carried out within the TV set and not by switching in the central office. This reduces problems in connection with signaling bursts and is an important privacy advantage. Key components for CMC techniques are electronically tunable distributed feedback lasers, which should not be affected by reflections or compact laser isolator modules. GRA

N90-10313*# Michigan Univ., Ann Arbor. Radiation Lab.

A COMBINED FINITE ELEMENT AND BOUNDARY INTEGRAL FORMULATION FOR SOLUTION VIA CGFFT OF 2-DIMENSIONAL SCATTERING PROBLEMS Technical Report, Feb. - Sep. 1989

Jeffery D. Collins and John L. Volakis Sep. 1989 77 p (Grant NAG2-541)

(NASA-CR-184781; NAS 1.26:184781; UM-025921-6-T) Avail: NTIS HC A05/MF A01 CSCL 20N

A new technique is presented for computing the scattering by 2-D structures of arbitrary composition. The proposed solution approach combines the usual finite element method with the boundary integral equation to formulate a discrete system. This is subsequently solved via the conjugate gradient (CG) algorithm. A particular characteristic of the method is the use of rectangular boundaries to enclose the scatterer. Several of the resulting boundary integrals are therefore convolutions and may be evaluated via the fast Fourier transform (FFT) in the implementation of the CG algorithm. The solution approach offers the principle advantage of having O(N) memory demand and employs a 1-D FFT versus a 2-D FFT as required with a traditional implementation of the CGFFT algorithm. The speed of the proposed solution method is compared with that of the traditional CGFFT algorithm, and results for rectangular bodies are given and shown to be in excellent agreement with the moment method. Author

N90-10314# Academy of Sciences of the Ukrainian SSR, Kiev. Inst. Yadernykh Issledovanij.

ON CANONICAL QUANTIZATION OF THE ELECTROMAGNETIC FIELD IN TERMS OF FIELD STRENGTHS

I. Yu. Krivskij and V. M. Simulik 1988 19 p In RUSSIAN; ENGLISH summary

(DE89-615389; KIYI-88-35) Avail: NTIS (US Sales Only) HC A03/MF A01

The program of canonical quantization of the electromagnetic field strengths B=(E-vector, H-vector) is performed. It was found that the simplest Lagrangian function in terms of field strengths which has allowed the interpretation of the electric field strength E-vector as the field coordinate and the magnetic field strength H-vector - as the field momentum. The 000-component of the Lipkin Zilch tensor plays the role of the Hamiltonian density in this scheme. The canonical amplitudes was connected to the scheme with the creation and annihilation operators of the real (transverse) photons. This allows the finding of the commutation relations for the quantized field strengths tensor (Bx) in the manifestly covariant form. DOE

N90-10315# Federal Aviation Administration, Atlantic City, NJ.

PHASE 2 TESTING AND EVALUATION OF LOW DATA RATE VOICE CODEC EQUIPMENT

Thomas Dehel, Marcus Grable, and Joseph Child (Computer Technology Associates, Inc., McLean, VA.) Aug. 1989 42 p (Contract FAA-T0704-F)

(ACD-330-Phase-2; DOT/FAA/CT-TN89/49-Phase-2) Avail: NTIS HC A03/MF A01

The Federal Aviation Administration (FAA) is currently evaluating low rate voice digitizing coder/decoder (CODEC's) for use with the Aeronautical Mobile Satellite Service (AMSS). Phase 2 of this evaluation consisted of air traffic control (ATC) personnel participating in an objective intelligibility test of several CODEC's under operational conditions. The results of the testing show that the intelligibility of the low rate 4.8 kilobits per second (kbps) CODEC's is essentially equivalent to the intelligibility of the 9.6 kbps CODEC. The results also show that the 4.8 kbps CODEC's can operate with high intelligibility under conditions of high bit error rates and operational background noise. Author

N90-10316 Brigham Young Univ., Provo, UT.

NEW ELECTRODYNAMIC AND ELECTROSTATIC MODELS WITH APPLICATIONS TO ANTENNA THEORY, SUPERCONDUCTOR SLOTS, AND LASERS Ph.D. Thesis

Steve W. Eggleston 1988 595 p

Avail: Univ. Microfilms Order No. DA8907606

The common set of functions used as a basis for the solution to Helmholtz and Laplace's equations is expanded to include solutions which are not found in the handbooks. With this complete set of basis functions of integer indexes a multicentered model is developed using Debye-like potentials for electrodynamics and standard potentials for electrostatics. The resonant modes of the model are the exact solution to a wide variety of thin linear antennas and antenna-like structures, narrow linear gaps in superconductors, microscopic linear lasers, and arbitrary linear charge distributions. The model is applied to a linear antenna of large-diameter, via Pocklington's and Hallen's integral equation. The nonsinusoidal current of this linear antenna of large-diameter is decomposed into idealized components using equal and unequal spacing, and single and many centered linear antennas. Babinet's principal is brought into play to apply the model to gaps in superconductors. The model of a laser is in the microscopic domain, a domain that was not previously explored. The electrostatic model allows the modeling of an arbitrary linear charge distribution between two points. Dissert. Abstr.

N90-10317*# Hawaii Univ., Manoa. Dept. of Electrical Engineering.
MULTI-LEVEL BANDWIDTH EFFICIENT BLOCK MODULATION CODES
Shu Lin 1 Oct. 1989 54 p
(Grant NAG5-931)
(NASA-CR-185484; NAS 1.26:185484; NASA-Rept-89-002)
Avail: NTIS HC A04/MF A01 CSCL 17B

The multilevel technique is investigated for combining block coding and modulation. There are four parts. In the first part, a formulation is presented for signal sets on which modulation codes are to be constructed. Distance measures on a signal set are defined and their properties are developed. In the second part, a general formulation is presented for multilevel modulation codes in terms of component codes with appropriate Euclidean distances. The distance properties, Euclidean weight distribution and linear structure of multilevel modulation codes are investigated. In the third part, several specific methods for constructing multilevel block modulation codes with interdependency among component codes are proposed. Given a multilevel block modulation code C with no interdependency among the binary component codes, the proposed methods give a multilevel block modulation code C which has the same rate as C, a minimum squared Euclidean distance not less than that of code C, a trellis diagram with the same number of states as that of C and a smaller number of nearest neighbor codewords than that of C. In the last part, error performance of block modulation codes is analyzed for an AWGN channel based on soft-decision maximum likelihood decoding. Error probabilities of some specific codes are evaluated based on their Euclidean weight distributions and simulation results. Author

N90-10318 British Broadcasting Corp., London (England). Engineering Div.
COMPARISON OF DPCM PREDICTION STRATEGIES FOR HIGH-QUALITY DIGITAL TELEVISION BIT-RATE REDUCTION
M. J. Knee and N. D. Wells 1989 15 p
(BBC-RD-1989/8) Avail: Issuing Activity

DPCM prediction strategies are compared for bit-rate reduction of YUV component-coded digital television signals for broadcast-quality contribution or distribution applications. Several systems are compared for two critical moving picture sequences as a test of worst-case performance. The effects of transmission errors on the decoded picture are also compared for some of the systems. The results show that, in terms of picture quality, many of the systems give similar performance on critical sequences but that the error performance of multi-element predictors is much better than that of some of the adaptive prediction strategies. The best performance is obtained from a least-mean-square (LMS) adaptive predictor. Author

N90-10319# Lawrence Livermore National Lab., CA.
MAXIMIZATION OF DIRECTED ELECTROMAGNETIC RADIATION WITH AN OPTIMIZED ANTENNA
R. M. Bevensee Jun. 1989 5 p Presented at the International Union of Radio Science International Symposium on Electromagnetic Theory, Stockholm, Sweden, 14-17 Aug. 1989
(Contract W-7405-eng-48)
(DE89-014045; UCRL-100242; CONF-8908101-1) Avail: NTIS HC A01/MF A01

The results of a study are summarized to obtain reasonable upperbounds to the maximum energy density W sub T (Omega sub 0) per steradian radiated during a time interval (-T,T) in a direction Omega sub 0 and also the maximum instantaneous far field r Epsilon (Omega sub 0). The constraints are: (1) the antenna elements are driven in series by a circuit of zero stored energy around a simple series resonance, (2) the antenna is enclosed within a spherical working volume of radius a/lambda sub min = 1, (3) signal frequencies are restricted to omega less than or equal to omega sub max = 2 pi c/lambda sub min, and (4) the total energy radiated is 1 J. DOE

N90-10320# National Telecommunications and Information Administration, Annapolis, MD.
MANUAL OF REGULATIONS AND PROCEDURES FOR FEDERAL RADIO FREQUENCY MANAGEMENT, MAY 1986 EDITION: REVISIONS FOR JANUARY 1989
14 Feb. 1989 122 p
(PB89-193791) Avail: NTIS HC A06/MF A01 CSCL 17B

This document contains revised pages of the January 1989 Manual of Regulations and Procedures for Federal Radio Frequency Management. GRA

N90-10321# IIT Research Inst., Chicago, IL.
ELF (EXTREMELY LOW FREQUENCY) COMMUNICATIONS SYSTEM ECOLOGICAL MONITORING PROGRAM: ELECTROMAGNETIC FIELD MEASUREMENTS AND ENGINEERING SUPPORT, 1988 Technical Report, 1982 - 1988
D. P. Haradem, J. R. Gauger, and J. E. Zapotosky May 1989 306 p
(Contracts N00039-88-C-0065; N00039-84-C-0070; N00039-81-C-0357)
(AD-A210200; IITRI-E06595-5) Avail: NTIS HC A14/MF A03 CSCL 20/14

A long-term program for studying possible effects from the operation of the Navy's ELF (extremely low frequency) Communications System is being conducted on biota and ecosystems components in north-western Wisconsin and the Upper Peninsula of Michigan. Sixteen general types of organisms from three major ecosystems in the ELF system area are being examined. Formulation of an ELF Ecological Monitoring Program was completed in early 1982 by the Department of the Navy, and studies were initiated in late summer of the same year. Beginning in 1983 and continuing during 1984, major activities of the program consisted of characterization of critical aspects of each study, collection of data to validate assumptions made in proposals, and selection of study sites. From 1985 through 1988, activities centered on the operation of full-scale studies. This report documents electromagnetic (EM) field measurements at investigator selected study sites from 1982 through 1988. Other engineering support activities are also described. GRA

N90-10322# Analytical Sciences Corp., Reading, MA.
OMEGA SYSTEM PERFORMANCE ASSESSMENT Final Report, Jun. 1988 - Mar. 1989
Peter B. Morris Mar. 1989 148 p
(Contract DTCG23-86-C-20024)
(AD-A210342; TASC-TR-5351-8-1; USCG/ONSCEN-01-89)
Avail: NTIS HC A07/MF A01 CSCL 17/7

A measure of system performance, termed the system availability index, is introduced as: (1) an indicator of operational performance; (2) a probability of system access and utility to the system subscriber; and (3) a means of comparing system options. Theoretical development of the index is given in terms of a system availability model which is based on receiver/station reliability, signal coverage, and user geographic priorities. Sample calculations of the index are presented to illustrate comparison of system

options, e.g., the effect of a station off-air. Techniques are presented to compute a station power level assignment and station off-air maintenance schedule. Comparison of signals from the VLF communications stations and the Omega system in terms of signal coverage, receiver utilization, and government policy is also given. GRA

N90-10323# Harry Diamond Labs., Adelphi, MD.
CONSUMER ELECTRONICS TESTING TO FAST-RISE EMP (ELECTROMAGNETIC PULSE) VEMPS (VERTICAL ELECTROMAGNETIC PULSE SIMULATOR) 2 DEVELOPMENT Final Report, Mar. 1987 - Mar. 1988
Vincent J. Ellis Jun. 1989 62 p
(AD-A210505; HDL-TR-2149) Avail: NTIS HC A04/MF A01 CSCL 20/15

The Army has initiated a research and development effort for a new free-field, fast-rise Electromagnetic Pulse (EMP) simulator, the second-generation Vertical Electromagnetic Pulse Simulator (VEMPS 2). Because of the unique performance characteristics of VEMPS 2 and the technological changes in consumer electronics over the past 10 years, there is a need to evaluate the incidental effects of VEMPS-2-like simulated EMP on modern consumer electronics. Although a similar evaluation of the effects of existing EMP simulators on consumer electronics was performed in 1978 the results obtained may not be directly applicable to the VEMPS 2 scenario and modern consumer electronics. One of the proposed site locations for the VEMPS 2 is the Woodbridge Research Facility (WRF), the location of the Army's lead laboratory for EMP research. The environment at WRF was used as a basis for developing the physical parameters associated with the test efforts described herein. Various types of consumer electronics identified through a survey of the Woodbridge, VA, community, were exposed to EMP environments similar to the predicted VEMPS 2 environments, and the results evaluated. The analysis indicates that the impact, if any, of VEMPS 2 operation on consumer electronics in the public areas outside WRF will be minimal. GRA

N90-10324# Naval Ocean Systems Center, San Diego, CA.
TWIRE: A TEST PROGRAM FOR VLF AIRBORNE TRANSMISSIONS Interim Report, May 1987 - Jan. 1988
R. A. Pappert and L. R. Hitney Apr. 1989 104 p
(AD-A210516; NOSC/TD-1499) Avail: NTIS HC A06/MF A01 CSCL 25/2

A computer program called TWIRE, which combines a TACAMO configuration code, a radiation resistance code and a VLF propagation code, has been assembled for the purpose of conducting case studies for airborne VLF transmissions and for the purpose of pointing out possible future areas of improvement for such transmissions. A major deficiency of the program is that it is not fully automated because the configuration code requires initial inputs which often have to be determined by trial and error. Nevertheless, the program is useful for case studies and provides a tool for assessing the adequacy for field calculation purposes of point dipoles as approximations to rationally determined TACAMO antenna configurations. Sample results of such comparisons are included. GRA

N90-10325# Air Force Geophysics Lab., Hanscom AFB, MA.
EFFECTS OF RAIN ATTENUATION ON SATELLITE EHF (EXTREMELY HIGH FREQUENCY) COMMUNICATIONS IN THE US Final Report, 1986 - 1988
Paul Tattelman and Kevin P. Larson 9 Jan. 1989 188 p
(AD-A210517; AFGL-TR-89-0012; AFGL-ERP-1017) Avail: NTIS HC A09/MF A01 CSCL 20/14

One-minute rain rate data over a 10-year period-of-record at each of 41 locations in the contiguous U.S., and for a 6 1/2-year period-of-record at 1 location in Puerto Rico, were extracted from original weighing raingage recordings. The data were analyzed to determine monthly, seasonal, and annual rain-rate frequencies, durations, and probabilities at locations representing a large variety of climatic rainfall regimes. These analyses are particularly useful for estimating EHF (Extremely High Frequency) communication outages due to the increasing effects of attenuation caused by rain at frequencies above 10 GHz. An attenuation model was used to estimate the effects of rain attenuation at all 42 locations. Analyses of the 1-min rain rates, and outage estimates for various frequencies and propagation-path elevation angles are presented. GRA

N90-10326# Army Research Inst. for the Behavioral and Social Sciences, Alexandria, VA.
SINCGARS (SINGLE-CHANNEL GROUND/AIRBORNE RADIO SYSTEM) OPERATOR PERFORMANCE DECAY Interim Report, Oct. 1983 - Feb. 1987
Richard L. Palmer and Louis W. Buckalew Nov. 1988 20 p
(AD-A210716; ARI-RR-1501) Avail: NTIS HC A02/MF A01 CSCL 17/4

The Single-Channel Ground/Airborne Radio System (SINCGARS) is scheduled to replace the Army's VRC-12 and PRC-77 radios. However, SINCGARS is more complex to operate and requires more training. This study examined the decay of operational skills and knowledge in two groups of recently trained operators who went without exposure to SINCGARS for several weeks. Performance levels were measured with the SINCGARS Learning-Retention Test (SLRT), a simulated hands-on performance test emphasizing skills and operational knowledge retention. The results provided tentative indications that operators may lose about 10 percent of their prior performance levels within the first few weeks. This figure is expected to vary considerably, depending on the type of soldier, the length of the nonexposure period, and other conditions. It was also found that performance level was correlated with soldiers' Armed Services Vocational Aptitude Battery (ASVAB) General Technical (GT) scores. Correlations between GT and SLRT scores obtained at two different times were .43 and .50, respectively. However, no relation was observed between performance decay and GT. Further evaluation of operator performance decay needs to be done to determine the effect of longer periods of nonexposure (e.g., 60 and 90 days). GRA

N90-10327# Mission Research Corp., Santa Barbara, CA.
IMPROVED PROPAGATION MODELS FOR DISCRETE RANDOM MEDIA Final Report, 15 Dec. 1986 - 14 Feb. 1989
Charles L. Rino 15 Apr. 1989 6 p
(Contract DAAL03-87-C-0002)
(AD-A211085; ARO-24723.1-GS-S) Avail: NTIS HC A02/MF A01 CSCL 20/14

An exact spectral-domain formulation was developed for characterizing wave propagation in continuous random media. The formulation consists of a pair of coupled first-order differential equations for waves propagating in the forward and backward directions. These generalized transmission line equations fully accommodate backscatter, and they impose no restriction on scattering angle. In the first application of these equations, the models that are commonly used for propagation of light in the atmosphere and radiowaves in ionized media are generalized to accommodate backscatter. The backscatter enhancement predicted by the cumulative forward scatter single backscatter approximation does not occur unless the finite correlation between the forward and backward propagating waves is included. The model is extended to discrete random media. A similar pair of differential equations is derived that characterize the propagation of vector waves in sparse discrete random media. The equations are exact for small numbers of particles, and can be used to compute the mutual interaction among scattering objects whose free-space scattering characteristics are known. From this model the effective wave number that is commonly used for coherent wave propagation was generalized to include both backscatter and cross polarization terms. When generalized to second order, the equations can be cast in the same form as equations of vector radiative transport, but they are derived directly from Maxwell's equations. GRA

N90-10149*# Lockheed Missiles and Space Co., Palo Alto, CA.
ANTENNA TECHNOLOGY FOR BEAMED SPACE-POWER
W. S. Gregorwich *In* NASA. Langley Research Center, Second

Beamed Space-Power Workshop Jul. 1989 p 159-170 (For primary document see N90-10140 01-20)
Avail: NTIS HC A19/MF A03 CSCL 20N

N90-10155*# National Aeronautics and Space Administration. Lewis Research Center, Cleveland, OH.
OVERVIEW OF MICROWAVE CONCEPTS
Karl A. Faymon *In* NASA. Langley Research Center, Second Beamed Space-Power Workshop Jul. 1989 p 287-290 (For primary document see N90-10140 01-20)
Avail: NTIS HC A19/MF A03 CSCL 20N

33 ELECTRONICS AND ELECTRICAL ENGINEERING

Includes test equipment and maintainability; components, e.g., tunnel diodes and transistors; microminiaturization; and integrated circuitry.

For related information see also *60 Computer Operations and Hardware* and *76 Solid-State Physics.*

N90-10328# J and D Scientific, Inc., Mesa, AZ.
SCANNING TUNNELING MICROSCOPY ETCHING OF MICROMETER LEVEL FEATURES ON p-TYPE GaAs Final Report, 15 Aug. 1988 - 14 Feb. 1989
Larry D. McCormick Mar. 1989 26 p
(Contract DAAL03-88-C-0019)
(AD-A209216; ARO-26209.1-EL-SBI) Avail: NTIS HC A03/MF A01 CSCL 09/1

The goal of the phase 1 research was to demonstrate that p-type GaAs could be imaged and etched using a scanning tunneling microscope (STM) tip to produce features smaller than the micrometer level. The material used in this study was Zn doped. The etching solution was 5mM NaOH, 1mM EDTA. Negative biases, i.e., tip positive, of 4 volts yielded etched regions after subsequent oxidation decomposition of the processed region. These regions could be produced much smaller than 1 micrometer. Therefore, the phase 1 research showed that STM can be used to selectively etch regions of p-type GaAs under electrochemical conditions. This procedure has potential application in the custom production of small, fast semi-conductor devices. GRA

N90-10329*# National Aeronautics and Space Administration. Pasadena Office, CA.
LATERALLY STACKED SCHOTTKY DIODES FOR INFRARED SENSOR APPLICATIONS Patent Application
True-Lon Lin, inventor (to NASA) (Jet Propulsion Lab., California Inst. of Tech., Pasadena.) 9 Jun. 1989 12 p Prepared in cooperation with Jet Propulsion Lab., California Inst. of Tech., Pasadena
(Contract NAS7-918)
(NASA-Case-NPO-17426-1-CU; NAS 1.71:NPO-17426-1-CU; US-Patent-Appl-SN-363815) Avail: NTIS HC A03/MF A01 CSCL 09A

Laterally stacked Schottky diodes for infrared sensor applications are fabricated utilizing porous silicon having pores. A Schottky metal contract is formed in the pores, such as by electroplating. The sensors may be integrated with silicon circuits on the same chip with a high quantum efficiency, which is ideal for IR focal plane array applications due to uniformity and reproducibility. NASA

N90-10330# City Coll. of the City Univ. of New York, NY. Inst. for Ultrafast Spectroscopy and Lasers.
SUBPICOSECOND OPTICAL DIGITAL COMPUTATION USING CONJUGATE PARAMETRIC GENERATORS Final Report, Dec. 1987 - Nov. 1988
Robert Alfano, George Eichmann, Roger Dorsinville, and Yao Li 31 Mar. 1989 8 p
(Grant AF-AFOSR-0039-88; AF Proj. 2305)
(AD-A207908; RF-447242; AFOSR-89-0647TR) Avail: NTIS HC A02/MF A01 CSCL 09/5

Fundamental optical nonlinear processes based on X3 of different materials: organic polymers and liquids, and semiconductors were investigated for size and speed. Ultrafast optical logic devices, switches, and processes based on these nonlinear optical materials were designed, built, and tested. GRA

N90-10331# Lawrence Livermore National Lab., CA.
COMMERCIAL HIGH CURRENT IGNITRON DEVELOPMENT
R. Kihara, D. B. Cummings, K. S. Leighton, and A. P. Shulski Jun. 1989 6 p Presented at the 7th Institute of Electrical and Electronics Engineers Pulsed Power Conference, Monterey, CA, 12-14 Jun. 1989
(Contract W-7405-eng-48)
(DE89-015077; UCRL-100358; CONF-890665-36) Avail: NTIS HC A02/MF A01

The overall goal is to develop and qualify devices capable of repetitively switching high peak currents (greater than 1 MA) and large quantities of charge (greater than 500 C). In 1988 a hollow-anode ignitron was designed and tested at levels of up 925 kA and 260 C per shot. This level is three times that previously achieved with standard, commercially available tubes. The latest designs, developed with the cooperation on industry, incorporate a hollow anode into an industrial ignitron. Prototypes have recently achieved levels of 770 kA and 270 C per shot. DOE

N90-10332# Lawrence Livermore National Lab., CA. Beam Research Program.
A BATTERY-POWERED, SOLID STATE MAGNETIC COMPRESSOR WITH APPLICATIONS FOR HIGH PRF ACCELERATORS AND LASERS
E. E. Bowles, B. L. Burley (General Dynamics Corp., San Diego, CA.), D. M. Barrett, H. C. Kirbie, and M. A. Newton 17 May 1989 6 p Presented at the 7th Institute of Electrical and Electronics Engineers Pulsed Power Conference, Monterey, CA, 12-14 Jun. 1989
(Contract W-7405-eng-48)
(DE89-015770; UCRL-100320; CONF-890665-38) Avail: NTIS HC A02/MF A01

An 8-J/pulse magnetic pulse compressor was built to demonstrate a power conditioning technique whereby battery power is converted into a train of 5 micrometer pulses at a maximum pulse repetition frequency of 11 kHz. The machine employs inverter-grade thyristors that switch with less than 120-ps pulse-to-pulse jitter. The network uses a phased-triggering scheme to obtain an output voltage regulation of (+ or -) 0.002 percent. Magnetic core reset is achieved by using a reflected portion of the output pulse from a mismatched load. DOE

N90-10333# Los Alamos National Lab., NM.
REPORT ON THE PERFORMANCE AND OPERATING CHARACTERISTICS OF THE BURLE C83061E QUANTACON (TRADEMARK) PHOTOMULTIPLIER TUBE
V. D. Sandberg, T. N. Thompson, and F. A. Helvy (Burle Industries, Inc., Lancaster, PA.) 1989 13 p Presented at the Workshop on Physics and Experimental Techniques of High Energy Neutrinos and VHE and UHE Gamma-Ray Particle Astrophysics, AR, 11-13 May 1989 Submitted for publication
(Contract W-7405-eng-36)
(DE89-015257; LA-UR-89-2404; CONF-8905193-1) Avail: NTIS HC A03/MF A01

The Burle C83061E QUANTACON (trademark) is a 10.4 inch diameter photomultiplier tube with improved photoelectron collection optics. We report here on the first tests of this newly developed tube. We find the single photoelectron charge resolution to be excellent, with a peak to (noise) valley ratio exceeding 3 and with a transit time spread of less than 2.3 ns (FWHM) for full photocathode illumination at the single photoelectron level. A design for a fast anode pulse base is also presented. DOE

N90-10334# Central Research Inst. of Electric Power Industry, Tokyo (Japan).
DEVELOPMENT OF AN EXPERT SYSTEM SUPPORTING SHORT-CIRCUIT TESTS FOR CIRCUIT BREAKERS
Kinya Sunabe and Ryuzo Horiuchi Jun. 1988 74 p In JAPANESE; ENGLISH summary
(DE89-760384; CRIE-W-87039) Avail: NTIS (US Sales Only) HC A04/MF A01

Test operator must be familiar with electrical and mechanical characteristics on the many and complicated equipments to operate the large capacity short circuit ones. The expert system supporting short circuit test for circuit breaker was developed to reduce the burden and to make unskilled workers operatable in a short period. A personal computer is operated by using expert system program language and C language. This system can be used by operating keys except character ones to improve man machine interface. The suitable testing circuit is selected and circuit constant to be inserted is presented to operate the system. The setting times for sequence timer and phase controller are calculated and presented. Optimal instruments are designated and presented on the basis of measuring items such as voltage and current. The calculated results by this system agreed well with the previous manual calculations by the comparison with the setting values for the conventional automatic analyzer of measurements. Anyone can carry out the short circuit test of circuit breaker rightly, easily and safely without complicated manual calculations. DOE

N90-10335# Allied-Signal Aerospace Co., Kansas City, MO. Technical Communications Div.
CHARACTERIZATION OF 4/3 TECHNOLOGY LARGE-SCALE INTEGRATED CIRCUIT ON POLYSILICON PROCESSES
Topical Report
E. C. Daskalos and J. M. Sobering Aug. 1988 30 p
(Contract DE-AC04-76DP-00613)
(BDX-613-3971) Avail: NTIS HC A03/MF A01

The major variables affecting the polysilicon process are discussed and evaluated. A process was developed to achieve a manufacturable process. Author

N90-10336# Allied-Signal Aerospace Co., Kansas City, MO. Technical Communications Div.
STATISTICAL MODELING OF ELECTRICAL COMPONENTS
Final Report
R. L. Jolly Jul. 1988 17 p
(Contract DE-AC04-76DP-00613)
(BDX-613-3939) Avail: NTIS HC A03/MF A01

A method of forecasting production yields based on SPICE (Computer Program) circuit simulation and Monte Carlo techniques was evaluated. This method involved calculating functionally accurate component models using statistical techniques and using these component models in a SPICE electrical circuit simulation program. The results of the simulation program allow production yields to be calculated using standard statistical techniques. Author

N90-10337# Sandia National Labs., Albuquerque, NM.
MECHANICAL STATES IN WOUND CAPACITORS. PART 1: PREDICTION
Robert C. Reuter, Jr. and James J. Allen 1989 20 p Presented at the ASME Design Conference, Montreal, Quebec, 17-20 Sep. 1989
(Contract DE-AC04-76DP-00078)
(DE89-008110; SAND-89-0544C-Pt-1; CONF-890987-1-Pt-1)
Avail: NTIS HC A03/MF A01

The problem of determining the mechanical states inside wound capacitor rolls is addressed through the application of two dimensional, linear elasticity. Allowances are made for heterogeneous wound construction of the capacitor, orthotropic material behavior of the capacitor constituents, and arbitrary winding tension. A key element in the formulation is the derivation of material properties for a wound, orthotropic layer which is equivalent in behavior to a stack of dissimilar plies such as are actually wound on the capacitor simultaneously during one turn of the mandrel. The dissimilar plies are necessary by virtue of the conductor and dielectric materials which must be present in a capacitor. The derivation of predictive equations is based on winding the equivalent layer on an appropriate mandrel, followed by a recovery of the individual ply responses. The capability to explicitly calculate the winding tensions which would be necessary to produce a required wound tension dependence upon capacitor radius is also developed. Numerical results for typical capacitor design and construction are presented, and justification for the application of optimization theory in capacitor development is demonstrated. DOE

N90-10338# Sandia National Labs., Albuquerque, NM.
MECHANICAL STATES IN WOUND CAPACITORS. PART 2: OPTIMIZATION
James J. Allen and Robert C. Reuter, Jr. 1989 32 p Presented at the ASME Design Conference, Montreal, Quebec, 17-20 Sep. 1989
(Contract DE-AC04-76DP-00078)
(DE89-008116; SAND-89-0545C-Pt-2; CONF-890987-2-Pt-2)
Avail: NTIS HC A03/MF A01

The winding process is encountered frequently in manufacturing, such as winding of polymer films and paper, laminated pressure vessel construction, and the manufacture of wound capacitors. The winding of capacitors will typically involve hundreds of plies of conductor and dielectric wound over a core. Due to the large number of layers, the calculation of the mechanical studies within a wound capacitor is a significant computational task. The focus of Part 2 is the formulation and application of optimization techniques for the design of wound capacitors. The design criteria to be achieved is a specified uniform wound tension in a capacitor. An optimization statement is formulated of the wound capacitor design problem, a technique is developed for reducing the numerical calculation required to repeatedly analyze the capacitor as required by the optimization algorithm, and the technique is applied to an example. DOE

N90-10339# Sandia National Labs., Albuquerque, NM.
PREPARATION AND EVALUATION OF COMPOSITE MEMBRANES FOR ZINC/BROMINE STORAGE BATTERIES
Charles Arnold, Jr. and Roger A. Assink 1989 12 p Presented at the American Chemical Society National Meeting, Miami Beach, FL, 10-15 Sep. 1989
(Contract DE-AC04-76DP-00078)
(DE89-009931; SAND-89-0700C; CONF-890902-2) Avail: NTIS HC A03/MF A01

Low coulombic efficiencies of zinc/bromine redox batteries were attributed to migration of bromine and negatively charged bromine moieties through the microporous separator used to separate the catholyte from the anolyte. While it was demonstrated that improvements in coulombic efficiency can be achieved by replacing the microporous separator with a cationic ion exchange membrane, these membranes are expensive and/or not sufficiently conductive to be practicable. It was found that the rate of bromine permeation can be reduced by two orders of magnitude with minimal decreases in conductivity by impregnating commercial microporous polyethylene type separators with sulfonated polysulfone, a cationic polyelectrolyte that was developed in earlier work for other redox storage batteries. DOE

N90-10340# Sandia National Labs., Albuquerque, NM. Explosive Subsystems Div.
HEAT TRANSFER CHARACTERISTICS OF IGNITER OUTPUT PLUMES
N. A. Evans and N. A. Durand 1989 11 p Presented at the 14th International Pyrotechnics Seminar, Jersey, England, 18-22 Sep. 1989
(Contract DE-AC04-76DP-00078)
(DE89-011449; SAND-89-0271C; CONF-8909113) Avail: NTIS HC A03/MF A01

Seven types of pyrotechnic igniters were each mounted at one end of a closed cylindrical bore hole representative of the center hole in a thermal battery. Measurements of local bore wall

temperature, T(sub w), using commercially available, fast response (10 microsec) sheathed chromel-constantan thermocouples allowed calculation of local heat transfer rates, q, and wall heat flows, Q. The principal charge constituents of all these igniters were titanium and potassium perchlorate, while three types also contained barium styphnate as an ignition sensitizer. Igniter closure disc materials included glass-ceramic, glass, metal (plain, scored, with and without capture cone), and kapton/RTV. All igniters produced the lowest values of T(sub w) and q at the beginning of the bore, and, except for the igniter with the kapton/RTV closure disc, these quantities increased with distance along the bore. For igniters containing only titanium/potassium perchlorate, the rates of increase of Q along the bore length, compared with those for T(sub w) and q, were generally lower and more variable. The inclusion of barium styphnate produced rates of change in Q that were essentially constant to the end of the bore. The highest overall average wall temperatures were achieved by two igniter types with metal closure discs and no capture cone. No clear correlation was established between peak bore pressure and maximum wall temperature. DOE

N90-10341# Sandia National Labs., Albuquerque, NM. Explosive Subsystems Div.
PYROTECHNIC IGNITION STUDIES USING A GUN TUNNEL
N. A. Evans 1989 11 p Presented at the 14th International Pyrotechnics Seminar, Jersey, England, 18-22 Sep. 1989
(Contract DE-AC04-76DP-00789)
(DE89-012496; SAND-89-0252C; CONF-8909113-1) Avail: NTIS HC A03/MF A01

A gun tunnel is being used to investigate the ignition characteristics of center-hole iron/potassium perchlorate thermal battery discs. Details are given of the construction, operation, and data reduction method for the gun tunnel. To simulate an igniter, this system can readily produce a pulse of hot argon at maximum pressures and temperatures up to P(sub max) = 8 MPa and T sub max = 4000K, respectively, with flow times of the order of 3 msec. For a single battery disc, a segment of the ignition boundary was found to lie in the region of T sub max = 1200 to 1300K and 0.7 MPa less than P sub max less than 2.0 MPa. The results also showed two types of ignition: prompt ignition, requiring an average delivered enthalpy (ovr (Delta)H) sub ig = 6 cal during an average flow time (ovr (Delta)t) sub ig = 0.7 msec, and delayed ignition, with (ovr (Delta)H) sub ig = 16 cal and (ovr (Delta)t) sub ig = 2.4 msec. In addition, near an ignition boundary, high speed motion photography showed the ignition delay increased to 6 msec with significant spatial non-uniformity. DOE

N90-10342# Sandia National Labs., Albuquerque, NM.
VARISTOR-PARTICLE LIGHTNING ARRESTOR CONNECTOR PERFORMANCE UNDER SIMULATED EXTREME LIGHTNING CURRENTS
R. J. Fisher and J. G. Kostas 1989 6 p Presented at the International Conference on Lightning and Static Electricity, Bath, England, 26-28 Sep. 1989
(Contract DE-AC04-76DP-00789)
(DE89-012663; SAND-88-3470C; CONF-8909124-2) Avail: NTIS HC A02/MF A01

Varistor-particle lightning arrestor connectors have been tested under simulated lightning currents of peak amplitude up to 185 kA. Each connector was attached to a circuit of representative interest, in which currents were measured at various points. These currents were reproduced in post-test circuit modeling, during which voltages were determined throughout the circuit and response sensitivity to statistical variations in post-breakdown contact-arc voltage was demonstrated. In all cases, resultant downstream circuit voltages were well below the 1500-V criterion. DOE

N90-10343# Pacific Northwest Labs., Richland, WA.
PERFORMANCE OF A BROADBANDED ULTRASONIC TRANSDUCER WITH COAXIALLY MOUNTED, NONDIRECTIONAL RECEIVER
G. J. Posakony and E. R. Green Jul. 1989 12 p Presented at the Conference on Review of Progress in Quantitative NDE, Brunswick, ME, 23-28 Jul. 1989
(Contract DE-AC06-76RL-00183)
(DE89-015838; PNL-SA-16946; CONF-890770-1) Avail: NTIS HC A03/MF A01

For a majority of ultrasonic nondestructive testing applications, the ultrasonic transducer used for transmission is also used for reception. When separate transducers are used, the receiving element is usually a duplicate of the transmitting element. In this situation, the directivity pattern of the transducer(s) is the same for transmission and reception. It is well established that the amount of energy and the directivity patterns reflected from a target (flaw or defect) are highly dependent on the type and shape of the target. Further, it is known that the directivity pattern of the receiving transducer can inhibit the ability to characterize the target. To study these effects, an experiment was designed using a nondirectional receiver, coaxially-mounted into the transmitting element. The objective was to demonstrate the influence of directionality as it relates to target orientation and size. DOE

N90-10344# Lawrence Livermore National Lab., CA.
MICRO-CAVITY INTEGRABLE VACUUM DIODES AND TRIODES
William J. Orvis, Charles F. McConaghy, Dino R. Ciarlo, Jick H. Yee, Ed W. Hee, Charles E. Hunt, and Johann Trujillo (California Univ., Davis.) Jul. 1989 5 p Presented at the 2nd International Conference on Vacuum Microelectronics, Bath, England, 24-26 Jul. 1989
(Contract W-7405-eng-48)
(DE89-016649; UCRL-100525; CONF-8907121-1) Avail: NTIS HC A01/MF A01

We are developing miniature, vacuum, field emission diodes, and triodes for use in electronics in hazardous environments. We have produced the structures for micrometer sized diodes and triodes. We are currently improving the emission rate of the field mission electron source, before inserting it into the diode and triode structures. DOE

N90-10345# Polytechnic Univ., Farmingdale, NY.
PHYSICS OF HIGH ENERGY PHOTOCONDUCTIVE SWITCHES Final Technical Report, 1 Aug. 1985 - 30 Sep. 1988
Erich E. Kunhardt Jun. 1989 25 p
(Grant AF-AFOSR-0249-85; AF Proj. 2301)
(AD-A210341; AFOSR-89-0994TR) Avail: NTIS HC A02/MF A01 CSCL 09/1

During this funding period, a semi-classical macro-kinetic theory that describes the dynamic behavior of carriers in a semiconductor under the influence of space-time varying fields was formulated. The macro-kinetic model is considerably easier to implement numerically than Monte Carlo methods or those based on the Boltzmann Transport Equation (BTE). Moreover, the macro-kinetic model requires orders of magnitude less computer time to run. A Monte Carlo method was developed for obtaining the electron energy distribution, transport parameters, and rate coefficients in multi-valley semiconductors. The procedure requires an order of magnitude less time than conventional Monte Carlo techniques. GRA

N90-10346# Ceramic Process Systems Corp., Milford, MA.
COMPOSITE CERAMIC SUPERCONDUCTING WIRES FOR ELECTRIC MOTOR APPLICATIONS Annual Report No. 1, 30 Jun. 1988 - 30 Jun. 1989
John W. Holloran 7 Jul. 1989 189 p
(Contract N00014-88-C-0512; ARPA Order 9525)
(AD-A210345; CPS-89-009) Avail: NTIS HC A09/MF A01 CSCL 09/1

Progress is described on developing Y-123 wire for an HTSC motor. The wire development involves synthesis of Y-123 powder, spinning polymer containing green fiber, heat treating the fiber to produce metallized superconducting filaments, and characterizing the electrical properties. A melt spinning process was developed for producing 125-micron diameter green fiber containing 50 vol percent Y-123. This fiber can be braided for producing transposed multifilamentary wire. A process was developed to coat green fiber

with silver alloys which can be continuous sintering. A second process for multifilamentary ribbon wire is also being developed. The Y-123 filaments have 77 deg self-field Jc values up to 2600 A/sq cm, but Jc is reduced to 10 A/cm squared at 800 G. Preliminary data is presented on mechanical properties. A dc homopolar motor with an iron magnetic circuit is being designed to operate with early HTSC wire. GRA

N90-10347# Ceramphysics, Inc., Westerville, OH.
CAPACITIVE ENERGY STORAGE AT CRYOGENIC TEMPERATURES, PHASE 2 Final Report, 1 Jan. 1986 - 31 Dec. 1988
C. F. Clark 14 Feb. 1989 148 p
(Contract F49620-86-C-0029; AF Proj. 3005)
(AD-A210366; AFOSR-89-0995TR-Phase-2) Avail: NTIS HC A07/MF A01 CSCL 09/1

The primary goal of this Phase 2 program was to improve the dielectric breakdown strength of ceramic multilayer capacitors (MLC's) in order to improve capacitive energy storage at liquid nitrogen temperatures. A secondary goal was to explore the reproducibility of a field enforced state switching effect discovered in the Phase 1 program. The ceramic composition involved in these programs is designated as CPN17 and has a dielectric constant in the range 8,000 to 10,000 at 77 K. Several variations in conventional ceramic processing parameters were studied, leading to systematic improvements in the breakdown strength at 77 K (160 to 250 to 400 kV/cm). GRA

N90-10348# Giner, Inc., Waltham, MA.
ADVANCED DOUBLE LAYER CAPACITOR Quarterly Report No. 3, 1 Nov. 1988 - 31 Jan. 1989
Anthony B. LaConti, Philip Lessner, and S. Sarangapani Jul. 1989 21 p
(Contract N00014-88-C-0391)
(AD-A210510; C87A-25) Avail: NTIS HC A03/MF A01 CSCL 10/3

The overall goal of this project is to develop electrochemical capacitors with no liquid electrolyte present. The liquid electrolyte is replaced by a solid ionomer electrolyte. An advantage of these devices over conventional electrochemical capacitors containing free acid would be greater safety and reliability. In the third quarter, we concentrated our efforts in three areas: (1) preparation and characterization of RuOx powders, (2) preparation of membrane and electrode (M and E) assemblies with high capacitance, and (3) ac impedance characterization of M and E assemblies. GRA

N90-10349# California Univ., San Diego. Dept. of Electrical Engineering and Computer Sciences.
STUDIES OF HIGH POWER DENSITY, PICO-SECOND RISE-TIME LIGHT ACTIVATED SEMICONDUCTOR SWITCH Final Report, 1 Sep. 1987 - 31 Dec. 1988
Paul L. Yu 31 Dec. 1988 107 p
(Grant AF-AFOSR-0351-87; AF Proj. 2301)
(AD-A210549; AFOSR-89-0993TR) Avail: NTIS HC A06/MF A01 CSCL 09/1

The carrier dynamics of the diode which is related to its electrical power switching behaviors is investigated in this program. A model is developed where the carrier transport and Maxwell equations are incorporated and self-consistent electrical field profiles, current density and carrier are obtained in the PIN diode. Both low and high level optical excitations as well as low and high applied bias situations can be described by this model. The transient behavior of the diode switch at different optical energy levels is now well understood, while conventional theory for photodiodes at low level excitation and at low bias cannot be applied to cases for high level excitation and high bias. As a circuit element, the rise time of the switch under these circumstances depends on the time the internal field is cancelled out by mobile carriers generated. The predicted input energy dependence and the transmission line impedance dependence of the rise time compare well with experimental results. The model also suggests the experimental configuration for obtaining power in the GW range. Finally, a preliminary investigation is made on the effects of avalanche multiplication on the performance of the diode switch. GRA

N90-10350# Minnesota Univ., Minneapolis. Corrosion Research Center.
THE USE OF LITHIUM BATTERIES IN BIOMEDICAL DEVICES Technical Report No. 8, Jul 1988 - Jun. 1989
Boone B. Owens 15 Jun. 1989 4 p
(Contract N00014-88-K-0360)
(AD-A210789) Avail: NTIS HC A01/MF A01 CSCL 10/4

Lithium batteries have played an important role in the development of useful implantable biomedical devices. The cardiac pacemaker is the most well known of these devices and high energy, long-life reliable lithium primary cells have effectively replaced all of the alkaline cells previously used in these electronic systems. The recent development of higher power devices such as drug pumps and cardiac defibrillators require the use of batteries with higher energy and power capabilities. High rate rechargeable batteries that can be configured as flat prismatic cells would be especially useful in some of these new applications. Lithium polymer electrolyte batteries may find a useful role in these new areas. GRA

N90-10351# Westinghouse Electric Corp., Lima, OH.
HIGH TEMPERATURE VSCF (VARIABLE SPEED CONSTANT FREQUENCY) GENERATOR SYSTEM Final Report, 16 Sep. 1985 - 30 Jun. 1988
Thomas Allen Maphet, Jack Lee McCabria, Carroll Charles Kouba, James Thomas Mitchell, and James Robert Kwiecinski Apr. 1989 66 p
(Contract F33615-85-C-2551; AF Proj. 3145)
(AD-A210823; AFWAL-TR-88-2144) Avail: NTIS HC A04/MF A01 CSCL 10/2

The high temperature VSCF generator program was designed to develop a generating system capable of withstanding constantly high oil-in temperatures of 200 C in an ambient environment of 200 C. This is a requirement due to anticipated new fighter aircraft designs that will not be capable of cooling the oil to 100 C as in today's designs due to size restrictions of the heat exchanger and/or extended operation of the aircraft at supersonic speeds. The generator uses composite material to withstand the constant use of 200 C inlet oil. GRA

N90-10352# Massachusetts Inst. of Tech., Cambridge. Lab. for Computer Science.
THE ORGANIZATION OF PERMUTATION ARCHITECTURES WITH BUSSED INTERCONNECTIONS
Joe Kilian, Sholomo Kipnis, and Charles E. Leiserson Jan. 1989 33 p
(Contract N00014-80-C-0622)
(AD-A210832; MIT/LCS/TM-379) Avail: NTIS HC A03/MF A01 CSCL 09/1

The problem of efficiently permuting data stored in VLSI chips is explored in accordance with a predetermined set of permutations. By connecting chips with shared bus interconnections, as opposed to point-to-point interconnections, it is shown that the number of pins per chip can often be reduced. Uniform permutation architectures were also considered that realize permutations in several clock ticks, instead of one, and show that further savings in the number of pins per chip can be obtained. GRA

N90-10353# Massachusetts Inst. of Tech., Cambridge. Artificial Intelligence Lab.
SUMMARIZING QUALITATIVE BEHAVIOR FROM MEASUREMENTS OF NONLINEAR CIRCUITS, REVISION M.S. Thesis
Michelle K. Lee 11 May 1989 87 p
(Contract N00014-86-K-0180)
(AD-A210919; AI-TR-1125) Avail: NTIS HC A05/MF A01 CSCL 09/1

The process of exploring the behavior of nonlinear, dynamical systems can be a time-consuming and tedious process. A program

was written which automates much of the work of an experimental dynamicist. In particular, the program automatically characterizes the behavior of any driven, nonlinear electrical circuit exhibiting interesting behavior below the 10 MHz range. In order to accomplish this task, the program can autonomously select interesting input parameters, drive the circuit, measure its response, perform a set of numeric computations on the measured data, interpret the results and decompose the circuit's parameter space into regions of qualitatively distinct behavior. The output is a two-dimensional portrait summarizing the high-level, qualitative behavior of the nonlinear circuit for every point in the graph as well as an accompanying textual explanation describing any interesting patterns observed in the diagram. In addition to the graph and the text, the program generates a symbolic description of the circuit's behavior. This intermediate data structure can then be passed onto other programs for further analysis. GRA

N90-10354# Minnesota Univ., Minneapolis. Dept. of Chemical Engineering and Materials Science.
RECHARGEABLE LITHIUM/POLYMER CATHODE BATTERIES Technical Report, Jul. 1988 - Jun. 1989
Tetsuya Osaka, Toshiki Nakajima, Koh Shiota, and Boone B. Owens 15 Jun. 1989 4 p
(Contract N00014-88-K-0360)
(AD-A210978; AD-E501135; TR-6-ONR) Avail: NTIS HC A01/MF A01 CSCL 10/3

Polypyrrole (PPy) and polyaniline (PAn) were investigated for cathode materials of rechargeable lithium batteries. PPy films prepared with PF6(-) anion and/or platinum substrate precoated with nitrile butadiene rubber (NBR) were excellent cathode materials because of rough and/or highly oriented film structure. PAn films were successfully prepared from non-aqueous propylene carbonate solution containing aniline, CF3COOH and lithium perchlorate. Its acidity strongly affects the anion doping-undoping behavior. The PAn cathode prepared in high acidic solution (e.g., 4:1 ratio of acid:aniline) gives the excellent battery performance. GRA

N90-10166*# National Aeronautics and Space Administration. Lewis Research Center, Cleveland, OH.
CENTRAL ELECTRICAL UTILITY POWER FOR A SATELLITE RING CITY IN LOW EARTH ORBIT SPACE
Ira T. Myers, Karl A. Faymon, and A. D. Patton (Texas A&M Univ., College Station.) *In* NASA. Langley Research Center, Second Beamed Space-Power Workshop Jul. 1989 p 409-418 (For primary document see N90-10140 01-20)
Avail: NTIS HC A19/MF A03 CSCL 10C

34 FLUID MECHANICS AND HEAT TRANSFER

Includes boundary layers; hydrodynamics; fluidics; mass transfer; and ablation cooling.

For related information see also *02 Aerodynamics* and *77 Thermodynamics and Statistical Physics.*

N90-10355# National Oceanic and Atmospheric Administration, Boulder, CO. Wave Propagation Lab.
OBSERVATIONS OF SPHERICAL-WAVE SCINTILLATION IN STRONG REFRACTIVE-INDEX TURBULENCE
G. R. Ochs and R. B. Fritz Oct. 1988 42 p
(PB89-124747; NOAA-TM-ERL-WPL-154) Avail: NTIS HC A03/MF A01 CSCL 20D

Observations of the fine structure of spherical wave intensity scintillation, with concurrent independent measurements of refractive index turbulence and inner scale, made over a 1 km path are presented. Quantitative measurements of the spatial covariance were made by continuously cycling the spacing of two 1-mm diameter detectors, by operating continuously at fixed spacings, and by converting the temporal frequency observed by a small-diameter detector, moving at high speed in a circular pattern, to spatial wavelength. Qualitative information was also obtained through high-speed photographs. Details much smaller than the inner scale, which did not arise from the last few meters of the path, were observed by all techniques. Author

N90-10356# Advisory Group for Aerospace Research and Development, Neuilly-Sur-Seine (France). Fluid Dynamics Panel.
FLUID DYNAMICS OF THREE-DIMENSIONAL TURBULENT SHEAR FLOWS AND TRANSITION
Apr. 1989 415 p In ENGLISH and FRENCH Symposium held in Cesme, Turkey, 3-6 Oct. 1988
(AGARD-CP-438; ISBN-92-835-0502-6) Copyright Avail: NTIS HC A18/MF A03

The trends and achievements of current research activities in three dimensional turbulent shear flows and transitions were determined and the problems on which future research should be focussed were highlighted. Seven sessions devoted to the topic of transition are included, and these sessions well represented the current state of the art. The characteristics of three dimensional turbulent shear flows were dealt with in five sessions, a reflection of the fact that here much more experimental work is needed, and the effort devoted to this difficult topic has not yet reached the level required. For individual titles, see N90-10357 through N90-10383.

N90-10357*# Arizona State Univ., Tempe. Mechanical and Aerospace Engineering.
STABILITY AND TRANSITION OF THREE-DIMENSIONAL BOUNDARY LAYERS
William S. Saric and Helen L. Reed *In* AGARD, Fluid Dynamics of Three-Dimensional Turbulent Shear Flows and Transition Apr. 1989 20 p (For primary document see N90-10356 01-34)
(Grants NAG1-280; NAG1-402; NAG1-731)
Copyright Avail: NTIS HC A18/MF A03 CSCL 20D

The most recent efforts on the stability and transition of three-dimensional flows are reviewed. These include flows over swept wings, rotating disks, and attachment lines. The generic similarities of their stability behavior is discussed. It is shown that the breakdown process if very complex, often leading to contradictory results. Particular attention is paid to opposing observations of stationary and traveling wave distances. Author

N90-10358# Royal Aircraft Establishment, Farnborough (England).
EXPERIMENTAL INVESTIGATION OF ATTACHMENT-LINE TRANSITION IN LOW-SPEED, HIGH-LIFT WIND-TUNNEL TESTING
B. C. Hardy *In* AGARD, Fluid Dynamics of Three-Dimensional Turbulent Shear Flows and Transition Apr. 1989 17 p (For primary document see N90-10356 01-34)
Copyright Avail: NTIS HC A18/MF A03

The state of the attachment-line boundary layer on two typical, low-speed, high-lift wind-tunnel models was investigated experimentally. Transition was observed on both models within the Reynolds number range of the Royal Aerospace Establishment 5 meter, low-speed, pressurized Wind Tunnel, but significant differences were found from the behavior previously observed using infinite swept and high-speed wing configurations. An adverse Reynolds number effect on maximum lift, which correlated quite well with the onset of attachment-line transition, was found for one of the models. No such effect was found with the other model but in this case laminarization following transition at the attachment line was observed and is suggested as a probable reason for the absence of any scale effect on the forces within the Reynolds number range of both tests. It is concluded that attachment-line transition and laminarization can both contribute to scale effect in low-speed, high-lift testing and that, for many aircraft, accurate simulation of the full-scale behavior in conventional wind tunnel is unlikely. It is suggested that further work is required to establish whether these effects are likely to give rise to significant discrepancies between high-lift performance measured in the tunnel and in flight. Author

N90-10359*# National Aeronautics and Space Administration. Langley Research Center, Hampton, VA.
STABILITY OF A SUPERSONIC BOUNDARY LAYER ALONG A SWEPT LEADING EDGE **c02**
Mujeeb R. Malik and Ivan E. Beckwith *In* AGARD, Fluid Dynamics of Three-Dimensional Turbulent Shear Flows and Transition Apr. 1989 9 p (For primary document see N90-10356 01-34)
Copyright Avail: NTIS HC A18/MF A03 CSCL 01A

The instability of an attachment-line boundary layer formed on a swept cylinder in a supersonic freestream is considered in the linear regime. The supersonic attachment-line boundary layer is shown to be susceptible to oblique Tollmien-Schlichting wave instability which may be controlled by wall cooling. The critical Reynolds number based upon momentum thickness is found to be about 230. The onset of transition in the attachment-line boundary layer is also studied using the e (sup N) method and results are compared with the experimental data obtained at M (sub infinity) = 3.5 in the absence of any trips or spanwise contamination. Author

N90-10360# Centre d'Etudes Aerodynamiques et Thermiques, Poitiers (France). Lab. d'Etudes Aerodynamiques.
LEADING EDGE TRANSITION BY CONTAMINATION IN HYPERSONIC FLOW [TRANSITION PAR CONTAMINATION DE BORD D'ATTAQUE EN ECOULEMENT HYPERSONIQUE] **c02**
J. L. DaCosta, D. Aymer delaChevalerie, and T. Alziary deRoquefort *In* AGARD, Fluid Dynamics of Three-Dimensional Turbulent Shear Flows and Transition Apr. 1989 14 p In FRENCH; ENGLISH summary (For primary document see N90-10356 01-34)
Copyright Avail: NTIS HC A18/MF A03

Transition by attachment-line contamination in hypersonic flow was studied. Experiments are carried out on a swept circular cylinder fitted with streamwise end plates at Mach number 7.1. The sweep angle is 74 degrees. Pressure and heat fluxes are measured along the attachment-line. The occurrence of transition is detected by an increase of the Stanton number. The cylinder can be cooled by liquid nitrogen which allows the influence of the wall temperature to be tested. Either a laminar or turbulent incoming boundary layer can be achieved at the cylinder base. Results compare favorably with the predictions given by Poll's criterion. Author

N90-10361*# National Aeronautics and Space Administration. Ames Research Center, Moffett Field, CA.
DIRECT NUMERICAL STUDY OF LEADING-EDGE CONTAMINATION **c02**
P. R. Spalart *In* AGARD, Fluid Dynamics of Three-Dimensional Turbulent Shear Flows and Transition Apr. 1989 13 p (For primary document see N90-10356 01-34)
Copyright Avail: NTIS HC A18/MF A03 CSCL 01A

Instability, turbulence, and relaminarization in the attachment-line region of swept and unswept cylindrical bodies are studied by numerical solution of the full Navier-Stokes equations. The flow is simulated over a strip containing the attachment-line and treated as homogeneous in the spanwise direction; the disturbances decay exponentially upstream. Transpiration through the wall may be prescribed. The new method, which admits completely general disturbance, agrees with published linear-stability results, which were limited to an apparently restrictive form of disturbance. Fully developed turbulent solutions with sweep are generated and compare well with the experiment. The turbulence is subcritical (except for blowing), resulting in large hysteresis loops. By lowering the sweep Reynolds number, or increasing the suction, the turbulent flow is made to relaminarize. The relaminarization Reynolds number is much less sensitive to suction than the linear-stability Reynolds number. Extensive attempts to detect the postulated nonlinear instability of the unswept flow failed, suggesting that this flow is linearly and nonlinearly stable. Author

N90-10362# Office National d'Etudes et de Recherches Aerospatiales, Toulouse (France).
EXPERIMENTAL STUDY OF TRANSITION AND LEADING EDGE CONTAMINATION ON SWEPT WINGS [ETUDE DE LA TRANSITION ET DE LA CONTAMINATION DE BORD D'ATTAQUE SUR AILES EN FLECHE]
D. Arnal and J. C. Juillen *In* AGARD, Fluid Dynamics of Three-Dimensional Turbulent Shear Flows and Transition Apr. 1989 14 p In FRENCH; ENGLISH summary (For primary document see N90-10356 01-34)
Copyright Avail: NTIS HC A18/MF A03

The transition mechanisms in an incompressible laminar boundary layer developing on swept wings is investigated experimentally. The transition is detected by using hot films glued on the model. Two series of experiments are presented: in the first one, the sensors are placed along the chord and the instantaneous signals allow us to analyse the problems of streamwise instability, crossflow instability, and leading edge contamination. In the second series of experiments, hot films are glued along the span direction, close to the leading edge. The leading edge contamination is studied in detail and the possibilities of relaminarization are examined. Author

N90-10363# Stuttgart Univ. (Germany, F.R.). Inst. A fuer Mechanik.
NUMERICAL INVESTIGATION OF THE EFFECTS OF LONGITUDINAL VORTICES ON THE ONSET OF TRANSITION IN A FLAT PLATE BOUNDARY LAYER
U. Konzelmann, U. Rist, and H. Fasel (Arizona Univ., Tucson.) *In* AGARD, Fluid Dynamics of Three-Dimensional Turbulent Shear Flows and Transition Apr. 1989 13 p (For primary document see N90-10356 01-34)
Copyright Avail: NTIS HC A18/MF A01

The Navier-Stokes equations for three-dimensional, incompressible flows are solved numerically to investigate spatially amplified disturbances in a growing flat plate boundary layer. The disturbances are introduced by time-periodic blowing and suction over a finite slot. The generated disturbances consisted of two-dimensional Tollmien-Schlichting waves, pairs of oblique three-dimensional Tollmien-Schlichting waves, and longitudinal vortices. To isolate nonlinear mechanisms and to identify the importance of longitudinal vortices, two numerical simulations with flow parameters similar to the experiment by Klebanoff with a two-dimensional Tollmien-Schlichting wave of moderate amplitude with two small oblique three-dimensional disturbances of fundamental and subharmonic frequency were performed. In the second calculation an additional longitudinal vortex disturbance was introduced. In both cases the amplification rates for three-dimensional models agreed with the secondary stability theory. The effect of additional longitudinal vortex was such that the initial amplitude for the fundamental three-dimensional disturbance was shifted to higher values. Because of the higher amplitude level for the three-dimensional fundamental disturbances, which is caused by the longitudinal vortices, in this case fundamental resonance would dominate over subharmonic resonance in spite of the lower amplification rate of the fundamental wave. In a numerical simulation of the experiment of Kachanov et al. with larger two-dimensional disturbance amplitudes, neither the subharmonic nor the fundamental resonance model agrees with the numerical Navier-Stokes results. Therefore an improved model was developed which includes two two-dimensional waves and longitudinal vortices. This model yields remarkable agreement with the numerical simulation and with experimental measurements and thus appears to capture the relevant mechanisms. Author

N90-10364*# National Aeronautics and Space Administration. Langley Research Center, Hampton, VA.
GOERTLER INSTABILITY ON AN AIRFOIL: COMPARISON OF MARCHING SOLUTION WITH EXPERIMENTAL OBSERVATIONS **c02**
Vijay Kalburgi, Siva M. Mangalam (Analytical Services and Materials, Inc., Hampton, VA.), and J. Ray Dagenhart *In* AGARD, Fluid Dynamics of Three-Dimensional Turbulent Shear Flows and

Transition Apr. 1989 16 p (For primary document see N90-10356 01-34)
Copyright Avail: NTIS HC A18/MF A03 CSCL 01A

Theoretical predictions based on the marching technique are compared with experimental observations on an airfoil with a concave region. Theoretical predictions of the wavelength of the most amplified Goertler vortex are in excellent agreement with the experimental observation for the range of chord Reynolds numbers from 1.0 to 3.67 million. In the convex zone, solutions from the marching technique showed that the initial counter-rotating vortex pairs lift off the surface and dissipate while another layer of vortex pairs of opposite rotation develops near the surface. This confirms the experimentally observed double peaked streamwise velocity perturbations. Furthermore, the streamwise velocity perturbations which dominate spanwise variation in the surface shear stress distribution shift by half a wavelength in the convex region. The experimental flow visualization photographs clearly confirm this phenomena. Author

N90-10365# Hellenic Air Force Technology Research Center, Athens (Greece).
THREE-DIMENSIONAL BOUNDARY LAYER TRANSITION ON A CONCAVE SURFACE
G. Leoutsakos and R. I. Crane (Imperial Coll. of Science and Technology, London, England) *In* AGARD, Fluid Dynamics of Three-Dimensional Turbulent Shear Flows and Transition Apr. 1989 11 p (For primary document see N90-10356 01-34)
Copyright Avail: NTIS HC A18/MF A03

Measurements of streamwise mean and rms velocity, intermittency factor, and energy spectra are reported for a laminar boundary layer undergoing transition on a concave wall in the presence of a naturally-occurring Goertler vortex system, concentrating on a particular vortex pair. The ratio of boundary layer thickness to wall radius at the start of curvature was 0.01. Nonlinear amplification of the vortices, followed by spanwise meandering and a secondary instability, preceeded transition, which was defined in terms of the intermittency factor after filtering out low frequencies associated with this vortex behavior. Transition was initiated in the vortex upwash region and apparently completed within a streamwise distance of only a few boundary-layer thicknesses at both upwash and downwash locations, implying rapid lateral spread of turbulence. With considerable velocity profile distortion prior to transition, values of momentum thickness Reynolds number and Goertler number at the start of transition, either upwash-localized or upwash-downwash averaged, did not correspond well with established correlations for flat surfaces or with earlier concave-wall studies. Author

N90-10366*# High Technology Corp., Hampton, VA.
CURVATURE EFFECTS ON THE STABILITY OF THREE-DIMENSIONAL LAMINAR BOUNDARY LAYERS
F. S. Collier, Jr. and Mujeeb R. Malik *In* AGARD, Fluid Dynamics of Three-Dimensional Turbulent Shear Flows and Transition Apr. 1989 15 p (For primary document see N90-10356 01-34) (Contract NAS1-18240)
Copyright Avail: NTIS HC A18/MF A03 CSCL 20D

The linear stability equations for compressible, three-dimensional laminar boundary layer flow are derived in an orthogonal curvilinear coordinate system. The system of equations is solved using a finite difference scheme in order to study the effects of streamline and surface curvature and compressibility on the stability of the flow past a swept wing. It is known that convex surface curvature can have a stabilizing effect on the laminar boundary layer. Conversely, concave surface curvature can be destabilizing. The magnitude of these effects for swept wings is determined. Results indicate that amplification rates and hence, N-factors, for the flow over the convex upper surface of a swept wing can be reduced by about 15 to 45 percent when curvature effects are included in the linear stability analysis. The results of the calculations show that concave curvature destabilizes crossflow type disturbances with a significant increase in amplification rate. In addition, comparisons are made with some experimental results on a swept concave-convex surface. Calculated velocity vector plots show good agreement with observed disturbances in the laminar boundary layer over the concave surface. Author

N90-10367# Bristol Univ. (England). Dept. of Aerospace Engineering.
THE THREE-DIMENSIONAL VORTEX SHEET STRUCTURE ON DELTA WINGS **c02**
Martin V. Lowson *In* AGARD, Fluid Dynamics of Three-Dimensional Turbulent Shear Flows and Transition Apr. 1989 16 p (For primary document see N90-10356 01-34)
Copyright Avail: NTIS HC A18/MF A03

Preliminary results are reported from flow visualization studies of the separated shear layers on slender delta wings in air at Reynolds numbers from 3000 to 100,000 based on chord. The work confirms the existence of a systematic structure in the shear layer paralleling the classic instabilities occurring in other cases. Both quasi two-dimensional instabilities traveling at mean flow velocities and a new form of streamwise instability, believed to result from curvature of the vortex sheet, were identified. Both instabilities are found to be stabilized by the stretching process towards the center of the core. For the case studied the interaction between the two instabilities causes the vortex sheet to become turbulent at Reynolds numbers above 20,000 based on local chord. Forced response studies of the vortex sheet have demonstrated the existence of new mechanisms for vortex formation in the shear layer. The results are believed to be relevant to more complex three dimensional shear layers, and have implications for full scale flows on aircraft at high angles of attack. Author

N90-10368*# National Aeronautics and Space Administration. Langley Research Center, Hampton, VA.
SIMULTANEOUS DETECTION OF SEPARATION AND TRANSITION IN SURFACE SHEAR LAYERS
Siva M. Mangalam (Analytical Services and Materials, Inc., Hampton, VA.), J. P. Stack, and W. G. Sewall *In* AGARD, Fluid Dynamics of Three-Dimensional Turbulent Shear Flows and Transition Apr. 1989 10 p (For primary document see N90-10356 01-34)
Copyright Avail: NTIS HC A18/MF A03 CSCL 20D

Flush-mounted hot-film gages have proved effective in detecting boundary-layer transition and in measuring skin friction but with limited success in detecting laminar separation and reattachment. The development of multielement micro hot-film sensors, and the recent discovery of the phase reversal phenomena associated with low-frequency dynamic shear stress signals across regions of laminar separation and turbulent reattachment, have made it possible to simultaneously and unambiguously detect these surface shear layer characteristics. Experiments were conducted on different airfoils at speeds ranging from low subsonic to transonic speeds to establish the technique for incompressible and compressible flow applications. The multielement dynamic shear stress sensor technique was successfully used to detect laminar separation, turbulent reattachment, as well as, shock induced laminar and turbulent separation. Author

N90-10369# Deutsche Forschungs- und Versuchsanstalt fuer Luft- und Raumfahrt, Goettingen (Germany, F.R.). Inst. for Experimental Fluid Mechanics.
EXPERIMENTAL STUDY OF INSTABILITY MODES IN A THREE-DIMENSIONAL BOUNDARY LAYER
B. Mueller and H. Bippes *In* AGARD, Fluid Dynamics of Three-Dimensional Turbulent Shear Flows and Transition Apr. 1989 15 p Sponsored in part by Deutschen Forschungsgemeinschaft (For primary document see N90-10356 01-34)
Copyright Avail: NTIS HC A18/MF A03

Hot-wire measurements were performed to examine the development of stationary and traveling waves in a three-dimensional boundary layer. The appearance of stationary vortices is discussed. The wavelength is independent from the Tu-level, however, if a spanwise periodicity is superimposed upon the flow, the wavelength is initiated by this disturbance. Otherwise,

there is evidence that the stationary vortices are triggered by model fixed disturbances like surface roughnesses or manufacturing tolerances of the leading edge of the flat plate. The development of the stationary vortices is examined. In the wind tunnel with a Tu-level Tu is approximately 0.15 percent, an experimental growth of alpha (sub i) is approximately 8 over 60 percent of the plate is first observed, then, the amplification slows down and the stationary vortices reach a final amplitude of about 10 percent for the U-component and 6 percent for the V-component. For a wind tunnel with a Tu-level of about Tu = 0.05 the growth rate for the stationary vortices agrees well with one predicted by linear stability theory for the swept flat plate. The mean velocity profiles are deformed by the stationary vortices. These profiles are very unstable and may introduce secondary oscillations. Besides the stationary vortices, travelling waves are examined. The range of amplified waves is between 50 and 200 Hz which agrees well with the linear stability theory. The areas where nonlinear effects are present is much larger than in two-dimensional flow. Therefore, transition criteria based on the linear stability theory might be limited. Author

N90-10370# Universidad Politecnica de Madrid (Spain). School of Aeronautics.
BIFURCATIONS IN POISEUILLE FLOW AND WALL TURBULENCE
Javier Jimenez *In* AGARD, Fluid Dynamics of Three-Dimensional Turbulent Shear Flows and Transition Apr. 1989 11 p (For primary document see N90-10356 01-34)
Copyright Avail: NTIS HC A18/MF A03

The fully nonlinear stage of two dimensional Poiseuille flow undergoes a limit cycle bifurcation, whose detailed mechanism is studied using full numerical simulations of simple, spatially periodic cases. It is also shown that this mechanism, a periodic ejection from the wall layer, underlies the production of turbulence in more complicated two dimensional situations. Vorticity ejections are also present in the sublayer of three dimensional channels. The behavior is studied briefly in three dimensional simulations. A simplified model system is then proposed and studied. There are important differences between the two ejections mechanisms, due to the presence of three dimensional vorticity. Author

N90-10371# Deutsche Forschungs- und Versuchsanstalt fuer Luft- und Raumfahrt, Goettingen (Germany, F.R.). Inst. for Theoretical Fluid Mechanics.
PRIMARY AND SECONDARY STABILITY ANALYSIS APPLIED TO THE DFVLR-TRANSITION SWEPT-PLATE EXPERIMENT
T. M. Fischer and U. Dallmann *In* AGARD, Fluid Dynamics of Three-Dimensional Turbulent Shear Flows and Transition Apr. 1989 11 p (For primary document see N90-10356 01-34)
Copyright Avail: NTIS HC A18/MF A03

A three-dimensional, incompressible boundary-layer flow is investigated theoretically with respect to primary and secondary instability. These investigations accompany a basic transition experiment. Primary stationary and secondary wave disturbances are used to model the measured mean flow and velocity fluctuations in the early transition regime. The analysis is based on a Falkner-Skan-Cooke approximation of the undisturbed flow. Author

N90-10372# Deutsche Forschungs- und Versuchsanstalt fuer Luft- und Raumfahrt, Goettingen (Germany, F.R.). Inst. for Theoretical Fluid Mechanics.
NUMERICAL INVESTIGATION OF TRANSITION IN 3D BOUNDARY LAYERS
F. Meyer and L. Kleiser *In* AGARD, Fluid Dynamics of Three-Dimensional Turbulent Shear Flows and Transition Apr. 1989 17 p (For primary document see N90-10356 01-34)
Copyright Avail: NTIS HC A18/MF A03

Linear and nonlinear stages of the laminar-turbulent transition process in a three-dimensional boundary layer initiated by crossflow instability are investigated by linear stability theory and numerical simulation. The conditions of the investigation are adapted to the swept flat plate transition experiment. The parallel basic flow is defined by Falkner-Skan-Cooke similarity profiles. The observed wavelengths of the crossflow vortices and frequencies of the travelling disturbances are well predicted by the linear theory. In the numerical simulations, the temporal evolution of spatially periodic disturbances are considered. Quasi two-dimensional calculations (excluding variations along the vortex axis) show a nonlinear saturation of stationary crossflow vortex disturbances. Nonlinear interactions of stationary and travelling disturbances are studied by three-dimensional simulations. The disturbance development depends significantly on the chosen initial disturbance field. Generally, close correspondence between the computed and the experimentally observed disturbances is obtained at corresponding stages of development. However, there are also some discrepancies. The ratio of the crossflow component of the disturbances to the streamwise component is always larger in the experiment. Nonlinear disturbance interactions produce a significant distortion of the streamwise and crosswise averaged mean boundary layer profiles and an increase of the wall shear stress. Author

N90-10373# California State Univ., Long Beach. Dept. of Aerospace Engineering.
A THREE-DIMENSIONAL LINEAR STABILITY APPROACH TO TRANSITION ON WINGS AT INCIDENCE **c02**
Tuncer Cebeci, H. H. Chen, and D. Arnal *In* AGARD, Fluid Dynamics of Three-Dimensional Turbulent Shear Flows and Transition Apr. 1989 13 p Sponsored in part by Navy (For primary document see N90-10356 01-34)
Copyright Avail: NTIS HC A18/MF A03

The calculation of transition of an infinite swept wing was investigated for a range of sweep angles, Reynolds numbers, and angles of attack. The method solves boundary layer and Orr-Sommerfeld equations by a finite-difference procedure and involves interaction with the inviscid flow. Amplification rates in the e (sup n) method are determined with an eigenvalue procedure which determines the relationship between the wave numbers. The calculation method is evaluated in terms of measurements reported for the flow around an ONERA-D wing equipped with a cambered leading edge and attached to a half fuselage. It is shown to be convenient to use, particularly because the neutral stability curves (zarfs) facilitate the calculation and avoid uncertainties associated with the choice of magnitude and location of the critical frequencies. In general, the calculated values of the onset of transition are in good agreement with measured values, for the eight cases examined. Author

N90-10374# Manchester Univ. (England). Dept. of Engineering.
NUMERICALLY DETERMINED TRANSITION IN SEPARATED INTERNAL FLOW
J. H. Gerrard *In* AGARD, Fluid Dynamics of Three-Dimensional Turbulent Shear Flows and Transition Apr. 1989 9 p (For primary document see N90-10356 01-34)
Copyright Avail: NTIS HC A18/MF A03

The oscillating axisymmetric flow in a conically tapered tube was studied experimentally and by numerical analysis. The investigation of transition to turbulence was concerned with the position of the tube and the phase at which turbulence occurs for different flow parameters. Numerical computation with an inherently unstable explicit finite difference scheme exhibits breakdown at a phase of the oscillation which can be made independent of the numerical parameters. In this condition it is found that numerical breakdown and observed transition occur at the same phase. Author

N90-10375# Centre National de la Recherche Scientifique, Toulouse (France). Inst. de Mecanique des Fluides.
NUMERICAL SOLUTION OF THREE-DIMENSIONAL UNSTEADY FLOWS: APPLICATION TO INSTABILITY PROBLEMS [RESOLUTION NUMERIQUE D'ECOULEMENTS TRIDIMENSIONNELS INSTATIONNAIRES: APPLICATION A DES PROBLEMES D'INSTABILITE]
J. B. Cazalbou, P. Chassaing, and H. Ha Minh *In* AGARD, Fluid Dynamics of Three-Dimensional Turbulent Shear Flows and

Transition Apr. 1989 11 p In FRENCH; ENGLISH summary (For primary document see N90-10356 01-34)
Copyright Avail: NTIS HC A18/MF A03

A numerical code solving the complete three dimensional unsteady flows is presented. The code is then applied to several flows presenting three dimensional instabilities. The unsteady Navier-Stokes equations, in velocity-pressure formulation, without or with heat transfers according to the Boussinesq approximation, are integrated by a semi-implicit finite volume method using staggered meshes. Four flow applications are given: purely convective flow in a 3-D driven cavity; mixed convective flow, with thermal aspects; natural convection flow in 3-D square cavity; and Rayleigh-Benard instability in small boxes. Using 2-D result comparison, an attempt is made to isolate the specific 3-D effects and the influence of three dimensional flow structures. Author

N90-10376# Princeton Univ., NJ. Gas Dynamics Lab.
A STUDY OF THE STRUCTURE OF HIGHLY SWEPT SHOCK WAVE TURBULENT BOUNDARY LAYER INTERACTIONS
Seymour M. Bogdonoff *In* AGARD, Fluid Dynamics of Three-Dimensional Turbulent Shear Flows and Transition Apr. 1989 14 p (For primary document see N90-10356 01-34)
Copyright Avail: NTIS HC A18/MF A03

The combination of detailed flow field studies and extensive calculations were used to construct a model of the three-dimensional interaction of shock waves and turbulent boundary layers. Although different configurations have somewhat different details, a general flow structure consisting of a flattened vortical field, aligned along the shock direction, was found for the fin and swept wedge geometries examined thus far. The lower part of the entering boundary layer is involved in this vortical structure, while the outer part of the layer flows over the initial structure, and is the initial phase of the flow developing downstream of the interaction. Concepts of separation, vortices, reattachment, surface flow visualization observations, and the assumption of steady flow are not supported by the detailed experimental data. Author

N90-10377# Office National d'Etudes et de Recherches Aerospatiales, Toulouse (France).
CONTROL AND MODIFICATION OF TURBULENCE [CONTROLE ET MODIFICATION DE LA TURBULENCE]
J. Cousteix, E. Coustols, and D. Arnal *In* AGARD, Fluid Dynamics of Three-Dimensional Turbulent Shear Flows and Transition Apr. 1989 34 p In FRENCH; ENGLISH summary (For primary document see N90-10356 01-34)
Copyright Avail: NTIS HC A18/MF A03

Means devoted to control turbulence in boundary layers developing on aircraft are presented in order to reduce their skin friction drag. These means deal with the laminar flow control and the use of internal or external boundary layer manipulators. The description of the phenomena which are involved is given after recalling a few essential features of the transition process and of the turbulence in boundary layers. Author

N90-10378# Messerschmitt-Boelkow-Blohm G.m.b.H., Munich (Germany, F.R.). Military Aircraft Div.
TURBULENCE MANAGEMENT: APPLICATION ASPECTS
E. H. Hirschel, P. Thiede (Messerschmitt-Boelkow-Blohm G.m.b.H., Bremen, Germany, F.R.), and F. Monnoyer *In* AGARD, Fluid Dynamics of Three-Dimensional Turbulent Shear Flows and Transition Apr. 1989 12 p (For primary document see N90-10356 01-34)
Copyright Avail: NTIS HC A18/MF A03

Turbulence management for the reduction of turbulent friction drag is an important topic. Numerous research programs in this field have demonstrated that valuable net drag reduction is obtainable by techniques which do not involve substantial, expensive modifications or redesign of existing aircraft. Hence, large projects aiming at short term introduction of turbulence management technology into airline service are presently under development. The various points that have to be investigated for this purpose are presented. Both design and operational aspects are considered, the first dealing with optimizing of turbulence management techniques at operating conditions, and the latter defining the technical problems involved by application of turbulence management to in-service aircraft. The cooperative activities of Airbus Industrie and its partners are cited as an example. Author

N90-10379# McDonnell-Douglas Research Labs., Saint Louis, MO.
TRAILING-EDGE SWEEP AND THREE-DIMENSIONAL VORTEX INTERACTIONS IN JETS AND MIXING LAYERS **c02**
V. Kibens, R. W. Wlezien, F. W. Roos, and J. T. Kegelman *In* AGARD, Fluid Dynamics of Three-Dimensional Turbulent Shear Flows and Transition Apr. 1989 12 p (For primary document see N90-10356 01-34)
Copyright Avail: NTIS HC A18/MF A03

Three-dimensional vortex interactions are investigated in jets with slanted indeterminate-origin exit nozzles, and in mixing layers behind a splitter plate with a swept trailing edge. Flow visualization images were quantitatively processed to characterize complex three-dimensional vortex interactions in non-axisymmetric jets. Phase-conditioned, pulsed laser-sheet illumination was used to obtain a series of sectional images while rotating the asymmetric nozzle. The section images were recombined into an unwrapped representation of the developing vortex systems in the shear layer. Partial pairing of sections of adjacent vortex systems was shown to be responsible for asymmetric shear-layer growth. Flow visualization in the flow behind the swept trailing edge showed that two families of instability waves can develop with different orientations with respect to the trailing-edge angle. Excitation was shown to enhance waves with orientation parallel to the trailing edge or perpendicular to the mean flow direction, depending on excitation frequency. The wavelengths of the two wave families were identical, and the streamwise spacing depended on the sweep angle. Author

N90-10380# National Aerospace Lab., Amsterdam (Netherlands). GARTEUR Action Group AD.
A EUROPEAN COLLABORATIVE INVESTIGATION OF THE THREE-DIMENSIONAL TURBULENT SHEAR LAYERS OF A SWEPT WING **c02**
B. vandenBerg *In* AGARD, Fluid Dynamics of Three-Dimensional Turbulent Shear Flows and Transition Apr. 1989 19 p (For primary document see N90-10356 01-34)
Copyright Avail: NTIS HC A18/MF A03

The turbulent shear layers of a swept wing are described. The measurements will comprise both the upper and lower wing boundary layer, as well as, the three-dimensional near-wake behind the wing. Starting from required viscous flow properties, a wing geometry was designed by flow calculations. The theoretical wing design was checked by pilot model tests. The results suggest that the viscous flow may become an interesting test case for turbulence models for three-dimensional shear flows. The measurements in the turbulent shear layers will comprise mean flow quantities, skin friction data, and the six Reynolds stress tensor components. To establish the measurement accuracy, several data checks will be performed, including independent tests with similar models in two different wind tunnels. Author

N90-10381# Manchester Univ. (England). Dept. of Mechanical Engineering.
TURBULENCE MODELLING OF THREE-DIMENSIONAL SHEAR FLOWS
B. E. Launder *In* AGARD, Fluid Dynamics of Three-Dimensional Turbulent Shear Flows and Transition Apr. 1989 20 p (For primary document see N90-10356 01-34)
Copyright Avail: NTIS HC A18/MF A03

Aspects of modeling the turbulent stress field in three-dimensional strain fields are considered. Special emphasis is given to the level of modeling known as second-moment closure in which, in place of an isotropic effective viscosity, nonlinear constitutive equations are solved for each of the non-zero turbulent stresses. The advantages of this approach over the simpler

eddy-viscosity modeling are strikingly brought out by examples of swirling free and confined flows and three-dimensional flows in straight and curved ducts. The impact of certain fundamental studies now in progress are studied for improving the realism of computations of three-dimensional turbulent flows in the future.
Author

N90-10382# Office National d'Etudes et de Recherches Aeronautiques, Paris (France).
NUMERICAL SIMULATION OF TURBULENT PLANE CHANNEL FLOWS [SIMULATIONS NUMERIQUES D'ECOULEMENTS TURBULENTS]
K. Dang and V. Deschamps *In* AGARD, Fluid Dynamics of Three-Dimensional Turbulent Shear Flows and Transition Apr. 1989 16 p In FRENCH Previously announced is IAA as A89-31814 (For primary document see N90-10356 01-34)
Copyright Avail: NTIS HC A18/MF A03

The unsteady Navier Stokes equations for incompressible fluids are solved by a fourth order finite difference method associated with a semi-implicit time scheme in which pressure is calculated iteratively in a way that satisfies a global incompressibility condition. This algorithm is used to simulate an unsteady, plane-channel turbulent flow with Reynolds numbers of the order of 2000 (based on the mean velocity at the center and half-way point of the channel). The flow, assumed to be homogeneous in both the longitudinal and transverse directions, is maintained with an external contribution of energy realized by imposing a constant mean pressure gradient or a constant flow rate. Although both procedures result in a similar asymptotic flow, the laminar Poiseuille flow is destabilized much more rapidly when the constant flow rate procedure is used. The influence of discretization on the precision of the results is discussed. Transl. by M.G.

N90-10383# Institut de Mecanique de Grenoble (France).
NUMERICAL SIMULATION OF COHERENT STRUCTURES IN AN INCOMPRESSIBLE MIXING LAYER [SIMULATION NUMERIQUE DES STRUCTURES COHERENTES DANS UNE COUCHE DE MELANGE INCOMPRESSIBLE]
Marcel Lesieur, Pierre Comte, Xavier Normand, and Yves Fouillet *In* AGARD, Fluid Dynamics of Three-Dimensional Turbulent Shear Flows and Transition Apr. 1989 11 p In FRENCH; ENGLISH summary (For primary document see N90-10356 01-34)
Copyright Avail: NTIS HC A18/MF A03

Numerical simulations are presented for mixing layers developing from a hyperbolic tangent basic velocity profile to which is superposed an infinitesimal random perturbation. The velocity and passive temperature charts are visualized. The following cases are envisaged: (1) a two dimensional mixing-layer with periodic boundary condition in the flow direction (the numerical code uses finite difference methods and calculations done at a Reynolds number of 1000 and 10,000); (2) a two dimensional spatially developing mixing layer; and (3) a three dimensional temporal mixing layer (large-eddy simulation, pseudospectral code). In the two dimensional case, it is shown that the coherent structures develop from the Kelvin-Helmholtz instability. The coherent structures undergo successive pairings, are shown to be unpredictable, and possess a broadband spatial spectrum of slope comprised between K(sup -3) and K(sup -4). In the three dimensional case, a spectral subgrid scale eddy-viscosity reaches the high Reynolds numbers. Thus the interaction is studied between large-scale coherent structures and small scale three dimensional turbulence which cascades along a K(sup -5/3) kinetic energy spectrum. Author

N90-10384# Lawrence Livermore National Lab., CA. Computing and Mathematics Research Div.
ANALYSIS OF A MODEL AND SEQUENTIAL NUMERICAL METHOD FOR THERMAL RESERVOIR SIMULATION
John A. Trangenstein 18 Jul. 1989 24 p Presented at the 2nd European Conference on the Mathematics of Oil Recovery, Cambridge, United Kingdom, 25-27 Jul. 1989 Submitted for publication Sponsored in part by DNA
(Contract W-7405-eng-48)
(DE89-015117; UCRL-101566; CONF-890759-1) Avail: NTIS HC A03/MF A01

A model is presented and analyzed for two-component, three-phase, nonisothermal fluid flow in a one-dimensional fluid reservoir. The thermodynamic principles are discussed that constrain the model functions, and analyze the effect of these thermodynamic principles on the flow equations. This analysis allows the formulation of a sequential approach to steam flooding: first a parabolic equation is solved to find the pressure and total fluid velocity, then a system of hyperbolic conservation laws is solved to update the fluid composition and energy. The thermodynamic principles allow the computation of the characteristic speeds and directions in the component/energy conservation equations, and the use of these in a second-order Godunov method. DOE

N90-10385*# National Aeronautics and Space Administration. Marshall Space Flight Center, Huntsville, AL.
CONSTITUTIVE RELATIONSHIPS AND MODELS IN CONTINUUM THEORIES OF MULTIPHASE FLOWS
Rand Decker, ed. Washington Sep. 1989 165 p Workshop held in Huntsville, AL, 5-7 Apr. 1989; sponsored by NASA, Washington and USRA, Washington, DC
(NASA-CP-3047; M-616; NAS 1.55:3047) Avail: NTIS HC A08/MF A01 CSCL 20D

In April, 1989, a workshop on constitutive relationships and models in continuum theories of multiphase flows was held at NASA's Marshall Space Flight Center. Topics of constitutive relationships for the partial or per phase stresses, including the concept of solid phase pressure are discussed. Models used for the exchange of mass, momentum, and energy between the phases in a multiphase flow are also discussed. The program, abstracts, and texts of the presentations from the workshop are included. For individual titles, see N90-10386 through N90-10394.

N90-10386*# Commissariat a l'Energie Atomique, Grenoble (France).
THE GENERALIZED DRIFT FLUX APPROACH: IDENTIFICATION OF THE VOID-DRIFT CLOSURE LAW
J. A. Boure *In* NASA, Marshall Space Flight Center, Constitutive Relationships and Models in Continuum Theories of Multiphase Flows Sep. 1989 p 1-17 (For primary document see N90-10385 01-34)
Avail: NTIS HC A08/MF A01 CSCL 20D

The main characteristics and the potential advantages of generalized drift flux models are presented. In particular it is stressed that the issue on the propagation properties and on the mathematical nature (hyperbolic or not) of the model and the problem of closure are easier to tackle than in two fluid models. The problem of identifying the differential void-drift closure law inherent to generalized drift flux models is then addressed. Such a void-drift closure, based on wave properties, is proposed for bubbly flows. It involves a drift relaxation time which is of the order of 0.25 s. It is observed that, although wave properties provide essential closure validity tests, they do not represent an easily usable source of quantitative information on the closure laws. Author

N90-10387*# Dartmouth Coll., Hanover, NH. School of Engineering.
TWO-PHASE POTENTIAL FLOW
Graham B. Wallis *In* NASA, Marshall Space Flight Center, Constitutive Relationships and Models in Continuum Theories of Multiphase Flows Sep. 1989 p 19-34 (For primary document see N90-10385 01-34)
Avail: NTIS HC A08/MF A01 CSCL 20D

Some features of two recent approaches of two-phase potential flow are presented. The first approach is based on a set of progressive examples that can be analyzed using common techniques, such as conservation laws, and taken together appear to lead in the direction of a general theory. The second approach is based on variational methods, a classical approach to

conservative mechanical systems that has a respectable history of application to single phase flows. This latter approach, exemplified by several recent papers by Geurst, appears generally to be consistent with the former approach, at least in those cases for which it is possible to obtain comparable results. Each approach has a justifiable theoretical base and is self-consistent. Moreover, both approaches appear to give the right prediction for several well-defined situations. K.C.D.

N90-10388*# Clarkson Univ., Potsdam, NY. Dept. of Civil and Environmental Engineering.
INTERPRETATION AND MODELING OF THE AVERAGED EQUATIONS FOR A FLUID-SOLID FLOW
Hayley H. Shen and Guann-Jiun Hwang *In* NASA, Marshall Space Flight Center, Constitutive Relationships and Models in Continuum Theories of Multiphase Flows Sep. 1989 p 35-55 (For primary document see N90-10385 01-34)
Avail: NTIS HC A08/MF A01 CSCL 20D

A self-consistent derivation of the conservation laws is given for flows of a fluid-solid mixture. A unified analytical framework for obtaining constitutive relations is provided. This analysis uses a control volume/control surface approach that is widely used in fluid mechanics. All terms in the governing equations and the constitutive relations are written in terms of the mass-weighted averages except solid concentration. It is believed that the mass-weighted average is the natural bridge between micromechanics and constitutive relations. The derived momentum equations contain terms that differ from all existing models except that of Prosperetti and Jones (1984). However, their assumptions are not needed here. Special attention is given to the solid phase pressure. The physical basis of the previously assumed form for this pressure (Givler 1987) becomes clear. A number of related phenomena are also discussed. These include the anti-diffusion and anisotropic normal stresses. The energy equations are also different from existing models. Author

N90-10389*# Pittsburgh Energy Technology Center, PA.
STRESS IN DILUTE SUSPENSIONS
Stephen L. Passman *In* NASA, Marshall Space Flight Center, Constitutive Relationships and Models in Continuum Theories of Multiphase Flows Sep. 1989 p 57-64 Prepared in cooperation with Sandia National Labs., Albuquerque, NM (For primary document see N90-10385 01-34)
Avail: NTIS HC A08/MF A01 CSCL 20D

Generally, two types of theory are used to describe the field equations for suspensions. The so-called postulated equations are based on the kinetic theory of mixtures, which logically should give reasonable equations for solutions. The basis for the use of such theory for suspensions is tenuous, though it at least gives a logical path for mathematical arguments. It has the disadvantage that it leads to a system of equations which is underdetermined, in a sense that can be made precise. On the other hand, the so-called averaging theory starts with a determined system, but the very process of averaging renders the resulting system underdetermined. A third type of theory is proposed in which the kinetic theory of gases is used to motivate continuum equations for the suspended particles. This entails an interpretation of the stress in the particles that is different from the usual one. Classical theory is used to describe the motion of the suspending medium. The result is a determined system for a dilute suspension. Extension of the theory to more concentrated systems is discussed. Author

N90-10390*# Illinois Univ., Chicago. Dept. of Mechanical Engineering.
THEORY OF DROPLET. PART 1: RENORMALIZED LAWS OF DROPLET VAPORIZATION IN NON-DILUTE SPRAYS
H. H. Chiu *In* NASA, Marshall Space Flight Center, Constitutive Relationships and Models in Continuum Theories of Multiphase Flows Sep. 1989 p 65-101 (For primary document see N90-10385 01-34)
Avail: NTIS HC A08/MF A01 CSCL 20D

The vaporization of a droplet, interacting with its neighbors in a non-dilute spray environment is examined as well as a vaporization scaling law established on the basis of a recently developed theory of renormalized droplet. The interacting droplet consists of a centrally located droplet and its vapor bubble which is surrounded by a cloud of droplets. The distribution of the droplets and the size of the cloud are characterized by a pair-distribution function. The vaporization of a droplet is retarded by the collective thermal quenching, the vapor concentration accumulated in the outer sphere, and by the limited percolative passages for mass, momentum and energy fluxes. The retardation is scaled by the local collective interaction parameters (group combustion number of renormalized droplet, droplet spacing, renormalization number and local ambient conditions). The numerical results of a selected case study reveal that the vaporization correction factor falls from unity monotonically as the group combustion number increases, and saturation is likely to occur when the group combustion number reaches 35 to 40 with interdroplet spacing of 7.5 diameters and an environment temperature of 500 K. The scaling law suggests that dense sprays can be classified into: (1) a diffusively dense cloud characterized by uniform thermal quenching in the cloud; (2) a stratified dense cloud characterized by a radial stratification in temperature by the differential thermal quenching of the cloud; or (3) a sharply dense cloud marked by fine structure in the quasi-droplet cloud and the corresponding variation in the correction factor due to the variation in the topological structure of the cloud characterized by a pair-distribution function of quasi-droplets. Author

N90-10391*# Rensselaer Polytechnic Inst., Troy, NY. Dept. of Mathematical Sciences.
EFFECT OF PARTICLE VELOCITY FLUCTUATIONS ON THE INERTIA COUPLING IN TWO-PHASE FLOW
Donald A. Drew *In* NASA, Marshall Space Flight Center, Constitutive Relationships and Models in Continuum Theories of Multiphase Flows Sep. 1989 p 103-125 Sponsored in part by DOE, and by Cornell Univ., Ithaca, NY (For primary document see N90-10385 01-34)
(Contract DAAL03-86-K-0126)
Avail: NTIS HC A08/MF A01 CSCL 20D

Consistent forms for the interfacial force, the interfacial pressure, the Reynolds stresses and the particle stress have been derived for the inviscid, irrotational incompressible flow of fluid in a dilute suspension of spheres. The particles are assumed to have a velocity distribution, giving rise to an effective pressure and stress in the particle phase. The velocity fluctuations also contribute in the fluid Reynolds stress and in the (elastic) stress field inside the spheres. The relation of these constitutive equations to the force on an individual sphere is discussed. Author

N90-10392*# Cornell Univ., Ithaca, NY. School of Mechanical and Aerospace Engineering.
THE ROLE OF PARTICLE COLLISIONS IN PNEUMATIC TRANSPORT
E. Mastorakos, M. Louge, and J. T. Jenkins *In* NASA, Marshall Space Flight Center, Constitutive Relationships and Models in Continuum Theories of Multiphase flows Sep. 1989 p 127-137 (For primary document see N90-10385 01-34)
(Contract DE-FG22-88PC-88929; NSF CBT-88-09347)
Avail: NTIS HC A08/MF A01 CSCL 20D

A model of dilute gas-solid flow in vertical risers is developed in which the particle phase is treated as a granular material, the balance equations for rapid granular flow are modified to incorporate the drag force from the gas, and boundary conditions, based on collisional exchanges of momentum and energy at the wall, are employed. In this model, it is assumed that the particle fluctuations are determined by inter-particle collisions only and that the turbulence of the gas is unaffected by the presence of the particles. The model is developed in the context of, but not limited to, steady, fully developed flow. A numerical solution of the resulting governing equations provides concentration profiles generally observed in dilute pneumatic flow, velocity profiles in good agreement with the measurements of Tsuji, et al. (1984),

and an explanation for the enhancement of turbulence that they observed. Author

N90-10393*# Alabama Univ., Huntsville. Dept. of Mechanical Engineering.
SCALING AND MODELING OF TURBULENT SUSPENSION FLOWS
C. P. Chen *In* NASA, Marshall Space Flight Center, Constitutive Relationships and Models in Continuum Theories of Multiphase Flows Sep. 1989 p 139-146 (For primary document see N90-10385 01-34)
(Contract NAS8-36718)
Avail: NTIS HC A08/MF A01 CSCL 20D

Scaling factors determining various aspects of particle-fluid interactions and the development of physical models to predict gas-solid turbulent suspension flow fields are discussed based on two-fluid, continua formulation. The modes of particle-fluid interactions are discussed based on the length and time scale ratio, which depends on the properties of the particles and the characteristics of the flow turbulence. For particle size smaller than or comparable with the Kolmogorov length scale and concentration low enough for neglecting direct particle-particle interaction, scaling rules can be established in various parameter ranges. The various particle-fluid interactions give rise to additional mechanisms which affect the fluid mechanics of the conveying gas phase. These extra mechanisms are incorporated into a turbulence modeling method based on the scaling rules. A multiple-scale two-phase turbulence model is developed, which gives reasonable predictions for dilute suspension flow. Much work still needs to be done to account for the poly-dispersed effects and the extension to dense suspension flows. K.C.D.

N90-10394*# Kentucky Univ., Lexington. Dept. of Mechanical Engineering.
TURBULENCE KINETIC ENERGY EQUATION FOR DILUTE SUSPENSIONS
T. W. Abou-Arab and M. C. Roco *In* NASA, Marshall Space Flight Center, Constitutive Relationships and Models in Continuum Theories of Multiphase Flows Sep. 1989 p 147-162 (For primary document see N90-10385 01-34)
Avail: NTIS HC A08/MF A01 CSCL 20D

A multiphase turbulence closure model is presented which employs one transport equation, namely the turbulence kinetic energy equation. The proposed form of this equation is different from the earlier formulations in some aspects. The power spectrum of the carrier fluid is divided into two regions, which interact in different ways and at different rates with the suspended particles as a function of the particle-eddy size ratio and density ratio. The length scale is described algebraically. A mass/time averaging procedure for the momentum and kinetic energy equations is adopted. The resulting turbulence correlations are modeled under less retrictive assumptions comparative to previous work. The closures for the momentum and kinetic energy equations are given. Comparisons of the predictions with experimental results on liquid-solid jet and gas-solid pipe flow show satisfactory agreement. Author

N90-10395# Materials Research Labs., Ascot Vale (Australia).
NUMERICAL SIMULATION OF DETONATION TRANSFER BETWEEN GASEOUS EXPLOSIVE LAYERS
David A. Jones, Raafat H. Guirguis, and Elaine S. Oran (Naval Research Lab., Washington, DC.) 1989 34 p
(MRL-RR-1-89; AR-005-706) Copyright Avail: NTIS HC A03/MF A01

The development of a two-dimensional computer code to simulate detonation transfer between explosive layers is described. The code is based on previous models developed at the Laboratory for Computational Physics and Fluid Dynamics at Naval Research Laboratory, Washington, DC to study the structure of layered detonations and the details of detonation transmission from one medium to another. The code was configured to simulate experiments conducted at the University of Michigan on the lateral transfer of detonation and shock phenomena between different gaseous layers. Preliminary calcuations with the code show that the computations produce many of the structures seen in the Michigan experiments and also provide detailed descriptions of the detonation transmission and evolving structure. Author

N90-10396 Cincinnati Univ., OH.
A COMPOSITE VELOCITY PROCEDURE FOR THE THREE-DIMENSIONAL REDUCED NAVIER-STOKES EQUATIONS Ph.D. Thesis
Raymond E. Gordnier 1988 176 p
Avail: Univ. Microfilms Order No. DA8908474

A composite velocity procedure is developed for the three-dimensional reduced Navier-Stokes equations. In the spirit of matched asymptotic expansions, the velocity components are written as a combination multiplicative and additive composite of viscous like velocities (U, W) and pseudo-potential or inviscid velocities (Phi sub x, Phi sub y, Phi sub z). The solution procedure is then consistent with both asymptotic inviscid flow and boundary layer theory. For transonic flow cases the Enquist-Osher flux biasing scheme developed for the full potential equation is used to capture shock waves. This scheme captures very sharp shocks with no oscillations at the shock. A quasi-conservation form of the governing equations is used in the shock region to capture the correct rotational shock with the standard non-conservation form of the equations used in non-shock regions. The consistent, coupled, strongly implicit procedure coupled with a plane relaxation procedure is used to solve the discretized equations. This provides a scheme that is unconditionally stable and requires no local iterations at each cross plane. Several techniques for accelerating the convergence of the scheme are described. The composite velocity technique is applied to a number of axisymmetric and non-axisymmetric geometries. Comparisons of the numerical results with experimental results for flow along a circular cylinder with a circular arc bump show good agreement except in separated flow regions where the turbulence model breaks down. Three-dimensional solutions for cylinders with both elliptic and square cross sections are also obtained. Dissert. Abstr.

N90-10397 Texas Univ., Austin.
ITERATIVE PERFORMANCE AND AN ADAPTIVE PROCEDURE FOR VISCOUS FLOW PROBLEMS Ph.D. Thesis
Kuo Chih Wang 1988 172 p
Avail: Univ. Microfilms Order No. DA8909759

The use of accelerated gradient-type iterative methods for the solution of Newtonian and generalized Newtonian viscous flow problems is presented. The formulations are based on penalty and mixed finite element methods and such factors as the effect of the penalty parameter, asymmetry, continuation, and preconditioning are examined. Also an adaptive grid refinement scheme in 2 dimensions for 9-node biquadratic quadrilateral elements is developed. It was incorporated in a two-dimensional finite element program for viscous flow problems. Numerical results are given for a variety of model and engineering problems to demonstrate the advantage of adaptive refinement, including free-surface problems and problems with energy transport. Dissert. Abstr.

N90-10398# Westinghouse Hanford Co., Richland, WA.
PORFLO-3: A MATHEMATICAL MODEL FOR FLUID FLOW, HEAT, AND MASS TRANSPORT IN VARIABLY SATURATED GEOLOGIC MEDIA: USERS MANUAL, VERSION 1.0
A. K. Runchal and B. Sagar (Pacific Northwest Labs., Richland, WA.) Jul. 1989 215 p
(Contract DE-AC06-87RL-10930)
(DE89-013977; WHC-EP-0041) Avail: NTIS HC A10/MF A02

This manual provides instructions for the use of the PORFLO-3 computer code. This computer code is based on mathematical formulation of fluid flow, heat transfer, and mass transport in variably saturated geologic media. The geologic medium may be heterogeneous and anisotropic and may contain linear and planar features such as boreholes and fractures. The code can be used to analyze 3-D problems of partially as well as fully saturated media with various types of fluid, heat, and mass sources.

PORFLO-3 is written in American National Standard FORTRAN 77. A summary of the theory of PORFLO-3 is provided. The 3 partial differential equations that govern fluid flow, heat, transfer, and mass transport and the method of their solution are discussed. The governing equations are discretized by the method of Nodal Point Integration and solved by any of the four alternate methods: Point-successive Over-relaxation, Alternating Direction Implicit Scheme, Choleski Decomposition, and Gaussian Elimination. The structure of the code and the information flow between its 89 subroutines are explained. Certain practical suggestions for the design of the spatial grid and choice of time steps are discussed. The format-free approach for data input is used in PORFLO-3 is also discussed. Detailed instructions for data input are provided. Input and output for two example problems are shown along with error messages from PORFLO-3. DOE

N90-10399# University of Southern California, Los Angeles.
CAPILLARY EFFECTS IN STEADY-STATE FLOW IN HETEROGENEOUS CORES
Yanis C. Yortsos and Jincai Chang Aug. 1989 32 p Prepared in cooperation with Dept. of Energy, Bartlesville, OK
(Contract DE-FG22-87BC-14126)
(DE89-000758; DOE/BC-14126/10) Avail: NTIS HC A03/MF A01

Effects of capillary heterogeneity at the macroscopic scale have previously been analyzed for static conditions or in the context of outflow end-effects. This paper presents a systematic study for the case of one-dimensional, steady-state flow, that complements recent work on transient displacement (Chang and Yortsos, 1989). We consider the saturation response to various forms of heterogeneity. Included are analytical results for certain model cases, some general results, and numerical solutions for variously correlated spatial variations. The sensitivity to process parameters, such as rate and heterogeneity length scale and correlation, is studied. Physical interpretations are offered, and potential applications in the estimation of heterogeneity are discussed. DOE

N90-10400# Sandia National Labs., Albuquerque, NM.
SHOCK BEHAVIOR OF EXPLOSIVES ABOUT THE C-J (CHAPMAN-JUGET) POINT
Paul W. Cooper 1989 6 p Presented at the 9th International Symposium on Detonation, Portland, OR, 28 Aug. - 1 Sep. 1989
(Contract DE-AC04-76DP-00078)
(DE89-007642; SAND-88-2766C; CONF-890811-6) Avail: NTIS HC A02/MF A01

Experimental data is presented for pressure and particle velocity along the Hugoniot of the detonation reaction products for a number of explosives in a reduced parameter form P/P(sub cj) versus u/u(sub cj). Two correlations are found: P/P(sub cj) = a + b(u/u(sub cj)) + c(u/u(sub cj))(sup 2) when P/P(sub cj) is greater than 0.08, and P/P(sub cj) = m(u/u(sub cj))(sup n) when P/P(sub cj) is less than 0.08. The correlations yield results that agree reasonably with code calculations. DOE

N90-10401# North Carolina State Univ., Raleigh. Dept. of Mechanical and Aerospace Engineering.
LAMINAR BOUNDARY LAYER ALONG INVISCID SURFACE STREAMLINES OVER INCLINED AXISYMMETRIC BODIES IN INCOMPRESSIBLE FLOW Final Report, Aug. 1981 - May 1983
Fred R. Dejarnette and Lee H. Kania Feb. 1989 145 p
(Contract F33615-81-K-3625)
(AD-A210202; AFWAL-TR-86-3094) Avail: NTIS HC A07/MF A01 CSCL 20/4

A computer program was developed to calculate laminar layers along inviscid surface streamlines over inclined axisymmetric bodies. The inviscid surface streamlines are computed from experimental pressure data using a doubly quadratic spline interpolation technique if an analytical potential solution is not provided. By application of the axisymmetric analog, or small cross flow assumption, the properties of this 3-D flow field may be approximated by solving the axisymmetric boundary layer equations over an equivalent axisymmetric body for each inviscid surface streamline. Hall's and Blottner's boundary layer solution methods, both of which utilize a finite difference technique to obtain the local velocity profile, were incorporated into the computational code. Results are presented for a sphere, an ellipsoid of revolution with thickness ratio of 1/4 at 12 and 30 degrees angle of attack, and a sphere-ogive-cylinder configuration at 45 degrees angle of attack. The latter case utilized experimental pressure data while an analytical potential solution was available for the other configurations. A technique for calculating the streamline metric along an inviscid surface streamline was developed. Boundary layer profiles were calculated along the streamlines from the stagnation point to the separation point. Calculations using the axisymmetric analog and ellipsoid of revolution at angle of attack. GRA

N90-10402# University of Southern California, Los Angeles. Dept. of Aerospace Engineering.
DYNAMICS AND CONTROL OF TURBULENT SHEAR FLOWS Report, Oct. 1986 - May 1989
May 1989 61 p
(Contract N00014-86-K-0679)
(AD-A210396) Avail: NTIS HC A04/MF A01 CSCL 20/4

Topics of study during this time period include: Bounded Shear Flow - Experimental Approaches, Control of Laminar Separated Shear Layer on Airfoils; Control of Large Scale Features in Turbulent Mixing Layers; Direct Numerical Simulations of Flow Control; Control of Entrainment in Confined Shear Layers; Theoretical Underpinnings: Amplitude and Phase Descriptions of Coherent Structures; Phase Control of Vortex Structures in Shear Flows; Mathematical Analysis of Navier Stokes Equations; and Effects of Longitudinal Roughness Elements upon Turbulent Boundary Layer. Other areas of concern are: Some ideas on the Control of Near Wall Eddies; A technique for Acoustic Excitation of Separated Shear Flow; Heat Transfer in Rayleigh-Benard Convection; Energy Transfer and Non local Interactions in Homogeneous Isotopic Turbulence. Invarient Manifold Theory for Hydrodynamic transition; The theory of nonstationary viscous flow Past Plane Domains with Noncompact Boundaries; and Stability Properties of Subsonic Mixing Layers. GRA

N90-10403# Flow Research, Inc., Kent, WA.
NUMERICAL CALCULATIONS OF THE COLLAPSE OF A CAVITY IN THE VICINITY OF A COMPLIANT WALL Final Report, 1 Aug. 1985 - 30 Nov. 1988
James H. Duncan 27 Apr. 1989 22 p
(Contract N00014-85-C-0747)
(AD-A210489; FLOW-TR-477) Avail: NTIS HC A03/MF A01 CSCL 20/4

The collapse of a spherical vapor cavity in the vicinity of a complaint boundary is examined numerically. The fluid is treated as a potential flow. Lagrangian boundary conditions are used on the cavity surface; fluid particles and the velocity potential on the surface are tracked in time. At each time step an integral method is used to solve Laplace's equation. The complaint wall is modeled as a membrane with a spring foundation. At the interface between the fluid and the membrane, the pressure and vertical velocity in the flow is matched to the pressure and vertical velocity of the membrane. These boundary conditions linearized and applied at the position of the undisturbed interface between the flow and the membrane. The results of a preliminary set of calculations are presented in which the initial cavity position and radius, the ratio of the time scale for a spherical collapse to the membrane's spring-mass time scale, and the ratio of the spring constant to the membrane tension are all held constant. The characteristics of the collapse as a function of the ratio of the spring constant to the fluid pressure far from the cavity are examined. It is shown that as the spring constant is reduced, the collapse characteristics change from those of a cavity adjacent to a rigid wall and tend toward those of a cavity in an infinite fluid. GRA

N90-10404# Naval Ship Research and Development Center, Bethesda, MD.
TWO COUNTER-ROTATING VORTICES APPROACHING A FREE SURFACE IN A VISCOUS FLUID Final Report

Samuel Ohring and Hans J. Lugt Jun. 1989 63 p
(AD-A210495; DTRC-89/013) Avail: NTIS HC A04/MF A01 CSCL 20/4

Numerical computations were performed to investigate the interaction of two counter-rotating vortices with a free surface in a viscous, incompressible fluid where the motion is considered two-dimensional and laminar. The decaying vortices deform the free surface during their approach and they can display the phenomenon of rebounding. The numerical scheme is based on the Navier-Stokes equations and uses boundary-fitted coordinates to accommodate the locally high vorticity of the moving vortices and the nonlinear deformation of the free surface. GRA

N90-10405# Wisconsin Univ., Madison. Center for Mathematical Sciences.
ANALYSIS OF SPURT PHENOMENA FOR A NON-NEWTONIAN FLUID Summary Report
David S. Malkus, John A. Nohel, and Bradley J. Plohr Mar. 1989 22 p
(Contract DAAL03-87-K-0036; AF-AFOSR-0191-87; NSF DMS-86-20303; AF-AFOSR-0141-85; NSF DMS-87-12058)
(AD-A210560; CMS-TSR-89-28) Avail: NTIS HC A03/MF A01 CSCL 20/4

This document discusses novel phenomena in dynamic shearing flows of non-Newtonian fluids of importance for polymer processing. A striking example is spurt which was observed experimentally in the flow of monodispersive polyisoprenes through capillaries. The volumetric flow rate increased dramatically at a critical stress independent of molecular weight. The authors show that satisfactory explanation of spurt requires studying the full dynamics of the equations of motion and constitutive relations characterized by a non-monotonic relation between the steady shear stress and strain rate. The increase in volumetric flow rate is shown to correspond to jumps in the strain rate when the driving pressure gradient exceeds a critical value. Motivated by scaling suggested by accurate numerical computations of the governing dynamic problem that yielded qualitative and quantitative agreement with experiment, we introduce a system of ordinary differential equation that approximates dynamic behavior of highly elastic and very viscous fluids. The complete dynamics of the system of ode's determined by phase plane analysis. These results are then used to explain not only spurt but also shape memory, hysteresis, latency, and other effects that have also been observed in numerical simulations. GRA

N90-10406# Wisconsin Univ., Madison. Center for Mathematical Sciences.
STABILITY OF DISCONTINUOUS SHEARING MOTIONS OF A NON-NEWTONIAN FLUID Technical Summary Report
John A. Nohel, Robert L. Pego (Michigan Univ., Ann Arbor.), and Athanasios E. Tzavaras 18 Jul. 1989 11 p
(Contracts DAAL03-87-K-0036; DAAL03-88-K-0185; AF-AFOSR-0919-87; NSF DMS-87-12058; NSF DMS-86-20303; NSF DMS-87-16132)
(AD-A210643; AD-E951366; CMS-TSR-90-4) Avail: NTIS HC A03/MF A01 CSCL 20/4

This paper discusses recent results on the nonlinear stability of discontinuous steady states of a model initial-boundary value problem in one space dimension for incompressible, isothermal shear flow of a non-Newtonian fluid between parallel plates located at x = + or - 1, and driven by a constant pressure gradient. The non-Newtonian contribution to the shear stress is assumed to satisfy a simple differential constitutive law. The key feature is a non-monotone relation between the total steady shear stress and steady shear strain rate that results in steady states having, in general, discontinuities in the strain rate. We explain why every solution tends to a steady state as it approaches limit of infinity, and we identify steady states that are stable. GRA

N90-10407# Wisconsin Univ., Madison. Center for Mathematical Sciences.
STABILITY OF DISCONTINUOUS STEADY STATES IN SHEARING MOTION OF A NON-NEWTONIAN FLUID Technical Summary Report
John A. Nohel, Robert L. Pego (Michigan Univ., Ann Arbor.), and Athanasios E. Tzavaras 18 Jul. 1989 24 p
(Contracts DAAL03-87-K-0036; DAAL03-88-K-0185; AF-AFOSR-0191-87; NSF DMS-87-12058; NSF DMS-86-20303; NSF DMS-87-16132)
(AD-A210644; AD-E951366; CMS-TSR-90-5) Avail: NTIS HC A03/MF A01 CSCL 20/4

This document studies the nonlinear stability of discontinuous steady states of a model initial-boundary value problem in one space dimension for incompressible, isothermal shear flow of a non-Newtonian fluid driven by a constant pressure gradient. The non-Newtonian contribution to the shear stress is assumed to satisfy a simple differential constitutive law. The key feature is a non-monotone relation between the total steady shear stress and shear strain-rate that results in steady states having, in general, discontinuities in the strain rate. It is shown that every solution tends to a steady state as t approaches limit of infinity, and we identify steady states that are stable. GRA

N90-10408# Wisconsin Univ., Madison. Center for Mathematical Sciences.
GLOBAL EXISTENCE AND ASYMPTOTIC STABILITY FOR A NONLINEAR INTEGRODIFFERENTIAL EQUATION MODELING HEAT FLOW Technical Summary Report
Deborah Brandon Jun. 1989 55 p
(Grants AF-AFOSR-0307-85; AF-AFOSR-0191-87)
(AD-A210647; AD-E951366; CMS-TSR-89-37) Avail: NTIS HC A04/MF A01 CSCL 20/4

Initial value problems were studied that arise from models for 1-D heat flow (with finite wave speeds) in materials with memory. Under assumptions that ensure compatibility of the constitutive relations with the second law of thermodynamics, the resulting integrodifferential equation is hyperbolic near equilibrium. The existence is established of unique, global (in time) defined, classical solutions to the problems under consideration, provided the data are smooth and sufficiently close to equilibrium. Both Dirichlet and Neumann boundary conditions are treated as well as the problem on the entire real line. Local existence is proved using a contraction mapping argument which involves estimates for linear hyperbolic PDE's with variable coefficients. Global existence is obtained by deriving a priori energy estimates. These estimates are based on inequalities for strongly positive Volterra kernels (including a new inequality that is needed due to the form of the constitutive relations). Furthermore, compatibility with the second law plays an essential role in the proof in order to obtain an existence result under less restrictive assumptions on the data. GRA

N90-10409*# National Aeronautics and Space Administration. Langley Research Center, Hampton, VA.
APPLICATION OF FORMAL OPTIMIZATION TECHNIQUES IN THERMAL/STRUCTURAL DESIGN OF A HEAT-PIPE-COOLED PANEL FOR A HYPERSONIC VEHICLE
Charles J. Camarda and Michael F. Riley (PRC Kentron, Inc., Hampton, VA.) Oct. 1987 32 p
(NASA-TM-89131; L-16134; NAS 1.15:89131) Avail: NTIS HC A03/MF A01 CSCL 20D

Nonlinear mathematical programming methods are used to design a radiantly cooled and heat-pipe-cooled panel for a Mach 6.7 transport. The cooled portion of the panel is a hybrid heat-pipe/actively cooled design which uses heat pipes to transport the absorbed heat to the ends of the panel where it is removed by active cooling. The panels are optimized for minimum mass and to satisfy a set of heat-pipe, structural, geometric, and minimum-gage constraints. Two panel concepts are investigated: cylindrical heat pipes embedded in a honeycomb core and an integrated design which uses a web-core heat-pipe sandwich concept. The latter was lighter and resulted in a design which

was less than 10 percent heavier than an all actively cooled concept. The heat-pipe concept, however, is redundant and can sustain a single-point failure, whereas the actively cooled concept cannot. An additional study was performed to determine the optimum number of coolant manifolds per panel for a minimum-mass design. Author

N90-10410# Minnesota Univ., Minneapolis. Dept. of Aerospace Engineering and Mechanics.
SIMILARITY SOLUTIONS THAT GIVE RISE TO HYPERBOLICITY AND CHANGE OF TYPE IN STEADY FLOW OF A VISCOELASTIC FLUID
Claude Verdier and Daniel D. Joseph 1989 24 p
(Contract DAAL03-88-K-0083)
(AD-A210920; ARO-25648.11-MA) Avail: NTIS HC A03/MF A01 CSCL 20/4

Similarity solutions have proved to be a very useful tool for the study of flows of viscoelastic fluids since they allow numerical computations to be checked against them. Hyperbolic regions of the vorticity are computed for an upper convected Maxwell model using the similarity solution of Phanthien for flow between rotating disks and using the similarity solution of Menon for an accelerated flow in cylindrical coordinates. It is shown that the extra tension becomes enormous at the edge of disks of ordinary rheometers and under operating conditions. GRA

N90-10411# Texas Univ., Austin. Dept. of Physics.
SYMMETRY BREAKING BIFURCATIONS AND THE GROWTH OF CHAOS IN A ROTATING FLUID Final Report, 1 Jun. 1986 - 31 Dec. 1989
Harry L. Swinney 1 Aug. 1989 8 p
(Contract N00014-86-K-0385)
(AD-A210969; TR-89-1) Avail: NTIS HC A02/MF A01 CSCL 20/4

Laboratory experiments and numerical simulation on flow between concentric independently rotating cylinders (the Couette-Taylor system) reveal a primary bifurcation to a new state, ribbons, which are traveling waves in the azimuthal direction but standing waves in the axial direction. Other experiments, conducted on a rigid rapidly rotating annulus, are designed to explore parameter regimes characteristics of planetary scale flows. Eastward jets are found to exhibit Rossby waves for a wide range of control parameters, and these jets (or, more precisely, the potential vorticity gradients in the core of the jets) act as a strong barrier to tracer transport; these observations have important implications for the transport of pollutants in oceans and the atmosphere. The behavior of westward jets is found to be markedly different from that of eastward jets. GRA

35 INSTRUMENTATION AND PHOTOGRAPHY

Includes remote sensors; measuring instruments and gages; detectors; cameras and photographic supplies; and holography.

For aerial photography see *43 Earth Resources and Remote Sensing*. For related information see also *06 Aircraft Instrumentation*, and *19 Spacecraft Instrumentation*.

N90-10412*# National Aeronautics and Space Administration. Langley Research Center, Hampton, VA.
INTRODUCTION TO TOTAL- AND PARTIAL-PRESSURE MEASUREMENTS IN VACUUM SYSTEMS
R. A. Outlaw and F. A. Kern Washington Nov. 1989 77 p
(NASA-RP-1219; L-16494; NAS 1.61:1219) Avail: NTIS HC A05/MF A01 CSCL 14B

An introduction to the fundamentals of total and partial pressure measurement in the vacuum regime (760 x 10 to the -16th power Torr) is presented. The instrument most often used in scientific fields requiring vacuum measurement are discussed with special emphasis on ionization type gauges and quadrupole mass spectrometers. Some attention is also given to potential errors in measurement as well as calibration techniques. Author

N90-10413*# Morton Thiokol, Brigham City, UT. Aerospace Group.
THREE-IN-ONE GAGE Final Test Report
D. M. Garecht Sep. 1988 93 p
(Contract NAS8-30490)
(NASA-CR-183714; NAS 1.26:183714; TWR-18519; WBS-HQ302-10-10; ECS-SS-1816) Avail: NTIS HC A05/MF A01 CSCL 14B

The Three-in-One Gage is a three way gage designed to measure pressure, temperature, and displacement at the same port continuously. The Two-in-One Gage is a two way gage designed to measure pressure and temperature in the same port continuously. The Two-in-One is an adaptation of the Three-in-One to incorporate dual seals, however, without the proximity sensor. The Three-in-One is assembled using two Type K thermocouples, 1 Kulite Pressure Transducer, and one Kaman Proximity Displacement Sensor. Tests of performance were completed. Author

N90-10414# Dynaco Corp., Derry, NH.
DEVELOPMENT OF A SEMIQUANTITATIVE CORROSION MONITOR Final Report, Oct. 1985 - Oct. 1988
Frank Ansuini Feb. 1989 65 p
(Contract F33615-85-C-5069)
(AD-A208132; AFWAL-TR-88-4245) Avail: NTIS HC A04/MF A01 CSCL 14/2

A prototype dual mode corrosion monitor is described which is capable of measuring both instantaneous corrosion rate and cumulative corrosion loss in atmospheric environments not boldly exposed to weather. The monitor system consists of two components: a small flat sensor to be located in the area to be monitored and a battery powered electronics unit to query the sensor. The sensor element is made of steel which is far more sensitive to atmospheric corrosion than most commonly used metals; thus the sensor will react before significant damage has been done to other materials. The sensor itself is actually two discrete sensors on the same substrate and photo-etched from the same foil. GRA

N90-10415*# National Aeronautics and Space Administration. Lewis Research Center, Cleveland, OH.
ADJUSTABLE DEPTH GAGE Patent Application
Roger C. Forsgren, inventor (to NASA) 7 Jul. 1989 10 p
(NASA-Case-LEW-14880-1; NAS 1.71:LEW-14880-1; US-Patent-Appl-SN-376738) Avail: NTIS HC A02/MF A01 CSCL 14B

A quick adjust depth gage includes a handle-clamp assembly wherein the clamp includes an opening in which a cylindrical shaft with suitable depth measurement markings thereon is reviewed. Turning the handle on the clamp enables the gage to be set to the desired depth. NASA

N90-10416# Massachusetts Inst. of Tech., Cambridge. Artificial Intelligence Lab.
ANALYSIS AND CONSTRUCTION OF CONTACT AND TACTILE SENSORS
Kenneth Salisbury, John Hollerbach, David Brock, and David Siegel Jul. 1989 35 p
(Contract DE-AC04-76DP-00789)
(DE89-013992; SAND-87-7120) Avail: NTIS HC A03/MF A01

The preliminary analysis and construction of two radically different touch sensors was performed. The sensors investigated provide complementary means for a robot finger to perceive information about contact with an object. The sensor developed by Siegel is a miniature array of 64 pressure sensitive elements which employ a capacitance measuring scheme to achieve good linearity and resolution in measurement of the normal force at each element. The other sensor, developed by Brock employs an entirely different technique for sensing contact. It uses a rigid, hollow fingertip mounted on a force sensing structure to measure

contact information. The structure employs strain gauges to permit the measurement of all six components of the net force acting on the fingertip. DOE

N90-10417# Allied-Signal Aerospace Co., Kansas City, MO.
A ROBOTIC ELECTRICAL AND TENSILE TESTING SYSTEM FOR DIODES
G. S. Darner Jul. 1989 15 p
(Contract DE-AC04-76DP-00613)
(DE89-014012; KCP-613-4081) Avail: NTIS HC A03/MF A01

A robotic system was developed to automate the die attachment electrical testing performed on a specific diode. An industrial robot was integrated with electrical test equipment and a nondestructive tensile tester to verify the integrity of the lead attachment to the diode die. Robotic manipulation is employed to route the diodes through the testing and bin sorting operations. DOE

N90-10418# Fermi National Accelerator Lab., Batavia, IL.
AN ALGORITHM TO CALCULATE THE BEAM MOMENTUM DISTRIBUTION FROM FLYING WIRE PROFILES
X. Q. Wang 27 Jul. 1989 12 p
(Contract DE-AC02-76CH-03000)
(DE89-015587; FNAL-TM-1612) Avail: NTIS HC A03/MF A01

Horizontal flying wire measurements give beam profiles from which information about the beam momentum distribution and betatron distribution can be extracted. When calculating these beam characteristics in the past, for the matter of simplicity, the beam was assumed Gaussian. For beam profiles which may not be Gaussian, an algorithm to obtain the general beam momentum distribution is developed using the Fourier transform to the beam profiles. Since the profile is the convolution of the momentum distribution and the betatron distribution, using a Fourier transform method makes calculations easier. DOE

N90-10419# Virginia Polytechnic Inst. and State Univ., Blacksburg. Dept. of Mechanical Engineering.
DEVELOPMENT OF AN AUTOMATED PROBE FOR THERMAL CONDUCTIVITY MEASUREMENTS Final Report
B. P. Dougherty and W. C. Thomas May 1989 131 p
(Grant NIST-60NANB6D0642)
(PB89-209324; NIST/GCR-89/563) Avail: NTIS HC A07/MF A01 CSCL 14B

A transient technique was validated for making thermal conductivity measurements. The technique incorporated a small, effectively spherical, heat source and temperature sensing probe. The actual thermal conductivity measurements lasted 30 seconds. After approximately 15 minutes of data reduction, a value for thermal conductivity was obtained. The probe yielded local thermal conductivity measurements. Spherical sample volumes less than 8 cu cm were required for the materials tested. Thermal conductivity (and moisture) distributors can be measured for relatively dry or wetted samples. Author

N90-10420# National Inst. of Standards and Technology, Gaithersburg, MD. Chemical Process Metrology Div.
THIN FILM THERMOCOUPLES FOR HIGH TEMPERATURE MEASUREMENT
Kenneth G. Kreider May 1989 26 p
(PB89-209290; NISTIR-89/4087) Avail: NTIS HC A03/MF A01 CSCL 14B

Thin film thermocouples have unique capabilities for measuring surface temperatures at high temperatures (above 800 K) under harsh conditions. Their low mass, approximately 2 x 10(-5) g/mm permits very rapid response and very little disturbance of heat transfer to the surface being measured. This has led to applications inside gas turbine engines and diesel engines measuring the surface temperature of first stage turbine blades and vanes and ceramic liners in diesel cylinders. The most successful high temperature (up to 1300 K) thin film thermocouples are sputter deposited from platinum and platinum-10 percent rhodium targets although results using base metal alloys, gold, and platinel will also be presented. The fabrication techniques used to form the thermocouples, approaches used to solve the high temperature insulation and adherence problems, current applications, and test results using the thin film thermocouples are reviewed. In addition a discussion will be presented on the current problems and future trends related to applications of thin film thermocouples at higher temperatures up to 1900 K. GRA

N90-10421# Midwest Research Inst., Golden, CO. Solar Energy Research Inst.
SOME SIGNIFICANT RESULTS FROM TESTING A REMOTE MULTIPLEXING UNIT (RMU) FOR TEMPERATURE-INDUCED ERRORS
Chester V. Wells Jun. 1989 24 p
(Contract DE-AC02-83CH-10093)
(DE89-009432; SERI/TR-215-3195) Avail: NTIS HC A03/MF A01

A key item of equipment used to acquire research data while testing wind turbines is the Remote Multiplexing Unit (RMU). To more adequately analyze and report data in the DOE Wind Program, and to provide the uncertainties associated with such data, performance data were needed on RMUs, especially in terms of their behavior under the influence of temperature and the rate of change in temperature. A special test was conducted on one RMU in 1986, with particular attention paid to the strain gage and voltage signal conditioning cards. Some significant findings from the analysis of the test data are presented. The information can be used to describe the uncertainties that are to be applied to wind energy research data acquired through RMU-based data acquisition systems. Operational recommendations suggested by the results include using longer warm-up times for the demultiplexing unit and possibly heating the RMU for operation at lower temperatures. DOE

N90-10422# Argonne National Lab., IL. Chemical Technology Div.
REAL-TIME OBSERVATIONS OF AEROSOL COMPOSITION CHANGES
Stanley A. Johnson and Romesh Kumar 1989 5 p Presented at the 1989 American Chemical Society National Meeting, Miami Beach, FL, 10-15 Sep. 1989
(Contract W-31-109-eng-38)
(DE89-012382; CONF-890902-7) Avail: NTIS HC A01/MF A01

We have developed a near real-time aerosol particle analyzer that uses a combination of filtration and impaction for particle size classification and collection, and Fourier-transform infrared (FTIR) spectroscopy for analysis. This infrared aerosol analyzer (IAA) supplies full range (2.0 to 20 (mu)m) infrared absorption spectra of the ambient aerosol separated into three different size fractions. The coarse size fraction, greater than 2.5 (mu)m aerodynamic diameter (a.d.), made up largely of crustal matter, is analyzed separately from the fine (0.5 to 2.5 (mu)m a.d.) and the ultra-fine (less than 0.5 (mu)m a.d.) size fractions which contain the secondary particulate matter that is formed in the atmosphere from gaseous and condensed-phase precursors. Separating the three size fractions avoids interactions between the possibly acidic fine fractions and the possibly basic coarse fraction. The collected particulate samples are analyzed in situ by infrared spectroscopy with analytical time resolutions approaching those of trace gas analyzers. DOE

N90-10423*# Lawrence Livermore National Lab., CA.
BRAGG CRYSTAL POLARIMETERS
E. Silver, A. Simionivici, S. Labov, R. Novick, P. Kaaret, C. Martin, T. Hamilton, M. Weisskopf, R. Elsner, and J. Beeman (California Univ., Berkeley. Lawrence Berkeley Lab.) et al 15 Jun. 1989 12 p Presented at the 33rd SPIE Annual International Technical Symposium on Optical and Optoelectronic Applied Science and Engineering, San Diego, CA, 6-11 Aug. 1989 Prepared in cooperation with California Univ., Irvine; Rome Univ. (Italy); and Leicester Univ., (England) Sponsored in part by NASA
(Contract W-7405-eng-48)
(NASA-CR-181331; NAS 1.26:181331; DE89-015775; UCRL-100710; CONF-890836-5) Avail: NTIS HC A03/MF A01 CSCL 14B

A Bragg crystal oriented at 45 deg to an incoming beam of X-rays acts as a polarization analyzer. This crystal geometry preferentially reflects those X-rays which satisfy the Bragg condition and whose electric vectors are perpendicular to the plane defined by the incident and reflected photons. X-rays with electric vectors parallel to this plane of incidence are photoelectrically absorbed. The energy bandwidth of nearly perfect crystals is extremely small which makes them very inefficient X-ray polarimeters. This limitation is particularly acute for observations of the relatively weak X-ray continuum of stellar sources. The bandwidth can be greatly increased by employing mosaic or ideally imperfect crystals. Mosaic crystals possess a high integrated reflectivity which results in a large increase in the reflection of continuum radiation. A review of the theory and performance characteristics of crystal polarimeters designed for observations of cosmic X-ray sources is presented. DOE

N90-10424# Waugh Controls Corp., Chatsworth, CA.
WIDE-RANGE FUEL FLOWMETER, PHASE 2 Final Report, 4 Jun. 1986 - 3 Feb. 1988
William Seiler, Jr. Jul. 1989 120 p
(Contract F40600-86-C-0003)
(AD-A210547; AEDC-TR-89-6) Avail: NTIS HC A06/MF A01 CSCL 13/7

The Wide-Range Fuel Flowmeter (WRFF) development program proved the viability of the recirculation method of wide-range flow measurement over a 140 to 1 or greater range with a 1-percent or better measurement uncertainty. The objectives were to: (1) Reduce the size of the flowmeter and electronic conditioner and provide a more functional and economically producible system; (2) Replace the recirculating pump with a smaller, more reliable unit and assure that all components in contact with the fluid are compatible with jet fuels; (3) Provide means to disable recirculating flow when operating at high flow rates; and (4) Evaluate the performance of an air-driven pump for possible use in hazardous atmospheres. The meter was redesigned to greatly reduce its size and weight; large and expensive manifolds were eliminated, and wherever possible, commercially available fittings were used. Inwardly pointing tubes were incorporated to inject and retrieve the recirculating flow, reducing recirculation flow variation and related recirculation flow errors. The electronic conditioner was repackaged in a standard 3-1/2-by 19-in. rack mount. An auto-zero feature was created and incorporated in the electronic conditioner, greatly simplifying the accelerating the zeroing process. GRA

N90-10425# Naval Research Lab., Washington, DC. High Power Electromagnetic Radiation Branch.
DESIGN AND OPERATING CHARACTERISTICS OF A CW RELEVANT QUASI-OPTICAL GYROTRON WITH VARIABLE MIRROR SEPARATION Memorandum Report, Jun. 1987 - Mar. 1989
A. W. Fliflet, T. A. Hargreaves, Wallace M. Manheimer, R. P. Fischer, M. L. Barsanti, B. Levush, and T. Antonsen (Science Applications International Corp., McLean, VA.) 26 Jun. 1989 86 p
(AD-A210611; NRL-MR-6459) Avail: NTIS HC A05/MF A01 CSCL 09/1

Results from a quasi-optical gyrotron experiment with a 20 to 28 cm mirror separation will be presented showing operation at powers up to 150 kW and efficiencies up to 12 percent. The output coupling could be varied from 0.4 to 3 percent by changing the mirror separation and operating frequency. Operation was obtained over frequencies ranging from 95 to 130 GHz by changing the axial magnetic field, limited on the low end by waveguide cutoff in the diagnostics and at the end by the maximum magnetic field achievable. The output power varied by approximately a factor of 2 over this range. Frequency variation of 4 percent was achieved by varying only the electron gun voltage; however, the output power also varied substantially due to the fact that the electron beam power was changing dramatically. Efficiency optimization by variation of output coupling and by tapering the magnetic field has been demonstrated. Regions of single-mode operation at powers up to 125 kW have been characterized and compared to recently developed theory. Details of the experimental design and its numerical modeling, along with the data obtained and its comparison to relevant theories are presented. GRA

N90-10426# Naval Surface Weapons Center, Silver Spring, MD. Research and Technology Dept.
PIN SWITCH CIRCUITS INSTRUMENT FOR MICROSECOND VELOCITY MEASUREMENTS Final Report
Harry E. Cleaver 8 Sep. 1988 55 p
(AD-A210638; AD-E951366; NSWC-MP-88-172) Avail: NTIS HC A04/MF A01 CSCL 14/2

The Pin Switch Circuits instrument combines signals generated by its 10-pin switch probe circuits into one coded output signal for recording on tape recorders on oscilloscopes. It has an internal test circuit for checking system performance and display generation purposes. The instrument plugs into a single-width compartment of the Tektronix TM500 Series Instrumentation Mainframes. GRA

N90-10148*# Naval Research Lab., Washington, DC. High Power Electromagnetic Radiation Branch.
GYROTRON DEVELOPMENT FOR SPACE POWER BEAMING
Wallace M. Manheimer *In* NASA. Langley Research Center, Second Beamed Space-Power Workshop Jul. 1989 p 139-158 (For primary document see N90-10140 01-20)
Avail: NTIS HC A19/MF A03 CSCL 14B

N90-10798*# American Science and Engineering, Inc., Cambridge, MA.
THE DETECTION OF SOFT X-RAYS WITH CHARGED COUPLED DETECTORS
P. Burstein and John M. Davis *In its* Solar X-ray Astronomy Sounding Rocket Program 22 Aug. 1989 6 p (For primary document see N90-10796 01-88)
Avail: NTIS HC A15/MF A02 CSCL 14B

36 LASERS AND MASERS

Includes parametric amplifiers.
For related information see also *76 Solid-State Physics.*

N90-10427# Optical Society of America, Washington, DC.
SHORTWAVELENGTH COHERENT RADIATION: GENERATION AND APPLICATIONS Final Report, 1 Jun. 1988 - 1 Mar. 1989
Jarus W. Quinn 1 Mar. 1989 171 p Topical Meeting held at Cape Cod, MA, 26-29 Sep. 1988
(Contracts N00014-88-J-1115; DE-FG05-88ER-13853; NSF PHY-88-09775; AF-AFOSR-0192-88; AF Proj. 2301)
(AD-A209847; AFOSR-89-0788TR; LC-88-60866; ISBN-1-55752-052-6) Avail: NTIS HC A08/MF A01 CSCL 20/5

The meeting dealt with the development and application of sources of coherent radiation from the extreme ultraviolet to the X-ray spectral region. Closely related areas of interest are multiphoton phenomena, soft X-ray optics, and laser produced plasmas. Topics covered included: short-wavelength lasers, free electron lasers and undulators, harmonic generation and frequency conversion, short wavelength optics and novel instrumentation, laser plasma radiation sources, multiphoton phenomena, ultrafast short-wavelength sources, applications in spectroscopy, and microfabrication, phase coherent applications, holography and interferometry, and unique applications of short-wavelength sources. GRA

N90-10428# Lawrence Livermore National Lab., CA.
NTES LASER FACILITY FOR PHYSICS EXPERIMENTS: BUILDING 381 HIGH BAY OPTION
D. J. Christie, R. J. Foley, D. N. Frank, M. A. Henesian, J. T. Hunt, W. G. Labiak, D. W. Larson, J. K. Lawson, R. W. Lee, and S. E. Mayo et al 12 Jul. 1989 218 p
(Contract W-7405-eng-48)
(DE89-014326; UCID-21725) Avail: NTIS HC A10/MF A02

This paper discusses the following topics on the NTES laser facility: Mission Statement and Project Description; Experiment Area; High-Energy, Double-Pass Laser; Facilities; Laser Control and Data Acquisition; and Auxiliary Lasers. DOE

N90-10429# Argonne National Lab., IL. Physics Div.
A LASER-DRIVEN SOURCE OF POLARIZED HYDROGEN AND DEUTERIUM
L. Young, R. J. Holt, R. A. Gilman, R. Kowalczyk, and K. Coulter 1989 3 p Presented at the 9th International Conference on Laser Spectroscopy, Bretton Woods, NH, 18-23 Jun. 1989
(Contract W-31-109-eng-38)
(DE89-015130; CONF-890618-3) Avail: NTIS HC A01/MF A01

A laser-driven polarized source of hydrogen and deuterium which operates on the principle of spin-exchange optical pumping is being developed. This source is designed to operate as an internal target in an electron storage ring for fundamental studies of spin-dependent structure of nuclei. It has the potential to exceed the flux from existing conventional sources (3 x 10(16)s) by an order of magnitude. Currently, the source delivers hydrogen at a flux of 8 x 10(16) atoms/s with an atomic polarization of 24 percent and deuterium at 6 x 10(16) atoms/s with a polarization of 29 percent. Technical obstacles which were overcome, with varying degrees of success are complete Doppler-coverage in the optical-pumping stage without the use of a buffer gas, wall-induced depolarization and radiation-trapping. Future improvements should allow achievement of the design goals of 4 x 10(17) atoms/s with a polarization of 50 percent. DOE

N90-10430# Hughes Aircraft Co., El Segundo, CA. Electro-Optical and Data Systems Group.
STIMULATED ROTATIONAL RAMAN SCATTERING Final Report, 1 Sep. 1986 - 31 Mar. 1989
C. G. Parazzoli, G. L. Rafanelli, D. M. Capps, and C. Drutman 31 Mar. 1989 230 p
(Contract DE-AC03-86SF-16495)
(DE89-016427; DOE/SF-16495/T2) Avail: NTIS HC A11/MF A02

The effect of Stimulated Rotational Raman Scattering (SRRS) processes on high energy laser directed energy weapon systems was studied. The program had 3 main objectives; achieving an accurate description of the physical processes involved in SRRS; developing a numerical algorithm to confidently evaluate SRRS-induced losses in the propagation of high energy laser beams in the uplink and downlink segments of the optical trains of various strategic defense system scenarios; and discovering possible methods to eliminate, or at least reduce, the deleterious effects of SRRS on the energy deposition on target. The following topics are discussed: the motivation for the accomplishments of the DOE program; the Semiclassical Theory of Non-Resonant SRRS for Diatomic Homonuclear Molecules; and then the following appendices; Calculation of the Dipole Transition Reduced Matrix Element, Guided Tour of Hughes SRRS Code, Running the Hughes SRRS Code, and Hughes SRRS Code Listing. DOE

N90-10431# Sandia National Labs., Albuquerque, NM.
LASER INITIATION OF SECONDARY EXPLOSIVES
Anita M. Renlund, Philip L. Stanton, and Wayne M. Trott 1989 8 p Presented at the 9th International Symposium on Detonation, Portland, OR, Sep. 1989
(Contract DE-AC04-76DP-00789)
(DE89-010229; SAND-88-2465C; CONF-890926-2) Avail: NTIS HC A02

Several experiments were performed to investigate the effects of explosive material parameters on energy thresholds for direct laser initiation of secondary explosives. Laser energy requirements for initiation of pentaerythritol tetranitrate (PETN) were decreased for small particle size powder and low density pressings. Promptness of detonation, however, was aided by higher densities. Initiation of PETN was achieved at energies at or below 10 mJ (power densities approximately 0.2 GW sq cm) at laser wavelengths of 1.06 micrometers, 532 nm and 355 nm and strong confinement of the explosive sample assisted build-up to detonation. At 355 and 308 nm PETN could be initiated by irradiation on the bare explosive surface. Hexahydro 1,3,5-trinitro-s-triazine (RDX) was initiated at 308 nm but not at 1.06 micrometers. Hexanitrostibene (HNS) by direct irradiation at any of these wavelengths was successful. The results suggest that if sufficient energy is deposited, a fast deflagration or convective burn is achieved and that this grows to detonation via a conventional deflagration-to-detonation transition. DOE

N90-10432# Aerospace Corp., El Segundo, CA. Aerophysics Lab.
MULTILINE MULTIMODE CW CHEMICAL LASER PERFORMANCE
Harold Mirels 1 Jul. 1989 44 p
(Contract F04701-85-C-0086)
(AD-A210613; TR-0088(3907)-1; SD-TR-89-47) Avail: NTIS HC A03/MF A01 CSCL 09/3

Effects of translational rotational nonequilibrium large scale CW chemical laser performance are evaluated for the case of a Fabry-Perot resonator with multiple longitudinal modes. Numerical results are presented for the limit Delta nu Sub c is dominated by Delta nu sub h is dominated by Delta nu sub d, where Delta nu sub c, Delta nu sub h, and Delta nu sub d denote longitudinal mode separation, homogeneous width, and Doppler width, respectively. Results include the effect of threshold gain on the power in each longitudinal mode, the power associated with each rotational energy level, and the net laser power. In the case of a saturated laser, an increase of threshold gain results in an increase in the output from strong rotational transitions at the expense of the output from weak rotational transitions. Total output is reduced. With further increase of threshold gain, the output from all rotational transitions is reduced. The case of rotational nonequilibrium and translational equilibrium is also considered. The latter case, a common assumption, is shown to provide net output power that is intermediate between the values for rotational and translational equilibrium and for rotational and translational nonequilibrium. GRA

N90-10433# Lightwave Electronics Corp., Mountain View, CA.
EFFICIENT NONLINEAR CONVERSION OF LASER DIODE PUMPED MINIATURE SOLID STATE LASER SOURCES Final Report, 1 May 1986 - 30 Apr. 1989
David C. Gerstenberger and Richard W. Wallace Jun. 1989 37 p
(Contract DAAL03-86-C-0007)
(AD-A210708; ARO-23290.2-PH-S) Avail: NTIS HC A03/MF A01 CSCL 09/3

This research program has dealt with the development of efficient and compact sources of visible laser light based on the nonlinear optical conversion of the outputs of diode pumped solid state lasers. Intracavity frequency doubling, frequency doubling of continuous wave single frequency nonplanar ring Nd:YAG lasers in external resonant cavities and single pass doubling of diode pumped Q-switched lasers were studied. Nonlinear materials including lithium diffused lithium niobate, magnesium oxide doped lithium niobate and potassium titanyl phosphate were examined. We obtained 45 mW of CW green light from an monolithic externally resonant cavity constructed of MgO:MiNbO3 pumped by a 200 mW single frequency Nd:YAG laser. This doubler was electro-optically locked into resonance with the laser oscillator and maintained at phasematching temperature by a miniature platinum hybrid heater-sensor element and control circuit. Peak powers LiNbO3 over 200 mW in the green were measured with this doubling device when pumped by a single frequency pulsed 500 mW source. GRA

N90-10434# Aerospace Corp., El Segundo, CA. Aerophysics Lab.
COUPLED MULTILINE CW HF LASERS: EXPERIMENTAL PERFORMANCE
Jay M. Bernard, Richard A. Chodzko, and Harold Mirels 1 Jul. 1989 26 p

(Contract F04701-85-C-0086)
(AD-A210844; TR-0086A(2060)-2; SD-TR-89-46) Avail: NTIS HC A03/MF A01 CSCL 09/3

The experimental performance of two coupled arc-driven continuous wave HF chemical lasers employing unstable resonators was measured. Mode-matched adjoint coupling of 20 percent was accomplished with a beamsplitter. Multiline interference fringes were obtained when the two laser output beams were overlapped in the near field. The mutual coherence of the two beams was inferred from measurement of the visibility of these fringes. Single line fringe visibility was measured as 98 percent + or - 2 percent for each of the two strongest lines. These data suggest that the two outputs are nearly completely phase-locked. This locking was found to be insensitive to perturbations in the lengths of the laser resonators. Mode-beating measurements also suggest complete phase locking, as the coupled system behaves like a single laser cavity. The coherent combination of the two laser output beams was attempted by minimizing the optical path difference between these beams, at an external measuring station. This was achieved by changing the external path length of one beam until maximum multiline visibility (97 percent) was obtained. Demonstration of the corresponding far-field peak intensity enhancement and reduction in spot size for the combined outputs was also accomplished. GRA

N90-10435# Aerospace Corp., El Segundo, CA. Lab. Operations.
MASTER OSCILLATOR WITH POWER AMPLIFIERS: PERFORMANCE OF A TWO-ELEMENT CW HF PHASED-LASER ARRAY
Jay M. Bernard, Richard A. Chodzko, and John G. Coffer 15 Jun. 1989 31 p
(Contract F04701-85-C-0086)
(AD-A211141; TR-0088(3060)-1; SD-TR-89-40) Avail: NTIS HC A03/MF A01 CSCL 09/3

The experimental performance of a two-element phased array of multiline continuous-wave hydrogen-fluoride chemical lasers in the master oscillator with power amplifiers (MOPA) configuration has been measured. The mutual coherence of the two amplified beams was inferred from measurements of the visibility of interference fringes obtained when the beams were overlapped in the near field. When the optical path difference for the two beams was minimized, multiline visibilities of 0.90 + or - 0.02 were measured. White-light interferometry was used to equalize the optical path lengths. Spectral mismatch between the master oscillator output and the amplifier's preferred gain distribution affected neither the amplification factor nor the mutual coherence of the amplified beams. The effect of spatial coherence of the master oscillator beam on these near-field measurements, and the eventual requirement of far-field measurements to precisely optimize path lengths, are discussed. Spectral data, amplification factors, and mutual coherence measurements are shown, and the resulting phased-array far-field performance is presented. GRA

N90-10151*# Lawrence Livermore National Lab., CA.
TECHNICAL OPTIONS FOR HIGH AVERAGE POWER FREE ELECTRON MILIMETER-WAVE AND LASER DEVICES
James C. Swingle *In* NASA. Langley Research Center, Second Beamed Space-Power Workshop Jul. 1989 p 191-219 (For primary document see N90-10140 01-20)
Avail: NTIS HC A19/MF A03 CSCL 20E

N90-10152*# Hampton Inst., VA. Dept. of Physics.
LASER ENERGY CONVERSION
N. W. Jalufka *In* NASA. Langley Research Center, Second Beamed Space-Power Workshop Jul. 1989 p 221-238 (For primary document see N90-10140 01-20)
Avail: NTIS HC A19/MF A03 CSCL 20E

N90-10154*# National Aeronautics and Space Administration. Langley Research Center, Hampton, VA.
OVERVIEW OF LASER CONCEPTS
Edmund J. Conway *In its* Second Beamed Space-Power Workshop Jul. 1989 p 261-286 (For primary document see N90-10140 01-20)
Avail: NTIS HC A19/MF A03 CSCL 20E

N90-10156*# National Aeronautics and Space Administration. Langley Research Center, Hampton, VA.
LASER-POWERED LUNAR BASE
R. Costen, Donald H. Humes, G. H. Walker, M. D. Williams, and Russell J. DeYoung *In its* Second Beamed Space-Power Workshop Jul. 1989 p 293-316 (For primary document see N90-10140 01-20)
Avail: NTIS HC A19/MF A03 CSCL 20E

N90-10157*# National Aeronautics and Space Administration. Langley Research Center, Hampton, VA.
LASER-POWERED MARTIAN ROVER
W. L. Harries, W. E. Meador, G. A. Miner, Gregory L. Schuster, G. H. Walker, and M. D. Williams *In its* Second Beamed Space-Power Workshop Jul. 1989 p 317-327 (For primary document see N90-10140 01-20)
Avail: NTIS HC A19/MF A03 CSCL 20E

N90-10161*# National Aeronautics and Space Administration. Langley Research Center, Hampton, VA.
LASER PROPULSION OPTION
Donald H. Humes *In its* Second Beamed Space-Power Workshop Jul. 1989 p 365-375 (For primary document see N90-10140 01-20)
Avail: NTIS HC A19/MF A03 CSCL 20E

N90-10162*# National Aeronautics and Space Administration. Langley Research Center, Hampton, VA.
EARTH ORBIT LASER SYSTEMS
Ja H. Lee *In its* Second Beamed Space-Power Workshop Jul. 1989 p 377-381 (For primary document see N90-10140 01-20)
Avail: NTIS HC A19/MF A03 CSCL 20E

N90-10163*# Miami Univ., Oxford, OH.
LASER DIODE ARRAY AND TRANSMISSION OPTICS
Jin H. Kwon *In* NASA. Langley Research Center, Second Beamed Space-Power Workshop Jul. 1989 p 383-389 (For primary document see N90-10140 01-20)
Avail: NTIS HC A19/MF A03 CSCL 20E

N90-10164*# Hampton Inst., VA. Dept. of Physics.
LASER THRUSTER
N. W. Jalufka *In* NASA. Langley Research Center, Second Beamed Space-Power Workshop Jul. 1989 p 391-396 (For primary document see N90-10140 01-20)
Avail: NTIS HC A19/MF A03 CSCL 20E

N90-10167*# National Aeronautics and Space Administration. Langley Research Center, Hampton, VA.
BEAMED LASER POWER IN SUPPORT OF NEAR-EARTH MISSIONS
Edmund J. Conway, Gregory L. Schuster, Willard Weaver, and Donald H. Humes *In its* Second Beamed Space-Power Workshop Jul. 1989 p 419-429 (For primary document see N90-10140 01-20)
Avail: NTIS HC A19/MF A03 CSCL 20E

37 MECHANICAL ENGINEERING

Includes auxiliary systems (nonpower); machine elements and processes; and mechanical equipment.

N90-10436# Science Applications International Corp., Billerica, MA.
ADAPTIVE MACHINE VISION Annual Report
William W. Stoner 25 Jan. 1989 120 p
(Contract N00014-86-C-0601)
(AD-A208130) Avail: NTIS HC A06/MF A01 CSCL 17/11

The results are presented of research on two topics, the adaptive photosensor array model and initiation of target tracking in a high clutter, high target density environment. The problem of tracking multiple targets occurs not only in Strategic Defense Initiative but also in natural and robotic vision. In psychology the problem is called the correspondence problem because in successive looks at a complex moving scene, the visual system must find corresponding objects in each look to perceive the objects as moving. Exactly how the visual system makes this correspondence is unknown. However, any animal that moves solves the problem, because nearby objects have higher apparent velocities than distant objects. GRA

N90-10437*# Hamilton Standard, Windsor Locks, CT.
TWO STAGE GEAR TOOTH DYNAMICS PROGRAM Final Report
Linda S. Boyd Aug. 1989 49 p
(Contract NAS3-25281)
(NASA-CR-185110; NAS 1.26:185110; AVSCOM-TM-89-C-003; HSER-12648) Avail: NTIS HC A03/MF A01 CSCL 13I

The epicyclic gear dynamics program was expanded to add the option of evaluating the tooth pair dynamics for two epicyclic gear stages with peripheral components. This was a practical extension to the program as multiple gear stages are often used for speed reduction, space, weight, and/or auxiliary units. The option was developed for either stage to be a basic planetary, star, single external-external mesh, or single external-internal mesh. The two stage system allows for modeling of the peripherals with an input mass and shaft, an output mass and shaft, and a connecting shaft. Execution of the initial test case indicated an instability in the solution with the tooth paid loads growing to excessive magnitudes. A procedure to trace the instability is recommended as well as a method of reducing the program's computation time by reducing the number of boundary condition iterations. Author

N90-10438*# ST Systems Corp., Lanham, MD.
AN ADAPTIVE CONTROLLER FOR ENHANCING OPERATOR PERFORMANCE DURING TELEOPERATION
Craig R. Carignan, Janice M. Tarrant, and Gary E. Mosier (National Aeronautics and Space Administration. Goddard Space Flight Center, Greenbelt, MD.) 1989 6 p
(Contract NAS5-28561)
(NASA-CR-183445; NAS 1.26:183445) Avail: NTIS HC A02/MF A01 CSCL 13I

An adaptive controller is developed for adjusting robot arm parameters while manipulating payloads of unknown mass and inertia. The controller is tested experimentally in a master/slave configuration where the adaptive slave arm is commanded via human operator inputs from a master. Kinematically similar six-joint master and slave arms are used with the last three joints locked for simplification. After a brief initial adaptation period for the unloaded arm, the slave arm retrieves different size payloads and maneuvers them about the workspace. Comparisons are then drawn with similar tasks where the adaptation is turned off. Several simplifications of the controller dynamics are also addressed and experimentally verified. Author

N90-10439 Vanderbilt Univ., Nashville, TN.
AN EXPERT SYSTEM FOR OPTIMAL GEAR DESIGN Ph.D. Thesis
Kuan-Chan Lin 1988 316 p
Avail: Univ. Microfilms Order No. DA8910860

An expert system is developed for optimal spur gear design. Design automation is accomplished by separating the design space into different categories, i.e. geometric design variables and non-geometric design variables. The geometric variables are further divided into terms that are related to the gear mathematical model and terms that are determined according to the designer's experience. By properly developing the mathematical model, numerical optimization can be used to seek the best solution for a given set of geometric constraints. The process of determining the non-geometric design variables is automated by using symbolic computation. This gear design expert system is built according to the AGMA standards and a survey of gear design experts. The recommendations of gear designers and the information provided by AGMA standards are integrated into knowledge bases and data bases. By providing fast information retrieval and design guidelines, this expert system greatly streamlines the spur gear design process and makes it possible for a novice designer to achieve a reliable design in a short period of time. The concept of separating the design space into geometric and non-geometric variables can also be applied to the design process for general mechanical elements. The expert system technique is used to simulate a human designer to optimize the process of determining non-geometric parameters, and the numerical optimization is used to identify the best geometric solution. The combination of the expert system technique with numerical optimization essentially eliminates the deficiencies of both methods and thus provides a better way of modeling the engineering design process. Dissert. Abstr.

N90-10440# California Univ., Berkeley. Dept. of Materials Science and Mineral Engineering.
MICROMECHANISMS OF SURFACE FRICTION IN ZINC ELECTROGALVANIZED STEEL SHEETS
S. J. Shaffer, A. M. Philip, and J. W. Morris, Jr. Apr. 1989 9 p Presented at the Galvatech 89 Conference, Tokyo (Japan), 5-7 Sep. 1989 Prepared in cooperation with California Univ., Berkeley, Lawrence Berkeley Lab. Sponsored in part by Ford Motor Co., Rouge Steel Co., and LTV Steel Co.
(Contract DE-AC03-76SF-00098)
(DE89-011819; LBL-26935; CONF-8909114) Avail: NTIS HC A03/MF A01

Significant variations are found in the measured coefficients of friction of commercial zinc electrogalvanized steel (EGS) sheets. The tribological mechanisms apparently differ from those in bare steel. Because of the relative softness of the zinc layer, its mechanical properties are important in determining the coefficient of friction. Since zinc is hexagonal, its mechanical properties are highly anisotropic. This suggests that the coefficient of friction should depend strongly on the crystallographic texture of the galvanized layer. Such a dependence was found in draw-bead simulator tests on a variety of commercial steels. Coatings with a strong basal texture had particularly high coefficients of friction. This result is interpreted on the basis of a simple model that considers the interaction between asperities on the rigid tool and the relatively deformable coating. DOE

N90-10441# Allied-Signal Aerospace Co., Kansas City, MO. Technical Communications Div.
HIGH-SPEED MACHINING OF ALUMINUM
S. J. Heine Jul. 1989 64 p
(Contract DE-AC04-76DP-00613)
(DE89-014011; KCP-613-4080) Avail: NTIS HC A03/MF A01

High-speed machining of aluminum alloys has become an established manufacturing process for a variety of production parts at Allied-Signal Inc., Kansas City Division. Some of these parts include a mounting deck, a forward retainer, and a mount. In the course of developing the production machining processes for these parts, general tooling and machining parameters were developed that aid in the application of this technology to future parts. High-speed machining is a cost effective, viable manufacturing process for aluminum material when correct part selection criteria and processing parameters are applied. DOE

N90-10442# Sandia National Labs., Albuquerque, NM.
THE ROLE OF SENSOR DIRECTED, MODEL BASED CONTROL IN ROBOTICS
R. W. Harrigan 1989 5 p Presented at the IROS 1989 International Workshop on Intelligent Robots and Systems: The Autonomous Robot and its Application, Tsukuba, Japan, 4-6 Sep. 1989
(Contract DE-AC04-76DP-00789)
(DE89-014133; SAND-89-0788C; CONF-8909167-1) Avail: NTIS HC A01/MF A01

This paper discusses the use of model based control of industrial robots to achieve automatic programming of robot trajectories, hybrid force/position control and computer assisted manual operation. Experiments at Sandia National Laboratories are reviewed to illustrate the impact of model based control on the operation of robotic systems. Computer models of the robots and their operating environments are complemented with environmental sensing. Sensing allows correlation of modeled geometries with the location of objects in the actual environment. In addition, sensors detect error situations which may require operator attention prior to continued system operation. Computer models are used to verify the validity of sensor data before the robotic system executes operations based upon those data. DOE

N90-10443# Oak Ridge National Lab., TN. Center for Engineering Systems Advanced Research.

AUTONOMOUS MOBILE ROBOT RESEARCH USING THE HERMIES-3 ROBOT

F. G. Pin, M. Beckerman, P. F. Spelt, J. T. Robinson, and C. R. Weisbin 1989 6 p Presented at the IROS '89: International Workshop on Intelligent Robots and Systems: The Autonomous Robot and its Application, Tsukuba (Japan), 4-6 Sep. 1989
(Contract DE-AC05-84OR-21400)
(DE89-015916; CONF-8909167-2) Avail: NTIS HC A02/MF A01

This paper reports on the status and future directions in the research, development and experimental validation of intelligent control techniques for autonomous mobile robots using the HERMIES-3 robot at the Center for Engineering Systems Advanced research (CESAR) at Oak Ridge National Laboratory (ORNL). HERMIES-3 is the fourth robot in a series of increasingly sophisticated and capable experimental test beds developed at CESAR. HERMIES-3 is comprised of a battery powered, onmi-directional wheeled platform with a seven degree-of-freedom manipulator arm, video cameras, sonar range sensors, laser imaging scanner and a dual computer system containing up to 128 NCUBE nodes in hypercube configuration. All electronics, sensors, computers, and communication equipment required for autonomous operation of HERMIES-3 are located on board along with sufficient battery power for three to four hours of operation. The paper first provides a more detailed description of the HERMIES-3 characteristics, focussing on the new areas of research and demonstration now possible at CESAR with this new test-bed. The initial experimental program is then described with emphasis placed on autonomous performance of human-scale tasks, integration of a dexterous manipulator and platform motion in geometrically complex environments. DOE

N90-10444# Oak Ridge Y-12 Plant, TN. Development Div.

CHARACTERIZATION OF ELECTRON-BEAM WELD PROCESSES IN URANIUM BY ACOUSTIC EMISSION MONITORING

J. W. Whittaker and J. L. Murphy 19 Aug. 1989 19 p
(Contract DE-AC05-84OS-21400)
(DE89-016044; Y/DW-890) Avail: NTIS HC A03

Work was begun to characterize electron-beam (EB) welding of uranium by use of acoustic emission (AE) monitoring at the Oak Ridge Y-12 Plant. One specific objective was to determine if a correlation existed between weld penetration and an AE parameter(s). AE monitoring techniques were developed which allowed detection and recording of AE information during welding. Initial results from bead-on-plate welds of uranium imply that the AE signal varies during different processes: weld initiation, process stabilization, steady-state weld formation, weld cessation, and material cool-down. A correlation was developed between the AE average signal level (ASL) parameter and weld penetration which implies that penetration can be predicted from a given measured ASL level. DOE

N90-10445# Carnegie-Mellon Univ., Pittsburgh, PA. Robotics Inst.

A NEW APPROACH TO CONTROL SINGLE-LINK FLEXIBLE ARMS. PART 1: MODELLING AND IDENTIFICATION IN THE PRESENCE OF JOINT FRICTION

Vicente Feliu, Kuldip S. Rattan (Wright State Univ., Dayton, OH.), and H. Benjamin Brown, Jr. Mar. 1989 33 p
(AD-A210590; CMU-RI-TR-89-8-Pt-1) Copyright Avail: NTIS HC A03/MF A01 CSCL 12/9

This report presents a new way to model and identify single-link flexible arms when Coulomb friction is present in the joint. In order to isolate the effects of this nonlinearity, the arm model is divided into two submodels: motor and beam. The two are coupled through the torque at the base of the beam. A systematic method is developed to obtain the dynamics of a lumped-mass flexible beam, and some properties are obtained from this model. The influence of the payload on the model is given special attention. This way of modelling is later extended to the general case of distributed-mass flexible arms. Identification in the presence of Coulomb friction is carried out. A new method is proposed to estimate this friction and to reconstruct the motor frequency response from experimental results, which are highly distorted by this nonlinear friction. GRA

N90-10446*# Carnegie-Mellon Univ., Pittsburgh, PA. Robotics Inst.

THE 1988 YEAR END REPORT FOR ROAD FOLLOWING AT CARNEGIE-MELLON Annual Report, 15 Jan. 1988 - 31 Mar. 1989

Charles Thorpe and Takeo Kanade Feb. 1989 131 p Sponsored in part by Digital Equipment Corp.
(Contract NAGw-1175; DACA76-85-C-0003; NSF DRC-86-04199; ARPA Order 5351)
(NASA-CR-185967; NAS 1.26:185967; AD-A210594; CMU-RI-TR-89-5; ETL-0537) Copyright Avail: NTIS HC A07/MF A01 CSCL 12/9

This report describes the progress in vision and navigation for outdoor mobile robots at the Carnegie Mellon Robotics Institute during 1988. This research was primarily sponsored by DARPA as part of the Strategic Computing Initiative. Portions of this research were also partially supported by the National Science Foundation and Digital Corporation. In the four years of the project, we have built perception modules for following roads, detecting obstacles, mapping terrain, and recognizing objects. Together with our sister Integration contract, we have built systems that drive mobile robots along roads and cross country, and have gained valuable insights into viable approaches for outdoor mobile robot research. Specifically in 1988, we have completed one color vision system for finding roads, begun two others that handle difficult lighting and structured public roads and highways, and built a road-following system that uses active scanning with a laser rangefinder. We have used 3-D information to build elevation maps for cross-country path planning, and have used maps to retraverse a route. Progress in 1988 on these projects is described. GRA

N90-10447*# Spectra Research Systems, Inc., Huntsville, AL. Systems Technology Div.

INTERCHANGEABLE END EFFECTOR TOOLS UTILIZED ON THE PROTOFLIGHT MANIPULATOR ARM Final Report

May 1987 153 p
(Contract NAS8-36307)
(NASA-CR-179374; NAS 1.26:179374; SRS/STD-TR86-011-549) Avail: NTIS HC A08/MF A01 CSCL 13I

A subset of teleoperator and effector tools was designed, fabricated, delivered and successfully demonstrated on the Marshall Space Flight Center (MSFC) protoflight manipulator arm (PFMA). The tools delivered included a rotary power tool with interchangeable collets and two fluid coupling mate/demate tools; one for a Fairchild coupling and the other for a Purolator coupling. An electrical interface connector was also provided for the rotary power tool. A tool set, from which the subset was selected, for performing on-orbit satellite maintenance was identified and conceptionally designed. Maintenance requirements were

synthesized, evaluated and prioritized to develop design requirements for a set of end effector tools representative of those needed to provide on-orbit maintenance of satellites to be flown in the 1986 to 2000 timeframe. Author

N90-10448# Missouri Univ., Rolla.
STUDIES IN PENETRATION MECHANICS Final Report, 23 Sep. 1985 - 22 Mar. 1989
R. C. Batra 14 Jun. 1989 119 p
(Contract DAAG29-85-K-0238)
(AD-A210713; ARO-22806.17-EG) Avail: NTIS HC A06/MF A01 CSCL 19/10

The details of a steadily growing plastic flow field a short while after a thick target has been impacted by a deformable penetrator have been studied with the ultimate objectives of identifying key material and kinematic variables that should be included in developing engineering models of target penetration. The problems studied include the axisymmetric thermomechanical deformations of a viscoplastic target being penetrated by a rigid cylindrical penetrator, and of a viscoplastic rod striking a known hemispherical rigid cavity. The effects of heat generated due to plastic deformations, compressibility of the material, work-hardening, strain-rate hardening, thermal softening, and the shape of the penetrator nose in the former case and the cavity shape for the latter problem have been investigated. GRA

N90-10449# Technische Univ., Munich (Germany, F.R.). Gear Research Lab.
DEVELOPMENT OF A HIGH TEMPERATURE FZG-RYDER GEAR LUBRICANT LOAD CAPACITY MACHINE Final Report, 1 Sep. 1986 - 31 Dec. 1988
K. Michaelis and H. Winter 16 May 1989 81 p
(Contract F49620-86-C-0081; AF Proj. 3048)
(AD-A210799; TUM-F515/2/MI; Rept-1583; WRDC-TR-89-2028)
Avail: NTIS HC A05/MF A01 CSCL 13/9

A modified FZG-Ryder gear machine was developed to run scuffing tests at high speed (n1 = 9700/min) and oil temperatures from 74 C to 200 C. Test oil volume is approximately 3 liters. Good correlation was found between FZG-Ryder and standard Ryder test results when rating ester base lubricants and using ester base reference oils such as Hercolube. Poor correlation was found when using mineral based reference oil. Tests on three oils at 200 C showed considerable lower load capacity as compared to ratings at 74 C. However, relative ranking of the lubricant was unchanged. GRA

38 QUALITY ASSURANCE AND RELIABILITY

Includes product sampling procedures and techniques; and quality control.

No abstracts in this category.

39 STRUCTURAL MECHANICS

Includes structural element design and weight analysis; fatigue; and thermal stress.

For applications see *05 Aircraft Design, Testing and Performance* and *18 Spacecraft Design, Testing and Performance.*

N90-10450*# MARC Analysis Research Corp., Palo Alto, CA. Finite Element Factory.
THE MHOST FINITE ELEMENT PROGRAM: 3-D INELASTIC ANALYSIS METHODS FOR HOT SECTION COMPONENTS. VOLUME 2: USER'S MANUAL Final Report
Shohei Nakazawa Jul. 1989 136 p
(Contract NAS3-23697)
(NASA-CR-182235-Vol-2; NAS 1.26:182235-Vol-2; FEF/PD/1101/89-Vol-2) Avail: NTIS HC A07/MF A01 CSCL 20K

The user options available for running the MHOST finite element analysis package is described. MHOST is a solid and structural analysis program based on the mixed finite element technology, and is specifically designed for 3-D inelastic analysis. A family of 2- and 3-D continuum elements along with beam and shell structural elements can be utilized, many options are available in the constitutive equation library, the solution algorithms and the analysis capabilities. The outline of solution algorithms is discussed along with the data input and output, analysis options including the user subroutines and the definition of the finite elements implemented in the program package. Author

N90-10451*# MARC Analysis Research Corp., Palo Alto, CA. Finite Element Factory.
THE MHOST FINITE ELEMENT PROGRAM: 3-D INELASTIC ANALYSIS METHODS FOR HOT SECTION COMPONENTS. VOLUME 3: SYSTEMS' MANUAL Final Report
Shohei Nakazawa Jul. 1989 216 p
(Contract NAS3-23697)
(NASA-CR-182236; NAS 1.26:182236; FEF/PD/1102/89-Vol-3)
Avail: NTIS HC A10/MF A02 CSCL 20K

The internal structure is discussed of the MHOST finite element program designed for 3-D inelastic analysis of gas turbine hot section components. The computer code is the first implementation of the mixed iterative solution strategy for improved efficiency and accuracy over the conventional finite element method. The control structure of the program is covered along with the data storage scheme and the memory allocation procedure and the file handling facilities including the read and/or write sequences. Author

N90-10452# Queensland Univ., Brisbane (Australia). Dept. of Civil Engineering.
LIMIT ANALYSIS OF WELDED TEE END CONNECTIONS FOR HOLLOW TUBES
N. J. Stevens (Crooks, Mitchell, Peacock and Stewart Proprietary Ltd., Australia) and S. Kitipornchai Nov. 1988 33 p
(PB89-191647; RR-CE95; ISBN-0-86776-310-8) Avail: NTIS HC A03/MF A01 CSCL 20K

A limit analysis is presented, based on the yield line approach, for predicting the ultimate capacity of welded tee end connections for hollow tubes. Five failure mechanisms are identified. The failure mechanisms range from simple mechanisms such as yielding of the cleat plate or the tube to the more complex mechanisms involving a combination of hinge formation in the cap plate and local yielding in the tube. It is shown that the dimensions of the connection components involving the tube, the cap and the cleat plate sizes determine which is the controlling failure mechanism. A further series of tests on tubes of square hollow section is presented. The theoretical predictions, based on the yield line approach, agree very well with test results from 36 welded tee end connections on circular and square hollow tubes. GRA

N90-10453# Royal Armament Research and Development Establishment, Wescott (England).
A DESIGN ASSESSMENT FOR METALLIC PRESSURE VESSELS CIRCUMFERENTIALLY REINFORCED WITH A PRE-TENSIONED HIGH-SPECIFIC-STRENGTH ANISOTROPIC COMPOSITE OVERWIND
A. Groves and J. Margetson Mar. 1989 29 p
(AD-A209108; RARDE-12/88; DRIC-BR-109774) Avail: NTIS HC A03/MF A01 CSCL 10/4

A design assessment is presented for thick-walled metallic pressure vessels circumferentially reinforced with a pre-tensioned high-specific-strength anisotropic fiber reinforced composite overwind. The assessment is restricted to the most important study of evaluating, for five potential composite overwinds, the relationship between the reinforcement thickness and metallic liner thickness to yield a vessel of comparable strength to an all-metal reference vessel. The resulting data are nevertheless used in a

series of ancillary analyses, namely weight comparisons, strain to failure studies and detailed stress computations, to establish optimum configurations and, moreover, to identify the most suitable overwinding material. The influence of variations in the considerably lower transverse moduli (radial and axial) of the circumferentially reinforcing material is also considered by repeating the assessment studies for both 10GPa and IGPa transverse moduli composite overwinds. GRA

N90-10454*# National Aeronautics and Space Administration. Langley Research Center, Hampton, VA.
AN INTERFEROMETRIC STRAIN-DISPLACEMENT MEASUREMENT SYSTEM
William N. Sharpe, Jr. Aug. 1989 67 p
(NASA-TM-101638; NAS 1.15:101638) Avail: NTIS HC A04/MF A01 CSCL 20K

A system for measuring the relative in-plane displacement over a gage length as short as 100 micrometers is described. Two closely spaced indentations are placed in a reflective specimen surface with a Vickers microhardness tester. Interference fringes are generated when they are illuminated with a He-Ne laser. As the distance between the indentations expands or contracts with applied load, the fringes move. This motion is monitored with a minicomputer-controlled system using linear diode arrays as sensors. Characteristics of the system are: (1) gage length ranging from 50 to 500 micrometers, but 100 micrometers is typical; (2) least-count resolution of approximately 0.0025 micrometer; and (3) sampling rate of 13 points per second. In addition, the measurement technique is non-contacting and non-reinforcing. It is useful for strain measurements over small gage lengths and for crack opening displacement measurements near crack tips. This report is a detailed description of a new system recently installed in the Mechanisms of Materials Branch at the NASA Langley Research Center. The intent is to enable a prospective user to evaluate the applicability of the system to a particular problem and assemble one if needed. Author

N90-10455*# Tulane Univ., New Orleans, LA.
MECHANICS OF THE CRACK PATH FORMATION Final Report
Asher A. Rubinstein Sep. 1989 21 p
(Grant NAG3-815)
(NASA-CR-185143; NAS 1.26:185143; E-5070) Avail: NTIS HC A03/MF A01 CSCL 20K

A detailed analysis of experimentally obtained curvilinear crack path trajectories formed in a heterogeneous stress field is presented. Experimental crack path trajectories were used as data for numerical simulations, recreating the actual stress field governing the development of the crack path. Thus, the current theories of crack curving and kinking could be examined by comparing them with the actual stress field parameters as they develop along the experimentally observed crack path. The experimental curvilinear crack path trajectories were formed in the tensile specimens with a hole positioned in the vicinity of a potential crack path. The numerical simulation, based on the solution of equivalent boundary value problems with the possible perturbations of the crack path, is presented here. Author

N90-10456*# National Aeronautics and Space Administration. Langley Research Center, Hampton, VA.
GLOBAL/LOCAL STRESS ANALYSIS OF COMPOSITE STRUCTURES M.S. Thesis
Jonathan B. Ransom Aug. 1989 114 p
(NASA-TM-101640; NAS 1.15:101640) Avail: NTIS HC A06/MF A01 CSCL 20K

A method for performing a global/local stress analysis is described and its capabilities are demonstrated. The method employs spline interpolation functions which satisfy the linear plate bending equation to determine displacements and rotations from a global model which are used as boundary conditions for the local model. Then, the local model is analyzed independent of the global model of the structure. This approach can be used to determine local, detailed stress states for specific structural regions using independent, refined local models which exploit information from less-refined global models. The method presented is not restricted to having a priori knowledge of the location of the regions requiring local detailed stress analysis. This approach also reduces the computational effort necessary to obtain the detailed stress state. Criteria for applying the method are developed. The effectiveness of the method is demonstrated using a classical stress concentration problem and a graphite-epoxy blade-stiffened panel with a discontinuous stiffener. Author

N90-10457*# National Aeronautics and Space Administration. Langley Research Center, Hampton, VA.
ANALYSIS AND TEST OF A 16-FOOT RADIAL RIB REFLECTOR DEVELOPMENTAL MODEL
Shawn A. Birchenough (Massachusetts Inst. of Tech., Cambridge.) Aug. 1989 28 p
(NASA-TM-101648; NAS 1.15:101648) Avail: NTIS HC A03/MF A01 CSCL 20K

Analytical and experimental modal tests were performed to determine the vibrational characteristics of a 16-foot diameter radial rib reflector model. Single rib analyses and experimental tests provided preliminary information relating to the reflector. A finite element model predicted mode shapes and frequencies of the reflector. The analyses correlated well with the experimental tests, verifying the modeling method used. The results indicate that five related, characteristic mode shapes form a group. The frequencies of the modes are determined by the relative phase of the radial ribs. Author

N90-10458# Sandia National Labs., Albuquerque, NM.
VIBRAFUGE: A COMBINED ENVIRONMENT TESTING FACILITY-VIBRATION TESTING ON A CENTRIFUGE
Jim Doggett and Fred Cericola 1989 18 p Presented at the Society of Automotive Engineers Aerotech 89, Anaheim, CA, 25-28 Sep. 1989
(Contract DE-AC04-76DP-00789)
(DE89-015120; SAND-89-1881C; CONF-8909168-1) Avail: NTIS HC A03/MF A01

Vibration testing in a centrifuge acceleration field (up to 50 gs) can be accomplished in either of two axes relative to the centrifuge acceleration with a modified, commercially available, electrodynamic shaker and the use of a specially designed orthogonal motion converter. Fixing the shaker armature axis in-line with the centrifuge arm (head towards the pivot) keeps the inertial forces on the head in the one direction which can be offset with servo controlled pneumatic bags located beneath the shaker head. Testing in an axis perpendicular to the principal axis is accomplished with the orthogonal motion converter which is driven by the shaker head. DOE

N90-10459# Washington State Univ., Pullman. Fracture Lab.
PARTICLE EMISSION AND CHARGING EFFECTS INDUCED BY FRACTURE Technical Report, 1 Jun. 1987 - 30 May 1989
J. Thomas Dickinson 15 Jun. 1989 357 p
(Contract N00014-87-K-0514)
(AD-A210215) Avail: NTIS HC A16/MF A02 CSCL 20/11

A series of studies involving the physical consequences of deformation and fracture of materials are presented. These measurements include fracto-emission (FE) experiments on model rocket propellent, two studies on properties of ejecta (macroscopic particles) from materials including explosive crystals, fracture induced electrical breakdown, the detection of free charge carriers accompanying fracture in single crystal Si, Fe studies on polymers, adhesives, single crystal and amorphous inorganics, studies of fracture surfaces using scanning tunneling microscopy and atomic force microscopy, and two studies on the interaction of intense UV laser radiation with materials. The appendix presents a review article on fracto-emission from interfacial failure. GRA

N90-10460# Army Armament Research, Development and Engineering Center, Watervliet, NY. Close Combat Armaments Center.
STRESS INTENSITY FACTORS AND DISPLACEMENTS FOR ARC BEND SAMPLES USING COLLOCATION Final Report

J. A. Kapp Jun. 1989 33 p Presented at the 18th ASTM National Symposium on Fracture Mechanics, Boulder, CO
(AD-A210404; AD-F000138; ARCCB-MR-89014) Avail: NTIS HC A03/MF A01 CSCL 20/11

Stress intensity, crack mouth opening displacements, and load-line displacements were determined for the arc bend-chord support specimen using boundary collocation. Several inner radius (r1) to outer radius (r2) ratios were studied at each of two span (S) to width (W) ratios. The actual solution matrix is for S/W = 3, r1/r2 = 0.8, 0.6 0.4, and for S/W = 4, R1/R2 = 0.8, 0.7, 0.6. Also, the three-point bend single-edge specimen (SE(B)) at both S/W = 3 and S/W = 4 was studied to examine the limiting behavior of the generated solutions. For all of the S/W = 3 cases, solutions were obtained for crack length to width ratios (a/W) from 0.2 to 0.6, and in the S/W = 4 cases, a/W was varied from 0.2 to 0.5. The solutions were obtained by the linear superposition of a pure bending stress, a pure shear stress, and a uniform normal stress on an annual segment. The magnitudes of the individual components depended upon the size of the annular segment and the S/W ratio. Wide range expressions were fit to the numerical solutions to make them applicable over a wider range of testing conditions and for inclusion in future revisions of E-399 on Plane Strain Fracture Toughness testing. GRA

N90-10461# Ballistic Research Labs., Aberdeen Proving Ground, MD.
EPIC-2 CALCULATED IMPACT LOADING HISTORIES OF THIN PLATES
Ennis F. Quigley Jun. 1989 28 p
(AD-A210557; BRL-TR-3011) Avail: NTIS HC A03/MF A01 CSCL 09/1

Although the EPIC-2 code can predict the ballistic shock environments in projectile-impacted targets, these targets must be axisymmetric. By modifying the code to calculate the history of an impacting projectile on the target, one can use the loading history as input for a finite element analysis of the ballistic shock in non-axisymmetric targets. Loading histories of 20 mm fragment simulator projectiles for impact velocities of 366 m/s and 1012 m/s on 38 mm x 914 mm circular rolled homogeneous armor plates have been calculated by the EPIC-2 code and have been used in ADINA finite element structural response analyses of the plate. Comparisons of EPIC-2 and ADINA responses calculations show that the EPIC-2 code can be used to calculate loading histories which do represent the loading of a target by nonperforating projectiles. GRA

N90-10462# Virginia Polytechnic Inst. and State Univ., Blacksburg.
FATIGUE GROWTH AND CLOSURE OF SHORT CRACKS Final Report, Jun. 1985 - Dec. 1988
Nagaraja S. Iyyer and Norman E. Dowling 3 Jun. 1989 298 p
(Contract F33615-85-K-3210; AF Proj. 2302)
(AD-A210824; AFWAL-TR-89-3008) Avail: NTIS HC A13/MF A02 CSCL 11/6

The growth and closure behavior of short cracks in 2024-T351 aluminum alloy and four different conditions of 4340 steel using through thickness cracks of straight fronts were investigated. The experiments were carried out to study the influence of stress level, stress ratio, yield strength and prior austenitic grain sizes in notched and unnotched specimens. The stereoimaging technique was developed and adapted to obtain crack closing and opening points, and also near tip displacement fields. Experimental results are presented with a general discussion. It was found that long cracks showed good correlation when analyzed in terms of effective stress intensity range. However, correlations were poor for short cracks. It was found that short cracks show less closure behavior than long cracks. The estimates of initial crack lengths based on linear elastic data were made. GRA

N90-10463# Army Armament Research and Development Command, Watervliet, NY.
FRACTURE AND THREE DIMENSIONAL STRESS ANALYSES OF 7075 ALUMINUM PROJECTILE COMPONENTS UNDER SPIN AND INERTIA LOAD Final Report
J. H. Underwood, M. A. Scavullo, G. P. OHara, and B. A. Konrad Jun. 1989 27 p
(AD-A210986; ARCCB-TR-89016) Avail: NTIS HC A03/MF A01 CSCL 19/1

A fracture case study of a high strength aluminum projectile component subjected to inertial and spin loading during launch from a cannon is presented. A 3-D finite element model was used to calculate the projectile stresses and to determine which of the several types of loading was the primary cause of failure. A design change to minimize spin loading resulted in a significantly reduced failure incidence. Mechanical and fracture mechanics tests of the aluminum were performed in order to determine material specifications which could prevent failures in the future. An energy-to-failure test similar to the Charpy test was found to be the most discriminating. GRA

N90-10464# Pennsylvania State Univ., University Park. Dept. of Materials Science and Engineering.
POROSITY AND CRACK INITIATION DURING LOW CYCLE FATIGUE
D. A. Gerard and D. A. Koss Jul. 1989 25 p
(Contract N00014-86-K-0381)
(AD-A210989; TR-13) Avail: NTIS HC A03/MF A01 CSCL 11/6

The influence of porosity on crack initiation during low cycle fatigue LCF has been examined by both experimental observations and theoretical modeling. Experimental data based on powder-processed titanium indicate a porosity-induced enhancement of crack initiation, which contributes to significant reductions in low cycle fatigue life. All of the levels of porosity examined, which range from 0.4 to 6 volume percent, cause an order of magnitude or greater decrease in the number of cycles to initiate a 15 micron crack. Based on a modification of a Neuber analysis, local strain profiles which develop adjacent to holes in uniaxial tension and large-strain amplitude fatigue testing have also been predicted and experimentally verified. Modeling porosity located at a surface as a through-thickness hole deforming under plane-stress conditions, adapting a Coffin-Manson law as a failure criterion and using cumulative damage theory, a theoretical analysis has been developed for predicting the number of cycles for microcrack initiation in the presence of porosity. The predictions, which rely on pore shapes and the low cycle fatigue response of the fully dense matrix, accurately predict the number of cycles necessary to initiate a 15 micron crack adjacent to both isolated and interconnected pores during low cycle fatigue. GRA

42 GEOSCIENCES (GENERAL)

No abstracts in this category.

43 EARTH RESOURCES AND REMOTE SENSING

Includes remote sensing of earth resources by aircraft and spacecraft; photogrammetry; and aerial photography.

For instrumentation see *35 Instrumentation and Photography.*

N90-10465*# Utah Univ., Salt Lake City. Dept. of Geography.
IMAGE-BASED TERRAIN MODELING WITH THEMATIC MAPPER APPLIED TO RESOLVING THE LIMIT OF HOLOCENE LAKE EXPANSION IN THE GREAT SALT LAKE DESERT, UTAH, PART 1 Final Report
John A. Merola 25 Jul. 1989 109 p
(Contract NAS5-28753)
(NASA-CR-185913; NAS 1.26:185913; LLTR-89-1) Avail: NTIS HC A06/MF A01 CSCL 08B

The LANDSAT Thematic Mapper (TM) scanner records reflected solar energy from the earth's surface in six wavelength regions, or bands, and one band that records emitted energy in the thermal region, giving a total of seven bands. Useful research was extracted about terrain morphometry from remote sensing measurements and this information is used in an image-based terrain model for selected coastal geomorphic features in the Great Salt Lake Desert (GSLD). Technical developments include the incorporation of Aerial Profiling of Terrain System (APTS) data in satellite image analysis, and the production and use of 3-D surface plots of TM reflectance data. Also included in the technical developments is the analysis of the ground control point spatial distribution and its affects on geometric correction, and the terrain mapping procedure; using satellite data in a way that eliminates the need to degrade the data by resampling. The most common approach for terrain mapping with multispectral scanner data includes the techniques of pattern recognition and image classification, as opposed to direct measurement of radiance for identification of terrain features. The research approach in this investigation was based on an understanding of the characteristics of reflected light resulting from the variations in moisture and geometry related to terrain as described by the physical laws of radiative transfer. The image-based terrain model provides quantitative information about the terrain morphometry based on the physical relationship between TM data, the physical character of the GSLD, and the APTS measurements. Author

N90-10466*# Utah Univ., Salt Lake City. Dept. of Geography.
FLUCTUATION HISTORY OF GREAT SALT LAKE, UTAH, DURING THE LAST 13,000 YEARS, PART 2 Final Report
Stuart B. Murchison 25 Jul. 1989 159 p
(Contract NAS5-28753)
(NASA-CR-185911; NAS 1.26:185911; LLTR-89-2) Avail: NTIS HC A08/MF A01 CSCL 08B

Great Salt Lake level fluctuations from 13,000 yr B.P. to the present were interpreted by examination of shoreline geomorphic features, shoreline deposits, archeologic sites, isotopic data, and palynologic data. After the conclusion of the Bonneville paleolake cycle, between 13,000 and 12,000 yr B.P. the lake regressed to levels low enough to deposit a littoral oxidized red bed stratum and a pelagic Glauber's salt layer. A late Pleistocene lake cycle occurred between 12,000 and 10,000 yr B.P. depositing several beaches, the highest reaching an altitude of about 4250 ft (1295.3 m). The lake regressed after 10,000 yr B.P., only to rise to 4230 ft (1289.2 m) between 9700 and 9400 yr B.P. and then gradually lower at least 15 ft (4.5 m) or more. Lake levels fluctuated between 4212 and 4180 ft (1284 and 1274 m) for the next 4000 years. A late Holocene lake cycle, constrained by radiocarbon ages between 3440 and 1400 yr B.P., is reported at a highest static level of 4221 ft (1286.5 m). After a lake level drop to altitudes ranging between 4210 and 4205 ft (1283.2 and 1281.6 m), a 4217 ft (1285.7 m) level was reached after 400 yr B.P. This level lowered to 4214 ft (1284.4 m) in the mid to late 1700 s A.D. The lake levels have since stabilized aroung a 4200 ft (1280 m) mean. Author

N90-10467# Wisconsin Univ., Madison. Dept. of Mathematics.
A COMPILATION OF DIGITIZED SATELLITE IMAGERY OF THE GULF STREAM (1982, 1983, AND 1985)
Jennifer Earles, Lawrence Pratt, Peter Cornillon, and Jean-Francois Cayula (Rhode Island Univ., Narragansett.) Nov. 1988 109 p
(Contract N00014-87-K-0007; NSF OCE-87-00601; NSF OCE-85-10828)
(AD-A210243; WHOI-88-57) Avail: NTIS HC A06/MF A01 CSCL 08/3

Ninety plots of digitized temperature boundaries from infrared satellite images of the Gulf Stream along with corresponding image snapshots were compiled to determine stream width propagation speed. The satellite images are from the years 1982, 1983, and 1985 and are often of consecutive days. In this report, these images and digitized plots are presented. GRA

N90-10468*# Woods Hole Oceanographic Inst., MA.
SATELLITE DATA PROCESSING SYSTEM (SDPS) USERS MANUAL V1.0
Michael Caruso and Chris Dunn May 1989 66 p
(Contracts JPL-957652; N00014-86-K-0751)
(NASA-CR-183054; NAS 1.26:183054; AD-A210278; WHOI-89-13)
Avail: NTIS HC A04/MF A01 CSCL 12/5

SDPS is a menu driven interactive program designed to facilitate the display and output of image and line-based data sets common to telemetry, modeling and remote sensing. This program can be used to display up to four separate raster images and overlay line-based data such as coastlines, ship tracks and velocity vectors. The program uses multiple windows to communicate information with the user. At any given time, the program may have up to four image display windows as well as auxiliary windows containing information about each image displayed. SDPS is not a commercial program. It does not contain complete type checking or error diagnostics which may allow the program to crash. Known anomalies will be mentioned in the appropriate section as notes or cautions. SDPS was designed to be used on Sun Microsystems Workstations running SunView1 (Sun Visual/Integrated Environment for Workstations). It was primarily designed to be used on workstations equipped with color monitors, but most of the line-based functions and several of the raster-based functions can be used with monochrome monitors. The program currently runs on Sun 3 series workstations running Sun OS 4.0 and should port easily to Sun 4 and Sun 386 series workstations with SunView1. Users should also be familiar with UNIX, Sun workstations and the SunView window system. GRA

44 ENERGY PRODUCTION AND CONVERSION

Includes specific energy conversion systems, e.g., fuel cells; global sources of energy; geophysical conversion; and windpower.

For related information see also *07 Aircraft Propulsion and Power, 20 Spacecraft Propulsion and Power,* and *28 Propellants and Fuels.*

N90-10469# Argonne National Lab., Idaho Falls, ID.
EXPERIENCE WITH MODEL BASED DISPLAY FOR ADVANCED DIAGNOSTICS AND CONTROL
Jeffrey D. Staffon and Richard W. Lindsay 1989 8 p Presented at the 7th Power Plant Dynamics, Control and Testing Symposium, Knoxville, TN, 15-17 May 1989
(Contract W-31-109-eng-38)
(DE89-015693; CONF-890555-18) Avail: NTIS HC A02/MF A01

A full color, model based display system based on the Rankine thermodynamic cycle has been developed for use at the Experimental Breeder Reactor 2 by plant operators, engineers, and experimenters. The displays generate a real time thermodynamic model of the plant processes on computer screens to provide a direct indication of the plant performance. Operators and others who view the displays are no longer required to mentally

construct a model of the process before acting. The model based display accurately depicts the plant states. It appears to effectively reduce the gulf of evaluation, which should result in a significant reduction in human operator errors if this plant display approach is adopted by the nuclear industry. Preliminary comments from users, including operators, indicate an overwhelming acceptance of the display approach. The displays incorporate alarm functions as well as levels of detail paging capability. The system is developed on a computer network which allows the easy addition of displays as well as extra computers. Constructing a complete console can be rapid and inexpensive. DOE

N90-10470# Midwest Research Inst., Golden, CO.
ENERGY STORAGE AND DISTRIBUTION PROGRAM SUMMARY. VOLUME 2: RESEARCH SUMMARIES, FISCAL YEAR 1988
Jun. 1989 167 p
(Contract DE-AC02-83CH-10093)
(DE89-000867; DOE/CH-10093/52-Vol-2) Avail: NTIS HC A08/MF A01

The status of research and development projects supported by the Office of Energy Storage and Distribution (OESD) is summarized. The purpose is to inform interested readers of the research progress in both the Electric Energy Systems and Energy Storage programs. Developing advanced electric system and energy storage technologies is contributing to the nation's energy goals. The focus is on the individual research projects and furnishes a more detailed version of the OESD program. A summary of each research project that was active in FY 1988 as a result of FY 1988 or prior-year funding is contained in this second volume. Each contract description contains base project information, the project's objectives, and the status of the research performed in FY 1988. A companion document, Energy Storage and Distribution Program Summary, Volume 1: Overview; Fiscal Year 1988, provides an overview of the mission, strategy, and content of the OESD program. DOE

N90-10471# Midwest Research Inst., Golden, CO. Solar Energy Research Inst.
HIGH-EFFICIENCY CuInSe2 AND CuInGaSe2 BASED CELLS AND MATERIALS RESEARCH Annual Report, 1 Nov. 1987 - 31 Dec. 1988
W. E. Devaney, W. S. Chen, and J. M. Stewart Jun. 1989 30 p Prepared in cooperation with Boeing Co., Seattle, WA
(Contract DE-AC02-83CH-10093)
(DE89-009449; SERI/STR-211-3238) Avail: NTIS HC A03/MF A01

The results of the first year of a two-year research program are presented. A 1 sq cm ZnO/CdZnS/CuInGaSe(sub 2) solar cell with total-area efficiency of 12.5 percent (AM1.5, 100mW/sq cm) was fabricated. The quantum efficiency of this device at 400 nm exceeds 0.7 as a result of the improved transmission of the ZnO/thin CdZnS window layers. The fabrication and characteristics of each of the three layers and of the complete devices are discussed. Results on gallium doping of CdZnS window layers are presented. Three-layer antireflection coatings for CdZnS/CuInSe2 cells are single-layer coatings for ZnO/CdZnS/CuInGaSe2 structures were designed and deposited. Results on devices made using high-gallium-content CuInGaSe2 are discussed. DOE

N90-10472# International Fuel Cells Corp., South Windsor, CT.
IMPACT OF FUNDAMENTAL TECHNICAL IMPROVEMENTS Annual Report
D. L. Maricle Jun. 1989 36 p
(Contract GRI-5086-260-1398)
(PB89-218010; FCR-9643A; GRI-89/0137) Avail: NTIS HC A03/MF A01 CSCL 10A

The objective of the program is to identify the fundamental limitations of phosphoric acid and solid oxide fuel cells and define research paths for solution of the high priority limitations. Thirty opportunities for improving the phosphoric acid power plant were identified in a comparison of an ideal power plant to the current capability of a 200-kilowatt, learned-out, commercial power plant. The highest priority technical opportunities were assessed and the benefit payoff calculated. The top four areas are: performance improvement (80 mV), performance stability, an anode catalyst which could shift CO and not be poisoned by its presence, and methods to reduce cell stack material cost by 50 percent.
Author

N90-10473# Oregon State Univ., Corvallis. Solar Energy Research Inst.
A COMPARISON OF WIND TURBULENCE SIMULATION MODELS FOR STOCHASTIC LOADS ANALYSIS FOR HORIZONTAL-AXIS WIND TURBINES
S. N. Walker, T. L. Weber, and R. E. Wilson Jun. 1989 33 p
(Contract DE-AC02-83CH-10093)
(DE89-009442; SERI/STR-217-3463) Avail: NTIS HC A03/MF A01

Four wind turbine turbulence codes, the Pacific Northwest Laboratory (PNL) Rotational Code, the PNL Simulation Code, the Holley Code, and the Sandia National Laboratories Code, were examined. Hub-height simulations were made with each code and were compared to hub-height wind data from the vertical plane array of anemometers at the Howden 330-kW horizontal-axis wind turbine (HAWT). Blade tip simulations were made with each code and were compared to rotational wind data taken from the Howden-330 kW HAWT. The PNL Rotational Code was given an overall rating of satisfactory for large wind turbine applications and an overall rating of good for small wind turbine applications. The PNL Simulation Code was given a rating of good when used with large turbines and a rating of very good when used with small turbines. The Holley Code and the Sandia Code were given ratings of good and satisfactory, respectively, for both large and small wind turbine applications. The Sandia Code could be upgraded if documentation were made available. Further upgrades for any of the codes would require major revision. DOE

N90-10474# Midwest Research Inst., Golden, CO. Solar Energy Research Inst.
ALTERNATIVE FABRICATION TECHNIQUES FOR HIGH-EFFICIENCY CuInSe2 AND CuInSe2-ALLOY FILMS AND CELLS
A. Rockett, T. C. Lommasson, and H. Talieh Jul. 1989 45 p Prepared in cooperation with Illinois Univ., Urbana
(Contract DE-AC02-83CH-10093)
(DE89-009451; SERI/STR-211-3539) Avail: NTIS HC A04/MF A01

This report, the first annual technical progress report for this project, covers the period from November 30, 1987 through December 31, 1988. Results of recent experiments characterizing CuInSe sub 2 deposited by reactive magnetron sputtering and by a hybrid sputtering and evaporation technique are presented. Both techniques produce films with chemical and structural properties comparable with those commonly accepted for polycrystalline CuInSe(sub 2) used in solar cells. Transmission electron microscopic analysis of the films produced by the reactive sputtering and hybrid techniques were found to be generally similar to those fabricated by three-source evaporation in terms of microstructure, composition, lattice-defect structure, and compositional uniformity. DOE

N90-10475# Sandia National Labs., Albuquerque, NM.
UNITED STATES PHOTOVOLTAIC CONCENTRATOR TECHNOLOGY PROCESS AND NEW PROGRAM INITIATIVE
J. L. Chamberlin and E. C. Boes 1989 5 p Presented at the 9th European Photovoltaic Solar Energy Conference and Exhibition, Freiburg, Fed. Republic of Germany, 25-29 Sep. 1989
(Contract DE-AC04-76DP-00789)
(DE89-013812; SAND-89-0339C; CONF-890925-1) Avail: NTIS HC A01/MF A01

We are continuing to see significant progress in the development of photovoltaic (PV) concentrator technology in the USA. This paper briefly summarizes the most significant developments which have occurred in the past 18 months, including descriptions of PV concentrator module development activities, PV concentrator array

installations, concentrator cell research progress, results of the latest costing studies, and plans for a Concentrator Initiative Program. DOE

N90-10476# Sandia National Labs., Albuquerque, NM. Solar Thermal Collector Technology.
STRETCHED-MEMBRANE HELIOSTATS FOR SOLAR CENTRAL-RECEIVER POWER PLANTS
Daniel J. Alpert and Richard M. Houser 1989 12 p
(Contract DE-AC04-76DP-00789)
(DE89-016034; SAND-89-0839C; CONF-890836-8) Avail: NTIS HC A03/MF A01

For more than 10 years, the U.S. Department of Energy's Solar Thermal Program has pioneered the development of heliostats, mirrors that track the sun, for solar central-receiver power plants. The field of heliostats is the single most expensive part of such plants, so their cost must be as low as possible for the technology to be commercially successful. Recent efforts have focused on the development of heliostats that use stretched-membrane reflectors in place of the more familiar glass mirrors. In a stretched-membrane heliostat, metal foils are stretched over both sides of a large-diameter metal ring. The reflective surface is a silvered-polymer film glued to the front membrane. A slight vacuum in the space between the two membranes is actively controlled to provide a concave, focused contour to the mirror, and in an emergency this space can be rapidly pressurized to defocus it. Because of their simplicity and lighter weight, stretched-membrane heliostats have the potential to cost significantly less than current glass-mirror designs. The first 50-m(sup 2) mirror modules, built under contract to Sandia in 1986, demonstrates that the optical performance of membrane heliostats would be at least as good as heliostats using glass mirrors. DOE

N90-10153*# National Aeronautics and Space Administration. Langley Research Center, Hampton, VA.
STRUCTURAL CONCEPTS FOR VERY LARGE (400-METER-DIAMETER) SOLAR CONCENTRATORS
Martin M. Mikulas, Jr. and John M. Hedgepeth (Astro Aerospace Corp., Carpinteria, CA.) *In its* Second Beamed Space-Power Workshop Jul. 1989 p 239-257 (For primary document see N90-10140 01-20)
Avail: NTIS HC A19/MF A03 CSCL 10A

45 ENVIRONMENT POLLUTION

Includes atmospheric, noise, thermal, and water pollution.

N90-10477 California Inst. of Tech., Pasadena.
PAPER 1. IMPACT OF VOLCANIC AEROSOLS ON STRATOSPHERIC CHEMISTRY. PAPER 2. O2 (1 SIGMA G +) AND O2 (1 DELTA G) IN THE H + O2 REACTION SYSTEM. PAPER 3. BAROTROPIC INSTABILITY OF ZONAL JETS ON MARS, EARTH AND VENUS Ph.D. Thesis
Diane Vera Michelangeli 1989 171 p
Avail: Univ. Microfilms Order No. DA8901776

In the first paper, consequences of the eruption of the El Chichon volcano on the Earth's stratospheric chemistry were studied. A one-dimensional radiative transfer model shows that the total radiation changes because of efficient scattering volcanic aerosols. The photolysis rates obtained from a one-dimensional photochemical model vary consistently with the total radiation changes. When a temperature perturbation is added, ozone decreases by 7 percent, and hydrochloric acid increases by 10 percent at 24 km. Direct injections of Cl2, HCl, and H2O into the stratosphere were investigated. Possible important heterogeneous reactions involving the aerosols were also evaluated. All results are compared to observations and are of general interest because of the relation to the Antarctic ozone hole problem. In the second paper, the generation of metastable O2 (1 sigma g +) and O2 (1 delta g) in the H + O2 system of reactions was studied by the flow discharge chemiluminescence detection method. The rate constants for the quenching of O2 (1 delta g +) by H and H2 were determined to be 5.1 + or - 1.4 x 10(-13) and 7.1 + or - 0.1 x 10(-13) cu cm/sec, respectively. An upper limit for the branching ratio to produce O2 (1 sigma g +) by the H + HO2 reaction was deduced from the experiments to be 2.1 percent. The contributions from other reactions producing singlet oxygen were investigated. In the third paper, a linearized nondivergent barotropic vorticity model is used to intercompare the fastest growing, barotropically unstable wave modes computed for zonal jets at high latitudes in the middle atmospheres of Venus, Earth, and Mars. For each of these planets, wave patterns were detected in the thermal radiance field in the vicinity of the zonal jets. For the terrestrial wintertime stratosphere and for Venus, these observed waves have characteristics similar to those computed for the fastest growing barotropic modes. For Mars, it is found that such modes would have zonal wavenumbers 1 or 2, with e-folding times of 2 to 3 days and periods of 0.75 to 2.5 days; the longer period, k = 2 equatorward mode would dominate for the faster and narrower zonal jets. Dissert. Abstr.

N90-10478*# National Aeronautics and Space Administration. John F. Kennedy Space Center, Cocoa Beach, FL.
CHARACTERIZATION AND EVALUATION OF ACID RAIN IN EAST CENTRAL FLORIDA FROM 1978 TO 1987: TEN YEAR SUMMARY REPORT
Brooks C. Madsen, Thomas W. Dreschel, and C. Ross Hinkle (Bionetics Corp., Cocoa Beach, FL.) Jan. 1989 42 p
(Contract NAS10-10285)
(NASA-TM-102149; NAS 1.15:102149) Avail: NTIS HC A03/MF A01 CSCL 13B

Rainfall was collected on the University of Central Florida (UCF) campus near Orlando since July 1977 and at the Kennedy Space Center (KSC), Florida since August 1977. Since November 1983, the KSC site has been affiliated with the National Atmospheric Deposition Network. Annual volume weighted pH was slightly above the 10 year mean of 4.58 during four of the past five years. Nitrate concentrations have risen somewhat during recent years while excess sulfate concentrations have remained below the 10 year mean during four of the past years. These observations hold for both the UCF and KSC data. The distribution of individual sample pH was nearly identical at UCF and KSC. Stepwise regression suggests that sulfate, nitrate, ammonium ion, and calcium play major roles in the description of rainwater acidity. Annual acid deposition and annual rainfall have varied from 30 to 50 meq/m2-yr and 100 to 180 cm/yr, respectively. Sea salt comprises about 25 percent (UCF) and greater than 50 percent (KSC) of total ionic composition. Author

N90-10479*# Environmental Research Inst. of Michigan, Ann Arbor. Advanced Concepts Div.
SPATIAL CHARACTERIZATION OF ACID RAIN STRESS IN CANADIAN SHIELD LAKES Final Report
F. J. Tanis and E. M. Marshall Mar. 1989 176 p
(Contract NAS5-28779)
(NASA-CR-183446; NAS 1.26:183446; E-189400-39-F) Avail: NTIS HC A09/MF A01 CSCL 13B

The lake acidification in Northern Ontario was investigated using LANDSAT TM to sense lake volume reflectance and also to provide important vegetation and terrain characteristics. The purpose of this project was to determine the ability of LANDSAT to assess water quality characteristics associated with lake acidification. Results demonstrate that a remote sensor can discriminate lake clarity based upon reflection. The basic hypothesis is that seasonal and multi-year changes in lake optical transparency are indicative of sensitivity to acidic deposition. In many acid-sensitive lakes optical transparency is controlled by the amount of dissolved organic carbon present. Seasonal changes in the optical transparency of lakes can potentially provide an indication of the stress due to acid deposition and loading. Author

N90-10480# National Center for Atmospheric Research, Boulder, CO. Atmospheric Chemistry Div.
STUDY OF THE NO3 RADICAL DECOMPOSITION REACTION AND THE N2O5 IN EQUILIBRIUM WITH NO3 + NO2 EQUILIBRIUM CONSTANT Final Report
James A. Davidson, Christopher A. Cantrell, and Richard E. Shetter 1989 97 p Sponsored by Coordinating Research Council, Inc., Atlanta, GA
(PB89-208961; CRC-APRAC-AP-17) Avail: NTIS HC A05/MF A01 CSCL 13B

A determination was made of several important spectroscopic and thermodynamic properties of three oxides of nitrogen which are important in atmospheric chemistry, NO2, NO3 and N2O5. In the first phase, a redetermination was made of the absorption cross sections of NO2 (visible and ultraviolet regions), NO3 (visible region), and N2O5 (infrared regions), the effects of temperature, concentration of gas and instrument resolution on the cross sections were determined. The new cross section data were used in the second phase of the study in the redetermination of the equilibrium constant for N2O5 dissociation: N2O5 greater than NO33 + NO2. The first studies designed to measure the apparent first order decay of the NO3 radical shed new light on the several conflicting results related to these parameters, and allow a clearer choice of reliable data for use in the simulation of the atmospheric chemistry of the oxides of nitrogen and in the prediction of reasonable control strategies for these oxides. GRA

N90-10481# National Oceanic and Atmospheric Administration, Silver Spring, MD. Air Resources Lab.
THE SUITABILITY OF DIFFUSION AND WIND-FIELD TECHNIQUES FOR AN EMERGENCY-RESPONSE DISPERSION MODEL
Richard M. Eckman and Ronald J. Dobosy (Atmospheric Turbulence and Diffusion Lab., Oak Ridge, TN.) Apr. 1989 38 p
(PB89-190219; NOAA-TM-ERL-ARL-171) Avail: NTIS HC A03/MF A01 CSCL 13B

Most atmospheric dispersion models have two separate components: a diffusion component that simulates the dilution of a contaminant by turbulence, and a wind-field component that transport the contaminant away from the source. Many modeling techniques were developed for each of these components. The suitability of these modeling techniques was examined for a near-field emergency response model that must simulate the dispersion of a hazardous contaminant out to several kilometers from a source. For an emergency response model that must provide real-time dispersion estimates (a Class A model), a puff model is the most appropriate diffusion technique, and simple interpolation is the most appropriate wind-field technique. For more-complex models that are used for emergency planning and post-accident assessments (Class B models), a puff model is still suitable, but the wind-field technique should be able to remove spurious velocity divergence and channel the wind flow in complex terrain. GRA

N90-10482# Oak Ridge National Lab., TN. Energy Div.
INTERNATIONAL IMPACTS OF GLOBAL CLIMATE CHANGE: TESTIMONY TO HOUSE APPROPRIATIONS SUBCOMMITTEE ON FOREIGN OPERATIONS, EXPORT FINANCING AND RELATED PROGRAMS
W. Fulkerson, R. M. Cushman, G. Marland, and S. Rayner 21 Feb. 1989 11 p
(Contract DE-AC05-84OR-21400)
(DE89-014004; ORNL/TM-11184) Avail: NTIS HC A03/MF A01

International impacts of global climate change are those for which the important consequences arise because of national sovereignty. Such impacts could be of two types: (1) migrations across national borders of people, of resources (such as agricultural productivity, or surface water, or natural ecosystems), of effluents, or of patterns of commerce; and (2) changes to the way nations use and manage their resources, particularly fossil fuels and forests, as a consequence of international concern over the global climate. Actions by a few resource-dominant nations may affect the fate of all. These two types of international impacts raise complex equity issues because one nation may perceive itself as gaining at the expense of its neighbors, or it may perceive itself as a victim of the actions of others. DOE

N90-10483# University Coll., Galway (Ireland).
INTERNATIONAL CONFERENCE ON AEROSOLS AND BACKGROUND POLLUTION ABSTRACTS
15 Jun. 1989 111 p Conference held in Galway (Ireland), 3-15 Jun. 1989
(Contract DAJA45-89-M-0053)
(AD-A210970; R/D-6061-EN-02) Avail: NTIS HC A06/MF A01 CSCL 04/2

Abstracts of papers presented at the conference are given. Session topics includes: Aerosol climatology; MariMarine aerosols; Properties of aerosols -- chemical, physical, carbonaceous, and optical; Transport, scavenging and deposition -- Transport and dispersal of aerosols, vertical and horizontal. GRA

46 GEOPHYSICS

Includes aeronomy; upper and lower atmosphere studies; ionospheric and magnetospheric physics; and geomagnetism.

For space radiation see *93 Space Radiation.*

N90-10484# Coast Guard, Groton, CT. Research and Development Center.
ATMOSPHERIC TRANSMISSIVITY UPDATE - 1988 Final Interim Report
Michael R. Wroblewski, Marc B. Mandler, and Miles A. Millbach Oct. 1988 65 p
(AD-A209130; CGR/DC-22/88; USCG-D-07-89) Avail: NTIS HC A04/MF A01 CSCL 04/1

The Coast Guard uses atmospheric visibility data collected in 1958 and 1959 when calculating the effective luminous range of aids to navigation. Presently, Coast Guard aid designers question whether or not increases in population and industry have changed atmospheric visibility along our coasts. Recent atmospheric visibility data in the form of transmissivity curves are presented to answer this question. National Weather Service (NWS) visibility records from the maritime zone form the basis for the study. Data from these records were sorted into 28 geographical zones. Curves were fit to frequency distributions within each zone, forming new atmospheric transmissivity curves, one for each zone. The new and old transmissivity curves differ considerably in many regions. The old transmissivity curves should not be used to estimate atmospheric conditions. Further study has shown that even the new transmissivity curves can be improved. Accurate, localized curves can be obtained by decreasing the area size to the limit that the NWS data will allow. It is recommend that the Coast Guard accept small, localized regions for calculating transmissivity curves. In addition, software needs to be developed which uses new localized curves and that aid design tables and calculations. This product would remove the need for the look up tables and tedious computations presently used during aid design. GRA

N90-10485# Pacific Northwest Labs., Richland, WA.
AN ANISOTROPIC SHADOWBAND CORRECTION FOR PARAMETERIZED SKY CONDITIONS AND GEOMETRY
B. A. LeBaron, J. J. Michalsky, and R. Perez (State Univ. of New York, Albany.) Mar. 1989 15 p Presented at the American Solar Energy Society Annual Meeting, Denver, CO, 19-23 Jun. 1989
(Contract DE-AC06-76RL-01830)
(DE89-014916; PNL-SA-16848; CONF-890610-5) Avail: NTIS HC A03/MF A01

A model is presented that corrects the horizontal diffuse irradiance measured using a polar-axis design shadowband. Ratios of true diffuse to uncorrected diffuse measurements are binned and averaged according to parameters describing the associated geometric screening and current sky conditions. The screening parameter is a geometric calculation for the amount of the sky

hemisphere eclipsed by the band. The sky condition parameters account for the anisotropic distribution of the diffuse irradiance across the sky hemisphere. An independent set of uncorrected diffuse data corrected using this parameterization technique has a root mean square error of 6.8 W/sw m and a regression slope of 0.99. Since the correction ratios are developed from parameters that are not site specific, the model should be generally applicable. DOE

N90-10486 Washington Univ., Seattle.
PLASMA WAVES IN THE EARTH'S FORESHOCK, BOW SHOCK, AND MAGNETOSHEATH Ph.D. Thesis
Terrance George Onsager 1988 137 p
Avail: Univ. Microfilms Order No. DA8911645

A detailed analysis is given of electrostatic waves in the earth's foreshock, bow shock, and magnetosheath. The wave modes measured in these regions, the possible generation mechanisms, and the process which drive the plasma to its unstable state are investigated. The measurements used here were obtained from the plasma wave receiver, the particle instrument, and the magnetometer on board the Active Magnetospheric Particle Tracer Explorer (AMPTE) Ion Release Module (IRM). Electron beam mode waves have been identified in the earth's foreshock. A technique is developed which allows the rest frame frequency and wave number of the electron beam mode waves to be determined from the measurements. The experimentally determined values are compared with theoretical predictions, and approximate limits are put on the beam temperatures. It is demonstrated that electrostatic waves are present in the bow shock and magnetosheath with frequencies above the maximum frequency for Doppler shifted ion acoustic waves, yet below the Langmuir frequency.
Dissert. Abstr.

N90-10487# Kiruna Geophysical Inst. (Sweden).
KIRUNA GEOPHYSICAL DATA: DATA SUMMARY 88/7-9, JULY - SEPTEMBER 1988
Bo Thelin 1989 41 p
(PB89-210249) Avail: NTIS HC A03/MF A01 CSCL 04A

Kiruna geophysical data is a collection of results of ground-based more or less continuous measurements of upper atmosphere variables carried out at Swedish Institute of Space Physics. The data is to present current geophysical data related to polar upper atmospheric conditions. GRA

N90-10488# Atmospheric and Environmental Research, Inc., Cambridge, MA.
A STUDY OF THE IMPACT OF SIMULATED SATELLITE LIDAR WIND OBSERVATIONS
R. N. Hoffman, J.-F. Louis, T. Nehrkorn, M. Mickelson, and R. Isaacs 30 Mar. 1989 85 p
(Contract F19628-86-C-0141)
(AD-A210430; AFGL-TR-89-0094; SR-7) Avail: NTIS HC A05/MF A01 CSCL 04/1

Observing system simulation experiments (OSSEs) are conducted to assess the impact of a space borne Doppler wind lidar sensor. Analyzed and forecast meteorological fields are greatly improved by the addition of the lidar wind profiles. The greatest impacts are in the Southern Hemisphere height and wind fields and the tropical wind fields. In order to calibrate the OSSE results, comparisons are made with real data observing system experiments (OSEs). These comparisons indicate that the expected impact of an actual lidar with the stated geographic coverage (equivalent to that of the current operational temperature sounders) and error characteristics (random, 1 m/s rms) would improve forecasts by approximately 36 hours in the Southern Hemisphere. GRA

N90-10489# Massachusetts Inst. of Tech., Cambridge. Dept. of Earth Atmospheric and Planetary Sciences.
ONR/NORDA WORKSHOP ON TERRAIN ANALYSIS AND QUANTITATIVE GEOMORPHOLOGY
Thomas H. Jordan 12 Jul. 1989 13 p Workshop held in Cambridge, MA, 5-7 Apr. 1988
(Contract N00014-88-J-1132)
(AD-A210464) Avail: NTIS HC A03/MF A01 CSCL 08/3

The purpose of the workshop on terrain analysis and quantitative geomorphology was to assess methods for the quantification and analysis of seafloor morphology, to examine their application to acoustic scattering problems, and to evaluate future research directions and needs. A broader goal was to foster cooperation among investigators and minimize the redundancy in Navy-sponsored research projects. This report summarizes the results of the workshop and makes recommendations regarding future research. GRA

N90-10490# Aerospace Corp., El Segundo, CA. Lab. Operations.
THE AURORAL ENERGY DEPOSITION OVER THE POLAR IONOSPHERE DURING SUBSTORMS
B.-H. Ahn, H. W. Kroehl, Y. Kamide, D. J. Gorney, and S.-I. Akasofu (Alaska Univ., Fairbanks.) 15 Jun. 1989 44 p
(Contract F04701-85-C-0086)
(AD-A210522; SD-TR-89-43) Avail: NTIS HC A03/MF A01 CSCL 04/1

The global Joule heating distributions are estimated through the magnetogram inversion method. This study employs instantaneous ionospheric conductance distributions deduced from the DMSP-F6 bremsstrahlung X-ray image data. Also estimated from the X-ray data are instantaneous global particle heating distributions. The two heating distributions thus obtained allow us to investigate various aspects of heat energy processes over the polar ionosphere on an instantaneous basis. A special emphasis is placed on their spatial and temporal behaviors. Several important results of this study are summarized as follows: (1) Regions of significant Joule heating are closely associated with the auroral electrojets prominently in the dawn and dusk sectors. (2) The major Joule heating usually occurs poleward of the major particle heating region, particularly in the morning sector. On the other hand, the two heating patterns are complementary in the longitudinal direction. (3) There is a higher correlation between the global Joule heating rate (U sub J) and AE(12) than between the global particle heating rate (U sub A) and AE(12). (4) The particle heating rate tends to be more prominent during the maximum phase of substorms and afterward than during the pre-expansion phase. (5) The U sub J/U sub A ratio varies by more than a factor of 10, suggesting the wide variability in the relative importance of the two heating rates. GRA

47 METEOROLOGY AND CLIMATOLOGY

Includes weather forecasting and modification.

N90-10491# National Oceanographic Data Center, Washington, DC.
MARINE WEATHER LOG, VOLUME 32, NUMBER 3, SUMMER 1988 Quarterly Report
Richard M. DeAngelis, ed. 1988 78 p
(PB88-248075) Avail: NTIS HC A05/MF A01 CSCL 04B

This Marine weather log includes articles on: (1) ships, shores and tsunamis; (2) tornadoes; (3) ship weather report collection (marine observations program); (4) tips to the radio officer; and (5) marine weather review logs for the North Atlantic and North Pacific oceans for January, February and March, 1988. K.C.D.

N90-10492# National Weather Service, Fort Worth, TX. Scientific Services Div.
FORECASTING CONVECTION WITH THE AFOS (AUTOMATION OF FIELD OPERATIONS AND SERVICES) DATA ANALYSIS PROGRAMS. (ADAP-VERSION 2.0) (AFOS DATA ANALYSIS PROGRAMS-VERSION 2.0)
Phillip D. Bothwell Mar. 1988 141 p
(PB89-145940; NOAA-TM-NWS-SR-122) Avail: NTIS HC A07/MF A01 CSCL 04B

Thunderstorm forecasting with the AFOS data analysis program (ADAP-version 2) is presented. The instability indices, cap strength,

surface moisture, pressure changes, and station change charts of the ADAP program are discussed. Warm and cold advection and surface streamlines/wind vector plots are also discussed. Forecasting convection with the ADAP decision tree is covered in detail. Three case studies are presented to illustrate the ADAP program. K.C.D.

N90-10493# National Severe Storms Lab., Norman, OK.
NATIONAL SEVERE STORMS LABORATORY, FISCAL YEAR 1988 Annual Report
Dec. 1988 50 p
(PB89-156145) Avail: NTIS HC A03/MF A01 CSCL 04B

The National Severe Storms Laboratory conducts a broad program of research to develop a basic understanding of severe weather phenomena, including the large and mesoscale environments that evolve and interact to produce intense storms. Research is focused upon observational and theoretical studies of hazardous, middle lattitude weather phenomena such as tornadoes, hailstorms, lightning, windstorms, floods and blizzards. Sophisticated numerical models are employed as research tools. Programs of the NSSL are discussed. A description of facilities and a listing of FY 1988 publications are included. K.C.D.

N90-10494# National Oceanic and Atmospheric Administration, Boulder, CO. Air Resources Lab.
GEOPHYSICAL MONITORING FOR CLIMATIC CHANGE NUMBER 16 Summary Report, 1987
Barry A. Bodhaine, ed. and Rita M. Rosson, ed. Dec. 1988 140 p
(PB89-159628) Avail: NTIS HC A07/MF A01 CSCL 04B

Research on the geophysical monitoring for climatic change includes observatory reports and reports from the following groups: (1) aerosols and radiation monitoring; (2) carbon cycle; (3) trace gas monitoring; (4) acquisition and data management; (5) station climatology; (6) air quality; and (7) nitrous oxide and halocarbons. Work on the alkaline aerosols program (dust emissions modeling) and the Arctic gas and aerosol sampling program (springtime tropospheric ozone destruction in the high Arctic) is also reported. Cooperative programs are also discussed. K.C.D.

N90-10495# HSS, Inc., Bedford, MA.
A PROGRAM TO IMPROVE PERFORMANCE OF AFGL (AIR FORCE GEOPHYSICAL LABORATORY) AUTOMATED PRESENT WEATHER OBSERVING SENSORS Final Report, 2 Apr. 1985 - 31 May 1988
D. F. Hansen, W. K. Shubert, and D. R. Rohleder 1 Aug. 1988 110 p
(Contract F19628-86-C-0061; AF Proj. 2688)
(AD-A207669; HSS-B-169; AFGL-TR-88-0329) Avail: NTIS HC A06/MF A01 CSCL 04/2

Under a prior Air Force (AFGL) program two prototype Automated Present Weather Sensors were developed. The present program supported hardware and software upgrades to those sensors which were intended to achieve two objectives. The first and primary objective was to improve the performance capability of the sensors to meet the performance specifications of the NWS-ASOS and FAA-AWOS automated present weather observing systems. The second objective was to provide additional sensor capabilities beyond those required for ASOS/AWOS systems, which would be of value in Air force applications of present weather sensors. Tests made on the sensors after the upgrades were performed, demonstrated their capability to now meet three of the four basic requirements for ASOS/AWOS present weather sensors, namely: (1) precipitation detection; (2) false alarm rate; and (3) precipitation identification. Their ability to meet the fourth requirement; i.e., rainrate accuracy, could not be verified for lack of adequate reference standards. GRA

N90-10496# Naval Postgraduate School, Monterey, CA.
THERMODYNAMIC AND DYNAMIC PROCESSES IN THE UPDRAFT REGION OF GALE (GENESIS OF ATLANTIC LOWS EXPERIMENT) IOP (INTENSIVE OBSERVATION PERIOD) 9 M.S. Thesis
Dianne K. Crittenden Mar. 1989 55 p
(AD-A208139) Avail: NTIS HC A04/MF A01 CSCL 04/2

A detailed diagnostic examination of the warm frontal region ahead of the surface cyclone in Intensive Observation Period (IOP) 9 of the Genesis of Atlantic Lows Experiment (GALE) is conducted. Data consists of normal synoptic observations and special GALE observations, analyzed by the Navy Operational Regional Analysis and Predictions System (NORAPS), which uses optimal interpolation. These analyses are enhanced by hand drawn fronts and cloud outlines from Geostationary Operational Environmental Satellite (GOES) imagery. Symmetric stability is evaluated on cross sectional analyses of pseudo-absolute momentum and equivalent potential temperature, and reveal conditions of moist symmetric neutrality in the warm frontal region. The planetary boundary layer theta budget is examined to determine what processes heated and moistened the region. Surface heat and moisture fluxes were found to contribute to significant theta increases only in the early stages of development. Upper level divergence and surface frontogenesis are studied to determine their contributions to forcing the warm frontal updraft. Results indicate that during the period of explosive development, upper level forcing was unfavorable for development. Low level frontogenetical forcing in the presence of symmetric neutrality was found to be strong enough to oppose this negative upper level forcing to force rapid development. GRA

N90-10497 Illinois Univ. at Urbana-Champaign, Savoy.
NUMERICAL SIMULATIONS OF A MIDLATITUDE SQUALL LINE Ph.D. Thesis
Robert Gerard Fovell 1988 225 p
Avail: Univ. Microfilms Order No. DA8908683

A two-dimensional, nonhydrostatic cloud model was used in attempts to numerically replicate the observed structure of a typical mid-latitude squall line. Basic simulations were made using common temperature and moisture profiles in the vertical, and emphasis was placed on varying the microphysics and the vertical wind shear. The temperature and moisture profiles chosen were adapted from the environmental conditions which were present prior to the development of the 22 May 1976 Oklahoma squall line and were typical of environments which supported severe springtime convection in that area. The model storms described herein were all similar in that they organized themselves into long-lasting mature states marked by behavior which was more or less multicellular, depending on the strength of the wind shear. Each storm persisted through the production of new cells at the leading edge of the storm, over the storm's gust front. This production proceeded in a quite regular manner in virtually every case, although specific details such as the length and composition of the repeat cycle and the total precipitation produced were sensitive to the microphysics and the strength of the vertical wind shear. However, each of the model storms appear to have achieved a very long-lasting, quasi-equilibrium state; the only major exceptions to this were among the smallest shear cases where random influences were more apparent. The incorporation of ice processes into the microphysics resulted in the production of more horizontally extensive storms which possessed estimated radar reflectivity fields which were more realistic in appearance. Increasing the vertical wind shear had the effect of producing narrower, more intense model storms which propagated more quickly. The response of the model convection to increasing wind shear was considered within the context of recent ideas concerning the vorticity dynamics of actual squall lines. Dynamically, however, all of the model storms were quite similar as there were general features which were common to all of the runs. Dissert. Abstr.

N90-10498# National Weather Service, Silver Spring, MD. Office of Hydrology.
EXTREME HURRICANES IN THE NINETEENTH CENTURY Final Report
Francis P. Ho Mar. 1989 144 p
(Contract EMW-84-E-1589)

(PB89-201305; NOAA-TM-NWS-HYDRO-43) Avail: NTIS HC A07/MF A01 CSCL 04B

This report provides available meteorological information pertinent to coastal flooding risk assessment of severe hurricanes in the nineteenth century. Pertinent hurricane parameters included are: the central pressure, the radius of maximum winds, and the direction and speed of the storm's forward motion. The report also gives brief discussions of available data and informative newspaper accounts of individual hurricanes which helped in determining the hurricane track and the point of landfall. Author

N90-10499# National Weather Service, Kansas City, MO. Central Region.

A CASE STUDY EVALUATION OF SATELLITE-DERIVED RAINFALL ESTIMATES AND THEIR APPLICATION TO NUMERICAL MODEL PRECIPITATION FORECAST VERIFICATION

Glenn A. Field (National Weather Service, Milwaukee, WI.) May 1989 84 p

(Grants NSF ATM-80-05369; NSF ATM-85-14730)

(PB89-194591; NOAA-TM-NWS-CR-96) Avail: NTIS HC A05/MF A01 CSCL 04B

Satellite-derived precipitation estimates are computed and then evaluated using a dense network of cooperative observer rain gauge reports as the verification. The feasibility of using these satellite rainfall estimates to evaluate numerical model precipitation forecasts is investigated. The correspondence between the numerical model forecast and the observations also is assessed. The satellite rainfall estimates are produced every half hour for the 24-hour period starting 1200 GMT, July 20, 1981. More than 300 cooperative observer rain gauge observations made during the same time period as the estimates are compiled. The numerical model evaluated is an Australian mesoscale model referred to as the Subsynoptic Scale Model (SSM). Its 24-hour precipitation forecast is examined for the same time period as the satellite estimates and ground-based observations. GRA

N90-10500# National Oceanic and Atmospheric Administration, Silver Spring, MD. Air Resources Lab.

METEOROLOGICAL SUPPORT: DESCRIPTIONS OF APPLICATION PROGRAMS FOR ACCESSING AND DISPLAYING DATA

Glenn D. Rolph and Barbara J. B. Stunder Mar. 1989 74 p

(PB89-194625; NOAA-TM-ERL-ARL-169) Avail: NTIS HC A04/MF A01 CSCL 04B

Programs for accessing and displaying meteorological data are described. Surface and upper-air observations and model-tenerated forecast data may be accessed. Step-by-step procedures and examples are provided for each application program. Brief descriptions of air-parcel trajectory models are also included. Most of the programs require access to the NAS 9000 computer in Suitland, MD. Meteorological data for these programs are provided by NOAA's National Meteorological Center in Camp Springs, MD. Author

N90-10501# National Weather Service, Silver Spring, MD.

RESEARCH HIGHLIGHTS OF THE NMC (NATIONAL METEOROLOGICAL CENTER) DEVELOPMENT DIVISION: 1987-1988

Mar. 1989 243 p

(PB89-206478) Avail: NTIS HC A11/MF A02 CSCL 04B

During 1987 and 1988, the forecast products of the National Meteorological Center (NMC) continued to improve. Two initiatives have been undertaken to increase the interaction between university investigators and NMC scientists. In 1984, NMC established a visiting scientist program through the University Corporation for Atmospheric Research (UCAR). More recently, a second program has been established jointly with the National Science Foundation to support academic research in numerical weather prediction and to foster collaborative research between university and NMC scientists, using NMC facilities. Several major changes have been implemented into the operational models and analysis procedures in the past two years. The document summarizes these changes and the research highlights of the NMC Development Division in the following three areas: regional modeling, global modeling, and marine products. A summary of the NMC Workshop on Operational Numerical Weather Prediction Systems of the Future, held in early March 1988, is presented. Some current developments are discussed and the near-term future plans are also outlined. Author

N90-10502# Sandia National Labs., Albuquerque, NM.

DATA PROCESSING IN LIGHTNING WARNING SYSTEMS

Thomas S. Edrington 1989 13 p Presented at the International Conference on Lightning and Static Electricity, Bath, England, 26-28 Sep. 1989

(Contract DE-AC04-76DP-00789)

(DE89-012495; SAND-89-1161C; CONF-8909124-1) Avail: NTIS HC A03/MF A01

Rata from an array of sixteen electric-field sensors have been used to evaluate the potential benefits to lightning warning systems of processing old data as well as data from off-site sensors. These specific topics are approached from a broad decision-theoretic viewpoint. DOE

N90-10503# Naval Air Systems Command, Washington, DC.

US NAVY REGIONAL CLIMATIC STUDY OF THE UNITED STATES ATLANTIC COAST AND ASSOCIATED WATERS

Jan. 1989 542 p

(AD-A210198; NAVAIR-50-1C-555) Avail: NTIS HC A23/MF A03 CSCL 04/2

This climatic study consists of monthly charts and tables of: (1) clouds; (2) precipitation; (3) visibility tables; (4) ceiling visibility (mid-range/low range); (5) wind visibility cloudiness; (6) scalar mean wind speed; (7) wind speed less than 11 and greater or equal to 34 knots; (8) wind speed 11-21 and 22-33 knots; (9) surface wind roses; (10) air and sea temperature; (11) wave height isopleths, (12) wave height tables; and (13) surface currents (seasonal). GRA

N90-10504# Atmospheric and Environmental Research, Inc., Cambridge, MA.

A STUDY OF THE IMPACT OF SIMULATED 183 GHz WATER VAPOR RETRIEVALS ON NUMERICAL WEATHER PREDICTION

C. Grassotti, R. Isaacs, R. N. Hoffman, J.-F. Louis, T. Nehrkorn, and M. Mickelson 31 Mar. 1989 185 p

(Contract F19628-86-C-0141)

(AD-A210431; AFGL-TR-89-0093; SR-6) Avail: NTIS HC A09/MF A01 CSCL 04/2

Observing system simulation experiments (OSSEs) are conducted to assess the impact of the Special Sensor Microwave 183 GHz (SSM/T-2) water vapor sounder and the associated SSM/T-1 temperature sounder. Analyzed and forecast meteorological fields are improved by the addition of the SSM/T-1,2 temperature and humidity profiles. The greatest impacts occur in the Southern Hemisphere in the scenario when the civilian infrared sounder data are not available, i.e., when TOVS data are not assimilated. To calibrate the OSSE results, comparisons are made with real data observing system experiments (OSEs). These comparisons indicate that the expected impact of adding actual SSM/T-1,2 data with the stated geographic coverage and error characteristics, in the absence of TOVS data, would improve 500 mb height forecasts by approximately 12 hours in the Southern Hemisphere. However adding SSM/T-1,2 would have smaller impacts (8 h or less) in the Southern Hemisphere if added to the available TOVS data. Improvements for 200 mb wind forecasts in the tropics are: 36 hours for SSM/T-1,2 alone and 12 hours for SSM/T-1,2 and TOVS together. Little impact was seen in moisture forecasts from the addition of the SSM data, but moisture and cloud analysis were clearly improved when the SSM data was assimilated; a decrease in global root mean square error of about 5 percent was indicated. GRA

N90-10505*# National Aeronautics and Space Administration. Langley Research Center, Hampton, VA.
THE 1984 DIRECT STRIKE LIGHTNING DATA, PART 1
Mitchel E. Thomas and Harold K. Carney Sep. 1986 512 p
(NASA-TM-87690-Pt-1; NAS 1.15:87690-Pt-1) Avail: NTIS HC A22/MF A03 CSCL 04B

Data waveforms are presented which were obtained during the 1984 direct-strike lightning tests utilizing the NASA F106-B aircraft specially instrumented for lightning electromagnetic measurements. The aircraft was operated in the vicinity of the NASA Langley Research Center, Hampton, Virginia, in a thunderstorm environment to elicit strikes. Electromagnetic field data and conduction currents on the aircraft were recorded for attached lightning. The entire transient recorder data obtained for 247 uses and 11 nearby flashes in the 1984 campaign are presented. This is part 1, consisting of summary and conclusion.
Author

N90-10506*# National Aeronautics and Space Administration. Langley Research Center, Hampton, VA.
THE 1984 DIRECT STRIKE LIGHTNING DATA, PART 2
Mitchel E. Thomas and Harold K. Carney Sep. 1986 474 p
(NASA-TM-87690-Pt-2; NAS 1.15:87690-Pt-2) Avail: NTIS HC A20/MF A03 CSCL 04B

Data waveforms are presented which were obtained during the 1984 direct-strike lightning tests utilizing the NASA F106-B aircraft specially instrumented for lightning electromagnetic measurements. The aircraft was operated in the vicinity of the NASA Langley Research Center, Hampton, Virginia, in a thunderstorm environment to elicit strikes. Electromagnetic field data and conduction currents on the aircraft were recorded for attached lightning. This is part 2, consisting entirely of charts and graphs.
Author

N90-10507*# National Aeronautics and Space Administration. Langley Research Center, Hampton, VA.
THE 1984 DIRECT STRIKE LIGHTNING DATA, PART 3
Mitchel E. Thomas and Harold K. Carney Sep. 1986 364 p
(NASA-TM-87690-Pt-3; NAS 1.15:87690-Pt-3) Avail: NTIS HC A16/MF A03 CSCL 04B

Data waveforms are presented which were obtained during the 1984 direct-strike lightning tests utilizing the NASA F106-B aircraft specially instrumented for lightning electromagnetic measurements. The aircraft was operated in the vicinity of the NASA Langley Research Center, Hampton, Virginia, in a thunderstorm environment to elicit strikes. Electromagnetic field data and conduction currents on the aircraft were recorded for attached lightning. This is part 3, consisting entirely of charts and graphs.
Author

N90-10508# Reading Univ. (England).
COORDINATION OF MESOSCALE METEOROLOGICAL RESEARCH BETWEEN ASL AND EUROPEAN GROUPS Final Report, Mar. 1987 - Mar. 1989
Robert P. Pearce 6 Jul. 1989 39 p
(Contract DAJA45-87-C-0014; DA Proj. 1L1-61102-BH-57)
(AD-A210902; R/D-5735-EN-01) Avail: NTIS HC A03/MF A01 CSCL 04/1

An account of the Mesoscale Panel's activities and a list of its recommendations to Army Atmospheric Science Lab (ASL) is contained. The Panel's work was concentrated into the mesometeorology workshop held at the Risoe National Lab. Roskilde, Denmark, 12th to 15th May, 1987, 2 Panel Meetings (Risoe, 14th to 15th May, Sept. 14th to 16th, 1988. Included are the report of the last Panel Meeting, together with a separate list of its recommendation. Recommendations R1-R9 reflect the Panel's concern with the status and direction of the mesoscale modeling activities at ASL and propose radical changes which must be implemented if the Army's needs are to make effective use of modern developments elsewhere in this rapidly developing area of research. Recommendations R10-R13 relate to the project WIND database and reflect the importance the Panel attaches to making this data as widely and speedily accessible as possible. The excellent work of the field phase now needs to be followed up by exploitation of the data by the wider commitments of atmospheric mesoscale modeling if the Army is to benefit from modelling advances elsewhere and improved predictions of mesoscale phenomena.
GRA

48 OCEANOGRAPHY

Includes biological, dynamic, and physical oceanography; and marine resources.

For related information see also *43 Earth Resources and Remote Sensing.*

N90-10509# National Oceanic and Atmospheric Administration, Rockville, MD. Office of Undersea Research.
BIOCHEMICAL CYCLING AND FLUXES BETWEEN THE DEEP EUPHOTIC ZONE AND OTHER OCEANIC REALMS
Catherine R. Agegian, ed. May 1988 182 p
(PB89-152458; NOAA-RR-NURP-88-1) Avail: NTIS HC A09/MF A01 CSCL 08C

Papers included in this report are the result of a symposium held in December 1986. The symposium was held to reconsider the processes which govern the uptake of carbon dioxide by marine plants and the transport of carbonate and organic carbon particles to the deep sea including: (1) a reassessment of the euphotic zone with respect to the biological and ecological adaptations of marine algae at low irradiance levels; (2) an evaluation of the depth distribution of recycled vs. new primary production in the euphotic zone of oligotrophic ocean waters; (3) an estimation of the importance of new primary production in global biogeochemical cycles of the ocean; and (4) a discussion of the evolutionary change in primary production of reconstructing the physico-chemical history of the euphotic zone over a geologic time scale.
Author

N90-10510# Woods Hole Oceanographic Inst., MA. Coastal Research Center.
COASTAL RESEARCH CENTER WOODS HOLE OCEANOGRAPHIC INSTITUTION Technical Report, Mar. 1986 - Jul. 1988
Bruce W. Tripp Mar. 1989 46 p Sponsored by Richard King Mellon Foundation, Pittsburgh, PA; Andrew W. Mellon Foundation, New York; Oliver S. and Jennie R. Donaldson Charitable Trust, Fall River, MA; and Mobil Foundation, Inc., New York, NY
(PB89-198238; WHOI-89-7; CRC-89-1) Avail: NTIS HC A03/MF A01 CSCL 08C

The activities of the Woods Hole Oceanographic Institution (WHOI) Coastal Research Center during the period of March 1986 to July 1988 are briefly described. Major research activities during this period include: (1) impacts of global climate change on the coastal zone; (2) coastal instrumentation (flumes and current profiler) (3) assimilative capacity of contaminants (e.g. PCB's) by marine organisms; and (4) rapid response (to natural and man caused catastrophes). During this period the Georges Bank book was completed and published.
GRA

N90-10511# Woods Hole Oceanographic Inst., MA.
THE INFLUENCE OF A STEADY BAROCLINIC DEEP OCEAN ON THE SHELF Ph.D. Thesis
M. Ross Vennell Oct. 1988 202 p
(Grant NSF OCE-85-18487)
(PB89-198188; WHOI-88-46) Copyright Avail: NTIS HC A10/MF A02 CSCL 08C

The degree to which a baroclinic deep ocean could be responsible for the mean flow on the shallow continental shelf is examined using steady, boundary forced models which incorporate bottom friction. One set of models, for a vertically well mixed shelf, includes the horizontal advection of density. The second set of models comprises a three-layer model without interfacial friction and a two-layer model with interfacial friction. It is found that near bottom flow has a short cross isobath scale due to the steep continental slope and consequently that the deep oceans

lower water column could not be responsible for the observed mean flow. The cross isobath scale of flow in the upper deep ocean is predominantly determined by the oceans velocity profile. In a barotropic or near barotropic flow the upper water column follows the near bottom flow and therefore has little influence on the shelf. Using oxygen isotope data, Chapman et al. (1986) found that the Scotian shelf is the major source of Mid-Atlantic Bight shelf water. Their barotropic modeling results are extended to show that a baroclinic deep ocean also acts to hold shelf water on the shelf. Author

N90-10512# National Oceanic and Atmospheric Administration, Miami, FL. Oceanographic and Meteorological Labs.
A SEASONAL ISOTHERM DEPTH CLIMATOLOGY FOR THE EASTERN TROPICAL PACIFIC
Donald V. Hansen and Alan Herman Dec. 1988 41 p Revised
(PB89-193577; NOAA-TR-ERL-434; AOML-33) Avail: NTIS HC A03/MF A01 CSCL 08C

A seasonal climatology of the depths of the 10C, 15C, and 20C isotherms in the eastern tropical Pacific is presented. The analyses used Kriging, which is a method for optimal interpolation of data fields. The data set consisted of 10,505 expendable bathythermograph (XBT) and conductivity temperature depth (CTD) stations collected during non-El Nino years. Results are presented on shaded contour maps with values overprinted at 2 degree intervals. The method of analysis also yields an estimate of the uncertainty of each interpolated point. Author

N90-10513# National Environmental Satellite Service, Washington, DC. Marine Environmental Assessment Div.
CHESAPEAKE BAY SURFACE SALINITIES, 1951-88
Michael J. Dowgiallo (National Oceanic and Atmospheric Administration, Washington, DC.) Feb. 1989 34 p
(PB89-194583; NOAA-TM-NESDIS-AISC-15) Avail: NTIS HC A03/MF A01 CSCL 08C

Surface salinities for five National Ocean Service stations around Chesapeake Bay are summarized for the 38 year period 1951 to 1988. Monthly average salinities and long term monthly averages are presented graphically for each station. Departures from normal (1951 to 1980 monthly average) salinities are color coded to highlight the above- and below-normal periods. Salinities were predominantly above normal in the 1960's, below normal in the 1970's, and above normal in the 1980's. The dataset shows such events as the greatly depressed salinities following Tropical Storm Agnes in 1972 and the above normal salinities evident following the dry periods in the 1980's. Author

N90-10514# Woods Hole Oceanographic Inst., MA.
A SEARCH FOR LAYERING IN THE OCEANIC CRUST Ph.D. Thesis
John Anthony Collins Feb. 1989 194 p
(Grants NSF OCE-81-17210; NSF EAR-80-26445; NSF EAR-83-09535; NSF OCE-80-25206; NSF OCE-84-10658; NSF OCE-87-00806)
(PB89-198220; WHOI-89-4) Avail: NTIS HC A09/MF A01 CSCL 08C

In Chapter 1, the geological structures that generate Moho reflections are investigated by calculating synthetic reflection profiles for laterally-varying velocity models appropriate to the fossil crust/mantle boundary exposed in the Bay of Islands Ophiolite. The similarities between the synthetic and observed data suggest that the complicated geological structures that comprise the fossil crust/mantle transition in ophiolites might also be characteristic of the oceanic crust. Analyses of the velocity and reflectivity structure at DSDP Site 504B are presented in Chapters 2 and 3 of the report. In contrast to standard oceanic models, a velocity-depth profile that better explains the observed data is characterized by high velocity gradients in the middle crust, a 1.8 km thick low-velocity zone immediately above Moho, and a total crustal thickness of only 5 km. The MCS data show no conclusive evidence for laterally coherent reflection events generated within the upper 1 to 2 km of the crust. This surprising observation is understandable on inspection of synthetic reflection seismograms calculated for velocity-depth profiles constructed from the logged downhole variations in physical properties. Low-amplitude reflections from the extrusives/sheeted-dike transition are obscured by sediment-column multiples and by source reverberation. Author

N90-10515# Oak Ridge National Lab., TN.
EVALUATION OF THE NORTH ATLANTIC SEASONAL NITROGEN MODEL, VERSION 2
Michael J. R. Fasham 29 Jul. 1989 7 p Prepared in cooperation with Institute of Oceanographic Sciences, Wormley (UK)
(Contract DE-AC05-84OR-21400)
(DE89-016157; ORNL/FTR-3342) Avail: NTIS HC A02/MF A01

The results of version 2 of the three-dimensional North Atlantic Seasonal Nitrogen Model were compared with chlorophyll distributions derived from Coastal Zone Optical Scanner (CZOS) images and found to be in better agreement than the version 1 results. Also, the model gave a more realistic simulation of regenerated primary production, giving a geographically averaged f-ratio of 0.4 compared with 0.78 for version 1. Although the qualitative agreement between the model and data was good, there were areas of significant quantitative disagreement. A number of possible reasons for this were discussed, and future model runs were determined to test these hypotheses. DOE

N90-10516# University of Southern California, Los Angeles. Dept. of Geological Sciences.
SURFACE WAVE RAY TRACING AND Ms:YIELD DETERMINATION IN A LATERALLY HETEROGENEOUS EARTH Final Report, 7 Jan. 1987 - 31 Dec. 1988
Yuehua Zeng, Ta-liang Teng, and Keiiti Aki Feb. 1989 62 p
(Contract F19628-87-K-0018)
(AD-A210241; AFGL-TR-89-0065) Avail: NTIS HC A04/MF A01 CSCL 08/11

Pure path Rayleigh wave group velocities for 24 regional grids inside the Arctic were obtained from 74 mixed path measurements. The vertical shear wave velocity structures under these 24 grids were then determined according to their pure path group velocity dispersion data. This result indicates that the crustal shear wave velocity in the Arctic region is generally lower than the world-wide average. In addition, a typical mid-ocean ridge structure was clearly shown under the Nansen Ridge. An abnormally high upper mantle shear wave velocity was found under the Alpha Ridge and Makarov Basin, and low velocity beneath the Canadian Arctic Islands. In general, the inversion result agrees with the known tectonics in the Arctic region. To further check the validity of the result, synthetic Rayleigh waves were computed; a comparison with the observations shows very good agreement. GRA

N90-10517# Naval Underwater Systems Center, New London, CT. Environmental and Tactical Support Dept.
IFD (IMPLICIT FINITE DIFFERENCE): INTERFACED WITH HARVARD OPEN OCEAN MODEL FORECASTS Summary Report
George Botseas, Ding Lee, and William L. Siegmann (Rensselaer Polytechnic Inst., Troy, NY.) 30 May 1989 27 p
(AD-A210521; NUSC-TR-8367) Avail: NTIS HC A03/MF A01 CSCL 20/1

In 1982, the implicit finite difference (IFD) computer model was developed by Lee and Botseas at NUSC for solving the parabolic wave equation. The IFD model was designed to predict acoustics propagation in both range-dependent and range-independent undersea environments. Given an environment, the IFD model marches the acoustics solution in the water column forward, step-by-step, until maximum range has been reached. The capability to interface the IFD computer model with mesoscale forecasts generated by the Harvard Open Model is announced. Given the latitude and longitude of the source location, the IFD model extracts from the 3-dimensional Harvard data set sound speed profiles encountered in the direction of propagation. Contour plots are set containing both warm- and cold-core eddies in the

vicinity of the Gulf Stream. Acoustic propagation loss through a cold-core eddy is presented. A listing of the subroutine that links IFD with the Harvard data set is included. GRA

N90-10518# Hawaii Univ., Honolulu. Inst. of Geophysics.
SEMI-MONTHLY TEMPERATURE AND GEOPOTENTIAL ANOMALY IN THE UPPER 500 METERS ALONG THE OAHU-FARALLON ISLANDS GREAT CIRCLE FROM NOVEMBER 15, 1967 THROUGH DECEMBER 15, 1979
James M. Price and Dailin Wang May 1989 264 p
(Contract N00014-82-C-0380)
(AD-A210640; AD-E951366; HIG-89-1) Avail: NTIS HC A12/MF A01 CSCL 08/3

Semi-monthly time series of expendable bathythermograph (XBT) observations, objectively mapped onto the great circle arc from Oahu, Hawaii to the Farallon Islands off San Francisco, California are presented. They reveal the temperature structure in the upper 500 meters from November 15, 1967 through December 15, 1979. In addition, sections of geopotential anomalies relative to 5 MPa (5 mega Pascals) derived from the temperature sections and temperature sections and temperature/salinity (T/S) relations are presented. Averages of temperature and geopotential anomalies over the 12 complete years of data coverage, 1968 to 1979, and over each semi-month (i.e., all January 1 sections, all January 15 sections, all February 1 sections, etc.) during the 12-year period accompany the time series. A modest bibliography of articles on other observations of the temperature structure and currents in the North Pacific is included along with a brief discussion of the various topics addressed in the studies referenced. GRA

51 LIFE SCIENCES (GENERAL)

N90-10519# California Univ., Irvine. Laser Inst. and Medical Clinic.
BIOMEDICAL STUDIES WITH THE FREE ELECTRON LASER Final Report, 1 Feb. 1986 - 31 Jan. 1988
Michael W. Berns 15 May 1989 215 p
(Contract N00014-86-K-0115)
(AD-A208927) Avail: NTIS HC A10/MF A02 CSCL 06/7

An electrostatic VandeGraff free electron laser (FEL) was used to study the effects of infrared radiation on the synthesis of DNA and RNA in living vertebrate cells in culture. The laser was operated at wavelengths of 165 and 200 microns at power densities of 0.1 to 30 KW/sq cm. Cells were incubated in radioactive precursors to either DNA or RNA following exposure to the FEL and analyzed by light microscope autoradiography. The results indicated that the 200 micron wavelength inhibited DNA but not RNA synthesis in a subpopulation of cells and the 165 micron wavelength inhibited RNA synthesis and not DNA synthesis. The statistical significance for the 200 micron wavelength studies was $p = 0.05$ and for the 165 micron wavelength studies $p = 0.001$ to 0.005. GRA

N90-10520# Massachusetts Inst. of Tech., Cambridge. Div. of Health Sciences and Technology.
ELECTROPORATION: THEORY OF BASIC MECHANISMS Annual Project Report, 1 Jun. 1988 - 31 May 1989
James C. Weaver 30 Jun. 1989 52 p
(Contract N00014-87-K-0497; RR04108)
(AD-A210196) Avail: NTIS HC A04/MF A01 CSCL 06/1

Electroporation is a dramatic and apparently universal phenomenon which occurs in all bilayer-containing membranes. For this reason electroporation has implications for basic understanding of cell membranes, and is also likely to lead to a number of new applications. A quantitative understanding of how electroporation occurs has been lacking. We report significant progress towards providing descriptions of mechanisms which can quantitatively account for most of the complex electrical behavior of planar bilayer membranes without proteins. This has set the stage for development of models which describe both electrical behavior and molecular transport. In summary form, electroporation is now believed to be a universal cell membrane phenomenon, involving both the lipid bilayer and membrane macromolecules, and is therefore fundamental to membrane understanding, and it provides a general method for introducing molecules into cells, or releasing molecules from cells, with potentially major applications in science and technology. GRA

N90-10521# SRI International Corp., Menlo Park, CA. Dept. of Molecular Biology.
GENETIC ENGINEERING OF SINGLE-DOMAIN MAGNETIC PARTICLES Progress Report, 1 Mar. - 15 Jun. 1989
Nahid S. Waleh 15 Jun. 1989 5 p
(Contract N00014-89-C-0085; RR04106)
(AD-A210332) Avail: NTIS HC A01/MF A01 CSCL 06/13

Magnetotactic bacteria selectively synthesize membrane-bound, nanometer-sized, single-domain magnetic particles known as magnetosomes. Because these bacteria have complex nutritional requirements, only one species, Aquaspirillum magnetotacticum has been grown in pure culture. This bacterium produces approximately twenty intracellular magnetic particles per cell of single-domain size. To synthesize these particles, A. magnetotacticum must possess a highly efficient system(s) to remove iron from the environment. To investigate the mechanism of iron-uptake and the synthesis of magnetic particles in this microorganism, we will construct and screen genomic libraries of A. magnetotacticum for the iron-uptake and magnetosome-synthesizing genes. We will also use the available information on the mechanisms of iron-uptake in other bacteria to identify and characterize analogous systems, related genes, or homologous sequences in this magnetotactic bacterium. We have determined already that the genes of A. magnetotacticum are functionally expressed in E. coli. Furthermore, we have identified in this bacterium a sequence homologous to the tonB gene of E. coli. The tonB gene is known to be required for iron assimilation in enteric bacteria. The long-term goal of this project is to clone the identified genes in suitable host organisms that would make the large-scale, regulated production of single-domain magnetic particles possible. GRA

N90-10522# Oklahoma Univ., Norman. Dept. of Botany and Microbiology.
MOLECULAR BIOLOGY AND PHYSIOLOGY OF METHANOGENIC ARCHAEBACTERIA Annual Report, Jul. 1988 - Jun. 1989
David P. Nagle, Jr., David R. McCarthy, and Ralph S. Tanner 27 Jun. 1989 17 p
(Contract N00014-86-K-0222; RR04106)
(AD-A210399; Rept-89-00014-01) Avail: NTIS HC A03/MF A01 CSCL 06/13

Methane-producing archaebacteria are worthy of their novel biology and potential in anaerobic bioprocessing. The biochemistry, genetics, and molecular biology of the thermophilic autotroph Methanobacterium thermoautotrophicum are studied. DNA from antimetabolite resistant mutant strains was used to transform sensitive recipient cells to resistance, and DNA was cloned into Escherichia coli plasmids. This DNA will be mutated with transposons in the E. coli host, then isolated and used to transform methanogen cells to selectable mutant phenotypes. Mutant strains resistant to purine analogs were used to determine that wild type cells of M. thermoautotrophicum possess an almost complete set of enzymes for uptake, activation, and interconversion of purine bases and nucleosides. These mutants and the information about the pathways will be the basis for generating a genetic map. Metabolic studies of a unique formate auxotroph revealed a new role for this one carbon compound in the anabolic metabolism of this methanogen. GRA

52 AEROSPACE MEDICINE

Includes physiological factors; biological effects of radiation; and effects of weightlessness on man and animals.

N90-10523# Army Research Inst. of Environmental Medicine, Natick, MA.
CONTROL OF THERMOREGULATORY SWEATING DURING EXERCISE IN THE HEAT
Michael N. Sawka, Richard R. Gonzalez, Andrew J. Young, Richard C. Dennis, C. Robert Valeri, and Kent B. Pandolf Oct. 1988 26 p
(Contract N00014-79-C-0168; DA Proj. 3E1-6287-A-879)
(AD-A206001; USARIEM-M4-89) Avail: NTIS HC A03/MF A01 CSCL 06/4

The purposes of this study are to: (1) determine if erythrocyte infusion alters the control of thermoregulatory sweating; and (2) demonstrate how increases and decreases of both plasma tonicity and blood volume influence the thermoregulatory control parameters of threshold temperature and sweating sensitivity. Six non-heat acclimated and five heat acclimated males attempted Heat Stress Tests (HST's) both before and shortly after (48 to 96h) autologous erythrocyte infusion. The non-heat acclimated subjects were euhydrated for both HST's; whereas, the heat acclimated subjects were studied in a euhydrated and a hypohydrated (-5 percent body weight) condition both pre- and post-infusion (500 ml of solution containing approximately 60 percent hct of autologous erythrocytes). The HST's consisted of treadmill exercise (335 W.m) in a hot (35 C, 45 percent relative humidity) environment, and esophageal temperature and local sweating rate were continuously measured during 25 minutes of exercise. These experiments resulted in a matrix of conditions where both plasma tonicity and blood volume were increased or decreased relative to control conditions (euhydration, pre-infusion). The findings concerning thermoregulatory sweating during exercise in the heat are summarized: acute polycythemia will decrease the threshold temperature and increase the sweating sensitivity; and both threshold temperature and sweating sensitivity are increased or decreased from control levels dependent upon the combined influence of plasma tonicity and blood volume; threshold temperature changes are primarily influenced by plasma tonicity, and sweating sensitivity changes are primarily influenced by blood volume. GRA

N90-10524* National Aeronautics and Space Administration, Washington, DC.
AEROSPACE MEDICINE AND BIOLOGY: A CONTINUING BIBLIOGRAPHY WITH INDEXES (SUPPLEMENT 328)
Feb. 1989 48 p
(NASA-SP-7011(328); NAS 1.21:7011(328)) Avail: NTIS HC A03; NTIS standing order as PB89-912300, $10.50 domestic, $21.00 foreign CSCL 21E

This bibliography lists 104 reports, articles and other documents introduced into the NASA Scientific and Technical Information System during September, 1989. Subject coverage includes: aerospace medicine and psychology, life support systems and controlled environments, safety equipment, exobiology and extraterrestrial life, and flight crew behavior and performance. Author

N90-10525# Lawrence Livermore National Lab., CA.
MANAGING HUMAN EXPOSURE AND HEALTH RISKS: AN INTEGRATED APPROACH AND THE ROLE OF UNCERTAINTY
Thomas E. McKone Mar. 1989 10 p Presented at the 8th World Clean Air Congress and Exhibition, The Hague, Netherlands, 11-15 Sep. 1989 Submitted for publication
(Contract W-7405-eng-48)
(DE89-008611; UCRL-100511; CONF-890909-1) Avail: NTIS HC A02/MF A01

Human populations contact environmental pollutants through food, water, and air in varying amounts each day throughout a lifetime. A realistic strategy for managing health risks of environmental contaminants therefore requires a comprehensive and integrated approach. Using examples for exposure to contaminants in potable water and to contaminants transferred from air to food, two important issues in exposure assessment are considered: the completeness of current exposure models and the treatment of uncertainty in exposure estimates. The results indicate that risk managers should consider the potential for multiple pathways, avoid risk assessments derived from single value estimates, be aware of the uncertainty in risk estimates, and include this awareness in their decisions. DOE

N90-10526# Tel-Aviv Univ. (Israel). Eye Research Inst.
TREATMENT OF LASER-INDUCED RETINAL INJURIES Final Report, 12 Feb. 1985 - 31 Jan. 1987
Michael Belkin and Nava Naveh 29 Jun. 1989 36 p
(Contract DAMD17-85-G-5013)
(AD-A210284) Avail: NTIS HC A03/MF A01 CSCL 06/15

The effect of steroids known for their inflammatory effect on the laser-induced retinal injury is investigated. In an attempt to minimize this, prostaglandin E2 (PGE2), known for their mediatory-role in any inflammatory reaction were studied as well as changes in protein leakage. The latter is indicative of blood retinal barrier disruption. The study revealed an enhanced PGE2 response as manifested by excessive production in vitro of PGE2 by the retina/choroid of laser-exposed eyes and accumulation of both PGE2 and protein in the vitreous body to above prelaser values. Corticosteroid treatment abolished the increase in the vitreal PGE2 response, but it only partially reduced the excessive PGE2 production in vitro by retina/choroid. Treatment was effective during the first weak, but later failed. The finding of the transient nature of the anti-PGE2 effect of the steroids does not necessarily point to the steroids inefficacy as anti-inflammatory agents, but rather may point to the cytoprotective nature of PGs themselves. GRA

N90-10527# Medical Coll. of Wisconsin, Milwaukee. Dept. of Neurosurgery.
BIOMEDICAL INFLUENCES ON SPINAL CORD FUNCTION Final Report, 1 Sep. 1977 - 31 Aug. 1987
Anthony Sances, Jr. 14 Jun. 1989 40 p
(Contract N00014-77-C-0749)
(AD-A210311) Avail: NTIS HC A03/MF A01 CSCL 06/10

These studies were directed to delineate the mechanisms of injury to the human brain and spinal cord during impact injury such as that experienced by Navy Air Force personnel and other military personnel during typical military and non-military maneuvers. The program was conducted in concert with the Office of Naval Research and the Biodynamics Laboratory in New Orleans, LA. Our group of biomedical engineers and neurosurgeons provided assistance for the biodynamics program in the evaluation of impact injury to non-human primates. Evoked potentials were used to measure the alterations in neurological function secondary to inertial impact produced on the HYGE sled in New Orleans at -x G levels up to approximately 100. The pathological evaluations were conducted in New Orleans by consultants and Navy personnel, and our personnel at the Medical College of Wisconsin provided the neurosurgical and biomechanical and bioengineering expertise to assist these studies. In addition, basic studies were conducted to evaluate spinal cord injury function in non-human primates and in human cadaveric tissues to determine the mechanical properties and strengths to further understand potential mechanisms of injury in military personnel. GRA

N90-10528# Health Effects Research Lab., Research Triangle Park, NC.
HUMAN HEALTH STUDIES OF CARBON MONOXIDE (CO) UNDER CONDITIONS OF MILITARY WEAPONS SYSTEMS CREWMAN EXPOSURES. PROTOCOL 1: FORMATION OF COHb Final Report, Sep. 1982 - Mar. 1985
Vernon A. Benignus, ed., Milan Hazucha, Mathew L. Petrovick, Michael L. McCartney, and Paul N. Kizakevich (Research Triangle Inst., Research Triangle Park, NC.) 29 Sep. 1988 128 p
(DA Proj. 3E1-62787-A-878)
(AD-A210344) Avail: NTIS HC A07/MF A01 CSCL 24/1

The present experiment was performed as a first step to evaluate the accuracy of prediction of carboxyhemoglobin (COHb)

formation due to quasi steady state carbon monoxide (CO) exposure by use of the Coburn-Forster-Kane equation (CFKE) and related models. Thirteen healthy young males were exposed to CO in room air for 120 minutes. While they were being exposed to CO, they either rested or performed bicycle exercise at one of two moderate work levels (25 or 40 Watts). Also during exposure to CO, blood samples were drawn every fine min to assess the COHb level. Many of the variables of the CFKE were measured in individual subjects rather than using published norms. GRA

N90-10529# Defence Research Establishment, Ottawa (Ontario). Environmental Protection Section.

MEASUREMENT OF RESPIRATORY AIR TEMPERATURES AND CALCULATION OF RESPIRATORY HEAT LOSS WHEN WORKING AT VARIOUS AMBIENT TEMPERATURES

J. B. Cain, S. D. Livingstone, R. W. Nolan, and A. A. Keefe Mar. 1989 23 p

(AD-A210378; DREO-1004) Avail: NTIS HC A02/MF A01 CSCL 06/4

Heat loss due to respiration can represent a sizable portion of the body's total heat loss. The temperature and humidity of expired air are important in determining the respiratory heat loss since this heat loss depends upon, among other things, the difference between the inspired and expired air temperatures and the change in the absolute humidity of the respired air. The purpose was to establish the temperature and humidity of the expired air of subjects working at various metabolic rates at ambient temperatures between -40 and 20 C in order to calculate the heat loss from the body due to respiration. Measurements of the respired air temperature and water vapor content were made for five subjects while they either stood or walked on a treadmill. The results indicated that the maximum respired air temperature varied slightly with the ambient air temperature but changes in metabolic rate, respiration rate and breathing frequency had no apparent effect on the expired air temperature under the conditions studied. The relative humidity of the respired air was found to be close to saturation in the extreme-cold environments. Heat loss due to respiration was calculated and the influence of various physiological and environmental variables on the respiratory heat loss is discussed. GRA

N90-10530# Army Aeromedical Research Lab., Fort Rucker, AL.

HUMAN PERFORMANCE IN CONTINUOUS/SUSTAINED OPERATIONS AND THE DEMANDS OF EXTENDED WORK/REST SCHEDULES: AN ANNOTATED BIBLIOGRAPHY, VOLUME 2 Final Report, 1985 - 1989

Gerald P. Krueger and Suzanne M. Barnes Jun. 1989 77 p

(AD-A210504; USAARL-89-8) Avail: NTIS HC A05/MF A01 CSCL 05/8

A society intent upon maintaining high productivity levels 24 hours per day, and on providing a variety of services around the clock, produced occupations and circumstances requiring prolonged, continuous work periods. The performance of workers under conditions of sustained or continuous work has become an important topic in industrial psychology, and in particular, in the military services. There are some traditional jobs, circumstances, and even some new occupations that involve prolonged, sustained work periods without rest, in which individual workers continue beyond the normal 8 to 10 hour work day. In many of these sustained work situations, the termination point for a shift is unknown. Such activities usually require prolonging physical stamina and sustaining high levels of organizational and cognitive effectiveness. These continuous operations are of two types: First, there are extended operations, jobs, or tasks that proceed continuously with only a short break or breaks, but that operate within a typical shift system for lengthy periods, longer that a normal duty day. The worker knows he or she will be relieved or able to rest. Second, there are sustained operations, planned or unplanned, goal-oriented, nonstop continuous performance/ operations without allowance for rest or sleep, in which the worker is expected to keep going as long as he or she can. Both have very important worker performance and behavioral implications. GRA

N90-10531# Naval Research Lab., Washington, DC. Polymeric Materials Branch.

EYE/SENSOR PROTECTION AGAINST LASER IRRADIATION ORGANIC NONLINEAR OPTICAL MATERIALS Final Report, Apr. - Dec. 1988

Michael E. Boyle and Robert F. Cozzens 12 Jun. 1989 100 p

(AD-A210599; NRL-MR-6482) Avail: NTIS HC A05/MF A01 CSCL 06/5

Recent developments in organic nonlinear optical materials for application to eye and sensor protection are reviewed. This compendium includes a brief discussion of the functioning of the eye, delineation of some of the important eye protection parameters and an introduction to the origin of nonlinear optical effects and how they are measured. Specific examples of proposed or prototyped protection devices are also presented. A compilation of noteworthy organic third-order nonlinear optical materials is included as an appendix. Lasers are playing an important and increasing role in modern society. Their present uses range from compact disc players to optical data storage and communication systems. Because of this wide spread use, the continuing expansion of lasers into other arenas and the low damage thresholds of human eyes and electro-optic sensors, there is increasing concern about eye and sensor protection from laser irradiation. GRA

N90-10532# California Univ., Irvine.

EXCITATORY AMINO ACIDS AS TRANSMITTERS IN THE BRAIN Final Report, 1 May 1986 - 30 Apr. 1989

C. W. Cotman 30 Apr. 1989 12 p

(Contract DAAL03-86-K-0067)

(AD-A210685; ARO-23200.9-LS) Avail: NTIS HC A03/MF A01 CSCL 06/5

The overall goal of this work was to carry out an indepth study of the properties of the excitatory amino acid neurotransmitter receptors. These receptors represent an integral part of the central nervous system, as they are responsible for the majority of the excitatory synaptic transmission, as well as being involved in higher order processes such as plasticity and excitotoxicity. Considerable advances have been made in our understanding of these receptors. The results of these studies are summarized below with respect to each of the receptor classes. GRA

N90-10533# Naval Health Research Center, San Diego, CA. Dept. of Sleep Research.

DAYTIME SLEEPINESS, PERFORMANCE, MOOD, NOCTURNAL SLEEP: THE EFFECT OF BENZODIAZEPINE AND CAFFEINE ON THEIR RELATIONSHIP Interim Report

L. C. Johnson, C. L. Spinweber, S. A. Gomez, and L. T. Matteson 1 Mar. 1989 27 p

(AD-A210915; NHRC-89-7) Avail: NTIS HC A03/MF A01 CSCL 06/10

Daytime sleepiness is not only a clinical and research problem, it can have consequences in operational settings. Sleepiness and alertness are generally viewed as reciprocal and were viewed as a function of the circadian cycle and of prior sleep and wakefulness. It was clearly established that total or partial sleep loss results in decreased alertness and impaired performance, but the magnitude of the relationship between sleepiness and performance decrement was not determined. The relationships between daytime sleepiness, performance, mood and nocturnal sleep and how these relationships were influenced by the nighttime use of a benzodiazepine and ingestion of caffeine in the morning were further examined. Objective measures of daytime sleepiness were not significantly related to either performance or mood through those with greater sleep tendency generally reported better mood. Subjects with greater daytime sleep tendency had significantly longer and more efficient nocturnal sleep. Neither benzodiazepine or caffeine influenced these relationships. In contrast, higher subjective estimates of sleepiness were significantly associated with poorer mood and tended to be related to poorer performance.

Subjects receiving caffeine did not show these relationships. Nocturnal sleep measures were not related to subjective estimates of daytime sleepiness. GRA

N90-10534# Massachusetts Univ., Amherst.
BIOLOGICAL INVESTIGATIONS OF ADAPTIVE NETWORKS: NEURONAL CONTROL OF CONDITIONED RESPONSES Final Report, 1 Jun. 1986 - 18 Jul. 1989
John W. Moore Jul. 1989 53 p
(Grant AF-AFOSR-0182-86)
(AD-A211043; AFOSR-89-1016TR) Avail: NTIS HC A04/MF A01 CSCL 05/8

Investigations of adaptive neutral networks were conducted using the classically conditioned nictitating membrane response (NMR) of rabbits. Work involved both neurobiological and theoretical approaches based on mathematical models and computer simulation. Recordings were done from single brain stem neurons in awake, behaving animals for the purpose of determining the loci and activity relationship to CRs (conditioned responses). Computational tools for applying systems analysis to neurophysiological data obtained from single-unit recordings from awake behaving animals were developed. The relationship between single neurons' dynamic behavior and the CR was characterized in terms of differential equations and sophisticated correlational analyses based on Fourier and Laplace transform methods. Theoretical studies revolved around two mathematical models of learning. The Sutton-Barto-Desmond (SBD) model was designed to describe real-time features of the NM CR. A cerebellar network implementation of this model was constructed by combining parametric constraints of the model dictated by behavioral data with constraints based on anatomy and physiology of the cerebellum. The second major theoretical development was the construction of a two-element neural-network architecture that elegantly describes adaptive timing as manifested in the fine-grain temporal characteristics of CRs. GRA

N90-10535# California Univ., San Diego, La Jolla. Dept. of Psychiatry.
EXTRATHALAMIC MODULATION OF CORTICAL FUNCTION Interim Report, 1 Apr. 1988 - 31 Mar. 1989
Stephen L. Foote 15 Jul. 1989 6 p
(Contract F49620-87-C-0038)
(AD-A211044; AFOSR-89-1012TR) Avail: NTIS HC A02/MF A01 CSCL 06/4

The focus of the research is to understand the role that the widely-divergent, globally-acting locus coeruleus (LC)-noradrenergic (NA) system plays in sensory information processing. Completed light-microscopic studies of the regional and laminar distribution of cortical innervation by extrathalamic systems (e.g., noradrenergic, cholinergic, serotonergic, and dopaminergic) indicate that axons of each system exhibit a different density and laminar distribution. They also display individual developmental sequences in terms of the time terms of the time when innervation begins and the evolution of its specialized laminar distribution in each cortical region. These anatomic data support the proposal that each extrathalamic system contacts a distinct population of neurons in specific cortical regions. Each population of neurons may be involved in different aspects of cortical regions. Cellular electrophysiology studies suggest that activity in the LC-NA has specific modulatory effects on the sensory responsiveness of cortical neurons. It alters the excitatory and inhibitory components of these sensory responses. Functionally, the LC-NA system may be involved in the orienting and attentional mechanisms. GRA

53 BEHAVIORAL SCIENCES

Includes psychological factors; individual and group behavior; crew training and evaluation; and psychiatric research.

N90-10536# Air Univ., Maxwell AFB, AL. Airpower Research Inst.
THE EFFECT OF HIGHER EDUCATION VARIABLES ON CADET PERFORMANCE DURING 1987 LIGHT AIRCRAFT TRAINING
Larry E. Baker May 1989 254 p
(AD-A210199; AU-ARI-88-9) Avail: NTIS HC A12/MF A02 CSCL 05/6

Based on the data analysis, it was concluded that a significant relationship is evident between 3 of the higher education curriculum variables: prior flying time, athletics, and portions of the Air Force Officer Qualifying Test; and subject performance in the light aircraft training (LATR) program for Air Force Reserve Officer Training Corps cadets conducted at Embry-Riddle Aeronautical University during the summer of 1987. The curricular variables that proved significant are identified, why the relationship occurred is analyzed, and the possible ramifications of such a relationship are discussed. The 1987 LATR program provided a unique opportunity to explore the question of what specific variables may influence a qualified individual's ability to pilot military aircraft. The specificity of the research design prevents accurate statistical inference to other subject populations and flight training programs. However, the implications of the study are clear: the men and women selected for Air Force pilot training over the past 20 years have been very similar, the basic selection criteria have remained consistent. The rate of attrition from the undergraduate pilot training program has also remained somewhat consistent, with variations being detected as supply and demand change. The LATR research study was clear in indicating that many of the selection criteria did not relate to flying performance. With the similarity of populations, it is very possible that these variables also have no effect on undergraduate pilot training or operational flying. GRA

N90-10537# University of Southern California, Los Angeles. Dept. of Psychology.
INTEGRATION OF NEUROBIOLOGICAL AND COMPUTATIONAL ANALYSES OF THE NEURAL NETWORK ESSENTIALS FOR CONDITIONED TASTE AVERSIONS Progress Report No. 1
Kathleen C. Chambers 30 Jun. 1989 52 p
(Contract N00014-89-J-1296)
(AD-A210228) Avail: NTIS HC A04/MF A01 CSCL 06/4

The general goal of the ONR project is to determine the neural basis of learning and memory, i.e., how the brain stores and retrieves memory. More specifically, how the hard-wired (innate) part of the neural system interfaces with the plastic (learned) part is determined. The special form of learning which is the focus of this project is conditioned taste aversions (CTAs), i.e., learned aversions to the taste of a food or fluid when consumption of that substance is followed by illness. In order to achieve this general goal, neurobiological and computational analyses of the neural network essentials for CTA are being integrated. The essential neurobiological network for models for the CTA neural circuit are being developed. GRA

N90-10538# Case Western Reserve Univ., Cleveland, OH. Dept. of Psychology.
MODELS OF MENTAL FUNCTIONING Final Report, 15 Jun. 1987 - 14 Dec. 1988
Douglas K. Detterman 14 May 1989 15 p
(Grant AF-AFOSR-0227-87; AF Proj. 2313)
(AD-A210456; AFOSR-89-0813TR) Avail: NTIS HC A03/MF A01 CSCL 05/8

The purpose of this research was to develop models of basic cognitive tasks developed in previous research. A model of choice reaction time was written in Simscript 2.5 but development of this model made it clear that additional information was required before good models of basic cognitive tasks could be devised. Therefore,

a number of experiments were conducted which were designed to provide the basic information needed. The experiments focused on several questions important to the construction of explicit models. Some of these questions were: How do subjects build mental models of instructions and to what extent do the goodness of these models affect subsequent performance. What aspects of stimulus structure are important in the encoding of the stimuli used in these tasks. Seven experiments addressing these issues were conducted. In general, results suggest that basic cognitive tasks are far more complex than had previously been thought.
GRA

N90-10539# Chicago Univ., IL. Speech Research Lab.
ATTENTION AND VIGILANCE IN SPEECH PERCEPTION Final Report, 1 Jul. 1987 - 31 Dec. 1988
Howard C. Nusbaum 23 Jun. 1989 72 p
(Grant AF-AFOSR-0271-87; AF Proj. 2313)
(AD-A210493; AFOSR-89-0963TR) Avail: NTIS HC A04/MF A01 CSCL 05/8

Research is described which was carried out in three related projects investigating the function and limitations of attention in speech perception. The projects were directed at investigating the distribution of attention in time during phoneme recognition, perceptual normalization of talker differences, and perceptual learning of synthetic speech. The first project demonstrates that in recognizing phonemes listeners attend to earlier and later phonetic context, even when that context is in another syllable. The second project demonstrated that there are two mechanisms underlying the ability of listeners to recognize speech across talkers. The first, structural estimation, is based on computing a talker-independent representation of each utterance on its own; the second, contextual tuning, is based on learning the vocal characteristics of the talker. Structural estimation requires more attention and effort than contextual tuning. The final project examined the attentional demands of synthetic speech and how they change with perceptual learning. The results demonstrated that the locus of attentional demands in perception of synthetic speech is in recognition rather than storage or recall of synthetic speech. Moreover, perceptual learning increases the efficiency with which listeners can use spare capacity in recognizing synthetic speech and this effect is not just due to increased intelligibility.
GRA

N90-10540# Advanced Decision Systems, Mountain View, CA.
TRACKING PERFORMANCE EVALUATION Final Report, 1 Dec. 1987 - 31 Aug. 1988
Shozo Mori, Kuo-Chu Chang, Chee-Yee Chong, and Steve Spain 7 Dec. 1988 76 p Prepared in cooperation with Massachusetts Inst. of Technology, Lexington
(Contract F19628-85-C-0002)
(AD-A210499; ESD-TR-89-128; ADS-TR-1196-1) Avail: NTIS HC A05/MF A01 CSCL 05/6

The research conducted at Advanced Decision Systems, sponsored by Lincoln Laboratory, Massachusetts Institute of Technology, under a project entitled, Discrimination Architecture Engineering Support, from 1 December 1987 to 31 August 1988, is documented. Simple analytic models were developed for predicting performance of tracking systems in terms of track purity under given tracking environments, in particular, multilayer ballistic missile defense environments concerning tracking-surveillance and object -discrimination. The main result is a simple analytic model which relates single-scan track-to-measurement association (correlation) performance to two key parameters, object density on sensors' focal planes, and average measurement prediction accuracy by tracks. Predicted track purity is then calculated, through this model, based on given object trajectories and sensor deployment patterns. Extended models were developed to account for false alarms and merged measurements (CSOs) due to limited sensor resolution. Small-scaled but fairly extensive Monte Carlo simulations support the analytic models for predicting track purity developed through this project.
GRA

54 MAN/SYSTEM TECHNOLOGY AND LIFE SUPPORT

Includes human engineering; biotechnology; and space suits and protective clothing.

For related information see also *16 Space Transportation.*

N90-10541# Army Research Inst. of Environmental Medicine, Natick, MA. Military Ergonomics Div.
THERMOREGULATORY RESPONSES TO INTERMITTENT EXERCISE ARE INFLUENCED BY KNIT STRUCTURE OF UNDERWEAR
Ruth Nielsen (National Inst. of Occupational Health, Solna, Sweden) and Thomas L. Endrusick Apr. 1989 26 p
(AD-A209087; USARIEM-M-34-189) Avail: NTIS HC A03/MF A01 CSCL 06/10

The purpose of this study was to evaluate the role of knit structure in underwear on thermoregulatory responses. Underwear manufactured from 100 percent polypropylene fibers in five different knit structures (1-by-1 rib, fleece, fishnet, interlock, double-layer rib) were evaluated. All five year underwear prototypes were tested as part of a prototype clothing system. Measured on a thermal manikin these clothing systems had total thermal resistances, I(tot), of 0.243, 0.268, 0.256. 0.248 and 0.250 square meter/k/w, respectively. Human testing was done on eight male subjects and took place at T(a) = 5 C, t(sp) = 3.5 c and V(a) = 0.32 m/s. The test comprised a repeated bout of 40 min cycle exercise (315 w/square meter; 52 + or - 4.9 percent maximum oxygen consumption followed by 20 min of rest (w/sqi M). VO2, heart rate, esophageal temperature, local skin temperatures, ambient air temperature, dew point temperature at three skin sites and in the ambient air were monitored. Onset of sweating was evaluated from the dew point sensor recordings. The differences in knit structure of the underwater in the clothing systems resulted in significant differences in mean skin temperature, local and average skin wetness, non-evaporated and evaporated sweat during the course of the core temperature.
GRA

N90-10542*# National Aeronautics and Space Administration. Ames Research Center, Moffett Field, CA.
VISION SCIENCE AND TECHNOLOGY AT NASA: RESULTS OF A WORKSHOP
Andrew B. Watson, ed. and Jeffrey B. Mulligan, ed. Aug. 1989 62 p Workshop held at Moffett Field, CA, 30 Nov. - 2 Dec. 1988
(NASA-TM-102214; A-89211; NAS 1.15:102214) Avail: NTIS HC A04/MF A01 CSCL 05H

A broad review is given of vision science and technology within NASA. The subject is defined and its applications in both NASA and the nation at large are noted. A survey of current NASA efforts is given, noting strengths and weaknesses of the NASA program. For individual titles, see N90-10543 through N90-10570.

N90-10543*# National Aeronautics and Space Administration. Ames Research Center, Moffett Field, CA.
VISION SCIENCE AND TECHNOLOGY AT NASA: RESULTS OF A WORKSHOP: EXECUTIVE SUMMARY
In its Vision Science and Technology at NASA: Results of a Workshop Aug. 1989 p 3-17 (For primary document see N90-10542 01-54)
Avail: NTIS HC A04/MF A01 CSCL 05H

Through Vision Science and Technology (VST), researchers seek to understand the process of vision at the biological, physical, and mathematical levels, and to translate that understanding into practical advances in human factors, visual displays, image processing, and autonomous vision. VST is an important element of many national initiatives in science and engineering, such as High-Definition Television, Human Genome Project, Superconducting Super Collider, and Strategic Defense Initiative, as well as in the efforts to revitalize American industry through increased automation. The NASA effort in VST is of high quality, but the level of effort is insufficient to meet the requirements of

future NASA missions. The NASA program in VST could be strengthened sufficiently to meet these future challenges. Steps in this direction should include: explicitly acknowledging VST in planning and funding; enhancing the complement of in-house researchers; encouraging selective excellence in a small number of VST areas; establishing an in-house center of excellence in VST; encouraging collaboration with universities and among centers; and adopting a long-term emphasis on fundamental work in VST to support future applications. Author

N90-10544*# National Aeronautics and Space Administration. Ames Research Center, Moffett Field, CA.
SAMPLING AND NOISE IN VISION NETWORKS Abstract Only
Albert J. Ahumada, Jr. *In its* Vision Science and Technology at NASA: Results of a Workshop Aug. 1989 p 19-20 (For primary document see N90-10542 01-54)
Avail: NTIS HC A04/MF A01 CSCL 05H

This research is part of the Human Interface Research Branch-Vision Group's program to develop computable models of biological solutions to general vision system problems. Two problem areas are addressed: (1) effects of discrete sampling by receptors, and (2) effects of visual system noise. Author

N90-10545*# National Aeronautics and Space Administration. Ames Research Center, Moffett Field, CA.
NETWORKS FOR IMAGE ACQUISITION, PROCESSING AND DISPLAY Abstract Only
Albert J. Ahumada, Jr. *In its* Vision Science and Technology at NASA: Results of a Workshop Aug. 1989 p 21 (For primary document see N90-10542 01-54)
Avail: NTIS HC A04/MF A01 CSCL 05H

The human visual system comprises layers of networks which sample, process, and code images. Understanding these networks is a valuable means of understanding human vision and of designing autonomous vision systems based on network processing. Ames Research Center has an ongoing program to develop computational models of such networks. The models predict human performance in detection of targets and in discrimination of displayed information. In addition, the models are artificial vision systems sharing properties with biological vision that has been tuned by evolution for high performance. Properties include variable density sampling, noise immunity, multi-resolution coding, and fault-tolerance. The research stresses analysis of noise in visual networks, including sampling, photon, and processing unit noises. Specific accomplishments include: models of sampling array growth with variable density and irregularity comparable to that of the retinal cone mosaic; noise models of networks with signal-dependent and independent noise; models of network connection development for preserving spatial registration and interpolation; multi-resolution encoding models based on hexagonal arrays (HOP transform); and mathematical procedures for simplifying analysis of large networks. Author

N90-10546*# Microtronics Associates, Pittsburgh, PA.
PARALLEL ASYNCHRONOUS HARDWARE IMPLEMENTATION OF IMAGE PROCESSING ALGORITHMS Abstract Only **c61**
Darryl D. Coon and A. G. U. Perera *In* NASA. Ames Research Center, Vision Science and Technology at NASA: Results of a Workshop Aug. 1989 p 22 (For primary document see N90-10542 01-54)
(Contract NAS1-18645)
Avail: NTIS HC A04/MF A01 CSCL 09B

Research is being carried out on hardware for a new approach to focal plane processing. The hardware involves silicon injection mode devices. These devices provide a natural basis for parallel asynchronous focal plane image preprocessing. The simplicity and novel properties of the devices would permit an independent analog processing channel to be dedicated to every pixel. A laminar architecture built from arrays of the devices would form a two-dimensional (2-D) array processor with a 2-D array of inputs located directly behind a focal plane detector array. A 2-D image data stream would propagate in neuron-like asynchronous pulse-coded form through the laminar processor. No multiplexing, digitization, or serial processing would occur in the preprocessing state. High performance is expected, based on pulse coding of input currents down to one picoampere with noise referred to input of about 10 femtoamperes. Linear pulse coding has been observed for input currents ranging up to seven orders of magnitude. Low power requirements suggest utility in space and in conjunction with very large arrays. Very low dark current and multispectral capability are possible because of hardware compatibility with the cryogenic environment of high performance detector arrays. The aforementioned hardware development effort is aimed at systems which would integrate image acquisition and image processing. Author

N90-10547*# National Aeronautics and Space Administration. Ames Research Center, Moffett Field, CA.
VISIONS OF VISUALIZATION AIDS: DESIGN PHILOSOPHY AND EXPERIMENTAL RESULTS Abstract Only **c61**
Stephen R. Ellis *In its* Vision Science and Technology at NASA: Results of a Workshop Aug. 1989 p 23 (For primary document see N90-10542 01-54)
Avail: NTIS HC A04/MF A01 CSCL 09B

Aids for the visualization of high-dimensional scientific or other data must be designed. Simply casting multidimensional data into a two- or three-dimensional spatial metaphor does not guarantee that the presentation will provide insight or parsimonious description of the phenomena underlying the data. Indeed, the communication of the essential meaning of some multidimensional data may be obscured by presentation in a spatially distributed format. Useful visualization is generally based on pre-existing theoretical beliefs concerning the underlying phenomena which guide selection and formatting of the plotted variables. Two examples from chaotic dynamics are used to illustrate how a visulaization may be an aid to insight. Two examples of displays to aid spatial maneuvering are described. The first, a perspective format for a commercial air traffic display, illustrates how geometric distortion may be introduced to insure that an operator can understand a depicted three-dimensional situation. The second, a display for planning small spacecraft maneuvers, illustrates how the complex counterintuitive character of orbital maneuvering may be made more tractable by removing higher-order nonlinear control dynamics, and allowing independent satisfaction of velocity and plume impingement constraints on orbital changes. Author

N90-10548*# National Aeronautics and Space Administration. Lyndon B. Johnson Space Center, Houston, TX.
VISION SCIENCE AND TECHNOLOGY FOR SUPERVISED INTELLIGENT SPACE ROBOTS Abstract Only
Jon D. Erickson *In* NASA. Ames Research Center, Vision Science and Technology at NASA: Results of a Workshop Aug. 1989 p 24 (For primary document see N90-10542 01-54)
Avail: NTIS HC A04/MF A01 CSCL 05H

The focus of recent work in robotic vision for application in intelligent space robots such as the Extravehicular Activity (EVA) Retriever is in visual function, that is, how information about the space world is derived and then conveyed to cognition. The goal of this work in visual function is first to understand how the relevant structure of the surrounding world is evidenced by regularities among the pixels of images, then to understand how these regularities are mapped on the premises that form the primitive elements of cognition, and then to apply these understandings with the elements of visual processing (algorithms) and visual mechanism (machine organization) to intelligent space robot simulations and test beds. Since visual perception is the process of recognizing regularities in images that are known on the basis of a model of the world to be reliable related to causal structure in the environment (because perception attaches meaning to the link between a conception of the environment and the objective environment), the work involves understanding generic, generally applicable models of world structure (not merely objects) and how that structure evidences itself in images. Author

N90-10549*# National Aeronautics and Space Administration. Goddard Space Flight Center, Greenbelt, MD.
COMPUTATION AND PARALLEL IMPLEMENTATION FOR EARLY VISION Abstract Only **c62**
J. Anthony Gualtieri *In* NASA. Ames Research Center, Vision Science and Technology at NASA: Results of a Workshop Aug. 1989 p 25-26 (For primary document see N90-10542 01-54)
Avail: NTIS HC A04/MF A01 CSCL 09B

The problem of early vision is to transform one or more retinal illuminance images-pixel arrays-to image representations built out of such primitive visual features such as edges, regions, disparities, and clusters. These transformed representations form the input to later vision stages that perform higher level vision tasks including matching and recognition. Researchers developed algorithms for: (1) edge finding in the scale space formulation; (2) correlation methods for computing matches between pairs of images; and (3) clustering of data by neural networks. These algorithms are formulated for parallel implementation of SIMD machines, such as the Massively Parallel Processor, a 128 x 128 array processor with 1024 bits of local memory per processor. For some cases, researchers can show speedups of three orders of magnitude over serial implementations. Author

N90-10550*# Odetics, Inc., Anaheim, CA.
INTENSITY DEPENDENT SPREAD THEORY Abstract Only
Richard Holben *In* NASA. Ames Research Center, Vision Science and Technology at NASA: Results of a Workshop Aug. 1989 p 27 (For primary document see N90-10542 01-54)
Avail: NTIS HC A04/MF A01 CSCL 05H

The Intensity Dependent Spread (IDS) procedure is an image-processing technique based on a model of the processing which occurs in the human visual system. IDS processing is relevant to many aspects of machine vision and image processing. For quantum limited images, it produces an ideal trade-off between spatial resolution and noise averaging, performs edge enhancement thus requiring only mean-crossing detection for the subsequent extraction of scene edges, and yields edge responses whose amplitudes are independent of scene illumination, depending only upon the ratio of the reflectance on the two sides of the edge. These properties suggest that the IDS process may provide significant bandwidth reduction while losing only minimal scene information when used as a preprocessor at or near the image plane. Author

N90-10551*# National Aeronautics and Space Administration. Langley Research Center, Hampton, VA.
IMAGE GATHERING, CODING, AND PROCESSING: END-TO-END OPTIMIZATION FOR EFFICIENT AND ROBUST ACQUISITION OF VISUAL INFORMATION Abstract Only
Friedrich O. Huck and Carl L. Fales *In* NASA. Ames Research Center, Vision Science and Technology at NASA: Results of a Workshop Aug. 1989 p 28-29 (For primary document see N90-10542 01-54)
Avail: NTIS HC A04/MF A01 CSCL 05H

Researchers are concerned with the end-to-end performance of image gathering, coding, and processing. The applications range from high-resolution television to vision-based robotics, wherever the resolution, efficiency and robustness of visual information acquisition and processing are critical. For the presentation at this workshop, it is convenient to divide research activities into the following two overlapping areas: The first is the development of focal-plane processing techniques and technology to effectively combine image gathering with coding, with an emphasis on low-level vision processing akin to the retinal processing in human vision. The approach includes the familiar Laplacian pyramid, the new intensity-dependent spatial summation, and parallel sensing/processing networks. Three-dimensional image gathering is attained by combining laser ranging with sensor-array imaging. The second is the rigorous extension of information theory and optimal filtering to visual information acquisition and processing. The goal is to provide a comprehensive methodology for quantitatively assessing the end-to-end performance of image gathering, coding, and processing. Author

N90-10552*# National Aeronautics and Space Administration. Lyndon B. Johnson Space Center, Houston, TX.
HYBRID VISION ACTIVITIES AT NASA JOHNSON SPACE CENTER Abstract Only
Richard D. Juday *In* NASA. Ames Research Center, Vision Science and Technology at NASA: Results of a Workshop Aug. 1989 p 30 (For primary document see N90-10542 01-54)
Avail: NTIS HC A04/MF A01 CSCL 05H

NASA's Johnson Space Center in Houston, Texas, is active in several aspects of hybrid image processing. (The term hybrid image processing refers to a system that combines digital and photonic processing). The major thrusts are autonomous space operations such as planetary landing, servicing, and rendezvous and docking. By processing images in non-Cartesian geometries to achieve shift invariance to canonical distortions, researchers use certain aspects of the human visual system for machine vision. That technology flow is bidirectional; researchers are investigating the possible utility of video-rate coordinate transformations for human low-vision patients. Man-in-the-loop teleoperations are also supported by the use of video-rate image-coordinate transformations, as researchers plan to use bandwidth compression tailored to the varying spatial acuity of the human operator. Technological elements being developed in the program include upgraded spatial light modulators, real-time coordinate transformations in video imagery, synthetic filters that robustly allow estimation of object pose parameters, convolutionally blurred filters that have continuously selectable invariance to such image changes as magnification and rotation, and optimization of optical correlation done with spatial light modulators that have limited range and couple both phase and amplitude in their response. Author

N90-10553*# National Aeronautics and Space Administration. Ames Research Center, Moffett Field, CA.
HUMAN MOTION PERCEPTION: HIGHER-ORDER ORGANIZATION Abstract Only
Mary K. Kaiser and Dennis R. Proffitt (Virginia Univ., Charlottesville.) *In its* Vision Science and Technology at NASA: Results of a Workshop Aug. 1989 p 31-32 (For primary document see N90-10542 01-54)
Avail: NTIS HC A04/MF A01 CSCL 05H

An overview is given of higher-order motion perception and organization. It is argued that motion is sufficient to fully specify a number of environmental properties, including: depth order, three-dimentional form, object displacement, and dynamics. A grammar of motion perception is proposed; applications of this work for display design are discussed. Author

N90-10554*# National Aeronautics and Space Administration. Ames Research Center, Moffett Field, CA.
TWO-DIMENSIONAL SHAPE RECOGNITION USING SPARSE DISTRIBUTED MEMORY Abstract Only
Pentti Kanerva and Bruno Olshausen *In its* Vision Science and Technology at NASA: Results of a Workshop Aug. 1989 p 33 (For primary document see N90-10542 01-54)
Avail: NTIS HC A04/MF A01 CSCL 05H

Researchers propose a method for recognizing two-dimensional shapes (hand-drawn characters, for example) with an associative memory. The method consists of two stages: first, the image is preprocessed to extract tangents to the contour of the shape; second, the set of tangents is converted to a long bit string for recognition with sparse distributed memory (SDM). SDM provides a simple, massively parallel architecture for an associative memory. Long bit vectors (256 to 1000 bits, for example) serve as both data and addresses to the memory, and patterns are grouped or classified according to similarity in Hamming distance. At the moment, tangents are extracted in a simple manner by progressively blurring the image and then using a Canny-type edge detector (Canny, 1986) to find edges at each stage of blurring. This results in a grid of tangents. While the technique used for obtaining the tangents is at present rather ad hoc, researchers plan to adopt an existing framework for extracting edge orientation information over a variety of resolutions, such as suggested by

Watson (1987, 1983), Marr and Hildreth (1980), or Canny (1986).
Author

N90-10555*# Odetics, Inc., Anaheim, CA.
THE INTENSITY DEPENDENT SPREAD MODEL AND COLOR CONSTANCY Abstract Only
Ellie Kurrasch *In* NASA. Ames Research Center, Vision Science and Technology at NASA: Results of a Workshop Aug. 1989 p 34 (For primary document see N90-10542 01-54)
Avail: NTIS HC A04/MF A01 CSCL 05H

Odetics is investigating the use of the intensity dependent spread (IDS) model for determining color constancy. Object segmentation is performed effortlessly by the human visual systems, but creating computer vision that takes an image as input and performs object identification on the basis of color has some difficulties. The unknown aspects of the light illuminating a scene in space or anywhere can seriously interfere with the use of color for object identification. The color of an image depends not only on the physical characteristics of the object, but also on the wavelength composition of the incident illumination. IDS processing provides the extraction of edges and of reflectance changes across edges, independent of variations in scene illumination. IDS depends solely on the ratio of the reflectances on the two sides of the edge. Researchers are in the process of using IDS to recover the reflectance image. Author

N90-10556*# National Aeronautics and Space Administration. Ames Research Center, Moffett Field, CA.
FILLING IN THE RETINAL IMAGE Abstract Only
James Larimer and Thomas Piantanida (SRI International Corp., Menlo Park, CA.) *In its* Vision Science and Technology at NASA: Results of a Workshop Aug. 1989 p 35 (For primary document see N90-10542 01-54)
Avail: NTIS HC A04/MF A01 CSCL 05H

The optics of the eye form an image on a surface at the back of the eyeball called the retina. The retina contains the photoreceptors that sample the image and convert it into a neural signal. The spacing of the photoreceptors in the retina is not uniform and varies with retinal locus. The central retinal field, called the macula, is densely packed with photoreceptors. The packing density falls off rapidly as a function of retinal eccentricity with respect to the macular region and there are regions in which there are no photoreceptors at all. The retinal regions without photoreceptors are called blind spots or scotomas. The neural transformations which convert retinal image signals into percepts fills in the gaps and regularizes the inhomogeneities of the retinal photoreceptor sampling mosaic. The filling-in mechamism plays an important role in understanding visual performance. The filling-in mechanism is not well understood. A systematic collaborative research program at the Ames Research Center and SRI in Menlo Park, California, was designed to explore this mechanism. It was shown that the perceived fields which are in fact different from the image on the retina due to filling-in, control some aspects of performance and not others. Researchers have linked these mechanisms to putative mechanisms of color coding and color constancy. Author

N90-10557*# National Aeronautics and Space Administration. Ames Research Center, Moffett Field, CA.
A3I VISIBILITY MODELING PROJECT Abstract Only
James Larimer, Aries Arditi, James Bergen, and Norman Badler (Pennsylvania Univ., Philadelphia.) *In its* Vision Science and Technology at NASA: Results of a Workshop Aug. 1989 p 36 (For primary document see N90-10542 01-54)
Avail: NTIS HC A04/MF A01 CSCL 05H

The Army-NASA Aircrew Aircraft Integration program is supporting a joint project to build a visibility computer-aided design (CAD) tool. CAD has become an essential tool in modern engineering applications. CAD tools are used to create engineering drawings and to evaluate potential designs before they are physically realized. The visibility CAD tool will provide the design engineer with a tool to aid in the location and specification of windows, displays, and control in crewstations. In an aircraft cockpit the location of instruments and the emissive and reflective characteristics of the surfaces must be determined to assure adequate aircrew performance. The visibility CAD tool will allow the designer to ask and answer many of these questions in the context of a three-dimensional graphical representation of the cockpit. The graphic representation of the cockpit is a geometrically valid model of the cockpit design. A graphic model of a pilot, called the pilot manikin, can be placed naturalistically in the cockpit model. The visibility tool has the capability of mapping the cockpit surfaces and other objects modeled in this graphic design space onto the simulated pilot's retinas for a given visual fixation.
Author

N90-10558*# National Aeronautics and Space Administration. Goddard Space Flight Center, Greenbelt, MD.
MOTION DETECTION IN ASTRONOMICAL AND ICE FLOE IMAGES Abstract Only
M. Manohar, H. K. Ramapriyan, and J. P. Strong *In* NASA. Ames Research Center, Vision Science and Technology at NASA: Results of a Workshop Aug. 1989 p 37 (For primary document see N90-10542 01-54)
Avail: NTIS HC A04/MF A01 CSCL 05H

Two approaches are presented for establishing correspondence between small areas in pairs of successive images for motion detection. The first one, based on local correlation, is used on a pair of successive Voyager images of the Jupiter which differ mainly in locally variable translations. This algorithm is implemented on a sequential machine (VAX 780) as well as the Massively Parallel Processor (MPP). In the case of the sequential algorithm, the pixel correspondence or match is computed on a sparse grid of points using nonoverlapping windows (typically 11 x 11) by local correlations over a predetermined search area. The displacement of the corresponding pixels in the two images is called the disparitries to cubic surfaces. The disparities at points where the error between the computed values and the surface values exceeds a particular threshold are replaced by the surface values. A bilinear interpolation is then used to estimate disparities at all other pixels between the grid points. When this algorithm was applied at the red spot in the Jupiter image, the rotating velocity field of the storm was determined. The second method of motion detection is applicable to pairs of images in which corresponding areas can experience considerable translation as well as rotation. Author

N90-10559*# National Aeronautics and Space Administration. Ames Research Center, Moffett Field, CA.
FACTORS AFFECTING THE PERCEPTION OF TRANSPARENT MOTION Abstract Only
Jeffrey B. Mulligan *In its* Vision Science and Technology at NASA: Results of a Workshop Aug. 1989 p 38 (For primary document see N90-10542 01-54)
Avail: NTIS HC A04/MF A01 CSCL 05H

It is possible to create a perception of transparency by combining patterns having different motions. Two particular combination rules, have specific interpretations in terms of physical phenomena: additive (specular reflection) and multiplicative (shadow illumination). Arbitrary combination rules applied to random patterns generate percepts in which the motions of the two patterns are visible, but have super-imposed noise. It is also possible to combine the patterns (using an exclusive-OR rule) so that only noise is visible. Within a one-dimensional family of combination rules which include addition and multiplication, there is a range where smooth motions are seen with no superimposed noise; this range is centered about the additive combination. This result suggests that the motion system deals with a linear representation of luminance, and is consistent with the analysis of motion by linear sensors. This research gives tentative validation the use in beam splitters (which combine images additively) in the construction of heads-up aviation displays. Further work is needed to determine if the superiority of additive combination generalizes to the case of full-color imagery (there are results in the literature suggesting that subtractive color mixture yields the best legibility of overlapping alphanumerics). Author

N90-10560*# National Aeronautics and Space Administration. Ames Research Center, Moffett Field, CA.
PHOTONIC PROCESSING AT NASA AMES RESEARCH CENTER Abstract Only
Ellen Ochoa and Max Reid *In its* Vision Science and Technology at NASA: Results of a Workshop Aug. 1989 p 39 (For primary document see N90-10542 01-54)
Avail: NTIS HC A04/MF A01 CSCL 05H

The Photonic Processing group is engaged in applied research on optical processors in support of the Ames vision to lead the development of autonomous intelligent systems. Optical processors, in conjunction with numeric and symbolic processors, are needed to provide the powerful processing capability that is required for many future agency missions. The research program emphasizes application of analog optical processing, where free-space propagation between components allows natural implementations of algorithms requiring a large degree of parallel computation. Special consideration is given in the Ames program to the integration of optical processors into larger, heterogeneous computational systems. Demonstration of the effective integration of optical processors within a broader knowledge-based system is essential to evaluate their potential for dependable operation in an autonomous environment such as space. The Ames Photonics program is currently addressing several areas of interest. One of the efforts is to develop an optical correlator system with two programmable spatial light modulators (SLMs) to perform distortion invariant pattern recognition. Another area of research is optical neural networks, also for use in distortion-invariant pattern recognition. Author

N90-10561*# National Aeronautics and Space Administration. Ames Research Center, Moffett Field, CA.
SPARSE DISTRIBUTED MEMORY OVERVIEW Abstract Only
Mike Raugh *In its* Vision Science and Technology at NASA: Results of a Workshop Aug. 1989 p 40-41 (For primary document see N90-10542 01-54)
Avail: NTIS HC A04/MF A01 CSCL 05H

The Sparse Distributed Memory (SDM) project is investigating the theory and applications of massively parallel computing architecture, called sparse distributed memory, that will support the storage and retrieval of sensory and motor patterns characteristic of autonomous systems. The immediate objectives of the project are centered in studies of the memory itself and in the use of the memory to solve problems in speech, vision, and robotics. Investigation of methods for encoding sensory data is an important part of the research. Examples of NASA missions that may benefit from this work are Space Station, planetary rovers, and solar exploration. Sparse distributed memory offers promising technology for systems that must learn through experience and be capable of adapting to new circumstances, and for operating any large complex system requiring automatic monitoring and control. Sparse distributed memory is a massively parallel architecture motivated by efforts to understand how the human brain works. Sparse distributed memory is an associative memory, able to retrieve information from cues that only partially match patterns stored in the memory. It is able to store long temporal sequences derived from the behavior of a complex system, such as progressive records of the system's sensory data and correlated records of the system's motor controls. Author

N90-10562*# Jet Propulsion Lab., California Inst. of Tech., Pasadena.
ALGORITHMS AND ARCHITECTURES FOR ROBOT VISION Abstract Only
Paul S. Schenker *In* NASA. Ames Research Center, Vision Science and Technology at NASA: Results of a Workshop Aug. 1989 p 42-43 (For primary document see N90-10542 01-54)
Avail: NTIS HC A04/MF A01 CSCL 05H

The scope of the current work is to develop practical sensing implementations for robots operating in complex, partially unstructured environments. A focus in this work is to develop object models and estimation techniques which are specific to requirements of robot locomation, approach and avoidance, and grasp and minipulation. Such problems have to date received limited attention in either computer or human vision - in essence, asking not only how perception is in general modeled, but also what is the functional purpose of its underlying representations. As in the past, researchers are drawing on ideas from both the psychological and machine vision literature. Of particular interest is the development 3-D shape and motion estimates for complex objects when given only partial and uncertain information and when such information is incrementally accrued over time. Current studies consider the use of surface motion, contour, and texture information, with the longer range goal of developing a fused sensing strategy based on these sources and others. Author

N90-10563*# California Univ., Berkeley. Telerobotics Unit.
INSTRUMENTATION AND ROBOTIC IMAGE PROCESSING USING TOP-DOWN MODEL CONTROL Abstract Only
Lawrence Stark, Barbara Mills, An H. Nguyen, and Huy X. Ngo *In* NASA. Ames Research Center, Vision Science and Technology at NASA: Results of a Workshop Aug. 1989 p 44 (For primary document see N90-10542 01-54)
Avail: NTIS HC A04/MF A01 CSCL 05H

A top-down image processing scheme is described. A three-dimensional model of a robotic working environment, with robot manipulators, workpieces, cameras, and on-the-scene visual enhancements is employed to control and direct the image processing, so that rapid, robust algorithms act in an efficient manner to continually update the model. Only the model parameters are communicated, so that savings in bandwidth are achieved. This image compression by modeling is especially important for control of space telerobotics. The background for this scheme lies in an hypothesis of human vision put forward by the senior author and colleagues almost 20 years ago - the Scanpath Theory. Evidence was obtained that repetitive sequences of saccadic eye movements, the scanpath, acted as the checking phase of visual pattern recognition. Further evidence was obtained that the scanpaths were apparently generated by a cognitive model and not directly by the visual image. This top-down theory of human vision was generalized in some sense to the frame in artificial intelligence. Another source of the concept arose from bioengineering instrumentation for measuring the pupil and eye movements with infrared video cameras and special-purpose hardware. Author

N90-10564*# National Aeronautics and Space Administration. Marshall Space Flight Center, Huntsville, AL.
COMPUTER VISION RESEARCH AT MARSHALL SPACE FLIGHT CENTER Abstract Only
Frank L. Vinz *In* NASA. Ames Research Center, Vision Science and Technology at NASA: Results of a Workshop Aug. 1989 p 45 (For primary document see N90-10542 01-54)
Avail: NTIS HC A04/MF A01 CSCL 05H

Orbital docking, inspection, and sevicing are operations which have the potential for capability enhancement as well as cost reduction for space operations by the application of computer vision technology. Research at MSFC has been a natural outgrowth of orbital docking simulations for remote manually controlled vehicles such as the Teleoperator Retrieval System and the Orbital Maneuvering Vehicle (OMV). Baseline design of the OMV dictates teleoperator control from a ground station. This necessitates a high data-rate communication network and results in several seconds of time delay. Operational costs and vehicle control difficulties could be alleviated by an autonomous or semi-autonomous control system onboard the OMV which would be based on a computer vision system having capability to recognize video images in real time. A concept under development at MSFC with these attributes is based on syntactic pattern recognition. It uses tree graphs for rapid recognition of binary images of known orbiting target vehicles. This technique and others being investigated at MSFC will be evaluated in realistic conditions by the use of MSFC orbital docking simulators. Computer vision is also being applied at MSFC as part of the supporting development for Work Package One of Space Station Freedom. Author

N90-10565*# Stanford Univ., CA.
STANFORD/NASA-AMES CENTER OF EXCELLENCE IN MODEL-BASED HUMAN PERFORMANCE Abstract Only
Brian A. Wandell *In* NASA. Ames Research Center, Vision Science and Technology at NASA: Results of a Workshop Aug. 1989 p 46 (For primary document see N90-10542 01-54)
Avail: NTIS HC A04/MF A01 CSCL 05H

The human operator plays a critical role in many aeronautic and astronautic missions. The Stanford/NASA-Ames Center of Excellence in Model-Based Human Performance (COE) was initiated in 1985 to further our understanding of the performance capabilities and performance limits of the human component of aeronautic and astronautic projects. Support from the COE is devoted to those areas of experimental and theoretical work designed to summarize and explain human performance by developing computable performance models. The ultimate goal is to make these computable models available to other scientists for use in design and evaluation of aeronautic and astronautic instrumentation. Within vision science, two topics have received particular attention. First, researchers did extensive work analyzing the human ability to recognize object color relatively independent of the spectral power distribution of the ambient lighting (color constancy). The COE has supported a number of research papers in this area, as well as the development of a substantial data base of surface reflectance functions, ambient illumination functions, and an associated software package for rendering and analyzing image data with respect to these spectral functions. Second, the COE supported new empirical studies on the problem of selecting colors for visual display equipment to enhance human performance in discrimination and recognition tasks. Author

N90-10566*# National Aeronautics and Space Administration. Ames Research Center, Moffett Field, CA.
AMES VISION GROUP RESEARCH OVERVIEW Abstract Only
Andrew B. Watson *In its* Vision Science and Technology at NASA: Results of a Workshop Aug. 1989 p 47 (For primary document see N90-10542 01-54)
Avail: NTIS HC A04/MF A01 CSCL 05H

A major goal of the reseach group is to develop mathematical and computational models of early human vision. These models are valuable in the prediction of human performance, in the design of visual coding schemes and displays, and in robotic vision. To date researchers have models of retinal sampling, spatial processing in visual cortex, contrast sensitivity, and motion processing. Based on their models of early human vision, researchers developed several schemes for efficient coding and compression of monochrome and color images. These are pyramid schemes that decompose the image into features that vary in location, size, orientation, and phase. To determine the perceptual fidelity of these codes, researchers developed novel human testing methods that have received considerable attention in the research community. Researchers constructed models of human visual motion processing based on physiological and psychophysical data, and have tested these models through simulation and human experiments. They also explored the application of these biological algorithms to applications in automated guidance of rotorcraft and autonomous landing of spacecraft. Researchers developed networks for inhomogeneous image sampling, for pyramid coding of images, for automatic geometrical correction of disordered samples, and for removal of motion artifacts from unstable cameras. Author

N90-10567*# National Aeronautics and Space Administration. Ames Research Center, Moffett Field, CA.
PYRAMID IMAGE CODES Abstract Only
Andrew B. Watson *In its* Vision Science and Technology at NASA: Results of a Workshop Aug. 1989 p 48 (For primary document see N90-10542 01-54)
Avail: NTIS HC A04/MF A01 CSCL 05H

All vision systems, both human and machine, transform the spatial image into a coded representation. Particular codes may be optimized for efficiency or to extract useful image features. Researchers explored image codes based on primary visual cortex in man and other primates. Understanding these codes will advance the art in image coding, autonomous vision, and computational human factors. In cortex, imagery is coded by features that vary in size, orientation, and position. Researchers have devised a mathematical model of this transformation, called the Hexagonal oriented Orthogonal quadrature Pyramid (HOP). In a pyramid code, features are segregated by size into layers, with fewer features in the layers devoted to large features. Pyramid schemes provide scale invariance, and are useful for coarse-to-fine searching and for progressive transmission of images. The HOP Pyramid is novel in three respects: (1) it uses a hexagonal pixel lattice, (2) it uses oriented features, and (3) it accurately models most of the prominent aspects of primary visual cortex. The transform uses seven basic features (kernels), which may be regarded as three oriented edges, three oriented bars, and one non-oriented blob. Application of these kernels to non-overlapping seven-pixel neighborhoods yields six oriented, high-pass pyramid layers, and one low-pass (blob) layer. Author

N90-10568*# Odetics, Inc., Anaheim, CA.
INTENSITY DEPENDENT SPREAD PROCESSOR AND WORKSTATION Abstract Only **c61**
George Westrom *In* NASA. Ames Research Center, Vision Science and Technology at NASA: Results of a Workshop Aug. 1989 p 49 (For primary document see N90-10542 01-54)
Avail: NTIS HC A04/MF A01 CSCL 09B

The Intensity Dependent Spread (IDS) is an adaptive algorithm which is modified according to the local intensity in the scene. (This results in a nonlinear process which cannot take advantage of rather nice linear transform methods.) The computation is similar to a neural net whereby intensity information is moving from each input pixel to a set of surrounding output pixels in a manner described by Cornsweet and Yellott. A prototype of a very large scale integration IDS processor is being developed and implemented in a workstation environment. The workstation consists of a SUN 3/260 and a DATACUBE pipeline processor. The IDS prototype is a board set which operates in the DATA CUBE processor. The SUN 3/260 performs control, background processing, IDS simulation and image display functions. Author

N90-10569*# National Aeronautics and Space Administration. Goddard Space Flight Center, Greenbelt, MD.
SPACE ENVIRONMENT ROBOT VISION SYSTEM Abstract Only
H. John Wood and William L. Eichhorn *In* NASA. Ames Research Center, Vision Science and Technology at NASA: Results of a Workshop Aug. 1989 p 50 (For primary document see N90-10542 01-54)
Avail: NTIS HC A04/MF A01 CSCL 05H

A prototype twin-camera stereo vision system for autonomous robots has been developed at Goddard Space Flight Center. Standard charge coupled device (CCD) imagers are interfaced with commercial frame buffers and direct memory access to a computer. The overlapping portions of the images are analyzed using photogrammetric techniques to obtain information about the position and orientation of objects in the scene. The camera head consists of two 510 x 492 x 8-bit CCD cameras mounted on individually adjustable mounts. The 16-mm efl lenses are designed for minimum geometric distortion. The cameras can be rotated in the pitch, roll, and yaw (pan angle) directions with respect to their optical axes. Calibration routines have been developed which automatically determine the lens focal lengths and pan angle between the two cameras. The calibration utilizes observations of a calibration structure with known geometry. Test results show the precision attainable is plus or minus 0.8 mm in range at 2 m distance using a camera separation of 171 mm. To demonstrate a task needed on Space Station Freedom, a target structure with a movable I beam was built. The camera head can autonomously direct actuators to dock the I-beam to another one so that they could be bolted together. Author

N90-10570*# National Aeronautics and Space Administration. Goddard Space Flight Center, Greenbelt, MD.
SELF-CALIBRATION OF ROBOT-SENSOR SYSTEM Abstract Only
Pen-Shu Yeh *In* NASA. Ames Research Center, Vision Science and Technology at NASA: Results of a Workshop Aug. 1989 p 51 (For primary document see N90-10542 01-54)
Avail: NTIS HC A04/MF A01 CSCL 05H

The process of finding the coordinate transformation between a robot and an external sensor system has been addressed. This calibration is equivalent to solving a nonlinear optimization problem for the parameters that characterize the transformation. A two-step procedure is herein proposed for solving the problem. The first step involves finding a nominal solution that is a good approximation of the final solution. A varational problem is then generated to replace the original problem in the next step. With the assumption that the variational parameters are small compared to unity, the problem that can be more readily solved with relatively small computation effort. Author

N90-10571*# Virginia Univ., Charlottesville. Dept. of Environmental Sciences.
A SIMPLE, MASS BALANCE MODEL OF CARBON FLOW IN A CONTROLLED ECOLOGICAL LIFE SUPPORT SYSTEM
Jay L. Garland Mar. 1989 37 p Prepared in cooperation with Bionetics Corp., Cocoa Beach, FL
(Contract NAS10-10285)
(NASA-TM-102151; NAS 1.15:102151) Avail: NTIS HC A03/MF A01 CSCL 05H

Internal cycling of chemical elements is a fundamental aspect of a Controlled Ecological Life Support System (CELSS). Mathematical models are useful tools for evaluating fluxes and reservoirs of elements associated with potential CELSS configurations. A simple mass balance model of carbon flow in CELSS was developed based on data from the CELSS Breadboard project at Kennedy Space Center. All carbon reservoirs and fluxes were calculated based on steady state conditions and modelled using linear, donor-controlled transfer coefficients. The linear expression of photosynthetic flux was replaced with Michaelis-Menten kinetics based on dynamical analysis of the model which found that the latter produced more adequate model output. Sensitivity analysis of the model indicated that accurate determination of the maximum rate of gross primary production is critical to the development of an accurate model of carbon flow. Atmospheric carbon dioxide was particularly sensitive to changes in photosynthetic rate. The small reservoir of CO2 relative to large CO2 fluxes increases the potential for volatility in CO2 concentration. Feedback control mechanisms regulating CO2 concentration will probably be necessary in a CELSS to reduce this system instability. Author

N90-10572# Georgia Inst. of Tech., Atlanta.
ACTIVE PARTICIPATION IN HIGHLY AUTOMATED SYSTEMS: TURNING THE WRONG STUFF INTO THE RIGHT STUFF Technical Report, 1 Jun. 1986 - 30 May 1989
Jacqueline R. Idaszak and Charles L. Hulin (Illinois Univ., Urbana.) 25 Jun. 1989 50 p
(Contract N00014-86-K-0332; RR04209)
(AD-A210218; ARL-89-7/ONR-89-1) Avail: NTIS HC A03/MF A01 CSCL 05/6

A failure of human operators to take an active monitoring role in complex automated systems has resulted in operators who are less able to improve the efficiency and stability of a system and unable to make a transition from normal scanning behavior to the detection, diagnosis, and correction of system failures. Passive monitoring is common when operator training follows an associative or stimulus-response model. In this study, we manipulated operator-system participation and operator-operator communication to investigate the effects of increases in active participation on operator monitoring and problem-solving performance. A total of 112 subjects worked as operators of a simulated process system. Operators worked in teams of two on both a monitoring task and, after the system failed, a diagnostic task. The results of this study suggest that active participation in the system improves both monitoring and diagnostic performance. In addition, active participation reduces boredom during monitoring, and stress while diagnosing a failure. Communication, on the other hand, was found to be a mixed blessing. Communication tended to facilitate performance of active participants, but degraded performance of passive participants. The implications of these results for system design, operator training, and future communication studies are discussed. GRA

N90-10573# Dayton Univ., OH.
EFFECTS OF MINIATURE CRT (CATHODE RAY TUBE) LOCATION UPON PRIMARY AND SECONDARY TASK PERFORMANCES Final Report, Sep. 1988 - Apr. 1989
Ronald M. Katsuyama, Evan P. Rolek, Suzanne Johnson, and Donald L. Monk (Aerospace Medical Research Labs., Wright-Patterson AFB, OH.) May 1989 47 p
(Contract F33615-85-C-0541)
(AD-A210223; AAMRL-TR-89-018) Avail: NTIS HC A03/MF A01 CSCL 23/2

Dual task performances were investigated as a function of the location of a peripherally mounted miniature CRT which presented secondary task information. The miniature CRT's location was varied across 3 levels of elevation and 4 levels of azimuth. Primary task information was presented by means of a stationary, centrally located CRT. The primary task required continuous monitoring of the primary display, while the secondary task required continuous tracking of an object on the secondary display. In general, the results indicated that performance decrements were not only a function of the absolute size of the viewing angle formed by the primary and secondary displays, but, in addition, by its direction. For example: (1) primary task performance decrements were generally greater when upward eye shifts were required to view the secondary display than when the corresponding downward eye shifts were required; (2) secondary task performance decrements were obtained only with upward eye shifts; and (3) lateral eye shifts produced smaller primary task decrements than comparable upward eye shifts. GRA

N90-10574# Carnegie-Mellon Univ., Pittsburgh, PA. Robotics Inst.
ON LEARNING FROM EXERCISES
B. K. Natarajan Feb. 1989 21 p
(AD-A210593; CMU-RI-TR-89-4) Copyright Avail: NTIS HC A03/MF A01 CSCL 05/8

This paper explores a new direction in the formal theory of learning--learning in the sense of improving computational efficiency as opposed to concept learning in the sense of Valient. Specifically, the paper concerns algorithms that learn to solve problems from sample instances of the problems. We develop a general framework for such learning and study the framework over two distinct random sources of sample instances. The first source provides sample instances together with their solutions, while the second source provides unsolved instances or exercises. We prove two theorems identifying conditions sufficient for learning over the two sources, our proofs being constructive in that they exhibit learning algorithms. To illustrate the scope of our results, we discuss their application to a program that learns to solve restricted classes of symbolic integrals. GRA

55 SPACE BIOLOGY

Includes exobiology; planetary biology; and extraterrestrial life.

No abstracts in this category.

59 MATHEMATICAL AND COMPUTER SCIENCES (GENERAL)

N90-10575*# National Aeronautics and Space Administration. Ames Research Center, Moffett Field, CA.
AN ALGORITHM FOR THE SYSTEMATIC DISTURBANCE OF OPTIMAL ROTATIONAL SOLUTIONS
Arthur J. Grunwald (Technion - Israel Inst. of Tech., Haifa.) and Mary K. Kaiser Aug. 1989 29 p
(NASA-TM-101089; A-89092; NAS 1.15:101089) Avail: NTIS HC A03/MF A01 CSCL 12A

An algorithm for introducing a systematic rotational disturbance into an optimal (i.e., single axis) rotational trajectory is described. This disturbance introduces a motion vector orthogonal to the quaternion-defined optimal rotation axis. By altering the magnitude of this vector, the degree of non-optimality can be controlled. The metric properties of the distortion parameter are described, with analogies to two-dimensional translational motion. This algorithm was implemented in a motion-control program on a three-dimensional graphic workstation. It supports a series of human performance studies on the detectability of rotational trajectory optimality by naive observers. Author

N90-10576*# Institute for Computer Applications in Science and Engineering, Hampton, VA.
CONVECTION OF A PATTERN OF VORTICITY THROUGH A REACTING SHOCK WAVE Final Report
T. L. Jackson, A. K. Kapila (Rensselaer Polytechnic Inst., Troy, NY.), and M. Y. Hussaini Sep. 1989 33 p Submitted for publication
(Contracts NAS1-18107; NAS1-18605)
(NASA-CR-181921; ICASE-89-68; NAS 1.26:181921) Avail: NTIS HC A03/MF A01 CSCL 12A

The passage of a weak vorticity disturbance through a reactive shock wave, or detonation, is examined by means of a linearized treatment. Of special interest is the effect of chemical heat release on the amplification of vorticity in particular, and on the disturbance pattern generated downstream of the detonation in general. It is found that the effect of exothermicity is to amplify the refracted waves. The manner in which the imposed disturbance alters the structure of the detonation itself is also discussed. Author

N90-10577*# National Aeronautics and Space Administration. Langley Research Center, Hampton, VA.
ADVANCING AUTOMATION AND ROBOTICS TECHNOLOGY FOR THE SPACE STATION FREEDOM AND FOR THE US ECONOMY Progress Report No. 8, Aug. 1988 - Feb. 1989
Jeremiah F. Creedon Apr. 1989 25 p
(NASA-TM-101561; NAS 1.15:101561) Avail: NTIS HC A03/MF A01 CSCL 12A

In April 1985, as required by Public Law 98-371, the NASA Advanced Technology Advisory Committee (ATAC) reported to Congress the results of its studies on advanced automation and robotics technology for use on the Freedom space station. This material was documented in the initial report (NASA Technical Memorandum 87566). A further requirement of the law was that ATAC follow NASA's progress in this area and report to Congress semiannually. This report is the eighth in a series of progress updates and covers the period between October 1, 1988, and March 31, 1989. NASA has accepted the basic recommendations of ATAC for its Space Station Freedom efforts. ATAC and NASA agree that the thrust of Congress is to build an advanced automation and robotics technology base that will support an evolutionary Space Station Freedom program and serve as a highly visible stimulator, affecting the U.S. long-term economy. The progress report identifies the work of NASA and the Freedom study contractors. It also describes research in progress, and it makes assessments of the advancement of automation and robotics technology on the Freedom space station. Author

60 COMPUTER OPERATIONS AND HARDWARE

Includes hardware for computer graphics, firmware, and data processing.

For components see *33 Electronics and Electrical Engineering.*

N90-10578# Massachusetts Inst. of Tech., Cambridge. Artificial Intelligence Lab.
PERFORMANCE EVALUATION OF THE SCHEME86 AND HP PRECISION ARCHITECTURES
Henry M. Wu Apr. 1989 40 p
(Contract N00014-86-K-0180)
(AD-A209418; AI-TR-1103) Avail: NTIS HC A03/MF A01 CSCL 12/6

The Scheme86 and the HP Precision Architectures represent different trends in computer processor design. The former uses wide micro-instructions, parallel hardware, and a low latency memory interface. The latter encourages pipelined implementation and visible interlocks. To compare the merits of these approaches, algorithms frequently encountered in numerical and symbolic computation were hand-coded for each architecture. Timings were done in simulators and the results were evaluated to determine the speed of each design. Based on these measurements conclusions were drawn as to which aspects of each architecture are suitable for a high performance computer. GRA

N90-10579# Massachusetts Inst. of Tech., Cambridge. Artificial Intelligence Lab.
A MULTIPROCESSOR ARCHITECTURE USING MODULAR ARITHMETIC FOR VERY HIGH PRECISION COMPUTATION
Henry M. Wu Apr. 1989 13 p
(Contract N00014-86-K-0180)
(AD-A208154; AI-M-1119) Avail: NTIS HC A03/MF A01 CSCL 12/6

A multiprocessor architecture is outlined that uses modular arithmetic to implement numerical computation with 900 bits of intermediate precision. A proposed prototype, to be implemented with off-the-shelf parts, will perform high precision arithmetic as fast as some workstations and minicomputers can perform IEEE double precision arithmetic. How the structure of modular arithmetic conveniently maps into a simple, pipelined multiprocessor architecture is discussed. Techniques developed to overcome a few classical drawbacks of modular arithmetic are presented. This architecture is suitable to and essential for the study of chaotic dynamical systems. GRA

N90-10580# Massachusetts Inst. of Tech., Cambridge. Microsystems Research Center.
GENERAL DECOMPOSITION OF SEQUENTIAL MACHINES: RELATIONSHIPS TO STATE ASSIGNMENT
Srinivas Devadas Mar. 1989 9 p
(Contract N00014-87-K-0825)
(AD-A208189; VLSI-MEMO-89-510) Avail: NTIS HC A02/MF A01 CSCL 12/3

In this paper, we present new techniques for state assignment of finite state machines based on state machine decomposition algorithms. A finite state machine can be decomposed into smaller interacting machines so as to optimize area and performance of the eventual logic implementation. A recently proposed form of decomposition, which has been shown to be superior to previous decomposition methods, involves identifying subroutines or factors in the original machine and extracting these factors to produce factored and factoring machines. Optimal state assignment corresponds to finding an optimal multiple general decomposition of a finite state machine. We present state assignment techniques targeting two-level and multi-level logic implementations based on factorization algorithms followed by state assignment algorithms. For the two-level case, we prove that one-hot encoding a non-trivially factored machine is guaranteed to produce a better result than one-hot encoding the original machine. GRA

N90-10581*# Institute for Computer Applications in Science and Engineering, Hampton, VA.
EVALUATING LOCAL INDIRECT ADDRESSING IN SIMD PROC ESSORS Final Report
David Middleton and Sherryl Tomboulian May 1989 20 p
(Contract NAS1-18605)
(NASA-CR-181845; ICASE-89-30; NAS 1.26:181845) Avail: NTIS HC A03/MF A01 CSCL 09B

In the design of parallel computers, there exists a tradeoff between the number and power of individual processors. The single instruction stream, multiple data stream (SIMD) model of parallel computers lies at one extreme of the resulting spectrum. The available hardware resources are devoted to creating the largest possible number of processors, and consequently each individual processor must use the fewest possible resources. Disagreement exists as to whether SIMD processors should be able to generate addresses individually into their local data memory, or all processors should access the same address. The tradeoff is examined between the increased capability and the reduced number of processors that occurs in this single instruction stream, multiple, locally addressed, data (SIMLAD) model. Factors are assembled that affect this design choice, and the SIMLAD model is compared with the bare SIMD and the MIMD models. Author

N90-10582# Lawrence Livermore National Lab., CA.
ADDRESSING USER DISPLAY REQUIREMENTS FROM A LARGE AND DIVERSE USER COMMUNITY
C. L. Hunter and E. E. Shultz, Jr. 19 Apr. 1989 9 p Presented at the 3rd International Conference on Human Computer Interaction, Boston, MA, 18-22 Sep. 1989 Submitted for publication
(Contract W-7405-eng-48)
(DE89-011403; UCRL-100958; CONF-8909126-1) Avail: NTIS HC A02/MF A01

A systematic, widely applicable methodology for defining user requirements for system functionality and user interface capabilities is described. This methodology is a variation of the user centered system design approach, which focuses on the user of a system. The methodology involves obtaining user input from questionnaires and interviews, utilizing a range of statistical techniques to analyze user data, then developing mathematical models to define user needs. This methodology was used successfully to define user requirements in a replacement for an absolute system at Lawrence Livermore National Laboratory. Advantages and disadvantages of this methodology are discussed. DOE

61 COMPUTER PROGRAMMING AND SOFTWARE

Includes computer programs, routines, alogorithms, and specific applications, e.g., CAD/CAM.

N90-10583*# Century Computing, Inc., Laurel, MD.
Ada (TRADEMARK) PROJECTS AT NASA. RUNTIME ENVIRONMENT ISSUES AND RECOMMENDATIONS
Daniel M. Roy and Randall W. Wilke Jan. 1988 148 p
(Contracts NAS5-30017; NAS5-27772)
(NASA-CR-183435; NAS 1.26:183435; DSTL-88-001) Avail: NTIS HC A07/MF A01 CSCL 09B

Ada practitioners should use this document to discuss and establish common short term requirements for Ada runtime environments. The major current Ada runtime environment issues are identified through the analysis of some of the Ada efforts at NASA and other research centers. The runtime environment characteristics of major compilers are compared while alternate runtime implementations are reviewed. Modifications and extensions to the Ada Language Reference Manual to address some of these runtime issues are proposed. Three classes of projects focusing on the most critical runtime features of Ada are recommended, including a range of immediately feasible full scale Ada development projects. Also, a list of runtime features and procurement issues is proposed for consideration by the vendors, contractors and the government. Author

N90-10584*# Michigan Univ., Ann Arbor. Robot Systems Div.
A COMMON DISTRIBUTED LANGUAGE APPROACH TO SOFTWARE INTEGRATION Final Report
Charles J. Antonelli, Richard A. Volz, and Trevor N. Mudge 9 Aug. 1989 32 p Prepared in cooperation with Texas A&M Univ., College Station
(Contract NCC9-16)
(NASA-CR-185499; NAS 1.26:185499) Avail: NTIS HC A03/MF A01 CSCL 09B

An important objective in software integration is the development of techniques to allow programs written in different languages to function together. Several approaches are discussed toward achieving this objective and the Common Distributed Language Approach is presented as the approach of choice. Author

N90-10585# Office of Naval Research European Office, FPO New York, NY.
PROCEEDINGS OF THE 2ND INTERNATIONAL CONFERENCE ON VECTOR AND PARALLEL COMPUTING
J. F. Blackburn 17 Jan. 1989 42 p Conference held in Bergen, Norway
(AD-A209401; ONREUR-9-1-C) Avail: NTIS HC A03/MF A01 CSCL 12/8

Summaries of the presentations by invited speakers to this conference, on Vector and Parallel Computing are given along with the author's abstracts of the contributed and student scholarship papers. In all, summaries of 16 papers and the abstracts of 91 other papers are included. GRA

N90-10586# National Aerospace Lab., Tokyo (Japan).
ON THE INTERACTIVE COMPUTER PROGRAM IPIS FOR AIRCRAFT PARAMETER IDENTIFICATION
Masahiko Nagayasu, Shuichi Sasa, and Masaaki Yanagihara Oct. 1988 45 p In JAPANESE; ENGLISH summary
(NAL-TR-1000; ISSN-0389-4010) Avail: NTIS HC A03/MF A01

A computer simulation program package, IPIS (Interactive Parameter Identification System), which was developed at the NAL for evaluation of flight test techniques concerning determination of aircraft performance characteristics from measured data in dynamic maneuvers, is described. The system is composed of programs for determination of parametric nonlinear aerodynamic model using wind tunnel test data, flight simulation, measurement simulation, motion reconstruction, identification of nonlinear aerodynamic models and calculation of performance characteristics. The system was evaluated using a simulation for the NAL STOL airplane. Author

N90-10587# Transportation Systems Center, Cambridge, MA.
WAVEFORM GENERATOR SIGNAL PROCESSING SOFTWARE Final Report, Jan. 1985 - Feb. 1988
Sep. 1988 171 p Prepared in cooperation with MGA Research Corp., Akron, NY
(Contracts DOT-HS-8-01936; DTNH22-82-C-07041; DTRS-57-84-C-00003; DTRS-57-86-P-81655)
(PB89-192660; DTS-74; DOT-TSC-NHTSA-88-2; DOT-HS-807-312) Avail: NTIS HC A08/MF A01 CSCL 09B

The report describes the software that was developed to process test waveforms that were recorded by crash test data acquisition systems. The test waveforms are generated by an electronic waveform generator which provides precise, repeatable signals designed to test the performance characteristics (amplitude and timing accuracy, and frequency response) of a data acquisition system. The waveform characteristics, processing algorithms, and instructions for use of the software are described in the report. Complete source listings are provided. Author

N90-10588*# College of William and Mary, Williamsburg, VA. Dept. of Computer Science.
SAFETY ANALYSIS OF KNOWLEDGE-BASED SYSTEMS Final Report
Larry J. Morell 15 Sep. 1989 31 p
(Grant NAG1-894)
(NASA-CR-184784; NAS 1.26:184784) Avail: NTIS HC A03/MF A01 CSCL 09B

The feasibility is investigated of designing a software specification language for knowledge based systems whose specifications are automatically verifiable. Two types of specifications are identified: (1) states what you want the software to do; and (2) states what you do not want the software to do. It is shown that type 1 specifications are less automatable than type 2 specifications in the following sense: for a given specification language, if type 1 specifications can be automatically verified, so can type 2 specifications. The converse is not true. The level of complexity of the specification language is defined to be the level in the Chomsky hierarchy of the sets of strings describable by that language. The result is that if the specification language has even the power to describe context-free languages, then type 1 specifications cannot be automatically verified, but type 2 can be. This result is disappointing because it severely limits the complexity of safety concerns. Author

N90-10589# Sandia National Labs., Albuquerque, NM.
A LOW-COST HYPERCUBE LOAD-BALANCE ALGORITHM
Karen M. Dragon (Rensselaer Polytechnic Inst., Troy, NY.) and John L. Gustafson 1989 15 p Presented at the 4th Hypercube, Concurrent Computers and Applications, Monterey, CA, 6-8 Mar. 1989
(Contract DE-AC04-76DP-00789)
(DE89-015739; SAND-88-2427C; CONF-890372-13) Avail: NTIS HC A03/MF A01

We have developed a divide-and-conquer approach to dynamic load balancing for a 1024-processor hypercube that requires only O(1) additional storage and O((log(sub 2)P)(sup 2)) additional operations. The balancing is done with global information rather than the nearest-neighbor information used in less effective techniques. Unlike previous global load balancers, the balancing is distributed over the ensemble rather than performed by a single processor. The algorithm has been tested using particle simulation, and is quite fast. The technique appears applicable to the efficient parallelization of Particle-In-Cell methods, finite difference and finite element methods with adaptive meshes, molecular dynamics calculations and other timestepping applications where dynamic load balancing is required. DOE

N90-10590# Sandia National Labs., Albuquerque, NM. Applied Mechanics Div.
BLOT: A MESH AND CURVE PLOT PROGRAM FOR THE OUTPUT OF A FINITE ELEMENT ANALYSIS
Amy P. Gilkey and John H. Glick Jun. 1989 143 p
(Contract DE-AC04-76DP-00789)
(DE89-013994; SAND-88-1432) Avail: NTIS HC A07/MF A01

BLOT is a graphics program for post processing of finite element analysis output that is presented in the EXODUS database format. It is command driven with free-format input and can drive any graphics device supported by the Sandia Virtual Device Interface. BLOT produces mesh plots with various representations of the analysis output variables. The major mesh plot capabilities are deformed mesh plots, line contours, banded contours, vector plots of two or three variables (e.g., velocity vectors), and symbol plots of scalar variables (e.g., temperature). Pathlines of analysis variables can also be drawn on the mesh. BLOT's features include element selection by material, element birth and death, multiple views for combining several displays on each plot, symmetry mirroring, and node and element numbering. BLOT can also produce X-Y curve plots of the analysis variables. BLOT generates time-vs-variable plots or variable-vs-variable plots. It also generates distance-vs-variable plots at selected time steps where the distance is the accumulated distance between pairs of nodes or element centers. DOE

N90-10591# Argonne National Lab., IL. Energy and Environmental Systems Div.
EVALUATION OF COMPUTER-AIDED SOFTWARE ENGINEERING TOOLS FOR DATA BASE DEVELOPMENT
Mark A. Woyna and C. Robert Carlson (Illinois Inst. of Tech., Chicago.) Feb. 1989 23 p
(Contract W-31-109-eng-38)
(DE89-014007; ANL/EES-TM-376) Avail: NTIS HC A03/MF A01

More than 80 computer aided software engineering (CASE) tools were evaluated to determine their usefulness in data base development projects. The goal was to review the current state of the CASE industry and recommend one or more tools for inclusion in the uniform development environment (UDE), a programming environment being designed by Argonne National Laboratory for the U.S. Department of Defense Organization of the Joint Chiefs of Staff, J-8 Directorate. This environment gives a computer programmer a consistent user interface and access to a full suite of tools and utilities for software development. In an effort to identify tools that would be useful in the planning, analysis, design, implementation, and maintenance of Argonne's data base development projects for the J-8 Directorate, 83 commercially available CASE products were evaluated. The method used are outlined and the results of the evaluation are presented. DOE

N90-10592# National Weather Service, Silver Spring, MD. Techniques Development Lab.
STRUCTURE FLOW DIAGRAM GENERATOR
Susan M. Adams Mar. 1989 18 p
(PB89-195978; NOAA-NWS-TDL-CP-89-1) Avail: NTIS HC A03/MF A01 CSCL 09B

The Structure Flow Diagram Generator provides the user with a convenient, easy-to-use, and less time-consuming way of diagramming the overall structure of a program. It allows for several options including segment and overlay numbers, and the inclusion of repetitive calls within a subroutine. The software can also be useful in preparing external documentation and publications which require an overall program structure diagram as part of the supporting documents. Author

N90-10593# National Weather Service, Silver Spring, MD. Techniques Development Lab.
STRING SEARCH
Susan M. Adams Mar. 1989 18 p
(PB89-195986; NOAA-NWS-TDL-CP-89-2) Avail: NTIS HC A03/MF A01 CSCL 09B

The String Search software performs a global search, a search on the main program and all its non-library functions and subroutines, for a specified text string. The support software is designed to be a useful tool in maintaining, enhancing, and developing programs. GRA

N90-10594# Lawrence Livermore National Lab., CA.
LOW-COST THREE-DIMENSIONAL STEREOSCOPIC DISPLAY TECHNIQUE FOR COMPUTER-AIDED DESIGN
Peter A. Luft and Gary Bradley 1 May 1989 10 p Presented at the Computer Graphics World Computervision International User Conference, Boston, 10-13 Sep. 1989
(Contract W-7405-eng-48)
(DE89-011635; UCRL-100718; CONF-8909111-1) Avail: NTIS HC A03/MF A01

This paper describes a procedure for obtaining low-cost stereoscopic imagery on any computer-aided design system that has color capability and models its data in 3-D form. This technique works independently of installed hardware or software. Stereoscopic imagery is valuable in the design process because it simplifies and clarifies complex computer-modeled parts and assemblies. Thus, the design and manufacturing processes benefit from better communication and fewer errors. DOE

N90-10595# California Univ., Berkeley. Lawrence Berkeley Lab. Information and Computing Sciences Div.
EFFECTIVE RESOURCE UTILIZATION FOR MULTIPROCESSOR JOIN EXECUTION
Marguerite C. Murphy (San Francisco State Univ., CA.) and Doron Rotem Jan. 1989 10 p Presented at the 15th International Conference on Very Large Data Bases, Amsterdam, Netherlands, 22-25 Aug. 1989
(Contract DE-AC03-76SF-00098)
(DE89-016303; LBL-26601; CONF-8908116-1) Avail: NTIS HC A02/MF A01

Conventional approaches to execution of database queries on general purpose multiprocessors attempt to maximize system throughput using inter-query parallelism with a fixed number of processors. Standard uniprocessor optimization techniques are used to minimize execution time of individual queries. Our approach is to increase performance by utilizing intra-query parallelism as well as minimizing overall resource requirements. Specifically, processor and i/o bandwidth requirements are minimized by coordinating the order in which data pages are read into memory and page joins assigned to available processors. We present a scheduling strategy based on join indices and prove lower and upper bounds on its resource requirements. We then describe a heuristic for estimating the number of processors required to complete join execution in minimal time. Our simulation results indicate that these techniques are effective with respect to processor utilization and buffer requirements. DOE

N90-10596# Naval Environmental Prediction Research Facility, Monterey, CA.
TESTS OF VARIOUS FINITE DIFFERENCE ALGORITHMS APPLIED TO A SIMPLE WATER VAPOR TRANSPORT PROBLEM ON A STAGGERED GRID Final Report, Oct. 1988 - Feb. 1989
Hung-Chi Kuo Apr. 1989 27 p
(AD-A210229; NEPRF-TR-89-04) Avail: NTIS HC A03/MF A01 CSCL 14/1

The 1-D constant advection of a Gaussian function is used to test four positive-definite schemes: Schemes 1, 2, Smolarkiwicz, and Arakawa; and three even-order accurate schemes: 3, 4, and 5, on the C staggered grid. It is shown that for the test problem, Schemes 1 and 2 produce identical numerical results. Arakawa's scheme produces the least damping among all the positive-definite schemes, but expensive computations are required with this scheme. With the advent of large digital computers, numerical modeling has taken an important place in atmospheric science. Constructing a numerical model often involves two steps. The first step is to formulate a set of continuous equations which represent the dynamics and the physics of interest in the atmosphere. The second step is to discretize these equations so that they may be solved on a computer. GRA

N90-10597# Naval Ocean Systems Center, San Diego, CA.
COST METRIC ALGORITHMS FOR INTERNETWORK APPLICATIONS Final Report
D. Olsen and R. Dillard Apr. 1989 47 p
(AD-A210324; NOSC/TR-1284) Avail: NTIS HC A03/MF A01 CSCL 12/7

The particular function of the Multi-Network Controller (MC) to be implemented for the 1990 Unified Networking Technology Advanced Technology Demonstration addressed in this Independent Exploratory Development (IED) project is the final selection of a subnet in response to a Transmit Service Request. The architectural description of the MC defines databases and performance measures used by this IED effort. In FY88, initial conclusions about the applicability of neural networks, fuzzy set methods, cost/value functions, and expert systems were investigated and documented. A Real Time Expert System (RTES), using subroutines that implement the decision techniques described, was selected as the best method for experimentation. A transportable, embeddable RTES shell (CLIPS) was chosen, and implementation of subnet selection algorithms began. An independent research effort for FY89 is also a spin-off of the FY88 IED effort, and is described. GRA

N90-10598# Cornell Univ., Ithaca, NY.
USING COMPUTER DESIGN AND SIMULATION TO IMPROVE MANUFACTURING PRODUCTIVITY Quarterly Status Report
John E. Hopcroft Jun. 1989 3 p
(Contract N00014-88-K-0591; ARPA Order 6419)
(AD-A210338) Avail: NTIS HC A01/MF A01 CSCL 13/8

The most significant development is the commitment to develop a uniform platform for specifying geometric objects and operations. The necessity for such a framework became obvious as the number of people in the project grew, and the reseach needed justification, and to avoid duplication of code. The platform, written in CLOS (Common Lisp Object System), will facilitate the use of various parallel architectures, and will allow programming at higher levels of abstraction, interchangeability of packages written at different institutions, and better documentation. The platform will include a geometric modeler, an algebra package, a utilities package (to include basic data structures and finite sets), a graphics package, and a finite element mesh generation package. Initial efforts will be focused on the geometric modeler and the algebra package. The finite element mesh generation package is an application that is built on top of these two packages. The utilities package will contain the basic data structures and other tools necessary for programming, and will be developed as needed. GRA

N90-10599# Aeronautical Research Labs., Melbourne (Australia).
A FORTRAN PROGRAM FOR THE CALCULATION OF THE CALIBRATION COEFFICIENTS OF A SIX-COMPONENT STRAIN GAUGE BALANCE Flight Mechanics Technical Memorandum
S. S. W. Lam Feb. 1989 55 p
(AD-A210375; ARL-FLIGHT-MECH-TM-410; DODA-AR-005-598)
Avail: NTIS HC A04/MF A01 CSCL 13/13

A computer program written in FORTRAN was developed to calculate the calibration coefficients of a six-component strain gauge balance. The method of Least Squares is used in the calculation procedures which do not require the components of the balance to be loaded independently. The procedures are, in fact, independent of the way the balance is loaded as long as the supplied load/output data provide sufficient information for the determination of the coefficients. The program incorporates several statistical estimations for the evaluation of the performance of the calibration process. It can therefore be used as an experimental tool for the investigation of different loading schemes which may be used to calibrate a strain gauge balance. GRA

N90-10600# Stanford Univ., CA. Systems Optimization Lab.
PRIMAL BARRIER METHODS FOR LINEAR PROGRAMMING
Aeneas Marxen Jun. 1989 80 p
(Contracts N00014-87-K-0142; DE-FG03-87ER-25030)
(AD-A210501; SU-SOL-89-6) Avail: NTIS HC A05/MF A01 CSCL 12/4

The linear program min c sub t sub x subject to Ax = b, x is greater or = 0, is solved by the projected Newton barrier method. The method consists of solving a sequence of subproblems of the form min c sub t sub x - micron sigma Ln x; subject to Ax = b. Extentions for upper bounds, free and fixed variables are given. A linear modification is made to the logarithmic barrier function, which results in the solution being bounded in all cases. It also facilitates the provision of a good starting point. The solution of each subproblem involves repeatedly computing a search direction and taking a step along this direction. Ways to find an initial feasible solution, step sizes and convergence criteria are discussed. Like other interior-point method for linear programming, this method solves a system of the form AH 1/AH A sub t sub q = y, where H is diagonal. This system can be very ill-conditioned and special precautions must be taken for the Cholesky factorization. The matrix A is assumed to be large and sparse. Data structures and algorithms for the sparse factorization are explained. In particular, the consequences of relatively dense columns in A are investigated

and a Schur-complement method is introduced to maintain the speed of the method in these cases. An implementation of the method was developed as part of the research. Results of extensive testing with medium to large problems are presented and the testing methodologies used are discussed. GRA

N90-10601# Teledyne Brown Engineering, Eatontown, NJ.
SOFTWARE METHODOLOGY CATALOG, SECOND EDITION, REVISION Technical Report, Apr. 1988 - Mar. 1989
Laurel VonGerichten, Marilyn Ginsberg, Richard Pirchner, and Richard Guilfoyle Mar. 1989 447 p
(Contract DAAB07-86-D-R001)
(AD-A210548; C01-091JB-0001-01) Avail: NTIS HC A19/MF A03 CSCL 12/5

This technical report provides a consolidated reference for software methods used over the total spectrum of software development. The primary objective is to provide, for each method included, a brief overview of the method and to give some insight into the underlying assumptions, the software development activities which it supports, and other characteristics associated with its use. A second objective is to provide sources for further information. The second edition of the catalog reports on 73 software methods. GRA

N90-10602*# National Aeronautics and Space Administration. Langley Research Center, Hampton, VA.
DOCUMENTATION OF THE CURRENT FAULT DETECTION, ISOLATION AND RECONFIGURATION SOFTWARE OF THE AIPS FAULT-TOLERANT PROCESSOR
David T. Lanning, Allen W. Shepard (Old Dominion Univ., Norfolk, VA.), and Sally C. Johnson Aug. 1987 31 p
(NASA-TM-89154; NAS 1.15:89154) Avail: NTIS HC A03/MF A01 CSCL 01B

Documentation is presented of the December 1986 version of the ADA code for the fault detection, isolation, and reconfiguration (FDIR) functions of the Advanced Information processing System (AIPS) Fault-Tolerant Processor (FTP). Because the FTP is still under development and the software is constantly undergoing changes, this should not be considered final documentation of the FDIR software of the FTP. Author

N90-10603# Massachusetts Inst. of Tech., Cambridge. Lab. for Computer Science.
THE IMPACT OF RECOVERY ON CONCURRENCY CONTROL
William E. Weihl Feb. 1989 21 p
(Contract N00014-83-K-0125; NSF CCR-87-16884)
(AD-A210828; MIT/LCS/TM-382) Avail: NTIS HC A03/MF A01 CSCL 12/5

It is widely recognized by practitioners that concurrency control an recovery for transaction systems interact in subtle ways. In most theoretical work, however, concurrency control and recovery are treated as separate, largely independent problems. The interactions between concurrency control and recovery are investigated. Two general recovery methods are considered for abstract data types, update-in-place and deferred-update. While each requires operations to conflict if they do not commute, the two recovery methods require subtly different notions of commutativity. A precise characterization is given of the conflict relations that work with each recovery method, and show that each permits conflict relations that the other does not. Thus, the two recovery methods place incomparable constraints on concurrency control. The analysis applies to arbitrary abstract data types, including those with operations that may be partial or non-deterministic. GRA

N90-10604# Massachusetts Inst. of Tech., Cambridge. Lab. for Computer Science.
AN INTRODUCTION TO INPUT/OUTPUT AUTOMATA
Nancy A. Lynch and Mark R. Tuttle Nov. 1988 27 p Revised
(Contracts N00014-83-K-0125; N00014-85-K-0168; NSF CCR-86-11442)
(AD-A210831; MIT/LCS/TM-373-Rev) Avail: NTIS HC A03/MF A01 CSCL 12/5

The input/output automation model was recently defined, in (LT1, LT2), as a tool for modeling concurrent and distributed discrete event systems of the sorts arising in computer science. Since its introduction, the model was used for describing and reasoning about several different types of systems, including network resource allocation algorithms, communication algorithms, concurrent database systems, shared atomic objects, and dataflow architectures. The model is introduced to researchers and is organized as follows. Section 2 contains an overview of the model. Section 3 defines the model formally and examines several illustrative examples concerning candy vending machines. Section 4 contains a second example, a leader election algorithm. Finally, Section 5 contains a survey of some of the uses that were so far made of the model. GRA

N90-10605# Massachusetts Inst. of Tech., Cambridge. Lab. for Computer Science.
TYPE RECONSTRUCTION WITH FIRST-CLASS POLYMORPHIC VALUES
James W. OToole and David K. Gifford May 1989 14 p
(Contract N00014-83-K-0125)
(AD-A210833; MIT/LCS/TM-380) Avail: NTIS HC A03/MF A01 CSCL 12/5

The first type reconstruction system which combines the implicit typing of ML with the full power of the explicity typed second-order polymorphic lambda calculus is presented. The system will accept ML-style programs, explicity typed programs, and programs that use explicit types for all first-class polymorphic values. This flexibility was accomplished by providing both generic and explicitly-quantified polymorphic types, as well as operators which convert between these two forms of polymorphism. This type reconstruction system is an integral part of the FX-89 programming language. A type reconstruction algorithm for the system is presented. The type reconstruction algorithm is proven sound and complete with respect to the formal typing rules. GRA

N90-10606# Massachusetts Inst. of Tech., Cambridge. Artificial Intelligence Lab.
DEPENDENCY-DIRECTED LOCALIZATION OF SOFTWARE BUGS
Ron I. Kuper May 1989 77 p Sponsored by IBM Corp.; NYNEX Corp.; and Siemens Corp.
(Contract N00014-88-K-0487; NSF IRI-86-16644)
(AD-A210837; AI-TR-1053) Avail: NTIS HC A05/MF A01 CSCL 12/5

A software bug manifests itself as a violated specification. Debugging is the process that culminates in repairing a program so that it satisfies its specification. An important part of debugging is localization, whereby the smallest region of the program that manifests the bug is found. The Debugging Assistant (DEBUSSI) is a system that localizes bugs by reasoning about logical dependencies. Via queries to the user and automated deduction, DEBUSSI manipulates the assumptions that underlie a bug manifestation, eventually localizing the bug to one particular assumption. At the same time DEBUSSI incrementally acquires specification information, thereby extending its understanding of the buggy program. As part of the Programmer's Apprentice, DEBUSSI will be useful for validating partial designs, as well as for testing fully implemented code. GRA

N90-10607# Institute for Defense Analyses, Alexandria, VA.
AEROSPACE SYSTEM UNIFIED LIFE CYCLE ENGINEERING PRODUCIBILITY MEASUREMENT ISSUES Final Report, Jan. 1988 - Sep. 1989
Dale E. Calkins, Richard S. Gaevert, Frederick J. Michel, and Karen J. Richter May 1989 177 p
(Contract MDA903-89-C-0003)
(AD-A210937; AD-E501132; IDA-P-2151; IDA/HQ-88-33817)
Avail: NTIS HC A09/MF A01 CSCL 05/1

The goal of the Unified Life Cycle Engineering (ULCE) program is to develop enhanced design environments that will allow supportability and producibility to be considered early in the product design cycle along with the usual factors of cost, performance,

and schedule. An investigation into methods for the incorporation of producibility issues in early design is reported. Producibility is a product characteristic inherent in its design denoting ease and economy of manufacture. Many aspects of producibility are judgmental in character. However, to design products that are properly balanced with regard to all of the ULCE design factors, these qualitative aspects of a design must be handled and methods of trading off such factors against quantitative factors such as performance and cost measures must be developed. Methods of measuring and evaluating factors related to producibility are discussed and a plan is presented for the development of a design environment of an aerospace design synthesis model with a producibility module. Included is a description of relevant design and manufacturing methodologies (e.g., Design for Manufacture and Assembly, Taguchi Methods, Quality Function Deployment, Statistical Process Control) and a discussion of the kinds of tools (hardware, software, and attitude) that can and have been established to ensure strong producibility characteristics in a product. In addition, an extensive bibliography is provided in an appendix. GRA

N90-10117*# Australian National Univ., Canberra.
OPTIMAL q-MARKOV COVER FOR FINITE PRECISION IMPLEMENTATION
Darrell Williamson and Robert E. Skelton (Purdue Univ., West Lafayette, IN.) *In* NASA. Langley Research Center, Proceedings of the Workshop on Computational Aspects in the Control of Flexible Systems, Part 2 May 1989 p 853-881 (For primary document see N90-10103 01-18)
Avail: NTIS HC A21/MF A03 CSCL 09B

N90-10546*# Microtronics Associates, Pittsburgh, PA.
PARALLEL ASYNCHRONOUS HARDWARE IMPLEMENTATION OF IMAGE PROCESSING ALGORITHMS Abstract Only
Darryl D. Coon and A. G. U. Perera *In* NASA. Ames Research Center, Vision Science and Technology at NASA: Results of a Workshop Aug. 1989 p 22 (For primary document see N90-10542 01-54)
(Contract NAS1-18645)
Avail: NTIS HC A04/MF A01 CSCL 09B

N90-10547*# National Aeronautics and Space Administration. Ames Research Center, Moffett Field, CA.
VISIONS OF VISUALIZATION AIDS: DESIGN PHILOSOPHY AND EXPERIMENTAL RESULTS Abstract Only
Stephen R. Ellis *In its* Vision Science and Technology at NASA: Results of a Workshop Aug. 1989 p 23 (For primary document see N90-10542 01-54)
Avail: NTIS HC A04/MF A01 CSCL 09B

N90-10568*# Odetics, Inc., Anaheim, CA.
INTENSITY DEPENDENT SPREAD PROCESSOR AND WORKSTATION Abstract Only
George Westrom *In* NASA. Ames Research Center, Vision Science and Technology at NASA: Results of a Workshop Aug. 1989 p 49 (For primary document see N90-10542 01-54)
Avail: NTIS HC A04/MF A01 CSCL 09B

62 COMPUTER SYSTEMS

Includes computer networks and special application computer systems.

N90-10608*# National Aeronautics and Space Administration. Pasadena Office, CA.
NETWORK OF DEDICATED PROCESSORS FOR FINDING LOWEST-COST MAP PATH Patent Application
Silvio P. Eberhardt, inventor (to NASA) (Jet Propulsion Lab., California Inst. of Tech., Pasadena.) 26 May 1989 12 p Prepared in cooperation with Jet Propulsion Lab., California Inst. of Tech., Pasadena
(Contract NAS7-918)
(NASA-Case-NPO-17716-1-CU; NAS 1.71:NPO-17716-1-CU; US-Patent-Appl-SN-357759) Avail: NTIS HC A03/MF A01 CSCL 09B

A method and associated apparatus are disclosed for finding the lowest cost path of several variable paths. The paths are comprised of a plurality of linked cost-incurring areas existing between an origin point and a destination point. The method comprises the steps of, connecting a purality of nodes together in the manner of the cost-incurring areas; programming each node to have a cost associated therewith corresponding to one of the cost-incurring areas; injecting a signal into one of the nodes representing the origin point; propagating the signal through the plurality of nodes from inputs to outputs; reducing the signal in magnitude at each node as a function of the respective cost of the node; and, starting at one of the nodes representing the destination point and following a path having the least reduction in magnitude of the signal from node to node back to one of the nodes representing the origin point whereby the lowest cost path from the origin point to the destination point is found. NASA

N90-10609 Syracuse Univ., Utica, NY.
A DECISION SUPPORT APPROACH TO THE FILE ALLOCATION PROBLEM IN A DISTRIBUTED COMPUTING SYSTEM Ph.D. Thesis
Debashish Ghosh 1988 285 p
Avail: Univ. Microfilms Order No. DA8907875

The file allocation problem in a distributed computing system involves the determination of the number of copies of each program/data file that must be maintained in the system, along with the computer nodes where these copies will be located. Available formulations for the file allocation problem incorporate either operating costs or system performance measures (e.g., response time), but not both, as design considerations. In addition, it is assumed that file access patterns and various cost factors remain unchanged over time. A decision support framework is provided for solving the file allocation problem. The proposed framework remedies the shortcomings of the available formulations, and explicitly recognizes the superior abilities of the human decision maker to perform complex tradeoffs (in this case between operating costs and response time). The proposed multi-period, multi-criteria methodology consists of three modules: an integer programming formulation, a system simulator, and a time-cost tradeoff module. To establish the suitability and applicability of the proposed approach, a prototype was developed and a sample problem was solved. Dissert. Abstr.

N90-10610*# National Aeronautics and Space Administration. Hugh L. Dryden Flight Research Facility, Edwards, CA.
THE AEROSPACE ENERGY SYSTEMS LABORATORY: HARDWARE AND SOFTWARE IMPLEMENTATION
Richard D. Glover and Nora ONeil-Rood Jul. 1989 21 p Presented at the 5th iRUG International Conference, Schaumberg, IL, 14-15 Nov. 1988
(NASA-TM-101706; H-1518; NAS 1.15:101706) Avail: NTIS HC A03/MF A01 CSCL 09B

For many years NASA Ames Research Center, Dryden Flight Research Facility has employed automation in the servicing of flight critical aircraft batteries. Recently a major upgrade to Dryden's computerized Battery Systems Laboratory was initiated to incorporate distributed processing and a centralized database. The new facility, called the Aerospace Energy Systems Laboratory (AESL), is being mechanized with iAPX86 and iAPX286 hardware running iRMX86. The hardware configuration and software structure for the AESL are described. Author

N90-10611# California Inst. of Tech., Pasadena. Concurrent Computation Program.
APPLICATIONS OF PARALLEL SUPERCOMPUTERS: SCIENTIFIC RESULTS AND COMPUTER SCIENCE LESSONS
Geoffrey C. Fox 12 Jul. 1989 92 p Presented at the Inaugural Symposium for Center for Science and Technology, Syracuse, NY, 2 Mar. 1989 Sponsored by IBM
(Contract DE-FG03-85ER-25009; NSF CCR-88-09615; NSF

ACS-87-19502)
(DE89-016385; DOE/ER-25009/806; CONF-8903158-1) Avail: NTIS HC A05/MF A01

Parallel Computing has come of age with several commercial and inhouse systems that deliver supercomputer performance. We illustrate this with several major computations completed or underway at Caltech on hypercubes, transputer arrays and the SIMD Connection Machine CM-2 and AMT DAP. Applications covered are lattice gauge theory, computational fluid dynamics, subatomic string dynamics, statistical and condensed matter physics, theoretical and experimental astronomy, quantum chemistry, plasma physics, grain dynamics, computer chess, graphics ray tracing, and Kalman filters. We use these applications to compare the performance of several advanced architecture computers including the conventional CRAY and ETA-10 supercomputers. We describe which problems are suitable for which computers in the terms of a matching between problem and computer architecture. This is part of a set of lessons we draw for hardware, software, and performance. We speculate on the emergence of new academic disciplines motivated by the growing importance of computers. DOE

N90-10612# Oregon State Univ., Newport. Marine Science Center.
PARALLEL PROCESSING AND LEARNING IN SIMPLE SYSTEMS Final Report, 10 Jan. 1986 - 14 Jan. 1989
George J. Mpitsos 15 Mar. 1989 6 p
(Grant AF-AFOSR-0076-86; AF Proj. 2312)
(AD-A210225; AFOSR-89-0809TR) Avail: NTIS HC A02/MF A01 CSCL 05/8

Work over the three year tenure of this grant has dealt with interrelated studies of: (1) neuropharmacology, (2) behavior, and (3) distributed and/or parallel processing in the generation of variable motor patterns in the buccal-oral system of the sea slug Pleurobranchaea californica. Computer simulations of simple neutral networks were undertaken to examine neurointegrative principles that could not be examined in biological preparations. The simulation work has set the basis for further simulations dealing with networks having characteristics relating to real neurons. All of the work had the goal of developing interdisciplinary tools for understanding the scale-independent problem of how individuals, each possessing only local knowledge of group activity, act within a group to produce different and variable adaptive outputs, and, in turn, of how the group influences the activity of the individual. The pharmacologic studies had the goal of developing biochemical tools with which to identify groups of neurons that perform specific tasks during the production of a given behavior but are multifunctional by being critically involved in generating several different behaviors. GRA

N90-10613# BBN Systems and Technologies Corp., Cambridge, MA.
TOOLS FOR APPLICATION DEVELOPMENT IN HETEROGENEOUS DISTRIBUTED ENVIRONMENTS
G. Falk, K. Anderson, M. Thome, M. Dean, and T. Reinhardt 29 Mar. 1989 50 p Sponsored by DARPA, Arlington, VA
(AD-A210238; BBN-6972) Avail: NTIS HC A03/MF A01 CSCL 12/5

Military software systems based on distributed heterogeneous computing resources are being deployed at an increasing rate. Existing networks, distributed operating systems, and software tools provide the basic elements of a system substrate for applications development in such environments. To improve programmer productivity, however, it is necessary to enhance these existing facilities with higher level programming constructs oriented toward concurrent programming in the large. The Tool for Large-grain Concurrency (TLC), described provides a basic set of such capabilities. TLC is based on COMMON LISP and CLOS (the Common Lisp Object System), translates high level functional programs into operations of the underlying systems, and coordinates concurrent execution of these subsystems on distributed heterogeneous resources. The usefulness of TLC was evaluated in the domain of the CASES decision support system of the Fleet Command Center Battle Management Program. GRA

N90-10614# Sparta, Inc., McLean, VA.
DDN TRUSTED GUARD GATEWAY: TRUSTED GUARD GATEWAY (TGG) TECHNOLOGY ASSESSMENT, PHASE 2 Final Report, 6 Jun. 1988 - 2 Feb. 1989
D. Solo, C. Eldridge, T. Rivers, G. Ellingwood, and I. Mainzer 2 Feb. 1989 106 p
(Contract DCA100-87-C-0095)
(AD-A210248) Avail: NTIS HC A06/MF A01 CSCL 12/7

The results are provided of a technology assessment effort made for the purpose of determining the acquisition and/or development potential of a specialized gateway that would interconnect communities with differing security characteristics (such as allowing multilevel secure, classified hosts operating at the unclassified level to communicate with hosts in the unclassified segment.) The Trusted Guard Gateway (TGG) definition and requirements as outlined in Phase 1 of this effort are reviewed. The Technology Assessment approach and methodology provides profiles of the various trusted operating system and gateway vendors surveyed are detailed. An overview is presented of an alternative approach to the TGG in the form of an application relay. GRA

N90-10615# Stanford Univ., CA. Computer Systems Lab.
SHARED MEMORY VERSUS MESSAGE PASSING ARCHITECTURES: AN APPLICATION BASED STUDY
Margaret Martonosi and Anoop Gupta 9 Nov. 1988 19 p
(Contract N00014-87-K-0828)
(AD-A210312) Avail: NTIS HC A03/MF A01 CSCL 12/6

The diminishing differences between the hardware structure of shared memory and message passing parallel computers mandate a new evaluation of the tradeoffs these architectures impose on the development and performance of applications. In a message passing computer, some message traffic is used to perform interprocessor updates which maintain consistency between the various processors data. Consider this traffic to be analogous to global bus traffic needed in shared memory computer for hardware cache consistency. Using Locus-Route, a global router for standard cell, as a case study, we investigate the level of traffic required to maintain consistency of data with each of the two architectures. By explicitly varying the frequency of interprocessor updates, the level of traffic in the message passing approach can be reduced to as little as 1 percent of the traffic in the shared memory approach while still obtaining solution quality within 10 percent of the quality given by the shared memory version. We show that exploiting locality, in the way wires to be routed are assigned to processors, can further lower this message traffic by as much as 67 percent. However, the degree to which locality can be exploited may be limited by the opposing requirement that the application be load balanced, as well as by limited locality in the data set. GRA

N90-10616# Stanford Univ., CA. Computer Systems Lab.
EXPLORING THE BENEFITS OF MULTIPLE HARDWARE CONTEXTS IN A MULTIPROCESSOR ARCHITECTURE: PRELIMINARY RESULTS
Wolf-Detrich Weber and Anoop Gupta 16 Nov. 1988 10 p Sponsored in part by Digital Equipment Corp., Hudson, MA
(Contract N00014-87-K-0828)
(AD-A210349) Avail: NTIS HC A02/MF A01 CSCL 12/6

A fundamental problem that any scalable multiprocessor must address is the ability to tolerate high latency memory operations. The extent to which multiple hardware contexts per processor can help to mitigate the negative effects of high latency is explored. In particular, the performance is evaluated of a directory-based cache coherent multiprocessor using memory reference traces obtained from three parallel applications. The case is explored where there are a small fixed number (2 to 4) of hardware contexts per processor and the context switch overhead is low. In contrast to previously proposed approaches, a simple context-switch

criterion is used, namely a cache miss or a write-hit to shared data. The results show that the effectiveness of multiple contexts depends on the nature of the applications, the context switch overhead, and the inherent latency of the machine architecture. Given reasonably low overhead hardware context switches, it is shown that two of four contexts can achieve substantial performance gains over a single context. For one application, the processor utilization increased by about 65 percent with two contexts and by about 100 percent with four contexts. GRA

N90-10617# SRI International Corp., Menlo Park, CA.
THE REWRITE RULE MACHINE PROJECT Final Report
Joseph A. Goguen, Jose Meseguer, Sany Leinwand, Timothy Winkler, and Hitoshi Aida 1 May 1989 24 p
(Contracts N00014-85-C-0417; N00014-88-C-0450; NSF CCR-87-07155)
(AD-A210528; SRI-ECU-1243) Avail: NTIS HC A03/MF A01 CSCL 12/5

Current generation parallel machines are typically either coarse-grain or fine-grain. Each design has certain limits, either in the amount of parallelism that it can effectively exploit, or else in the types of problem for which it is suitable. For example, only very homogeneous computations can make efficient use of today's fine-grained machines. However, many complex computations are locally homogeneous, but not globally homogeneous. The Rewrite Rule Machine (RRM) resolves this dilemma through its hierarchical architecture, which has several levels of organization. The lowest level is the cell, which stores a token and pointers to other cells; this organization avoids the von Neumann memory access bottleneck. Next, an ensemble contains many cells, representing a complex data structure to which rewrite rules are applied under the direction of a common controller. A cluster consists of many ensembles which cooperate in larger computations. Ensembles support fine-grained homogeneous parallelism, while clusters support coarse-grained inhomogeneous parallelism. This multi-grained parallelism allows the RRM to exploit the local homogeneity that is typical of many complex computations. The RRM can support the efficient execution of many different programming paradigms by compiling them into its concurrent rewriting model of computation. GRA

N90-10549*# National Aeronautics and Space Administration. Goddard Space Flight Center, Greenbelt, MD.
COMPUTATION AND PARALLEL IMPLEMENTATION FOR EARLY VISION Abstract Only
J. Anthony Gualtieri *In* NASA. Ames Research Center, Vision Science and Technology at NASA: Results of a Workshop Aug. 1989 p 25-26 (For primary document see N90-10542 01-54)
Avail: NTIS HC A04/MF A01 CSCL 09B

63 CYBERNETICS

Includes feedback and control theory, artificial intelligence, robotics and expert systems.

For related information see also *54 Man/System Technology and Life Support.*

N90-10618*# National Aeronautics and Space Administration. Langley Research Center, Hampton, VA.
OPTIMIZED RESOLVED RATE CONTROL OF SEVEN-DEGREE-OF-FREEDOM LABORATORY TELEROBOTIC MANIPULATOR (LTM) WITH APPLICATION TO THREE-DIMENSIONAL GRAPHICS SIMULATION
L. Keith Barker and William S. McKinney, Jr. Washington Oct. 1989 80 p
(NASA-TP-2938; L-16562; NAS 1.60:2938) Avail: NTIS HC A05/MF A01 CSCL 09B

The Laboratory Telerobotic Manipulator (LTM) is a seven-degree-of-freedom robot arm. Two of the arms were delivered to Langley Research Center for ground-based research to assess the use of redundant degree-of-freedom robot arms in space operations. Resolved-rate control equations for the LTM are derived. The equations are based on a scheme developed at the Oak Ridge National Laboratory for computing optimized joint angle rates in real time. The optimized joint angle rates actually represent a trade-off, as the hand moves, between small rates (least-squares solution) and those rates which work toward satisfying a specified performance criterion of joint angles. In singularities where the optimization scheme cannot be applied, alternate control equations are devised. The equations developed were evaluated using a real-time computer simulation to control a 3-D graphics model of the LTM. Author

N90-10619# Rutgers - The State Univ., New Brunswick, NJ.
REGULATION OF NONLINEAR AND GENERALIZED LINEAR SYSTEMS Final Report, 15 Jul. 1985 - 14 Jul. 1988
Eduardo D. Sontag 14 Sep. 1988 11 p
(Grant AF-AFOSR-0247-85; AF Proj. 2304)
(AD-A207725; AFOSR-89-0529TR) Avail: NTIS HC A02/MF A01 CSCL 12/4

Research during the grant period can be classified into these areas: Equilinearization, Sampling and Discrete Time Controllability, Input/Output Equations, Input/Output Stability, Families of Systems, Image Processing and Robotics, Nonlinear Stabilization, Computational Complexity in Control, and Neural Networks and Piecewise Linear Control. The progress achieved in each of these areas is described. GRA

N90-10620 Illinois Univ., Urbana-Champaign.
ADAPTIVE ROBUST CONTROL Ph.D. Thesis
Salvatore Joseph Cusumano 1988 90 p
Avail: Univ. Microfilms Order No. DA8908661

An approach is presented for the problem of adaptive robust control. The essential idea involved is to fragment the modeling uncertainty in a physical plant into small families of plant models for which robust linear time-invariant controllers can be readily designed. A convex combination of these controllers is then implemented, the parameters of which are tuned based on error measurements. Using this approach, absolute bounds are provided on the ability to adaptively stabilize against unmodeled dynamics. These computations enable the nonlinear feedback to be quantitively compared with linear feedback in the context of robust stabilization problems. These results offer support to a maxim which holds in broad generality: the accuracy to within which a physical plant is modeled determines the type of feedback best suited to control that plant. Dissert. Abstr.

N90-10621# Northeast Artificial Intelligence Consortium, Syracuse, NY.
NORTHEAST ARTIFICIAL INTELLIGENCE CONSORTIUM ANNUAL REPORT FOR 1987. VOLUME 5: BUILDING AN INTELLIGENT ASSISTANT: THE ACQUISITION, INTEGRATION AND MAINTENANCE OF COMPLEX DISTRIBUTED TASKS Interim Report, Dec. 1986 - Dec. 1987
Victor Lesser, W. Bruce Croft, and Beverly Woolf (Massachusetts Univ., Amherst.) Mar. 1989 591 p
(Contract F30602-85-C-0008; AF Proj. 2304; AF Proj. 5581)
(AD-A210330; RADC-TR-88-324-Vol-5) Avail: NTIS HC A25/MF A04 CSCL 12/9

The Northeast Artificial Intelligence Consortium (NAIC) was created to conduct pertinent research in artificial intelligence and to perform activities ancillary to this research. The topics covered in general are: versatile expert system for equipment maintenance distributed AI for communications system control, automatic photo interpretation, time oriented problem solving, speech understanding systems, knowledge base maintenance, hardware architectures for very large systems, knowledge based reasoning and planning, and a knowledge acquisition, assistance, and explanation system. The specific topic for this volume is the development of intelligent interfaces to support cooperating computer users in their interactions with a computer. GRA

N90-10622# Northeast Artificial Intelligence Consortium, Syracuse, NY.
NORTHEAST ARTIFICIAL INTELLIGENCE CONSORTIUM ANNUAL REPORT FOR 1987. VOLUME 7, PART A: TIME ORIENTED PROBLEM SOLVING Interim Report, Dec. 1986 - Dec. 1987
James F. Allen (Rochester Univ., NY.) Mar. 1989 342 p
(Contract F30602-85-C-0008; AF Proj. 5581)
(AD-A210331; RADC-TR-88-324-Vol-7-Pt-A) Avail: NTIS HC A15/MF A02 CSCL 12/9

The Northeast Artificial Intelligence Consortium (NAIC) was created to conduct pertinent research in artificial intelligence. The topics covered in general are: versatile expert system for equipment maintenance, distributed AI for communications system control, automatic photo interpretation, time oriented problem solving, speech understanding systems, knowledge base maintenance, hardware architectures for very large systems, knowledge-based reasoning and planning, and a knowledge acquisition, assistance, and explanation system. The specific topic for this volume is a model theory and axiomatization of a logic for reasoning about planning in domains of concurrent actions. GRA

N90-10623# APTEK, Inc., Scottsdale, AZ.
SCIENTIFIC AND TECHNICAL REPORT VOICE ACTIVATED GUN TURRENT CONTROL Final Report, Oct. 1987 - Aug. 1988
Frank Toney 20 Aug. 1988 11 p
(Contract DAAA21-82-C-0184)
(AD-A210350) Avail: NTIS HC A02/MF A01 CSCL 25/4

The objective of the research project was to determine the feasibility of using a Low Memory Requirement Voice Recognizer to activate gun turrent control. Such a system would enable a single individual to manually pilot the helicopter while activating gun functions by voice command. To develop an effective voice recognition system, major limitations of existing voice recognition technology needed to be overcome. The major limitations of current voice recognition systems are: (1) they are normally capable of recognizing only one speaker and one mode of speaking, (2) recognition time is slow when working with sizeable vocabularies, (3) they require extensive hardware with resultant excessive weight and size limitations (for aircraft applications), and (4) they are difficult to interface with, and access artificial intelligence/expert software systems. GRA

N90-10624# Carnegie-Mellon Univ., Pittsburgh, PA. Robotics Inst.
SOME RESULTS ON LEARNING
B. K. Natarajan Feb. 1989 29 p
(AD-A210591; CMU-RI-TR-89-6) Copyright Avail: NTIS HC A03/MF A01 CSCL 12/1

This paper presents some formal results on learning. In particular, it concerns algorithms that learn sets and functions from examples. We seek conditions necessary and sufficient for learning over a range of probabilistic models for such algorithms. The motivation behind the study is a need to better understand the class of problems known as concept learning problems in the artificial intelligence literature. GRA

N90-10625# Texas Univ., Austin. Applied Research Labs.
THE APPLICABILITY AND LIMITATIONS OF EXPERT SYSTEM SHELLS
James K. Kroger 30 May 1989 42 p
(AD-A210801; ARL-TR-89-32) Avail: NTIS HC A03/MF A01 CSCL 12/5

As expert system technology has moved from the laboratory into the field, tools for building expert systems have become commercially available. This report reviews the major aspects of these tools, or shells. It discusses in-depth two sample projects using expert systems shells. Finally, it discusses problems which exist with current expert system shells, and makes recommendations for overcoming them. GRA

N90-10626# Transition Research, Inc., Danbury, CT.
ROBOT VEHICLE VIDEO IMAGE COMPRESSION, PHASE 1 Final Report, Jul. 1988 - Jan. 1989
Carl F. Weiman Jan. 1989 71 p
(Contract DAAE07-88-C-R068)
(AD-A210974) Avail: NTIS HC A04/MF A01 CSCL 23/3

This Phase 1 SBIR study analyzed and simulated in software a new approach to image data compression for remote vehicle driving. Results show feasibility for 1,000-to-1 compression rates for full color, wide field of view, real time imagery. The approach is based on a three stage process. The first stage consists of reducing resolution of peripheral imagery to match the drop in human visual resolution away from the center of view. This is accomplished by resampling video camera output in real time. The second stage consists of coding color and contrast edges in separate channels. The third stage consists of applying a simple, efficient data compression technique. A hybrid DCT/DPCM data compression method proved to be the most suitable. All three stages of the compression process and reconstruction of imagery can be implemented in real time on equipment which can be compactly mounted in remote vehicles. This is a fundamentally new and valuable attack on the problem of remote driving, which has been with us for decades. The solution is critical for deployment of Army remote systems. GRA

N90-10627# Army Tank-Automotive Systems Development Center, Warren, MI.
ROBOTIC VEHICLE MESSAGE FORMAT Final Report
Daniele Mariani and Yue Min Wong (FMC Corp., Santa Clara, CA.) Jul. 1989 59 p
(AD-A210996; TACOM-TR-13458) Avail: NTIS HC A04/MF A01 CSCL 12/9

The digital message format described in this report will be used in the following robotic vehicles/systems: (1) Robotic Command Center (RCC); (2) Tech-base Enhancements for Autonomous Machines (TEAM); (3) Robotic Wiesels; and (4) The United Kingdom's Mobile Advanced Research and Development Initiative (MARDI). Robotic vehicle systems requiring or desiring compatibility with Army assets should consider using the robotic vehicle message format (RVMF). For the past decade, different agencies throughout the Department of Defense (DOD) and industry have been involved in the development of unmanned ground-vehicle systems. Most of these vehicle systems were designed to meet certain requirements. Communications interoperability between systems was not one of these requirements. As the effort to develop unmanned vehicle systems matures and increases in magnitude, communications interoperability between the different systems has become very desirable. This is because systems which can talk to each other have the potential to allow flexible testing in the development phase, and to make possible more effective deployment of these systems once they are mature enough to be fielded. GRA

N90-10628# Columbia Univ., New York, NY. Dept. of Mechanical Engineering.
THE DEVELOPMENT OF AN EXPERT SYSTEM FOR THE CREATIVE DESIGN OF MECHANISMS Report, 1 May 1986 - 30 Apr. 1989
Ferdinand Freudenstein and David A. Hoeltzel 26 Jun. 1989 114 p
(Contract DAAL03-86-K-0071)
(AD-A211115; ARO-23439.6-EG) Avail: NTIS HC A06/MF A01 CSCL 12/9

A unified design methodology has been developed for the creative design of mechanisms. This is based on an abstract representation of the kinematic structure of mechanisms, which we have called the stratified representation of mechanisms. This transforms the basic structure of a mechanism into an essentially unique spanning tree with a minimum number of edges, each associated with a fundamental loop. In this fashion hundreds of thousands of mechanisms have been generated automatically, thus providing a creative design tool of extraordinary power and efficiency. The same basic approach has been developed for the

automatic determination of favorable mechanism dimensions by means of algorithms for the determination of the rotatability and assemblability of the links, while eliminating crossing links. GRA

64 NUMERICAL ANALYSIS

Includes iteration, difference equations, and numerical approximation.

N90-10629# Naval Postgraduate School, Monterey, CA.
FINITE METHODS FOR A NONLINEAR ALLOCATION PROBLEM Technical Report, Oct. 1987 - Sep. 1988
Alan R. Washburn Apr. 1989 20 p
(AD-A209719; NPS55-89-03) Avail: NTIS HC A03/MF A01 CSCL 12/3

The author considers the problem of allocating m resources to n tasks. The potential effectiveness, y(j) for the jth task is a linear function of the allocations to that task, and the objective function is a convex function f (y sub 1 ,..., y sub n) to be minimized. Two finite algorithms for obtaining an optimal solution are proposed and evaluated. GRA

N90-10630# National Aerospace Lab., Tokyo (Japan).
GRID GENERATION PROCEDURE USING THE INTEGRAL EQUATION METHOD
Susumu Takanashi Dec. 1988 12 p In JAPANESE; ENGLISH summary
(NAL-TR-1009; ISSN-0389-4010) Avail: NTIS HC A03/MF A01

A grid generation method for arbitrary aircraft configurations, based on the singular integral equation for electrostatic fields, is presented. The electrostatic field can be visually represented by two families of lines, i.e., electrostatic potential and electrostatic force lines, which can also be utilized as one of the most promising computational grids. The singular integral equation is numerically solved by dividing the boundaries including body surface into a number of small triangular elements, as in the standard panel method. Typical examples obtained by the present method are also presented. Author

N90-10631*# Institute for Computer Applications in Science and Engineering, Hampton, VA.
A HIGH-ORDER LAGRANGIAN-DECOUPLING METHOD FOR THE INCOMPRESSIBLE NAVIER-STOKES EQUATIONS Final Report
Lee-Wing Ho, Yvon Maday, Anthony T. Patera, and Einar M. Ronquist (Massachusetts Inst. of Tech., Cambridge.) Sep. 1989 48 p Presented at the ICOSAMOM Meeting, 1989
(Contracts NAS1-18605; N00014-89-J-1610; N00014-88-K-0188; NSF ASC-88-06925)
(NASA-CR-181903; NAS 1.26:181903; ICASE-89-57) Avail: NTIS HC A03/MF A01 CSCL 12A

A high-order Lagrangian-decoupling method is presented for the unsteady convection-diffusion and incompressible Navier-Stokes equations. The method is based upon: (1) Lagrangian variational forms that reduce the convection-diffusion equation to a symmetric initial value problem; (2) implicit high-order backward-differentiation finite-difference schemes for integration along characteristics; (3) finite element or spectral element spatial discretizations; and (4) mesh-invariance procedures and high-order explicit time-stepping schemes for deducing function values at convected space-time points. The method improves upon previous finite element characteristic methods through the systematic and efficient extension to high order accuracy, and the introduction of a simple structure-preserving characteristic-foot calculation procedure which is readily implemented on modern architectures. The new method is significantly more efficient than explicit-convection schemes for the Navier-Stokes equations due to the decoupling of the convection and Stokes operators and the attendant increase in temporal stability. Numerous numerical examples are given for the convection-diffusion and Navier-Stokes equations for the particular case of a spectral element spatial discretization. Author

N90-10632# Lawrence Livermore National Lab., CA. Computing and Mathematics Research Div.
NUMERICAL METHODS FOR DIFFERENTIAL-ALGEBRAIC EQUATIONS: CURRENT STATUS AND FUTURE DIRECTIONS
Linda R. Petzold 20 Jun. 1989 17 p Presented at the Conference on Computational Ordinary Differential Equations, London, United Kingdom, 3-7 Jul. 1989 Submitted for publication
(Contract W-7405-eng-48)
(DE89-015116; UCRL-101209; CONF-8907106-2) Avail: NTIS HC A03/MF A01

Many physical systems are naturally described as systems of differential-algebraic equations (DAEs). These types of systems occur in the modeling of electrical networks, flow of incompressible fluids, control, mechanical systems subject to constraints, and in many other applications. This class of problems include systems which are in many ways quite different from ODEs. Some of the recent developments in the numerical solution of DAE systems, including problem structure and formulation, convergence and order results for multistep and Runge-Kutta methods, and general purpose codes are outlined. Finally, some directions are indicated for future progress. DOE

N90-10633# International Centre for Theoretical Physics, Trieste (Italy).
FINDING ISOLATED ZERO POINTS OF COMPLEX POLYNOMIAL MAPPINGS
Senlin Xu Dec. 1988 16 p Submitted for publication
(DE89-617523; IC-88/403) Avail: NTIS (US Sales Only) HC A03/MF A01

At first the properties of isolated zero points of complex polynomial mappings are discussed using the integral expression of a degree of C sup 1 mapping, Sard's Theorems and homotopy. Then we prove that for almost every complex polynomial mapping P:C sup n yields C sup n, the zero set H sup -1 (0) of the homotopy H(z,t) = tP(z) + (1-t)Q(z) consists of s = PI (sub j = 1)(sup n) s sub j disjoint differential curves, and the zero set phi sub delta (sub j) sup -1 (0) of its piecewise linear approximation phi sub delta (sub j) consists of some broken lines which do not meet (nu)-dimensional simplexes (0 is less than or = nu is less than or = to 2n-1) where Q(z) = (Q sub 1(z),...,Q sub n (z)), Q sub j (z) = z sub j (sup sj) - b sub j sup sj, b sub j is not = 0, j = 1,...,n. When (lim sub j yields infinity delta sub j = 0), these broken lines tend to corresponding differential curves in H sup -1 (0). DOE

N90-10634# International Centre for Theoretical Physics, Trieste (Italy).
EXTENDED WEYL GROUP FOR KAC-MOODY ALGEBRAS
V. K. Dobrev Dec. 1988 15 p Presented at the 17th International Conference on Differential Geometric Methods in Theoretical Physics, Chester, United Kingdom, Aug. 1988 Submitted for publication
(DE89-617525; IC-88/419) Avail: NTIS (US Sales Only) HC A03/MF A01

An extended Weyl group W sup e is introduced for the highest weight modules over A sub 1 sup (1). This group is the direct product of the standard affine Weyl (or Weyl-Kac) group W and a new group W sub a. The latter was introduced recently in order to rewrite the character formulae for certain factor modules of singular Verma modules (i.e., Verma modules for which the central charge is equal to minus the dual Coxeter number) in the form of the classical Weyl character formula for the finite-dimensional irreducible representations of semisimple Lie algebras (resp. Weyl-Kac character formula for the integrable highest weight modules over affine Kac-Moody algebras) so that W sub a was playing the role of the usual Weyl group (resp. affine Weyl group). The extended group W sup e was used to rewrite in a similar manner the characters of factor modules of a larger class of Verma modules including also all Verma modules with integral highest weights. Thus the new formula includes as partial cases the Weyl-Kac character formula and the character formulae

obtained. The conjecture was also made that the formulae holds for any affine Kac-Moody algebra. DOE

N90-10635*# National Aeronautics and Space Administration. Lewis Research Center, Cleveland, OH.
QUOTIENT-DIFFERENCE TYPE GENERALIZATIONS OF THE POWER METHOD AND THEIR ANALYSIS
Avram Sidi and William F. Ford Sep. 1989 18 p Prepared in cooperation with Technion-Israel Inst. of Tech., Haifa
(NASA Order C-99066-G)
(NASA-TM-102361; ICOMP-89-25; E-5077; NAS 1.15:102361)
Avail: NTIS HC A03/MF A01 CSCL 12A

The recursion relations that were proposed by W. F. Ford and A. Sidi (Appl. Numer. Math, 4 (1988), pp. 477-489) for implementing vector extrapolation methods are used for devising generalizations of the power method for linear operators. These generalizations are shown to produce approximations to largest eigenvalues of a linear operator under certain conditions. They are similar in form to the quotient-difference algorithm and share similar convergence properties with the latter. These convergence properties also resemble those obtained for the basic LR and QR algorithms. Finally, it is shown that the convergence rate produced by one fo these generalizations is twice as fast for normal operators as it is for nonnormal operators. Author

N90-10636# National Inst. of Standards and Technology, Gaithersburg, MD. Applied and Computational Mathematics Div.
ON THE EXPECTED COMPLEXITY OF THE THREE-DIMENSIONAL VORONOI DIAGRAM
Javier Bemal May 1989 23 p
(PB89-209332; NISTIR-89/4100) Avail: NTIS HC A03/MF A01 CSCL 12A

Let S be a set of n sites chosen independently from a uniform distribution in a cube in three-dimensional Euclidean space. Work by Bentley, Weide and Yao is extended to show that the Voronoi diagram for S has an expected O(n) number of faces. A consequence of the proof of the result is that the Voronoi diagram for S can be constructed in expected O(n) time. Finally, it is shown that with the exception of at most an expected O(n sup(2/3)) number of polyhedra, each polyhedron in the Voronoi diagram for S has an expected constant number of faces. GRA

N90-10637*# Institute for Computer Applications in Science and Engineering, Hampton, VA.
ON THE COEFFICIENTS OF DIFFERENTIATED EXPANSIONS OF ULTRASPHERICAL POLYNOMIALS Final Report
Andreas Karageorghis (Southern Methodist Univ., Dallas, TX.) and Timothy N. Phillips Sep. 1989 11 p Prepared in cooperation with University Coll. of Wales, Aberystwyth Submitted for publication
(Contract NAS1-18605)
(NASA-CR-181913; ICASE-89-65; NAS 1.26:181913) Avail: NTIS HC A03/MF A01 CSCL 12A

A formula expressing the coefficients of an expression of ultraspherical polynomials which has been differentiated an arbitrary number of times in terms of the coefficients of the original expansion is proved. The particular examples of Chebyshev and Legendre polynomials are considered. Author

N90-10638*# Institute for Computer Applications in Science and Engineering, Hampton, VA.
AN ITERATIVE METHOD FOR SYSTEMS OF NONLINEAR HYPERBOLIC EQUATIONS Final Report
Jeffrey S. Scroggs Aug. 1989 15 p Submitted for publication
(Contract NAS1-18605)
(NASA-CR-181919; NAS 1.26:181919; ICASE-89-62) Avail: NTIS HC A03/MF A01 CSCL 12A

An iterative algorithm for the efficient solution of systems of nonlinear hyperbolic equations is presented. Parallelism is evident at several levels. In the formation of the iteration, the equations are decoupled, thereby providing large grain parallelism. Parallelism may also be exploited within the solves for each equation. Convergence of the interation is established via a bounding function argument. Experimental results in two-dimensions are presented. Author

N90-10639*# Institute for Computer Applications in Science and Engineering, Hampton, VA.
SHOCK CAPTURING BY THE SPECTRAL VISCOSITY METHOD Final Report
Eitan Tadmor Sep. 1989 15 p Presented at the ICOSAHOM Meeting, Italy, Jun. 1989 Submitted for publication
(Contract NAS1-18605; BSF-85-00346)
(NASA-CR-181920; NAS 1.26:181920; ICASE-89-67) Avail: NTIS HC A03/MF A01 CSCL 12A

A main disadvantage of using spectral methods for nonlinear conservation laws lies in the formation of Gibbs phenomenon, once spontaneous shock discontinuities appear in the solution. The global nature of spectral methods than pollutes the unstable Gibbs oscillations overall the computational domain, and the lack of entropy dissipation prevents convergences in these cases. The Spectral Viscosity method, which is based on high frequency dependent vanishing viscosity regularization of the classical spectral methods is discussed. It is shown that this method enforces the convergence of nonlinear spectral approximations without sacrificing their overall spectral accuracy. Author

N90-10640*# Institute for Computer Applications in Science and Engineering, Hampton, VA.
NUMERICAL OPTIMIZATION IN HILBERT SPACE USING INEXACT FUNCTION AND GRADIENT EVALUATIONS Final Report
Richard G. Carter Jun. 1989 25 p Submitted for publication
(Contract NAS1-18605)
(NASA-CR-181926; NAS 1.26:181926; ICASE-89-45) Avail: NTIS HC A03/MF A01 CSCL 12A

Trust region algorithms provide a robust iterative technique for solving non-convex unstrained optimization problems, but in many instances it is prohibitively expensive to compute high accuracy function and gradient values for the method. Of particular interest are inverse and parameter estimation problems, since function and gradient evaluations involve numerically solving large systems of differential equations. A global convergence theory is presented for trust region algorithms in which neither function nor gradient values are known exactly. The theory is formulated in a Hilbert space setting so that it can be applied to variational problems as well as the finite dimensional problems normally seen in trust region literature. The conditions concerning allowable error are remarkably relaxed: relative errors in the gradient error condition is automatically satisfied if the error is orthogonal to the gradient approximation. A technique for estimating gradient error and improving the approximation is also presented. Author

N90-10641# Stanford Univ., CA. Dept. of Statistics.
IMPROVED ESTIMATION OF THE DISTURBANCE VARIANCE IN A LINEAR REGRESSION MODEL
Alan E. Gelfand and Dipak K. Dey 11 Jul. 1989 14 p
(Contract N00014-89-J-1627)
(AD-A210272; TR-418) Avail: NTIS HC A03/MF A01 CSCL 12/3

This paper considers estimation of the disturbance variance in a linear regression model. A new class of improved estimators is obtained by extending results dating to Stein (1964). These estimators dominate the ordinary least square estimator under squared error loss. GRA

N90-10642# Otago Univ., Dunedin (New Zealand). Dept. of Mathematics and Statistics.
ON THE 2-EXTENDABILITY OF PLANAR GRAPHS
D. A. Holton, Dingjun Lou, and Michael D. Plummer (Vanderbilt Univ., Nashville, TN.) 1989 24 p
(Contract N00014-85-K-0488; UGC-32-635; NSF INT-85-21818)
(AD-A210289) Avail: NTIS HC A03/MF A01 CSCL 12/1

Some sufficient conditions for the 2-extendability of k-connected k-regular (k greater than or = 3) planar graphs are given. In

particular, it is proved that for k greater than or = 3, a k-connected k-regular planar graph with each cyclic cutset of sufficiently large size is 2-extendable. All graphs are finite, undirected, connected and simple, although some parallel edge situations will occur after some contractions are made. However, any loops formed by these contractions will be deleted. Let nu and n be positive integers with n less than or = (v - 2)/2 and let G be a graph with nu vertices and epsilon edges having a perfect matching. The graph G is said to be n-extendable if every matching of size n in G lies in a perfect matching of G. GRA

N90-10643# Vanderbilt Univ., Nashville, TN. Dept. of Mathematics.
EXTENDING MATCHINGS IN PLANAR GRAPHS 4
Michael D. Plummer 1989 36 p
(Contract N00014-85-K-0488)
(AD-A210315) Avail: NTIS HC A03/MF A01 CSCL 12/2

The structure of certain non-2-extendable planar graphs is studied first. In particular, 4-connected 5-regular planar graphs which are not 2-extendable are investigated and examples of these are presented. It is then proved that all 5-connected even planar graphs are 2-extendable. Finally, a certain configuration called a generalized butterfly is defined and it is shown that 4-connected maximal planar even graphs which contain no generalized butterfly are 2-extendable. GRA

N90-10644# Naval Research Lab., Washington, DC. Lab. for Computational Physics and Fluid Dynamics.
TESTS OF GATING ALGORITHMS FOR TRACKING OF MULTIPLE OBJECTS. PART 1: THEORY, REQUIREMENTS AND PERFORMANCE MEASURES Interim Report, Feb. 1988 - Feb. 1989
J. M. Picone, M. Zuniga, J. Uhlmann (Berkeley Research Association, Springfield, VA.), and J. P. Boris 30 Jun. 1989 24 p
(AD-A210519; NRL-MR-6479) Avail: NTIS HC A03/MF A01 CSCL 12/1

This report provides the necessary foundation for tests of selected gating algorithms for multiple-target tracking. We investigate a nonhierarchical cluster algorithm and several near-neighbor algorithms. The discussion covers accuracy and scaling of cost with the number of objects being tracked. We estimate the scaling theory and discuss data set requirements and appropriate quantitative measures of performance. GRA

N90-10645# Iowa State Univ. of Science and Technology, Ames. Dept. of Mathematics.
APPLICATIONS OF ALGEBRAIC LOGIC AND UNIVERSAL ALGEBRA TO COMPUTER SCIENCE Final Report, 1 May 1989 - 30 Apr. 1989
21 Jun. 1989 28 p
(Contract N00014-88-J-1182)
(AD-A210556) Avail: NTIS HC A03/MF A01 CSCL 12/5

A four-day conference was held at Iowa State University oriented around the topics stated in the title. Approximately 80 people attended the conference, with roughly equal representation from mathematics and computer science. The conference consisted of eight invited lectures and 26 contributed talks. There was also a round-table discussion on the role of algebra and logic in computer science. GRA

N90-10646# Wisconsin Univ., Madison. Center for Mathematical Sciences.
ON TWO POLYNOMIAL SPACES ASSOCIATED WITH A BOX SPLINE Summary Report
Carl DeBoor, Nira Dyn (Tel-Aviv Univ., Israel), and Amos Ron Apr. 1989 77 p
(Contract DAAL03-87-K-0030; NSF DMS-87-01275)
(AD-A210559; CMS-TSR-89-29) Avail: NTIS HC A05/MF A01 CSCL 12/2

The polynomial space H in the span of the integer translates of a box spline M admits a well-known characterization as the joint kernel of a set of homogeneous differential operators with constant coefficients. The dual space H has a convenient representation by a polynomial space P, explicity known, which plays an important role in box spline theory as well as in multivariate polynomial interpolation. This paper characterized the dual space P as the joint kernel of simple differential operators, each one a power of a directional derivative. Various applications of this result to multivariate polynomial interpolation, multivariate splines and quality between polynomial and exponential spaces are discussed. GRA

N90-10647# Wisconsin Univ., Madison. Center for Mathematical Sciences.
A STRAIGHTFORWARD METHOD FOR FINDING IMPLICIT SOLITARY WAVE SOLUTIONS OF NONLINEAR EVOLUTION AND WAVE EQUATIONS Summary Report
Partha P. Banerjee, Faker Daoud (Syracuse Univ., NY.), and Willy Hereman Jun. 1989 30 p
(Grants AF-AFOSR-0263-87; NSF MIP-86-58865; NSF ECS-86-03643)
(AD-A210561; CMS-TSR-89-38) Avail: NTIS HC A03/MF A01 CSCL 12/1

The authors present a straightforward method of finding implicit solutions for nonlinear evolution and wave equations. The method is illustrated by finding single implicit solitary wave solutions for the Harry Dym, Korteweg-de Vries, modified Korteweg-de Vries and Boussinesq equations. GRA

N90-10648# Massachusetts Univ., Amherst. Dept. of Chemistry.
COMPUTATIONAL MODELING OF pi-CONJUGATED POLYRADICALS Technical Report No. 6, 30 Sep. 1988 - 30 May 1989
Paul M. Lahti and Andrew Ichimura 30 May 1989 15 p
(Contract N00014-87-K-0464)
(AD-A210573) Avail: NTIS HC A03/MF A01 CSCL 07/3

Spin-spin coupling in a number of aryloxyl-based polyradicals is computationally investigated using the AM1 semiempirical molecular method with configuration interaction. The qualitative accuracy of ground spin state prediction by parity based models is confirmed by computational predictions, and experimental results to date for a variety of model diradical systems is in accord with computationally predicted ground state multiplicities. The method is of general utility in identifying polyradical systems of potential interest for synthesis a possible organic high spin magnetic materials. GRA

N90-10649# Wisconsin Univ., Madison. Center for Mathematical Sciences.
PERIODIC SOLUTIONS OF SPATIALLY PERIODIC HAMILTONIAN SYSTEMS Technical Summary Report
Patricio L. Felmer 10 Jul. 1989 26 p
(Grants AF-AFOSR-0202-87; NSF DMS-85-20905)
(AD-A210645; AD-E951366; CMS-TSR-90-3) Avail: NTIS HC A03/MF A01 CSCL 12/1

This work is concerned with the study of existence and multiplicity of periodic solutions of Hamiltonian systems of ordinary differential equations $z=J(Hz(z,t) + f(t))$ when the Hamiltonian $H(z,t) = H(p,q,t)$ is periodic in the variable q and superlinear in the variable p. By imposing a growth condition on the derivative of H, we obtain the existence of at least $n + 1$ periodic solutions, where n is the dimension of the system. The existence of periodic solutions is obtained by using a Saddle Point Theorem recently proved by Lui. We consider a functional over E X M, where E is a Hilbert space and M is a compact manifold, satisfying a saddle point condition on E, uniformly on M. We present a proof of this Saddle Point Theorem using standard minimax techniques based on the cup length of M. GRA

N90-10650# Wisconsin Univ., Madison. Center for Mathematical Sciences.
MULTIPLE SOLUTIONS FOR LAGRANGIAN SYSTEMS IN T SUPERSCRIPT n Technical Summary Report
Patricio L. Felmer 10 Jul. 1989 23 p

(Grants AF-AFOSR-0202-87; NSF DMS-85-20905)
(AD-A210646; AD-E951366; CMS-TSR-90-2) Avail: NTIS HC A03/MF A01 CSCL 12/1

The existence is studied of multiple periodic solutions of a general Lagrangean system having as a configuration space the n-dimensional torus T raised to the n power. The critical points of the potential energy correspond to equilibrium of the system when no external forces are present. The author studies the number of T-periodic solutions of the system, inherited by the equilibrium solutions, when the external force is not zero. In particular it is proven that the forced system has at least the same number of periodic solutions as critical points the potential has, when certain condition is satisfied. The proof of the results are based of the notion of Ljusternik-Schnirelmann relative category. The author relates the level sets of the potential with the level sets of the functional associated to the Lagrangean system. The ideas developed are applied to study some multiplicity result for the existence of solutions of an elliptic partial difference equation with Neumann boundary condition. GRA

N90-10651# Chemical Research and Development Center, Aberdeen Proving Ground, MD.
INHERENT BIAS IN NONLINEAR LEAST SQUARES ANALYSIS OF FIRST-ORDER KINETIC DATA Technical Report, Jun. 1985 - Sep. 1986
Barry L. Knier and Frederick R. Longo (Drexel Univ., Philadelphia, PA.) Jun. 1989 13 p
(DA Proj. 1L1-62706-A-553)
(AD-A210677; CRDEC-TR-88157) Avail: NTIS HC A03/MF A01 CSCL 12/1

Generally, it is assumed in analyzing first-order kinetic data that the unweighted fit to the exponential function, at bEXP(-KT), is superior to that of the logarithmic function, ln b - kt. A careful analysis shows that this conclusion is not justified. In addition, a comparison of fits of actual data to both functions demonstrates that the methods are essentially equivalent. GRA

N90-10652# Stanford Univ., CA. Dept. of Operations Research.
A UNIFIED VIEW OF INFINITESIMAL PERTURBATION ANALYSIS AND LIKELIHOOD RATIOS Technical Report No. 32
Pierre LEcuyer (Universite Laval, Quebec) Feb. 1989 26 p
(Contract DAAL03-88-K-0063)
(AD-A210682; TR-32; ARO-25839.5-MA) Avail: NTIS HC A03/MF A01 CSCL 12/4

A view of the likelihood ratio (LR) gradient estimation technique (also called the score function (SF) method) is presented under which infinitesimal perturbation analysis (IPA) can be viewed as a (degenerate) special case, by selecting appropriately what the random component omega effectively represents. Varying the actual meaning of omega (i.e., defining the underlying sample space in different ways) might define different variants of the LR method, some of them mixing IPA with more traditional LR. We illustrate this by many examples. We also give general conditions under which the gradient estimators are unbiased. GRA

N90-10653# Stanford Univ., CA. Dept. of Electrical Engineering.
STUDIES IN ESTIMATION THEORY, APPLICATIONS AND IMPLEMENTATIONS Final Report, Mar. 1986 - Mar. 1989
Thomas Kailath 22 Jun. 1989 51 p
(Contract DAAL03-86-K-0045)
(AD-A210712; ARO-23453.34-MA) Avail: NTIS HC A04/MF A01 CSCL 12/1

This report contains results of studies of factorization of matrices with displacement structure; a unified treatment of matrices with strongly regular and arbitrary rank profiles; linear system stability and root distribution of polynomials; a unified approach via inertia computation of Bezoutians; and fast parallelizable array algorithms via displacement of matrices. GRA

N90-10654# Stanford Univ., CA. Dept. of Statistics.
ASYMPTOTIC ROBUSTNESS IN REGRESSION AND AUTOREGRESSION BASED ON LINDEBERG CONDITIONS Technical Report No. 23
T. W. Anderson and Naoto Kunitomo Jun. 1989 36 p
(Contract DAAL03-89-K-0033)
(AD-A210725; TR-23; ARO-26394.2-MA) Avail: NTIS HC A03/MF A01 CSCL 12/3

A statistical procedure is asymptotically robust if its large-sample properties hold under conditions more general than the conditions under which the procedure is derived. The justification of such procedures is often based directly or indirectly on a central limit theorem. In this paper Lindeberg-type conditions are utilized to establish asymptotic normality of sample regression and autoregression coefficients. GRA

N90-10655# Texas Inst. for Computational Mechanics, Austin.
NUMERICAL ANALYSIS OF A CLASS OF PROBLEMS IN THE MATHEMATICAL THEORY OF PLASTICITY AND DAMAGE Final Report, 15 Apr. 1986 - 14 Apr. 1989
J. Tinsley Oden 14 Jun. 1989 130 p
(Contract DAAL03-86-K-0043)
(AD-A210731; ARO-23120.3-MA) Avail: NTIS HC A07/MF A01 CSCL 12/2

A fairly detailed study of many existing theories of damage was conducted. One conclusion, perhaps not surprising, is that there is poor agreement among researchers in this field as to what constitutes a physically correct measure of damage in both brittle and ductile materials. For anisotropic damage, scalar-, vector-, and tensor-valued damage variables have been proposed for materials that undergo elastic and elastoplastic deformation. Numerous deficiencies and inconsistencies, both physical and mathematical, exist in some of the more publicized theories. In general, the field is still quite immature and the general acceptance of basic principles and definition of terms have neither the experimental support nor the consensus of workers in the field to form the nucleus of a general mathematical theory. The field of isotropic damage is in somewhat better shape. In the present study, a critical look at the subject was conducted and several new results were produced. GRA

N90-10656# Massachusetts Inst. of Tech., Cambridge. Lab. for Computer Science.
A SPECIAL CASE OF SECOND-ORDER STRICTNESS ANALYSIS
Paul P. Wang Feb. 1989 22 p
(Contract N00014-83-K-0125; NSF 98477-8511190-CCR)
(AD-A210829; MIT/LCS/TM-383) Avail: NTIS HC A02/MF A01 CSCL 12/5

A function declaration is called strict in one of its formal parameters if, in all calls to the function, either the actual corresponding parameter is evaluated, or the call does not terminate. Approximating strictness analysis with abstract interpretation reduces to the evaluation of recursive monotone Boolean functions. This evaluation problem is complete in deterministic exponential time when the functions are declared with only base type formal parameters, and is deterministic super-exponential time hard when functions are formal parameters. However, by coarsening the strictness analysis approximation to be conjunctive, the first-order case can be completed in linear time. It is shown that the second-order case is NP-hard. GRA

65 STATISTICS AND PROBABILITY

Includes data sampling and smoothing; Monte Carlo method; and stochastic processes.

N90-10657# Minnesota Univ., Minneapolis. Inst. for Mathematics and its Applications.
STOCHASTIC CONTROL THEORY, NONLINEAR STRUCTURAL MECHANICS AND APPLIED COMBINATORICS Final Report, 15 Mar. 1986 - 24 Mar. 1989

Willard Miller, Jr. 12 May 1989 39 p
(Contract DAAL03-86-K-0044)
(AD-A209042; ARO-23305.1-MA) Avail: NTIS HC A03/MF A01 CSCL 12/1

During this workshop there will be lectures and informal exchanges and discussions on recent advances in design theory and differences sets (t-designs without repeated blocks, (s, r, mu)-nets and their automorphisms, quasi-symmetric designs, Fourier transforms of difference sets, design on partially ordered sets etc.). Interactions between design theory and coding theory will be emphasized. Combinatorial and graph-theoretical methods are increasingly important in the social sciences. This workshop will emphasize mathematical techniques and open mathematical problems arising in such fields as anthropology, economics, political science, psychology, and sociology. Combinatorial models and methods also play a fundamental role in modern biology. A major portion of this workshop will focus on the combinatorics of sequence analysis. The presentations will emphasize open mathematical questions arising from biological modeling in the hope of enriching both mathematics and biology. GRA

N90-10658# Naval Postgraduate School, Monterey, CA.
NUMBER OF TEST SAMPLES NEEDED TO OBTAIN A DESIRED BAYESIAN CONFIDENCE INTERVAL FOR A PROPORTION M.S. Thesis
Ahmet Z. Ipekkan Mar. 1989 85 p
(AD-A208157) Avail: NTIS HC A05/MF A01 CSCL 12/3

One recurring problem in military operational test and evaluation is determination of the number of items to test. A Bayesian method is described to determine the sample size that is needed to estimate a proportion or probability with a (1-alpha)100 confidence when a prior distribution is given to that programs, graphs, and tables to assist in finding the required sample size. These results are compared with other approaches in determining the required sample sizes that are needed to obtain a desired confidence interval for a proportion or probability. GRA

N90-10659# National Inst. of Standards and Technology, Gaithersburg, MD. Applied and Computational Mathematics Div.
THE COMPUTATION AND USE OF THE ASYMPTOTIC COVARIANCE MATRIX FOR MEASUREMENT ERROR MODELS
Paul T. Boggs and Janet R. Donaldson Jun. 1989 30 p
(PB89-215321; NISTIR-89/4102) Avail: NTIS HC A03/MF A01 CSCL 12A

The measurement error model assumes that errors occur in both the response variables and the predictor variables. In using this model, it is of interest to compute confidence regions and intervals for the estimators of the model parameters. An asymptotic form for the covariance matrix is used to construct approximate confidence regions and intervals. The solution of the minimization problem resulting from the use of the measurement error model is discussed, and a procedure for accurately computing the covariance matrix is developed. Then the quality of the confidence regions and intervals constructed from this matrix is assessed via a Monte Carlo study. Author

N90-10660# Wayne State Univ., Detroit, MI. Dept. of Mathematics.
EMPIRICAL BAYES SELECTION FOR THE HIGHEST PROBABILITY OF SUCCESS IN NEGATIVE BINOMIAL DISTRIBUTIONS
TaChen Liang Jun. 1989 21 p Prepared in cooperation with Purdue Univ., West Lafayette, IN
(Contract N00014-88-K-0170; NSF DMS-86-06964; NSF DMS-87-02620)
(AD-A210273; TR-89-18C) Avail: NTIS HC A03/MF A01 CSCL 12/3

The problem of selecting the highest probability of success from among several negative binomial distributions via the nonparametric empirical Bayes approach is studied. A monotone selection rule is proposed on basis of monotone empirical Bayes estimators of the negative binomial success probabilities which are obtained by using the antitonic and isotonic regression methods. The asymptotic optimality property of the proposed empirical Bayes selection rule is also established. GRA

N90-10661# Purdue Univ., West Lafayette, IN. Dept. of Statistics.
ON LOWER CONFIDENCE FOR PCS IN TRUNCATED LOCATION PARAMETER MODELS
Shanti S. Gupta, Lii-Yuh Leu, and TaChen Liang (Wayne State Univ., Detroit, MI.) Jun. 1989 24 p Sponsored in part by National Science Council, Republic of China, Taiwan
(Contract N00014-88-K-0170; NSF DMS-88-06964; NSF DMS-87-02620)
(AD-A210274; TR-89-17C) Avail: NTIS HC A03/MF A01 CSCL 12/3

How to derive lower confidence bounds for the probability of a correct selection in truncated location parameter models is examined. Two cases are considered according to whether the scale parameter is known or unknown. For each case, a lower confidence bound for the difference between the best and the second best is obtained. These lower confidence bounds are used to construct lower confidence bounds for the probability of a correct selection. The results are then applied to the problem of selecting the best exponential population having the largest truncated location parameter. Useful tables are provided for implementing the proposed methods. GRA

N90-10662# Purdue Univ., West Lafayette, IN. Dept. of Statistics.
SELECTION OF THE BEST WITH A PRELIMINARY TEST FOR TWO-PARAMETER EXPONENTIAL DISTRIBUTIONS
Lii-Yuh Leu and TaChen Liang (Wayne State Univ., Detroit, MI.) Jun. 1989 18 p
(Contract N00014-88-K-0170; NSF DMS-86-06964)
(AD-A210275; TR-89-14) Avail: NTIS HC A03/MF A01 CSCL 12/3

The problem of selecting the best population from among k (greater than or -) two parameter exponential populations is examined. New selection procedures are proposed for selecting the unique best. The procedures include preliminary tests which allow the experimenter to have an option to not select if the statistical evidences is not significant. Two probabilities, the probability to make a selection and the probability of a correct selection, are controlled by these selection procedures. Comparisons between the proposed selection procedures and certain earlier existing procedures are also made. The results show the superiority of the proposed selection procedures in terms of the required sample size. GRA

N90-10663# Purdue Univ., West Lafayette, IN. Dept. of Statistics.
A BRIEF BIBLIOGRAPHY OF STATISTICAL CLASSIFICATION PROCEDURES: DECISION-THEORETIC APPROACH
Lii-Yuh Leu (National Central Univ., Chung-Li, Taiwan) Jun. 1989 7 p
(Contract N00014-88-K-0170)
(AD-A210276; TR-89-15) Avail: NTIS HC A02/MF A01 CSCL 12/3

This bibliography lists references pertaining to the classification problem based on a decision-theoretic approach. In spite of efforts to make it an exhaustive bibliography, this claim may not be justified. Any responsibility for any omissions rests solely with the author. GRA

N90-10664# Qualcomm, Inc., San Diego, CA.
RESEARCH IN MATHEMATICS AND COMPUTER SCIENCE: CALCULATION OF THE PROBABILITY OF UNDETECTED ERROR FOR CERTAIN ERROR DETECTION CODES, PHASE 1 Final Technical Report, 1 Aug. 1988 - 31 Jan. 1989
Jack K. Wolf, Lyle J. Fredrickson, and Andrew J. Viterbi 31 Mar. 1989 60 p
(Contract F49620-88-C-0088)

(AD-A210302; AFOSR-89-0841TR) Avail: NTIS HC A04/MF A01 CSCL 12/5

Cyclic redundancy check codes (or CRC codes) have become the standard means for insuring the integrity of messages that have been transmitted over a noisy communications channel. The sole purpose of these codes is to detect transmission errors (in contrast to error correction codes (or ECC codes) which attempt to correct transmissions in errors). Sometimes both CRC and ECC codes are utilized and in that case the burden is on the CRC code to detect errors that were not correctly decoded by the ECC code. Unfortunately, even the very best CRC codes cannot detect all transmission errors. The probability of CRC failure is called the probability of undetected error. An efficient method of calculating this probability of undetected error was searched for and then to use this method to find good (or even the best) CRC codes. A new algorithm was implemented to find good choices for the generator polynomial of CRC codes, that is, generator polynomials for which the probability of undetected error was less than a given bound for all shortened block lengths and for all values of the binary symmetric channel error rate. Results are given for generator polynomials corresponding to 8, 16, 24 and 32 parity bits. All possible generator polynomial corresponding to 8 and 16 parity bits and some of the generator polynomials corresponding to 24 and 32 parity bits were tested. GRA

N90-10665# Utah Univ., Salt Lake City. Dept. of Chemistry.

ADVANCES IN REGRESSION: USE OF MODELS IN SPECTROSCOPIC DATA ANALYSIS Technical Report No. 13, Jul. 1988 - Jul. 1989

Joel M. Harris, S. D. Frans, P. E. Poston, and A. L. Wong 1 Jul. 1989 41 p

(Contract N00014-89-J-1412)
(AD-A210541) Avail: NTIS HC A03/MF A01 CSCL 12/3

Regression analysis or the method of least squares is one of the oldest methods of statistical data analysis, which provides a general approach to extracting underlying relationships from data, including the parameters which describe the relationship between points and the uncertainties in those parameters. Regression methods have their roots in the method of maximum likelihood which assures that the parameter estimates are unbiased and efficient. Regression analysis of spectroscopic data will be presented, with emphasis on using models to describe the correlations which are expected in the data, on proper weighting of observations, and on determining uncertainties in estimated parameters. While this approach is particularly powerful for multidimensional, hyphenated spectroscopic methods (time-resolved fluorescence, GC-MS, LC-UV, etc.), the theory of regression methods will first be developed with examples from measurements of lower dimensionality. The basis of regression methods for multidimensional data in the simple statistics of estimating a mean and standard deviation provides an intuitive basis for understanding more powerful analysis procedures, while extending our background simple statistics into methods for manipulating spectroscopic data. GRA

N90-10666# Stanford Univ., CA. Dept. of Operations Research.

DISCRETE-TIME CONVERSION FOR SIMULATING FINITE-HORIZON MARKOV PROCESSES Technical Report No. 34

Bennett L. Fox and Peter W. Glynn (Wisconsin Univ., Madison.) May 1989 26 p Sponsored in part by Natural Sciences and Engineering Research Council of Canada
(Contracts DAAL03-88-K-0063; DAAG29-84-K-0030; NSF ECS-84-04809)
(AD-A210683; TR-34; ARO-25839.7-MA) Avail: NTIS HC A03/MF A01 CSCL 12/3

The expectation of certain integrals of functionals of continuous-time Markov chains is estimated by simulation over a finite horizon, fixed or random. By computing conditional expectations given the sequence of states visited (and possibly other information), we reduce variance. This is discrete-time conversion. Efficiency is further increased by combining discrete-time conversion with stratification and splitting. GRA

N90-10667# Stanford Univ., CA. Dept. of Operations Research.

MARKOV CHAIN MOMENT FORMULAS FOR REGENERATIVE SIMULATION Technical Report No. 35

James M. Calvin Jun. 1989 14 p

(Contract DAAL03-88-K-0063)
(AD-A210684; TR-35; ARO-25839.8-MA) Avail: NTIS HC A03/MF A01 CSCL 12/3

Let (X sub n : n greater than or =) be a regenerative Markov chain on a general state space, and f a real-valued bounded function. Let tau and Z be random variables that have the distribution of a regeneration cycle length and the sum of f(Xk) over a cycle, respectively. This paper derives expressions for moments of the form E (tau superscript j) (Z superscript k), which are then used to gain insight into the qualities of regenerative estimators based on different regeneration points. GRA

N90-10668# Stanford Univ., CA. Dept. of Operations Research.

COMPUTATIONAL AND STATISTICAL ISSUES IN DISCRETE-EVENT SIMULATION

Peter W. Glynn and Donald L. Iglehart Mar. 1989 18 p

(Contract DAAL03-88-K-0063)
(AD-A210743; TR-33; ARO-25839.6-MA) Avail: NTIS HC A02/MF A01 CSCL 12/3

Discrete-event simulation is one of the most important techniques available for studying complex stochastic systems. The principal methods available for analyzing both the transient and steady-state simulation problems are reviewed in sequential and parallel computing environments. Next several of the variance reduction methods designed to make simulations run more efficiently are discussed. Finally, a short discussion is given of the methods available to study optimization using simulation. GRA

N90-10669# Ballistic Research Labs., Aberdeen Proving Ground, MD.

ASSESSING THE ACCURACY OF VULNERABILITY MODELS BY COMPARISON WITH VULNERABILITY EXPERIMENTS Final Report

Michael W. Starks Jul. 1989 24 p

(AD-A210871; BRL-TR-3018) Avail: NTIS HC A02/MF A01 CSCL 12/5

Over the past three decades the business of vulnerability analysis was conducted more as art than as science. For a number of reasons, there is recent movement away from art and towards science. One reason is internal to the Ballistic Research Laboratory. If a substantial work force of scientists and engineers spends several decades doing vulnerability analysis it would be both surprising and disappointing if improved clarity and on the foundations of the subject were not achieved. A second reason is the declining cachet associated with computer models. Several decades ago it was virtually the case that if a quantitative result issued from a computer model, it was sufficiently warranted as correct. The crude extrapolations which then passed as vulnerability models benefited from that halo effect. Today, people are understandably more skeptical about models. Questions are asked and answers expected about accuracy and validation. The pressure of such questioning has forced vulnerability analysts into seeking greater scientific respectability for the fruits of their labors. A third cause of the scientific turn is the recent explosion of computer technology. Vulnerability phenomena are complex; realistic simulation was out of the question with the tools available to early vulnerability analysts. GRA

N90-10670# Massachusetts Inst. of Tech., Cambridge. Dept. of Electrical Engineering and Computer Science.

TOWARD A THEORY OF REPRESENTATION DESIGN Ph.D. Thesis

Jeffrey VanBaalen May 1989 222 p

(Contract N00014-85-K-0124)
(AD-A210885; AI-TR-1128) Avail: NTIS HC A10/MF A02
CSCL 12/5

Designing representations for analytical reasoning problems (of the sort found on the GRE and LSAT) are examined. These problems are intended to test the ability to draw logical conclusions from information presented and to synthesize that information in order to deduce interrelationships. A computer program was developed that takes as input a straightforward predicate calculus translation of a problem, requests additional information if necessary, decides what to represent and how, designs representations that capture the constraints of the problem, and finally, creates and executes a LISP program that uses those representations to produce a solution. Even though these problems are typically difficult for theorem provers to solve, the LISP program that uses the designed representations is very efficient. The representations designed by the system are powerful because they capture the constraints of a problem in two ways: The structure of the representation resembles the structure of the thing represented. For example, consider representing married couples as sets of size two. The structure of this representation resembles the structure of married couples because both have exactly two individuals in them. The structure enables efficient behaviors that enforce a problem's constraints by keeping them invariant in the structure. For example, as a set representing a married couple is manipulated, a behavior associated with it maintains its fixed size. GRA

N90-10671# Massachusetts Inst. of Tech., Cambridge.
STOCHASTIC QUANTIZATION
Sanjoy K. Mitter 1989 10 p
(Contract DAAL03-86-K-0171)
(AD-A210942; ARO-24635.101-MA-UIR) Avail: NTIS HC
A02/MF A01 CSCL 12/3

Stochastic differential equations were studied which relate to the free field and other fields in finite volume following the earlier work of Jona-Lasinio and Mitter. Also studied were lattice approximations to these stochastic differential equations and a limit theorem was proved when the lattice spacing goes to zero. The nature of the results obtained are now described. GRA

N90-10672# Texas A&M Univ., College Station. Dept. of Statistics.
A UNIFIED APPROACH TO ESTIMATING TAIL BEHAVIOR
Scott D. Grimshaw May 1989 116 p
(Contract DAAL03-87-K-0003)
(AD-A210961; TR-55; ARO-23010.4-MA) Avail: NTIS HC
A06/MF A01 CSCL 12/3

Tail estimators are proposed which make minimal assumptions and let the data dictate the form of the probability model. These estimators use only the observations in the tail and are based on a unifying density-quantile model. The fundamental result is a representation motivates a unified parameterization for tail estimators of the underlying probability model, motivates methods for obtaining parameter estimates and simplifies the derivation of the asymptotic properties of the proposed parameter estimates. Parameter estimates may be obtained using a Generalized Pareto Distribution or a Generalized Extreme Value Distribution model of the exceedences. Assuming the underlying distribution can be correctly classified as either short tailed or long tailed, other estimates are formed. The asymptotic properties of these estimates are derived under rate of convergence conditions to show the effect of threshold selection on parameters properties. GRA

N90-10673# Texas A&M Univ., College Station. Dept. of Statistics.
MULTI-SAMPLE FUNCTIONAL STATISTICAL DATA ANALYSIS
Emanuel Parzen May 1989 14 p
(Contract DAAL03-87-K-0003)
(AD-A210992; TR-54; ARO-23010.3-MA) Avail: NTIS HC
A03/MF A01 CSCL 12/3

This paper discusses a functional approach to the problem of comparison of multi-samples (two samples or c samples, where c is greater than or = 2). The data consists of c random samples whose probability distributions are to be tested for equality. A diversity of statistics to test equality of c samples is presented in a unified framework with the aim of helping the researcher choose the optimal procedures which provide greatest insight about how the samples differ in their distributions. Concepts discussed are: sample distribution functions; ranks; mid-distribution function; two-sample t test and nonparametric Wilcoxon test; multi-sample analysis of variance and Kruskal Wallis test; Anderson Darling and Cramer von Mises tests; components and linear rank statistics; comparison distribution and comparison density functions, especially for discrete distributions; components with orthogonal polynomial score functions; chi-square tests and their components. GRA

66 SYSTEMS ANALYSIS

Includes mathematical modeling; network analysis; and operations research.

N90-10674*# National Aeronautics and Space Administration. Lewis Research Center, Cleveland, OH.
APPLICATION OF A HYBRID GENERATION/UTILITY ASSESSMENT HEURISTIC TO A CLASS OF SCHEDULING PROBLEMS
Ann O. Heyward 1989 13 p Prepared for presentation at the International Conference on Systems, Man, and Cybernetics, Cambridge, MA, 14-17 Nov. 1989; sponsored by IEEE
(NASA-TM-102367; E-5086; NAS 1.15:102367) Avail: NTIS HC
A03/MF A01 CSCL 12B

A two-stage heuristic solution approach for a class of multiobjective, n-job, 1-machine scheduling problems is described. Minimization of job-to-job interference for n jobs is sought. The first stage generates alternative schedule sequences by interchanging pairs of schedule elements. The set of alternative sequences can represent nodes of a decision tree; each node is reached via decision to interchange job elements. The second stage selects the parent node for the next generation of alternative sequences through automated paired comparison of objective performance for all current nodes. An application of the heuristic approach to communications satellite systems planning is presented. Author

67 THEORETICAL MATHEMATICS

Includes topology and number theory.

N90-10675# Air Force Academy, CO.
AN INTRODUCTION TO FRACTALS AND CHAOS Final Report
John W. Haussermann Jun. 1989 174 p
(AD-A210257; USAFA-TR-89-04) Avail: NTIS HC A08/MF A01
CSCL 12/2

Fractals and chaos have gained immense popularity in the last few years. Fractal objects and chaotic dynamics are being postulated and observed in diverse areas of science. A mathematical introduction is given to fractals and chaos, including some necessary background for the technical definitions. Partial Contents: Fractal -- Observations and representations; Topology and open covers; Topological dimension; Hausdorff dimension (A definition of fractal); Similarity dimension; The Cantor set; Koch snowflakes; Random coastlines; Another approach - IFS (Iterated Function System); and Further examples; Chaos -- The Poincare map; Iterations of continuous functions -- Orbits; Periodic points; Invariant sets/Attractors; Scrambled Sets -- Definitions of chaos; Universality -- The bifurcation diagram; Higher dimensions; Complex dynamics; and Randomness. GRA

70 PHYSICS (GENERAL)

For precision time and time interval (PTTI) see *35 Instrumentation and Photography;* for geophysics, astrophysics or solar physics see *46 Geophysics, 90 Astrophysics,* or *92 Solar Physics.*

N90-10676# International Centre for Theoretical Physics, Trieste (Italy).
ENERGY DEPENDENT TRANSPORT PROBLEM WITH GENERALIZED BOUNDARY CONDITIONS
S. A. ElWakil, M. T. Attia, M. S. Abdel Krim, and A. A. ElGhazaly (Atomic Energy Authority, Anhass, Egypt) Dec. 1988 18 p Submitted for publication
(DE89-617843; IC-88/415) Avail: NTIS (US Sales Only) HC A03/MF A01

The slowing down of the Boltzmann Equation for generalized boundary conditions is considered and transformed into one speed equation in Laplace space. Exact relations between energy reflection and transmission coefficients for a problem with diffuse reflecting boundary conditions and the albedos for the problem with isotropic boundary conditions are obtained. The Galerkin method is used to calculate the energy reflection coefficient for a finite slab at different thicknesses for different mass ratios A, target to projectile mass ratio, for different synthetic scattering kernels. The methods for partial heat fluxes for isotropic and anisotropic scattering in dispersive medium are given. The results obtained for isotropic boundary conditions compare well with the exact results. DOE

N90-10677*# Institute for Computer Applications in Science and Engineering, Hampton, VA.
ANALYTIC THEORY FOR THE SELECTION OF SAFFMAN-TAYLOR FINGERS IN THE PRESENCE OF THIN FILM EFFECTS Final Report
S. Tanveer (Ohio State Univ., Columbus.) Sep. 1989 59 p Submitted for publication
(Contract NAS1-18605)
(NASA-CR-181910; NAS 1.26:181910; ICASE-89-63) Avail: NTIS HC A04/MF A01 CSCL 20C

An analytic theory is presented for the width selection of Saffman-Taylor fingers in the presence of thin film effect. In the limit of small capillary number Ca and small gap to width ratio epsilon, such that epsilon much less than Ca much less than 1, it is found that fingers with relative width lambda less than 1/2 are possible such that lambda squared (1-lambda)/(1-2 lambda) = k epsilon/Ca(sup 3/2), where the positive constant k depends on the branch of solution and equals 2.776 for the first branch. A fully nonlinear analysis is necessary in this problem even to obtain the correct scaling law. It is also shown how in principle, the selection rule for arbitrary Ca can be obtained. Author

N90-10678*# Cornell Univ., Ithaca, NY. Dept. of Computer Science.
THE ARCHITECTURE OF NEWTON: A GENERAL-PURPOSE DYNAMICS SIMULATOR
James F. Cremer and A. James Stewart 1989 6 p
(Contracts NGT-50337; N00014-88-K-0591; N00014-88-K-0281; NSF DMC-88-17355; AMSI-U03-8300)
(NASA-CR-185489; NAS 1.26:185489; AD-A210247) Avail: NTIS HC A02/MF A01 CSCL 20/11

The architecture of Newton, a general-purpose system for simulating the dynamics of complex physical objects is described. The system automatically formulates and analyzes equations of motion, and performs automatic modification of this system of equations when necessitated by changes in kinematic relationships between objects. Impact and temporary contact are handled, though currently using simple models. User directed influence of simulations is achieved using Newton's control module, which can be used to experiment with the control of many degree-of-freedom articulated objects. GRA

71 ACOUSTICS

Includes sound generation, transmission and attenuation. For noise pollution see *45 Environmental Pollution.*

N90-10679*# National Aeronautics and Space Administration. Langley Research Center, Hampton, VA.
MEASUREMENT RESOLUTION OF NOISE DIRECTIVITY PATTERNS FROM ACOUSTIC FLIGHT TESTS
David A. Conner Washington Oct. 1989 43 p
(NASA-TM-4134; L-16456; NAS 1.15:4134; AVSCOM-TR-89-B-004) Avail: NTIS HC A03/MF A01 CSCL 20A

The measurement resolution of noise directivity patterns from acoustic flight tests was investigated. Directivity angle resolution is affected by the data reduction parameters, the aircraft velocity and flyover altitude, and by deviations of the aircraft from the desired flight path. Equations are developed which determine bounds for the lateral and longitudinal directivity angle resolution as a function of the nominal directivity angle. The equations are applied to a flight test data base and the effects of several flight conditions and data reduction parameters on the directivity angle resolution are presented. The maximum directivity angle resolution typically occurs when the aircraft is at or near the overhead position. In general, directivity angle resolution improves with decreasing velocity, increasing altitude, increasing sampling rate, decreasing block size, and decreasing block averages. Deviations from the desired ideal flight path will increase the resolution. For the flight experiment considered in this study, an average of two flyovers were required at each test condition to obtain an acceptable flight path. The ability of the pilot to maintain the flight track improved with decreasing altitude, decreasing velocity, and practice. Due to the prevailing wind conditions, yaw angles of as much as 20 deg were required to maintain the desired flight path. Author

N90-10680*# National Aeronautics and Space Administration. Langley Research Center, Hampton, VA.
FLUCTUATING PRESSURES MEASURED BENEATH A HIGH-TEMPERATURE, TURBULENT BOUNDARY LAYER ON A FLAT PLATE AT MACH NUMBER OF 5
Tony L. Parrott, Michael G. Jones (Planning Research Corp., Hampton, VA.), and Cindy W. Albertson Washington Nov. 1989 39 p
(NASA-TP-2947; L-16596; NAS 1.60:2947) Avail: NTIS HC A03/MF A01 CSCL 20A

Fluctuating pressures were measured beneath a Mach 5, turbulent boundary layer on a flat plate with an array of piezoresistive sensors. The data were obtained with a digital signal acquisition system during a test run of 4 seconds. Data sampling rate was such that frequency analysis up to 62.5 kHz could be performed. To assess in situ frequency response of the sensors, a specially designed waveguide calibration system was employed to measure transfer functions of all sensors and related instrumentation. Pressure time histories were approximated well by a Gaussian prohibiting distribution. Pressure spectra were very repeatable over the array span of 76 mm. Total rms pressures ranged from 0.0017 to 0.0046 of the freestream dynamic pressure. Streamwise, space-time correlations exhibited expected decaying behavior of a turbulence generated pressure field. Average convection speed was 0.87 of freestream velocity. The trendless behavior with sensor separation indicated possible systematic errors. Author

N90-10681*# Old Dominion Univ., Norfolk, VA.
DESIGN GUIDE FOR PREDICTING NONLINEAR RANDOM RESPONSE (INCLUDING SNAP-THROUGH) OF BUCKLED PLATES
Chung Fai Ng Sep. 1989 33 p
(Grant NAG1-363)
(NASA-CR-181877; NAS 1.26:181877) Avail: NTIS HC A03/MF A01 CSCL 20A

This design guide describes a method for predicting the random response of flat and curved plates which is based on theoretical analyses and experimental results. The plate curvature can be

due to postbuckling, in-plane mechanical or thermal stresses. Based on a single mode formula, root mean square values of the strain response to broadband excitation are evaluated for different static buckled configurations using the equivalent linearization technique. The effects on the overall strain response due to instability motion of snap-through are included. Panel parameters include clamped and simply-supported boundaries, aspect ratio, thickness and length. Analytical results are compared with experimental results from tests with 12 in. x 15 in. aluminum plates under thermal loading in a progressive wave facility. Comparisons are also made with results from tests with a 2 in. x 15 in. x 0.032 in. aluminum beam under base mechanical excitation. The comparisons help to assess the accuracy of the theory and the conditions under which deviations from the theory due to effects of imperfection and higher modes are significant. Author

N90-10682 Southampton Univ. (England).
THE THEORY AND APPLICATION OF QUADRATIC MINIMIZATION IN THE ACTIVE REDUCTION OF SOUND AND VIBRATION Ph.D. Thesis
A. R. D. Curtis 1988 143 p
Avail: Univ. Microfilms Order No. BRDX85088

Active sound reduction is the use of active sources of sound, that is devices which are potentially sources of sound energy, to modify a pre-existing sound field in such a way that the overall effect is a reduction in sound. Until recently the most common approach in active sound control was to attempt to achieve complete cancellation of the sound. This is possible at single points but is practically impossible over an appreciable region. A more modest and practical aim is to try to reduce the sound field by as much as possible by minimizing some overall measure of the amplitude of the sound field. The technique of sound field minimization is examined. Candidate sound field measures which are suitable for minimization are presented and discussed. The quantities include acoustic energy, intensity and power flow as well as a practical measure, the sum of the squares of the signals from a number of sensors. Theoretical simulations and experimental implementations are used to evaluate sound field minimization techniques. The discussion and experiments are extended to the active reduction of structural vibrations. Dissert. Abstr.

N90-10683*# Hamilton Standard, Windsor Locks, CT.
ACOUSTIC TEST AND ANALYSIS OF A COUNTERROTATING PROP-FAN MODEL Final Report
Bernard Magliozzi, Paul Brown, and David Parzych Oct. 1987 156 p
(Contract NAS3-24222)
(NASA-CR-179590; NAS 1.26:179590) Avail: NTIS HC A08/MF A01 CSCL 20A

Results of acoustic tests of a 62.2 cm (24.5 in) diameter model counterrotating Prop-Fan are presented. The model was tested as a tractor and a pusher downstream of a pylon, both at 0 degrees and at 4 degrees angle-of-attack. The effects on noise of spacing between rotors and between the pylons and the rotors were also measured. Effects of rotor spacing were found to cause small changes in noise over the range of spacings tested. The presence of the pylon resulted in a 2 to 3 EPNdB increase in noise. Angle-of-attack effects showed an increase of 3 to 4 EPNdB for the tractor and only about 1 EPNdB for the pusher configuration. Speed was found to be the strongest parameter in minimizing noise. However, the decrease in noise with tip speeds below 200 m/sec (650 ft/sec) became significantly smaller than at higher tip speeds. Comparison of noise spectra between single rotation and counterrotating Prop-Fans showed that the counterrotating Prop-Fan has significantly higher levels of higher frequency noise which radiates in the forward direction. Correlations between measurement and prediction are discussed. Predictions are made of far-field noise during takeoff and near-field noise during cruise. Author

72 ATOMIC AND MOLECULAR PHYSICS

Includes atomic structure, electron properties, and molecular spectra.

N90-10684# Colorado State Univ., Fort Collins. Dept. of Chemistry.
MONTE CARLO SIMULATIONS OF SMALL SOLUTE/SOLVENT CLUSTERS: CLUSTER PROPERTIES AND PHASE TRANSITIONS
S. Li and E. R. Bernstein 1 Jun. 1989 41 p Submitted for publication
(Contract N00014-79-C-0647)
(AD-A209559; AD-E900860; TR-55) Avail: NTIS HC A03/MF A01 CSCL 07/4

Atom-atom L-J (6-12-1) potentials are employed to calculate the cluster configurations of all local energy minima of benzene(N2)n and (N2)n clusters for n=1, 2,.....10 and some benzene(Ar)n and N2(Ar)n clusters. The number of configurations increases exponentially and the binding energy range increases linearly with the number of solvent molecules for these clusters. Monte Carlo simulations are performed on the temperature behavior of the cluster potential energy, intermolecular distance, and some angular variables for benzene(Ar)n, and benzene(N2)n clusters. Molecules comprising the cluster can undergo tunneling between the different potential energy minima at particular transition temperatures. This tunneling process can be viewed as a solid-solid or solid-liquid phase transition for the cluster. GRA

N90-10685# Michigan Univ., Ann Arbor. Dept. of Physics.
STUDIES OF ELEMENTARY PARTICLES Progress Report and Proposal
16 May 1989 86 p
(Contract DE-AC02-76ER-01112)
(DE89-014859; DOE/ER-01112/14) Avail: NTIS HC A05/MF A01

Some task highlights discussed in this report are: Task B has completed and successfully operated 8 Michigan muon array patches for the UMC experiment; the Task C built luminosity monitor for the Mark II detector is functioning well and fulfilling its key role in the determination of the Z mass and width; major Task C contributions to the machine diagnostics, the bremsstrahlung monitor and wire scanner, have provided critical tuning information for the SLC; and Task E ((gamma)*) has recently reported the detection of 200 GeV gamma rays from the Crab Nebula with a statistical significance of 5.8 (sigma). This observation confirms the importance of imaging techniques for VHE gamma ray astronomy. The Michigan theory group (Task G) has focused on: working to understand the systematics of gluon dynamics in poorly understood pseudoscalar meson decays; exploring the consequences of heavy Higgs boson and/or a top quark more massive than the W(sup (plus minus)) or Z; surveying the potentially attractive ways of experimentally searching for the Higgs boson of the minimal Standard Model or the spectrum of Higgs bosons to be expected in extensions of the Standard Model; calculating the radiative corrections for W sup + W sup - yields W sup + W sup - as a precision test of the Standard Model, especially in its sensitivity to the Higgs sector; investigating the modifications of general relativity arising from quantum fluctuations of matter; exploring phenomenological test of CP violation dynamics; developing relations between the strong CP problem and ElectroWeak CP violation; and investigating 4-Fermi interactions in Technicolor models. DOE

N90-10686# Oak Ridge National Lab., TN. Physics Div.
ON THE UTILITY AND UBIQUITY OF ATOMIC COLLISION PHYSICS
Sheldon Datz 1989 12 p Presented at the 16th International Conference on the Physics of Electronic and Atomic Collisions, New York, NY, 26 Jul. - 1 Aug. 1989 Sponsored by Martin Marietta Energy Systems, Inc.
(Contract DE-AC05-84OR-21400)
(DE89-015356; CONF-890708-3) Avail: NTIS HC A03/MF A01

In the introduction, the history and makeup of ICPEAC are

discussed. In the second part, the extent of applicability of atomic collision physics is covered. In the third part, one subject (dielectronic excitation) was chosen to show the interrelationship of various subbranches of atomic collision physics. DOE

N90-10687# Argonne National Lab., IL. Chemistry Div.
A STRUCTURAL BASIS FOR ELECTRON TRANSFER IN BACTERIAL PHOTOSYNTHESIS
James R. Norris, Theodore J. DiMagno, Alexander Angerhofer (Stuttgart Univ., Germany, F.R.), C. H. Chang, Osamma El-Kabbani, and M. Schiffer 1989 16 p Presented at the 22nd Jerusalem Symposium on Quantum Chemistry, Jerusalem, Israel, 15-18 May 1989
(Contract W-31-109-eng-38)
(DE89-015702; CONF-8905146-2) Avail: NTIS HC A03/MF A01

Triplet data for the primary donor in single crystals of bacterial reaction centers of Rhodobacter sphaeroides and Rhodopseudomonas viridis are interpreted in terms of the corresponding X-ray structures. The analysis of electron paramagnetic resonance data from single crystals (triplet zero field splitting and cation and triplet linewidth of the primary special pair donor of bacterial reaction centers) is extended to systems of a non-crystalline nature. A unified interpretation based on frontier molecular orbitals concludes that the special pair behaves like a supermolecule in all wild-type bacteria investigated. However, in heterodimers of Rb. capsulatus (His sup M200) changed to Leu or Phe with the result that the M-half of the special pair is converted to bacteriopheophytin) the special pair possesses the EPR properties more appropriately described in terms of a monomer. In all cases the triplet state and cation EPR properties appear to be dominated by the highest occupied molecular orbitals. These conclusions derived from EPR experiments are supplemented by data from Stark spectroscopy of reaction centers from Rb capsulatus. DOE

N90-10688# Los Alamos National Lab., NM.
OBSERVATION OF EXCITED H(SUP 0) ATOMS PRODUCED BY RELATIVISTIC H(SUP (MINUS)) IONS IN CARBON AND FORMVAR FOILS
A. H. Mohagheghi, H. C. Bryant, P. G. Harris, C. Y. Tang, C. R. Quick, R. A. Reeder, S. Cohen, W. W. Smith, and J. E. Stewart (University of Western Washington, Bellingham.) Feb. 1989 27 p Presented at the 16th International Conference on the Physics of Electronic and Atomic Collisions, New York, NY, 26 Jul. - 1 Aug. 1989
(Contracts W-7405-eng-36; DE-AS04-77ER-03998)
(DE89-015301; LA-UR-89-2473; CONF-890708-2) Avail: NTIS HC A03/MF A01

The relative yield was measured for several low-lying excited states of neutral hydrogen atoms produced by the passage of 226-MeV and 581-MeV H(-) ions through thin carbon foils and a tilted formvar foil. The relative yields of H(0*) (n = 2, 3, 4) were measured for 17 different carbon foils ranging in thickness from 662 to 5386 A at 581 MeV. The relative yield of H(0*) (n = 2) was also measured for these carbon foils at 226 MeV. These data exhibit a significant deviation from a simple yield curve indicating that a more complex mechanism than was previously thought is responsible for producing the excited states. The relative yields of H(0*) (n = 2, 3) were measured for a tilting formvar foil at 226 MeV; unexplained dips appear at incidence angles of theta is approximately 12 degrees and theta is approximately 15 degrees in the yield of n = 2 and n = 3 states, respectively. DOE

N90-10689# Brookhaven National Lab., Upton, NY. Accelerator Development Dept.
TANGENT MAP ANALYSIS OF THE BEAM-BEAM INTERACTION
S. Y. Lee and S. Tepikian 1989 5 p Presented at the 3rd Advanced Inertial Confinement Fusion Accelerator Beam Dynamics Workshop: Beam-Beam Effects in Circular Colliders, Novosibirsk, USSR, 20 May - 3 Jun. 1989
(Contract DE-AC02-76CH-00016)
(DE89-015857; BNL-42954; CONF-890594-4) Avail: NTIS HC A01/MF A01

The tangent map of the beam-beam interaction was studied and no evidence was found of beam-beam instability for (epsilon) = 0.04. Tracking study with tune modulation shows, however, large emittance growth due to the sum resonances. The emittance growth is due to the multiple crossing of the sum resonances. DOE

N90-10690# Purdue Univ., West Lafayette, IN. Dept. of Chemistry.
SOLVENT DYNAMICAL EFFECTS IN ELECTRON TRANSFER: PREDICTED INFLUENCES OF ELECTRON COUPLING UPON THE RATE-DIELECTRIC FRICTION DEPENDENCE Technical Report No. 86, 1 Oct. 1987 - 30 Jun. 1989
Alexander Gochev, George E. McManis, and Michael J. Weaver 1 Jul. 1989 48 p
(Contract N00014-86-K-0556)
(AD-A210193) Avail: NTIS HC A03/MF A01 CSCL 07/4

The predicted dependence of the bimolecular rate constant for outer-sphere electron exchange, k sub ex, upon the longitudinal relaxation time, tau sub L, for Debye solvents is examined numerically on the basis of a suitably combined rate formulation in order to examine the manner and extent to which the rate-solvent friction dependence, of particular experimental significance, should be sensitive to the degree of donor-acceptor electronic coupling and related factors. The treatment accounts for the contributions to k sub ex from a spatial distribution of reactant pairs as well as for the effects of donor-acceptor interactions upon the unimolecular rate constant, k sub et (1/s), for each encounter geometry. The latter include the influence of electronic interactions as prescribed by the matrix coupling element, H12, upon the effective frequency for adiabatic barrier crossings, nu sub n, as well as upon the electronic transmission coefficient, K sub el (i.e. the degree of reaction nonadiabaticity). The anticipated dependence of the free-energy barrier, as well as nu sub n and K sub el, upon the donor-acceptor separation is accounted for in the k sub ex calculations. Numerical comparisons are made with corresponding log k sub ex - log(1/tau sub L) plots obtained using the simple encounter preequilibrium treatment which presumes that only a fixed narrow range of encounter-pair geometries contribute to k sub ex. GRA

N90-10691# Purdue Univ., West Lafayette, IN. Dept. of Chemistry.
SOLVENT EFFECTS ON INTERVALENCE ELECTRON-TRANSFER ENERGIES FOR BIFERROCENE CATIONS: COMPARISONS WITH MOLECULAR MODELS OF SOLVENT REORGANIZATION Technical Report No. 91, 1 Oct. 1987 - 30 Jun. 1989
George E. McManis, Alexander Gochev, Roger M. Nielson, and Michael J. Weaver 1 Jul. 1989 33 p Submitted for publication
(Contract N00014-86-K-0556)
(AD-A210263) Avail: NTIS HC A03/MF A01 CSCL 07/4

Outer shell electron transfer reorganization energies, lambda sub O, as evaluated from intervalence band maxima, E sub op, for biferrocenylacetylene (BFA+), 1,4-biferrocenyl butadiyne (BFB+), and biferrocene (BF+) cations in thirteen solvents are compared with the predictions of some contemporary models of solvent reorganization in order to ascertain the importance of non-continuum, or solvent molecularity, factors to lambda sub O. Measurements of E sub op were made in relatively polar media in solutions containing low concentrations of PF6(-) so to minimize complications from ion pairing. The relative E sub op values for all three biferrocenes are essentially independent of the solvent; E sub op for BFB+ relative to BFA+ is in good agreement with the predictions of the two-sphere model (but not ellipsoid models), although the Eop values for BF+ are larger than expected, most probably due to electron delocalization effects. Comparisons are made with the recent mean spherical approximation (MSA) treatment of solvent reorganization. The MSA model can account

semiquantitatively for the smaller E sub op values relative to E sub op (con) observed in a number of solvents, but does not predict the especially large such deviations observed for methanol and D20. The latter are shown to be qualitatively consistent with local solvent structuring effects deduced on the basis of a nonlocal dielectric approach as well as on empirical grounds. GRA

N90-10692# Purdue Univ., West Lafayette, IN. Dept. of Chemistry.
SOLVENT DYNAMICAL EFFECTS IN ELECTRON TRANSFER: EVALUATION OF ELECTRONIC MATRIX COUPLING ELEMENTS FOR METALLOCENE SELF-EXCHANGE REACTIONS Technical Report, 1 Oct. 1987 - 30 Jun. 1989
George E. McManis, Roger M. Nielson, Alexander Gochev, and Michael J. Weaver 1 Jul. 1989 50 p Submitted for publication
(Contract N00014-86-K-0556)
(AD-A210306; TR-90) Avail: NTIS HC A03/MF A01 CSCL 07/4

The functional dependence of the rate constants for self exchange, k sub ex, for a series of metallocene redox couples to solvent-induced variations in the nuclear frequency factor, nu, engendered by alterations in the longitudinal solvent relaxation time, tau sub L, are utilized to deduce values of the electronic matrix coupling element, H12, for electron exchange. The analysis exploits the sensitivity of the k sub ex tau sub L -1 dependence to the degree of reaction adiabaticity and hence H12 for a given electron exchange reaction. Six metallocene couples are examined: Cp2Co+/o, Cp2Fe+/o (Cp = cyclopentadienyl) and the decamethyl derivatives Cp2Co+/o and Cp2Fe+/o scrutinized previously, additional solvent-dependent k sub ex values for carboxymethyl (cobaltocenium-cobaltocene) (Cp(e)Z Co+/o, e= ester) and hydroxymethyl (ferrocenium-ferrocene) (HMFc+/o.) Kinetic data are examined in 15 solvents, including 11 debye solvents for which it is anticipated that is proportioned to 1/tau sub L. Corrections to k sub ex for the solvent-dependent variations in the barrier height were obtained by corresponding measurements of the optical electron transfer energies for the related binuclear complex biferrocenylacetylene, yielding barrier corrected rate constants, k sub ex. The relationship between H12 superscript o and metallocene electronic structure is briefly discussed. The analysis also enables effective solvent relaxation times for adiabatic barrier crossing in non-Debye media including primary alcohols, to be extracted. GRA

N90-10693# Lowell Univ., MA. Polymer Science Program.
MONOLAYER FORMATION CHARACTERISTICS OF NOVEL ORGANIC MOLECULES WITH NONLINEAR OPTICALLY ACTIVE MOIETIES Technical Report, Jul. 1988 - Jul. 1989
Sai S. Kumar, R. S. Kumar, L. A. Samuelson, Jayant Kumar, A. Blumstein, and Sukant K. Tripathy 31 May 1989 24 p Presented at the 4th International Conference on Langmuir-Blodgett Films, Tsukuba (Japan), 24-29 Apr. 1989 Submitted for publication
(Contract N00014-87-K-0131)
(AD-A210496; TR-5) Avail: NTIS HC A03/MF A01 CSCL 07/3

Organic materials were recently recognized as promising candidates for nonlinear optics (NLO) applications in view of their fast response time and large non-resonant nonlinear effects in comparison with their inorganic counterparts. Organic materials that form molecular crystals and polymers with optimized molecular structure are therefore being synthesized and their NLO response assessed in attempts to obtain superior material performance. Another advantage of organic and polymeric materials is their relative ease of processing. It is possible to fabricate ultra thin films of organic NLO material that are suitably designed using the Langmuir-Blodgett (L-B) technique. A number of novel electroactive materials with amphibolic molecular structure containing COOH, OH, NMe2, OMe, NO2, and CN were synthesized. The monolayer forming ability of these compounds is discussed. The stability of the monolayer as a function of pH, temperature, composition of the material in mixed monolayers and the nature of the subphase are investigated. Appropriate choice of experimental conditions under which a stable monolayer is obtained for each material is indicated. GRA

N90-10694# North Texas State Univ., Denton. Dept. of Physics.
TWO PHOTON ABSORPTION CHARACTERIZATION Quarterly Report No. 6, 28 Nov. 1988 - 27 Feb. 1989
Chris L. Littler and David G. Seiler 15 May 1989 14 p
(Contract DAAB07-87-C-F094; DA Proj. 1L1-61102-A-31-B)
(AD-A210508) Avail: NTIS HC A03/MF A01 CSCL 20/3

Magnetooptical measurements of Hg(1-x)Cd(x)Te alloys have provided a new means of studying impurities and defects in this important II-VI material. Two-photon magnetoabsorption (TMPA) has been used to accurately determine the temperature dependence of the energy gap of various HgCdTe alloys, revealing behavior that deviates from currently accepted models. In addition, magnetooptical techniques have been used to detect the presence of both shallow and deep impurities/defects and accurately determine their activation energies, thus providing information necessary for understanding the electrical and optical properties of the material. GRA

73 NUCLEAR AND HIGH-ENERGY PHYSICS

Includes elementary and nuclear particles; and reactor theory.

For space radiation see *93 Space Radiation.*

N90-10695# Brown Univ., Providence, RI. Dept. of Physics.
RESEARCH PROGRAM IN THEORETICAL HIGH ENERGY PHYSICS Progress Report
David Feldman, Herbert M. Fried, Antal Jevicki, Kyungsik Kang, and Chung-I Tan 30 Jun. 1989 26 p
(Contract DE-AC02-76ER-03130)
(DE89-013963; DOE/ER-03130/425) Avail: NTIS HC A03/MF A01

This year's research has dealt with: superstrings in the early universe; the invisible axion emissions from SN1987A; quartic interaction in Witten's superstring field theory; W-boson associated multiplicity and the dual parton model; cosmic strings and galaxy formation; cosmic strings and baryogenesis; quark flavor mixing; p p(-) scattering at TeV energies; random surfaces; ordered exponentials and differential equations; initial value and back-reaction problems in quantum field theory; string field theory and Weyl invariance; the renormalization group and string field theory; the evolution of scalar fields in an inflationary universe, with and without the effects of gravitational perturbations; cosmic string catalysis of skyrmion decay; inflation and cosmic strings from dynamical symmetry breaking; the physic of flavor mixing; string-inspired cosmology; strings at high-energy densities and complex temperatures; the problem of non-locality in string theory; string statistical mechanics; large-scale structures with cosmic strings and neutrinos; the delta expansion for stochastic quantization; high-energy neutrino flux from ordinary cosmic strings; a physical picture of loop bremsstrahlung; cylindrically-symmetric solutions of four-dimensional sigma models; large-scale structure with hot dark matter and cosmic strings; the unitarization of the odderon; string thermodynamics and conservation laws; the dependence of inflationary-universe models on initial conditions; the delta expansion and local gauge invariance; particle physics and galaxy formation; chaotic inflation with metric and matter perturbations; grand-unified theories, galaxy formation, and large-scale structure; neutrino clustering in cosmic-string-induced wakes; and infrared approximations to nonlinear differential equations. DOE

N90-10696# Purdue Univ., West Lafayette, IN. Dept. of Physics.
A THEORETICAL HIGH ENERGY PHYSICS PROGRAM Annual Progress Report, 1989

T. E. Clark, T. K. Kuo, S. T. Love, and C. N. Leung 1989 28 p Sponsored by Purdue Research Foundation, West Lafayette, IN
(Contract DE-AC02-76ER-01428)
(DE89-012685; DOE/ER-01428/T2) Avail: NTIS HC A03/MF A01

The following research topics are briefly described: aspects of dynamical symmetry breaking in gauge field theory; supersymmetric quantum electrodynamics and dynamical chiral symmetry breaking; anti-symmetric tensor gauge theories; extensions of the standard model; and neutrino oscillations in matter. DOE

N90-10697# Fermi National Accelerator Lab., Batavia, IL.
FERMILAB FIXED TARGET BEAMS FROM THE MAIN INJECTOR
S. Childress, R. Coleman, G. Koizumi, A. Malensek, C. Moore, R. Schailey, R. Stefanski, and L. Stutte May 1989 60 p Presented at the Workshop on Physics at the Main Injector, Batavia, IL, 16-18 May 1989
(Contract DE-AC02-76CH-03000)
(DE89-014355; FNAL-TM-1599; CONF-8905183-3) Avail: NTIS HC A04/MF A01

The following topics at Fermilab are discussed: 120 to 150 GeV beam extraction; link to switchyard; primary beam splits and transport; and experimental facilities at 120 to 150 GeV. DOE

N90-10698# California Univ., Berkeley. Lawrence Berkeley Lab.
TELLURIUM-118/ANTIMONY-118 GENERATOR
Y. Yano and M. Lagunas-Solar (California Univ., Davis.) Jun. 1989 15 p Presented at the 36th Annual Meeting of the Society of Nuclear Medicine, St. Louis, MO, 13-16 Jun. 1989
(Contract DE-AC03-76SF-00098)
(DE89-015225; LBL-27314; CONF-890680-1) Avail: NTIS HC A03/MF A01

This research develops a radioisotope generator to obtain Sb-118 (3.5 m half-life, 75 percent positron s) from the 6.0 d Te-118 parent. About 2 mCi of Te-118 was produced per run. Gamma ray analysis with a GeLi detector indicated the production of Te-118/Sb-118, Sb-120, Sb-122, Te-119/Sb-119, Te-119m/Sb-119, Te-121, and Te-121m. The Sb target was brought into solution with HCl and HNO3 acid. Six percent sodium tartrate was added to the target solution to form the Sb-tartrate complex for loading onto an inorganic ion exchange column of neutal alumina (Al2O3) and SnO2. Six percent sodium tartrate at various pH's ranging from 2 to 8 were used as the eluent solutions. Elution yields of Sn-118 and breakthroughs of Te radioisotopes were determined by dose calibrator measurements and GeLi analysis. Results indicate that the Sn-118 yield at pH 7.0 from the SnO2 was twice the yield from Al2O3 with 6 percent tartrate, while the breakthroughs of Te radioactivity were nearly comparable for the two columns. However, elutions with 6 percent tartrate at pH 3.5 doubled the yield of Sb-118 from Al2O3 while elutions at pH 3.5 from SnO2 increased the Sb-118 yield about 28 percent. Cumulative elution volumes of 6 percent tartrate at pH 7.0 from either Al2O3 or SnO2 led to a gradual reduction in Sb-118 yield from about 25 percent down to 5 to 6 percent. Elutions at pH 3.5, led to a higher yield without a gradual reduction in yield with cumulative elution volumes of 6 percent tartrate. A pH of 5.0 was finally chosen as the best compromise between sustained levels of Sb-118 yield and the biological and chemical advantages of working at a pH higher than 3.5. Exchange labeling was used to label thio compounds with the Sb-118-tartrate from the generator. DOE

N90-10699# Oak Ridge National Lab., TN. Solid State Div.
THE TEMPORAL DEVELOPMENT OF COLLISION CASCADES IN THE BINARY COLLISION APPROXIMATION
Mark T. Robinson Jul. 1989 23 p Presented at the 13th International Conference on Atomic Collisions in Solids, Aarhus, Denmark, 7-11 Aug. 1989
(Contract DE-AC05-84OR-21400)
(DE89-015860; CONF-890821-1) Avail: NTIS HC A03/MF A01

A modified binary collision approximation (BCA) was developed to allow explicit evaluation of the times at which projectiles in a collision cascade reach significant points in their trajectories, without altering the event-driven character of the model. The modified BCA was used to study the temporal development of cascades in copper and gold, initiated by primary atoms of up to 10 KeV initial kinetic energy. Cascades generated with time-ordered collisions show fewer distant Frenkel pairs than do cascades generated with velocity-ordered collisions. In the former, the slower projectiles tend to move in less-damaged crystal than they do in the latter. The effect is larger in Au than in Cu and increases with primary energy. As an approach to cascade nonlinearities, cascades were generated in which stopped cascade atoms were allowed to be redisplaced in later encounters. There were many more redisplacements in time-ordered cascades than in velocity-ordered ones. Because of the additional stopping introduced by the redisplacement events, the cascades in which they were allowed had fewer defects than occurred otherwise. This effect also was larger in Au than in Cu and larger at high energies although most of the redisplacement encounters involved only low-energy particles. DOE

N90-10700# Battelle Memorial Inst., Columbus, OH.
DEVELOPMENT OF THE ELECTROACOUSTIC DEWATERING (EAD) PROCESS FOR FINE/ULTRAFINE COAL Quarterly Progress Report No. 3, Apr. - Jun. 1989
18 Jul. 1989 9 p
(Contract DE-AC22-88PC-88883)
(DE89-015883; DOE/PC-88883/T3) Avail: NTIS HC A03/MF A01

Battelle, in cooperation with the Electric Power Research Institute (EPRI), Ashbrook-Simon-Hartley (ASH), Kaiser Engineers (KE), Lewis Corporation, and Professor S. H. Chiang of the University of Pittsburgh, is developing an advanced process for the dewatering of fine and ultrafine coals. The advanced process, called Electroacoustic Dewatering (EAD), capitalizes on the adaptation of synergistic effects of electric and acoustic fields to commercial coal dewatering systems, such as belt filter presses. DOE

N90-10701# California Univ., Berkeley. Lawrence Berkeley Lab. Exploratory Studies Group.
A SYMPLECTIC COHERENT BEAM-BEAM MODEL
Miguel A. Furman May 1989 8 p Presented at the 3rd Advanced Inertial Confinement Fusion Accelerator Beam Dynamics Workshop: Beam-Beam Effects in Circular Colliders, 20 May - 3 Jun. 1989
(Contract DE-AC03-76SF-00098)
(DE89-015386; LBL-27351; CONF-890594-3) Avail: NTIS HC A02/MF A01

A one-dimensional model was considered to study the effects of the beam-beam force on the coherent dynamics of colliding beams. The key ingredient is a linearized beam-beam kick. Only the quadrupole modes were studied, with the dynamical variables being the 2nd-order moments of the canonical variables q, p. The model is self-consistent in the sense that no higher order moments are generated by the linearized beam-beam kicks, and that the only source of violation of symplecticity is the radiation. The round beam case only was studied, in which vertical and horizontal quantities are assumed to be equal (though they may be different in the two beams). Depending on the values of the tune and beam intensity, steady states were observed in which otherwise identical bunches have sizes that are equal, or unequal, or periodic, or behave chaotically from turn to turn. Possible implications of luminosity saturation with increasing beam intensity are discussed. Finally, some preliminary applications to an asymmetric collider were presented. DOE

74 OPTICS

Includes light phenomena; and optical devices.
For lasers see *36 Lasers and Masers.*

N90-10702# Carnegie-Mellon Univ., Pittsburgh, PA.
RADON TRANSFORM ANALYSIS OF A PROBABILISTIC METHOD FOR IMAGE GENERATION Annual Report No. 2, 1 Apr. 1988 - 31 Mar. 1989
Marc A. Berger (Georgia Inst. of Tech., Atlanta.) 12 Apr. 1989 20 p
(Grant AF-AFOSR-0137-87)
(AD-A207814; AFOSR-89-0606TR) Avail: NTIS HC A03/MF A01 CSCL 20/6

The research performed for this grant over the past year involved affine iterated function system (IFS) encoding and IFS mixing for digital images. This relates to a technique of Michael Barnsley's for generating fractal and other images by randomly iterating affine transformations of the plane into itself. By this technique an image is both generated and represented as the long-term probability distribution for a 2-D or 3-D Markov chain. The encoding involves finding an affine collage of the image, whereby it is identified as a convex combination of affinely scaled versions of itself. This permits some remarkable data compression. The mixing involves a merging of IFS's so as to produce images with combined textures. It ties in with the encoding in that a broader class of images can then be efficiently encoded, and there are more degrees of freedom in the encoding search. The mathematical methods used involve stochastic optimization, computational geometry, the Radon transform, dynamical systems and ergodic theory for Markov chains. GRA

N90-10703# Sandia National Labs., Albuquerque, NM.
SECOND-ORDER NONLINEAR OPTICAL DEVICES IN POLED POLYMERS
K. D. Singer, W. R. Holland, M. G. Kuzyk, G. L. Wolk, H. E. Katz, M. L. Schilling (Bell Telephone Labs., Inc., Murray Hill, NJ.), and P. A. Cahill 1989 12 p Presented at the SPIE Symposium on Nonlinear Optical Properties of Organic Materials II, San Diego, CA, 10-11 Aug. 1989
(Contract DE-AC04-76DP-00789)
(DE89-015842; SAND-89-1696C; CONF-8908100-1) Avail: NTIS HC A03/MF A01

Guest-host poled polymer films have become an active area of research as potential candidates for second-order nonlinear optical and electro-optic devices. This interest derives mainly from their large nonlinear optical coefficients, ease of fabrication, and high optical quality. Progress was rapid in producing stable, efficient materials, and in building demonstration devices. The second-order nonlinear optical properties arise from the orientational order induced in a collection of highly nonlinear molecules incorporated in a glassy polymer matrix. After reviewing the alignment physics, results are presented for nonlinear optical measurements on a methacrylate polymer functionalized with a dicyanovinyl terminated azo dye. Device issues concerning nonlinear optical devices are described with particular attention to phase-matching. Data are presented for the demonstration of anomalous dispersion phase matched second harmonic generation in dye solutions. Also presented are the results on electro-optic modulators. DOE

N90-10704# California Univ., Berkeley. Lawrence Berkeley Lab. Accelerator and Fusion Research Div.
DESIGN OF GRAZING INCIDENCE MONOCHROMATORS INVOLVING UNCONVENTIONAL GRATINGS
Wayne R. McKinney and Christopher Palmer (Milton Roy Co., Rochester, NY.) Jan. 1989 5 p Presented at the Symposium on Lasers and Optics, Los Angeles, CA, 5-20 Jan. 1989
(Contract DE-AC03-76SF-00098)
(DE89-016341; LBL-26882; CONF-890142-5) Avail: NTIS HC A01/MF A01

The basic aspects of second order focusing of straight and parallel grooved varied line space gratings are reviewed in both converging and collimated light in a more explicit and detailed manner that found in the literature. The effects of the VLS correction to the location of the focal curve for grazing incidence geometries are found to be very significant. DOE

N90-10705# Sandia National Labs., Albuquerque, NM.
A COMPARISON OF REAL-TIME OPTICAL CORRELATORS FOR PATTERN RECOGNITION
K. Terry Stalker, Perry A. Molley, and Bruce D. Hansche 1989 15 p Presented at the International Congress on Optical Science and Engineering, 24-28 Apr. 1989
(Contract DE-AC04-76DP-00789)
(DE89-016416; SAND-88-2911C; CONF-8904242-3) Avail: NTIS HC A03/MF A01

Two types of optical correlators were built to investigate real time pattern recognition. The first employs 1-D devices to perform the two dimensional correlation in real time. This architecture uses an array of light emitting diodes (LED's) to input an electronically stored reference image into the processor in parallel. The input scene data is introduced into the processor one line at a time using an acousto-optic device (AOD). Multichannel time integrating correlations are performed in the row direction using the AOD and in the column direction using a charge coupled device (CCD) operating in the time delay and integrate mode. A processor was built using this technology which correlates a 64 x 44 pixel binary reference image with a 256 x 232 input scene at video rates. The second correlator is a space integrating Fourier transform based correlator. A magneto optic-device (MOD) is used at the Fourier transform plane to rapidly change filter functions. The binary nature of the MOD device necessitates using either a binary phase or binary amplitude representation of the desired complex filter function. For this reason, several types of Binary Phase-Only Filter (BPOF) representations were analyzed and experimentally investigated. Experimental correlation results were obtained using both the Hartley BPOF and a newly developed class of complex binary filters, called Quad-Phase-Only Filters (QPOF). The performance of the two systems are compared on the basis of processing speed, space bandwidth product, processor size and light efficiency. The inherent differences between incoherent and coherent processing and their implications for filter design are also discussed. Finally, estimates of future performance are presented. DOE

N90-10706# Los Alamos National Lab., NM.
MULTIMODE FIBER INTERFEROMETRY AND SEVERAL-MODE FIBER POLARIMETRY VIA PHASE CONJUGATION
P. R. Forman, F. C. Jahoda, B. L. Mason, and C. B. Netterfield 1989 10 p Presented at the 6th International Conference on Optical Fiber Sensors, Paris (France), 17-20 Sep. 1989
(Contract W-7405-eng-36)
(DE89-014226; LA-UR-89-2112; CONF-8909161-1) Avail: NTIS HC A02/MF A01

While the simplest fiber optics are realized by transmission intensity modulations impressed on multimode fibers, great enhancements in sensitivity are achieved by interferometric or polarimetric methods with light propagated through single-mode fibers. In this paper we report preliminary experiments on retaining the sensitivity of interferometric and/or polarimetric measurements while using only multimode fiber components. The utility of success in this endeavor can be measured by greater experimental simplicity (light injection and alignment tolerances), by cost factors (cheaper fiber optics components), or by larger intensity transmission limits (which can be translated to higher time resolution for a given signal-to-noise ratio). DOE

N90-10707# Kaptron, Inc., Palo Alto, CA.
AUTOMATION OF FIBER-OPTIC PIGTAILING PROCESS: LASER WELDING DEMONSTRATION PROGRAM Final Report
F. C. Unterleitner 26 May 1989 28 p
(Contract N00014-88-C-2050)
(AD-A210351) Avail: NTIS HC A03/MF A01 CSCL 20/6

This demonstration program is intended to demonstrate the feasibility of coupling a commercially available Nd:YAG laser with the Kaptron POLYTROPE 3000 automatic alignment system for

the production of single mode fiber pigtailed semiconductor lasers. It has been demonstrated that 30 watts of Nd:YAG laser power can produce repeatable welds of 0.18mm thick Kovar saddles to gold plated substrates of the type used for semiconductor laser modules. It has also been shown that beam geometry stabilization by passing the beam through a step index fiber (or reflective tube channel) is essential for reliable and repeatable welding with this type of multimode laser. Laser and delivery system requirements for a production Nd:YAG laser welding accessory for the Polytrope 3000 have been defined, and recommendations for such an accessory are included in this report. GRA

N90-10708# Mississippi Univ., University. Physical Acoustics Research Lab.
THEORETICAL AND EXPERIMENTAL INVESTIGATION OF NONLINEAR OPTOACOUSTICS IN LIQUIDS Ph.D. Thesis
Stanley A. Cheyne and Henry E. Bass 30 Jun. 1989 62 p
(Contract N00014-84-C-0193)
(AD-A210427; PARGUM-89-01) Avail: NTIS HC A04/MF A01 CSCL 09/6

The optoacoustic effect in liquids has been studied theoretically and experimentally. Measurements were taken in various liquids studying the thermal expansion mechanism and comparing these results to existing theoretical predictions. Among the quantities investigated were the dependence of optoacoustic amplitude on optical absorption coefficient, thermal expansion coefficient and laser pulse energy. These experimental observations were found to be in agreement with theory. The signal amplitude was also measured as a function of propagation distance. It was found that the optoacoustic amplitude varies as 1/sq rt(r) which is characteristic of a cylindrical source. Measurements were also taken in liquid Carbon Disulfide (CS2). The strong absorption of the 337 nm radiation resulted in a nonlinear relationship between optoacoustic amplitude and input energy. These nonlinear variations were explained in terms of dynamically changing temperature dependent coefficients of thermal expansion and optical absorption. GRA

N90-10709# Lowell Univ., MA. Polymer Science Program.
NONLINEAR OPTICS AND ORGANIC MATERIALS Technical Report No. 7, Jul. 1988 - Jul. 1989
Elizabeth Cavicchi, Jayant Kumar, Sai S. Kumar, and Sukant K. Tripathy 31 May 1989 29 p Submitted for publication
(Contract N00014-87-K-0131)
(AD-A210570) Avail: NTIS HC A03/MF A01 CSCL 20/6

The origin and nature of nonlinear optical effects in organic and polymeric materials is discussed. Approaches to the applications of these nonlinear optical effects in prototypical devices is explored. In glancing through a flat windowpane, light's interaction with glass is immediately confronted, but ignore it. It is assumed that the world's image is not perceptibly altered when light passes through the glass. Yet glass does play tricks with light: a penny viewed through a variety of lenses may appear the same size, magnified, reduced, or blurred. Contemporary optics research is distant from common experience, seeking clues far more subtle than the shape of a piece of glass, with techniques more esoteric than abrasive polishing of a glass lens. The traditional dominance of glass in optics is now challenged by a host of synthetic materials exhibiting unusual optical behavior. GRA

N90-10710# Carnegie-Mellon Univ., Pittsburgh, PA. Robotics Inst.
SURFACE REFLECTION: PHYSICAL AND GEOMETRICAL PERSPECTIVES
Shree K. Nayar, Katsushi Ikeuchi, and Takeo Kanade Mar. 1989 59 p Sponsored in part by Westinghouse Electric Corp.
(Contract F33615-87-C-1499)
(AD-A210592; CMU-RI-TR-89-7) Copyright Avail: NTIS HC A04/MF A01 CSCL 20/6

Machine vision can greatly benefit from the development of accurate reflectance models. There are two approaches to the study of reflection: physical and geometrical optics. While geometrical models may be construed as mere approximations to physical models, they possess simpler mathematical forms that often render them more usable than physical models. However, geometrical models are applicable only when the wavelength of incident light is small compared to the dimensions of the surface imperfections. Therefore, it is incorrect to use these models to interpret or predict reflections from smooth surfaces, and only physical models are capable of describing the underlying reflection mechanism. This paper is directed towards unifying physical and geometrical approaches to describe reflection from surfaces that may vary from smooth to rough. More specifically, we consider the Beckmann-Spizzichino (physical optics) model and the Torrance-Sparrow (geometrical optics) model. These two models were chosen in particular as they have been reported to fit experimental data very well. Each model is described in detail, and the conditions that determine the validity of the model are clearly stated. From studying the behaviors of both models, a model is proposed comprising three reflection components: the diffuse lobe, the specular lobe, and the specular spike. The dependencies of the three components on the surface roughness and the angles of incidence and reflection are analyzed in detail. GRA

N90-10711# Naval Ocean Systems Center, San Diego, CA. Office of Naval Technology.
DEMONSTRATION OF A DUAL-LIDAR METHOD FOR MEASURING OPTICAL DEPTHS IN THE VERTICAL Final Report, Oct. 1988 - May 1989
Merle R. Paulson and Douglas R. Jensen May 1989 31 p
(AD-A210598; NOSC/TD-1544) Avail: NTIS HC A03/MF A01 CSCL 17/9

Experimental results are reported of optical depth measurements in the vertical direction. A dual-lidar method for measuring extinction coefficient profiles was employed. The mathematical derivations of the method are described. GRA

N90-10712# Cambridge Consultants Ltd.. (England).
CUSTOM DIFFRACTION GRATINGS Final Report, Apr. 1988 - Apr. 1989
T. R. Empson 7 Jul. 1989 66 p
(Contract DAJA45-88-C-0014; DA Proj. 1L1-61103-BH-07)
(AD-A211002; C3086-FR-001A; R/D-5970-MS-01-F) Avail: NTIS HC A04/MF A01 CSCL 20/6

The objective of this work was to design, develop and manufacture a batch of custom transmission diffraction gratings with a low zero-order optical transmission across the visible and near-infrared waveband. A high laser damage threshold was also desirable. It was shown that neither conventional blazed gratings nor holographically fabricated sinusoidal photoresist gratings were entirely suitable. The preferred approach was to use reactive ion etching to transfer a quasi-sinusoidal groove profile into the surface of a hard substrate such as fused silica. Differential etch rates were exploited to achieve a larger groove amplitude in the etched gratings than in the photoresist mask. Of the batch of ten gratings which were supplied, the best grating exhibited a zero-order transmission which did not exceed 6 percent over the wavelength range 543nm to 875nm. The main conclusion of the work was that a deep grooved surface relief transmission diffraction grating can provide a broad band optical attenuation of around 95 percent across the visible and near infrared waveband. The use of reactive ion etching techniques can enable the production of such gratings with high laser damage thresholds. GRA

N90-10713# California Univ., Santa Barbara. Dept. of Electrical and Computer Engineering.
USE OF DEPLETION EDGE TRANSLATION FOR HIGH-SPEED MODULATION AND SWITCHING OF LIGHTWAVES Final Report, 1 Mar. 1988 - 30 Apr. 1989
Larry A. Coldren May 1989 35 p
(Grant AF-AFOSR-0323-85; AF Proj. 2305)
(AD-A211186; CU-ECE-TR-89-01; AFOSR-89-1054TR) Avail: NTIS HC A03/MF A01 CSCL 20/6

We report on our work for the period 1 March 1988 to 28 February 1989. The primary emphasis has been the Fabry-Perot

modulator which we introduced in last year's interim report. Over the past year, we have completed the design, optimization and sensitivity analysis for the modulator. Experimentally, we have made good progress in improving the device performance going from a 2:1 on:off ratio for a 25 V drive to a 10:1 on:off ratio for a 7 V drive. We present a brief comparison of our modulator results with those of other groups. With supplemental support from other contracts, we have also made significant advances in fundamental areas which should open new avenues for continued improvement of existing devices and lead to new device structures. We have observed a new effect in superlattices (Field-induced Stark localization) which leads to a blue-shift in absorption edge rather than a conventional red shift. We have also observed optical properties ascribable only to quantum well effects in quantum well structures grown directly by molecular beam epitaxy using a process pioneered at UCSB. Both of these new structures should prove to be promising active regions for the Fabry-Perot device. Additionally, the Fabry-Perot will serve as an excellent vehicle with which to fully characterize the electro-optic properties of these new structures. GRA

N90-10799*# American Science and Engineering, Inc., Cambridge, MA.
THE DESIGN AND EVALUATION OF GRAZING INCIDENCE RELAY OPTICS
John M. Davis, R. C. Chase, J. K. Silk, and A. S. Krieger *In its* Solar X-ray Astronomy Sounding Rocket Program 22 Aug. 1989 6 p (For primary document see N90-10796 01-88)
Avail: NTIS HC A15/MF A02 CSCL 20F

75 PLASMA PHYSICS

Includes magnetohydrodynamics and plasma fusion.
For ionospheric plasmas see *46 Geophysics*. For space plasmas see *90 Astrophysics*.

N90-10714# California Univ., Berkeley. Electronics Research Lab.
PLASMA THEORY AND SIMULATION Quarterly Progress Report Nos. 1-2, 1 Jan. - 30 Jun. 1988
Charles K. Birdsall 30 Jun. 1988 38 p
(Contracts N00014-85-K-0809; DE-FG03-86ER-53220; RR0109)
(AD-A207952) Avail: NTIS HC A03/MF A01 CSCL 04/1

A magnetized plasma next to an absorbing wall is simulated, showing positive wall charging causing a large E-field near the wall, then a large ExB drift, then a Kelvin-Helmholtz instability, vortices and coalescence. Particle transport to the walls is Bohm-like, for omega sub pi greater than omega sub ci. Plasma transport across B sub O to a wall is studied without and with an active antenna buried in the wall. Particle losses are increased appreciably by the fields of the antenna. Small angle Coulomb collisions produce a drag force and diffusion tensor, which are calculated self-consistently. This produces a FP-PIC method. An example is shown for a beam scattering off fixed ions. Implicit particle simulations are discussed for bounded plasma. The effect of source distribution on the sheath potential is discussed. Initiation of an effort to simulate a traveling-wave tube is discussed. Substantial progress has been made in making our standard periodic code ES1 work efficiently on a fast PC. A plasma sheath reference listing is discussed. GRA

N90-10715# TRW Space Technology Labs., Redondo Beach, CA. Applied Technology Div.
MHD SEED RECOVERY AND REGENERATION Final Report
14 Oct. 1988 317 p Prepared in cooperation with Fluor Daniel, Inc., Irvine, CA
(Contract DE-AC22-87PC-79672)
(DE89-002711; DOE/PC-79672/T1) Avail: NTIS HC A14/MF A02

The TRW Econoseed MHD Seed Regeneration Process is based on the reaction of calcium formate with potassium sulfate spent seed from an MHD electric power generation plant. The process was tested at bench scale, design a proof of concept (POC) test plant, plan and cost a Phase 2 project for a POC plant evaluation and prepare a conceptual design of a 300 MW (t) commercial plant. The results of the project are as follows: (1) each of the unit operations is demonstrated, and (2) the data are incorporated into a POC plant design and project cost, as well as a 300 MW (t) commercial retrofit plant design and cost estimate. Specific results are as follows: (1) calcium formate can be produced at 100 percent yield in a total retention time of less than 5 minutes, (2) utilizing the calcium formate, spent seed can quantitatively be converted to potassium formate, potassium carbonate or mixtures of these with potassium sulfate as per the commercial design without measurable loss of potassium to insolubles at a total retention time under 20 minutes and ambient pressure, (3) the solid rejects form the process meet RCRA EP Toxicity requirements for safe disposal, and (4) filtration and evaporation data, as well as reaction data cited above, show that the Econoseed technology is ready for scale up to POC plant scale. Economics forecast studies show that the total cost per unit of potassium for seed regeneration by the Econoseed Process is in the range of $0.23 to $0.27/lb, a cost which is less than half the potassium cost of $0.63/lb for purchasing new potassium carbonate. DOE

N90-10716# Oak Ridge National Lab., TN.
IGNITION AND BURN CRITERIA FOR D3He TOKAMAK AND SPHERICAL TORUS REACTORS
J. D. Galambos and Y.-K. M. Peng 1989 34 p Presented at the 2nd International Symposium on Aneutronic Power, Washington, DC, 28-29 Apr. 1989 Sponsored by Martin Marietta Energy Systems, Inc.
(Contract DE-AC05-84OR-21400)
(DE89-015059; CONF-8904214-1) Avail: NTIS HC A03/MF A01

D sup 3 He ignition and burn criteria for tokamaks and spherical torus reactors are examined in a global analysis with profile corrections. Particle confinement and ash buildup effects are included with the power balance, which results in an increased sensitivity of the ignition criteria to losses via brehmsstrahlung and synchrotron radiation. Plasma beta scaling via an epsilon beta sub p limit provides the needed aspect ratio (A) dependence, and permits an analysis in all A values of the first and second stability regimes. Energy confinement time (tau sub E) associated with particle diffusion (tau sub p) and energy conduction (tau sub c) are used; parabolic profile are assumed with exponents alpha sub n = 1.0 and alpha sub T = 1.5; and we set tau sub p = 2 tau sub c. The ignition condition for minimum n tau sub E is found to be sensitive to (beta) but not to the magnetic field. Steady state burn in second stability tokamaks (epsilon beta sub p (ge) 0.6) at high A (greater than 4) with average synchrotron wall reflectivities below 95 percent requires n tau sub E above 5 x 10(21) m sup -3)s or strong plasma elongation (kappa greater than 3). Ignition in a spherical tori can be achieved with wall reflectivities below 80 percent and at n tau sub E (le) 10(21) m sup -3)s, without requiring strong plasma shaping or epsilon beta sub p greater than 0.6. The need to minimize n tau sub E for ignition and burn strongly limits the synchrotron radiation loss to less than 20 percent of the fusion power for all values of A. Synchrotron power fractions can be increased to 40 percent by increasing n tau sub E to its upperbound of ignition. Further increases of this fraction can be obtained only by assuming preferential ash removal. DOE

N90-10717*# National Aeronautics and Space Administration. Marshall Space Flight Center, Huntsville, AL.
METHOD AND APPARATUS FOR MAINTAINING THERMAL CONTROL IN PLASMA CONDITIONS Patent Application
Ann F. Whitaker, inventor (to NASA) 28 Jul. 1989 10 p
(NASA-Case-MFS-28368-1; NAS 1.71:MFS-28368-1; US-Patent-Appl-SN-386174) Avail: NTIS HC A02/MF A01 CSCL 20I

An apparatus and method are disclosed for determining the effects of exposure of oxygen plasma on a thin film polymer whose bulk is maintained at a predetermined temperature. The apparatus includes a chamber having a specimen therein. A plasma

environment is provided in the chamber. A closure member is provided for sealing the chamber after the specimen is introduced into the chamber. The closure member also serves as a support for the test apparatus which includes a cooling coil. A platform having the test specimen thereon is supported on the cooling coil to be cooled by coolant flowing through the cooling coils. A thermoelectric module is supported on the platform to assist in maintaining a low test temperature for the test samples. The temperature of the sample is monitored by a thermocouple probe which is in contact with the sample. Any change in bulk sample temperature caused by the thermocouple probe is quickly adjusted to maintain the initial bulk temperature by the thermoelectric module. NASA

N90-10718*# National Aeronautics and Space Administration. Lewis Research Center, Cleveland, OH.
PLASMA GUN WITH COAXIAL POWDER FEED AND ADJUSTABLE CATHODE Patent Application
Isidor Zaplatynsky, inventor (to NASA) 7 Jul. 1989 12 p
(NASA-Case-LEW-14901-1; NAS 1.71:LEW-14901-1; US-Patent-Appl-SN-376488) Avail: NTIS HC A03/MF A01 CSCL 20I

An improved plasma gun coaxially injects particles of ceramic materials having high melting temperatures into the central portion of a plasma jet. This results in a more uniform and higher temperature and velocity distribution of the sprayed particles. The position of the cathode is adjustable to facilitate optimization of the performance of the gun wherein grains of the ceramic material are melted at lower power input levels. NASA

N90-10719# Lawrence Livermore National Lab., CA. Physics Dept.
SIMULTANEOUS MULTIPLE FREQUENCY INTERFEROMETRY: AN APPLICATION OF HOMODYNE PHASE MEASUREMENT
Paul R. Bolton 1 May 1989 19 p
(Contract W-7405-eng-48)
(DE89-013975; UCID-21636) Avail: NTIS HC A03/MF A01

Microwave interferometry of plasmas involving only multiple homodyne phase measurement is considered in the limits of very low and very high collisionality. Starting with an assumed Langevin model of a weakly ionized gaseous plasma, the expressions for the complex propagation constant(s) of probe(s) are simplified for these limiting cases. Emphasis is on the imaginary component of the propagation constant which accounts for the phase shifting phenomena. Simultaneous use of two probing frequencies enables phase determination of both the time dependent electron density and effective collision rate which are line integrated along the probe propagation length. Extension to a triple frequency interferrometric system allows additional determination of the line integrated square of the electron density due to the incorporation of higher order terms in a Taylor series expansion. If a reasonable functional form for the longitudinal variation in plasma density is assumed, the plasma spatial profile can then be estimated. Throughout, plasmas are assumed to be transversely uniform. In addition, physical interpretation of a real effective collision rate can be simplified in these collisional limits to be directly proportional to an energy distribution averaged momentum transfer rate. DOE

N90-10720# California Univ., Berkeley. Lawrence Berkeley Lab.
SCATTERING OF AN ICRF MAGNETOSONIC WAVE BY PLASMA DENSITY TURBULENCE
Daniel R. Cook and Allan N. Kaufman Apr. 1989 6 p Presented at the 8th American Physical Society Topical Conference on Radio Frequency Power in Plasmas, Irvine, CA, 1-3 May 1989 Prepared in cooperation with California Univ., Berkeley
(Contract DE-AC03-76SF-00098)
(DE89-015223; LBL-27108; CONF-8905120-20) Avail: NTIS HC A02/MF A01

A fast Inertial Confinement Reactor Fusion (ICRF) magnetosonic wave, launched into a tokamak plasma, scatters off turbulent density fluctuations in the plasma edge. We use cold-fluid theory to calculate the angular distribution of the scattered wave and find it to be predominantly perpendicular to the incident wavevector for second harmonic majority heating. We calculate the mean free path and find it to be large compared to the size of tokamak devices. Therefore, scattering of ICRF magnetosonic waves by density turbulence is an utterly negligible effect. DOE

N90-10721# Los Alamos National Lab., NM.
OBSERVATIONS OF AZIMUTHAL ASYMMETRY FOR CERTAIN FRC OPERATING REGIMES
B. Wright, D. Barnes, R. Chrien, E. Crawford, R. Milroy, S. Okada (Osaka Univ., Japan), R. Siemon, M. Tuszewski, and R. Webster 1989 3 p Presented at the 9th US Compact Toroid Symposium, Union, WA, 14-15 Mar. 1989
(Contract W-7405-eng-36)
(DE89-015300; LA-UR-89-2474; CONF-8903100-4) Avail: NTIS HC A01/MF A01

The FRX-C/LSM experiment was operated with additional diagnostics for studies of FRC structure in the (theta)-pinch source. Data were taken over ranges of fill pressure and bias field that lead to the formation of FRCs with confinement properties that are consistently good (e.g., at 3 mtorr at 0.7 kG bias) and consistently poor (e.g., at 5 mtorr at any bias). The pertinent diagnostics were end-on soft X-ray imaging, arrays of external B sub theta and B sub r probes, and five chords of interferometry. The data show that easily observed departures from azimuthal (theta) symmetry occur in some cases and that further research into the cause and nature of these asymmetries would benefit the studies of FRC stability and confinement. DOE

N90-10722# Lawrence Livermore National Lab., CA.
GENERATION OF 3/2 OMEGA SUB o RADIATION IN INHOMOGENEOUS PLASMAS UNDER THE IRRADIATION OF INTENSE ELECTROMAGNETIC WAVES Final Report, 3 Apr. 1987 - 30 Sep. 1988
A. Y. Wong and B. S. Bauer Feb. 1989 116 p Prepared in cooperation with California Univ., Los Angeles, CA
(Contract W-7405-eng-48)
(DE89-015723; UCRL-21188) Avail: NTIS HC A06/MF A01

Several phenomena of importance to laser-plasma interactions that are associated with cavitons generated at the critical layer of a nonuniform plasma by resonant absorption of intense electromagnetic radiation were investigated. The emission, from deep cavitons, of electromagnetic radiation at half-harmonics of the pump frequency, was examined. Caviton formation was shown to be most efficient for shallow density gradients at the critical layer. Huge electron plasma waves, with attendant wave-breaking and energetic particle production, were generated. Experimental results are consistent with LLNL and UCLA computer simulations. DOE

N90-10723# Massachusetts Inst. of Tech., Cambridge. Plasma Fusion Center.
MASSACHUSETTS INSTITUTE OF TECHNOLOGY PLASMA FUSION CENTER Report to the President, 1988 - 1989
Jul. 1989 26 p
(Contract DE-AC02-78ET-51013)
(DE89-016050; DOE/ET-51013/273; PFC/IR-89-1) Avail: NTIS HC A03/MF A01

This report discusses the following topics on fusion energy: cold fusion; alcator confinement experiments; applied plasma physics research; fusion systems; coherent electromagnetic wave generation; and fusion technology and engineering. DOE

N90-10724# Texas Univ., Austin. Fusion Research Center.
KINETIC EFFECTS IN ALFVEN WAVE HEATING. PART 2: PROPAGATION AND ABSORPTION WITH A SINGLE MINORITY SPECIES
Wann-Quan Li, David W. Ross, and Swadesh M. Mahajan Jun. 1989 29 p
(Contracts DE-FG05-88ER-53266; DE-FG05-80ET-53088)
(DE89-016619; DOE/ER-53266/25-Pt-2; FRCR-337-Pt-2) Avail: NTIS HC A03/MF A01

Kinetic effects of Alfven wave spatial resonances near the plasma edge are investigated numerically and analytically in a cylindrical tokamak model. In Part 1, cold plasma surface Alfven eigenmodes (SAE's) in a pure plasma are examined. Numerical calculations of antenna-driven waves exhibiting absorption resonances at certain discrete frequencies are first reviewed. From a simplified kinetic equation, an analytical dispersion relation is then obtained with the antenna current set equal to zero. The real and imaginary parts of its roots, which are the complex eigenfrequencies, agree with the central frequencies and widths, respectively, of the numerical antenna-driven resonances. These results serve as an introduction to the companion paper, in which it is shown that, in the presence of a minority species, certain SAE's, instead of heating the plasma exterior, can dissipate substantial energy in the two-ion hybrid layer near the plasma center. DOE

N90-10725# Naval Research Lab., Washington, DC. Lab. for Computational Physics and Fluid Dynamics.
NUMERICAL SIMULATION OF THE COMPRESSIBLE ORSZAG-TANG VORTEX Interim Report, Jun. 1988 - Feb. 1989
R. B. Dahlburg and J. M. Picone 8 Jun. 1989 53 p
(AD-A210465; NRL-MR-6486) Avail: NTIS HC A04/MF A01 CSCL 20/9

Results of fully compressible, Fourier collocation, numerical simulations of the Orszag-Tang vortex system are presented. Initial conditions consist of a nonrandom, periodic field in which the magnetic and velocity fields contain X-points but differ in modal structure along one spatial direction. The velocity field is initially solenoidal, with the total initial pressure-field consisting of the superposition of the appropriate incompressible pressure distribution upon a flat pressure field corresponding to the initial, average flow Mach number of the flow. In our numerical simulations, we vary this initial Mach number from 0.2 to 0.6. These values correspond to average plasma beta values ranging from 30.0 to 3.3 respectively. Compressible effects develop within one or two Alfven transit times, as manifested in the spectra of compressible quantities such as mass density and nonsolenoidal flow field. These effects include: (1) retardation of growth of correlation between the magnetic field and the velocity field, (2) emergence of compressible small scale structure such as massive jets, and (3) bifurcation of eddies in the compressible flow field. Differences between the incompressible and compressible results tend to increase with increasing initial average Mach number. GRA

N90-10726# Air Force Weapons Lab., Kirtland AFB, NM.
AN EXPERIMENTAL STUDY OF MICROWAVE TRANSMISSION THROUGH A DECAYING PLASMA Final Report, Jan. 1986 - Feb. 1988
Kyle James Hendricks May 1989 31 p
(AF Proj. 5797)
(AD-A210586; AFWL-TR-89-35) Avail: NTIS HC A03/MF A01 CSCL 20/9

The physics of pulsed microwave, or radio frequency (RF), transmission through a decaying plasma column, is studied experimentally. A plasma column is formed in argon or nitrogen gases, to represent the neutral gas breakdown due to an RF pulse. Initially the electron frequency is greater than the microwave frequency. An RF pulse capable of plasma reionization is applied across the plasma column at varying times in the plasma's decay phase (the plasma afterglow). The variations were studied of the transmitted RF pulse characteristics, pulse width and amplitude, as a function of the time into the afterglow. The ionization frequency of argon by a microwave pulse is found experimentally to be within 20 percent of the theoretical value. The comparison of ionization frequency is useful in establishing the applicability of earlier cavity measurements to present day open geometry systems used in transmission/propagation experiments. GRA

N90-10727# Naval Research Lab., Washington, DC. Plasma Radiation Branch.
THE DENSE Z-PINCH AS A PLASMA RADIATION SOURCE. 1: QUASI-STATIC BENNETT MODEL Interim Report
W. Thornhill, J. L. Giuliani, Jr., and J. Davis 10 Jul. 1989 37 p Sponsored by DNA and ONR
(AD-A210600; NRL-MR-6500) Avail: NTIS HC A03/MF A01 CSCL 20/9

The radiative yield from a slowly rising current, pulsed power driven, frozen deuterium z pinch is investigated. This novel approach differs from the conventional z pinch plasma radiation source which is driven by a rapid current rise leading to a fast implosion. The slow pinch is modeled as an adiabatic contraction subject to Bennet pressure equilibrium and driven by a constant generator voltage of 500 kV. Electron degeneracy effects are included in the pressure, but, the resistivity is taken as purely classical. The Bremsstrahlung radiation spectrum evolves from thin to nearly thick during the collapse phase. The present simple model predicts results that suggest that such plasmas may be useful as a Plasma Radiation Source. GRA

76 SOLID-STATE PHYSICS

Includes superconductivity.

For related information, see also *33 Electronics and Electrical Engineering* and *36 Lasers and Masers.*

N90-10728# Texas A&M Univ., College Station. Dept. of Physics.
A COMPACT X-RAY LITHOGRAPHY LATTICE USING SUPERFERRIC MAGNETS
C. A. Swenson, F. R. Huson, W. W. MacKay, L. K. Chen, and S. Ohnuma (Houston Univ., TX.) 1989 3 p Presented at the 13th Particle Accelerator Conference, Chicago, IL, 20-23 Mar. 1989 Prepared in cooperation with Texas Accelerator Center, The Woodlands
(Contract DE-FG05-87ER-40374)
(DE89-013947; DOE/ER-40374/21; CONF-890335-217) Avail: NTIS HC A01/MF A01

A conceptual lattice design for a very compact superconducting synchrotron dedicated to X-ray lithography is presented. The synchrotron radiation produced in the high field superconducting magnets has a critical wavelength of 10 angstrom at a beam energy of about 787 MeV. The size and angular divergence of the beam in this lattice can satisfy future requirements for X-ray lithography. An optimization of the lithography parameters is presented. DOE

N90-10729# Kopin Corp., Taunton, MA.
EPITAXIAL GaAs ON SOI WAFERS Final Report, 1 Aug. 1988 - 31 Jan. 1989
J. P. Salerno 29 Mar. 1989 34 p
(Contract DAAL03-88-C-0016)
(AD-A209009; ARO-26206.1-EL-SBI) Avail: NTIS HC A03/MF A01 CSCL 20/12

The feasibility of the heteroepitaxy of high quality GaAs on silicon-on-insulator (SOI) substrates by the OMCVD process was investigated. The motivation for this is the potential to obtain large area GaAs wafers with improved radiation hardness and, eventually, the monolithic integration of radiation hardened Si and GaAs components. Epitaxial GaAs has been grown on SOI wafers prepared by both isolated silicon epitaxy (ISE) and high-dose oxygen implantation (SIMOX). The use of SIMOX provided an efficient means to obtain SOI wafers with the proper Si surface orientation compatible with a standard GaAs on Si growth technology and an excellent surface morphology was achieved. An optimally oriented ISE surface was apparently not obtained with the resulting surface morphology typical of growth on a singular (100) surface. However, the GaAs grown on ISE shows an improved defect structure while the high quality oxide/silicon interface characteristic of the ISE process is maintained. A n-channel GaAs

on SOI FET profile was achieved by doping during the epitaxy process. GRA

N90-10730# Minnesota Univ., Minneapolis. Dept. of Electrical Engineering.
QUANTUM 1/F NOISE IN SOLID STATE DEVICES IN PARTICULAR Hg1-(SUB x)Cd(SUB x)Te N(+)-P DIODES Final Report, 16 Sep. 1985 - 28 Feb. 1989
A. vanderZiel and A. D. vanRheenen 15 May 1989 10 p
(Contract DAAG29-85-K-0235)
(AD-A209365; ARO-22874.14-EL) Avail: NTIS HC A02/MF A01 CSCL 20/12

The research results are documented in the fourteen reports and publications issued under this contract. Solid state devices; diodes, quantum noise, quantum theory, and Hg(1-x)Cd(x)Te N(+)-P are discussed. GRA

N90-10731# State Univ. of New York, Buffalo. Dept. of Chemistry.
DENSITY OF STATES IN A RESONANT TUNNELING STRUCTURE
W. Trzeciakowski, D. Sahu, and Thomas F. George Jun. 1989 26 p Submitted for publication
(Contract N00014-86-K-0043)
(AD-A209508; UBUFFALO/DC/89/TR-100) Avail: NTIS HC A03/MF A01 CSCL 20/12

The change in the density of states Delta (E) brought about by the double-barrier structure is calculated. The positions and widths narrow resonances coincide with those obtained from transmission T(E), but in many cases Delta (E) is a better quantity for characterizing the resonances than T(E). GRA

N90-10732# Massachusetts Inst. of Tech., Cambridge. Dept. of Chemistry.
FACE-SPECIFIC INTERACTION OF MoS4(2-1) WITH ORIENTED CRYSTALS OF (0001) CdX (X = Se, S) Interim Technical Report No. 28, 1-12 Jun. 1988
James J. Hickman and Mark S. Wrighton 12 Jun. 1989 17 p
(Contract N00014-84-K-0553)
(AD-A209519) Avail: NTIS HC A03/MF A01 CSCL 20/2

Oriented (0001) CdX (X = S, Se) crystals selectively adsorb MoS4(2) onto the cadmium rich faces. Binding of MoS4(2) is effected by dipping the CdX crystals into CH3CN containing 20 mM (Et4N)2MoS4. Removal of the crystal from the solution followed by rinsing with CH3CN leaves MoS4(2) on the Cd but not X-rich face of the crystal as detected by X-ray photoelectron spectroscopy (XPS) and Auger electron spectroscopy (AES). The specificity for Cd-face vs. X-face binding is typically greater than 5:1 as determined by XPS and AES data for both faces of the same crystal. GRA

N90-10733# Cornell Univ., Ithaca, NY. School of Chemical Engineering.
NEGATIVE-WORKING ELECTRON BEAM RESIST BASED ON POLY(METHYL METHACRYLATE)
Y. M. Namastet, S. Kay Obendorf, Bernard C. Dems, and F. Rodriguez 12 May 1989 9 p Presented at the SPIE Symposium on Microlithography, San Jose, CA, 26 Feb. - 3 Mar. 1989
(Contract N00014-85-K-0474)
(AD-A207834; TR-12) Avail: NTIS HC A02/MF A01 CSCL 20/12

Blends of polymethylmethacrylate (PMMA) and dipentaerythritol pentaacrylate (DPEPA) respond to electron beam exposure as negative resists, with sensitivity that increases with increasing DPEPA concentration. Blends of 80 wt. pct PMMA and 20 wt. pct DPEPA exhibit an electron sensitivity of 4 microcoulombs/sq cm and a contrast gamma of 1.2. Resolution of 0.25 micrometers has been demonstrated with this blend without the use of non-solvent rinses or plasma de-scumming. This superior resolution for a negative electron resist is attributed to the small degree of swelling of the PMMA host polymer. Increasing the molecular weight of the PMMA component to 450,000 increases the sensitivity to 1 microcoulomb/sq cm, but results in poorer resolution. Use of nearly monodisperse PMMA improves the contrast to a gamma value of 2.3 without affecting resolution or sensitivity relative to the blends with low molecular weight PMMA. GRA

N90-10734# Midwest Research Inst., Golden, CO. Solar Energy Research Inst.
STRUCTURE OF AMORPHOUS SILICON ALLOY FILMS Annual Subcontract Report, 15 Jan. 1988 - 14 Jan. 1989
R. E. Norberg and P. A. Fedders Jun. 1989 31 p
(Contract DE-AC02-83CH-10093)
(DE89-009441; SERI/STR-211-3530) Avail: NTIS HC A03/MF A01

The understanding was improved at the microsccpic level of amorphous silicon-germanium-alloy films deposited under various conditions to assist researchers to produce higher quality films. The method was a joint theoretical and experimental approach to the correlation of NMR, ESR, and other characterizations, especially relating to rearrangements of hydrogen. Deuteron magnetic resonance reveals the presence of (and changes in) tightly bonded hydrogen (deuterium), weakly bonded hydrogen, molecular hydrogen, and rotating silyl groups. Microvoids are investigated via observation of para D2 for which Delta M sub J transitions are frozen out. Solid echoes reveal HD and ortho D2 trapped as singles in the semiconductor matrix. Theoretical calculations show dangling bonds to be more likely than floating bonds. DOE

N90-10735# Argonne National Lab., IL. Chemistry Div.
CONTROLLING PHOTOINDUCED ELECTRON TRANSFER RATES IN DONOR-SPACER-ACCEPTOR MOLECULES BY CHANGING THE ELECTRONIC PROPERTIES OF THE SPACER
Michael R. Wasielewski, Mark P. Niemczyk, and Douglas G. Johnson 1989 4 p Presented at the 13th DOE Solar Photochemistry Conference, Silvercreek, CO, 11-15 Jun. 1989
(Contract W-31-109-eng-38)
(DE89-015128; CONF-8906129-1) Avail: NTIS HC A01/MF A01

Electron transfer in photosynthetic reaction centers was examined. Specifically, the nature of the medium that lies between the electron donors and acceptors in the reaction centers was studied. The approach was to synthesize four fixed-distance porphyrin-quinone molecules in order to study the effects of changing the orbital energies of the donor, acceptor, and intervening spacer molecules. DOE

N90-10736# Argonne National Lab., IL.
CERAMIC PROCESSING OF BULK HIGH-T(SUB C) SUPERCONDUCTORS
Hongi J. Leu Apr. 1989 4 p Presented at the Mid-America Chinese Professional Annual Convention, Chicago, IL, 2-4 Jun. 1989
(Contract W-31-109-eng-38)
(DE89-015703; CONF-8906179-1) Avail: NTIS HC A01/MF A01

Processes are presented for the fabrication of high-T(sub c) YBa2Cu3O(7-delta) bulk oxide superconductors. The electrical and mechanical properties of the tapes cast by the doctor blade technique and wires prepared by extrusion have been characterized. Microstructural effects on these properties are discussed. Characteristics of new Bi- and Tl-based oxide superconductors are briefly reviewed. DOE

N90-10737*# National Aeronautics and Space Administration. Lewis Research Center, Cleveland, OH.
STUDY OF DEPOSITION OF YBa2Cu3O7-x ON CUBIC ZIRCONIA
Joseph D. Warner, Joseph E. Meola, and Kimberly A. Jenkins (Ohio Univ., Athens.) 1989 7 p Presented at the 3rd Annual Conference on Superconductivity and Applications, Buffalo, NY, 19-21 Sep. 1989; sponsored by New York State Inst. on Superconductivity
(NASA-TM-102350; E-5059; NAS 1.15:102350) Avail: NTIS HC A02/MF A01 CSCL 20L

Films of YBa2Cu3O7-x were grown on (100) cubic zirconia

with 8 percent yttria by laser ablation from sintered targets of YBa2Cu3O7-x. The temperature of the zirconia substrate during growth was varied between 700 and 780 C. The atmosphere during growth was 170 mtorr of O2. The films were subsequently slowly cooled in-situ in 1 atm of O2. The best films were c-axis aligned and had a transition temperature of 87.7 K. The superconducting transition temperature and the X-ray diffraction analysis is reported as a function of the substrate temperature and of the angle between the laser beam and the target's normal. Author

N90-10738*# National Aeronautics and Space Administration. Lewis Research Conter, Cleveland, OH.
OPTICAL DISPERSION RELATIONS FOR DIAMONDLIKE CARBON FILMS
Samuel A. Alterovitz, Robert M. Sieg, Neil S. Shoemaker (Case Western Reserve Univ., Cleveland, OH.), and John J. Pouch 1989 9 p Presented at the 1989 Spring Meeting of the Materials Research Society, San Diego, CA, 24-29 Apr. 1989
(NASA-TM-102356; E-4769; NAS 1.15:102356) Avail: NTIS HC A02/MF A01 CSCL 20L

Ellipsometric measurements on plasma deposited diamondlike amorphous carbon (a-C:H) films were taken in the visible, (E=1.75 to 3.5 eV). The films were deposited on Si and their properties were varied using high temperature (up to 750 C) anneals. The real (n) and imaginary (k) parts of the complex index of refraction N were obtained simultaneously. Following the theory of Forouhi and Bloomer, a least squares fit was used to find the dispersion relations n(E) and k(E). Reasonably good fits were obtained, showing that the theory can be used for a-C:H films. Moreover, the value of the energy gap (Eg) obtained in this way was compared to the Eg value using conventional Tauc plots and reasonably good agreement was obtained. Author

N90-10739# Lawrence Livermore National Lab., CA.
ANALYSIS OF THE PERFORMANCE OF GALLIUM ARSENIDE PHOTOAVALANCHE SWITCHES
W. T. White, III, C. G. Dease, and G. H. Khanaka Jul. 1989 5 p Presented at the 7th IEEE Pulsed Power Conference, Monterey, CA, 12-14 Jun. 1989 Submitted for publication
(Contract W-7405-eng-48)
(DE89-015774; UCRL-100355; CONF-890665-42) Avail: NTIS HC A01/MF A01

This work investigates how the dielectric relaxation that occurs after optical absorption can raise the electrical field from below avalanche threshold to above threshold inside a simple GaAs photoconductor. The process of optically raising the electrical field above its initial value we call dynamic field enhancement. Trade-offs between optical intensity, doping, optical absorption depth, and sample thickness are discussed with respect to obtaining useful performance of a dynamically field enhanced photoavalanche switch. We trace the origin of various contributions to field enhancement and deduce certain bounds on the magnitude of the process. In this work, response time is not considered. From a one-dimensional analysis, we conclude that, in homogeneous photoconductors with ohmic contacts, dynamic field enhancement is limited at low fields to roughly a factor of two increase. We compare our analysis to one- and two-dimensional calculations obtained with computer codes based on a drift/diffusion model. DOE

N90-10740# Australian Nuclear Science and Technology Organization, Lucas Heights.
LITHIUM COMPENSATION OF GaAs
D. Alexiev and A. J. Tavendale Aug. 1988 16 p
(DE89-616080; ANSTO/E-676; ISSN-1030-7745; ISBN-0-642-59890-8) Avail: NTIS (US Sales Only) HC A03/MF A01

Defects generated following Li diffusion into GaAs were studied by optical deep level transient spectroscopy (ODLTS) and deep level transient spectroscopy (DLTS). In an exploratory series of experiments, the effect of Li diffusion on existing trap spectra, and defect generation as a means for the compensation of GaAs was studied. The variables included diffusion temperature, initial trap spectra of GaAs and annealing periods. Detailed measurements of trap energies were made. DOE

N90-10741# International Centre for Theoretical Physics, Trieste (Italy).
MOTT TRANSITION: LOW-ENERGY EXCITATIONS AND SUPERCONDUCTIVITY
L. B. Ioffe and A. I. Larkin (Landau Inst. for Theoretical Physics, Moscow, USSR) Sep. 1988 17 p Submitted for publication
(DE89-617778; IC-88/340) Avail: NTIS (US Sales Only) HC A03/MF A01

It is possible that metal-dielectric transition does not result in changes of magnetic or crystallographic symmetry. In this case a fermionic spectrum is not changed at the transition, but additional low-energy excitations appear which can be described as a gauge field that has the same symmetry as an electromagnetic one. In the case of a non half-filled band, gapless scalar Bose excitations also appear. Due to the presence of additional gauge field the physical conductivity is determined by the lowest conductivity of the Fermi or Bose subsystems. DOE

N90-10742# Los Alamos National Lab., NM.
SUPERCONDUCTIVITY FROM VALENCE FLUCTUATIONS WITH FINITE U
B. H. Brandow 1989 3 p Presented at the International Conference on Materials and Mechanisms of Superconductivity - High-Temperature Superconductors, 23-28 Jul. 1989
(Contract W-7405-eng-36)
(DE89-015302; LA-UR-89-2469; CONF-890718-17) Avail: NTIS HC A01/MF A01

The finite-U paring mechanism of Newns is found to be opposed by a magnetic tendency arising from Gutzwiller renormalization of the hybridization. This competition restricts superconductivity and also reproduces the parabolic rise and fall of T sub c in La(2-x)Sr(x)CuO4 with increasing x. DOE

N90-10743# Temple Univ., Philadelphia, PA. Dept. of Physics.
MIXED-VALENT AND HEAVY FERMIONS AND RELATED SYSTEMS Progress Report No. 2, May 1987 - Jun. 1988
Pedro Schlottmann 14 Jul. 1989 14 p
(Contract DE-FG02-87ER-45333)
(DE89-016335; DOE/ER-45333/2) Avail: NTIS HC A03/MF A01

Brief discussions are given in this progress report on the following topics: the 4f-quadrupolar moment of Yb in YbCu sub 2 Si sub 2; thermodynamics of the n-channel Kondo problem in a magnetic field; the two-impurity Kondo problem; critical behavior of Heisenberg chains; spin-wave theory of the two-dimensional antiferromagnet with impurities; one-dimensional Hubbard model with attractive on-site U; the Gutzwiller dynamic susceptibility; and high-temperature superconductivity. DOE

N90-10744# Utah Univ., Salt Lake City. Coll. of Engineering.
ORDERED STRUCTURES AND METASTABLE ALLOYS GROWN BY OMVPE
G. B. Stringfellow 1989 18 p
(Contract DE-FG02-84ER-45061)
(DE89-016370; DOE/ER-45061/T5) Avail: NTIS HC A03/MF A01

The understanding of the thermodynamics of mixing in semiconductor solids has evolved from the purely empirical regular solution model to models based on the electron energy states in the solid, including the delta-lattice parameter (DLP) model and, more recently, first principles calculations. These models are in agreement that the enthalpy of mixing is invariably (ge)0 for III/V and II/VI alloys, and increases with increasing difference in lattice constant for the constituent binary compounds. In terms of the simple thermochemical mixing models, this suggests the occurrence of miscibility gaps. Solid phase immiscibility was indeed observed in a number of systems. Nevertheless, such alloys can be grown by OMVPE, including the highly metastable alloys GaPSb and InPSb. Ordered structures are now observed in several III/V

alloy systems including the ternary systems GaAsSb, GaInP, AlInAs, AlGaAs, and GaInAs, and the quaternaries GaInAsP, GaInAsSb, and AlGaInP. Ordering in other alloy systems such as GaPSb, InPSb, InAsSb, and GaAsP will be described. An unexpected observation is that the preferred ordered structure for the ternaries GaInP, GaPSb, InAsSb, and GaAsP involves ordering along the (111) directions, forming the CuPt (L1 sub 1) structure. This is also true of GaAsSb grown by MBE. Both the first principles calculations and simple strain energy calculations indicate that such ordered structures are more stable than the disordered solid solution, but less stable than the other ordered structures. DOE

N90-10745# Brookhaven National Lab., Upton, NY.
CRITICAL MAGNETIC FIELDS (H(SUB c2), H(SUB c1)) AND KAPPA IN YBa2(Cu0.98M0.02)3O(7+DELTA), M=Ni, Al, AND Cu
Youwen Xu, M. Suenaga, and A. R. Moodenbaugh 1989 2 p Presented at the International Conference on Materials and Mechanisms of Superconductivity - High-Temperature Superconductors, Stanford, CA, 23-28 Jul. 1989
(Contract DE-AC02-76CH-00016)
(DE89-016412; BNL-43065; CONF-890718-22) Avail: NTIS HC A01/MF A01

The upper critical magnetic field H sub c2 up to 5T and (dM(T)/dH) sub Hc2 for aligned powders of pure and Al and Ni substituted YBa2(Cu.98M.02)3O(7+delta) are measured magnetically. The (dH sub c2 /dT)tc is linear with slopes of -2.2T/K, -2.4T/K and -2.8T/K for the pure, Ni and Al samples respectively. The values of H sub c1, kappa, and delta C/T sub c were deduced from (dM(T)/dH) sub Hc2. DOE

N90-10746# Brookhaven National Lab., Upton, NY.
MAGNETIC CORRELATIONS IN HIGH T(SUB c) OXIDES IN THE SUPERCONDUCTING STATE
G. Shirane 21 May 1989 10 p
(Contract DE-AC02-76CH-00016)
(DE89-016421; BNL-43034) Avail: NTIS HC A02/MF A01

A review is given of recent neutron scattering measurements on La(2-x)Sr(x)CuO4 and YBa2Cu3O(6+x) single crystals. Well defined, modulated magnetic excitations are observed in a high quality single crystal of La(1.85)Sr(0.15)CuO4. This crystal exhibits a sharp superconducting transition at 33 K with a high Meissner effect. For magnetic excitation energies of 9 MeV and lower, the intensity drops substantially below 150K. Similar magnetic scattering of YBa2Cu3O(6-x) in the superconducting region is now being sought. DOE

N90-10747# Fermi National Accelerator Lab., Batavia, IL.
PERFORMANCE OF THE CAMEX64 SILICON STRIP READOUT CHIP
R. J. Yarema Jun. 1989 22 p
(Contract DE-AC02-76CH-03000)
(DE89-014015; FNAL-TM-1604) Avail: NTIS HC A03

The CAMEX64 is a 64 channel full custom CMOS chip designed specifically for the readout of silicon strip detectors. CAMEX which stands for CMOS Multichannel Analog MultiplEXer for Silicon Strip Detectors was designed by members of the Franhofer Institute for Microelectronic Circuits and Systems and the Max Planck Institute for Physics and Astrophysics. Each CAMEX channel has a switched capacitor charge sensitive amplifier with 4 sampling capacitors and a multiplexing scheme for reading out each of the channels on an analog bus. The device uses multiple sampling capacitors to filter and reduce input noise. Filtering is controlled through sampling techniques using external clocks. The device operates in a double correlated sampling mode and therefore cannot separate detector leakage current from a charge input. Normal operation is similar to all other silicon readout chips designed and built thus far in that there is a data acquisition cycle during which charge is simultaneously accepted on all channels for a short period of time from a detector array, followed by a readout cycle where that charge or hit information is read out. This device works especially well for colliding beam experiments where the time of charge arrival is accurately known. However it can be used in fixed target or asynchronous mode where the time of charge arrival is not well known. In the asynchronous mode it appears that gain is somewhat dependent on the time interval required to decide whether or not to accept charge input information and thus the maximum signal to noise performance found with the synchronous mode may not be achieved in the asynchronous mode. DOE

N90-10748# California Univ., Berkeley. Lawrence Berkeley Lab.
ATOMIC IMAGING AND INTERFACIAL ANALYSIS
C. J. D. Hetherington and G. Thomas Jan. 1989 13 p Presented at the Ceramics-Metal Interfaces Conference, Santa Cruz, NM, 16-18 Jan. 1989
(Contract DE-AC03-76SF-00098)
(DE89-015339; LBL-26734; CONF-8901153-1) Avail: NTIS HC A03/MF A01

The structure and composition of interfaces are important in influencing the overall physical properties of materials. Thus, a methodical development of the growth and processing of metal/ceramic composites with a view to improving their properties should be accompanied by a characterization of the interfacial structures. In this paper, the contribution of atomic imaging by electron microscopy to such an analysis is indicated with examples of research utilizing the Atomic Resolution Microscope (ARM) at the National Center for Electron Microscopy. DOE

N90-10749# Massachusetts Inst. of Tech., Cambridge. Dept. of Materials Science and Engineering.
PROGRESS REPORT ON GRAIN BOUNDARIES
R. W. Balluffi and P. D. Bristowe Jun. 1989 23 p
(Contract DE-FG02-87ER-45310)
(DE89-015541; DOE/ER-45310/19) Avail: NTIS HC A03/MF A01

The research was focused on the following three major areas: (1) study of the atomic structure of grain boundaries by means of X-ray diffraction, transmission electron microscopy and computer modeling; (2) study of grain boundary phase transitions by electron microscopy and computer modeling; (3) investigation of the mechanism of high angle grain boundary migration. Results are briefly discussed. DOE

N90-10750# Oak Ridge National Lab., TN. Metals and Ceramics Div.
MORPHOLOGICAL ASPECTS OF THE FRICTION OF HOT-FILAMENT-GROWN DIAMOND THIN FILMS
Peter J. Blau, Charles S. Yust, and Robert E. Clausing 1989 10 p Presented at the 16th Leeds-Lyon Symposium on Tribology, Lyon (France), 5-8 Sep. 1989
(Contract DE-AC05-84OR-21400)
(DE89-015986; CONF-8909174-1) Avail: NTIS HC A02/MF A01

Recent developments in chemical vapor deposition (CVD) technology have made it possible to produce thin diamond film on a variety of substrate materials. Diamond, having a very high hardness and low sliding friction coefficient, is a good candidate for tribological applications. Diamond films produced by a hot-filament CVD method often have irregular surfaces owning to the preferred growth mode of the crystals which form on the surface. This investigation using sapphire and bearing steel spherically tipped sliders demonstrated that the morphology of the diamond film surface produced friction coefficient up to ten times those observed in previous experiments which involved smooth diamond surfaces sliding against various solids in air. DOE

N90-10751# Sandia National Labs., Albuquerque, NM.
STRUCTURAL ASPECTS OF THE PHASE SEPARATION IN La2CuO4.032
C. Chaillout, J. Chenavas, S. W. Cheong, Z. Fisk, M. S. Lehmann, M. Marezio (Bell Telephone Labs., Inc., Murray Hill, NJ.), B. Morosin, and J. E. Schirber 1989 3 p Presented at the International Conference on Materials and Mechanisms of Superconductivity -

High-Temperature Superconductors, Stanford, CA, 23-28 Jul. 1989
(Contract DE-AC04-76DP-00789)
(DE89-016183; SAND-89-1876C; CONF-890718-24) Avail: NTIS HC A01/MF A01

The average structure of superconducting La sub 2 CuO sub 4.032 has been determined by single-crystal neutron diffraction data. The excess oxygen is located between two adjacent LaO layers. Its presence distorts the apical-oxygen sublattice in such a way that a short O--O bond is formed (1.64(angstrom)). By scanning several hkl reflections, we have confirmed that a phase separation occurs below room temperature. The peaks of one phase are in agreement with the space group Cmca and the unit cell proposed by Jorgensen et al., and Cox et al., however, a monoclinic unit cell is needed to index the second phase reflections. DOE

N90-10752# California Univ., Berkeley. Lawrence Berkeley Lab. Center for Advanced Materials.
CHARACTERIZATION OF GaAs/Si/GaAs HETEROINTERFACES
Zuzanna Liliental-Weber and Raymond P. Mariella, Jr. (Lawrence Livermore National Lab., CA.) Jun. 1989 7 p Presented at the Spring Meeting of the Materials Research Society, San Diego, CA, 24-28 Apr. 1989
(Contracts DE-AC03-76SF-00098; W-7405-eng-48)
(DE89-016302; LBL-27498; CONF-890426-25) Avail: NTIS HC A02/MF A01

Transmission electron microscopy of GaAs grown on Si for metal-semiconductor-metal photodetectors is presented in this paper. Two kinds of samples are compared: GaAs grown on a 15 (angstrom) Si epilayer grown on GaAs, and GaAs grown at low temperature (300 C) on Si substrates. It is shown that the GaAs epitaxial layer grown on thin Si layer has reverse polarity to the substrate (antiphase relation). Higher defect density is observed for GaAs grown on Si substrate. This higher defect density correlates with an increased device speed, but with reduced sensitivity. DOE

N90-10753# California Univ., Berkeley. Lawrence Berkeley Lab. Center for Advanced Materials.
METHODS TO DECREASE DEFECT DENSITY IN GaAs/Si HETEROEPITAXY
Zuzanna Liliental-Weber Jun. 1989 12 p Presented at the Spring Meeting of the Materials Research Society, San Diego, CA, 24-28 Apr. 1989
(Contract DE-AC03-76SF-00098)
(DE89-016306; LBL-27356; CONF-890426-26) Avail: NTIS HC A03/MF A01

In this paper, the fundamental mechanisms of procedures improving the structural quality of GaAs grown on Si are discussed. Patterned growth, strained layer superlattices and power thermal cycling are promising approaches to achieve a high quality of GaAs layers grown on Si substrates. DOE

N90-10754# Arizona State Univ., Tempe. Semiconductor Materials Research Lab.
AUTONOMOUS CONTROL SYSTEM FOR CZOCHRALSKI GROWTH OF LEC GaAs Final Technical Report, 1 Oct. 1986 - 30 Nov. 1989
B. Luger and R. C. White 1989 29 p
(Contract F49620-86-C-0012)
(AD-A210190; AFOSR-89-0801TR) Avail: NTIS HC A03/MF A01 CSCL 20/2

The consolidation of the Czochralski Growth Control System (CGCS) is a revision of the hardware and software within the constraints of the first generation. The consolidation consists of: a cabinet that is physically more compatible with the Cambridge console; a more modular hardware arrangement that facilitates calibration, servicing, and expansion; increased accuracy and stability of the system variable measurements; and many software enhancements, including increased controller flexibility and improved diameter estimation and control. The hardware and software installation was completed and crystal growth with complete digital control was demonstrated. GRA

N90-10755# SRI International Corp., Menlo Park, CA.
PROCESSING AND FABRICATION OF HIGH TEMPERATURE OXIDE SUPERCONDUCTORS Annual Report, 1 Aug. 1988 - 30 Jun. 1989
Sylvia M. Johnson 7 Jul. 1989 15 p
(Contract N00014-88-C-0705)
(AD-A210197) Avail: NTIS HC A03/MF A01 CSCL 20/12

During the past year, a process for synthesizing superconductor powders by freeze drying was optimized. The objectives were to develop an understanding of the processing of these powders and to fabricate simple shapes from freeze dried powders. A series of powders were synthesized from solutions of barium acetate, copper nitrate, and yttrium nitrate, with pH values of 2.8 to 9.8 and calcined at temperatures from 510 to 908 C. The surface area of these powders were determined by BET AND XRD. Selected powders are being characterized by SEM, DTA, ICP analysis (performed at Stanford University), carbon analysis, and tap density. The highest surface area (in lightly milled powders) of 4.4 sq m/g was achieved with a pH of 4 in a series of experiments in which the Ba and Y solutions were mixed together before the Cu nitrate solution was added, then calcined at 825 C. Surface areas decrease with increasing calcining temperature, however. It appears that calcining at 750 or 850 C gives the best critical temperature, with complete transitions at greater than 90 K. Critical temperature measurements performed at Standford show that the goal of a critical temperature of Tc greater than 90 K and a temperature difference, W, between 10 and 90 percent of transition of less than 2 K, were achieved. GRA

N90-10756# Air Force Wright Aeronautical Labs., Wright-Patterson AFB, OH. Materials Lab.
EFFECTS OF COHERENT SCATTERING ON INFRARED ABSORPTION IN DOPED SEMICONDUCTORS Final Report, Jun. 1985 - Aug. 1986
Peggy J. Grigsby (Universal Energy Systems, Inc., Dayton, OH.) and Gail J. Brown Apr. 1989 39 p
(AD-A210224; AFWAL-TR-88-4205) Avail: NTIS HC A03/MF A01 CSCL 20/12

An improved theoretical model was developed for interpreting the infrared absorption spectra of doped semiconductors. The model focused on the specific problem of coherent scattering effects or optical channeling. These effects are produced by coherent multiple internal reflections from the polished plane-parallel faces of an optically thin sample. The coherent scattering produces oscillating noise on the infrared absorption spectrum. This noise makes it difficult to determine the correct absorption coefficient from the spectrum. The effect occurs in both silicon and gallium arsenide. The specific expression for the transmittance in the presence of scattering was determined and the inversion of this relation was calculated to obtain the absorption coefficient. In cases where the equation based on coherent scattering did not give results, a combination of coherent and incoherent scattering equations was used to minimize the channeling oscillations. GRA

N90-10757# Aerospace Corp., El Segundo, CA. Electronics Research Lab.
BIAS AND OXIDE THICKNESS DEPENDENCE OF TRAPPED CHARGE BUILDUP IN MOS DEVICES
R. J. Krantz and T. C. Zietlow 31 Jan. 1989 27 p
(Contract F04701-88-C-0089)
(AD-A210264; TR-0089(4925-07)-1; SD-TR-89-42) Avail: NTIS HC A03/MF A01 CSCL 20/12

A rate equation for charge buildup, which includes sweep-out, hole/electron trapping, tunneling, recombination, and the effects of internal fields, is generalized to apply to negative gate biases and include electron injection from the silicon and aluminum gate interfaces. The dependence of the midgap voltage shift on oxide thickness is explicitly examined. The theoretical results are verified

by comparison with experimental results obtained on p-type silicon test capacitors of different oxide thicknesses under varying positive and negative gate biases. GRA

N90-10758# University of Southern California, Los Angeles. Dept. of Materials Science and Engineering.
EXPERIMENTAL INVESTIGATIONS OF TRANSPORT AND OPTICAL PROPERTIES OF 3-5 QUANTUM WELL STRUCTURES GROWN VIA MOLECULAR BEAM EPITAXY UNDER OPTIMAL GROWTH CONDITIONS Progress Report, 1 Jan. 1987 - 31 Dec. 1988
A. Madhukar 18 Apr. 1989 57 p
(Contract DAAL03-86-K-0102)
(AD-A210269; ARO-23736.1-EL) Avail: NTIS HC A04/MF A01 CSCL 20/12

Zero field mobilities in GaAs/Al(x)Ga(1-x)As(100) inverted HEMT structures in excess of 100,000 sq cm/V-Sec at LN2 temperatures were achieved . The possibility of high mobilities in square single quantum wells with modulation doping on the inverted interface side only is demonstrated. Photoluminescences linewidth dependence on the square single quantum well width shows inverse proportion rather than the inverse cubic proportion behavior expected from the popularly used notion of well width fluctuations. The observed behavior is shown to be consistent with fluctuations in the band edge discontinuity (i.e., well depth) arising from in-plane fluctuations in the alloy composition of the AlxGa(1-x)As barrier layers in high quality structures. Influence of an electric field across single and coupled-double quantum wells on their optical characteristics is examined theoretically and through photoluminescence, photocurrent, electroreflectance, photoreflectance and Photovoltage measurements. Exploiting growth conditions controlled thermodynamic and kinetic effects on facet formation and inter-facet migration, a unique in-situ method for realization of quantum wire and quantum box structures without the need for lithography or direct-write patterning on such small dimensions is demonstrated. Finally, some initial results on resonant tunneling diodes are reported. GRA

N90-10759# Duke Univ., Durham, NC.
PROPERTIES OF DEVICES PREPARED WITH EPITAXIAL LAYERS ON InP Final Report, Jul. 1985 - Jun. 1987
H. C. Casey, Jr. Mar. 1989 36 p
(Contract F19628-85-K-0040)
(AD-A210304; RADC-TR-89-30) Avail: NTIS HC A03/MF A01 CSCL 20/12

Electrical measurements were made on capacitors prepared with remote plasma-enhanced chemical vapor deposition (RPECVD) SiO2 films on p-type Ga(0.47)In(0.53)As at low substrate temperatures. These measurements demonstrated that the RPECVD dielectric is suitable for use in the fabrication of MISFETs. Measurements on RPECVD SiO2 layers on Si showed that care must be taken in cleaning and processing to prevent Na ions from being introduced into the dielectric layers. To provide stable characteristics, surface cleaning before deposition must be investigated and processing techniques must be used to prevent the introduction of mobile ions into the deposited dielectric layers. Techniques to reduce the temperature sensitivity of the threshold current density of InP-Ga(x)In(1-y) DH (double heterostructure) lasers were investigated. The most promising technique is the use of thin pseudomorphic active layers and wide energy gap cladding layers. GRA

N90-10760# North Carolina State Univ., Raleigh. Dept. of Materials Science and Engineering.
THE GROWTH OF GALLIUM NITRIDE FILMS VIA THE INNOVATIVE TECHNIQUE OF ATOMIC LAYER EPITAXY Annual Progress Report, 1 Jun. 1988 - 31 May 1989
Robert F. Davis, Michael J. Paisley, and Zlatko Sitar 1 Jun. 1989 28 p
(Contract N00014-86-K-0686)
(AD-A210380; NCSU/MTE-6) Avail: NTIS HC A03/MF A01 CSCL 20/2

This contract involves investigating the efficacy of atomic layer and molecular beam epitaxy techniques for the growth of GaN (a wide bandgap semiconductor). Growth of materials in the Al-Ga-In-N solid solution series was extended as well as pure AlN and InN, and heterostructures of these materials. In addition, work was begun on the growth of cubic boron nitride. The first reported heterostructures of cubic GaN/AlN were produced. Work also continued on characterization of the cubic GaN already produced. Much improved material and higher growth rates were observed with the installation of a NCSU-designed, constructed, and commissioned electron cyclotron resonance plasma source. GRA

N90-10761# Stanford Univ., CA. Electronics Lab.
ADVANCED GaAs PROCESS MODELING, VOLUME 1 Final Report, Dec. 1985 - Oct. 1988
Thomas W. Sigmon May 1989 96 p
(Contract F33615-85-C-5048; AF Proj. 2423)
(AD-A210385; WRDC-TR-89-4024-Vol-1) Avail: NTIS HC A05/MF A01 CSCL 20/12

Physical models were developed for substrate and process defects and variations which affect the electrical parameters of MESFET structures fabricated on this material by direction implantation processes. Verification of these models was to be carried out where possible by fabrication of specially designed device structures capable of providing statistically significant data. In order to remove, as much as possible, unwanted process variations all device processing was carried our under a subcontract with the Rockwell MRDC GaAs pilot line facility. The primary successes of the program include: (1) development of a physical model to explain the effect of dislocations on the fluctuations threshold voltage observed experimentally; (2) development of analytical Pearson IV models for the profiles of the technologically significant ions Si, Se, and Be in 100 oriented GaAs for specific tilt and rotational angles of the substrates with respect to the implant beam; and (3) development of a one dimensional device and process simulator which allows exploration of the effect of certain process variables on the significant MESFET electrical parameters. GRA

N90-10762# Massachusetts Inst. of Tech., Lexington. Lincoln Lab.
SUBMILLIMETER QUANTUM ELECTRONICS Final Report, 1 Apr. 1985 - 1 Nov. 1988
T. C. L. G. Sollner 14 Jun. 1989 78 p
(Contracts F19628-85-C-0002; MIPR-ARO-105-88)
(AD-A210439; ESD-TR-89-142; ARO-22746.11-PH) Avail: NTIS HC A05/MF A01 CSCL 20/12

The phenomena of resonant tunneling was explored in GaAs/AlGaAs heterostructures that were grown by molecular-beam epitaxy. The physics and fundamental speed limitations were studied, and devices such as oscillators, multipliers, and mixers are demonstrated. Useful output was obtained at room temperature for frequencies up to 425 GHz. The feasibility of resonant-tunneling transistors was examined, suggesting cutoff frequencies above 100 GHz. Planar antenna arrays were developed and tested up to 1.7 THz. In the area of compact solid-state instrumentation, a 555 GHz receiver was developed that had a noise temperature of 45000 K and weighed 3 kg. GRA

N90-10763# Aerospace Corp., El Segundo, CA. Electronics Research Lab.
HIGH ENERGY NEUTRON IRRADIATION EFFECTS IN GaAs MODULATION-DOPED FIELD EFFECT TRANSISTORS (MODFETS): THRESHOLD VOLTAGE
R. J. Krantz, W. L. Bloss, and M. J. OLoughlin 15 Jun. 1989 40 p
(Contract F04701-88-C-0089)
(AD-A210502; TR-0089(4925-07)-3; SD-TR-89-44) Avail: NTIS HC A03/MF A01 CSCL 20/12

The effects of high energy neutrons of fluences approaching 1 x 10 to the 15th power per sq cm on MODFETs have been studied. Neutron-induced threshold voltage shifts are described by application of a finite temperature strong inversion, depletion

layer, charge control model. The results of this model show that the neutron-induced threshold voltage is a consequence of electron trapping the GaAs layer near the AlGaAs/GaAs interface. This allows a convenient parameterization of the neutron degradation by accounting for these trapped electrons as effective acceptors, defining an effective acceptor introduction rate, and applying the charge control model to describe the threshold voltage. Our analysis shows that neutron degradation in these AlGaAs/GaAs heterostructures is dominated by the change in the depletion layer charge and the shift in the Fermi level with neutron fluence. The dominant mechanisms are shown to depend on GaAs material parameters, only. The contribution due to the AlGaAs layer carrier removal is less than 3 percent of the total threshold voltage shift. GRA

N90-10764# State Univ. of New York, Buffalo. Dept. of Chemistry.
DWELL TIME AND AVERAGE LOCAL SPEED IN A RESONANT TUNNELING STRUCTURE
L. N. Pandey, D. Sahu, and Thomas F. George Jul. 1989 22 p
(Contract N00014-86-K-0043)
(AD-A210566; UBUFFALO/DC/89/TR-106) Avail: NTIS HC A03/MF A01 CSCL 20/12

The dwell times and the average local speeds of an electron in a resonant tunneling structure depend sensitively on the matching parameter at the interfaces. There is a need to carry out microscopic calculations to find out which matching parameter is appropriate for a given structure. GRA

N90-10765# Arizona State Univ., Tempe. Dept. of Electrical Engineering.
DEEP TRAPS AND SIDEGATING IN GaAs DEVICES Final Report, 15 May 1986 - 14 May 1989
George N. Maracas and David A. Johnson 15 Jul. 1989 12 p
(Contract DAAL03-86-K-0070)
(AD-A210740; ARO-23494.12-EL) Avail: NTIS HC A03/MF A01 CSCL 20/12

This is the final technical report for ARO contract DAALO3-86-K-0070. Progress in the areas of semi-insulating GaAs conduction mechanisms and how they apply to the phenomena of sidegating and backgating in GaAs based devices are described. The experimental and theoretical program evolved into a highly collaborative effort between industry and university with several joint publications resulting. The sidegating/backgating problem was finally acknowledged as can be seen by the recent creation of a highly interactive workshop dedicated to such effects. Research included the establishment of electrical and optical characterization facilities specifically designed for the study of the high resistivity materials and their effects on devices. Advances were made in several exponential signals for Deep Level Transient Spectroscopy (DLTS), imaging of deep level domains using voltage contrast in a scanning electron microscope (SEM), surface stability of various passivation techniques and one dimensional, steady state and transient numerical simulations of semi-insulating GaAs transport properties. Additionally the chaotic properties of the low frequency oscillations were discovered. GRA

N90-10766# Arizona Univ., Tucson. Optical Sciences Center.
FEMTOSECOND DYNAMICS OF FLUORO-ALUMINUM PHTHALOCYANINE AND LINEAR ALKANE MOLECULES Progress Report
Z. Z. Ho, V. William, N. Peyghambarian, and W. M. Hetherington (Oregon State Univ., Corvallis.) Aug. 1989 10 p
(Contract DAAL03-86-G-0024)
(AD-A210939; ARO-23757.8-PH-F) Avail: NTIS HC A02/MF A01 CSCL 07/4

The dynamics of fluoro-aluminum phthalocyanine polycrystalline thin films is studied using differential transmission spectroscopy with femtosecond laser pulses. Following excitation by 620 nm pulses into the first electronic transition a very rapid energy redistribution of the excitons is directly observed within the 55 fs duration of the pump pulse. Following this process two extremely fast decay routes lead to the recovery of the ground state: exciton annihilation with an intensity dependent decay of 550 fs at power density of 1.2 GW/sq cm and exciton-phonon coupling with a 4 ps decay time. A complete interpretation of the decay mechanisms based on the Frenkel exciton terminology successfully accounts for the observed results. The nonlinear dynamics of a series of linear alkane molecules in pure liquid state were analyzed using the time resolved optical Kerr effect. The results show that the Kerr nonlinearity increases linearly with the number of atoms. However, for those molecules with more than eight carbons, a surprisingly large deviation from the bond additivity approximation was observed. The molecular orientational contribution to the nonlinear response is negligible for these types of molecules. GRA

N90-10767# Massachusetts Inst. of Tech., Cambridge. Research Lab. of Electronics.
FOCUSED ION BEAM IMPLANTATION Semiannual Progress Report, 1 Jan. - 30 Jun. 1989
John Melngailis 13 Jul. 1989 9 p
(Contract DAAL03-88-K-0108)
(AD-A210977; ARO-26051-EL) Avail: NTIS HC A02/MF A01 CSCL 20/12

The capability to transfer the positions of features from a given level of an integrated circuit layout to the focused ion beam machine is important in most of the intended applications of focused ion beams implantation. The capability is developed to transfer patterns written in MAGIC (a layout software system) to the focused ion beam format. The machine development was used to implant the channels on Si-NMOS devices. A test structure was used where each die had 256 transistors each one with probe contact pads. Each die was aligned to the focused ion beam and then all 256 channels were implanted with a variety of doses and geometrics. In the area of GaAs devices, Gunn diodes were implanted with variety of doping gradients between the contacts. The doping gradients were chosen according to calculated computer models. The fine pattern writing of the focused ion beam system is used to generate electrodes on GaAs/GaAlAs modulation doped structures. These electrodes had a minimum width of 0.05 microns and were used to observe resonant tunneling parallel to the surface. GRA

N90-10768# Cambridge Univ. (England).
THE EFFECT OF TWINS ON CRITICAL CURRENTS OF HIGH Tc SUPERCONDUCTORS Interim Report No. 4
A. M. Campbell and M. F. Ashby 1989 4 p
(Contract DAJA45-87-C-0059)
(AD-A210988; R/D-5909-MS-01) Avail: NTIS HC A01/MF A01 CSCL 20/3

The initial work on levitation forces and separation of superconducting powders has divided into two projects. The first is the nature of the frictional forces and damping on levitated magnets. Although it is reasonable to suppose this arises from ac losses in the superconductor, magnets rotating about their center of symmetry should not give fluctuating fields and should form almost frictionless bearings. The second is the direct use of magnetic forces to separate particles of superconducting from non superconducting material. The major problem here has been the tendency of fine particles to stick together due to electrostatic forces. To overcome this we have formed a slurry of the material in liquid nitrogen and flash evaporated the nitrogen to blow particles apart. This is reasonably successful but we do not yet know to what extent they will reaglomerate. A second problem is ensuring thermal equilibrium of the particles. This can be done fairly easily in a liquid slurry, but this limits the temperature range we can use and the liquid convection tends to counteract the separation process. GRA

N90-10769# Carnegie-Mellon Univ., Pittsburgh, PA.
TRAP GETTERING BY ISOELECTRONIC DOPING OF p-GaAs AND n-GaAs GROWN BY MOLECULAR BEAM EPITAXY
A. G. Milnes, Aizhen Li (Shanghai Inst. of Metallurgy, China), H. K. Kim, J. C. Jeong, D. Wong, J. H. Zhao, Z.-Q. Fang, and T. E. Schlesinger 1989 5 p Submitted for publication

(Contract DAAL03-86-K-0066)
(AD-A211162; ARO-23520.8-EL) Avail: NTIS HC A01/MF A01 CSCL 20/2

The effects of isoelectronic In and Sb doping on the hole traps in Be doped p-GaAs and electron traps in Si-doped n-GaAs(100) grown by molecular beam epitaxy (MBE) have been investigated. The dominant hole traps in our Be doped layers are at about E sub v + 0.56 eV (H4) and may be the HL8 trap (0.52 to 0.54 eV) reported previously and at E sub v + 0.29 eV (H2). The concentrations of H4 and H2 are reduced by three orders of magnitude (from 10 to the 15th power/cu cm for H4, 10 to the 14th power/cu cm for H2) by increasing the growth temperature from 500 to 600 C. Photocapacitance measurements support the view that this trap is As(++) sub Ga and not a trap associated with FeGa. Additions of 0.2 percent to 2 percent In or Sb for growths at 500 or 550 C have no affect on the concentration of this anti-site defect trap but cause a considerable reduction of the trap at 0.29 eV (H2). The two dominant electron traps M3 (E sub c - 0.33 eV) and M6 (E sub c - 0.62 eV) in our n-GaAs layers are drastically reduced in concentration by up to three orders of magnitude by introducing 0.2 to 1 at. percent In or Sb and increasing growth temperature from 500 to 600 C. In and Sb appear to have rather similar effects in trap gettering the concentration of the M3, M6 and H2. This suggests that these traps are in some way related to (V sub As V sub Ga) complexes or (V sub As(X) V sub Ga) complexes. GRA

77 THERMODYNAMICS AND STATISTICAL PHYSICS

Includes quantum mechanics; theoretical physics; and Bose and Fermi statistics.

For related information see also *25 Inorganic and Physical Chemistry* and *34 Fluid Mechanics and Heat Transfer.*

N90-10770# Universidade Federal do Rio de Janeiro (Brazil).
ARE THERE CAUSAL VACUUM SOLUTIONS WITH THE SYMMETRIES OF THE GOEDEL UNIVERSE IN HIGHER-DERIVATIVE GRAVITY
A. J. Accioly and G. E. A. Matsas (Universidade Estadual de Paulista, Sao Paulo, Brazil) 1988 11 p
(DE89-611966; IFT-P-29/88) Avail: NTIS (US Sales Only) HC A03/MF A01

A globally causal vacuum solution with the symmetries of the Godel universe is obtained in the framework of higher derivative gravity. This very peculiar and rare result has no similar one in the standard general relativity. The Reboucas-Tiomno universe, i.e., the unique completely causal Goedel-type solution of Einstein's field equations with the algebraic Segre characteristics ((1,11)) is shown to be a special case of our solution. It is also shown that one model is an imbedding of the 3-D anti-de Litter universe in 4-D space-time. DOE

N90-10771# International Centre for Theoretical Physics, Trieste (Italy).
N=1,2 SUPERGRAVITIES IN 2+1 DIMENSIONS AS CHERN-SIMONS THEORIES
Miao Li Dec. 1988 10 p Submitted for publication Prepared in cooperation with International Centre for Relativistic Astrophysics, Rome, Italy and Rome Univ., Italy
(DE89-612006; IC-88/406) Avail: NTIS (US Sales Only) HC A02/MF A01

The results are reported on the explanation of the Lagrangians of 2+1 supergravities as graded Chern-Simons terms, which are derived from inspiration of Witten's recent work on exact solvability of 2+1 Einstein gravity. DOE

N90-10772# Maryland Univ., College Park.
THEORETICAL INVESTIGATIONS OF CHAOTIC DYNAMICS Final Report, 1 Dec. 1986 - 30 Nov. 1988
James A. Yorke 30 Nov. 1988 6 p
(Grant AF-AFOSR-0110-87; AF Proj. 2304)
(AD-A207724; AFOSR-89-0572TR) Avail: NTIS HC A02/MF A01 CSCL 12/2

Ten papers were published: Pseudo-orbit shadowing in the family of tent maps; Is every approximate trajectory of some process near an exact trajectory of a nearby process; Noise reduction in dynamical systems; Using dynamic embedding methods to analyze experimental data; Period halving for x sub H+1 = MF sub N where F has negative Schwarzian derivative; Numerical orbits of chaotic processes represent true orbits; A procedure for finding numerical trajectories on chaotic saddles; Antimonotonicity: Concurrent creation and annihilation of periodic orbits; Accessible saddles on fractal basin boundaries. Analysis of a procedure for finding numerical trajectories close to chaotic saddle hyperbolic sets. GRA

N90-10773# Pisa Univ. (Italy). Facolta di Ingegneria.
THERMODYNAMIC TRANSPORT PROPERTIES OF NITROGEN TETROXIDE IN HYPERCRITICAL CONDITIONS FOR REGENERATIVE COOLING OF A ROCKET ENGINE. VOLUME 1: TESTS Ph.D. Thesis [PROPRIETA' TERMODINAMICHE E DI TRASPORTO DEL TETROSSIDO DI AZOTO IN CONDIZIONI IPERCRITICHE PER IL RAFFREDDAMENTO RIGENERATIVO DI UN MOTORE A RAZZO. VOL. 1: TESTO DELLA TESI]
Giorgio Saccoccia 1988 236 p In ITALIAN
(ETN-89-94975) Avail: NTIS HC A11/MF A02

The thermodynamical and transport properties are studied for nitrogen tetroxide (N2O4), which is utilized in hypercritical conditions as oxidants and cooling fluids in rocket propulsion with regenerative cooling systems. An equation of state was performed in the varied zone of the state diagram, taking into account the phase change and two dissociation reactions. The study of the transport properties and state effects is based on the results of the fluid molecular theory. In addition to the state effects, the simple application results obtained for a case of thermal exchange in a cooling channel was studied through the behavior of the substance. B.G.

N90-10774# Pisa Univ. (Italy). Facolta di Ingegneria.
THERMODYNAMIC TRANSPORT PROPERTIES OF NITROGEN TETROXIDE IN HYPERCRITICAL CONDITIONS FOR REGENERATIVE COOLING OF A ROCKET ENGINE. VOLUME 2: APPENDICES Ph.D. Thesis [PROPRIETA' TERMODINAMICHE E DI TRASPORTO DEL TETROSSIDO DI AZOTO IN CONDIZIONI IPERCRITICHE PER IL RAFFREDDAMENTO RIGENERATIVO DI UN MOTORE A RAZZO. VOL. 2: APPENDICI ALLA TESI]
Giorgio Saccoccia 1988 255 p In ITALIAN
(ETN-89-94977) Avail: NTIS HC A12/MF A02

The N2O4 thermodynamical and transport properties were studied by computerized simulation based on experimental data and numerical analysis. The analysis is applicable to rockets where the N2O4 is used both as oxidant and hypercritical cooling agent. The content of the computer programs developed is detailed. The results obtained by the state equations, viscosity, thermal conductivity and Prandtl number are comparable to available experimental data. ESA

N90-10775# International Centre for Theoretical Physics, Trieste (Italy).
D=3 CHERN-SIMONS ACTION, SUPERGRAVITY AND QUANTIZATION
Omer F. Dayi Jan. 1989 12 p Submitted for publication
(DE89-617530; IC-89/6) Avail: NTIS (US Sales Only) HC A03/MF A01

An interpretation of three-dimensional simple supergravity as a pure Chern-Simons gauge action is shown to be valid up to the one loop level. Canonical quantization of this system does not lead to an explicit definition of the physical Hilbert space. Hence another formulation of the N = 1 three-dimensional supergravity is introduced. In this formalism an explicit definition of the physical Hilbert space is possible, but still one has to solve the problems of showing that there exists a global set of coordinates and of defining the inner product. DOE

N90-10776# Brookhaven National Lab., Upton, NY. Dept. of Physics.
QUANTIZATION OF ANOMALOUS GAUGE THEORIES ON A LATTICE
Sinya Aoki 1989 5 p Presented at the Lattice 1988 Symposium, Batavia, IL, 22-25 Sep. 1989
(Contract DE-AC02-76CH-00016)
(DE89-010247; BNL-42493; CONF-8909112-1) Avail: NTIS HC A01/MF A01

Advantages and disadvantages of three equivalent lattice actions proposed before for anomalous chiral gauge theories are discussed. Applications to the chiral Scwinger model and the four-dimensional chiral QED are presented. DOE

N90-10777# Brookhaven National Lab., Upton, NY. Physics Dept.
LATTICE FIELDS AND STRONG INTERACTIONS
Michael Creutz Jun. 1989 24 p Presented at the NATO International Advanced Course on the Nuclear Equation of State, Peniscola (Spain), 12 May - 3 Jun. 1989
(Contract DE-AC02-76CH-00016)
(DE89-015099; BNL-42968; CONF-8905143-3) Avail: NTIS HC A03/MF A01

The lattice formulation of gauge theories and the use of numerical methods to investigate nonperturbative phenomena are reviewed. These methods are directly applicable to studying hadronic matter at high temperatures. Considerable recent progress has been made in numerical algorithms for including dynamical fermions in such calculations. Dealing with a nonvanishing baryon density adds new unsolved challenges. DOE

80 SOCIAL SCIENCES (GENERAL)

Includes educational matters.

No abstracts in this category.

81 ADMINISTRATION AND MANAGEMENT

Includes management planning and research.

N90-10778# Director, Operational Test and Evaluation, Washington, DC.
DIRECTOR, OPERATIONAL TEST AND EVALUATION REPORT FY-88 Annual Report
John E. Krings 19 Jan. 1989 325 p
(AD-A206784) Avail: NTIS HC A14/MF A02 CSCL 05/1

This is an unclassified version of the FY 1988 Annual Report of the Director, Operational Test and Evaluation. The original, classified version of this report was submitted to the Secretary of Defense and the House and Senate Committees on Armed Services and on Appropriations on 19 January 1989 pursuant to the provisions of Section 138, Title 10, U.S. Code. This unclassified version is published in order to promote wider understanding of the role of operational testing in the development and acquisition of effective and affordable weapon systems. GRA

N90-10779# Chicago Univ., IL. Center for Decision Research.
LEARNING TO MAKE DECISIONS: WHEN INCENTIVES HELP AND HINDER
Robin M. Hogarth, Craig R. McKenzie, Brain J. Gibbs, and Margaret A. Marquis Jun. 1989 56 p
(Contract N00014-84-C-0018; RR04209)
(AD-A210185; TR-24) Avail: NTIS HC A04/MF A01 CSCL 05/8

Under what conditions do explicit incentives affect learning and performance in decision making. Noting that feedback often confounds information concerning the underlying structure of decision-making tasks (i.e., how variables are related) and levels of performance, we distinguish tasks on dimensions of: (1) complexity, and (2) exactingness. By 1 we mean the ease or difficulty of inferring the underlying structure of the task, by 2 the extent to which erroneous decisions are penalized. Errors are heavily penalized in exacting environments but lenient environments are forgiving. It is assumed that incentives increase effort and attention but do not have a direct effect on performance. Instead, by increasing effort and attention, incentives increase expectations of performance. When higher aspirations are not satisfied, however, frustration ensues leading to lower performance. It is argued that exactingness is unlikely to be important in tasks that are inferentially simple or complex because of ceiling and floor effects: in the former, there is little room for improvement; in the latter, little possibility for decrements in performance. In tasks of intermediate complexity, exactingness is predicted to have an inverted-U shaped relation with performance. This occurs because feedback in exacting environments induces contrary forces. On the one hand, it is more refined, providing greater opportunities for learning; on the other, it is liable to be more frustrating with outcomes GRA

N90-10780# Illinois Univ., Urbana. Dept. of Psychology.
A THEORY OF COLLECTIVE INDUCTION Final Report, 1 Jun. 1986 - 31 May 1989
Patrick R. Laughlin 3 Jul. 1989 12 p
(Contract N00014-86-K-0322)
(AD-A210553) Avail: NTIS HC A03/MF A01 CSCL 05/1

The mission of this contract was to develop and test a theory of collective induction, the cooperative search for descriptive, predictive, and explanatory generalizations, rules, and principles. The report consists of five parts: (1) a general theory of group problem solving and decision making in the form of four postulates; (2) competitive tests of the predictions of 20 a priori social combination models for 200 four-person groups on a rule induction task; (3) an a posteriori theory of collective induction in the form of three further postulates to account for the social combination processes of these 200 groups; (4) competitive tests of the predictions of these three postulates as a 21st a priori consideration of the generality of the theory. GRA

N90-10781# Colorado Univ., Boulder. Center for Research on Judgment and Policy.
EFFECTS OF STRESS ON JUDGMENT AND DECISION MAKING IN DYNAMIC TASKS Interim Report, Sep. 1987 - Aug. 1988
Kenneth R. Hammond May 1989 37 p
(Contract MDA903-86-C-0142; Proj. 74F)
(AD-A210605; ARI-RN-89-22) Avail: NTIS HC A03/MF A01 CSCL 05/8

Studies of expert microburst forecasters were conducted. Two studies yielded results confirming the validity of a linear model of expert judgement and the meaningfulness of profiles as representations of weather phenomena. A simulation demonstrated that a simple scientifically and empirically ignorant forecasting model could perform as well as a sophisticated scientifically informed algorithm. A study conducted under dynamic and highly representative forecasting conditions yielded the following major findings: (1) agreement on precursor values was low to moderate, setting the possible upper limit on forecasting accuracy; (2) agreement on microburst probabilities was lower under the highly representative situation than in our best case scenario study; and (3) new information received over time had very little impact on the experts' judgements. GRA

82 DOCUMENTATION AND INFORMATION SCIENCE

Includes information management; information storage and retrieval technology; technical writing; graphic arts; and micrography.

For computer documentation see *61 Computer Programming and Software.*

N90-10782*# National Aeronautics and Space Administration, Washington, DC.
NASA SCIENTIFIC AND TECHNICAL PUBLICATIONS: A CATALOG OF SPECIAL PUBLICATIONS, REFERENCE PUBLICATIONS, CONFERENCE PUBLICATIONS, AND TECHNICAL PAPERS, 1988
Feb. 1989 57 p
(NASA-SP-7063(03); NAS 1.21:7063(03)) Avail: NTIS HC free as PR-849; NASA Scientific and Technical Information Facility, BWI Airport, MD free CSCL 05B

This catalog lists 179 citations of all NASA Special Publications, NASA Reference Publications, NASA Conference Publications, and NASA Technical Papers that were entered into the NASA scientific and technical information database during accession year 1988. The entries are grouped by subject category. Indexes of subject terms, personal authors, and NASA report numbers are provided.
Author

N90-10783# Naval Postgraduate School, Monterey, CA.
PLANNING AN INTEGRATED ON-LINE LIBRARY SYSTEM (IOLS) M.S. Thesis
Caroline J. Miller Mar. 1989 121 p
(AD-A209406) Avail: NTIS HC A06/MF A01 CSCL 05/2

Requirements for an Integrated On-line Library System (IOLS) to automate the acquisitions, cataloging and circulation functions of the Dudley Knox Library of the Naval Postgraduate School were matched against the capabilities of commercial IOLSs available for purchase. NOTIS was the recommended choice. A cost analysis and implementation plan were developed for installing NOTIS on the Naval Postgraduate School's IBM mainframe computer.
GRA

N90-10784 Liverpool Univ. (England).
ONLINE SUPPORT FOR THE INTELLECTUAL ACTIVITY OF BROWSING Ph.D. Thesis
Joanne Frances Cove 1987 217 p
Avail: Univ. Microfilms Order No. BRDX84621

The human browsing process is difficult to understand and consequently is hard to define. As society comes increasingly to accumulate electronically stored information, the need for online access to this information becomes paramount. Existing Information Retrieval systems are successful in assisting the user whose needs are well-defined, to isolate significant text items. The problem of providing retrieval assistance to the browser whose information requirement is ill-defined, is examined. Two prototype browsing systems are designed to test ideas about optimal methods of providing online assistance with commencing a browse, query formulation and reformulation and navigation through an information source to elicit relevant text items. Simple evaluations of the prototypes and conclusions drawn concerning assistance provided are reported.
Dissert. Abstr.

N90-10785 Missouri Univ., Rolla.
AN ANALYTICAL HIERARCHY PROCESS APPROACH TO ESTABLISH THE SYSTEMS ANALYST'S KNOWLEDGE BASE FOR SELECTING AN INFORMATION REQUIREMENTS DETERMINATION STRATEGY Ph.D. Thesis
Veera Veerakool 1988 109 p
Avail: Univ. Microfilms Order No. DA8909817

The Analytical Hierarchy Process (AHP) in establishing a systems analyst knowledge base for selecting an information requirements determination strategy is applied. Experienced systems analysts were asked to evaluate a four level hierarchy consisting of the objective of effective organizational information systems, the types of applications under consideration, the alternative information requirements determination strategies, and the knowledge and skills categories. The use of AHP was demonstrated as an efficient knowledge engineering tool. The underlying knowledge used by the systems analysts in achieving an overall effective organizational information system was codified as the specific knowledge required to use an information requirements determination strategy for application development. Behavioral knowledge elements were found to be the dominant knowledge elements. In general, these behavioral knowledge elements were more important than the technical knowledge elements. Prototyping was found to be the most effective information requirements determination strategy and Electronic Data Processing was found to be the most important type of application.
Dissert. Abstr.

N90-10786# California Univ., Berkeley. School of Education.
MOTIVATING THE NOTION OF GENERIC DESIGN WITHIN INFORMATION PROCESSING THEORY: THE DESIGN PROBLEM SPACE Technical Report, Dec. 1987 - Dec. 1988
Vinod Goel and Peter Pirolli 9 Dec. 1988 46 p
(Contract N00014-88-K-0233; RR04206)
(AD-A210266; DPS-1) Avail: NTIS HC A03/MF A01 CSCL 23/2

A preliminary attempt is made to differentiate design problem solving from non-design problem solving by identifying major invariants in the design problem space. There are four major steps in the strategy: (1) characterize design as a radial category and flesh out the task environment of the central or prototypical cases; (2) take the design task environment seriously; (3) explicate the impact of this task environment on the design problem space; and (4) argue that, given the structure of the information processing system as a constant, the features noted in the problem spaces of design tasks will not all occur in problem spaces where the task environment is vastly different. This analysis leads to the claim that these features are invariants in the problem spaces of design situations, and collectively constitute a design problem space. Descriptive protocol studies are used to explore the problem spaces of three prototypical design tasks from the disciplines of architecture, mechanical engineering, and instructional design.
GRA

N90-10787# Defense Logistics Agency, Alexandria, VA. Operations Research and Economic Analysis Office.
COMPUTER AVAILABILITY IMPACT ON THE ARCHIVING OF SCIENTIFIC AND TECHNICAL REPORTS Final Report
Charles W. Elliott Jul. 1989 47 p
(AD-A210283) Avail: NTIS HC A03/MF A01 CSCL 05/2

This is an examination of the impact the DTIC-Z DROLS Mainframe computer availability has on the ability to efficiently input scientific and technical reports. There is an interesting approach to problem identification and resolution using cause and effect diagrams, the Pareto principle, quality circles and task teams.
GRA

N90-10788# Carnegie-Mellon Univ., Pittsburgh, PA.
DIFFERENCES IN WRITERS INITIAL TASK REPRESENTATIONS
Linda Carey, Linda Flower, John R. Hayes, Karen A. Schriver, and Christina Haas May 1989 29 p
(Contract N00014-85-K-0423)
(AD-A210433) Avail: NTIS HC A03/MF A01 CSCL 05/7

This exploratory study investigates how writers represent their task to themselves before beginning to write. Using data from verbal protocols, we examine the initial plans of twelve writers (five experts and seven student writers) who were working on an expository writing task. The protocols were coded for types of planning. We also obtained independent measures of the quality of the subjects' plans and of the quality of their texts. The analysis suggests that both the quantity and quality of a writer's initial planning may make a difference in the quality of the final text. We found a positive correlation between the amount of initial planning and text quality, and between the quality of planning and

text quality. In particular, we found that writers who developed rhetorical plans (i.e., plans for audience and purpose) tended to produce higher-rated texts. From our analysis, we hypothesize that experienced writers build a rhetorical representation of their task. We defined a rhetorical representation as one which is rich in rhetorical goals and plans relating to the audience, purpose, form and language of the text, and in which the writer integrates his plans to form a coherent theory of the task. GRA

N90-10789# Teledyne Brown Engineering, Augusta, GA. Analysis and Technology Directorate.
COMMUNICATIONS DATA BASE (CDB), PHASE 3 (WITH SOFTWARE DOCUMENTATION) Final Report
30 Mar. 1989 83 p
(Contract DABT60-85-C-0520)
(AD-A210540; MD89-CDSF-0013) Avail: NTIS HC A05/MF A01 CSCL 25/5

The Communications Data Base (CDB) has been developed by the Signal Center (SIGCEN) to be used as an analytical tool supporting various studies and analysis applications, both automated and manual. The CDB describes mission essential communications requirements for a set of organizations notionally comprising a U.S. Theater in a North Atlantic Treaty Organization (NATO) environment. Communications requirements are expressed in terms of needlines in the CDB. A needline is a set of related data elements describing a need to exchange information between two or more battlefield communicators. The Report's introduction discusses the reasons for developing the CDB and the data base's importance to Army tactical communications analysis. The background section describes earlier attempts to quantify tactical communications requirements and CDB strategies to overcome previous difficulties. Also included is an important discussion fo the CDB and its relation to the Network Assessment Model (NAM) and the Operational Facilities (OPFAC) Data Base. GRA

N90-10790# Defence Research Establishment Suffield, Ralston (Alberta).
WEEDING POLICY AND PROCEDURES: INFORMATION SERVICES
John G. Currie and Anne M. Dickason May 1989 20 p
(AD-A210568; DRES-SP-128) Avail: NTIS HC A03/MF A01 CSCL 05/2

The policy concerning the weeding of material from the DRES libraries is presented. Specific procedures to be followed for the weeding of monographs, periodicals, Sci-Tech reports and government documents are stated. A bibliography is included. GRA

N90-10791# Vector Research, Inc., Ann Arbor, MI.
DEVELOPMENT OF INFORMATION QUALITY ENGINEERING (IQE) METHODOLOGY FOR INFORMATION RESOURCE MANAGEMENT Final Report
James R. Bambery 22 Jul. 1989 12 p
(Contract DAAH01-88-C-0105; DARPA Order 6208)
(AD-A210615; VRI-DARPA-1-FR89-1(R)) Avail: NTIS HC A03/MF A01 CSCL 05/2

The applicability and efficacy was demonstrated of the IQE methodology to develop a Quality Assurance/Quality Control system approach to enhance quality and productivity of the information support activity of DARPA. The IQE methodology was used to develop a model for the DARPA information system and a system architecture. Work was then suspended on the project because of an internal realignment within DARPA which resulted in revised IRM policies. Study effort was then directed at finding an alternative area where the IQE technique could be applied. The use of IQE in developing war game/protocols for the exchange of information between concurrently running war games appear to have merit. GRA

N90-10792# Defense Technical Information Center, Alexandria, VA.
DEFENSE TECHNICAL INFORMATION CENTER CATALOGING GUIDELINES
Jul. 1989 151 p Supersedes DTIC/TR-88/4 dated Apr. 1988, AD-A192200
(AD-A211000; DTIC/TR-89/10; DTIC/TR-88/4) Avail: NTIS HC A08/MF A01 CSCL 05/2

The guidelines for descriptive cataloging is a procedure manual published by the Defense Technical Information Center (DTIC). It outlines the cataloging information to be included in the data fields for online input of technical publications. The text is arranged numerically, by field number, and includes appendices with separate sections of special handling and search procedures for duplicate checking. Changes to the security classifications fields have been added to implement DOD 5200.1-R, Information Security Program Regulation. An enhanced version of this guideline for remote input is available as the Shared Bibliographic Input Manual. GRA

83 ECONOMICS AND COST ANALYSIS

Includes cost effectiveness studies.

No abstracts in this category.

84 LAW, POLITICAL SCIENCE AND SPACE POLICY

Includes NASA appropriation hearings; aviation law; space law and policy; international law; international cooperation; and patent policy.

No abstracts in this category.

85 URBAN TECHNOLOGY AND TRANSPORTATION

Includes applications of space technology to urban problems; technology transfer; technology assessment; and surface and mass transportation.

For related information see also *03 Air Transportation and Safety, 16 Space Transportation,* and *44 Energy Production and Conversion.*

N90-10793# Office of the Under Secretary of Defense (Acquisitions), Washington, DC.
DOMESTIC TECHNOLOGY TRANSFER PROGRAM REGULATION Regulation Report
D. Appler Dec. 1988 15 p
(PB89-195374; DOD-3200.12-R-4) Avail: NTIS HC A01/MF A01 CSCL 05A

This regulation authorizes the DoD Domestic Technology Transfer Program and responds to the requirements of Public Law 96-480, the Federal Technology Transfer Act of 1986, and Executive Order 12591. Its purpose is to ensure the full use of the nation's federal investment in research and development, stimulating improved use by state and local governments and the private sector. GRA

88 SPACE SCIENCES (GENERAL)

N90-10794# Lawrence Livermore National Lab., CA. Inst. of Geophysics and Planetary Physics.
INSTITUTE OF GEOPHYSICS AND PLANETARY PHYSICS, 1988 Annual Report, 1 Jul. 1987 - 30 Sep. 1988
Charles R. Alcock, ed. and Christina M. Budwine, ed. 1 Jul.

1989 102 p
(Contract W-7405-eng-48)
(DE89-014363; UCRL-53809-88) Avail: NTIS HC A06/MF A01

The purpose of the Institute of Geophysics and Planetary Physics (IGPP) is to enrich the opportunities of University of California campus researchers by making available to them some of the laboratory's unique facilities and expertise, and to broaden the scientific horizon of LLNL researchers by encouraging collaborative or interdisciplinary work with other UC scientists. This report contains brief summaries on research conducted at the IGPP-LLNL on the following topics: geoscience, high-pressure sciences, and astrophysics. DOE

N90-10795*# National Aeronautics and Space Administration. Lyndon B. Johnson Space Center, Houston, TX.
ORBITAL DEBRIS RESEARCH AT NASA JOHNSON SPACE CENTER, 1986-1988
Robert C. Reynolds and Andrew E. Potter, Jr. (Lockheed Engineering and Sciences Co., Houston, TX.) Sep. 1989 60 p
(NASA-TM-102155; S-595; NAS 1.15:102155) Avail: NTIS HC A04/MF A01 CSCL 03B

Research on orbital debris has intensified in recent years as the number of debris objects in orbit has grown. The population of small debris has now reached the level that orbital debris has become an important design factor for the Space Station. The most active center of research in this field has been the NASA Lyndon B. Johnson Space Center. Work is being done on the measurement of orbital debris, development of models of the debris population, and development of improved shielding against hypervelocity impacts. Significant advances have been made in these areas. The purpose of this document is to summarize these results and provide references for further study. Author

N90-10796*# American Science and Engineering, Inc., Cambridge, MA.
SOLAR X-RAY ASTRONOMY SOUNDING ROCKET PROGRAM Final Report, 1 Feb. 1979 - 31 Jul. 1989
J. Daniel Moses 22 Aug. 1989 335 p
(Contract NAS5-25496)
(NASA-CR-183447; NAS 1.26:183447; ASE-5568) Copyright Avail: NTIS HC A15/MF A02 CSCL 03A

Several broad objectives were pursued by the development and flight of the High Resolution Soft X-Ray Imaging Sounding Rocket Payload, followed by the analysis of the resulting data and by comparison with both ground based and space based observations from other investigators. The scientific objectives were: to study the thermal equilibrium of active region loop systems by analyzing the X-ray observations to determine electron temperatures, densities, and pressures; by recording the changes in the large scale coronal structures from the maximum and descending phases of Cycle 21 to the ascending phase of Cycle 22; and to extend the study of small scale coronal structures through the minimum of Cycle 21 with new emphasis on correlative observations. For individual titles, see N90-10797 through N90-10804.

N90-10797*# American Science and Engineering, Inc., Cambridge, MA.
SOFT X-RAY ASTRONOMY USING GRAZING INCIDENCE OPTICS **c89**
John M. Davis *In its* Solar X-ray Astronomy Sounding Rocket Program 22 Aug. 1989 4 p Presented at the Symposium of High Energy Solar Physics, Tokyo, Japan (For primary document see N90-10796 01-88)
Avail: NTIS HC A15/MF A02 CSCL 03A

The instrumental background of X-ray astronomy with an emphasis on high resolution imagery is outlined. Optical and system performance, in terms of resolution, are compared and methods for improving the latter in finite length instruments described. The method of analysis of broadband images to obtain diagnostic information is described and is applied to the analysis of coronal structures. Author

N90-10798*# American Science and Engineering, Inc., Cambridge, MA.
THE DETECTION OF SOFT X-RAYS WITH CHARGED COUPLED DETECTORS **c35**
P. Burstein and John M. Davis *In its* Solar X-ray Astronomy Sounding Rocket Program 22 Aug. 1989 6 p (For primary document see N90-10796 01-88)
Avail: NTIS HC A15/MF A02 CSCL 14B

The characteristics of an ideal soft X-ray imaging detector are enumerated. Of recent technical developments the CCD or charge coupled device goes furthest to meeting these requirements. Several properties of CCDs are described with reference to experimental work and their application to practical instruments is reviewed. Author

N90-10799*# American Science and Engineering, Inc., Cambridge, MA.
THE DESIGN AND EVALUATION OF GRAZING INCIDENCE RELAY OPTICS **c74**
John M. Davis, R. C. Chase, J. K. Silk, and A. S. Krieger *In its* Solar X-ray Astronomy Sounding Rocket Program 22 Aug. 1989 6 p (For primary document see N90-10796 01-88)
Avail: NTIS HC A15/MF A02 CSCL 20F

X-ray astronomy, both solar and celestial, has many needs for high spatial resolution observations which have to be performed with electronic detectors. If the resolution is not to be detector limited, plate scales in excess of 25 microns arc/sec, corresponding to focal lengths greater than 5 m, are required. In situations where the physical size is restricted, the problem can be solved by the use of grazing incidence relay optics. A system was developed which employs externally polished hyperboloid-hyperboloid surfaces to be used in conjunction with a Wolter-Schwarzschild primary. The secondary is located in front of the primary focus and provides a magnification of 4, while the system has a plate scale of 28 microns arc/sec and a length of 1.9 m. The design, tolerance specification, fabrication and performance at visible and X-ray wavelengths of this optical system are described. Author

N90-10800*# Emmanuel Coll., Boston, MA.
THE CORRESPONDENCE BETWEEN SMALL-SCALE CORONAL STRUCTURES AND THE EVOLVING SOLAR MAGNETIC FIELD **c92**
D. F. Webb and J. Daniel Moses (American Science and Engineering, Inc., Cambridge, MA.) *In* American Science and Engineering, Inc., Solar X-Ray Astronomy Sounding Rocket Program 22 Aug. 1989 8 p (For primary document see N90-10796 01-88)
(Contracts F19628-87-K-0033; N00173-87-T0-06614)
Avail: NTIS HC A15/MF A02 CSCL 03B

Solar coronal bright points, first identified in soft X-rays as X-ray Bright Points (XBPs), are compact, short lived and associated with small bipolar magnetic flux. Contradictory studies have suggested that XBPs are either a primary signature of the emerging flux spectrum of the quiet Sun, or that they are representative of the disappearance of pre-existing flux. Results are presented using coordinated data obtained during recent X-ray sounding rocket flights on 15 August and 11 December 1987 to determine the correspondence of XBPs with time-series, ground based observations of evolving bipolar magnetic structures, He-I dark points, and the network. The results are consistent with the view that coronal bright points are more likely to be associated with the annihilation of pre-existing flux than with emerging flux.
Author

N90-10801*# Emmanuel Coll., Boston, MA. Physics Research Div.
THE OBSERVATION OF POSSIBLE RECONNECTION EVENTS IN THE BOUNDARY CHANGES OF SOLAR CORONAL HOLES **c92**
S. W. Kahler and J. Daniel Moses (American Science and Engineering, Inc., Cambridge, MA.) *In* American Science and Engineering, Inc., Solar X-Ray Astronomy Sounding Rocket Program 22 Aug. 1989 12 p (For primary document see

N90-10796 01-88)
(Contract F19628-87-K-0033)
Avail: NTIS HC A15/MF A02 CSCL 03B

Coronal holes are large scale regions of magnetically open fields which are easily observed in solar soft X-ray images. The boundaries of coronal holes are separatrices between large scale regions of open and closed magnetic fields where one might expect to observe evidence of solar magnetic reconnection. Previous studies by Nolte and colleagues using Skylab X-ray images established that large scale (greater than or equal to 9 x 10(4) km) changes in coronal hole boundaries were due to coronal processes, i.e., magnetic reconnection, rather than to photospheric motions. Those studies were limited to time scales of about one day, and no conclusion could be drawn about the size and time scales of the reconnection process at hole boundaries. Sequences of appropriate Skylab X-ray images were used with a time resolution of about 90 min during times of the central meridian passages of the coronal hole labelled Coronal Hole 1 to search for hole boundary changes which can yield the spatial and temporal scales of coronal magnetic reconnection. It was found that 29 of 32 observed boundary changes could be associated with bright points. The appearance of the bright point may be the signature of reconnection between small scale and large scale magnetic fields. The observed boundary changes contributed to the quasi-rigid rotation of Coronal Hole 1. Author

N90-10802*# Smithsonian Astrophysical Observatory, Cambridge, MA.
X-RAY BRIGHT POINTS AND He I LAMBDA 10830 DARK POINTS **c89**
L. Golub, K. L. Harvey, M. Herant, and D. F. Webb (Emmanuel Coll., Boston, MA.) *In* American Science and Engineering, Inc., Solar X-ray Astronomy Sounding Rocket Program 22 Aug. 1989 8 p Prepared in cooperation with American Science and Engineering, Inc., Cambridge, MA (For primary document see N90-10796 01-88)
(Contract NAGw-112; F19628-87-K-0033)
Avail: NTIS HC A15/MF A02 CSCL 03A

Using near-simultaneous full disk Solar X-ray images and He I 10830 lambda, spectroheliograms from three recent rocket flights, dark points identified on the He I maps were compared with X-ray bright points identified on the X-ray images. It was found that for the largest and most obvious features there is a strong correlation: most He I dark points correspond to X-ray bright points. However, about 2/3 of the X-ray bright points were not identified on the basis of the helium data alone. Once an X-ray feature is identified it is almost always possible to find an underlying dark patch of enhanced He I absorption which, however, would not a priori have been selected as a dark point. Therefore, the He I dark points, using current selection criteria, cannot be used as a one-to-one proxy for the X-ray data. He I dark points do, however, identify the locations of the stronger X-ray bright points. Author

N90-10803*# National Aeronautics and Space Administration. Marshall Space Flight Center, Huntsville, AL.
ADVANCES IN PHOTOGRAPHIC X-RAY IMAGING FOR SOLAR ASTRONOMY **c89**
J. Daniel Moses, R. Schueller, K. Waljeski (Brandeis Univ., Waltham, MA.), and John M. Davis *In* American Science and Engineering, Inc., Solar X-ray Astronomy Sounding Rocket Program 22 Aug. 1989 14 p (For primary document see N90-10796 01-88)
(Grant NGT-50308)
Copyright Avail: NTIS HC A15/MF A02 CSCL 03A

The technique of obtaining quantitative data from high resolution soft X-ray photographic images produced by grazing incidence optics was successfully developed to a high degree during the Solar Research Sounding Rocket Program and the S-054 X-Ray Spectrographic Telescope Experiment Program on Skylab. Continued use of soft X-ray photographic imaging in sounding rocket flights of the High Resolution Solar Soft X-Ray Imaging Payload has provided opportunities to further develop these techniques. The developments discussed include: (1) The calibration and use of an inexpensive, commercially available microprocessor controlled drum type film processor for photometric film development; (2) The use of Kodak Technical Pan 2415 film and Kodak SO-253 High Speed Holographic film for improved resolution; and (3) The application of a technique described by Cook, Ewing, and Sutton for determining the film characteristics curves from density histograms of the flight film. Although the superior sensitivity, noise level, and linearity of microchannel plate and CCD detectors attracts the development efforts of many groups working in soft X-ray imaging, the high spatial resolution and dynamic range as well as the reliability and ease of application of photographic media assures the continued use of these techniques in solar X-ray astronomy observations. Author

N90-10804*# National Aeronautics and Space Administration. Marshall Space Flight Center, Huntsville, AL.
CORRESPONDENCE BETWEEN SOLAR FINE-SCALE STRUCTURES IN THE CORONA, TRANSITION REGION, AND LOWER ATMOSPHERE FROM COLLABORATIVE OBSERVATIONS **c92**
J. Daniel Moses, J. W. Cook, J.-D. F. Bartoe, G. E. Brueckner, K. P. Dere, D. F. Webb, John M. Davis, F. Recely, S. F. Martin, and H. Zirin (California Inst. of Tech., Pasadena.) *In* American Science and Engineering, Inc., Solar X-ray Astronomy Sounding Rocket Program 22 Aug. 1989 26 p Submitted for publication (For primary document see N90-10796 01-88)
Copyright Avail: NTIS HC A15/MF A02 CSCL 03A

The Soft X-Ray Imaging Payload and the High Resolution Telescope and Spectrograph (HRTS) instrument were launched from White Sands on 11 December 1987 in coordinated sounding rocket flights to investigate the correspondence of coronal and transition region structures, especially the relationship between X-ray bright points (XBPs) and transition region small spatial scale energetic events. The coaligned data from X-ray images are presented along with maps of sites of transition region energetic events observed in C IV (100,000 K), HRTS 1600 A spectroheliograms of the T sub min region and ground based magnetogram and He I 10830 A images. Author

89 ASTRONOMY

Includes radio, gamma-ray, and infrared astronomy, and astrometry.

N90-10805*# New Mexico Univ., Albuquerque. Inst. for Astrophysics.
A LUNAR FAR-SIDE VERY LOW FREQUENCY ARRAY
Jack O. Burns, ed., Nebojsa Duric, ed., Stewart Johnson, ed. (BDM Corp., Albuquerque, NM.), and G. Jeffrey Taylor, ed. Nov. 1989 75 p Workshop held in Albuquerque, NM, 18-19 Feb. 1988; sponsored by NASA, Washington, New Mexico Univ., Albuquerque, and BDM Corp., Albuquerque, NM Sponsored by NASA, Washington
(NASA-CP-3039; NAS 1.55:3039) Avail: NTIS HC A04/MF A01 CSCL 03A

Papers were presented to consider very low frequency (VLF) radio astronomical observations from the moon. In part 1, the environment in which a lunar VLF radio array would function is described. Part 2 is a review of previous and proposed low-frequency observatories. The science that could be conducted with a lunar VLF array is described in part 3. The design of a lunar VLF array and site selection criteria are considered, respectively, in parts 4 and 5. Part 6 is a proposal for precursor lunar VLF observations. Finally, part 7 is a summary and statement of conclusions, with suggestions for future science and engineering studies. The workshop concluded with a general consensus on the scientific goals and preliminary design for a lunar VLF array. Author

N90-10806 Florida Univ., Gainesville.
ANALYSIS OF NEARLY SIMULTANEOUS X-RAY AND OPTICAL OBSERVATIONS OF ACTIVE GALACTIC NUCLEI

Ph.D. Thesis
James Raymond Webb 1988 192 p
Avail: Univ. Microfilms Order No. DA8912101

Rosemary Hill optical and EINSTEIN X-ray observations of a sample of 36 active galactic nuclei (AGN) were reduced and analyzed. Seventy-two X-ray observations of these sources were reduced, nineteen of which yielded spectral information. Of these spectral observations, significant hydrogen column densities above the galactic value were required for nine of the eleven sources which were observed more than once by EINSTEIN. Correlations between the X-ray and optical luminosities were investigated using the Jefferys method of least squares. This method allows for errors in both variables. The results indicate a strong correlation between the X-ray and optical luminosities for the entire sample. Division of the sample into groups with similar optical variability characteristics show that the less violently violent variable AGN are more highly correlated than the violently variable blazars. Infrared and radio observations were combined with the X-ray and optical observations of six AGN. These sources were modelled in terms of the synchrotron-self-Compton model. The turnover frequency falls between the infrared and radio data and reliable estimates of this parameter are difficult to estimate. Therefore the results were found as a function of the turnover frequency. Four sources required relativistic bulk motion or beaming. Multifrequency spectra made at different times for one individual source, 0235+164, required different amounts of beaming to satisfy the X-ray observations. Sizes of the emitting regions for the sources modelled ranged from 0.5 parsec to 1.0 parsec. Dissert. Abstr.

N90-10807*# National Aeronautics and Space Administration. Ames Research Center, Moffett Field, CA.
AUTOMATIC CLASSIFICATION OF SPECTRA FROM THE INFRARED ASTRONOMICAL SATELLITE (IRAS)
Peter Cheeseman, John Stutz, Matthew Self, William Taylor (Sterling Federal Systems, Inc., Palo Alto, CA.), John Goebel, Kevin Volk, and Helen Walker Mar. 1989 595 p
(NASA-RP-1217; NAS 1.61:1217) Avail: NTIS HC A25/MF A04 CSCL 03A

A new classification of Infrared spectra collected by the Infrared Astronomical Satellite (IRAS) is presented. The spectral classes were discovered automatically by a program called Auto Class 2. This program is a method for discovering (inducing) classes from a data base, utilizing a Bayesian probability approach. These classes can be used to give insight into the patterns that occur in the particular domain, in this case, infrared astronomical spectroscopy. The classified spectra are the entire Low Resolution Spectra (LRS) Atlas of 5,425 sources. There are seventy-seven classes in this classification and these in turn were meta-classified to produce nine meta-classes. The classification is presented as spectral plots, IRAS color-color plots, galactic distribution plots and class commentaries. Cross-reference tables, listing the sources by IRAS name and by Auto Class class, are also given. These classes show some of the well known classes, such as the black-body class, and silicate emission classes, but many other classes were unsuspected, while others show important subtle differences within the well known classes. Author

N90-10808*# National Aeronautics and Space Administration. Ames Research Center, Moffett Field, CA.
ASTROMETRIC TELESCOPE FACILITY. PRELIMINARY SYSTEMS DEFINITION STUDY. VOLUME 3: COST ESTIMATE
Charlie Sobeck, ed. Jul. 1987 10 p
(NASA-TM-89429-Vol-3; A-87239; NAS 1.15:89429-Vol-3) Avail: NTIS HC A02/MF A01 CSCL 03A

The results of the Astrometric Telescope Facility (ATF) Preliminary System Definition Study conducted in the period between March and September 1986 are described. The main body of the report consists primarily of the charts presented at the study final review which was held at NASA Ames Research Center on July 30 and 31, 1986. The charts have been revised to reflect the results of that review. Explanations for the charts are provided on the adjoining pages where required. Note that charts which have been changed or added since the review are dated 10/1/86; unchanged charts carry the review date 7/30/86. In addition, a narrative summary is presented of the study results and two appendices. The first appendix is a copy of the ATF Characteristics and Requirements Document generated as part of the study. The second appendix shows the inputs to the Space Station Mission Requirements Data Base submitted in May 1986. The report is issued in three volumes. Volume 1 contains an executive summary of the ATF mission, strawman design, and study results. Volume 2 contains the detailed study information. Volume 3 has the ATF cost estimate, and will have limited distribution. Author

N90-10797*# American Science and Engineering, Inc., Cambridge, MA.
SOFT X-RAY ASTRONOMY USING GRAZING INCIDENCE OPTICS
John M. Davis *In its* Solar X-ray Astronomy Sounding Rocket Program 22 Aug. 1989 4 p Presented at the Symposium of High Energy Solar Physics, Tokyo, Japan (For primary document see N90-10796 01-88)
Avail: NTIS HC A15/MF A02 CSCL 03A

N90-10802*# Smithsonian Astrophysical Observatory, Cambridge, MA.
X-RAY BRIGHT POINTS AND He I LAMBDA 10830 DARK POINTS
L. Golub, K. L. Harvey, M. Herant, and D. F. Webb (Emmanuel Coll., Boston, MA.) *In* American Science and Engineering, Inc., Solar X-ray Astronomy Sounding Rocket Program 22 Aug. 1989 8 p Prepared in cooperation with American Science and Engineering, Inc., Cambridge, MA (For primary document see N90-10796 01-88)
(Contract NAGw-112; F19628-87-K-0033)
Avail: NTIS HC A15/MF A02 CSCL 03A

N90-10803*# National Aeronautics and Space Administration. Marshall Space Flight Center, Huntsville, AL.
ADVANCES IN PHOTOGRAPHIC X-RAY IMAGING FOR SOLAR ASTRONOMY
J. Daniel Moses, R. Schueller, K. Waljeski (Brandeis Univ., Waltham, MA.), and John M. Davis *In* American Science and Engineering, Inc., Solar X-ray Astronomy Sounding Rocket Program 22 Aug. 1989 14 p (For primary document see N90-10796 01-88)
(Grant NGT-50308)
Copyright Avail: NTIS HC A15/MF A02 CSCL 03A

90 ASTROPHYSICS

Includes cosmology; celestial mechanics; space plasmas; and interstellar and interplanetary gases and dust.
For related information see also *75 Plasma Physics*.

N90-10809*# Fermi National Accelerator Lab., Batavia, IL.
ASTROPHYSICAL AND COSMOLOGICAL CONSTRAINTS TO NEUTRINO PROPERTIES
Edward W. Kolb, David N. Schramm, and Michael S. Turner Mar. 1989 37 p Prepared in cooperation with Chicago Univ., IL Submitted for publication
(Grant NAGw-1340)
(NASA-CR-185031; NAS 1.26:185031; FERMILAB-Pub-89/97-A)
Avail: NTIS HC A03/MF A01 CSCL 03B

The astrophysical and cosmological constraints on neutrino properties (masses, lifetimes, numbers of flavors, etc.) are reviewed. The freeze out of neutrinos in the early Universe are discussed and then the cosmological limits on masses for stable neutrinos are derived. The freeze out argument coupled with observational limits is then used to constrain decaying neutrinos as well. The limits to neutrino properties which follow from SN1987A are then reviewed. The constraint from the big bang nucleosynthesis on the number of neutrino flavors is also considered. Astrophysical constraints on neutrino-mixing as well as future observations of relevance to neutrino physics are briefly discussed. Author

N90-10810 Illinois Univ. at Urbana-Champaign, Savoy.
THEORETICAL STATISTICS OF ZERO-AGE CATACLYSMIC VARIABLES Ph.D. Thesis
Michael James Politano 1988 159 p
Avail: Univ. Microfilms Order No. DA8908806

The distribution of the white dwarf masses, the distribution of the mass ratios and the distribution of the orbital periods in cataclysmic variables which are forming at the present time are calculated. These systems are referred to as zero-age cataclysmic variables. Results show that 60 percent of the systems being formed contain helium white dwarfs and 40 percent contain carbon-oxygen white dwarfs. The mean white dwarf mass in those systems containing helium white dwarfs is 0.34 solar mass. The mean white dwarf mass in those systems containing carbon-oxygen white dwarfs is 0.75 solar mass. The distribution of white dwarf masses in zero-age cataclysmic variables is similar to the distribution of masses in single white dwarfs for masses above approximately 0.6 solar mass. The distribution of white dwarf masses in zero-age cataclysmic variables is not sufficient to account for the observed high white dwarf masses in cataclysmic variables, emphasizing the possible importance of selection effects. The orbital period distribution identifies four main classes of zero-age cataclysmic variables: (1) short-period systems containing helium white dwarfs; (2) systems containing carbon-oxygen white dwarfs whose secondaries are convectively stable against rapid mass transfer to the white dwarf; (3) systems containing carbon-oxygen white dwarfs whose secondaries are radiatively stable against rapid mass transfer to the white dwarf; and (4) long period systems with evolved secondaries. The ranges of progenitor lobe-filling giant masses and radii are also better identified. The white dwarf mass distribution in zero-age cataclysmic variables has direct application to the calculation of the frequency of outbursts in classical novae as a function of the mass of the white dwarf. The method developed to calculate the distributions of the orbital parameters in zero-age cataclysmic variables can be used to calculate theoretical statistics of any class of binary systems. This method provides a theoretical framework from which to investigate the statistical properties and the evolution of the orbital parameters of binary systems. Dissert. Abstr.

N90-10811 New York Univ., New York.
ATOMIC EFFECTS OF BETA DECAY IN ASTROPHYSICS AND IN ELEMENTARY PARTICLE PHYSICS Ph.D. Thesis
Zonghua Chen 1988 67 p
Avail: Univ. Microfilms Order No. DA8910558

The bound-state beta decay of Re-187 and its application in Astrophysics is studied. There existed an uncertainty in the ratio of rho sub p of bound-state to continuum beta decay of Re-187 in both theory and experiment. A more definite theoretical result of rho sub p of approximately 1 percent is obtained by using single-configuration and multi-configuration Hartree-Fock-Dirac approximations. The results obtained are close to those obtained by Williams, Fowler, and Koonin by a modified Thomas-Fermi model. The bound-state beta decay of Re-187 at high temperatures is also studied. A generalization of the Thomas-Fermi results of various energy contributions to the ground-state energy of a neutral atom is also presented. An analytical expression for the ratio of the electron-electron to electron-nuclear interaction is obtained by the corrected Thomas-Fermi result, the ratio obtained gives a better agreement with the Hartree-Fock numerical results.
Dissert. Abstr.

N90-10812 New York Univ., New York.
HOMOGENEOUS GRAVITATIONAL FIELDS AND LIMITS OF GRAVITATIONAL FIELDS Ph.D. Thesis
Eugene Joseph Surowitz 1988 136 p
Avail: Univ. Microfilms Order No. DA8910610

A rigorous definition of homogeneous gravitational fields is given and their connection with gauge transformations is described. These fields are limits for physically significant gravitational fields derived from Einstein's theory of gravitation. Examples are developed to demonstrate the features of the theory. A limit of the Schwarzschild solution is investigated. Dissert. Abstr.

N90-10813# Naval Postgraduate School, Monterey, CA.
THE ORIGIN OF THE UNIVERSE FROM QUANTUM CHAOS: AN INTRODUCTION TO CURRENT IDEAS
Karlheinz E. Woehler May 1989 45 p Presented at the Colloquium in Honor of Memory of John Dyer, Monterey, CA, 31 Dec. 1988
(AD-A210441; NPS61-89-010) Avail: NTIS HC A03/MF A01 CSCL 03/2

In his recently published book, A Brief History of Time, S. Hawking describes his remarkable insights into the problem of the origin of our universe. In this talk a more quantitative description of some of the important principles from this book is presented as a mathematical appendix to it. A brief review of the ideas of the standard Big Bang model of the Universe is given in terms of the evolution equation that follows from Einstein's theory. The meaning of the cosmological constant, its relation to vacuum energy, the model of the empty DeSitter space and gravity is derived. By analogy to Schrodinger mechanics one can give the general features of quantum cosmology, in which the origin of the universe can be viewed as a quantum tunneling process in imaginary time from a quantum chaos state of no space, no time, no matter to an inflationary expanding DeSitter space which eventually transits into the hot Big Bang expansion that we see.
GRA

91 LUNAR AND PLANETARY EXPLORATION

Includes planetology; and manned and unmanned flights. For spacecraft design or space stations see *18 Spacecraft Design, Testing and Performance.*

N90-10814*# National Aeronautics and Space Administration. Langley Research Center, Hampton, VA.
CONCEPTUAL DESIGN OF A SYNCHRONOUS MARS TELECOMMUNICATIONS SATELLITE
Deborah M. Badi, Jeffrey T. Farmer, Paul A. Garn, and Gary L. Martin (George Washington Univ., Hampton, VA.) Washington Nov. 1989 18 p
(NASA-TP-2942; L-16580; NAS 1.60:2942) Avail: NTIS HC A03/MF A01 CSCL 03B

Future missions to Mars will require a communications system to link activities on the Martian surface with each other and with mission controllers on Earth. A conceptual design is presented for an aerosynchronous communications satellite to provide these links. The satellite provides the capability for voice, data/command, and video transmissions. The mission scenario assumed for the design is described, and a description of a single aerosynchronous satellite is explained. A viable spacecraft design is then presented. Communication band selection and channel allocation are discussed. The communications system conceptual design is presented along with the trades used in sizing each of the required antennas. Also, the analyses used to develop the supporting subsystem designs are described as is the communications impact on each subsystem design. Author

N90-10815*# Georgia Inst. of Tech., Atlanta. School of Electrical Engineering.
LABORATORY MEASUREMENTS OF MICROWAVE AND MILLIMETER-WAVE PROPERTIES OF PLANETARY ATMOSPHERIC CONSTITUENTS
Paul G. Steffes 1989 22 p Presented at the 1st International Conference on Laboratory Research for Planetary Atmospheres, Bowie, MD, 25-27 Oct. 1989
(Grant NAGw-533)
(NASA-CR-185914; NAS 1.26:185914) Avail: NTIS HC A03/MF A01 CSCL 03B

Accurate data on microwave and millimeter-wave properties of potential planetary atmospheric constituents is critical for the proper interpretation of radio occultation measurements, and of radio astronomical observations of both continuum and spectral line emissions. Such data is also needed to correct for atmospheric

effects on radar studies of surface reflectivity. Since the refractive and absorptive properties of atmospheric constituents often vary drastically from theoretically-predicted profiles, especially under the extreme conditions characteristic of the planetary atmosphere, laboratory measurements under simulated planetary conditions are required. This paper reviews the instrumentation and techniques used for laboratory measurement of the refractivity and absorptivity of atmospheric constituents at wavelengths longward of 1 mm, under simulated planetary conditions (temperature, pressure, and broadening gases). Techniques for measuring both gases and condensates are considered. Also reviewed are the relative accuracies of the various techniques. Laboratory measurements are reviewed which have already been made, and additional measurements which are needed for interpretation of data from Venus and the outer planets, are highlighted. Author

N90-10816 Brigham Young Univ., Provo, UT.
COMPUTER SIMULATION OF PLASMA INTERACTIONS NEAR TITAN Ph.D. Thesis
Michael T. Johnson 1989 161 p
Avail: Univ. Microfilms Order No. DA8904919

A disturbance in the plasma flow behind Titan was detected by Pioneer 11. A year later Voyager 1 passed directly behind Titan. Voyager obtained data on an extended atmosphere of Titan which is responsible for the disturbance. A computer simulation that utilizes the parameters of the flow and the makeup of the upper atmosphere and ionosphere, in combination with the laws of plasma dynamics, was generated and is presented here. Using this simulation, an analysis of the system has been executed for different positions of Titan in its orbit and as a function of time at each place. Different regions of the reaction are clearly depicted, including the flow upstream, a bow wave that apparently is not a shock and varies in intensity at different points in the orbit, an ionosheath, and a low density region inside a stretched ionosphere. The electric field looks as if a conducting ring were placed in the tail. The results of this study could be used in the planning of the Cassini mission. Dissert. Abstr.

92 SOLAR PHYSICS

Includes solar activity, solar flares, solar radiation and sunspots.

For related information see *93 Space Radiation.*

N90-10817# National Geophysical Data Center, Boulder, CO.
SOLAR-GEOPHYSICAL DATA NUMBER 531, PART 2. DATA FOOR MAY 1988 AND MISCELLANEOUS Comprehensive Reports, Nov. 1988
Helen E. Coffey and John A. McKinnon Nov. 1988 61 p
(PB89-139950; SGD-531-Pt-2; LC-79-640375; ISSN-0038-0911)
Avail: NTIS HC A04/MF A01 CSCL 03B

A detailed index of solar geophysical data is presented for May, 1988. It includes Meudon carte synoptique, solar flares, solar radio bursts at fixed frequencies, solar X-ray radiation from GOES satellite, mass ejections from the sun, and active prominences and filaments. Author

N90-10818# National Geophysical Data Center, Boulder, CO.
SOLAR-GEOPHYSICAL DATA NUMBER 532, DECEMBER 1988. PART 1: DATA FOR NOVEMBER, OCTOBER 1988, AND LATE DATA Prompt Reports
Helen E. Coffey, ed. and John A. McKinnon, ed. Dec. 1988 144 p
(PB89-152086; SGD-532-Pt-1; LC-79-640375; ISSN-0038-0911)
Avail: NTIS HC A07/MF A01 CSCL 03B

A detailed solar geophysical index is presented. The data for November 1988 includes: (1) IUWDS (International Ursigram and World Days Service) alert periods (advance and worldwide); (2) solar activity indices; (3) solar flares; (4) solar radio emissions; and (5) standard mean solar magnetic field graphs. The data for October 1988 includes: (1) solar active regions; (2) sudden ionospheric disturbances; (3) solar radio spectral observations; (4) cosmic ray measurements by neutron monitor; (5) geomagnetic indices; and (6) radio propagation indices. Solar radio spectral observations for July-Aug. 1988, and geomagnetic sudden commencements/solar flare effects for Sept. 1988, are also listed. K.C.D.

N90-10819# National Geophysical Data Center, Boulder, CO.
SOLAR-GEOPHYSICAL DATA NUMBER 532, DECEMBER 1988. PART 2: DATA FOR JUNE 1988 AND MISCELLANEOUS Comprehensive Reports
Helen E. Coffey, ed. and John A. McKinnon, ed. Dec. 1988 86 p
(PB89-152094; SGD-532-Pt-2; LC-79-640375; ISSN-0038-0911)
Avail: NTIS HC A05/MF A01 CSCL 03B

A detailed index of solar geophysical data for 1988 is presented. Data for June 1988 includes: (1) Meudon carte synoptique; (2) solar flares; (3) solar radio bursts at fixed frequencies; (4) solar X-ray radiation from GOES satellite; (5) mass ejections from the sun; and (6) active prominences and filaments. K.C.D.

N90-10820# National Geophysical Data Center, Boulder, CO.
SOLAR-GEOPHYSICAL DATA NUMBER 533. PART 1: DATA FOR DECEMBER, NOVEMBER 1988, AND LATE DATA Prompt Reports, Jan. 1989
Helen E. Coffey, ed. Jan. 1989 150 p
(PB89-162481; SGD-533-Pt-1; LC-79-640375; ISSN-0038-0911)
Avail: NTIS HC A07/MF A01 CSCL 03B

A detailed solar geophysical index for 1988 is given. Data for December 1988 includes: (1) IUWDS (International Ursigram and World Days Service) alert periods (advance and worldwide); (2) solar activity indices; (3) solar flares; (4) solar radio emissions; and (5) Stanford mean solar magnetic field graphs. Data for November 1988 includes: (1) solar active regions; (2) sudden ionospheric disturbances; (3) solar radio spectral observations; (4) cosmic ray measurements by neutron monitor; (5) geomagnetic indices; and (6) radio propagation indices. Other data includes: (1) Pioneer 12 interplanetary magnetic field magnitudes (January to June 1988); and (2) cosmic ray measurements by neutron monitor and geomagnetic sudden commencements/solar flare effects (October 1988). K.C.D.

N90-10821# National Geophysical Data Center, Boulder, CO.
SOLAR-GEOPHYSICAL DATA NUMBER 533. PART 2: DATA FOR JULY 1988 AND MISCELLANEOUS Comprehensive Reports, Jan. 1989
Helen E. Coffey, ed. Jan. 1989 99 p
(PB89-162499; SGD-533-Pt-2; LC-79-640375; ISSN-0038-0911)
Avail: NTIS HC A05/MF A01 CSCL 03B

A detailed solar geophysical index for 1988 is presented. Data for July 1988 includes: (1) Meudon carte synoptique; (2) solar flares; (3) solar radio bursts at fixed frequencies; (4) solar X-ray radiation for GOES satellite; (5) mass ejections from the sun; and (6) active prominences and filaments. K.C.D.

N90-10822# National Geophysical Data Center, Boulder, CO.
SOLAR-GEOPHYSICAL DATA NUMBER 534, FEBRUARY 1989. PART 1: (PROMPT REPORTS). DATA FOR JANUARY 1989, DECEMBER 1988 AND LATE DATA
Helen E. Coffey, ed. Feb. 1989 172 p
(PB89-173041; SGD-534-Pt-1; ISSN-0038-0911; LC-79-640375)
Avail: NTIS HC A08/MF A01 CSCL 03B

A detailed solar geophysical index for 1988 through 1989 is given. Data for January 1989 includes: (1) IUWDS (International Ursigram and World Days Service) alert periods (advance and worldwide); (2) solar activity indices; (3) solar flares; (4) solar radio emission; and (5) Stanford mean solar magnetic field graphs. Data for December 1988 includes: (1) solar active regions; (2) sudden ionospheric disturbances; (3) solar radio spectral observations; (4) cosmic ray measurements by neutron monitor; (5) geomagnetic indices; and (6) radio propagation indices. Other data reported includes solar radio emissions, cosmic ray measurements by neutron monitor (errata), and geomagnetic sudden commencements. K.C.D.

N90-10823# National Geophysical Data Center, Boulder, CO.
SOLAR-GEOPHYSICAL DATA NUMBER 534, FEBRUARY 1989. PART 2: (COMPREHENSIVE REPORTS). DATA FOR AUGUST 1988 AND MISCELLANEOUS
Helen E. Coffey, ed. Feb. 1989 68 p
(PB89-173058; SGD-534-Pt-2; ISSN-0038-0911; LC-79-640375)
Avail: NTIS HC A04/MF A01 CSCL 03B

A detailed solar geophysical index for 1988 through 1989 is given. Data for August 1988 includes: (1) solar flares; (2) solar radio bursts at fixed frequencies; (3) solar X-ray radiation from GOES satellite; (4) mass ejections from the sun; and (5) active prominences and filaments. Meudon carte synoptique data for July 1988 is also reported. K.C.D.

N90-10824# National Geophysical Data Center, Boulder, CO.
SOLAR-GEOPHYSICAL DATA NUMBER 536, PART 2. DATA FOR OCTOBER 1988 AND MISCELLANEOUS Comprehensive Reports, Apr. 1989
Helen E. Coffey, ed. Apr. 1989 89 p
(PB89-194658; SGD-536-Pt-2; LC-79-640375; ISSN-0038-0911)
Avail: NTIS HC A05/MF A01 CSCL 03B

A detailed solar geophysical index for 1988 and 1989 is given. Data for October 1988 includes: (1) solar flares; (2) solar radio bursts at fixed frequencies; (3) solar X-ray radiation from GOES satellite; (4) mass ejections from the sun; and (5) active prominences and filaments. A Meudon Carte Synoptique for July and August 1988 is also included. K.C.D.

N90-10825# National Academy of Sciences - National Research Council, Washington, DC. Panel on Long-Term Observations.
LONG-TERM SOLAR-TERRESTRIAL OBSERVATIONS
1988 72 p
(Contract DE-AI01-87ER-60590)
(DE89-016318; DOE/ER-60590/T1) Avail: NTIS HC A05/MF A01

In the fall of 1985, the Committee on Solar-Terrestrial Research (CSTR) created a panel to study the requirements for long-term monitoring and archiving of solar-terrestrial data. The panel comprised specialists in all four areas that constitute solar-terrestrial science: the sun, interplanetary medium, magnetosphere-thermosphere-ionosphere, and upper atmosphere. It interviewed many individuals from the solar-terrestrial monitoring and data archiving communities, along with administrators and directors from appropriate government agencies. It circulated nearly 500 questionnaires to obtain information and opinions from the broader community to learn which observational data should be considered essential over the long term to support the operational and research needs of solar-terrestrial science. This report summarizes the panel's principal findings, and the panel's recommendations follow. A separate section listing the critical observational needs by area is presented together with the scientific rationale for each area. The recommendations are defended in terms of this explicit scientific rationale and the multifold uses of current and long-term solar-terrestrial observations for continued operational solar-terrestrial forecasts and services. DOE

N90-10800*# Emmanuel Coll., Boston, MA.
THE CORRESPONDENCE BETWEEN SMALL-SCALE CORONAL STRUCTURES AND THE EVOLVING SOLAR MAGNETIC FIELD
D. F. Webb and J. Daniel Moses (American Science and Engineering, Inc., Cambridge, MA.) *In* American Science and Engineering, Inc., Solar X-Ray Astronomy Sounding Rocket Program 22 Aug. 1989 8 p (For primary document see N90-10796 01-88)
(Contracts F19628-87-K-0033; N00173-87-T0-06614)
Avail: NTIS HC A15/MF A02 CSCL 03B

N90-10801*# Emmanuel Coll., Boston, MA. Physics Research Div.
THE OBSERVATION OF POSSIBLE RECONNECTION EVENTS IN THE BOUNDARY CHANGES OF SOLAR CORONAL HOLES
S. W. Kahler and J. Daniel Moses (American Science and Engineering, Inc., Cambridge, MA.) *In* American Science and Engineering, Inc., Solar X-Ray Astronomy Sounding Rocket Program 22 Aug. 1989 12 p (For primary document see N90-10796 01-88)
(Contract F19628-87-K-0033)
Avail: NTIS HC A15/MF A02 CSCL 03B

N90-10804*# National Aeronautics and Space Administration. Marshall Space Flight Center, Huntsville, AL.
CORRESPONDENCE BETWEEN SOLAR FINE-SCALE STRUCTURES IN THE CORONA, TRANSITION REGION, AND LOWER ATMOSPHERE FROM COLLABORATIVE OBSERVATIONS
J. Daniel Moses, J. W. Cook, J.-D. F. Bartoe, G. E. Brueckner, K. P. Dere, D. F. Webb, John M. Davis, F. Recely, S. F. Martin, and H. Zirin (California Inst. of Tech., Pasadena.) *In* American Science and Engineering, Inc., Solar X-ray Astronomy Sounding Rocket Program 22 Aug. 1989 26 p Submitted for publication (For primary document see N90-10796 01-88)
Copyright Avail: NTIS HC A15/MF A02 CSCL 03A

93 SPACE RADIATION

Includes cosmic radiation; and inner and outer earth's radiation belts.

For biological effects of radiation see *52 Aerospace Medicine.* For theory see *73 Nuclear and High-Energy Physics.*

No abstracts in this category.

99 GENERAL

N90-10826# Department of National Education, Pretoria (South Africa).
NATIONAL REGISTER OF RESEARCH PROJECTS, 1986/87. PART 2B: NATURAL SCIENCES: PHYSICAL, ENGINEERING AND RELATED SCIENCES (NEW PROJECTS)
Aug. 1988 183 p In AFRICAANS; ENGLISH summary
(DE89-015033; DNE-9015033-Pt-2B; NASOP-11-009(88/08); NATED-11-009(88/08); ISBN-0-7970-1561-2; ISBN-0-7970-1566-3) Avail: NTIS (US Sales Only) HC A09

This Register is intended to serve as a source of information on research which is being conducted in all fields (both natural and human sciences) in the Republic of South Africa. New and current research projects that were commenced or modified during 1986 and 1987, on which information was received by the compilers until January 1988, are included, with the exception of confidential projects. Project titles and keywords are presented in the language as supplied, and the classifications are based on those provided by the primary sources. DOE

N90-10827# Assistant Secretary of the Army (Research, Development and Acquisition), Washington, DC.
ARMY SCIENCE CONFERENCE PROCEEDINGS (16TH) HELD IN FORT MONROE, VIRGINIA ON 25-27 OCTOBER 1988: ADDENDA
27 Oct. 1988 92 p Conference held in Fort Monroe, VA, 25-27 Oct. 1988
(AD-A210235) Avail: NTIS HC A05/MF A01 CSCL 05/2

The proceedings of the conference are presented. Some areas of discussion are: the near millimeter wave properties of high temperature superconductors; to preserve and defend the tech base; and an overview of biotechnology. GRA

Typical Subject Index Listing

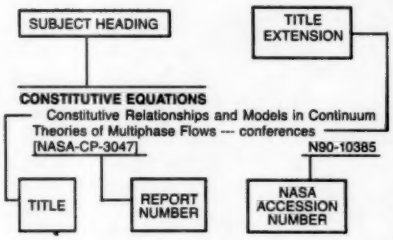

The subject heading is a key to the subject content of the document. Titles, report numbers, and accession numbers of pertinent documents are provided under each subject heading. When the title is insufficiently descriptive of the document content, a title extension has been added, separated from the title by three hyphens. The report number helps to indicate the type of document cited (e.g., NASA report, NASA translation, NASA contractor report). The NASA accession number is the number by which the document abstracts are arranged in this journal and by which the document is sold or requested. The titles, with title extensions if present, are arranged under each subject heading in ascending accession number order. The subject headings have been selected from the latest revision of the *NASA Thesaurus* (NASA SP-7064).

A

ABILITIES
SINCGARS (Single-Channel Ground/Airborne Radio System) operator performance decay
[AD-A210716] N90-10326

ABRASION
The response of isotropic brittle materials to abrasive processes
[DE89-016637] N90-10251

ABSORPTIVITY
Theoretical and experimental investigation of nonlinear optoacoustics in liquids
[AD-A210427] N90-10708
Laboratory measurements of microwave and millimeter-wave properties of planetary atmospheric constituents
[NASA-CR-185914] N90-10815

ACCELERATED LIFE TESTS
Predictive aging of polymers
[NASA-CASE-NPO-17524-1-CU] N90-10261

ACCELERATION (PHYSICS)
VIBRAFUGE: A combined environment testing facility-vibration testing on a centrifuge
[DE89-015120] N90-10458

ACCURACY
Assessing the accuracy of vulnerability models by comparison with vulnerability experiments
[AD-A210871] N90-10669

ACID RAIN
Characterization and evaluation of acid rain in East Central Florida from 1978 to 1987: Ten year summary report
[NASA-TM-102149] N90-10478
Spatial characterization of acid rain stress in Canadian Shield Lakes
[NASA-CR-183446] N90-10479

ACOUSTIC ATTENUATION
Investigation of materials and bonding using the scanning laser acoustic microscope
[KCP-613-4033] N90-10270

ACOUSTIC EMISSION
Characterization of electron-beam weld processes in uranium by acoustic emission monitoring
[DE89-016044] N90-10444

ACOUSTIC MEASUREMENT
Acoustic test and analysis of a counterrotating prop-fan model
[NASA-CR-179590] N90-10683

ACOUSTIC MICROSCOPES
Investigation of materials and bonding using the scanning laser acoustic microscope
[KCP-613-4033] N90-10270

ACOUSTIC PROPAGATION
Investigation of materials and bonding using the scanning laser acoustic microscope
[KCP-613-4033] N90-10270

ACOUSTIC PROPERTIES
IFD (Implicit Finite Difference): Interfaced with Harvard open ocean model forecasts
[AD-A210521] N90-10517

ACOUSTIC VELOCITY
IFD (Implicit Finite Difference): Interfaced with Harvard open ocean model forecasts
[AD-A210521] N90-10517

ACOUSTICS
The theory and application of quadratic minimization in the active reduction of sound and vibration N90-10682
Development of the electroacoustic dewatering (EAD) process for fine/ultrafine coal
[DE89-015883] N90-10700

ACOUSTO-OPTICS
Theoretical and experimental investigation of nonlinear optoacoustics in liquids
[AD-A210427] N90-10708

ACRYLATES
Negative-working electron beam resist based on poly(methyl methacrylate)
[AD-A207834] N90-10733

ACRYLIC RESINS
UV-curable polyurethane-methacrylate co-networks and interpenetrating networks
[AD-A210445] N90-10285
Synthesis and interfacial properties of new generation polyurethane systems
[AD-A210446] N90-10286

ACTIVATION
Scientific and technical report voice activated gun turrent control
[AD-A210350] N90-10623

ACTIVATION ENERGY
Two photon absorption characterization
[AD-A210508] N90-10694

ACTIVE CONTROL
Control law synthesis and optimization software for large order aeroservoelastic systems N90-10111
Combustion instabilities in liquid-fueled propulsion systems: An overview N90-10192
Attenuation of reheat buzz by active control N90-10201
Application of formal optimization techniques in thermal/structural design of a heat-pipe-cooled panel for a hypersonic vehicle
[NASA-TM-89131] N90-10409

ACTIVE GALACTIC NUCLEI
Analysis of nearly simultaneous X-ray and optical observations of active galactic nuclei N90-10806

ADA (PROGRAMMING LANGUAGE)
Ada (trademark) projects at NASA. Runtime environment issues and recommendations
[NASA-CR-183435] N90-10583

ADAPTIVE CONTROL
Adaptive machine vision
[AD-A208130] N90-10436
An adaptive controller for enhancing operator performance during teleoperation
[NASA-CR-183445] N90-10438
Adaptive robust control N90-10620

ADDRESSING
Evaluating local indirect addressing in SIMD processors
[NASA-CR-181845] N90-10581

ADHESION
Adhesion of encapsulating elastomer to polyolefin sleeve
[BDX-613-3985] N90-10271

ADHESION TESTS
Adhesion of encapsulating elastomer to polyolefin sleeve
[BDX-613-3985] N90-10271

ADHESIVE BONDING
Adhesion of encapsulating elastomer to polyolefin sleeve
[BDX-613-3985] N90-10271

ADSORPTION
Multiple internal reflection Fourier transform infrared spectroscopy studies of thiocyanate adsorption on silver and gold
[AD-A210245] N90-10223
The structure determination of molecular adsorbates with large unit cells or lattice-gas disorder on metal surfaces
[AD-A210926] N90-10230

AEROACOUSTICS
Large-scale Advanced Prop-fan (LAP) technology assessment report
[NASA-CR-182142] N90-10046
Measurement resolution of noise directivity patterns from acoustic flight tests
[NASA-TM-4134] N90-10679

AEROBRAKING
Preliminary design of a large tetrahedral truss/hexagonal heatshield panel aerobrake
[NASA-TM-101612] N90-10127

AERODYNAMIC CHARACTERISTICS
Development of a flight test methodology for a US Navy half-scale unmanned air vehicle
[AD-A210563] N90-10029
Stability and Control of Tactical Missile Systems
[AGARD-CP-451] N90-10050
The present status and the future of missile aerodynamics N90-10051
Wind tunnel tests: The role of the model N90-10064
High temperature VSCF (Variable Speed Constant Frequency) generator system
[AD-A210823] N90-10351

AERODYNAMIC CONFIGURATIONS
Prediction of stability derivatives for missiles using the HISSS panel code N90-10053
Experience gained in the improvement of the Aspide aerodynamic configuration for the surface to air role N90-10072
Analysis of flight data from a High-Incidence Research Model by system identification methods
[NASA-TP-2940] N90-10074

AERODYNAMIC FORCES
An integrated CFD/experimental analysis of aerodynamic forces and moments
[NASA-TM-102195] N90-10006

AERODYNAMIC INTERFERENCE
Wind tunnel support system effects on a fighter aircraft model at Mach numbers from 0.6 to 2.0
[AD-A210614] N90-10010

AERODYNAMIC STABILITY
Airworthiness and flight characteristics test of the UH-60A Black Hawk helicopter equipped with the XM-139 multiple mine dispensing system (VOLCANO)
[AD-A210271] N90-10025
Prediction of the aerodynamic stability of missiles N90-10052
Analysis of flight data from a High-Incidence Research Model by system identification methods
[NASA-TP-2940] N90-10074

AERODYNAMICS
The application of TSIM software to act design and analysis on flexible aircraft N90-10086

AEROELASTICITY
Static aeroelastic analysis for generic configuration aircraft
[NASA-TM-89423] N90-10042

Large-scale Advanced Prop-fan (LAP) technology assessment report
[NASA-CR-182142] N90-10046
Aeroelastic tailoring procedure for controlling fin hinge moments N90-10058
Aeroelastic analysis of missile control surfaces with structural non-linearity N90-10071
The application of TSIM software to act design and analysis on flexible aircraft N90-10086
Modifying high-order aeroelastic math model of a jet transport using maximum likelihood estimation N90-10106
Control law synthesis and optimization software for large order aeroservoelastic systems N90-10111
Flexible aircraft dynamic modeling for dynamic analysis and control synthesis N90-10112
The active flexible wing aeroservoelastic wind-tunnel test program N90-10119

AEROLOGY
Meeting Review: Workshop on Airborne Instrumentation
[PB89-174775] N90-10032

AERONAUTICAL ENGINEERING
A review of Australian and New Zealand investigations on aeronautical fatigue during the period April 1987 to March 1989
[AD-A210373] N90-10026

AEROSOLS
Real-time observations of aerosol composition changes
[DE89-012382] N90-10422
Paper 1. Impact of volcanic aerosols on stratospheric chemistry. Paper 2. O2 (1 sigma g +) and O2 (1 delta g) in the H + O2 reaction system. Paper 3. Barotropic instability of zonal jets on Mars, Earth and Venus N90-10477
International Conference on Aerosols and Background Pollution Abstracts
[AD-A210970] N90-10483
Geophysical monitoring for climatic change number 16
[PB89-159628] N90-10494

AEROSPACE ENGINEERING
Technology for large space systems: A bibliography with indexes (supplement 21)
[NASA-SP-7046(21)] N90-10130

AEROSPACE MEDICINE
Aerospace medicine and biology: A continuing bibliography with indexes (supplement 328)
[NASA-SP-7011(328)] N90-10524

AEROSPACE SAFETY
Liquid rocket booster study. Volume 2, book 2, appendix 1: Trades studies
[NASA-CR-183601] N90-10136

AEROSPACE SCIENCES
NASA scientific and technical publications: A catalog of special publications, reference publications, conference publications, and technical papers, 1988
[NASA-SP-7063(03)] N90-10782

AEROSPACE SYSTEMS
Supersonic flow computations over aerospace configurations using an Euler marching solver
[NASA-CR-4085] N90-10012
Conference on Aerospace Transparent Materials and Enclosures (15th) 16-20 January 1989. Volume 2: Sessions 6-9
[AD-A210201] N90-10024
Proceedings of the Workshop on Computational Aspects in the Control of Flexible Systems, part 1
[NASA-TM-101578-PT-1] N90-10080
Computational controls for aerospace systems N90-10082
A comparison of software for the modeling and control of flexible systems N90-10092
Proceedings of the Workshop on Computational Aspects in the Control of Flexible Systems, part 2
[NASA-TM-101578-PT-2] N90-10103
Aerospace system unified life cycle engineering producibility measurement issues
[AD-A210937] N90-10607

AEROSPACE VEHICLES
Hierarchical damage tolerant controllers for smart structures
[AD-A209422] N90-10022

AEROTHERMODYNAMICS
Boost-phase discrimination research activities
[NASA-TM-101889] N90-10176

AFTERBURNING
Characteristics of combustion driven pressure oscillations in advanced turbo-fan engines with afterburner N90-10194
Reheat buzz: An acoustically coupled combustion instability N90-10200
Attenuation of reheat buzz by active control N90-10201

AGING (MATERIALS)
Predictive aging of polymers
[NASA-CASE-NPO-17524-1-CU] N90-10261

AGING (METALLURGY)
Strain aging in tungsten-heavy alloys
[AD-A211166] N90-10259

AGREEMENTS
Effects of stress on judgment and decision making in dynamic tasks
[AD-A210605] N90-10781

AIR POLLUTION
International impacts of global climate change: Testimony to House Appropriations Subcommittee on Foreign Operations, Export Financing and Related Programs
[DE89-014004] N90-10482
International Conference on Aerosols and Background Pollution Abstracts
[AD-A210970] N90-10483
Geophysical monitoring for climatic change number 16
[PB89-159628] N90-10494
Managing human exposure and health risks: An integrated approach and the role of uncertainty
[DE89-008611] N90-10525

AIR QUALITY
Geophysical monitoring for climatic change number 16
[PB89-159628] N90-10494

AIR TO AIR MISSILES
Analysis and testing of a high performance air-air missile N90-10069

AIR TRAFFIC
Safer skies with TCAS: Traffic Alert and Collision Avoidance System
[PB89-169221] N90-10016

AIR TRAFFIC CONTROL
National airspace system approach and departure sequencing operational concept
[NAS-SR-1322] N90-10017

AIR TRANSPORTATION
New energy conversion techniques in space, applicable to propulsion
[AIAA-79-1338] N90-10145

AIRBORNE EQUIPMENT
Meeting Review: Workshop on Airborne Instrumentation
[PB89-174775] N90-10032

AIRCRAFT ACCIDENT INVESTIGATION
Aircraft accident report: Aloha Airlines, Flight 243, Boeing 737-200, N73711, near Maui, Hawaii, April 28, 1988
[PB89-910404] N90-10013

AIRCRAFT ACCIDENTS
Aircraft accident report: Aloha Airlines, Flight 243, Boeing 737-200, N73711, near Maui, Hawaii, April 28, 1988
[PB89-910404] N90-10013
Classification and reduction of pilot error
[NASA-CR-181867] N90-10014

AIRCRAFT APPROACH SPACING
National airspace system approach and departure sequencing operational concept
[NAS-SR-1322] N90-10017

AIRCRAFT CONFIGURATIONS
A numerical method for solving transonic flow past aircraft in Cartesian coordinates
[NAL-TR-1008] N90-10003
Computation of transonic flow about stores
[AD-A210402] N90-10009
Supersonic flow computations over aerospace configurations using an Euler marching solver
[NASA-CR-4085] N90-10012
Static aeroelastic analysis for generic configuration aircraft
[NASA-TM-89423] N90-10042
Grid generation procedure using the integral equation method
[NAL-TR-1009] N90-10630

AIRCRAFT CONSTRUCTION MATERIALS
Conference on Aerospace Transparent Materials and Enclosures (15th) 16-20 January 1989. Volume 2: Sessions 6-9
[AD-A210201] N90-10024
Composite Blade Structural Analyzer (COBSTRAN) theoretical/programmer's manual
[NASA-TM-101958] N90-10181
Materials for engine applications above 3000 deg F: An overview
[NASA-TM-100169] N90-10188
Castings Airworthiness
[AGARD-R-762] N90-10231
Casting factors imposed by the French regulation for foundry castings used in military aircraft N90-10233
The question of the casting factor N90-10238

AIRCRAFT CONTROL
Classification and reduction of pilot error
[NASA-CR-181867] N90-10014
Real-time support for high performance aircraft operation
[NASA-CR-185475] N90-10075
The active flexible wing aeroservoelastic wind-tunnel test program N90-10119

AIRCRAFT DESIGN
Prediction of dynamic derivatives N90-10055
Marginal release disturbances on advanced missiles N90-10070
High temperature VSCF (Variable Speed Constant Frequency) generator system
[AD-A210823] N90-10351
Turbulence management: Application aspects N90-10378
A3I visibility modeling project N90-10557

AIRCRAFT ENGINES
A supersonic through-flow fan engine airframe integration study
[NASA-CR-185140] N90-10004
Full scale technology demonstration of a modern counterrotating unducted fan engine concept: Component test
[NASA-CR-180868] N90-10047
Full scale technology demonstration of a modern counterrotating unducted fan engine concept. Design report
[NASA-CR-180867] N90-10048
Full scale technology demonstration of a modern counterrotating unducted fan engine concept. Engine test
[NASA-CR-180869] N90-10049
Combustor influence on fighter engine operability N90-10193
Dynamic instability characteristics of aircraft turbine engine combustors N90-10195

AIRCRAFT EQUIPMENT
Electro-impulse de-icing testing analysis and design
[NASA-CR-4175] N90-10031
Meeting Review: Workshop on Airborne Instrumentation
[PB89-174775] N90-10032

AIRCRAFT GUIDANCE
Guidance simulation and test support for differential GPS flight experiment
[NASA-CR-177471] N90-10021

AIRCRAFT INDUSTRY
A review of Australian and New Zealand investigations on aeronautical fatigue during the period April 1987 to March 1989
[AD-A210373] N90-10026

AIRCRAFT INSTRUMENTS
Cockpit lighting compatibility with image intensification night imaging systems: Issues and answers
[AD-A210503] N90-10028
Optimal integral controller with sensor failure accommodation N90-10123

AIRCRAFT MAINTENANCE
Aircraft accident report: Aloha Airlines, Flight 243, Boeing 737-200, N73711, near Maui, Hawaii, April 28, 1988
[PB89-910404] N90-10013
An appraisal of a number of power assessment procedures being proposed for use in Chinook-Lycoming T55 engine
[AD-A210482] N90-10041

AIRCRAFT NOISE
Measurement resolution of noise directivity patterns from acoustic flight tests
[NASA-TM-4134] N90-10679

AIRCRAFT PARTS
Castings Airworthiness
[AGARD-R-762] N90-10231
Casting factors imposed by the French regulation for foundry castings used in military aircraft N90-10233
The question of the casting factor N90-10238

AIRCRAFT PERFORMANCE
On the interactive computer program IPIS for aircraft parameter identification
[NAL-TR-1000] N90-10586

AIRCRAFT PILOTS
Scientific and technical report voice activated gun turrent control
[AD-A210350] N90-10623

AIRCRAFT POWER SUPPLIES
The aerospace energy systems laboratory: Hardware and software implementation
[NASA-TM-101706] N90-10610

AIRCRAFT RELIABILITY
Aircraft accident report: Aloha Airlines, Flight 243, Boeing 737-200, N73711, near Maui, Hawaii, April 28, 1988
[PB89-910404] N90-10013
Airworthiness and flight characteristics test of the UH-60A Black Hawk helicopter equipped with the XM-139 multiple mine dispensing system (VOLCANO)
[AD-A210271] N90-10025

Castings Airworthiness
[AGARD-R-782] N90-10231
Casting airworthiness joint European civil authorities view-point N90-10234
Royal Aerospace Establishment: No place for a castings factor N90-10235
Combined advanced foundry and quality control techniques to enhance reliability of castings for the aerospace industry N90-10240

AIRCRAFT SAFETY
Aircraft accident report: Aloha Airlines, Flight 243, Boeing 737-200, N73711, near Maui, Hawaii, April 28, 1988
[PB89-910404] N90-10013
Safer skies with TCAS: Traffic Alert and Collision Avoidance System
[PB89-169221] N90-10016
Electro-impulse de-icing testing analysis and design
[NASA-CR-4175] N90-10031

AIRCRAFT STABILITY
Structural stability augmentation system design using BODEDIRECT: A quick and accurate approach N90-10116

AIRCRAFT STRUCTURES
The application of TSIM software to act design and analysis on flexible aircraft N90-10086
Modifying high-order aeroelastic math model of a jet transport using maximum likelihood estimation N90-10106
Flexible aircraft dynamic modeling for dynamic analysis and control synthesis N90-10112
Aircraft modal supression system: Existing design approach and its shortcomings N90-10115
Structural stability augmentation system design using BODEDIRECT: A quick and accurate approach N90-10116
Thin walled cast high-strength structural parts N90-10242
Fatigue crack initiation mechanics of metal aircraft structures
[AD-A210567] N90-10255

AIRFOILS
Basic studies of the unsteady flow past high angle of attack airfoils
[AD-A210252] N90-10008
Goertler instability on an airfoil: Comparison of marching solution with experimental observations N90-10364
Simultaneous detection of separation and transition in surface shear layers N90-10368

AIRFRAMES
A supersonic through-flow fan engine airframe integration study
[NASA-CR-185140] N90-10004
A review of Australian and New Zealand investigations on aeronautical fatigue during the period April 1987 to March 1989
[AD-A210373] N90-10026
How to control unstable missile airframes: Methodology and limitations N90-10060
Winged versus wingless airframes N90-10073

AIRPORTS
ILS (Instrument Landing System) mathematical modeling study on the effects of proposed hangar construction west of runway 18R on localizer performance at Dallas-Fort Worth International Airport
[AD-A210631] N90-10019

ALERTNESS
Attention and vigilance in speech perception
[AD-A210493] N90-10539

ALGAE
Biochemical cycling and fluxes between the deep euphotic zone and other oceanic realms
[PB89-152458] N90-10509

ALGEBRA
Numerical methods for differential-algebraic equations: Current status and future directions
[DE89-015116] N90-10632
Extended Weyl group for Kac-Moody algebras
[DE89-617525] N90-10634
Applications of algebraic logic and universal algebra to computer science
[AD-A210556] N90-10645

ALGORITHMS
Computation of transonic flow about stores
[AD-A210402] N90-10009
A structured singular value approach to missile autopilot analysis 2 N90-10068
A performance comparison of integration algorithms in simulating flexible structures N90-10101
Minimum-variance reduced-order estimation algorithms from Pontrygin's minimum principle N90-10105
Use of the quasilinearization algorithm for the simulation of LSS slewing N90-10110
Boost-phase discrimination research activities
[NASA-TM-101889] N90-10176
Mechanical states in wound capacitors. Part 2: Optimization
[DE89-008116] N90-10338
An algorithm to calculate the beam momentum distribution from flying wire profiles
[DE89-015587] N90-10418
Stimulated rotational Raman scattering
[DE89-016427] N90-10430
Parallel asynchronous hardware implementation of image processing algorithms N90-10546
Computation and parallel implementation for early vision N90-10549
Algorithms and architectures for robot vision N90-10562
Intensity dependent spread processor and workstation N90-10568
On learning from exercises
[AD-A210593] N90-10574
An algorithm for the systematic disturbance of optimal rotational solutions
[NASA-TM-101089] N90-10575
Performance evaluation of the Scheme86 and HP precision architectures
[AD-A209418] N90-10578
A low-cost hypercube load-balance algorithm
[DE89-015739] N90-10589
Tests of various finite difference algorithms applied to a simple water vapor transport problem on a staggered grid
[AD-A210229] N90-10596
Cost metric algorithms for internetwork applications
[AD-A210324] N90-10597
Primal barrier methods for linear programming
[AD-A210501] N90-10600
Some results on learning
[AD-A210591] N90-10624
Quotient-difference type generalizations of the power method and their analysis
[NASA-TM-102361] N90-10635
An iterative method for systems of nonlinear hyperbolic equations
[NASA-CR-181919] N90-10638
Tests of gating algorithms for tracking of multiple objects. Part 1: Theory, requirements and performance measures
[AD-A210519] N90-10644
Research in mathematics and computer science: Calculation of the probability of undetected error for certain error detection codes, phase 1
[AD-A210302] N90-10664

ALLOCATIONS
Finite methods for a nonlinear allocation problem
[AD-A209719] N90-10629

ALUMINUM
Application of superplastically formed and diffusion bonded aluminum to a laminar flow control leading edge
[NASA-CR-178316] N90-10030
High-speed machining of aluminum
[DE89-014011] N90-10441

ALUMINUM ALLOYS
Microstructure morphology and quality of Al-Si castings N90-10244
Emittance, catalysis, and dynamic oxidation of Ti-14Al-21Nb
[NASA-TP-2955] N90-10248
Fatigue crack initiation mechanics of metal aircraft structures
[AD-A210567] N90-10255
Fracture and three dimensional stress analyses of 7075 aluminum projectile components under spin and inertia load
[AD-A210986] N90-10463

ALUMINUM GALLIUM ARSENIDES
Experimental investigations of transport and optical properties of 3-5 quantum well structures grown via molecular beam epitaxy under optimal growth conditions
[AD-A210269] N90-10758
High energy neutron irradiation effects in GaAs modulation-Doped Field Effect Transistors (MODFETS): Threshold voltage
[AD-A210502] N90-10763

ALUMINUM GRAPHITE COMPOSITES
Space structures concepts and materials
[NASA-CR-183727] N90-10128

ALUMINUM OXIDES
Zirconia toughened SiC whisker reinforced alumina composites small business innovation research
[NASA-CR-179629] N90-10294

AMBIENT TEMPERATURE
Measurement of respiratory air temperatures and calculation of respiratory heat loss when working at various ambient temperatures
[AD-A210378] N90-10529

AMINES
Reactions of hydrogen chloride and boron trichloride with trimethylsilylamino groups
[AD-A209006] N90-10209

AMINO ACIDS
Control of synthetic peptide tertiary structure
[AD-A210339] N90-10281
Excitatory amino acids as transmitters in the brain
[AD-A210685] N90-10532

AMMUNITION
Remarks on certain aspects of solid explosive detonation via small projectile impact
[AD-A210648] N90-10307

AMORPHOUS MATERIALS
Optical dispersion relations for diamondlike carbon films
[NASA-TM-102356] N90-10738

AMORPHOUS SILICON
Structure of amorphous silicon alloy films
[DE89-009441] N90-10734

AMPLIFICATION
Master oscillator with power amplifiers: Performance of a two-element CW HF phased-laser array
[AD-A211141] N90-10435

ANALYZERS
Real-time observations of aerosol composition changes
[DE89-012382] N90-10422

ANGLE OF ATTACK
Basic studies of the unsteady flow past high angle of attack airfoils
[AD-A210252] N90-10008
Analysis of flight data from a High-Incidence Research Model by system identification methods
[NASA-TP-2940] N90-10074

ANILINE
Rechargeable lithium/polymer cathode batteries
[AD-A210978] N90-10354

ANNEALING
Gaussmeter determination of 302 stainless steel material condition
[BDX-613-3941] N90-10249
The effects of normal annealing cycles during IGFET fabrication on initial and radiation induced gate insulator defects
[AD-A210282] N90-10278
Characterization of GaAs/Si/GaAs heterointerfaces
[DE89-016302] N90-10752
Methods to decrease defect density in GaAs/Si heteroepitaxy
[DE89-016306] N90-10753

ANNIHILATION REACTIONS
Femtosecond dynamics of fluoro-aluminum phthalocyanine and linear alkane molecules
[AD-A210939] N90-10766

ANNUAL VARIATIONS
ELF (Extremely Low Frequency) Communications System Ecological Monitoring Program: Electromagnetic field measurements and engineering support, 1988
[AD-A210200] N90-10321
A seasonal isotherm depth climatology for the eastern tropical Pacific
[PB89-193577] N90-10512

ANOMALIES
Semi-monthly temperature and geopotential anomaly in the upper 500 meters along the Oahu-Farallon Islands great circle from November 15, 1967 through December 15, 1979
[AD-A210640] N90-10518
Quantization of anomalous gauge theories on a lattice
[DE89-010247] N90-10776

ANTENNA ARRAYS
Submillimeter quantum electronics
[AD-A210439] N90-10762

ANTENNA DESIGN
Technology for large space systems: A bibliography with indexes (supplement 21)
[NASA-SP-7046(21)] N90-10130
New electrodynamic and electrostatic models with applications to antenna theory, superconductor slots, and lasers N90-10316
Maximization of directed electromagnetic radiation with an optimized antenna
[DE89-014045] N90-10319
TWIRE: A test program for VLF airborne transmissions
[AD-A210516] N90-10324

ANTENNA RADIATION PATTERNS
The addition of Bendix MLS (Microwave Landing System) antenna patterns to MLS mathematical model
[AD-A210633] N90-10020
Maximization of directed electromagnetic radiation with an optimized antenna
[DE89-014045] N90-10319

ANTENNAS
The addition of Bendix MLS (Microwave Landing System) antenna patterns to MLS mathematical model
[AD-A210633] N90-10020

ANTIMISSILE DEFENSE
Tracking performance evaluation
[AD-A210499] N90-10540

ANTIMONY
Trap gettering by isoelectronic doping of p-GaAs and n-GaAs grown by molecular beam epitaxy
[AD-A211162] N90-10769

ANTIMONY COMPOUNDS
The synthesis and structure of novel antimony thiametallacycles
[AD-A210868] N90-10229

ANTIMONY ISOTOPES
Tellurium-118/antimony-118 generator
[DE89-015225] N90-10696

ANTIREFLECTION COATINGS
High-efficiency CuInSe2 and CuInGaSe2 based cells and materials research
[DE89-009449] N90-10471

APPLICATIONS PROGRAMS (COMPUTERS)
Forecasting convection with the AFOS (Automation of Field Operations and Services) data analysis programs. (ADAP-version 2.0) (AFOS data analysis programs-version 2.0)
[PB89-145940] N90-10492
String Search
[PB89-195986] N90-10593

APPROACH CONTROL
National airspace system approach and departure sequencing operational concept
[NAS-SR-1322] N90-10017

APPROXIMATION
On lower confidence for PCS in truncated location parameter models
[AD-A210274] N90-10661
The temporal development of collision cascades in the binary collision approximation
[DE89-015860] N90-10699

ARCHAEBACTERIA
Molecular biology and physiology of methanogenic archaebacteria
[AD-A210399] N90-10522

ARCHITECTURE (COMPUTERS)
The organization of permutation architectures with bussed interconnections
[AD-A210632] N90-10352
The role of sensor directed, model based control in robotics
[DE89-014133] N90-10442
Parallel asynchronous hardware implementation of image processing algorithms N90-10546
Sparse distributed memory overview N90-10561
Algorithms and architectures for robot vision N90-10562
Performance evaluation of the Scheme86 and HP precision architectures
[AD-A209418] N90-10578
A multiprocessor architecture using modular arithmetic for very high precision computation
[AD-A208154] N90-10579
Effective resource utilization for multiprocessor join execution
[DE89-016303] N90-10595
Cost metric algorithms for internetwork applications
[AD-A210324] N90-10597
Using computer design and simulation to improve manufacturing productivity
[AD-A210336] N90-10598
Applications of parallel supercomputers: Scientific results and computer science lessons
[DE89-016385] N90-10611
Shared memory versus message passing architectures: An application based study
[AD-A210312] N90-10615
Exploring the benefits of multiple hardware contexts in a multiprocessor architecture: Preliminary results
[AD-A210349] N90-10616
The rewrite rule machine project
[AD-A210528] N90-10617
Northeast Artificial Intelligence Consortium annual report for 1987. Volume 5: Building an intelligent assistant: The acquisition, integration and maintenance of complex distributed tasks
[AD-A210330] N90-10621
The architecture of NEWTON: A general-purpose dynamics simulator
[NASA-CR-185489] N90-10678
A comparison of real-time optical correlators for pattern recognition
[DE89-016416] N90-10705
Development of Information Quality Engineering (IQE) methodology for information resource management
[AD-A210615] N90-10791

ARGON LASERS
Treatment of laser-induced retinal injuries
[AD-A210284] N90-10526

ARGON PLASMA
An experimental study of microwave transmission through a decaying plasma
[AD-A210586] N90-10726

ARITHMETIC
A multiprocessor architecture using modular arithmetic for very high precision computation
[AD-A208154] N90-10579

ARMED FORCES (UNITED STATES)
Human performance in continuous/sustained operations and the demands of extended work/rest schedules: An annotated bibliography, volume 2
[AD-A210504] N90-10530

ARMOR
Alternative test methodology for ballistic performance ranking of armor ceramics
[AD-A210587] N90-10290
Studies in penetration mechanics
[AD-A210713] N90-10448

ARRAYS
Laser diode array and transmission optics N90-10163
A lunar far-side very low frequency array
[NASA-CP-3039] N90-10805

ARTIFICIAL CARDIAC PACEMAKER
The use of lithium batteries in biomedical devices
[AD-A210789] N90-10350

ARTIFICIAL INTELLIGENCE
Identification of stability and control parameters of a brilliant ammunition N90-10065
Real-time support for high performance aircraft operation
[NASA-CR-185475] N90-10075
Knowledge-based machine vision systems for space station automation
[NASA-CR-185710] N90-10124
Analysis and construction of contact and tactile sensors
[DE89-013992] N90-10416
Autonomous mobile robot research using the HERMIES-3 robot
[DE89-015916] N90-10443
Vision Science and Technology at NASA: Results of a Workshop
[NASA-TM-102214] N90-10542
Sparse distributed memory overview N90-10561
Advancing automation and robotics technology for the space station Freedom and for the US economy
[NASA-TM-101561] N90-10577
Northeast Artificial Intelligence Consortium annual report for 1987. Volume 5: Building an intelligent assistant: The acquisition, integration and maintenance of complex distributed tasks
[AD-A210330] N90-10621
Northeast Artificial Intelligence Consortium annual report for 1987. Volume 7, part A: Time oriented problem solving
[AD-A210331] N90-10622
Some results on learning
[AD-A210591] N90-10624
The applicability and limitations of expert system shells
[AD-A210801] N90-10625
The development of an expert system for the creative design of mechanisms
[AD-A211115] N90-10628

ARTIFICIAL SATELLITES
On analytic modeling of lunar perturbations of artificial satellites of the earth
[AD-A210440] N90-10078
Gyrotron development for space power beaming N90-10148
Effects of rain attenuation on satellite EHF (Extremely High Frequency) communications in the US
[AD-A210517] N90-10325

ASPARTATES
Polypeptide inhibitors of mineral scaling and corrosion
[AD-A210507] N90-10225

ASTROMETRY
Astrometric telescope facility. Preliminary systems definition study. Volume 3: Cost estimate
[NASA-TM-89429-VOL-3] N90-10808

ASTRONOMICAL OBSERVATORIES
Analysis of nearly simultaneous X-ray and optical observations of active galactic nuclei N90-10806

ASTRONOMICAL PHOTOGRAPHY
Advances in photographic X-ray imaging for solar astronomy N90-10803

ASTRONOMICAL PHOTOMETRY
Analysis of nearly simultaneous X-ray and optical observations of active galactic nuclei N90-10806

ASTRONOMY
Motion detection in astronomical and ice floe images N90-10558
Institute of Geophysics and Planetary Physics, 1988
[DE89-014383] N90-10794
National register of research projects, 1986/87. Part 2B: Natural sciences: Physical, engineering and related sciences (new projects)
[DE89-015033] N90-10826

ASTROPHYSICS
On the utility and ubiquity of atomic collision physics
[DE89-015356] N90-10686
Institute of Geophysics and Planetary Physics, 1988
[DE89-014363] N90-10794
Astrophysical and cosmological constraints to neutrino properties
[NASA-CR-185031] N90-10809
Atomic effects of beta decay in astrophysics and in elementary particle physics N90-10811

ASYMMETRY
A symplectic coherent beam-beam model
[DE89-015986] N90-10701
Observations of azimuthal asymmetry for certain FRC operating regimes
[DE89-015300] N90-10721

ASYMPTOTIC METHODS
Asymptotic robustness in regression and autoregression based on Lindeberg conditions
[AD-A210725] N90-10654

ASYMPTOTIC SERIES
Global existence and asymptotic stability for a nonlinear integrodifferential equation modeling heat flow
[AD-A210647] N90-10408
A unified approach to estimating tail behavior
[AD-A210961] N90-10672

ATLANTIC OCEAN
Marine weather log, volume 32, number 3, summer 1988
[PB88-248075] N90-10491
US Navy regional climatic study of the United States Atlantic Coast and associated waters
[AD-A210198] N90-10503
Evaluation of the North Atlantic seasonal nitrogen model, version 2
[DE89-016157] N90-10515

ATMOSPHERIC ATTENUATION
Atmospheric transmissivity update - 1988
[AD-A209130] N90-10484

ATMOSPHERIC CHEMISTRY
Paper 1. Impact of volcanic aerosols on stratospheric chemistry. Paper 2. O2 (1 sigma g +) and O2 (1 delta g) in the H + O2 reaction system. Paper 3. Barotropic instability of zonal jets on Mars, Earth and Venus N90-10477
Study of the NO3 radical decomposition reaction and the N2O5 in equilibrium with NO3 + NO2 equilibrium constant
[PB89-208961] N90-10480

ATMOSPHERIC COMPOSITION
Meeting Review: Workshop on Airborne Instrumentation
[PB89-174775] N90-10032
Kiruna geophysical data: Data Summary 88/7-9, July - September 1988
[PB89-210249] N90-10487
Geophysical monitoring for climatic change number 16
[PB89-159628] N90-10494
Human health studies of carbon monoxide (CO) under conditions of military weapons systems crewman exposures. Protocol 1: Formation of COHb
[AD-A210344] N90-10528
Laboratory measurements of microwave and millimeter-wave properties of planetary atmospheric constituents
[NASA-CR-185914] N90-10815

ATMOSPHERIC DIFFUSION
The suitability of diffusion and wind-field techniques for an emergency-response dispersion model
[PB89-190219] N90-10481

ATMOSPHERIC EFFECTS
Development of a semiquantitative corrosion monitor
[AD-A208132] N90-10414

ATMOSPHERIC ELECTRICITY
The 1984 direct strike lightning data, part 1
[NASA-TM-87690-PT-1] N90-10505
The 1984 direct strike lightning data, part 2
[NASA-TM-87690-PT-2] N90-10506
The 1984 direct strike lightning data, part 3
[NASA-TM-87690-PT-3] N90-10507

ATMOSPHERIC MODELS
The suitability of diffusion and wind-field techniques for an emergency-response dispersion model
[PB89-190219] N90-10481
Numerical simulations of a midlatitude squall line N90-10497
Coordination of mesoscale meteorological research between ASL and European groups
[AD-A210902] N90-10508

ATMOSPHERIC SOUNDING
A study of the impact of simulated 183 GHz water vapor retrievals on numerical weather prediction
[AD-A210431] N90-10504

ATMOSPHERIC TEMPERATURE
A study of the impact of simulated 183 GHz water vapor retrievals on numerical weather prediction
[AD-A210431] N90-10504
Measurement of respiratory air temperatures and calculation of respiratory heat loss when working at various ambient temperatures
[AD-A210378] N90-10529
ATOMIC COLLISIONS
On the utility and ubiquity of atomic collision physics
[DE89-015356] N90-10686
ATOMIC EXCITATIONS
Observation of excited H(sup 0) atoms produced by relativistic H(sup (minus)) ions in carbon and formvar foils
[DE89-015301] N90-10688
ATOMIC PHYSICS
Atomic effects of beta decay in astrophysics and in elementary particle physics N90-10811
ATOMIC STRUCTURE
Bonding in transition metal silyl dimers. Molecular orbital theory
[AD-A208269] N90-10260
Superconductivity from valence fluctuations with finite U
[DE89-015302] N90-10742
ATOMS
The temporal development of collision cascades in the binary collision approximation
[DE89-015860] N90-10699
ATTENTION
Daytime sleepiness, performance, mood, nocturnal sleep: The effect of benzodiazepine and caffeine on their relationship
[AD-A210915] N90-10533
Attention and vigilance in speech perception
[AD-A210493] N90-10539
ATTENUATION
Effects of rain attenuation on satellite EHF (Extremely High Frequency) communications in the US
[AD-A210517] N90-10325
ATTITUDE CONTROL
The Spartan 1 mission
[NASA-TM-101887] N90-10077
Explicit modeling and computational load distribution for concurrent processing simulation of the space station N90-10096
Modeling, simulation, and analyses of attitude control for the Crew/Equipment Retriever (CER) proposed for space station
[AD-A208140] N90-10125
ATTITUDE STABILITY
Modeling, simulation, and analyses of attitude control for the Crew/Equipment Retriever (CER) proposed for space station
[AD-A208140] N90-10125
AUDITORY PERCEPTION
Attention and vigilance in speech perception
[AD-A210493] N90-10539
AURORAL ELECTROJETS
The auroral energy deposition over the polar ionosphere during substorms
[AD-A210522] N90-10490
AUSTENITE
Fatigue growth and closure of short cracks
[AD-A210824] N90-10462
AUTOMATA THEORY
An introduction to input/output automata
[AD-A210831] N90-10604
AUTOMATIC CONTROL
Active participation in highly automated systems: Turning the wrong stuff into the right stuff
[AD-A210218] N90-10572
Advancing automation and robotics technology for the space station Freedom and for the US economy
[NASA-TM-101561] N90-10577
Autonomous control system for Czochralski growth of LEC GaAs
[AD-A210190] N90-10754
Automatic classification of spectra from the Infrared Astronomical Satellite (IRAS)
[NASA-RP-1217] N90-10807
AUTOMATIC PILOTS
How to control unstable missile airframes: Methodology and limitations N90-10060
A structured singular value approach to missile autopilot analysis 2 N90-10068
Flexible missile autopilot design studies with PC-MATLAB/386 N90-10088
AUTOMATIC WEATHER STATIONS
A program to improve performance of AFGL (Air Force Geophysical Laboratory) automated present weather observing sensors
[AD-A207669] N90-10495
AUTOMOBILE ENGINES
Advanced Turbine Technology Applications Project (ATTAP)
[NASA-CR-185133] N90-10036
AUTONOMIC NERVOUS SYSTEM
Extrathalamic modulation of cortical function
[AD-A211044] N90-10535
AUTONOMY
Autonomous mobile robot research using the HERMIES-3 robot
[DE89-015916] N90-10443
AUTORADIOGRAPHY
Biomedical studies with the free electron laser
[AD-A208927] N90-10519
AXISYMMETRIC BODIES
Laminar boundary layer along inviscid surface streamlines over inclined axisymmetric bodies in incompressible flow
[AD-A210202] N90-10401
AZIMUTH
ILS/MLS comparison tests at Miami/Tamiami, Florida Airport
[ACD-330] N90-10018
Observations of azimuthal asymmetry for certain FRC operating regimes
[DE89-015300] N90-10721
AZULENE
Impedance analysis of ionic transport in polypyrrole-polyazulene copolymer and its charge-discharge characteristics
[AD-A210979] N90-10299
Rechargeable lithium/polymer cathode batteries
[AD-A210978] N90-10354

B

BACTERIA
Genetic engineering of single-domain magnetic particles
[AD-A210332] N90-10521
A structural basis for electron transfer in bacterial photosynthesis
[DE89-015702] N90-10687
BANDWIDTH
Multi-level bandwidth efficient block modulation codes
[NASA-CR-185484] N90-10317
BAROCLINITY
The influence of a steady baroclinic deep ocean on the shelf
[PB89-198188] N90-10511
BAROTROPIC FLOW
Paper 1. Impact of volcanic aerosols on stratospheric chemistry. Paper 2. O2 (1 sigma g +) and O2 (1 delta g) in the H + O2 reaction system. Paper 3. Barotropic instability of zonal jets on Mars, Earth and Venus N90-10477
BAYES THEOREM
Number of test samples needed to obtain a desired Bayesian confidence interval for a proportion
[AD-A208157] N90-10658
Empirical Bayes selection for the highest probability of success in negative binomial distributions
[AD-A210273] N90-10660
A brief bibliography of statistical classification procedures: Decision-theoretic approach
[AD-A210276] N90-10663
BAYS (TOPOGRAPHIC FEATURES)
Coastal Research Center Woods Hole Oceanographic Institution
[PB89-198238] N90-10510
BEAM INJECTION
Fermilab fixed target beams from the main injector
[DE89-014355] N90-10697
BEAM INTERACTIONS
Tangent map analysis of the beam-beam interaction
[DE89-015857] N90-10689
BEAM SPLITTERS
Fermilab fixed target beams from the main injector
[DE89-014355] N90-10697
BEAMS (RADIATION)
Gyrotron development for space power beaming N90-10148
Laser-powered Martian rover N90-10157
Applicability of the beamed power concept to lunar rovers, construction, mining, explorers and other mobile equipment N90-10159
Laser diode array and transmission optics N90-10163
Beamed laser power in support of near-earth missions N90-10167
An algorithm to calculate the beam momentum distribution from flying wire profiles
[DE89-015587] N90-10418
A symplectic coherent beam-beam model
[DE89-015386] N90-10701
BEHAVIOR
Summarizing qualitative behavior from measurements of nonlinear circuits, revisior
[AD-A210919] N90-10353
Biological investigations of adaptive networks: Neuronal control of conditioned responses
[AD-A211043] N90-10534
BEND TESTS
Stress intensity factors and displacements for arc bend samples using collocation
[AD-A210404] N90-10460
BENDING
Aircraft modal supression system: Existing design approach and its shortcomings N90-10115
Structural stability augmentation system design using BODEDIRECT: A quick and accurate approach N90-10116
BENDING FATIGUE
Stress intensity factors and displacements for arc bend samples using collocation
[AD-A210404] N90-10460
BENZENE
Monte Carlo simulations of small solute/solvent clusters: Cluster properties and phase transitions
[AD-A209559] N90-10684
BETA PARTICLES
Atomic effects of beta decay in astrophysics and in elementary particle physics N90-10811
BIAS
Inherent bias in nonlinear least squares analysis of first-order kinetic data
[AD-A210677] N90-10651
Bias and oxide thickness dependence of trapped charge buildup in MOS devices
[AD-A210264] N90-10757
BIBLIOGRAPHIES
Technology for large space systems: A bibliography with indexes (supplement 21)
[NASA-SP-7046(21)] N90-10130
Space station systems: A bibliography with indexes (supplement 8)
[NASA-SP-7056(08)] N90-10131
Aerospace medicine and biology: A continuing bibliography with indexes (supplement 328)
[NASA-SP-7011(328)] N90-10524
Human performance in continuous/sustained operations and the demands of extended work/rest schedules: An annotated bibliography, volume 2
[AD-A210504] N90-10530
NASA scientific and technical publications: A catalog of special publications, reference publications, conference publications, and technical papers, 1988
[NASA-SP-7063(03)] N90-10782
National register of research projects, 1986/87. Part 2B: Natural sciences: Physical, engineering and related sciences (new projects)
[DE89-015033] N90-10826
BIG BANG COSMOLOGY
The origin of the universe from quantum chaos: An introduction to current ideas
[AD-A210441] N90-10813
BINARY DIGITS
Comparison of DPCM prediction strategies for high-quality digital television bit-rate reduction
[BBC-RD-1989/8] N90-10318
BINDERS (MATERIALS)
Effects of binder concentration on the properties of plastic-bonded explosives
[DE89-007744] N90-10301
BINOMIALS
Empirical Bayes selection for the highest probability of success in negative binomial distributions
[AD-A210273] N90-10660
BIOASTRONAUTICS
Aerospace medicine and biology: A continuing bibliography with indexes (supplement 328)
[NASA-SP-7011(328)] N90-10524
BIOCHEMISTRY
Biochemical cycling and fluxes between the deep euphotic zone and other oceanic realms
[PB89-152458] N90-10509
Electroporation: Theory of basic mechanisms
[AD-A210196] N90-10520
BIODYNAMICS
Biomedical influences on spinal cord function
[AD-A210311] N90-10527
BIOENGINEERING
Instrumentation and robotic image processing using top-down model control N90-10563
BIOINSTRUMENTATION
Synthetic polypeptide composites for sensor applications
[AD-A210797] N90-10296
The use of lithium batteries in biomedical devices
[AD-A210789] N90-10350

BIOLOGICAL EFFECTS
Organic explosives and related compounds. Environmental and health considerations [AD-A210554] N90-10306
Aerospace medicine and biology: A continuing bibliography with indexes (supplement 328) [NASA-SP-7011(328)] N90-10524
Biological investigations of adaptive networks: Neuronal control of conditioned responses [AD-A211043] N90-10534
BIOPROCESSING
Molecular biology and physiology of methanogenic archaebacteria [AD-A210399] N90-10522
BIOSYNTHESIS
Biomedical studies with the free electron laser [AD-A206927] N90-10519
BIOTECHNOLOGY
Army Science Conference Proceedings (16th) held in Fort Monroe, Virginia on 25-27 October 1988: Addenda [AD-A210235] N90-10827
BIRD-AIRCRAFT COLLISIONS
Definition and reduction of the F-16 windshield birdstrike hazard [AD-A210700] N90-10015
BL LACERTAE OBJECTS
Analysis of nearly simultaneous X-ray and optical observations of active galactic nuclei N90-10806
BLOOD VOLUME
Control of thermoregulatory sweating during exercise in the heat [AD-A206001] N90-10523
BODY TEMPERATURE
Measurement of respiratory air temperatures and calculation of respiratory heat loss when working at various ambient temperatures [AD-A210378] N90-10529
BOEING 737 AIRCRAFT
Aircraft accident report: Aloha Airlines, Flight 243, Boeing 737-200, N73711, near Maui, Hawaii, April 28, 1988 [PB89-910404] N90-10013
BOLTZMANN DISTRIBUTION
Physics of high energy photoconductive switches [AD-A210341] N90-10345
BOLTZMANN TRANSPORT EQUATION
Energy dependent transport problem with generalized boundary conditions [DE89-017843] N90-10676
BOMBER AIRCRAFT
Encyclopedia of US Air Force aircraft and missile systems. Volume 2: Post-World War 2 bombers, 1945-1973 [AD-A209273] N90-10001
BOOSTER ROCKET ENGINES
Liquid rocket booster study. Volume 2, book 1 [NASA-CR-183600] N90-10133
Liquid rocket booster study. Volume 2, book 5, appendix 9: LRB alternate applications and evolutionary growth [NASA-CR-183604] N90-10134
Liquid rocket booster study. Volume 2, book 4, appendices 6-8: Reports of Rocketdyne, Pratt and Whitney, and TRW [NASA-CR-183603] N90-10135
Liquid rocket booster study. Volume 2, book 2, appendix 1: Trades studies [NASA-CR-183601] N90-10136
Liquid rocket booster study. Volume 1: Executive summary [NASA-CR-183599] N90-10137
Liquid rocket booster study. Volume 2, book 6, appendix 10: Vehicle systems effects [NASA-CR-183605] N90-10138
Liquid rocket booster study. Volume 2, book 3, appendices 2-5: PPIP, transition plan, AMOS plan, and environmental analysis [NASA-CR-183602] N90-10139
BORANES
Metal-assisted syntheses of boranes and carboranes [AD-A210728] N90-10227
BORON
Photoreflectance study of boron ion-implanted (100) cadmium telluride [SD-TR-88-89] N90-10300
BORON CARBIDES
Shock compression and release in high-strength ceramics [DE89-013995] N90-10265
BORON CHLORIDES
Reactions of hydrogen chloride and boron trichloride with trimethylsilylamino groups [AD-A209006] N90-10209
BORON NITRIDES
New polymer precursors to boron and silicon nitrides [AD-A210287] N90-10279
BOUNDARY INTEGRAL METHOD
A combined finite element and boundary integral formulation for solution via CGFFT of 2-dimensional scattering problems [NASA-CR-184781] N90-10313
BOUNDARY LAYER CONTROL
Application of superplastically formed and diffusion bonded aluminum to a laminar flow control leading edge [NASA-CR-178316] N90-10030
Laminar flow control perforated wing panel development [NASA-CR-178166] N90-10187
Stability of a supersonic boundary layer along a swept leading edge N90-10359
Control and modification of turbulence N90-10377
Turbulence management: Application aspects N90-10378
Dynamics and control of turbulent shear flows [AD-A210396] N90-10402
BOUNDARY LAYER EQUATIONS
A three-dimensional linear stability approach to transition on wings at incidence N90-10373
BOUNDARY LAYER FLOW
On the interaction of stationary crossflow vortices and Tollmien-Schlichting waves in the boundary layer on a rotating disc [NASA-CR-181859] N90-10007
The three-dimensional vortex sheet structure on delta wings N90-10367
A composite velocity procedure for the three-dimensional reduced Navier-Stokes equations N90-10396
BOUNDARY LAYER SEPARATION
Laminar boundary layer along inviscid surface streamlines over inclined axisymmetric bodies in incompressible flow [AD-A210202] N90-10401
Dynamics and control of turbulent shear flows [AD-A210396] N90-10402
BOUNDARY LAYER STABILITY
Fluid Dynamics of Three-Dimensional Turbulent Shear Flows and Transition [AGARD-CP-438] N90-10356
Stability and transition of three-dimensional boundary layers N90-10357
Stability of a supersonic boundary layer along a swept leading edge N90-10359
Direct numerical study of leading-edge contamination N90-10361
Experimental study of transition and leading edge contamination on swept wings N90-10362
Three-dimensional boundary layer transition on a concave surface N90-10365
Curvature effects on the stability of three-dimensional laminar boundary layers N90-10366
The three-dimensional vortex sheet structure on delta wings N90-10367
Simultaneous detection of separation and transition in surface shear layers N90-10368
Experimental study of instability modes in a three-dimensional boundary layer N90-10369
Primary and secondary stability analysis applied to the DFVLR-transition swept-plate experiment N90-10371
Numerical investigation of transition in 3D boundary layers N90-10372
A three-dimensional linear stability approach to transition on wings at incidence N90-10373
Trailing-edge sweep and three-dimensional vortex interactions in jets and mixing layers N90-10379
Numerical simulation of coherent structures in an incompressible mixing layer N90-10383
BOUNDARY LAYER TRANSITION
On the interaction of stationary crossflow vortices and Tollmien-Schlichting waves in the boundary layer on a rotating disc [NASA-CR-181859] N90-10007
The measurement of boundary layers on a compressor blade in cascade. Volume 1: Experimental technique, analysis and results [NASA-CR-185118-VOL-1] N90-10038
The measurement of boundary layers on a compressor blade in cascade. Volume 2: Data tables [NASA-CR-185118-VOL-2] N90-10039
Fluid Dynamics of Three-Dimensional Turbulent Shear Flows and Transition [AGARD-CP-438] N90-10356
Stability and transition of three-dimensional boundary layers N90-10357
Experimental investigation of attachment-line transition in low-speed, high-lift wind-tunnel testing N90-10358
Leading edge transition by contamination in hypersonic flow N90-10360
Direct numerical study of leading-edge contamination N90-10361
Experimental study of transition and leading edge contamination on swept wings N90-10362
Numerical investigation of the effects of longitudinal vortices on the onset of transition in a flat plate boundary layer N90-10363
Three-dimensional boundary layer transition on a concave surface N90-10365
Simultaneous detection of separation and transition in surface shear layers N90-10368
Experimental study of instability modes in a three-dimensional boundary layer N90-10369
Primary and secondary stability analysis applied to the DFVLR-transition swept-plate experiment N90-10371
Numerical investigation of transition in 3D boundary layers N90-10372
A three-dimensional linear stability approach to transition on wings at incidence N90-10373
Numerically determined transition in separated internal flow N90-10374
Control and modification of turbulence N90-10377
BOUNDARY VALUE PROBLEMS
Use of the quasilinearization algorithm for the simulation of LSS slewing N90-10110
Two counter-rotating vortices approaching a free surface in a viscous fluid [AD-A210495] N90-10404
Stability of discontinuous shearing motions of a non-Newtonian fluid [AD-A210643] N90-10406
Stability of discontinuous steady states in shearing motion of a non-Newtonian fluid [AD-A210644] N90-10407
Global existence and asymptotic stability for a nonlinear integrodifferential equation modeling heat flow [AD-A210647] N90-10408
Mechanics of the crack path formation [NASA-CR-185143] N90-10455
Numerical methods for differential-algebraic equations: Current status and future directions [DE89-015116] N90-10632
BOUSSINESQ APPROXIMATION
Numerical solution of three-dimensional unsteady flows: Application to instability problems N90-10375
BOW WAVES
Plasma waves in the earth's foreshock, bow shock, and magnetosheath N90-10486
Computer simulation of plasma interactions near Titan N90-10816
BRAGG ANGLE
Bragg crystal polarimeters [NASA-CR-181331] N90-10423
BRAIN
Biomedical influences on spinal cord function [AD-A210311] N90-10527
Excitatory amino acids as transmitters in the brain [AD-A210685] N90-10532
Sparse distributed memory overview N90-10561
Pyramid image codes N90-10567
BRANCHING (MATHEMATICS)
An introduction to fractals and chaos [AD-A210257] N90-10675
BRAYTON CYCLE
Performance potential of an advanced technology Mach 3 turbojet engine installed on a conceptual high-speed civil transport [NASA-TM-4144] N90-10034
BREEDER REACTORS
Experience with model based display for advanced diagnostics and control [DE89-015693] N90-10469
BREMSSTRAHLUNG
The auroral energy deposition over the polar ionosphere during substorms [AD-A210522] N90-10490
BRITTLE MATERIALS
The response of isotropic brittle materials to abrasive processes [DE89-016637] N90-10251
BRITTLENESS
The response of isotropic brittle materials to abrasive processes [DE89-016637] N90-10251
BROADBAND
Coherent multichannel techniques for integrated broadband communications subscriber lines [AD-A209323] N90-10312
Performance of a broadbanded ultrasonic transducer with coaxially mounted, nondirectional receiver [DE89-015838] N90-10343
BROKEN SYMMETRY
Symmetry breaking bifurcations and the growth of chaos in a rotating fluid [AD-A210969] N90-10411
A theoretical high energy physics program [DE89-012685] N90-10696
BUBBLES
Theory of droplet. Part 1: Renormalized laws of droplet vaporization in non-dilute sprays N90-10390

Analytic theory for the selection of Saffman-Taylor fingers in the presence of thin film effects
[NASA-CR-181910] N90-10677

BUCKLING
Design guide for predicting nonlinear random response (including snap-through) of buckled plates
[NASA-CR-181877] N90-10681

BUDGETING
Energy storage and distribution program summary. Volume 2: Research summaries, fiscal year 1988
[DE89-000667] N90-10470

BURNS (INJURIES)
Treatment of laser-induced retinal injuries
[AD-A210284] N90-10526

C

CADMIUM TELLURIDES
Photoreflectance study of boron ion-implanted (100) cadmium telluride
[SD-TR-88-89] N90-10300

CAFFEINE
Daytime sleepiness, performance, mood, nocturnal sleep: The effect of benzodiazepine and caffeine on their relationship
[AD-A210915] N90-10533

CALCIUM CARBONATES
Polypeptide inhibitors of mineral scaling and corrosion
[AD-A210507] N90-10225

CALCIUM COMPOUNDS
MHD seed recovery and regeneration
[DE89-002711] N90-10715

CALCIUM PHOSPHATES
Polypeptide inhibitors of mineral scaling and corrosion
[AD-A210507] N90-10225

CALIBRATING
Introduction to total- and partial-pressure measurements in vacuum systems
[NASA-RP-1219] N90-10412
Self-calibration of robot-sensor system N90-10570
A FORTRAN program for the calculation of the calibration coefficients of a six-component strain gauge balance
[AD-A210375] N90-10599
Autonomous control system for Czochralski growth of LEC GaAs
[AD-A210190] N90-10754
Automatic classification of spectra from the Infrared Astronomical Satellite (IRAS)
[NASA-RP-1217] N90-10807

CALORIMETERS
Thermophysical properties of ceramics. Part 2: Development of specific-heat-measurement apparatus at high temperature
[DE89-760382] N90-10268

CAMERAS
Space environment robot vision system N90-10569

CAPACITORS
Mechanical states in wound capacitors. Part 1: Prediction
[DE89-006110] N90-10337
Mechanical states in wound capacitors. Part 2: Optimization
[DE89-008116] N90-10338
Capacitive energy storage at cryogenic temperatures, phase 2
[AD-A210366] N90-10347
Advanced double layer capacitor
[AD-A210510] N90-10348
Properties of devices prepared with epitaxial layers on InP
[AD-A210304] N90-10759

CAPILLARY FLOW
Capillary effects in steady-state flow in heterogeneous cores
[DE89-000758] N90-10399
Analysis of spurt phenomena for a non-Newtonian fluid
[AD-A210560] N90-10405

CARBON
Research on ultra low wear materials for energy conservation
[DE89-015096] N90-10263
Observation of excited H(sup 0) atoms produced by relativistic H(sup (minus)) ions in carbon and formvar foils
[DE89-015301] N90-10688
Optical dispersion relations for diamondlike carbon films
[NASA-TM-102356] N90-10738

CARBON CYCLE
Biochemical cycling and fluxes between the deep euphotic zone and other oceanic realms
[PB89-152458] N90-10509
A simple, mass balance model of carbon flow in a controlled ecological life support system
[NASA-TM-102151] N90-10571

CARBON DIOXIDE
Biochemical cycling and fluxes between the deep euphotic zone and other oceanic realms
[PB89-152458] N90-10509

CARBON DIOXIDE LASERS
Laser propulsion to earth orbit. Has its time come? N90-10143

CARBON MONOXIDE
Human health studies of carbon monoxide (CO) under conditions of military weapons systems crewman exposures. Protocol 1: Formation of COHb
[AD-A210344] N90-10528

CARBORANE
Monomers, polymers and transition metal complexes based upon carboranes
[AD-A210226] N90-10221
Metal-assisted syntheses of boranes and carboranes
[AD-A210728] N90-10227

CARBOXYLATES
Comparison of carboxylated and sulfonated model polyurethane ionomers
[AD-A210438] N90-10284

CARBOXYLIC ACIDS
Cubane derivatives for propellant applications
[AD-A210368] N90-10305

CARRIAGES
New test techniques to evaluate near field effects for supersonic store carriage and separation N90-10062

CARTESIAN COORDINATES
A numerical method for solving transonic flow past aircraft in Cartesian coordinates
[NAL-TR-1008] N90-10003

CASCADE FLOW
The measurement of boundary layers on a compressor blade in cascade. Volume 1: Experimental technique, analysis and results
[NASA-CR-185118-VOL-1] N90-10038
The measurement of boundary layers on a compressor blade in cascade. Volume 2: Data tables
[NASA-CR-185118-VOL-2] N90-10039

CASTINGS
Castings Airworthiness
[AGARD-R-762] N90-10231
US Air Force certification of castings N90-10232
Casting factors imposed by the French regulation for foundry castings used in military aircraft N90-10233
Casting airworthiness joint European civil authorities view-point N90-10234
Royal Aerospace Establishment: No place for a castings factor N90-10235
Castings, from theory to practical application N90-10236
Evaluation of titanium castings for aerospace components N90-10237
The question of the casting factor N90-10238
Quality control of castings N90-10239
Combined advanced foundry and quality control techniques to enhance reliability of castings for the aerospace industry N90-10240
The creation of quality: New directions in the production of aeronautics castings N90-10241
Thin walled cast high-strength structural parts N90-10242
Advances in the technology of titanium castings N90-10243
Microstructure morphology and quality of Al-Si castings N90-10244
The improved corrosion resistance of ultra high purity magnesium alloy castings N90-10245

CASTOR OIL
UV-curable polyurethane-methacrylate co-networks and interpenetrating networks
[AD-A210445] N90-10285

CATACLYSMIC VARIABLES
Theoretical statistics of zero-age cataclysmic variables N90-10810

CATALOGS (PUBLICATIONS)
Software methodology catalog, second edition, revision
[AD-A210548] N90-10601
NASA scientific and technical publications: A catalog of special publications, reference publications, conference publications, and technical papers, 1988
[NASA-SP-7063(03)] N90-10782

CATALYSIS
Heterogeneous catalysts in water
[AD-A210742] N90-10228
Emittance, catalysis, and dynamic oxidation of Ti-14Al-21Nb
[NASA-TP-2955] N90-10248
Control of synthetic peptide tertiary structure
[AD-A210339] N90-10281
Inherent bias in nonlinear least squares analysis of first-order kinetic data
[AD-A210677] N90-10651

CATALYSTS
Structural and surface characterization of dispersed metal catalysts
[DE89-014530] N90-10206
Heterogeneous catalysts in water
[AD-A210742] N90-10228

CATHODE RAY TUBES
Effects of miniature CRT (Cathode Ray Tube) location upon primary and secondary task performances
[AD-A210223] N90-10573

CATHODES
Rechargeable lithium/polymer cathode batteries
[AD-A210978] N90-10354
Plasma gun with coaxial powder feed and adjustable cathode
[NASA-CASE-LEW-14901-1] N90-10718

CATIONS
Solvent effects on intervalence electron-transfer energies for biferrocene cations: Comparisons with molecular models of solvent reorganization
[AD-A210263] N90-10691

CAVITIES
Numerical calculations of the collapse of a cavity in the vicinity of a compliant wall
[AD-A210489] N90-10403

CAVITY RESONATORS
Efficient nonlinear conversion of laser diode pumped miniature solid state laser sources
[AD-A210708] N90-10433
Coupled multiline CW HF lasers: Experimental performance
[AD-A210844] N90-10434
Use of depletion edge translation for high-speed modulation and switching of lightwaves
[AD-A211186] N90-10713

CELLS (BIOLOGY)
Electroporation: Theory of basic mechanisms
[AD-A210196] N90-10520
Genetic engineering of single-domain magnetic particles
[AD-A210332] N90-10521

CENTRIFUGES
VIBRAFUGE: A combined environment testing facility-vibration testing on a centrifuge
[DE89-015120] N90-10458

CERAMIC COATINGS
Japanese structural ceramics research and development N90-10272

CERAMIC MATRIX COMPOSITES
Ceramic components in machines, Cologne and Aachen, West Germany; Maastricht, The Netherlands and Brussels, Belgium
[DE89-015831] N90-10264
Zirconia toughened SiC whisker reinforced alumina composites small business innovation research
[NASA-CR-179629] N90-10294

CERAMICS
Advanced Turbine Technology Applications Project (ATTAP)
[NASA-CR-185133] N90-10036
Materials for engine applications above 3000 deg F: An overview
[NASA-TM-100169] N90-10188
Raman characterization of high temperature materials using an imaging detector
[DE89-016308] N90-10219
New structural materials
[AD-A209425] N90-10246
Friction and wear of oxide-ceramic sliding against IN-718 nickel base alloy at 25 to 800 C in atmospheric air
[NASA-TM-102291] N90-10262
Ceramic components in machines, Cologne and Aachen, West Germany; Maastricht, The Netherlands and Brussels, Belgium
[DE89-015831] N90-10264
Shock compression and release in high-strength ceramics
[DE89-013995] N90-10265
Thermophysical properties of ceramics. Part 2: Development of specific-heat-measurement apparatus at high temperature
[DE89-760382] N90-10268
Japanese structural ceramics research and development N90-10272
Structure-mechanical property relationships in ion implanted ceramics
[DE89-010129] N90-10274
Alternative test methodology for ballistic performance ranking of armor ceramics
[AD-A210587] N90-10290
The measurement of infrared spectra of dense ceramics by specular reflectance spectroscopy
[AD-A210609] N90-10291

Improved silicon carbide for advanced heat engines [NASA-CR-180831] N90-10293
Zirconia toughened SiC whisker reinforced alumina composites small business innovation research [NASA-CR-179629] N90-10294
Composite ceramic superconducting wires for electric motor applications [AD-A210345] N90-10346
Capacitive energy storage at cryogenic temperatures, phase 2 [AD-A210366] N90-10347
Plasma gun with coaxial powder feed and adjustable cathode [NASA-CASE-LEW-14901-1] N90-10718
Ceramic processing of bulk high-T(sub c) superconductors [DE89-015703] N90-10736

CEREBELLUM
Biological investigations of adaptive networks: Neuronal control of conditioned responses [AD-A211043] N90-10534

CEREBRAL CORTEX
Extrathalamic modulation of cortical function [AD-A211044] N90-10535

CERTIFICATION
US Air Force certification of castings N90-10232
Royal Aerospace Establishment: No place for a castings factor N90-10235

CHANNEL FLOW
Numerical simulation of turbulent plane channel flows N90-10362

CHAOS
Symmetry breaking bifurcations and the growth of chaos in a rotating fluid [AD-A210969] N90-10411
An introduction to fractals and chaos [AD-A210257] N90-10675
Theoretical investigations of chaotic dynamics [AD-A207724] N90-10772
The origin of the universe from quantum chaos: An introduction to current ideas [AD-A210441] N90-10813

CHARGE CARRIERS
Studies of high power density, pico-second rise-time light activated semiconductor switch [AD-A210549] N90-10349
Particle emission and charging effects induced by fracture [AD-A210215] N90-10459
Trap gettering by isoelectronic doping of p-GaAs and n-GaAs grown by molecular beam epitaxy [AD-A211162] N90-10769

CHARGE COUPLED DEVICES
Space environment robot vision system N90-10569
The detection of soft X-rays with charged coupled detectors N90-10798

CHECKOUT
Dependency-directed localization of software bugs [AD-A210837] N90-10606

CHEMICAL ANALYSIS
Analysis of surface modified colloidal silicas [DE89-015849] N90-10267

CHEMICAL BONDS
International Conference on Organometallic Chemistry (13th) held in Torino, Europe on 4-9 September 1988: Abstracts [AD-A210617] N90-10178
Reaction of oxygen with allene [DE89-015219] N90-10216
Bonding in transition metal silyl dimers. Molecular orbital theory [AD-A208269] N90-10260
New polymer precursors to boron and silicon nitrides [AD-A210287] N90-10279

CHEMICAL COMPOSITION
New structural materials [AD-A209425] N90-10246
Properties of HY-100 for naval construction [MRL-R-1149] N90-10247
Characterization and evaluation of acid rain in East Central Florida from 1978 to 1987: Ten year summary report [NASA-TM-102149] N90-10478

CHEMICAL ENERGY
Acoustic-vortex-chemical interactions in an idealized ramjet N90-10206

CHEMICAL EXPLOSIONS
Effects of binder concentration on the properties of plastic-bonded explosives [DE89-007744] N90-10301

CHEMICAL LASERS
Multiline multimode CW chemical laser performance [AD-A210613] N90-10432
Master oscillator with power amplifiers: Performance of a two-element CW HF phased-laser array [AD-A211141] N90-10435

CHEMICAL PROPERTIES
Investigation of the pyrometallurgical, physical and mechanical behavior of weld metal [AD-A211114] N90-10258
Properties of F-34 (JP-8) fuel for 1988 [AD-A210188] N90-10303

CHEMICAL PROPULSION
Low-earth-orbit to low-lunar-orbit laser freighter N90-10160
Laser propulsion option N90-10161

CHEMICAL REACTIONS
Reactions of hydrogen chloride and boron trichloride with trimethylsilylamino groups [AD-A209006] N90-10209
Chemistry of nitromethane at very high pressure [DE89-006016] N90-10215
Reaction of oxygen with allene [DE89-015219] N90-10216
Direct numerical simulation of turbulent free shear flows [AD-A210161] N90-10218
Monomers, polymers and transition metal complexes based upon carboranes [AD-A210226] N90-10221
Metal-assisted syntheses of boranes and carboranes [AD-A210728] N90-10227
Cubane derivatives for propellant applications [AD-A210368] N90-10305
On the utility and ubiquity of atomic collision physics [DE89-015356] N90-10686
Solvent dynamical effects in electron transfer: Predicted influences of electron coupling upon the rate-dielectric friction dependence [AD-A210193] N90-10690

CHESAPEAKE BAY (US)
Chesapeake Bay surface salinities, 1951-88 [PB89-194583] N90-10513

CHIPS (ELECTRONICS)
Laterally stacked Schottky diodes for infrared sensor applications [NASA-CASE-NPO-17426-1-CU] N90-10329
The organization of permutation architectures with bussed interconnections [AD-A210832] N90-10352
Performance of the CAMEX64 silicon strip readout chip [DE89-014015] N90-10747

CHIRAL DYNAMICS
Quantization of anomalous gauge theories on a lattice [DE89-010247] N90-10776

CIRCADIAN RHYTHMS
Human performance in continuous/sustained operations and the demands of extended work/rest schedules: An annotated bibliography, volume 2 [AD-A210504] N90-10530

CIRCUIT BREAKERS
Development of an expert system supporting short-circuit tests for circuit breakers [DE89-760384] N90-10334

CIRCUIT DIAGRAMS
Circuit level modeling of inductive elements [DE89-015122] N90-10173
Focused ion beam implantation [AD-A210977] N90-10767

CIRCUIT RELIABILITY
Development of an expert system supporting short-circuit tests for circuit breakers [DE89-760384] N90-10334

CIRCUITS
Statistical modeling of electrical components [BDX-613-3939] N90-10336
Summarizing qualitative behavior from measurements of nonlinear circuits, revision [AD-A210919] N90-10353

CIRCULAR CYLINDERS
Leading edge transition by contamination in hypersonic flow N90-10360

CIRCULAR TUBES
Limit analysis of welded tee end connections for hollow tubes [PB89-191647] N90-10452

CIVIL AVIATION
Casting airworthiness joint European civil authorities view-point N90-10234

CLASSIFICATIONS
Classification and reduction of pilot error [NASA-CR-181867] N90-10014
Defense Technical Information Center cataloging guidelines [AD-A211000] N90-10792
Automatic classification of spectra from the Infrared Astronomical Satellite (IRAS) [NASA-RP-1217] N90-10807

CLEARANCES
Marginal release disturbances on advanced missiles N90-10070

CLIMATE
Effects of rain attenuation on satellite EHF (Extremely High Frequency) communications in the US [AD-A210517] N90-10325
US Navy regional climatic study of the United States Atlantic Coast and associated waters [AD-A210198] N90-10503

CLIMATE CHANGE
International impacts of global climate change: Testimony to House Appropriations Subcommittee on Foreign Operations, Export Financing and Related Programs [DE89-014004] N90-10482
Geophysical monitoring for climatic change number 16 [PB89-159628] N90-10494
Coastal Research Center Woods Hole Oceanographic Institution [PB89-198238] N90-10510

CLIMATOLOGY
International impacts of global climate change: Testimony to House Appropriations Subcommittee on Foreign Operations, Export Financing and Related Programs [DE89-014004] N90-10482
US Navy regional climatic study of the United States Atlantic Coast and associated waters [AD-A210198] N90-10503
A seasonal isotherm depth climatology for the eastern tropical Pacific [PB89-193577] N90-10512

CLINICAL MEDICINE
Daytime sleepiness, performance, mood, nocturnal sleep: The effect of benzodiazepine and caffeine on their relationship [AD-A210915] N90-10533

CLOSED ECOLOGICAL SYSTEMS
Power from space for use on earth: An emerging global option N90-10144
A simple, mass balance model of carbon flow in a controlled ecological life support system [NASA-TM-102151] N90-10571

CLOSURE LAW
Turbulence modelling of three-dimensional shear flows N90-10381
The generalized drift flux approach: Identification of the void-drift closure law N90-10386

CLOTHING
Thermoregulatory responses to intermittent exercise are influenced by knit structure of underwear [AD-A209087] N90-10541

CLOUD COVER
US Navy regional climatic study of the United States Atlantic Coast and associated waters [AD-A210198] N90-10503

CLOUD PHYSICS
Numerical simulations of a midlatitude squall line N90-10497

CLOUDS (METEOROLOGY)
Numerical simulations of a midlatitude squall line N90-10497

CMOS
Performance of the CAMEX64 silicon strip readout chip [DE89-014015] N90-10747

COAL
Development of the electroacoustic dewatering (EAD) process for fine/ultrafine coal [DE89-015883] N90-10700

COASTS
US Navy regional climatic study of the United States Atlantic Coast and associated waters [AD-A210198] N90-10503
Coastal Research Center Woods Hole Oceanographic Institution [PB89-196238] N90-10510

COBALT
Structural and surface characterization of dispersed metal catalysts [DE89-014530] N90-10208

COCKPITS
Cockpit lighting compatibility with image intensification night imaging systems: Issues and answers [AD-A210503] N90-10028
A3I visibility modeling project N90-10557

CODING
Electrostatically suspended rotor for angular encoder [NASA-CASE-MFS-28294-1] N90-10310
Multi-level bandwidth efficient block modulation codes [NASA-CR-185484] N90-10317
Networks for image acquisition, processing and display N90-10545
Image gathering, coding, and processing: End-to-end optimization for efficient and robust acquisition of visual information N90-10551
Ames vision group research overview N90-10566
Pyramid image codes N90-10567

Radon transform analysis of a probabilistic method for image generation
[AD-A207814] N90-10702

COEFFICIENTS
A FORTRAN program for the calculation of the calibration coefficients of a six-component strain gauge balance
[AD-A210375] N90-10599

COGNITION
Models of mental functioning
[AD-A210456] N90-10538
Visions of visualization aids: Design philosophy and experimental results N90-10547
Vision science and technology for supervised intelligent space robots N90-10548
Sparse distributed memory overview N90-10561

COHERENT RADIATION
Shortwavelength coherent radiation: Generation and applications
[AD-A209847] N90-10427

COHERENT SCATTERING
Effects of coherent scattering on infrared absorption in doped semiconductors
[AD-A210224] N90-10756

COLLAPSE
Numerical calculations of the collapse of a cavity in the vicinity of a compliant wall
[AD-A210489] N90-10403

COLLIMATION
An algorithm to calculate the beam momentum distribution from flying wire profiles
[DE89-015587] N90-10418

COLLISION AVOIDANCE
Safer skies with TCAS: Traffic Alert and Collision Avoidance System
[PB89-169221] N90-10016

COLLISIONAL PLASMAS
Simultaneous multiple frequency interferometry: An application of homodyne phase measurement
[DE89-013975] N90-10719

COLLISIONS
The temporal development of collision cascades in the binary collision approximation
[DE89-015860] N90-10699

COLLOIDS
Analysis of surface modified colloidal silicas
[DE89-015849] N90-10267

COLOR
The intensity dependent spread model and color constancy N90-10555

COLOR VISION
The 1988 year end report for road following at Carnegie-Mellon
[NASA-CR-185967] N90-10446
Stanford/NASA-Ames Center of Excellence in model-based human performance N90-10565
Ames vision group research overview N90-10566

COMBINATIONS (MATHEMATICS)
On the 2-extendability of planar graphs
[AD-A210289] N90-10642

COMBINATORIAL ANALYSIS
Stochastic control theory, nonlinear structural mechanics and applied combinatorics
[AD-A209042] N90-10657

COMBUSTIBLE FLOW
Upward flame spread on vertical walls
[PB89-214787] N90-10217
Numerical simulation of detonation transfer between gaseous explosive layers
[MRL-RR-1-89] N90-10395

COMBUSTION CHAMBERS
Combustor influence on fighter engine operability N90-10193
Dynamic instability characteristics of aircraft turbine engine combustors N90-10195
Recent developments in Ramjet pressure oscillation technology N90-10199
Numerical simulation of pressure oscillations in a ramjet combustor N90-10202

COMBUSTION EFFICIENCY
Cycle analysis of scramjet engines
[NAL-TR-1002] N90-10035
Direct numerical simulation of turbulent free shear flows
[AD-A210161] N90-10218

COMBUSTION STABILITY
Combustion Instabilities in Liquid-Fuelled Propulsion Systems
[AGARD-CP-450] N90-10191
Combustion instabilities in liquid-fueled propulsion systems: An overview N90-10192
Experimental study on the stability of small rocket engines with storable liquid propellants N90-10196
Low frequency and high frequency combustion oscillation phenomena inside a rocket combustion chamber fed by liquid or gaseous propellants N90-10197
Effects of low-frequency instabilities on the operation of Ramjet air inlets N90-10198
Reheat buzz: An acoustically coupled combustion instability N90-10200
Attenuation of reheat buzz by active control N90-10201
Numerical simulation of unsteady combustion in a dump combustor N90-10203
Very-low-frequency oscillations in liquid-fueled ramjets N90-10204
Oscillations in non-axisymmetric dump combustors N90-10205
Acoustic-vortex-chemical interactions in an idealized ramjet N90-10206
Combustion-driven oscillation in large combustion systems for power generation N90-10207
Upward flame spread on vertical walls
[PB89-214787] N90-10217

COMMAND AND CONTROL
Conceptual design of a synchronous Mars telecommunications satellite
[NASA-TP-2942] N90-10814

COMMERCE
Assessing the accuracy of vulnerability models by comparison with vulnerability experiments
[AD-A210871] N90-10669

COMMUNICATION CABLES
Coherent multilchannel techniques for integrated broadband communications subscriber lines
[AD-A209323] N90-10312

COMMUNICATION SATELLITES
Conceptual design of a synchronous Mars telecommunications satellite
[NASA-TP-2942] N90-10814

COMPARISON
A performance comparison of integration algorithms in simulating flexible structures N90-10101
Low-earth-orbit to low-lunar-orbit laser freighter N90-10160

COMPLEX COMPOUNDS
NMR evidence for a planar arene intermediate in the electron-transfer induced eta 6 to eta 4 hapticity change of a rhodium arene complex
[AD-A210211] N90-10177
International Conference on Organometallic Chemistry (13th) held in Torino, Europe on 4-9 September 1988: Abstracts
[AD-A210617] N90-10178
Monomers, polymers and transition metal complexes based upon carboranes
[AD-A210226] N90-10221

COMPLEXITY
On the expected complexity of the three-dimensional Voronoi diagram
[PB89-209332] N90-10636

COMPOSITE MATERIALS
Composite Blade Structural Analyzer (COBSTRAN) theoretical/programmer's manual
[NASA-TM-101958] N90-10181
Failure behavior of PEEK and its short-fiber composite systems
[AD-A210729] N90-10189
New structural materials
[AD-A209425] N90-10246
Preparation and evaluation of composite membranes for zinc/bromine storage batteries
[DE89-009931] N90-10339

COMPOSITE STRUCTURES
PMR graphite engine duct development
[NASA-CR-182228] N90-10037
Hygrothermal effects on the complex moduli of composite laminates N90-10182
Development of pressure containment and damage tolerance technology for composite fuselage structures in large transport aircraft
[NASA-CR-3996] N90-10186
Global/local stress analysis of composite structures
[NASA-TM-101640] N90-10456

COMPRESSIBLE FLOW
Three-dimensional unsteady transonic viscous-inviscid interaction N90-10005
Numerical simulation of the compressible Orszag-Tang vortex
[AD-A210465] N90-10725

COMPRESSION LOADS
Dynamically compressed metals: Theory
[AD-A210741] N90-10257

COMPRESSOR BLADES
The measurement of boundary layers on a compressor blade in cascade. Volume 1: Experimental technique, analysis and results
[NASA-CR-185118-VOL-1] N90-10038
The measurement of boundary layers on a compressor blade in cascade. Volume 2: Data tables
[NASA-CR-185118-VOL-2] N90-10039

COMPUTATION
Proceedings of the Workshop on Computational Aspects in the Control of Flexible Systems, part 1
[NASA-TM-101578-PT-1] N90-10080
Proceedings of the Workshop on Computational Aspects in the Control of Flexible Systems, part 2
[NASA-TM-101578-PT-2] N90-10103
Computation and parallel implementation for early vision N90-10549
On learning from exercises
[AD-A210593] N90-10574
Regulation of nonlinear and generalized linear systems
[AD-A207725] N90-10619

COMPUTATIONAL FLUID DYNAMICS
Three-dimensional unsteady transonic viscous-inviscid interaction N90-10005
An integrated CFD/experimental analysis of aerodynamic forces and moments
[NASA-TM-102195] N90-10006
The measurement of boundary layers on a compressor blade in cascade. Volume 1: Experimental technique, analysis and results
[NASA-CR-185118-VOL-1] N90-10038
The measurement of boundary layers on a compressor blade in cascade. Volume 2: Data tables
[NASA-CR-185118-VOL-2] N90-10039
Stability and Control of Tactical Missile Systems
[AGARD-CP-451] N90-10050
The present status and the future of missile aerodynamics N90-10051
Prediction of tactical missile dynamics N90-10056
Fluid Dynamics of Three-Dimensional Turbulent Shear Flows and Transition
[AGARD-CP-438] N90-10356
Stability and transition of three-dimensional boundary layers N90-10357
Direct numerical study of leading-edge contamination N90-10361
Numerical investigation of the effects of longitudinal vortices on the onset of transition in a flat plate boundary layer N90-10363
Primary and secondary stability analysis applied to the DFVLR-transition swept-plate experiment N90-10371
Numerical investigation of transition in 3D boundary layers N90-10372
Numerically determined transition in separated internal flow N90-10374
Control and modification of turbulence N90-10377
Turbulence modelling of three-dimensional shear flows N90-10381
Numerical simulation of turbulent plane channel flows N90-10382
Numerical simulation of coherent structures in an incompressible mixing layer N90-10383
A composite velocity procedure for the three-dimensional reduced Navier-Stokes equations N90-10396
A high-order Lagrangian-decoupling method for the incompressible Navier-Stokes equations
[NASA-CR-181903] N90-10631

COMPUTATIONAL GEOMETRY
On the expected complexity of the three-dimensional Voronoi diagram
[PB89-209332] N90-10636

COMPUTATIONAL GRIDS
Iterative performance and an adaptive procedure for viscous flow problems N90-10397
Tests of various finite difference algorithms applied to a simple water vapor transport problem on a staggered grid
[AD-A210229] N90-10596

COMPUTER AIDED DESIGN
Remote control missile model test N90-10063
Proceedings of the Workshop on Computational Aspects in the Control of Flexible Systems, part 1
[NASA-TM-101578-PT-1] N90-10080
Computational controls for aerospace systems N90-10082
Additional software developments wanted for modeling and control of flexible space systems N90-10083
Flexible structure control experiments using a real-time workstation for computer-aided control engineering N90-10084
CONSOLE: A CAD tandem for optimization-based design interacting with user-supplied simulators N90-10085
Flexible missile autopilot design studies with PC-MATLAB/386 N90-10088
DYSCO: A software system for modeling general dynamic systems N90-10089
Modeling and control system design and analysis tools for flexible structures N90-10090

Proceedings of the Workshop on Computational Aspects in the Control of Flexible Systems, part 2 [NASA-TM-101578-PT-2] N90-10103
Relating tolerances and kinematic behavior [AD-A211125] N90-10311
An expert system for optimal gear design N90-10439
Atmospheric transmissivity update - 1988 [AD-A209130] N90-10484
A3I visibility modeling project N90-10557
Evaluation of computer-aided software engineering tools for data base development [DE89-014007] N90-10591
Low-cost three-dimensional stereoscopic display technique for computer-aided design [DE89-011635] N90-10594
Aerospace system unified life cycle engineering producibility measurement issues [AD-A210937] N90-10607
The development of an expert system for the creative design of mechanisms [AD-A211115] N90-10628

COMPUTER AIDED MANUFACTURING
Relating tolerances and kinematic behavior [AD-A211125] N90-10311

COMPUTER ASSISTED INSTRUCTION
Northeast Artificial Intelligence Consortium annual report for 1987. Volume 5: Building an intelligent assistant: The acquisition, integration and maintenance of complex distributed tasks [AD-A210330] N90-10621

COMPUTER DESIGN
Evaluating local indirect addressing in SIMD processors [NASA-CR-181845] N90-10581
Using computer design and simulation to improve manufacturing productivity [AD-A210338] N90-10598
The rewrite rule machine project [AD-A210528] N90-10617

COMPUTER GRAPHICS
A3I visibility modeling project N90-10557
BLOT: A mesh and curve plot program for the output of a finite element analysis [DE89-013994] N90-10590

COMPUTER INFORMATION SECURITY
DDN Trusted Guard Gateway: Trusted Guard Gateway (TGG) technology assessment, phase 2 [AD-A210248] N90-10614

COMPUTER NETWORKS
Ada (trademark) projects at NASA. Runtime environment issues and recommendations [NASA-CR-183435] N90-10583
Cost metric algorithms for internetwork applications [AD-A210324] N90-10597
An introduction to input/output automata [AD-A210831] N90-10604
Network of dedicated processors for finding lowest-cost map path [NASA-CASE-NPO-17716-1-CU] N90-10608
Tools for application development in heterogeneous distributed environments [AD-A210238] N90-10613
DDN Trusted Guard Gateway: Trusted Guard Gateway (TGG) technology assessment, phase 2 [AD-A210248] N90-10614

COMPUTER PROGRAMMING
Automated model formulation for time-varying flexible structures N90-10107
Evaluation of computer-aided software engineering tools for data base development [DE89-014007] N90-10591
Structure flow diagram generator [PB89-195978] N90-10592
String Search [PB89-195986] N90-10593
Using computer design and simulation to improve manufacturing productivity [AD-A210338] N90-10598
Software methodology catalog, second edition, revision [AD-A210548] N90-10601
The impact of recovery on concurrency control [AD-A210828] N90-10603
Type reconstruction with first-class polymorphic values [AD-A210833] N90-10605
Tools for application development in heterogeneous distributed environments [AD-A210238] N90-10613
The applicability and limitations of expert system shells [AD-A210801] N90-10625
Applications of algebraic logic and universal algebra to computer science [AD-A210556] N90-10645
Toward a theory of representation design [AD-A210885] N90-10670

COMPUTER PROGRAMS
Initial flight qualification and operational maintenance of X-29A flight software [NASA-TM-101703] N90-10023
Stability and Control of Tactical Missile Systems [AGARD-CP-451] N90-10050
Missile Datcom: Enhancements for design applications N90-10054
Prediction of dynamic derivatives N90-10055
Prediction of tactical missile dynamics N90-10056
Remote control missile model test N90-10063
Analysis and testing of a high performance air-air missile N90-10069
Marginal release disturbances on advanced missiles N90-10070
The application of TSIM software to act design and analysis on flexible aircraft N90-10086
DYSCO: A software system for modeling general dynamic systems N90-10089
Control law synthesis and optimization software for large order aeroservoelastic systems N90-10111
TWIRE: A test program for VLF airborne transmissions [AD-A210516] N90-10324
Summarizing qualitative behavior from measurements of nonlinear circuits, revision [AD-A210919] N90-10353
Numerical simulation of detonation transfer between gaseous explosive layers [MRL-RR-1-89] N90-10395
Two stage gear tooth dynamics program [NASA-CR-185110] N90-10437
The MHOST finite element program: 3-D inelastic analysis methods for hot section components. Volume 2: User's manual [NASA-CR-182235-VOL-2] N90-10450
The MHOST finite element program: 3-D inelastic analysis methods for hot section components. Volume 3: Systems' manual [NASA-CR-182236] N90-10451
A common distributed language approach to software integration [NASA-CR-185499] N90-10584
On the interactive computer program IPIS for aircraft parameter identification [NAL-TR-1000] N90-10586
Waveform generator signal processing software [PB89-192660] N90-10587
BLOT: A mesh and curve plot program for the output of a finite element analysis [DE89-013994] N90-10590
A FORTRAN program for the calculation of the calibration coefficients of a six-component strain gauge balance [AD-A210375] N90-10599
Software methodology catalog, second edition, revision [AD-A210548] N90-10601
Dependency-directed localization of software bugs [AD-A210837] N90-10606
Tools for application development in heterogeneous distributed environments [AD-A210238] N90-10613
Northeast Artificial Intelligence Consortium annual report for 1987. Volume 7, part A: Time oriented problem solving [AD-A210331] N90-10622
Robot vehicle video image compression, phase 1 [AD-A210974] N90-10626
The architecture of NEWTON: A general-purpose dynamics simulator [NASA-CR-185489] N90-10678
Autonomous control system for Czochralski growth of LEC GaAs [AD-A210190] N90-10754
Focused ion beam implantation [AD-A210977] N90-10767

COMPUTER STORAGE DEVICES
Two-dimensional shape recognition using sparse distributed memory N90-10554
Sparse distributed memory overview N90-10561
Shared memory versus message passing architectures: An application based study [AD-A210312] N90-10615
Exploring the benefits of multiple hardware contexts in a multiprocessor architecture: Preliminary results [AD-A210349] N90-10616

COMPUTER SYSTEMS DESIGN
Performance evaluation of the Scheme86 and HP precision architectures [AD-A209418] N90-10578
The development of an expert system for the creative design of mechanisms [AD-A211115] N90-10628

COMPUTER SYSTEMS PERFORMANCE
Generic system components of the Thiokol ultrasonic RSRM case-to-insulation bondline inspection system [NASA-CR-183738] N90-10171
Performance evaluation of the Scheme86 and HP precision architectures [AD-A209418] N90-10578
Evaluation of computer-aided software engineering tools for data base development [DE89-014007] N90-10591
Computer availability impact on the archiving of scientific and technical reports [AD-A210283] N90-10787

COMPUTER SYSTEMS SIMULATION
Using computer design and simulation to improve manufacturing productivity [AD-A210338] N90-10598

COMPUTER TECHNIQUES
Relating tolerances and kinematic behavior [AD-A211125] N90-10311
General decomposition of sequential machines: Relationships to state assignment [AD-A208189] N90-10580
The aerospace energy systems laboratory: Hardware and software implementation [NASA-TM-101706] N90-10610

COMPUTER VISION
Knowledge-based machine vision systems for space station automation [NASA-CR-185710] N90-10124
Adaptive machine vision [AD-A208130] N90-10436
The 1988 year end report for road following at Carnegie-Mellon [NASA-CR-185967] N90-10446
Vision Science and Technology at NASA: Results of a Workshop [NASA-TM-102214] N90-10542
Parallel asynchronous hardware implementation of image processing algorithms N90-10546
Vision science and technology for supervised intelligent space robots N90-10548
Computation and parallel implementation for early vision N90-10549
Intensity dependent spread theory N90-10550
Image gathering, coding, and processing: End-to-end optimization for efficient and robust acquisition of visual information N90-10551
Hybrid vision activities at NASA Johnson Space Center N90-10552
Two-dimensional shape recognition using sparse distributed memory N90-10554
The intensity dependent spread model and color constancy N90-10555
Algorithms and architectures for robot vision N90-10562
Computer vision research at Marshall Space Flight Center N90-10564
Ames vision group research overview N90-10566
Space environment robot vision system N90-10569

COMPUTERIZED SIMULATION
Validation of missile simulation N90-10066
Additional software developments wanted for modeling and control of flexible space systems N90-10083
Flexible structure control experiments using a real-time workstation for computer-aided control engineering N90-10084
The application of TSIM software to act design and analysis on flexible aircraft N90-10086
A comparison of software for the modeling and control of flexible systems N90-10092
Efficiency and capabilities of multi-body simulations N90-10095
Explicit modeling and computational load distribution for concurrent processing simulation of the space station N90-10096
Simulation of flexible structures with impact: Experimental validation N90-10097
Simulation and control problems in elastic robots N90-10098
Linearized flexibility models in multibody dynamics and control N90-10099
Simulation of shuttle flight control system structural interaction with RMS deployed payloads N90-10100
A performance comparison of integration algorithms in simulating flexible structures N90-10101
Use of the quasilinearization algorithm for the simulation of LSS slewing N90-10110
Modeling, simulation, and analyses of attitude control for the Crew/Equipment Retriever (CER) proposed for space station [AD-A208140] N90-10125
Boost-phase discrimination research activities [NASA-TM-101889] N90-10176
Numerical simulation of pressure oscillations in a ramjet combustor N90-10202

Numerical simulation of unsteady combustion in a dump combustor N90-10203
Computer simulations of polymer dynamics in the solid state
[DE89-010337] N90-10275
Statistical modeling of electrical components
[BDX-613-3939] N90-10336
Numerical simulation of coherent structures in an incompressible mixing layer N90-10383
Analysis of a model and sequential numerical method for thermal reservoir simulation
[DE89-015117] N90-10384
Numerical simulation of detonation transfer between gaseous explosive layers
[MRL-RR-1-89] N90-10395
The role of sensor directed, model based control in robotics
[DE89-014133] N90-10442
A comparison of wind turbulence simulation models for stochastic loads analysis for horizontal-axis wind turbines
[DE89-009442] N90-10473
Tracking performance evaluation
[AD-A210499] N90-10540
On the interactive computer program IPIS for aircraft parameter identification
[NAL-TR-1000] N90-10586
A low-cost hypercube load-balance algorithm
[DE89-015739] N90-10589
An introduction to input/output automata
[AD-A210831] N90-10604
Computational and statistical issues in discrete-event simulation
[AD-A210743] N90-10668
Assessing the accuracy of vulnerability models by comparison with vulnerability experiments
[AD-A210871] N90-10669
Generation of 3/2 omega sub o radiation in inhomogeneous plasmas under the irradiation of intense electromagnetic waves
[DE89-015723] N90-10722
Computer simulation of plasma interactions near Titan N90-10816

COMPUTERS
Computer availability impact on the archiving of scientific and technical reports
[AD-A210283] N90-10787

CONCAVITY
Three-dimensional boundary layer transition on a concave surface N90-10365

CONCENTRATION (COMPOSITION)
Electrical field dependence of protein conformation and channel function in lipid membranes of different compositions
[AD-A210236] N90-10222
Effects of binder concentration on the properties of plastic-bonded explosives
[DE89-007744] N90-10301

CONCENTRATORS
Structural concepts for very large (400-meter-diameter) solar concentrators N90-10153
United States photovoltaic concentrator technology process and new program initiative
[DE89-013812] N90-10475

CONCURRENT PROCESSING
The impact of recovery on concurrency control
[AD-A210828] N90-10603
Tools for application development in heterogeneous distributed environments
[AD-A210238] N90-10613
The rewrite rule machine project
[AD-A210528] N90-10617
Northeast Artificial Intelligence Consortium annual report for 1987. Volume 7, part A: Time oriented problem solving
[AD-A210331] N90-10622

CONDITIONING (LEARNING)
Biological investigations of adaptive networks: Neuronal control of conditioned responses
[AD-A211043] N90-10534
Integration of neurobiological and computational analyses of the neural network essentials for conditioned taste aversions
[AD-A210228] N90-10537

CONDUCTION BANDS
High energy neutron irradiation effects in GaAs modulation-Doped Field Effect Transistors (MODFETS): Threshold voltage
[AD-A210502] N90-10763

CONFERENCES
Conference on Aerospace Transparent Materials and Enclosures (15th) 16-20 January 1989. Volume 2: Sessions 6-9
[AD-A210201] N90-10024
Stability and Control of Tactical Missile Systems
[AGARD-CP-451] N90-10050
Proceedings of the Workshop on Computational Aspects in the Control of Flexible Systems, part 1
[NASA-TM-101578-PT-1] N90-10080
Proceedings of the Workshop on Computational Aspects in the Control of Flexible Systems, part 2
[NASA-TM-101578-PT-2] N90-10103
Second Beamed Space-Power Workshop
[NASA-CP-3037] N90-10140
International Conference on Organometallic Chemistry (13th) held in Torino, Europe on 4-9 September 1988: Abstracts
[AD-A210617] N90-10178
Combustion Instabilities in Liquid-Fuelled Propulsion Systems
[AGARD-CP-450] N90-10191
Castings Airworthiness
[AGARD-R-762] N90-10231
Fluid Dynamics of Three-Dimensional Turbulent Shear Flows and Transition
[AGARD-CP-438] N90-10356
International Conference on Aerosols and Background Pollution Abstracts
[AD-A210970] N90-10483
Coordination of mesoscale meteorological research between ASL and European groups
[AD-A210902] N90-10508
Vision Science and Technology at NASA: Results of a Workshop
[NASA-TM-102214] N90-10542
Proceedings of the 2nd International Conference on Vector and Parallel Computing
[AD-A209401] N90-10585
Deep traps and sidegating in GaAs devices
[AD-A210740] N90-10765
A lunar far-side very low frequency array
[NASA-CP-3039] N90-10805
Army Science Conference Proceedings (16th) held in Fort Monroe, Virginia on 25-27 October 1988: Addenda
[AD-A210235] N90-10827

CONFIDENCE LIMITS
Number of test samples needed to obtain a desired Bayesian confidence interval for a proportion
[AD-A208157] N90-10658
The computation and use of the asymptotic covariance matrix for measurement error models
[PB89-215321] N90-10659
On lower confidence for PCS in truncated location parameter models
[AD-A210274] N90-10661

CONFIGURATION INTERACTION
Computational modeling of pi-conjugated polyradicals
[AD-A210573] N90-10648

CONGRESSIONAL REPORTS
Safer skies with TCAS: Traffic Alert and Collision Avoidance System
[PB89-169221] N90-10016
Advancing automation and robotics technology for the space station Freedom and for the US economy
[NASA-TM-101561] N90-10577

CONNECTORS
Varistor-particle lightning arrestor connector performance under simulated extreme lightning currents
[DE89-012663] N90-10342

CONSERVATION LAWS
Interpretation and modeling of the averaged equations for a fluid-solid flow N90-10388

CONSTITUTIVE EQUATIONS
Constitutive Relationships and Models in Continuum Theories of Multiphase Flows --- conferences
[NASA-CP-3047] N90-10385
Interpretation and modeling of the averaged equations for a fluid-solid flow N90-10388

CONSTRAINTS
Astrophysical and cosmological constraints to neutrino properties
[NASA-CR-185031] N90-10809

CONSTRUCTION
Properties of HY-100 for naval construction
[MRL-R-1149] N90-10247

CONSUMERS
Consumer electronics testing to fast-rise EMP (Electromagnetic Pulse) VEMPS (Vertical Electromagnetic Pulse Simulator) 2 development
[AD-A210505] N90-10323

CONTACT LOADS
Analysis and construction of contact and tactile sensors
[DE89-013992] N90-10416

CONTAMINATION
Direct numerical study of leading-edge contamination N90-10361

CONTINENTAL SHELVES
The influence of a steady baroclinic deep ocean on the shelf
[PB89-198188] N90-10511

CONTINUOUS RADIATION
Design and operating characteristics of a CW relevant quasi-optical gyrotron with variable mirror separation
[AD-A210611] N90-10425

CONTINUOUS WAVE LASERS
Multiline multimode CW chemical laser performance
[AD-A210613] N90-10432
Coupled multiline CW HF lasers: Experimental performance
[AD-A210844] N90-10434
Master oscillator with power amplifiers: Performance of a two-element CW HF phased-laser array
[AD-A211141] N90-10435
Biomedical studies with the free electron laser
[AD-A206927] N90-10519

CONTINUUM MECHANICS
Mechanics of damping for fiber composite laminates including hygro-thermal effects
[NASA-TM-102329] N90-10185
Constitutive Relationships and Models in Continuum Theories of Multiphase Flows --- conferences
[NASA-CP-3047] N90-10385

CONTROL SURFACES
Aeroelastic tailoring procedure for controlling fin hinge moments N90-10058
Aeroelastic analysis of missile control surfaces with structural non-linearity N90-10071
The active flexible wing aeroservoelastic wind-tunnel test program N90-10119

CONTROL SYSTEMS DESIGN
Identification of stability and control parameters of a brilliant ammunition N90-10065
Investigations of thrust vector control for high-alpha pitchover N90-10067
Real-time support for high performance aircraft operation
[NASA-CR-185475] N90-10075
Proceedings of the Workshop on Computational Aspects in the Control of Flexible Systems, part 1
[NASA-TM-101578-PT-1] N90-10080
NASA'S controls-structures interaction program N90-10081
Computational controls for aerospace systems N90-10082
Additional software developments wanted for modeling and control of flexible space systems N90-10083
Flexible structure control experiments using a real-time workstation for computer-aided control engineering N90-10084
CONSOLE: A CAD tandem for optimization-based design interacting with user-supplied simulators N90-10085
Control/structure interaction methods for space station power systems N90-10087
Flexible missile autopilot design studies with PC-MATLAB/386 N90-10088
Modeling and control system design and analysis tools for flexible structures N90-10090
A comparison of software for the modeling and control of flexible systems N90-10092
Proceedings of the Workshop on Computational Aspects in the Control of Flexible Systems, part 2
[NASA-TM-101578-PT-2] N90-10103
Controlling flexible structures: A survey of methods N90-10114
Structural stability augmentation system design using BODEDIRECT: A quick and accurate approach N90-10116
Input-output oriented computation algorithms for the control of large flexible structures N90-10118
Active vibration mitigation of distributed parameter, smart-type structures using Pseudo-Feedback Optimal Control (PFOC) N90-10121
Bidirectional power converter control electronics
[NASA-CR-175070] N90-10175

CONTROL THEORY
How to control unstable missile airframes: Methodology and limitations N90-10060
Proceedings of the Workshop on Computational Aspects in the Control of Flexible Systems, part 1
[NASA-TM-101578-PT-1] N90-10080
Simulation and control problems in elastic robots N90-10098
Linearized flexibility models in multibody dynamics and control N90-10099
Optical processing for distributed sensors in control of flexible spacecraft N90-10102
Flexible robot control: Modeling and experiments N90-10104
Modifying high-order aeroelastic math model of a jet transport using maximum likelihood estimation N90-10106
Automated model formulation for time-varying flexible structures N90-10107
Control law synthesis and optimization software for large order aeroservoelastic systems N90-10111

Flexible aircraft dynamic modeling for dynamic analysis and control synthesis N90-10112
Experimental validation of flexible robot arm modeling and control N90-10113
Controlling flexible structures: A survey of methods N90-10114
Aircraft modal supression system: Existing design approach and its shortcomings N90-10115
Optimal q-Markov COVER for finite precision implementation N90-10117
Stochastic control theory, nonlinear structural mechanics and applied combinatorics [AD-A209042] N90-10657

CONTROLLED FUSION
Massachusetts Institute of Technology Plasma Fusion Center [DE89-016050] N90-10723

CONTROLLERS
Explicit modeling and computational load distribution for concurrent processing simulation of the space station N90-10096
Optical processing for distributed sensors in control of flexible spacecraft N90-10102
Proceedings of the Workshop on Computational Aspects in the Control of Flexible Systems, part 2 [NASA-TM-101578-PT-2] N90-10103
Flexible robot control: Modeling and experiments N90-10104
Flexible aircraft dynamic modeling for dynamic analysis and control synthesis N90-10112
Experimental validation of flexible robot arm modeling and control N90-10113
Controlling flexible structures: A survey of methods N90-10114
Optimal q-Markov COVER for finite precision implementation N90-10117
Active vibration mitigation of distributed parameter, smart-type structures using Pseudo-Feedback Optimal Control (PFOC) N90-10121
Optimal integral controller with sensor failure accommodation N90-10123
An adaptive controller for enhancing operator performance during teleoperation [NASA-CR-183445] N90-10438
Adaptive robust control N90-10620

CONVECTION
Forecasting convection with the AFOS (Automation of Field Operations and Services) data analysis programs. (ADAP-version 2.0) (AFOS data analysis programs-version 2.0) [PB89-145940] N90-10492

CONVECTIVE FLOW
Symmetry breaking bifurcations and the growth of chaos in a rotating fluid [AD-A210969] N90-10411
Convection of a pattern of vorticity through a reacting shock wave [NASA-CR-181921] N90-10576

CONVERGENCE
Primal barrier methods for linear programming [AD-A210501] N90-10600
Numerical methods for differential-algebraic equations: Current status and future directions [DE89-015116] N90-10632

COOLING
Application of formal optimization techniques in thermal/structural design of a heat-pipe-cooled panel for a hypersonic vehicle [NASA-TM-89131] N90-10409

COOPERATION
A comparison of software for the modeling and control of flexible systems N90-10092

COORDINATE TRANSFORMATIONS
Self-calibration of robot-sensor system N90-10570

COPOLYMERS
Comparison of carboxylated and sulfonated model polyurethane ionomers [AD-A210438] N90-10284
Synthesis and physical properties of poly(perfluoroalkylether) urethanes [AD-A210500] N90-10287
Polyheterocycle Langmuir-Blodgett films [AD-A210625] N90-10292
Hierarchical structure in polymeric solids and its influence on properties [AD-A210918] N90-10297
Impedance analysis of ionic transport in polypyrrole-polyazulene copolymer and its charge-discharge characteristics [AD-A210979] N90-10299

COPPER
Solvent effects on the kinetics of electroreduction of Cu(I) at mercury [AD-A209423] N90-10211

COPPER OXIDES
Study of deposition of YBa2Cu3O7-x on cubic zirconia [NASA-TM-102350] N90-10737

CORES
Capillary effects in steady-state flow in heterogeneous cores [DE89-000758] N90-10399

CORONAL HOLES
The observation of possible reconnection events in the boundary changes of solar coronal holes N90-10801
Correspondence between solar fine-scale structures in the corona, transition region, and lower atmosphere from collaborative observations N90-10804

CORONAL LOOPS
Solar X-ray Astronomy Sounding Rocket Program [NASA-CR-183447] N90-10796

CORRELATION
Motion detection in astronomical and ice floe images N90-10558
Differences in writers initial task representations [AD-A210433] N90-10788

CORRELATORS
A comparison of real-time optical correlators for pattern recognition [DE89-016416] N90-10705

CORROSION
Polypeptide inhibitors of mineral scaling and corrosion [AD-A210507] N90-10225
Development of a semiquantitative corrosion monitor [AD-A208132] N90-10414

CORROSION PREVENTION
Polypeptide inhibitors of mineral scaling and corrosion [AD-A210507] N90-10225

CORROSION RESISTANCE
The improved corrosion resistance of ultra high purity magnesium alloy castings N90-10245

CORROSION TESTS
Development of a semiquantitative corrosion monitor [AD-A208132] N90-10414

COSMOLOGY
Research program in theoretical high energy physics [DE89-013963] N90-10695
Astrophysical and cosmological constraints to neutrino properties [NASA-CR-185031] N90-10809
The origin of the universe from quantum chaos: An introduction to current ideas [AD-A210441] N90-10813

COST ANALYSIS
Statistical modeling of electrical components [BDX-613-3939] N90-10336
Cost metric algorithms for internetwork applications [AD-A210324] N90-10597
Planning an Integrated On-line Library System (IOLS) [AD-A209406] N90-10783

COSTS
Energy storage and distribution program summary. Volume 2: Research summaries, fiscal year 1988 [DE89-000867] N90-10470

COUNTER ROTATION
Full scale technology demonstration of a modern counterrotating unducted fan engine concept: Component test [NASA-CR-180868] N90-10047
Full scale technology demonstration of a modern counterrotating unducted fan engine concept. Design report [NASA-CR-180867] N90-10048
Full scale technology demonstration of a modern counterrotating unducted fan engine concept. Engine test [NASA-CR-180869] N90-10049
Two counter-rotating vortices approaching a free surface in a viscous fluid [AD-A210495] N90-10404
Acoustic test and analysis of a counterrotating prop-fan model [NASA-CR-179590] N90-10683

COUPLING
Effect of particle velocity fluctuations on the inertia coupling in two-phase flow N90-10391
Design and operating characteristics of a CW relevant quasi-optical gyrotron with variable mirror separation [AD-A210611] N90-10425

COUPLING COEFFICIENTS
Solvent dynamical effects in electron transfer: Predicted influences of electron coupling upon the rate-dielectric friction dependence [AD-A210193] N90-10690

COUPLINGS
Interchangeable end effector tools utilized on the protoflight manipulator arm [NASA-CR-179374] N90-10447

COVARIANCE
Optimal q-Markov COVER for finite precision implementation N90-10117

CRACK CLOSURE
Fatigue growth and closure of short cracks [AD-A210824] N90-10462

CRACK INITIATION
Fatigue crack initiation mechanics of metal aircraft structures [AD-A210567] N90-10255
Porosity and crack initiation during low cycle fatigue [AD-A210989] N90-10484

CRACK OPENING DISPLACEMENT
An interferometric strain-displacement measurement system [NASA-TM-101638] N90-10454
Stress intensity factors and displacements for arc bend samples using collocation [AD-A210404] N90-10480

CRACK PROPAGATION
Raman characterization of high temperature materials using an imaging detector [DE89-016308] N90-10219
Mechanics of the crack path formation [NASA-CR-185143] N90-10455
Particle emission and charging effects induced by fracture [AD-A210215] N90-10459
Fatigue growth and closure of short cracks [AD-A210824] N90-10462

CRACKING (FRACTURING)
Porosity and crack initiation during low cycle fatigue [AD-A210989] N90-10484

CRACKS
Mechanics of the crack path formation [NASA-CR-185143] N90-10455

CRASHES
Waveform generator signal processing software [PB89-192660] N90-10587
The impact of recovery on concurrency control [AD-A210828] N90-10603

CREEP STRENGTH
Development of metastable processing paths for high temperature alloys [AD-A210550] N90-10254

CRITICAL POINT
Critical magnetic fields (H(sub c2), H(sub c1)) and kappa in YBa2(Cu0.98M0.02)3O(7+delta), M=Ni, Al, and Cu [DE89-016412] N90-10745

CRITICAL TEMPERATURE
The effect of twins on critical currents of high Tc superconductors [AD-A210988] N90-10768

CROSS FLOW
On the interaction of stationary crossflow vortices and Tollmien-Schlichting waves in the boundary layer on a rotating disc [NASA-CR-181859] N90-10007

CRYOGENIC TEMPERATURE
Capacitive energy storage at cryogenic temperatures, phase 2 [AD-A210366] N90-10347

CRYSTAL DEFECTS
The effects of normal annealing cycles during IGFET fabrication on initial and radiation induced gate insulator defects [AD-A210282] N90-10278

CRYSTAL GROWTH
Quartz crystal microbalance studies of electrochemical growth of conducting polymers [AD-A210788] N90-10295
Morphological aspects of the friction of hot-filament-grown diamond thin films [DE89-015986] N90-10750
Autonomous control system for Czochralski growth of LEC GaAs [AD-A210190] N90-10754

CRYSTAL LATTICES
The structure determination of molecular adsorbates with large unit cells or lattice-gas disorder on metal surfaces [AD-A210926] N90-10230

CRYSTAL STRUCTURE
Structural and surface characterization of dispersed metal catalysts [DE89-014530] N90-10208
Raman spectroscopic study of the rare earth sesquisulfides [AD-A210610] N90-10226
The measurement of infrared spectra of dense ceramics by specular reflectance spectroscopy [AD-A210609] N90-10291
Face-specific interaction of MoS4(2-1) with oriented crystals of (0001) CdX (X = Se, S) [AD-A209519] N90-10732
Ordered structures and metastable alloys grown by OMVPE [DE89-016370] N90-10744

Atomic imaging and interfacial analysis
[DE89-015339] N90-10748
Structural aspects of the phase separation in La2CuO4.032
[DE89-016183] N90-10751
The effect of twins on critical currents of high Tc superconductors
[AD-A210988] N90-10768

CRYSTALLIZATION
Computer simulations of polymer dynamics in the solid state
[DE89-010337] N90-10275

CRYSTALLOGRAPHY
Mott transition: Low-energy excitations and superconductivity
[DE89-617778] N90-10741
The growth of gallium nitride films via the innovative technique of atomic layer epitaxy
[AD-A210380] N90-10760

CRYSTALS
Bragg crystal polarimeters
[NASA-CR-181331] N90-10423
Face-specific interaction of MoS4(2-1) with oriented crystals of (0001) CdX (X = Se, S)
[AD-A209519] N90-10732

CUBANE
Cubane derivatives for propellant applications
[AD-A210368] N90-10305

CULTURE TECHNIQUES
Genetic engineering of single-domain magnetic particles
[AD-A210332] N90-10521

CUMULATIVE DAMAGE
Porosity and crack initiation during low cycle fatigue
[AD-A210989] N90-10464

CURING
UV-curable polyurethane-methacrylate co-networks and interpenetrating networks
[AD-A210445] N90-10285

CURRENT DENSITY
Studies of high power density, pico-second rise-time light activated semiconductor switch
[AD-A210549] N90-10349

CURVATURE
Curvature effects on the stability of three-dimensional laminar boundary layers N90-10366

CUTTERS
High-speed machining of aluminum
[DE89-014011] N90-10441

CYANATES
Multiple internal reflection Fourier transform infrared spectroscopy studies of thiocyanate adsorption on silver and gold
[AD-A210245] N90-10223

CYCLIC COMPOUNDS
The synthesis and structure of novel antimony thiametallacycles
[AD-A210888] N90-10229

CYCLIC HYDROCARBONS
NMR evidence for a planar arene intermediate in the electron-transfer induced eta 6 to eta 4 hapticity change of a rhodium arene complex
[AD-A210211] N90-10177

CYCLOGENESIS
Thermodynamic and dynamic processes in the updraft region of GALE (Genesis of Atlantic Lows Experiment) IOP (Intensive Observation Period) 9
[AD-A208139] N90-10496

CYCLOTRON RESONANCE DEVICES
Gyrotron development for space power beaming N90-10148
History and status of beamed power technology and applications at 2.45 Gigahertz N90-10150
Design and operating characteristics of a CW relevant quasi-optical gyrotron with variable mirror separation
[AD-A210611] N90-10425

CZOCHRALSKI METHOD
Autonomous control system for Czochralski growth of LEC GaAs
[AD-A210190] N90-10754

D

DAMAGE
US Air Force certification of castings N90-10232
Numerical analysis of a class of problems in the mathematical theory of plasticity and damage
[AD-A210731] N90-10655

DAMAGE ASSESSMENT
Hierarchical damage tolerant controllers for smart structures
[AD-A209422] N90-10022
Debris/ice/TPS assessment and photographic analysis for Shuttle Mission STS-28R
[NASA-TM-102152] N90-10079
Development of pressure containment and damage tolerance technology for composite fuselage structures in large transport aircraft
[NASA-CR-3996] N90-10186

DAMPING
Prediction of dynamic derivatives N90-10055
On modelling nonlinear damping in distributed parameter systems N90-10109
Aircraft modal supression system: Existing design approach and its shortcomings N90-10115
Mechanics of damping for fiber composite laminates including hygro-thermal effects
[NASA-TM-102329] N90-10185
Numerical simulation of unsteady combustion in a dump combustor N90-10203
The effect of twins on critical currents of high Tc superconductors
[AD-A210988] N90-10768

DATA ACQUISITION
Development of an automated probe for thermal conductivity measurements
[PB89-209324] N90-10419
Kiruna geophysical data: Data Summary 88/7-9, July - September 1988
[PB89-210249] N90-10487
Extreme hurricanes in the nineteenth century
[PB89-201305] N90-10498
Meteorological support: Descriptions of application programs for accessing and displaying data
[PB89-194625] N90-10500
Research highlights of the NMC (National Meteorological Center) Development Division: 1987-1988
[PB89-206478] N90-10501
Networks for image acquisition, processing and display N90-10545
Waveform generator signal processing software
[PB89-192660] N90-10587

DATA BASE MANAGEMENT SYSTEMS
Evaluation of computer-aided software engineering tools for data base development
[DE89-014007] N90-10591
Effective resource utilization for multiprocessor join execution
[DE89-016303] N90-10595

DATA BASES
Evaluation of computer-aided software engineering tools for data base development
[DE89-014007] N90-10591
An introduction to input/output automata
[AD-A210831] N90-10604
Communications Data Base (CDB), phase 3 (with software documentation)
[AD-A210540] N90-10789

DATA COMPRESSION
Robot vehicle video image compression, phase 1
[AD-A210974] N90-10626
Radon transform analysis of a probabilistic method for image generation
[AD-A207814] N90-10702

DATA FLOW ANALYSIS
Structure flow diagram generator
[PB89-195978] N90-10592

DATA PROCESSING
Guidance simulation and test support for differential GPS flight experiment
[NASA-CR-177471] N90-10021
Satellite Data Processing System (SDPS) users manual V1.0
[NASA-CR-183054] N90-10468
Meteorological support: Descriptions of application programs for accessing and displaying data
[PB89-194625] N90-10500
Data processing in lightning warning systems
[DE89-012495] N90-10502
Advances in regression: Use of models in spectroscopic data analysis
[AD-A210541] N90-10665
Motivating the notion of generic design within information processing theory: The design problem space
[AD-A210266] N90-10786
Defense Technical Information Center cataloging guidelines
[AD-A211000] N90-10792

DATA REDUCTION
System identification for large space structures N90-10126

DATA RETRIEVAL
The impact of recovery on concurrency control
[AD-A210828] N90-10603

DATA SAMPLING
Number of test samples needed to obtain a desired Bayesian confidence interval for a proportion
[AD-A208157] N90-10658

DATA SMOOTHING
Minimum-variance reduced-order estimation algorithms from Pontrygin's minimum principle N90-10105

DATA STORAGE
The MHOST finite element program: 3-D inelastic analysis methods for hot section components. Volume 3: Systems' manual
[NASA-CR-182236] N90-10451
Computer availability impact on the archiving of scientific and technical reports
[AD-A210283] N90-10787

DEBRIS
Debris/ice/TPS assessment and photographic analysis for Shuttle Mission STS-28R
[NASA-TM-102152] N90-10079

DECAY
Atomic effects of beta decay in astrophysics and in elementary particle physics N90-10811

DECISION MAKING
Cost metric algorithms for internetwork applications
[AD-A210324] N90-10597
A decision support approach to the file allocation problem in a distributed computing system N90-10609
Learning to make decisions: When incentives help and hinder
[AD-A210185] N90-10779
A theory of collective induction
[AD-A210553] N90-10780
Effects of stress on judgment and decision making in dynamic tasks
[AD-A210605] N90-10781

DECISION THEORY
A brief bibliography of statistical classification procedures: Decision-theoretic approach
[AD-A210276] N90-10663
Application of a hybrid generation/utility assessment heuristic to a class of scheduling problems
[NASA-TM-102367] N90-10674

DECOMPOSITION
Chemistry of nitromethane at very high pressure
[DE89-008016] N90-10215
Development of metastable processing paths for high temperature alloys
[AD-A210550] N90-10254
Study of the NO3 radical decomposition reaction and the N2O5 in equilibrium with NO3 + NO2 equilibrium constant
[PB89-208961] N90-10480

DECONTAMINATION
Heterogeneous catalysts in water
[AD-A210742] N90-10228

DECOUPLING
A high-order Lagrangian-decoupling method for the incompressible Navier-Stokes equations
[NASA-CR-181903] N90-10631

DEFECTS
Two photon absorption characterization
[AD-A210508] N90-10694
Methods to decrease defect density in GaAs/Si heteroepitaxy
[DE89-016306] N90-10753

DEFENSE INDUSTRY
Domestic technology transfer program regulation
[PB89-195374] N90-10793

DEGASSING
Trap gettering by isoelectronic doping of p-GaAs and n-GaAs grown by molecular beam epitaxy
[AD-A211162] N90-10769

DEGREES OF FREEDOM
Shape control of high degree-of-freedom variable geometry trusses N90-10122
Optimized resolved rate control of seven-degree-of-freedom Laboratory Telerobotic Manipulator (LTM) with application to three-dimensional graphics simulation
[NASA-TP-2938] N90-10618

DEICING
Electro-impulse de-icing testing analysis and design
[NASA-CR-4175] N90-10031

DELTA WINGS
An integrated CFD/experimental analysis of aerodynamic forces and moments
[NASA-TM-102195] N90-10006
The three-dimensional vortex sheet structure on delta wings N90-10367

DENSE PLASMAS
The dense Z-pinch as a plasma radiation source. 1: Quasi-static Bennett model
[AD-A210600] N90-10727

DENSIFICATION
Preparation, purification and densification of zinc sulfide powder from organometallics
[AD-A210943] N90-10298

DENSITY (MASS/VOLUME)
Density of states in a resonant tunneling structure
[AD-A209508] N90-10731

DEOXYRIBONUCLEIC ACID
Biomedical studies with the free electron laser
[AD-A208927] N90-10519
DEPLOYMENT
Simulation of shuttle flight control system structural interaction with RMS deployed payloads N90-10100
DEPOSITION
Alternative fabrication techniques for high-efficiency CuInSe2 and CuInSe2-alloy films and cells
[DE89-009451] N90-10474
The auroral energy deposition over the polar ionosphere during substorms
[AD-A210522] N90-10490
DEPTH MEASUREMENT
Adjustable depth gage
[NASA-CASE-LEW-14880-1] N90-10415
DESIGN ANALYSIS
Large scale prop-fan structural design study. Volume 1: Initial concepts
[NASA-CR-174992] N90-10043
Large scale prop-fan structural design study. Volume 2: Preliminary design of SR-7
[NASA-CR-174993] N90-10044
Full scale technology demonstration of a modern counterrotating unducted fan engine concept. Design report
[NASA-CR-180867] N90-10048
Computational controls for aerospace systems N90-10082
Castings, from theory to practical application N90-10236
Relating tolerances and kinematic behavior
[AD-A211125] N90-10311
Design and operating characteristics of a CW relevant quasi-optical gyrotron with variable mirror separation
[AD-A210611] N90-10425
A design assessment for metallic pressure vessels circumferentially reinforced with a pre-tensioned high-specific-strength anisotropic composite overwind
[AD-A209108] N90-10453
Human motion perception: Higher-order organization N90-10553
Stochastic control theory, nonlinear structural mechanics and applied combinatorics
[AD-A209042] N90-10657
DETECTION
Data processing in lightning warning systems
[DE89-012495] N90-10502
Networks for image acquisition, processing and display N90-10545
Computation and parallel implementation for early vision N90-10549
Intensity dependent spread theory N90-10550
Motion detection in astronomical and ice floe images N90-10558
DETECTORS
Raman characterization of high temperature materials using an imaging detector
[DE89-016306] N90-10219
DETONATION
Free-expansion experiments and modeling in detonation: Chemistry and hydrodynamics on a laboratory scale
[DE89-007748] N90-10302
Remarks on certain aspects of solid explosive detonation via small projectile impact
[AD-A210648] N90-10307
Shock behavior of explosives about the C-J (Chapman-Juget) point
[DE89-007642] N90-10400
Laser initiation of secondary explosives
[DE89-010229] N90-10431
DETONATION WAVES
Laser propulsion to earth orbit. Has its time come? N90-10143
Numerical simulation of detonation transfer between gaseous explosive layers
[MRL-RR-1-89] N90-10395
Convection of a pattern of vorticity through a reacting shock wave
[NASA-CR-181921] N90-10576
DEUTERIUM
A laser-driven source of polarized hydrogen and deuterium
[DE89-015130] N90-10429
Structure of amorphous silicon alloy films
[DE89-009441] N90-10734
DEUTERONS
Ignition and burn criteria for D3He tokamak and spherical torus reactors
[DE89-015059] N90-10716
DEWATERING
Development of the electroacoustic dewatering (EAD) process for fine/ultrafine coal
[DE89-015883] N90-10700
DIAGNOSIS
Experience with model based display for advanced diagnostics and control
[DE89-015693] N90-10469
DIAGRAMS
On the expected complexity of the three-dimensional Voronoi diagram
[PB89-209332] N90-10636
DIAMAGNETISM
Measuring the shielding effectiveness of superconductive composites
[DE89-015164] N90-10180
DIAMONDS
Characterization of diamond films by thermogravimetric analysis and infrared spectroscopy
[AD-A210564] N90-10288
Morphological aspects of the friction of hot-filament-grown diamond thin films
[DE89-015986] N90-10750
DIELECTRIC PROPERTIES
Dynamically compressed metals: Theory
[AD-A210741] N90-10257
The high-frequency dielectric properties of glass fibre reinforced plastic and honeycomb layers
[AD-A210581] N90-10289
The measurement of infrared spectra of dense ceramics by specular reflectance spectroscopy
[AD-A210609] N90-10291
Analysis of the performance of gallium arsenide photoavalanche switches
[DE89-015774] N90-10739
Mott transition: Low-energy excitations and superconductivity
[DE89-617778] N90-10741
DIELECTRICS
The high-frequency dielectric properties of glass fibre reinforced plastic and honeycomb layers
[AD-A210581] N90-10289
Mott transition: Low-energy excitations and superconductivity
[DE89-617778] N90-10741
Properties of devices prepared with epitaxial layers on InP
[AD-A210304] N90-10759
DIFFERENTIAL EQUATIONS
Improved propagation models for discrete random media
[AD-A211085] N90-10327
Numerical methods for differential-algebraic equations: Current status and future directions
[DE89-015116] N90-10632
On the coefficients of differentiated expansions of ultraspherical polynomials
[NASA-CR-181913] N90-10637
Periodic solutions of spatially periodic Hamiltonian systems
[AD-A210645] N90-10649
Stochastic quantization
[AD-A210942] N90-10671
DIFFRACTION RADIATION
Custom diffraction gratings
[AD-A211002] N90-10712
DIFFUSION
Lithium compensation of GaAs
[DE89-616080] N90-10740
DIFFUSION WELDING
Application of superplastically formed and diffusion bonded aluminum to a laminar flow control leading edge
[NASA-CR-178316] N90-10030
DIGITAL COMMAND SYSTEMS
Robotic vehicle message format
[AD-A210996] N90-10627
DIGITAL COMPUTERS
Parallel asynchronous hardware implementation of image processing algorithms N90-10546
DIGITAL FILTERS
Optimal q-Markov COVER for finite precision implementation N90-10117
DIGITAL SIMULATION
Analysis and testing of a high performance air-air missile N90-10069
DIGITAL SYSTEMS
Subpicosecond optical digital computation using conjugate parametric generators
[AD-A207908] N90-10330
Radon transform analysis of a probabilistic method for image generation
[AD-A207814] N90-10702
Autonomous control system for Czochralski growth of LEC GaAs
[AD-A210190] N90-10754
DIGITAL TELEVISION
Comparison of DPCM prediction strategies for high-quality digital television bit-rate reduction
[BBC-RD-1989/8] N90-10318
DIMERS
Bonding in transition metal silyl dimers. Molecular orbital theory
[AD-A208269] N90-10260
DIODES
Laser diode array and transmission optics N90-10163
Micro-cavity integrable vacuum diodes and triodes
[DE89-016649] N90-10344
Studies of high power density, pico-second rise-time light activated semiconductor switch
[AD-A210549] N90-10349
Efficient nonlinear conversion of laser diode pumped miniature solid state laser sources
[AD-A210708] N90-10433
Quantum 1/F noise in solid state devices in particular Hg1-(sub x)Cd(sub x)Te N(+)-P diodes
[AD-A209365] N90-10730
DIPOLE ANTENNAS
Millimeter-wave/infrared rectenna development at Georgia Tech N90-10147
DIRECTIONAL ANTENNAS
Maximization of directed electromagnetic radiation with an optimized antenna
[DE89-014045] N90-10319
DIRECTIVITY
Measurement resolution of noise directivity patterns from acoustic flight tests
[NASA-TM-4134] N90-10679
DISCRETE FUNCTIONS
Discrete-time conversion for simulating finite-horizon Markov processes
[AD-A210683] N90-10666
Computational and statistical issues in discrete-event simulation
[AD-A210743] N90-10668
Multi-sample functional statistical data analysis
[AD-A210992] N90-10673
DISCRIMINANT ANALYSIS (STATISTICS)
A brief bibliography of statistical classification procedures: Decision-theoretic approach
[AD-A210276] N90-10663
DISPERSING
The suitability of diffusion and wind-field techniques for an emergency-response dispersion model
[PB89-190219] N90-10481
DISPLACEMENT
Two stage gear tooth dynamics program
[NASA-CR-185110] N90-10437
DISPLACEMENT MEASUREMENT
Three-in-one gage
[NASA-CR-183714] N90-10413
An interferometric strain-displacement measurement system
[NASA-TM-101638] N90-10454
DISPLAY DEVICES
Classification and reduction of pilot error
[NASA-CR-181867] N90-10014
Satellite Data Processing System (SDPS) users manual V1.0
[NASA-CR-183054] N90-10468
Experience with model based display for advanced diagnostics and control
[DE89-015693] N90-10469
Vision science and technology at NASA: Results of a workshop: Executive summary N90-10543
Visions of visualization aids: Design philosophy and experimental results N90-10547
Human motion perception: Higher-order organization N90-10553
Stanford/NASA-Ames Center of Excellence in model-based human performance N90-10565
Low-cost three-dimensional stereoscopic display technique for computer-aided design
[DE89-011635] N90-10594
DISTANCE MEASURING EQUIPMENT
Adjustable depth gage
[NASA-CASE-LEW-14880-1] N90-10415
DISTRIBUTED PARAMETER SYSTEMS
On modelling nonlinear damping in distributed parameter systems N90-10109
Active vibration mitigation of distributed parameter, smart-type structures using Pseudo-Feedback Optimal Control (PFOC) N90-10121
DISTRIBUTED PROCESSING
Two-dimensional shape recognition using sparse distributed memory N90-10554
A decision support approach to the file allocation problem in a distributed computing system N90-10609
The aerospace energy systems laboratory: Hardware and software implementation
[NASA-TM-101706] N90-10610
Parallel processing and learning in simple systems
[AD-A210225] N90-10612

Tools for application development in heterogeneous distributed environments
[AD-A210238] N90-10613
Northeast Artificial Intelligence Consortium annual report for 1987. Volume 5: Building an intelligent assistant: The acquisition, integration and maintenance of complex distributed tasks
[AD-A210330] N90-10621
Northeast Artificial Intelligence Consortium annual report for 1987. Volume 7, part A: Time oriented problem solving
[AD-A210331] N90-10622

DISTRIBUTION FUNCTIONS
Multi-sample functional statistical data analysis
[AD-A210992] N90-10673

DISTURBING FUNCTIONS
An algorithm for the systematic disturbance of optimal rotational solutions
[NASA-TM-101089] N90-10575
Improved estimation of the disturbance variance in a linear regression model
[AD-A210272] N90-10641

DIVERTERS
Analysis of results from wind tunnel tests of inlets for an advanced turboprop nacelle installation
[NASA-CR-174937] N90-10011

DOCUMENT STORAGE
Computer availability impact on the archiving of scientific and technical reports
[AD-A210283] N90-10787

DOCUMENTATION
Documentation of the current fault detection, isolation and reconfiguration software of the AIPS fault-tolerant processor
[NASA-TM-89154] N90-10602

DOPED CRYSTALS
Effects of coherent scattering on infrared absorption in doped semiconductors
[AD-A210224] N90-10756

DOPPLER EFFECT
Multiline multimode CW chemical laser performance
[AD-A210613] N90-10432

DOPPLER RADAR
A study of the impact of simulated satellite lidar wind observations
[AD-A210430] N90-10488

DRAG
New test techniques to evaluate near field effects for supersonic store carriage and separation N90-10062

DRAG REDUCTION
Control and modification of turbulence N90-10377
Turbulence management: Application aspects N90-10378

DRILLING
Adjustable depth gage
[NASA-CASE-LEW-14880-1] N90-10415

DROPS (LIQUIDS)
Theory of droplet. Part 1: Renormalized laws of droplet vaporization in non-dilute sprays N90-10390

DUCTILITY
Numerical analysis of a class of problems in the mathematical theory of plasticity and damage
[AD-A210731] N90-10655

DUCTS
PMR graphite engine duct development
[NASA-CR-182228] N90-10037
Reheat buzz: An acoustically coupled combustion instability N90-10200
Oscillations in non-axisymmetric dump combustors N90-10205

DUMP COMBUSTORS
Numerical simulation of unsteady combustion in a dump combustor N90-10203
Very-low-frequency oscillations in liquid-fueled ramjets N90-10204
Oscillations in non-axisymmetric dump combustors N90-10205

DYNAMIC CHARACTERISTICS
Prediction of dynamic derivatives N90-10055
Summarizing qualitative behavior from measurements of nonlinear circuits, revision
[AD-A210919] N90-10353
Analysis of spurt phenomena for a non-Newtonian fluid
[AD-A210560] N90-10405
Solvent dynamical effects in electron transfer: Predicted influences of electron coupling upon the rate-dielectric friction dependence
[AD-A210193] N90-10690

DYNAMIC CONTROL
Analysis of flight data from a High-Incidence Research Model by system identification methods
[NASA-TP-2940] N90-10074

DYNAMIC LOADS
Two stage gear tooth dynamics program
[NASA-CR-185110] N90-10437

DYNAMIC RESPONSE
Analysis of spurt phenomena for a non-Newtonian fluid
[AD-A210560] N90-10405
Design guide for predicting nonlinear random response (including snap-through) of buckled plates
[NASA-CR-181877] N90-10681

DYNAMIC STABILITY
Combustor influence on fighter engine operability N90-10193
Dynamic instability characteristics of aircraft turbine engine combustors N90-10195

DYNAMIC STRUCTURAL ANALYSIS
Proceedings of the Workshop on Computational Aspects in the Control of Flexible Systems, part 1
[NASA-TM-101578-PT-1] N90-10080
A finite element approach for large motion dynamic analysis of multibody structures in space N90-10093
Enhanced element-specific modal formulations for flexible multibody dynamics N90-10094
A performance comparison of integration algorithms in simulating flexible structures N90-10101
Proceedings of the Workshop on Computational Aspects in the Control of Flexible Systems, part 2
[NASA-TM-101578-PT-2] N90-10103
Flexible aircraft dynamic modeling for dynamic analysis and control synthesis N90-10112
Experimental validation of flexible robot arm modeling and control N90-10113
Controlling flexible structures: A survey of methods N90-10114

DYNAMIC TESTS
Full scale technology demonstration of a modern counterrotating unducted fan engine concept: Component test
[NASA-CR-180868] N90-10047

DYNAMICAL SYSTEMS
The application of TSIM software to act design and analysis on flexible aircraft N90-10086
DYSCO: A software system for modeling general dynamic systems N90-10089
Explicit modeling and computational load distribution for concurrent processing simulation of the space station N90-10096
Proceedings of the Workshop on Computational Aspects in the Control of Flexible Systems, part 2
[NASA-TM-101578-PT-2] N90-10103
Theoretical investigations of chaotic dynamics
[AD-A207724] N90-10772

E

EARTH CRUST
A search for layering in the oceanic crust
[PB89-198220] N90-10514
Surface wave ray tracing and Ms:yield determination in a laterally heterogeneous earth
[AD-A210241] N90-10516
Institute of Geophysics and Planetary Physics, 1988
[DE89-014363] N90-10794

EARTH IONOSPHERE
The auroral energy deposition over the polar ionosphere during substorms
[AD-A210522] N90-10490
Long-term solar-terrestrial observations
[DE89-016318] N90-10825

EARTH MANTLE
A search for layering in the oceanic crust
[PB89-198220] N90-10514

EARTH ORBITAL ENVIRONMENTS
Orbital debris research at NASA Johnson Space Center, 1986-1988
[NASA-TM-102155] N90-10795

EARTH ORBITS
Laser propulsion to earth orbit. Has its time come? N90-10143
Low-earth-orbit to low-lunar-orbit laser freighter N90-10160
Earth orbit laser systems N90-10162

ECOLOGY
ELF (Extremely Low Frequency) Communications System Ecological Monitoring Program: Electromagnetic field measurements and engineering support, 1988
[AD-A210200] N90-10321

ECONOMIC FACTORS
New energy conversion techniques in space, applicable to propulsion
[AIAA-79-1338] N90-10145

ECOSYSTEMS
ELF (Extremely Low Frequency) Communications System Ecological Monitoring Program: Electromagnetic field measurements and engineering support, 1988
[AD-A210200] N90-10321
Biochemical cycling and fluxes between the deep euphotic zone and other oceanic realms
[PB89-152458] N90-10509
Coastal Research Center Woods Hole Oceanographic Institution
[PB89-198238] N90-10510

EDGES
Computation and parallel implementation for early vision N90-10549
Intensity dependent spread theory N90-10550

EFFICIENCY
Efficiency and capabilities of multi-body simulations N90-10095
On learning from exercises
[AD-A210593] N90-10574

EIGENVALUES
Quotient-difference type generalizations of the power method and their analysis
[NASA-TM-102361] N90-10635

EINSTEIN EQUATIONS
Are there causal vacuum solutions with the symmetries of the Goedel universe in higher-derivative gravity
[DE89-611966] N90-10770

ELASTIC ANISOTROPY
Numerical analysis of a class of problems in the mathematical theory of plasticity and damage
[AD-A210731] N90-10655

ELASTIC BODIES
Simulation and control problems in elastic robots N90-10098

ELASTIC DEFORMATION
Numerical analysis of a class of problems in the mathematical theory of plasticity and damage
[AD-A210731] N90-10655

ELASTIC PROPERTIES
Mechanical states in wound capacitors. Part 1: Prediction
[DE89-008110] N90-10337
Fatigue growth and closure of short cracks
[AD-A210824] N90-10462

ELASTOMERS
Adhesion of encapsulating elastomer to polyolefin sleeve
[BDX-613-3985] N90-10271
Development of elastomeric polypeptide biomaterials
[AD-A210295] N90-10280

ELASTOPLASTICITY
The MHOST finite element program: 3-D inelastic analysis methods for hot section components. Volume 2: User's manual
[NASA-CR-182235-VOL-2] N90-10450
The MHOST finite element program: 3-D inelastic analysis methods for hot section components. Volume 3: Systems' manual
[NASA-CR-182236] N90-10451

ELECTRIC BATTERIES
The use of lithium batteries in biomedical devices
[AD-A210789] N90-10350
The aerospace energy systems laboratory: Hardware and software implementation
[NASA-TM-101706] N90-10610

ELECTRIC COILS
Mechanical states in wound capacitors. Part 1: Prediction
[DE89-008110] N90-10337

ELECTRIC DISCHARGES
Method and apparatus for determining time, direction and composition of impacting space particles
[NASA-CASE-LAR-13392-1-CU] N90-10132

ELECTRIC EQUIPMENT TESTS
Development of an expert system supporting short-circuit tests for circuit breakers
[DE89-760384] N90-10334

ELECTRIC FIELDS
Electrical field dependence of protein conformation and channel function in lipid membranes of different compositions
[AD-A210236] N90-10222
Studies of high power density, pico-second rise-time light activated semiconductor switch
[AD-A210549] N90-10349
Grid generation procedure using the integral equation method
[NAL-TR-1009] N90-10630
Development of the electroacoustic dewatering (EAD) process for fine/ultrafine coal
[DE89-015883] N90-10700
Analysis of the performance of gallium arsenide photoavalanche switches
[DE89-015774] N90-10739

ELECTRIC GENERATORS
Laser-powered lunar base N90-10156

ELECTRIC MOTORS
Composite ceramic superconducting wires for electric motor applications
[AD-A210345] N90-10346

ELECTRIC POTENTIAL
Deep traps and sidegating in GaAs devices
[AD-A210740] N90-10765
ELECTRIC POWER PLANTS
Impact of fundamental technical improvements
[PB89-218010] N90-10472
Stretched-membrane heliostats for solar central-receiver power plants
[DE89-016034] N90-10476
ELECTRIC POWER SUPPLIES
Impact of fundamental technical improvements
[PB89-218010] N90-10472
ELECTRIC SWITCHES
Physics of high energy photoconductive switches
[AD-A210341] N90-10345
Studies of high power density, pico-second rise-time light activated semiconductor switch
[AD-A210549] N90-10349
ELECTRICAL PROPERTIES
Impact of fundamental technical improvements
[PB89-218010] N90-10472
Electroporation: Theory of basic mechanisms
[AD-A210196] N90-10520
Two photon absorption characterization
[AD-A210508] N90-10694
Ceramic processing of bulk high-T(sub c) superconductors
[DE89-015703] N90-10736
Properties of devices prepared with epitaxial layers on InP
[AD-A210304] N90-10759
Advanced GaAs process modeling, volume 1
[AD-A210385] N90-10761
ELECTRO-OPTICS
Stimulated rotational Raman scattering
[DE89-016427] N90-10430
Second-order nonlinear optical devices in poled polymers
[DE89-015842] N90-10703
Use of depletion edge translation for high-speed modulation and switching of lightwaves
[AD-A211166] N90-10713
ELECTROCHEMICAL OXIDATION
Scanning tunneling microscopy etching of micrometer level features on p-type GaAs
[AD-A209216] N90-10328
ELECTROCHEMISTRY
Potential dependence of the elementary steps in the kinetics of electrode reactions involving amalgam formation
[AD-A209424] N90-10212
Combining spontaneous molecular assembly with microfabrication to pattern surfaces: Selective binding of isonitriles to platinum microwires and characterization by electrochemistry and surface spectroscopy
[AD-A209528] N90-10213
Electrochemistry in near-critical and supercritical fluids. Part 7: SO2
[AD-A209207] N90-10214
Polyheterocycle Langmuir-Blodgett films
[AD-A210625] N90-10292
Quartz crystal microbalance studies of electrochemical growth of conducting polymers
[AD-A210788] N90-10295
Advanced double layer capacitor
[AD-A210510] N90-10348
Electroporation: Theory of basic mechanisms
[AD-A210196] N90-10520
Face-specific interaction of MoS4(2-1) with oriented crystals of (0001) CdX (X = Se, S)
[AD-A209519] N90-10732
ELECTRODES
Potential dependence of the elementary steps in the kinetics of electrode reactions involving amalgam formation
[AD-A209424] N90-10212
Combining spontaneous molecular assembly with microfabrication to pattern surfaces: Selective binding of isonitriles to platinum microwires and characterization by electrochemistry and surface spectroscopy
[AD-A209528] N90-10213
ELECTRODYNAMICS
New electrodynamic and electrostatic models with applications to antenna theory, superconductor slots, and lasers N90-10316
ELECTROENCEPHALOGRAPHY
Extrathalamic modulation of cortical function
[AD-A211044] N90-10535
ELECTROLYTIC CELLS
Impedance studies of the cell Pt/Ag+ conducting glass/Ag beta-alumina/Pt
[AD-A209820] N90-10210
ELECTROMAGNETIC ABSORPTION
Two photon absorption characterization
[AD-A210508] N90-10694
ELECTROMAGNETIC FIELDS
Electro-impulse de-icing testing analysis and design
[NASA-CR-4175] N90-10031
On canonical quantization of the electromagnetic field in terms of field strengths
[DE89-015389] N90-10314
ELF (Extremely Low Frequency) Communications System Ecological Monitoring Program: Electromagnetic field measurements and engineering support, 1988
[AD-A210200] N90-10321
ELECTROMAGNETIC MEASUREMENT
The 1984 direct strike lightning data, part 1
[NASA-TM-87690-PT-1] N90-10505
The 1984 direct strike lightning data, part 2
[NASA-TM-87690-PT-2] N90-10506
The 1984 direct strike lightning data, part 3
[NASA-TM-87690-PT-3] N90-10507
ELECTROMAGNETIC NOISE
Quantum 1/F noise in solid state devices in particular Hg1-(sub x)Cd(sub x)Te N(+)-P diodes
[AD-A209365] N90-10730
ELECTROMAGNETIC PULSES
Consumer electronics testing to fast-rise EMP (Electromagnetic Pulse) VEMPS (Vertical Electromagnetic Pulse Simulator) 2 development
[AD-A210505] N90-10323
ELECTROMAGNETIC RADIATION
Maximization of directed electromagnetic radiation with an optimized antenna
[DE89-014045] N90-10319
ELECTROMAGNETIC SCATTERING
Plasma theory and simulation
[AD-A207952] N90-10714
ELECTROMAGNETIC WAVE TRANSMISSION
TWIRE: A test program for VLF airborne transmissions
[AD-A210516] N90-10324
Improved propagation models for discrete random media
[AD-A211085] N90-10327
ELECTRON BEAM WELDING
Characterization of electron-beam weld processes in uranium by acoustic emission monitoring
[DE89-016044] N90-10444
ELECTRON BEAMS
Characterization of electron-beam weld processes in uranium by acoustic emission monitoring
[DE89-016044] N90-10444
Negative-working electron beam resist based on poly(methyl methacrylate)
[AD-A207834] N90-10733
ELECTRON DISTRIBUTION
Physics of high energy photoconductive switches
[AD-A210341] N90-10345
ELECTRON ENERGY
Physics of high energy photoconductive switches
[AD-A210341] N90-10345
ELECTRON MICROSCOPY
Atomic imaging and interfacial analysis
[DE89-015339] N90-10748
Progress report on grain boundaries
[DE89-015541] N90-10749
ELECTRON TRANSFER
NMR evidence for a planar arene intermediate in the electron-transfer induced eta 6 to eta 4 hapticity change of a rhodium arene complex
[AD-A210211] N90-10177
Solvent relaxation in electron-transfer reactions: Comparisons between barrier-crossing dynamics in water and polar aprotic media
[AD-A210212] N90-10220
A structural basis for electron transfer in bacterial photosynthesis
[DE89-015702] N90-10687
Solvent dynamical effects in electron transfer: Predicted influences of electron coupling upon the rate-dielectric friction dependence
[AD-A210193] N90-10690
Solvent effects on intervalence electron-transfer energies for biferrocene cations: Comparisons with molecular models of solvent reorganization
[AD-A210263] N90-10691
Solvent dynamical effects in electron transfer: Evaluation of electronic matrix coupling elements for metallocene self-exchange reactions
[AD-A210306] N90-10692
Controlling photoinduced electron transfer rates in donor-spacer-acceptor molecules by changing the electronic properties of the spacer
[DE89-015128] N90-10735
ELECTRON TUNNELING
Dwell time and average local speed in a resonant tunneling structure
[AD-A210566] N90-10764
ELECTRONIC EQUIPMENT
Electronic encapsulation using foam with bonded metal covers for a filter pack
[DE89-014010] N90-10276
Director, Operational Test and Evaluation report FY-88
[AD-A206784] N90-10778
ELECTRONIC EQUIPMENT TESTS
Consumer electronics testing to fast-rise EMP (Electromagnetic Pulse) VEMPS (Vertical Electromagnetic Pulse Simulator) 2 development
[AD-A210505] N90-10323
ELECTRONIC FILTERS
Electronic encapsulation using foam with bonded metal covers for a filter pack
[DE89-014010] N90-10276
ELECTRONS
Solvent dynamical effects in electron transfer: Predicted influences of electron coupling upon the rate-dielectric friction dependence
[AD-A210193] N90-10690
ELECTROPHYSIOLOGY
Electroporation: Theory of basic mechanisms
[AD-A210196] N90-10520
Extrathalamic modulation of cortical function
[AD-A211044] N90-10535
ELECTROPLATING
Micromechanisms of surface friction in zinc electrogalvanized steel sheets
[DE89-011819] N90-10440
ELECTROSTATICS
Electrostatically suspended rotor for angular encoder
[NASA-CASE-MFS-28294-1] N90-10310
New electrodynamic and electrostatic models with applications to antenna theory, superconductor slots, and lasers N90-10316
ELEVATION ANGLE
Effects of miniature CRT (Cathode Ray Tube) location upon primary and secondary task performances
[AD-A210223] N90-10573
EMERGENCIES
The suitability of diffusion and wind-field techniques for an emergency-response dispersion model
[PB89-190219] N90-10481
EMISSION SPECTRA
X-ray bright points and He I lambda 10830 dark points N90-10802
EMISSIVITY
Total hemispherical emittance measured at high temperatures by the calorimetric method
[NASA-TM-102322] N90-10309
EMITTANCE
Emittance, catalysis, and dynamic oxidation of Ti-14Al-21Nb
[NASA-TP-2955] N90-10248
Total hemispherical emittance measured at high temperatures by the calorimetric method
[NASA-TM-102322] N90-10309
ENCAPSULATING
Electronic encapsulation using foam with bonded metal covers for a filter pack
[DE89-014010] N90-10276
END EFFECTORS
Interchangeable end effector tools utilized on the protoflight manipulator arm
[NASA-CR-179374] N90-10447
END PLATES
Limit analysis of welded tee end connections for hollow tubes
[PB89-191647] N90-10452
ENERGETIC PARTICLES
Particle emission and charging effects induced by fracture
[AD-A210215] N90-10459
ENERGY CONSERVATION
Research on ultra low wear materials for energy conservation
[DE89-015096] N90-10263
ENERGY CONVERSION
Second Beamed Space-Power Workshop
[NASA-CP-3037] N90-10140
Bidirectional power converter control electronics
[NASA-CR-175070] N90-10175
ENERGY CONVERSION EFFICIENCY
High-efficiency CuInSe2 and CuInGaSe2 based cells and materials research
[DE89-009449] N90-10471
ENERGY GAPS (SOLID STATE)
Two photon absorption characterization
[AD-A210508] N90-10694
Optical dispersion relations for diamondlike carbon films
[NASA-TM-102356] N90-10738
ENERGY STORAGE
Capacitive energy storage at cryogenic temperatures, phase 2
[AD-A210366] N90-10347

Energy storage and distribution program summary. Volume 2: Research summaries, fiscal year 1988
[DE89-000867] N90-10470

ENERGY TECHNOLOGY
Gyrotron development for space power beaming N90-10148
History and status of beamed power technology and applications at 2.45 Gigahertz N90-10150

ENERGY TRANSFER
Numerical simulation of detonation transfer between gaseous explosive layers
[MRL-RR-1-89] N90-10395
The auroral energy deposition over the polar ionosphere during substorms
[AD-A210522] N90-10490
Energy dependent transport problem with generalized boundary conditions
[DE89-617843] N90-10676

ENGINE AIRFRAME INTEGRATION
A supersonic through-flow fan engine airframe integration study
[NASA-CR-185140] N90-10004

ENGINE CONTROL
Full scale technology demonstration of a modern counterrotating unducted fan engine concept. Engine test
[NASA-CR-180869] N90-10049

ENGINE DESIGN
A supersonic through-flow fan engine airframe integration study
[NASA-CR-185140] N90-10004
Performance potential of an advanced technology Mach 3 turbojet engine installed on a conceptual high-speed civil transport
[NASA-TM-4144] N90-10034
Advanced Turbine Technology Applications Project (ATTAP)
[NASA-CR-185133] N90-10036
Large-scale Advanced Prop-fan (LAP) technology assessment report
[NASA-CR-182142] N90-10046
Full scale technology demonstration of a modern counterrotating unducted fan engine concept. Design report
[NASA-CR-180867] N90-10048
Revolutionary opportunities for materials and structures study
[NASA-CR-179642] N90-10184
Combustor influence on fighter engine operability N90-10193
Effects of low-frequency instabilities on the operation of Ramjet air inlets N90-10198

ENGINE FAILURE
Report on an overseas visit, June 1988
[AD-A210374] N90-10040
X-ray spectroscopy of the SSME plume
[NASA-CR-185308] N90-10168

ENGINE MONITORING INSTRUMENTS
X-ray spectroscopy of the SSME plume
[NASA-CR-185308] N90-10168

ENGINE PARTS
Full scale technology demonstration of a modern counterrotating unducted fan engine concept: Component test
[NASA-CR-180868] N90-10047
Materials for engine applications above 3000 deg F: An overview
[NASA-TM-100169] N90-10188
Improved silicon carbide for advanced heat engines
[NASA-CR-180831] N90-10293

ENGINE TESTS
Performance potential of an advanced technology Mach 3 turbojet engine installed on a conceptual high-speed civil transport
[NASA-TM-4144] N90-10034
Full scale technology demonstration of a modern counterrotating unducted fan engine concept: Component test
[NASA-CR-180868] N90-10047
Full scale technology demonstration of a modern counterrotating unducted fan engine concept. Engine test
[NASA-CR-180869] N90-10049

ENVIRONMENT POLLUTION
Organic explosives and related compounds. Environmental and health considerations
[AD-A210554] N90-10306

ENVIRONMENTAL CHEMISTRY
Characterization and evaluation of acid rain in East Central Florida from 1978 to 1987: Ten year summary report
[NASA-TM-102149] N90-10478

ENVIRONMENTAL MONITORING
Meeting Review: Workshop on Airborne Instrumentation
[PB89-174775] N90-10032
ELF (Extremely Low Frequency) Communications System Ecological Monitoring Program: Electromagnetic field measurements and engineering support, 1988
[AD-A210200] N90-10321
Characterization and evaluation of acid rain in East Central Florida from 1978 to 1987: Ten year summary report
[NASA-TM-102149] N90-10478
Spatial characterization of acid rain stress in Canadian Shield Lakes
[NASA-CR-183446] N90-10479
Geophysical monitoring for climatic change number 16
[PB89-159628] N90-10494

EPITAXY
Epitaxial GaAs on SOI wafers
[AD-A209009] N90-10729
Methods to decrease defect density in GaAs/Si heteroepitaxy
[DE89-016306] N90-10753
Properties of devices prepared with epitaxial layers on InP
[AD-A210304] N90-10759

EQUATIONS OF MOTION
Two-phase potential flow N90-10387
The architecture of NEWTON: A general-purpose dynamics simulator
[NASA-CR-185489] N90-10678
Tangent map analysis of the beam-beam interaction
[DE89-015857] N90-10689

EQUATIONS OF STATE
Analysis of a model and sequential numerical method for thermal reservoir simulation
[DE89-015117] N90-10384

ERGODIC PROCESS
Radon transform analysis of a probabilistic method for image generation
[AD-A207814] N90-10702

ERROR ANALYSIS
Phase 2 testing and evaluation of low data rate voice CODEC equipment
[ACD-330-PHASE-2] N90-10315
Inherent bias in nonlinear least squares analysis of first-order kinetic data
[AD-A210677] N90-10651
The computation and use of the asymptotic covariance matrix for measurement error models
[PB89-215321] N90-10659
Research in mathematics and computer science: Calculation of the probability of undetected error for certain error detection codes, phase 1
[AD-A210302] N90-10664

ERROR CORRECTING CODES
Multi-level bandwidth efficient block modulation codes
[NASA-CR-185484] N90-10317

ERROR DETECTION CODES
Research in mathematics and computer science: Calculation of the probability of undetected error for certain error detection codes, phase 1
[AD-A210302] N90-10664

ERRORS
Optimal q-Markov COVER for finite precision implementation N90-10117
Dependency-directed localization of software bugs
[AD-A210837] N90-10606

ESTIMATES
Minimum-variance reduced-order estimation algorithms from Pontrygin's minimum principle N90-10105
A unified view of infinitesimal perturbation analysis and likelihood ratios
[AD-A210682] N90-10652
Studies in estimation theory, applications and implementations
[AD-A210712] N90-10653

ESTIMATING
Improved estimation of the disturbance variance in a linear regression model
[AD-A210272] N90-10641
Studies in estimation theory, applications and implementations
[AD-A210712] N90-10653

ETCHING
Scanning tunneling microscopy etching of micrometer level features on p-type GaAs
[AD-A209216] N90-10328
Characterization of 4/3 technology large-scale integrated circuit on polysilicon processes
[BDX-613-3971] N90-10335
Custom diffraction gratings
[AD-A211002] N90-10712

ETHYLENE OXIDE
Synthesis and physical properties of poly(perfluoroalkylether) urethanes
[AD-A210500] N90-10287

EUCLIDEAN GEOMETRY
On the expected complexity of the three-dimensional Voronoi diagram
[PB89-209332] N90-10636

EULER EQUATIONS OF MOTION
Supersonic flow computations over aerospace configurations using an Euler marching solver
[NASA-CR-4085] N90-10012
Remote control missile model test N90-10063

EVALUATION
Director, Operational Test and Evaluation report FY-88
[AD-A206784] N90-10778

EVENTS
Computational and statistical issues in discrete-event simulation
[AD-A210743] N90-10668

EXCITONS
Femtosecond dynamics of fluoro-aluminum phthalocyanine and linear alkane molecules
[AD-A210939] N90-10766

EXOBIOLOGY
Aerospace medicine and biology: A continuing bibliography with indexes (supplement 328)
[NASA-SP-7011(328)] N90-10524

EXPERT SYSTEMS
Hierarchical damage tolerant controllers for smart structures
[AD-A209422] N90-10022
Validation of missile simulation N90-10066
Real-time support for high performance aircraft operation
[NASA-CR-185475] N90-10075
Knowledge-based machine vision systems for space station automation
[NASA-CR-185710] N90-10124
A rocket engine design expert system
[NASA-TM-102373] N90-10172
Development of an expert system supporting short-circuit tests for circuit breakers
[DE89-760384] N90-10334
An expert system for optimal gear design N90-10439
Photonic processing at NASA Ames Research Center N90-10560
Advancing automation and robotics technology for the space station Freedom and for the US economy
[NASA-TM-101561] N90-10577
Cost metric algorithms for internetwork applications
[AD-A210324] N90-10597
The applicability and limitations of expert system shells
[AD-A210801] N90-10625
The development of an expert system for the creative design of mechanisms
[AD-A211115] N90-10628
An analytical hierarchy process approach to establish the systems analyst's knowledge base for selecting an information requirements determination strategy N90-10785

EXPLOSIONS
Remarks on certain aspects of solid explosive detonation via small projectile impact
[AD-A210648] N90-10307
Shock behavior of explosives about the C-J (Chapman-Juget) point
[DE89-007642] N90-10400

EXPLOSIVES
Effects of binder concentration on the properties of plastic-bonded explosives
[DE89-007744] N90-10301
Free-expansion experiments and modeling in detonation: Chemistry and hydrodynamics on a laboratory scale
[DE89-007748] N90-10302
Organic explosives and related compounds. Environmental and health considerations
[AD-A210554] N90-10306
Shock behavior of explosives about the C-J (Chapman-Juget) point
[DE89-007642] N90-10400
Laser initiation of secondary explosives
[DE89-010229] N90-10431

EXPONENTIAL FUNCTIONS
Inherent bias in nonlinear least squares analysis of first-order kinetic data
[AD-A210677] N90-10651

EXPOSURE
Method and apparatus for maintaining thermal control in plasma conditions
[NASA-CASE-MFS-28368-1] N90-10717

EXTERNAL STORE SEPARATION
New test techniques to evaluate near field effects for supersonic store carriage and separation N90-10062
Marginal release disturbances on advanced missiles N90-10070

EXTERNAL STORES
Computation of transonic flow about stores
[AD-A210402] N90-10009
EXTERNAL SURFACE CURRENTS
The 1984 direct strike lightning data, part 1
[NASA-TM-87690-PT-1] N90-10505
EXTRAPOLATION
Approximate simulation model for analysis and optimization in engineering system design
[NASA-TM-101616] N90-10308
EXTRAVEHICULAR ACTIVITY
Vision science and technology for supervised intelligent space robots N90-10548
EXTREMELY HIGH FREQUENCIES
Effects of rain attenuation on satellite EHF (Extremely High Frequency) communications in the US
[AD-A210517] N90-10325
EXTREMELY LOW FREQUENCIES
ELF (Extremely Low Frequency) Communications System Ecological Monitoring Program: Electromagnetic field measurements and engineering support, 1988
[AD-A210200] N90-10321
EYE (ANATOMY)
Sampling and noise in vision networks N90-10544
EYE MOVEMENTS
Effects of miniature CRT (Cathode Ray Tube) location upon primary and secondary task performances
[AD-A210223] N90-10573
EYE PROTECTION
Eye/sensor protection against laser irradiation organic nonlinear optical materials
[AD-A210599] N90-10531

F

F-18 AIRCRAFT
Definition and reduction of the F-18 windshield birdstrike hazard
[AD-A210700] N90-10015
FABRICATION
PMR graphite engine duct development
[NASA-CR-182228] N90-10037
The effects of normal annealing cycles during IGFET fabrication on initial and radiation induced gate insulator defects
[AD-A210282] N90-10278
Preparation and evaluation of composite membranes for zinc/bromine storage batteries
[DE89-009931] N90-10339
Thin film thermocouples for high temperature measurement
[PB89-209290] N90-10420
High-efficiency CuInSe2 and CuInGaSe2 based cells and materials research
[DE89-009449] N90-10471
Alternative fabrication techniques for high-efficiency CuInSe2 and CuInSe2-alloy films and cells
[DE89-009451] N90-10474
Second-order nonlinear optical devices in poled polymers
[DE89-015842] N90-10703
Ceramic processing of bulk high-T(sub c) superconductors
[DE89-015703] N90-10736
FABRICS
The interlaminar fracture toughness of woven graphite/epoxy composites
[NASA-TP-2950] N90-10179
Thermoregulatory responses to intermittent exercise are influenced by knit structure of underwear
[AD-A209087] N90-10541
FABRY-PEROT INTERFEROMETERS
Use of depletion edge translation for high-speed modulation and switching of lightwaves
[AD-A211186] N90-10713
FAILURE
Optimal integral controller with sensor failure accommodation N90-10123
Failure behavior of PEEK and its short-fiber composite systems
[AD-A210729] N90-10189
Delayed failure of silver-aided diffusion welds between steel
[DE89-016652] N90-10252
Limit analysis of welded tee end connections for hollow tubes
[PB89-191647] N90-10452
FAST FOURIER TRANSFORMATIONS
A combined finite element and boundary integral formulation for solution via CGFFT of 2-dimensional scattering problems
[NASA-CR-184781] N90-10313
FATIGUE (BIOLOGY)
Human performance in continuous/sustained operations and the demands of extended work/rest schedules: An annotated bibliography, volume 2
[AD-A210504] N90-10530
FATIGUE (MATERIALS)
A review of Australian and New Zealand investigations on aeronautical fatigue during the period April 1987 to March 1989
[AD-A210373] N90-10026
Evaluation of titanium castings for aerospace components N90-10237
Limit analysis of welded tee end connections for hollow tubes
[PB89-191647] N90-10452
Porosity and crack initiation during low cycle fatigue
[AD-A210989] N90-10464
FATIGUE LIFE
A review of Australian and New Zealand investigations on aeronautical fatigue during the period April 1987 to March 1989
[AD-A210373] N90-10026
Porosity and crack initiation during low cycle fatigue
[AD-A210989] N90-10464
FAULT TOLERANCE
Development of pressure containment and damage tolerance technology for composite fuselage structures in large transport aircraft
[NASA-CR-3996] N90-10186
Documentation of the current fault detection, isolation and reconfiguration software of the AIPS fault-tolerant processor
[NASA-TM-89154] N90-10602
FEASIBILITY ANALYSIS
A feasibility assessment of installation, operation and disposal options for nuclear reactor power system concepts for a NASA growth space station
[NASA-TM-89823] N90-10174
FEEDBACK CONTROL
Structural stability augmentation system design using BODEDIRECT: A quick and accurate approach N90-10116
Modeling and stabilization of large flexible space stations N90-10120
Optimal integral controller with sensor failure accommodation N90-10123
A simple, mass balance model of carbon flow in a controlled ecological life support system
[NASA-TM-102151] N90-10571
FEEDERS
Plasma gun with coaxial powder feed and adjustable cathode
[NASA-CASE-LEW-14901-1] N90-10718
FERMIONS
Mixed-valent and heavy fermions and related systems
[DE89-016335] N90-10743
Quantization of anomalous gauge theories on a lattice
[DE89-010247] N90-10776
Lattice fields and strong interactions
[DE89-015099] N90-10777
FERROCENES
Solvent relaxation in electron-transfer reactions: Comparisons between barrier-crossing dynamics in water and polar aprotic media
[AD-A210212] N90-10220
Solvent effects on intervalence electron-transfer energies for biferrocene cations: Comparisons with molecular models of solvent reorganization
[AD-A210263] N90-10691
FIBER COMPOSITES
Space structures concepts and materials
[NASA-CR-183727] N90-10128
Mechanics of damping for fiber composite laminates including hygro-thermal effects
[NASA-TM-102329] N90-10185
Failure behavior of PEEK and its short-fiber composite systems
[AD-A210729] N90-10189
Field repair of composite materials in Army service: Planning for the future
[AD-A210732] N90-10190
Zirconia toughened SiC whisker reinforced alumina composites small business innovation research
[NASA-CR-179629] N90-10294
FIBER OPTICS
Multimode fiber interferometry and several-mode fiber polarimetry via phase conjugation
[DE89-014226] N90-10706
Automation of fiber-optic pigtailing process: Laser welding demonstration program
[AD-A210351] N90-10707
FIELD EFFECT TRANSISTORS
Vacuum microelectronics for beam power and rectennas N90-10146
The effects of normal annealing cycles during IGFET fabrication on initial and radiation induced gate insulator defects
[AD-A210282] N90-10278
Epitaxial GaAs on SOI wafers
[AD-A209009] N90-10729
Advanced GaAs process modeling, volume 1
[AD-A210385] N90-10761
FIELD EMISSION
Micro-cavity integrable vacuum diodes and triodes
[DE89-016649] N90-10344
FIELD STRENGTH
On canonical quantization of the electromagnetic field in terms of field strengths
[DE89-615389] N90-10314
FIELD THEORY (PHYSICS)
A theoretical high energy physics program
[DE89-012685] N90-10696
FIGHTER AIRCRAFT
Wind tunnel support system effects on a fighter aircraft model at Mach numbers from 0.6 to 2.0
[AD-A210614] N90-10010
FILE MAINTENANCE (COMPUTERS)
Initial flight qualification and operational maintenance of X-29A flight software
[NASA-TM-101703] N90-10023
FILTRATION
Properties of F-34 (JP-8) fuel for 1988
[AD-A210188] N90-10303
FINITE DIFFERENCE THEORY
Numerically determined transition in separated internal flow N90-10374
Numerical simulation of turbulent plane channel flows N90-10382
Numerical simulation of coherent structures in an incompressible mixing layer N90-10383
IFD (Implicit Finite Difference): Interfaced with Harvard open ocean model forecasts
[AD-A210521] N90-10517
Tests of various finite difference algorithms applied to a simple water vapor transport problem on a staggered grid
[AD-A210229] N90-10596
FINITE ELEMENT METHOD
Aeroelastic tailoring procedure for controlling fin hinge moments N90-10058
A finite element approach for large motion dynamic analysis of multibody structures in space N90-10093
Enhanced element-specific modal formulations for flexible multibody dynamics N90-10094
Combustion-driven oscillation in large combustion systems for power generation N90-10207
A combined finite element and boundary integral formulation for solution via CGFFT of 2-dimensional scattering problems
[NASA-CR-184781] N90-10313
Iterative performance and an adaptive procedure for viscous flow problems N90-10397
The MHOST finite element program: 3-D inelastic analysis methods for hot section components. Volume 2: User's manual
[NASA-CR-182235-VOL-2] N90-10450
The MHOST finite element program: 3-D inelastic analysis methods for hot section components. Volume 3: Systems' manual
[NASA-CR-182236] N90-10451
Analysis and test of a 16-foot radial rib reflector developmental model
[NASA-TM-101648] N90-10457
BLOT: A mesh and curve plot program for the output of a finite element analysis
[DE89-013994] N90-10590
FINITE VOLUME METHOD
Numerical solution of three-dimensional unsteady flows: Application to instability problems N90-10375
FINS
Aeroelastic tailoring procedure for controlling fin hinge moments N90-10058
Remote control missile model test N90-10063
FIRE DAMAGE
Upward flame spread on vertical walls
[PB89-214787] N90-10217
FLAME PROPAGATION
Upward flame spread on vertical walls
[PB89-214787] N90-10217
FLAT PLATES
Numerical investigation of the effects of longitudinal vortices on the onset of transition in a flat plate boundary layer N90-10363
Experimental study of instability modes in a three-dimensional boundary layer N90-10369
Primary and secondary stability analysis applied to the DFVLR-transition swept-plate experiment N90-10371
Numerical investigation of transition in 3D boundary layers N90-10372

Design guide for predicting nonlinear random response (including snap-through) of buckled plates
[NASA-CR-181877] N90-10661

FLEXIBLE BODIES
The application of TSIM software to act design and analysis on flexible aircraft N90-10086
Modeling and control system design and analysis tools for flexible structures N90-10090
Lumped mass formulations for modeling flexible body systems N90-10091
Simulation of flexible structures with impact: Experimental validation N90-10097
Linearized flexibility models in multibody dynamics and control N90-10099
A performance comparison of integration algorithms in simulating flexible structures N90-10101
Flexible robot control: Modeling and experiments N90-10104
Automated model formulation for time-varying flexible structures N90-10107
Flexible aircraft dynamic modeling for dynamic analysis and control synthesis N90-10112
Experimental validation of flexible robot arm modeling and control N90-10113
Controlling flexible structures: A survey of methods N90-10114
Aircraft modal supression system: Existing design approach and its shortcomings N90-10115
Structural stability augmentation system design using BODEDIRECT: A quick and accurate approach N90-10116
Active vibration mitigation of distributed parameter, smart-type structures using Pseudo-Feedback Optimal Control (PFOC) N90-10121
A new approach to control single-link flexible arms. Part 1: Modelling and identification in the presence of joint friction
[AD-A210590] N90-10445

FLEXIBLE SPACECRAFT
Proceedings of the Workshop on Computational Aspects in the Control of Flexible Systems, part 1
[NASA-TM-101578-PT-1] N90-10080
Additional software developments wanted for modeling and control of flexible space systems N90-10083
Flexible structure control experiments using a real-time workstation for computer-aided control engineering N90-10084
A comparison of software for the modeling and control of flexible systems N90-10092
Enhanced element-specific modal formulations for flexible multibody dynamics N90-10094
Explicit modeling and computational load distribution for concurrent processing simulation of the space station N90-10096
Optical processing for distributed sensors in control of flexible spacecraft N90-10102
Proceedings of the Workshop on Computational Aspects in the Control of Flexible Systems, part 2
[NASA-TM-101578-PT-2] N90-10103
Control law synthesis and optimization software for large order aeroservoelastic systems N90-10111
Input-output oriented computation algorithms for the control of large flexible structures N90-10118
Modeling and stabilization of large flexible space stations N90-10120

FLEXIBLE WINGS
The active flexible wing aeroservoelastic wind-tunnel test program N90-10119

FLIGHT CHARACTERISTICS
Airworthiness and flight characteristics test of the UH-60A Black Hawk helicopter equipped with the XM-139 multiple mine dispensing system (VOLCANO)
[AD-A210271] N90-10025
Analysis of flight data from a High-Incidence Research Model by system identification methods
[NASA-TP-2940] N90-10074

FLIGHT CONTROL
Hierarchical damage tolerant controllers for smart structures
[AD-A209422] N90-10022
Initial flight qualification and operational maintenance of X-29A flight software
[NASA-TM-101703] N90-10023
Simulation of shuttle flight control system structural interaction with RMS deployed payloads N90-10100

FLIGHT MECHANICS
Validation of missile simulation N90-10066

FLIGHT SAFETY
Safer skies with TCAS: Traffic Alert and Collision Avoidance System
[PB89-169221] N90-10016

FLIGHT SIMULATION
Stability and Control of Tactical Missile Systems
[AGARD-CP-451] N90-10050

FLIGHT STABILITY TESTS
Airworthiness and flight characteristics test of the UH-60A Black Hawk helicopter equipped with the XM-139 multiple mine dispensing system (VOLCANO)
[AD-A210271] N90-10025

FLIGHT TEST VEHICLES
Development of a flight test methodology for a US Navy half-scale unmanned air vehicle
[AD-A210563] N90-10029

FLIGHT TESTS
ILS/MLS comparison tests at Miami/Tamiami, Florida Airport
[ACD-330] N90-10018
Development of a flight test methodology for a US Navy half-scale unmanned air vehicle
[AD-A210563] N90-10029
Electro-impulse de-icing testing analysis and design
[NASA-CR-4175] N90-10031
Identification of stability and control parameters of a brilliant ammunition N90-10065
Marginal release disturbances on advanced missiles N90-10070
Experience gained in the improvement of the Aspide aerodynamic configuration for the surface to air role N90-10072
On the interactive computer program IPIS for aircraft parameter identification
[NAL-TR-1000] N90-10586
Measurement resolution of noise directivity patterns from acoustic flight tests
[NASA-TM-4134] N90-10679

FLOOD DAMAGE
Extreme hurricanes in the nineteenth century
[PB89-201305] N90-10498

FLOW CHARTS
Structure flow diagram generator
[PB89-195978] N90-10592

FLOW DISTRIBUTION
A numerical method for solving transonic flow past aircraft in Cartesian coordinates
[NAL-TR-1008] N90-10003
Computation of transonic flow about stores
[AD-A210402] N90-10009
The present status and the future of missile aerodynamics N90-10051
Boost-phase discrimination research activities
[NASA-TM-101889] N90-10176
Experimental investigation of attachment-line transition in low-speed, high-lift wind-tunnel testing N90-10358
Stability of a supersonic boundary layer along a swept leading edge N90-10359
Curvature effects on the stability of three-dimensional laminar boundary layers N90-10366
Experimental study of instability modes in a three-dimensional boundary layer N90-10369
A composite velocity procedure for the three-dimensional reduced Navier-Stokes equations N90-10396
Laminar boundary layer along inviscid surface streamlines over inclined axisymmetric bodies in incompressible flow
[AD-A210202] N90-10401
Studies in penetration mechanics
[AD-A210713] N90-10448
Numerical simulation of the compressible Orszag-Tang vortex
[AD-A210465] N90-10725

FLOW EQUATIONS
Boost-phase discrimination research activities
[NASA-TM-101889] N90-10176

FLOW GEOMETRY
A composite velocity procedure for the three-dimensional reduced Navier-Stokes equations N90-10396

FLOW MEASUREMENT
Wide-range fuel flowmeter, phase 2
[AD-A210547] N90-10424

FLOW STABILITY
Recent developments in Ramjet pressure oscillation technology N90-10199
Numerical solution of three-dimensional unsteady flows: Application to instability problems N90-10375
Wide-range fuel flowmeter, phase 2
[AD-A210547] N90-10424

FLOW THEORY
Two-phase potential flow N90-10387

FLOW VELOCITY
The role of particle collisions in pneumatic transport N90-10392
A composite velocity procedure for the three-dimensional reduced Navier-Stokes equations N90-10396
Capillary effects in steady-state flow in heterogeneous cores
[DE89-000758] N90-10399
Wide-range fuel flowmeter, phase 2
[AD-A210547] N90-10424

FLOWMETERS
Wide-range fuel flowmeter, phase 2
[AD-A210547] N90-10424

FLUID BOUNDARIES
Numerical calculations of the collapse of a cavity in the vicinity of a compliant wall
[AD-A210489] N90-10403

FLUID FLOW
Analysis of a model and sequential numerical method for thermal reservoir simulation
[DE89-015117] N90-10384
PORFLO-3: A mathematical model for fluid flow, heat, and mass transport in variably saturated geologic media: Users manual, version 1.0
[DE89-013977] N90-10398

FLUID-SOLID INTERACTIONS
Interpretation and modeling of the averaged equations for a fluid-solid flow N90-10388

FLUORESCENCE
Advances in regression: Use of models in spectroscopic data analysis
[AD-A210541] N90-10665

FLUORINE COMPOUNDS
Femtosecond dynamics of fluoro-aluminum phthalocyanine and linear alkane molecules
[AD-A210939] N90-10766

FLYBY MISSIONS
NASA Voyager 2 Neptune encounter press kit
[NASA-TM-101851] N90-10076

FOCAL PLANE DEVICES
Laterally stacked Schottky diodes for infrared sensor applications
[NASA-CASE-NPO-17426-1-CU] N90-10329
Parallel asynchronous hardware implementation of image processing algorithms N90-10546

FOCUSING
Millimeter-wave/infrared rectenna development at Georgia Tech N90-10147

FOILS (MATERIALS)
Observation of excited H(sup 0) atoms produced by relativistic H(sup (minus)) ions in carbon and formvar foils
[DE89-015301] N90-10688

FORECASTING
IFD (Implicit Finite Difference): Interfaced with Harvard open ocean model forecasts
[AD-A210521] N90-10517

FORMAT
Robotic vehicle message format
[AD-A210996] N90-10627

FORMATES
MHD seed recovery and regeneration
[DE89-002711] N90-10715

FORMING TECHNIQUES
Application of superplastically formed and diffusion bonded aluminum to a laminar flow control leading edge
[NASA-CR-178316] N90-10030

FOURIER TRANSFORMATION
An algorithm to calculate the beam momentum distribution from flying wire profiles
[DE89-015587] N90-10418

FRACTALS
The quantitative analysis of fracture surfaces using fractals
[DE89-015361] N90-10250
An introduction to fractals and chaos
[AD-A210257] N90-10675

FRACTOGRAPHY
The quantitative analysis of fracture surfaces using fractals
[DE89-015361] N90-10250
Ceramic components in machines, Cologne and Aachen, West Germany; Maastricht, The Netherlands and Brussels, Belgium
[DE89-015831] N90-10264

FRACTURE MECHANICS
Failure behavior of PEEK and its short-fiber composite systems
[AD-A210729] N90-10189
Influence of microstructure and microdamage processes on fracture at high loading rates
[AD-A210307] N90-10253
Mechanics of the crack path formation
[NASA-CR-185143] N90-10455
Particle emission and charging effects induced by fracture
[AD-A210215] N90-10459
Fatigue growth and closure of short cracks
[AD-A210824] N90-10462

FRACTURE STRENGTH
The interlaminar fracture toughness of woven graphite/epoxy composites
[NASA-TP-2950] N90-10179

Influence of microstructure and microdamage processes on fracture at high loading rates
[AD-A210307] N90-10253
Mechanisms of strength and toughness in a microalloyed, precipitation hardened steel
[AD-A210571] N90-10256
Stress intensity factors and displacements for arc bend samples using collocation
[AD-A210404] N90-10460

FRACTURES (MATERIALS)
Fracture and three dimensional stress analyses of 7075 aluminum projectile components under spin and inertia load
[AD-A210986] N90-10463

FRACTURING
The quantitative analysis of fracture surfaces using fractals
[DE89-015361] N90-10250

FREE ELECTRON LASERS
Technical options for high average power free electron milimeter-wave and laser devices N90-10151
Laser energy conversion N90-10152
Shortwavelength coherent radiation: Generation and applications
[AD-A209847] N90-10427
Biomedical studies with the free electron laser
[AD-A208927] N90-10519

FREE FLOW
Direct numerical simulation of turbulent free shear flows
[AD-A210161] N90-10218

FREEZE DRYING
Processing and fabrication of high temperature oxide superconductors
[AD-A210197] N90-10755

FREQUENCY CONTROL
Efficient nonlinear conversion of laser diode pumped miniature solid state laser sources
[AD-A210706] N90-10433

FREQUENCY RESPONSE
Numerically efficient algorithm for model development of high-order systems N90-10108

FRICTION
Friction and wear of oxide-ceramic sliding against IN-718 nickel base alloy at 25 to 800 C in atmospheric air
[NASA-TM-102291] N90-10262
Research on ultra low wear materials for energy conservation
[DE89-015096] N90-10263
Micromechanisms of surface friction in zinc electrogalvanized steel sheets
[DE89-011819] N90-10440
A new approach to control single-link flexible arms. Part 1: Modelling and identification in the presence of joint friction
[AD-A210590] N90-10445
Solvent dynamical effects in electron transfer: Predicted influences of electron coupling upon the rate-dielectric friction dependence
[AD-A210193] N90-10690
Morphological aspects of the friction of hot-filament-grown diamond thin films
[DE89-015986] N90-10750
The effect of twins on critical currents of high Tc superconductors
[AD-A210988] N90-10768

FRICTION DRAG
Control and modification of turbulence N90-10377
Turbulence management: Application aspects N90-10378

FROST
Debris/ice/TPS assessment and photographic analysis for Shuttle Mission STS-28R
[NASA-TM-102152] N90-10079

FUEL COMBUSTION
Revolutionary opportunities for materials and structures study
[NASA-CR-179642] N90-10184
High energy density solid and liquid hydrocarbon fuels
[AD-A210195] N90-10304

FUEL INJECTION
Experimental study on the stability of small rocket engines with storable liquid propellants N90-10196
Numerical simulation of unsteady combustion in a dump combustor N90-10203
Oscillations in non-axisymmetric dump combustors N90-10205

FUEL PUMPS
Compatibility of fuel system components with high density fuel
[AD-A210381] N90-10027
SSME Alternate Turbopump Development Program: Design verification specification for high-pressure fuel turbopump
[NASA-CR-183676] N90-10033

FUEL SPRAYS
Theory of droplet. Part 1: Renormalized laws of droplet vaporization in non-dilute sprays N90-10390

FUEL SYSTEMS
Compatibility of fuel system components with high density fuel
[AD-A210381] N90-10027

FUEL-AIR RATIO
Very-low-frequency oscillations in liquid-fueled ramjets N90-10204

FUNCTIONAL ANALYSIS
Discrete-time conversion for simulating finite-horizon Markov processes
[AD-A210683] N90-10666

FUNCTIONAL DESIGN SPECIFICATIONS
The development of an expert system for the creative design of mechanisms
[AD-A211115] N90-10628

FUNCTIONS (MATHEMATICS)
An introduction to fractals and chaos
[AD-A210257] N90-10675

FUSELAGES
Development of pressure containment and damage tolerance technology for composite fuselage structures in large transport aircraft
[NASA-CR-3996] N90-10186

G

GALACTIC EVOLUTION
Research program in theoretical high energy physics
[DE89-013963] N90-10695
The origin of the universe from quantum chaos: An introduction to current ideas
[AD-A210441] N90-10813

GALLIUM ARSENIDES
Scanning tunneling microscopy etching of micrometer level features on p-type GaAs
[AD-A209216] N90-10328
Epitaxial GaAs on SOI wafers
[AD-A209009] N90-10729
Analysis of the performance of gallium arsenide photoavalanche switches
[DE89-015774] N90-10739
Lithium compensation of GaAs
[DE89-616080] N90-10740
Characterization of GaAs/Si/GaAs heterointerfaces
[DE89-016302] N90-10752
Methods to decrease defect density in GaAs/Si heteroepitaxy
[DE89-016306] N90-10753
Effects of coherent scattering on infrared absorption in doped semiconductors
[AD-A210224] N90-10756
Advanced GaAs process modeling, volume 1
[AD-A210385] N90-10761
High energy neutron irradiation effects in GaAs modulation-Doped Field Effect Transistors (MODFETS): Threshold voltage
[AD-A210502] N90-10763
Deep traps and sidegating in GaAs devices
[AD-A210740] N90-10765
Trap gettering by isoelectronic doping of p-GaAs and n-GaAs grown by molecular beam epitaxy
[AD-A211162] N90-10769

GALLIUM NITRIDES
The growth of gallium nitride films via the innovative technique of atomic layer epitaxy
[AD-A210380] N90-10760

GAMMA RAY ASTRONOMY
Studies of elementary particles
[DE89-014859] N90-10685

GAMMA RAYS
Raman spectroscopic study of the rare earth sesquisulfides
[AD-A210610] N90-10226

GAS EXPLOSIONS
Numerical simulation of detonation transfer between gaseous explosive layers
[MRL-RR-1-89] N90-10395

GAS FLOW
Supersonic flow computations over aerospace configurations using an Euler marching solver
[NASA-CR-4085] N90-10012
The role of particle collisions in pneumatic transport N90-10392

GAS TURBINE ENGINES
Performance potential of an advanced technology Mach 3 turbojet engine installed on a conceptual high-speed civil transport
[NASA-TM-4144] N90-10034
Advanced Turbine Technology Applications Project (ATTAP)
[NASA-CR-185133] N90-10036
Report on an overseas visit, June 1988
[AD-A210374] N90-10040
Combustor influence on fighter engine operability N90-10193
The MHOST finite element program: 3-D inelastic analysis methods for hot section components. Volume 3: Systems' manual
[NASA-CR-182236] N90-10451

GAS TURBINES
Laser energy conversion N90-10152
Improved silicon carbide for advanced heat engines
[NASA-CR-180831] N90-10293

GAS-SOLID INTERACTIONS
The structure determination of molecular adsorbates with large unit cells or lattice-gas disorder on metal surfaces
[AD-A210926] N90-10230
The role of particle collisions in pneumatic transport N90-10392
Scaling and modeling of turbulent suspension flows N90-10393

GASEOUS ROCKET PROPELLANTS
Low frequency and high frequency combustion oscillation phenomena inside a rocket combustion chamber fed by liquid or gaseous propellants N90-10197

GASES
Boost-phase discrimination research activities
[NASA-TM-101889] N90-10176

GATES (CIRCUITS)
The effects of normal annealing cycles during IGFET fabrication on initial and radiation induced gate insulator defects
[AD-A210282] N90-10278
DDN Trusted Guard Gateway: Trusted Guard Gateway (TGG) technology assessment, phase 2
[AD-A210248] N90-10614
Bias and oxide thickness dependence of trapped charge buildup in MOS devices
[AD-A210264] N90-10757

GAUGE INVARIANCE
D=3 Chern-Simons action, supergravity and quantization
[DE89-617530] N90-10775

GAUGE THEORY
Quantization of anomalous gauge theories on a lattice
[DE89-010247] N90-10776
Lattice fields and strong interactions
[DE89-015099] N90-10777
Homogeneous gravitational fields and limits of gravitational fields N90-10812

GEAR TEETH
Two stage gear tooth dynamics program
[NASA-CR-185110] N90-10437

GEARS
An expert system for optimal gear design N90-10439

GENETIC ENGINEERING
Genetic engineering of single-domain magnetic particles
[AD-A210332] N90-10521
Molecular biology and physiology of methanogenic archaebacteria
[AD-A210399] N90-10522

GENETICS
Molecular biology and physiology of methanogenic archaebacteria
[AD-A210399] N90-10522

GEOCHEMISTRY
Institute of Geophysics and Planetary Physics, 1988
[DE89-014363] N90-10794

GEOCHRONOLOGY
Fluctuation history of Great Salt Lake, Utah, during the last 13,000 years, part 2
[NASA-CR-185911] N90-10466

GEOLOGY
National register of research projects, 1986/87. Part 2B: Natural sciences: Physical, engineering and related sciences (new projects)
[DE89-015033] N90-10826

GEOMETRICAL OPTICS
Surface reflection: Physical and geometrical perspectives
[AD-A210592] N90-10710

GEOMETRY
Face-specific interaction of MoS4(2-1) with oriented crystals of (0001) CdX (X = Se, S)
[AD-A209519] N90-10732

GEOMORPHOLOGY
Fluctuation history of Great Salt Lake, Utah, during the last 13,000 years, part 2
[NASA-CR-185911] N90-10466
ONR/NORDA Workshop on Terrain Analysis and Quantitative Geomorphology
[AD-A210464] N90-10489

GEOPHYSICS
Kiruna geophysical data: Data Summary 88/7-9, July - September 1988
[PB89-210249] N90-10487
Institute of Geophysics and Planetary Physics, 1988
[DE89-014363] N90-10794
Solar-geophysical data number 532, December 1988. Part 1: Data for November, October 1988, and late data
[PB89-152086] N90-10818
GEOPOTENTIAL
Semi-monthly temperature and geopotential anomaly in the upper 500 meters along the Oahu-Farallon Islands great circle from November 15, 1967 through December 15, 1979
[AD-A210640] N90-10518
GERMANIUM ALLOYS
Structure of amorphous silicon alloy films
[DE89-009441] N90-10734
GIBBS PHENOMENON
Shock capturing by the spectral viscosity method
[NASA-CR-181920] N90-10639
GLASS FIBER REINFORCED PLASTICS
The high-frequency dielectric properties of glass fibre reinforced plastic and honeycomb layers
[AD-A210581] N90-10289
GLASS LASERS
Overview of laser concepts N90-10154
GLOBAL POSITIONING SYSTEM
Guidance simulation and test support for differential GPS flight experiment
[NASA-CR-177471] N90-10021
GLYCOLS
Synthesis and physical properties of poly(perfluoroalkylether) urethanes
[AD-A210500] N90-10287
GOERTLER INSTABILITY
Goertler instability on an airfoil: Comparison of marching solution with experimental observations N90-10364
GOLD
Multiple internal reflection Fourier transform infrared spectroscopy studies of thiocyanate adsorption on silver and gold
[AD-A210245] N90-10223
GRADIENTS
A unified view of infinitesimal perturbation analysis and likelihood ratios
[AD-A210682] N90-10652
GRAIN BOUNDARIES
Progress report on grain boundaries
[DE89-015541] N90-10749
GRAIN SIZE
Fatigue crack initiation mechanics of metal aircraft structures
[AD-A210567] N90-10255
The measurement of infrared spectra of dense ceramics by specular reflectance spectroscopy
[AD-A210609] N90-10291
Preparation, purification and densification of zinc sulfide powder from organometallics
[AD-A210943] N90-10298
GRANTS
Energy storage and distribution program summary. Volume 2: Research summaries, fiscal year 1988
[DE89-000867] N90-10470
GRAPH THEORY
On the 2-extendability of planar graphs
[AD-A210289] N90-10642
Extending matchings in planar graphs 4
[AD-A210315] N90-10643
GRAPHITE
PMR graphite engine duct development
[NASA-CR-182228] N90-10037
GRAPHITE-EPOXY COMPOSITES
The interlaminar fracture toughness of woven graphite/epoxy composites
[NASA-TP-2950] N90-10179
GRAPHS (CHARTS)
The 1984 direct strike lightning data, part 2
[NASA-TM-87690-PT-2] N90-10506
The 1984 direct strike lightning data, part 3
[NASA-TM-87690-PT-3] N90-10507
Extending matchings in planar graphs 4
[AD-A210315] N90-10643
GRATINGS (SPECTRA)
Design of grazing incidence monochromators involving unconventional gratings
[DE89-016341] N90-10704
Custom diffraction gratings
[AD-A211002] N90-10712
GRAVITATION
Are there causal vacuum solutions with the symmetries of the Goedel universe in higher-derivative gravity
[DE89-611966] N90-10770
GRAVITATION THEORY
Homogeneous gravitational fields and limits of gravitational fields N90-10812
GRAVITATIONAL FIELDS
On analytic modeling of lunar perturbations of artificial satellites of the earth
[AD-A210440] N90-10078
Homogeneous gravitational fields and limits of gravitational fields N90-10812
GRAZING INCIDENCE
Design of grazing incidence monochromators involving unconventional gratings
[DE89-016341] N90-10704
GRAZING INCIDENCE TELESCOPES
Soft X-ray astronomy using grazing incidence optics N90-10797
The design and evaluation of grazing incidence relay optics N90-10799
Advances in photographic X-ray imaging for solar astronomy N90-10803
GREENHOUSE EFFECT
International impacts of global climate change: Testimony to House Appropriations Subcommittee on Foreign Operations, Export Financing and Related Programs
[DE89-014004] N90-10482
GRID GENERATION (MATHEMATICS)
Computation of transonic flow about stores
[AD-A210402] N90-10009
BLOT: A mesh and curve plot program for the output of a finite element analysis
[DE89-013994] N90-10590
Grid generation procedure using the integral equation method
[NAL-TR-1009] N90-10630
A high-order Lagrangian-decoupling method for the incompressible Navier-Stokes equations
[NASA-CR-181903] N90-10631
GROOVING
Custom diffraction gratings
[AD-A211002] N90-10712
GROUND STATE
Computational modeling of pi-conjugated polyradicals
[AD-A210573] N90-10648
GROUND STATIONS
Omega system performance assessment
[AD-A210342] N90-10322
GROUND TESTS
Full scale technology demonstration of a modern counterrotating unducted fan engine concept. Engine test
[NASA-CR-180869] N90-10049
GROUP DYNAMICS
Parallel processing and learning in simple systems
[AD-A210225] N90-10612
A theory of collective induction
[AD-A210553] N90-10780
GROUP THEORY
The organization of permutation architectures with bussed interconnections
[AD-A210832] N90-10352
GULF STREAM
A compilation of digitized satellite imagery of the Gulf Stream (1982, 1983, and 1985)
[AD-A210243] N90-10467
IFD (Implicit Finite Difference): Interfaced with Harvard open ocean model forecasts
[AD-A210521] N90-10517
GUN TURRETS
Scientific and technical report voice activated gun turrent control
[AD-A210350] N90-10623

H

HAMILTONIAN FUNCTIONS
Periodic solutions of spatially periodic Hamiltonian systems
[AD-A210645] N90-10649
HANGARS
ILS (Instrument Landing System) mathematical modeling study on the effects of proposed hangar construction west of runway 18R on localizer performance at Dallas-Fort Worth International Airport
[AD-A210831] N90-10019
HARDNESS
Structure-mechanical property relationships in ion implanted ceramics
[DE89-010129] N90-10274
HARTREE APPROXIMATION
Atomic effects of beta decay in astrophysics and in elementary particle physics N90-10811
HAZARDS
Definition and reduction of the F-18 windshield birdstrike hazard
[AD-A210700] N90-10015
HEALTH
Organic explosives and related compounds. Environmental and health considerations
[AD-A210554] N90-10306
Managing human exposure and health risks: An integrated approach and the role of uncertainty
[DE89-008611] N90-10525
HEAT
Control of thermoregulatory sweating during exercise in the heat
[AD-A206001] N90-10523
HEAT EXCHANGERS
High temperature VSCF (Variable Speed Constant Frequency) generator system
[AD-A210823] N90-10351
HEAT OF COMBUSTION
High energy density solid and liquid hydrocarbon fuels
[AD-A210195] N90-10304
HEAT OF FORMATION
Convection of a pattern of vorticity through a reacting shock wave
[NASA-CR-181921] N90-10576
HEAT PIPES
Application of formal optimization techniques in thermal/structural design of a heat-pipe-cooled panel for a hypersonic vehicle
[NASA-TM-89131] N90-10409
HEAT RESISTANT ALLOYS
New structural materials
[AD-A209425] N90-10246
Development of metastable processing paths for high temperature alloys
[AD-A210550] N90-10254
HEAT SHIELDING
Preliminary design of a large tetrahedral truss/hexagonal heatshield panel aerobrake
[NASA-TM-101612] N90-10127
HEAT TRANSFER
Heat transfer characteristics of igniter output plumes
[DE89-011449] N90-10340
PORFLO-3: A mathematical model for fluid flow, heat, and mass transport in variably saturated geologic media: Users manual, version 1.0
[DE89-013977] N90-10398
Global existence and asymptotic stability for a nonlinear integrodifferential equation modeling heat flow
[AD-A210647] N90-10408
Thermoregulatory responses to intermittent exercise are influenced by knit structure of underwear
[AD-A209087] N90-10541
Energy dependent transport problem with generalized boundary conditions
[DE89-617843] N90-10676
HEAT TREATMENT
Development of metastable processing paths for high temperature alloys
[AD-A210550] N90-10254
Strain aging in tungsten-heavy alloys
[AD-A211166] N90-10259
HEATING
Attenuation of reheat buzz by active control N90-10201
HELICOPTER ENGINES
An appraisal of a number of power assessment procedures being proposed for use in Chinook-Lycoming T55 engine
[AD-A210482] N90-10041
HELICOPTER PERFORMANCE
Airworthiness and flight characteristics test of the UH-60A Black Hawk helicopter equipped with the XM-139 multiple mine dispensing system (VOLCANO)
[AD-A210271] N90-10025
HELICOPTERS
Scientific and technical report voice activated gun turrent control
[AD-A210350] N90-10623
HELIOSTATS
Stretched-membrane heliostats for solar central-receiver power plants
[DE89-016034] N90-10476
HELIUM
X-ray bright points and He I lambda 10830 dark points N90-10802
HEMOGLOBIN
Human health studies of carbon monoxide (CO) under conditions of military weapons systems crewman exposures. Protocol 1: Formation of COHb
[AD-A210344] N90-10528
HETEROGENEITY
Capillary effects in steady-state flow in heterogeneous cores
[DE89-000758] N90-10399
Tools for application development in heterogeneous distributed environments
[AD-A210238] N90-10613

HETEROJUNCTIONS
High energy neutron irradiation effects in GaAs modulation-Doped Field Effect Transistors (MODFETS): Threshold voltage
[AD-A210502] N90-10763
HEURISTIC METHODS
Application of a hybrid generation/utility assessment heuristic to a class of scheduling problems
[NASA-TM-102367] N90-10674
HF LASERS
Coupled multiline CW HF lasers: Experimental performance
[AD-A210844] N90-10434
Master oscillator with power amplifiers: Performance of a two-element CW HF phased-laser array
[AD-A211141] N90-10435
HIERARCHIES
Hierarchical structure in polymeric solids and its influence on properties
[AD-A210918] N90-10297
An analytical hierarchy process approach to establish the systems analyst's knowledge base for selecting an information requirements determination strategy N90-10785
HIGH CURRENT
Commercial high current ignitron development
[DE89-015077] N90-10331
HIGH ELECTRON MOBILITY TRANSISTORS
Experimental investigations of transport and optical properties of 3-5 quantum well structures grown via molecular beam epitaxy under optimal growth conditions
[AD-A210269] N90-10758
HIGH ENERGY ELECTRONS
Physics of high energy photoconductive switches
[AD-A210341] N90-10345
HIGH ENERGY FUELS
High energy density solid and liquid hydrocarbon fuels
[AD-A210195] N90-10304
HIGH ENERGY INTERACTIONS
Studies of elementary particles
[DE89-014859] N90-10685
Research program in theoretical high energy physics
[DE89-013963] N90-10695
A theoretical high energy physics program
[DE89-012685] N90-10696
HIGH PRESSURE
SSME Alternate Turbopump Development Program: Design verification specification for high-pressure fuel turbopump
[NASA-CR-183676] N90-10033
Chemistry of nitromethane at very high pressure
[DE89-008016] N90-10215
Institute of Geophysics and Planetary Physics, 1988
[DE89-014363] N90-10794
HIGH REYNOLDS NUMBER
A study of high-lift airfoils at high Reynolds numbers in the Langley low-turbulence pressure tunnel
[NASA-TM-89125] N90-10002
HIGH SPEED
Large-scale Advanced Prop-fan (LAP) high speed wind tunnel test report
[NASA-CR-182125] N90-10045
High-speed machining of aluminum
[DE89-014011] N90-10441
HIGH STRENGTH ALLOYS
Strain aging in tungsten-heavy alloys
[AD-A211166] N90-10259
HIGH STRENGTH STEELS
Mechanisms of strength and toughness in a microalloyed, precipitation hardened steel
[AD-A210571] N90-10256
HIGH TEMPERATURE
Materials for engine applications above 3000 deg F: An overview
[NASA-TM-100169] N90-10188
Thin film thermocouples for high temperature measurement
[PB89-209290] N90-10420
Fluctuating pressures measured beneath a high-temperature, turbulent boundary layer on a flat plate at Mach number of 5
[NASA-TP-2947] N90-10580
HIGH TEMPERATURE ENVIRONMENTS
High temperature VSCF (Variable Speed Constant Frequency) generator system
[AD-A210823] N90-10351
HIGH TEMPERATURE LUBRICANTS
Development of a high temperature FZG-Ryder gear lubricant load capacity machine
[AD-A210799] N90-10449
HIGH TEMPERATURE SUPERCONDUCTORS
Study of deposition of YBa2Cu3O7-x on cubic zirconia
[NASA-TM-102350] N90-10737
Magnetic correlations in high T(sub c) oxides in the superconducting state
[DE89-016421] N90-10746
Processing and fabrication of high temperature oxide superconductors
[AD-A210197] N90-10755
The effect of twins on critical currents of high Tc superconductors
[AD-A210988] N90-10768
HIGH TEMPERATURE TESTS
Total hemispherical emittance measured at high temperatures by the calorimetric method
[NASA-TM-102322] N90-10309
HILBERT SPACE
Numerical optimization in Hilbert space using inexact function and gradient evaluations
[NASA-CR-181926] N90-10640
Periodic solutions of spatially periodic Hamiltonian systems
[AD-A210645] N90-10649
D=3 Chern-Simons action, supergravity and quantization
[DE89-017530] N90-10775
HISTORIES
Encyclopedia of US Air Force aircraft and missile systems. Volume 2: Post-World War 2 bombers, 1945-1973
[AD-A209273] N90-10001
HMX
Effects of binder concentration on the properties of plastic-bonded explosives
[DE89-007744] N90-10301
HOHLRAUMS
Total hemispherical emittance measured at high temperatures by the calorimetric method
[NASA-TM-102322] N90-10309
HOLES (ELECTRON DEFICIENCIES)
Trap gettering by isoelectronic doping of p-GaAs and n-GaAs grown by molecular beam epitaxy
[AD-A211162] N90-10769
HOLOGRAPHY
Optical processing for distributed sensors in control of flexible spacecraft N90-10102
HOMING DEVICES
Alternative polar homing strategies N90-10059
HOMOGENEITY
The rewrite rule machine project
[AD-A210528] N90-10617
Homogeneous gravitational fields and limits of gravitational fields N90-10812
HOMOTOPY THEORY
Finding isolated zero points of complex polynomial mappings
[DE89-617523] N90-10633
HONEYCOMB STRUCTURES
The high-frequency dielectric properties of glass fibre reinforced plastic and honeycomb layers
[AD-A210581] N90-10289
HOVERING STABILITY
Airworthiness and flight characteristics test of the UH-60A Black Hawk helicopter equipped with the XM-139 multiple mine dispensing system (VOLCANO)
[AD-A210271] N90-10025
HUMAN BEHAVIOR
Active participation in highly automated systems: Turning the wrong stuff into the right stuff
[AD-A210218] N90-10572
HUMAN BEINGS
Thermoregulatory responses to intermittent exercise are influenced by knit structure of underwear
[AD-A209087] N90-10541
Networks for image acquisition, processing and display N90-10545
Human motion perception: Higher-order organization N90-10553
HUMAN FACTORS ENGINEERING
Classification and reduction of pilot error
[NASA-CR-181867] N90-10014
Vision science and technology at NASA: Results of a workshop: Executive summary N90-10543
Pyramid image codes N90-10567
Addressing user display requirements from a large and diverse user community
[DE89-011403] N90-10582
HUMAN PERFORMANCE
Human performance in continuous/sustained operations and the demands of extended work/rest schedules: An annotated bibliography, volume 2
[AD-A210504] N90-10530
Daytime sleepiness, performance, mood, nocturnal sleep: The effect of benzodiazepine and caffeine on their relationship
[AD-A210915] N90-10533
Networks for image acquisition, processing and display N90-10545
Stanford/NASA-Ames Center of Excellence in model-based human performance N90-10565
Learning to make decisions: When incentives help and hinder
[AD-A210185] N90-10779
HUMAN TOLERANCES
Biomedical influences on spinal cord function
[AD-A210311] N90-10527
HUMIDITY
A study of the impact of simulated 183 GHz water vapor retrievals on numerical weather prediction
[AD-A210431] N90-10504
Measurement of respiratory air temperatures and calculation of respiratory heat loss when working at various ambient temperatures
[AD-A210378] N90-10529
HURRICANES
Extreme hurricanes in the nineteenth century
[PB89-201305] N90-10498
HYDROCARBON FUELS
High energy density solid and liquid hydrocarbon fuels
[AD-A210195] N90-10304
HYDRODYNAMICS
Free-expansion experiments and modeling in detonation: Chemistry and hydrodynamics on a laboratory scale
[DE89-007748] N90-10302
HYDROGEN
A laser-driven source of polarized hydrogen and deuterium
[DE89-015130] N90-10429
HYDROGEN CHLORIDES
Reactions of hydrogen chloride and boron trichloride with trimethylsilylamino groups
[AD-A209006] N90-10209
HYDROGEN IONS
Observation of excited H(sup 0) atoms produced by relativistic H(sup (minus)) ions in carbon and formvar foils
[DE89-015301] N90-10688
HYDROGEN OXYGEN ENGINES
Cycle analysis of scramjet engines
[NAL-TR-1002] N90-10035
A rocket engine design expert system
[NASA-TM-102373] N90-10172
HYDROLYSIS
Analysis of surface modified colloidal silicas
[DE89-015849] N90-10267
Preparation, purification and densification of zinc sulfide powder from organometallics
[AD-A210943] N90-10298
HYDROTHERMAL STRESS ANALYSIS
Hygrothermal effects on the complex moduli of composite laminates N90-10182
HYGRAL PROPERTIES
Hygrothermal effects on the complex moduli of composite laminates N90-10182
Mechanics of damping for fiber composite laminates including hygro-thermal effects
[NASA-TM-102329] N90-10185
HYPERBOLIC COORDINATES
Similarity solutions that give rise to hyperbolicity and change of type in steady flow of a viscoelastic fluid
[AD-A210920] N90-10410
HYPERBOLIC DIFFERENTIAL EQUATIONS
Global existence and asymptotic stability for a nonlinear integrodifferential equation modeling heat flow
[AD-A210647] N90-10408
An iterative method for systems of nonlinear hyperbolic equations
[NASA-CR-181919] N90-10638
HYPERCUBE MULTIPROCESSORS
A low-cost hypercube load-balance algorithm
[DE89-015739] N90-10589
Shared memory versus message passing architectures: An application based study
[AD-A210312] N90-10615
HYPERSONIC BOUNDARY LAYER
Leading edge transition by contamination in hypersonic flow N90-10360
HYPERSONIC VEHICLES
Application of formal optimization techniques in thermal/structural design of a heat-pipe-cooled panel for a hypersonic vehicle
[NASA-TM-89131] N90-10409
HYPERVELOCITY IMPACT
Orbital debris research at NASA Johnson Space Center, 1986-1988
[NASA-TM-102155] N90-10795
HYSTERESIS
Circuit level modeling of inductive elements
[DE89-015122] N90-10173
Analysis of spurt phenomena for a non-Newtonian fluid
[AD-A210560] N90-10405

I

ICE
Debris/ice/TPS assessment and photographic analysis for Shuttle Mission STS-28R
[NASA-TM-102152] N90-10079
IDENTIFYING
The intensity dependent spread model and color constancy N90-10555
IGNITERS
Heat transfer characteristics of igniter output plumes
[DE89-011449] N90-10340
IGNITION
Heat transfer characteristics of igniter output plumes
[DE89-011449] N90-10340
Pyrotechnic ignition studies using a gun tunnel
[DE89-012496] N90-10341
Ignition and burn criteria for D3He tokamak and spherical torus reactors
[DE89-015059] N90-10716
IGNITRONS
Commercial high current ignitron development
[DE89-015077] N90-10331
ILLUMINATING
Factors affecting the perception of transparent motion N90-10559
IMAGE ANALYSIS
Image-based terrain modeling with thematic mapper applied to resolving the limit of Holocene Lake expansion in the Great Salt Lake Desert, Utah, part 1
[NASA-CR-185913] N90-10465
Algorithms and architectures for robot vision N90-10562
Soft X-ray astronomy using grazing incidence optics N90-10797
The design and evaluation of grazing incidence relay optics N90-10799
The correspondence between small-scale coronal structures and the evolving solar magnetic field N90-10800
IMAGE INTENSIFIERS
Cockpit lighting compatibility with image intensification night imaging systems: Issues and answers
[AD-A210503] N90-10028
IMAGE PROCESSING
Optical processing for distributed sensors in control of flexible spacecraft N90-10102
Satellite Data Processing System (SDPS) users manual V1.0
[NASA-CR-183054] N90-10468
Vision Science and Technology at NASA: Results of a Workshop
[NASA-TM-102214] N90-10542
Vision science and technology at NASA: Results of a workshop: Executive summary N90-10543
Parallel asynchronous hardware implementation of image processing algorithms N90-10546
Computation and parallel implementation for early vision N90-10549
Intensity dependent spread theory N90-10550
Image gathering, coding, and processing: End-to-end optimization for efficient and robust acquisition of visual information N90-10551
Hybrid vision activities at NASA Johnson Space Center N90-10552
Two-dimensional shape recognition using sparse distributed memory N90-10554
The intensity dependent spread model and color constancy N90-10555
Motion detection in astronomical and ice floe images N90-10558
Photonic processing at NASA Ames Research Center N90-10560
Instrumentation and robotic image processing using top-down model control N90-10563
Computer vision research at Marshall Space Flight Center N90-10564
Ames vision group research overview N90-10566
Pyramid image codes N90-10567
Intensity dependent spread processor and workstation N90-10568
Space environment robot vision system N90-10569
Regulation of nonlinear and generalized linear systems
[AD-A207725] N90-10619
Robot vehicle video image compression, phase 1
[AD-A210974] N90-10626
Tellurium-118/antimony-118 generator
[DE89-015225] N90-10698
Radon transform analysis of a probabilistic method for image generation
[AD-A207814] N90-10702
A comparison of real-time optical correlators for pattern recognition
[DE89-016416] N90-10705
IMAGES
Raman characterization of high temperature materials using an imaging detector
[DE89-016308] N90-10219
A compilation of digitized satellite imagery of the Gulf Stream (1982, 1983, and 1985)
[AD-A210243] N90-10467
Sampling and noise in vision networks N90-10544
Networks for image acquisition, processing and display N90-10545
Computation and parallel implementation for early vision N90-10549
Image gathering, coding, and processing: End-to-end optimization for efficient and robust acquisition of visual information N90-10551
Motion detection in astronomical and ice floe images N90-10558
Factors affecting the perception of transparent motion N90-10559
IMAGING TECHNIQUES
Raman characterization of high temperature materials using an imaging detector
[DE89-016308] N90-10219
Low-cost three-dimensional stereoscopic display technique for computer-aided design
[DE89-011635] N90-10594
Negative-working electron beam resist based on poly(methyl methacrylate)
[AD-A207834] N90-10733
Atomic imaging and interfacial analysis
[DE89-015339] N90-10748
IMPACT
Definition and reduction of the F-18 windshield birdstrike hazard
[AD-A210700] N90-10015
Method and apparatus for determining time, direction and composition of impacting space particles
[NASA-CASE-LAR-13392-1-CU] N90-10132
IMPACT DAMAGE
Simulation of flexible structures with impact: Experimental validation N90-10097
IMPACT LOADS
Shock compression and release in high-strength ceramics
[DE89-013995] N90-10265
Remarks on certain aspects of solid explosive detonation via small projectile impact
[AD-A210648] N90-10307
EPIC-2 calculated impact loading histories of thin plates
[AD-A210557] N90-10461
IMPACT PREDICTION
Remarks on certain aspects of solid explosive detonation via small projectile impact
[AD-A210648] N90-10307
IMPACT STRENGTH
Definition and reduction of the F-18 windshield birdstrike hazard
[AD-A210700] N90-10015
Conference on Aerospace Transparent Materials and Enclosures (15th) 16-20 January 1989. Volume 2: Sessions 6-9
[AD-A210201] N90-10024
IMPACT TESTS
Alternative test methodology for ballistic performance ranking of armor ceramics
[AD-A210587] N90-10290
IMPACT TOLERANCES
Biomedical influences on spinal cord function
[AD-A210311] N90-10527
IMPEDANCE
Impedance analysis of ionic transport in polypyrrole-polyazulene copolymer and its charge-discharge characteristics
[AD-A210979] N90-10299
IMPEDANCE MEASUREMENT
Impedance studies of the cell Pt/Ag+ conducting glass/Ag beta-alumina/Pt
[AD-A209820] N90-10210
IMPURITIES
Two photon absorption characterization
[AD-A210508] N90-10694
IN-FLIGHT MONITORING
Flight Motor Set 360L003 (STS-29R)
[NASA-CR-183739-VOL-1] N90-10170
INCENTIVES
Learning to make decisions: When incentives help and hinder
[AD-A210185] N90-10779
INCOMPRESSIBLE BOUNDARY LAYER
Primary and secondary stability analysis applied to the DFVLR-transition swept-plate experiment N90-10371
Numerical simulation of coherent structures in an incompressible mixing layer N90-10383
INCOMPRESSIBLE FLOW
Numerical investigation of the effects of longitudinal vortices on the onset of transition in a flat plate boundary layer N90-10363
Numerical simulation of turbulent plane channel flows N90-10382
Effect of particle velocity fluctuations on the inertia coupling in two-phase flow N90-10391
Laminar boundary layer along inviscid surface streamlines over inclined axisymmetric bodies in incompressible flow
[AD-A210202] N90-10401
Two counter-rotating vortices approaching a free surface in a viscous fluid
[AD-A210495] N90-10404
Stability of discontinuous shearing motions of a non-Newtonian fluid
[AD-A210643] N90-10406
Stability of discontinuous steady states in shearing motion of a non-Newtonian fluid
[AD-A210644] N90-10407
A high-order Lagrangian-decoupling method for the incompressible Navier-Stokes equations
[NASA-CR-181903] N90-10631
Numerical simulation of the compressible Orszag-Tang vortex
[AD-A210465] N90-10725
INDEXES (DOCUMENTATION)
Space station systems: A bibliography with indexes (supplement 8)
[NASA-SP-7056(08)] N90-10131
Aerospace medicine and biology: A continuing bibliography with indexes (supplement 328)
[NASA-SP-7011(328)] N90-10524
NASA scientific and technical publications: A catalog of special publications, reference publications, conference publications, and technical papers, 1988
[NASA-SP-7063(03)] N90-10782
INDIUM
Trap gettering by isoelectronic doping of p-GaAs and n-GaAs grown by molecular beam epitaxy
[AD-A211162] N90-10769
INDIUM PHOSPHIDES
Properties of devices prepared with epitaxial layers on InP
[AD-A210304] N90-10759
INDUCTION (MATHEMATICS)
A theory of collective induction
[AD-A210553] N90-10780
INDUCTORS
Circuit level modeling of inductive elements
[DE89-015122] N90-10173
INDUSTRIAL SAFETY
Human performance in continuous/sustained operations and the demands of extended work/rest schedules: An annotated bibliography, volume 2
[AD-A210504] N90-10530
INERTIA
Effect of particle velocity fluctuations on the inertia coupling in two-phase flow N90-10391
Fracture and three dimensional stress analyses of 7075 aluminum projectile components under spin and inertia load
[AD-A210986] N90-10463
INERTIAL CONFINEMENT FUSION
NTES laser facility for physics experiments: Building 381 high bay option
[DE89-014326] N90-10428
INFLATABLE SPACECRAFT
Structural concepts for very large (400-meter-diameter) solar concentrators N90-10153
INFORMATION MANAGEMENT
Extreme hurricanes in the nineteenth century
[PB89-201305] N90-10498
Meteorological support: Descriptions of application programs for accessing and displaying data
[PB89-194625] N90-10500
Waveform generator signal processing software
[PB89-192660] N90-10587
Weeding policy and procedures: Information services
[AD-A210568] N90-10790
Development of Information Quality Engineering (IQE) methodology for information resource management
[AD-A210615] N90-10791
INFORMATION PROCESSING (BIOLOGY)
Extrathalamic modulation of cortical function
[AD-A211044] N90-10535
Integration of neurobiological and computational analyses of the neural network essentials for conditioned taste aversions
[AD-A210228] N90-10537
Models of mental functioning
[AD-A210456] N90-10538
INFORMATION RETRIEVAL
The impact of recovery on concurrency control
[AD-A210828] N90-10603

Online support for the intellectual activity of browsing
N90-10784

INFORMATION SYSTEMS
Satellite Data Processing System (SDPS) users manual V1.0
[NASA-CR-183054] N90-10468
Planning an Integrated On-line Library System (IOLS)
[AD-A209406] N90-10783
Online support for the intellectual activity of browsing
N90-10784
Motivating the notion of generic design within information processing theory: The design problem space
[AD-A210266] N90-10786
Weeding policy and procedures: Information services
[AD-A210568] N90-10790
Development of Information Quality Engineering (IQE) methodology for information resource management
[AD-A210615] N90-10791
Defense Technical Information Center cataloging guidelines
[AD-A211000] N90-10792

INFORMATION THEORY
Vision science and technology for supervised intelligent space robots N90-10548
Image gathering, coding, and processing: End-to-end optimization for efficient and robust acquisition of visual information N90-10551
Motivating the notion of generic design within information processing theory: The design problem space
[AD-A210266] N90-10786

INFORMATION TRANSFER
An introduction to input/output automata
[AD-A210831] N90-10604

INFRARED ABSORPTION
Effects of coherent scattering on infrared absorption in doped semiconductors
[AD-A210224] N90-10756

INFRARED ASTRONOMY
Analysis of nearly simultaneous X-ray and optical observations of active galactic nuclei N90-10806
Automatic classification of spectra from the Infrared Astronomical Satellite (IRAS)
[NASA-RP-1217] N90-10807

INFRARED DETECTORS
Laterally stacked Schottky diodes for infrared sensor applications
[NASA-CASE-NPO-17426-1-CU] N90-10329

INFRARED IMAGERY
A compilation of digitized satellite imagery of the Gulf Stream (1982, 1983, and 1985)
[AD-A210243] N90-10467

INFRARED RADIATION
Millimeter-wave/infrared rectenna development at Georgia Tech N90-10147
Biomedical studies with the free electron laser
[AD-A208927] N90-10519

INFRARED SPECTRA
Multiple internal reflection Fourier transform infrared spectroscopy studies of thiocyanate adsorption on silver and gold
[AD-A210245] N90-10223
Automatic classification of spectra from the Infrared Astronomical Satellite (IRAS)
[NASA-RP-1217] N90-10807

INFRARED SPECTROSCOPY
Attenuated total reflection FTIR spectroscopy for measuring interfacial reaction kinetics at silica surfaces
[AD-A210314] N90-10224
Characterization of diamond films by thermogravimetric analysis and infrared spectroscopy
[AD-A210564] N90-10288
Real-time observations of aerosol composition changes
[DE89-012382] N90-10422

INHIBITORS
Polypeptide inhibitors of mineral scaling and corrosion
[AD-A210507] N90-10225

INITIATION
Laser initiation of secondary explosives
[DE89-010229] N90-10431

INJECTION MOLDING
Improved silicon carbide for advanced heat engines
[NASA-CR-180831] N90-10293

INJECTORS
A rocket engine design expert system
[NASA-TM-102373] N90-10172

INJURIES
Biomedical influences on spinal cord function
[AD-A210311] N90-10527

INPUT
Computer availability impact on the archiving of scientific and technical reports
[AD-A210283] N90-10787

INPUT/OUTPUT ROUTINES
An introduction to input/output automata
[AD-A210831] N90-10604

INSPECTION
Generic system components of the Thiokol ultrasonic RSRM case-to-insulation bondline inspection system
[NASA-CR-183738] N90-10171
The creation of quality: New directions in the production of aeronautics castings N90-10241

INSTRUMENT LANDING SYSTEMS
ILS/MLS comparison tests at Miami/Tamiami, Florida Airport
[ACD-330] N90-10018
ILS (Instrument Landing System) mathematical modeling study on the effects of proposed hangar construction west of runway 18R on localizer performance at Dallas-Fort Worth International Airport
[AD-A210631] N90-10019

INSULATION
Deep traps and sidegating in GaAs devices
[AD-A210740] N90-10765

INSULATORS
The effects of normal annealing cycles during IGFET fabrication on initial and radiation induced gate insulator defects
[AD-A210282] N90-10278

INTAKE SYSTEMS
Analysis of results from wind tunnel tests of inlets for an advanced turboprop nacelle installation
[NASA-CR-174937] N90-10011
Effects of low-frequency instabilities on the operation of Ramjet air inlets N90-10198
Recent developments in Ramjet pressure oscillation technology N90-10199

INTEGRAL EQUATIONS
Grid generation procedure using the integral equation method
[NAL-TR-1009] N90-10630

INTEGRATED CIRCUITS
Circuit level modeling of inductive elements
[DE89-015122] N90-10173
Micro-cavity integrable vacuum diodes and triodes
[DE89-016649] N90-10344
Focused ion beam implantation
[AD-A210977] N90-10767

INTELLIGIBILITY
Attention and vigilance in speech perception
[AD-A210493] N90-10539

INTERACTIONS
Three-dimensional unsteady transonic viscous-inviscid interaction N90-10005
NASA'S controls-structures interaction program N90-10081
Lumped mass formulations for modeling flexible body systems N90-10091
Computer simulation of plasma interactions near Titan N90-10816

INTERFACE STABILITY
Synthesis and interfacial properties of new generation polyurethane systems
[AD-A210446] N90-10266

INTERFACES
Attenuated total reflection FTIR spectroscopy for measuring interfacial reaction kinetics at silica surfaces
[AD-A210314] N90-10224
Delayed failure of silver-aided diffusion welds between steel
[DE89-016652] N90-10252
Atomic imaging and interfacial analysis
[DE89-015339] N90-10748
Characterization of GaAs/Si/GaAs heterointerfaces
[DE89-016302] N90-10752

INTERFACIAL TENSION
Characterization of polymeric surfaces and interfaces
[AD-A210227] N90-10277
Analytic theory for the selection of Saffman-Taylor fingers in the presence of thin film effects
[NASA-CR-181910] N90-10677

INTERFERENCE DRAG
Wind tunnel support system effects on a fighter aircraft model at Mach numbers from 0.6 to 2.0
[AD-A210614] N90-10010

INTERFEROMETRY
Master oscillator with power amplifiers: Performance of a two-element CW HF phased-laser array
[AD-A211141] N90-10435
An interferometric strain-displacement measurement system
[NASA-TM-101638] N90-10454
Multimode fiber interferometry and several-mode fiber polarimetry via phase conjugation
[DE89-014226] N90-10706
Simultaneous multiple frequency interferometry: An application of homodyne phase measurement
[DE89-013975] N90-10719

INTERMETALLICS
New structural materials
[AD-A209425] N90-10248
Development of metastable processing paths for high temperature alloys
[AD-A210550] N90-10254

INTERPOLATION
Thermodynamic and dynamic processes in the updraft region of GALE (Genesis of Atlantic Lows Experiment) IOP (Intensive Observation Period) 9
[AD-A208139] N90-10496
Motion detection in astronomical and ice floe images
N90-10558
On two polynomial spaces associated with a box spline
[AD-A210559] N90-10646

INTERPROCESSOR COMMUNICATION
DDN Trusted Guard Gateway: Trusted Guard Gateway (TGG) technology assessment, phase 2
[AD-A210248] N90-10614

INVISCID FLOW
Three-dimensional unsteady transonic viscous-inviscid interaction N90-10005
A three-dimensional linear stability approach to transition on wings at incidence N90-10373
Effect of particle velocity fluctuations on the inertia coupling in two-phase flow N90-10391
Laminar boundary layer along inviscid surface streamlines over inclined axisymmetric bodies in incompressible flow
[AD-A210202] N90-10401

IODINE LASERS
Earth orbit laser systems N90-10162
Beamed laser power in support of near-earth missions
N90-10167

ION BEAMS
Custom diffraction gratings
[AD-A211002] N90-10712
Focused ion beam implantation
[AD-A210977] N90-10767

ION IMPLANTATION
Structure-mechanical property relationships in ion implanted ceramics
[DE89-010129] N90-10274
Photoreflectance study of boron ion-implanted (100) cadmium telluride
[SD-TR-88-89] N90-10300
Advanced GaAs process modeling, volume 1
[AD-A210385] N90-10761
Focused ion beam implantation
[AD-A210977] N90-10767

IONIZATION
Improved propagation models for discrete random media
[AD-A211085] N90-10327

IONIZATION FREQUENCIES
An experimental study of microwave transmission through a decaying plasma
[AD-A210586] N90-10726

IONOSPHERES
Computer simulation of plasma interactions near Titan
N90-10816

IONOSPHERIC DISTURBANCES
Plasma theory and simulation
[AD-A207952] N90-10714

IRIDIUM
Monomers, polymers and transition metal complexes based upon carboranes
[AD-A210226] N90-10221

IRON
Genetic engineering of single-domain magnetic particles
[AD-A210332] N90-10521

IRON ALLOYS
Establishment and initial operation of a resource facility for RSR (Rapid Solidification Rate) processed alloys in pilot quantities
[AD-A210369] N90-10283

IRON COMPOUNDS
Electrochemistry in near-critical and supercritical fluids. Part 7: SO2
[AD-A206207] N90-10214

IRRADIANCE
An anisotropic shadowband correction for parameterized sky conditions and geometry
[DE89-014916] N90-10485

IRRADIATION
Eye/sensor protection against laser irradiation organic nonlinear optical materials
[AD-A210599] N90-10531
Generation of 3/2 omega sub o radiation in inhomogeneous plasmas under the irradiation of intense electromagnetic waves
[DE89-015723] N90-10722

ISOCYANATES
An investigation of the degradation and stabilization of polymer systems
[AD-A210362] N90-10282

ISOLATION
Documentation of the current fault detection, isolation and reconfiguration software of the AIPS fault-tolerant processor
[NASA-TM-89154] N90-10602
ISOTHERMS
A seasonal isotherm depth climatology for the eastern tropical Pacific
[PB89-193577] N90-10512
ISOTOPIC LABELING
Tellurium-118/antimony-118 generator
[DE89-015225] N90-10698
ITERATION
Numerical optimization in Hilbert space using inexact function and gradient evaluations
[NASA-CR-181926] N90-10640
An introduction to fractals and chaos
[AD-A210257] N90-10675
ITERATIVE SOLUTION
Iterative performance and an adaptive procedure for viscous flow problems N90-10397
The MHOST finite element program: 3-D inelastic analysis methods for hot section components. Volume 3: Systems' manual
[NASA-CR-182236] N90-10451
An iterative method for systems of nonlinear hyperbolic equations
[NASA-CR-181919] N90-10638

J

JAPAN
Japanese structural ceramics research and development N90-10272
JET AIRCRAFT
Modifying high-order aeroelastic math model of a jet transport using maximum likelihood estimation N90-10106
JET ENGINE FUELS
Compatibility of fuel system components with high density fuel
[AD-A210381] N90-10027
Wide-range fuel flowmeter, phase 2
[AD-A210547] N90-10424
JET FLOW
Symmetry breaking bifurcations and the growth of chaos in a rotating fluid
[AD-A210969] N90-10411
JET VANES
Investigations of thrust vector control for high-alpha pitchover N90-10067
JOINING
The organization of permutation architectures with bussed interconnections
[AD-A210832] N90-10352
JOINTS (JUNCTIONS)
Flight set 360T004 (STS-30) insulation component, interim release, volume 3
[NASA-CR-183746] N90-10169
JP-8 JET FUEL
Properties of F-34 (JP-8) fuel for 1988
[AD-A210188] N90-10303
JUDGMENTS
Effects of stress on judgment and decision making in dynamic tasks
[AD-A210605] N90-10781

K

KALMAN FILTERS
Guidance simulation and test support for differential GPS flight experiment
[NASA-CR-177471] N90-10021
KINEMATIC EQUATIONS
The architecture of NEWTON: A general-purpose dynamics simulator
[NASA-CR-185489] N90-10678
KINEMATICS
Winged versus wingless airframes N90-10073
Lumped mass formulations for modeling flexible body systems N90-10091
Efficiency and capabilities of multi-body simulations N90-10095
Shape control of high degree-of-freedom variable geometry trusses N90-10122
Relating tolerances and kinematic behavior
[AD-A211125] N90-10311
The generalized drift flux approach: Identification of the void-drift closure law N90-10386
Studies in penetration mechanics
[AD-A210713] N90-10448
The development of an expert system for the creative design of mechanisms
[AD-A211115] N90-10628
KINETIC ENERGY
The structure determination of molecular adsorbates with large unit cells or lattice-gas disorder on metal surfaces
[AD-A210926] N90-10230
Turbulence kinetic energy equation for dilute suspensions N90-10394
Studies in penetration mechanics
[AD-A210713] N90-10448
KINETIC HEATING
Kinetic effects in Alfven wave heating. Part 2: Propagation and absorption with a single minority species
[DE89-016619] N90-10724
KINETIC THEORY
Energy dependent transport problem with generalized boundary conditions
[DE89-617843] N90-10676
KINETICS
Lumped mass formulations for modeling flexible body systems N90-10091
Hierarchical structure in polymeric solids and its influence on properties
[AD-A210918] N90-10297
Inherent bias in nonlinear least squares analysis of first-order kinetic data
[AD-A210677] N90-10651
KNOWLEDGE BASES (ARTIFICIAL INTELLIGENCE)
Knowledge-based machine vision systems for space station automation
[NASA-CR-185710] N90-10124
Safety analysis of knowledge-based systems
[NASA-CR-184784] N90-10588
KNOWLEDGE REPRESENTATION
Toward a theory of representation design
[AD-A210885] N90-10670

L

LAGRANGIAN EQUILIBRIUM POINTS
Multiple solutions for Lagrangian systems in T superscript n
[AD-A210646] N90-10650
LAKES
Spatial characterization of acid rain stress in Canadian Shield Lakes
[NASA-CR-183446] N90-10479
LAMINAR BOUNDARY LAYER
Curvature effects on the stability of three-dimensional laminar boundary layers N90-10366
Control and modification of turbulence N90-10377
Laminar boundary layer along inviscid surface streamlines over inclined axisymmetric bodies in incompressible flow
[AD-A210202] N90-10401
LAMINAR FLOW
Application of superplastically formed and diffusion bonded aluminum to a laminar flow control leading edge
[NASA-CR-178316] N90-10030
Laminar flow control perforated wing panel development
[NASA-CR-178166] N90-10187
Bifurcations in Poiseuille flow and wall turbulence N90-10370
Numerically determined transition in separated internal flow N90-10374
LAMINAR FLOW AIRFOILS
Dynamics and control of turbulent shear flows
[AD-A210396] N90-10402
LAMINATES
Mechanics of damping for fiber composite laminates including hygro-thermal effects
[NASA-TM-102329] N90-10185
LANDAU-GINZBURG EQUATIONS
Critical magnetic fields (H(sub c2), H(sub c1)) and kappa in YBa2(Cu0.98M0.02)3O(7+delta), M=Ni, Al, and Cu
[DE89-016412] N90-10745
LANGUAGE PROGRAMMING
A common distributed language approach to software integration
[NASA-CR-185499] N90-10584
LANTHANUM OXIDES
Magnetic correlations in high T(sub c) oxides in the superconducting state
[DE89-016421] N90-10746
LARGE SCALE INTEGRATION
Characterization of 4/3 technology large-scale integrated circuit on polysilicon processes
[BDX-613-3971] N90-10335
LARGE SPACE STRUCTURES
Flexible structure control experiments using a real-time workstation for computer-aided control engineering N90-10084
A finite element approach for large motion dynamic analysis of multibody structures in space N90-10093
Proceedings of the Workshop on Computational Aspects in the Control of Flexible Systems, part 2
[NASA-TM-101578-PT-2] N90-10103
Use of the quasilinearization algorithm for the simulation of LSS slewing N90-10110
Input-output oriented computation algorithms for the control of large flexible structures N90-10118
Modeling and stabilization of large flexible space stations N90-10120
Active vibration mitigation of distributed parameter, smart-type structures using Pseudo-Feedback Optimal Control (PFOC) N90-10121
System identification for large space structures N90-10126
Preliminary design of a large tetrahedral truss/hexagonal heatshield panel aerobrake
[NASA-TM-101612] N90-10127
Space structures concepts and materials
[NASA-CR-183727] N90-10128
Technology for large space systems: A bibliography with indexes (supplement 21)
[NASA-SP-7046(21)] N90-10130
Structural concepts for very large (400-meter-diameter) solar concentrators N90-10153
LASER APPLICATIONS
New energy conversion techniques in space, applicable to propulsion
[AIAA-79-1338] N90-10145
Technical options for high average power free electron milimeter-wave and laser devices N90-10151
Overview of laser concepts N90-10154
Laser-powered lunar base N90-10156
Laser-powered Martian rover N90-10157
Beamed laser power in support of near-earth missions N90-10167
New electrodynamic and electrostatic models with applications to antenna theory, superconductor slots, and lasers N90-10316
A laser-driven source of polarized hydrogen and deuterium
[DE89-015130] N90-10429
Laser initiation of secondary explosives
[DE89-010229] N90-10431
LASER BEAMS
Stimulated rotational Raman scattering
[DE89-016427] N90-10430
Efficient nonlinear conversion of laser diode pumped miniature solid state laser sources
[AD-A210708] N90-10433
Coupled multiline CW HF lasers: Experimental performance
[AD-A210844] N90-10434
Eye/sensor protection against laser irradiation organic nonlinear optical materials
[AD-A210599] N90-10531
Study of deposition of YBa2Cu3O7-x on cubic zirconia
[NASA-TM-102350] N90-10737
LASER CAVITIES
NTES laser facility for physics experiments: Building 981 high bay option
[DE89-014326] N90-10428
Coupled multiline CW HF lasers: Experimental performance
[AD-A210844] N90-10434
LASER DAMAGE
Treatment of laser-induced retinal injuries
[AD-A210284] N90-10526
LASER GYROSCOPES
Miniaturized triaxial laser gyro N90-10061
LASER INTERFEROMETRY
Shortwavelength coherent radiation: Generation and applications
[AD-A209847] N90-10427
LASER OUTPUTS
Laser initiation of secondary explosives
[DE89-010229] N90-10431
Multiline multimode CW chemical laser performance
[AD-A210613] N90-10432
Master oscillator with power amplifiers: Performance of a two-element CW HF phased-laser array
[AD-A211141] N90-10435
LASER PLASMA INTERACTIONS
Generation of 3/2 omega sub o radiation in inhomogeneous plasmas under the irradiation of intense electromagnetic waves
[DE89-015723] N90-10722
LASER PLASMAS
X-ray lithography studies of polysilane using a laser plasma X-ray source
[DE89-015390] N90-10266
Shortwavelength coherent radiation: Generation and applications
[AD-A209847] N90-10427

Generation of 3/2 omega sub o radiation in inhomogeneous plasmas under the irradiation of intense electromagnetic waves
[DE89-015723] N90-10722

LASER POWER BEAMING
Second Beamed Space-Power Workshop
[NASA-CP-3037] N90-10140
Power beaming options N90-10142
New energy conversion techniques in space, applicable to propulsion
[AIAA-79-1338] N90-10145
Laser energy conversion N90-10152
Overview of laser concepts N90-10154
Laser-powered lunar base N90-10156
Laser-powered Martian rover N90-10157
Low-earth-orbit to low-lunar-orbit laser freighter N90-10160
Earth orbit laser systems N90-10162
Laser diode array and transmission optics N90-10163
Laser thruster N90-10164

LASER PROPULSION
Second Beamed Space-Power Workshop
[NASA-CP-3037] N90-10140
Power beaming options N90-10142
Laser propulsion to earth orbit. Has its time come? N90-10143
Laser energy conversion N90-10152
Overview of laser concepts N90-10154
Low-earth-orbit to low-lunar-orbit laser freighter N90-10160
Laser propulsion option N90-10161
Earth orbit laser systems N90-10162
Laser thruster N90-10164

LASER PUMPING
Overview of laser concepts N90-10154
Efficient nonlinear conversion of laser diode pumped miniature solid state laser sources
[AD-A210708] N90-10433

LASER RANGE FINDERS
The 1988 year end report for road following at Carnegie-Mellon
[NASA-CR-185967] N90-10446

LASER WEAPONS
Stimulated rotational Raman scattering
[DE89-016427] N90-10430

LASER WELDING
Automation of fiber-optic pigtailing process: Laser welding demonstration program
[AD-A210351] N90-10707

LASERS
NTES laser facility for physics experiments: Building 381 high bay option
[DE89-014326] N90-10428
Custom diffraction gratings
[AD-A211002] N90-10712

LATTICES (MATHEMATICS)
Stochastic quantization
[AD-A210942] N90-10671

LAUNCH VEHICLES
Liquid rocket booster study. Volume 2, book 5, appendix 9: LRB alternate applications and evolutionary growth
[NASA-CR-183804] N90-10134
Liquid rocket booster study. Volume 2, book 6, appendix 10: Vehicle systems effects
[NASA-CR-183605] N90-10138

LEADING EDGE SWEEP
Stability of a supersonic boundary layer along a swept leading edge N90-10359
Direct numerical study of leading-edge contamination N90-10361

LEADING EDGES
Application of superplastically formed and diffusion bonded aluminum to a laminar flow control leading edge
[NASA-CR-178316] N90-10030
Laminar flow control perforated wing panel development
[NASA-CR-178166] N90-10187
Leading edge transition by contamination in hypersonic flow N90-10360
Experimental study of transition and leading edge contamination on swept wings N90-10362

LEARNING
On learning from exercises
[AD-A210593] N90-10574
Parallel processing and learning in simple systems
[AD-A210225] N90-10612
Some results on learning
[AD-A210591] N90-10624
Learning to make decisions: When incentives help and hinder
[AD-A210185] N90-10779

LEARNING THEORY
Biological investigations of adaptive networks: Neuronal control of conditioned responses
[AD-A211043] N90-10534

LEAST SQUARES METHOD
A FORTRAN program for the calculation of the calibration coefficients of a six-component strain gauge balance
[AD-A210375] N90-10599
Inherent bias in nonlinear least squares analysis of first-order kinetic data
[AD-A210677] N90-10651
Advances in regression: Use of models in spectroscopic data analysis
[AD-A210541] N90-10665

LIBRARIES
Planning an Integrated On-line Library System (IOLS)
[AD-A209406] N90-10783
Weeding policy and procedures: Information services
[AD-A210568] N90-10790

LIBRATION
A lunar far-side very low frequency array
[NASA-CP-3039] N90-10805

LIE GROUPS
Extended Weyl group for Kac-Moody algebras
[DE89-617525] N90-10634
N=1,2 supergravities in 2+1 dimensions as Chern-Simons theories
[DE89-612006] N90-10771

LIFE (DURABILITY)
US Air Force certification of castings N90-10232
Aerospace system unified life cycle engineering producibility measurement issues
[AD-A210937] N90-10607

LIFE CYCLE COSTS
Compatibility of fuel system components with high density fuel
[AD-A210361] N90-10027
Aerospace system unified life cycle engineering producibility measurement issues
[AD-A210937] N90-10607

LIFT
Experimental investigation of attachment-line transition in low-speed, high-lift wind-tunnel testing N90-10358

LIGHT (VISIBLE RADIATION)
Raman characterization of high temperature materials using an imaging detector
[DE89-016308] N90-10219

LIGHT AIRCRAFT
The effect of higher education variables on cadet performance during 1987 light aircraft training
[AD-A210199] N90-10536

LIGHT SCATTERING
An anisotropic shadowband correction for parameterized sky conditions and geometry
[DE89-014916] N90-10485

LIGHT SOURCES
Cockpit lighting compatibility with image intensification night imaging systems: Issues and answers
[AD-A210503] N90-10028

LIGHT TRANSMISSION
Coherent multichannel techniques for integrated broadband communications subscriber lines
[AD-A209323] N90-10312
Improved propagation models for discrete random media
[AD-A211085] N90-10327

LIGHTING EQUIPMENT
Cockpit lighting compatibility with image intensification night imaging systems: Issues and answers
[AD-A210503] N90-10028

LIGHTNING
Varistor-particle lightning arrestor connector performance under simulated extreme lightning currents
[DE89-012663] N90-10342
National Severe Storms Laboratory, fiscal year 1988
[PB89-156145] N90-10493
Data processing in lightning warning systems
[DE89-012495] N90-10502
The 1984 direct strike lightning data, part 1
[NASA-TM-87690-PT-1] N90-10505
The 1984 direct strike lightning data, part 2
[NASA-TM-87690-PT-2] N90-10506
The 1984 direct strike lightning data, part 3
[NASA-TM-87690-PT-3] N90-10507

LIGHTNING SUPPRESSION
Varistor-particle lightning arrestor connector performance under simulated extreme lightning currents
[DE89-012663] N90-10342

LIMITS (MATHEMATICS)
Limit analysis of welded tee end connections for hollow tubes
[PB89-191647] N90-10452

LINE SPECTRA
X-ray bright points and He I lambda 10830 dark points N90-10802

LINEAR ACCELERATORS
A battery-powered, solid state magnetic compressor with applications for high PRF accelerators and lasers
[DE89-015770] N90-10332

LINEAR PROGRAMMING
Primal barrier methods for linear programming
[AD-A210501] N90-10600

LINEAR SYSTEMS
Regulation of nonlinear and generalized linear systems
[AD-A207725] N90-10619
Studies in estimation theory, applications and implementations
[AD-A210712] N90-10653

LINEARITY
Improved estimation of the disturbance variance in a linear regression model
[AD-A210272] N90-10641

LINKAGES
Shape control of high degree-of-freedom variable geometry trusses N90-10122

LIPIDS
Electrical field dependence of protein conformation and channel function in lipid membranes of different compositions
[AD-A210236] N90-10222

LIQUID CRYSTALS
Mechanical properties, solubilities, and processabilities in the design of the first super-strong liquid-crystalline polymers
[DE89-009252] N90-10273

LIQUID FUELS
Very-low-frequency oscillations in liquid-fueled ramjets N90-10204
High energy density solid and liquid hydrocarbon fuels
[AD-A210195] N90-10304

LIQUID HYDROGEN
Liquid rocket booster study. Volume 2, book 1
[NASA-CR-183600] N90-10133

LIQUID OXYGEN
Liquid rocket booster study. Volume 2, book 1
[NASA-CR-183600] N90-10133

LIQUID PROPELLANT ROCKET ENGINES
Liquid rocket booster study. Volume 2, book 1
[NASA-CR-183600] N90-10133
Liquid rocket booster study. Volume 2, book 5, appendix 9: LRB alternate applications and evolutionary growth
[NASA-CR-183604] N90-10134
Liquid rocket booster study. Volume 2, book 4, appendices 6-8: Reports of Rocketdyne, Pratt and Whitney, and TRW
[NASA-CR-183603] N90-10135
Liquid rocket booster study. Volume 2, book 2, appendix 1: Trades studies
[NASA-CR-183601] N90-10136
Liquid rocket booster study. Volume 1: Executive summary
[NASA-CR-183599] N90-10137
Liquid rocket booster study. Volume 2, book 6, appendix 10: Vehicle systems effects
[NASA-CR-183605] N90-10138
Liquid rocket booster study. Volume 2, book 3, appendices 2-5: PPIP, transition plan, AMOS plan, and environmental analysis
[NASA-CR-183602] N90-10139
A rocket engine design expert system
[NASA-TM-102373] N90-10172
Combustion Instabilities in Liquid-Fuelled Propulsion Systems
[AGARD-CP-450] N90-10191
Experimental study on the stability of small rocket engines with storable liquid propellants N90-10196

LIQUID ROCKET PROPELLANTS
Liquid rocket booster study. Volume 2, book 4, appendices 6-8: Reports of Rocketdyne, Pratt and Whitney, and TRW
[NASA-CR-183603] N90-10135
Combustion Instabilities in Liquid-Fuelled Propulsion Systems
[AGARD-CP-450] N90-10191
Combustion instabilities in liquid-fueled propulsion systems: An overview N90-10192
Low frequency and high frequency combustion oscillation phenomena inside a rocket combustion chamber fed by liquid or gaseous propellants N90-10197

LIQUID SURFACES
Characterization of polymeric surfaces and interfaces
[AD-A210227] N90-10277

LIQUID-SOLID INTERFACES
Interpretation and modeling of the averaged equations for a fluid-solid flow N90-10388

LIQUIDS
Theoretical and experimental investigation of nonlinear optoacoustics in liquids
[AD-A210427] N90-10708

LITHIUM
The use of lithium batteries in biomedical devices
[AD-A210789] N90-10350

Lithium compensation of GaAs
[DE89-616080] N90-10740
LITHIUM OXIDES
Synthetic polypeptide composites for sensor applications
[AD-A210797] N90-10296
LITHIUM PERCHLORATES
Rechargeable lithium/polymer cathode batteries
[AD-A210978] N90-10354
LITHOGRAPHY
X-ray lithography studies of polysilane using a laser plasma X-ray source
[DE89-015390] N90-10266
A compact X-ray lithography lattice using superferric magnets
[DE89-013947] N90-10728
LOAD TESTING MACHINES
Development of a high temperature FZG-Ryder gear lubricant load capacity machine
[AD-A210799] N90-10449
LOAD TESTS
Fatigue crack initiation mechanics of metal aircraft structures
[AD-A210567] N90-10255
Development of a high temperature FZG-Ryder gear lubricant load capacity machine
[AD-A210799] N90-10449
Fracture and three dimensional stress analyses of 7075 aluminum projectile components under spin and inertia load
[AD-A210986] N90-10463
LOADING RATE
Influence of microstructure and microdamage processes on fracture at high loading rates
[AD-A210307] N90-10253
LOADS (FORCES)
A comparison of wind turbulence simulation models for stochastic loads analysis for horizontal-axis wind turbines
[DE89-009442] N90-10473
LOGIC CIRCUITS
Northeast Artificial Intelligence Consortium annual report for 1987. Volume 7, part A: Time oriented problem solving
[AD-A210331] N90-10622
LOGIC PROGRAMMING
Applications of algebraic logic and universal algebra to computer science
[AD-A210556] N90-10645
LONGITUDINAL STABILITY
Prediction of dynamic derivatives N90-10055
LOW CARBON STEELS
Mechanisms of strength and toughness in a microalloyed, precipitation hardened steel
[AD-A210571] N90-10256
LOW COST
Network of dedicated processors for finding lowest-cost map path
[NASA-CASE-NPO-17716-1-CU] N90-10608
LOW TEMPERATURE
Reactions of hydrogen chloride and boron trichloride with trimethylsilylamino groups
[AD-A209006] N90-10209
LOWER ATMOSPHERE
Correspondence between solar fine-scale structures in the corona, transition region, and lower atmosphere from collaborative observations N90-10804
LUBRICANT TESTS
Development of a high temperature FZG-Ryder gear lubricant load capacity machine
[AD-A210799] N90-10449
LUBRICATING OILS
Development of a high temperature FZG-Ryder gear lubricant load capacity machine
[AD-A210799] N90-10449
LUNAR BASES
Second Beamed Space-Power Workshop
[NASA-CP-3037] N90-10140
Office of exploration overview N90-10141
Laser-powered lunar base N90-10156
Power for the moon: Is microwave power beaming an option? N90-10158
Low-earth-orbit to low-lunar-orbit laser freighter N90-10160
Laser propulsion option N90-10161
Laser thruster N90-10164
A lunar far-side very low frequency array
[NASA-CP-3039] N90-10805
LUNAR EFFECTS
On analytic modeling of lunar perturbations of artificial satellites of the earth
[AD-A210440] N90-10078
LUNAR EVOLUTION
Office of exploration overview N90-10141
LUNAR EXPLORATION
Applicability of the beamed power concept to lunar rovers, construction, mining, explorers and other mobile equipment N90-10159
LUNAR ORBITS
Gyrotron development for space power beaming N90-10148
Low-earth-orbit to low-lunar-orbit laser freighter N90-10160
Laser propulsion option N90-10161
Earth orbit laser systems N90-10162
LUNAR ROVING VEHICLES
Applicability of the beamed power concept to lunar rovers, construction, mining, explorers and other mobile equipment N90-10159

M

MACH NUMBER
A study of high-lift airfoils at high Reynolds numbers in the Langley low-turbulence pressure tunnel
[NASA-TM-89125] N90-10002
Wind tunnel support system effects on a fighter aircraft model at Mach numbers from 0.6 to 2.0
[AD-A210614] N90-10010
Fluctuating pressures measured beneath a high-temperature, turbulent boundary layer on a flat plate at Mach number of 5
[NASA-TP-2947] N90-10680
MACHINING
High-speed machining of aluminum
[DE89-014011] N90-10441
MAGNESIUM ALLOYS
The improved corrosion resistance of ultra high purity magnesium alloy castings N90-10245
MAGNETIC COMPRESSION
A battery-powered, solid state magnetic compressor with applications for high PRF accelerators and lasers
[DE89-015770] N90-10332
MAGNETIC FIELD RECONNECTION
The observation of possible reconnection events in the boundary changes of solar coronal holes N90-10801
MAGNETIC FIELDS
On canonical quantization of the electromagnetic field in terms of field strengths
[DE89-615389] N90-10314
The 1984 direct strike lightning data, part 1
[NASA-TM-87690-PT-1] N90-10505
Observations of azimuthal asymmetry for certain FRC operating regimes
[DE89-015300] N90-10721
Mixed-valent and heavy fermions and related systems
[DE89-016335] N90-10743
Critical magnetic fields (H(sub c2), H(sub c1)) and kappa in YBa2(Cu0.98M0.02)3O(7+delta), M=Ni, Al, and Cu
[DE89-016412] N90-10745
Magnetic correlations in high T(sub c) oxides in the superconducting state
[DE89-016421] N90-10746
MAGNETIC FLUX
Gaussmeter determination of 302 stainless steel material condition
[BDX-613-3941] N90-10249
MAGNETIC MATERIALS
Genetic engineering of single-domain magnetic particles
[AD-A210332] N90-10521
MAGNETIC RESONANCE
Solvent relaxation in electron-transfer reactions: Comparisons between barrier-crossing dynamics in water and polar aprotic media
[AD-A210212] N90-10220
MAGNETIC SHIELDING
Measuring the shielding effectiveness of superconductive composites
[DE89-015164] N90-10180
MAGNETIC STORMS
The auroral energy deposition over the polar ionosphere during substorms
[AD-A210522] N90-10490
MAGNETO-OPTICS
Two photon absorption characterization
[AD-A210508] N90-10694
MAGNETOACOUSTIC WAVES
Scattering of an ICRF magnetosonic wave by plasma density turbulence
[DE89-015223] N90-10720
MAGNETOHYDRODYNAMIC FLOW
Computer simulation of plasma interactions near Titan N90-10816
MAGNETOHYDRODYNAMIC GENERATORS
Laser energy conversion N90-10152
MAGNETOHYDRODYNAMIC TURBULENCE
Numerical simulation of the compressible Orszag-Tang vortex
[AD-A210465] N90-10725
MAGNETOHYDRODYNAMIC WAVES
Kinetic effects in Alfven wave heating. Part 2: Propagation and absorption with a single minority species
[DE89-016619] N90-10724
MAGNETOHYDRODYNAMICS
MHD seed recovery and regeneration
[DE89-002711] N90-10715
MAGNETOMETERS
Gaussmeter determination of 302 stainless steel material condition
[BDX-613-3941] N90-10249
MAGNETOSHEATH
Plasma waves in the earth's foreshock, bow shock, and magnetosheath N90-10486
MAGNETRONS
Alternative fabrication techniques for high-efficiency CuInSe2 and CuInSe2-alloy films and cells
[DE89-009451] N90-10474
Massachusetts Institute of Technology Plasma Fusion Center
[DE89-016050] N90-10723
MAINTENANCE
A review of Australian and New Zealand investigations on aeronautical fatigue during the period April 1987 to March 1988
[AD-A210373] N90-10026
Field repair of composite materials in Army service: Planning for the future
[AD-A210732] N90-10190
MAN MACHINE SYSTEMS
CONSOLE: A CAD tandem for optimization-based design interacting with user-supplied simulators N90-10085
Hybrid vision activities at NASA Johnson Space Center N90-10552
Addressing user display requirements from a large and diverse user community
[DE89-011403] N90-10582
MAN COMPUTER INTERFACE
Northeast Artificial Intelligence Consortium annual report for 1987. Volume 5: Building an intelligent assistant: The acquisition, integration and maintenance of complex distributed tasks
[AD-A210330] N90-10621
MANAGEMENT PLANNING
Structure flow diagram generator
[PB89-195978] N90-10592
MANEUVERABILITY
Vortex induced characteristics of missiles in unsteady maneuvers N90-10057
Winged versus wingless airframes N90-10073
MANIFOLDS (MATHEMATICS)
Finding isolated zero points of complex polynomial mappings
[DE89-617523] N90-10633
MANIPULATORS
Simulation and control problems in elastic robots N90-10098
Flexible robot control: Modeling and experiments N90-10104
Experimental validation of flexible robot arm modeling and control N90-10113
Shape control of high degree-of-freedom variable geometry trusses N90-10122
Autonomous mobile robot research using the HERMIES-3 robot
[DE89-015916] N90-10443
Interchangeable end effector tools utilized on the protoflight manipulator arm
[NASA-CR-179374] N90-10447
Vision science and technology for supervised intelligent space robots N90-10548
Instrumentation and robotic image processing using top-down model control N90-10563
Optimized resolved rate control of seven-degree-of-freedom Laboratory Telerobotic Manipulator (LTM) with application to three-dimensional graphics simulation
[NASA-TP-2938] N90-10618
MANUALS
Manual of regulations and procedures for federal radio frequency management, May 1988 edition: Revisions for January 1989
[PB89-193791] N90-10320
Defense Technical Information Center cataloging guidelines
[AD-A211000] N90-10792
MANUFACTURING
Using computer design and simulation to improve manufacturing productivity
[AD-A210338] N90-10598

MAPPING
The 1988 year end report for road following at Carnegie-Mellon
[NASA-CR-185967] N90-10446
Network of dedicated processors for finding lowest-cost map path
[NASA-CASE-NPO-17716-1-CU] N90-10608
MARINE BIOLOGY
Biochemical cycling and fluxes between the deep euphotic zone and other oceanic realms
[PB89-152458] N90-10509
MARINE ENVIRONMENTS
International Conference on Aerosols and Background Pollution Abstracts
[AD-A210970] N90-10483
MARINE METEOROLOGY
Marine weather log, volume 32, number 3, summer 1988
[PB88-248075] N90-10491
US Navy regional climatic study of the United States Atlantic Coast and associated waters
[AD-A210198] N90-10503
MARKETING
Japanese structural ceramics research and development N90-10272
MARKOV CHAINS
Markov chain moment formulas for regenerative simulation
[AD-A210684] N90-10667
MARKOV PROCESSES
Optimal q-Markov COVER for finite precision implementation N90-10117
Discrete-time conversion for simulating finite-horizon Markov processes
[AD-A210683] N90-10666
Radon transform analysis of a probabilistic method for image generation
[AD-A207814] N90-10702
MARS (PLANET)
Office of exploration overview N90-10141
Laser-powered Martian rover N90-10157
MASS DISTRIBUTION
Theoretical statistics of zero-age cataclysmic variables N90-10810
MASS FLOW
A simple, mass balance model of carbon flow in a controlled ecological life support system
[NASA-TM-102151] N90-10571
MASS RATIOS
Theoretical statistics of zero-age cataclysmic variables N90-10810
MASS TRANSFER
PORFLO-3: A mathematical model for fluid flow, heat, and mass transport in variably saturated geologic media: Users manual, version 1.0
[DE89-013977] N90-10398
MASSIVELY PARALLEL PROCESSORS
The rewrite rule machine project
[AD-A210528] N90-10617
MATCHING
Extending matchings in planar graphs 4
[AD-A210315] N90-10643
MATHEMATICAL LOGIC
Applications of algebraic logic and universal algebra to computer science
[AD-A210556] N90-10645
MATHEMATICAL MODELS
ILS (Instrument Landing System) mathematical modeling study on the effects of proposed hangar construction west of runway 18R on localizer performance at Dallas-Fort Worth International Airport
[AD-A210631] N90-10019
The addition of Bendix MLS (Microwave Landing System) antenna patterns to MLS mathematical model
[AD-A210633] N90-10020
Compatibility of fuel system components with high density fuel
[AD-A210381] N90-10027
The measurement of boundary layers on a compressor blade in cascade. Volume 1: Experimental technique, analysis and results
[NASA-CR-185118-VOL-1] N90-10038
Missile Datcom: Enhancements for design applications N90-10054
Aeroelastic tailoring procedure for controlling fin hinge moments N90-10058
Identification of stability and control parameters of a brilliant ammunition N90-10065
On analytic modeling of lunar perturbations of artificial satellites of the earth
[AD-A210440] N90-10078
DYSCO: A software system for modeling general dynamic systems N90-10089
Lumped mass formulations for modeling flexible body systems N90-10091
Explicit modeling and computational load distribution for concurrent processing simulation of the space station N90-10096
Simulation and control problems in elastic robots N90-10098
Linearized flexibility models in multibody dynamics and control N90-10099
Flexible robot control: Modeling and experiments N90-10104
Modifying high-order aeroelastic math model of a jet transport using maximum likelihood estimation N90-10106
Automated model formulation for time-varying flexible structures N90-10107
Numerically efficient algorithm for model development of high-order systems N90-10108
On modelling nonlinear damping in distributed parameter systems N90-10109
Flexible aircraft dynamic modeling for dynamic analysis and control synthesis N90-10112
Aircraft modal supression system: Existing design approach and its shortcomings N90-10115
Modeling and stabilization of large flexible space stations N90-10120
System identification for large space structures N90-10126
Boost-phase discrimination research activities
[NASA-TM-101889] N90-10176
Dynamic instability characteristics of aircraft turbine engine combustors N90-10195
Very-low-frequency oscillations in liquid-fueled ramjets N90-10204
Combustion-driven oscillation in large combustion systems for power generation N90-10207
Reaction of oxygen with allene
[DE89-015219] N90-10216
Direct numerical simulation of turbulent free shear flows
[AD-A210161] N90-10218
Approximate simulation model for analysis and optimization in engineering system design
[NASA-TM-101616] N90-10308
New electrodynamic and electrostatic models with applications to antenna theory, superconductor slots, and lasers N90-10316
Improved propagation models for discrete random media
[AD-A211085] N90-10327
Statistical modeling of electrical components
[BDX-613-3939] N90-10336
Experimental study of instability modes in a three-dimensional boundary layer N90-10369
Constitutive Relationships and Models in Continuum Theories of Multiphase Flows --- conferences
[NASA-CP-3047] N90-10385
Iterative performance and an adaptive procedure for viscous flow problems N90-10397
PORFLO-3: A mathematical model for fluid flow, heat, and mass transport in variably saturated geologic media: Users manual, version 1.0
[DE89-013977] N90-10398
Global existence and asymptotic stability for a nonlinear integrodifferential equation modeling heat flow
[AD-A210647] N90-10408
Similarity solutions that give rise to hyperbolicity and change of type in steady flow of a viscoelastic fluid
[AD-A210920] N90-10410
Symmetry breaking bifurcations and the growth of chaos in a rotating fluid
[AD-A210969] N90-10411
Design and operating characteristics of a CW relevant quasi-optical gyrotron with variable mirror separation
[AD-A210611] N90-10425
The MHOST finite element program: 3-D inelastic analysis methods for hot section components. Volume 2: User's manual
[NASA-CR-182235-VOL-2] N90-10450
Global/local stress analysis of composite structures
[NASA-TM-101640] N90-10456
Analysis and test of a 16-foot radial rib reflector developmental model
[NASA-TM-101648] N90-10457
Image-based terrain modeling with thematic mapper applied to resolving the limit of Holocene Lake expansion in the Great Salt Lake Desert, Utah, part 1
[NASA-CR-185913] N90-10465
Evaluation of the North Atlantic seasonal nitrogen model, version 2
[DE89-016157] N90-10515
Surface wave ray tracing and Ms:yield determination in a laterally heterogeneous earth
[AD-A210241] N90-10516
Managing human exposure and health risks: An integrated approach and the role of uncertainty
[DE89-008811] N90-10525
Tracking performance evaluation
[AD-A210499] N90-10540
A simple, mass balance model of carbon flow in a controlled ecological life support system
[NASA-TM-102151] N90-10571
Tests of various finite difference algorithms applied to a simple water vapor transport problem on a staggered grid
[AD-A210229] N90-10596
Adaptive robust control N90-10620
Numerical optimization in Hilbert space using inexact function and gradient evaluations
[NASA-CR-181926] N90-10640
On lower confidence for PCS in truncated location parameter models
[AD-A210274] N90-10661
A unified approach to estimating tail behavior
[AD-A210961] N90-10672
Analytic theory for the selection of Saffman-Taylor fingers in the presence of thin film effects
[NASA-CR-181910] N90-10677
A symplectic coherent beam-beam model
[DE89-015386] N90-10701
Numerical simulation of the compressible Orszag-Tang vortex
[AD-A210465] N90-10725
Effects of stress on judgment and decision making in dynamic tasks
[AD-A210605] N90-10781
MATRICES (MATHEMATICS)
Studies in estimation theory, applications and implementations
[AD-A210712] N90-10653
The computation and use of the asymptotic covariance matrix for measurement error models
[PB89-215321] N90-10659
MAXIMUM LIKELIHOOD ESTIMATES
Modifying high-order aeroelastic math model of a jet transport using maximum likelihood estimation N90-10106
Advances in regression: Use of models in spectroscopic data analysis
[AD-A210541] N90-10665
MAXWELL EQUATION
Improved propagation models for discrete random media
[AD-A211085] N90-10327
MEASURING INSTRUMENTS
Method and apparatus for determining time, direction and composition of impacting space particles
[NASA-CASE-LAR-13392-1-CU] N90-10132
Three-in-one gage
[NASA-CR-183714] N90-10413
Development of an automated probe for thermal conductivity measurements
[PB89-209324] N90-10419
Data processing in lightning warning systems
[DE89-012495] N90-10502
MECHANICAL PROPERTIES
Failure behavior of PEEK and its short-fiber composite systems
[AD-A210729] N90-10189
Castings, from theory to practical application N90-10236
Combined advanced foundry and quality control techniques to enhance reliability of castings for the aerospace industry N90-10240
Thin walled cast high-strength structural parts N90-10242
Advances in the technology of titanium castings N90-10243
Properties of HY-100 for naval construction
[MRL-R-1149] N90-10247
The quantitative analysis of fracture surfaces using fractals
[DE89-015361] N90-10250
Dynamically compressed metals: Theory
[AD-A210741] N90-10257
Investigation of the pyrometallurgical, physical and mechanical behavior of weld metal
[AD-A211114] N90-10258
Ceramic components in machines, Cologne and Aachen, West Germany; Maastricht, The Netherlands and Brussels, Belgium
[DE89-015831] N90-10264
Japanese structural ceramics research and development N90-10272
Mechanical properties, solubilities, and processabilities in the design of the first super-strong liquid-crystalline polymers
[DE89-009252] N90-10273
Structure-mechanical property relationships in ion implanted ceramics
[DE89-010129] N90-10274

Synthesis and interfacial properties of new generation polyurethane systems
[AD-A210446] N90-10286
Synthesis and physical properties of poly(perfluoroalkylether) urethanes
[AD-A210500] N90-10287
A design assessment for metallic pressure vessels circumferentially reinforced with a pre-tensioned high-specific-strength anisotropic composite overwind
[AD-A209106] N90-10453
Ceramic processing of bulk high-T(sub c) superconductors
[DE89-015703] N90-10736

MEDICAL ELECTRONICS
The use of lithium batteries in biomedical devices
[AD-A210789] N90-10350

MELT SPINNING
Establishment and initial operation of a resource facility for RSR (Rapid Solidification Rate) processed alloys in pilot quantities
[AD-A210369] N90-10283

MEMBRANES
Electrical field dependence of protein conformation and channel function in lipid membranes of different compositions
[AD-A210236] N90-10222
Polyheterocycle Langmuir-Blodgett films
[AD-A210625] N90-10292
Preparation and evaluation of composite membranes for zinc/bromine storage batteries
[DE89-009931] N90-10339
Stretched-membrane heliostats for solar central-receiver power plants
[DE89-016034] N90-10476
Electroporation: Theory of basic mechanisms
[AD-A210196] N90-10520

MEMORY
Integration of neurobiological and computational analyses of the neural network essentials for conditioned taste aversions
[AD-A210228] N90-10537

MEMORY (COMPUTERS)
The MHOST finite element program: 3-D inelastic analysis methods for hot section components. Volume 3: Systems' manual
[NASA-CR-182236] N90-10451
Sparse distributed memory overview N90-10561
Effective resource utilization for multiprocessor join execution
[DE89-016303] N90-10595
Shared memory versus message passing architectures: An application based study
[AD-A210312] N90-10615

MENTAL PERFORMANCE
Models of mental functioning
[AD-A210456] N90-10538
Toward a theory of representation design
[AD-A210885] N90-10670

MERCURY AMALGAMS
Solvent effects on the kinetics of electroreduction of Cu(I) at mercury
[AD-A209423] N90-10211
Potential dependence of the elementary steps in the kinetics of electrode reactions involving amalgam formation
[AD-A209424] N90-10212

MESOMETEOROLOGY
Coordination of mesoscale meteorological research between ASL and European groups
[AD-A210902] N90-10508

MESOSCALE PHENOMENA
Coordination of mesoscale meteorological research between ASL and European groups
[AD-A210902] N90-10508

MESSAGE PROCESSING
Robotic vehicle message format
[AD-A210996] N90-10627

METABOLISM
Molecular biology and physiology of methanogenic archaebacteria
[AD-A210399] N90-10522

METAL COATINGS
Multiple internal reflection Fourier transform infrared spectroscopy studies of thiocyanate adsorption on silver and gold
[AD-A210245] N90-10223

METAL FATIGUE
Fatigue crack initiation mechanics of metal aircraft structures
[AD-A210567] N90-10255

METAL FILMS
Structure of amorphous silicon alloy films
[DE89-009441] N90-10734

METAL FOILS
Stretched-membrane heliostats for solar central-receiver power plants
[DE89-016034] N90-10476

METAL OXIDE SEMICONDUCTORS
Bias and oxide thickness dependence of trapped charge buildup in MOS devices
[AD-A210264] N90-10757

METAL SHEETS
Micromechanisms of surface friction in zinc electrogalvanized steel sheets
[DE89-011819] N90-10440

METAL SURFACES
Structural and surface characterization of dispersed metal catalysts
[DE89-014530] N90-10208

METALLIC GLASSES
Establishment and initial operation of a resource facility for RSR (Rapid Solidification Rate) processed alloys in pilot quantities
[AD-A210369] N90-10283

METALLIC PLASMAS
Dynamically compressed metals: Theory
[AD-A210741] N90-10257

METALS
The structure determination of molecular adsorbates with large unit cells or lattice-gas disorder on metal surfaces
[AD-A210926] N90-10230
Investigation of the pyrometallurgical, physical and mechanical behavior of weld metal
[AD-A211114] N90-10258

METASTABLE STATE
Development of metastable processing paths for high temperature alloys
[AD-A210550] N90-10254
Ordered structures and metastable alloys grown by OMVPE
[DE89-016370] N90-10744

METEOROLOGICAL CHARTS
Meteorological support: Descriptions of application programs for accessing and displaying data
[PB89-194625] N90-10500
Research highlights of the NMC (National Meteorological Center) Development Division: 1987-1988
[PB89-206478] N90-10501

METEOROLOGICAL INSTRUMENTS
Meeting Review: Workshop on Airborne Instrumentation
[PB89-174775] N90-10032
A program to improve performance of AFGL (Air Force Geophysical Laboratory) automated present weather observing sensors
[AD-A207669] N90-10495

METEOROLOGICAL PARAMETERS
Atmospheric transmissivity update - 1988
[AD-A209130] N90-10484
Marine weather log, volume 32, number 3, summer 1988
[PB88-248075] N90-10491
National Severe Storms Laboratory, fiscal year 1988
[PB89-156145] N90-10493
A case study evaluation of satellite-derived rainfall estimates and their application to numerical model precipitation forecast verification
[PB89-194591] N90-10499

METEOROLOGICAL RADAR
A study of the impact of simulated satellite lidar wind observations
[AD-A210430] N90-10488

METEOROLOGICAL SATELLITES
Thermodynamic and dynamic processes in the updraft region of GALE (Genesis of Atlantic Lows Experiment) IOP (Intensive Observation Period) 9
[AD-A208139] N90-10496
A case study evaluation of satellite-derived rainfall estimates and their application to numerical model precipitation forecast verification
[PB89-194591] N90-10499
A study of the impact of simulated 183 GHz water vapor retrievals on numerical weather prediction
[AD-A210431] N90-10504

METEOROLOGICAL SERVICES
Forecasting convection with the AFOS (Automation of Field Operations and Services) data analysis programs. (ADAP-version 2.0) (AFOS data analysis programs-version 2.0)
[PB89-145940] N90-10492
National Severe Storms Laboratory, fiscal year 1988
[PB89-156145] N90-10493
A program to improve performance of AFGL (Air Force Geophysical Laboratory) automated present weather observing sensors
[AD-A207669] N90-10495
Meteorological support: Descriptions of application programs for accessing and displaying data
[PB89-194625] N90-10500

METHANE
Molecular biology and physiology of methanogenic archaebacteria
[AD-A210399] N90-10522

METHYL ALCOHOL
Liquid rocket booster study. Volume 2, book 1
[NASA-CR-183600] N90-10133

MICROBALANCES
Quartz crystal microbalance studies of electrochemical growth of conducting polymers
[AD-A210788] N90-10295

MICROBURSTS (METEOROLOGY)
Effects of stress on judgment and decision making in dynamic tasks
[AD-A210605] N90-10781

MICROELECTRONICS
Vacuum microelectronics for beam power and rectennas N90-10146
Polyheterocycle Langmuir-Blodgett films
[AD-A210625] N90-10292
Micro-cavity integrable vacuum diodes and triodes
[DE89-016649] N90-10344
Performance of the CAMEX64 silicon strip readout chip
[DE89-014015] N90-10747

MICROMECHANICS
Hygrothermal effects on the complex moduli of composite laminates N90-10182
Micromechanisms of surface friction in zinc electrogalvanized steel sheets
[DE89-011819] N90-10440

MICROSTRIP ANTENNAS
Millimeter-wave/infrared rectenna development at Georgia Tech N90-10147

MICROSTRUCTURE
Microstructure morphology and quality of Al-Si castings N90-10244
The quantitative analysis of fracture surfaces using fractals
[DE89-015361] N90-10250
Influence of microstructure and microdamage processes on fracture at high loading rates
[AD-A210307] N90-10253
Mechanisms of strength and toughness in a microalloyed, precipitation hardened steel
[AD-A210571] N90-10256
Ceramic components in machines, Cologne and Aachen, West Germany; Maastricht, The Netherlands and Brussels, Belgium
[DE89-015831] N90-10264
Structure-mechanical property relationships in ion implanted ceramics
[DE89-010129] N90-10274
Structure of amorphous silicon alloy films
[DE89-009441] N90-10734
Ceramic processing of bulk high-T(sub c) superconductors
[DE89-015703] N90-10736

MICROWAVE ANTENNAS
Power for the moon: Is microwave power beaming an option? N90-10158

MICROWAVE INTERFEROMETERS
Simultaneous multiple frequency interferometry: An application of homodyne phase measurement
[DE89-013975] N90-10719

MICROWAVE LANDING SYSTEMS
ILS/MLS comparison tests at Miami/Tamiami, Florida Airport
[ACD-330] N90-10018
The addition of Bendix MLS (Microwave Landing System) antenna patterns to MLS mathematical model
[AD-A210633] N90-10020

MICROWAVE POWER BEAMING
Second Beamed Space-Power Workshop
[NASA-CP-3037] N90-10140
Power beaming options N90-10142
History and status of beamed power technology and applications at 2.45 Gigahertz N90-10150
Overview of microwave concepts N90-10155
Power for the moon: Is microwave power beaming an option? N90-10158
Microwave beam power N90-10165

MICROWAVE SOUNDING
A study of the impact of simulated 183 GHz water vapor retrievals on numerical weather prediction
[AD-A210431] N90-10504

MICROWAVE TRANSMISSION
Power for the moon: Is microwave power beaming an option? N90-10158
An experimental study of microwave transmission through a decaying plasma
[AD-A210586] N90-10726

MICROWAVES
Antenna technology for beamed space-power N90-10149
Technical options for high average power free electron milimeter-wave and laser devices N90-10151
Overview of microwave concepts N90-10155
Power for the moon: Is microwave power beaming an option? N90-10158
Microwave beam power N90-10165
Laboratory measurements of microwave and millimeter-wave properties of planetary atmospheric constituents
[NASA-CR-185914] N90-10815

MIDLATITUDE ATMOSPHERE
Numerical simulations of a midlatitude squall line N90-10497

MILITARY OPERATIONS
Communications Data Base (CDB), phase 3 (with software documentation)
[AD-A210540] N90-10789

MILITARY TECHNOLOGY
Encyclopedia of US Air Force aircraft and missile systems. Volume 2: Post-World War 2 bombers, 1945-1973
[AD-A209273] N90-10001
Consumer electronics testing to fast-rise EMP (Electromagnetic Pulse) VEMPS (Vertical Electromagnetic Pulse Simulator) 2 development
[AD-A210505] N90-10323

MILLIMETER WAVES
Millimeter-wave/infrared rectenna development at Georgia Tech N90-10147
Laboratory measurements of microwave and millimeter-wave properties of planetary atmospheric constituents
[NASA-CR-185914] N90-10815

MILLING
PMR graphite engine duct development
[NASA-CR-182228] N90-10037

MINERAL OILS
Development of a high temperature FZG-Ryder gear lubricant load capacity machine
[AD-A210799] N90-10449

MINIATURIZATION
Miniaturized triaxial laser gyro N90-10061
Efficient nonlinear conversion of laser diode pumped miniature solid state laser sources
[AD-A210708] N90-10433
Effects of miniature CRT (Cathode Ray Tube) location upon primary and secondary task performances
[AD-A210223] N90-10573

MINIMAX TECHNIQUE
Periodic solutions of spatially periodic Hamiltonian systems
[AD-A210645] N90-10649

MIRRORS
Design and operating characteristics of a CW relevant quasi-optical gyrotron with variable mirror separation
[AD-A210611] N90-10425

MIS (SEMICONDUCTORS)
Properties of devices prepared with epitaxial layers on InP
[AD-A210304] N90-10759

MISSILE CONTROL
Stability and Control of Tactical Missile Systems
[AGARD-CP-451] N90-10050
The present status and the future of missile aerodynamics N90-10051
Prediction of the aerodynamic stability of missiles N90-10052
Missile Datcom: Enhancements for design applications N90-10054
Vortex induced characteristics of missiles in unsteady maneuvers N90-10057
Alternative polar homing strategies N90-10059
How to control unstable missile airframes: Methodology and limitations N90-10060
Miniaturized triaxial laser gyro N90-10061
Remote control missile model test N90-10063
Investigations of thrust vector control for high-alpha pitchover N90-10067
A structured singular value approach to missile autopilot analysis 2 N90-10068
Analysis and testing of a high performance air-air missile N90-10069
Aeroelastic analysis of missile control surfaces with structural non-linearity N90-10071

MISSILE DESIGN
Stability and Control of Tactical Missile Systems
[AGARD-CP-451] N90-10050
The present status and the future of missile aerodynamics N90-10051
Prediction of stability derivatives for missiles using the HISSS panel code N90-10053
Missile Datcom: Enhancements for design applications N90-10054
Prediction of dynamic derivatives N90-10055
Prediction of tactical missile dynamics N90-10056
Vortex induced characteristics of missiles in unsteady maneuvers N90-10057
Aeroelastic tailoring procedure for controlling fin hinge moments N90-10058
Alternative polar homing strategies N90-10059
Remote control missile model test N90-10063
Wind tunnel tests: The role of the model N90-10064
Validation of missile simulation N90-10066
Marginal release disturbances on advanced missiles N90-10070
Experience gained in the improvement of the Aspide aerodynamic configuration for the surface to air role N90-10072
Winged versus wingless airframes N90-10073

MISSILE DETECTION
Tracking performance evaluation
[AD-A210499] N90-10540

MISSILE SYSTEMS
Encyclopedia of US Air Force aircraft and missile systems. Volume 2: Post-World War 2 bombers, 1945-1973
[AD-A209273] N90-10001

MISSILE TRACKING
Tracking performance evaluation
[AD-A210499] N90-10540

MISSILES
Encyclopedia of US Air Force aircraft and missile systems. Volume 2: Post-World War 2 bombers, 1945-1973
[AD-A209273] N90-10001
Flexible missile autopilot design studies with PC-MATLAB/386 N90-10088

MISSION PLANNING
Space station RT and E utilization study
[NASA-CR-181707] N90-10129

MIXED CRYSTALS
Monolayer formation characteristics of novel organic molecules with nonlinear optically active moieties
[AD-A210496] N90-10693

MIXING LAYERS (FLUIDS)
Trailing-edge sweep and three-dimensional vortex interactions in jets and mixing layers N90-10379
Numerical simulation of coherent structures in an incompressible mixing layer N90-10383

MODEL REFERENCE ADAPTIVE CONTROL
The role of sensor directed, model based control in robotics
[DE89-014133] N90-10442
Experience with model based display for advanced diagnostics and control
[DE89-015693] N90-10469

MODELS
Models of mental functioning
[AD-A210456] N90-10538
Acoustic test and analysis of a counterrotating prop-fan model
[NASA-CR-179590] N90-10683

MODFETS
High energy neutron irradiation effects in GaAs modulation-Doped Field Effect Transistors (MODFETS): Threshold voltage
[AD-A210502] N90-10763

MODULATION
Use of depletion edge translation for high-speed modulation and switching of lightwaves
[AD-A211186] N90-10713

MODULATORS
Use of depletion edge translation for high-speed modulation and switching of lightwaves
[AD-A211186] N90-10713

MODULUS OF ELASTICITY
Development of elastomeric polypeptide biomaterials
[AD-A210295] N90-10280

MOISTURE CONTENT
Hygrothermal effects on the complex moduli of composite laminates N90-10182

MOLDS
Advances in the technology of titanium castings N90-10243

MOLECULAR BEAM EPITAXY
Use of depletion edge translation for high-speed modulation and switching of lightwaves
[AD-A211186] N90-10713
Experimental investigations of transport and optical properties of 3-5 quantum well structures grown via molecular beam epitaxy under optimal growth conditions
[AD-A210269] N90-10758
The growth of gallium nitride films via the innovative technique of atomic layer epitaxy
[AD-A210380] N90-10760
Trap gettering by isoelectronic doping of p-GaAs and n-GaAs grown by molecular beam epitaxy
[AD-A211162] N90-10769

MOLECULAR BEAMS
Reaction of oxygen with allene
[DE89-015219] N90-10216

MOLECULAR BIOLOGY
Molecular biology and physiology of methanogenic archaebacteria
[AD-A210399] N90-10522
Army Science Conference Proceedings (16th) held in Fort Monroe, Virginia on 25-27 October 1988: Addenda
[AD-A210235] N90-10827

MOLECULAR ENERGY LEVELS
Multiline multimode CW chemical laser performance
[AD-A210613] N90-10432
Solvent effects on intervalence electron-transfer energies for biferrocene cations: Comparisons with molecular models of solvent reorganization
[AD-A210263] N90-10691

MOLECULAR EXCITATION
Controlling photoinduced electron transfer rates in donor-spacer-acceptor molecules by changing the electronic properties of the spacer
[DE89-015128] N90-10735

MOLECULAR INTERACTIONS
Monte Carlo simulations of small solute/solvent clusters: Cluster properties and phase transitions
[AD-A209559] N90-10684

MOLECULAR ORBITALS
Bonding in transition metal silyl dimers. Molecular orbital theory
[AD-A208269] N90-10260
Computational modeling of pi-conjugated polyradicals
[AD-A210573] N90-10648
A structural basis for electron transfer in bacterial photosynthesis
[DE89-015702] N90-10687

MOLECULAR RELAXATION
Solvent relaxation in electron-transfer reactions: Comparisons between barrier-crossing dynamics in water and polar aprotic media
[AD-A210212] N90-10220

MOLECULAR ROTATION
Multiline multimode CW chemical laser performance
[AD-A210613] N90-10432

MOLECULAR SPECTROSCOPY
Two photon absorption characterization
[AD-A210508] N90-10694

MOLECULAR STRUCTURE
International Conference on Organometallic Chemistry (13th) held in Torino, Europe on 4-9 September 1988: Abstracts
[AD-A210617] N90-10178
Control of synthetic peptide tertiary structure
[AD-A210339] N90-10281
Hierarchical structure in polymeric solids and its influence on properties
[AD-A210918] N90-10297
Monolayer formation characteristics of novel organic molecules with nonlinear optically active moieties
[AD-A210496] N90-10693

MOLECULAR WEIGHT
Synthesis and interfacial properties of new generation polyurethane systems
[AD-A210446] N90-10286

MOLECULES
Combining spontaneous molecular assembly with microfabrication to pattern surfaces: Selective binding of isonitriles to platinum microwires and characterization by electrochemistry and surface spectroscopy
[AD-A209528] N90-10213
Characterization of polymeric surfaces and interfaces
[AD-A210227] N90-10277
Monolayer formation characteristics of novel organic molecules with nonlinear optically active moieties
[AD-A210496] N90-10693

MOLYBDENUM COMPOUNDS
Face-specific interaction of MoS4(2-1) with oriented crystals of (0001) CdX (X = Se, S)
[AD-A209519] N90-10732

MOMENTS
An integrated CFD/experimental analysis of aerodynamic forces and moments
[NASA-TM-102195] N90-10006

MOMENTUM
An algorithm to calculate the beam momentum distribution from flying wire profiles
[DE89-015587] N90-10418

MONITORS
An appraisal of a number of power assessment procedures being proposed for use in Chinook-Lycoming T55 engine
[AD-A210482] N90-10041

MONOCHROMATORS
Design of grazing incidence monochromators involving unconventional gratings
[DE89-016341] N90-10704

MONOMERS
Monomers, polymers and transition metal complexes based upon carboranes
[AD-A210226] N90-10221
UV-curable polyurethane-methacrylate co-networks and interpenetrating networks
[AD-A210445] N90-10285
MONOTONE FUNCTIONS
A special case of second-order strictness analysis
[AD-A210829] N90-10656
MONTE CARLO METHOD
A structured singular value approach to missile autopilot analysis 2 N90-10068
Tracking performance evaluation
[AD-A210499] N90-10540
The computation and use of the asymptotic covariance matrix for measurement error models
[PB89-215321] N90-10659
Monte Carlo simulations of small solute/solvent clusters: Cluster properties and phase transitions
[AD-A209559] N90-10684
MOODS
Daytime sleepiness, performance, mood, nocturnal sleep: The effect of benzodiazepine and caffeine on their relationship
[AD-A210915] N90-10533
MOON
On analytic modeling of lunar perturbations of artificial satellites of the earth
[AD-A210440] N90-10078
Office of exploration overview N90-10141
A lunar far-side very low frequency array
[NASA-CP-3039] N90-10805
MORPHOLOGY
Microstructure morphology and quality of Al-Si castings N90-10244
Epitaxial GaAs on SOI wafers
[AD-A209009] N90-10729
Morphological aspects of the friction of hot-filament-grown diamond thin films
[DE89-015986] N90-10750
MOTION
Motion detection in astronomical and ice floe images N90-10558
MOTION PERCEPTION
Human motion perception: Higher-order organization N90-10553
Factors affecting the perception of transparent motion N90-10559
Ames vision group research overview N90-10566
MOTOR VEHICLES
Waveform generator signal processing software
[PB89-192660] N90-10587
MULTICHANNEL COMMUNICATION
Coherent multilchannel techniques for integrated broadband communications subscriber lines
[AD-A209323] N90-10312
MULTILAYER INSULATION
Composite multilayer insulations for thermal protection of aerospace vehicles
[NASA-TM-101071] N90-10183
MULTIPHASE FLOW
Analysis of a model and sequential numerical method for thermal reservoir simulation
[DE89-015117] N90-10384
Constitutive Relationships and Models in Continuum Theories of Multiphase Flows — conferences
[NASA-CP-3047] N90-10385
Stress in dilute suspensions N90-10389
Scaling and modeling of turbulent suspension flows N90-10393
Turbulence kinetic energy equation for dilute suspensions N90-10394
MULTIPHOTON ABSORPTION
Shortwavelength coherent radiation: Generation and applications
[AD-A209847] N90-10427
MULTIPLEXING
Some significant results from testing a Remote Multiplexing Unit (RMU) for temperature-induced errors
[DE89-009432] N90-10421
Performance of the CAMEX64 silicon strip readout chip
[DE89-014015] N90-10747
MULTIPROCESSING (COMPUTERS)
A multiprocessor architecture using modular arithmetic for very high precision computation
[AD-A208154] N90-10579
A common distributed language approach to software integration
[NASA-CR-185499] N90-10584
Effective resource utilization for multiprocessor join execution
[DE89-016303] N90-10595
Exploring the benefits of multiple hardware contexts in a multiprocessor architecture: Preliminary results
[AD-A210349] N90-10616
MULTIVARIATE STATISTICAL ANALYSIS
On two polynomial spaces associated with a box spline
[AD-A210559] N90-10646

N

NACELLES
Analysis of results from wind tunnel tests of inlets for an advanced turboprop nacelle installation
[NASA-CR-174937] N90-10011
NASA PROGRAMS
Development of pressure containment and damage tolerance technology for composite fuselage structures in large transport aircraft
[NASA-CR-3996] N90-10186
Vision Science and Technology at NASA: Results of a Workshop
[NASA-TM-102214] N90-10542
Vision science and technology at NASA: Results of a workshop: Executive summary N90-10543
NASTRAN
Aeroelastic analysis of missile control surfaces with structural non-linearity N90-10071
Control/structure interaction methods for space station power systems N90-10087
Composite Blade Structural Analyzer (COBSTRAN) theoretical/programmer's manual
[NASA-TM-101958] N90-10181
NAVIER-STOKES EQUATION
Stability and transition of three-dimensional boundary layers N90-10357
Direct numerical study of leading-edge contamination N90-10361
Numerical investigation of the effects of longitudinal vortices on the onset of transition in a flat plate boundary layer N90-10363
Primary and secondary stability analysis applied to the DFVLR-transition swept-plate experiment N90-10371
Numerical solution of three-dimensional unsteady flows: Application to instability problems N90-10375
Numerical simulation of turbulent plane channel flows N90-10382
A composite velocity procedure for the three-dimensional reduced Navier-Stokes equations N90-10396
Two counter-rotating vortices approaching a free surface in a viscous fluid
[AD-A210495] N90-10404
A high-order Lagrangian-decoupling method for the incompressible Navier-Stokes equations
[NASA-CR-181903] N90-10631
NAVIGATION
The role of sensor directed, model based control in robotics
[DE89-014133] N90-10442
NAVIGATION AIDS
Guidance simulation and test support for differential GPS flight experiment
[NASA-CR-177471] N90-10021
NAVY
Properties of HY-100 for naval construction
[MRL-R-1149] N90-10247
NEAR FIELDS
New test techniques to evaluate near field effects for supersonic store carriage and separation N90-10062
NEODYMIUM LASERS
Overview of laser concepts N90-10154
NEPTUNE (PLANET)
NASA Voyager 2 Neptune encounter press kit
[NASA-TM-101851] N90-10076
NETWORK ANALYSIS
Networks for image acquisition, processing and display N90-10545
NEURAL NETS
Real-time support for high performance aircraft operation
[NASA-CR-185475] N90-10075
Integration of neurobiological and computational analyses of the neural network essentials for conditioned taste aversions
[AD-A210228] N90-10537
Parallel processing and learning in simple systems
[AD-A210225] N90-10612
Regulation of nonlinear and generalized linear systems
[AD-A207725] N90-10619
NEUROLOGY
Biomedical influences on spinal cord function
[AD-A210311] N90-10527
Excitatory amino acids as transmitters in the brain
[AD-A210685] N90-10532
Biological investigations of adaptive networks: Neuronal control of conditioned responses
[AD-A211043] N90-10534
Parallel processing and learning in simple systems
[AD-A210225] N90-10612
NEUROMUSCULAR TRANSMISSION
Excitatory amino acids as transmitters in the brain
[AD-A210685] N90-10532
Extrathalamic modulation of cortical function
[AD-A211044] N90-10535
NEUROPHYSIOLOGY
Biological investigations of adaptive networks: Neuronal control of conditioned responses
[AD-A211043] N90-10534
NEUTRINO BEAMS
Fermilab fixed target beams from the main injector
[DE89-014355] N90-10697
NEUTRINOS
Research program in theoretical high energy physics
[DE89-013963] N90-10695
Astrophysical and cosmological constraints to neutrino properties
[NASA-CR-185031] N90-10809
NEUTRON DIFFRACTION
Structural aspects of the phase separation in La2CuO4.032
[DE89-016183] N90-10751
NEUTRON IRRADIATION
High energy neutron irradiation effects in GaAs modulation-Doped Field Effect Transistors (MODFETS): Threshold voltage
[AD-A210502] N90-10763
NEUTRON SCATTERING
Magnetic correlations in high T(sub c) oxides in the superconducting state
[DE89-016421] N90-10746
NEUTRONS
Energy dependent transport problem with generalized boundary conditions
[DE89-617843] N90-10676
NICKEL
Structural and surface characterization of dispersed metal catalysts
[DE89-014530] N90-10208
NICKEL ALLOYS
Friction and wear of oxide-ceramic sliding against IN-718 nickel base alloy at 25 to 800 C in atmospheric air
[NASA-TM-102291] N90-10262
NIGHT VISION
Cockpit lighting compatibility with image intensification night imaging systems: Issues and answers
[AD-A210503] N90-10028
NIOBIUM ALLOYS
Emittance, catalysis, and dynamic oxidation of Ti-14Al-21Nb
[NASA-TP-2955] N90-10248
NITRATES
Processing and fabrication of high temperature oxide superconductors
[AD-A210197] N90-10755
NITROGEN
Evaluation of the North Atlantic seasonal nitrogen model, version 2
[DE89-016157] N90-10515
NITROGEN OXIDES
Study of the NO3 radical decomposition reaction and the N2O5 in equilibrium with NO3 + NO2 equilibrium constant
[PB89-208961] N90-10480
NITROGEN PLASMA
An experimental study of microwave transmission through a decaying plasma
[AD-A210586] N90-10726
NITROGEN TETROXIDE
Thermodynamic transport properties of nitrogen tetroxide in hypercritical conditions for regenerative cooling of a rocket engine. Volume 1: Tests
[ETN-89-94975] N90-10773
Thermodynamic transport properties of nitrogen tetroxide in hypercritical conditions for regenerative cooling of a rocket engine. Volume 2: Appendices
[ETN-89-94977] N90-10774
NITROMETHANE
Chemistry of nitromethane at very high pressure
[DE89-008016] N90-10215
NOISE MEASUREMENT
Measurement resolution of noise directivity patterns from acoustic flight tests
[NASA-TM-4134] N90-10679
NOISE REDUCTION
The theory and application of quadratic minimization in the active reduction of sound and vibration N90-10682
NONDESTRUCTIVE TESTS
Generic system components of the Thiokol ultrasonic RSRM case-to-insulation bondline inspection system
[NASA-CR-183738] N90-10171

Gaussmeter determination of 302 stainless steel material condition
[BDX-613-3941] N90-10249
Investigation of materials and bonding using the scanning laser acoustic microscope
[KCP-613-4033] N90-10270

NONLINEAR EQUATIONS
An iterative method for systems of nonlinear hyperbolic equations
[NASA-CR-181919] N90-10638

NONLINEAR EVOLUTION EQUATIONS
A straightforward method for finding implicit solitary wave solutions of nonlinear evolution and wave equations
[AD-A210561] N90-10647

NONLINEAR OPTICS
Monolayer formation characteristics of novel organic molecules with nonlinear optically active moieties
[AD-A210496] N90-10693
Second-order nonlinear optical devices in poled polymers
[DE89-015842] N90-10703
Nonlinear optics and organic materials
[AD-A210570] N90-10709

NONLINEAR SYSTEMS
The application of TSIM software to act design and analysis on flexible aircraft N90-10086
Summarizing qualitative behavior from measurements of nonlinear circuits, revision
[AD-A210919] N90-10353
A new approach to control single-link flexible arms. Part 1: Modelling and identification in the presence of joint friction
[AD-A210590] N90-10445
Regulation of nonlinear and generalized linear systems
[AD-A207725] N90-10619
Finite methods for a nonlinear allocation problem
[AD-A209719] N90-10629
Stochastic control theory, nonlinear structural mechanics and applied combinatorics
[AD-A209042] N90-10657

NONLINEARITY
Aeroelastic analysis of missile control surfaces with structural non-linearity N90-10071
On modelling nonlinear damping in distributed parameter systems N90-10109
Use of the quasilinearization algorithm for the simulation of LSS slewing N90-10110
Inherent bias in nonlinear least squares analysis of first-order kinetic data
[AD-A210677] N90-10651
Theoretical and experimental investigation of nonlinear optoacoustics in liquids
[AD-A210427] N90-10708

NONNEWTONIAN FLUIDS
Analysis of spurt phenomena for a non-Newtonian fluid
[AD-A210560] N90-10405
Stability of discontinuous shearing motions of a non-Newtonian fluid
[AD-A210643] N90-10406
Stability of discontinuous steady states in shearing motion of a non-Newtonian fluid
[AD-A210644] N90-10407

NONPARAMETRIC STATISTICS
Empirical Bayes selection for the highest probability of success in negative binomial distributions
[AD-A210273] N90-10660

NOVAE
Theoretical statistics of zero-age cataclysmic variables N90-10610

NOZZLE DESIGN
Investigations of thrust vector control for high-alpha pitchover N90-10067

NUCLEAR ELECTRIC PROPULSION
Low-earth-orbit to low-lunar-orbit laser freighter N90-10160
Laser propulsion option N90-10161
Laser thruster N90-10164

NUCLEAR EXPLOSIONS
Dynamically compressed metals: Theory
[AD-A210741] N90-10257

NUCLEAR FUEL REPROCESSING
MHD seed recovery and regeneration
[DE89-002711] N90-10715

NUCLEAR MAGNETIC RESONANCE
NMR evidence for a planar arene intermediate in the electron-transfer induced eta 6 to eta 4 hapticity change of a rhodium arene complex
[AD-A210211] N90-10177

NUCLEAR REACTORS
Laser-powered lunar base N90-10156
Earth orbit laser systems N90-10162
Central electrical utility power for a satellite ring city in low earth orbit space N90-10166

NUCLEATION
Monte Carlo simulations of small solute/solvent clusters: Cluster properties and phase transitions
[AD-A209559] N90-10684
Methods to decrease defect density in GaAs/Si heteroepitaxy
[DE89-016306] N90-10753

NUMERICAL ANALYSIS
Numerical simulations of a midlatitude squall line N90-10497
Numerical analysis of a class of problems in the mathematical theory of plasticity and damage
[AD-A210731] N90-10655

NUMERICAL CONTROL
Combined advanced foundry and quality control techniques to enhance reliability of castings for the aerospace industry N90-10240

NUMERICAL DATA BASES
Defense Technical Information Center cataloging guidelines
[AD-A211000] N90-10792

NUMERICAL WEATHER FORECASTING
A study of the impact of simulated satellite lidar wind observations
[AD-A210430] N90-10488
A case study evaluation of satellite-derived rainfall estimates and their application to numerical model precipitation forecast verification
[PB89-194591] N90-10499
A study of the impact of simulated 183 GHz water vapor retrievals on numerical weather prediction
[AD-A210431] N90-10504

O

OBLIQUE SHOCK WAVES
Convection of a pattern of vorticity through a reacting shock wave
[NASA-CR-181921] N90-10576

OBLIQUE WINGS
Static aeroelastic analysis for generic configuration aircraft
[NASA-TM-89423] N90-10042

OCEAN BOTTOM
ONR/NORDA Workshop on Terrain Analysis and Quantitative Geomorphology
[AD-A210464] N90-10489
The influence of a steady baroclinic deep ocean on the shelf
[PB89-198188] N90-10511
A search for layering in the oceanic crust
[PB89-198220] N90-10514
Surface wave ray tracing and Ms:yield determination in a laterally heterogeneous earth
[AD-A210241] N90-10516

OCEAN DYNAMICS
The influence of a steady baroclinic deep ocean on the shelf
[PB89-198188] N90-10511

OCEAN MODELS
The influence of a steady baroclinic deep ocean on the shelf
[PB89-198188] N90-10511
IFD (Implicit Finite Difference): Interfaced with Harvard open ocean model forecasts
[AD-A210521] N90-10517

OCEAN SURFACE
Chesapeake Bay surface salinities, 1951-88
[PB89-194583] N90-10513

OCEAN TEMPERATURE
Semi-monthly temperature and geopotential anomaly in the upper 500 meters along the Oahu-Farallon Islands great circle from November 15, 1967 through December 15, 1979
[AD-A210640] N90-10518

OCEANOGRAPHIC PARAMETERS
Meeting Review: Workshop on Airborne Instrumentation
[PB89-174775] N90-10032
US Navy regional climatic study of the United States Atlantic Coast and associated waters
[AD-A210198] N90-10503
Coastal Research Center Woods Hole Oceanographic Institution
[PB89-198238] N90-10510

OCEANOGRAPHY
ONR/NORDA Workshop on Terrain Analysis and Quantitative Geomorphology
[AD-A210464] N90-10489
Coastal Research Center Woods Hole Oceanographic Institution
[PB89-198238] N90-10510

OILS
High temperature VSCF (Variable Speed Constant Frequency) generator system
[AD-A210823] N90-10351

OMEGA NAVIGATION SYSTEM
Omega system performance assessment
[AD-A210342] N90-10322

ON-LINE SYSTEMS
Planning an Integrated On-line Library System (IOLS)
[AD-A209406] N90-10783
Online support for the intellectual activity of browsing N90-10784
Defense Technical Information Center cataloging guidelines
[AD-A211000] N90-10792

OPERATING COSTS
Revolutionary opportunities for materials and structures study
[NASA-CR-179642] N90-10184

OPERATING SYSTEMS (COMPUTERS)
DDN Trusted Guard Gateway: Trusted Guard Gateway (TGG) technology assessment, phase 2
[AD-A210248] N90-10614
Computer availability impact on the archiving of scientific and technical reports
[AD-A210283] N90-10787

OPERATIONS RESEARCH
Regulation of nonlinear and generalized linear systems
[AD-A207725] N90-10619

OPERATOR PERFORMANCE
SINCGARS (Single-Channel Ground/Airborne Radio System) operator performance decay
[AD-A210716] N90-10326
An adaptive controller for enhancing operator performance during teleoperation
[NASA-CR-183445] N90-10438
Active participation in highly automated systems: Turning the wrong stuff into the right stuff
[AD-A210218] N90-10572

OPERATORS (MATHEMATICS)
On two polynomial spaces associated with a box spline
[AD-A210559] N90-10646

OPERATORS (PERSONNEL)
Active participation in highly automated systems: Turning the wrong stuff into the right stuff
[AD-A210218] N90-10572

OPTICAL COMMUNICATION
Coherent multichannel techniques for integrated broadband communications subscriber lines
[AD-A209323] N90-10312

OPTICAL DATA PROCESSING
Optical processing for distributed sensors in control of flexible spacecraft N90-10102
Photonic processing at NASA Ames Research Center N90-10560

OPTICAL EQUIPMENT
Polyheterocycle Langmuir-Blodgett films
[AD-A210625] N90-10292
Subpicosecond optical digital computation using conjugate parametric generators
[AD-A207908] N90-10330
Second-order nonlinear optical devices in poled polymers
[DE89-015842] N90-10703

OPTICAL FIBERS
Multimode fiber interferometry and several-mode fiber polarimetry via phase conjugation
[DE89-014226] N90-10706

OPTICAL MEASUREMENT
Demonstration of a dual-lidar method for measuring optical depths in the vertical
[AD-A210598] N90-10711

OPTICAL PATHS
Subpicosecond optical digital computation using conjugate parametric generators
[AD-A207908] N90-10330
Coupled multiline CW HF lasers: Experimental performance
[AD-A210844] N90-10434

OPTICAL PROPERTIES
Laser diode array and transmission optics N90-10163
Stretched-membrane heliostats for solar central-receiver power plants
[DE89-016034] N90-10476
Two photon absorption characterization
[AD-A210508] N90-10694
Design of grazing incidence monochromators involving unconventional gratings
[DE89-016341] N90-10704
Theoretical and experimental investigation of nonlinear optoacoustics in liquids
[AD-A210427] N90-10708

Nonlinear optics and organic materials
[AD-A210570] N90-10709

OPTICAL PUMPING
A laser-driven source of polarized hydrogen and deuterium
[DE89-015130] N90-10429

OPTICAL RADAR
A study of the impact of simulated satellite lidar wind observations
[AD-A210430] N90-10488
Demonstration of a dual-lidar method for measuring optical depths in the vertical
[AD-A210598] N90-10711

OPTICAL THICKNESS
Demonstration of a dual-lidar method for measuring optical depths in the vertical
[AD-A210598] N90-10711

OPTIMAL CONTROL
Active vibration mitigation of distributed parameter, smart-type structures using Pseudo-Feedback Optimal Control (PFOC) N90-10121
Optimized resolved rate control of seven-degree-of-freedom Laboratory Telerobotic Manipulator (LTM) with application to three-dimensional graphics simulation
[NASA-TP-2938] N90-10618
Stochastic control theory, nonlinear structural mechanics and applied combinatorics
[AD-A209042] N90-10657

OPTIMIZATION
CONSOLE: A CAD tandem for optimization-based design interacting with user-supplied simulators N90-10085
Numerically efficient algorithm for model development of high-order systems N90-10108
Control law synthesis and optimization software for large order aeroservoelastic systems N90-10111
Optimal q-Markov COVER for finite precision implementation N90-10117
Approximate simulation model for analysis and optimization in engineering system design
[NASA-TM-101616] N90-10308
An expert system for optimal gear design N90-10439
General decomposition of sequential machines: Relationships to state assignment
[AD-A208189] N90-10580
Effective resource utilization for multiprocessor join execution
[DE89-016303] N90-10595
Finite methods for a nonlinear allocation problem
[AD-A209719] N90-10629
Numerical optimization in Hilbert space using inexact function and gradient evaluations
[NASA-CR-181926] N90-10640
Monolayer formation characteristics of novel organic molecules with nonlinear optically active moieties
[AD-A210496] N90-10693
A compact X-ray lithography lattice using superferric magnets
[DE89-013947] N90-10728

ORBIT TRANSFER VEHICLES
Laser propulsion option N90-10161
Laser thruster N90-10164
Microwave beam power N90-10165

ORBITAL MANEUVERING VEHICLES
Computer vision research at Marshall Space Flight Center N90-10564

ORBITS
Theoretical investigations of chaotic dynamics
[AD-A207724] N90-10772

ORDER-DISORDER TRANSFORMATIONS
Raman spectroscopic study of the rare earth sesquisulfides
[AD-A210610] N90-10226
The structure determination of molecular adsorbates with large unit cells or lattice-gas disorder on metal surfaces
[AD-A210926] N90-10230
Ordered structures and metastable alloys grown by OMVPE
[DE89-016370] N90-10744

ORGANIC CHEMISTRY
The synthesis and structure of novel antimony thiametallacycles
[AD-A210888] N90-10229
Cubane derivatives for propellant applications
[AD-A210368] N90-10305

ORGANIC COMPOUNDS
Organic explosives and related compounds. Environmental and health considerations
[AD-A210554] N90-10306

ORGANIC LASERS
Eye/sensor protection against laser irradiation organic nonlinear optical materials
[AD-A210599] N90-10531

ORGANIC MATERIALS
Computational modeling of pi-conjugated polyradicals
[AD-A210573] N90-10648
Nonlinear optics and organic materials
[AD-A210570] N90-10709

ORGANOMETALLIC COMPOUNDS
International Conference on Organometallic Chemistry (13th) held in Torino, Europe on 4-9 September 1988: Abstracts
[AD-A210617] N90-10178
The synthesis and structure of novel antimony thiametallacycles
[AD-A210888] N90-10229
Bonding in transition metal silyl dimers. Molecular orbital theory
[AD-A208269] N90-10260
Solvent dynamical effects in electron transfer: Evaluation of electronic matrix coupling elements for metallocene self-exchange reactions
[AD-A210306] N90-10692

ORGANOMETALLIC POLYMERS
Metal-assisted syntheses of boranes and carboranes
[AD-A210728] N90-10227

ORIENTATION
Face-specific interaction of MoS4(2-1) with oriented crystals of (0001) CdX (X = Se, S)
[AD-A209519] N90-10732

OSCILLATORS
Master oscillator with power amplifiers: Performance of a two-element CW HF phased-laser array
[AD-A211141] N90-10435
Submillimeter quantum electronics
[AD-A210439] N90-10762

OSCILLOSCOPES
Pin switch circuits instrument for microsecond velocity measurements
[AD-A210638] N90-10426

OXIDATION
Heterogeneous catalysts in water
[AD-A210742] N90-10228
Emittance, catalysis, and dynamic oxidation of Ti-14Al-21Nb
[NASA-TP-2955] N90-10248

OXIDATION RESISTANCE
Emittance, catalysis, and dynamic oxidation of Ti-14Al-21Nb
[NASA-TP-2955] N90-10248

OXIDATION-REDUCTION REACTIONS
Combining spontaneous molecular assembly with microfabrication to pattern surfaces: Selective binding of isonitriles to platinum microwires and characterization by electrochemistry and surface spectroscopy
[AD-A209528] N90-10213
Solvent relaxation in electron-transfer reactions: Comparisons between barrier-crossing dynamics in water and polar aprotic media
[AD-A210212] N90-10220
Heterogeneous catalysts in water
[AD-A210742] N90-10228
Solvent dynamical effects in electron transfer: Evaluation of electronic matrix coupling elements for metallocene self-exchange reactions
[AD-A210306] N90-10692

OXIDES
Materials for engine applications above 3000 deg F: An overview
[NASA-TM-100169] N90-10188
Processing and fabrication of high temperature oxide superconductors
[AD-A210197] N90-10755

OXYGEN
Reaction of oxygen with allene
[DE89-015219] N90-10216
Method and apparatus for maintaining thermal control in plasma conditions
[NASA-CASE-MFS-28368-1] N90-10717

OZONE DEPLETION
Geophysical monitoring for climatic change number 16
[PB89-159628] N90-10494

P

P-I-N JUNCTIONS
Studies of high power density, pico-second rise-time light activated semiconductor switch
[AD-A210549] N90-10349

P-TYPE SEMICONDUCTORS
Scanning tunneling microscopy etching of micrometer level features on p-type GaAs
[AD-A209216] N90-10328

PACIFIC OCEAN
Marine weather log, volume 32, number 3, summer 1988
[PB88-248075] N90-10491
Semi-monthly temperature and geopotential anomaly in the upper 500 meters along the Oahu-Farallon Islands great circle from November 15, 1967 through December 15, 1979
[AD-A210640] N90-10518

PALEONTOLOGY
Fluctuation history of Great Salt Lake, Utah, during the last 13,000 years, part 2
[NASA-CR-185911] N90-10486

PANEL METHOD (FLUID DYNAMICS)
Prediction of stability derivatives for missiles using the HISSS panel code N90-10053

PARALLEL COMPUTERS
Shared memory versus message passing architectures: An application based study
[AD-A210312] N90-10615
The rewrite rule machine project
[AD-A210528] N90-10617

PARALLEL PROCESSING (COMPUTERS)
Parallel asynchronous hardware implementation of image processing algorithms N90-10546
Computation and parallel implementation for early vision N90-10549
Image gathering, coding, and processing: End-to-end optimization for efficient and robust acquisition of visual information N90-10551
Photonic processing at NASA Ames Research Center N90-10560
Sparse distributed memory overview N90-10561
Evaluating local indirect addressing in SIMD processors
[NASA-CR-181845] N90-10581
Proceedings of the 2nd International Conference on Vector and Parallel Computing
[AD-A209401] N90-10585
A low-cost hypercube load-balance algorithm
[DE89-015739] N90-10589
Effective resource utilization for multiprocessor join execution
[DE89-016303] N90-10595
Applications of parallel supercomputers: Scientific results and computer science lessons
[DE89-016385] N90-10611
Parallel processing and learning in simple systems
[AD-A210225] N90-10612
Shared memory versus message passing architectures: An application based study
[AD-A210312] N90-10615
An iterative method for systems of nonlinear hyperbolic equations
[NASA-CR-181919] N90-10638
Computational and statistical issues in discrete-event simulation
[AD-A210743] N90-10668

PARALLEL PROGRAMMING
The rewrite rule machine project
[AD-A210528] N90-10617

PARAMETER IDENTIFICATION
Numerically efficient algorithm for model development of high-order systems N90-10108
On the interactive computer program IPIS for aircraft parameter identification
[NAL-TR-1000] N90-10586
A unified approach to estimating tail behavior
[AD-A210961] N90-10672

PARAMETERIZATION
Quality control of castings N90-10239
Subpicosecond optical digital computation using conjugate parametric generators
[AD-A207908] N90-10330

PARTIAL DIFFERENTIAL EQUATIONS
A straightforward method for finding implicit solitary wave solutions of nonlinear evolution and wave equations
[AD-A210561] N90-10647
Multiple solutions for Lagrangian systems in T superscript n
[AD-A210646] N90-10650

PARTICLE ACCELERATOR TARGETS
Fermilab fixed target beams from the main injector
[DE89-014355] N90-10697

PARTICLE COLLISIONS
The role of particle collisions in pneumatic transport N90-10392
A symplectic coherent beam-beam model
[DE89-015386] N90-10701

PARTICLE DIFFUSION
Plasma theory and simulation
[AD-A207952] N90-10714

PARTICLE EMISSION
Particle emission and charging effects induced by fracture
[AD-A210215] N90-10459

PARTICLE INTERACTIONS
Tangent map analysis of the beam-beam interaction
[DE89-015857] N90-10689

Atomic effects of beta decay in astrophysics and in elementary particle physics N90-10811

PARTICLE MOTION

Effect of particle velocity fluctuations on the inertia coupling in two-phase flow N90-10391

The role of particle collisions in pneumatic transport N90-10392

PARTICLE SIZE DISTRIBUTION

The measurement of infrared spectra of dense ceramics by specular reflectance spectroscopy [AD-A210609] N90-10291

Real-time observations of aerosol composition changes [DE89-012382] N90-10422

PARTICLE THEORY

Plasma theory and simulation [AD-A207952] N90-10714

PARTICLES

Heterogeneous catalysts in water [AD-A210742] N90-10228

Numerical calculations of the collapse of a cavity in the vicinity of a compliant wall [AD-A210489] N90-10403

PARTICULATES

Properties of F-34 (JP-8) fuel for 1988 [AD-A210188] N90-10303

PATTERN RECOGNITION

Photonic processing at NASA Ames Research Center N90-10560

Algorithms and architectures for robot vision N90-10562

Instrumentation and robotic image processing using top-down model control N90-10563

Computer vision research at Marshall Space Flight Center N90-10564

A comparison of real-time optical correlators for pattern recognition [DE89-016416] N90-10705

PAYLOADS

Simulation of shuttle flight control system structural interaction with RMS deployed payloads N90-10100

Microwave beam power N90-10165

PEEK

Failure behavior of PEEK and its short-fiber composite systems [AD-A210729] N90-10189

PENETRATION

Studies in penetration mechanics [AD-A210713] N90-10448

PEPTIDES

Control of synthetic peptide tertiary structure [AD-A210339] N90-10281

PERFORATED PLATES

Laminar flow control perforated wing panel development [NASA-CR-178166] N90-10187

PERFORMANCE PREDICTION

ILS (Instrument Landing System) mathematical modeling study on the effects of proposed hangar construction west of runway 18R on localizer performance at Dallas-Fort Worth International Airport [AD-A210631] N90-10019

Large-scale Advanced Prop-fan (LAP) high speed wind tunnel test report [NASA-CR-182125] N90-10045

Stability and Control of Tactical Missile Systems [AGARD-CP-451] N90-10050

Prediction of stability derivatives for missiles using the HISSS panel code N90-10053

Missile Datcom: Enhancements for design applications N90-10054

Prediction of dynamic derivatives N90-10055

Prediction of tactical missile dynamics N90-10056

Vortex induced characteristics of missiles in unsteady maneuvers N90-10057

New test techniques to evaluate near field effects for supersonic store carriage and separation N90-10062

Comparison of DPCM prediction strategies for high-quality digital television bit-rate reduction [BBC-RD-1989/8] N90-10318

PERFORMANCE TESTS

Commercial high current ignitron development [DE89-015077] N90-10331

Report on the performance and operating characteristics of the Burle C83061E QUANTACON (trademark) photomultiplier tube [DE89-015257] N90-10333

Heat transfer characteristics of igniter output plumes [DE89-011449] N90-10340

Some significant results from testing a Remote Multiplexing Unit (RMU) for temperature-induced errors [DE89-009432] N90-10421

Analysis and test of a 16-foot radial rib reflector developmental model [NASA-TM-101648] N90-10457

Tracking performance evaluation [AD-A210499] N90-10540

Director, Operational Test and Evaluation report FY-88 [AD-A206784] N90-10778

PERIODIC FUNCTIONS

Periodic solutions of spatially periodic Hamiltonian systems [AD-A210645] N90-10649

PERIODIC VARIATIONS

Chesapeake Bay surface salinities, 1951-88 [PB89-194583] N90-10513

PERMEABILITY

Electrical field dependence of protein conformation and channel function in lipid membranes of different compositions [AD-A210236] N90-10222

PERMITTIVITY

Capacitive energy storage at cryogenic temperatures, phase 2 [AD-A210366] N90-10347

PERMUTATIONS

The organization of permutation architectures with bussed interconnections [AD-A210832] N90-10352

PERSONNEL

SINCGARS (Single-Channel Ground/Airborne Radio System) operator performance decay [AD-A210716] N90-10326

PERSPIRATION

Control of thermoregulatory sweating during exercise in the heat [AD-A206001] N90-10523

PERTURBATION THEORY

On analytic modeling of lunar perturbations of artificial satellites of the earth [AD-A210440] N90-10078

A unified view of infinitesimal perturbation analysis and likelihood ratios [AD-A210682] N90-10652

PETN

Free-expansion experiments and modeling in detonation: Chemistry and hydrodynamics on a laboratory scale [DE89-007748] N90-10302

Laser initiation of secondary explosives [DE89-010229] N90-10431

PHARMACOLOGY

Parallel processing and learning in simple systems [AD-A210225] N90-10612

PHASE CONJUGATION

Multimode fiber interferometry and several-mode fiber polarimetry via phase conjugation [DE89-014226] N90-10706

PHASE CONTROL

Dynamics and control of turbulent shear flows [AD-A210396] N90-10402

PHASE LOCKED SYSTEMS

Coupled multiline CW HF lasers: Experimental performance [AD-A210844] N90-10434

PHASE SHIFT

Simultaneous multiple frequency interferometry: An application of homodyne phase measurement [DE89-013975] N90-10719

PHASE TRANSFORMATIONS

Computer simulations of polymer dynamics in the solid state [DE89-010337] N90-10275

Monte Carlo simulations of small solute/solvent clusters: Cluster properties and phase transitions [AD-A209559] N90-10684

Mott transition: Low-energy excitations and superconductivity [DE89-617778] N90-10741

Progress report on grain boundaries [DE89-015541] N90-10749

PHASED ARRAYS

Gyrotron development for space power beaming N90-10148

Coupled multiline CW HF lasers: Experimental performance [AD-A210844] N90-10434

Master oscillator with power amplifiers: Performance of a two-element CW HF phased-laser array [AD-A211141] N90-10435

PHONEMES

Attention and vigilance in speech perception [AD-A210493] N90-10539

PHONETICS

Attention and vigilance in speech perception [AD-A210493] N90-10539

PHOSPHORIC ACID FUEL CELLS

Impact of fundamental technical improvements [PB89-218010] N90-10472

PHOTOCHEMICAL REACTIONS

Silicon dioxide deposition at 100 deg C using vacuum ultraviolet light [TR-0088(3945-07)-6] N90-10269

Paper 1. Impact of volcanic aerosols on stratospheric chemistry. Paper 2. O2 (1 sigma g +) and O2 (1 delta g) in the H + O2 reaction system. Paper 3. Barotropic instability of zonal jets on Mars, Earth and Venus N90-10477

PHOTOCONDUCTIVITY

Physics of high energy photoconductive switches [AD-A210341] N90-10345

PHOTOCONDUCTORS

Analysis of the performance of gallium arsenide photoavalanche switches [DE89-015774] N90-10739

PHOTODECOMPOSITION

An investigation of the degradation and stabilization of polymer systems [AD-A210362] N90-10282

PHOTOELECTRIC EMISSION

Superconductivity from valence fluctuations with finite U [DE89-015302] N90-10742

PHOTOGRAMMETRY

Space environment robot vision system N90-10569

PHOTOLITHOGRAPHY

Characterization of 4/3 technology large-scale integrated circuit on polysilicon processes [BDX-613-3971] N90-10335

Negative-working electron beam resist based on poly(methyl methacrylate) [AD-A207834] N90-10733

PHOTOLYSIS

An investigation of the degradation and stabilization of polymer systems [AD-A210362] N90-10282

PHOTOMETERS

Adaptive machine vision [AD-A208130] N90-10436

Characterization of GaAs/Si/GaAs heterointerfaces [DE89-016302] N90-10752

PHOTOMULTIPLIER TUBES

Report on the performance and operating characteristics of the Burle C83061E QUANTACON (trademark) photomultiplier tube [DE89-015257] N90-10333

PHOTONS

Two photon absorption characterization [AD-A210508] N90-10694

PHOTOOXIDATION

An investigation of the degradation and stabilization of polymer systems [AD-A210362] N90-10282

PHOTOSYNTHESIS

Biochemical cycling and fluxes between the deep euphotic zone and other oceanic realms [PB89-152458] N90-10509

A structural basis for electron transfer in bacterial photosynthesis [DE89-015702] N90-10687

Controlling photoinduced electron transfer rates in donor-spacer-acceptor molecules by changing the electronic properties of the spacer [DE89-015128] N90-10735

PHOTOTHERMAL CONVERSION

Predictive aging of polymers [NASA-CASE-NPO-17524-1-CU] N90-10261

PHOTOVOLTAIC CELLS

United States photovoltaic concentrator technology process and new program initiative [DE89-013812] N90-10475

PHTHALOCYANIN

Femtosecond dynamics of fluoro-aluminum phthalocyanine and linear alkane molecules [AD-A210939] N90-10766

PHYSICAL EXERCISE

Control of thermoregulatory sweating during exercise in the heat [AD-A206001] N90-10523

PHYSICAL OPTICS

Surface reflection: Physical and geometrical perspectives [AD-A210592] N90-10710

PHYSIOLOGICAL RESPONSES

Daytime sleepiness, performance, mood, nocturnal sleep: The effect of benzodiazepine and caffeine on their relationship [AD-A210915] N90-10533

Biological investigations of adaptive networks: Neuronal control of conditioned responses [AD-A211043] N90-10534

Thermoregulatory responses to intermittent exercise are influenced by knit structure of underwear [AD-A209087] N90-10541

PIEZORESISTIVE TRANSDUCERS
Fluctuating pressures measured beneath a high-temperature, turbulent boundary layer on a flat plate at Mach number of 5
[NASA-TP-2947] N90-10680
PILOT ERROR
Classification and reduction of pilot error
[NASA-CR-181867] N90-10014
PILOT PERFORMANCE
The effect of higher education variables on cadet performance during 1987 light aircraft training
[AD-A210199] N90-10536
PILOT SELECTION
The effect of higher education variables on cadet performance during 1987 light aircraft training
[AD-A210199] N90-10536
PILOT TRAINING
The effect of higher education variables on cadet performance during 1987 light aircraft training
[AD-A210199] N90-10536
PILOTS (PERSONNEL)
Human performance in continuous/sustained operations and the demands of extended work/rest schedules: An annotated bibliography, volume 2
[AD-A210504] N90-10530
PIPELINING (COMPUTERS)
Intensity dependent spread processor and workstation N90-10568
PLANAR STRUCTURES
On the 2-extendability of planar graphs
[AD-A210289] N90-10642
PLANETARY ATMOSPHERES
Paper 1. Impact of volcanic aerosols on stratospheric chemistry. Paper 2. O2 (1 sigma g +) and O2 (1 delta g) in the H + O2 reaction system. Paper 3. Barotropic instability of zonal jets on Mars, Earth and Venus N90-10477
Laboratory measurements of microwave and millimeter-wave properties of planetary atmospheric constituents
[NASA-CR-185914] N90-10815
PLANETARY BOUNDARY LAYER
Thermodynamic and dynamic processes in the updraft region of GALE (Genesis of Atlantic Lows Experiment) IOP (Intensive Observation Period) 9
[AD-A208139] N90-10496
PLANETARY EVOLUTION
Office of exploration overview N90-10141
PLANNING
Differences in writers initial task representations
[AD-A210433] N90-10788
PLASMA CONTROL
Observations of azimuthal asymmetry for certain FRC operating regimes
[DE89-015300] N90-10721
Massachusetts Institute of Technology Plasma Fusion Center
[DE89-016050] N90-10723
PLASMA DECAY
An experimental study of microwave transmission through a decaying plasma
[AD-A210586] N90-10726
PLASMA DENSITY
Simultaneous multiple frequency interferometry: An application of homodyne phase measurement
[DE89-013975] N90-10719
Scattering of an ICRF magnetosonic wave by plasma density turbulence
[DE89-015223] N90-10720
Numerical simulation of the compressible Orszag-Tang vortex
[AD-A210465] N90-10725
PLASMA DIAGNOSTICS
Observations of azimuthal asymmetry for certain FRC operating regimes
[DE89-015300] N90-10721
Generation of 3/2 omega sub o radiation in inhomogeneous plasmas under the irradiation of intense electromagnetic waves
[DE89-015723] N90-10722
Massachusetts Institute of Technology Plasma Fusion Center
[DE89-016050] N90-10723
PLASMA DRIFT
Plasma theory and simulation
[AD-A207952] N90-10714
PLASMA EQUILIBRIUM
The dense Z-pinch as a plasma radiation source. 1: Quasi-static Bennett model
[AD-A210600] N90-10727
PLASMA FREQUENCIES
Simultaneous multiple frequency interferometry: An application of homodyne phase measurement
[DE89-013975] N90-10719
PLASMA GUNS
Plasma gun with coaxial powder feed and adjustable cathode
[NASA-CASE-LEW-14901-1] N90-10718
PLASMA HEATING
Scattering of an ICRF magnetosonic wave by plasma density turbulence
[DE89-015223] N90-10720
Kinetic effects in Alfven wave heating. Part 2: Propagation and absorption with a single minority species
[DE89-016619] N90-10724
PLASMA INTERACTIONS
Dynamically compressed metals: Theory
[AD-A210741] N90-10257
PLASMA PHYSICS
Plasma waves in the earth's foreshock, bow shock, and magnetosheath N90-10486
Plasma theory and simulation
[AD-A207952] N90-10714
PLASMA PINCH
The dense Z-pinch as a plasma radiation source. 1: Quasi-static Bennett model
[AD-A210600] N90-10727
PLASMA RADIATION
The dense Z-pinch as a plasma radiation source. 1: Quasi-static Bennett model
[AD-A210600] N90-10727
PLASMA SHEATHS
Plasma theory and simulation
[AD-A207952] N90-10714
PLASMA SPECTRA
Numerical simulation of the compressible Orszag-Tang vortex
[AD-A210465] N90-10725
PLASMA SPRAYING
Plasma gun with coaxial powder feed and adjustable cathode
[NASA-CASE-LEW-14901-1] N90-10718
PLASMA TURBULENCE
Scattering of an ICRF magnetosonic wave by plasma density turbulence
[DE89-015223] N90-10720
PLASMA WAVES
Plasma waves in the earth's foreshock, bow shock, and magnetosheath N90-10486
PLASMAS (PHYSICS)
Method and apparatus for maintaining thermal control in plasma conditions
[NASA-CASE-MFS-28368-1] N90-10717
Scattering of an ICRF magnetosonic wave by plasma density turbulence
[DE89-015223] N90-10720
PLASTIC DEFORMATION
Fatigue crack initiation mechanics of metal aircraft structures
[AD-A210567] N90-10255
Studies in penetration mechanics
[AD-A210713] N90-10448
PLASTIC FLOW
Studies in penetration mechanics
[AD-A210713] N90-10448
PLASTIC PROPERTIES
Numerical analysis of a class of problems in the mathematical theory of plasticity and damage
[AD-A210731] N90-10655
PLATES (STRUCTURAL MEMBERS)
Design guide for predicting nonlinear random response (including snap-through) of buckled plates
[NASA-CR-181877] N90-10681
PLATINUM
Structural and surface characterization of dispersed metal catalysts
[DE89-014530] N90-10208
PLUMES
Boost-phase discrimination research activities
[NASA-TM-101889] N90-10176
Heat transfer characteristics of igniter output plumes
[DE89-011449] N90-10340
PNEUMATICS
The role of particle collisions in pneumatic transport N90-10392
POINTING CONTROL SYSTEMS
The Spartan 1 mission
[NASA-TM-101887] N90-10077
POLAR REGIONS
Kiruna geophysical data: Data Summary 88/7-9, July - September 1988
[PB89-210249] N90-10487
POLAR SUBSTORMS
The auroral energy deposition over the polar ionosphere during substorms
[AD-A210522] N90-10490
POLARIMETERS
Bragg crystal polarimeters
[NASA-CR-181331] N90-10423
POLARIMETRY
Multimode fiber interferometry and several-mode fiber polarimetry via phase conjugation
[DE89-014226] N90-10706
POLARIZATION (SPIN ALIGNMENT)
A laser-driven source of polarized hydrogen and deuterium
[DE89-015130] N90-10429
POLLUTION TRANSPORT
The suitability of diffusion and wind-field techniques for an emergency-response dispersion model
[PB89-190219] N90-10481
POLYCARBONATES
Conference on Aerospace Transparent Materials and Enclosures (15th) 16-20 January 1989. Volume 2: Sessions 6-9
[AD-A210201] N90-10024
An investigation of the degradation and stabilization of polymer systems
[AD-A210362] N90-10282
POLYCRYSTALS
Alternative fabrication techniques for high-efficiency CuInSe2 and CuInSe2-alloy films and cells
[DE89-009451] N90-10474
Femtosecond dynamics of fluoro-aluminum phthal ocyanine and linear alkane molecules
[AD-A210939] N90-10766
POLYISOPRENES
Analysis of spurt phenomena for a non-Newtonian fluid
[AD-A210560] N90-10405
POLYMER CHEMISTRY
New polymer precursors to boron and silicon nitrides
[AD-A210287] N90-10279
Development of elastomeric polypeptide biomaterials
[AD-A210295] N90-10280
POLYMERIC FILMS
Polyheterocycle Langmuir-Blodgett films
[AD-A210625] N90-10292
Quartz crystal microbalance studies of electrochemical growth of conducting polymers
[AD-A210788] N90-10295
Impedance analysis of ionic transport in polypyrrole-polyazulene copolymer and its charge-discharge characteristics
[AD-A210979] N90-10299
Rechargeable lithium/polymer cathode batteries
[AD-A210978] N90-10354
Second-order nonlinear optical devices in poled polymers
[DE89-015842] N90-10703
Method and apparatus for maintaining thermal control in plasma conditions
[NASA-CASE-MFS-28368-1] N90-10717
Negative-working electron beam resist based on poly(methyl methacrylate)
[AD-A207834] N90-10733
Femtosecond dynamics of fluoro-aluminum phthal ocyanine and linear alkane molecules
[AD-A210939] N90-10766
POLYMERIZATION
Predictive aging of polymers
[NASA-CASE-NPO-17524-1-CU] N90-10261
Mechanical properties, solubilities, and processabilities in the design of the first super-strong liquid-crystalline polymers
[DE89-009252] N90-10273
Computer simulations of polymer dynamics in the solid state
[DE89-010337] N90-10275
POLYMERS
Monomers, polymers and transition metal complexes based upon carboranes
[AD-A210226] N90-10221
Characterization of polymeric surfaces and interfaces
[AD-A210227] N90-10277
POLYMETHYL METHACRYLATE
Negative-working electron beam resist based on poly(methyl methacrylate)
[AD-A207834] N90-10733
POLYMORPHISM
Type reconstruction with first-class polymorphic values
[AD-A210833] N90-10605
POLYNOMIALS
Finding isolated zero points of complex polynomial mappings
[DE89-617523] N90-10633
On the coefficients of differentiated expansions of ultraspherical polynomials
[NASA-CR-181913] N90-10637
On two polynomial spaces associated with a box spline
[AD-A210559] N90-10646
Studies in estimation theory, applications and implementations
[AD-A210712] N90-10653

POLYPEPTIDES
Electrical field dependence of protein conformation and channel function in lipid membranes of different compositions
[AD-A210236] N90-10222
Polypeptide inhibitors of mineral scaling and corrosion
[AD-A210507] N90-10225
Development of elastomeric polypeptide biomaterials
[AD-A210295] N90-10280
Synthetic polypeptide composites for sensor applications
[AD-A210797] N90-10296
POLYURETHANE FOAM
Electronic encapsulation using foam with bonded metal covers for a filter pack
[DE89-014010] N90-10276
POLYURETHANE RESINS
An investigation of the degradation and stabilization of polymer systems
[AD-A210362] N90-10282
Comparison of carboxylated and sulfonated model polyurethane ionomers
[AD-A210438] N90-10284
UV-curable polyurethane-methacrylate co-networks and interpenetrating networks
[AD-A210445] N90-10285
Synthesis and interfacial properties of new generation polyurethane systems
[AD-A210446] N90-10286
Synthesis and physical properties of poly(perfluoroalkylether) urethanes
[AD-A210500] N90-10287
PONTRYAGIN PRINCIPLE
Minimum-variance reduced-order estimation algorithms from Pontryagin's minimum principle N90-10105
Modeling, simulation, and analyses of attitude control for the Crew/Equipment Retriever (CER) proposed for space station
[AD-A208140] N90-10125
POROSITY
Porosity and crack initiation during low cycle fatigue
[AD-A210989] N90-10464
POSITION (LOCATION)
Dependency-directed localization of software bugs
[AD-A210837] N90-10506
POSITION SENSING
The 1988 year end report for road following at Carnegie-Mellon
[NASA-CR-185967] N90-10446
POSTFLIGHT ANALYSIS
Flight Motor Set 360L003 (STS-29R)
[NASA-CR-183739-VOL-1] N90-10170
POSTLAUNCH REPORTS
Flight Motor Set 360L003 (STS-29R)
[NASA-CR-183739-VOL-1] N90-10170
POTASSIUM PERCHLORATES
Pyrotechnic ignition studies using a gun tunnel
[DE89-012496] N90-10341
POTENTIAL ENERGY
Multiple solutions for Lagrangian systems in T superscript n
[AD-A210646] N90-10650
Monte Carlo simulations of small solute/solvent clusters: Cluster properties and phase transitions
[AD-A209559] N90-10684
POTENTIAL FLOW
Two-phase potential flow N90-10387
Numerical calculations of the collapse of a cavity in the vicinity of a compliant wall
[AD-A210489] N90-10403
POWDER (PARTICLES)
Japanese structural ceramics research and development N90-10272
Preparation, purification and densification of zinc sulfide powder from organometallics
[AD-A210943] N90-10298
Processing and fabrication of high temperature oxide superconductors
[AD-A210197] N90-10755
POWDER METALLURGY
Establishment and initial operation of a resource facility for RSR (Rapid Solidification Rate) processed alloys in pilot quantities
[AD-A210369] N90-10283
POWER AMPLIFIERS
Master oscillator with power amplifiers: Performance of a two-element CW HF phased-laser array
[AD-A211141] N90-10435
POWER BEAMING
Power beaming options N90-10142
Gyrotron development for space power beaming N90-10148
Antenna technology for beamed space-power N90-10149
Technical options for high average power free electron milimeter-wave and laser devices N90-10151
Applicability of the beamed power concept to lunar rovers, construction, mining, explorers and other mobile equipment N90-10159
Central electrical utility power for a satellite ring city in low earth orbit space N90-10166
POWER CONDITIONING
A battery-powered, solid state magnetic compressor with applications for high PRF accelerators and lasers
[DE89-015770] N90-10332
PRECIPITATION (CHEMISTRY)
Characterization and evaluation of acid rain in East Central Florida from 1978 to 1987: Ten year summary report
[NASA-TM-102149] N90-10478
PRECIPITATION (METEOROLOGY)
A program to improve performance of AFGL (Air Force Geophysical Laboratory) automated present weather observing sensors
[AD-A207669] N90-10495
US Navy regional climatic study of the United States Atlantic Coast and associated waters
[AD-A210198] N90-10503
PRECIPITATION HARDENING
Mechanisms of strength and toughness in a microalloyed, precipitation hardened steel
[AD-A210571] N90-10256
Strain aging in tungsten-heavy alloys
[AD-A211166] N90-10259
PRECISION GUIDED PROJECTILES
Identification of stability and control parameters of a brilliant ammunition N90-10065
PREDICTION ANALYSIS TECHNIQUES
Prediction of the aerodynamic stability of missiles N90-10052
Leading edge transition by contamination in hypersonic flow N90-10360
Goertler instability on an airfoil: Comparison of marching solution with experimental observations N90-10364
IFD (Implicit Finite Difference): Interfaced with Harvard open ocean model forecasts
[AD-A210521] N90-10517
Tracking performance evaluation
[AD-A210499] N90-10540
PREDICTIONS
Predictive aging of polymers
[NASA-CASE-NPO-17524-1-CU] N90-10261
Turbulence modelling of three-dimensional shear flows N90-10381
Networks for image acquisition, processing and display N90-10545
PREPOLYMERS
UV-curable polyurethane-methacrylate co-networks and interpenetrating networks
[AD-A210445] N90-10285
PREPROCESSING
Automatic classification of spectra from the Infrared Astronomical Satellite (IRAS)
[NASA-RP-1217] N90-10807
PRESSURE EFFECTS
A study of high-lift airfoils at high Reynolds numbers in the Langley low-turbulence pressure tunnel
[NASA-TM-89125] N90-10002
PRESSURE GRADIENTS
Stability of discontinuous shearing motions of a non-Newtonian fluid
[AD-A210643] N90-10406
Stability of discontinuous steady states in shearing motion of a non-Newtonian fluid
[AD-A210644] N90-10407
PRESSURE MEASUREMENT
Introduction to total- and partial-pressure measurements in vacuum systems
[NASA-RP-1219] N90-10412
Three-in-one gage
[NASA-CR-183714] N90-10413
Fluctuating pressures measured beneath a high-temperature, turbulent boundary layer on a flat plate at Mach number of 5
[NASA-TP-2947] N90-10680
PRESSURE OSCILLATIONS
Combustion instabilities in liquid-fueled propulsion systems: An overview N90-10192
Characteristics of combustion driven pressure oscillations in advanced turbo-fan engines with afterburner N90-10194
Low frequency and high frequency combustion oscillation phenomena inside a rocket combustion chamber fed by liquid or gaseous propellants N90-10197
Effects of low-frequency instabilities on the operation of Ramjet air inlets N90-10198
Recent developments in Ramjet pressure oscillation technology N90-10199
Attenuation of reheat buzz by active control N90-10201
Numerical simulation of pressure oscillations in a ramjet combustor N90-10202
Very-low-frequency oscillations in liquid-fueled ramjets N90-10204
Oscillations in non-axisymmetric dump combustors N90-10205
Combustion-driven oscillation in large combustion systems for power generation N90-10207
PRESSURE SENSORS
Analysis and construction of contact and tactile sensors
[DE89-013992] N90-10416
PRESSURE VESSELS
A design assessment for metallic pressure vessels circumferentially reinforced with a pre-tensioned high-specific-strength anisotropic composite overwind
[AD-A209108] N90-10453
PRESSURIZED CABINS
Development of pressure containment and damage tolerance technology for composite fuselage structures in large transport aircraft
[NASA-CR-3996] N90-10186
PROBABILITY DISTRIBUTION FUNCTIONS
Discrete-time conversion for simulating finite-horizon Markov processes
[AD-A210683] N90-10666
Multi-sample functional statistical data analysis
[AD-A210992] N90-10673
PROBABILITY THEORY
Empirical Bayes selection for the highest probability of success in negative binomial distributions
[AD-A210273] N90-10660
On lower confidence for PCS in truncated location parameter models
[AD-A210274] N90-10661
Selection of the best with a preliminary test for two-parameter exponential distributions
[AD-A210275] N90-10662
Research in mathematics and computer science: Calculation of the probability of undetected error for certain error detection codes, phase 1
[AD-A210302] N90-10664
A unified approach to estimating tail behavior
[AD-A210961] N90-10672
Radon transform analysis of a probabilistic method for image generation
[AD-A207814] N90-10702
PROBLEM SOLVING
Iterative performance and an adaptive procedure for viscous flow problems N90-10397
A decision support approach to the file allocation problem in a distributed computing system N90-10609
Northeast Artificial Intelligence Consortium annual report for 1987. Volume 7, part A: Time oriented problem solving
[AD-A210331] N90-10622
Finite methods for a nonlinear allocation problem
[AD-A209719] N90-10629
Numerical optimization in Hilbert space using inexact function and gradient evaluations
[NASA-CR-181926] N90-10640
Application of a hybrid generation/utility assessment heuristic to a class of scheduling problems
[NASA-TM-102367] N90-10674
Motivating the notion of generic design within information processing theory: The design problem space
[AD-A210266] N90-10786
PROCESS CONTROL (INDUSTRY)
Establishment and initial operation of a resource facility for RSR (Rapid Solidification Rate) processed alloys in pilot quantities
[AD-A210369] N90-10283
Advanced GaAs process modeling, volume 1
[AD-A210385] N90-10761
PRODUCT DEVELOPMENT
Japanese structural ceramics research and development N90-10272
PRODUCTION ENGINEERING
Aerospace system unified life cycle engineering producibility measurement issues
[AD-A210937] N90-10607
PRODUCTIVITY
Using computer design and simulation to improve manufacturing productivity
[AD-A210338] N90-10598
PROGRAM VERIFICATION (COMPUTERS)
Initial flight qualification and operational maintenance of X-29A flight software
[NASA-TM-101703] N90-10023
Validation of missile simulation N90-10066
Safety analysis of knowledge-based systems
[NASA-CR-184784] N90-10588
PROGRAMMING LANGUAGES
A common distributed language approach to software integration
[NASA-CR-185499] N90-10584

Safety analysis of knowledge-based systems
[NASA-CR-184784] N90-10588
A special case of second-order strictness analysis
[AD-A210829] N90-10656

PROJECT PLANNING
Liquid rocket booster study. Volume 2, book 3, appendices 2-5: PPIP, transition plan, AMOS plan, and environmental analysis
[NASA-CR-183602] N90-10139

PROJECTILES
Remarks on certain aspects of solid explosive detonation via small projectile impact
[AD-A210648] N90-10307
Studies in penetration mechanics
[AD-A210713] N90-10448
EPIC-2 calculated impact loading histories of thin plates
[AD-A210557] N90-10461
Fracture and three dimensional stress analyses of 7075 aluminum projectile components under spin and inertia load
[AD-A210986] N90-10463
The temporal development of collision cascades in the binary collision approximation
[DE89-015860] N90-10699

PROP-FAN TECHNOLOGY
Large scale prop-fan structural design study. Volume 1: Initial concepts
[NASA-CR-174992] N90-10043
Large scale prop-fan structural design study. Volume 2: Preliminary design of SR-7
[NASA-CR-174993] N90-10044
Large-scale Advanced Prop-fan (LAP) high speed wind tunnel test report
[NASA-CR-182125] N90-10045
Large-scale Advanced Prop-fan (LAP) technology assessment report
[NASA-CR-182142] N90-10046
Full scale technology demonstration of a modern counterrotating unducted fan engine concept: Component test
[NASA-CR-180868] N90-10047
Full scale technology demonstration of a modern counterrotating unducted fan engine concept. Design report
[NASA-CR-180867] N90-10048
Full scale technology demonstration of a modern counterrotating unducted fan engine concept. Engine test
[NASA-CR-180869] N90-10049
Acoustic test and analysis of a counterrotating prop-fan model
[NASA-CR-179590] N90-10683

PROPAGATION VELOCITY
A compilation of digitized satellite imagery of the Gulf Stream (1982, 1983, and 1985)
[AD-A210243] N90-10467

PROPELLANT CHEMISTRY
Cubane derivatives for propellant applications
[AD-A210368] N90-10305

PROPELLANT COMBUSTION
Combustion instabilities in Liquid-Fuelled Propulsion Systems
[AGARD-CP-450] N90-10191
Low frequency and high frequency combustion oscillation phenomena inside a rocket combustion chamber fed by liquid or gaseous propellants N90-10197

PROPELLANTS
Cubane derivatives for propellant applications
[AD-A210368] N90-10305
Organic explosives and related compounds. Environmental and health considerations
[AD-A210554] N90-10306

PROPELLERS
Large scale prop-fan structural design study. Volume 2: Preliminary design of SR-7
[NASA-CR-174993] N90-10044

PROPULSION SYSTEM CONFIGURATIONS
Cycle analysis of scramjet engines
[NAL-TR-1002] N90-10035
Liquid rocket booster study. Volume 2, book 4, appendices 6-8: Reports of Rocketdyne, Pratt and Whitney, and TRW
[NASA-CR-183603] N90-10135
Liquid rocket booster study. Volume 2, book 2, appendix 1: Trades studies
[NASA-CR-183601] N90-10136
Liquid rocket booster study. Volume 1: Executive summary
[NASA-CR-183599] N90-10137
History and status of beamed power technology and applications at 2.45 Gigahertz N90-10150
Materials for engine applications above 3000 deg F: An overview
[NASA-TM-100169] N90-10188
Combustion Instabilities in Liquid-Fuelled Propulsion Systems
[AGARD-CP-450] N90-10191
Combustion instabilities in liquid-fueled propulsion systems: An overview N90-10192

PROPULSION SYSTEM PERFORMANCE
Performance potential of an advanced technology Mach 3 turbojet engine installed on a conceptual high-speed civil transport
[NASA-TM-4144] N90-10034
Report on an overseas visit, June 1988
[AD-A210374] N90-10040
Flight Motor Set 360L003 (STS-29R)
[NASA-CR-183739-VOL-1] N90-10170
A rocket engine design expert system
[NASA-TM-102373] N90-10172
Experimental study on the stability of small rocket engines with storable liquid propellants N90-10196

PROPYLENE
Rechargeable lithium/polymer cathode batteries
[AD-A210978] N90-10354

PROTEIN SYNTHESIS
Control of synthetic peptide tertiary structure
[AD-A210339] N90-10281

PROTEINS
Electrical field dependence of protein conformation and channel function in lipid membranes of different compositions
[AD-A210236] N90-10222

PROTOCOL (COMPUTERS)
Robotic vehicle message format
[AD-A210996] N90-10627

PROTOTYPES
A decision support approach to the file allocation problem in a distributed computing system N90-10609

PSYCHOLOGY
Human performance in continuous/sustained operations and the demands of extended work/rest schedules: An annotated bibliography, volume 2
[AD-A210504] N90-10530

PUBLIC HEALTH
Human health studies of carbon monoxide (CO) under conditions of military weapons systems crewman exposures. Protocol 1: Formation of COHb
[AD-A210344] N90-10528

PULSE CODE MODULATION
Multi-level bandwidth efficient block modulation codes
[NASA-CR-185484] N90-10317

PUPIL SIZE
Effects of miniature CRT (Cathode Ray Tube) location upon primary and secondary task performances
[AD-A210223] N90-10573

PURIFICATION
Preparation, purification and densification of zinc sulfide powder from organometallics
[AD-A210943] N90-10298

PURITY
The improved corrosion resistance of ultra high purity magnesium alloy castings N90-10245

PYRIDINES
Electrochemistry in near-critical and supercritical fluids. Part 7: SO2
[AD-A208207] N90-10214

PYROELECTRICITY
Synthetic polypeptide composites for sensor applications
[AD-A210797] N90-10296

PYROMETALLURGY
Investigation of the pyrometallurgical, physical and mechanical behavior of weld metal
[AD-A211114] N90-10258

PYROTECHNICS
Heat transfer characteristics of igniter output plumes
[DE89-011449] N90-10340
Pyrotechnic ignition studies using a gun tunnel
[DE89-012496] N90-10341

PYRROLES
Quartz crystal microbalance studies of electrochemical growth of conducting polymers
[AD-A210788] N90-10295
Impedance analysis of ionic transport in polypyrrole-polyazulene copolymer and its charge-discharge characteristics
[AD-A210979] N90-10299
Rechargeable lithium/polymer cathode batteries
[AD-A210978] N90-10354

Q

Q SWITCHED LASERS
Efficient nonlinear conversion of laser diode pumped miniature solid state laser sources
[AD-A210708] N90-10433

QUALITY
Differences in writers initial task representations
[AD-A210433] N90-10788

QUALITY CONTROL
Generic system components of the Thiokol ultrasonic RSRM case-to-insulation bondline inspection system
[NASA-CR-183738] N90-10171
Castings Airworthiness
[AGARD-R-762] N90-10231
US Air Force certification of castings N90-10232
Casting factors imposed by the French regulation for foundry castings used in military aircraft N90-10233
The question of the casting factor N90-10238
Quality control of castings N90-10239
Combined advanced foundry and quality control techniques to enhance reliability of castings for the aerospace industry N90-10240
The creation of quality: New directions in the production of aeronautics castings N90-10241
Thin walled cast high-strength structural parts N90-10242
Microstructure morphology and quality of Al-S. castings N90-10244
Development of Information Quality Engineering (IQE) methodology for information resource management
[AD-A210615] N90-10791

QUANTITATIVE ANALYSIS
The quantitative analysis of fracture surfaces using fractals
[DE89-015361] N90-10250

QUANTUM ELECTRODYNAMICS
A theoretical high energy physics program
[DE89-012685] N90-10696
Critical magnetic fields (H(sub c2), H(sub c1)) and kappa in YBa2(Cu0.98M0.02)3O(7+delta), M=Ni, Al, and Cu
[DE89-016412] N90-10745

QUANTUM ELECTRONICS
Quantum 1/F noise in solid state devices in particular Hg1-(sub x)Cd(sub x)Te N(+)-P diodes
[AD-A209365] N90-10730
Submillimeter quantum electronics
[AD-A210439] N90-10762

QUANTUM MECHANICS
Lattice fields and strong interactions
[DE89-015099] N90-10777

QUANTUM THEORY
Quantum 1/F noise in solid state devices in particular Hg1-(sub x)Cd(sub x)Te N(+)-P diodes
[AD-A209365] N90-10730
The origin of the universe from quantum chaos: An introduction to current ideas
[AD-A210441] N90-10813

QUANTUM WELLS
Use of depletion edge translation for high-speed modulation and switching of lightwaves
[AD-A211186] N90-10713
Experimental investigations of transport and optical properties of 3-5 quantum well structures grown via molecular beam epitaxy under optimal growth conditions
[AD-A210269] N90-10758
Submillimeter quantum electronics
[AD-A210439] N90-10762

QUARTZ CRYSTALS
Quartz crystal microbalance studies of electrochemical growth of conducting polymers
[AD-A210788] N90-10295

QUATERNARY ALLOYS
High-efficiency CuInSe2 and CuInGaSe2 based cells and materials research
[DE89-009449] N90-10471

QUATERNIONS
An algorithm for the systematic disturbance of optimal rotational solutions
[NASA-TM-101089] N90-10575

QUENCHING
Development of metastable processing paths for high temperature alloys
[AD-A210550] N90-10254

R

RADIATION COUNTERS
Report on the performance and operating characteristics of the Burle C83061E QUANTACON (trademark) photomultiplier tube
[DE89-015257] N90-10333

RADIATION DAMAGE
Particle emission and charging effects induced by fracture
[AD-A210215] N90-10459

RADIATION DETECTORS
Studies of elementary particles
[DE89-014859] N90-10685
The detection of soft X-rays with charged coupled detectors N90-10798

RADIATION EFFECTS
Biomedical studies with the free electron laser
[AD-A208927] N90-10519
Eye/sensor protection against laser irradiation organic nonlinear optical materials
[AD-A210599] N90-10531
RADIATION HARDENING
Vacuum microelectronics for beam power and rectennas N90-10146
Micro-cavity integrable vacuum diodes and triodes
[DE89-016649] N90-10344
RADIATION INJURIES
Treatment of laser-induced retinal injuries
[AD-A210284] N90-10526
RADIATION SOURCES
The dense Z-pinch as a plasma radiation source. 1: Quasi-static Bennett model
[AD-A210600] N90-10727
RADIATION TOLERANCE
TWIRE: A test program for VLF airborne transmissions
[AD-A210516] N90-10324
RADICALS
Computational modeling of pi-conjugated polyradicals
[AD-A210573] N90-10648
RADIO ASTRONOMY
A lunar far-side very low frequency array
[NASA-CP-3039] N90-10805
Analysis of nearly simultaneous X-ray and optical observations of active galactic nuclei N90-10806
RADIO EQUIPMENT
SINCGARS (Single-Channel Ground/Airborne Radio System) operator performance decay
[AD-A210716] N90-10326
RADIO FREQUENCIES
Manual of regulations and procedures for federal radio frequency management, May 1986 edition: Revisions for January 1989
[PB89-193791] N90-10320
An experimental study of microwave transmission through a decaying plasma
[AD-A210586] N90-10726
RADIO FREQUENCY INTERFERENCE
Coupled multiline CW HF lasers: Experimental performance
[AD-A210844] N90-10434
RADON
Radon transform analysis of a probabilistic method for image generation
[AD-A207814] N90-10702
RAIN
Effects of rain attenuation on satellite EHF (Extremely High Frequency) communications in the US
[AD-A210517] N90-10325
A case study evaluation of satellite-derived rainfall estimates and their application to numerical model precipitation forecast verification
[PB89-194591] N90-10499
RAIN GAGES
A case study evaluation of satellite-derived rainfall estimates and their application to numerical model precipitation forecast verification
[PB89-194591] N90-10499
RAMAN SPECTRA
Stimulated rotational Raman scattering
[DE89-016427] N90-10430
RAMAN SPECTROSCOPY
Raman characterization of high temperature materials using an imaging detector
[DE89-016308] N90-10219
Raman spectroscopic study of the rare earth sesquisulfides
[AD-A210610] N90-10226
RAMJET ENGINES
Recent developments in Ramjet pressure oscillation technology N90-10199
Numerical simulation of pressure oscillations in a ramjet combustor N90-10202
Very-low-frequency oscillations in liquid-fueled ramjets N90-10204
Acoustic-vortex-chemical interactions in an idealized ramjet N90-10206
RANDOM SAMPLING
Multi-sample functional statistical data analysis
[AD-A210992] N90-10673
RANDOM VARIABLES
Asymptotic robustness in regression and autoregression based on Lindeberg conditions
[AD-A210725] N90-10654
Markov chain moment formulas for regenerative simulation
[AD-A210684] N90-10667
RANGE FINDERS
Vision science and technology for supervised intelligent space robots N90-10548
RANKING
Studies in estimation theory, applications and implementations
[AD-A210712] N90-10653
RAPID QUENCHING (METALLURGY)
Establishment and initial operation of a resource facility for RSR (Rapid Solidification Rate) processed alloys in pilot quantities
[AD-A210369] N90-10283
RATIOS
Synthesis and physical properties of poly(perfluoroalkylether) urethanes
[AD-A210500] N90-10287
RAY TRACING
Surface wave ray tracing and Ms:yield determination in a laterally heterogeneous earth
[AD-A210241] N90-10516
RAYLEIGH WAVES
Surface wave ray tracing and Ms:yield determination in a laterally heterogeneous earth
[AD-A210241] N90-10516
REACTION KINETICS
Solvent effects on the kinetics of electroreduction of Cu(I) at mercury
[AD-A209423] N90-10211
Potential dependence of the elementary steps in the kinetics of electrode reactions involving amalgam formation
[AD-A209424] N90-10212
Reaction of oxygen with allene
[DE89-015219] N90-10216
Direct numerical simulation of turbulent free shear flows
[AD-A210161] N90-10218
Attenuated total reflection FTIR spectroscopy for measuring interfacial reaction kinetics at silica surfaces
[AD-A210314] N90-10224
Free-expansion experiments and modeling in detonation: Chemistry and hydrodynamics on a laboratory scale
[DE89-007748] N90-10302
REACTION TIME
Monolayer formation characteristics of novel organic molecules with nonlinear optically active moieties
[AD-A210496] N90-10693
REACTIVITY
Preparation, purification and densification of zinc sulfide powder from organometallics
[AD-A210943] N90-10298
REACTOR TECHNOLOGY
Experience with model based display for advanced diagnostics and control
[DE89-015693] N90-10469
READOUT
Performance of the CAMEX64 silicon strip readout chip
[DE89-014015] N90-10747
REAL TIME OPERATION
Analysis and testing of a high performance air-air missile N90-10069
Real-time support for high performance aircraft operation
[NASA-CR-185475] N90-10075
Real-time observations of aerosol composition changes
[DE89-012382] N90-10422
Optimized resolved rate control of seven-degree-of-freedom Laboratory Telerobotic Manipulator (LTM) with application to three-dimensional graphics simulation
[NASA-TP-2938] N90-10618
A comparison of real-time optical correlators for pattern recognition
[DE89-016416] N90-10705
REATTACHED FLOW
Simultaneous detection of separation and transition in surface shear layers N90-10368
RECEIVERS
Vacuum microelectronics for beam power and rectennas N90-10146
Antenna technology for beamed space-power N90-10149
Performance of a broadbanded ultrasonic transducer with coaxially mounted, nondirectional receiver
[DE89-015838] N90-10343
RECONSTRUCTION
Type reconstruction with first-class polymorphic values
[AD-A210833] N90-10605
RECOVERABLE SPACECRAFT
The Spartan 1 mission
[NASA-TM-101887] N90-10077
RECTENNAS
Vacuum microelectronics for beam power and rectennas N90-10146
Millimeter-wave/infrared rectenna development at Georgia Tech N90-10147
Antenna technology for beamed space-power N90-10149
Technical options for high average power free electron millimeter-wave and laser devices N90-10151
RECTIFICATION
Millimeter-wave/infrared rectenna development at Georgia Tech N90-10147
RECURSIVE FUNCTIONS
Quotient-difference type generalizations of the power method and their analysis
[NASA-TM-102361] N90-10635
A special case of second-order strictness analysis
[AD-A210829] N90-10656
REDUCTION (CHEMISTRY)
Solvent effects on the kinetics of electroreduction of Cu(I) at mercury
[AD-A209423] N90-10211
REDUNDANCY ENCODING
Research in mathematics and computer science: Calculation of the probability of undetected error for certain error detection codes, phase 1
[AD-A210302] N90-10664
REENTRY SHIELDING
Debris/ice/TPS assessment and photographic analysis for Shuttle Mission STS-28R
[NASA-TM-102152] N90-10079
REFLECTANCE
The measurement of infrared spectra of dense ceramics by specular reflectance spectroscopy
[AD-A210609] N90-10291
Image-based terrain modeling with thematic mapper applied to resolving the limit of Holocene Lake expansion in the Great Salt Lake Desert, Utah, part 1
[NASA-CR-185913] N90-10465
The intensity dependent spread model and color constancy N90-10555
Surface reflection: Physical and geometrical perspectives
[AD-A210592] N90-10710
Experimental investigations of transport and optical properties of 3-5 quantum well structures grown via molecular beam epitaxy under optimal growth conditions
[AD-A210269] N90-10758
REFLECTION
Attenuated total reflection FTIR spectroscopy for measuring interfacial reaction kinetics at silica surfaces
[AD-A210314] N90-10224
Energy dependent transport problem with generalized boundary conditions
[DE89-617843] N90-10676
Surface reflection: Physical and geometrical perspectives
[AD-A210592] N90-10710
REFLECTOR ANTENNAS
Analysis and test of a 16-foot radial rib reflector developmental model
[NASA-TM-101648] N90-10457
REFRACTIVITY
Observations of spherical-wave scintillation in strong refractive-index turbulence
[PB89-124747] N90-10355
Laboratory measurements of microwave and millimeter-wave properties of planetary atmospheric constituents
[NASA-CR-185914] N90-10815
REGENERATIVE COOLING
Thermodynamic transport properties of nitrogen tetroxide in hypercritical conditions for regenerative cooling of a rocket engine. Volume 1: Tests
[ETN-89-94975] N90-10773
Thermodynamic transport properties of nitrogen tetroxide in hypercritical conditions for regenerative cooling of a rocket engine. Volume 2: Appendices
[ETN-89-94977] N90-10774
REGENERATIVE FUEL CELLS
Rechargeable lithium/polymer cathode batteries
[AD-A210978] N90-10354
REGRESSION ANALYSIS
Improved estimation of the disturbance variance in a linear regression model
[AD-A210272] N90-10641
Asymptotic robustness in regression and autoregression based on Lindeberg conditions
[AD-A210725] N90-10654
Advances in regression: Use of models in spectroscopic data analysis
[AD-A210541] N90-10665
REGULATIONS
Castings Airworthiness
[AGARD-R-762] N90-10231
The question of the casting factor N90-10238
Manual of regulations and procedures for federal radio frequency management, May 1986 edition: Revisions for January 1989
[PB89-193791] N90-10320

Domestic technology transfer program regulation
[PB89-195374] N90-10793

REINFORCING FIBERS
Field repair of composite materials in Army service: Planning for the future
[AD-A210732] N90-10190

REINFORCING MATERIALS
A design assessment for metallic pressure vessels circumferentially reinforced with a pre-tensioned high-specific-strength anisotropic composite overwind
[AD-A209108] N90-10453

RELAXATION TIME
Solvent dynamical effects in electron transfer: Evaluation of electronic matrix coupling elements for metallocene self-exchange reactions
[AD-A210306] N90-10692

REMOTE CONTROL
Remote control missile model test N90-10063

REMOTE MANIPULATOR SYSTEM
Simulation of shuttle flight control system structural interaction with RMS deployed payloads N90-10100

REMOTE SENSORS
Some significant results from testing a Remote Multiplexing Unit (RMU) for temperature-induced errors
[DE89-009432] N90-10421
Satellite Data Processing System (SDPS) users manual V1.0
[NASA-CR-183054] N90-10468

REMOTELY PILOTED VEHICLES
Robot vehicle video image compression, phase 1
[AD-A210974] N90-10626

REPORTS
NASA scientific and technical publications: A catalog of special publications, reference publications, conference publications, and technical papers, 1988
[NASA-SP-7063(03)] N90-10782

REQUIREMENTS
Casting factors imposed by the French regulation for foundry castings used in military aircraft N90-10233

RESCUE OPERATIONS
Modeling, simulation, and analyses of attitude control for the Crew/Equipment Retriever (CER) proposed for space station
[AD-A208140] N90-10125

RESEARCH
National register of research projects, 1986/87. Part 2B: Natural sciences: Physical, engineering and related sciences (new projects)
[DE89-015033] N90-10826

RESEARCH AND DEVELOPMENT
Japanese structural ceramics research and development N90-10272
Domestic technology transfer program regulation
[PB89-195374] N90-10793

RESEARCH FACILITIES
NTES laser facility for physics experiments: Building 381 high bay option
[DE89-014326] N90-10428
Hybrid vision activities at NASA Johnson Space Center N90-10552

RESEARCH MANAGEMENT
Coordination of mesoscale meteorological research between ASL and European groups
[AD-A210902] N90-10508
Vision science and technology at NASA: Results of a workshop: Executive summary N90-10543
Army Science Conference Proceedings (16th) held in Fort Monroe, Virginia on 25-27 October 1988: Addenda
[AD-A210235] N90-10827

RESEARCH PROJECTS
Research highlights of the NMC (National Meteorological Center) Development Division: 1987-1988
[PB89-206478] N90-10501

RESERVOIRS
Analysis of a model and sequential numerical method for thermal reservoir simulation
[DE89-015117] N90-10384

RESIDUAL STRESS
Ceramic components in machines, Cologne and Aachen, West Germany; Maastricht, The Netherlands and Brussels, Belgium
[DE89-015831] N90-10264

RESOLUTION
Measurement resolution of noise directivity patterns from acoustic flight tests
[NASA-TM-4134] N90-10679

RESONANCE
Density of states in a resonant tunneling structure
[AD-A209508] N90-10731

RESONANT TUNNELING
Density of states in a resonant tunneling structure
[AD-A209508] N90-10731
Submillimeter quantum electronics
[AD-A210439] N90-10762
Dwell time and average local speed in a resonant tunneling structure
[AD-A210566] N90-10764

RESPIRATION
Managing human exposure and health risks: An integrated approach and the role of uncertainty
[DE89-008611] N90-10525
Measurement of respiratory air temperatures and calculation of respiratory heat loss when working at various ambient temperatures
[AD-A210378] N90-10529

RETINA
Treatment of laser-induced retinal injuries
[AD-A210284] N90-10526
Filling in the retinal image N90-10556
A3I visibility modeling project N90-10557

REVERSE FIELD PINCH
Observations of azimuthal asymmetry for certain FRC operating regimes
[DE89-015300] N90-10721

RHODIUM COMPOUNDS
NMR evidence for a planar arene intermediate in the electron-transfer induced eta 6 to eta 4 hapticity change of a rhodium arene complex
[AD-A210211] N90-10177
Monomers, polymers and transition metal complexes based upon carboranes
[AD-A210226] N90-10221

RIBONUCLEIC ACIDS
Biomedical studies with the free electron laser
[AD-A208927] N90-10519

RIGID STRUCTURES
Lumped mass formulations for modeling flexible body systems N90-10091

RISK
Managing human exposure and health risks: An integrated approach and the role of uncertainty
[DE89-008611] N90-10525

ROBOTICS
Flexible robot control: Modeling and experiments N90-10104
Experimental validation of flexible robot arm modeling and control N90-10113
A robotic electrical and tensile testing system for diodes
[DE89-014012] N90-10417
Adaptive machine vision
[AD-A208130] N90-10436
An adaptive controller for enhancing operator performance during teleoperation
[NASA-CR-183445] N90-10438
The role of sensor directed, model based control in robotics
[DE89-014133] N90-10442
A new approach to control single-link flexible arms. Part 1: Modelling and identification in the presence of joint friction
[AD-A210590] N90-10445
Interchangeable end effector tools utilized on the protoflight manipulator arm
[NASA-CR-179374] N90-10447
Instrumentation and robotic image processing using top-down model control N90-10563
Space environment robot vision system N90-10569
Advancing automation and robotics technology for the space station Freedom and for the US economy
[NASA-TM-101561] N90-10577
Optimized resolved rate control of seven-degree-of-freedom Laboratory Telerobotic Manipulator (LTM) with application to three-dimensional graphics simulation
[NASA-TP-2938] N90-10618
Robotic vehicle message format
[AD-A210996] N90-10627

ROBOTS
Proceedings of the Workshop on Computational Aspects in the Control of Flexible Systems, part 1
[NASA-TM-101578-PT-1] N90-10080
Simulation and control problems in elastic robots N90-10098
Proceedings of the Workshop on Computational Aspects in the Control of Flexible Systems, part 2
[NASA-TM-101578-PT-2] N90-10103
Flexible robot control: Modeling and experiments N90-10104
Experimental validation of flexible robot arm modeling and control N90-10113
Shape control of high degree-of-freedom variable geometry trusses N90-10122
Analysis and construction of contact and tactile sensors
[DE89-013992] N90-10416
The role of sensor directed, model based control in robotics
[DE89-014133] N90-10442
Autonomous mobile robot research using the HERMIES-3 robot
[DE89-015916] N90-10443
The 1988 year end report for road following at Carnegie-Mellon
[NASA-CR-185967] N90-10446
Vision Science and Technology at NASA: Results of a Workshop
[NASA-TM-102214] N90-10542
Vision science and technology for supervised intelligent space robots N90-10548
Algorithms and architectures for robot vision N90-10562
Ames vision group research overview N90-10566
Space environment robot vision system N90-10569
Self-calibration of robot-sensor system N90-10570
Robot vehicle video image compression, phase 1
[AD-A210974] N90-10626

ROBUSTNESS (MATHEMATICS)
Adaptive robust control N90-10620
Asymptotic robustness in regression and autoregression based on Lindeberg conditions
[AD-A210725] N90-10654

ROCKET ENGINE CASES
Flight set 360T004 (STS-30) insulation component, interim release, volume 3
[NASA-CR-183746] N90-10169

ROCKET ENGINE DESIGN
Liquid rocket booster study. Volume 2, book 5, appendix 9: LRB alternate applications and evolutionary growth
[NASA-CR-183604] N90-10134
Liquid rocket booster study. Volume 2, book 4, appendices 6-8: Reports of Rocketdyne, Pratt and Whitney, and TRW
[NASA-CR-183603] N90-10135
A rocket engine design expert system
[NASA-TM-102373] N90-10172
Thermodynamic transport properties of nitrogen tetroxide in hypercritical conditions for regenerative cooling of a rocket engine. Volume 1: Tests
[ETN-89-94975] N90-10773
Thermodynamic transport properties of nitrogen tetroxide in hypercritical conditions for regenerative cooling of a rocket engine. Volume 2: Appendices
[ETN-89-94977] N90-10774

ROCKET EXHAUST
X-ray spectroscopy of the SSME plume
[NASA-CR-185308] N90-10168

ROCKET NOZZLES
Flight set 360T004 (STS-30) insulation component, interim release, volume 3
[NASA-CR-183746] N90-10169

ROCKET SOUNDING
Solar X-ray Astronomy Sounding Rocket Program
[NASA-CR-183447] N90-10796

ROLL
Prediction of dynamic derivatives N90-10055

ROTATING DISKS
Electrostatically suspended rotor for angular encoder
[NASA-CASE-MFS-28294-1] N90-10310

ROTATING FLUIDS
On the interaction of stationary crossflow vortices and Tollmien-Schlichting waves in the boundary layer on a rotating disc
[NASA-CR-181859] N90-10007
Symmetry breaking bifurcations and the growth of chaos in a rotating fluid
[AD-A210969] N90-10411

ROTATION
Similarity solutions that give rise to hyperbolicity and change of type in steady flow of a viscoelastic fluid
[AD-A210920] N90-10410
An algorithm for the systematic disturbance of optimal rotational solutions
[NASA-TM-101089] N90-10575

ROTORS
Improved silicon carbide for advanced heat engines
[NASA-CR-180831] N90-10293

ROVING VEHICLES
Laser-powered Martian rover N90-10157

RP-1 ROCKET PROPELLANTS
Liquid rocket booster study. Volume 2, book 1
[NASA-CR-183600] N90-10133

RUN TIME (COMPUTERS)
Efficiency and capabilities of multi-body simulations N90-10095
Performance evaluation of the Scheme86 and HP precision architectures
[AD-A209418] N90-10578
A multiprocessor architecture using modular arithmetic for very high precision computation
[AD-A208154] N90-10579
Ada (trademark) projects at NASA. Runtime environment issues and recommendations
[NASA-CR-183435] N90-10583

S

SAFETY FACTORS
US Air Force certification of castings N90-10232
SALINITY
Chesapeake Bay surface salinities, 1951-88 [PB89-194583] N90-10513
Semi-monthly temperature and geopotential anomaly in the upper 500 meters along the Oahu-Farallon Islands great circle from November 15, 1967 through December 15, 1979 [AD-A210640] N90-10518
SAMPLES
Multi-sample functional statistical data analysis [AD-A210992] N90-10673
SAMPLING
Method and apparatus for determining time, direction and composition of impacting space particles [NASA-CASE-LAR-13392-1-CU] N90-10132
Sampling and noise in vision networks N90-10544
Networks for image acquisition, processing and display N90-10545
Asymptotic robustness in regression and autoregression based on Lindeberg conditions [AD-A210725] N90-10654
Selection of the best with a preliminary test for two-parameter exponential distributions [AD-A210275] N90-10662
SATELLITE COMMUNICATION
Effects of rain attenuation on satellite EHF (Extremely High Frequency) communications in the US [AD-A210517] N90-10325
SATELLITE IMAGERY
A compilation of digitized satellite imagery of the Gulf Stream (1982, 1983, and 1985) [AD-A210243] N90-10467
SATELLITE OBSERVATION
A case study evaluation of satellite-derived rainfall estimates and their application to numerical model precipitation forecast verification [PB89-194591] N90-10499
SATELLITE ORBITS
On analytic modeling of lunar perturbations of artificial satellites of the earth [AD-A210440] N90-10078
SATELLITE POWER TRANSMISSION
Second Beamed Space-Power Workshop [NASA-CP-3037] N90-10140
Power beaming options N90-10142
Power from space for use on earth: An emerging global option N90-10144
History and status of beamed power technology and applications at 2.45 Gigahertz N90-10150
Overview of microwave concepts N90-10155
Power for the moon: Is microwave power beaming an option? N90-10158
SATELLITE SOLAR ENERGY CONVERSION
Power from space for use on earth: An emerging global option N90-10144
New energy conversion techniques in space, applicable to propulsion [AIAA-79-1338] N90-10145
Technical options for high average power free electron milimeter-wave and laser devices N90-10151
Laser energy conversion N90-10152
SCALE (CORROSION)
Polypeptide inhibitors of mineral scaling and corrosion [AD-A210507] N90-10225
SCALING LAWS
Scaling and modeling of turbulent suspension flows N90-10393
SCANNING
Synthesis and physical properties of poly(perfluoroalkylether) urethanes [AD-A210500] N90-10287
The 1988 year end report for road following at Carnegie-Mellon [NASA-CR-185967] N90-10446
Active participation in highly automated systems: Turning the wrong stuff into the right stuff [AD-A210218] N90-10572
Online support for the intellectual activity of browsing N90-10784
SCANNING TUNNELING MICROSCOPY
Scanning tunneling microscopy etching of micrometer level features on p-type GaAs [AD-A209216] N90-10328
SCENE ANALYSIS
Knowledge-based machine vision systems for space station automation [NASA-CR-185710] N90-10124
The 1988 year end report for road following at Carnegie-Mellon [NASA-CR-185967] N90-10446
SCHEDULING
Effective resource utilization for multiprocessor join execution [DE89-016303] N90-10595
Application of a hybrid generation/utility assessment heuristic to a class of scheduling problems [NASA-TM-102367] N90-10674
SCHOTTKY DIODES
Laterally stacked Schottky diodes for infrared sensor applications [NASA-CASE-NPO-17426-1-CU] N90-10329
SCINTILLATION
Observations of spherical-wave scintillation in strong refractive-index turbulence [PB89-124747] N90-10355
SEA ICE
Motion detection in astronomical and ice floe images N90-10558
SEARCHING
String Search [PB89-195986] N90-10593
Online support for the intellectual activity of browsing N90-10784
SECONDARY FLOW
Basic studies of the unsteady flow past high angle of attack airfoils [AD-A210252] N90-10008
SEDIMENTS
A search for layering in the oceanic crust [PB89-196220] N90-10514
SEISMIC WAVES
A search for layering in the oceanic crust [PB89-196220] N90-10514
Institute of Geophysics and Planetary Physics, 1988 [DE89-014363] N90-10794
SEMICONDUCTOR DEVICES
Scanning tunneling microscopy etching of micrometer level features on p-type GaAs [AD-A209216] N90-10328
SEMICONDUCTOR DIODES
A robotic electrical and tensile testing system for diodes [DE89-014012] N90-10417
Dwell time and average local speed in a resonant tunneling structure [AD-A210566] N90-10764
SEMICONDUCTOR LASERS
Laser diode array and transmission optics N90-10163
Efficient nonlinear conversion of laser diode pumped miniature solid state laser sources [AD-A210708] N90-10433
Automation of fiber-optic pigtailing process: Laser welding demonstration program [AD-A210351] N90-10707
Properties of devices prepared with epitaxial layers on InP [AD-A210304] N90-10759
SEMICONDUCTORS (MATERIALS)
Photoreflectance study of boron ion-implanted (100) cadmium telluride [SD-TR-88-89] N90-10300
Density of states in a resonant tunneling structure [AD-A209508] N90-10731
Ordered structures and metastable alloys grown by OMVPE [DE89-016370] N90-10744
Effects of coherent scattering on infrared absorption in doped semiconductors [AD-A210224] N90-10756
The growth of gallium nitride films via the innovative technique of atomic layer epitaxy [AD-A210380] N90-10760
SENSORS
A program to improve performance of AFGL (Air Force Geophysical Laboratory) automated present weather observing sensors [AD-A207669] N90-10495
SEPARATED FLOW
Basic studies of the unsteady flow past high angle of attack airfoils [AD-A210252] N90-10008
The three-dimensional vortex sheet structure on delta wings N90-10367
Simultaneous detection of separation and transition in surface shear layers N90-10368
Bifurcations in Poiseuille flow and wall turbulence N90-10370
Numerically determined transition in separated internal flow N90-10374
SEQUENCING
National airspace system approach and departure sequencing operational concept [NAS-SR-1322] N90-10017
General decomposition of sequential machines: Relationships to state assignment [AD-A208189] N90-10580
Application of a hybrid generation/utility assessment heuristic to a class of scheduling problems [NASA-TM-102367] N90-10674
SEQUENTIAL COMPUTERS
General decomposition of sequential machines: Relationships to state assignment [AD-A208189] N90-10580
SERIES EXPANSION
On the coefficients of differentiated expansions of ultraspherical polynomials [NASA-CR-181913] N90-10637
SERVICE LIFE
Predictive aging of polymers [NASA-CASE-NPO-17524-1-CU] N90-10261
SET THEORY
On the expected complexity of the three-dimensional Voronoi diagram [PB89-209332] N90-10636
SHADOWS
An anisotropic shadowband correction for parameterized sky conditions and geometry [DE89-014916] N90-10485
Factors affecting the perception of transparent motion N90-10559
SHAKERS
VIBRAFUGE: A combined environment testing facility-vibration testing on a centrifuge [DE89-015120] N90-10458
SHAPE CONTROL
Shape control of high degree-of-freedom variable geometry trusses N90-10122
SHAPES
The measurement of infrared spectra of dense ceramics by specular reflectance spectroscopy [AD-A210609] N90-10291
Two-dimensional shape recognition using sparse distributed memory N90-10554
SHEAR FLOW
Direct numerical simulation of turbulent free shear flows [AD-A210161] N90-10218
Fluid Dynamics of Three-Dimensional Turbulent Shear Flows and Transition [AGARD-CP-438] N90-10356
Turbulence modelling of three-dimensional shear flows N90-10381
Dynamics and control of turbulent shear flows [AD-A210396] N90-10402
Analysis of spurt phenomena for a non-Newtonian fluid [AD-A210560] N90-10405
SHEAR PROPERTIES
Stability of discontinuous shearing motions of a non-Newtonian fluid [AD-A210643] N90-10406
SHEAR STRESS
Simultaneous detection of separation and transition in surface shear layers N90-10368
Analysis of spurt phenomena for a non-Newtonian fluid [AD-A210560] N90-10405
Stability of discontinuous steady states in shearing motion of a non-Newtonian fluid [AD-A210644] N90-10407
Stress intensity factors and displacements for arc bend samples using collocation [AD-A210404] N90-10460
SHOCK DISCONTINUITY
Shock capturing by the spectral viscosity method [NASA-CR-181920] N90-10639
SHOCK LOADS
Dynamically compressed metals: Theory [AD-A210741] N90-10257
Shock compression and release in high-strength ceramics [DE89-013995] N90-10265
SHOCK SPECTRA
EPIC-2 calculated impact loading histories of thin plates [AD-A210557] N90-10461
SHOCK TESTS
Remarks on certain aspects of solid explosive detonation via small projectile impact [AD-A210648] N90-10307
SHOCK WAVE INTERACTION
A study of the structure of highly swept shock wave turbulent boundary layer interactions N90-10376
SHOCK WAVES
A numerical method for solving transonic flow past aircraft in Cartesian coordinates [NAL-TR-1008] N90-10003

A composite velocity procedure for the three-dimensional reduced Navier-Stokes equations N90-10396
Shock behavior of explosives about the C-J (Chapman-Juget) point
[DE89-007642] N90-10400
SHORT CIRCUITS
Development of an expert system supporting short-circuit tests for circuit breakers
[DE89-760384] N90-10334
SHORT CRACKS
Fatigue growth and closure of short cracks
[AD-A210824] N90-10462
SHORT WAVE RADIATION
Shortwavelength coherent radiation: Generation and applications
[AD-A209847] N90-10427
SHROUDED TURBINES
Advanced Turbine Technology Applications Project (ATTAP)
[NASA-CR-185133] N90-10036
SIGNAL ANALYSIS
Combustion-driven oscillation in large combustion systems for power generation N90-10207
SIGNAL DETECTION
Sampling and noise in vision networks N90-10544
SIGNAL ENCODING
Pin switch circuits instrument for microsecond velocity measurements
[AD-A210638] N90-10426
SIGNAL GENERATORS
Waveform generator signal processing software
[PB89-192660] N90-10587
SIGNAL MEASUREMENT
Pin switch circuits instrument for microsecond velocity measurements
[AD-A210638] N90-10426
SIGNAL PROCESSING
System identification for large space structures N90-10126
Sampling and noise in vision networks N90-10544
Network of dedicated processors for finding lowest-cost map path
[NASA-CASE-NPO-17716-1-CU] N90-10608
Fluctuating pressures measured beneath a high-temperature, turbulent boundary layer on a flat plate at Mach number of 5
[NASA-TP-2947] N90-10680
SIGNAL RECEPTION
ILS/MLS comparison tests at Miami/Tamiami, Florida Airport
[ACD-330] N90-10018
SIGNAL REFLECTION
A search for layering in the oceanic crust
[PB89-198220] N90-10514
SIGNAL TRANSMISSION
Omega system performance assessment
[AD-A210342] N90-10322
SIGNATURES
Two counter-rotating vortices approaching a free surface in a viscous fluid
[AD-A210495] N90-10404
SILANES
X-ray lithography studies of polysilane using a laser plasma X-ray source
[DE89-015390] N90-10266
New polymer precursors to boron and silicon nitrides
[AD-A210287] N90-10279
SILICON
The effects of normal annealing cycles during IGFET fabrication on initial and radiation induced gate insulator defects
[AD-A210282] N90-10278
Performance of the CAMEX64 silicon strip readout chip
[DE89-014015] N90-10747
Methods to decrease defect density in GaAs/Si heteroepitaxy
[DE89-016306] N90-10753
Effects of coherent scattering on infrared absorption in doped semiconductors
[AD-A210224] N90-10756
Bias and oxide thickness dependence of trapped charge buildup in MOS devices
[AD-A210264] N90-10757
SILICON ALLOYS
Microstructure morphology and quality of Al-Si castings N90-10244
Structure of amorphous silicon alloy films
[DE89-009441] N90-10734
SILICON CARBIDES
Shock compression and release in high-strength ceramics
[DE89-013995] N90-10265
Thermophysical properties of ceramics. Part 2: Development of specific-heat-measurement apparatus at high temperature
[DE89-760382] N90-10268
Improved silicon carbide for advanced heat engines
[NASA-CR-180831] N90-10293
Zirconia toughened SiC whisker reinforced alumina composites small business innovation research
[NASA-CR-179629] N90-10294
SILICON COMPOUNDS
Reactions of hydrogen chloride and boron trichloride with trimethylsilylamino groups
[AD-A209006] N90-10209
Bonding in transition metal silyl dimers. Molecular orbital theory
[AD-A208269] N90-10260
SILICON DIOXIDE
Attenuated total reflection FTIR spectroscopy for measuring interfacial reaction kinetics at silica surfaces
[AD-A210314] N90-10224
Analysis of surface modified colloidal silicas
[DE89-015849] N90-10267
Silicon dioxide deposition at 100 deg C using vacuum ultraviolet light
[TR-0086(3945-07)-6] N90-10269
SILICON FILMS
Characterization of diamond films by thermogravimetric analysis and infrared spectroscopy
[AD-A210564] N90-10288
SILICON NITRIDES
Combining spontaneous molecular assembly with microfabrication to pattern surfaces: Selective binding of isonitriles to platinum microwires and characterization by electrochemistry and surface spectroscopy
[AD-A209528] N90-10213
New polymer precursors to boron and silicon nitrides
[AD-A210287] N90-10279
SILICON POLYMERS
Characterization of 4/3 technology large-scale integrated circuit on polysilicon processes
[BDX-613-3971] N90-10335
SILVER
Multiple internal reflection Fourier transform infrared spectroscopy studies of thiocyanate adsorption on silver and gold
[AD-A210245] N90-10223
SIMD (COMPUTERS)
Evaluating local indirect addressing in SIMD proc essors
[NASA-CR-181845] N90-10581
SIMPLEX METHOD
Finite methods for a nonlinear allocation problem
[AD-A209719] N90-10629
SIMULATION
Basic studies of the unsteady flow past high angle of attack airfoils
[AD-A210252] N90-10008
Study of the NO3 radical decomposition reaction and the N2O5 in equilibrium with NO3 + NO2 equilibrium constant
[PB89-208961] N90-10480
Numerical simulations of a midlatitude squall line N90-10497
Discrete-time conversion for simulating finite-horizon Markov processes
[AD-A210683] N90-10666
Markov chain moment formulas for regenerative simulation
[AD-A210684] N90-10667
SIMULATORS
CONSOLE: A CAD tandem for optimization-based design interacting with user-supplied simulators N90-10085
Consumer electronics testing to fast-rise EMP (Electromagnetic Pulse) VEMPS (Vertical Electromagnetic Pulse Simulator) 2 development
[AD-A210505] N90-10323
SINGLE CRYSTALS
The measurement of infrared spectra of dense ceramics by specular reflectance spectroscopy
[AD-A210609] N90-10291
Magnetic correlations in high T(sub c) oxides in the superconducting state
[DE89-016421] N90-10746
SINGULARITY (MATHEMATICS)
A structured singular value approach to missile autopilot analysis 2 N90-10068
SINTERING
Ceramic processing of bulk high-T(sub c) superconductors
[DE89-015703] N90-10736
SKIN FRICTION
Simultaneous detection of separation and transition in surface shear layers N90-10368
Control and modification of turbulence N90-10377
SLEEP DEPRIVATION
Daytime sleepiness, performance, mood, nocturnal sleep: The effect of benzodiazepine and caffeine on their relationship
[AD-A210915] N90-10533
SLEWING
Use of the quasilinearization algorithm for the simulation of LSS slewing N90-10110
SLIDING
Friction and wear of oxide-ceramic sliding against IN-718 nickel base alloy at 25 to 800 C in atmospheric air
[NASA-TM-102291] N90-10262
SOFTWARE ENGINEERING
Proceedings of the Workshop on Computational Aspects in the Control of Flexible Systems, part 1
[NASA-TM-101578-PT-1] N90-10080
Additional software developments wanted for modeling and control of flexible space systems N90-10083
A comparison of software for the modeling and control of flexible systems N90-10092
Control law synthesis and optimization software for large order aeroservoelastic systems N90-10111
Safety analysis of knowledge-based systems
[NASA-CR-184784] N90-10588
Structure flow diagram generator
[PB89-195978] N90-10592
String Search
[PB89-195986] N90-10593
SOFTWARE TOOLS
Computational controls for aerospace systems N90-10082
CONSOLE: A CAD tandem for optimization-based design interacting with user-supplied simulators N90-10085
Control/structure interaction methods for space station power systems N90-10087
Modeling and control system design and analysis tools for flexible structures N90-10090
String Search
[PB89-195986] N90-10593
The applicability and limitations of expert system shells
[AD-A210801] N90-10625
SOI (SEMICONDUCTORS)
Epitaxial GaAs on SOI wafers
[AD-A209009] N90-10729
SOLAR ACTIVITY
Solar-geophysical data number 532, December 1988. Part 1: Data for November, October 1988, and late data
[PB89-152086] N90-10818
Solar-geophysical data number 533. Part 1: Data for December, November 1988, and late data
[PB89-162481] N90-10820
Solar-geophysical data number 534, February 1989. Part 1: (Prompt reports). Data for January 1989, December 1988 and late data
[PB89-173041] N90-10822
Long-term solar-terrestrial observations
[DE89-016318] N90-10825
SOLAR ARRAYS
Power beaming options N90-10142
Applicability of the beamed power concept to lunar rovers, construction, mining, explorers and other mobile equipment N90-10159
Earth orbit laser systems N90-10162
Central electrical utility power for a satellite ring city in low earth orbit space N90-10166
SOLAR CELLS
Laser energy conversion N90-10152
Laser-powered lunar base N90-10156
High-efficiency CuInSe2 and CuInGaSe2 based cells and materials research
[DE89-009449] N90-10471
Alternative fabrication techniques for high-efficiency CuInSe2 and CuInSe2-alloy films and cells
[DE89-009451] N90-10474
SOLAR COLLECTORS
Structural concepts for very large (400-meter-diameter) solar concentrators N90-10153
SOLAR CORONA
Soft X-ray astronomy using grazing incidence optics N90-10797
The design and evaluation of grazing incidence relay optics N90-10799
The correspondence between small-scale coronal structures and the evolving solar magnetic field N90-10800
SOLAR COSMIC RAYS
Solar-geophysical data number 532, December 1988. Part 1: Data for November, October 1988, and late data
[PB89-152086] N90-10818
Solar-geophysical data number 533. Part 1: Data for December, November 1988, and late data
[PB89-162481] N90-10820

Solar-geophysical data number 534, February 1989. Part 1: (Prompt reports). Data for January 1989, December 1988 and late data
[PB89-173041] N90-10822

SOLAR ENERGY
Power from space for use on earth: An emerging global option N90-10144

SOLAR ENERGY CONVERSION
Power beaming options N90-10142
Laser-powered Martian rover N90-10157
United States photovoltaic concentrator technology process and new program initiative
[DE89-013812] N90-10475
Stretched-membrane heliostats for solar central-receiver power plants
[DE89-016034] N90-10476

SOLAR FLARES
Solar-geophysical data number 531, part 2. Data foor May 1988 and miscellaneous
[PB89-139950] N90-10817
Solar-geophysical data number 532, December 1988. Part 1: Data for November, October 1988, and late data
[PB89-152086] N90-10818
Solar-geophysical data number 532, December 1988. Part 2: Data for June 1988 and miscellaneous
[PB89-152094] N90-10819
Solar-geophysical data number 533. Part 2: Data for July 1988 and miscellaneous
[PB89-162499] N90-10821
Solar-geophysical data number 534, February 1989. Part 2: (Comprehensive reports). Data for August 1988 and miscellaneous
[PB89-173058] N90-10823
Solar-geophysical data number 536, part 2. Data for October 1988 and miscellaneous
[PB89-194658] N90-10824

SOLAR FLUX
The correspondence between small-scale coronal structures and the evolving solar magnetic field N90-10800

SOLAR MAGNETIC FIELD
The correspondence between small-scale coronal structures and the evolving solar magnetic field N90-10800
The observation of possible reconnection events in the boundary changes of solar coronal holes N90-10801
Solar-geophysical data number 532, December 1988. Part 1: Data for November, October 1988, and late data
[PB89-152086] N90-10818
Solar-geophysical data number 533. Part 1: Data for December, November 1988, and late data
[PB89-162481] N90-10820
Solar-geophysical data number 534, February 1989. Part 1: (Prompt reports). Data for January 1989, December 1988 and late data
[PB89-173041] N90-10822

SOLAR PHYSICS
Solar X-ray Astronomy Sounding Rocket Program
[NASA-CR-183447] N90-10796

SOLAR POWER SATELLITES
Second Beamed Space-Power Workshop
[NASA-CP-3037] N90-10140
Power from space for use on earth: An emerging global option N90-10144
New energy conversion techniques in space, applicable to propulsion
[AIAA-79-1336] N90-10145
History and status of beamed power technology and applications at 2.45 Gigahertz N90-10150
Technical options for high average power free electron millimeter-wave and laser devices N90-10151
Laser-powered Martian rover N90-10157
Applicability of the beamed power concept to lunar rovers, construction, mining, explorers and other mobile equipment N90-10159

SOLAR PROMINENCES
Solar-geophysical data number 531, part 2. Data foor May 1988 and miscellaneous
[PB89-139950] N90-10817
Solar-geophysical data number 532, December 1988. Part 2: Data for June 1988 and miscellaneous
[PB89-152094] N90-10819
Solar-geophysical data number 533. Part 2: Data for July 1988 and miscellaneous
[PB89-162499] N90-10821
Solar-geophysical data number 534, February 1989. Part 2: (Comprehensive reports). Data for August 1988 and miscellaneous
[PB89-173058] N90-10823
Solar-geophysical data number 536, part 2. Data for October 1988 and miscellaneous
[PB89-194658] N90-10824

SOLAR RADIATION
An anisotropic shadowband correction for parameterized sky conditions and geometry
[DE89-014916] N90-10485
Geophysical monitoring for climatic change number 16
[PB89-159628] N90-10494

SOLAR RADIO BURSTS
Solar-geophysical data number 531, part 2. Data foor May 1988 and miscellaneous
[PB89-139950] N90-10817
Solar-geophysical data number 532, December 1988. Part 2: Data for June 1988 and miscellaneous
[PB89-152094] N90-10819
Solar-geophysical data number 533. Part 2: Data for July 1988 and miscellaneous
[PB89-162499] N90-10821
Solar-geophysical data number 534, February 1989. Part 2: (Comprehensive reports). Data for August 1988 and miscellaneous
[PB89-173058] N90-10823
Solar-geophysical data number 536, part 2. Data for October 1988 and miscellaneous
[PB89-194658] N90-10824

SOLAR RADIO EMISSION
Solar-geophysical data number 532, December 1988. Part 1: Data for November, October 1988, and late data
[PB89-152086] N90-10818
Solar-geophysical data number 533. Part 1: Data for December, November 1988, and late data
[PB89-162481] N90-10820
Solar-geophysical data number 534, February 1989. Part 1: (Prompt reports). Data for January 1989, December 1988 and late data
[PB89-173041] N90-10822

SOLAR SPECTRA
Solar X-ray Astronomy Sounding Rocket Program
[NASA-CR-183447] N90-10796
X-ray bright points and He I lambda 10830 dark points N90-10802
Advances in photographic X-ray imaging for solar astronomy N90-10803
Correspondence between solar fine-scale structures in the corona, transition region, and lower atmosphere from collaborative observations N90-10804

SOLAR WIND
Numerical simulation of the compressible Orszag-Tang vortex
[AD-A210465] N90-10725

SOLAR X-RAYS
The correspondence between small-scale coronal structures and the evolving solar magnetic field N90-10800
Solar-geophysical data number 531, part 2. Data foor May 1988 and miscellaneous
[PB89-139950] N90-10817
Solar-geophysical data number 532, December 1988. Part 2: Data for June 1988 and miscellaneous
[PB89-152094] N90-10819
Solar-geophysical data number 533. Part 2: Data for July 1988 and miscellaneous
[PB89-162499] N90-10821
Solar-geophysical data number 534, February 1989. Part 2: (Comprehensive reports). Data for August 1988 and miscellaneous
[PB89-173058] N90-10823
Solar-geophysical data number 536, part 2. Data for October 1988 and miscellaneous
[PB89-194658] N90-10824

SOLID ELECTROLYTES
Impedance studies of the cell Pt/Ag+ conducting glass/Ag beta-alumina/Pt
[AD-A209820] N90-10210
Advanced double layer capacitor
[AD-A210510] N90-10348

SOLID PROPELLANTS
Laser propulsion to earth orbit. Has its time come? N90-10143

SOLID STATE
Computer simulations of polymer dynamics in the solid state
[DE89-010337] N90-10275

SOLID STATE DEVICES
Vacuum microelectronics for beam power and rectennas N90-10146
Quantum 1/F noise in solid state devices in particular Hg1-(sub x)Cd(sub x)Te N(+)-P diodes
[AD-A209365] N90-10730
Submillimeter quantum electronics
[AD-A210439] N90-10762

SOLID STATE LASERS
Earth orbit laser systems N90-10162
A battery-powered, solid state magnetic compressor with applications for high PRF accelerators and lasers
[DE89-015770] N90-10332
Efficient nonlinear conversion of laser diode pumped miniature solid state laser sources
[AD-A210708] N90-10433

SOLID SUSPENSIONS
Scaling and modeling of turbulent suspension flows N90-10393
Turbulence kinetic energy equation for dilute suspensions N90-10394

SOLIDIFICATION
Development of metastable processing paths for high temperature alloys
[AD-A210550] N90-10254
Establishment and initial operation of a resource facility for RSR (Rapid Solidification Rate) processed alloys in pilot quantities
[AD-A210369] N90-10283

SOLIDS
Hierarchical structure in polymeric solids and its influence on properties
[AD-A210918] N90-10297

SOLITARY WAVES
A straightforward method for finding implicit solitary wave solutions of nonlinear evolution and wave equations
[AD-A210561] N90-10647

SOLUBILITY
Mechanical properties, solubilities, and processabilities in the design of the first super-strong liquid-crystalline polymers
[DE89-009252] N90-10273
Synthetic polypeptide composites for sensor applications
[AD-A210797] N90-10296

SOLUTES
Monte Carlo simulations of small solute/solvent clusters: Cluster properties and phase transitions
[AD-A209559] N90-10684

SOLUTIONS
Stress in dilute suspensions N90-10389

SOLVATION
Potential dependence of the elementary steps in the kinetics of electrode reactions involving amalgam formation
[AD-A209424] N90-10212

SOLVENTS
Solvent effects on the kinetics of electroreduction of Cu(I) at mercury
[AD-A209423] N90-10211
Solvent relaxation in electron-transfer reactions: Comparisons between barrier-crossing dynamics in water and polar aprotic media
[AD-A210212] N90-10220
Monte Carlo simulations of small solute/solvent clusters: Cluster properties and phase transitions
[AD-A209559] N90-10684
Solvent effects on intervalence electron-transfer energies for biferrocene cations: Comparisons with molecular models of solvent reorganization
[AD-A210263] N90-10691
Solvent dynamical effects in electron transfer: Evaluation of electronic matrix coupling elements for metallocene self-exchange reactions
[AD-A210306] N90-10692

SOUND FIELDS
The theory and application of quadratic minimization in the active reduction of sound and vibration N90-10682

SOUND TRANSMISSION
IFD (Implicit Finite Difference): Interfaced with Harvard open ocean model forecasts
[AD-A210521] N90-10517

SOUND WAVES
Acoustic-vortex-chemical interactions in an idealized ramjet N90-10206

SPACE DEBRIS
Orbital debris research at NASA Johnson Space Center, 1986-1988
[NASA-TM-102155] N90-10795

SPACE ERECTABLE STRUCTURES
Structural concepts for very large (400-meter-diameter) solar concentrators N90-10153

SPACE EXPLORATION
Overview of laser concepts N90-10154

SPACE MAINTENANCE
Interchangeable end effector tools utilized on the protoflight manipulator arm
[NASA-CR-179374] N90-10447

SPACE PLASMAS
Computer simulation of plasma interactions near Titan N90-10816

SPACE PLATFORMS
Input-output oriented computation algorithms for the control of large flexible structures N90-10118

SPACE POWER REACTORS
A feasibility assessment of installation, operation and disposal options for nuclear reactor power system concepts for a NASA growth space station
[NASA-TM-89923] N90-10174

SPACE SHUTTLE ASCENT STAGE
Flight Motor Set 360L003 (STS-29R)
[NASA-CR-183739-VOL-1] N90-10170

SPACE SHUTTLE BOOSTERS
Flight set 360T004 (STS-30) insulation component, interim release, volume 3
[NASA-CR-183746] N90-10169
Flight Motor Set 360L003 (STS-29R)
[NASA-CR-183739-VOL-1] N90-10170
Generic system components of the Thiokol ultrasonic RSRM case-to-insulation bondline inspection system
[NASA-CR-183738] N90-10171

SPACE SHUTTLE MAIN ENGINE
X-ray spectroscopy of the SSME plume
[NASA-CR-185308] N90-10168

SPACE SHUTTLE MISSION 51-J
Debris/ice/TPS assessment and photographic analysis for Shuttle Mission STS-28R
[NASA-TM-102152] N90-10079

SPACE SHUTTLE MISSIONS
Flight Motor Set 360L003 (STS-29R)
[NASA-CR-183739-VOL-1] N90-10170

SPACE SHUTTLE PAYLOADS
The Spartan 1 mission
[NASA-TM-101887] N90-10077

SPACE SHUTTLES
Simulation of shuttle flight control system structural interaction with RMS deployed payloads N90-10100
Liquid rocket booster study. Volume 1: Executive summary
[NASA-CR-183599] N90-10137
Liquid rocket booster study. Volume 2, book 6, appendix 10: Vehicle systems effects
[NASA-CR-183605] N90-10138

SPACE STATION PAYLOADS
Space station RT and E utilization study
[NASA-CR-181707] N90-10129

SPACE STATION POWER SUPPLIES
Space station RT and E utilization study
[NASA-CR-181707] N90-10129
Space station systems: A bibliography with indexes (supplement 8)
[NASA-SP-7056(08)] N90-10131
Beamed laser power in support of near-earth missions N90-10167
A feasibility assessment of installation, operation and disposal options for nuclear reactor power system concepts for a NASA growth space station
[NASA-TM-89923] N90-10174
Bidirectional power converter control electronics
[NASA-CR-175070] N90-10175

SPACE STATION PROPULSION
Space station systems: A bibliography with indexes (supplement 8)
[NASA-SP-7056(08)] N90-10131

SPACE STATION STRUCTURES
Space station systems: A bibliography with indexes (supplement 8)
[NASA-SP-7056(08)] N90-10131

SPACE STATIONS
Control/structure interaction methods for space station power systems N90-10087
Explicit modeling and computational load distribution for concurrent processing simulation of the space station N90-10096
Modeling and stabilization of large flexible space stations N90-10120
Knowledge-based machine vision systems for space station automation
[NASA-CR-185710] N90-10124
System identification for large space structures N90-10126
Space station RT and E utilization study
[NASA-CR-181707] N90-10129
Space station systems: A bibliography with indexes (supplement 8)
[NASA-SP-7056(08)] N90-10131
Central electrical utility power for a satellite ring city in low earth orbit space N90-10166
Beamed laser power in support of near-earth missions N90-10167
Advancing automation and robotics technology for the space station Freedom and for the US economy
[NASA-TM-101561] N90-10577
Orbital debris research at NASA Johnson Space Center, 1986-1988
[NASA-TM-102155] N90-10795

SPACE TOOLS
Interchangeable end effector tools utilized on the protoflight manipulator arm
[NASA-CR-179374] N90-10447

SPACE TRANSPORTATION
Low-earth-orbit to low-lunar-orbit laser freighter N90-10160
Laser propulsion option N90-10161
Laser thruster N90-10164

SPACE TRANSPORTATION SYSTEM
Liquid rocket booster study. Volume 2, book 2, appendix 1: Trades studies
[NASA-CR-183601] N90-10136
Liquid rocket booster study. Volume 2, book 3, appendices 2-5: PPIP, transition plan, AMOS plan, and environmental analysis
[NASA-CR-183602] N90-10139

SPACE-TIME FUNCTIONS
Are there causal vacuum solutions with the symmetries of the Goedel universe in higher-derivative gravity
[DE89-611966] N90-10770

SPACECRAFT COMMUNICATION
Space station RT and E utilization study
[NASA-CR-181707] N90-10129

SPACECRAFT COMPONENTS
Materials for engine applications above 3000 deg F: An overview
[NASA-TM-100169] N90-10188
Evaluation of titanium castings for aerospace components N90-10237

SPACECRAFT CONSTRUCTION MATERIALS
Conference on Aerospace Transparent Materials and Enclosures (15th) 16-20 January 1989. Volume 2: Sessions 6-9
[AD-A210201] N90-10024

SPACECRAFT CONTROL
Computational controls for aerospace systems N90-10082
Additional software developments wanted for modeling and control of flexible space systems N90-10083
Flexible structure control experiments using a real-time workstation for computer-aided control engineering N90-10084
Control/structure interaction methods for space station power systems N90-10087
Simulation of shuttle flight control system structural interaction with RMS deployed payloads N90-10100
Optical processing for distributed sensors in control of flexible spacecraft N90-10102
Input-output oriented computation algorithms for the control of large flexible structures N90-10118
Space station RT and E utilization study
[NASA-CR-181707] N90-10129

SPACECRAFT DESIGN
NASA'S controls-structures interaction program N90-10081
Computational controls for aerospace systems N90-10082
Orbital debris research at NASA Johnson Space Center, 1986-1988
[NASA-TM-102155] N90-10795

SPACECRAFT DOCKING
Computer vision research at Marshall Space Flight Center N90-10564

SPACECRAFT EQUIPMENT
Space station RT and E utilization study
[NASA-CR-181707] N90-10129

SPACECRAFT GUIDANCE
Computational controls for aerospace systems N90-10082

SPACECRAFT LAUNCHING
The Spartan 1 mission
[NASA-TM-101887] N90-10077

SPACECRAFT MOTION
Lumped mass formulations for modeling flexible body systems N90-10091
Enhanced element-specific modal formulations for flexible multibody dynamics N90-10094

SPACECRAFT POWER SUPPLIES
Second Beamed Space-Power Workshop
[NASA-CP-3037] N90-10140
Overview of microwave concepts N90-10155
Central electrical utility power for a satellite ring city in low earth orbit space N90-10166
Circuit level modeling of inductive elements
[DE89-015122] N90-10173

SPACECRAFT PROPULSION
Liquid rocket booster study. Volume 1: Executive summary
[NASA-CR-183599] N90-10137
Second Beamed Space-Power Workshop
[NASA-CP-3037] N90-10140
Overview of microwave concepts N90-10155
Microwave beam power N90-10165

SPACECRAFT RADIATORS
Total hemispherical emittance measured at high temperatures by the calorimetric method
[NASA-TM-102322] N90-10309

SPACECRAFT RELIABILITY
Liquid rocket booster study. Volume 2, book 2, appendix 1: Trades studies
[NASA-CR-183601] N90-10136

SPACECRAFT SHIELDING
Preliminary design of a large tetrahedral truss/hexagonal heatshield panel aerobrake
[NASA-TM-101612] N90-10127
Orbital debris research at NASA Johnson Space Center, 1986-1988
[NASA-TM-102155] N90-10795

SPACECRAFT STRUCTURES
Hierarchical damage tolerant controliers for smart structures
[AD-A209422] N90-10022
NASA'S controls-structures interaction program N90-10081
Flexible structure control experiments using a real-time workstation for computer-aided control engineering N90-10084
Explicit modeling and computational load distribution for concurrent processing simulation of the space station N90-10096

SPARTAN SATELLITES
The Spartan 1 mission
[NASA-TM-101887] N90-10077

SPATIAL DISTRIBUTION
Evaluation of the North Atlantic seasonal nitrogen model, version 2
[DE89-016157] N90-10515
Solvent dynamical effects in electron transfer: Predicted influences of electron coupling upon the rate-dielectric friction dependence
[AD-A210193] N90-10690

SPATIAL MARCHING
Supersonic flow computations over aerospace configurations using an Euler marching solver
[NASA-CR-4085] N90-10012

SPECIFIC HEAT
Thermophysical properties of ceramics. Part 2: Development of specific-heat-measurement apparatus at high temperature
[DE89-760382] N90-10268

SPECIFICATIONS
Dependency-directed localization of software bugs
[AD-A210837] N90-10606

SPECTRAL METHODS
On the coefficients of differentiated expansions of ultraspherical polynomials
[NASA-CR-181913] N90-10637
Shock capturing by the spectral viscosity method
[NASA-CR-181920] N90-10639

SPECTRAL REFLECTANCE
Photoreflectance study of boron ion-implanted (100) cadmium telluride
[SD-TR-88-89] N90-10300
Spatial characterization of acid rain stress in Canadian Shield Lakes
[NASA-CR-183446] N90-10479

SPECTROSCOPIC ANALYSIS
Advances in regression: Use of models in spectroscopic data analysis
[AD-A210541] N90-10665
Laboratory measurements of microwave and millimeter-wave properties of planetary atmospheric constituents
[NASA-CR-185914] N90-10815

SPECTROSCOPY
Advances in regression: Use of models in spectroscopic data analysis
[AD-A210541] N90-10665
Lithium compensation of GaAs
[DE89-616080] N90-10740

SPECULAR REFLECTION
The measurement of infrared spectra of dense ceramics by specular reflectance spectroscopy
[AD-A210609] N90-10291

SPEECH RECOGNITION
Phase 2 testing and evaluation of low data rate voice CODEC equipment
[ACD-330-PHASE-2] N90-10315
Attention and vigilance in speech perception
[AD-A210493] N90-10539
Scientific and technical report voice activated gun turrent control
[AD-A210350] N90-10623

SPENT FUELS
MHD seed recovery and regeneration
[DE89-002711] N90-10715

SPHERICAL HARMONICS
On the coefficients of differentiated expansions of ultraspherical polynomials
[NASA-CR-181913] N90-10637

SPHERICAL WAVES
Observations of spherical-wave scintillation in strong refractive-index turbulence
[PB89-124747] N90-10355

SPIN TESTS
Fracture and three dimensional stress analyses of 7075 aluminum projectile components under spin and inertia load
[AD-A210986] N90-10463
SPIN-SPIN COUPLING
Computational modeling of pi-conjugated polyradicals
[AD-A210573] N90-10648
SPINAL CORD
Biomedical influences on spinal cord function
[AD-A210311] N90-10527
SPLINE FUNCTIONS
Global/local stress analysis of composite structures
[NASA-TM-101640] N90-10456
SPLINES
On two polynomial spaces associated with a box spline
[AD-A210559] N90-10646
SPRAYERS
Theory of droplet. Part 1: Renormalized laws of droplet vaporization in non-dilute sprays N90-10390
SPRINGS (ELASTIC)
Numerical calculations of the collapse of a cavity in the vicinity of a compliant wall
[AD-A210489] N90-10403
SPUTTERING
Alternative fabrication techniques for high-efficiency CuInSe2 and CuInSe2-alloy films and cells
[DE89-009451] N90-10474
SQUALLS
Numerical simulations of a midlatitude squall line N90-10497
STABILITY
Stability of discontinuous shearing motions of a non-Newtonian fluid
[AD-A210643] N90-10406
Tangent map analysis of the beam-beam interaction
[DE89-015857] N90-10689
STABILITY AUGMENTATION
Structural stability augmentation system design using BODEDIRECT: A quick and accurate approach N90-10116
STABILITY DERIVATIVES
Analysis of flight data from a High-Incidence Research Model by system identification methods
[NASA-TP-2940] N90-10074
The active flexible wing aeroservoelastic wind-tunnel test program N90-10119
STABILIZATION
Regulation of nonlinear and generalized linear systems
[AD-A207725] N90-10619
STABLE OSCILLATIONS
Deep traps and sidegating in GaAs devices
[AD-A210740] N90-10765
STAINLESS STEELS
Gaussmeter determination of 302 stainless steel material condition
[BDX-613-3941] N90-10249
STANDARDS
Castings Airworthiness
[AGARD-R-762] N90-10231
Quality control of castings N90-10239
The creation of quality: New directions in the production of aeronautics castings N90-10241
STATIC AERODYNAMIC CHARACTERISTICS
Prediction of the aerodynamic stability of missiles N90-10052
Prediction of tactical missile dynamics N90-10056
STATIC PRESSURE
The measurement of boundary layers on a compressor blade in cascade. Volume 2: Data tables
[NASA-CR-185118-VOL-2] N90-10039
STATIC STABILITY
Airworthiness and flight characteristics test of the UH-60A Black Hawk helicopter equipped with the XM-139 multiple mine dispensing system (VOLCANO)
[AD-A210271] N90-10025
Combustor influence on fighter engine operability N90-10193
STATIC TESTS
Static aeroelastic analysis for generic configuration aircraft
[NASA-TM-89423] N90-10042
STATISTICAL ANALYSIS
Statistical modeling of electrical components
[BDX-613-3939] N90-10336
The computation and use of the asymptotic covariance matrix for measurement error models
[PB89-215321] N90-10650
On lower confidence for PCS in truncated location parameter models
[AD-A210274] N90-10661
Computational and statistical issues in discrete-event simulation
[AD-A210743] N90-10668
STATISTICAL DISTRIBUTIONS
Asymptotic robustness in regression and autoregression based on Lindeberg conditions
[AD-A210725] N90-10654
Selection of the best with a preliminary test for two-parameter exponential distributions
[AD-A210275] N90-10662
A unified approach to estimating tail behavior
[AD-A210961] N90-10672
Multi-sample functional statistical data analysis
[AD-A210992] N90-10673
STATISTICAL TESTS
A unified view of infinitesimal perturbation analysis and likelihood ratios
[AD-A210682] N90-10652
Number of test samples needed to obtain a desired Bayesian confidence interval for a proportion
[AD-A206157] N90-10658
Selection of the best with a preliminary test for two-parameter exponential distributions
[AD-A210275] N90-10662
Multi-sample functional statistical data analysis
[AD-A210992] N90-10673
STEADY FLOW
Similarity solutions that give rise to hyperbolicity and change of type in steady flow of a viscoelastic fluid
[AD-A210920] N90-10410
STEADY STATE
Capillary effects in steady-state flow in heterogeneous cores
[DE89-000758] N90-10399
Stability of discontinuous shearing motions of a non-Newtonian fluid
[AD-A210643] N90-10406
Stability of discontinuous steady states in shearing motion of a non-Newtonian fluid
[AD-A210644] N90-10407
Computational and statistical issues in discrete-event simulation
[AD-A210743] N90-10668
Deep traps and sidegating in GaAs devices
[AD-A210740] N90-10765
STEELS
Properties of HY-100 for naval construction
[MRL-R-1149] N90-10247
Delayed failure of silver-aided diffusion welds between steel
[DE89-016652] N90-10252
Investigation of the pyrometallurgical, physical and mechanical behavior of weld metal
[AD-A211114] N90-10258
Development of a semiquantitative corrosion monitor
[AD-A208132] N90-10414
Micromechanisms of surface friction in zinc electrogalvanized steel sheets
[DE89-011819] N90-10440
STELLAR MASS
Theoretical statistics of zero-age cataclysmic variables N90-10810
STEREOSCOPIC VISION
Space environment robot vision system N90-10569
STEREOSCOPY
Low-cost three-dimensional stereoscopic display technique for computer-aided design
[DE89-011635] N90-10594
STIMULI
Models of mental functioning
[AD-A210456] N90-10538
STIRLING ENGINES
Laser-powered lunar base N90-10156
STOCHASTIC PROCESSES
A comparison of wind turbulence simulation models for stochastic loads analysis for horizontal-axis wind turbines
[DE89-009442] N90-10473
Stochastic control theory, nonlinear structural mechanics and applied combinatorics
[AD-A209042] N90-10657
Stochastic quantization
[AD-A210942] N90-10671
Radon transform analysis of a probabilistic method for image generation
[AD-A207814] N90-10702
STORABLE PROPELLANTS
Experimental study on the stability of small rocket engines with storable liquid propellants N90-10196
STORAGE BATTERIES
Rechargeable lithium/polymer cathode batteries
[AD-A210978] N90-10354
STORM DAMAGE
Extreme hurricanes in the nineteenth century
[PB89-201305] N90-10498
STORMS (METEOROLOGY)
National Severe Storms Laboratory, fiscal year 1988
[PB89-158145] N90-10493
Numerical simulations of a midlatitude squall line N90-10497
Extreme hurricanes in the nineteenth century
[PB89-201305] N90-10498
STRAIN GAGE BALANCES
A FORTRAN program for the calculation of the calibration coefficients of a six-component strain gauge balance
[AD-A210375] N90-10599
STRAIN HARDENING
Delayed failure of silver-aided diffusion welds between steel
[DE89-016652] N90-10252
Strain aging in tungsten-heavy alloys
[AD-A211166] N90-10259
STRAIN MEASUREMENT
An interferometric strain-displacement measurement system
[NASA-TM-101638] N90-10454
STRAIN RATE
Delayed failure of silver-aided diffusion welds between steel
[DE89-016652] N90-10252
Analysis of spurt phenomena for a non-Newtonian fluid
[AD-A210560] N90-10405
Stability of discontinuous shearing motions of a non-Newtonian fluid
[AD-A210643] N90-10406
STRATEGY
Comparison of DPCM prediction strategies for high-quality digital television bit-rate reduction
[BBC-RD-1989/8] N90-10318
An analytical hierarchy process approach to establish the systems analyst's knowledge base for selecting an information requirements determination strategy N90-10785
STRATOSPHERE
Paper 1. Impact of volcanic aerosols on stratospheric chemistry. Paper 2. O2 (1 sigma g +) and O2 (1 delta g) in the H + O2 reaction system. Paper 3. Barotropic instability of zonal jets on Mars, Earth and Venus N90-10477
STRESS (PHYSIOLOGY)
Control of thermoregulatory sweating during exercise in the heat
[AD-A206001] N90-10523
STRESS ANALYSIS
Analysis of results from wind tunnel tests of inlets for an advanced turboprop nacelle installation
[NASA-CR-174937] N90-10011
Casting airworthiness joint European civil authorities view-point N90-10234
Analysis of spurt phenomena for a non-Newtonian fluid
[AD-A210560] N90-10405
Limit analysis of welded tee end connections for hollow tubes
[PB89-191647] N90-10452
A design assessment for metallic pressure vessels circumferentially reinforced with a pre-tensioned high-specific-strength anisotropic composite overwind
[AD-A209108] N90-10453
Global/local stress analysis of composite structures
[NASA-TM-101640] N90-10456
Fracture and three dimensional stress analyses of 7075 aluminum projectile components under spin and inertia load
[AD-A210986] N90-10463
STRESS CYCLES
Porosity and crack initiation during low cycle fatigue
[AD-A210989] N90-10464
STRESS DISTRIBUTION
Stress in dilute suspensions N90-10389
STRESS INTENSITY FACTORS
Stress intensity factors and displacements for arc bend samples using collocation
[AD-A210404] N90-10460
STRESS RATIO
Fatigue growth and closure of short cracks
[AD-A210824] N90-10462
STRESS-STRAIN RELATIONSHIPS
Fatigue crack initiation mechanics of metal aircraft structures
[AD-A210567] N90-10255
STRESSES
Two stage gear tooth dynamics program
[NASA-CR-185110] N90-10437
Effects of stress on judgment and decision making in dynamic tasks
[AD-A210605] N90-10781
STRING THEORY
Research program in theoretical high energy physics
[DE89-013963] N90-10695

STRONG INTERACTIONS (FIELD THEORY)
Lattice fields and strong interactions
[DE89-015099] N90-10777
STRONGLY COUPLED PLASMAS
Dynamically compressed metals: Theory
[AD-A210741] N90-10257
STRUCTURAL ANALYSIS
SSME Alternate Turbopump Development Program: Design verification specification for high-pressure fuel turbopump
[NASA-CR-183676] N90-10033
Static aeroelastic analysis for generic configuration aircraft
[NASA-TM-89423] N90-10042
Aeroelastic analysis of missile control surfaces with structural non-linearity N90-10071
Control/structure interaction methods for space station power systems N90-10087
Modeling and control system design and analysis tools for flexible structures N90-10090
Lumped mass formulations for modeling flexible body systems N90-10091
Efficiency and capabilities of multi-body simulations N90-10095
Simulation of flexible structures with impact: Experimental validation N90-10097
Linearized flexibility models in multibody dynamics and control N90-10099
Composite Blade Structural Analyzer (COBSTRAN) theoretical/programmer's manual
[NASA-TM-101958] N90-10181
Structure-mechanical property relationships in ion implanted ceramics
[DE89-010129] N90-10274
The MHOST finite element program: 3-D inelastic analysis methods for hot section components. Volume 2: User's manual
[NASA-CR-182235-VOL-2] N90-10450
Design guide for predicting nonlinear random response (including snap-through) of buckled plates
[NASA-CR-181877] N90-10681
STRUCTURAL DESIGN
Large scale prop-fan structural design study. Volume 1: Initial concepts
[NASA-CR-174992] N90-10043
Large scale prop-fan structural design study. Volume 2: Preliminary design of SR-7
[NASA-CR-174993] N90-10044
Royal Aerospace Establishment: No place for a castings factor N90-10235
Application of formal optimization techniques in thermal/structural design of a heat-pipe-cooled panel for a hypersonic vehicle
[NASA-TM-89131] N90-10409
Analysis and test of a 16-foot radial rib reflector developmental model
[NASA-TM-101648] N90-10457
Design of grazing incidence monochromators involving unconventional gratings
[DE89-016341] N90-10704
A lunar far-side very low frequency array
[NASA-CP-3039] N90-10805
Conceptual design of a synchronous Mars telecommunications satellite
[NASA-TP-2942] N90-10814
STRUCTURAL DESIGN CRITERIA
Analysis of results from wind tunnel tests of inlets for an advanced turboprop nacelle installation
[NASA-CR-174937] N90-10011
Preliminary design of a large tetrahedral truss/hexagonal heatshield panel aerobrake
[NASA-TM-101612] N90-10127
Design guide for predicting nonlinear random response (including snap-through) of buckled plates
[NASA-CR-181877] N90-10681
STRUCTURAL ENGINEERING
CONSOLE: A CAD tandem for optimization-based design interacting with user-supplied simulators N90-10085
Control/structure interaction methods for space station power systems N90-10087
The development of an expert system for the creative design of mechanisms
[AD-A211115] N90-10628
STRUCTURAL FAILURE
Composite Blade Structural Analyzer (COBSTRAN) theoretical/programmer's manual
[NASA-TM-101958] N90-10181
STRUCTURAL STABILITY
Modeling and stabilization of large flexible space stations N90-10120
STRUCTURAL VIBRATION
Flexible structure control experiments using a real-time workstation for computer-aided control engineering N90-10084
A performance comparison of integration algorithms in simulating flexible structures N90-10101
Modifying high-order aeroelastic math model of a jet transport using maximum likelihood estimation N90-10106
Aircraft modal supression system: Existing design approach and its shortcomings N90-10115
Modeling and stabilization of large flexible space stations N90-10120
SUBMILLIMETER WAVES
Submillimeter quantum electronics
[AD-A210439] N90-10762
SUBSTRATES
Characterization of GaAs/Si/GaAs heterointerfaces
[DE89-016302] N90-10752
SUDDEN IONOSPHERIC DISTURBANCES
Solar-geophysical data number 533. Part 1: Data for December, November 1988, and late data
[PB89-162481] N90-10820
Solar-geophysical data number 534, February 1989. Part 1: (Prompt reports). Data for January 1989, December 1988 and late data
[PB89-173041] N90-10822
SULFONATES
Comparison of carboxylated and sulfonated model polyurethane ionomers
[AD-A210438] N90-10284
SULFUR
Properties of F-34 (JP-8) fuel for 1988
[AD-A210188] N90-10303
SULFUR DIOXIDES
Electrochemistry in near-critical and supercritical fluids. Part 7: SO2
[AD-A208207] N90-10214
SUN
Long-term solar-terrestrial observations
[DE89-016318] N90-10825
SUPERCOMPUTERS
Proceedings of the 2nd International Conference on Vector and Parallel Computing
[AD-A209401] N90-10585
Applications of parallel supercomputers: Scientific results and computer science lessons
[DE89-016385] N90-10611
SUPERCONDUCTING FILMS
Study of deposition of YBa2Cu3O7-x on cubic zirconia
[NASA-TM-102350] N90-10737
SUPERCONDUCTING MAGNETS
A compact X-ray lithography lattice using superferric magnets
[DE89-013947] N90-10728
The effect of twins on critical currents of high Tc superconductors
[AD-A210988] N90-10768
SUPERCONDUCTIVITY
Measuring the shielding effectiveness of superconductive composites
[DE89-015164] N90-10180
Mott transition: Low-energy excitations and superconductivity
[DE89-617778] N90-10741
Superconductivity from valence fluctuations with finite U
[DE89-015302] N90-10742
Critical magnetic fields (H(sub c2), H(sub c1)) and kappa in YBa2(Cu0.98M0.02)3O(7+delta), M=Ni, Al, and Cu
[DE89-016412] N90-10745
Structural aspects of the phase separation in La2CuO4.032
[DE89-016183] N90-10751
SUPERCONDUCTORS
Measuring the shielding effectiveness of superconductive composites
[DE89-015164] N90-10180
New electrodynamic and electrostatic models with applications to antenna theory, superconductor slots, and lasers N90-10316
Composite ceramic superconducting wires for electric motor applications
[AD-A210345] N90-10346
Ceramic processing of bulk high-T(sub c) superconductors
[DE89-015703] N90-10736
Mixed-valent and heavy fermions and related systems
[DE89-016335] N90-10743
Critical magnetic fields (H(sub c2), H(sub c1)) and kappa in YBa2(Cu0.98M0.02)3O(7+delta), M=Ni, Al, and Cu
[DE89-016412] N90-10745
SUPERCRITICAL AIRFOILS
A study of high-lift airfoils at high Reynolds numbers in the Langley low-turbulence pressure tunnel
[NASA-TM-89125] N90-10002
SUPERCRITICAL FLUIDS
Electrochemistry in near-critical and supercritical fluids. Part 7: SO2
[AD-A208207] N90-10214
SUPERGRAVITY
N=1,2 supergravities in 2+1 dimensions as Chern-Simons theories
[DE89-612006] N90-10771
D=3 Chern-Simons action, supergravity and quantization
[DE89-617530] N90-10775
SUPERLATTICES
Methods to decrease defect density in GaAs/Si heteroepitaxy
[DE89-016306] N90-10753
SUPERNOVA 1987A
Astrophysical and cosmological constraints to neutrino properties
[NASA-CR-185031] N90-10809
SUPERNOVAE
Research program in theoretical high energy physics
[DE89-013963] N90-10695
SUPERPLASTICITY
Application of superplastically formed and diffusion bonded aluminum to a laminar flow control leading edge
[NASA-CR-178316] N90-10030
SUPERSONIC AIRCRAFT
A supersonic through-flow fan engine airframe integration study
[NASA-CR-185140] N90-10004
SUPERSONIC BOUNDARY LAYERS
Stability of a supersonic boundary layer along a swept leading edge N90-10359
SUPERSONIC COMBUSTION RAMJET ENGINES
Cycle analysis of scramjet engines
[NAL-TR-1002] N90-10035
Effects of low-frequency instabilities on the operation of Ramjet air inlets N90-10198
SUPERSONIC CRUISE AIRCRAFT RESEARCH
A supersonic through-flow fan engine airframe integration study
[NASA-CR-185140] N90-10004
SUPERSONIC FLOW
Supersonic flow computations over aerospace configurations using an Euler marching solver
[NASA-CR-4085] N90-10012
New test techniques to evaluate near field effects for supersonic store carriage and separation N90-10062
SUPERSONIC SPEED
High temperature VSCF (Variable Speed Constant Frequency) generator system
[AD-A210823] N90-10351
SUPERSONIC TRANSPORTS
Revolutionary opportunities for materials and structures study
[NASA-CR-179642] N90-10184
SUPERSONIC TURBINES
Revolutionary opportunities for materials and structures study
[NASA-CR-179642] N90-10184
SUPERSYMMETRY
N=1,2 supergravities in 2+1 dimensions as Chern-Simons theories
[DE89-612006] N90-10771
SUPPORT SYSTEMS
Space station RT and E utilization study
[NASA-CR-181707] N90-10129
SUPPORTS
Wind tunnel support system effects on a fighter aircraft model at Mach numbers from 0.6 to 2.0
[AD-A210614] N90-10010
SURFACE FINISHING
Advances in the technology of titanium castings N90-10243
Adhesion of encapsulating elastomer to polyolefin sleeve
[BDX-613-3985] N90-10271
SURFACE LAYERS
Attenuated total reflection FTIR spectroscopy for measuring interfacial reaction kinetics at silica surfaces
[AD-A210314] N90-10224
SURFACE PROPERTIES
Analysis of surface modified colloidal silicas
[DE89-015849] N90-10267
Synthesis and physical properties of poly(perfluoroalkylether) urethanes
[AD-A210500] N90-10287
Epitaxial GaAs on SOI wafers
[AD-A209009] N90-10729
SURFACE REACTIONS
The structure determination of molecular adsorbates with large unit cells or lattice-gas disorder on metal surfaces
[AD-A210926] N90-10230
SURFACE ROUGHNESS
Surface reflection: Physical and geometrical perspectives
[AD-A210592] N90-10710

SURFACE STABILITY
Deep traps and sidegating in GaAs devices
[AD-A210740] N90-10765
SURFACE TO AIR MISSILES
Experience gained in the improvement of the Aspide aerodynamic configuration for the surface to air role
N90-10072
SURFACE WAVES
Surface wave ray tracing and Ms:yield determination in a laterally heterogeneous earth
[AD-A210241] N90-10516
SURGES
Deep traps and sidegating in GaAs devices
[AD-A210740] N90-10765
SUSPENDING (HANGING)
Electrostatically suspended rotor for angular encoder
[NASA-CASE-MFS-28294-1] N90-10310
SWEAT COOLING
Control of thermoregulatory sweating during exercise in the heat
[AD-A206001] N90-10523
SWEEP ANGLE
A study of the structure of highly swept shock wave turbulent boundary layer interactions N90-10376
Trailing-edge sweep and three-dimensional vortex interactions in jets and mixing layers N90-10379
SWEPT WINGS
Experimental study of transition and leading edge contamination on swept wings N90-10362
A three-dimensional linear stability approach to transition on wings at incidence N90-10373
A European collaborative investigation of the three-dimensional turbulent shear layers of a swept wing
N90-10380
SWITCHES
Analysis of the performance of gallium arsenide photoavalanche switches
[DE89-015774] N90-10739
SWITCHING
Use of depletion edge translation for high-speed modulation and switching of lightwaves
[AD-A211186] N90-10713
SWITCHING CIRCUITS
Commercial high current ignitron development
[DE89-015077] N90-10331
Pin switch circuits instrument for microsecond velocity measurements
[AD-A210638] N90-10426
SYNCHROTRONS
A compact X-ray lithography lattice using superferric magnets
[DE89-013947] N90-10728
SYNOPTIC METEOROLOGY
Research highlights of the NMC (National Meteorological Center) Development Division: 1987-1988
[PB89-206478] N90-10501
SYNTHESIS (CHEMISTRY)
International Conference on Organometallic Chemistry (13th) held in Torino, Europe on 4-9 September 1988: Abstracts
[AD-A210617] N90-10178
Measuring the shielding effectiveness of superconductive composites
[DE89-015164] N90-10180
Raman spectroscopic study of the rare earth sesquisulfides
[AD-A210610] N90-10226
Metal-assisted syntheses of boranes and carboranes
[AD-A210728] N90-10227
The synthesis and structure of novel antimony thiametallacycles
[AD-A210888] N90-10229
Analysis of surface modified colloidal silicas
[DE89-015849] N90-10267
New polymer precursors to boron and silicon nitrides
[AD-A210287] N90-10279
Control of synthetic peptide tertiary structure
[AD-A210339] N90-10281
Comparison of carboxylated and sulfonated model polyurethane ionomers
[AD-A210438] N90-10284
Synthesis and interfacial properties of new generation polyurethane systems
[AD-A210446] N90-10286
Monolayer formation characteristics of novel organic molecules with nonlinear optically active moieties
[AD-A210496] N90-10693
SYNTHETIC RESINS
Nonlinear optics and organic materials
[AD-A210570] N90-10709
SYSTEM EFFECTIVENESS
Director, Operational Test and Evaluation report FY-88
[AD-A206784] N90-10778
SYSTEM IDENTIFICATION
System identification for large space structures
N90-10126
SYSTEMS COMPATIBILITY
Cockpit lighting compatibility with image intensification night imaging systems: Issues and answers
[AD-A210503] N90-10028
SYSTEMS ENGINEERING
An appraisal of a number of power assessment procedures being proposed for use in Chinook-Lycoming T55 engine
[AD-A210482] N90-10041
Investigations of thrust vector control for high-alpha pitchover N90-10067
NASA'S controls-structures interaction program
N90-10081
Flexible structure control experiments using a real-time workstation for computer-aided control engineering
N90-10084
CONSOLE: A CAD tandem for optimization-based design interacting with user-supplied simulators
N90-10085
Control/structure interaction methods for space station power systems N90-10087
Approximate simulation model for analysis and optimization in engineering system design
[NASA-TM-101616] N90-10308
Aerospace system unified life cycle engineering producibility measurement issues
[AD-A210937] N90-10607
An analytical hierarchy process approach to establish the systems analyst's knowledge base for selecting an information requirements determination strategy
N90-10785
SYSTEMS INTEGRATION
Liquid rocket booster study. Volume 2, book 3, appendices 2-5: PPIP, transition plan, AMOS plan, and environmental analysis
[NASA-CR-183602] N90-10139
Planning an Integrated On-line Library System (IOLS)
[AD-A209406] N90-10783
SYSTEMS MANAGEMENT
Planning an Integrated On-line Library System (IOLS)
[AD-A209406] N90-10783
SYSTEMS SIMULATION
Approximate simulation model for analysis and optimization in engineering system design
[NASA-TM-101616] N90-10308

T

TABLES (DATA)
The 1984 direct strike lightning data, part 2
[NASA-TM-87690-PT-2] N90-10506
The 1984 direct strike lightning data, part 3
[NASA-TM-87690-PT-3] N90-10507
TACTICS
Communications Data Base (CDB), phase 3 (with software documentation)
[AD-A210540] N90-10789
TACTILE DISCRIMINATION
Analysis and construction of contact and tactile sensors
[DE89-013992] N90-10416
TANGENTS
Tangent map analysis of the beam-beam interaction
[DE89-015857] N90-10689
TANTALUM OXIDES
Synthetic polypeptide composites for sensor applications
[AD-A210797] N90-10296
TARGET RECOGNITION
Tracking performance evaluation
[AD-A210499] N90-10540
TARGET THICKNESS
Studies in penetration mechanics
[AD-A210713] N90-10448
TARGETS
EPIC-2 calculated impact loading histories of thin plates
[AD-A210557] N90-10461
Networks for image acquisition, processing and display N90-10545
Tests of gating algorithms for tracking of multiple objects. Part 1: Theory, requirements and performance measures
[AD-A210519] N90-10644
TASK COMPLEXITY
Effects of miniature CRT (Cathode Ray Tube) location upon primary and secondary task performances
[AD-A210223] N90-10573
TASKS
Models of mental functioning
[AD-A210456] N90-10538
Differences in writers initial task representations
[AD-A210433] N90-10788
TASTE
Integration of neurobiological and computational analyses of the neural network essentials for conditioned taste aversions
[AD-A210228] N90-10537
TECHNICAL WRITING
Differences in writers initial task representations
[AD-A210433] N90-10788
TECHNOLOGY ASSESSMENT
Large scale prop-fan structural design study. Volume 1: Initial concepts
[NASA-CR-174992] N90-10043
Large scale prop-fan structural design study. Volume 2: Preliminary design of SR-7
[NASA-CR-174993] N90-10044
Castings, from theory to practical application
N90-10236
Japanese structural ceramics research and development N90-10272
TECHNOLOGY TRANSFER
Domestic technology transfer program regulation
[PB89-195374] N90-10793
TELECOMMUNICATION
ELF (Extremely Low Frequency) Communications System Ecological Monitoring Program: Electromagnetic field measurements and engineering support, 1988
[AD-A210200] N90-10321
SINCGARS (Single-Channel Ground/Airborne Radio System) operator performance decay
[AD-A210716] N90-10326
Active participation in highly automated systems: Turning the wrong stuff into the right stuff
[AD-A210218] N90-10572
Communications Data Base (CDB), phase 3 (with software documentation)
[AD-A210540] N90-10789
TELEOPERATORS
An adaptive controller for enhancing operator performance during teleoperation
[NASA-CR-183445] N90-10438
Interchangeable end effector tools utilized on the protoflight manipulator arm
[NASA-CR-179374] N90-10447
Hybrid vision activities at NASA Johnson Space Center N90-10552
Instrumentation and robotic image processing using top-down model control N90-10563
Computer vision research at Marshall Space Flight Center N90-10564
TELESCOPES
Astrometric telescope facility. Preliminary systems definition study. Volume 3: Cost estimate
[NASA-TM-89429-VOL-3] N90-10808
TELEVISION SYSTEMS
Vision science and technology at NASA: Results of a workshop: Executive summary N90-10543
TELEVISION TRANSMISSION
Comparison of DPCM prediction strategies for high-quality digital television bit-rate reduction
[BBC-RD-1989/8] N90-10318
TELLURIUM ISOTOPES
Tellurium-118/antimony-118 generator
[DE89-015225] N90-10698
TEMPER (METALLURGY)
Gaussmeter determination of 302 stainless steel material condition
[BDX-613-3941] N90-10249
TEMPERATURE CONTROL
Method and apparatus for maintaining thermal control in plasma conditions
[NASA-CASE-MFS-28368-1] N90-10717
TEMPERATURE EFFECTS
Hygrothermal effects on the complex moduli of composite laminates N90-10182
New structural materials
[AD-A209425] N90-10246
Predictive aging of polymers
[NASA-CASE-NPO-17524-1-CU] N90-10261
Some significant results from testing a Remote Multiplexing Unit (RMU) for temperature-induced errors
[DE89-009432] N90-10421
TEMPERATURE GRADIENTS
A seasonal isotherm depth climatology for the eastern tropical Pacific
[PB89-193577] N90-10512
TEMPERATURE MEASUREMENT
Three-in-one gage
[NASA-CR-183714] N90-10413
Thin film thermocouples for high temperature measurement
[PB89-209290] N90-10420
Some significant results from testing a Remote Multiplexing Unit (RMU) for temperature-induced errors
[DE89-009432] N90-10421

TEMPERATURE PROBES
Development of an automated probe for thermal conductivity measurements
[PB89-209324] N90-10419
TENSILE CREEP
Delayed failure of silver-aided diffusion welds between steel
[DE89-016652] N90-10252
TENSILE PROPERTIES
Mechanical properties, solubilities, and processabilities in the design of the first super-strong liquid-crystalline polymers
[DE89-009252] N90-10273
TENSILE TESTS
A robotic electrical and tensile testing system for diodes
[DE89-014012] N90-10417
Mechanics of the crack path formation
[NASA-CR-185143] N90-10455
TERMINAL BALLISTICS
Alternative test methodology for ballistic performance ranking of armor ceramics
[AD-A210587] N90-10290
Studies in penetration mechanics
[AD-A210713] N90-10448
EPIC-2 calculated impact loading histories of thin plates
[AD-A210557] N90-10461
TERRAIN ANALYSIS
Image-based terrain modeling with thematic mapper applied to resolving the limit of Holocene Lake expansion in the Great Salt Lake Desert, Utah, part 1
[NASA-CR-185913] N90-10465
ONR/NORDA Workshop on Terrain Analysis and Quantitative Geomorphology
[AD-A210464] N90-10489
TEST FACILITIES
The aerospace energy systems laboratory: Hardware and software implementation
[NASA-TM-101706] N90-10610
Astrometric telescope facility. Preliminary systems definition study. Volume 3: Cost estimate
[NASA-TM-89429-VOL-3] N90-10808
TEXTS
Differences in writers initial task representations
[AD-A210433] N90-10788
TEXTURES
Radon transform analysis of a probabilistic method for image generation
[AD-A207814] N90-10702
THALAMUS
Extrathalamic modulation of cortical function
[AD-A211044] N90-10535
THEMATIC MAPPERS (LANDSAT)
Image-based terrain modeling with thematic mapper applied to resolving the limit of Holocene Lake expansion in the Great Salt Lake Desert, Utah, part 1
[NASA-CR-185913] N90-10465
Spatial characterization of acid rain stress in Canadian Shield Lakes
[NASA-CR-183446] N90-10479
THEORETICAL PHYSICS
Studies of elementary particles
[DE89-014859] N90-10685
Research program in theoretical high energy physics
[DE89-013963] N90-10695
A theoretical high energy physics program
[DE89-012685] N90-10696
THERMAL BATTERIES
Pyrotechnic ignition studies using a gun tunnel
[DE89-012496] N90-10341
THERMAL CONDUCTIVITY GAGES
Development of an automated probe for thermal conductivity measurements
[PB89-209324] N90-10419
THERMAL INSULATION
Flight set 360T004 (STS-30) insulation component, interim release, volume 3
[NASA-CR-183746] N90-10169
Composite multilayer insulations for thermal protection of aerospace vehicles
[NASA-TM-101071] N90-10183
THERMAL PROTECTION
Composite multilayer insulations for thermal protection of aerospace vehicles
[NASA-TM-101071] N90-10183
THERMAL SIMULATION
Analysis of a model and sequential numerical method for thermal reservoir simulation
[DE89-015117] N90-10384
THERMAL STABILITY
Space structures concepts and materials
[NASA-CR-183727] N90-10128
Mechanics of damping for fiber composite laminates including hygro-thermal effects
[NASA-TM-102329] N90-10185
THERMISTORS
Development of an automated probe for thermal conductivity measurements
[PB89-209324] N90-10419
THERMOCOUPLES
Thin film thermocouples for high temperature measurement
[PB89-209290] N90-10420
THERMODYNAMIC CYCLES
Cycle analysis of scramjet engines
[NAL-TR-1002] N90-10035
THERMODYNAMIC EQUILIBRIUM
Global existence and asymptotic stability for a nonlinear integrodifferential equation modeling heat flow
[AD-A210647] N90-10408
THERMODYNAMIC PROPERTIES
Dynamically compressed metals: Theory
[AD-A210741] N90-10257
Study of the NO3 radical decomposition reaction and the N2O5 in equilibrium with NO3 + NO2 equilibrium constant
[PB89-208961] N90-10480
Thermoregulatory responses to intermittent exercise are influenced by knit structure of underwear
[AD-A209087] N90-10541
Thermodynamic transport properties of nitrogen tetroxide in hypercritical conditions for regenerative cooling of a rocket engine. Volume 1: Tests
[ETN-89-94975] N90-10773
Thermodynamic transport properties of nitrogen tetroxide in hypercritical conditions for regenerative cooling of a rocket engine. Volume 2: Appendices
[ETN-89-94977] N90-10774
THERMODYNAMICS
Hierarchical structure in polymeric solids and its influence on properties
[AD-A210918] N90-10297
Ordered structures and metastable alloys grown by OMVPE
[DE89-016370] N90-10744
THERMOGRAVIMETRY
Characterization of diamond films by thermogravimetric analysis and infrared spectroscopy
[AD-A210564] N90-10288
THERMONUCLEAR REACTIONS
On the utility and ubiquity of atomic collision physics
[DE89-015356] N90-10686
Ignition and burn criteria for D3He tokamak and spherical torus reactors
[DE89-015059] N90-10716
Massachusetts Institute of Technology Plasma Fusion Center
[DE89-016050] N90-10723
THERMOPHYSICAL PROPERTIES
Thermophysical properties of ceramics. Part 2: Development of specific-heat-measurement apparatus at high temperature
[DE89-760382] N90-10268
Development of an automated probe for thermal conductivity measurements
[PB89-209324] N90-10419
THERMOREGULATION
Control of thermoregulatory sweating during exercise in the heat
[AD-A206001] N90-10523
Thermoregulatory responses to intermittent exercise are influenced by knit structure of underwear
[AD-A209087] N90-10541
THICKNESS
Alternative test methodology for ballistic performance ranking of armor ceramics
[AD-A210587] N90-10290
Bias and oxide thickness dependence of trapped charge buildup in MOS devices
[AD-A210264] N90-10757
THIN FILMS
Raman characterization of high temperature materials using an imaging detector
[DE89-016308] N90-10219
Silicon dioxide deposition at 100 deg C using vacuum ultraviolet light
[TR-0088(3945-07)-6] N90-10269
Characterization of diamond films by thermogravimetric analysis and infrared spectroscopy
[AD-A210564] N90-10288
Thin film thermocouples for high temperature measurement
[PB89-209290] N90-10420
Alternative fabrication techniques for high-efficiency CuInSe2 and CuInSe2-alloy films and cells
[DE89-009451] N90-10474
Analytic theory for the selection of Saffman-Taylor fingers in the presence of thin film effects
[NASA-CR-181910] N90-10677
Second-order nonlinear optical devices in poled polymers
[DE89-015842] N90-10703
Optical dispersion relations for diamondlike carbon films
[NASA-TM-102356] N90-10738
Morphological aspects of the friction of hot-filament-grown diamond thin films
[DE89-015986] N90-10750
THIN PLATES
EPIC-2 calculated impact loading histories of thin plates
[AD-A210557] N90-10461
THIN WALLS
Thin walled cast high-strength structural parts
N90-10242
THIOLS
Multiple internal reflection Fourier transform infrared spectroscopy studies of thiocyanate adsorption on silver and gold
[AD-A210245] N90-10223
THREE DIMENSIONAL BOUNDARY LAYER
Stability and transition of three-dimensional boundary layers N90-10357
Three-dimensional boundary layer transition on a concave surface N90-10365
Curvature effects on the stability of three-dimensional laminar boundary layers N90-10366
Experimental study of instability modes in a three-dimensional boundary layer N90-10369
Primary and secondary stability analysis applied to the DFVLR-transition swept-plate experiment N90-10371
Numerical investigation of transition in 3D boundary layers N90-10372
A three-dimensional linear stability approach to transition on wings at incidence N90-10373
A European collaborative investigation of the three-dimensional turbulent shear layers of a swept wing N90-10380
THREE DIMENSIONAL FLOW
Boost-phase discrimination research activities
[NASA-TM-101889] N90-10176
Fluid Dynamics of Three-Dimensional Turbulent Shear Flows and Transition
[AGARD-CP-438] N90-10356
Numerical solution of three-dimensional unsteady flows: Application to instability problems N90-10375
Trailing-edge sweep and three-dimensional vortex interactions in jets and mixing layers N90-10379
Turbulence modelling of three-dimensional shear flows N90-10381
A composite velocity procedure for the three-dimensional reduced Navier-Stokes equations N90-10396
THREE DIMENSIONAL MODELS
Numerical investigation of the effects of longitudinal vortices on the onset of transition in a flat plate boundary layer N90-10363
Bifurcations in Poiseuille flow and wall turbulence N90-10370
Numerical investigation of transition in 3D boundary layers N90-10372
A study of the structure of highly swept shock wave turbulent boundary layer interactions N90-10376
THRESHOLD VOLTAGE
High energy neutron irradiation effects in GaAs modulation-Doped Field Effect Transistors (MODFETS): Threshold voltage
[AD-A210502] N90-10763
THRUST AUGMENTATION
Characteristics of combustion driven pressure oscillations in advanced turbo-fan engines with afterburner N90-10194
THRUST CHAMBERS
A rocket engine design expert system
[NASA-TM-102373] N90-10172
THRUST VECTOR CONTROL
Investigations of thrust vector control for high-alpha pitchover N90-10067
THUNDERSTORMS
Forecasting convection with the AFOS (Automation of Field Operations and Services) data analysis programs. (ADAP-version 2.0) (AFOS data analysis programs-version 2.0)
[PB89-145940] N90-10492
TIME
Northeast Artificial Intelligence Consortium annual report for 1987. Volume 7, part A: Time oriented problem solving
[AD-A210331] N90-10622
TIME SERIES ANALYSIS
Method and apparatus for determining time, direction and composition of impacting space particles
[NASA-CASE-LAR-13392-1-CU] N90-10132

TIME SHARING
Shared memory versus message passing architectures: An application based study
[AD-A210312] N90-10615
TISSUES (BIOLOGY)
Electroporation: Theory of basic mechanisms
[AD-A210196] N90-10520
TITAN
Computer simulation of plasma interactions near Titan N90-10816
TITANIUM ALLOYS
Evaluation of titanium castings for aerospace components N90-10237
Advances in the technology of titanium castings N90-10243
Emittance, catalysis, and dynamic oxidation of Ti-14Al-21Nb
[NASA-TP-2955] N90-10248
Influence of microstructure and microdamage processes on fracture at high loading rates
[AD-A210307] N90-10253
TITANIUM BORIDES
New structural materials
[AD-A209425] N90-10246
Shock compression and release in high-strength ceramics
[DE89-013995] N90-10265
TOKAMAK DEVICES
Ignition and burn criteria for D3He tokamak and spherical torus reactors
[DE89-015059] N90-10716
Kinetic effects in Alfven wave heating. Part 2: Propagation and absorption with a single minority species
[DE89-016619] N90-10724
TOLERANCES (MECHANICS)
Casting airworthiness joint European civil authorities view-point N90-10234
Advances in the technology of titanium castings N90-10243
Relating tolerances and kinematic behavior
[AD-A211125] N90-10311
TOLLMIEN-SCHLICHTING WAVES
On the interaction of stationary crossflow vortices and Tollmien-Schlichting waves in the boundary layer on a rotating disc
[NASA-CR-181859] N90-10007
TOMOGRAPHY
Ceramic components in machines, Cologne and Aachen, West Germany; Maastricht, The Netherlands and Brussels, Belgium
[DE89-015831] N90-10264
Tellurium-116/antimony-118 generator
[DE89-015225] N90-10696
TOOLS
Adjustable depth gage
[NASA-CASE-LEW-14880-1] N90-10415
TOPOLOGY
Finding isolated zero points of complex polynomial mappings
[DE89-617523] N90-10633
TOXICITY
Heterogeneous catalysts in water
[AD-A210742] N90-10228
Organic explosives and related compounds. Environmental and health considerations
[AD-A210554] N90-10306
TOXICOLOGY
Organic explosives and related compounds. Environmental and health considerations
[AD-A210554] N90-10306
TRACKING (POSITION)
Alternative polar homing strategies N90-10059
Tests of gating algorithms for tracking of multiple objects. Part 1: Theory, requirements and performance measures
[AD-A210519] N90-10644
TRAILING EDGES
Trailing-edge sweep and three-dimensional vortex interactions in jets and mixing layers N90-10379
TRAINING ANALYSIS
SINCGARS (Single-Channel Ground/Airborne Radio System) operator performance decay
[AD-A210716] N90-10326
TRAINING DEVICES
Visions of visualization aids: Design philosophy and experimental results N90-10547
TRAJECTORIES
The role of sensor directed, model based control in robotics
[DE89-014133] N90-10442
The temporal development of collision cascades in the binary collision approximation
[DE89-015860] N90-10699
TRAJECTORY MEASUREMENT
Tracking performance evaluation
[AD-A210499] N90-10540
TRANSDUCERS
Performance of a broadbanded ultrasonic transducer with coaxially mounted, nondirectional receiver
[DE89-015838] N90-10343
TRANSFER FUNCTIONS
Numerically efficient algorithm for model development of high-order systems N90-10108
TRANSFORMERS
Circuit level modeling of inductive elements
[DE89-015122] N90-10173
TRANSITION METALS
Metal-assisted syntheses of boranes and carboranes
[AD-A210728] N90-10227
Heterogeneous catalysts in water
[AD-A210742] N90-10228
Bonding in transition metal silyl dimers. Molecular orbital theory
[AD-A208269] N90-10260
TRANSITION TEMPERATURE
Structural aspects of the phase separation in La2CuO4.032
[DE89-016183] N90-10751
TRANSMISSION CIRCUITS
Studies of high power density, pico-second rise-time light activated semiconductor switch
[AD-A210549] N90-10349
TRANSMISSION EFFICIENCY
Multi-level bandwidth efficient block modulation codes
[NASA-CR-185484] N90-10317
Omega system performance assessment
[AD-A210342] N90-10322
TRANSMISSION LINES
Improved propagation models for discrete random media
[AD-A211085] N90-10327
TRANSMISSIVITY
Atmospheric transmissivity update - 1988
[AD-A209130] N90-10484
TRANSMITTANCE
Solvent dynamical effects in electron transfer: Predicted influences of electron coupling upon the rate-dielectric friction dependence
[AD-A210193] N90-10690
Density of states in a resonant tunneling structure
[AD-A209508] N90-10731
TRANSMITTERS
Excitatory amino acids as transmitters in the brain
[AD-A210685] N90-10532
TRANSONIC FLOW
A numerical method for solving transonic flow past aircraft in Cartesian coordinates
[NAL-TR-1008] N90-10003
Computation of transonic flow about stores
[AD-A210402] N90-10009
TRANSPARENCE
Conference on Aerospace Transparent Materials and Enclosures (15th) 16-20 January 1989. Volume 2: Sessions 6-9
[AD-A210201] N90-10024
Factors affecting the perception of transparent motion N90-10559
TRANSPORT AIRCRAFT
Modifying high-order aeroelastic math model of a jet transport using maximum likelihood estimation N90-10106
Development of pressure containment and damage tolerance technology for composite fuselage structures in large transport aircraft
[NASA-CR-3996] N90-10186
TRANSPORT PROPERTIES
Impedance analysis of ionic transport in polypyrrole-polyazulene copolymer and its charge-discharge characteristics
[AD-A210979] N90-10299
Electroporation: Theory of basic mechanisms
[AD-A210196] N90-10520
Experimental investigations of transport and optical properties of 3-5 quantum well structures grown via molecular beam epitaxy under optimal growth conditions
[AD-A210269] N90-10758
Deep traps and sidegating in GaAs devices
[AD-A210740] N90-10765
Thermodynamic transport properties of nitrogen tetroxide in hypercritical conditions for regenerative cooling of a rocket engine. Volume 1: Tests
[ETN-89-94975] N90-10773
Thermodynamic transport properties of nitrogen tetroxide in hypercritical conditions for regenerative cooling of a rocket engine. Volume 2: Appendices
[ETN-89-94977] N90-10774
TRAPPED PARTICLES
Method and apparatus for determining time, direction and composition of impacting space particles
[NASA-CASE-LAR-13392-1-CU] N90-10132
Bias and oxide thickness dependence of trapped charge buildup in MOS devices
[AD-A210264] N90-10757
TREADMILLS
Control of thermoregulatory sweating during exercise in the heat
[AD-A208001] N90-10523
TREES (MATHEMATICS)
Automated model formulation for time-varying flexible structures N90-10107
TRIBOLOGY
Morphological aspects of the friction of hot-filament-grown diamond thin films
[DE89-015986] N90-10750
TRIMETHYL COMPOUNDS
Reactions of hydrogen chloride and boron trichloride with trimethylsilylamino groups
[AD-A209006] N90-10209
TRINITROTOLUENE
Free-expansion experiments and modeling in detonation: Chemistry and hydrodynamics on a laboratory scale
[DE89-007748] N90-10302
Remarks on certain aspects of solid explosive detonation via small projectile impact
[AD-A210648] N90-10307
TRIODES
Micro-cavity integrable vacuum diodes and triodes
[DE89-016649] N90-10344
TRITIUM
Ignition and burn criteria for D3He tokamak and spherical torus reactors
[DE89-015059] N90-10716
TROPICAL METEOROLOGY
A study of the impact of simulated satellite lidar wind observations
[AD-A210430] N90-10488
A seasonal isotherm depth climatology for the eastern tropical Pacific
[PB89-193577] N90-10512
TRUSSES
Shape control of high degree-of-freedom variable geometry trusses N90-10122
Preliminary design of a large tetrahedral truss/hexagonal heatshield panel aerobrake
[NASA-TM-101612] N90-10127
Space structures concepts and materials
[NASA-CR-183727] N90-10128
TUNGSTEN ALLOYS
Strain aging in tungsten-heavy alloys
[AD-A211166] N90-10259
TURBINE BLADES
Large scale prop-fan structural design study. Volume 1: initial concepts
[NASA-CR-174992] N90-10043
Large scale prop-fan structural design study. Volume 2: Preliminary design of SR-7
[NASA-CR-174993] N90-10044
TURBINE ENGINES
Dynamic instability characteristics of aircraft turbine engine combustors N90-10195
TURBINE PUMPS
SSME Alternate Turbopump Development Program: Design verification specification for high-pressure fuel turbopump
[NASA-CR-183676] N90-10033
TURBOCOMPRESSORS
Improved silicon carbide for advanced heat engines
[NASA-CR-180831] N90-10293
TURBOFAN ENGINES
PMR graphite engine duct development
[NASA-CR-182228] N90-10037
Full scale technology demonstration of a modern counterrotating unducted fan engine concept: Component test
[NASA-CR-180868] N90-10047
Full scale technology demonstration of a modern counterrotating unducted fan engine concept. Design report
[NASA-CR-180867] N90-10048
Full scale technology demonstration of a modern counterrotating unducted fan engine concept. Engine test
[NASA-CR-180869] N90-10049
New energy conversion techniques in space, applicable to propulsion
[AIAA-79-1338] N90-10145
Characteristics of combustion driven pressure oscillations in advanced turbo-fan engines with afterburner N90-10194
TURBOMACHINE BLADES
Composite Blade Structural Analyzer (COBSTRAN) theoretical/programmer's manual
[NASA-TM-101958] N90-10181

TURBOPROP ENGINES
Large-scale Advanced Prop-fan (LAP) high speed wind tunnel test report
[NASA-CR-182125] N90-10045
Full scale technology demonstration of a modern counterrotating unducted fan engine concept. Design report
[NASA-CR-180867] N90-10048
TURBULENCE
Observations of spherical-wave scintillation in strong refractive-index turbulence
[PB89-124747] N90-10355
Bifurcations in Poiseuille flow and wall turbulence N90-10370
Control and modification of turbulence N90-10377
Turbulence management: Application aspects N90-10378
A comparison of wind turbulence simulation models for stochastic loads analysis for horizontal-axis wind turbines
[DE89-009442] N90-10473
TURBULENCE EFFECTS
A study of high-lift airfoils at high Reynolds numbers in the Langley low-turbulence pressure tunnel
[NASA-TM-89125] N90-10002
Convection of a pattern of vorticity through a reacting shock wave
[NASA-CR-181921] N90-10576
TURBULENCE MODELS
Fluid Dynamics of Three-Dimensional Turbulent Shear Flows and Transition
[AGARD-CP-438] N90-10356
A European collaborative investigation of the three-dimensional turbulent shear layers of a swept wing N90-10380
Turbulence modelling of three-dimensional shear flows N90-10381
Numerical simulation of turbulent plane channel flows N90-10382
Scaling and modeling of turbulent suspension flows N90-10393
Turbulence kinetic energy equation for dilute suspensions N90-10394
A comparison of wind turbulence simulation models for stochastic loads analysis for horizontal-axis wind turbines
[DE89-009442] N90-10473
TURBULENT BOUNDARY LAYER
The measurement of boundary layers on a compressor blade in cascade. Volume 1: Experimental technique, analysis and results
[NASA-CR-185118-VOL-1] N90-10038
A study of the structure of highly swept shock wave turbulent boundary layer interactions N90-10376
Fluctuating pressures measured beneath a high-temperature, turbulent boundary layer on a flat plate at Mach number of 5
[NASA-TP-2947] N90-10680
TURBULENT FLOW
Three-dimensional unsteady transonic viscous-inviscid interaction N90-10005
Direct numerical simulation of turbulent free shear flows
[AD-A210161] N90-10218
Fluid Dynamics of Three-Dimensional Turbulent Shear Flows and Transition
[AGARD-CP-438] N90-10356
A European collaborative investigation of the three-dimensional turbulent shear layers of a swept wing N90-10380
Numerical simulation of turbulent plane channel flows N90-10382
Scaling and modeling of turbulent suspension flows N90-10393
Dynamics and control of turbulent shear flows
[AD-A210396] N90-10402
The suitability of diffusion and wind-field techniques for an emergency-response dispersion model
[PB89-190219] N90-10481
TURING MACHINES
General decomposition of sequential machines: Relationships to state assignment
[AD-A208189] N90-10580
TWINNING
The effect of twins on critical currents of high Tc superconductors
[AD-A210988] N90-10768
TWO DIMENSIONAL FLOW
Two counter-rotating vortices approaching a free surface in a viscous fluid
[AD-A210495] N90-10404
TWO FLUID MODELS
The generalized drift flux approach: Identification of the void-drift closure law N90-10386
The role of particle collisions in pneumatic transport N90-10392
TWO PHASE FLOW
The generalized drift flux approach: Identification of the void-drift closure law N90-10386
Two-phase potential flow N90-10387
Interpretation and modeling of the averaged equations for a fluid-solid flow N90-10388
Effect of particle velocity fluctuations on the inertia coupling in two-phase flow N90-10391
The role of particle collisions in pneumatic transport N90-10392

U

UH-60A HELICOPTER
Airworthiness and flight characteristics test of the UH-60A Black Hawk helicopter equipped with the XM-139 multiple mine dispensing system (VOLCANO)
[AD-A210271] N90-10025
ULTRASONIC FLAW DETECTION
Investigation of materials and bonding using the scanning laser acoustic microscope
[KCP-613-4033] N90-10270
ULTRASONIC SCANNERS
Investigation of materials and bonding using the scanning laser acoustic microscope
[KCP-613-4033] N90-10270
ULTRASONIC TESTS
Generic system components of the Thiokol ultrasonic RSRM case-to-insulation bondline inspection system
[NASA-CR-183738] N90-10171
ULTRASONICS
Performance of a broadbanded ultrasonic transducer with coaxially mounted, nondirectional receiver
[DE89-015838] N90-10343
ULTRAVIOLET RADIATION
Silicon dioxide deposition at 100 deg C using vacuum ultraviolet light
[TR-0088(3945-07)-6] N90-10269
ULTRAVIOLET SPECTROSCOPY
Shortwavelength coherent radiation: Generation and applications
[AD-A209847] N90-10427
UNIVERSE
Are there causal vacuum solutions with the symmetries of the Goedel universe in higher-derivative gravity
[DE89-611966] N90-10770
The origin of the universe from quantum chaos: An introduction to current ideas
[AD-A210441] N90-10813
UNMANNED SPACECRAFT
Development of a flight test methodology for a US Navy half-scale unmanned air vehicle
[AD-A210563] N90-10029
UNSTEADY FLOW
Basic studies of the unsteady flow past high angle of attack airfoils
[AD-A210252] N90-10008
Vortex induced characteristics of missiles in unsteady maneuvers N90-10057
Reheat buzz: An acoustically coupled combustion instability N90-10200
Numerical simulation of unsteady combustion in a dump combustor N90-10203
Numerical solution of three-dimensional unsteady flows: Application to instability problems N90-10375
Numerical simulation of turbulent plane channel flows N90-10382
UPPER ATMOSPHERE
Kiruna geophysical data: Data Summary 88/7-9, July - September 1988
[PB89-210249] N90-10487
URANIUM
Characterization of electron-beam weld processes in uranium by acoustic emission monitoring
[DE89-016044] N90-10444
URETHANES
UV-curable polyurethane-methacrylate co-networks and interpenetrating networks
[AD-A210445] N90-10285
Synthesis and physical properties of poly(perfluoroalkylether) urethanes
[AD-A210500] N90-10287
USER MANUALS (COMPUTER PROGRAMS)
Composite Blade Structural Analyzer (COBSTRAN) theoretical/programmer's manual
[NASA-TM-101958] N90-10181
PORFLO-3: A mathematical model for fluid flow, heat, and mass transport in variably saturated geologic media: Users manual, version 1.0
[DE89-013977] N90-10398
The MHOST finite element program: 3-D inelastic analysis methods for hot section components. Volume 2: User's manual
[NASA-CR-182235-VOL-2] N90-10450
Satellite Data Processing System (SDPS) users manual V1.0
[NASA-CR-183054] N90-10468
USER REQUIREMENTS
Addressing user display requirements from a large and diverse user community
[DE89-011403] N90-10582

V

VACUUM
Are there causal vacuum solutions with the symmetries of the Goedel universe in higher-derivative gravity
[DE89-611966] N90-10770
VACUUM DEPOSITION
Silicon dioxide deposition at 100 deg C using vacuum ultraviolet light
[TR-0088(3945-07)-6] N90-10269
VACUUM SYSTEMS
Introduction to total- and partial-pressure measurements in vacuum systems
[NASA-RP-1219] N90-10412
VACUUM TUBES
Vacuum microelectronics for beam power and rectennas N90-10146
VALENCE
Solvent relaxation in electron-transfer reactions: Comparisons between barrier-crossing dynamics in water and polar aprotic media
[AD-A210212] N90-10220
Solvent effects on intervalence electron-transfer energies for biferrocene cations: Comparisons with molecular models of solvent reorganization
[AD-A210263] N90-10691
Superconductivity from valence fluctuations with finite U
[DE89-015302] N90-10742
VALUE
Type reconstruction with first-class polymorphic values
[AD-A210833] N90-10605
VAPOR DEPOSITION
Characterization of diamond films by thermogravimetric analysis and infrared spectroscopy
[AD-A210564] N90-10288
Properties of devices prepared with epitaxial layers on InP
[AD-A210304] N90-10759
VAPOR PHASE EPITAXY
Ordered structures and metastable alloys grown by OMVPE
[DE89-016370] N90-10744
VAPORIZING
Theory of droplet. Part 1: Renormalized laws of droplet vaporization in non-dilute sprays N90-10390
VARIANCE (STATISTICS)
Improved estimation of the disturbance variance in a linear regression model
[AD-A210272] N90-10641
VARIATIONAL PRINCIPLES
Self-calibration of robot-sensor system N90-10570
VARIATIONS
Discrete-time conversion for simulating finite-horizon Markov processes
[AD-A210683] N90-10666
VECTOR PROCESSING (COMPUTERS)
Proceedings of the 2nd International Conference on Vector and Parallel Computing
[AD-A209401] N90-10585
VECTORS (MATHEMATICS)
Extended Weyl group for Kac-Moody algebras
[DE89-617525] N90-10634
Quotient-difference type generalizations of the power method and their analysis
[NASA-TM-102361] N90-10635
VELOCITY MEASUREMENT
Pin switch circuits instrument for microsecond velocity measurements
[AD-A210638] N90-10426
VERTICAL AIR CURRENTS
Thermodynamic and dynamic processes in the updraft region of GALE (Genesis of Atlantic Lows Experiment) IOP (Intensive Observation Period) 9
[AD-A208139] N90-10496
VERTICAL ORIENTATION
Demonstration of a dual-lidar method for measuring optical depths in the vertical
[AD-A210598] N90-10711
VERY LARGE SCALE INTEGRATION
The organization of permutation architectures with bussed interconnections
[AD-A210832] N90-10352
Network of dedicated processors for finding lowest-cost map path
[NASA-CASE-NPO-17716-1-CU] N90-10608

VERY LOW FREQUENCIES
Omega system performance assessment
[AD-A210342] N90-10322
TWIRE: A test program for VLF airborne transmissions
[AD-A210516] N90-10324
A lunar far-side very low frequency array
[NASA-CP-3039] N90-10805
VIBRATION DAMPING
Flexible structure control experiments using a real-time workstation for computer-aided control engineering N90-10084
Active vibration mitigation of distributed parameter, smart-type structures using Pseudo-Feedback Optimal Control (PFOC) N90-10121
Analysis and test of a 16-foot radial rib reflector development model
[NASA-TM-101648] N90-10457
The theory and application of quadratic minimization in the active reduction of sound and vibration N90-10682
VIBRATION TESTS
SSME Alternate Turbopump Development Program: Design verification specification for high-pressure fuel turbopump
[NASA-CR-183676] N90-10033
VIBRAFUGE: A combined environment testing facility-vibration testing on a centrifuge
[DE89-015120] N90-10458
VIBRATIONAL SPECTRA
Raman spectroscopic study of the rare earth sesquisulfides
[AD-A210610] N90-10226
Computer simulations of polymer dynamics in the solid state
[DE89-010337] N90-10275
VIDEO SIGNALS
Robot vehicle video image compression, phase 1
[AD-A210974] N90-10626
VISCOELASTIC CYLINDERS
Similarity solutions that give rise to hyperbolicity and change of type in steady flow of a viscoelastic fluid
[AD-A210920] N90-10410
VISCOSITY
Shock capturing by the spectral viscosity method
[NASA-CR-181920] N90-10639
VISCOUS FLOW
Iterative performance and an adaptive procedure for viscous flow problems N90-10397
Two counter-rotating vortices approaching a free surface in a viscous fluid
[AD-A210495] N90-10404
VISCOUS FLUIDS
Two counter-rotating vortices approaching a free surface in a viscous fluid
[AD-A210495] N90-10404
Analytic theory for the selection of Saffman-Taylor fingers in the presence of thin film effects
[NASA-CR-181910] N90-10677
VISIBILITY
Atmospheric transmissivity update - 1988
[AD-A209130] N90-10484
US Navy regional climatic study of the United States Atlantic Coast and associated waters
[AD-A210198] N90-10503
A3I visibility modeling project N90-10557
VISION
Vision science and technology at NASA: Results of a workshop: Executive summary N90-10543
Sampling and noise in vision networks N90-10544
Networks for image acquisition, processing and display N90-10545
Visions of visualization aids: Design philosophy and experimental results N90-10547
Human motion perception: Higher-order organization N90-10553
Filling in the retinal image N90-10556
Instrumentation and robotic image processing using top-down model control N90-10563
Pyramid image codes N90-10567
VISUAL DISCRIMINATION
Networks for image acquisition, processing and display N90-10545
Two-dimensional shape recognition using sparse distributed memory N90-10554
Stanford/NASA-Ames Center of Excellence in model-based human performance N90-10565
VISUAL FIELDS
Filling in the retinal image N90-10556
VISUAL PERCEPTION
Filling in the retinal image N90-10556
VOICE COMMUNICATION
Phase 2 testing and evaluation of low data rate voice CODEC equipment
[ACD-330-PHASE-2] N90-10315
VOICE CONTROL
Scientific and technical report voice activated gun turrent control
[AD-A210350] N90-10623
VOICE DATA PROCESSING
Phase 2 testing and evaluation of low data rate voice CODEC equipment
[ACD-330-PHASE-2] N90-10315
VOLCANOES
Paper 1. Impact of volcanic aerosols on stratospheric chemistry. Paper 2. O2 (1 sigma g +) and O2 (1 delta g) in the H + O2 reaction system. Paper 3. Barotropic instability of zonal jets on Mars, Earth and Venus N90-10477
VORTEX SHEETS
The three-dimensional vortex sheet structure on delta wings N90-10367
VORTICES
On the interaction of stationary crossflow vortices and Tollmien-Schlichting waves in the boundary layer on a rotating disc
[NASA-CR-181859] N90-10007
Basic studies of the unsteady flow past high angle of attack airfoils
[AD-A210252] N90-10008
Vortex induced characteristics of missiles in unsteady maneuvers N90-10057
Acoustic-vortex-chemical interactions in an idealized ramjet N90-10206
Numerical investigation of the effects of longitudinal vortices on the onset of transition in a flat plate boundary layer N90-10363
Goertler instability on an airfoil: Comparison of marching solution with experimental observations N90-10364
Three-dimensional boundary layer transition on a concave surface N90-10365
Trailing-edge sweep and three-dimensional vortex interactions in jets and mixing layers N90-10379
A European collaborative investigation of the three-dimensional turbulent shear layers of a swept wing N90-10380
Convection of a pattern of vorticity through a reacting shock wave
[NASA-CR-181921] N90-10576
Plasma theory and simulation
[AD-A207952] N90-10714
VORTICITY EQUATIONS
Similarity solutions that give rise to hyperbolicity and change of type in steady flow of a viscoelastic fluid
[AD-A210920] N90-10410
VOYAGER PROJECT
NASA Voyager 2 Neptune encounter press kit
[NASA-TM-101851] N90-10076
VOYAGER 2 SPACECRAFT
NASA Voyager 2 Neptune encounter press kit
[NASA-TM-101851] N90-10076
VULNERABILITY
Assessing the accuracy of vulnerability models by comparison with vulnerability experiments
[AD-A210871] N90-10669

W

WAFERS
Epitaxial GaAs on SOI wafers
[AD-A209009] N90-10729
WALL FLOW
Bifurcations in Poiseuille flow and wall turbulence N90-10370
WALLS
Plasma theory and simulation
[AD-A207952] N90-10714
WARM FRONTS
Thermodynamic and dynamic processes in the updraft region of GALE (Genesis of Atlantic Lows Experiment) IOP (Intensive Observation Period) 9
[AD-A208139] N90-10496
WARNING SYSTEMS
Safer skies with TCAS: Traffic Alert and Collision Avoidance System
[PB89-169221] N90-10016
Data processing in lightning warning systems
[DE89-012495] N90-10502
WATER
Heterogeneous catalysts in water
[AD-A210742] N90-10228
WATER POLLUTION
Coastal Research Center Woods Hole Oceanographic Institution
[PB89-198238] N90-10510
Managing human exposure and health risks: An integrated approach and the role of uncertainty
[DE89-008611] N90-10525
WATER QUALITY
Spatial characterization of acid rain stress in Canadian Shield Lakes
[NASA-CR-183446] N90-10479
WATER TABLES
Fluctuation history of Great Salt Lake, Utah, during the last 13,000 years, part 2
[NASA-CR-185911] N90-10466
WATER VAPOR
A study of the impact of simulated 183 GHz water vapor retrievals on numerical weather prediction
[AD-A210431] N90-10504
Tests of various finite difference algorithms applied to a simple water vapor transport problem on a staggered grid
[AD-A210229] N90-10596
WAVE DIFFRACTION
Custom diffraction gratings
[AD-A211002] N90-10712
WAVE DISPERSION
Optical dispersion relations for diamondlike carbon films
[NASA-TM-102356] N90-10738
WAVE EQUATIONS
A straightforward method for finding implicit solitary wave solutions of nonlinear evolution and wave equations
[AD-A210561] N90-10647
WAVE INTERACTION
Reheat buzz: An acoustically coupled combustion instability N90-10200
Acoustic-vortex-chemical interactions in an idealized ramjet N90-10206
WAVE PROPAGATION
Observations of spherical-wave scintillation in strong refractive-index turbulence
[PB89-124747] N90-10355
Stimulated rotational Raman scattering
[DE89-016427] N90-10430
Kinetic effects in Alfven wave heating. Part 2: Propagation and absorption with a single minority species
[DE89-016619] N90-10724
WAVE SCATTERING
A combined finite element and boundary integral formulation for solution via CGFFT of 2-dimensional scattering problems
[NASA-CR-184781] N90-10313
Scattering of an ICRF magnetosonic wave by plasma density turbulence
[DE89-015223] N90-10720
WEAPON SYSTEMS
Human health studies of carbon monoxide (CO) under conditions of military weapons systems crewman exposures. Protocol 1: Formation of COHb
[AD-A210344] N90-10528
Director, Operational Test and Evaluation report FY-88
[AD-A206784] N90-10778
WEAR
The response of isotropic brittle materials to abrasive processes
[DE89-016637] N90-10251
Friction and wear of oxide-ceramic sliding against IN-718 nickel base alloy at 25 to 800 C in atmospheric air
[NASA-TM-102291] N90-10262
Research on ultra low wear materials for energy conservation
[DE89-015096] N90-10263
WEAR RESISTANCE
Friction and wear of oxide-ceramic sliding against IN-718 nickel base alloy at 25 to 800 C in atmospheric air
[NASA-TM-102291] N90-10262
WEAR TESTS
Compatibility of fuel system components with high density fuel
[AD-A210381] N90-10027
WEATHER
Marine weather log, volume 32, number 3, summer 1988
[PB88-248075] N90-10491
A program to improve performance of AFGL (Air Force Geophysical Laboratory) automated present weather observing sensors
[AD-A207669] N90-10495
WEATHER FORECASTING
Forecasting convection with the AFOS (Automation of Field Operations and Services) data analysis programs. (ADAP-version 2.0) (AFOS data analysis programs-version 2.0)
[PB89-145940] N90-10492
National Severe Storms Laboratory, fiscal year 1988
[PB89-156145] N90-10493
Meteorological support: Descriptions of application programs for accessing and displaying data
[PB89-194625] N90-10500

Research highlights of the NMC (National Meteorological Center) Development Division: 1987-1988
[PB89-206478] N90-10501
Effects of stress on judgment and decision making in dynamic tasks
[AD-A210605] N90-10781

WEATHERING
Development of a semiquantitative corrosion monitor
[AD-A208132] N90-10414

WEAVING
The interlaminar fracture toughness of woven graphite/epoxy composites
[NASA-TP-2950] N90-10179

WELDED JOINTS
Delayed failure of silver-aided diffusion welds between steel
[DE89-016652] N90-10252
Limit analysis of welded tee end connections for hollow tubes
[PB89-191647] N90-10452

WELDING
Investigation of the pyrometallurgical, physical and mechanical behavior of weld metal
[AD-A211114] N90-10258
Automation of fiber-optic pigtailing process: Laser welding demonstration program
[AD-A210351] N90-10707

WHISKER COMPOSITES
Friction and wear of oxide-ceramic sliding against IN-718 nickel base alloy at 25 to 800 C in atmospheric air
[NASA-TM-102291] N90-10262
Ceramic components in machines, Cologne and Aachen, West Germany; Maastricht, The Netherlands and Brussels, Belgium
[DE89-015831] N90-10264
Zirconia toughened SiC whisker reinforced alumina composites small business innovation research
[NASA-CR-179629] N90-10294

WHITE DWARF STARS
Theoretical statistics of zero-age cataclysmic variables N90-10810

WHITE NOISE
Sampling and noise in vision networks N90-10544

WIND (METEOROLOGY)
A study of the impact of simulated satellite lidar wind observations
[AD-A210430] N90-10488
National Severe Storms Laboratory, fiscal year 1988
[PB89-156145] N90-10493

WIND EFFECTS
The suitability of diffusion and wind-field techniques for an emergency-response dispersion model
[PB89-190219] N90-10481

WIND PROFILES
A study of the impact of simulated satellite lidar wind observations
[AD-A210430] N90-10488

WIND TUNNEL APPARATUS
Wind tunnel support system effects on a fighter aircraft model at Mach numbers from 0.6 to 2.0
[AD-A210614] N90-10010

WIND TUNNEL MODELS
An integrated CFD/experimental analysis of aerodynamic forces and moments
[NASA-TM-102195] N90-10006
Wind tunnel support system effects on a fighter aircraft model at Mach numbers from 0.6 to 2.0
[AD-A210614] N90-10010
Wind tunnel tests: The role of the model N90-10064
Experimental investigation of attachment-line transition in low-speed, high-lift wind-tunnel testing N90-10358

WIND TUNNEL TESTS
A study of high-lift airfoils at high Reynolds numbers in the Langley low-turbulence pressure tunnel
[NASA-TM-89125] N90-10002
An integrated CFD/experimental analysis of aerodynamic forces and moments
[NASA-TM-102195] N90-10006
Wind tunnel support system effects on a fighter aircraft model at Mach numbers from 0.6 to 2.0
[AD-A210614] N90-10010
Analysis of results from wind tunnel tests of inlets for an advanced turboprop nacelle installation
[NASA-CR-174937] N90-10011
Development of a flight test methodology for a US Navy half-scale unmanned air vehicle
[AD-A210563] N90-10029
Large-scale Advanced Prop-fan (LAP) high speed wind tunnel test report
[NASA-CR-182125] N90-10045
Wind tunnel tests: The role of the model N90-10064
Identification of stability and control parameters of a brilliant ammunition N90-10065
The active flexible wing aeroservoelastic wind-tunnel test program N90-10119
Experimental investigation of attachment-line transition in low-speed, high-lift wind-tunnel testing N90-10358

WIND TUNNELS
Wind tunnel support system effects on a fighter aircraft model at Mach numbers from 0.6 to 2.0
[AD-A210614] N90-10010

WIND TURBINES
Some significant results from testing a Remote Multiplexing Unit (RMU) for temperature-induced errors
[DE89-009432] N90-10421
A comparison of wind turbulence simulation models for stochastic loads analysis for horizontal-axis wind turbines
[DE89-009442] N90-10473

WIND VELOCITY
US Navy regional climatic study of the United States Atlantic Coast and associated waters
[AD-A210198] N90-10503

WINDSHIELDS
Definition and reduction of the F-18 windshield birdstrike hazard
[AD-A210700] N90-10015

WING PANELS
Laminar flow control perforated wing panel development
[NASA-CR-178166] N90-10187

WINGS
Winged versus wingless airframes N90-10073

WIRE
Composite ceramic superconducting wires for electric motor applications
[AD-A210345] N90-10346
An algorithm to calculate the beam momentum distribution from flying wire profiles
[DE89-015587] N90-10418

WIRE WINDING
Mechanical states in wound capacitors. Part 1: Prediction
[DE89-008110] N90-10337
Mechanical states in wound capacitors. Part 2: Optimization
[DE89-008116] N90-10338

WORK-REST CYCLE
Human performance in continuous/sustained operations and the demands of extended work/rest schedules: An annotated bibliography, volume 2
[AD-A210504] N90-10530

WORKSTATIONS
Flexible structure control experiments using a real-time workstation for computer-aided control engineering N90-10084
Intensity dependent spread processor and workstation N90-10568

X

X RAY ASTRONOMY
The Spartan 1 mission
[NASA-TM-101887] N90-10077
Solar X-ray Astronomy Sounding Rocket Program
[NASA-CR-183447] N90-10796
Soft X-ray astronomy using grazing incidence optics N90-10797
The detection of soft X-rays with charged coupled detectors N90-10798
The design and evaluation of grazing incidence relay optics N90-10799
The observation of possible reconnection events in the boundary changes of solar coronal holes N90-10801
X-ray bright points and He I lambda 10830 dark points N90-10802
Advances in photographic X-ray imaging for solar astronomy N90-10803
Correspondence between solar fine-scale structures in the corona, transition region, and lower atmosphere from collaborative observations N90-10804
Analysis of nearly simultaneous X-ray and optical observations of active galactic nuclei N90-10806

X RAY DIFFRACTION
Bragg crystal polarimeters
[NASA-CR-181331] N90-10423
Progress report on grain boundaries
[DE89-015541] N90-10749

X RAY IMAGERY
Advances in photographic X-ray imaging for solar astronomy N90-10803
Correspondence between solar fine-scale structures in the corona, transition region, and lower atmosphere from collaborative observations N90-10804

X RAY LASERS
X-ray lithography studies of polysilane using a laser plasma X-ray source
[DE89-015390] N90-10266

X RAY SOURCES
X-ray lithography studies of polysilane using a laser plasma X-ray source
[DE89-015390] N90-10266
X-ray bright points and He I lambda 10830 dark points N90-10802

X RAY SPECTROSCOPY
X-ray spectroscopy of the SSME plume
[NASA-CR-185308] N90-10168
Shortwavelength coherent radiation: Generation and applications
[AD-A209847] N90-10427

X RAYS
A compact X-ray lithography lattice using superferric magnets
[DE89-013947] N90-10728
The detection of soft X-rays with charged coupled detectors N90-10798

X-29 AIRCRAFT
Initial flight qualification and operational maintenance of X-29A flight software
[NASA-TM-101703] N90-10023

Y

YAG LASERS
Efficient nonlinear conversion of laser diode pumped miniature solid state laser sources
[AD-A210708] N90-10433
Automation of fiber-optic pigtailing process: Laser welding demonstration program
[AD-A210351] N90-10707

YAW
Aircraft modal supression system: Existing design approach and its shortcomings N90-10115

YIELD STRENGTH
Fatigue growth and closure of short cracks
[AD-A210824] N90-10462

YTTRIUM OXIDES
Magnetic correlations in high T(sub c) oxides in the superconducting state
[DE89-016421] N90-10746

Z

ZINC COATINGS
Micromechanisms of surface friction in zinc electrogalvanized steel sheets
[DE89-011819] N90-10440

ZINC SULFIDES
Preparation, purification and densification of zinc sulfide powder from organometallics
[AD-A210943] N90-10298

ZINC-BROMIDE BATTERIES
Preparation and evaluation of composite membranes for zinc/bromine storage batteries
[DE89-009931] N90-10339

ZIRCONIUM OXIDES
Structural and surface characterization of dispersed metal catalysts
[DE89-014530] N90-10208
Shock compression and release in high-strength ceramics
[DE89-013995] N90-10265
Zirconia toughened SiC whisker reinforced alumina composites small business innovation research
[NASA-CR-179629] N90-10294
Study of deposition of YBa2Cu3O7-x on cubic zirconia
[NASA-TM-102350] N90-10737

ZONAL FLOW (METEOROLOGY)
Paper 1. Impact of volcanic aerosols on stratospheric chemistry. Paper 2. O2 (1 sigma g +) and O2 (1 delta g) in the H + O2 reaction system. Paper 3. Barotropic instability of zonal jets on Mars, Earth and Venus N90-10477

Typical Personal Author Index Listing

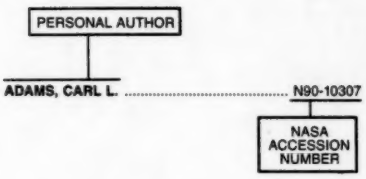

Listings in this index are arranged alphabetically by personal author. The NASA accession number denotes the number by which the citation is identified.

A

ABOU-ARAB, T. W. N90-10394
ACCIOLY, A. J. N90-10770
ADAMS, CARL L. N90-10307
ADAMS, SUSAN M. N90-10592
N90-10593
AGEGIAN, CATHERINE R. N90-10509
AGNEW, STEPHEN F. N90-10215
AHMED, N. U. N90-10120
AHN, B.-H. N90-10490
AHUMADA, ALBERT J., JR. N90-10544
N90-10545
AIDA, HITOSHI N90-10617
AIELLO, ROBERT A. N90-10181
AKASOFU, S.-I. N90-10490
AKI, KEIITI N90-10516
ALBERTS, T. N90-10123
ALBERTSON, CINDY W. N90-10680
ALCOCK, CHARLES R. N90-10794
ALEXANDER, D. J. N90-10250
ALEXIEV, D. N90-10740
ALFANO, ROBERT N90-10330
ALLEN, JAMES F. N90-10622
ALLEN, JAMES J. N90-10337
N90-10338
ALLEN, JERRY M. N90-10063
ALLEN, S. M. N90-10022
ALPERT, DANIEL J. N90-10476
ALRED, JOHN N90-10141
ALT, R. L. N90-10300
ALTEROVITZ, SAMUEL A. N90-10738
AMIRTHARAJ, P. M. N90-10300
ANDERSON, ALFRED B. N90-10250
ANDERSON, K. N90-10613
ANDERSON, P. H. N90-10129
ANDERSON, T. W. N90-10654
ANGERHOFER, ALEXANDER N90-10687
ANISSIPOUR, AMIR A. N90-10090
N90-10106
ANSUINI, FRANK N90-10414
ANTONELLI, CHARLES J. N90-10584
ANTONSEN, T. N90-10425
AOKI, SINYA N90-10776
APPLER, D. N90-10793
ARCHIBALD, T. G. N90-10305
ARDITI, ARIES N90-10557
ARNAL, D. N90-10362
N90-10373
N90-10377
ARNOLD, CHARLES, JR. N90-10339
ARSENEAUX, PETER J. N90-10045
ARSENTO, G. N90-10237
ASHBY, M. F. N90-10768
ASHCROFT, N. W. N90-10257
ASHLEY, KEVIN N90-10223
ASSINK, ROGER A. N90-10267
N90-10339
ATTIA, M. T. N90-10676
AYLER, S. E. N90-10199

B

BADI, DEBORAH M. N90-10814
BADLER, NORMAN N90-10557
BADLEY, RICKY D. N90-10267
BAHR, D. W. N90-10195
BAINUM, P. M. N90-10110
BAKER, LARRY E. N90-10536
BALAKRISHNAN, A. V. N90-10109
BALDWIN, N. J. N90-10247
BALLUFFI, R. W. N90-10749
BAMBERY, JAMES R. N90-10791
BANERJEE, PARTHA P. N90-10647
BANKS, BRUCE A. N90-10309
BARD, ALLEN J. N90-10214
BARKER, L. KEITH N90-10618
BARNES, D. N90-10721
BARNES, SUZANNE M. N90-10530
BARNHART, PAUL J. N90-10004
BARRETT, D. M. N90-10332
BARSANTI, M. L. N90-10425
BARSKY, MICHAEL F. N90-10102
BARTOE, J.-D. F. N90-10804
BARUH, H. N90-10098
BASS, HENRY E. N90-10708
BASSOM, ANDREW P. N90-10007
BATRA, R. C. N90-10448
BATTERSON, JAMES G. N90-10074
BAUER, B. S. N90-10722
BAUM, K. N90-10305
BAUMGARDNER, DARREL N90-10032
BECKERMAN, M. N90-10443
BECKWITH, IVAN E. N90-10359
BEEMAN, J. N90-10423
BELKIN, MICHAEL N90-10526
BEMAL, JAVIER N90-10636
BENELLI, G. N90-10207
BENIGNUS, VERNON A. N90-10528
BENSON, RUSSELL A. N90-10090
N90-10106
N90-10114
BENTLEY, J. N90-10208
BERGEN, JAMES N90-10557
BERGER, MARC A. N90-10702
BERMAN, ALEX N90-10089
BERNARD, JAY M. N90-10434
N90-10435
BERNHART, W. D. N90-10031
BERNS, MICHAEL W. N90-10519
BERNSTEIN, E. R. N90-10684
BETZ, G. N90-10241
BEVENSEE, R. M. N90-10319
BHALLA, A. N90-10296
BILLINGSLEY, JAMES P. N90-10307
BILLMAN, L. C. N90-10043
N90-10044
BIPPES, H. N90-10369
BIRCHENOUGH, SHAWN A. N90-10457
BIRDSALL, CHARLES K. N90-10714
BLACKBURN, J. F. N90-10312
N90-10585
BLAIR, A. B., JR. N90-10062
BLAIS, NORMAND N90-10302
BLAKE, WILLIAM B. N90-10054
BLAU, PETER J. N90-10750
BLELLOCH, PAUL N90-10087
BLISS, MARY N90-10291
BLOOMFIELD, HARVEY S. N90-10174
BLOSS, W. L. N90-10763
BLUMSTEIN, A. N90-10693
BODHAINE, BARRY A. N90-10494
BOEHNING, C. W. N90-10270
BOES, E. C. N90-10475
BOETTINGER, WILLIAM J. N90-10254
BOGDONOFF, SEYMOUR M. N90-10376
BOGGS, PAUL T. N90-10659
BOLEY, G. D. N90-10014
BOLTON, PAUL R. N90-10719
BONSU, F. O. N90-10305
BORIS, J. P. N90-10208
N90-10644
BOTHWELL, PHILLIP D. N90-10492
BOTSEAS, GEORGE N90-10517
BOUADI, HACENE N90-10182
BOURE, J. A. N90-10386
BOURNE, D. A. N90-10311
BOWLES, E. E. N90-10332
BOWMAN, D. R. N90-10015
BOWMAN, R. C., JR. N90-10300
BOYD, LINDA S. N90-10437
BOYLE, MICHAEL E. N90-10531
BRADLEY, GARY N90-10594
BRADT, R. C. N90-10272
BRANDENSTEIN, D. J. N90-10077
BRANDON, DEBORAH N90-10408
BRANDOW, B. H. N90-10742
BRAY, MARTIN N90-10244
BREITER, M. W. N90-10210
BRIDGES, P. J. N90-10243
BRISTOWE, P. D. N90-10749
BROCK, DAVID N90-10416
BROWN, GAIL J. N90-10756
BROWN, H. BENJAMIN, JR. N90-10445
BROWN, NORMAN J. N90-10251
BROWN, PAUL N90-10683
BROWN, WILLIAM C. N90-10150
BRUECKNER, G. E. N90-10804
BRUNGS, D. N90-10241
BRYANT, H. C. N90-10688
BUB, WERNER N90-10066
BUCHWALD, STEPHEN L. N90-10229
BUCKALEW, LOUIS W. N90-10326
BUDWINE, CHRISTINA M. N90-10794
BURLEY, B. L. N90-10332
BURNS, JACK O. N90-10805
BURROWS, ELIZABETH P. N90-10306
BURRUS, D. L. N90-10195
BURSTEIN, P. N90-10798
BURTON, R. GAINES N90-10263
BURTON, RALPH A. N90-10263

C

CABAK, A. N90-10021
CABRERA, CARLOS R. N90-10214
CAGLAYAN, A. K. N90-10022
CAHILL, P. A. N90-10703
CAIN, J. B. N90-10529
CALKINS, DALE E. N90-10607
CALVIN, JAMES M. N90-10667
CAMARDA, CHARLES J. N90-10409
CAMPBELL, A. M. N90-10768
CAMPBELL, WILLIAM A. N90-10045
CANTRELL, CHRISTOPHER A. N90-10480
CAPELLO, G. P. N90-10240
CAPPS, D. M. N90-10430
CARDRICK, A. W. N90-10235
CAREY, LINDA N90-10788
CARIGNAN, CRAIG R. N90-10438
CARLIER, J. C. N90-10243
CARLSON, C. ROBERT N90-10591
CARNEY, HAROLD K. N90-10505
N90-10506
N90-10507
CAROSSO, M. N90-10240
CARTER, RICHARD G. N90-10640
CARUSO, MICHAEL N90-10468
CASEY, H. C., JR. N90-10759
CASON, RANDALL W. N90-10025
CAVICCHI, ELIZABETH N90-10709
CAYULA, JEAN-FRANCOIS N90-10467
CAZALBOU, J. B. N90-10375
CEBECI, TUNCER N90-10373
CERICOLA, FRED N90-10458
CHADWICK, G. A. N90-10239
CHAILLOUT, C. N90-10751
CHAKRAVARTHY, SUKUMAR N90-10012
CHAMBERLIN, J. L. N90-10475
CHAMBERS, KATHLEEN C. N90-10537
CHAMIS, CHRISTOS C. N90-10181
N90-10185
CHAMPIGNY, P. N90-10052
CHANG, C. H. N90-10687
CHANG, CHE-WEI N90-10093
CHANG, JINCAI N90-10399
CHANG, KUO-CHU N90-10540

CHARGIN, MLADEN K. N90-10042
CHASE, R. C. N90-10799
CHASSAING, P. N90-10375
CHEESEMAN, PETER N90-10807
CHEN, C. P. N90-10393
CHEN, H. H. N90-10373
CHEN, J. N90-10292
CHEN, L. K. N90-10728
CHEN, W. S. N90-10471
CHEN, ZONGHUA N90-10811
CHENAVAS, J. N90-10751
CHEONG, S. W. N90-10751
CHEYNE, STANLEY A. N90-10708
CHILD, JOSEPH N90-10315
CHILDRESS, S. N90-10697
CHIPMAN, LAURE J. N90-10124
CHIU, H. H. N90-10390
CHODZKO, RICHARD A. N90-10434
N90-10435
CHONG, CHEE-YEE N90-10540
CHRIEN, R. N90-10721
CHRISTIAN, JOSE L., JR. N90-10159
CHRISTIE, D. J. N90-10428
CHUN, P. A. N90-10199
CIARLO, DINO R. N90-10344
CIFONE, ANTHONY J. N90-10193
N90-10195
CIMINO, WILLIAM W. N90-10099
CLARK, C. F. N90-10347
CLARK, R. K. N90-10248
CLARK, T. E. N90-10696
CLAUSING, ROBERT E. N90-10750
CLEAVER, HARRY E. N90-10426
CLOSSET, BERNARD N90-10244
COEN, PETER G. N90-10034
COFFER, JOHN G. N90-10435
COFFEY, HELEN E. N90-10817
N90-10818
N90-10819
N90-10820
N90-10821
N90-10822
N90-10823
N90-10824
COHEN, S. N90-10688
COLDREN, LARRY A. N90-10713
COLEMAN, EDWARD E. N90-10090
N90-10114
COLEMAN, R. N90-10697
COLLIER, F. S., JR. N90-10366
COLLINS, JEFFERY D. N90-10313
COLLINS, JOHN ANTHONY N90-10514
COMTE, PIERRE N90-10383
CONNER, DAVID A. N90-10679
CONNOR, TIMOTHY J. N90-10285
CONWAY, EDMUND J. N90-10154
N90-10167
COOK, DANIEL R. N90-10720
COOK, J. W. N90-10804
COOK, M. N90-10171
COON, DARRYL D. N90-10546
COOPER, DAVID M. N90-10176
COOPER, PAUL W. N90-10400
COOPER, STUART L. N90-10284
N90-10285
N90-10286
N90-10287
COOPER, WILLIAM A. N90-10032
CORNILLON, PETER N90-10467
COSSALTER, V. N90-10207
COSTEN, R. N90-10156
COTMAN, C. W. N90-10532
COULTER, K. N90-10429
COUSTEIX, J. N90-10377
COUSTOLS, E. N90-10377
COVE, JOANNE FRANCES N90-10784
COX, B. N. N90-10255
COZZENS, ROBERT F. N90-10531
CRANE, R. I. N90-10365
CRAWFORD, E. N90-10721
CREEDON, JEREMIAH F. N90-10577
CREIGHTON, D. C. N90-10077
CREMER, JAMES F. N90-10578
CREUTZ, MICHAEL N90-10777
CRITTENDEN, DIANNE K. N90-10496
CROFT, W. BRUCE N90-10621
CROSS, E. L. N90-10296
CRUDDACE, RAYMOND G. N90-10077
CUDDIHY, EDWARD F. N90-10261
CULICK, F. E. C. N90-10192
CULL, RONALD C. N90-10158
CUMMINGS, D. B. N90-10331
CURRIE, JOHN G. N90-10790
CURTIS, A. R. D. N90-10582
CUSHMAN, R. M. N90-10482
CUSUMANO, SALVATORE JOSEPH N90-10620

D

DACOSTA, J. L. N90-10360
DAGENHART, J. RAY N90-10364
DAHLBURG, R. B. N90-10725
DALLMANN, U. N90-10371
DANG, K. N90-10382
DANIELSON, A. O. N90-10067
DANYLUK, STEVEN N90-10180
DAOUD, FAKER N90-10647
DARNER, G. S. N90-10417
DASKALOS, E. C. N90-10335
DATZ, SHELDON N90-10686
DAVIDIAN, KENNETH J. N90-10172
DAVIDSON, EDWARD A. N90-10232
DAVIDSON, JAMES A. N90-10480
DAVIS, J. N90-10727
DAVIS, JOHN M. N90-10797
N90-10798
N90-10799
N90-10803
N90-10804
DAVIS, L. C. N90-10276
DAVIS, R. F. N90-10272
DAVIS, ROBERT F. N90-10760
DAVIS, WILLIAM M. N90-10229
DAYI, OMER F. N90-10775
DEADMORE, DANIEL L. N90-10262
DEAN, M. N90-10513
DEANGELIS, R. J. N90-10208
DEANGELIS, RICHARD M. N90-10491
DEASE, C. G. N90-10739
DEATON, JERRY W. N90-10179
DEBOOR, CARL N90-10646
DECKER, RAND N90-10385
DEGEORGE, C. L. N90-10046
DEHEL, THOMAS N90-10315
DEIWERT, GEORGE S. N90-10176
DEJARNETTE, FRED R. N90-10401
DELACHEVALERIE, D. AYMER N90-10360
DEMICHELE, G. N90-10207
DEMS, BERNARD C. N90-10733
DENNIS, RICHARD C. N90-10523
DERE, K. P. N90-10804
DEROQUEFORT, T. ALZIARY N90-10360
DESCHAMPS, V. N90-10382
DESLANDES, RONALD N90-10070
DESPINEY, P. N90-10053
DETTERMAN, DOUGLAS K. N90-10538
DEUTSCH, STEVEN N90-10038
N90-10039
DEVADAS, SRINIVAS N90-10580
DEVANEY, W. E. N90-10471
DEY, DIPAK K. N90-10641
DEYOUNG, RUSSELL J. N90-10140
N90-10156
N90-10160
DICARLO, JAMES A. N90-10188
DICKASON, ANNE M. N90-10790
DICKINSON, J. THOMAS N90-10459
DIFILIPPO, FRANK N90-10309
DILLARD, R. N90-10597
DILLENIUS, M. F. E. N90-10058
DILLINGER, R. B. N90-10067
DIMAGNO, THEODORE J. N90-10687
DOBOSY, RONALD J. N90-10481
DOBREV, V. K. N90-10634
DOGGETT, JIM N90-10458
DOHERR, K.-F. N90-10065
DONALDSON, JANET R. N90-10659
DORSEY, JOHN T. N90-10127
DORSINVILLE, ROGER N90-10330
DOUGHERTY, B. P. N90-10419
DOWDING, ROBERT J. N90-10259
DOWELL, F. N90-10273
DOWGIALLO, MICHAEL J. N90-10513
DOWLING, A. P. N90-10200
DOWLING, NORMAN E. N90-10462
DRAGON, KAREN M. N90-10589
DRESCHEL, THOMAS W. N90-10478
DREW, DONALD A. N90-10391
DRUTMAN, C. N90-10430
DUBELL, THOMAS L. N90-10193
DUNCAN, JAMES H. N90-10403
DUNN, CHRIS N90-10468
DURAKPASA, H. N90-10210
DURAND, N. A. N90-10340
DURIC, NEBOJSA N90-10805
DYN, NIRA N90-10646

E

EARLES, JENNIFER N90-10467
EARLS, MICHAEL R. N90-10023
EBERHARDT, SILVIO P. N90-10608
EBRAHIMI, YAGHOOB S. N90-10105
ECKMAN, RICHARD M. N90-10481
EDRINGTON, THOMAS S. N90-10502
EDWARDS, S. J. N90-10022
EGGLESTON, STEVE W. N90-10316
EICHHORN, WILLIAM L. N90-10569
EICHMANN, GEORGE N90-10330
EL-KABBANI, OSAMMA N90-10687
ELDRIDGE, C. N90-10614
ELGHAZALY, A. A. N90-10676
ELLINGWOOD, G. N90-10614
ELLIOTT, CHARLES W. N90-10787
ELLIS, STEPHEN R. N90-10547
ELLIS, VINCENT J. N90-10323
ELSNER, R. N90-10423
ELWAKIL, S. A. N90-10676
EMPSON, T. R. N90-10712
ENDRUSICK, THOMAS L. N90-10541
ERHAN, S. N90-10296
ERICKSON, JON D. N90-10548
ERICSSON, L. E. N90-10056
EVANS, N. A. N90-10340
N90-10341

F

FABIAN, J. M. N90-10077
FALES, CARL L. N90-10551
FALK, G. N90-10613
FAN, MICHAEL K. H. N90-10085
FANG, Z.-Q. N90-10769
FARLOW, G. C. N90-10274
FARMER, JEFFREY T. N90-10814
FASEL, H. N90-10363
FASHAM, MICHAEL J. R. N90-10515
FAWCETT, W. RONALD N90-10211
N90-10212
FAYMON, KARL A. N90-10155
N90-10165
N90-10166
FEDDERS, P. A. N90-10734
FELDMAN, DAVID N90-10695
FELIU, VICENTE N90-10445
FELMER, PATRICIO L. N90-10649
N90-10650
FERRIS, JAMES C. N90-10002
FIELD, GLENN A. N90-10499
FISCHER, D. A. N90-10292
FISCHER, R. P. N90-10425
FISCHER, T. M. N90-10371
FISCHLER, J. E. N90-10187
FISHER, R. J. N90-10342
FISHER, RICHARD A. N90-10229
FISK, Z. N90-10751
FLIFLET, A. W. N90-10425
FLOWER, LINDA N90-10788
FOLEY, R. J. N90-10428
FOOTE, STEPHEN L. N90-10535
FORD, WARREN T. N90-10228
N90-10267
FORD, WILLIAM F. N90-10635
FORMAN, P. R. N90-10706
FORNASIER, L. N90-10053
FORSGREN, ROGER C. N90-10415
FOSS, COLBY A., JR. N90-10211
FOUCAUD, ROBERT N90-10196
FOUILLET, YVES N90-10383
FOVELL, ROBERT GERARD N90-10497
FOX, BENNETT L. N90-10666
FOX, GEOFFREY C. N90-10611
FRANK, D. N. N90-10428
FRANS, S. D. N90-10665
FREDRICKSON, LYLE J. N90-10664
FREUDENSTEIN, FERDINAND N90-10628
FRIED, HERBERT M. N90-10695
FRIEDBERG, R. A. N90-10031
FRITZ, G. G. N90-10077
FRITZ, R. B. N90-10355
FROST, R. H. N90-10258
FUCHS, BARUCH A. N90-10251
FUCHS, HEINZ N90-10055
FULKERSON, W. N90-10482
FUNK, JOAN G. N90-10179
FURMAN, MIGUEL A. N90-10701

G

GAEVERT, RICHARD S. N90-10607
GALAMBOS, J. D. N90-10716
GALLIMORE, IAN T. N90-10102
GARCIA, EDWIN N90-10214
GARDNER, J. H. N90-10206
GARECHT, D. M. N90-10413

GARLAND, JAY L. N90-10571
GARN, PAUL A. N90-10814
GARNIER, F. N90-10203
GATE, M. S. N90-10059
GAUGER, J. R. N90-10321
GAZZINA, A. N90-10060
N90-10073
GEIER, G. J. N90-10021
GEIGER, WILLIAM E. N90-10177
GEISELHART, KARL A. N90-10034
GELFAND, ALAN E. N90-10641
GENOUX, R. N90-10236
GEORGE, THOMAS F. N90-10731
N90-10764
GERARD, D. A. N90-10464
GERRARD, J. H. N90-10374
GERSTENBERGER, DAVID C. N90-10433
GHOSH, DEBASHISH N90-10609
GIBBS, BRAIN J. N90-10779
GIESSEN, B. C. N90-10283
GIFFORD, DAVID K. N90-10605
GILKEY, AMY P. N90-10590
GILMAN, R. A. N90-10429
GINSBERG, MARILYN N90-10601
GIOVANOLA, J. H. N90-10253
GIULIANI, J. L., JR. N90-10727
GLASER, PETER E. N90-10144
GLASS, B. J. N90-10107
GLENNY, D. E. N90-10040
N90-10041
GLICK, JOHN H. N90-10590
GLOVER, RICHARD D. N90-10610
GLUCK, R. N90-10096
GLYNN, PETER W. N90-10666
N90-10668
GOCHEV, ALEXANDER N90-10690
N90-10691
N90-10692
GOEBEL, JOHN N90-10807
GOEL, VINOD N90-10786
GOGUEN, JOSEPH A. N90-10617
GOLUB, L. N90-10802
GOMEZ, S. A. N90-10533
GONZALEZ, RICHARD R. N90-10523
GOODYEAR, M. D. N90-10030
GORDNIER, RAYMOND E. N90-10396
GORNEY, D. J. N90-10490
GOSLIN, T. J. N90-10115
N90-10116
GOUKER, MARK A. N90-10147
GRABLE, MARCUS N90-10315
GRADY, DENNIS E. N90-10265
GRASSOTTI, C. N90-10504
GRAY, HENRY F. N90-10146
GREEN, E. R. N90-10343
GREGORWICH, W. S. N90-10149
GREINER, N. ROY N90-10302
GRENICH, A. F. N90-10027
GRIGSBY, PEGGY J. N90-10756
GRIMES, RUSSELL N. N90-10227
GRIMSHAW, SCOTT D. N90-10672
GROVES, A. N90-10453
GRUNWALD, ARTHUR J. N90-10575
GRUSKA, C. J. N90-10043
N90-10044
GUALTIERI, J. ANTHONY N90-10549
GUILFOYLE, RICHARD N90-10601
GUIRGUIS, RAAFAT H. N90-10395
GUPTA, ANOOP N90-10615
N90-10616
GUPTA, SHANTI S. N90-10661
GUSTAFSON, JOHN L. N90-10589
GUTMARK, E. N90-10205
GUTSCHEWSKI, G. N90-10077

H

HAAS, CHRISTINA N90-10788
HALE, P. D. N90-10292
HALL, PHILIP N90-10007
HAMAMATSU, TERUHIDE N90-10268
HAMILTON, T. N90-10423
HAMMOND, KENNETH R. N90-10781
HANAGUD, S. N90-10107
HANCOCK, J. P. N90-10011
HANKS, BRANTLEY R. N90-10081
HANSCHE, BRUCE D. N90-10705
HANSEN, D. F. N90-10495
HANSEN, DANIEL L. N90-10125
HANSEN, DONALD V. N90-10512
HARADEM, D. P. N90-10321
HARDING, S. A. N90-10305
HARDY, B. C. N90-10358
HARGREAVES, T. A. N90-10425
HARRIES, W. L. N90-10157
HARRIGAN, R. W. N90-10442
HARRIS, DANIEL C. N90-10298
HARRIS, DAVID C. N90-10288
HARRIS, JOEL M. N90-10223
N90-10224
N90-10665
HARRIS, P. G. N90-10688
HARVEY, K. L. N90-10802
HARVEY, PIERRE D. N90-10213
HAUSSERMANN, JOHN W. N90-10675
HAWTHORNE, M. FREDERICK N90-10221
HAYES, JOHN R. N90-10788
HAZUCHA, MILAN N90-10528
HED, P. PAUL N90-10251
HEDGEPETH, JOHN M. N90-10153
HEE, ED W. N90-10344
HEINE, S. J. N90-10441
HELLER, JACK A. N90-10174
HELVY, F. A. N90-10333
HENDERSON, B. E. N90-10194
HENDRICKS, KYLE JAMES N90-10726
HENESIAN, M. A. N90-10428
HENSHALL, G. A. N90-10252
HERANT, M. N90-10802
HEREMAN, WILLY N90-10647
HERMAN, ALAN N90-10512
HERTZBERG, A. N90-10145
HETHERINGTON, C. J. D. N90-10748
HETHERINGTON, W. M. N90-10766
HEWER, G. A. N90-10068
HEYWARD, ANN O. N90-10674
HICKMAN, JAMES J. N90-10213
N90-10732
HIGGINBOTHAM, SCOTT A. N90-10079
HINKLE, C. ROSS N90-10478
HIRSCHEL, E. H. N90-10378
HITNEY, L. R. N90-10324
HO, FRANCIS P. N90-10498
HO, J. K. N90-10115
N90-10116
HO, LEE-WING N90-10631
HO, Z. Z. N90-10766
HOELTZEL, DAVID A. N90-10628
HOFFMAN, R. N. N90-10488
N90-10504
HOGARTH, ROBIN M. N90-10779
HOLBEN, RICHARD N90-10550
HOLLAND, W. R. N90-10703
HOLLERBACH, JOHN N90-10416
HOLLORAN, JOHN W. N90-10346
HOLT, R. D. N90-10271
HOLT, R. J. N90-10429
HOLTON, D. A. N90-10642
HOMAN, JAMES G. N90-10285
HONG, K. N90-10292
HOOPER, N. N90-10201
HOPCROFT, JOHN E. N90-10598
HOPKINS, PAUL B. N90-10281
HORIUCHI, RYUZO N90-10334
HOULIHAN, T. N90-10123
HOUSER, RICHARD M. N90-10476
HOWE, R. M. N90-10101
HOYLE, CHARLES E. N90-10282
HUANG, SHENG-YU N90-10216
HUCK, FRIEDRICH O. N90-10551
HULIN, CHARLES L. N90-10572
HUMES, DONALD H. N90-10132
N90-10156
N90-10161
N90-10167
HUNT, CHARLES E. N90-10344
HUNT, J. T. N90-10428
HUNTER, C. L. N90-10582
HUSON, F. R. N90-10728
HUSSAIN, F. N90-10218
HUSSAINI, M. Y. N90-10576
HWANG, GUANN-JIUN N90-10388

I

IADELUCA, JOSEPH P. N90-10017
ICHIMURA, ANDREW N90-10648
IDASZAK, JACQUELINE R. N90-10572
IGLEHART, DONALD L. N90-10668
IKEUCHI, KATSUSHI N90-10710
INAGAKI, T. N90-10292
IOFFE, L. B. N90-10741
IPEKKAN, AHMET Z. N90-10658
ISAACS, R. N90-10488
N90-10504
ISHIKAWA, HIROSHI N90-10268
IYYER, NAGARAJA S. N90-10462

J

JACKSON, T. L. N90-10576
JACOBSON, NATHAN S. N90-10188
JAHODA, F. C. N90-10706
JALUFKA, N. W. N90-10152
N90-10164
JAMES, M. R. N90-10255
JENKINS, J. T. N90-10392
JENKINS, JERRY E. N90-10054
JENKINS, KIMBERLY A. N90-10737
JENSEN, DOUGLAS R. N90-10711
JEONG, J. C. N90-10769
JEVICKI, ANTAL N90-10695
JIMENEZ, JAVIER N90-10370
JOHNSON, A. M. N90-10027
JOHNSON, CURTIS E. N90-10268
N90-10298
JOHNSON, DAVID N90-10180
JOHNSON, DAVID A. N90-10765
JOHNSON, DOUGLAS G. N90-10735
JOHNSON, L. C. N90-10533
JOHNSON, MICHAEL T. N90-10816
JOHNSON, SALLY C. N90-10602
JOHNSON, STANLEY A. N90-10422
JOHNSON, STEWART N90-10805
JOHNSON, SUZANNE N90-10573
JOHNSON, SYLVIA M. N90-10755
JOLLY, R. L. N90-10336
JONES, B. A. N90-10270
JONES, DAVID A. N90-10395
JONES, JESSE D. N90-10020
JONES, MICHAEL G. N90-10680
JORDAN, THOMAS H. N90-10489
JOSEPH, DANIEL D. N90-10410
JOSLIN, D. L. N90-10274
JOST, G. S. N90-10026
JOU, WEN-HUEI N90-10202
JUDAY, RICHARD D. N90-10552
JUILLEN, J. C. N90-10362

K

KAARET, P. N90-10423
KAHLER, S. W. N90-10801
KAILASANATH, K. N90-10206
KAILATH, THOMAS N90-10653
KAISER, MARY K. N90-10553
N90-10575
KALBURGI, VIJAY N90-10364
KAMIDE, Y. N90-10490
KANADE, TAKEO N90-10446
N90-10710
KANDA, TAKESHI N90-10035
KANERVA, PENTTI N90-10554
KANG, KYUNGSIK N90-10695
KANIA, LEE H. N90-10401
KANTROWITZ, ARTHUR N90-10143
KAPILA, A. K. N90-10576
KAPP, J. A. N90-10460
KARAGEORGHIS, ANDREAS N90-10637
KASSEL, PHILIP C., JR. N90-10132
KASSNER, M. E. N90-10252
KATNIK, GREGORY N. N90-10079
KATSUYAMA, RONALD M. N90-10573
KATZ, H. E. N90-10703
KAUFMAN, ALLAN N. N90-10720
KAYNES, IAN W. N90-10086
KEEFE, A. A. N90-10529
KEGELMAN, J. T. N90-10379
KELLER, A. N90-10297
KENNEY, CHARLES N90-10068
KENNEY, INGA N90-10215
KENNEY, JOHN N90-10215
KENWORTHY, M. J. N90-10195
KERN, F. A. N90-10412
KHANAKA, G. H. N90-10739
KIBENS, V. N90-10379
KIHARA, R. N90-10331
KILIAN, JOE N90-10352
KIM, H. K. N90-10769
KIM, HYOUNG MAN N90-10126
KINARD, WILLIAM H. N90-10132
KING, W. E. N90-10252
KIPNIS, SHOLOMO N90-10352
KIPP, MARLIN E. N90-10265
KIRBIE, H. C. N90-10332
KITIPORNCHAI, S. N90-10452
KIZAKEVICH, PAUL N. N90-10528
KLABUNDE, RICHARD N90-10068
KLEIN, VLADISLAV N90-10074
KLEISER, L. N90-10372
KLOOP, R. W. N90-10253
KNAACK, MARCELLE S. N90-10001

KNEE, M. J. N90-10318
KNIER, BARRY L. N90-10651
KNIGHT, DIANE S. N90-10226
KOBAYASHI, T. N90-10253
KOBERSTEIN, JEFFREY T. N90-10277
KOIZUMI, G. N90-10697
KOKIDKO, DAVID N90-10290
KOLB, EDWARD W. N90-10809
KONINCKX, JAN N90-10085
KONRAD, B. A. N90-10463
KONZELMANN, U. N90-10363
KOSS, D. A. N90-10464
KOSTAS, J. G. N90-10342
KOUBA, CARROLL CHARLES N90-10351
KOURTIDES, D. A. N90-10183
KOWALCZYK, R. N90-10429
KRANTZ, R. J. N90-10757
N90-10763
KRATZER, R. H. N90-10209
KREIDER, KENNETH G. N90-10420
KRIEGER, A. S. N90-10799
KRIM, M. S. ABDEL N90-10676
KRINGS, JOHN E. N90-10778
KRIVSKIJ, I. YU. N90-10314
KROEHL, H. W. N90-10490
KROGER, JAMES K. N90-10625
KRONE-SCHMIDT, W. N90-10209
KROTHAPALLI, ANJANEYULU N90-10008
KRUEGER, GERALD P. N90-10530
KUBIAK, GLENN D. N90-10266
KULKARNI, ANIL K. N90-10217
KUMAR, JAYANT N90-10693
N90-10709
KUMAR, R. S. N90-10693
KUMAR, ROMESH N90-10422
KUMAR, SAI S. N90-10693
N90-10709
KUNHARDT, ERICH E. N90-10345
KUNITOMO, NAOTO N90-10654
KUO, HUNG-CHI N90-10596
KUO, T. K. N90-10696
KUPER, RON I. N90-10606
KURRASCH, ELLIE N90-10555
KUSSMAUL, MICHAEL N90-10309
KUZYK, M. G. N90-10703
KWIECINSKI, JAMES ROBERT N90-10351
KWON, JIN H. N90-10163

L

LABEGORRE, B. N90-10203
LABIAK, W. G. N90-10428
LABOV, S. N90-10423
LACONTI, ANTHONY B. N90-10348
LADDEN, R. M. N90-10043
N90-10044
LAGUNAS-SOLAR, M. N90-10698
LAHTI, PAUL M. N90-10648
LAM, S. S. W. N90-10599
LANAGAN, M. T. N90-10180
LANE, M. T. N90-10078
LANGHORNE, P. J. N90-10201
LANNING, DAVID T. N90-10602
LARIMER, JAMES N90-10556
N90-10557
LARKIN, A. I. N90-10741
LARSON, D. W. N90-10428
LARSON, KEVIN P. N90-10325
LASKIN, ROBERT A. N90-10082
LAUGHLIN, PATRICK R. N90-10780
LAUNDER, B. E. N90-10381
LAVERDANT, A. N90-10203
LAWSON, J. K. N90-10428
LEBARON, B. A. N90-10485
LECOURT, RENAUD N90-10196
LECUYER, PIERRE N90-10652
LEE, C. T. N90-10294
LEE, CHIA-FON N90-10218
LEE, DING N90-10517
LEE, IN N90-10042
LEE, JA H. N90-10162
LEE, MICHELLE K. N90-10353
LEE, R. W. N90-10428
LEE, S. Y. N90-10689
LEHMANN, G. N90-10065
LEHMANN, M. S. N90-10751
LEIGHTON, K. S. N90-10331
LEINWAND, SANY N90-10617
LEISERSON, CHARLES E. N90-10352
LEISHMAN, D. K. N90-10043
N90-10044
LEOUTSAKOS, G. N90-10365
LESIEUR, MARCEL N90-10383
LESSER, VICTOR N90-10621
LESSNER, PHILIP N90-10348
LEU, HONGI J. N90-10736
LEU, LII-YUH N90-10661
N90-10662
N90-10663
LEUNG, C. H. N90-10696
LEVINE, STANLEY R. N90-10188
LEVUSH, B. N90-10425
LEWIS, J. S. N90-10194
LEWIS, WILLIAM D. N90-10025
LI, AIZHEN N90-10769
LI, FEIYUE N90-10110
LI, MIAO N90-10771
LI, S. N90-10684
LI, WANN-QUAN N90-10724
LI, YAO N90-10330
LIANG, TACHEN N90-10660
N90-10661
N90-10662
LIEN, MARY M. N90-10295
LIESNER, CH. N90-10242
LILIENTAL-WEBER, ZUZANNA N90-10752
N90-10753
LIM, S. S. N90-10120
LIN, JIGUAN GENE N90-10083
LIN, KUAN-CHAN N90-10439
LIN, SHU N90-10317
LIN, TRUE-LON N90-10329
LINDSAY, RICHARD W. N90-10469
LINHARDT, P. N90-10210
LITTLE, BRENDA J. N90-10225
LITTLER, CHRIS L. N90-10694
LIVINGSTONE, S. D. N90-10529
LOGAN, A. L. N90-10014
LOMMASSON, T. C. N90-10474
LONG, E. L., JR. N90-10264
LONGO, FREDERICK R. N90-10651
LOOMIS, P. V. W. N90-10021
LOSIER, PAUL W. N90-10025
LOU, DINGJUN N90-10642
LOUGE, M. N90-10392
LOUIS, J.-F. N90-10488
N90-10504
LOUNDAGIN, J. A. N90-10199
LOURENCO, LUIZ N90-10008
LOUTFY, R. O. N90-10294
LOVE, S. T. N90-10696
LOWSON, MARTIN V. N90-10367
LUCID, S. W. N90-10077
LUFT, PETER A. N90-10594
LUGER, B. N90-10754
LUGT, HANS J. N90-10404
LYMAN, V. N90-10011
LYNCH, NANCY A. N90-10604

M

MACKAY, W. W. N90-10728
MADAY, YVON N90-10631
MADHUKAR, A. N90-10758
MADSEN, BROOKS C. N90-10478
MAGLIOZZI, BERNARD N90-10683
MAHAJAN, SWADESH M. N90-10724
MAINZER, I. N90-10614
MALENSEK, A. N90-10697
MALIK, MUJEEB R. N90-10359
N90-10366
MALKUS, DAVID S. N90-10405
MAN, GUY K. N90-10082
MANDLER, MARC B. N90-10484
MANGALAM, SIVA M. N90-10364
N90-10368
MANHEIMER, WALLACE M. N90-10148
N90-10425
MANNANT, J. P. N90-10238
MANOHAR, M. N90-10558
MAPHET, THOMAS ALLEN N90-10351
MARACAS, GEORGE N. N90-10765
MARCHAND, ALAN P. N90-10304
MAREZIO, M. N90-10751
MARGETSON, J. N90-10453
MARIANI, DANIELE N90-10627
MARIANO, STEPHEN A. N90-10290
MARICLE, D. L. N90-10472
MARIELLA, RAYMOND P., JR. N90-10752
MARKS, J. N90-10269
MARLAND, G. N90-10482
MAROLO, SAMUEL A. N90-10024
MARQUIS, MARGARET A. N90-10779
MARSHALL, E. M. N90-10479
MARTEL, CHARLES R. N90-10303
MARTIN, C. N90-10423
MARTIN, GARY L. N90-10814
MARTIN, S. F. N90-10804
MARTONOSI, MARGARET N90-10615
MARXEN, AENEAS N90-10600
MASON, B. L. N90-10706
MASTORAKOS, E. N90-10392
MASUYA, GORO N90-10035
MATSAS, G. E. A. N90-10770
MATTESON, L. T. N90-10533
MAYO, S. E. N90-10428
MAZZUCA, S. N90-10064
N90-10072
N90-10073
MCCABRIA, JACK LEE N90-10351
MCCARTHY, DAVID R. N90-10522
MCCARTNEY, MICHAEL L. N90-10528
MCCONAGHY, CHARLES F. N90-10344
MCCORMICK, LARRY D. N90-10328
MCENROE, FRANK J. N90-10267
MCGHEE, ROBERT J. N90-10002
MCGRAIN, MOIRA N90-10272
MCGUIRE, M. N90-10180
MCHARGUE, C. J. N90-10274
MCINTOSH, S. C., JR. N90-10058
MCKENNEY, BARBARA L. N90-10272
MCKENZIE, CRAIG R. N90-10779
MCKINNEY, WAYNE R. N90-10704
MCKINNEY, WILLIAM S., JR. N90-10618
MCKINNON, JOHN A. N90-10817
N90-10818
N90-10819
MCKONE, THOMAS E. N90-10525
MCMANIS, GEORGE E. N90-10220
N90-10690
N90-10691
N90-10692
MEADOR, W. E. N90-10157
MEHTA, J. M. N90-10195
MELNGAILIS, JOHN N90-10767
MELTON, JOHN E. N90-10006
MENDENHALL, MICHAEL R. N90-10057
MENON, SURESH N90-10202
MEOLA, JOSEPH E. N90-10737
MERKERT, JON N90-10177
MEROLA, JOHN A. N90-10465
MESEGUER, JOSE N90-10617
METCALFE, RALPH W. N90-10218
MEYER, F. N90-10372
MICHAELIS, K. N90-10449
MICHALSKY, J. J. N90-10485
MICHEL, FREDERICK J. N90-10607
MICHELANGELI, DIANE VERA N90-10477
MICKELSON, M. N90-10488
N90-10504
MIDDLETON, DAVID N90-10581
MIKULAS, MARTIN M., JR. N90-10127
N90-10153
MILDICE, J. W. N90-10175
MILLBACH, MILES A. N90-10484
MILLER, CAROLINE J. N90-10783
MILLER, ISRAEL R. N90-10222
MILLER, WILLARD, JR. N90-10657
MILLS, BARBARA N90-10563
MILNES, A. G. N90-10769
MILROY, R. N90-10721
MINER, G. A. N90-10157
MINH, H. HA N90-10375
MINTO, K. D. N90-10118
MIRELS, HAROLD N90-10432
N90-10434
MIRTICH, MICHAEL J. N90-10309
MITCHELL, JAMES THOMAS N90-10351
MITCHELL, WAYNE R. N90-10306
MITTER, SANJOY K. N90-10671
MIURA, HIROKAZU N90-10042
MOHAGHEGHI, A. H. N90-10688
MOLLEY, PERRY A. N90-10705
MONK, DONALD L. N90-10573
MONNOYER, F. N90-10378
MONTA, WILLIAM J. N90-10062
MONTGOMERY, RAYMOND C. N90-10102
MOODENBAUGH, A. R. N90-10745
MOORE, C. N90-10697
MOORE, JOHN W. N90-10534
MORELL, LARRY J. N90-10588
MORGAN, HARRY L., JR. N90-10002
MORI, SHOZO N90-10540
MOROSIN, B. N90-10751
MORRIS, J. W., JR. N90-10440
MORRIS, PETER B. N90-10322
MORRIS, SHELBY J., JR. N90-10034
MORRIS, W. L. N90-10255
MORROW, CASEY N90-10280
MOSES, J. DANIEL N90-10796
N90-10800
N90-10801
N90-10803
N90-10804
MOSIER, GARY E. N90-10438
MOYER, SETH A. N90-10006

MPITSOS, GEORGE J. N90-10612
MUDGE, TREVOR N. N90-10584
MUELLER, B. N90-10369
MUKHOPADHYAY, V. N90-10111
MULLIGAN, JEFFREY B. N90-10542
N90-10559
MUNQUR, P. N90-10195
MURCHISON, STUART B. N90-10466
MURPHY, J. L. N90-10444
MURPHY, MARGUERITE C. N90-10595
MUYSHONDT, G. P. N90-10173
MYERS, CRAIG W. N90-10286
MYERS, IRA T. N90-10166

N

NABITY, J. A. N90-10199
NAGATA, JOHN I. N90-10025
NAGAYASU, MASAHIKO N90-10586
NAGEL, J. M. N90-10077
NAGLE, DAVID P., JR. N90-10522
NAKAHARA, J. H. N90-10209
NAKAJIMA, TOSHIKI N90-10354
NAKAMURA, MASAYOSHI N90-10003
NAKAZAWA, SHOHEI N90-10450
N90-10451
NAMASTET, Y. M. N90-10733
NAOI, KATSUHIKO N90-10295
N90-10299
NATARAJAN, B. K. N90-10574
N90-10624
NATISHAN, M. E. N90-10256
NAVEH, NAVA N90-10526
NAVINCHANDRA, D. N90-10311
NAYAR, SHREE K. N90-10710
NEHRKORN, T. N90-10488
N90-10504
NELSON, GORDON L. N90-10282
NESBITT, JAMES A. N90-10188
NETTERFIELD, C. B. N90-10706
NEWTON, M. A. N90-10332
NG, CHUNG FAI N90-10681
NGO, HUY X. N90-10563
NGUYEN, AN H. N90-10563
NGUYEN, N. V. N90-10305
NIELSEN, JACK N. N90-10051
NIELSEN, RUTH N90-10541
NIELSON, ROGER M. N90-10177
N90-10220
N90-10691
N90-10692
NIEMCZYK, MARK P. N90-10735
NOHEL, JOHN A. N90-10405
N90-10406
N90-10407
NOID, D. W. N90-10275
NOLAN, R. W. N90-10529
NOLL, THOMAS N90-10111
N90-10119
NORBERG, R. E. N90-10734
NORMAN, ARLAN D. N90-10279
NORMAND, XAVIER N90-10383
NORRIS, JAMES R. N90-10687
NOVICK, R. N90-10423
NOWITZKY, A. M. N90-10128
NUSBAUM, HOWARD C. N90-10539

O

OBENDORF, S. KAY N90-10733
OCHOA, ELLEN N90-10560
OCHS, G. R. N90-10355
ODELL, M. S. N90-10300
ODEN, J. TINSLEY N90-10655
ODONNELL, R. E. N90-10249
OFER, DAVID N90-10213
OHARA, G. P. N90-10463
OHERN, M. E. N90-10274
OHNUMA, S. N90-10728
OHRING, SAMUEL N90-10404
OKADA, S. N90-10721
OKAMOTO, Y. N90-10292
OKKEMA, ANN Z. N90-10287
OLIVE, DAN F. N90-10168
OLOUGHLIN, M. J. N90-10763
OLSEN, D. N90-10597
OLSHAUSEN, BRUNO N90-10554
OLSON, D. L. N90-10258
ONEIL-ROOD, NORA N90-10610
ONSAGER, TERRANCE GEORGE N90-10486
OPPENHEIM, IRVING J. N90-10104
ORAN, ELAINE S. N90-10206
N90-10395
ORVIS, WILLIAM J. N90-10344
OSAKA, TETSUYA N90-10299
N90-10354
OTOOLE, JAMES W. N90-10605
OUTKA, DUANE A. N90-10266
OUTLAW, R. A. N90-10412
OWENS, BOONE B. N90-10350
N90-10354

P

PACIOREK, K. J. N90-10209
PAISLEY, MICHAEL J. N90-10760
PALMER, CHRISTOPHER N90-10704
PALMER, RICHARD L. N90-10326
PANDEY, L. N. N90-10764
PANDOLF, KENT B. N90-10523
PAPPERT, R. A. N90-10324
PARADA, L. O. N90-10108
PARAZZOLI, C. G. N90-10430
PARMER, DAVID L. N90-10306
PARROTT, TONY L. N90-10680
PARRY, DIANE B. N90-10223
N90-10224
PARZEN, EMANUEL N90-10673
PARZYCH, DAVID N90-10683
PASSMAN, JAMES A. N90-10169
PASSMAN, STEPHEN L. N90-10389
PATERA, ANTHONY T. N90-10631
PATTEN, W. N. N90-10121
PATTON, A. D. N90-10166
PAULSON, MERLE R. N90-10711
PEARCE, ROBERT P. N90-10508
PEEL, C. J. N90-10235
PEGO, ROBERT L. N90-10406
N90-10407
PENG, Y.-K. M. N90-10716
PENNOCK, A. P. N90-10011
PERERA, A. G. U. N90-10546
PEREZ, R. N90-10485
PERKINS, STANLEY C., JR. N90-10057
PERRY, BOYD N90-10119
PETIT, SERGE N90-10061
PETROVICK, MATHEW L. N90-10528
PETZOLD, LINDA R. N90-10632
PEYGHAMBARIAN, N. N90-10766
PHILIP, A. M. N90-10440
PHILLIPS, TIMOTHY N. N90-10637
PIACENTINI, B. N90-10064
PIANTANIDA, THOMAS N90-10556
PICONE, J. M. N90-10644
N90-10725
PIENKOWSKI, THOMAS N90-10180
PIERPONT, D. N90-10121
PIN, F. G. N90-10443
PIRCHNER, RICHARD N90-10601
PIROLLI, PETER N90-10786
PIRZADEH, SHAHYAR N90-10005
PITTS, W. C. N90-10183
PLENTOVICH, ELIZABETH B. N90-10062
PLOHR, BRADLEY J. N90-10405
PLUMMER, MICHAEL D. N90-10642
N90-10643
POEPPEL, R. B. N90-10180
POLITANO, MICHAEL JAMES N90-10810
POLSTORFF, WALTER N90-10310
PORTNOY, W. M. N90-10173
POSAKONY, G. J. N90-10343
POSTON, P. E. N90-10865
POTOTZKY, A. N90-10111
POTTER, ANDREW E., JR. N90-10795
POUCH, JOHN J. N90-10738
PRASAD, K. U. N90-10280
PRATT, LAWRENCE N90-10467
PRECLIK, D. N90-10197
PRESTON, S. B. N90-10305
PRICE, JAMES M. N90-10518
PROBST, HUBERT B. N90-10188
PROFFITT, DENNIS R. N90-10553

Q

QUICK, C. R. N90-10688
QUIGLEY, ENNIS F. N90-10461
QUINN, JARUS W. N90-10427

R

RAFANELLI, G. L. N90-10430
RAJ, R. N90-10272
RAMAPRIYAN, H. K. N90-10558
RAMASWAMY, R. N90-10311
RAMBONE, JAMES D. N90-10019
RAMPALLI, RAJIV N90-10091
RANDALL, R. S. N90-10059
RANGANATH, HEGGERE S. N90-10124
RANSOM, JONATHAN B. N90-10456
RASH, CLARENCE E. N90-10028
RATHER, JOHN D. G. N90-10142
RATTAN, KULDIP S. N90-10445
RAUGH, MIKE N90-10561
RAYNER, S. N90-10482
REARDON, FREDERICK H. N90-10204
RECELY, F. N90-10804
REED, HELEN L. N90-10357
REEDER, R. A. N90-10688
REID, MAX N90-10560
REINHARDT, T. N90-10613
REINHOLTZ, C. F. N90-10122
REISMAN, A. N90-10278
RENLUND, ANITA M. N90-10431
REUCROFT, P. J. N90-10208
REUTER, ROBERT C., JR. N90-10337
N90-10338
REYNOLDS, ROBERT C. N90-10795
RICHERSON, D. W. N90-10272
RICHTER, KAREN J. N90-10607
RIEHR, GLEN A. N90-10170
RILEY, MICHAEL F. N90-10409
RINO, CHARLES L. N90-10327
RIST, U. N90-10363
RITTER, J. C. N90-10247
RIVERA, THOMAS N90-10301
RIVERS, T. N90-10614
ROBERT, MICHEL N90-10233
ROBERTSHAW, H. H. N90-10121
N90-10122
ROBERTSON, DAVID D. N90-10006
ROBERTSON, R. E. N90-10269
ROBINSON, J. T. N90-10443
ROBINSON, MARK T. N90-10699
ROCKETT, A. N90-10474
ROCO, M. C. N90-10394
RODRIGUEZ, F. N90-10733
ROGERS, W. H. N90-10014
ROHLEDER, D. R. N90-10495
ROLEK, EVAN P. N90-10573
ROLPH, GLENN D. N90-10500
RON, AMOS N90-10648
RONQUIST, EINAR M. N90-10631
ROOS, F. W. N90-10379
ROSEN, R. S. N90-10252
ROSENBLATT, DAVID H. N90-10306
ROSENBLATT, GERD M. N90-10219
ROSS, DAVID W. N90-10724
ROSSON, RITA M. N90-10494
ROTEM, DORON N90-10595
ROY, DANIEL M. N90-10583
RUBINSTEIN, ASHER A. N90-10455
RUNCHAL, A. K. N90-10398
RUTH, MICHAEL J. N90-10088
RYAN, ROBERT R. N90-10094

S

SACCOCCIA, GIORGIO N90-10773
N90-10774
SAGAR, B. N90-10398
SAHU, D. N90-10731
N90-10764
SALERNO, J. P. N90-10729
SALERNO, R. J. N90-10122
SALISBURY, KENNETH N90-10416
SAMUELSEN, L. A. N90-10292
SAMUELSON, L. A. N90-10693
SANCES, ANTHONY, JR. N90-10527
SANCHO, MICHEL N90-10234
SANDBERG, V. D. N90-10333
SANDERS, WILLIAM A. N90-10188
SANKARAN, S. N. N90-10248
SANS, C. N90-10198
SARANGAPANI, S. N90-10348
SARAVANOS, D. A. N90-10185
SARIC, WILLIAM S. N90-10357
SASA, SHUICHI N90-10586
SAWKA, MICHAEL N. N90-10523
SAWYER, WALLACE C. N90-10062
N90-10063
SCAVULLO, M. A. N90-10483
SCHADOW, K. C. N90-10205
SCHAILEY, R. N90-10697
SCHENKER, PAUL S. N90-10562
SCHIFFER, M. N90-10687
SCHILLING, H. N90-10065
SCHILLING, M. L. N90-10703
SCHIRBER, J. E. N90-10751
SCHLESINGER, T. E. N90-10769
SCHLOTTMANN, PEDRO N90-10743
SCHMIDT, DAVID K. N90-10112
SCHRAG, R. L. N90-10031

SCHRAMM, DAVID N. N90-10809
SCHRIVER, KAREN A. N90-10788
SCHUELLER, R. N90-10803
SCHULTZ, JEROLD M. N90-10189
SCHUSTER, GREGORY L. N90-10157
N90-10167
SCHWEIGER, F. A. N90-10184
SCROGGS, JEFFREY S. N90-10638
SEILER, DAVID G. N90-10694
SEILER, WILLIAM, JR. N90-10424
SELF, MATTHEW N90-10807
SENNETT, MICHAEL S. N90-10190
SEPAHY, D. N90-10071
SERRANO, M. N90-10203
SEWALL, W. G. N90-10368
SHAFFER, S. J. N90-10440
SHANKAR, VIJAYA N90-10012
SHARPE, WILLIAM N., JR. N90-10454
SHAW, DAVID S. N90-10063
SHAW, NANCY J. N90-10186
SHEN, HAYLEY H. N90-10388
SHEPARD, ALLEN W. N90-10602
SHETTER, RICHARD E. N90-10480
SHILLER, PAUL N90-10260
SHIMOYAMA, ISAO N90-10104
SHIOTA, KOH N90-10354
SHIRANE, G. N90-10746
SHOCKEY, D. A. N90-10253
SHOEMAKER, NEIL S. N90-10738
SHREWSBERRY, D. J. N90-10077
SHUBERT, W. K. N90-10495
SHULSKI, A. P. N90-10331
SHULTZ, E. E., JR. N90-10582
SIDI, AVRAM N90-10635
SIEG, ROBERT M. N90-10736
SIEGEL, DAVID N90-10416
SIEGMANN, WILLIAM L. N90-10517
SIEMON, R. N90-10721
SIGMON, THOMAS W. N90-10761
SIKES, C. S. N90-10225
SILK, J. K. N90-10799
SILVER, E. N90-10423
SIMIONIVICI, A. N90-10423
SIMONS, J. W. N90-10253
SIMULIK, V. M. N90-10314
SINGER, FRED S. N90-10132
SINGER, K. D. N90-10703
SITAR, ZLATKO N90-10760
SITZ, JOEL R. N90-10023
SIVASEGARAM, S. N90-10205
SKELTON, ROBERT E. N90-10117
SKLAD, P. S. N90-10274
SKOTHEIM, T. A. N90-10292
SLINEY, HAROLD E. N90-10262
SMITH, P. J. N90-10186
SMITH, W. W. N90-10688
SMYRL, WILLIAM H. N90-10295
N90-10299
SOBECK, CHARLIE N90-10808
SOBERING, J. M. N90-10335
SOBIESZCZANSKI-SOBIESKI, JAROSLAW N90-10308
SOLLNER, T. C. L. G. N90-10762
SOLO, D. N90-10614
SONTAG, EDUARDO D. N90-10619
SPAGNA, P. N90-10197
SPAIN, STEVE N90-10540
SPALART, P. R. N90-10361
SPELT, P. F. N90-10443
SPINWEBER, C. L. N90-10533
STACK, J. P. N90-10368
STAFFON, JEFFREY D. N90-10469
STALKER, K. TERRY N90-10705
STALLINGS, ROBERT L., JR. N90-10062
STANLEY, JOHN E. N90-10132
STANTON, PHILIP L. N90-10431
STARK, LAWRENCE N90-10563
STARKS, MICHAEL W. N90-10669
STEARNS, CARL A. N90-10188
STEELE, RAYMOND D. N90-10301
STEFANSKI, R. N90-10697
STEFFES, PAUL G. N90-10815
STENGER, G. J. N90-10015
STEVENS, GERALD L. N90-10069
STEVENS, N. J. N90-10452
STEVENSON, CHARLES G. N90-10079
STEWART, A. JAMES N90-10678
STEWART, J. E. N90-10688
STEWART, J. M. N90-10471
STIDHAM, CURTIS N90-10309
STIEBER, MICHAEL E. N90-10084
STONER, WILLIAM W. N90-10436
STOTLER, C. L. N90-10037
STOWERS, IRVING F. N90-10251
STRETZ, LAWRENCE A. N90-10301
STRINGFELLOW, G. B. N90-10744
STRONG, J. P. N90-10558
STUFFLE, K. L. N90-10294
STUNDER, BARBARA J. B. N90-10500
STUTTE, L. N90-10697
STUTZ, JOHN N90-10807
SUENAGA, M. N90-10745
SUMPTER, B. G. N90-10275
SUN, K. C. N90-10145
SUNABE, KINYA N90-10334
SUPAN, E. C. N90-10128
SUROWITZ, EUGENE JOSEPH N90-10812
SWANSON, BASIL I. N90-10215
SWENSON, C. A. N90-10728
SWINGLE, JAMES C. N90-10151
SWINNEY, HARRY L. N90-10411
SZEMA, KUO-YEN N90-10012

T

TADIKONDA, S. S. K. N90-10098
TADMOR, EITAN N90-10639
TAKAHASHI, TAKESHI N90-10268
TAKANASHI, SUSUMU N90-10630
TALIEH, H. N90-10474
TAN, CHUNG-I N90-10695
TANG, C. Y. N90-10688
TANIS, F. J. N90-10479
TANNER, JAMES C. N90-10029
TANNER, RALPH S. N90-10522
TANVEER, S. N90-10677
TARRANT, JANICE M. N90-10438
TATTELMAN, PAUL N90-10325
TAUB, RENEE G. N90-10272
TAUER, KENNETH J. N90-10259
TAVENDALE, A. J. N90-10740
TAYLOR, G. JEFFREY N90-10805
TAYLOR, GENE W. N90-10301
TAYLOR, LAWRENCE W., JR. N90-10080
N90-10092
N90-10103
TAYLOR, WILLIAM N90-10807
TENG, TA-LIANG N90-10516
TENNERY, V. J. N90-10264
TEPIKIAN, S. N90-10689
TESSIER-YOUNGS, CLAIRE A. N90-10260
THELIN, BO N90-10487
THIEDE, P. N90-10378
THOMAS, G. N90-10748
THOMAS, MITCHEL E. N90-10505
N90-10506
N90-10507
THOMAS, W. C. N90-10419
THOME, M. N90-10613
THOMPSON, JOE F. N90-10009
THOMPSON, T. N. N90-10333
THOMSON, L. W. N90-10186
THORNHILL, W. N90-10727
THORPE, CHARLES N90-10446
TIGHE, N. J. N90-10272
TITS, ANDRE L. N90-10085
TOLIVAR, A. FERNANDO N90-10082
TOMBOULIAN, SHERRYL N90-10581
TONEY, FRANK N90-10623
TORREY, WALTER L. N90-10232
TOWNSEND, JOHN N90-10018
TRAN, C. B. N90-10115
TRANGENSTEIN, JOHN A. N90-10384
TRIPATHY, SUKANT K. N90-10292
N90-10693
N90-10709
TRIPP, BRUCE W. N90-10510
TROTT, WAYNE M. N90-10431
TRUJILLO, JOHANN N90-10344
TRZECIAKOWSKI, W. N90-10731
TURNBALL, JOE N90-10100
TURNBERG, J. E. N90-10043
N90-10044
TURNER, MICHAEL S. N90-10809
TUSZEWSKI, M. N90-10721
TUTTLE, MARK R. N90-10604
TZAVARAS, ATHANASIOS E. N90-10406
N90-10407

U

UEYAMA, KEN-ICHI N90-10299
UHLMANN, J. N90-10644
ULSOY, A. GALIP N90-10097
N90-10113
UNDERWOOD, J. H. N90-10463
UNTERLEITNER, F. C. N90-10707
URRY, DAN W. N90-10280

V

VALERI, C. ROBERT N90-10523
VANBAALEN, JEFFREY N90-10670
VANDENBERG, B. N90-10380
VANDERVOORT, R. J. N90-10095
VANDERZIEL, A. N90-10730
VANDOMMELEN, LEON N90-10008
VANHOVE, M. A. N90-10230
VANRHEENEN, A. D. N90-10730
VEERAKOOL, VEERA N90-10785
VEIRS, D. KIRK N90-10219
VENNELL, M. ROSS N90-10511
VERDIER, CLAUDE N90-10410
VERONA, ROBERT W. N90-10028
VIDAL, JACQUES J. N90-10075
VINZ, FRANK L. N90-10564
VISSER, SUSAN A. N90-10284
VITERBI, ANDREW J. N90-10664
VOLAKIS, JOHN L. N90-10313
VOLK, KEVIN N90-10807
VOLZ, RICHARD A. N90-10584
VONGERICHTEN, LAUREL N90-10601

W

WACHTMAN, J. B., JR. N90-10272
WAINAUSKI, HAROLD S. N90-10045
WAKAMATSU, YOSHIO N90-10035
WALDEN, BARBARA L. N90-10291
WALEH, NAHID S. N90-10521
WALJESKI, K. N90-10803
WALKER, G. H. N90-10156
N90-10157
WALKER, HELEN N90-10807
WALKER, S. N. N90-10473
WALLACE, RICHARD W. N90-10433
WALLIS, GRAHAM B. N90-10387
WALLS, JOHN E. N90-10019
WALTERS, M. N90-10278
WANDELL, BRIAN A. N90-10565
WANG, DAILIN N90-10518
WANG, KUO CHIH N90-10397
WANG, LI-SHENG N90-10085
WANG, PAUL P. N90-10656
WANG, X. Q. N90-10418
WARNER, JOSEPH D. N90-10737
WASHBURN, ALAN R. N90-10629
WASIELEWSKI, MICHAEL R. N90-10735
WATSON, ANDREW B. N90-10542
N90-10566
N90-10567
WEAVER, JAMES C. N90-10520
WEAVER, MICHAEL J. N90-10177
N90-10220
N90-10690
N90-10691
N90-10692
WEAVER, WILLARD N90-10167
WEBB, D. F. N90-10800
N90-10802
N90-10804
WEBB, JAMES RAYMOND N90-10806
WEBER, T. L. N90-10473
WEBER, WOLF-DETRICH N90-10616
WEBSTER, R. N90-10721
WEIHL, WILLIAM E. N90-10603
WEIMAN, CARL F. N90-10626
WEIMER, WAYNE A. N90-10268
WEISBIN, C. R. N90-10443
WEISSKOPF, M. N90-10423
WELCH, SHARON S. N90-10102
WELLS, CHESTER V. N90-10421
WELLS, N. D. N90-10318
WEST, B. S. N90-10015
WESTROM, GEORGE N90-10568
WHALEN, THOMAS J. N90-10293
WHEELER, A. P. N90-10225
WHITAKER, ANN F. N90-10717
WHITBY, DAVID G. N90-10010
WHITE, C. W. N90-10274
WHITE, R. C. N90-10754
WHITE, W. T., III N90-10739
WHITE, WILLIAM B. N90-10226
N90-10291
WHITELAW, J. H. N90-10205
WHITFIELD, DAVID L. N90-10009
WHITTAKER, J. W. N90-10444
WIEDEMANN, K. E. N90-10248
WILCOX, FLOYD J., JR. N90-10062
WILKE, RANDALL W. N90-10583
WILLIAM, V. N90-10766
WILLIAMS, M. D. N90-10156
N90-10157

WILLIAMSON, DARRELL N90-10117
WILLINGHAM, CHARLES B. N90-10298
WILLIS, PAUL B. N90-10261
WILSON, R. D. N90-10186
WILSON, R. E. N90-10473
WINKLER, TIMOTHY N90-10617
WINTER, H. N90-10449
WITHERS, J. C. N90-10294
WLEZIEN, R. W. N90-10379
WOEHLER, KARLHEINZ E. N90-10613
WOLF, JACK K. N90-10664
WOLK, G. L. N90-10703
WONG, A. L. N90-10665
WONG, A. Y. N90-10722
WONG, D. N90-10769
WONG, YUE MIN N90-10627
WOOD, H. JOHN N90-10569
WOOLF, BEVERLY N90-10621
WOOLSEY, PATRICK N90-10290
WORTMAN, JIM J. N90-10132
WOYNA, MARK A. N90-10591
WRIGHT, B. N90-10721
WRIGHTON, MARK S. N90-10213
N90-10732
WROBLEWSKI, MICHAEL R. N90-10484
WU, HENRY M. N90-10578
N90-10579
WUNDERLICH, B. N90-10275
WUNSCH, P. K. N90-10129
WYNN, R. H. N90-10121

X

XU, SENLIN N90-10633
XU, YOUWEN N90-10745

Y

YANAGIHARA, MASAAKI N90-10586
YANG, X. Q. N90-10292
YANO, Y. N90-10698
YAREMA, R. J. N90-10747
YEE, JICK H. N90-10344
YEH, PEN-SHU N90-10570
YOKEL, S. A. N90-10037
YORKE, JAMES A. N90-10772
YORTSOS, YANIS C. N90-10399
YOUNG, ANDREW J. N90-10523
YOUNG, CHRISTOPHER J. N90-10025
YOUNG, L. N90-10429
YOUNGS, WILEY J. N90-10260
YU, PAUL L. N90-10349
YU, XUE-HAI N90-10285
N90-10287
YUST, CHARLES S. N90-10750

Z

ZAPLATYNSKY, ISIDOR N90-10718
ZAPOTOSKY, J. E. N90-10321
ZARATE, EUGENE A. N90-10260
ZEIGLER, JOHN M. N90-10266
ZENG, YUEHUA N90-10516
ZEUMER, N. N90-10241
ZHAO, J. H. N90-10769
ZHOU, ZHULIN N90-10289
ZIERKE, WILLIAM C. N90-10038
N90-10039
ZIETLOW, T. C. N90-10757
ZIMMERMAN, D. N90-10077
ZIRIN, H. N90-10804
ZOU, CHAOFENG N90-10213
ZULIANI, D. J. N90-10245
ZUMWALT, G. W. N90-10031
ZUNIGA, M. N90-10644

Typical Corporate Source Index Listing

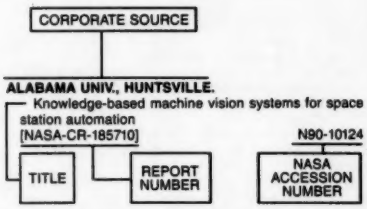

Listings in this index are arranged alphabetically by corporate source. The title of the document provides the user with a brief description of the subject matter. The report number helps to indicate the type of document cited (e.g., NASA report, translation, NASA contractor report). The NASA accession number denotes the number by which the citation is identified. The titles are arranged under each corporate source in ascending accession number order.

A

ACADEMY OF SCIENCES OF THE UKRAINIAN SSR, KIEV.
On canonical quantization of the electromagnetic field in terms of field strengths
[DE89-615389] N90-10314

ADVANCED DECISION SYSTEMS, MOUNTAIN VIEW, CA.
Tracking performance evaluation
[AD-A210499] N90-10540

ADVISORY GROUP FOR AEROSPACE RESEARCH AND DEVELOPMENT, NEUILLY-SUR-SEINE (FRANCE).
Stability and Control of Tactical Missile Systems
[AGARD-CP-451] N90-10050
Combustion Instabilities in Liquid-Fuelled Propulsion Systems
[AGARD-CP-450] N90-10191
Castings Airworthiness
[AGARD-R-762] N90-10231
Fluid Dynamics of Three-Dimensional Turbulent Shear Flows and Transition
[AGARD-CP-438] N90-10356

AERITALIA S.P.A., TURIN (ITALY).
Evaluation of titanium castings for aerospace components N90-10237

AERONAUTICAL RESEARCH LABS., MELBOURNE (AUSTRALIA).
A review of Australian and New Zealand investigations on aeronautical fatigue during the period April 1987 to March 1989
[AD-A210373] N90-10026
Report on an overseas visit, June 1988
[AD-A210374] N90-10040
An appraisal of a number of power assessment procedures being proposed for use in Chinook-Lycoming T55 engine
[AD-A210482] N90-10041
A FORTRAN program for the calculation of the calibration coefficients of a six-component strain gauge balance
[AD-A210375] N90-10599

AERONAUTICAL SYSTEMS DIV., WRIGHT-PATTERSON AFB, OH.
US Air Force certification of castings N90-10232

AEROSPACE CORP., EL SEGUNDO, CA.
Silicon dioxide deposition at 100 deg C using vacuum ultraviolet light
[TR-0088(3945-07)-6] N90-10269
Multiline multimode CW chemical laser performance
[AD-A210613] N90-10432
Coupled multiline CW HF lasers: Experimental performance
[AD-A210844] N90-10434
Master oscillator with power amplifiers: Performance of a two-element CW HF phased-laser array
[AD-A211141] N90-10435
The auroral energy deposition over the polar ionosphere during substorms
[AD-A210522] N90-10490
Bias and oxide thickness dependence of trapped charge buildup in MOS devices
[AD-A210264] N90-10757
High energy neutron irradiation effects in GaAs modulation-Doped Field Effect Transistors (MODFETS): Threshold voltage
[AD-A210502] N90-10763

AIR FORCE ACADEMY, CO.
An introduction to fractals and chaos
[AD-A210257] N90-10675

AIR FORCE GEOPHYSICS LAB., HANSCOM AFB, MA.
Effects of rain attenuation on satellite EHF (Extremely High Frequency) communications in the US
[AD-A210517] N90-10325

AIR FORCE SYSTEMS COMMAND, WRIGHT-PATTERSON AFB, OH.
The high-frequency dielectric properties of glass fibre reinforced plastic and honeycomb layers
[AD-A210581] N90-10289
Properties of F-34 (JP-8) fuel for 1988
[AD-A210188] N90-10303

AIR FORCE WEAPONS LAB., KIRTLAND AFB, NM.
An experimental study of microwave transmission through a decaying plasma
[AD-A210586] N90-10726

AIR FORCE WRIGHT AERONAUTICAL LABS., WRIGHT-PATTERSON AFB, OH.
Missile Datcom: Enhancements for design applications N90-10054
Effects of coherent scattering on infrared absorption in doped semiconductors
[AD-A210224] N90-10756

AIR UNIV., MAXWELL AFB, AL.
The effect of higher education variables on cadet performance during 1987 light aircraft training
[AD-A210199] N90-10536

ALABAMA UNIV., BIRMINGHAM.
Development of elastomeric polypeptide biomaterials
[AD-A210295] N90-10280

ALABAMA UNIV., HUNTSVILLE.
Knowledge-based machine vision systems for space station automation
[NASA-CR-185710] N90-10124
Scaling and modeling of turbulent suspension flows N90-10393

ALBERT EINSTEIN MEDICAL CENTER, PHILADELPHIA, PA.
Synthetic polypeptide composites for sensor applications
[AD-A210797] N90-10296

ALLIED-SIGNAL AEROSPACE CO., KANSAS CITY, MO.
Gaussmeter determination of 302 stainless steel material condition
[BDX-613-3941] N90-10249
Investigation of materials and bonding using the scanning laser acoustic microscope
[KCP-613-4033] N90-10270
Adhesion of encapsulating elastomer to polyolefin sleeve
[BDX-613-3985] N90-10271
Electronic encapsulation using foam with bonded metal covers for a filter pack
[DE89-014010] N90-10276
Characterization of 4/3 technology large-scale integrated circuit on polysilicon processes
[BDX-613-3971] N90-10335
Statistical modeling of electrical components
[BDX-613-3939] N90-10336
A robotic electrical and tensile testing system for diodes
[DE89-014012] N90-10417
High-speed machining of aluminum
[DE89-014011] N90-10441

AMERICAN SCIENCE AND ENGINEERING, INC., CAMBRIDGE, MA.
Solar X-ray Astronomy Sounding Rocket Program
[NASA-CR-183447] N90-10796
Soft X-ray astronomy using grazing incidence optics N90-10797
The detection of soft X-rays with charged coupled detectors N90-10798
The design and evaluation of grazing incidence relay optics N90-10799
X-ray bright points and He I lambda 10830 dark points N90-10802

ANALYTICAL SCIENCES CORP., READING, MA.
Omega system performance assessment
[AD-A210342] N90-10322

APTEK, INC., SCOTTSDALE, AZ.
Scientific and technical report voice activated gun turrent control
[AD-A210350] N90-10623

ARGONNE NATIONAL LAB., IDAHO FALLS, ID.
Experience with model based display for advanced diagnostics and control
[DE89-015693] N90-10469

ARGONNE NATIONAL LAB., IL.
Real-time observations of aerosol composition changes
[DE89-012382] N90-10422
A laser-driven source of polarized hydrogen and deuterium
[DE89-015130] N90-10429
Evaluation of computer-aided software engineering tools for data base development
[DE89-014007] N90-10591
A structural basis for electron transfer in bacterial photosynthesis
[DE89-015702] N90-10687
Controlling photoinduced electron transfer rates in donor-spacer-acceptor molecules by changing the electronic properties of the spacer
[DE89-015128] N90-10735
Ceramic processing of bulk high-T(sub c) superconductors
[DE89-015703] N90-10736

ARIZONA STATE UNIV., TEMPE.
Stability and transition of three-dimensional boundary layers N90-10357
Autonomous control system for Czochralski growth of LEC GaAs
[AD-A210190] N90-10754
Deep traps and sidegating in GaAs devices
[AD-A210740] N90-10765

ARIZONA UNIV., TUCSON.
Femtosecond dynamics of fluoro-aluminum phthal ocyanine and linear alkane molecules
[AD-A210939] N90-10766

ARMY AEROMEDICAL RESEARCH LAB., FORT RUCKER, AL.
Cockpit lighting compatibility with image intensification night imaging systems: Issues and answers
[AD-A210503] N90-10028
Human performance in continuous/sustained operations and the demands of extended work/rest schedules: An annotated bibliography, volume 2
[AD-A210504] N90-10530

ARMY ARMAMENT RESEARCH, DEVELOPMENT AND ENGINEERING CENTER, WATERVLIET, NY.
Stress intensity factors and displacements for arc bend samples using collocation
[AD-A210404] N90-10460

ARMY ARMAMENT RESEARCH AND DEVELOPMENT COMMAND, WATERVLIET, NY.
Fracture and three dimensional stress analyses of 7075 aluminum projectile components under spin and inertia load
[AD-A210986] N90-10463

ARMY AVIATION ENGINEERING FLIGHT ACTIVITY, EDWARDS AFB, CA.
Airworthiness and flight characteristics test of the UH-60A Black Hawk helicopter equipped with the XM-139 multiple mine dispensing system (VOLCANO)
[AD-A210271] N90-10025

ARMY BIOMEDICAL RESEARCH AND DEVELOPMENT LAB., FORT DETRICK, MD.
Organic explosives and related compounds. Environmental and health considerations
[AD-A210554] N90-10306
ARMY LAB. COMMAND, WATERTOWN, MA.
Strain aging in tungsten-heavy alloys
[AD-A211166] N90-10259
Alternative test methodology for ballistic performance ranking of armor ceramics
[AD-A210587] N90-10290
ARMY MATERIALS TECHNOLOGY LAB., WATERTOWN, MA.
Field repair of composite materials in Army service: Planning for the future
[AD-A210732] N90-10190
ARMY MISSILE COMMAND, REDSTONE ARSENAL, AL.
Remarks on certain aspects of solid explosive detonation via small projectile impact
[AD-A210648] N90-10307
ARMY RESEARCH INST. FOR THE BEHAVIORAL AND SOCIAL SCIENCES, ALEXANDRIA, VA.
SINCGARS (Single-Channel Ground/Airborne Radio System) operator performance decay
[AD-A210716] N90-10326
ARMY RESEARCH INST. OF ENVIRONMENTAL MEDICINE, NATICK, MA.
Control of thermoregulatory sweating during exercise in the heat
[AD-A206001] N90-10523
Thermoregulatory responses to intermittent exercise are influenced by knit structure of underwear
[AD-A209087] N90-10541
ARMY TANK-AUTOMOTIVE SYSTEMS DEVELOPMENT CENTER, WARREN, MI.
Robotic vehicle message format
[AD-A210998] N90-10627
ARNOLD ENGINEERING DEVELOPMENT CENTER, ARNOLD AIR FORCE STATION, TN.
Wind tunnel support system effects on a fighter aircraft model at Mach numbers from 0.6 to 2.0
[AD-A210614] N90-10010
ASSISTANT SECRETARY OF THE ARMY (RESEARCH, DEVELOPMENT AND ACQUISITION), WASHINGTON, DC.
Army Science Conference Proceedings (16th) held in Fort Monroe, Virginia on 25-27 October 1988: Addenda
[AD-A210235] N90-10827
ATMOSPHERIC AND ENVIRONMENTAL RESEARCH, INC., CAMBRIDGE, MA.
A study of the impact of simulated satellite lidar wind observations
[AD-A210430] N90-10488
A study of the impact of simulated 183 GHz water vapor retrievals on numerical weather prediction
[AD-A210431] N90-10504
AUSTRALIAN NATIONAL UNIV., CANBERRA.
Optimal q-Markov COVER for finite precision implementation N90-10117
AUSTRALIAN NUCLEAR SCIENCE AND TECHNOLOGY ORGANIZATION, LUCAS HEIGHTS.
Lithium compensation of GaAs
[DE89-616060] N90-10740

B

BALLISTIC RESEARCH LABS., ABERDEEN PROVING GROUND, MD.
EPIC-2 calculated impact loading histories of thin plates
[AD-A210557] N90-10461
Assessing the accuracy of vulnerability models by comparison with vulnerability experiments
[AD-A210871] N90-10669
BATTELLE MEMORIAL INST., COLUMBUS, OH.
Development of the electroacoustic dewatering (EAD) process for fine/ultrafine coal
[DE89-015863] N90-10700
BBN SYSTEMS AND TECHNOLOGIES CORP., CAMBRIDGE, MA.
Tools for application development in heterogeneous distributed environments
[AD-A210236] N90-10613
BELDEN WIRE AND CABLE, GENEVA, IL.
Measuring the shielding effectiveness of superconductive composites
[DE89-015164] N90-10180
BIONETICS CORP., COCOA BEACH, FL.
A simple, mass balance model of carbon flow in a controlled ecological life support system
[NASA-TM-102151] N90-10571
BOEING ADVANCED SYSTEMS CO., SEATTLE, WA.
Compatibility of fuel system components with high density fuel
[AD-A210381] N90-10027
BOEING AEROSPACE CO., SEATTLE, WA.
Linearized flexibility models in multibody dynamics and control N90-10099
Development of pressure containment and damage tolerance technology for composite fuselage structures in large transport aircraft
[NASA-CR-3996] N90-10186
BOEING CO., SEATTLE, WA.
Modeling and control system design and analysis tools for flexible structures N90-10090
Modifying high-order aeroelastic math model of a jet transport using maximum likelihood estimation N90-10106
Controlling flexible structures: A survey of methods N90-10114
Aircraft modal supression system: Existing design approach and its shortcomings N90-10115
High-efficiency CuInSe2 and CuInGaSe2 based cells and materials research
[DE89-009449] N90-10471
BOEING COMMERCIAL AIRPLANE CO., SEATTLE, WA.
Classification and reduction of pilot error
[NASA-CR-181867] N90-10014
Minimum-variance reduced-order estimation algorithms from Pontrygin's minimum principle N90-10105
Structural stability augmentation system design using BODEDIRECT: A quick and accurate approach N90-10116
BRIGHAM YOUNG UNIV., PROVO, UT.
New electrodynamic and electrostatic models with applications to antenna theory, superconductor slots, and lasers N90-10316
Computer simulation of plasma interactions near Titan N90-10816
BRISTOL UNIV. (ENGLAND).
Hierarchical structure in polymeric solids and its influence on properties
[AD-A210918] N90-10297
The three-dimensional vortex sheet structure on delta wings N90-10367
BRITISH AEROSPACE DYNAMICS GROUP, HATFIELD (ENGLAND).
Alternative polar homing strategies N90-10059
Aeroelastic analysis of missile control surfaces with structural non-linearity N90-10071
BRITISH BROADCASTING CORP., LONDON (ENGLAND).
Comparison of DPCM prediction strategies for high-quality digital television bit-rate reduction
[BBC-RD-1989/8] N90-10318
BROOKHAVEN NATIONAL LAB., UPTON, NY.
Polyheterocycle Langmuir-Blodgett films
[AD-A210625] N90-10292
Tangent map analysis of the beam-beam interaction
[DE89-015857] N90-10689
Critical magnetic fields (H(sub c2), H(sub c1)) and kappa in YBa2(Cu0.98M0.02)3O(7+delta), M=Ni, Al, and Cu
[DE89-016412] N90-10745
Magnetic correlations in high T(sub c) oxides in the superconducting state
[DE89-016421] N90-10746
Quantization of anomalous gauge theories on a lattice
[DE89-010247] N90-10776
Lattice fields and strong interactions
[DE89-015099] N90-10777
BROWN UNIV., PROVIDENCE, RI.
Research program in theoretical high energy physics
[DE89-013963] N90-10695
BURTON TECHNOLOGIES, INC., RALEIGH, NC.
Research on ultra low wear materials for energy conservation
[DE89-015096] N90-10263

C

CALIFORNIA INST. OF TECH., PASADENA.
Combustion instabilities in liquid-fueled propulsion systems: An overview N90-10192
Paper 1. Impact of volcanic aerosols on stratospheric chemistry. Paper 2. O2 (1 sigma g +) and O2 (1 delta g) in the H + O2 reaction system. Paper 3. Barotropic instability of zonal jets on Mars, Earth and Venus N90-10477
Applications of parallel supercomputers: Scientific results and computer science lessons
[DE89-016385] N90-10611
CALIFORNIA STATE UNIV., LONG BEACH.
A three-dimensional linear stability approach to transition on wings at incidence N90-10373
CALIFORNIA STATE UNIV., SACRAMENTO.
Very-low-frequency oscillations in liquid-fueled ramjets N90-10204
CALIFORNIA UNIV., BERKELEY.
Reaction of oxygen with allene
[DE89-015219] N90-10216
Micromechanisms of surface friction in zinc electrogalvanized steel sheets
[DE89-011819] N90-10440
Instrumentation and robotic image processing using top-down model control N90-10563
Plasma theory and simulation
[AD-A207952] N90-10714
Scattering of an ICRF magnetosonic wave by plasma density turbulence
[DE89-015223] N90-10720
Motivating the notion of generic design within information processing theory: The design problem space
[AD-A210266] N90-10786
CALIFORNIA UNIV., BERKELEY. LAWRENCE BERKELEY LAB.
Reaction of oxygen with allene
[DE89-015219] N90-10216
Raman characterization of high temperature materials using an imaging detector
[DE89-016308] N90-10219
The structure determination of molecular adsorbates with large unit cells or lattice-gas disorder on metal surfaces
[AD-A210926] N90-10230
Micromechanisms of surface friction in zinc electrogalvanized steel sheets
[DE89-011819] N90-10440
Effective resource utilization for multiprocessor join execution
[DE89-016303] N90-10595
Tellurium-118/antimony-118 generator
[DE89-015225] N90-10698
A symplectic coherent beam-beam model
[DE89-015386] N90-10701
Design of grazing incidence monochromators involving unconventional gratings
[DE89-016341] N90-10704
Scattering of an ICRF magnetosonic wave by plasma density turbulence
[DE89-015223] N90-10720
Atomic imaging and interfacial analysis
[DE89-015339] N90-10748
Characterization of GaAs/Si/GaAs heterointerfaces
[DE89-016302] N90-10752
Methods to decrease defect density in GaAs/Si heteroepitaxy
[DE89-016306] N90-10753
CALIFORNIA UNIV., DAVIS.
Solvent effects on the kinetics of electroreduction of Cu(I) at mercury
[AD-A209423] N90-10211
Potential dependence of the elementary steps in the kinetics of electrode reactions involving amalgam formation
[AD-A209424] N90-10212
CALIFORNIA UNIV., IRVINE.
Bragg crystal polarimeters
[NASA-CR-181331] N90-10423
Biomedical studies with the free electron laser
[AD-A208927] N90-10519
Excitatory amino acids as transmitters in the brain
[AD-A210685] N90-10532
CALIFORNIA UNIV., LOS ANGELES.
Real-time support for high performance aircraft operation
[NASA-CR-185475] N90-10075
On modelling nonlinear damping in distributed parameter systems N90-10109
Monomers, polymers and transition metal complexes based upon carboranes
[AD-A210226] N90-10221
Generation of 3/2 omega sub o radiation in inhomogeneous plasmas under the irradiation of intense electromagnetic waves
[DE89-015723] N90-10722
CALIFORNIA UNIV., SAN DIEGO.
Studies of high power density, pico-second rise-time light activated semiconductor switch
[AD-A210549] N90-10349
CALIFORNIA UNIV., SAN DIEGO, LA JOLLA.
Extrathalamic modulation of cortical function
[AD-A211044] N90-10535
CALIFORNIA UNIV., SANTA BARBARA.
Use of depletion edge translation for high-speed modulation and switching of lightwaves
[AD-A211186] N90-10713
CALSPAN ADVANCED TECHNOLOGY CENTER, BUFFALO, NY.
Numerically efficient algorithm for model development of high-order systems N90-10108
CALSPAN CORP., ARNOLD AFS, TN.
Wind tunnel support system effects on a fighter aircraft model at Mach numbers from 0.6 to 2.0
[AD-A210614] N90-10010

CAMBRIDGE CONSULTANTS LTD., (ENGLAND).
Custom diffraction gratings
[AD-A211002] N90-10712
CAMBRIDGE UNIV. (ENGLAND).
Reheat buzz: An acoustically coupled combustion instability N90-10200
The effect of twins on critical currents of high Tc superconductors
[AD-A210988] N90-10768
CARNEGIE-MELLON UNIV., PITTSBURGH, PA.
Flexible robot control: Modeling and experiments N90-10104
Relating tolerances and kinematic behavior
[AD-A211125] N90-10311
A new approach to control single-link flexible arms. Part 1: Modelling and identification in the presence of joint friction
[AD-A210590] N90-10445
The 1988 year end report for road following at Carnegie-Mellon
[NASA-CR-185967] N90-10446
On learning from exercises
[AD-A210593] N90-10574
Some results on learning
[AD-A210591] N90-10624
Radon transform analysis of a probabilistic method for image generation
[AD-A207814] N90-10702
Surface reflection: Physical and geometrical perspectives
[AD-A210592] N90-10710
Trap gettering by isoelectronic doping of p-GaAs and n-GaAs grown by molecular beam epitaxy
[AD-A211162] N90-10769
Differences in writers initial task representations
[AD-A210433] N90-10788
CASE INST. OF TECH., CLEVELAND, OH.
Bonding in transition metal silyl dimers. Molecular orbital theory
[AD-A208269] N90-10260
CASE WESTERN RESERVE UNIV., CLEVELAND, OH.
Models of mental functioning
[AD-A210456] N90-10538
CENTER FOR NIGHT VISION AND ELECTRO-OPTICS, FORT BELVOIR, VA.
Photoreflectance study of boron ion-implanted (100) cadmium telluride
[SD-TR-88-89] N90-10300
CENTRAL RESEARCH INST. OF ELECTRIC POWER INDUSTRY, TOKYO (JAPAN).
Thermophysical properties of ceramics. Part 2: Development of specific-heat-measurement apparatus at high temperature
[DE89-760382] N90-10268
Development of an expert system supporting short-circuit tests for circuit breakers
[DE89-760384] N90-10334
CENTRE D'ETUDES AERODYNAMIQUES ET THERMIQUES, POITIERS (FRANCE).
Leading edge transition by contamination in hypersonic flow N90-10360
CENTRE NATIONAL DE LA RECHERCHE SCIENTIFIQUE, TOULOUSE (FRANCE).
Numerical solution of three-dimensional unsteady flows: Application to instability problems N90-10375
CENTURY COMPUTING, INC., LAUREL, MD.
Ada (trademark) projects at NASA. Runtime environment issues and recommendations
[NASA-CR-183435] N90-10583
CERAMIC PROCESS SYSTEMS CORP., MILFORD, MA.
Composite ceramic superconducting wires for electric motor applications
[AD-A210345] N90-10346
CERAMPHYSICS, INC., WESTERVILLE, OH.
Capacitive energy storage at cryogenic temperatures, phase 2
[AD-A210366] N90-10347
CHARLES RIVER ANALYTICS, INC., CAMBRIDGE, MA.
Hierarchical damage tolerant controllers for smart structures
[AD-A209422] N90-10022
CHEMICAL RESEARCH AND DEVELOPMENT CENTER, ABERDEEN PROVING GROUND, MD.
Inherent bias in nonlinear least squares analysis of first-order kinetic data
[AD-A210677] N90-10651
CHICAGO UNIV., IL.
Attention and vigilance in speech perception
[AD-A210493] N90-10539
Learning to make decisions: When incentives help and hinder
[AD-A210185] N90-10779
Astrophysical and cosmological constraints to neutrino properties
[NASA-CR-185031] N90-10809
CINCINNATI UNIV., OH.
A composite velocity procedure for the three-dimensional reduced Navier-Stokes equations N90-10396
CITY COLL. OF THE CITY UNIV. OF NEW YORK, NY.
Subpicosecond optical digital computation using conjugate parametric generators
[AD-A207908] N90-10330
CLARKSON UNIV., POTSDAM, NY.
Interpretation and modeling of the averaged equations for a fluid-solid flow N90-10388
COAST GUARD, GROTON, CT.
Atmospheric transmissivity update - 1988
[AD-A209130] N90-10484
COLLEGE OF WILLIAM AND MARY, WILLIAMSBURG, VA.
Safety analysis of knowledge-based systems
[NASA-CR-184784] N90-10588
COLORADO SCHOOL OF MINES, GOLDEN.
Investigation of the pyrometallurgical, physical and mechanical behavior of weld metal
[AD-A211114] N90-10258
COLORADO STATE UNIV., FORT COLLINS.
Monte Carlo simulations of small solute/solvent clusters: Cluster properties and phase transitions
[AD-A209559] N90-10684
COLORADO UNIV., BOULDER.
New polymer precursors to boron and silicon nitrides
[AD-A210287] N90-10279
Effects of stress on judgment and decision making in dynamic tasks
[AD-A210605] N90-10781
COLUMBIA UNIV., NEW YORK, NY.
The development of an expert system for the creative design of mechanisms
[AD-A211115] N90-10628
COMMISSARIAT A L'ENERGIE ATOMIQUE, GRENOBLE (FRANCE).
The generalized drift flux approach: Identification of the void-drift closure law N90-10386
COMMUNICATIONS RESEARCH CENTRE, OTTAWA (ONTARIO).
Flexible structure control experiments using a real-time workstation for computer-aided control engineering N90-10084
COMTEK CO., GRAFTON, VA.
A finite element approach for large motion dynamic analysis of multibody structures in space N90-10093
CONNECTICUT UNIV., STORRS.
Characterization of polymeric surfaces and interfaces
[AD-A210227] N90-10277
CONTROL RESEARCH CORP., LEXINGTON, MA.
Additional software developments wanted for modeling and control of flexible space systems N90-10083
CORNELL UNIV., ITHACA, NY.
Dynamically compressed metals: Theory
[AD-A210741] N90-10257
The role of particle collisions in pneumatic transport N90-10392
Using computer design and simulation to improve manufacturing productivity
[AD-A210338] N90-10598
The architecture of NEWTON: A general-purpose dynamics simulator
[NASA-CR-185489] N90-10678
Negative-working electron beam resist based on poly(methyl methacrylate)
[AD-A207834] N90-10733

D

DARTMOUTH COLL., HANOVER, NH.
Laser propulsion to earth orbit. Has its time come? N90-10143
Two-phase potential flow N90-10387
DAYTON UNIV., OH.
Definition and reduction of the F-18 windshield birdstrike hazard
[AD-A210700] N90-10015
Conference on Aerospace Transparent Materials and Enclosures (15th) 16-20 January 1989. Volume 2: Sessions 6-9
[AD-A210201] N90-10024
Effects of miniature CRT (Cathode Ray Tube) location upon primary and secondary task performances
[AD-A210223] N90-10573
DEFENCE RESEARCH ESTABLISHMENT, OTTAWA (ONTARIO).
Measurement of respiratory air temperatures and calculation of respiratory heat loss when working at various ambient temperatures
[AD-A210378] N90-10529
DEFENCE RESEARCH ESTABLISHMENT SUFFIELD, RALSTON (ALBERTA).
Weeding policy and procedures: Information services
[AD-A210568] N90-10790
DEFENSE LOGISTICS AGENCY, ALEXANDRIA, VA.
Computer availability impact on the archiving of scientific and technical reports
[AD-A210283] N90-10787
DEFENSE TECHNICAL INFORMATION CENTER, ALEXANDRIA, VA.
Defense Technical Information Center cataloging guidelines
[AD-A211000] N90-10792
DELAWARE UNIV., NEWARK.
Failure behavior of PEEK and its short-fiber composite systems
[AD-A210729] N90-10189
DEPARTMENT OF ENERGY, BARTLESVILLE, OK.
Capillary effects in steady-state flow in heterogeneous cores
[DE89-000758] N90-10399
DEPARTMENT OF NATIONAL EDUCATION, PRETORIA (SOUTH AFRICA).
National register of research projects, 1986/87. Part 2B: Natural sciences: Physical, engineering and related sciences (new projects)
[DE89-015033] N90-10826
DETROIT DIESEL ALLISON, INDIANAPOLIS, IN.
Advanced Turbine Technology Applications Project (ATTAP)
[NASA-CR-185133] N90-10036
DEUTSCHE FORSCHUNGS- UND VERSUCHSANSTALT FUER LUFT- UND RAUMFAHRT, GOETTINGEN (GERMANY, F.R.).
Experimental study of instability modes in a three-dimensional boundary layer N90-10369
Primary and secondary stability analysis applied to the DFVLR-transition swept-plate experiment N90-10371
Numerical investigation of transition in 3D boundary layers N90-10372
DIRECTOR, OPERATIONAL TEST AND EVALUATION, WASHINGTON, DC.
Director, Operational Test and Evaluation report FY-88
[AD-A206784] N90-10778
DORNIER-WERKE G.M.B.H., FRIEDRICHSHAFEN (GERMANY, F.R.).
Prediction of dynamic derivatives N90-10055
DRAPER (CHARLES STARK) LAB., INC., CAMBRIDGE, MA.
Simulation of shuttle flight control system structural interaction with RMS deployed payloads N90-10100
DUKE UNIV., DURHAM, NC.
Properties of devices prepared with epitaxial layers on InP
[AD-A210304] N90-10759
DWA COMPOSITE SPECIALITIES, INC., CHATSWORTH, CA.
Space structures concepts and materials
[NASA-CR-183727] N90-10128
DYNACO CORP., DERRY, NH.
Development of a semiquantitative corrosion monitor
[AD-A208132] N90-10414
DYNACS ENGINEERING CO., INC., CLEARWATER, FL.
Efficiency and capabilities of multi-body simulations N90-10095

E

EAGLE ENGINEERING, INC., HOUSTON, TX.
Liquid rocket booster study. Volume 2, book 6, appendix 10: Vehicle systems effects
[NASA-CR-183605] N90-10138
EMMANUEL COLL., BOSTON, MA.
The correspondence between small-scale coronal structures and the evolving solar magnetic field N90-10800
The observation of possible reconnection events in the boundary changes of solar coronal holes N90-10801
ENTE NAZIONALE PER L'ENERGIA ELETTRICA, PISA (ITALY).
Combustion-driven oscillation in large combustion systems for power generation N90-10207
ENVIRONMENTAL RESEARCH INST. OF MICHIGAN, ANN ARBOR.
Spatial characterization of acid rain stress in Canadian Shield Lakes
[NASA-CR-183446] N90-10479

F

FEDERAL AVIATION ADMINISTRATION, ATLANTIC CITY, NJ.
ILS/MLS comparison tests at Miami/Tamiami, Florida Airport
[ACD-330] N90-10018
ILS (Instrument Landing System) mathematical modeling study on the effects of proposed hangar construction west of runway 18R on localizer performance at Dallas-Fort Worth International Airport
[AD-A210631] N90-10019
The addition of Bendix MLS (Microwave Landing System) antenna patterns to MLS mathematical model
[AD-A210633] N90-10020
Phase 2 testing and evaluation of low data rate voice CODEC equipment
[ACD-330-PHASE-2] N90-10315

FERMI NATIONAL ACCELERATOR LAB., BATAVIA, IL.
An algorithm to calculate the beam momentum distribution from flying wire profiles
[DE89-015587] N90-10418
Fermilab fixed target beams from the main injector
[DE89-014355] N90-10697
Performance of the CAMEX64 silicon strip readout chip
[DE89-014015] N90-10747
Astrophysical and cosmological constraints to neutrino properties
[NASA-CR-185031] N90-10809

FLORIDA AGRICULTURAL AND MECHANICAL UNIV., TALLAHASSEE.
Basic studies of the unsteady flow past high angle of attack airfoils
[AD-A210252] N90-10008

FLORIDA UNIV., GAINESVILLE.
Hygrothermal effects on the complex moduli of composite laminates N90-10182
Analysis of nearly simultaneous X-ray and optical observations of active galactic nuclei N90-10606

FLOW RESEARCH, INC., KENT, WA.
Numerical simulation of pressure oscillations in a ramjet combustor N90-10202
Direct numerical simulation of turbulent free shear flows
[AD-A210161] N90-10218
Numerical calculations of the collapse of a cavity in the vicinity of a compliant wall
[AD-A210489] N90-10403

FLUOR DANIEL, INC., IRVINE, CA.
MHD seed recovery and regeneration
[DE89-002711] N90-10715

FLUOROCHEM, INC., AZUSA, CA.
Cubane derivatives for propellant applications
[AD-A210368] N90-10305

FORD MOTOR CO., DEARBORN, MI.
Improved silicon carbide for advanced heat engines
[NASA-CR-180831] N90-10293

G

GENERAL DYNAMICS CORP., SAN DIEGO, CA.
Liquid rocket booster study. Volume 2, book 1
[NASA-CR-183600] N90-10133
Liquid rocket booster study. Volume 2, book 5, appendix 9: LRB alternate applications and evolutionary growth
[NASA-CR-183604] N90-10134
Liquid rocket booster study. Volume 2, book 4, appendices 6-8: Reports of Rocketdyne, Pratt and Whitney, and TRW
[NASA-CR-183603] N90-10135
Liquid rocket booster study. Volume 2, book 2, appendix 1: Trades studies
[NASA-CR-183601] N90-10136
Liquid rocket booster study. Volume 1: Executive summary
[NASA-CR-183599] N90-10137
Liquid rocket booster study. Volume 2, book 6, appendix 10: Vehicle systems effects
[NASA-CR-183605] N90-10138
Liquid rocket booster study. Volume 2, book 3, appendices 2-5: PPIP, transition plan, AMOS plan, and environmental analysis
[NASA-CR-183602] N90-10139
Bidirectional power converter control electronics
[NASA-CR-175070] N90-10175

GENERAL ELECTRIC CO., CINCINNATI, OH.
PMR graphite engine duct development
[NASA-CR-182228] N90-10037
Full scale technology demonstration of a modern counterrotating unducted fan engine concept: Component test
[NASA-CR-180868] N90-10047
Full scale technology demonstration of a modern counterrotating unducted fan engine concept. Design report
[NASA-CR-180867] N90-10048
Full scale technology demonstration of a modern counterrotating unducted fan engine concept. Engine test
[NASA-CR-180869] N90-10049
Revolutionary opportunities for materials and structures study
[NASA-CR-179642] N90-10184
Dynamic instability characteristics of aircraft turbine engine combustors N90-10195

GENERAL ELECTRIC CO., SCHENECTADY, NY.
Input-output oriented computation algorithms for the control of large flexible structures N90-10118

GENERAL SCIENCES CORP., PLYMOUTH MEETING, PA.
New structural materials
[AD-A209425] N90-10246

GEO-CENTERS, INC., NEWTON, MA.
High energy density solid and liquid hydrocarbon fuels
[AD-A210195] N90-10304

GEORGIA INST. OF TECH., ATLANTA.
Automated model formulation for time-varying flexible structures N90-10107
Millimeter-wave/infrared rectenna development at Georgia Tech N90-10147
Active participation in highly automated systems: Turning the wrong stuff into the right stuff
[AD-A210218] N90-10572
Laboratory measurements of microwave and millimeter-wave properties of planetary atmospheric constituents
[NASA-CR-185914] N90-10815

GETTI SPECIALI S.P.A., TORINO (ITALY).
Combined advanced foundry and quality control techniques to enhance reliability of castings for the aerospace industry N90-10240

GINER, INC., WALTHAM, MA.
Advanced double layer capacitor
[AD-A210510] N90-10348

H

HAMILTON STANDARD, WINDSOR LOCKS, CT.
Large scale prop-fan structural design study. Volume 1: Initial concepts
[NASA-CR-174992] N90-10043
Large scale prop-fan structural design study. Volume 2: Preliminary design of SR-7
[NASA-CR-174993] N90-10044
Large-scale Advanced Prop-fan (LAP) high speed wind tunnel test report
[NASA-CR-182125] N90-10045
Large-scale Advanced Prop-fan (LAP) technology assessment report
[NASA-CR-182142] N90-10046
Two stage gear tooth dynamics program
[NASA-CR-185110] N90-10437
Acoustic test and analysis of a counterrotating prop-fan model
[NASA-CR-179590] N90-10683

HAMPTON INST., VA.
Laser energy conversion N90-10152
Laser thruster N90-10164

HARRY DIAMOND LABS., ADELPHI, MD.
Consumer electronics testing to fast-rise EMP (Electromagnetic Pulse) VEMPS (Vertical Electromagnetic Pulse Simulator) 2 development
[AD-A210505] N90-10323

HAWAII UNIV., HONOLULU.
Semi-monthly temperature and geopotential anomaly in the upper 500 meters along the Oahu-Farallon Islands great circle from November 15, 1967 through December 15, 1979
[AD-A210640] N90-10518

HAWAII UNIV., MANOA.
Multi-level bandwidth efficient block modulation codes
[NASA-CR-185484] N90-10317

HEALTH EFFECTS RESEARCH LAB., RESEARCH TRIANGLE PARK, NC.
Human health studies of carbon monoxide (CO) under conditions of military weapons systems crewman exposures. Protocol 1: Formation of COHb
[AD-A210344] N90-10528

HELLENIC AIR FORCE TECHNOLOGY RESEARCH CENTER, ATHENS (GREECE).
Three-dimensional boundary layer transition on a concave surface N90-10365

HI-TEC METALS R AND D LTD., CHANDLER'S FORD (ENGLAND).
Quality control of castings N90-10239

HIGH TECHNOLOGY CORP., HAMPTON, VA.
Curvature effects on the stability of three-dimensional laminar boundary layers N90-10366

HONSEL WERKE A.G., MESCHEDE (GERMANY, F.R.).
The creation of quality: New directions in the production of aeronautics castings N90-10241

HOWARD UNIV., WASHINGTON, DC.
Use of the quasilinearization algorithm for the simulation of LSS slewing N90-10110

HSS, INC., BEDFORD, MA.
A program to improve performance of AFGL (Air Force Geophysical Laboratory) automated present weather observing sensors
[AD-A207669] N90-10495

HUGHES AIRCRAFT CO., EL SEGUNDO, CA.
Stimulated rotational Raman scattering
[DE89-016427] N90-10430

HUNTER COLL., NEW YORK, NY.
Polyheterocycle Langmuir-Blodgett films
[AD-A210625] N90-10292

I

IIT RESEARCH INST., CHICAGO, IL.
ELF (Extremely Low Frequency) Communications System Ecological Monitoring Program: Electromagnetic field measurements and engineering support, 1988
[AD-A210200] N90-10321

ILLINOIS UNIV. AT URBANA-CHAMPAIGN, SAVOY.
Numerical simulations of a midlatitude squall line N90-10497
Theoretical statistics of zero-age cataclysmic variables N90-10810

ILLINOIS UNIV., CHICAGO.
Theory of droplet. Part 1: Renormalized laws of droplet vaporization in non-dilute sprays N90-10390

ILLINOIS UNIV., URBANA.
Alternative fabrication techniques for high-efficiency CuInSe2 and CuInSe2-alloy films and cells
[DE89-009451] N90-10474
A theory of collective induction
[AD-A210553] N90-10780

ILLINOIS UNIV., URBANA-CHAMPAIGN.
Adaptive robust control N90-10620

IMPERIAL COLL. OF SCIENCE AND TECHNOLOGY, LONDON (ENGLAND).
Oscillations in non-axisymmetric dump combustors N90-10205

INSTITUT DE MECANIQUE DE GRENOBLE (FRANCE).
Numerical simulation of coherent structures in an incompressible mixing layer N90-10383

INSTITUT FUER FLUGMECHANIK, BRUNSWICK (GERMANY, F.R.).
Identification of stability and control parameters of a brilliant ammunition N90-10065

INSTITUTE FOR COMPUTER APPLICATIONS IN SCIENCE AND ENGINEERING, HAMPTON, VA.
On the interaction of stationary crossflow vortices and Tollmien-Schlichting waves in the boundary layer on a rotating disc
[NASA-CR-181859] N90-10007
Convection of a pattern of vorticity through a reacting shock wave
[NASA-CR-181921] N90-10576
Evaluating local indirect addressing in SIMD proc essors
[NASA-CR-181845] N90-10581
A high-order Lagrangian-decoupling method for the incompressible Navier-Stokes equations
[NASA-CR-181903] N90-10631
On the coefficients of differentiated expansions of ultraspherical polynomials
[NASA-CR-181913] N90-10637
An iterative method for systems of nonlinear hyperbolic equations
[NASA-CR-181919] N90-10638
Shock capturing by the spectral viscosity method
[NASA-CR-181920] N90-10639
Numerical optimization in Hilbert space using inexact function and gradient evaluations
[NASA-CR-181926] N90-10640
Analytic theory for the selection of Saffman-Taylor fingers in the presence of thin film effects
[NASA-CR-181910] N90-10677

INSTITUTE FOR DEFENSE ANALYSES, ALEXANDRIA, VA.
Aerospace system unified life cycle engineering producibility measurement issues
[AD-A210937] N90-10607

INSTITUTE OF OCEANOGRAPHIC SCIENCES, WORMLEY (ENGLAND).
Evaluation of the North Atlantic seasonal nitrogen model, version 2
[DE89-016157] N90-10515

INTERNATIONAL CENTRE FOR RELATIVISTIC ASTROPHYSICS, ROME (ITALY).
N=1,2 supergravities in 2+1 dimensions as Chern-Simons theories
[DE89-612006] N90-10771
INTERNATIONAL CENTRE FOR THEORETICAL PHYSICS, TRIESTE (ITALY).
Finding isolated zero points of complex polynomial mappings
[DE89-617523] N90-10633
Extended Weyl group for Kac-Moody algebras
[DE89-617525] N90-10634
Energy dependent transport problem with generalized boundary conditions
[DE89-617843] N90-10676
Mott transition: Low-energy excitations and superconductivity
[DE89-617778] N90-10741
N=1,2 supergravities in 2+1 dimensions as Chern-Simons theories
[DE89-612006] N90-10771
D=3 Chern-Simons action, supergravity and quantization
[DE89-617530] N90-10775
INTERNATIONAL FUEL CELLS CORP., SOUTH WINDSOR, CT.
Impact of fundamental technical improvements
[PB89-218010] N90-10472
IOWA STATE UNIV. OF SCIENCE AND TECHNOLOGY, AMES.
Applications of algebraic logic and universal algebra to computer science
[AD-A210556] N90-10645

J

J AND D SCIENTIFIC, INC., MESA, AZ.
Scanning tunneling microscopy etching of micrometer level features on p-type GaAs
[AD-A209216] N90-10328
JET PROPULSION LAB., CALIFORNIA INST. OF TECH., PASADENA.
Computational controls for aerospace systems N90-10082
Predictive aging of polymers
[NASA-CASE-NPO-17524-1-CU] N90-10261
Laterally stacked Schottky diodes for infrared sensor applications
[NASA-CASE-NPO-17426-1-CU] N90-10329
Algorithms and architectures for robot vision N90-10562
Network of dedicated processors for finding lowest-cost map path
[NASA-CASE-NPO-17716-1-CU] N90-10608
JOHNS HOPKINS UNIV., LAUREL, MD.
Flexible missile autopilot design studies with PC-MATLAB/386 N90-10088

K

KAMAN AEROSPACE CORP., ARLINGTON, VA.
Power beaming options N90-10142
KAMAN AEROSPACE CORP., BLOOMFIELD, CT.
DYSCO: A software system for modeling general dynamic systems N90-10089
KAPTRON, INC., PALO ALTO, CA.
Automation of fiber-optic pigtailing process: Laser welding demonstration program
[AD-A210351] N90-10707
KENTUCKY UNIV., LEXINGTON.
Structural and surface characterization of dispersed metal catalysts
[DE89-014530] N90-10208
Turbulence kinetic energy equation for dilute suspensions N90-10394
KIRUNA GEOPHYSICAL INST. (SWEDEN).
Kiruna geophysical data: Data Summary 88/7-9, July - September 1988
[PB89-210249] N90-10487
KOPIN CORP., TAUNTON, MA.
Epitaxial GaAs on SOI wafers
[AD-A209009] N90-10729

L

LAWRENCE LIVERMORE NATIONAL LAB., CA.
Technical options for high average power free electron milimeter-wave and laser devices N90-10151
The response of isotropic brittle materials to abrasive processes
[DE89-016637] N90-10251
Delayed failure of silver-aided diffusion welds between steel
[DE89-016652] N90-10252
Maximization of directed electromagnetic radiation with an optimized antenna
[DE89-014045] N90-10319
Commercial high current ignitron development
[DE89-015077] N90-10331
A battery-powered, solid state magnetic compressor with applications for high PRF accelerators and lasers
[DE89-015770] N90-10332
Micro-cavity integrable vacuum diodes and triodes
[DE89-016649] N90-10344
Analysis of a model and sequential numerical method for thermal reservoir simulation
[DE89-015117] N90-10384
Bragg crystal polarimeters
[NASA-CR-181331] N90-10423
NTES laser facility for physics experiments: Building 381 high bay option
[DE89-014326] N90-10428
Managing human exposure and health risks: An integrated approach and the role of uncertainty
[DE89-008611] N90-10525
Addressing user display requirements from a large and diverse user community
[DE89-011403] N90-10582
Low-cost three-dimensional stereoscopic display technique for computer-aided design
[DE89-011635] N90-10594
Numerical methods for differential-algebraic equations: Current status and future directions
[DE89-015116] N90-10632
Simultaneous multiple frequency interferometry: An application of homodyne phase measurement
[DE89-013975] N90-10719
Generation of 3/2 omega sub o radiation in inhomogeneous plasmas under the irradiation of intense electromagnetic waves
[DE89-015723] N90-10722
Analysis of the performance of gallium arsenide photoavalanche switches
[DE89-015774] N90-10739
Institute of Geophysics and Planetary Physics, 1988
[DE89-014363] N90-10794
LEICESTER UNIV. (ENGLAND).
Bragg crystal polarimeters
[NASA-CR-181331] N90-10423
LIGHTWAVE ELECTRONICS CORP., MOUNTAIN VIEW, CA.
Efficient nonlinear conversion of laser diode pumped miniature solid state laser sources
[AD-A210708] N90-10433
LITTLE (ARTHUR D.), INC., CAMBRIDGE, MA.
Power from space for use on earth: An emerging global option N90-10144
LIVERPOOL UNIV. (ENGLAND).
Online support for the intellectual activity of browsing N90-10784
LOCKHEED-GEORGIA CO., MARIETTA.
Analysis of results from wind tunnel tests of inlets for an advanced turboprop nacelle installation
[NASA-CR-174937] N90-10011
Application of superplastically formed and diffusion bonded aluminum to a laminar flow control leading edge
[NASA-CR-178316] N90-10030
LOCKHEED MISSILES AND SPACE CO., PALO ALTO, CA.
Antenna technology for beamed space-power N90-10149
LOCKHEED MISSILES AND SPACE CO., SUNNYVALE, CA.
Prediction of tactical missile dynamics N90-10056
LOS ALAMOS NATIONAL LAB., NM.
The Spartan 1 mission
[NASA-TM-101887] N90-10077
Chemistry of nitromethane at very high pressure
[DE89-008016] N90-10215
Mechanical properties, solubilities, and processabilities in the design of the first super-strong liquid-crystalline polymers
[DE89-009252] N90-10273
Effects of binder concentration on the properties of plastic-bonded explosives
[DE89-007744] N90-10301
Free-expansion experiments and modeling in detonation: Chemistry and hydrodynamics on a laboratory scale
[DE89-007748] N90-10302
Report on the performance and operating characteristics of the Burle C83061E QUANTACON (trademark) photomultiplier tube
[DE89-015257] N90-10333
Observation of excited H(sup 0) atoms produced by relativistic H(sup (minus)) ions in carbon and formvar foils
[DE89-015301] N90-10688
Multimode fiber interferometry and several-mode fiber polarimetry via phase conjugation
[DE89-014226] N90-10706
Observations of azimuthal asymmetry for certain FRC operating regimes
[DE89-015300] N90-10721
Superconductivity from valence fluctuations with finite U
[DE89-015302] N90-10742
LOWELL UNIV., MA.
Monolayer formation characteristics of novel organic molecules with nonlinear optically active moieties
[AD-A210496] N90-10693
Nonlinear optics and organic materials
[AD-A210570] N90-10709

M

MANCHESTER UNIV. (ENGLAND).
Numerically determined transition in separated internal flow N90-10374
Turbulence modelling of three-dimensional shear flows N90-10381
MARC ANALYSIS RESEARCH CORP., PALO ALTO, CA.
The MHOST finite element program: 3-D inelastic analysis methods for hot section components. Volume 2: User's manual
[NASA-CR-182235-VOL-2] N90-10450
The MHOST finite element program: 3-D inelastic analysis methods for hot section components. Volume 3: Systems' manual
[NASA-CR-182236] N90-10451
MARYLAND UNIV., COLLEGE PARK.
CONSOLE: A CAD tandem for optimization-based design interacting with user-supplied simulators N90-10085
Theoretical investigations of chaotic dynamics
[AD-A207724] N90-10772
MASSACHUSETTS INST. OF TECH., CAMBRIDGE.
Combining spontaneous molecular assembly with microfabrication to pattern surfaces: Selective binding of isonitriles to platinum microwires and characterization by electrochemistry and surface spectroscopy
[AD-A209528] N90-10213
The synthesis and structure of novel antimony thiametallacycles
[AD-A210888] N90-10229
The organization of permutation architectures with bussed interconnections
[AD-A210832] N90-10352
Summarizing qualitative behavior from measurements of nonlinear circuits, revision
[AD-A210919] N90-10353
Analysis and construction of contact and tactile sensors
[DE89-013992] N90-10416
ONR/NORDA Workshop on Terrain Analysis and Quantitative Geomorphology
[AD-A210464] N90-10489
The influence of a steady baroclinic deep ocean on the shelf
[PB89-198188] N90-10511
A search for layering in the oceanic crust
[PB89-198220] N90-10514
Electroporation: Theory of basic mechanisms
[AD-A210196] N90-10520
Performance evaluation of the Scheme86 and HP precision architectures
[AD-A209418] N90-10578
A multiprocessor architecture using modular arithmetic for very high precision computation
[AD-A208154] N90-10579
General decomposition of sequential machines: Relationships to state assignment
[AD-A208189] N90-10580
The impact of recovery on concurrency control
[AD-A210828] N90-10603
An introduction to input/output automata
[AD-A210831] N90-10604
Type reconstruction with first-class polymorphic values
[AD-A210833] N90-10605
Dependency-directed localization of software bugs
[AD-A210837] N90-10606
A special case of second-order strictness analysis
[AD-A210829] N90-10656
Toward a theory of representation design
[AD-A210885] N90-10670
Stochastic quantization
[AD-A210942] N9C-10671
Massachusetts Institute of Technology Plasma Fusion Center
[DE89-016050] N90-10723
Face-specific interaction of MoS4(2-1) with oriented crystals of (0001) CdX (X = Se, S)
[AD-A209519] N90-10732

Progress report on grain boundaries
[DE89-015541] N90-10749
Focused ion beam implantation
[AD-A210977] N90-10767

MASSACHUSETTS INST. OF TECH., LEXINGTON.
On analytic modeling of lunar perturbations of artificial satellites of the earth
[AD-A210440] N90-10078
Tracking performance evaluation
[AD-A210499] N90-10540
Submillimeter quantum electronics
[AD-A210439] N90-10762

MASSACHUSETTS UNIV., AMHERST.
Biological investigations of adaptive networks: Neuronal control of conditioned responses
[AD-A211043] N90-10534
Computational modeling of pi-conjugated polyradicals
[AD-A210573] N90-10648

MATERIALS AND ELECTROCHEMICAL RESEARCH CORP., TUCSON, AZ.
Zirconia toughened SiC whisker reinforced alumina composites small business innovation research
[NASA-CR-179629] N90-10294

MATERIALS RESEARCH LABS., ASCOT VALE (AUSTRALIA).
Numerical simulation of detonation transfer between gaseous explosive layers
[MRL-RR-1-89] N90-10395

MATERIALS RESEARCH LABS., MELBOURNE (AUSTRALIA).
Properties of HY-100 for naval construction
[MRL-R-1149] N90-10247

MCDONNELL-DOUGLAS CORP., LONG BEACH, CA.
Laminar flow control perforated wing panel development
[NASA-CR-178166] N90-10187

MCDONNELL-DOUGLAS CORP., SAINT LOUIS, MO.
The Spartan 1 mission
[NASA-TM-101887] N90-10077

MCDONNELL-DOUGLAS RESEARCH LABS., SAINT LOUIS, MO.
Trailing-edge sweep and three-dimensional vortex interactions in jets and mixing layers N90-10379

MECHANICAL DYNAMICS, INC., ANN ARBOR, MI.
Lumped mass formulations for modeling flexible body systems N90-10091

MEDICAL COLL. OF WISCONSIN, MILWAUKEE.
Biomedical influences on spinal cord function
[AD-A210311] N90-10527

MESSERSCHMITT-BOELKOW-BLOHM G.M.B.H., BREMEN (GERMANY, F.R.).
Castings, from theory to practical application N90-10236

MESSERSCHMITT-BOELKOW-BLOHM G.M.B.H., MUNICH (GERMANY, F.R.).
Prediction of stability derivatives for missiles using the HISSS panel code N90-10053
Validation of missile simulation N90-10066
Marginal release disturbances on advanced missiles N90-10070
Low frequency and high frequency combustion oscillation phenomena inside a rocket combustion chamber fed by liquid or gaseous propellants N90-10197
Turbulence management: Application aspects N90-10378

MESSIER FONDERIE, ARUDY (FRANCE).
The question of the casting factor N90-10238

MGA RESEARCH CORP., AKRON, NY.
Waveform generator signal processing software
[PB89-192660] N90-10587

MIAMI UNIV., OXFORD, OH.
Laser diode array and transmission optics N90-10163

MICHIGAN UNIV., ANN ARBOR.
Enhanced element-specific modal formulations for flexible multibody dynamics N90-10094
Simulation of flexible structures with impact: Experimental validation N90-10097
A performance comparison of integration algorithms in simulating flexible structures N90-10101
Experimental validation of flexible robot arm modeling and control N90-10113
A combined finite element and boundary integral formulation for solution via CGFFT of 2-dimensional scattering problems
[NASA-CR-184781] N90-10313
A common distributed language approach to software integration
[NASA-CR-185499] N90-10584
Studies of elementary particles
[DE89-014859] N90-10685

MICROELECTRONICS CENTER OF NORTH CAROLINA, RESEARCH TRIANGLE PARK.
The effects of normal annealing cycles during IGFET fabrication on initial and radiation induced gate insulator defects
[AD-A210282] N90-10278

MICROTRONICS ASSOCIATES, PITTSBURGH, PA.
Parallel asynchronous hardware implementation of image processing algorithms N90-10546

MIDWEST RESEARCH INST., GOLDEN, CO.
Some significant results from testing a Remote Multiplexing Unit (RMU) for temperature-induced errors
[DE89-009432] N90-10421
Energy storage and distribution program summary. Volume 2: Research summaries, fiscal year 1988
[DE89-000867] N90-10470
High-efficiency CuInSe2 and CuInGaSe2 based cells and materials research
[DE89-009449] N90-10471
Alternative fabrication techniques for high-efficiency CuInSe2 and CuInSe2-alloy films and cells
[DE89-009451] N90-10474
Structure of amorphous silicon alloy films
[DE89-009441] N90-10734

MINNESOTA UNIV., MINNEAPOLIS.
Quartz crystal microbalance studies of electrochemical growth of conducting polymers
[AD-A210788] N90-10295
Impedance analysis of ionic transport in polypyrrole-polyazulene copolymer and its charge-discharge characteristics
[AD-A210979] N90-10299
The use of lithium batteries in biomedical devices
[AD-A210789] N90-10350
Rechargeable lithium/polymer cathode batteries
[AD-A210978] N90-10354
Similarity solutions that give rise to hyperbolicity and change of type in steady flow of a viscoelastic fluid
[AD-A210920] N90-10410
Stochastic control theory, nonlinear structural mechanics and applied combinatorics
[AD-A209042] N90-10657
Quantum 1/F noise in solid state devices in particular Hg1-(sub x)Cd(sub x)Te N(+)-P diodes
[AD-A209365] N90-10730

MISSION RESEARCH CORP., SANTA BARBARA, CA.
Improved propagation models for discrete random media
[AD-A211085] N90-10327

MISSISSIPPI STATE UNIV., MISSISSIPPI STATE.
Computation of transonic flow about stores
[AD-A210402] N90-10009

MISSISSIPPI STATE UNIV., STATE COLLEGE.
Three-dimensional unsteady transonic viscous-inviscid interaction N90-10005

MISSISSIPPI UNIV., UNIVERSITY.
Theoretical and experimental investigation of nonlinear optoacoustics in liquids
[AD-A210427] N90-10708

MISSOURI UNIV., ROLLA.
Studies in penetration mechanics
[AD-A210713] N90-10448
An analytical hierarchy process approach to establish the systems analyst's knowledge base for selecting an information requirements determination strategy N90-10785

MITRE CORP., MCLEAN, VA.
National airspace system approach and departure sequencing operational concept
[NAS-SR-1322] N90-10017

MORTON THIOKOL, BRIGHAM CITY, UT.
Flight set 360T004 (STS-30) insulation component, interim release, volume 3
[NASA-CR-183746] N90-10169
Three-in-one gage
[NASA-CR-183714] N90-10413

N

NATIONAL ACADEMY OF SCIENCES - NATIONAL RESEARCH COUNCIL, WASHINGTON, DC.
Long-term solar-terrestrial observations
[DE89-016318] N90-10825

NATIONAL AERONAUTICS AND SPACE ADMINISTRATION, WASHINGTON, DC.
NASA Voyager 2 Neptune encounter press kit
[NASA-TM-101851] N90-10076
Technology for large space systems: A bibliography with indexes (supplement 21)
[NASA-SP-7046(21)] N90-10130
Space station systems: A bibliography with indexes (supplement 8)
[NASA-SP-7056(08)] N90-10131
Aerospace medicine and biology: A continuing bibliography with indexes (supplement 328)
[NASA-SP-7011(328)] N90-10524
NASA scientific and technical publications: A catalog of special publications, reference publications, conference publications, and technical papers, 1988
[NASA-SP-7063(03)] N90-10782

NATIONAL AERONAUTICS AND SPACE ADMINISTRATION. AMES RESEARCH CENTER, MOFFETT FIELD, CA.
An integrated CFD/experimental analysis of aerodynamic forces and moments
[NASA-TM-102195] N90-10006
Static aeroelastic analysis for generic configuration aircraft
[NASA-TM-89423] N90-10042
The present status and the future of missile aerodynamics N90-10051
Boost-phase discrimination research activities
[NASA-TM-101889] N90-10176
Composite multilayer insulations for thermal protection of aerospace vehicles
[NASA-TM-101071] N90-10183
Direct numerical study of leading-edge contamination N90-10361
Vision Science and Technology at NASA: Results of a Workshop
[NASA-TM-102214] N90-10542
Vision science and technology at NASA: Results of a workshop: Executive summary N90-10543
Sampling and noise in vision networks N90-10544
Networks for image acquisition, processing and display N90-10545
Visions of visualization aids: Design philosophy and experimental results N90-10547
Human motion perception: Higher-order organization N90-10553
Two-dimensional shape recognition using sparse distributed memory N90-10554
Filling in the retinal image N90-10556
A3I visibility modeling project N90-10557
Factors affecting the perception of transparent motion N90-10559
Photonic processing at NASA Ames Research Center N90-10560
Sparse distributed memory overview N90-10561
Ames vision group research overview N90-10566
Pyramid image codes N90-10567
An algorithm for the systematic disturbance of optimal rotational solutions
[NASA-TM-101089] N90-10575
Automatic classification of spectra from the Infrared Astronomical Satellite (IRAS)
[NASA-RP-1217] N90-10807
Astrometric telescope facility. Preliminary systems definition study. Volume 3: Cost estimate
[NASA-TM-89429-VOL-3] N90-10808

NATIONAL AERONAUTICS AND SPACE ADMINISTRATION. GODDARD SPACE FLIGHT CENTER, GREENBELT, MD.
The Spartan 1 mission
[NASA-TM-101887] N90-10077
Computation and parallel implementation for early vision N90-10549
Motion detection in astronomical and ice floe images N90-10558
Space environment robot vision system N90-10569
Self-calibration of robot-sensor system N90-10570

NATIONAL AERONAUTICS AND SPACE ADMINISTRATION. HUGH L. DRYDEN FLIGHT RESEARCH FACILITY, EDWARDS, CA.
Initial flight qualification and operational maintenance of X-29A flight software
[NASA-TM-101703] N90-10023
The aerospace energy systems laboratory: Hardware and software implementation
[NASA-TM-101706] N90-10610

NATIONAL AERONAUTICS AND SPACE ADMINISTRATION. JOHN F. KENNEDY SPACE CENTER, COCOA BEACH, FL.
Debris/ice/TPS assessment and photographic analysis for Shuttle Mission STS-28R
[NASA-TM-102152] N90-10079
Characterization and evaluation of acid rain in East Central Florida from 1978 to 1987: Ten year summary report
[NASA-TM-102149] N90-10478

NATIONAL AERONAUTICS AND SPACE ADMINISTRATION. LYNDON B. JOHNSON SPACE CENTER, HOUSTON, TX.
Office of exploration overview N90-10141
Vision science and technology for supervised intelligent space robots N90-10548
Hybrid vision activities at NASA Johnson Space Center N90-10552

Orbital debris research at NASA Johnson Space Center, 1986-1988
[NASA-TM-102155] N90-10795

NATIONAL AERONAUTICS AND SPACE ADMINISTRATION. LANGLEY RESEARCH CENTER, HAMPTON, VA.

A study of high-lift airfoils at high Reynolds numbers in the Langley low-turbulence pressure tunnel
[NASA-TM-89125] N90-10002
Performance potential of an advanced technology Mach 3 turbojet engine installed on a conceptual high-speed civil transport
[NASA-TM-4144] N90-10034
New test techniques to evaluate near field effects for supersonic store carriage and separation N90-10062
Remote control missile model test N90-10063
Analysis of flight data from a High-Incidence Research Model by system identification methods
[NASA-TP-2940] N90-10074
Proceedings of the Workshop on Computational Aspects in the Control of Flexible Systems, part 1
[NASA-TM-101578-PT-1] N90-10080
NASA'S controls-structures interaction program N90-10081
A comparison of software for the modeling and control of flexible systems N90-10092
Optical processing for distributed sensors in control of flexible spacecraft N90-10102
Proceedings of the Workshop on Computational Aspects in the Control of Flexible Systems, part 2
[NASA-TM-101578-PT-2] N90-10103
Control law synthesis and optimization software for large order aeroservoelastic systems N90-10111
The active flexible wing aeroservoelastic wind-tunnel test program N90-10119
Preliminary design of a large tetrahedral truss/hexagonal heatshield panel aerobrake
[NASA-TM-101612] N90-10127
Method and apparatus for determining time, direction and composition of impacting space particles
[NASA-CASE-LAR-13392-1-CU] N90-10132
Second Beamed Space-Power Workshop
[NASA-CP-3037] N90-10140
Structural concepts for very large (400-meter-diameter) solar concentrators N90-10153
Overview of laser concepts N90-10154
Laser-powered lunar base N90-10156
Laser-powered Martian rover N90-10157
Low-earth-orbit to low-lunar-orbit laser freighter N90-10160
Laser propulsion option N90-10161
Earth orbit laser systems N90-10162
Beamed laser power in support of near-earth missions N90-10167
The interlaminar fracture toughness of woven graphite/epoxy composites
[NASA-TP-2950] N90-10179
Emittance, catalysis, and dynamic oxidation of Ti-14Al-21Nb
[NASA-TP-2955] N90-10248
Approximate simulation model for analysis and optimization in engineering system design
[NASA-TM-101616] N90-10308
Stability of a supersonic boundary layer along a swept leading edge N90-10359
Goertler instability on an airfoil: Comparison of marching solution with experimental observations N90-10364
Simultaneous detection of separation and transition in surface shear layers N90-10368
Application of formal optimization techniques in thermal/structural design of a heat-pipe-cooled panel for a hypersonic vehicle
[NASA-TM-89131] N90-10409
Introduction to total- and partial-pressure measurements in vacuum systems
[NASA-RP-1219] N90-10412
An interferometric strain-displacement measurement system
[NASA-TM-101638] N90-10454
Global/local stress analysis of composite structures
[NASA-TM-101640] N90-10456
Analysis and test of a 16-foot radial rib reflector developmental model
[NASA-TM-101648] N90-10457
The 1984 direct strike lightning data, part 1
[NASA-TM-87690-PT-1] N90-10505
The 1984 direct strike lightning data, part 2
[NASA-TM-87690-PT-2] N90-10506
The 1984 direct strike lightning data, part 3
[NASA-TM-87690-PT-3] N90-10507
Image gathering, coding, and processing: End-to-end optimization for efficient and robust acquisition of visual information N90-10551
Advancing automation and robotics technology for the space station Freedom and for the US economy
[NASA-TM-101561] N90-10577
Documentation of the current fault detection, isolation and reconfiguration software of the AIPS fault-tolerant processor
[NASA-TM-89154] N90-10602
Optimized resolved rate control of seven-degree-of-freedom Laboratory Telerobotic Manipulator (LTM) with application to three-dimensional graphics simulation
[NASA-TP-2938] N90-10618
Measurement resolution of noise directivity patterns from acoustic flight tests
[NASA-TM-4134] N90-10679
Fluctuating pressures measured beneath a high-temperature, turbulent boundary layer on a flat plate at Mach number of 5
[NASA-TP-2947] N90-10680
Conceptual design of a synchronous Mars telecommunications satellite
[NASA-TP-2942] N90-10814

NATIONAL AERONAUTICS AND SPACE ADMINISTRATION. LEWIS RESEARCH CENTER, CLEVELAND, OH.

Overview of microwave concepts N90-10155
Power for the moon: Is microwave power beaming an option? N90-10158
Applicability of the beamed power concept to lunar rovers, construction, mining, explorers and other mobile equipment N90-10159
Microwave beam power N90-10165
Central electrical utility power for a satellite ring city in low earth orbit space N90-10166
A rocket engine design expert system
[NASA-TM-102373] N90-10172
A feasibility assessment of installation, operation and disposal options for nuclear reactor power system concepts for a NASA growth space station
[NASA-TM-89923] N90-10174
Composite Blade Structural Analyzer (COBSTRAN) theoretical/programmer's manual
[NASA-TM-101958] N90-10181
Mechanics of damping for fiber composite laminates including hygro-thermal effects
[NASA-TM-102329] N90-10185
Materials for engine applications above 3000 deg F: An overview
[NASA-TM-100169] N90-10188
Friction and wear of oxide-ceramic sliding against IN-718 nickel base alloy at 25 to 800 C in atmospheric air
[NASA-TM-102291] N90-10262
Total hemispherical emittance measured at high temperatures by the calorimetric method
[NASA-TM-102322] N90-10309
Adjustable depth gage
[NASA-CASE-LEW-14880-1] N90-10415
Quotient-difference type generalizations of the power method and their analysis
[NASA-TM-102361] N90-10635
Application of a hybrid generation/utility assessment heuristic to a class of scheduling problems
[NASA-TM-102367] N90-10674
Plasma gun with coaxial powder feed and adjustable cathode
[NASA-CASE-LEW-14901-1] N90-10718
Study of deposition of YBa2Cu3O7-x on cubic zirconia
[NASA-TM-102350] N90-10737
Optical dispersion relations for diamondlike carbon films
[NASA-TM-102356] N90-10738

NATIONAL AERONAUTICS AND SPACE ADMINISTRATION. MARSHALL SPACE FLIGHT CENTER, HUNTSVILLE, AL.

Electrostatically suspended rotor for angular encoder
[NASA-CASE-MFS-28294-1] N90-10310
Constitutive Relationships and Models in Continuum Theories of Multiphase Flows
[NASA-CP-3047] N90-10385
Computer vision research at Marshall Space Flight Center N90-10564
Method and apparatus for maintaining thermal control in plasma conditions
[NASA-CASE-MFS-28368-1] N90-10717
Advances in photographic X-ray imaging for solar astronomy N90-10803
Correspondence between solar fine-scale structures in the corona, transition region, and lower atmosphere from collaborative observations N90-10804

NATIONAL AERONAUTICS AND SPACE ADMINISTRATION. PASADENA OFFICE, CA.

Predictive aging of polymers
[NASA-CASE-NPO-17524-1-CU] N90-10261
Laterally stacked Schottky diodes for infrared sensor applications
[NASA-CASE-NPO-17426-1-CU] N90-10329
Network of dedicated processors for finding lowest-cost map path
[NASA-CASE-NPO-17716-1-CU] N90-10608

NATIONAL AEROSPACE LAB., AMSTERDAM (NETHERLANDS).

A European collaborative investigation of the three-dimensional turbulent shear layers of a swept wing N90-10380

NATIONAL AEROSPACE LAB., TOKYO (JAPAN).

A numerical method for solving transonic flow past aircraft in Cartesian coordinates
[NAL-TR-1008] N90-10003
Cycle analysis of scramjet engines
[NAL-TR-1002] N90-10035
On the interactive computer program IPIS for aircraft parameter identification
[NAL-TR-1000] N90-10586
Grid generation procedure using the integral equation method
[NAL-TR-1009] N90-10630

NATIONAL CENTER FOR ATMOSPHERIC RESEARCH, BOULDER, CO.

Meeting Review: Workshop on Airborne Instrumentation
[PB89-174775] N90-10032
Study of the NO3 radical decomposition reaction and the N2O5 in equilibrium with NO3 + NO2 equilibrium constant
[PB89-208961] N90-10480

NATIONAL ENVIRONMENTAL SATELLITE SERVICE, WASHINGTON, DC.

Chesapeake Bay surface salinities, 1951-88
[PB89-194583] N90-10513

NATIONAL GEOPHYSICAL DATA CENTER, BOULDER, CO.

Solar-geophysical data number 531, part 2. Data foor May 1988 and miscellaneous
[PB89-139950] N90-10817
Solar-geophysical data number 532, December 1988. Part 1: Data for November, October 1988, and late data
[PB89-152086] N90-10818
Solar-geophysical data number 532, December 1988. Part 2: Data for June 1988 and miscellaneous
[PB89-152094] N90-10819
Solar-geophysical data number 533. Part 1: Data for December, November 1988, and late data
[PB89-162481] N90-10820
Solar-geophysical data number 533. Part 2: Data for July 1988 and miscellaneous
[PB89-162499] N90-10821
Solar-geophysical data number 534, February 1989. Part 1: (Prompt reports). Data for January 1989, December 1988 and late data
[PB89-173041] N90-10822
Solar-geophysical data number 534, February 1989. Part 2: (Comprehensive reports). Data for August 1988 and miscellaneous
[PB89-173058] N90-10823
Solar-geophysical data number 536, part 2. Data for October 1988 and miscellaneous
[PB89-194658] N90-10824

NATIONAL INST. OF STANDARDS AND TECHNOLOGY, GAITHERSBURG, MD.

Development of metastable processing paths for high temperature alloys
[AD-A210550] N90-10254
Thin film thermocouples for high temperature measurement
[PB89-209290] N90-10420
On the expected complexity of the three-dimensional Voronoi diagram
[PB89-209332] N90-10636
The computation and use of the asymptotic covariance matrix for measurement error models
[PB89-215321] N90-10659

NATIONAL OCEANIC AND ATMOSPHERIC ADMINISTRATION, BOULDER, CO.

Observations of spherical-wave scintillation in strong refractive-index turbulence
[PB89-124747] N90-10355
Geophysical monitoring for climatic change number 16
[PB89-159628] N90-10494

NATIONAL OCEANIC AND ATMOSPHERIC ADMINISTRATION, MIAMI, FL.

A seasonal isotherm depth climatology for the eastern tropical Pacific
[PB89-193577] N90-10512

NATIONAL OCEANIC AND ATMOSPHERIC ADMINISTRATION, ROCKVILLE, MD.

Biochemical cycling and fluxes between the deep euphotic zone and other oceanic realms
[PB89-152458] N90-10509

NATIONAL OCEANIC AND ATMOSPHERIC ADMINISTRATION, SILVER SPRING, MD.

The suitability of diffusion and wind-field techniques for an emergency-response dispersion model
[PB89-190219] N90-10481

Meteorological support: Descriptions of application programs for accessing and displaying data
[PB89-194625] N90-10500

NATIONAL OCEANOGRAPHIC DATA CENTER, WASHINGTON, DC.
Marine weather log, volume 32, number 3, summer 1988
[PB88-248075] N90-10491

NATIONAL SEVERE STORMS LAB., NORMAN, OK.
National Severe Storms Laboratory, fiscal year 1988
[PB89-156145] N90-10493

NATIONAL TELECOMMUNICATIONS AND INFORMATION ADMINISTRATION, ANNAPOLIS, MD.
Manual of regulations and procedures for federal radio frequency management, May 1986 edition: Revisions for January 1989
[PB89-193791] N90-10320

NATIONAL TRANSPORTATION SAFETY BOARD, WASHINGTON, DC.
Aircraft accident report: Aloha Airlines, Flight 243, Boeing 737-200, N73711, near Maui, Hawaii, April 28, 1988
[PB89-910404] N90-10013

NATIONAL WEATHER SERVICE, FORT WORTH, TX.
Forecasting convection with the AFOS (Automation of Field Operations and Services) data analysis programs. (ADAP-version 2.0) (AFOS data analysis programs-version 2.0)
[PB89-145940] N90-10492

NATIONAL WEATHER SERVICE, KANSAS CITY, MO.
A case study evaluation of satellite-derived rainfall estimates and their application to numerical model precipitation forecast verification
[PB89-194591] N90-10499

NATIONAL WEATHER SERVICE, SILVER SPRING, MD.
Extreme hurricanes in the nineteenth century
[PB89-201305] N90-10498
Research highlights of the NMC (National Meteorological Center) Development Division: 1987-1988
[PB89-206478] N90-10501
Structure flow diagram generator
[PB89-195978] N90-10592
String Search
[PB89-195986] N90-10593

NAVAL AIR SYSTEMS COMMAND, WASHINGTON, DC.
US Navy regional climatic study of the United States Atlantic Coast and associated waters
[AD-A210198] N90-10503

NAVAL ENVIRONMENTAL PREDICTION RESEARCH FACILITY, MONTEREY, CA.
Tests of various finite difference algorithms applied to a simple water vapor transport problem on a staggered grid
[AD-A210229] N90-10596

NAVAL HEALTH RESEARCH CENTER, SAN DIEGO, CA.
Daytime sleepiness, performance, mood, nocturnal sleep: The effect of benzodiazepine and caffeine on their relationship
[AD-A210915] N90-10533

NAVAL OCEAN SYSTEMS CENTER, SAN DIEGO, CA.
TWIRE: A test program for VLF airborne transmissions
[AD-A210516] N90-10324
Cost metric algorithms for internetwork applications
[AD-A210324] N90-10597
Demonstration of a dual-lidar method for measuring optical depths in the vertical
[AD-A210598] N90-10711

NAVAL POSTGRADUATE SCHOOL, MONTEREY, CA.
Development of a flight test methodology for a US Navy half-scale unmanned air vehicle
[AD-A210563] N90-10029
Modeling, simulation, and analyses of attitude control for the Crew/Equipment Retriever (CER) proposed for space station
[AD-A208140] N90-10125
Thermodynamic and dynamic processes in the updraft region of GALE (Genesis of Atlantic Lows Experiment) IOP (Intensive Observation Period) 9
[AD-A208139] N90-10496
Finite methods for a nonlinear allocation problem
[AD-A209719] N90-10629
Number of test samples needed to obtain a desired Bayesian confidence interval for a proportion
[AD-A208157] N90-10658
Planning an Integrated On-line Library System (IOLS)
[AD-A209406] N90-10783
The origin of the universe from quantum chaos: An introduction to current ideas
[AD-A210441] N90-10813

NAVAL RESEARCH LAB., WASHINGTON, DC.
The Spartan 1 mission
[NASA-TM-101887] N90-10077
Vacuum microelectronics for beam power and rectennas N90-10146
Gyrotron development for space power beaming N90-10148
Acoustic-vortex-chemical interactions in an idealized ramjet N90-10206
Design and operating characteristics of a CW relevant quasi-optical gyrotron with variable mirror separation
[AD-A210611] N90-10425
Eye/sensor protection against laser irradiation organic nonlinear optical materials
[AD-A210599] N90-10531
Tests of gating algorithms for tracking of multiple objects. Part 1: Theory, requirements and performance measures
[AD-A210519] N90-10644
Numerical simulation of the compressible Orszag-Tang vortex
[AD-A210485] N90-10725
The dense Z-pinch as a plasma radiation source. 1: Quasi-static Bennett model
[AD-A210600] N90-10727

NAVAL SHIP RESEARCH AND DEVELOPMENT CENTER, BETHESDA, MD.
Mechanisms of strength and toughness in a microalloyed, precipitation hardened steel
[AD-A210571] N90-10256
Two counter-rotating vortices approaching a free surface in a viscous fluid
[AD-A210495] N90-10404

NAVAL SURFACE WEAPONS CENTER, SILVER SPRING, MD.
Pin switch circuits instrument for microsecond velocity measurements
[AD-A210638] N90-10426

NAVAL UNDERWATER SYSTEMS CENTER, NEW LONDON, CT.
IFD (Implicit Finite Difference): Interfaced with Harvard open ocean model forecasts
[AD-A210521] N90-10517

NAVAL WEAPONS CENTER, CHINA LAKE, CA.
Investigations of thrust vector control for high-alpha pitchover N90-10067
A structured singular value approach to missile autopilot analysis 2 N90-10068
Analysis and testing of a high performance air-air missile N90-10069
Recent developments in Ramjet pressure oscillation technology N90-10199
Characterization of diamond films by thermogravimetric analysis and infrared spectroscopy
[AD-A210564] N90-10288
Preparation, purification and densification of zinc sulfide powder from organometallics
[AD-A210943] N90-10298

NEW MEXICO UNIV., ALBUQUERQUE.
A lunar far-side very low frequency array
[NASA-CP-3039] N90-10805

NEW YORK UNIV., NEW YORK.
Atomic effects of beta decay in astrophysics and in elementary particle physics N90-10811
Homogeneous gravitational fields and limits of gravitational fields N90-10812

NIELSEN ENGINEERING AND RESEARCH, INC., MOUNTAIN VIEW, CA.
Vortex induced characteristics of missiles in unsteady maneuvers N90-10057
Aeroelastic tailoring procedure for controlling fin hinge moments N90-10058

NORTH CAROLINA STATE UNIV., RALEIGH.
The effects of normal annealing cycles during IGFET fabrication on initial and radiation induced gate insulator defects
[AD-A210262] N90-10278
Laminar boundary layer along inviscid surface streamlines over inclined axisymmetric bodies in incompressible flow
[AD-A210202] N90-10401
The growth of gallium nitride films via the innovative technique of atomic layer epitaxy
[AD-A210360] N90-10760

NORTH TEXAS STATE UNIV., DENTON.
Two photon absorption characterization
[AD-A210508] N90-10694

NORTHEAST ARTIFICIAL INTELLIGENCE CONSORTIUM, SYRACUSE, NY.
Northeast Artificial Intelligence Consortium annual report for 1987. Volume 5: Building an intelligent assistant: The acquisition, integration and maintenance of complex distributed tasks
[AD-A210330] N90-10621
Northeast Artificial Intelligence Consortium annual report for 1987. Volume 7, part A: Time oriented problem solving
[AD-A210331] N90-10622

NORTHEASTERN UNIV., BOSTON, MA.
Establishment and initial operation of a resource facility for RSR (Rapid Solidification Rate) processed alloys in pilot quantities
[AD-A210369] N90-10283

O

OAK RIDGE NATIONAL LAB., TN.
The quantitative analysis of fracture surfaces using fractals
[DE89-015361] N90-10250
Ceramic components in machines, Cologne and Aachen, West Germany; Maastricht, The Netherlands and Brussels, Belgium
[DE89-015831] N90-10264
Structure-mechanical property relationships in ion implanted ceramics
[DE89-010129] N90-10274
Computer simulations of polymer dynamics in the solid state
[DE89-010337] N90-10275
Autonomous mobile robot research using the HERMIES-3 robot
[DE89-015916] N90-10443
International impacts of global climate change: Testimony to House Appropriations Subcommittee on Foreign Operations, Export Financing and Related Programs
[DE89-014004] N90-10482
Evaluation of the North Atlantic seasonal nitrogen model, version 2
[DE89-016157] N90-10515
On the utility and ubiquity of atomic collision physics
[DE89-015356] N90-10686
The temporal development of collision cascades in the binary collision approximation
[DE89-015860] N90-10699
Ignition and burn criteria for D3He tokamak and spherical torus reactors
[DE89-015059] N90-10716
Morphological aspects of the friction of hot-filament-grown diamond thin films
[DE89-015986] N90-10750

OAK RIDGE Y-12 PLANT, TN.
Characterization of electron-beam weld processes in uranium by acoustic emission monitoring
[DE89-016044] N90-10444

ODETICS, INC., ANAHEIM, CA.
Intensity dependent spread theory N90-10550
The intensity dependent spread model and color constancy N90-10555
Intensity dependent spread processor and workstation N90-10568

OFFICE NATIONAL D'ETUDES ET DE RECHERCHES AERONAUTIQUES, PARIS (FRANCE).
Numerical simulation of turbulent plane channel flows N90-10362

OFFICE NATIONAL D'ETUDES ET DE RECHERCHES AEROSPATIALES, PARIS (FRANCE).
Prediction of the aerodynamic stability of missiles N90-10052
Experimental study on the stability of small rocket engines with storable liquid propellants N90-10196
Effects of low-frequency instabilities on the operation of Ramjet air inlets N90-10198
Numerical simulation of unsteady combustion in a dump combustor N90-10203

OFFICE NATIONAL D'ETUDES ET DE RECHERCHES AEROSPATIALES, TOULOUSE (FRANCE).
Experimental study of transition and leading edge contamination on swept wings N90-10362
Control and modification of turbulence N90-10377

OFFICE OF AIR FORCE HISTORY, WASHINGTON, DC.
Encyclopedia of US Air Force aircraft and missile systems. Volume 2: Post-World War 2 bombers, 1945-1973
[AD-A209273] N90-10001

OFFICE OF NAVAL RESEARCH EUROPEAN OFFICE, FPO NEW YORK, NY.
Coherent multichannel techniques for integrated broadband communications subscriber lines
[AD-A209323] N90-10312
Proceedings of the 2nd International Conference on Vector and Parallel Computing
[AD-A209401] N90-10585

OFFICE OF TECHNOLOGY ASSESSMENT, WASHINGTON, DC.
Safer skies with TCAS: Traffic Alert and Collision Avoidance System
[PB89-169221] N90-10016

OFFICE OF THE UNDER SECRETARY OF DEFENSE (ACQUISITIONS), WASHINGTON, DC.
Domestic technology transfer program regulation
[PB89-195374] N90-10793

OKLAHOMA STATE UNIV., STILLWATER.
Heterogeneous catalysts in water
[AD-A210742] N90-10228
OKLAHOMA UNIV., NORMAN.
Molecular biology and physiology of methanogenic archaebacteria
[AD-A210399] N90-10522
OLD DOMINION UNIV., NORFOLK, VA.
Optimal integral controller with sensor failure accommodation N90-10123
Design guide for predicting nonlinear random response (including snap-through) of buckled plates
[NASA-CR-181877] N90-10681
OPTICAL SOCIETY OF AMERICA, WASHINGTON, DC.
Shortwavelength coherent radiation: Generation and applications
[AD-A209847] N90-10427
OREGON STATE UNIV., CORVALLIS.
A comparison of wind turbulence simulation models for stochastic loads analysis for horizontal-axis wind turbines
[DE89-009442] N90-10473
OREGON STATE UNIV., NEWPORT.
Parallel processing and learning in simple systems
[AD-A210225] N90-10612
OTAGO UNIV., DUNEDIN (NEW ZEALAND).
Attenuation of reheat buzz by active control N90-10201
On the 2-extendability of planar graphs
[AD-A210289] N90-10642
OTTAWA UNIV. (ONTARIO).
Modeling and stabilization of large flexible space stations N90-10120

P

PACIFIC NORTHWEST LABS., RICHLAND, WA.
Performance of a broadbanded ultrasonic transducer with coaxially mounted, nondirectional receiver
[DE89-015838] N90-10343
An anisotropic shadowband correction for parameterized sky conditions and geometry
[DE89-014916] N90-10485
PENNSYLVANIA STATE UNIV., STATE COLLEGE.
The measurement of boundary layers on a compressor blade in cascade. Volume 1: Experimental technique, analysis and results
[NASA-CR-185118-VOL-1] N90-10038
The measurement of boundary layers on a compressor blade in cascade. Volume 2: Data tables
[NASA-CR-185118-VOL-2] N90-10039
PENNSYLVANIA STATE UNIV., UNIVERSITY PARK.
Upward flame spread on vertical walls
[PB89-214787] N90-10217
Raman spectroscopic study of the rare earth sesquisulfides
[AD-A210610] N90-10226
The measurement of infrared spectra of dense ceramics by specular reflectance spectroscopy
[AD-A210609] N90-10291
Porosity and crack initiation during low cycle fatigue
[AD-A210989] N90-10464
PISA UNIV. (ITALY).
Thermodynamic transport properties of nitrogen tetroxide in hypercritical conditions for regenerative cooling of a rocket engine. Volume 1: Tests
[ETN-89-94975] N90-10773
Thermodynamic transport properties of nitrogen tetroxide in hypercritical conditions for regenerative cooling of a rocket engine. Volume 2: Appendices
[ETN-89-94977] N90-10774
PITTSBURGH ENERGY TECHNOLOGY CENTER, PA.
Stress in dilute suspensions N90-10389
POLYTECHNIC UNIV., FARMINGDALE, NY.
Physics of high energy photoconductive switches
[AD-A210341] N90-10345
PRATT AND WHITNEY AIRCRAFT, WEST PALM BEACH, FL.
SSME Alternate Turbopump Development Program: Design verification specification for high-pressure fuel turbopump
[NASA-CR-183676] N90-10033
Combustor influence on fighter engine operability N90-10193
PRINCETON UNIV., NJ.
A study of the structure of highly swept shock wave turbulent boundary layer interactions N90-10376
PURDUE UNIV., WEST LAFAYETTE, IN.
Flexible aircraft dynamic modeling for dynamic analysis and control synthesis N90-10112
NMR evidence for a planar arene intermediate in the electron-transfer induced eta 6 to eta 4 hapticity change of a rhodium arene complex
[AD-A210211] N90-10177
Solvent relaxation in electron-transfer reactions: Comparisons between barrier-crossing dynamics in water and polar aprotic media
[AD-A210212] N90-10220
Empirical Bayes selection for the highest probability of success in negative binomial distributions
[AD-A210273] N90-10660
On lower confidence for PCS in truncated location parameter models
[AD-A210274] N90-10661
Selection of the best with a preliminary test for two-parameter exponential distributions
[AD-A210275] N90-10662
A brief bibliography of statistical classification procedures: Decision-theoretic approach
[AD-A210276] N90-10663
Solvent dynamical effects in electron transfer: Predicted influences of electron coupling upon the rate-dielectric friction dependence
[AD-A210193] N90-10690
Solvent effects on intervalence electron-transfer energies for biferrocene cations: Comparisons with molecular models of solvent reorganization
[AD-A210263] N90-10691
Solvent dynamical effects in electron transfer: Evaluation of electronic matrix coupling elements for metallocene self-exchange reactions
[AD-A210306] N90-10692
A theoretical high energy physics program
[DE89-012685] N90-10696

Q

QUALCOMM, INC., SAN DIEGO, CA.
Research in mathematics and computer science: Calculation of the probability of undetected error for certain error detection codes, phase 1
[AD-A210302] N90-10664
QUEENSLAND UNIV., BRISBANE (AUSTRALIA).
Limit analysis of welded tee end connections for hollow tubes
[PB89-191647] N90-10452

R

RAYTHEON CO., WALTHAM, MA.
History and status of beamed power technology and applications at 2.45 Gigahertz N90-10150
READING UNIV. (ENGLAND).
Coordination of mesoscale meteorological research between ASL and European groups
[AD-A210902] N90-10508
RENSSELAER POLYTECHNIC INST., TROY, NY.
Effect of particle velocity fluctuations on the inertia coupling in two-phase flow N90-10391
ROCKWELL INTERNATIONAL SCIENCE CENTER, THOUSAND OAKS, CA.
Supersonic flow computations over aerospace configurations using an Euler marching solver
[NASA-CR-4085] N90-10012
Fatigue crack initiation mechanics of metal aircraft structures
[AD-A210567] N90-10255
ROLLS-ROYCE LTD., BRISTOL (ENGLAND).
Characteristics of combustion driven pressure oscillations in advanced turbo-fan engines with afterburner N90-10194
ROME UNIV. (ITALY).
Bragg crystal polarimeters
[NASA-CR-181331] N90-10423
N=1,2 supergravities in 2+1 dimensions as Chern-Simons theories
[DE89-612006] N90-10771
ROYAL AEROSPACE ESTABLISHMENT, FARNBOROUGH (ENGLAND).
The application of TSIM software to act design and analysis on flexible aircraft N90-10086
ROYAL AIRCRAFT ESTABLISHMENT, FARNBOROUGH (ENGLAND).
Royal Aerospace Establishment: No place for a castings factor N90-10235
Experimental investigation of attachment-line transition in low-speed, high-lift wind-tunnel testing N90-10358
ROYAL ARMAMENT RESEARCH AND DEVELOPMENT ESTABLISHMENT, WESCOTT (ENGLAND).
A design assessment for metallic pressure vessels circumferentially reinforced with a pre-tensioned high-specific-strength anisotropic composite overwind
[AD-A209108] N90-10453
RUTGERS - THE STATE UNIV., NEW BRUNSWICK, NJ.
Regulation of nonlinear and generalized linear systems
[AD-A207725] N90-10619
RUTGERS UNIV., NEW BRUNSWICK, NJ.
Simulation and control problems in elastic robots N90-10098

S

SANDIA NATIONAL LABS., ALBUQUERQUE, NM.
Circuit level modeling of inductive elements
[DE89-015122] N90-10173
Shock compression and release in high-strength ceramics
[DE89-013995] N90-10265
Analysis of surface modified colloidal silicas
[DE89-015849] N90-10267
Mechanical states in wound capacitors. Part 1: Prediction
[DE89-008110] N90-10337
Mechanical states in wound capacitors. Part 2: Optimization
[DE89-008116] N90-10338
Preparation and evaluation of composite membranes for zinc/bromine storage batteries
[DE89-009931] N90-10339
Heat transfer characteristics of igniter output plumes
[DE89-011449] N90-10340
Pyrotechnic ignition studies using a gun tunnel
[DE89-012496] N90-10341
Varistor-particle lightning arrestor connector performance under simulated extreme lightning currents
[DE89-012663] N90-10342
Stress in dilute suspensions N90-10389
Shock behavior of explosives about the C-J (Chapman-Juget) point
[DE89-007642] N90-10400
Laser initiation of secondary explosives
[DE89-010229] N90-10431
The role of sensor directed, model based control in robotics
[DE89-014133] N90-10442
VIBRAFUGE: A combined environment testing facility-vibration testing on a centrifuge
[DE89-015120] N90-10458
United States photovoltaic concentrator technology process and new program initiative
[DE89-013812] N90-10475
Stretched-membrane heliostats for solar central-receiver power plants
[DE89-016034] N90-10476
Data processing in lightning warning systems
[DE89-012495] N90-10502
A low-cost hypercube load-balance algorithm
[DE89-015739] N90-10589
BLOT: A mesh and curve plot program for the output of a finite element analysis
[DE89-013994] N90-10590
Second-order nonlinear optical devices in poled polymers
[DE89-015842] N90-10703
A comparison of real-time optical correlators for pattern recognition
[DE89-016416] N90-10705
Structural aspects of the phase separation in La2CuO4.032
[DE89-016183] N90-10751
SANDIA NATIONAL LABS., LIVERMORE, CA.
X-ray lithography studies of polysilane using a laser plasma X-ray source
[DE89-015390] N90-10266
SCIENCE APPLICATIONS INTERNATIONAL CORP., BILLERICA, MA.
Adaptive machine vision
[AD-A208130] N90-10436
SCIENCE APPLICATIONS INTERNATIONAL CORP., MCLEAN, VA.
Japanese structural ceramics research and development N90-10272
SELENIA S.P.A., ROME (ITALY).
How to control unstable missile airframes: Methodology and limitations N90-10060
Wind tunnel tests: The role of the model N90-10064
Experience gained in the improvement of the Aspide aerodynamic configuration for the surface to air role N90-10072
Winged versus wingless airframes N90-10073
SERVICE TECHNIQUES DES PROGRAMMES AERONAUTIQUES, PARIS (FRANCE).
Casting factors imposed by the French regulation for foundry castings used in military aircraft N90-10233
Casting airworthiness joint European civil authorities view-point N90-10234
SETTAS S.A., JUMET (BELGIUM).
Advances in the technology of titanium castings N90-10243

SMITHSONIAN ASTROPHYSICAL OBSERVATORY, CAMBRIDGE, MA.
X-ray bright points and He I lambda 10830 dark points N90-10802
SOCIETE FRANCAISE D'EQUIPMENTS POUR LA NAVIGATION AERIENNE, CHATELLERAULT (FRANCE).
Miniaturized triaxial laser gyro N90-10061
SOUTHAMPTON UNIV. (ENGLAND).
The theory and application of quadratic minimization in the active reduction of sound and vibration N90-10682
SPARTA, INC., MCLEAN, VA.
DDN Trusted Guard Gateway: Trusted Guard Gateway (TGG) technology assessment, phase 2
[AD-A210248] N90-10614
SPECTRA RESEARCH SYSTEMS, INC., HUNTSVILLE, AL.
Interchangeable end effector tools utilized on the protoflight manipulator arm
[NASA-CR-179374] N90-10447
SRI INTERNATIONAL CORP., MENLO PARK, CA.
Influence of microstructure and microdamage processes on fracture at high loading rates
[AD-A210307] N90-10253
Genetic engineering of single-domain magnetic particles
[AD-A210332] N90-10521
The rewrite rule machine project
[AD-A210528] N90-10617
Processing and fabrication of high temperature oxide superconductors
[AD-A210197] N90-10755
ST SYSTEMS CORP., LANHAM, MD.
An adaptive controller for enhancing operator performance during teleoperation
[NASA-CR-183445] N90-10438
STANFORD UNIV., CA.
Stanford/NASA-Ames Center of Excellence in model-based human performance N90-10585
Primal barrier methods for linear programming
[AD-A210501] N90-10600
Shared memory versus message passing architectures: An application based study
[AD-A210312] N90-10615
Exploring the benefits of multiple hardware contexts in a multiprocessor architecture: Preliminary results
[AD-A210349] N90-10616
Improved estimation of the disturbance variance in a linear regression model
[AD-A210272] N90-10641
A unified view of infinitesimal perturbation analysis and likelihood ratios
[AD-A210682] N90-10652
Studies in estimation theory, applications and implementations
[AD-A210712] N90-10653
Asymptotic robustness in regression and autoregression based on Lindeberg conditions
[AD-A210725] N90-10654
Discrete-time conversion for simulating finite-horizon Markov processes
[AD-A210683] N90-10666
Markov chain moment formulas for regenerative simulation
[AD-A210684] N90-10667
Computational and statistical issues in discrete-event simulation
[AD-A210743] N90-10668
Advanced GaAs process modeling, volume 1
[AD-A210385] N90-10761
STATE UNIV. OF NEW YORK, BUFFALO.
Density of states in a resonant tunneling structure
[AD-A209508] N90-10731
Dwell time and average local speed in a resonant tunneling structure
[AD-A210566] N90-10764
STRUCTURAL DYNAMICS RESEARCH CORP., SAN DIEGO, CA.
Control/structure interaction methods for space station power systems N90-10087
STUTTGART UNIV. (GERMANY, F.R.).
Numerical investigation of the effects of longitudinal vortices on the onset of transition in a flat plate boundary layer N90-10363
SVERDRUP TECHNOLOGY, INC., BAY SAINT LOUIS, MS.
X-ray spectroscopy of the SSME plume
[NASA-CR-185308] N90-10168
SVERDRUP TECHNOLOGY, INC., CLEVELAND, OH.
A supersonic through-flow fan engine airframe integration study
[NASA-CR-185140] N90-10004
SYRACUSE UNIV., UTICA, NY.
A decision support approach to the file allocation problem in a distributed computing system N90-10609

T

TECHNION - ISRAEL INST. OF TECH., HAIFA.
Quotient-difference type generalizations of the power method and their analysis
[NASA-TM-102361] N90-10635
TECHNISCHE UNIV., MUNICH (GERMANY, F.R.).
Development of a high temperature FZG-Ryder gear lubricant load capacity machine
[AD-A210799] N90-10449
TECHNISCHE UNIV., VIENNA (AUSTRIA).
Impedance studies of the cell Pt/Ag+ conducting glass/Ag beta-alumina/Pt
[AD-A209820] N90-10210
TEL-AVIV UNIV. (ISRAEL).
Treatment of laser-induced retinal injuries
[AD-A210284] N90-10526
TELEDYNE BROWN ENGINEERING, AUGUSTA, GA.
Communications Data Base (CDB), phase 3 (with software documentation)
[AD-A210540] N90-10789
TELEDYNE BROWN ENGINEERING, EATONTOWN, NJ.
Software methodology catalog, second edition, revision
[AD-A210548] N90-10601
TELEDYNE BROWN ENGINEERING, HUNTSVILLE, AL.
Space station RT and E utilization study
[NASA-CR-181707] N90-10129
TEMPLE UNIV., PHILADELPHIA, PA.
Mixed-valent and heavy fermions and related systems
[DE89-016335] N90-10743
TENNESSEE UNIV., KNOXVILLE.
Computer simulations of polymer dynamics in the solid state
[DE89-010337] N90-10275
TEXAS A&M UNIV., COLLEGE STATION.
A common distributed language approach to software integration
[NASA-CR-185499] N90-10584
A unified approach to estimating tail behavior
[AD-A210961] N90-10672
Multi-sample functional statistical data analysis
[AD-A210992] N90-10673
A compact X-ray lithography lattice using superferric magnets
[DE89-013947] N90-10728
TEXAS ACCELERATOR CENTER, THE WOODLANDS.
A compact X-ray lithography lattice using superferric magnets
[DE89-013947] N90-10728
TEXAS INST. FOR COMPUTATIONAL MECHANICS, AUSTIN.
Numerical analysis of a class of problems in the mathematical theory of plasticity and damage
[AD-A210731] N90-10655
TEXAS UNIV., AUSTIN.
System identification for large space structures N90-10126
Electrochemistry in near-critical and supercritical fluids. Part 7: SO2
[AD-A208207] N90-10214
Iterative performance and an adaptive procedure for viscous flow problems N90-10397
Symmetry breaking bifurcations and the growth of chaos in a rotating fluid
[AD-A210969] N90-10411
The applicability and limitations of expert system shells
[AD-A210801] N90-10625
Kinetic effects in Alfven wave heating. Part 2: Propagation and absorption with a single minority species
[DE89-016619] N90-10724
THEORY AND APPLICATIONS UNLIMITED CORP., LOS GATOS, CA.
Guidance simulation and test support for differential GPS flight experiment
[NASA-CR-177471] N90-10021
THIOKOL CORP., BRIGHAM CITY, UT.
Flight Motor Set 360L003 (STS-29R)
[NASA-CR-183739-VOL-1] N90-10170
Generic system components of the Thiokol ultrasonic RSRM case-to-insulation bondline inspection system
[NASA-CR-183738] N90-10171
TIMMINCO METALS, HALEY (ONTARIO).
The improved corrosion resistance of ultra high purity magnesium alloy castings N90-10245
TIMMINCO METALS, TORONTO (ONTARIO).
Microstructure morphology and quality of Al-Si castings N90-10244
TITAN-ALUMINUM-FEINGUSS G.M.B.H., BESTWIG (GERMANY, F.R.).
Thin walled cast high-strength structural parts N90-10242
TRANSITION RESEARCH, INC., DANBURY, CT.
Robot vehicle video image compression, phase 1
[AD-A210974] N90-10626
TRANSPORTATION SYSTEMS CENTER, CAMBRIDGE, MA.
Waveform generator signal processing software
[PB89-192660] N90-10587
TRW SPACE TECHNOLOGY LABS., REDONDO BEACH, CA.
Explicit modeling and computational load distribution for concurrent processing simulation of the space station N90-10096
MHD seed recovery and regeneration
[DE89-002711] N90-10715
TULANE UNIV., NEW ORLEANS, LA.
Mechanics of the crack path formation
[NASA-CR-185143] N90-10455
TURIN UNIV. (ITALY).
International Conference on Organometallic Chemistry (13th) held in Torino, Europe on 4-9 September 1988: Abstracts
[AD-A210617] N90-10178

U

ULTRASYSTEMS, INC., IRVINE, CA.
Reactions of hydrogen chloride and boron trichloride with trimethylsilylamino groups
[AD-A209006] N90-10209
UNIVERSIDAD POLITECNICA DE MADRID (SPAIN).
Bifurcations in Poiseuille flow and wall turbulence N90-10370
UNIVERSIDADE FEDERAL DO RIO DE JANEIRO (BRAZIL).
Are there causal vacuum solutions with the symmetries of the Goedel universe in higher-derivative gravity
[DE89-611966] N90-10770
UNIVERSITY COLL., GALWAY (IRELAND).
International Conference on Aerosols and Background Pollution Abstracts
[AD-A210970] N90-10483
UNIVERSITY COLL. OF WALES, ABERYSTWYTH.
On the coefficients of differentiated expansions of ultraspherical polynomials
[NASA-CR-181913] N90-10637
UNIVERSITY OF NORTH TEXAS, DENTON.
High energy density solid and liquid hydrocarbon fuels
[AD-A210195] N90-10304
UNIVERSITY OF SOUTH ALABAMA, MOBILE.
Polypeptide inhibitors of mineral scaling and corrosion
[AD-A210507] N90-10225
UNIVERSITY OF SOUTHERN CALIFORNIA, LOS ANGELES.
Capillary effects in steady-state flow in heterogeneous cores
[DE89-000758] N90-10399
Dynamics and control of turbulent shear flows
[AD-A210396] N90-10402
Surface wave ray tracing and Ms:yield determination in a laterally heterogeneous earth
[AD-A210241] N90-10516
Integration of neurobiological and computational analyses of the neural network essentials for conditioned taste aversions
[AD-A210228] N90-10537
Experimental investigations of transport and optical properties of 3-5 quantum well structures grown via molecular beam epitaxy under optimal growth conditions
[AD-A210269] N90-10758
UNIVERSITY OF SOUTHERN MISSISSIPPI, HATTIESBURG.
An investigation of the degradation and stabilization of polymer systems
[AD-A210362] N90-10282
UTAH UNIV., SALT LAKE CITY.
Multiple internal reflection Fourier transform infrared spectroscopy studies of thiocyanate adsorption on silver and gold
[AD-A210245] N90-10223
Attenuated total reflection FTIR spectroscopy for measuring interfacial reaction kinetics at silica surfaces
[AD-A210314] N90-10224
Image-based terrain modeling with thematic mapper applied to resolving the limit of Holocene Lake expansion in the Great Salt Lake Desert, Utah, part 1
[NASA-CR-185913] N90-10465
Fluctuation history of Great Salt Lake, Utah, during the last 13,000 years, part 2
[NASA-CR-185911] N90-10466
Advances in regression: Use of models in spectroscopic data analysis
[AD-A210541] N90-10665
Ordered structures and metastable alloys grown by OMVPE
[DE89-016370] N90-10744

V

VANDERBILT UNIV., NASHVILLE, TN.
An expert system for optimal gear design N90-10439
Extending matchings in planar graphs 4
[AD-A210315] N90-10643

VECTOR RESEARCH, INC., ANN ARBOR, MI.
Development of Information Quality Engineering (IQE) methodology for information resource management
[AD-A210615] N90-10791

VIRGINIA POLYTECHNIC INST. AND STATE UNIV., BLACKSBURG.
Active vibration mitigation of distributed parameter, smart-type structures using Pseudo-Feedback Optimal Control (PFOC) N90-10121
Shape control of high degree-of-freedom variable geometry trusses N90-10122
Development of an automated probe for thermal conductivity measurements
[PB89-209324] N90-10419
Fatigue growth and closure of short cracks
[AD-A210824] N90-10462

VIRGINIA UNIV., CHARLOTTESVILLE.
Metal-assisted syntheses of boranes and carboranes
[AD-A210728] N90-10227
A simple, mass balance model of carbon flow in a controlled ecological life support system
[NASA-TM-102151] N90-10571

W

WASHINGTON STATE UNIV., PULLMAN.
Particle emission and charging effects induced by fracture
[AD-A210215] N90-10459

WASHINGTON UNIV., SEATTLE.
New energy conversion techniques in space, applicable to propulsion
[AIAA-79-1338] N90-10145
Control of synthetic peptide tertiary structure
[AD-A210339] N90-10281
Plasma waves in the earth's foreshock, bow shock, and magnetosheath N90-10486

WAUGH CONTROLS CORP., CHATSWORTH, CA.
Wide-range fuel flowmeter, phase 2
[AD-A210547] N90-10424

WAYNE STATE UNIV., DETROIT, MI.
Empirical Bayes selection for the highest probability of success in negative binomial distributions
[AD-A210273] N90-10660

WEIZMANN INST. OF SCIENCE, REHOVOTH (ISRAEL).
Electrical field dependence of protein conformation and channel function in lipid membranes of different compositions
[AD-A210236] N90-10222

WESTINGHOUSE ELECTRIC CORP., LIMA, OH.
High temperature VSCF (Variable Speed Constant Frequency) generator system
[AD-A210823] N90-10351

WESTINGHOUSE HANFORD CO., RICHLAND, WA.
PORFLO-3: A mathematical model for fluid flow, heat, and mass transport in variably saturated geologic media: Users manual, version 1.0
[DE89-013977] N90-10398

WICHITA STATE UNIV., KS.
Electro-impulse de-icing testing analysis and design
[NASA-CR-4175] N90-10031

WISCONSIN UNIV., MADISON.
Comparison of carboxylated and sulfonated model polyurethane ionomers
[AD-A210438] N90-10284
UV-curable polyurethane-methacrylate co-networks and interpenetrating networks
[AD-A210445] N90-10285
Synthesis and interfacial properties of new generation polyurethane systems
[AD-A210446] N90-10286
Synthesis and physical properties of poly(perfluoroalkylether) urethanes
[AD-A210500] N90-10287
Analysis of spurt phenomena for a non-Newtonian fluid
[AD-A210560] N90-10405
Stability of discontinuous shearing motions of a non-Newtonian fluid
[AD-A210643] N90-10406
Stability of discontinuous steady states in shearing motion of a non-Newtonian fluid
[AD-A210644] N90-10407
Global existence and asymptotic stability for a nonlinear integrodifferential equation modeling heat flow
[AD-A210647] N90-10408
A compilation of digitized satellite imagery of the Gulf Stream (1982, 1983, and 1985)
[AD-A210243] N90-10467
On two polynomial spaces associated with a box spline
[AD-A210559] N90-10646
A straightforward method for finding implicit solitary wave solutions of nonlinear evolution and wave equations
[AD-A210561] N90-10647
Periodic solutions of spatially periodic Hamiltonian systems
[AD-A210645] N90-10649
Multiple solutions for Lagrangian systems in T superscript n
[AD-A210646] N90-10650

WOODS HOLE OCEANOGRAPHIC INST., MA.
Satellite Data Processing System (SDPS) users manual V1.0
[NASA-CR-183054] N90-10468
Coastal Research Center Woods Hole Oceanographic Institution
[PB89-198238] N90-10510
The influence of a steady baroclinic deep ocean on the shelf
[PB89-198188] N90-10511
A search for layering in the oceanic crust
[PB89-198220] N90-10514

Typical Contract Number Index Listing

Listings in this index are arranged alphanumerically by contract number. Under each contract number the NASA accession numbers denoting documents that have been produced as a result of research done under that contract are arranged in ascending order. The NASA accession number denotes the number by which the citation is identified.

AF PROJ. 1926 ..... N90-10015
AF PROJ. 2301 ..... N90-10345
N90-10349
N90-10427
AF PROJ. 2302 ..... N90-10462
AF PROJ. 2304 ..... N90-10619
N90-10621
N90-10772
AF PROJ. 2305 ..... N90-10330
N90-10713
AF PROJ. 2307 ..... N90-10008
N90-10009
AF PROJ. 2312 ..... N90-10612
AF PROJ. 2313 ..... N90-10538
N90-10539
AF PROJ. 2423 ..... N90-10761
AF PROJ. 2480 ..... N90-10027
AF PROJ. 2688 ..... N90-10495
AF PROJ. 3005 ..... N90-10347
AF PROJ. 3048 ..... N90-10449
AF PROJ. 3145 ..... N90-10351
AF PROJ. 5581 ..... N90-10821
N90-10822
AF PROJ. 5797 ..... N90-10726
AF-AFOSR-0039-88 ..... N90-10330
AF-AFOSR-0076-86 ..... N90-10612
AF-AFOSR-0110-87 ..... N90-10772
AF-AFOSR-0137-87 ..... N90-10702
AF-AFOSR-0141-85 ..... N90-10405
AF-AFOSR-0182-86 ..... N90-10534
AF-AFOSR-0191-87 ..... N90-10405
N90-10407
N90-10408
AF-AFOSR-0192-88 ..... N90-10427
AF-AFOSR-0202-87 ..... N90-10649
N90-10650
AF-AFOSR-0227-87 ..... N90-10538
AF-AFOSR-0243-86 ..... N90-10008
AF-AFOSR-0247-85 ..... N90-10619
AF-AFOSR-0249-85 ..... N90-10345
AF-AFOSR-0263-87 ..... N90-10647
AF-AFOSR-0271-87 ..... N90-10539
AF-AFOSR-0307-85 ..... N90-10408
AF-AFOSR-0323-85 ..... N90-10713
AF-AFOSR-0351-87 ..... N90-10349
AF-AFOSR-0919-87 ..... N90-10406
AFWL PROJ. 88-162 ..... N90-10251
AMSI-U03-8300 ..... N90-10678
ARPA ORDER 5351 ..... N90-10446
ARPA ORDER 6419 ..... N90-10598
ARPA ORDER 9525 ..... N90-10346
BSF-85-00348 ..... N90-10639
DA PROJ. 1L1-61102-A-31-B N90-10694
DA PROJ. 1L1-61102-BH-57 ..... N90-10297
N90-10508
DA PROJ. 1L1-61103-BH-07 ..... N90-10712
DA PROJ. 1L1-62105-AH-84 ..... N90-10290
DA PROJ. 1L1-62706-A-553 ..... N90-10651
DA PROJ. 1L2-63102-DO-71 ..... N90-10190
DA PROJ. 3E1-6287-A-879 ..... N90-10523
DA PROJ. 3E1-62787-A-878 ..... N90-10528
DAAA21-82-C-0184 ..... N90-10823
DAAB07-86-D-R001 ..... N90-10601
DAAB07-87-C-F094 ..... N90-10694
DAAE07-88-C-R068 ..... N90-10626
DAAG29-84-K-0030 ..... N90-10686
DAAG29-85-K-0042 ..... N90-10189
DAAG29-85-K-0235 ..... N90-10730
DAAG29-85-K-0238 ..... N90-10448
DAAG29-85-K-0243 ..... N90-10296
DAAH01-88-C-0105 ..... N90-10791
DAAL03-86-C-0007 ..... N90-10433
DAAL03-86-G-0024 ..... N90-10766
DAAL03-86-K-0038 ..... N90-10257
DAAL03-86-K-0043 ..... N90-10655
DAAL03-86-K-0044 ..... N90-10657
DAAL03-86-K-0045 ..... N90-10653
DAAL03-86-K-0048 ..... N90-10227
DAAL03-86-K-0049 ..... N90-10228
DAAL03-86-K-0064 ..... N90-10258
DAAL03-86-K-0066 ..... N90-10769
DAAL03-86-K-0067 ..... N90-10532
DAAL03-86-K-0070 ..... N90-10765
DAAL03-86-K-0071 ..... N90-10628
DAAL03-86-K-0102 ..... N90-10758
DAAL03-86-K-0126 ..... N90-10391
DAAL03-86-K-0133 ..... N90-10277
DAAL03-86-K-0171 ..... N90-10671
DAAL03-87-C-0002 ..... N90-10327
DAAL03-87-K-0003 ..... N90-10672
N90-10673
DAAL03-87-K-0030 ..... N90-10646
DAAL03-87-K-0036 ..... N90-10405
N90-10406
N90-10407
DAAL03-88-C-0016 ..... N90-10729
DAAL03-88-C-0019 ..... N90-10328
DAAL03-88-K-0063 ..... N90-10652
N90-10666
N90-10667
N90-10668
DAAL03-88-K-0083 ..... N90-10410
DAAL03-88-K-0108 ..... N90-10767
DAAL03-88-K-0185 ..... N90-10406
N90-10407
DAAL03-89-K-0033 ..... N90-10654
DABT60-85-C-0520 ..... N90-10789
DACA76-85-C-0003 ..... N90-10446
DAJA45-85-C-0004 ..... N90-10297
DAJA45-87-C-0014 ..... N90-10508
DAJA45-87-C-0059 ..... N90-10768
DAJA45-88-C-0014 ..... N90-10712
DAJA45-88-M-0295 ..... N90-10178
DAJA45-89-M-0053 ..... N90-10483
DAMD17-85-G-5013 ..... N90-10526
DARPA ORDER 6208 ..... N90-10791
DCA100-87-C-0095 ..... N90-10614
DE-AC02-76CH-00016 ..... N90-10689
N90-10745
N90-10746
N90-10776
N90-10777
DE-AC02-76CH-03000 ..... N90-10418
N90-10697
N90-10747
DE-AC02-76ER-01112 ..... N90-10685
DE-AC02-76ER-01428 ..... N90-10696
DE-AC02-76ER-03130 ..... N90-10695
DE-AC02-78ET-51013 ..... N90-10723
DE-AC02-83CH-10093 ..... N90-10421
N90-10470
N90-10471
N90-10473
N90-10474
N90-10734
DE-AC02-88CE-90027 ..... N90-10263
DE-AC03-76SF-00098 ..... N90-10216
N90-10219
N90-10440
N90-10595
N90-10698
N90-10701
N90-10704
N90-10720
N90-10748
N90-10752
N90-10753
DE-AC03-86SF-16495 ..... N90-10430
DE-AC04-76DP-00078 ..... N90-10337
N90-10338
N90-10339
N90-10340
N90-10400
DE-AC04-76DP-00613 ..... N90-10249
N90-10270
N90-10271
N90-10276
N90-10335
N90-10336
N90-10417
N90-10441
DE-AC04-76DP-00789 ..... N90-10173
N90-10265
N90-10266
N90-10267
N90-10341
N90-10342
N90-10416
N90-10431
N90-10442
N90-10458
N90-10475
N90-10476
N90-10502
N90-10589
N90-10590
N90-10703
N90-10705
N90-10751
DE-AC05-84OR-02140 ..... N90-10274
DE-AC05-84OR-21400 ..... N90-10250
N90-10264
N90-10275
N90-10443
N90-10482
N90-10515
N90-10686
N90-10699
N90-10716
N90-10750
DE-AC05-84OS-21400 ..... N90-10444
DE-AC06-76RL-00183 ..... N90-10343
DE-AC06-76RL-01830 ..... N90-10485
DE-AC06-87RL-10930 ..... N90-10398
DE-AC22-87PC-79672 ..... N90-10715
DE-AC22-88PC-88883 ..... N90-10700
DE-AI01-85CE-50111 ..... N90-10036
DE-AI01-87ER-60590 ..... N90-10825
DE-AS04-77ER-03998 ..... N90-10688
DE-FG02-84ER-45061 ..... N90-10744
DE-FG02-87ER-45310 ..... N90-10749
DE-FG02-87ER-45333 ..... N90-10743
DE-FG03-85ER-25009 ..... N90-10611
DE-FG03-86ER-53220 ..... N90-10714
DE-FG03-87ER-25030 ..... N90-10600
DE-FG05-90ET-53088 ..... N90-10724
DE-FG05-85ER-45186 ..... N90-10208
DE-FG05-87ER-40374 ..... N90-10728
DE-FG05-88ER-13853 ..... N90-10427
DE-FG05-88ER-53266 ..... N90-10724
DE-FG22-87BC-14126 ..... N90-10399
DE-FG22-88PC-88929 ..... N90-10392
DEN3-336 ..... N90-10036
DOT-HS-8-01936 ..... N90-10587
DTCG23-88-C-20024 ..... N90-10322
DTFA01-89-C-00001 ..... N90-10017
DTNH22-82-C-07041 ..... N90-10587
DTRS-57-84-C-00003 ..... N90-10587
DTRS-57-86-P-81655 ..... N90-10587
EMW-84-E-1589 ..... N90-10498
FAA-T0604-L N90-10018
FAA-T0704-F N90-10315
F04701-85-C-0086 ..... N90-10269
N90-10432
N90-10434
N90-10435
N90-10490

F04701-85-C-0086-P00019 ..... N90-10300
F04701-88-C-0089 ..... N90-10757
N90-10763
F08635-84-C-0228 ..... N90-10009
F19628-85-C-0002 ..... N90-10078
N90-10540
N90-10762
F19628-85-K-0040 ..... N90-10759
F19628-86-C-0061 ..... N90-10495
F19628-86-C-0141 ..... N90-10486
N90-10504
F19628-87-K-0018 ..... N90-10516
F19628-87-K-0033 ..... N90-10800
N90-10801
N90-10802
F30602-85-C-0006 ..... N90-10621
N90-10622
F33615-81-C-2078 ..... N90-10204
F33615-81-K-3625 ..... N90-10401
F33615-84-C-2412 ..... N90-10304
F33615-84-C-3404 ..... N90-10015
N90-10024
F33615-85-C-0541 ..... N90-10573
F33615-85-C-2551 ..... N90-10351
F33615-85-C-5048 ..... N90-10761
F33615-85-C-5069 ..... N90-10414
F33615-85-K-3210 ..... N90-10462
F33615-87-C-1499 ..... N90-10710
F33615-87-C-2711 ..... N90-10027
F33615-88-C-3212 ..... N90-10022
F40600-86-C-0003 ..... N90-10424
F49620-86-C-0012 ..... N90-10754
F49620-86-C-0029 ..... N90-10347
F49620-86-C-0081 ..... N90-10449
F49620-86-K-0010 ..... N90-10253
F49620-87-C-0036 ..... N90-10535
F49620-88-C-0086 ..... N90-10664
GRI-5086-260-1396 ..... N90-10472
JPL-957652 ..... N90-10468
MDA903-86-C-0142 ..... N90-10781
MDA903-89-C-0003 ..... N90-10607
MIPR-ARO-105-88 ..... N90-10762
MIPR-ARO-118-87 ..... N90-10176
MIPR-102-88 ..... N90-10230
MIPR-121-86 ..... N90-10230
NAGW-112 ..... N90-10602
NAGW-533 ..... N90-10815
NAGW-1175 ..... N90-10446
NAGW-1340 ..... N90-10809
NAG1-280 ..... N90-10357
NAG1-363 ..... N90-10681
NAG1-402 ..... N90-10357
NAG1-731 ..... N90-10357
NAG1-894 ..... N90-10588
NAG2-302 ..... N90-10075
NAG2-541 ..... N90-10313
NAG3-202 ..... N90-10147
NAG3-284 ..... N90-10031
NAG3-815 ..... N90-10455
NAG5-931 ..... N90-10317
NASA ORDER C-99066-G N90-10635
NAS1-15820 ..... N90-10012
NAS1-17506 ..... N90-10187
NAS1-17740 ..... N90-10186
NAS1-18027 ..... N90-10014
NAS1-18036 ..... N90-10030
NAS1-18107 ..... N90-10576
NAS1-18228 ..... N90-10129
NAS1-18240 ..... N90-10366
NAS1-18605 ..... N90-10007
N90-10576
N90-10581
N90-10631
N90-10637
N90-10638
N90-10639
N90-10640
N90-10677
NAS1-18645 ..... N90-10546
NAS2-12378 ..... N90-10021
NAS3-21854 ..... N90-10037
NAS3-22394 ..... N90-10043
N90-10044
NAS3-23051 ..... N90-10045
N90-10046
NAS3-23697 ..... N90-10450
N90-10451
NAS3-23710 ..... N90-10011
NAS3-23878 ..... N90-10175
NAS3-24210 ..... N90-10047
N90-10048
N90-10049
NAS3-24222 ..... N90-10683
NAS3-24384 ..... N90-10293
NAS3-24622 ..... N90-10184
NAS3-24872 ..... N90-10294
NAS3-25266 ..... N90-10004
NAS3-25281 ..... N90-10437
NAS5-25496 ..... N90-10796
NAS5-27772 ..... N90-10583
NAS5-28561 ..... N90-10438
NAS5-28753 ..... N90-10465
N90-10466
NAS5-28779 ..... N90-10479
NAS5-30017 ..... N90-10583
NAS7-918 ..... N90-10261
N90-10329
N90-10608
NAS8-30490 ..... N90-10169
N90-10170
N90-10171
N90-10413
NAS8-36307 ..... N90-10447
NAS8-36716 ..... N90-10393
NAS8-36801 ..... N90-10033
NAS8-37137 ..... N90-10133
N90-10134
N90-10135
N90-10136
N90-10137
N90-10138
N90-10139
NAS8-37257 ..... N90-10128
NAS10-10285 ..... N90-10478
N90-10571
NAS13-290 ..... N90-10168
NCC8-016 ..... N90-10124
NCC9-16 ..... N90-10584
NGT-50308 ..... N90-10803
NGT-50337 ..... N90-10678
NIST-60NANB4D0037 ..... N90-10217
NIST-60NANB6D0642 ..... N90-10419
NR PROJ. 039-212 ..... N90-10283
NSF ACS-87-19502 ..... N90-10611
NSF ASC-88-06925 ..... N90-10631
NSF ATM-80-05369 ..... N90-10499
NSF ATM-85-14730 ..... N90-10499
NSF ATM-87-09659 ..... N90-10032
NSF CBT-88-09347 ..... N90-10392
NSF CCR-86-11442 ..... N90-10604
NSF CCR-87-07155 ..... N90-10617
NSF CCR-87-16884 ..... N90-10603
NSF CCR-88-09615 ..... N90-10611
NSF DMC-88-17355 ..... N90-10678
NSF DMR-88-18412 ..... N90-10275
NSF DMS-85-20905 ..... N90-10649
N90-10650
NSF DMS-86-06964 ..... N90-10660
N90-10662
NSF DMS-86-20303 ..... N90-10405
N90-10406
N90-10407
NSF DMS-87-01275 ..... N90-10646
NSF DMS-87-02620 ..... N90-10660
N90-10661
NSF DMS-87-12058 ..... N90-10405
N90-10406
N90-10407
NSF DMS-87-16132 ..... N90-10406
N90-10407
N90-10661
NSF DMS-88-06964 ..... N90-10446
NSF DRC-86-04199 ..... N90-10514
NSF EAR-80-26445 ..... N90-10514
NSF EAR-83-09535 ..... N90-10666
NSF ECS-84-04809 ..... N90-10647
NSF ECS-86-03643 ..... N90-10642
NSF INT-85-21818 ..... N90-10606
NSF IRI-86-16644 ..... N90-10647
NSF MIP-86-58865 ..... N90-10514
NSF OCE-80-25206 ..... N90-10514
NSF OCE-81-17210 ..... N90-10514
NSF OCE-84-10658 ..... N90-10467
NSF OCE-85-10828 ..... N90-10511
NSF OCE-85-18487 ..... N90-10467
NSF OCE-87-00601 ..... N90-10514
NSF OCE-87-00606 ..... N90-10427
NSF PHY-88-09775 ..... N90-10656
NSF 98477-8511190-CCR N90-10038
NSG-3264 ..... N90-10039
N90-10527
N00014-77-C-0749 ..... N90-10523
N00014-79-C-0168 ..... N90-10684
N00014-79-C-0647 ..... N90-10352
N00014-80-C-0622 ..... N90-10283
N00014-80-C-0986 ..... N90-10518
N00014-82-C-0360 ..... N90-10218
N00014-82-C-0600 ..... N90-10603
N00014-83-K-0125 ..... N90-10604
N90-10605
N90-10656
N00014-83-K-0423 ..... N90-10284
N90-10285
N90-10286
N90-10287
N00014-83-K-0498 ..... N90-10210
N00014-84-C-0016 ..... N90-10779
N00014-84-C-0193 ..... N90-10708
N00014-84-C-0359 ..... N90-10202
N00014-84-K-0428 ..... N90-10214
N00014-84-K-0553 ..... N90-10213
N90-10732
N00014-85-C-0417 ..... N90-10617
N00014-85-C-0747 ..... N90-10403
N00014-85-K-0124 ..... N90-10670
N00014-85-K-0129 ..... N90-10226
N90-10291
N00014-85-K-0168 ..... N90-10604
N00014-85-K-0423 ..... N90-10788
N00014-85-K-0474 ..... N90-10733
N00014-85-K-0488 ..... N90-10642
N90-10643
N00014-85-K-0748 ..... N90-10262
N00014-85-K-0809 ..... N90-10714
N00014-86-C-0601 ..... N90-10436
N00014-86-K-0043 ..... N90-10731
N90-10764
N00014-86-K-0115 ..... N90-10519
N00014-86-K-0180 ..... N90-10353
N90-10578
N90-10579
N00014-86-K-0222 ..... N90-10522
N00014-86-K-0282 ..... N90-10221
N00014-86-K-0322 ..... N90-10780
N00014-86-K-0332 ..... N90-10572
N00014-86-K-0361 ..... N90-10464
N00014-86-K-0385 ..... N90-10411
N00014-86-K-0402 ..... N90-10280
N00014-86-K-0556 ..... N90-10177
N90-10220
N90-10690
N90-10691
N90-10692
N00014-86-K-0640 ..... N90-10260
N00014-86-K-0679 ..... N90-10402
N00014-86-K-0686 ..... N90-10760
N00014-86-K-0751 ..... N90-10468
N00014-87-C-0676 ..... N90-10305
N00014-87-C-0713 ..... N90-10209
N00014-87-G-0203 ..... N90-10222
N00014-87-K-0007 ..... N90-10467
N00014-87-K-0131 ..... N90-10292
N90-10693
N90-10709
N00014-87-K-0142 ..... N90-10600
N00014-87-K-0464 ..... N90-10648
N00014-87-K-0497 ..... N90-10520
N00014-87-K-0514 ..... N90-10459
N00014-87-K-0541 ..... N90-10211
N90-10212
N00014-87-K-0791 ..... N90-10279
N00014-87-K-0825 ..... N90-10580
N00014-87-K-0828 ..... N90-10615
N90-10616
N00014-88-C-0391 ..... N90-10348
N00014-88-C-0450 ..... N90-10617
N00014-88-C-0512 ..... N90-10346
N00014-88-C-0601 ..... N90-10246
N00014-88-C-0705 ..... N90-10755
N00014-88-C-0746 ..... N90-10278
N00014-88-C-2050 ..... N90-10707
N00014-88-J-1115 ..... N90-10427
N00014-88-J-1132 ..... N90-10489
N00014-88-J-1182 ..... N90-10645
N00014-88-K-0170 ..... N90-10660
N90-10661
N90-10662
N90-10663
N00014-88-K-0188 ..... N90-10631
N00014-88-K-0201 ..... N90-10281
N00014-88-K-0233 ..... N90-10786
N00014-88-K-0281 ..... N90-10678
N00014-88-K-0307 ..... N90-10229
N00014-88-K-0360 ..... N90-10295
N90-10299
N90-10350
N90-10354
N00014-88-K-0428 ..... N90-10225
N00014-88-K-0487 ..... N90-10606
N00014-88-K-0591 ..... N90-10598
N90-10678
N00014-89-C-0085 ..... N90-10521
N00014-89-J-1296 ..... N90-10537
N00014-89-J-1412 ..... N90-10223
N90-10224
N90-10665
N00014-89-J-1610 ..... N90-10631
N00014-89-J-1627 ..... N90-10641

N00019-86-C-0032	N90-10058
N00039-81-C-0357	N90-10321
N00039-84-C-0070	N90-10321
N00039-88-C-0065	N90-10321
N00173-87-T0-06614	N90-10800
N62269-86-C-0261	N90-10255
PROJ. 74F	N90-10781
RR0109	N90-10714
RR04106	N90-10280
	N90-10281
	N90-10521
	N90-10522
RR04108	N90-10222
	N90-10520
RR04206	N90-10786
RR04209	N90-10572
	N90-10779
UGC-32-635	N90-10642
W-31-109-ENG-38	N90-10180
	N90-10422
	N90-10429
	N90-10469
	N90-10591
	N90-10687
	N90-10735
	N90-10736
W-7405-ENG-36	N90-10215
	N90-10273
	N90-10301
	N90-10302
	N90-10333
	N90-10688
	N90-10706
	N90-10721
	N90-10742
W-7405-ENG-48	N90-10251
	N90-10252
	N90-10319
	N90-10331
	N90-10332
	N90-10344
	N90-10384
	N90-10423
	N90-10428
	N90-10525
	N90-10582
	N90-10594
	N90-10632
	N90-10719
	N90-10722
	N90-10739
	N90-10752
	N90-10794
186-30-21	N90-10808
307-51-00	N90-10737
307-51-08-04	N90-10412
324-01-00	N90-10294
326-23-30-01	N90-10814
480-51-23-03	N90-10129
505-31-3B	N90-10011
505-45-72	N90-10175
505-60-21-01	N90-10002
505-60-31-01	N90-10187
505-61-91	N90-10006
505-62-0K	N90-10437
505-62-21	N90-10038
	N90-10039
	N90-10635
505-62-81-05	N90-10409
505-63-1B	N90-10181
505-63-5A	N90-10437
505-63-01-05	N90-10454
505-63-01-06	N90-10179
505-63-01-10	N90-10456
505-63-11	N90-10185
505-63-31	N90-10455
505-63-51-07	N90-10679
505-66-01-02	N90-10074
505-66-11	N90-10021
505-66-21-01	N90-10602
505-66-21-04	N90-10505
	N90-10506
	N90-10507
505-67-00	N90-10542
505-68-11	N90-10031
505-68-91-02	N90-10012
505-69-61	N90-10004
505-69-71-03	N90-10034
505-90-21-01	N90-10007
	N90-10576
	N90-10581
	N90-10631
	N90-10637
	N90-10638
	N90-10639
	N90-10640
	N90-10677
506-41-3G	N90-10174
506-42-11	N90-10172
506-43-11	N90-10262
506-43-31	N90-10183
506-43-41-01	N90-10308
506-43-71	N90-10248
506-44-21	N90-10738
506-46-11-01	N90-10080
	N90-10103
506-47-11	N90-10575
506-80-31-02	N90-10681
506-80-31-06	N90-10680
510-01-0A	N90-10037
533-02-51	N90-10023
	N90-10610
533-04-11	N90-10450
	N90-10451
533-06-01	N90-10042
534-06-23-10	N90-10186
535-03-01	N90-10045
	N90-10046
	N90-10047
	N90-10048
	N90-10049
535-05-01	N90-10188
549-02-41-01	N90-10618
585-01-61-01	N90-10457
586-01-11	N90-10309
591-22-21-01	N90-10127
643-10-01	N90-10674
906-85-44-50	N90-10140

Typical Report Number Index Listing

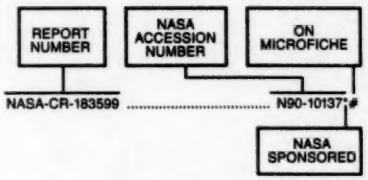

Listings in this index are arranged alphanumerically by report number. The NASA accession number denotes the number by which the citation is identified. An asterisk (*) indicates that the itemis a NASA report. A pound sign (#) indicates that the item is available on microfiche.

A-87091 ..... N90-10042* #
A-87239 ..... N90-10808* #
A-89035 ..... N90-10183* #
A-89092 ..... N90-10575* #
A-89145 ..... N90-10006* #
A-89211 ..... N90-10542* #

AAMRL-TR-89-018 ..... N90-10573 #

ACD-330 ..... N90-10018 #
ACD-330-PHASE-2 ..... N90-10315 #

AD-A206001 ..... N90-10523 #
AD-A206784 ..... N90-10778 #
AD-A207669 ..... N90-10495 #
AD-A207724 ..... N90-10772 #
AD-A207725 ..... N90-10619 #
AD-A207814 ..... N90-10702 #
AD-A207834 ..... N90-10733 #
AD-A207908 ..... N90-10330 #
AD-A207952 ..... N90-10714 #
AD-A208130 ..... N90-10436 #
AD-A208132 ..... N90-10414 #
AD-A208139 ..... N90-10496 #
AD-A208140 ..... N90-10125 #
AD-A208154 ..... N90-10579 #
AD-A208157 ..... N90-10658 #
AD-A208189 ..... N90-10580 #
AD-A208207 ..... N90-10214 #
AD-A208269 ..... N90-10260 #
AD-A208927 ..... N90-10519 #
AD-A209006 ..... N90-10209 #
AD-A209009 ..... N90-10729 #
AD-A209042 ..... N90-10657 #
AD-A209087 ..... N90-10541 #
AD-A209108 ..... N90-10453 #
AD-A209130 ..... N90-10484 #
AD-A209216 ..... N90-10328 #
AD-A209273 ..... N90-10001 #
AD-A209323 ..... N90-10312 #
AD-A209365 ..... N90-10730 #
AD-A209401 ..... N90-10585 #
AD-A209406 ..... N90-10783 #
AD-A209418 ..... N90-10578 #
AD-A209422 ..... N90-10022 #
AD-A209423 ..... N90-10211 #
AD-A209424 ..... N90-10212 #
AD-A209425 ..... N90-10246 #
AD-A209508 ..... N90-10731 #
AD-A209519 ..... N90-10732 #
AD-A209528 ..... N90-10213 #
AD-A209559 ..... N90-10684 #
AD-A209719 ..... N90-10629 #
AD-A209820 ..... N90-10210 #
AD-A209847 ..... N90-10427 #
AD-A210161 ..... N90-10218 #
AD-A210185 ..... N90-10779 #
AD-A210188 ..... N90-10303 #
AD-A210190 ..... N90-10754 #
AD-A210193 ..... N90-10690 #
AD-A210195 ..... N90-10304 #
AD-A210196 ..... N90-10520 #
AD-A210197 ..... N90-10755 #
AD-A210198 ..... N90-10503 #
AD-A210199 ..... N90-10536 #
AD-A210200 ..... N90-10321 #
AD-A210201 ..... N90-10024 #
AD-A210202 ..... N90-10401 #
AD-A210211 ..... N90-10177 #
AD-A210212 ..... N90-10220 #
AD-A210215 ..... N90-10459 #
AD-A210218 ..... N90-10572 #
AD-A210223 ..... N90-10573 #
AD-A210224 ..... N90-10756 #
AD-A210225 ..... N90-10612 #
AD-A210226 ..... N90-10221 #
AD-A210227 ..... N90-10277 #
AD-A210228 ..... N90-10537 #
AD-A210229 ..... N90-10596 #
AD-A210235 ..... N90-10827 #
AD-A210236 ..... N90-10222 #
AD-A210238 ..... N90-10613 #
AD-A210241 ..... N90-10516 #
AD-A210243 ..... N90-10467 #
AD-A210245 ..... N90-10223 #
AD-A210247 ..... N90-10678* #
AD-A210248 ..... N90-10614 #
AD-A210252 ..... N90-10008 #
AD-A210257 ..... N90-10675 #
AD-A210263 ..... N90-10691 #
AD-A210264 ..... N90-10757 #
AD-A210266 ..... N90-10786 #
AD-A210269 ..... N90-10758 #
AD-A210271 ..... N90-10025 #
AD-A210272 ..... N90-10641 #
AD-A210273 ..... N90-10660 #
AD-A210274 ..... N90-10661 #
AD-A210275 ..... N90-10662 #
AD-A210276 ..... N90-10663 #
AD-A210278 ..... N90-10468* #
AD-A210282 ..... N90-10278 #
AD-A210283 ..... N90-10787 #
AD-A210284 ..... N90-10526 #
AD-A210287 ..... N90-10279 #
AD-A210289 ..... N90-10642 #
AD-A210295 ..... N90-10280 #
AD-A210302 ..... N90-10664 #
AD-A210304 ..... N90-10759 #
AD-A210306 ..... N90-10692 #
AD-A210307 ..... N90-10253 #
AD-A210311 ..... N90-10527 #
AD-A210312 ..... N90-10615 #
AD-A210314 ..... N90-10224 #
AD-A210315 ..... N90-10643 #
AD-A210324 ..... N90-10597 #
AD-A210330 ..... N90-10621 #
AD-A210331 ..... N90-10622 #
AD-A210332 ..... N90-10521 #
AD-A210338 ..... N90-10598 #
AD-A210339 ..... N90-10281 #
AD-A210341 ..... N90-10345 #
AD-A210342 ..... N90-10322 #
AD-A210344 ..... N90-10528 #
AD-A210345 ..... N90-10346 #
AD-A210349 ..... N90-10616 #
AD-A210350 ..... N90-10623 #
AD-A210351 ..... N90-10707 #
AD-A210362 ..... N90-10282 #
AD-A210366 ..... N90-10347 #
AD-A210368 ..... N90-10305 #
AD-A210369 ..... N90-10283 #
AD-A210373 ..... N90-10026 #
AD-A210374 ..... N90-10040 #
AD-A210375 ..... N90-10599 #
AD-A210378 ..... N90-10529 #
AD-A210380 ..... N90-10760 #
AD-A210381 ..... N90-10027 #
AD-A210385 ..... N90-10761 #
AD-A210396 ..... N90-10402 #
AD-A210399 ..... N90-10522 #
AD-A210402 ..... N90-10009 #
AD-A210404 ..... N90-10460 #
AD-A210427 ..... N90-10708 #
AD-A210430 ..... N90-10488 #
AD-A210431 ..... N90-10504 #
AD-A210433 ..... N90-10788 #
AD-A210438 ..... N90-10284 #
AD-A210439 ..... N90-10762 #
AD-A210440 ..... N90-10078 #
AD-A210441 ..... N90-10813 #
AD-A210445 ..... N90-10285 #
AD-A210446 ..... N90-10286 #
AD-A210456 ..... N90-10538 #
AD-A210464 ..... N90-10489 #
AD-A210465 ..... N90-10725 #
AD-A210482 ..... N90-10041 #
AD-A210489 ..... N90-10403 #
AD-A210493 ..... N90-10539 #
AD-A210495 ..... N90-10404 #
AD-A210496 ..... N90-10693 #
AD-A210499 ..... N90-10540 #
AD-A210500 ..... N90-10287 #
AD-A210501 ..... N90-10600 #
AD-A210502 ..... N90-10763 #
AD-A210503 ..... N90-10028 #
AD-A210504 ..... N90-10530 #
AD-A210505 ..... N90-10323 #
AD-A210507 ..... N90-10225 #
AD-A210508 ..... N90-10694 #
AD-A210510 ..... N90-10348 #
AD-A210516 ..... N90-10324 #
AD-A210517 ..... N90-10325 #
AD-A210519 ..... N90-10644 #
AD-A210521 ..... N90-10517 #
AD-A210522 ..... N90-10490 #
AD-A210528 ..... N90-10617 #
AD-A210540 ..... N90-10789 #
AD-A210541 ..... N90-10665 #
AD-A210547 ..... N90-10424 #
AD-A210548 ..... N90-10601 #
AD-A210549 ..... N90-10349 #
AD-A210550 ..... N90-10254 #
AD-A210553 ..... N90-10780 #
AD-A210554 ..... N90-10306 #
AD-A210556 ..... N90-10645 #
AD-A210557 ..... N90-10461 #
AD-A210559 ..... N90-10646 #
AD-A210560 ..... N90-10405 #
AD-A210561 ..... N90-10647 #
AD-A210563 ..... N90-10029 #
AD-A210564 ..... N90-10288 #
AD-A210566 ..... N90-10764 #
AD-A210567 ..... N90-10255 #
AD-A210568 ..... N90-10790 #
AD-A210570 ..... N90-10709 #
AD-A210571 ..... N90-10256 #
AD-A210573 ..... N90-10648 #
AD-A210581 ..... N90-10289 #
AD-A210586 ..... N90-10726 #
AD-A210587 ..... N90-10290 #
AD-A210590 ..... N90-10445 #
AD-A210591 ..... N90-10624 #
AD-A210592 ..... N90-10710 #
AD-A210593 ..... N90-10574 #
AD-A210594 ..... N90-10446* #
AD-A210597 ..... N90-10077* #
AD-A210598 ..... N90-10711 #
AD-A210599 ..... N90-10531 #
AD-A210600 ..... N90-10727 #
AD-A210605 ..... N90-10781 #
AD-A210609 ..... N90-10291 #
AD-A210610 ..... N90-10226 #
AD-A210611 ..... N90-10425 #
AD-A210613 ..... N90-10432 #
AD-A210614 ..... N90-10010 #
AD-A210615 ..... N90-10791 #
AD-A210617 ..... N90-10178 #
AD-A210625 ..... N90-10292 #
AD-A210631 ..... N90-10019 #
AD-A210633 ..... N90-10020 #
AD-A210638 ..... N90-10426 #
AD-A210640 ..... N90-10518 #
AD-A210643 ..... N90-10406 #
AD-A210644 ..... N90-10407 #
AD-A210645 ..... N90-10649 #
AD-A210646 ..... N90-10650 #
AD-A210647 ..... N90-10408 #

AD-A210648 ..... N90-10307 #
AD-A210677 ..... N90-10651 #
AD-A210682 ..... N90-10652 #
AD-A210683 ..... N90-10666 #
AD-A210684 ..... N90-10667 #
AD-A210685 ..... N90-10532 #
AD-A210700 ..... N90-10015 #
AD-A210706 ..... N90-10433 #
AD-A210712 ..... N90-10653 #
AD-A210713 ..... N90-10448 #
AD-A210716 ..... N90-10326 #
AD-A210725 ..... N90-10654 #
AD-A210728 ..... N90-10227 #
AD-A210729 ..... N90-10189 #
AD-A210731 ..... N90-10655 #
AD-A210732 ..... N90-10190 #
AD-A210740 ..... N90-10765 #
AD-A210741 ..... N90-10257 #
AD-A210742 ..... N90-10228 #
AD-A210743 ..... N90-10668 #
AD-A210786 ..... N90-10295 #
AD-A210789 ..... N90-10350 #
AD-A210797 ..... N90-10296 #
AD-A210799 ..... N90-10449 #
AD-A210801 ..... N90-10625 #
AD-A210823 ..... N90-10351 #
AD-A210824 ..... N90-10462 #
AD-A210826 ..... N90-10603 #
AD-A210829 ..... N90-10656 #
AD-A210831 ..... N90-10604 #
AD-A210832 ..... N90-10352 #
AD-A210833 ..... N90-10605 #
AD-A210837 ..... N90-10606 #
AD-A210844 ..... N90-10434 #
AD-A210871 ..... N90-10669 #
AD-A210885 ..... N90-10670 #
AD-A210886 ..... N90-10229 #
AD-A210902 ..... N90-10508 #
AD-A210912 ..... N90-10176* #
AD-A210915 ..... N90-10533 #
AD-A210918 ..... N90-10297 #
AD-A210919 ..... N90-10353 #
AD-A210920 ..... N90-10410 #
AD-A210926 ..... N90-10230 #
AD-A210937 ..... N90-10607 #
AD-A210939 ..... N90-10766 #
AD-A210942 ..... N90-10671 #
AD-A210943 ..... N90-10298 #
AD-A210961 ..... N90-10672 #
AD-A210969 ..... N90-10411 #
AD-A210970 ..... N90-10483 #
AD-A210974 ..... N90-10626 #
AD-A210977 ..... N90-10767 #
AD-A210978 ..... N90-10354 #
AD-A210979 ..... N90-10299 #
AD-A210986 ..... N90-10463 #
AD-A210988 ..... N90-10768 #
AD-A210989 ..... N90-10464 #
AD-A210992 ..... N90-10673 #
AD-A210996 ..... N90-10627 #
AD-A211000 ..... N90-10792 #
AD-A211002 ..... N90-10712 #
AD-A211043 ..... N90-10534 #
AD-A211044 ..... N90-10535 #
AD-A211085 ..... N90-10327 #
AD-A211114 ..... N90-10258 #
AD-A211115 ..... N90-10628 #
AD-A211125 ..... N90-10311 #
AD-A211141 ..... N90-10435 #
AD-A211162 ..... N90-10769 #
AD-A211166 ..... N90-10259 #
AD-A211186 ..... N90-10713 #

AD-E501132 ..... N90-10607 #
AD-E501135 ..... N90-10299 #
AD-E501135 ..... N90-10354 #
AD-E801954 ..... N90-10009 #
AD-E900860 ..... N90-10684 #
AD-E951366 ..... N90-10307 #
AD-E951366 ..... N90-10406 #
AD-E951366 ..... N90-10407 #
AD-E951366 ..... N90-10408 #
AD-E951366 ..... N90-10426 #
AD-E951366 ..... N90-10518 #
AD-E951366 ..... N90-10649 #
AD-E951366 ..... N90-10650 #

AD-F000138 ..... N90-10460 #

ADS-TR-1196-1 ..... N90-10540 #

AEDC-TR-89-4 ..... N90-10010 #
AEDC-TR-89-6 ..... N90-10424 #

AFATL-TR-89-20 ..... N90-10009 #

AFGL-ERP-1017 ..... N90-10325 #

AFGL-TR-88-0329 ..... N90-10495 #
AFGL-TR-89-0012 ..... N90-10325 #
AFGL-TR-89-0065 ..... N90-10516 #
AFGL-TR-89-0093 ..... N90-10504 #
AFGL-TR-89-0094 ..... N90-10488 #

AFOSR-89-0529TR ..... N90-10619 #
AFOSR-89-0572TR ..... N90-10772 #
AFOSR-89-0606TR ..... N90-10702 #
AFOSR-89-0647TR ..... N90-10330 #
AFOSR-89-0780TR ..... N90-10008 #
AFOSR-89-0788TR ..... N90-10427 #
AFOSR-89-0801TR ..... N90-10754 #
AFOSR-89-0809TR ..... N90-10612 #
AFOSR-89-0813TR ..... N90-10538 #
AFOSR-89-0841TR ..... N90-10664 #
AFOSR-89-0983TR ..... N90-10539 #
AFOSR-89-0992TR ..... N90-10253 #
AFOSR-89-0993TR ..... N90-10349 #
AFOSR-89-0994TR ..... N90-10345 #
AFOSR-89-0995TR-PHASE-2 ..... N90-10347 #
AFOSR-89-1012TR ..... N90-10535 #
AFOSR-89-1016TR ..... N90-10534 #
AFOSR-89-1054TR ..... N90-10713 #

AFWAL-TR-86-3094 ..... N90-10401 #
AFWAL-TR-88-2128 ..... N90-10304 #
AFWAL-TR-88-2144 ..... N90-10351 #
AFWAL-TR-88-3110 ..... N90-10015 #
AFWAL-TR-88-4205 ..... N90-10756 #
AFWAL-TR-88-4245 ..... N90-10414 #
AFWAL-TR-89-3008 ..... N90-10462 #
AFWAL-TR-89-3009 ..... N90-10022 #

AFWL-TR-89-35 ..... N90-10726 #

AGARD-CP-438 ..... N90-10356 #
AGARD-CP-450 ..... N90-10191 #
AGARD-CP-451 ..... N90-10050 #

AGARD-R-762 ..... N90-10231 #

AI-M-1119 ..... N90-10579 #

AI-TR-1053 ..... N90-10606 #
AI-TR-1103 ..... N90-10578 #
AI-TR-1125 ..... N90-10353 #
AI-TR-1128 ..... N90-10670 #

AIAA-79-1338 ..... N90-10145* #
AIAA-89-2140 ..... N90-10004* #
AIAA-89-3596 ..... N90-10023* #

AMSMI/TR-RD-SS-88-11 ..... N90-10307 #

ANL/EES-TM-376 ..... N90-10591 #

ANSTO/E-676 ..... N90-10740 #

AOML-33 ..... N90-10512 #

AR-005-677 ..... N90-10247 #
AR-005-706 ..... N90-10395 #

ARCCB-MR-89014 ..... N90-10460 #

ARCCB-TR-89016 ..... N90-10463 #

ARI-RN-89-22 ..... N90-10781 #

ARI-RR-1501 ..... N90-10326 #

ARL-FLIGHT-MECH-TM-410 ..... N90-10599 #

ARL-PROP-TM-454 ..... N90-10041 #
ARL-PROP-TM-455 ..... N90-10040 #

ARL-STRUC-TM-506 ..... N90-10026 #

ARL-TR-89-32 ..... N90-10625 #

ARL-89-7/ONR-89-1 ..... N90-10572 #

ARO-22301.7-MS ..... N90-10189 #
ARO-22746.11-PH ..... N90-10762 #
ARO-22776.17-CH ..... N90-10228 #
ARO-22806.17-EG ..... N90-10448 #
ARO-22874.14-EL ..... N90-10730 #
ARO-23010.3-MA ..... N90-10673 #
ARO-23010.4-MA ..... N90-10672 #
ARO-23011.6-CH ..... N90-10230 #
ARO-23120.3-MA ..... N90-10655 #
ARO-23200.9-LS ..... N90-10532 #
ARO-23230.2-LS-A ..... N90-10296 #
ARO-23238.1-PH ..... N90-10257 #
ARO-23290.2-PH-S ..... N90-10433 #
ARO-23305.1-MA ..... N90-10657 #
ARO-23439.6-EG ..... N90-10628 #
ARO-23453.34-MA ..... N90-10653 #
ARO-23474.28-MS ..... N90-10258 #
ARO-23494.12-EL ..... N90-10765 #
ARO-23508.7-CH ..... N90-10227 #
ARO-23520.8-EL ..... N90-10769 #
ARO-23736.1-EL ..... N90-10758 #
ARO-23757.8-PH-F ..... N90-10766 #
ARO-24165.6-MS ..... N90-10277 #
ARO-24539.1-EG-SDI ..... N90-10176* #
ARO-24635.101-MA-UIR ..... N90-10671 #
ARO-24723.1-GS-S ..... N90-10327 #
ARO-25648.11-MA ..... N90-10410 #
ARO-25839.5-MA ..... N90-10652 #
ARO-25839.6-MA ..... N90-10668 #
ARO-25839.7-MA ..... N90-10666 #
ARO-25839.8-MA ..... N90-10667 #
ARO-26051-EL ..... N90-10767 #
ARO-26206.1-EL-SBI ..... N90-10729 #
ARO-26209.1-EL-SBI ..... N90-10328 #
ARO-26394.2-MA ..... N90-10654 #

ASE-5568 ..... N90-10796* #

AU-ARI-88-9 ..... N90-10536 #

AVSCOM-TM-89-C-003 ..... N90-10437* #

AVSCOM-TR-89-B-004 ..... N90-10679* #

BBC-RD-1989/8 ..... N90-10318

BBN-6972 ..... N90-10613 #

BDX-613-3939 ..... N90-10336 #
BDX-613-3941 ..... N90-10249 #
BDX-613-3971 ..... N90-10335 #
BDX-613-3985 ..... N90-10271 #

BNL-42493 ..... N90-10776 #
BNL-42954 ..... N90-10689 #
BNL-42968 ..... N90-10777 #
BNL-43034 ..... N90-10746 #
BNL-43065 ..... N90-10745 #

BRL-TR-3011 ..... N90-10461 #
BRL-TR-3018 ..... N90-10669 #

CGR/DC-22/88 ..... N90-10484 #

CMS-TSR-89-28 ..... N90-10405 #
CMS-TSR-89-29 ..... N90-10646 #
CMS-TSR-89-37 ..... N90-10408 #
CMS-TSR-89-38 ..... N90-10647 #
CMS-TSR-90-2 ..... N90-10650 #
CMS-TSR-90-3 ..... N90-10649 #
CMS-TSR-90-4 ..... N90-10406 #
CMS-TSR-90-5 ..... N90-10407 #

CMU-RI-TR-89-4 ..... N90-10574 #
CMU-RI-TR-89-5 ..... N90-10446* #
CMU-RI-TR-89-6 ..... N90-10624 #
CMU-RI-TR-89-7 ..... N90-10710 #
CMU-RI-TR-89-8-PT-1 ..... N90-10445 #
CMU-RI-TR-89-10 ..... N90-10311 #

CONF-881155-75 ..... N90-10266 #
CONF-890142-5 ..... N90-10704 #
CONF-890335-217 ..... N90-10728 #
CONF-890372-13 ..... N90-10589 #
CONF-890426-25 ..... N90-10752 #
CONF-890426-26 ..... N90-10753 #
CONF-890435-5 ..... N90-10219 #
CONF-890508-1 ..... N90-10180 #
CONF-890555-18 ..... N90-10469 #
CONF-890594-3 ..... N90-10701 #
CONF-890594-4 ..... N90-10689 #
CONF-890610-5 ..... N90-10485 #
CONF-890618-3 ..... N90-10429 #
CONF-890665-36 ..... N90-10331 #
CONF-890665-38 ..... N90-10332 #
CONF-890665-42 ..... N90-10739 #
CONF-890680-1 ..... N90-10698 #
CONF-890708-2 ..... N90-10688 #
CONF-890708-3 ..... N90-10686 #
CONF-890718-17 ..... N90-10742 #
CONF-890718-22 ..... N90-10745 #
CONF-890718-24 ..... N90-10751 #
CONF-890759-1 ..... N90-10384 #
CONF-890770-1 ..... N90-10343 #
CONF-890811-6 ..... N90-10400 #
CONF-890811-7 ..... N90-10215 #
CONF-890811-18 ..... N90-10301 #

CONF-890811-19 ..... N90-10302 #
CONF-890815-18 ..... N90-10173 #
CONF-890821-1 ..... N90-10699 #
CONF-890836-5 ..... N90-10423* #
CONF-890836-8 ..... N90-10476 #
CONF-890902-1 ..... N90-10273 #
CONF-890902-2 ..... N90-10339 #
CONF-890902-7 ..... N90-10422 #
CONF-890909-1 ..... N90-10525 #
CONF-890925-1 ..... N90-10475 #
CONF-890926-2 ..... N90-10431 #
CONF-890987-1-PT-1 ..... N90-10337 #
CONF-890987-2-PT-2 ..... N90-10338 #
CONF-890995-1 ..... N90-10274 #
CONF-8811253-1 ..... N90-10250 #
CONF-8901153-1 ..... N90-10748 #
CONF-8903100-4 ..... N90-10721 #
CONF-8903158-1 ..... N90-10611 #
CONF-8904214-1 ..... N90-10716 #
CONF-8904242-3 ..... N90-10705 #
CONF-8904259-1 ..... N90-10251 #
CONF-8905120-20 ..... N90-10720 #
CONF-8905143-3 ..... N90-10777 #
CONF-8905146-2 ..... N90-10687 #
CONF-8905183-3 ..... N90-10697 #
CONF-8905193-1 ..... N90-10333 #
CONF-8906129-1 ..... N90-10735 #
CONF-8906179-1 ..... N90-10736 #
CONF-8906187-1 ..... N90-10267 #
CONF-8907106-2 ..... N90-10632 #
CONF-8907121-1 ..... N90-10344 #
CONF-8908100-1 ..... N90-10703 #
CONF-8908101-1 ..... N90-10319 #
CONF-8908116-1 ..... N90-10595 #
CONF-8909111-1 ..... N90-10594 #
CONF-8909112-1 ..... N90-10776 #
CONF-8909113 ..... N90-10340 #
CONF-8909113-1 ..... N90-10341 #
CONF-8909114 ..... N90-10440 #
CONF-8909120-1 ..... N90-10275 #
CONF-8909124-1 ..... N90-10502 #
CONF-8909124-2 ..... N90-10342 #
CONF-8909126-1 ..... N90-10582 #
CONF-8909161-1 ..... N90-10706 #
CONF-8909167-1 ..... N90-10442 #
CONF-8909167-2 ..... N90-10443 #
CONF-8909168-1 ..... N90-10458 #
CONF-8909171-1 ..... N90-10252 #
CONF-8909174-1 ..... N90-10750 #

CPS-89-009 ..... N90-10346 #

CRC-APRAC-AP-17 ..... N90-10480 #

CRC-89-1 ..... N90-10510 #

CRDEC-TR-88157 ..... N90-10651 #

CRIE-W-87039 ..... N90-10334 #
CRIE-W-87042 ..... N90-10268 #

CU-ECE-TR-89-01 ..... N90-10713 #

CU-1-533835 ..... N90-10279 #

C01-091JB-0001-01 ..... N90-10601 #
C87A-25 ..... N90-10348 #
C3086-FR-001A ..... N90-10712 #

DE89-000758 ..... N90-10399 #
DE89-000867 ..... N90-10470 #
DE89-002711 ..... N90-10715 #
DE89-007642 ..... N90-10400 #
DE89-007744 ..... N90-10301 #
DE89-007748 ..... N90-10302 #
DE89-008016 ..... N90-10215 #
DE89-008110 ..... N90-10337 #
DE89-008116 ..... N90-10338 #
DE89-008611 ..... N90-10525 #
DE89-009252 ..... N90-10273 #
DE89-009432 ..... N90-10421 #
DE89-009441 ..... N90-10734 #
DE89-009442 ..... N90-10473 #
DE89-009449 ..... N90-10471 #
DE89-009451 ..... N90-10474 #
DE89-009931 ..... N90-10339 #
DE89-010129 ..... N90-10274 #
DE89-010229 ..... N90-10431 #
DE89-010247 ..... N90-10776 #
DE89-010337 ..... N90-10275 #
DE89-011403 ..... N90-10582 #
DE89-011449 ..... N90-10340 #
DE89-011635 ..... N90-10594 #
DE89-011819 ..... N90-10440 #
DE89-012382 ..... N90-10422 #
DE89-012495 ..... N90-10502 #
DE89-012496 ..... N90-10341 #
DE89-012663 ..... N90-10342 #
DE89-012685 ..... N90-10696 #
DE89-013812 ..... N90-10475 #
DE89-013947 ..... N90-10728 #
DE89-013963 ..... N90-10695 #
DE89-013975 ..... N90-10719 #
DE89-013977 ..... N90-10398 #
DE89-013992 ..... N90-10416 #
DE89-013994 ..... N90-10590 #
DE89-013995 ..... N90-10265 #
DE89-014004 ..... N90-10482 #
DE89-014007 ..... N90-10591 #
DE89-014010 ..... N90-10276 #
DE89-014011 ..... N90-10441 #
DE89-014012 ..... N90-10417 #
DE89-014015 ..... N90-10747 #
DE89-014045 ..... N90-10319 #
DE89-014133 ..... N90-10442 #
DE89-014226 ..... N90-10706 #
DE89-014326 ..... N90-10428 #
DE89-014355 ..... N90-10697 #
DE89-014363 ..... N90-10794 #
DE89-014530 ..... N90-10208 #
DE89-014859 ..... N90-10685 #
DE89-014916 ..... N90-10485 #
DE89-015033 ..... N90-10626 #
DE89-015059 ..... N90-10716 #
DE89-015077 ..... N90-10331 #
DE89-015096 ..... N90-10263 #
DE89-015099 ..... N90-10777 #
DE89-015116 ..... N90-10632 #
DE89-015117 ..... N90-10384 #
DE89-015120 ..... N90-10458 #
DE89-015122 ..... N90-10173 #
DE89-015128 ..... N90-10735 #
DE89-015130 ..... N90-10429 #
DE89-015164 ..... N90-10180 #
DE89-015219 ..... N90-10216 #
DE89-015223 ..... N90-10720 #
DE89-015225 ..... N90-10698 #
DE89-015257 ..... N90-10333 #
DE89-015300 ..... N90-10721 #
DE89-015301 ..... N90-10688 #
DE89-015302 ..... N90-10742 #
DE89-015339 ..... N90-10748 #
DE89-015356 ..... N90-10686 #
DE89-015361 ..... N90-10250 #
DE89-015386 ..... N90-10701 #
DE89-015390 ..... N90-10266 #
DE89-015541 ..... N90-10749 #
DE89-015587 ..... N90-10418 #
DE89-015693 ..... N90-10469 #
DE89-015702 ..... N90-10687 #
DE89-015703 ..... N90-10736 #
DE89-015723 ..... N90-10722 #
DE89-015739 ..... N90-10589 #
DE89-015770 ..... N90-10332 #
DE89-015774 ..... N90-10739 #
DE89-015775 ..... N90-10423* #
DE89-015831 ..... N90-10264 #
DE89-015838 ..... N90-10343 #
DE89-015842 ..... N90-10703 #
DE89-015849 ..... N90-10267 #
DE89-015857 ..... N90-10689 #
DE89-015860 ..... N90-10699 #
DE89-015883 ..... N90-10700 #
DE89-015916 ..... N90-10443 #
DE89-015986 ..... N90-10750 #
DE89-016034 ..... N90-10476 #
DE89-016044 ..... N90-10444 #
DE89-016050 ..... N90-10723 #
DE89-016157 ..... N90-10515 #
DE89-016183 ..... N90-10751 #
DE89-016302 ..... N90-10752 #
DE89-016303 ..... N90-10595 #
DE89-016306 ..... N90-10753 #
DE89-016308 ..... N90-10219 #
DE89-016318 ..... N90-10825 #
DE89-016335 ..... N90-10743 #
DE89-016341 ..... N90-10704 #
DE89-016370 ..... N90-10744 #
DE89-016385 ..... N90-10611 #
DE89-016412 ..... N90-10745 #
DE89-016416 ..... N90-10705 #
DE89-016421 ..... N90-10746 #
DE89-016427 ..... N90-10430 #
DE89-016619 ..... N90-10724 #
DE89-016637 ..... N90-10251 #
DE89-016649 ..... N90-10344 #
DE89-016652 ..... N90-10252 #
DE89-611966 ..... N90-10770 #
DE89-612006 ..... N90-10771 #
DE89-615389 ..... N90-10314 #
DE89-616080 ..... N90-10740 #
DE89-617523 ..... N90-10633 #
DE89-617525 ..... N90-10634 #
DE89-617530 ..... N90-10775 #
DE89-617778 ..... N90-10741 #
DE89-617843 ..... N90-10676 #
DE89-760382 ..... N90-10268 #
DE89-760384 ..... N90-10334 #

DNE-9015033-PT-2B ..... N90-10826 #

DOD-3200.12-R-4 ..... N90-10793 #

DODA-AR-005-574 ..... N90-10041 #
DODA-AR-005-575 ..... N90-10040 #
DODA-AR-005-598 ..... N90-10599 #
DODA-AR-005-604 ..... N90-10026 #

DOE/BC-14126/10 ..... N90-10399 #

DOE/CE-90027/1 ..... N90-10263 #

DOE/CH-10093/52-VOL-2 ..... N90-10470 #

DOE/ER-01112/14 ..... N90-10685 #
DOE/ER-01428/T2 ..... N90-10696 #
DOE/ER-03130/425 ..... N90-10695 #
DOE/ER-25009/806 ..... N90-10611 #
DOE/ER-40374/21 ..... N90-10728 #
DOE/ER-45061/T5 ..... N90-10744 #
DOE/ER-45186/T1 ..... N90-10208 #
DOE/ER-45310/19 ..... N90-10749 #
DOE/ER-45333/2 ..... N90-10743 #
DOE/ER-53266/25-PT-2 ..... N90-10724 #
DOE/ER-60590/T1 ..... N90-10825 #

DOE/ET-51013/273 ..... N90-10723 #

DOE/NASA/0336-1 ..... N90-10036* #

DOE/PC-79672/T1 ..... N90-10715 #
DOE/PC-88883/T3 ..... N90-10700 #

DOE/SF-16495/T2 ..... N90-10430 #

DOT-HS-807-312 ..... N90-10587 #

DOT-TSC-NHTSA-88-2 ..... N90-10587 #

DOT/FAA/CT-TN89/26 ..... N90-10020 #
DOT/FAA/CT-TN89/29 ..... N90-10019 #
DOT/FAA/CT-TN89/39 ..... N90-10018 #
DOT/FAA/CT-TN89/49-PHASE-2 ..... N90-10315 #

DOT/FAA/DS-89/24 ..... N90-10014* #
DOT/FAA/DS-89/25 ..... N90-10017 #

DPS-1 ..... N90-10786 #

DREO-1004 ..... N90-10529 #

DRES-SP-128 ..... N90-10790 #

DRIC-BR-109774 ..... N90-10453 #

DSTL-88-001 ..... N90-10583* #

DTIC/TR-88/4 ..... N90-10792 #
DTIC/TR-89/10 ..... N90-10792 #

DTRC-89/013 ..... N90-10404 #

DTRC/SME-88-81 ..... N90-10256 #

DTS-74 ..... N90-10587 #

DVS-30-REV-3 ..... N90-10033* #

E-3622 ..... N90-10174* #
E-3734 ..... N90-10188* #
E-4279 ..... N90-10031* #
E-4704 ..... N90-10309* #
E-4769 ..... N90-10738* #
E-4963 ..... N90-10262* #
E-4986 ..... N90-10181* #
E-5034 ..... N90-10185* #
E-5059 ..... N90-10737* #
E-5068 ..... N90-10004* #
E-5070 ..... N90-10455* #
E-5077 ..... N90-10635* #
E-5086 ..... N90-10674* #
E-5107 ..... N90-10172* #
E-189400-39-F ..... N90-10479* #

ECS-SS-1011 ..... N90-10170* #
ECS-SS-1012 ..... N90-10169* #
ECS-SS-1816 ..... N90-10413* #
ECS-SS-2412 ..... N90-10171* #

EDR-14232 ..... N90-10036* #

ESD-TR-88-315 ..... N90-10078 #
ESD-TR-89-128 ..... N90-10540 #
ESD-TR-89-142 ..... N90-10762 #

ETL-0537 ..... N90-10446* #

ETN-89-94975 ..... N90-10773 #
ETN-89-94977 ..... N90-10774 #

FCR-9643A ..... N90-10472 #

FEF/PD/1101/89-VOL-2 ..... N90-10450* #
FEF/PD/1102/89-VOL-3 ..... N90-10451* #

FERMILAB-PUB-89/97-A ..... N90-10809* #

FLOW-RR-480 ..... N90-10218 #

FLOW-TR-477 ..... N90-10403 #

FNAL-TM-1599 ..... N90-10697 #
FNAL-TM-1604 ..... N90-10747 #
FNAL-TM-1612 ..... N90-10418 #

FRCR-337-PT-2 ..... N90-10724 #

FTD-ID(RS)T-0349-89 ..... N90-10289 #

GDSS-LRB-MEM-88-01-VOL-2-BK-2 ..... N90-10136* #

GRI-89/0137 ..... N90-10472 #

H-1518 ..... N90-10610* #
H-1558 ..... N90-10023* #

HDL-TR-2149 ..... N90-10323 #

HIG-89-1 ..... N90-10518 #

HSER-11518-VOL-1 ..... N90-10043* #
HSER-11518-VOL-2 ..... N90-10044* #
HSER-11804 ..... N90-10046* #
HSER-11894 ..... N90-10045* #
HSER-12548 ..... N90-10437* #

HSS-B-169 ..... N90-10495 #

IC-88/340 ..... N90-10741 #
IC-88/403 ..... N90-10633 #
IC-88/406 ..... N90-10771 #
IC-88/415 ..... N90-10676 #
IC-88/419 ..... N90-10634 #
IC-89/6 ..... N90-10775 #

ICASE-89-30 ..... N90-10581* #
ICASE-89-34 ..... N90-10007* #
ICASE-89-45 ..... N90-10640* #
ICASE-89-57 ..... N90-10631* #
ICASE-89-62 ..... N90-10638* #
ICASE-89-63 ..... N90-10677* #
ICASE-89-65 ..... N90-10637* #
ICASE-89-67 ..... N90-10639* #
ICASE-89-68 ..... N90-10576* #

ICOMP-89-25 ..... N90-10635* #

IDA-P-2151 ..... N90-10607 #

IDA/HQ-88-33817 ..... N90-10607 #

IFT-P-29/88 ..... N90-10770 #

IITRI-E06595-5 ..... N90-10321 #

ISBN-0-642-59890-8 ..... N90-10740 #
ISBN-0-7970-1561-2 ..... N90-10826 #
ISBN-0-7970-1566-3 ..... N90-10826 #
ISBN-0-86776-310-8 ..... N90-10452 #
ISBN-1-55752-052-6 ..... N90-10427 #
ISBN-92-835-0494-1 ..... N90-10050 #
ISBN-92-835-0502-6 ..... N90-10356 #
ISBN-92-835-0503-4 ..... N90-10191 #
ISBN-92-835-0507-7 ..... N90-10231 #

ISSN-0036-0911 ..... N90-10817 #
ISSN-0038-0911 ..... N90-10818 #
ISSN-0038-0911 ..... N90-10819 #
ISSN-0038-0911 ..... N90-10820 #
ISSN-0038-0911 ..... N90-10821 #
ISSN-0038-0911 ..... N90-10822 #
ISSN-0038-0911 ..... N90-10823 #
ISSN-0038-0911 ..... N90-10824 #
ISSN-0389-4010 ..... N90-10003 #
ISSN-0389-4010 ..... N90-10035 #
ISSN-0389-4010 ..... N90-10586 #
ISSN-0389-4010 ..... N90-10630 #
ISSN-1030-7745 ..... N90-10740 #

KCP-613-4033 ..... N90-10270 #
KCP-613-4076 ..... N90-10276 #
KCP-613-4080 ..... N90-10441 #
KCP-613-4081 ..... N90-10417 #

KIYI-88-35 ..... N90-10314 #

L-16134 ..... N90-10409* #
L-16266 ..... N90-10002* #
L-16456 ..... N90-10679* #
L-16494 ..... N90-10412* #
L-16531 ..... N90-10034* #
L-16562 ..... N90-10618* #
L-16571 ..... N90-10074* #
L-16580 ..... N90-10814* #
L-16590 ..... N90-10140* #
L-16596 ..... N90-10680* #
L-16606 ..... N90-10248* #
L-16629 ..... N90-10179* #

LA-UR-89-376 ..... N90-10302 #
LA-UR-89-407 ..... N90-10301 #
LA-UR-89-689 ..... N90-10215 #
LA-UR-89-1127 ..... N90-10273 #
LA-UR-89-2112 ..... N90-10706 #
LA-UR-89-2404 ..... N90-10333 #
LA-UR-89-2469 ..... N90-10742 #
LA-UR-89-2473 ..... N90-10688 #
LA-UR-89-2474 ..... N90-10721 #

LBL-26130 ..... N90-10219 #
LBL-26537 ..... N90-10216 #
LBL-26601 ..... N90-10595 #
LBL-26734 ..... N90-10748 #
LBL-26882 ..... N90-10704 #
LBL-26935 ..... N90-10440 #
LBL-27108 ..... N90-10720 #
LBL-27314 ..... N90-10698 #
LBL-27351 ..... N90-10701 #
LBL-27356 ..... N90-10753 #
LBL-27496 ..... N90-10752 #

LC-79-640375 ..... N90-10817 #
LC-79-640375 ..... N90-10818 #
LC-79-640375 ..... N90-10819 #
LC-79-640375 ..... N90-10820 #
LC-79-640375 ..... N90-10821 #
LC-79-640375 ..... N90-10822 #
LC-79-640375 ..... N90-10823 #
LC-79-640375 ..... N90-10824 #
LC-88-60866 ..... N90-10427 #
LC-89-600725 ..... N90-10016 #

LG85ER0105 ..... N90-10011* #
LG86ER0060 ..... N90-10030* #

LLTR-89-1 ..... N90-10465* #
LLTR-89-2 ..... N90-10466* #

M-616 ..... N90-10385* #

MD89-CDSF-0013 ..... N90-10789 #

MIT/LCS/TM-373-REV ..... N90-10604 #
MIT/LCS/TM-379 ..... N90-10352 #
MIT/LCS/TM-380 ..... N90-10605 #
MIT/LCS/TM-382 ..... N90-10603 #
MIT/LCS/TM-383 ..... N90-10656 #

MRL-R-1149 ..... N90-10247 #

MRL-RR-1-89 ..... N90-10395 #

MT-CWJR-089-034 ..... N90-10258 #

MTL-TR-89-43 ..... N90-10290 #
MTL-TR-89-45 ..... N90-10190 #
MTL-TR-89-63 ..... N90-10259 #

NADC-89044-60 ..... N90-10255 #

NAL-TR-1000 ..... N90-10586 #
NAL-TR-1002 ..... N90-10035 #
NAL-TR-1006 ..... N90-10003 #
NAL-TR-1009 ..... N90-10630 #

NAS 1.15:4134 ..... N90-10679* #
NAS 1.15:4144 ..... N90-10034* #
NAS 1.15:87690-PT-1 ..... N90-10505* #
NAS 1.15:87690-PT-2 ..... N90-10506* #
NAS 1.15:87690-PT-3 ..... N90-10507* #
NAS 1.15:89125 ..... N90-10002* #
NAS 1.15:89131 ..... N90-10409* #
NAS 1.15:89154 ..... N90-10602* #
NAS 1.15:89423 ..... N90-10042* #
NAS 1.15:89429-VOL-3 ..... N90-10808* #
NAS 1.15:89923 ..... N90-10174* #
NAS 1.15:100169 ..... N90-10188* #
NAS 1.15:101071 ..... N90-10183* #
NAS 1.15:101089 ..... N90-10575* #
NAS 1.15:101561 ..... N90-10577* #
NAS 1.15:101578-PT-1 ..... N90-10080* #
NAS 1.15:101578-PT-2 ..... N90-10103* #
NAS 1.15:101612 ..... N90-10127* #
NAS 1.15:101616 ..... N90-10308* #
NAS 1.15:101638 ..... N90-10454* #
NAS 1.15:101640 ..... N90-10456* #
NAS 1.15:101648 ..... N90-10457* #
NAS 1.15:101703 ..... N90-10023* #
NAS 1.15:101706 ..... N90-10610* #
NAS 1.15:101851 ..... N90-10076*
NAS 1.15:101887 ..... N90-10077* #
NAS 1.15:101889 ..... N90-10176* #
NAS 1.15:101958 ..... N90-10181* #
NAS 1.15:102149 ..... N90-10478* #
NAS 1.15:102151 ..... N90-10571* #
NAS 1.15:102152 ..... N90-10079* #
NAS 1.15:102155 ..... N90-10795* #
NAS 1.15:102195 ..... N90-10006* #
NAS 1.15:102214 ..... N90-10542* #
NAS 1.15:102291 ..... N90-10262* #
NAS 1.15:102322 ..... N90-10309* #
NAS 1.15:102329 ..... N90-10185* #
NAS 1.15:102350 ..... N90-10737* #
NAS 1.15:102356 ..... N90-10738* #
NAS 1.15:102361 ..... N90-10635* #
NAS 1.15:102367 ..... N90-10674* #
NAS 1.15:102373 ..... N90-10172* #
NAS 1.21:7011(328) N90-10524*
NAS 1.21:7046(21) N90-10130*
NAS 1.21:7056(08) N90-10131*
NAS 1.21:7063(03) ..... N90-10782* #
NAS 1.26:3996 ..... N90-10186* #
NAS 1.26:4065 ..... N90-10012* #
NAS 1.26:4175 ..... N90-10031* #
NAS 1.26:174937 ..... N90-10011* #
NAS 1.26:174992 ..... N90-10043* #
NAS 1.26:174993 ..... N90-10044* #
NAS 1.26:175070 ..... N90-10175* #
NAS 1.26:177471 ..... N90-10021* #
NAS 1.26:178166 ..... N90-10187* #
NAS 1.26:178316 ..... N90-10030* #
NAS 1.26:179374 ..... N90-10447* #
NAS 1.26:179590 ..... N90-10683* #
NAS 1.26:179629 ..... N90-10294* #
NAS 1.26:179642 ..... N90-10184* #
NAS 1.26:180831 ..... N90-10293* #
NAS 1.26:180867 ..... N90-10048* #
NAS 1.26:180868 ..... N90-10047* #
NAS 1.26:180869 ..... N90-10049* #
NAS 1.26:181331 ..... N90-10423* #
NAS 1.26:181707 ..... N90-10129* #
NAS 1.26:181845 ..... N90-10581* #
NAS 1.26:181859 ..... N90-10007* #
NAS 1.26:181867 ..... N90-10014* #
NAS 1.26:181877 ..... N90-10681* #
NAS 1.26:181903 ..... N90-10631* #
NAS 1.26:181910 ..... N90-10677* #
NAS 1.26:181913 ..... N90-10637* #
NAS 1.26:181919 ..... N90-10638* #
NAS 1.26:181920 ..... N90-10639* #
NAS 1.26:181921 ..... N90-10576* #
NAS 1.26:181926 ..... N90-10640* #
NAS 1.26:182125 ..... N90-10045* #
NAS 1.26:182142 ..... N90-10046* #
NAS 1.26:182228 ..... N90-10037* #
NAS 1.26:182235-VOL-2 ..... N90-10450* #
NAS 1.26:182236 ..... N90-10451* #
NAS 1.26:183054 ..... N90-10468* #
NAS 1.26:183435 ..... N90-10583* #
NAS 1.26:183445 ..... N90-10438* #
NAS 1.26:183446 ..... N90-10479* #
NAS 1.26:183447 ..... N90-10796* #
NAS 1.26:183599 ..... N90-10137* #
NAS 1.26:183600 ..... N90-10133* #
NAS 1.26:183601 ..... N90-10136* #
NAS 1.26:183602 ..... N90-10139* #
NAS 1.26:183603 ..... N90-10135* #
NAS 1.26:183604 ..... N90-10134* #
NAS 1.26:183605 ..... N90-10138* #
NAS 1.26:183676 ..... N90-10033* #
NAS 1.26:183714 ..... N90-10413* #
NAS 1.26:183727 ..... N90-10128* #
NAS 1.26:183738 ..... N90-10171* #
NAS 1.26:183739-VOL-1 ..... N90-10170* #
NAS 1.26:183746 ..... N90-10169* #
NAS 1.26:184781 ..... N90-10313* #
NAS 1.26:184784 ..... N90-10588* #

NAS 1.26:185031 ..... N90-10809* #
NAS 1.26:185110 ..... N90-10437* #
NAS 1.26:185118-VOL-1 ..... N90-10038* #
NAS 1.26:185118-VOL-2 ..... N90-10039* #
NAS 1.26:185133 ..... N90-10036* #
NAS 1.26:185140 ..... N90-10004* #
NAS 1.26:185143 ..... N90-10455* #
NAS 1.26:185308 ..... N90-10168* #
NAS 1.26:185475 ..... N90-10075* #
NAS 1.26:185484 ..... N90-10317* #
NAS 1.26:185489 ..... N90-10678* #
NAS 1.26:185499 ..... N90-10584* #
NAS 1.26:185710 ..... N90-10124* #
NAS 1.26:185911 ..... N90-10466* #
NAS 1.26:185913 ..... N90-10465* #
NAS 1.26:185914 ..... N90-10815* #
NAS 1.26:185967 ..... N90-10446* #
NAS 1.55:3037 ..... N90-10140* #
NAS 1.55:3039 ..... N90-10805* #
NAS 1.55:3047 ..... N90-10385* #
NAS 1.60:2938 ..... N90-10618* #
NAS 1.60:2940 ..... N90-10074* #
NAS 1.60:2942 ..... N90-10814* #
NAS 1.60:2947 ..... N90-10680* #
NAS 1.60:2950 ..... N90-10179* #
NAS 1.60:2955 ..... N90-10248* #
NAS 1.61:1217 ..... N90-10807* #
NAS 1.61:1219 ..... N90-10412* #
NAS 1.71:LAR-13392-1-CU ..... N90-10132* #
NAS 1.71:LEW-14880-1 ..... N90-10415* #
NAS 1.71:LEW-14901-1 ..... N90-10718* #
NAS 1.71:MFS-28294-1 ..... N90-10310* #
NAS 1.71:MFS-28368-1 ..... N90-10717* #
NAS 1.71:NPO-17426-1-CU ..... N90-10329* #
NAS 1.71:NPO-17524-1-CU ..... N90-10261* #
NAS 1.71:NPO-17716-1-CU ..... N90-10608* #

NAS-SR-1322 ..... N90-10017 #

NASA-CASE-LAR-13392-1-CU ..... N90-10132* #

NASA-CASE-LEW-14880-1 ..... N90-10415* #
NASA-CASE-LEW-14901-1 ..... N90-10718* #

NASA-CASE-MFS-28294-1 ..... N90-10310* #
NASA-CASE-MFS-28368-1 ..... N90-10717* #

NASA-CASE-NPO-17426-1-CU ..... N90-10329* #
NASA-CASE-NPO-17524-1-CU ..... N90-10261* #
NASA-CASE-NPO-17716-1-CU ..... N90-10608* #

NASA-CP-3037 ..... N90-10140* #
NASA-CP-3039 ..... N90-10805* #
NASA-CP-3047 ..... N90-10385* #

NASA-CR-3996 ..... N90-10186* #
NASA-CR-4085 ..... N90-10012* #
NASA-CR-4175 ..... N90-10031* #
NASA-CR-174937 ..... N90-10011* #
NASA-CR-174992 ..... N90-10043* #
NASA-CR-174993 ..... N90-10044* #
NASA-CR-175070 ..... N90-10175* #
NASA-CR-177471 ..... N90-10021* #
NASA-CR-178166 ..... N90-10187* #
NASA-CR-178316 ..... N90-10030* #
NASA-CR-179374 ..... N90-10447* #
NASA-CR-179590 ..... N90-10683* #
NASA-CR-179629 ..... N90-10294* #
NASA-CR-179642 ..... N90-10184* #
NASA-CR-180831 ..... N90-10293* #
NASA-CR-180867 ..... N90-10048* #
NASA-CR-180868 ..... N90-10047* #
NASA-CR-180869 ..... N90-10049* #
NASA-CR-181331 ..... N90-10423* #
NASA-CR-181707 ..... N90-10129* #
NASA-CR-181845 ..... N90-10581* #
NASA-CR-181859 ..... N90-10007* #
NASA-CR-181867 ..... N90-10014* #
NASA-CR-181877 ..... N90-10681* #
NASA-CR-181903 ..... N90-10631* #
NASA-CR-181910 ..... N90-10677* #
NASA-CR-181913 ..... N90-10637* #
NASA-CR-181919 ..... N90-10638* #
NASA-CR-181920 ..... N90-10639* #
NASA-CR-181921 ..... N90-10576* #
NASA-CR-181926 ..... N90-10640* #
NASA-CR-182125 ..... N90-10045* #
NASA-CR-182142 ..... N90-10046* #
NASA-CR-182228 ..... N90-10037* #
NASA-CR-182235-VOL-2 ..... N90-10450* #
NASA-CR-182236 ..... N90-10451* #
NASA-CR-183054 ..... N90-10468* #
NASA-CR-183435 ..... N90-10583* #
NASA-CR-183445 ..... N90-10438* #
NASA-CR-183446 ..... N90-10479* #
NASA-CR-183447 ..... N90-10796* #
NASA-CR-183599 ..... N90-10137* #
NASA-CR-183600 ..... N90-10133* #
NASA-CR-183601 ..... N90-10136* #
NASA-CR-183602 ..... N90-10139* #
NASA-CR-183603 ..... N90-10135* #
NASA-CR-183604 ..... N90-10134* #
NASA-CR-183605 ..... N90-10138* #
NASA-CR-183676 ..... N90-10033* #
NASA-CR-183714 ..... N90-10413* #
NASA-CR-183727 ..... N90-10128* #
NASA-CR-183738 ..... N90-10171* #
NASA-CR-183739-VOL-1 ..... N90-10170* #
NASA-CR-183746 ..... N90-10169* #
NASA-CR-184781 ..... N90-10313* #
NASA-CR-184784 ..... N90-10588* #
NASA-CR-185031 ..... N90-10809* #
NASA-CR-185110 ..... N90-10437* #
NASA-CR-185118-VOL-1 ..... N90-10038* #
NASA-CR-185118-VOL-2 ..... N90-10039* #
NASA-CR-185133 ..... N90-10036* #
NASA-CR-185140 ..... N90-10004* #
NASA-CR-185143 ..... N90-10455* #
NASA-CR-185308 ..... N90-10168* #
NASA-CR-185475 ..... N90-10075* #
NASA-CR-185484 ..... N90-10317* #
NASA-CR-185489 ..... N90-10678* #
NASA-CR-185499 ..... N90-10584* #
NASA-CR-185710 ..... N90-10124* #
NASA-CR-185911 ..... N90-10466* #
NASA-CR-185913 ..... N90-10465* #
NASA-CR-185914 ..... N90-10815* #
NASA-CR-185967 ..... N90-10446* #

NASA-REPT-89-002 ..... N90-10317* #

NASA-RP-1217 ..... N90-10807* #
NASA-RP-1219 ..... N90-10412* #

NASA-SP-7011(328) N90-10524*
NASA-SP-7046(21) N90-10130*
NASA-SP-7056(08) N90-10131*
NASA-SP-7063(03) ..... N90-10782* #

NASA-TM-4134 ..... N90-10679* #
NASA-TM-4144 ..... N90-10034* #
NASA-TM-87690-PT-1 ..... N90-10505* #
NASA-TM-87690-PT-2 ..... N90-10506* #
NASA-TM-87690-PT-3 ..... N90-10507* #
NASA-TM-89125 ..... N90-10002* #
NASA-TM-89131 ..... N90-10409* #
NASA-TM-89154 ..... N90-10602* #
NASA-TM-89423 ..... N90-10042* #
NASA-TM-89429-VOL-3 ..... N90-10808* #
NASA-TM-89923 ..... N90-10174* #
NASA-TM-100169 ..... N90-10188* #
NASA-TM-101071 ..... N90-10183* #
NASA-TM-101089 ..... N90-10575* #
NASA-TM-101561 ..... N90-10577* #
NASA-TM-101578-PT-1 ..... N90-10080* #
NASA-TM-101578-PT-2 ..... N90-10103* #
NASA-TM-101612 ..... N90-10127* #
NASA-TM-101616 ..... N90-10308* #
NASA-TM-101638 ..... N90-10454* #
NASA-TM-101640 ..... N90-10456* #
NASA-TM-101648 ..... N90-10457* #
NASA-TM-101703 ..... N90-10023* #
NASA-TM-101706 ..... N90-10610* #
NASA-TM-101851 ..... N90-10076*
NASA-TM-101887 ..... N90-10077* #
NASA-TM-101889 ..... N90-10176* #
NASA-TM-101958 ..... N90-10181* #
NASA-TM-102149 ..... N90-10478* #
NASA-TM-102151 ..... N90-10571* #
NASA-TM-102152 ..... N90-10079* #
NASA-TM-102155 ..... N90-10795* #
NASA-TM-102195 ..... N90-10006* #
NASA-TM-102214 ..... N90-10542* #
NASA-TM-102291 ..... N90-10262* #
NASA-TM-102322 ..... N90-10309* #
NASA-TM-102329 ..... N90-10185* #
NASA-TM-102350 ..... N90-10737* #
NASA-TM-102356 ..... N90-10738* #
NASA-TM-102361 ..... N90-10635* #
NASA-TM-102367 ..... N90-10674* #
NASA-TM-102373 ..... N90-10172* #

NASA-TP-2938 ..... N90-10618* #
NASA-TP-2940 ..... N90-10074* #
NASA-TP-2942 ..... N90-10814* #
NASA-TP-2947 ..... N90-10680* #
NASA-TP-2950 ..... N90-10179* #
NASA-TP-2955 ..... N90-10248* #

NASOP-11-009(88/08) ..... N90-10826 #

NATED-11-009(88/08) ..... N90-10826 #

NAVAIR-50-1C-555 ..... N90-10503 #

NCAR/TN-330+PROC ..... N90-10032 #

NCSU/MTE-6 ..... N90-10760 #

NEPRF-TR-89-04 ..... N90-10596 #

NHRC-89-7 ..... N90-10533 #

NIST/GCR-89/563 ..... N90-10419 #
NIST/GCR-89/565 ..... N90-10217 #

NISTIR-89/4087 ..... N90-10420 #
NISTIR-89/4100 ..... N90-10636 #
NISTIR-89/4102 ..... N90-10659 #

NOAA-NWS-TDL-CP-89-1 ..... N90-10592 #
NOAA-NWS-TDL-CP-89-2 ..... N90-10593 #

NOAA-RR-NURP-88-1 ..... N90-10509 #

NOAA-TM-ERL-ARL-169 ..... N90-10500 #
NOAA-TM-ERL-ARL-171 ..... N90-10481 #

NOAA-TM-ERL-WPL-154 ..... N90-10355 #

NOAA-TM-NESDIS-AISC-15 ..... N90-10513 #

NOAA-TM-NWS-CR-96 ..... N90-10499 #

NOAA-TM-NWS-HYDRO-43 ..... N90-10498 #

NOAA-TM-NWS-SR-122 ..... N90-10492 #

NOAA-TR-ERL-434 ..... N90-10512 #

NOSC/TD-1499 ..... N90-10324 #
NOSC/TD-1544 ..... N90-10711 #

NOSC/TR-1284 ..... N90-10597 #

NPS55-89-03 ..... N90-10629 #
NPS61-89-010 ..... N90-10813 #

NRL-MR-6459 ..... N90-10425 #
NRL-MR-6479 ..... N90-10644 #
NRL-MR-6482 ..... N90-10531 #
NRL-MR-6486 ..... N90-10725 #
NRL-MR-6500 ..... N90-10727 #

NRL-9207 ..... N90-10077* #

NSWC-MP-88-172 ..... N90-10426 #

NTSB/AAR-89/03 ..... N90-10013 #

NUSC-TR-8367 ..... N90-10517 #

ONR-TR-12 ..... N90-10223 #

ONREUR-9-1-C ..... N90-10585 #
ONREUR-9-2-R ..... N90-10312 #

ORNL/FTR-3319 ..... N90-10264 #
ORNL/FTR-3342 ..... N90-10515 #

ORNL/TM-11184 ..... N90-10482 #

OTA-SET-431 ..... N90-10016 #

PARGUM-89-01 ..... N90-10708 #

PB88-248075 ..... N90-10491 #
PB89-124747 ..... N90-10355 #
PB89-139950 ..... N90-10817 #
PB89-145940 ..... N90-10492 #
PB89-152086 ..... N90-10818 #
PB89-152094 ..... N90-10819 #
PB89-152458 ..... N90-10509 #
PB89-156145 ..... N90-10493 #
PB89-159628 ..... N90-10494 #
PB89-162481 ..... N90-10820 #
PB89-162499 ..... N90-10821 #
PB89-169221 ..... N90-10016 #
PB89-173041 ..... N90-10822 #
PB89-173058 ..... N90-10823 #
PB89-174775 ..... N90-10032 #
PB89-190219 ..... N90-10481 #
PB89-191647 ..... N90-10452 #
PB89-192660 ..... N90-10587 #
PB89-193577 ..... N90-10512 #
PB89-193791 ..... N90-10320 #
PB89-194583 ..... N90-10513 #
PB89-194591 ..... N90-10499 #
PB89-194625 ..... N90-10500 #

PB89-194658 ..... N90-10824 #
PB89-195374 ..... N90-10793 #
PB89-195978 ..... N90-10592 #
PB89-195986 ..... N90-10593 #
PB89-196188 ..... N90-10511 #
PB89-196220 ..... N90-10514 #
PB89-196238 ..... N90-10510 #
PB89-201305 ..... N90-10498 #
PB89-206478 ..... N90-10501 #
PB89-206961 ..... N90-10480 #
PB89-209290 ..... N90-10420 #
PB89-209324 ..... N90-10419 #
PB89-209332 ..... N90-10636 #
PB89-210249 ..... N90-10487 #
PB89-214787 ..... N90-10217 #
PB89-215321 ..... N90-10659 #
PB89-218010 ..... N90-10472 #
PB89-910404 ..... N90-10013 #

PFC/IR-89-1 ..... N90-10723 #

PNL-SA-16848 ..... N90-10485 #
PNL-SA-16946 ..... N90-10343 #

P89-10131 ..... N90-10076*

R/D-4794-MS-01 ..... N90-10297 #
R/D-5735-EN-01 ..... N90-10508 #
R/D-5909-MS-01 ..... N90-10768 #
R/D-5970-MS-01-F ..... N90-10712 #
R/D-6012-CH-02 ..... N90-10178 #
R/D-6061-EN-02 ..... N90-10483 #

RADC-TR-88-324-VOL-5 ..... N90-10621 #
RADC-TR-88-324-VOL-7-PT-A ..... N90-10622 #
RADC-TR-89-30 ..... N90-10759 #

RARDE-12/88 ..... N90-10453 #

REPT-89-00014-01 ..... N90-10522 #
REPT-1583 ..... N90-10449 #

RF-447242 ..... N90-10330 #

RR-CE95 ..... N90-10452 #

S-595 ..... N90-10795* #

SAND-87-7120 ..... N90-10416 #
SAND-88-1432 ..... N90-10590 #
SAND-88-2427C ..... N90-10589 #
SAND-88-2465C ..... N90-10431 #
SAND-88-2766C ..... N90-10400 #
SAND-88-2911C ..... N90-10705 #
SAND-88-3060C ..... N90-10266 #
SAND-88-3470C ..... N90-10342 #
SAND-89-0252C ..... N90-10341 #
SAND-89-0271C ..... N90-10340 #
SAND-89-0287C ..... N90-10267 #
SAND-89-0339C ..... N90-10475 #
SAND-89-0544C-PT-1 ..... N90-10337 #
SAND-89-0545C-PT-2 ..... N90-10338 #
SAND-89-0700C ..... N90-10339 #
SAND-89-0788C ..... N90-10442 #
SAND-89-0839C ..... N90-10476 #
SAND-89-1161C ..... N90-10502 #
SAND-89-1461 ..... N90-10265 #
SAND-89-1625C ..... N90-10173 #
SAND-89-1696C ..... N90-10703 #
SAND-89-1876C ..... N90-10751 #
SAND-89-1881C ..... N90-10458 #

SD-TR-88-88 ..... N90-10269 #
SD-TR-88-89 ..... N90-10300 #
SD-TR-89-40 ..... N90-10435 #
SD-TR-89-42 ..... N90-10757 #
SD-TR-89-43 ..... N90-10490 #
SD-TR-89-44 ..... N90-10763 #
SD-TR-89-46 ..... N90-10434 #
SD-TR-89-47 ..... N90-10432 #

SDI-2-1 ..... N90-10305 #

SERI/STR-211-3238 ..... N90-10471 #
SERI/STR-211-3530 ..... N90-10734 #
SERI/STR-211-3539 ..... N90-10474 #
SERI/STR-217-3463 ..... N90-10473 #

SERI/TR-215-3195 ..... N90-10421 #

SGD-531-PT-2 ..... N90-10817 #
SGD-532-PT-1 ..... N90-10818 #
SGD-532-PT-2 ..... N90-10819 #
SGD-533-PT-1 ..... N90-10820 #
SGD-533-PT-2 ..... N90-10821 #
SGD-534-PT-1 ..... N90-10822 #
SGD-534-PT-2 ..... N90-10823 #
SGD-536-PT-2 ..... N90-10824 #

SR-6 ..... N90-10504 #
SR-7 ..... N90-10488 #

SRI-ECU-1243 ..... N90-10617 #

SRS/STD-TR86-011-549 ..... N90-10447* #

SU-SOL-89-6 ..... N90-10600 #

TACOM-TR-13458 ..... N90-10627 #

TASC-TR-5351-8-1 ..... N90-10322 #

TR-1 ..... N90-10226 #
TR-1 ..... N90-10229 #
TR-2 ..... N90-10260 #
TR-2 ..... N90-10278 #
TR-2 ..... N90-10291 #
TR-5 ..... N90-10693 #
TR-6-ONR ..... N90-10354 #
TR-7 ..... N90-10212 #
TR-7-ONR ..... N90-10299 #
TR-8 ..... N90-10209 #
TR-11 ..... N90-10211 #
TR-12 ..... N90-10733 #
TR-13 ..... N90-10214 #
TR-13 ..... N90-10464 #
TR-20 ..... N90-10284 #
TR-21 ..... N90-10287 #
TR-22 ..... N90-10285 #
TR-23 ..... N90-10654 #
TR-24 ..... N90-10779 #
TR-32 ..... N90-10652 #
TR-33 ..... N90-10668 #
TR-34 ..... N90-10666 #
TR-35 ..... N90-10667 #
TR-54 ..... N90-10673 #
TR-55 ..... N90-10672 #
TR-55 ..... N90-10684 #
TR-89-1 ..... N90-10411 #
TR-89-14 ..... N90-10662 #
TR-89-15 ..... N90-10663 #
TR-89-17C ..... N90-10661 #
TR-89-18C ..... N90-10660 #
TR-90 ..... N90-10253 #
TR-90 ..... N90-10692 #
TR-418 ..... N90-10641 #
TR-841 ..... N90-10078 #
TR-0086A(2060)-2 ..... N90-10434 #
TR-0088(3060)-1 ..... N90-10435 #
TR-0088(3907)-1 ..... N90-10432 #
TR-0088(3945-07)-1 ..... N90-10300 #
TR-0088(3945-07)-6 ..... N90-10269 #
TR-0089(4925-07)-1 ..... N90-10757 #
TR-0089(4925-07)-3 ..... N90-10763 #

TUM-F515/2/MI ..... N90-10449 #

TWR-17542-1 ..... N90-10170* #
TWR-17543-VOL-3 ..... N90-10169* #
TWR-18519 ..... N90-10413* #
TWR-18894 ..... N90-10171* #

UBUFFALO/DC/89/TR-100 ..... N90-10731 #
UBUFFALO/DC/89/TR-106 ..... N90-10764 #

UCID-21636 ..... N90-10719 #
UCID-21725 ..... N90-10428 #

UCRL-21188 ..... N90-10722 #
UCRL-53809-88 ..... N90-10794 #
UCRL-100242 ..... N90-10319 #
UCRL-100320 ..... N90-10332 #
UCRL-100355 ..... N90-10739 #
UCRL-100358 ..... N90-10331 #
UCRL-100511 ..... N90-10525 #
UCRL-100525 ..... N90-10344 #
UCRL-100647 ..... N90-10251 #
UCRL-100710 ..... N90-10423* #
UCRL-100718 ..... N90-10594 #
UCRL-100958 ..... N90-10582 #
UCRL-101209 ..... N90-10632 #
UCRL-101547 ..... N90-10252 #
UCRL-101566 ..... N90-10384 #

UDR-TR-87-27 ..... N90-10015 #

UM-025921-6-T ..... N90-10313* #

US-PATENT-APPL-SN-357759 ..... N90-10608* #
US-PATENT-APPL-SN-363815 ..... N90-10329* #
US-PATENT-APPL-SN-366957 ..... N90-10261* #
US-PATENT-APPL-SN-369490 ..... N90-10132* #
US-PATENT-APPL-SN-376488 ..... N90-10718* #
US-PATENT-APPL-SN-376738 ..... N90-10415* #
US-PATENT-APPL-SN-386174 ..... N90-10717* #
US-PATENT-APPL-SN-396262 ..... N90-10310* #

USAAEFA-86-12 ..... N90-10025 #

USAARL-88-6 ..... N90-10028 #
USAARL-89-8 ..... N90-10530 #

USABRDL-TR-8901 ..... N90-10306 #

USAFA-TR-89-04 ..... N90-10675 #

USARIEM-M-34-189 ..... N90-10541 #

USARIEM-M4-89 ..... N90-10523 #

USCG-D-07-89 ..... N90-10484 #

USCG/ONSCEN-01-89 ..... N90-10322 #

VLSI-MEMO-89-510 ..... N90-10580 #

VRI-DARPA-1-FR89-1(R) ..... N90-10791 #

WBS-HQ302-10-10 ..... N90-10413* #

WBS-4B102-10-10 ..... N90-10171* #
WBS-4B601-03-08 ..... N90-10170* #
WBS-4B601-04-01 ..... N90-10169* #

WHC-EP-0041 ..... N90-10398 #

WHOI-88-46 ..... N90-10511 #
WHOI-88-57 ..... N90-10467 #
WHOI-89-4 ..... N90-10514 #
WHOI-89-7 ..... N90-10510 #
WHOI-89-13 ..... N90-10468* #

WRDC-TR-89-2021 ..... N90-10303 #
WRDC-TR-89-2028 ..... N90-10449 #
WRDC-TR-89-2034 ..... N90-10027 #
WRDC-TR-89-4024-VOL-1 ..... N90-10761 #
WRDC-TR-89-4044-VOL-2 ..... N90-10024 #

Y/DW-890 ..... N90-10444 #

Appendix—About STAR

Scientific and Technical Aerospace Reports (STAR) is a major component of a comprehensive National Aeronautics and Space Administration information system covering aeronautics, space, and supporting disciplines. *STAR* is issued on the 8th and 23rd of each month and announces current publications of the following types:

- NASA, NASA contractor, and NASA grantee reports
- Reports issued by other U.S. Government agencies, domestic and foreign institutions, universities, and private firms
- Translations in report form
- NASA-owned patents and patent applications
- Other U.S. Government agency and foreign patents and patent applications
- Domestic and foreign dissertations and theses

Journal, book, and conference literature, cover-to-cover journal translations, and certain foreign dissertations are announced in a companion journal, *International Aerospace Abstracts (IAA),* available on subscription from the American Institute of Aeronautics and Astronautics, Technical Information Service, 555 West 57th Street, 12th Floor, New York, NY 10019.

SUBJECT SCOPE

The subject scope of *STAR* and *IAA* includes all aspects of aeronautics and space research and development, supporting basic and applied research, and applications. Aerospace aspects of earth resources, energy development, conservation, oceanography, environmental protection, urban transportation, and other topics of high national priority are also covered.

OTHER NASA PUBLICATIONS

Other NASA publications and information services are described in the publication, *The NASA Scientific and Technical Information System ... and How to Use It,* available without charge from the NASA Scientific and Technical Information Facility, P.O. Box 8757, BWI Airport, MD 21240.

HOW TO USE *STAR* SUBJECT CATEGORIES

STAR is categorized by 10 major subject divisions broken down further into 76 specific subject categories and one general division/category. The major subject divisions are listed on page ii in the Table of Contents, together with a note for each that defines its scope and provides any cross-references. For example:

AERONAUTICS

Includes aeronautics (general); aerodynamics; air transportation and safety; aircraft communications and navigation; aircraft design, testing and performance; aircraft instrumentation; aircraft propulsion and power; aircraft stability and control; and research and support facilities (air).

For related information see also *Astronautics.*

Each major division is further divided into as many as nine specific categories, which are identified by category numbers.

Abstracts in *STAR* are grouped by subject category, the categories appearing in sequential order. Category breaks in the abstract section are identified by the category number and title, and a scope note. Cross-references to other categories are provided as appropriate. For example:

02 AERODYNAMICS

Includes aerodynamics of bodies, combinations, wings, rotors, and control surfaces; and internal flow in ducts and turbomachinery.

For related information see also *34 Fluid Mechanics and Heat Transfer.*

CROSS-REFERENCES

Individual *STAR* abstracts are not ordinarily cross-referenced, except for certain conference reports or book translations that have had separate abstracts written for their component papers or chapters. Citations and abstracts of the components follow immediately after those of the parent document. When the subject content of a component differs sufficiently from the general content of the parent, a cross-reference citation also is printed at the end of the category to which it normally would have been assigned if it were independent.

DOCUMENTS ON MICROFICHE

Documents on microfiche[1] are designated by a pound sign (#) following the accession number. The pound sign is used without regard to the source or quality of the microfiche.

LIMITED REPRODUCIBILITY

A Note of Limited Reproducibility appears in the citation, if one or a combination of the following factors affect the reproducibility of more than 20% of the document. These factors include: faint or broken type, color photographs, black and white photographs, foldouts, dot matrix print, charts/graphs with script notation, non-Roman alphabet, or some other factor that limits the reproducibility of that document. This notation also appears on the microfiche header, with the specific causing factor checked off on a list visible in the second frame.

AVAILABILITIES

One or more sources from which a document announced in *STAR* is available to the public is given in each citation. The most commonly indicated sources and their acronyms or abbreviations are listed below. If the publication is available from a source other than those listed, the publisher and his address will be displayed on the availability line or in combination with the corporate source line.

Avail: NTIS. Sold by the National Technical Information Service. Prices for hard copy (HC) and microfiche (MF) are indicated by a price code following the letters HC or MF in the *STAR* citation. Current values for the price codes are given in the tables on page A-7.

Initially distributed microfiche under the NTIS SRIM (Selected Research in Microfiche) is available at greatly reduced unit prices. For this service and for information concerning subscription to NASA printed reports, consult the NTIS Subscription Section, Springfield, VA 22161.

NOTE ON ORDERING DOCUMENTS: When ordering NASA publications (those followed by the * symbol), use the N accession number. NASA patent applications (only the specifications are offered) should be ordered by the US-Patent-Appl-SN number. Non-NASA publications (no asterisk) should be ordered by the AD, PB, or other *report number* shown on the last line of the citation, not by the N accession number. It is also advisable to cite the title and other bibliographic identification.

(1) A microfiche is a transparent sheet of film, 105 by 148 mm in size, containing as many as 60 to 98 pages of information reduced to micro images (not to exceed 26:1 reduction).

Avail: SOD (or GPO). Sold by the Superintendent of Documents, U.S. Government Printing Office, in hard copy. The current price and order number are given following the availability line. (NTIS will fill microfiche requests, as indicated above, for those documents identified by a # symbol.)

Avail: BLL (formerly NLL): British Library Lending Division, Boston Spa, Wetherby, Yorkshire, England. Photocopies available from this organization at the price shown. (If none is given, inquiry should be addressed to the BLL.)

Avail: DOE Depository Libraries. Organizations in U.S. cities and abroad that maintain collections of Department of Energy reports, usually in microfiche form, are listed in *Energy Research Abstracts*. Services available from the DOE and its depositories are described in a booklet, *DOE Technical Information Center - Its Functions and Services* (TID-4660), which may be obtained without charge from the DOE Technical Information Center.

Avail: ESDU. Pricing information on specific data, computer programs, and details on Engineering Sciences Data Unit (ESDU) topic categories can be obtained from ESDU International Ltd. Requesters in North America should use the Virginia address while all other requesters should use the London address, both of which are on page A-6.

Avail: Fachinformationszentrum, Karlsruhe. Sold by the Fachinformationszentrum Energie, Physik, Mathematik GMBH, Eggenstein Leopoldshafen, Federal Republic of Germany, at the price shown in deutschmarks (DM).

Avail: HMSO. Publications of Her Majesty's Stationery Office are sold in the U.S. by Pendragon House, Inc. (PHI), Redwood City, CA. The U.S. price (including a service and mailing charge) is given, or a conversion table may be obtained from PHI.

Avail: NASA Public Document Rooms. Documents so indicated may be examined at or purchased from the National Aeronautics and Space Administration, Public Documents Room (Room 126), 600 Independence Ave., S.W., Washington, DC 20546, or public document rooms located at NASA installations, and the NASA Pasadena Office at the Jet Propulsion Laboratory.

Avail: Univ. Microfilms. Documents so indicated are dissertations selected from *Dissertation Abstracts* and are sold by University Microfilms as xerographic copy (HC) and microfilm. All requests should cite the author and the Order Number as they appear in the citation.

Avail: US Patent and Trademark Office. Sold by Commissioner of Patents and Trademarks, U.S. Patent and Trademark Office, at the standard price of $1.50 each, postage free. (See discussion of NASA patents and patent applications below.)

Avail: (US Sales Only). These foreign documents are available to users within the United States from the National Technical Information Service (NTIS). They are available to users outside the United States through the International Nuclear Information Service (INIS) representative in their country, or by applying directly to the issuing organization.

Avail: USGS. Originals of many reports from the U.S. Geological Survey, which may contain color illustrations, or otherwise may not have the quality of illustrations preserved in the microfiche or facsimile reproduction, may be examined by the public at the libraries of the USGS field offices whose addresses are listed in this Introduction. The libraries may be queried

concerning the availability of specific documents and the possible utilization of local copying services, such as color reproduction.

Avail: Issuing Activity, or Corporate Author, or no indication of availability. Inquiries as to the availability of these documents should be addressed to the organization shown in the citation as the corporate author of the document.

NASA PATENTS AND PATENT APPLICATIONS

Patents and patent applications owned by NASA are announced in *STAR* under appropriate subject categories and are referenced in the *STAR* indexes. In the Report/Accession Number Index, patents are indexed by the NASA Case Number (which appears in lieu of the report number in other indexes), the U.S. Patent Number, the U.S. Patent Application Serial Number, and the U.S. Patent Class. Patent applications for which patents have not yet been issued are indexed by the NASA Case Number and the U.S. Patent Application Serial Number.

NASA *patent application specifications* are sold in paper copy and microfiche by the National Technical Information Service (NTIS). The US-Patent-Appl-SN- number should be used in ordering either paper copy or microfiche from NTIS. Printed copies of *patents* (which are not microfiched) are available for purchase from:

Commissioner of Patents and Trademarks
U.S. Patent and Trademark Office
Washington, DC 20231

When ordering patents, the U.S. Patent Number should be used, and payment must be remitted in advance, by money order or check payable to the Commissioner of Patents and Trademarks. Prepaid purchase coupons for ordering are also available from the Patent and Trademark Office. The patents and patent applications announced in *STAR* are owned by NASA and are available for royalty-free licensing. Requests for licensing terms and further information should be addressed to:

Associate General Counsel for Intellectual Property/Code GP
National Aeronautics and Space Administration
Washington, DC 20546

ELIGIBILITY AND REGISTRATION FOR NASA INFORMATION PRODUCTS AND SERVICES

A variety of services is available to organizations of the following types that have registered with NASA to receive specific services or products:

1. NASA offices and installations, contractors, subcontractors, grantees, and consultants;
2. Other U.S. Government agencies and their contractors;
3. Libraries in the United States that have arrangements with NASA to maintain collections of NASA documents for public reference;
4. Other organizations in the United States having a need for NASA documents in work related to aeronautics and space research;
5. Organizations abroad that have established reciprocal document exchange arrangements with NASA.

Only the central service points or central points of document acquisition and control within qualified organizations are eligible to register for NASA products and services. Domestic organizations that may be eligible to receive various classes of NASA publications and services should address their requests for registration or for further information to:

NASA Scientific and Technical Information Facility
ATTN: Registration Services
P.O. Box 8757
BWI Airport, MD 21240
301-621-0153

Organizations abroad should direct requests to Manager, International STI Activities, NTT, NASA Headquarters, Washington, DC 20546.

AVAILABILITY OF *STAR* ABSTRACTS ON MICROFICHE

Microfiche of the abstract sections of this issue and other issues of *STAR* are available on annual subscription from NTIS as PB90-911300, Attn: Subscriptions, 5285 Port Royal Road, Springfield, VA 22161. Annual subscription rates are $75.50 North America; $151.00 foreign. Abstract sections for previous years retroactive to 1964 are available at the current rates. Microfiche for individual *STAR* issue abstract sections are not available.

PUBLIC COLLECTIONS OF NASA DOCUMENTS

DOMESTIC: NASA and NASA-sponsored documents and a large number of aerospace publications are available to the public for reference purposes at the library maintained by the American Institute of Aeronautics and Astronautics, Technical Information Service, 555 West 57th Street, 12th Floor, New York, NY 10019

EUROPEAN: An extensive collection of NASA and NASA-sponsored publications is maintained by the British Library Lending Division, Boston Spa, Wetherby, Yorkshire, England, for public access. The British Library Lending Division also has available many of the non-NASA publications cited in *STAR*. European requesters may purchase facsimile copy or microfiche of NASA and NASA-sponsored documents, those identified by both the symbols # and * from ESA - Information Retrieval Service, European Space Agency, 8-10 rue Mario-Nikis, 75738 Paris CEDEX 15, France.

FEDERAL DEPOSITORY LIBRARY PROGRAM

In order to provide the general public with greater access to U.S. Government publications, Congress established the Federal Depository Library Program under the Government Printing Office (GPO), with 51 regional depositories responsible for permanent retention of material, inter-library loan, and reference services. At least one copy of nearly every NASA and NASA-sponsored publication, either in printed or microfiche format, is received and retained by the 51 regional depositories. A list of the regional GPO libraries, arranged alphabetically by state, appears on the inside back cover. These libraries are *not* sales outlets. A local library can contact a Regional Depository to help locate specific reports, or direct contact may be made by an individual.

ADDRESSES OF ORGANIZATIONS

American Institute of Aeronautics and Astronautics
Technical Information Service
555 West 57th Street, 12th Floor
New York, New York 10019

British Library Lending Division,
Boston Spa, Wetherby, Yorkshire,
England

Commissioner of Patents and Trademarks
U.S. Patent and Trademark Office
Washington, DC 20231

Department of Energy
Technical Information Center
P.O. Box 62
Oak Ridge, Tennessee 37830

European Space Agency-Information Retrieval Service
ESRIN
Via Galileo Galilei
00044 Frascati (Rome) Italy

Engineering Sciences Data Unit International
P.O. Box 1633
Manassas, Virginia 22110

Engineering Sciences Data Unit International, Ltd.
251-259 Regent Street
London, W1R 7AD, England

Fachinformationszentrum Energie, Physik, Mathematik
GMBH
7514 Eggenstein Leopoldshafen
Federal Republic of Germany

Her Majesty's Stationery Office
P.O. Box 569, S.E. 1
London, England

NASA Scientific and Technical Information Facility
P.O. Box 8757
BWI Airport, Maryland 21240

National Aeronautics and Space Administration
Scientific and Technical Information Division (NTT)
Washington, DC 20546

National Technical Information Service
5285 Port Royal Road
Springfield, Virginia 22161

Pendragon House, Inc.
899 Broadway Avenue
Redwood City, California 94063

Superintendent of Documents
U.S. Government Printing Office
Washington, DC 20402

University Microfilms
A Xerox Company
300 North Zeeb Road
Ann Arbor, Michigan 48106

University Microfilms, Ltd.
Tylers Green
London, England

U.S. Geological Survey Library National Center
MS 950
12201 Sunrise Valley Drive
Reston, Virginia 22092

U.S. Geological Survey Library
2255 North Gemini Drive
Flagstaff, Arizona 86001

U.S. Geological Survey
345 Middlefield Road
Menlo Park, California 94025

U.S. Geological Survey Library
Box 25046
Denver Federal Center, MS914
Denver, Colorado 80225

NTIS PRICE SCHEDULES

(Effective January 1, 1990)

Schedule A
STANDARD PRICE DOCUMENTS AND MICROFICHE

PRICE CODE	NORTH AMERICAN PRICE	FOREIGN PRICE
A01	$ 8.00	$ 16.00
A02	11.00	22.00
A03	15.00	30.00
A04-A05	17.00	34.00
A06-A09	23.00	46.00
A10-A13	31.00	62.00
A14-A17	39.00	78.00
A18-A21	45.00	90.00
A22-A25	53.00	106.00
A99	*	*
NO1	55.00	70.00
NO2	55.00	80.00

Schedule E
EXCEPTION PRICE DOCUMENTS AND MICROFICHE

PRICE CODE	NORTH AMERICAN PRICE	FOREIGN PRICE
E01	$10.00	$ 20.00
E02	12.00	24.00
E03	14.00	28.00
E04	16.50	33.00
E05	18.50	37.00
E06	21.50	43.00
E07	24.00	48.00
E08	27.00	54.00
E09	29.50	59.00
E10	32.50	65.00
E11	35.00	70.00
E12	38.50	77.00
E13	41.00	82.00
E14	45.00	90.00
E15	48.50	97.00
E16	53.00	106.00
E17	57.50	115.00
E18	62.00	124.00
E19	69.00	138.00
E20	80.00	160.00
E99	*	*

* Contact NTIS for price quote.

IMPORTANT NOTICE

NTIS Shipping and Handling Charges

U.S., Canada, Mexico — ADD $3.00 per TOTAL ORDER

All Other Countries — ADD $4.00 per TOTAL ORDER

Exceptions — Does NOT apply to:

ORDERS REQUESTING NTIS RUSH HANDLING

ORDERS FOR SUBSCRIPTION OR STANDING ORDER PRODUCTS *ONLY*

NOTE: Each additional delivery address on an order requires a separate shipping and handling charge.

FEDERAL REGIONAL DEPOSITORY LIBRARIES

ALABAMA

AUBURN UNIV. AT MONTGOMERY LIBRARY
Documents Department
Montgomery, AL 36193
(205) 279-9110 ext.253

UNIV. OF ALABAMA LIBRARY
Reference Department/Documents
Box S
Tuscaloosa, AL 35486
(205) 348-6046

ARIZONA

DEPT. OF LIBRARY, ARCHIVES, AND PUBLIC RECORDS
Third Floor State Capitol
1700 West Washington
Phoenix, AZ 85007
(602) 255-4121

ARKANSAS

ARKANSAS STATE LIBRARY
Documents Service Section
One Capitol Mall
Little Rock, AR 72201
(501) 371-2090

CALIFORNIA

CALIFORNIA STATE LIBRARY
Govt. Publications Section
914 Capitol Mall
Sacramento, CA 95814
(916) 322-4572

COLORADO

UNIV. OF COLORADO
Norlin Library
Government Publications Division
Campus Box 184
Boulder, CO 80309
(303) 492-8834

DENVER PUBLIC LIBRARY
Govt. Pub. Department
1357 Broadway
Denver, CO 80203
(303) 571-2346

CONNECTICUT

CONNECTICUT STATE LIBRARY
231 Capitol Avenue
Hartford, CT 06106
(203) 566-4971

FLORIDA

UNIV. OF FLORIDA LIBRARIES
Documents Department
Library West
Gainesville, FL 32611
(904) 392-0367

GEORGIA

UNIV. OF GEORGIA LIBRARIES
Government Documents Dept.
Athens, GA 30602
(404) 542-8949

HAWAII

UNIV. OF HAWAII
Hamilton Library
Government Documents Collection
2550 The Mall
Honolulu, HI 96822
(808) 948-8230

IDAHO

UNIV. OF IDAHO LIBRARY
Documents Section
Moscow, ID 83843
(208) 885-6344

ILLINOIS

ILLINOIS STATE LIBRARY
Federal Documents
Centennial Building
Springfield, IL 62756
(217) 782-5012

INDIANA

INDIANA STATE LIBRARY
Serials Section
140 North Senate Avenue
Indianapolis, IN 46204
(317) 232-3686

IOWA

UNIV. OF IOWA LIBRARIES
Government Publications Dept.
Iowa City, IA 52242
(319) 335-5926

KANSAS

UNIVERSITY OF KANSAS
Spencer Research Library
Government Documents
Lawrence, KS 66045
(913) 864-4662

KENTUCKY

UNIV. OF KENTUCKY LIBRARIES
Government Publications/Maps Dept.
Lexington, KY 40506
(606) 257-8400

LOUISIANA

LOUISIANA STATE UNIVERSITY
Middleton Library
Government Documents Dept.
Baton Rouge, LA 70803
(504) 388-2570

LOUISIANA TECHNICAL UNIV.
Prescott Memorial Library
Government Documents Dept.
Ruston, LA 71272
(318) 257-4962

MAINE

UNIVERSITY OF MAINE
Raymond H. Fogler Library
Govt. Documents & Microforms Dept.
Orono, ME 04469
(207) 581-1680

MARYLAND

UNIVERSITY OF MARYLAND
McKeldin Library
Documents/Maps Room
College Park, MD 20742
(301) 454-3034

MASSACHUSETTS

BOSTON PUBLIC LIBRARY
Government Documents Dept.
666 Boylston Street
Boston, MA 02117
(617) 536-5400 ext.226

MICHIGAN

DETROIT PUBLIC LIBRARY
5201 Woodward Avenue
Detroit, MI 48202
(313) 833-1409

LIBRARY OF MICHIGAN
Government Documents
P.O. Box 30007
735 E. Michigan Avenue
Lansing, MI 48909
(517) 373-1593

MINNESOTA

UNIVERSITY OF MINNESOTA
Wilson Library
Government Publications
309 Nineteenth Avenue South
Minneapolis, MN 55455
(612) 373-7813

MISSISSIPPI

UNIV. OF MISSISSIPPI LIB.
Government Documents Dept.
106 Old Gym Bldg.
University, MS 38677
(601) 232-5857

MISSOURI

University of Missouri at Columbia Library
Government Documents
Columbia, MO 65201
(314) 882-6733

MONTANA

UNIV. OF MONTANA
Mansfield Library
Documents Division
Missoula, MT 59812
(406) 243-6700

NEBRASKA

UNIVERSITY OF NEBRASKA - LINCOLN
Love Memorial Library
Documents Department
Lincoln, NE 68588
(402) 472-2562

NEVADA

UNIV. OF NEVADA-RENO LIB.
Govt. Pub. Department
Reno, NV 89557
(702) 784-6579

NEW JERSEY

NEWARK PUBLIC LIBRARY
U.S. Documents Division
5 Washington Street
P.O. Box 630
Newark, NJ 07101
(201) 733-7812

NEW MEXICO

UNIVERSITY OF NEW MEXICO
General Library
Government Publications/Maps Dept.
Albuquerque, NM 87131
(505) 277-5441

NEW MEXICO STATE LIBRARY
325 Don Gaspar Avenue
Santa Fe, NM 87501
(505) 827-3826

NEW YORK

NEW YORK STATE LIBRARY
Documents Sect. Cultural Educ. Ctr.
Empire State Plaza
Albany, NY 12230
(518) 474-5563

NORTH CAROLINA

UNIVERSITY OF NORTH CAROLINA AT CHAPEL HILL
Davis Library 080A
BA/SS Department Documents
Chapel Hill, NC 27514
(919) 962-1151

NORTH DAKOTA

NORTH DAKOTA STATE UNIVERSITY LIBRARY
Government Documents Dept.
Fargo, ND 58105
(701) 237-8352
In cooperation with Univ. of North Dakota, Chester Fritz Library
Grand Forks

OHIO

STATE LIBRARY OF OHIO
Documents Section
65 South Front Street
Columbus, OH 43266
(614) 644-7051

OKLAHOMA

OKLAHOMA DEPT. OF LIBRARIES
Government Documents
200 NE 18th Street
Oklahoma City, OK 73105
(405) 521-2502, ext. 252

OKLAHOMA STATE UNIV. LIB.
Documents Department
Stillwater, OK 74078
(405) 624-0489

OREGON

PORTLAND STATE UNIV.
Millar Library
934 SW Harrison - P.O. Box 1151
Portland, OR 97207
(503) 229-3673

PENNSYLVANIA

STATE LIBRARY OF PENN.
Government Publications Section
Box 1601
Walnut St. & Commonwealth Ave.
Harrisburg, PA 17105
(717) 787-3752

SOUTH CAROLINA

CLEMSON UNIV. COOPER LIB.
Documents Department
Clemson, SC 29634
(803) 656-5174
In cooperation with Univ. of South Carolina, Thomas Cooper Library, Columbia

TEXAS

TEXAS STATE LIBRARY
Public Services Department
P.O. Box 12927 - 1201 Brazos
Austin, TX 78711
(512) 463-5455

TEXAS TECH. UNIV. LIBRARY
Documents Department
Lubbock, TX 79409
(806) 742-2268

UTAH

UTAH STATE UNIVERSITY
Merrill Library & Learning Resources Center, UMC-30
Documents Department
Logan, UT 84322
(801) 750-2682

VIRGINIA

UNIVERSITY OF VIRGINIA
Alderman Library
Government Documents
Charlottesville, VA 22903
(804) 924-3133

WASHINGTON

WASHINGTON STATE LIBRARY
Document Section
Olympia, WA 98504
(206) 753-4027

WEST VIRGINIA

WEST VIRGINIA UNIV. LIB.
Government Documents Section
P.O. Box 6069
Morgantown, WV 26506
(304) 293-3640

WISCONSIN

ST. HIST SOC. OF WISCONSIN LIB.
Government Pub. Section
816 State Street
Madison, WI 53706
(608) 262-2781
In cooperation with Univ. of Wisconsin-Madison, Memorial Library

MILWAUKEE PUBLIC LIBRARY
Documents Division
814 West Wisconsin Avenue
Milwaukee, WI 53233
(414) 278-3065

WYOMING

WYOMING STATE LIBRARY
Supreme Court & Library Bldg.
Cheyenne, WY 82002
(307) 777-5919

National Aeronautics and
Space Administration
Code NTT
Washington, D.C.
20546
Official Business
Penalty for Private Use, $300

SPECIAL FOURTH-CLASS RATE
POSTAGE & FEES PAID
NASA
PERMIT No. G27

NASA

POSTMASTER: If Undeliverable (Section 158
Postal Manual) Do Not Return